

Oil & Natural Gas Technology

DOE Award No.: DE-FC26-01NT41248

Final Technical Report

Arctic Energy Technology Development Laboratory

Submitted by:
Institute of Northern Engineering
University of Alaska Fairbanks
PO Box 755910
Fairbanks, AK 99775-5910

Prepared for:
United States Department of Energy
National Energy Technology Laboratory

April 2009



Office of Fossil Energy



Arctic Energy Technology Development Laboratory

Final Technical Report

Reporting Period Start: August 1, 2001
Reporting Period End: December 31, 2008

Dennis Witmer, Editor
(Complete list of authors on next page)
Institute of Northern Engineering
University of Alaska Fairbanks
ffdew@uaf.edu
907-474-7082

Report Issued: April 2009

DOE Award Number:
DE-FC26-01NT41248

Submitted by:
Institute of Northern Engineering
Arctic Energy Technology Development Laboratory
University of Alaska Fairbanks
PO Box 755910
Fairbanks, AK 99775-5910

Contributing Authors

Bandopadhyay, Sukumar – University of Alaska Fairbanks
Chamberlin, Charles – Humboldt State University
Chaney, Robert – Science Applications International Corporation
Chen, Gang – University of Alaska Fairbanks
Chukwu, Godwin – University of Alaska Fairbanks
Clough, James – Alaska Department of Natural Resources
Colt, Steve – University of Alaska Anchorage
Covscek, Anthony – Stanford University
Crosby, Robert – Remote Utility Systems Group
Dandekar, Abhijit – University of Alaska Fairbanks
Decker, Paul – Alaska Division of Geological and Geophysical Surveys
Galloway, Brandon – University of Alaska Fairbanks
Ganguli, Rajive – University of Alaska Fairbanks
Hanks, Catherine – University of Alaska Fairbanks
Haut, Rich – Houston Advanced Research Center
Hilton, Kristie – University of Alaska Fairbanks
Hinzman, Larry – University of Alaska Fairbanks
Holdman, Gwen – University of Alaska Fairbanks
Holland, Kristie – GW Scientific
Hunter, Robert – BP
Johnson, Ron – University of Alaska Fairbanks
Johnson, Thomas – University of Alaska Fairbanks
Kane, Doug – University of Alaska Fairbanks
Kaneveskiy, Mikhail – University of Alaska Fairbanks
Kenny, Tristan – University of Alaska Fairbanks
Khataniar, Santanu – University of Alaska Fairbanks
Kulkami, Abhijeet – University of Alaska Fairbanks
Lehman, Peter – Humboldt State University
Leigh, Mary Beth – University of Alaska Fairbanks
Liang, Jenn-Tai – University of Kansas
Lilly, Michael – GW Scientific
Lin, Chuen-Sen – University of Alaska Fairbanks
Martin, Paul – Pacific Northwest National Laboratory
McGrail, Pete – Pacific Northwest National Laboratory
Miller, Dan – University of Alaska Fairbanks
Misra, Debasmita – University of Alaska Fairbanks
Nagabhushana, Nagendra – University of Alaska Fairbanks
Ogbe, David – University of Alaska Fairbanks
Osborne, Amanda – University of Alaska Anchorage
Owen, Antoinette – Pacific Northwest National Laboratory
Patil, Sharish – University of Alaska Fairbanks
Reifenstuhl, Rocky – Alaska Division of Geological and Geophysical Surveys
Reynolds, Doug – University of Alaska Fairbanks
Robertson, Eric – Idaho National Engineering and Environmental Laboratory
Schaefer, H. Todd – Pacific Northwest National Laboratory
Schmid, Jack – University of Alaska Fairbanks
Shur, Yuri – University of Alaska Fairbanks
Tussing, Arlon – Institute of the North
Walker, Jack – ConocoPhillips Alaska
Walter, Katey – University of Alaska Fairbanks
Watson, Shannon – University of Alaska Fairbanks
White, Daniel – University of Alaska Fairbanks
White, Gregory – Idaho National Engineering and Environmental Laboratory
White, Mark – Pacific Northwest National Laboratory
Wies, Richard – University of Alaska Fairbanks
Williams, Tom – Houston Advanced Research Center
Witmer, Dennis – University of Alaska Fairbanks
Wollard, Craig – University of Alaska Anchorage
Zhu, Tao – University of Alaska Fairbanks

Disclaimer

This report was prepared as an account of work sponsored by an agency of the United States Government. Neither the United States Government nor any agency thereof, nor any of their employees, makes any warranty, express or implied, or assumes any legal liability or responsibility for the accuracy, completeness, or usefulness of any information, apparatus, product, or process disclosed, or represents that its use would not infringe privately owned rights. Reference herein to any specific commercial product, process, or service by trade name, trademark, manufacturer, or otherwise does not necessarily constitute or imply its endorsement, recommendation, or favoring by the United States Government or any agency thereof. The views and opinions of authors expressed herein do not necessarily state or reflect those of the United States Government or any agency thereof.

Abstract

The Arctic Energy Technology Development Laboratory was created by the University of Alaska Fairbanks in response to a congressionally mandated funding opportunity through the U.S. Department of Energy (DOE), specifically to encourage research partnerships between the university, the Alaskan energy industry, and the DOE. The enabling legislation permitted research in a broad variety of topics particularly of interest to Alaska, including providing more efficient and economical electrical power generation in rural villages, as well as research in coal, oil, and gas. The contract was managed as a cooperative research agreement, with active project monitoring and management from the DOE.

In the eight years of this partnership, approximately 30 projects were funded and completed. These projects, which were selected using an industry panel of Alaskan energy industry engineers and managers, cover a wide range of topics, such as diesel engine efficiency, fuel cells, coal combustion, methane gas hydrates, heavy oil recovery, and water issues associated with ice road construction in the oil fields of the North Slope. Each project was managed as a separate DOE contract, and the final technical report for each completed project is included with this final report.

The intent of this process was to address the energy research needs of Alaska and to develop research capability at the university. As such, the intent from the beginning of this process was to encourage development of partnerships and skills that would permit a transition to direct competitive funding opportunities managed from funding sources. This project has succeeded at both the individual project level and at the institutional development level, as many of the researchers at the university are currently submitting proposals to funding agencies, with some success.

Contents

Contributing Authors	iii
Disclaimer.....	iv
Abstract.....	v
Contents.....	vi
Executive Summary.....	1
Legislative Authorization and Overall Strategy.....	2
Project Selection Process	2
Industry Participation in the AETDL Process.....	4
Project Management	5
Project Summaries	6
Task 1.01.1 Energy Information Clearinghouse for Energy Technology Issues in Alaska	7
Task 1.01.2 Small-Scale Fuel Cell and Reformer Systems for Remote Power.....	8
Task 1.01.3 Crack Growth and Reliability Analysis of Solid Oxide Fuel Cells	9
Task 1.02.1 Low-Rank Coal Grinding Performance Versus Boiler Performance	10
Task 1.03.1 Effects of Village Power Quality on Fuel Consumption and Operating Expenses	11
Task 1.03.4 Methanol-Fired Fuel Cell for Use in Remote Applications.....	12
Task 1.03.5 Capture of Heat Energy from Diesel Engine After-Cooler Circuit	13
Task 1.03.6 Reliable and Affordable Energy Conference	14
Task 1.04.1 Galena Electric Power Situation Options Analysis	15
Task 1.04.2 Development and Assessment of Options for Potential CO ₂ Sequestration in Alaska	16
Task 1.04.3 A Compilation and Review of Proposed Alaska Development Projects	17
Task 1.05.1 Economic Analysis of Beluga Coal Gasification.....	18
Task 2.01.1 Transportation Issues in the Delivery of GTL Products from the Alaskan North Slope to Market	19
Task 2.02.1 Solid Oxide Fuel Cell System for Remote Power Generation	20
Task 2.03.1 Injection of CO ₂ for Recovery of Methane from Gas Hydrate Reservoirs	21
Task 2.03.2 Rural Alaska Coalbed Methane: Application of New Technologies to Explore and Produce Energy	22
Task 2.04.1 Testing of a 5 kW SOFC on Diesel Reformate for Remote Power Applications.....	23
Task 2.04.2 Analysis of Actual Operating Conditions of an Off-Grid Solid Oxide Fuel Cell.....	24

Task 2.04.3 Alaska Coalbed Methane Water Disposal Methods: A Review of Available CBM Information and Disposal and Treatment Options for Alaska	25
Task 2.08.2 Atqasuk Methane Seep	26
Task 3.01.1 Solvent-Based Enhanced Oil Recovery Process to Develop West Sak Alaska North Slope Heavy Oil Resources	27
Task 3.03.1 Characterization and Alteration of Wettability States of Alaskan Reservoirs to Improve Oil Recovery Efficiency	28
Task 3.03.2 Physical, Biological, and Chemical Implications of Mid-Winter Pumping of Tundra Ponds.....	29
Task 3.04.1 Reservoir Characterization, Source Rock Potential, Fossil Fuel Resources, and Basin Analyses, Bristol Bay Basin, Alaska	30
Task 3.04.2 Unraveling the Timing of Fluid Migration and Trap Formation in the Brooks Range Foothills: A Key to Discovering Hydrocarbons	31
Task 3.04.3 Novel Chemically Bonded Phosphate Ceramic Borehole Sealants for the Arctic Environment.....	32
Task 3.05.1 Evaluation of Wax Deposition and Its Control During Production of Alaska North Slope Oils.....	33
Task 3.05.2 Phase Behavior, Solid Organic Precipitation and Mobility Characterization Studies in Support of Enhanced Heavy Oil Recovery on the Alaska North Slope.....	34
Task 3.05.3 Chemical and Microbial Characterization of North Slope Heavy Oils to Assess Viscosity Reduction and Enhanced Recovery with Microbial Methods.....	35
Task 3.05.4 Operational Watershed Modeling Tools to Support North Slope Field Operations and Water Use	36
Task 3.08.1 Resource Characterization and Quantification of Natural Gas-Hydrate and Associated Free-Gas Accumulations in the Prudhoe Bay–Kuparuk River Area on the North Slope of Alaska.....	37
Task 3.08.2 DOE HARC Concept Study	38
Task 6.01.1 Administration	39
Acknowledgments.....	40
Appendix A Request for Proposals.....	41
Appendix B Enabling Legislation	49

Executive Summary

The Arctic Energy Technology Development Laboratory was created by the University of Alaska Fairbanks in response to a congressionally mandated funding opportunity through the U.S. Department of Energy (DOE), specifically to encourage research partnerships between the university, the Alaskan energy industry, and the DOE. The enabling legislation permitted research in a broad variety of topics particularly of interest to Alaska, including providing more efficient and economical electrical power generation in rural villages, as well as research in coal, oil, and gas. The contract was managed as a cooperative research agreement, with active project monitoring and management from the DOE.

In the eight years of this partnership, approximately thirty projects were funded and completed. These projects, which were selected using an industry panel of Alaskan energy industry engineers and managers, cover a wide range of topics, such as diesel engine efficiency, fuel cells, coal combustion, methane gas hydrates, heavy oil recovery, and water issues associated with ice road construction in the oil fields of the North Slope. Each project was managed as a separate DOE contract, and the final technical report for each completed project is included with this final report.

The intent of this process was to address the energy research needs of Alaska and to develop research capability at the university. As such, the intent from the beginning of this process was to encourage development of partnerships and skills that would permit a transition to direct competitive funding opportunities managed from funding sources. This project has succeeded at both the individual project level and at the institutional development level, as many of the researchers at the university are currently submitting proposals to funding agencies, with some success.

This final technical report includes individual stand-alone reports for each funded project. A brief one-page summary document is provided to assist the reader in finding information that is of interest. The broad research areas covered include heavy oil recovery, enhanced oil recovery methods, wax deposition issues, methane hydrates, environmental impacts of oil development (including water use and the deployment of new low-impact platform structures), new cementing techniques for arctic conditions, geological fracture mechanisms for oil migration, reservoir characterization of the Bristol Bay area, coal bed methane (including issues with produced water), methane seeps near Atkasuk, combustion properties of high-volatility low-rank Alaskan coals, testing of solid oxide fuel cells on diesel fuel and propane, testing of proton exchange membrane fuel cells on methanol, heat recovery from diesel engines, CO₂ sequestration options for Alaska, power options for the village of Galena (including the Toshiba 4S nuclear reactor), and review of energy options (including web sites and conferences).

Legislative Authorization and Overall Strategy

The Arctic Energy Technology Development Laboratory (AETDL) at the University of Alaska Fairbanks originated in legislation passed in 2001 PUBLIC LAW 106–398, section 3197. This legislation authorized the U.S. Department of Energy (DOE) to set up an Office of Arctic Energy. In 2001 initial funding of \$1,000,000 was provided.

As defined in the enabling legislation, the purpose of the Office of Arctic Energy was to promote research, development, and deployment of

- electrical power technology that is cost-effective and especially well-suited to meet the needs of rural and remote Alaska;
- alternative energy, including fuel cells, geothermal, and wind;
- natural gas hydrates, coal bed methane, and shallow bed natural gas;
- small hydroelectric facilities, river turbines, and tidal power;
- natural gas development, including gas-to-liquids technology and liquefied natural gas (along with associated transportation systems); and
- enhanced oil recovery technology, including heavy oil recovery, reinjection of carbon, and extended drilling reach technologies.

Project Selection Process

Given the breadth of the allowable research topics (well beyond the evaluation expertise of any individual), a process was needed to evaluate proposed projects. A system modeled on the National Laboratory Partnership program was instituted, and involved several steps. One-page pre-proposals were solicited in a general call for proposals, and were ranked by an industry panel. The highest-scoring projects were asked to submit a two-page pre-proposal with additional information and to make an oral presentation before the industry panel. The highest-ranking projects from this process were then asked to submit a complete DOE proposal, all of which were packaged and submitted to DOE for review and funding. Because of the diversity of allowable technologies, two panels were formed to review proposals: one for remote electrical issues and one for the oil, gas, and coal issues.

This process, which was used for four years, attracted 210 pre-proposals for consideration. Of these, 28 projects were submitted to the DOE National Energy Technology Laboratory (DOE/NETL) for funding consideration, from which 23 were approved and funded. Thirteen other projects were added to the contract through means other than the competitive process: five during the first funding year before the project selection process was in place, three during the last year (2008) as extensions of existing work or seed funding, and five at the direction of DOE/NETL. An administrative task was added to the project to cover the effort of administering such a complex contract, especially to assure that the cost share

needed on each individual task was documented. Four projects approved for funding were not completed (some were never started), so the 32 technical reports presented here represent the total of the work completed by this project.

When the contract was initially written in 2001, the overall contract covered a five-year period, not to exceed \$22,400,000 in federal funds, with an additional \$5,600,000 in cost share required. The contract, in fact, lasted eight years, with total funding to the university of approximately \$13,900,000, and a documented cost share of more than \$4,400,000.

There was much discussion about how this contract should be managed, in particular what the reporting requirements should be for each task, and how cost share should be assessed. Initially, the agreement was that the entire project was a single contract; that a single quarterly report sufficed for the whole; and that cost share would be assessed over the entire contract and needed to meet the minimum by the end of the contract. However, early in the project, these rules were changed to require complete reporting for each task, and cost-share matching on a project-by-project basis. Eventually, cost-share requirements were changed back to being based on the total contract (the DOE waived cost-share requirements on several directed tasks), although nearly all individual tasks met or exceeded cost-share requirements.

The project-selection process is described in Appendix A, Call for Proposals – FY 2003 and FY 2004 Funding Cycles (a similar process was used in 2002 and 2005). This process involved several steps:

- Circulation of the Request for Proposals (RFP).
- Formation of two industry review panels—one for fossil energy and one for remote power. (Panel members were volunteers, but needed to present a resume showing industry experience as well as academic credentials.)
- Deadline for one-page pre-proposals for submission electronically.
- Circulation and ranking of one-page pre-proposals by industry panel.
- Notification of top ten to twelve projects of advancement to second round, request for additional technical and financial information, and request to give oral presentation to review panel.
- Meeting of industry panel to hear oral presentations and rank projects.
- Preparation of complete DOE proposal by highest-ranking projects.
- Addition of new projects to existing project mix and submission to DOE as annual work plan.
- Review of proposals by DOE and funding of some projects.

Since one of the contract's major aims was to encourage university/industry partnerships, the scoring process included a category worth ten percent of the total score for a partnership.

Industry Participation in the AETDL Process

Inspection of the database from the AETDL proposal review process shows a diverse group of industry partners attracted to the opportunity. Seventy-six different external organizations are listed as prime external contacts on the proposals, including nine universities (in addition to the University of Alaska), nine agencies (state and federal), five national laboratories (including NETL), three major oil companies, four utilities, eight oil-support companies, fifteen consultants or engineering consulting companies, sixteen equipment manufacturers, three native corporations, and five small businesses.

Type	Proposals	Projects
Universities	9	2
Agencies	9	6
National labs	5	3
Oil companies	3	2
Oil support companies	8	2
Utilities	4	4
Consultants	15	5
Equipment suppliers	16	5
Native corporations	3	2
Small businesses	4	1
Total	76	32

Table 1. Summary of external involvement in proposal and projects at AETDL

A similar distribution of partnerships can be seen upon inspection of the funded projects. Two external universities, six agencies, three national labs, two oil companies, two oil-support companies, four utilities, five consultants, five equipment manufacturers, two native corporations, and one small business participated in approved projects.

At the University of Alaska, sixteen faculty participated as principal investigators on contract-related projects. These faculty are with the UAF Petroleum Engineering, Mechanical Engineering, and Electrical Engineering Departments, the Geophysical Institute, and the UA Institute of Social and Economic Research.

The wide variety of participants in the AETDL projects is demonstrated by the numerous authors who participated in this final report, including thirty-five associated with University of Alaska Fairbanks, three with University of Alaska Anchorage, five from other universities, seven from National Laboratories, four from private industry, three from government agencies, and five from private research organizations.

Project Management

Because the contract with NETL was written as a cooperative research agreement, reporting was a required task for each selected project, including a written quarterly report. However, AETDL also required attendance at quarterly review meetings, at which each project's principal investigator (PI) presented information on the project's progress during the quarter. This progress report was a twenty-minute PowerPoint presentation, followed by a question-and-answer period. Some of these quarterly reviews were broadcast via web from electronic meeting rooms; but this proved somewhat awkward, as the university and DOE subscribed to two different systems and communication between the two was difficult. During the last several years, a simpler system of webcasting the PowerPoint presentations with telephone conferencing was used, which proved more reliable.

One issue that occurred repeatedly during the contract was the relatively frequent change in DOE's project COTR. During the eight-year contract period, five individuals were assigned this role, with only one of them stationed in Alaska. Each new COTR needed time to become familiar with the wide variety of projects in progress under this contract, and as the cumulative history of the overall project grew, the task became more difficult. Fortunately, DOE's Arctic Energy Office representative, Mr. Brent Sheets, remained in place during the entire contract period, as did the PI at the university, so some continuity was maintained.

One of the project's complications was the necessary accounting required to track funding for each task. Adding to the complexity was the confusion of project funding, which came from multiple congressional budget line accounts at DOE. Furthermore, during the proposal-writing process, project names were selected by individual project PIs who sometimes selected titles similar to those of other funded projects. After several attempts to designate a mutually understandable designation for each task, a code was adopted based on the DOE BNR code, the initial year of funding, and a sequence number. More confusion was generated by project funding that was added from multiple fiscal year budgets, requiring inclusion in multiple work-plan budgets and multiple passes through the approval process. The process of vetting and approving annual work plans required patience on all sides, and the ultimate success of this project speaks volumes to the professionalism and good will of all participants. On the university side, great care was taken to keep all projects discrete so that no confusion arose from the accounting process.

Project Summaries

Given the wide variety of research topics permitted under the AETDL process, attempting to summarize the research requires a discussion of each individual project. A thorough understanding of the research requires reading each final report. Each project's final report was prepared as a stand-alone document, and many were submitted during the course of the contract as individual tasks were completed.

This final report contains a one-page overview of each funded project, including a project abstract, the objectives of the study, and a brief summary of the findings. The summary section is intended solely to allow the reader to locate projects of interest.

Project titles were assigned based on the title of proposals submitted under the project-selection process above, and thus were selected by the project PI. Some titles were quite similar to each other, so project numbers were assigned by NETL in an attempt to keep track of the discrete projects. The numbering is based on the funding stream and the initial year of the project, followed by a sequence number within that year.

Project Title:

Task 1.01.1 Energy Information Clearinghouse for Energy Technology Issues in Alaska

Program/Project Identification Number

DE-FC26-01NT41248 1.01.1

UAF PI Name and address

Ron Johnson
University of Alaska Fairbanks
PO Box 755905
Fairbanks, AK 99775-5905
(907) 474-6096 ffraj@uaf.edu

Abstract

Due to lack of roads and electrical grids, energy use and production patterns in Alaska are significantly different from other parts of the U.S. This project is designed to create a web site that addresses the range of available technologies for production of electrical power in remote areas, including analysis of cost, reliability, and state of development.

Objectives

Create a web site containing an unbiased assessment of emerging technologies and their potential for use in remote areas of Alaska.

Final Summary

The Energy Information Clearinghouse is useful as one site that integrates a wide variety of information relating to energy issues both worldwide and within Alaska. The information is presented in such a way as to be intelligible to the general public, as well as to provide details with links to relevant web sites for those with technical backgrounds.

[Link to final report](#)

Project Title:

Task 1.01.2 Small-Scale Fuel Cell and Reformer Systems for Remote Power

Program/Project Identification Number

DE-FC26-01NT41248 1.01.2

UAF PI Name and address

Dennis Witmer

University of Alaska Fairbanks
PO Box 755910
Fairbanks, AK 99775
(907) 474-7082 fdew@uaf.edu

Abstract

Due to lack of roads and electrical grids, much of the electricity is generated in rural Alaska using diesel electric generators, which are expensive to maintain and cause a wide variety of environmental problems. Fuel cells may prove to be a better alternative, offering higher efficiency, reduced emissions, improved heat recovery, and lower operating costs. However, the most readily available fuel in remote locations is diesel, which is difficult to reform to produce a hydrogen-rich gas necessary for operation of the fuel cell. This project is designed to evaluate the thermodynamic efficiency and operational reliability of fuel cells and reformers in the laboratory, to establish baseline performance prior to field testing.

Objectives

- 1) Continue to assess the viability of fuel cells for applications in remote areas of Alaska.
- 2) Purchase and test available hardware in the pre-commercial stages from vendors, and test systems for thermodynamic efficiency, reliability, and suitability for application in remote areas of Alaska.
- 3) Test reformer systems, especially those operating on readily available liquid fuels suitable for transport and storage in remote Alaskan regions.
- 4) Share information collected with Alaskan, national, and international fuel cell communities.

Final Summary

While the fuel cell industry advertises the rapid commercialization of their technology, attempts to purchase hardware from individual companies at prices comparable to that for conventional energy systems proved to be difficult. During this study, several technologies were identified that were tested in subsequent AETDL projects, but the prices were considerably higher than expected, and the durability and reliability of these products were lower than expected.

[Link to final report](#)

Project Title:

Task 1.01.3 Crack Growth and Reliability Analysis of Solid Oxide Fuel Cells

Program/Project Identification Number

DE-FC26-01NT41248 1.01.3

UAF PI Name and address

Sukumar Bandopadhyay
University of Alaska Fairbanks
P.O. Box 755960, 311 Duckering
Fairbanks, AK 99775-5960
(907) 474-7730 fs0b@uaf.edu

External PI Name and address

Naqendra Nagabhushana
University of Alaska Fairbanks
(907) 474-5150
ffnn@uaf.edu

Abstract

Solid oxide fuel cells (SOFCs) operate at high temperatures (800°C) and require that a material be stable in both oxidizing and reducing environments. Oxides are generally brittle materials, and materials processing flaws may cause premature failure, especially under thermal stresses during heat-up, and stress gradients caused by oxygen gradients.

Objectives

This project is designed to measure the crack propagation properties of yttria stabilized zirconia (YSZ) used in SOFCs.

Final Summary

Yttria stabilized zirconia (YSZ) of 9.6 mol% yttria composition was procured in the form of tubes 100 mm long. The composition is of interest as tubular electrolytes for SOFCs. Rings cut from the tubes were characterized for microstructure, phase stability, mechanical strength (Weibull modulus), and fracture mechanisms. The strength at operating condition of SOFCs (1000°C) decreased to 95 MPa as compared with room temperature strength of 230 MPa. However, the Weibull modulus remains relatively unchanged. Slow crack growth (SCG) parameter, $n = 17$ evaluated at room temperature in air was representative of well-studied brittle materials. Based on the results, further work is planned to evaluate the strength degradation, modulus, and failure in a more representative environment of the fuel cell.

[Link to final report](#)

Project Title:

Task 1.02.1 Low-Rank Coal Grinding Performance Versus Boiler Performance

Program/Project Identification Number

DE-FC26-01NT41248 1.02.1

UAF PI Name and address

Rajive Ganguli
University of Alaska Fairbanks,
Mining and Geological Engineering
PO Box 755800
Fairbanks, AK 99775-5800
(907) 474-6396 ffrg@uaf.edu

External PI Name and address

Alan Renshaw
Usibelli Coal Mine
(907) 683-9739
alan@usibelli.com

Abstract

Alaskan low-rank coal (LRC) from the Usibelli Mine in Healy, Alaska, is used to generate electrical power in pulverized boilers in Alaska and Asia. However, standards for particle size distribution (PSD) for pulverized coal are based on experience with higher-rank coals. This project will investigate the possibility that LRC can be burned at larger particle sizes, as the highly volatile coal components will fragment the coal during the combustion process. If this can be shown, lower operating costs, lower energy consumption during grinding, and larger markets could result.

Objectives

Establish optimal particle size distribution for Alaskan LRC used in pulverized coal boiler operations, and increase marketability of Alaskan LRCs by establishing combustion properties from reduced grinding.

Final Summary

The intent of this project was to demonstrate that Alaskan LRC, which is high in volatile content, need not be ground as fine as bituminous coal (typically low in volatile content) for optimum combustion in power plants. The grind or PSD, which is quantified by percentage of pulverized coal passing 74 microns (200 mesh), affects the pulverizer throughput in power plants; the finer the grind, the lower the throughput. For a power plant to maintain combustion levels, throughput needs to be high. The problem of particle size is compounded for Alaskan coal, since it has a low Hardgrove grindability index (HGI); that is, it is difficult to grind.

This project studied the relationship between PSD and power plant efficiency, emissions, and mill power consumption for low-rank high-volatile-content Alaskan coal. The emissions studied were CO, CO₂, NO_x, SO₂, and Hg (only two tests). The tested PSD range was 42% to 81% passing 76 microns. Within the tested range, there was very little correlation between PSD and power plant efficiency, CO, NO_x, and SO₂. Mercury emissions were very low and, therefore, did not allow comparison between grind sizes. Mill power consumption was lower for coarser grinds.

[Link to final report](#)

Project Title:

Task 1.03.1 Effects of Village Power Quality on Fuel Consumption and Operating Expenses

Program/Project Identification Number

DE-FC26-01NT41248 1.03.1

UAF PI Name and address

Richard Wies
University of Alaska Fairbanks
PO Box 755915
Fairbanks, AK 99775
(907)474-7071 frww@uaf.edu

External PI Name and address

Lumas Kendrick
Sentech, Inc.
(240) 223-5552
lkendrick@sentech.org

Abstract

Poor power quality in village power systems increases the cost of meeting the load. These costs take the form of increased fuel use and increased generator maintenance. Power quality problems may consist of poor power factor (PF) or waveform disturbances. The poor PF problem results when 3-phase generators serve unbalanced resistive (lighting) and inductive (motors) loads. Power factor values outside of the generator's optimum operating range result in inefficient generator operation, excessive fuel consumption, and increased maintenance. Waveform disturbances may be voltage sags, spikes, or other effects resulting from nonlinear loads, like energy-efficient fluorescent lighting that increase the amount of undesirable electrical noise in the system. The amount of noise in the system is measured using total harmonic distortion (THD), which is the ratio of the amount of useable voltage or current at the system operating frequency (60 Hz) to the overall amount of voltage or current. All of these power-quality conditions, alone or in combination, can act to degrade the overall system performance and increase energy costs. This project will measure the PF and the THD due to line noise in remote villages, and determine if this is affecting efficiency.

Objectives

This project involves collecting, formatting, and analyzing power system data from a representative number of rural villages in Alaska served by the Alaska Energy Authority (AEA).

Final Summary

Over its five-year history, this project has investigated approaches to improving power quality and implementing fuel-saving measures through the use of performance assessment software tools developed in MATLAB® Simulink®. The project has also investigated the implementation of remote monitoring, automated generation control, and the addition of renewable energy sources in select villages. Results have shown how many of these communities would benefit from the use of automated generation control by implementing a simple economic dispatch scheme and the integration of renewable energy sources, such as wind generation.

[Link to final report](#)

Project Title:

Task 1.03.4 Methanol-Fired Fuel Cell for Use in Remote Applications

Program/Project Identification Number

DE-FC26-01NT41248 1.03.4

UAF PI Name and address

Dennis Witmer
University of Alaska Fairbanks
PO Box 755910
Fairbanks, AK 99775
(907) 474-7082 fdew@uaf.edu

External PI Name and address

Peter Lehman
Schatz Energy Research Center
707-826-4345
pal1@axe.humboldt.edu

Abstract

Proton exchange membrane (PEM) fuel cells have been demonstrated to provide reliable power in remote sites at the 1 kW level when operated on hydrogen. However, hydrogen is not a readily available fuel in Alaska, and heavy hydrocarbon fuels are difficult to reform at small scale. This project will demonstrate the use of a methanol-water mix (freezing point – 126°F) as a fuel source for PEM fuel cells. Methanol is also readily available in bulk quantities in Fairbanks, and fuel costs are similar to those of conventional fuels. The reformer technology involves a palladium membrane, which will provide high-quality hydrogen suitable for the PEM fuel cell.

Objectives

- 1) Demonstrate in the laboratory the operation of a PEM fuel cell operating on liquid fuel suitable for use in remote areas of Alaska.
- 2) Demonstrate this technology in a suitably chosen field location in Alaska.

Final Summary

This project was designed to demonstrate an alternative to existing conventional technologies by developing an integrated power supply at 1 kW using a PEM fuel cell operated on methanol. During the course of this project, a methanol reformer was procured, and the efficiency of conversion of methanol to hydrogen was measured. This reformer was then integrated with a 1 kW PEM fuel cell, and system efficiency was measured using a 24-hour varying load profile. Results indicate that methanol reformation is relatively efficient, approaching 80% (LHV, methanol fuel in/hydrogen out). PEM fuel cells operating on pure hydrogen have been demonstrated to operate at efficiencies of about 50%. System efficiencies of greater than 30% were anticipated for the integrated system, but measured values were somewhat lower than this, due largely to a mismatch between reformer output and fuel cell size.

This project successfully demonstrated the use of methanol as a fuel for powering a fuel cell, but the project was terminated before a field demonstration could be undertaken due to issues associated with the source of funds. However, significant issues remain with PEM fuel cells, including system costs and reliability; and further work is needed before these devices can be used for providing electrical power in remote areas of Alaska.

[Link to final report](#)

Project Title:

Task 1.03.5 Capture of Heat Energy from Diesel Engine After-Cooler Circuit

Program/Project Identification Number

DE-FC26-01NT41248 1.03.5

UAF PI Name and address

Chuen-Sen Lin
University of Alaska Fairbanks
325 Duckering Building
Fairbanks, AK 99775
(907) 474-5126 fcsl@uaf.edu

External PI Name and address

Mark Teitzel
AVEC
(907) 565-5337
mteitzel@avec.org

Abstract

Diesel electrical generators produce waste heat as well as electrical power. New diesel generators, which use turbochargers, release a significant amount of heat from the turbocharger after-coolers and have no systems currently designed to capture the released heat for useful applications. Another significant amount of heat energy is the heat released from exhaust manifolds. This project will design, build, and test heat recovery systems for this energy. This project will also study the feasibility of recovering exhaust heat from a laboratory diesel engine using an ultra low-sulfur fuel. The feasibility will be evaluated according to quality and quantity of exhaust heat recovered, changes in engine efficiency and emissions, and possible manifold damages caused by applying exhaust heat recovery.

Objectives

This project will study different waste heat applications, select the most desirable application, design and fabricate prototypes for performance measurements, and determine the feasibility and economic impact of the selected application for Alaska villages. This project will also study the feasibility of recovering exhaust heat from an engine using an ultra low-sulfur fuel.

Final Summary

An exhaust-heat recovery system was fabricated, and 350 hours of testing was conducted. Based on testing data, the exhaust heat recovery heating system showed insignificant effects on engine performance and maintenance requirements. From measurements, it was determined that the amount of heat recovered from the system was about 50% of the heat energy contained in the exhaust (heat contained in exhaust was evaluated based on environment temperature). The estimated payback time for 100% use of recovered heat would be less than 3 years at a fuel price of \$3.50 per gallon, an interest rate of 10%, and an engine operation of 8 hours per day. During the performance of this study, several existing field projects utilizing this exhaust-heat recovery technology were identified and analyzed. Further investigations into using waste heat for additional electrical generation in Rankine cycle engines or chilling turbo-charged air are currently being funded by the Alaska Energy Authority and the EPA.

[Link to final report](#)

Project Title:

Task 1.03.6 Reliable and Affordable Energy Conference

Program/Project Identification Number

DE-FC26-01NT41248 1.03.6

UAF PI Name and address

Dennis Witmer
University of Alaska Fairbanks
PO Box 755910
Fairbanks, AK 99775
(907) 474-7082 fdew@uaf.edu

External PI Name and address

Peter Crimp
Alaska Energy Authority
(907) 771-3039
PCrimp@aidea.org

Abstract

In the enabling legislation for the Arctic Energy Office in 2001, specific inclusion was made for the study of ways to reduce the cost of electrical power in remote Alaskan communities. As part of this mandate, the University of Alaska, in conjunction with DOE, the Denali Commission, and the Alaska Energy Authority, has organized a series of rural energy conferences, held approximately every 18 months. The goal of these meeting is to bring together rural utility operators, rural community leaders, government agency representatives, equipment suppliers, and researchers from universities and national laboratories to discuss the current state of the art in rural power generation and to discuss current projects, including successes as well as near-successes.

Objectives

Bring Alaska Rural Energy providers, researchers, government agencies, and other interested parties together to discuss recent progress in providing energy to rural Alaska.

Final Summary

Five conferences were held at approximately 18-month intervals. At each of these conferences, presenters were encouraged to prepare PowerPoint files, which were collected and then made public on the UAF AETDL web site. This web site, which has become the best record of the conference, is located at <http://www.alaska.edu/uaf/cem/ine/aetdl/conferences/>.

There are thousands of pages of information on this web site, on many topics. Given the uncertain longevity of web information, we are providing copies of all the information in electronic form as documentation for this final report.

Link to final report

Project Title:

Task 1.04.1 Galena Electric Power Situation Options Analysis

Program/Project Identification Number

DE-FC26-01NT41248 1.04.1

UAF PI Name and address

Ron Johnson
University of Alaska Fairbanks
PO Box 755905
Fairbanks, AK 99775-5905
(907) 474-6096 ffrai@uaf.edu

External PI Name and address

Robert Chaney
SAIC
(907) 271-3633
Robert.E.Chaney@saic.com

Abstract

Providing electrical power in remote Alaskan villages is difficult due to a lack of electrical grids and roads. Currently, diesel generators provide power in most communities, but this technology is significantly more expensive than power on the grid, with significant environmental issues related to air emissions and fuel spills. The city of Galena, Alaska, has been offered a small nuclear power plant as a demonstration, but also has other options, including coal (there is a known coal seam several miles from town) and renewables.

Objectives

Assess the cost and feasibility of power options available to the city of Galena, including the current diesel generators, the proposed Toshiba nuclear power plant, a coal-fired power plant, and other renewable options, including low-head hydro, wind, and solar power.

Final Summary

Under the assumptions used in this study, the nuclear system is the clear economic winner when compared with diesel, even when diesel prices are low and nuclear security staff requirements are high. This result is due to the ability of the 10-MW nuclear plant to serve the entire residential heat load (about 8,000 MWh/yr and 2.3 MW peak) and the entire air station heat load (52 B Btu/yr). We have used a daily dispatch model to verify that nuclear capacity is always adequate to meet daily energy requirements for both of these large loads. When the nuclear power plant is unavailable, the air base can back up its own heat load, and the Galena diesel system almost surely can back up the Galena residential loads.

[Link to final report](#)

Project Title:

Task 1.04.2 Development and Assessment of Options for Potential CO₂ Sequestration in Alaska

Program/Project Identification Number

DE-FC26-01NT41248 1.04.2

UAF PI Name and address

Shirish Patil
University of Alaska Fairbanks
306 Tanana Drive, Room 415
Fairbanks, AK 99775
(907) 474-5127 ffslp@uaf.edu

External PI Name and address

Peter McGrail
PNNL
pete.mcgrail@pnl.gov

Abstract

As evidence for global warming becomes more convincing, concern with the CO₂ emissions from fossil fuel burning has led to suggestions of CO₂ separation and sequestration. In Alaska, significant CO₂ emissions are generated by the Alaska North Slope (ANS) oil fields, both as a byproduct of electrical production and as a component in natural gas. The ANS also has significant deposits of viscous oil, and injecting CO₂ into these structures would enhance the production of heavy oils as well as sequester the CO₂. This task is intended to evaluate the feasibility of such a project.

Objectives

- 1) Determine sources and potential sinks for CO₂ on the ANS.
- 2) Evaluate the economics of CO₂ flooding for improved oil recovery
- 3) Characterize sources and sinks of CO₂ statewide.

Final Summary

This study investigated CO₂ storage options by screening ANS oil pools amenable to enhanced oil recovery (EOR), by evaluating the phase behavior of viscous oil and CO₂ mixtures, and by simulating EOR through CO₂ flooding and migration of CO₂ in a saline aquifer. Phase-behavior studies revealed that CO₂ gas was partially miscible with West Sak viscous oil at a pressure close to the reservoir pressure. Compositional simulation of CO₂ flooding for a five-spot West Sak reservoir pattern showed an increase in percent recovery with an increase in pore volume (PV) injected, but at the expense of an early breakthrough. A sensitivity analysis of this CO₂ flooding project was found to be strongly dependent on such variables as oil price and discount rate. Investigation of supercritical CO₂ injection in a saline formation did not indicate an increase in temperature in this region of nearly continuous permafrost.

[Link to final report](#)

Project Title:

Task 1.04.3 A Compilation and Review of Proposed Alaska Development Projects

Program/Project Identification Number

DE-FC26-01NT41248 1.04.3

UAF PI Name and address

Steve Colt
University of Alaska Anchorage
3211 Providence Dr.
Anchorage, AK 99508
(907) 786-1753 afsgc@uaa.alask

External PI Name and address

Arlon R. Tussing
Alaska Pacific University
(206) 275-0665
tussing@mindspring.com

Abstract

Alaska has abundant known natural resources, but much of this natural wealth remains untapped due to lack of infrastructure. Public investment in infrastructure such as roads and power grids could encourage development, but this infrastructure is expensive, given the vast distances and difficult construction required in the Arctic. Economic analysis of many individual projects have been undertaken in the past, but finding clusters of projects that could share infrastructure could change the economics sufficiently to justify investment in one region of Alaska.

Objectives

This study will catalog timely and available economic-feasibility, benefit-cost, and similar study reports regarding potential energy infrastructure and resource development projects in Alaska. Potential inferences from this data will be summarized to suggest the most useful lines of further research to remove development bottlenecks in energy supply and energy-related infrastructure.

Final Summary

Many energy projects have been proposed in Alaska over the past several decades. Proposed energy projects have ranged from large-scale hydro projects that have never been built, to small-scale village power projects for use of local alternative energy sources, many of which also have not been built. This project was initially intended to review these rejected projects to evaluate the economic feasibility of the ideas in light of current economics. This review included contacting the agencies responsible for reviewing and funding these projects in Alaska, including the Alaska Energy Authority, the Denali Commission, and the Arctic Energy Technology Development Laboratory; obtaining available information about these projects; and analyzing the economic data. Unfortunately, the most apparent result of this effort was that the data associated with these projects was not collected in a systematic way that allowed this information to be analyzed in a coherent fashion.

[Link to final report](#)

Project Title:

Task 1.05.1 Economic Analysis of Beluga Coal Gasification

Program/Project Identification Number

DE-FC26-01NT41248 1.05.1

UAF PI Name and address

Steve Colt

University of Alaska Anchorage
3211 Providence Dr.
Anchorage, AK 99508
(907) 786-1753 afsgc@uaa.alask

Abstract

The Institute of Social and Economic Research (ISER) will provide economic analysis of options for the gasification and use of coal from Alaska's Beluga Coal Field. Project partners organized by the DOE/NETL will provide engineering costs of mining, gasification, and product production options, as well as projected market prices for possible products of gasification. In project phase 1, the model will consider the feasibility of a gasification plant located at the Agrium fertilizer plant. In project phase 2, a generalized plant located in Cook Inlet will be analyzed.

Objectives

Conduct economic analysis of Beluga Coal Field gasification project.

Final Summary

The ISER was requested to conduct an economic analysis of a possible "Cook Inlet Syngas Pipeline." The economic analysis was incorporated as section 7.4 of the larger report entitled "Beluga Coal Gasification Feasibility Study, DOE/NETL-2006/1248, Phase 2 Final Report, October 2006, for Subtask 41817.333.01.01." The pipeline would carry CO₂ and N₂-H₂ from a synthetic gas plant on the western side of Cook Inlet to Agrium's facility. Economic analysis determined that the net present value of the total capital and operating life-cycle costs for the pipeline ranges from \$318 to \$588 million. The greatest contributor to this spread is the cost of electricity, which ranged from \$0.05 to \$0.10/kWh in this analysis. The financial analysis shows that the delivery cost of gas may range from \$0.33 to \$0.55/Mcf in the first year, depending primarily on the price for electricity.

[Link to final report](#)

Project Title:

Task 2.01.1 Transportation Issues in the Delivery of GTL Products from the Alaskan North Slope to Market

Program/Project Identification Number

DE-FC26-01NT41248 2.01.1

UAF PI Name and address

Gang Chen

University of Alaska Fairbanks
315 Duckering Building
Fairbanks, AK 99775
(907) 474-6875 fgc@uaf.edu

Abstract

Alaska's North Slope oil fields contain large quantities of natural gas, currently being re-injected to maintain pressure in the oil fields. A natural gas pipeline is proposed, but economic viability of such a project is questionable. An alternative method of marketing the gas would be to use a gas-to-liquids (GTL) process to create diesel length chains that could be shipped through the existing Trans Alaskan Pipeline System (TAPS), thus extending the life of the pipeline by ensuring adequate liquid flow to keep the system viable. This GTL product is sulfur-free, and properties can be altered during processing, resulting in a high-value product. However, transporting this product in the pipeline presents some issues. First, long length chains created in the Fischer-Tropsch (FT) process could cause waxing problems in the pipeline and possible gelling of the liquid. Secondly, the liquid could be shipped either by mixing with the crude oil (with a loss in value due to mixing with sulfur-containing crudes) or in slugs with pigs at either end (but some mixing would occur due to bypass and mixing at pump stations)

Objectives

- 1) Measure properties of GTL product that affect transportation in the TAPS, including viscosity, gel strength, and wax content.
- 2) Model the mixing behavior of GTL/crude slug methods.

Final Summary

The focus of this project was to study the operational challenges involved in transporting gas in converted liquid form through the existing TAPS.

A three-year, comprehensive research program was undertaken by the Petroleum Development Laboratory, University of Alaska Fairbanks, under Cooperative Agreement No. DE-FC26-98FT40016 to study the feasibility of transporting GTL products through TAPS. Cold restart of TAPS following an extended winter shutdown and solids deposition in the pipeline were identified as the main transportation issues in moving GTL products through the pipeline. The scope of work in the current project (Cooperative Agreement No. DE-FC26-01NT41248) included preparation of fluid samples for the experiments to be conducted to augment the comprehensive research program.

[Link to final report](#)

Project Title:

Task 2.02.1 Solid Oxide Fuel Cell System for Remote Power Generation

Program/Project Identification Number

DE-FC26-01NT41248 2.02.1

UAF PI Name and address

Dennis Witmer
University of Alaska Fairbanks
PO Box 755910
Fairbanks, AK 99775
(907) 474-7082 fdew@uaf.edu

External PI Name and address

Gary Allen
Fuel Cell Technologies, Ltd.
(613) 541-6114
gallen@fct.ca

Abstract

Solid oxide fuel cells (SOFCs) have been successfully demonstrated at the 200 kW size to be the most efficient and reliable of the fuel cell technologies currently available. However, many applications in Alaska require smaller power loads. This project will evaluate the performance of a small 5-kW fuel cell system for possible use in remote Alaskan applications. The first task will be to establish the thermodynamic energy balance for the system.

Objectives

- 1) Demonstrate the successful operation of a 5 kW SOFC, operating on natural gas.
- 2) Measure thermodynamic efficiency of a 5 kW unit, including net electrical energy out and recoverable useful heat.
- 3) Demonstrate a unit operating on propane, methanol, and GTL products.
- 4) Place unit in field for demonstration.

Final Summary

In this work, a 5 kW fuel cell was delivered to UAF from Fuel Cell Technologies of Kingston, Ontario. The cell stack was a tubular design, and was built by Siemens Westinghouse Fuel Cell Division. This stack achieved a run of more than one year while delivering grid-quality electricity from natural gas with virtually no degradation and at an electrical efficiency of nearly 40%. The project was ended after two control-system failures resulted in system damage.

While this demonstration was successful, considerable additional product development is required before this technology can provide electrical energy in remote Alaska. The major issue is cost, and currently, the largest component of system cost is the fuel cell stack cost, although the cost of the balance of plant is not insignificant. While several manufacturers are working on schemes for significant cost reduction, these systems do not yet provide the same level of performance and reliability as the larger-scale Siemens systems, or levels that would justify commercial deployment.

[Link to final report](#)

Project Title:

Task 2.03.1 Injection of CO₂ for Recovery of Methane from Gas Hydrate Reservoirs

Program/Project Identification Number

DE-FC26-01NT41248 2.03.1

UAF PI Name and address

Tao Zhu
University of Alaska Fairbanks
411 Duckering Building
Fairbanks, AK 99775
(907) 474-5141 fftz@uaf.edu

External PI Name and address

James Bush
PNNL
(509) 376-6555
jg.bush@pnl.gov

Abstract

Methane hydrates are clathrate structures that trap methane molecules in a solid phase, and are formed under conditions of high pressure and temperatures just above 0°C. If natural gas can be produced from these structures, total energy reserves are estimated to be far larger than from conventional geological natural gas deposits. Methane hydrate formations are known to exist in the North Slope oil fields, embedded with and just below permafrost soils. This project will investigate the possible use of CO₂ to displace methane in hydrate structures for production of natural gas from methane hydrates. This process is thermodynamically favorable, would stabilize the structures (important on North Slope applications where even a few feet of subsidence would put the area below sea level), and would be carbon neutral.

Objectives

- 1) Establish the feasibility of using CO₂ to displace CH₄ in hydrate structures in porous media in laboratory experiments.
- 2) Model reservoir behavior to assess feasibility of using this method to produce natural gas on the North Slope.

Final Summary

The EGHR (enhanced gas hydrate recovery) concept discussed in this report takes advantage of the physical and thermodynamic properties of mixtures in the H₂O-CO₂ system, combined with controlled multiphase flow, heat, and mass transport processes in hydrate-bearing porous media. The results were verified with computer modeling using the STOMP-HYD simulator, which showed more than three times enhancement in production rate using the EGHR technique when compared with warm water injection alone. The gas exchange technology (including EHGR) releases methane by replacing it with a more thermodynamic molecule (e.g., carbon dioxide). This technology has four advantages: 1) it sequesters a greenhouse gas (CO₂); 2) it releases energy via an exothermic reaction; 3) it retains the mechanical stability of the hydrate reservoir; and 4) the produced water can be used to form the emulsion and recycled into the reservoir, thus eliminating a disposal problem in arctic settings.

[Link to final report](#)

Project Title:

Task 2.03.2 Rural Alaska Coalbed Methane: Application of New Technologies to Explore and Produce Energy

Program/Project Identification Number

DE-FC26-01NT41248 2.03.2

UAF PI Name and address

Shirish Patil
University of Alaska Fairbanks
306 Tanana Drive, Room 415
Fairbanks, AK 99775
(907) 474-5127 fsip@uaf.edu

External PI Name and address

James Clough
Alaska DGGs
(907) 451-5030
jim.clough@alaska.gov

Abstract

Coal is widely distributed in Alaska, but most remote power generation depends on diesel electric generators. Over 37 rural Alaska villages are situated on or are immediately adjacent to coalfields that are potential coalbed methane (CBM) sources. Coalbed methane, particularly from low-rank coals, might be an ideal alternative to current technology, but significant reductions must be made to the cost of drilling production wells before this alternative is economic. Produced water management and gas production rates need to be determined. This three-year program will test the producibility of low-rank coals using slim-hole drilling techniques that are essential to reducing mobilization and drilling

Objectives

The objectives of this program are several:

- 1) To determine the actual CBM energy requirements and surface facility needs for a medium-sized rural village like Fort Yukon (population ~650).
- 2) To determine if low-rank coals, such as are present at Fort Yukon, are capable of CBM production.
- 3) To determine if slim-hole drilling technology can be used to reduce gas production and dewatering costs.
- 4) To determine if production of low volumes of gas, at temperatures well below freezing during winter months, can be achieved.
- 5) To assemble a database of information on gas and water flow rates, gas content, coal seam properties, well drilling, completion and stimulation techniques, and pumping and injection systems for dewatering and water management.

Final Summary

It was concluded that the Fort Yukon coal deposit has neither an adequate gas content nor sufficient permeability to supply the amount of gas required to meet the energy needs of Fort Yukon village. Even if the required amount of methane could be produced, the cost of electricity may not be competitive with the current method of diesel power generation. However, the project did show that slim-hole drilling with lightweight, portable rigs is a technically feasible method for CBM gas production in remote areas. An initially unanticipated outcome of the project was that drilling waste generated in the project could be successfully used as a sealant in landfill areas without any significant environmental risk. This provides for a method to dispose of drilling waste in remote areas at reduced cost.

[Link to final report](#)

Project Title:

Task 2.04.1 Testing of a 5 kW SOFC on Diesel Reformate for Remote Power Applications

Program/Project Identification Number

DE-FC26-01NT41248 2.04.1

UAF PI Name and address

Dennis Witmer
University of Alaska Fairbanks
PO Box 755910
Fairbanks, AK 99775
(907) 474-7082 fdew@uaf.edu

External PI Name and address

Lyman Frost
INEEL
(208) 526-2491
frosli@inel.gov

Abstract

Solid oxide fuel cells (SOFC) have been demonstrated to generate electrical power at high efficiency at the 5 kW range when operated on natural gas (this demonstration continues). However, natural gas is not a readily available fuel in remote locations, where the value of electrical power is high. Thus, operating these fuel cells on liquid fuels, preferably diesel fuels, is critical to the use of fuel cells in these locations. This program is designed to test a SOFC on a diesel reformate, first using a large-scale fuel processor currently being built at INEEL. The second phase of this program is to use the same fuel cell, but operate it on a small 5 kW Pox fuel processor to be designed and built by SOFCo.

Objectives

- 1) Continue operating existing fuel cell on natural gas to establish stack degradation and lifetime data.
- 2) Demonstrate tubular SOFC system operating on dilute reformate stream provided by INEEL 500 kW diesel reformer.
- 3) Develop small-scale 5 kW diesel Pox reformer.
- 4) Demonstrate SOFC and diesel reformer operation in breadboard configuration.

Final Summary

Results from this project were somewhat encouraging, with laboratory breadboard integration of a small-scale diesel reformer and demonstration of a SOFC in the first 18 months of the project. This initial demonstration was conducted at INEEL in the spring of 2005, using a small-scale diesel reformer provided by SOFCo and a fuel cell provided by Acumentrics. However, attempts to integrate and automate the available technology have not proved successful yet. This is due both to the lack of movement on the fuel processing side as well as to the rather poor stack lifetimes exhibited by the fuel cells. A commercial product is still unavailable, and pre-commercial devices are extremely expensive and require extensive field support.

[Link to final report](#)

Project Title:

Task 2.04.2 Analysis of Actual Operating Conditions of an Off-Grid Solid Oxide Fuel Cell

Program/Project Identification Number

DE-FC26-01NT41248 2.04.2

UAF PI Name and address

Dennis Witmer
University of Alaska Fairbanks
PO Box 755910
Fairbanks, AK 99775
(907) 474-7082 ffdew@uaf.edu

External PI Name and address

Tim Hudson
National Park Service
(907) 644-3381
tim_hudson@nps.gov

Abstract

The National Park Service (NPS) has purchased a 5 kW solid oxide fuel cell (SOFC) that operates on propane to be deployed at the Exit Glacier Visitor Center in Seward, Alaska. This project will monitor the performance of this fuel cell and provide independent third-party reporting and analysis of this demonstration.

Objectives

- 1) Establish the efficiency, reliability, and suitability of small-scale SOFCs for use in remote areas of Alaska.
- 2) Demonstrate the operation of a SOFC operating on propane.

Final Summary

This project was intended to demonstrate the operation of a 5 kW fuel cell that uses propane at a remote site (defined as one without access to grid power, Internet, or cell phone, but on the road system). A fuel cell was purchased by the NPS for installation in their newly constructed visitor center at Exit Glacier, Kenai Fjords National Park. The DOE participation in this project as initially scoped was for independent verification of the operation of this demonstration.

This project met with mixed success. The fuel cell has operated over six seasons at the facility with varying degrees of success; it had one very good run of about 1049 hours late in the summer of 2006. In general, however, the operation was below expectations. There were numerous stack failures, the efficiency of electrical generation was lower than expected, and the field support effort required was far higher than expected.

Based on the results, this technology has not developed to the point where demonstrations in off-road sites are justified.

[Link to final report](#)

Project Title:

Task 2.04.3 Alaska Coalbed Methane Water Disposal Methods: A Review of Available CBM Information and Disposal and Treatment Options for Alaska

Program/Project Identification Number

DE-FC26-01NT41248 2.04.3

UAF PI Name and address

Debasmita Misra
University of Alaska Fairbanks
307Duckering Building
Fairbanks, AK 99775
(907) 474-5339 ffdm1@uaf.edu

External PI Name and address

Mike Lilly
GW Scientific
(907) 479-8891
mlilly@gwscientific.com

Abstract

Natural gas produced from coal seams—also referred to as coal bed methane (CBM)—is becoming an increasingly important source of natural gas in the U.S. Coal seams suitable for this process are relatively shallow (1000–3000 feet), but are saturated with groundwater. Production of natural gas requires that the seam be de-watered before the methane can be released, resulting in large volumes of produced water. While this water could be re-injected to the earth, such processes are expensive, and the water may be of suitable quality for other uses. This study is intended to survey the issue of produced water and to consider the water-use options available for Alaska.

Objectives

- 1) Review relevant studies of CBM-produced water in the Lower 48, and the uses for this water (re-injected, surface disposal, agricultural uses).
- 2) Review available relevant data on water quality from Alaskan shallow coal seams in the Matanuska-Susitna Valley and other parts of the state.
- 3) Evaluate the possible uses of produced water in Alaska.

Final Summary

The review of CBM-produced water quantity and quality indicates that generalizations about what should be expected in rural Alaska communities is very difficult without site information about the CBM reservoir properties, formation water chemistry, infrastructure, and needs in each setting. The production of CBM water can vary from near zero to requirements to pump for many years. The range of water quality can also vary from near-drinking-water standards to water quality that could be costly to treat.

[Link to final report](#)

Project Title:

Task 2.08.2 Atqasuk Methane Seep

Program/Project Identification Number

DE-FC26-01NT41248 2.08.2

UAF PI Name and address

Katey Walter
University of Alaska Fairbanks
PO Box 755910
Fairbanks, AK 99775-5910
(907) 474-6095 ftkmw1@uaf.edu

Abstract

Methane gas is both an energy source, being the primary component in natural gas, and an atmospheric gas of concern in global climate change models. Methane is produced in nature as a byproduct of the decay of vegetation. Alaska's North Slope contains large amounts of frozen peat that are significant reservoirs of carbon, but as temperatures warm, there is concern that additional biological activity could release significant quantities of methane, thus accelerating climate change. For this reason, researchers have been attempting to quantify the rate of methane production from these areas. In January 2008, the PI led a small team of researchers to measure the flow rate of methane from a seep near Atqasuk. The measurements consistently indicated that the flow rate was approximately 3000 cubic feet per day, and that the gas is methane. This flow rate is considerably higher than found in typical lakes, where methane is produced from decaying vegetation on the bottom of the lake at a rate of less than 1 cubic foot per day, so the source of the seep near Atqasuk is of scientific interest. This quantity of methane is also enough to supply energy for several homes, although, based on preliminary economic calculations, this single seep is likely too far from the village and too small to power the entire village. However, if the seep is related to either coal deposits or a deeper gas source, drilling for gas in or near the village may be feasible.

Objectives

The objectives of this study were to measure Atqasuk seep flow rates, characterize gas from this seep, locate other seeps nearby, and evaluate the possible use of this gas in the village of Atqasuk to displace diesel fuel.

Final Summary

The research team (1) quantified the amount of CH₄ generated by several seeps, and evaluated its potential use as an unconventional gas source for the village of Atqasuk; (2) collected gas and analyzed its composition from multiple seeps several miles apart to see if the source is the same, or if gas is being generated locally from isolated biogenic sources; and (3) assessed the potential magnitude of natural CH₄ gas seeps for future use in climate change modeling. This study determined that the seeps have a mixed biogenic-thermogenic signature and likely have a coal seam origin. Our recommendation is that transporting gas from the seep sites to Atqasuk is not cost-effective, but given the widespread distribution of seeps, there is the potential for shallow drilling of coal seams beneath the town.

[Link to final report](#)

Project Title:

Task 3.01.1 Solvent-Based Enhanced Oil Recovery Process to Develop West Sak Alaska North Slope Heavy Oil Resources

Program/Project Identification Number

DE-FC26-01NT41248 3.01.1

UAF PI Name and address

David O. Ogbe
University of Alaska Fairbanks
PO Box 755880
429 Duckering Bldg.
Fairbanks, AK 99775-5880
(907) 474-7998 fdoo@uaf.edu

Abstract

The Alaska North Slope (ANS) oil fields contain large reserves (in excess of 15 billion barrels) of cold, heavy crude oil that cannot be produced without some form of enhanced oil recovery (EOR). These reserves are relatively shallow (only a few thousand feet) and lie beneath permafrost. The presence of permafrost prohibits the use of steam injection for EOR, and thus other methods are needed. Vapor extraction, where light hydrocarbons are injected, shows promise as a method of reducing the viscosity of these oils and allowing them to be produced.

Objectives

- 1) Develop model for vapor extraction processes.
- 2) Compare vapor extraction model with laboratory experiments (at Stanford).
- 3) Compare model predictions with pilot well tests from the North Slope.

Final Summary

A one-year research program was conducted to evaluate the feasibility of applying solvent-based EOR processes to develop West Sak and Ugnu heavy oil resources found on the ANS. During the first phase of the research, background information was collected, and experimental and numerical studies of the vapor extraction process (VAPEX) in West Sak and Ugnu were conducted. The experimental study is designed to foster understanding of the processes governing vapor chamber formation and growth, and to optimize oil recovery. A specially designed core holder and a computed tomography scanner were used to measure the in-situ distribution of phases. A numerical simulation study of the VAPEX was initiated during the first year. The numerical work completed during this period includes setting up a numerical model and using the analog data to simulate lab experiments of the VAPEX process.

[Link to final report](#)

Project Title:

Task 3.03.1 Characterization and Alteration of Wettability States of Alaskan Reservoirs to Improve Oil Recovery Efficiency

Program/Project Identification Number

DE-FC26-01NT41248 3.03.1

UAF PI Name and address

Abhijit Dandekar
University of Alaska Fairbanks
435 Duckering Building
Fairbanks, AK 99775
(907) 474-6427 ffayd@uaf.edu

External PI Name and address

Prasad Saripalli
PNNL

Abstract

Wettability has a strong influence on the efficiency of oil recovery (EOR). Limited available data suggest that the Alaska North Slope (ANS) reservoirs may be suitable targets for application of improved EOR techniques based on wettability changes. New methods using interfacial tracers will be developed for rapid, nondestructive characterization of mixed-wettability states of oil-bearing rocks in laboratory and field settings. The new methods will be used to experimentally demonstrate the influence of injected and reservoir fluid composition on wettability and, hence, on oil recovery efficiency in a variety of EOR processes currently favored in ANS exploration, using representative Alaskan cores. The resulting wettability, relative permeability, sweep and oil drainage, and imbibition data will be modeled as a function of capillary number and bond number, in a form suitable for incorporation into a numerical simulator. The new model will be used to predict optimal injection conditions for EOR operations that assist in expansion of oil reserves on the ANS and to support Alaska's historic lead in the development of new petroleum production technology.

Objectives

In this project, new methods for a rapid, nondestructive wettability characterization will be developed. The new techniques will be used to ascertain experimentally the influence of wettability on oil recovery efficiency in representative Alaskan cores. Results from experiments and data analysis will be used to demonstrate how influencing the wettability through injection of fluids with different salinity and altered composition can be used to improve recovery efficiency in typical EOR processes of interest to ANS exploration.

Final Summary

Numerous corefloods were conducted on reservoir rock material from representative formations on the ANS. The corefloods consisted of injecting water (reservoir water and ultra low-salinity ANS lake water) of different salinities in secondary as well as tertiary mode. Additionally, complete reservoir-condition corefloods were conducted using live oil. In all the tests, wettability indices, residual oil saturation, and oil recovery were measured. All results consistently led to one conclusion: that is, a decrease in injection water salinity causes a reduction in residual oil saturation and a slight increase in water-wetness, both of which are comparable with literature observations.

[Link to final report](#)

Project Title:

Task 3.03.2 Physical, Biological, and Chemical Implications of Mid-Winter Pumping of Tundra Ponds

Program/Project Identification Number

DE-FC26-01NT41248 3.03.2

UAF PI Name and address

Larry Hinzman
University of Alaska Fairbanks
PO Box 757340
Fairbanks, AK 99775-7340
(907) 474-6016 fldh@uaf.edu

External PI Name and address

Mike Lilly
GW Scientific
(907) 479-8891
mlilly@gwscientific.com

Abstract

Oil and gas development on the North Slope of Alaska is difficult due to the lack of roads, which are expensive to build and maintain because of the presence of unstable permafrost soils. Ice roads are the preferred method for providing access to drilling sites. Water to build these ice roads is pumped from tundra ponds, which has resulted in some controversy, as there is little precipitation on the North Slope and little water flow except during snowmelt in the spring. Current permitting regulations stipulate that a maximum of 15% of the water in any lake may be pumped for ice road construction, but no scientific justification for this limit exists. Direct impacts to fish and wildlife populations are difficult to quantify, and may require the intentional stressing of a wetland to measure changes in water chemistry.

Objectives

The objective of this study was to establish a scientific basis for permitting regulations affecting the pumping of tundra ponds for ice road construction.

Final Summary

Tundra lakes on the North Slope of Alaska are an important resource for energy development and petroleum field operations. A majority of exploration activities, pipeline maintenance, and restoration activities take place on winter ice roads that depend on water availability at key times of the winter operating season. These same lakes provide important fisheries and ecosystem functions. In particular, overwintering habitat for fish is one important management concern. This study focused on the evaluation of winter water use in the current field operating areas to provide a better understanding of current water-use practices. It found that under current water-use practices, there were no measurable negative effects of winter pumping on the lakes studied, and current water-use management practices were appropriately conservative. The study did find many areas where improvements in the understanding of tundra lake hydrology and water usage would benefit industry, management agencies, and the protection of fisheries and ecosystems.

[Link to final report](#)

Project Title:

Task 3.04.1 Reservoir Characterization, Source Rock Potential, Fossil Fuel Resources, and Basin Analyses, Bristol Bay Basin, Alaska

Program/Project Identification Number

DE-FC26-01NT41248 3.04.1

UAF PI Name and address

Paul McCarthy
Geophysical Institute
PO Box 757320
Fairbanks, AK
(907) 474-6894 mccarthy@gi.alas

External PI Name and address

Rocky Reifentstahl
Dept. of Natural Resources
(907) 451-5026
rocky@dnr.state.ak.us

Abstract

The Bristol Bay region of Alaska is known to have significant hydrocarbon resources, but exploration in the region has been limited because of the lack of nearby infrastructure. As the natural gas industry in the Cook Inlet region matures, however, finding nearby sources of abundant natural gas has increased the interest in the Bristol Bay region. This project is designed to improve the understanding of the hydrocarbon potential in the Bristol Bay region as a necessary step in attracting exploration in the region.

Objectives

- 1) Develop a more complete understanding of the geology of the Bristol Bay region.
- 2) Prepare public reports and maps of this information for use by oil and gas exploration companies.

Final Summary

From 2004 through 2007, four partial field seasons focused on energy-related geology in the Port Moller, Chignik, Ugashik Lakes, and Puale Bay areas of the Bristol Bay region, Alaska Peninsula. These new geologic field data and laboratory analyses codify fundamental reservoir, source, seal capacity, and thermal maturity characteristics of basin targets; places the Miocene Bear Lake Formation reservoir data in a stratigraphic and sequence stratigraphic framework; and summarizes the petroleum system geology and hydrocarbon potential of this frontier basin. All data are public. All data through the 2006 field season were published in peer-reviewed Division of Geological & Geophysical Surveys (AKDGGS) reports: www.dggs.dnr.state.ak.us/publications and www.dog.dnr.state.ak.us/oil.

Successful lease sales were held in Bristol Bay in 2006, with data from this study cited as an important factor in the new interest in this area.

[Link to final report](#)

Project Title:

Task 3.04.2 Unraveling the Timing of Fluid Migration and Trap Formation in the Brooks Range Foothills: A Key to Discovering Hydrocarbons

Program/Project Identification Number

DE-FC26-01NT41248 3.04.2

UAF PI Name and address

Catherine Hanks

P.O. Box 757320, 903 Koyukuk Dr.
Fairbanks, AK 99775-7320
(907) 474-5562 chanks@dino.gi.a

Abstract

Seventy-five percent of Alaska's operating budget comes from hydrocarbon production, mostly from the North Slope, especially from Prudhoe Bay, which is in the geologically simplest northern margin of the large Colville basin. As this field ages, finding additional hydrocarbon resources is critical for Alaska's economy. The southern Colville basin, near the Brooks Range, has abundant hydrocarbon potential, but the timing of hydrocarbon generation and migration and/or reservoir development with respect to trap formation is complex and poorly understood. This project is designed to study the geology of exposed outcroppings in the Brooks Range to develop a clear picture of when and where fractures developed in the Colville basin in order to better predict oil and gas migration pathways, timing of hydrocarbon migration, and timing of trap formation.

Objectives

Map the structural geology, both surface and subsurface, based on two transects in the Brooks Range. Document the fracture distribution and character throughout the stratigraphic column, the processes associated with fracture formation, temperatures, pressures, and fluid compositions during fracturing. Publish maps of information.

Final Summary

The results of the study indicate that fractures formed episodically throughout the evolution of northern Alaska, due to a variety of mechanisms. Four distinct fracture sets were observed. The earliest fractures formed in deep parts of the Colville basin and in the underlying Ellesmerian sequence rocks as these rocks experienced compression associated with the growing Brooks Range fold-and-thrust belt. Across northern Alaska, the early deep basin fractures were probably synchronous with hydrocarbon generation. Initially, these early fractures were good migration pathways, but were destroyed where they were subsequently overridden by the advancing Brooks Range fold-and-thrust belt. However, at these locations, younger fracture sets related to folding and thrusting could have enhanced reservoir permeability and/or served as vertical migration pathways to overlying structural traps.

[Link to final report](#)

Project Title:

Task 3.04.3 Novel Chemically Bonded Phosphate Ceramic Borehole Sealants for the Arctic Environment

Program/Project Identification Number

DE-FC26-01NT41248 3.04.3

UAF PI Name and address

Shirish Patil
University of Alaska Fairbanks
306 Tanana Drive, Room 415
Fairbanks, AK 99775
(907) 474-5127 ffslp@uaf.edu

External PI Name and address

Arun Wagh
Argonne National Laboratory
(630) 252-4295
wagh@anl.gov

Abstract

Chemically bonded phosphate ceramic sealants have been developed at Argonne National Laboratory, and are ideally suited for sealbore completions in arctic environments, especially in areas of permafrost. This project is intended to modify the sealants as necessary to allow for their use in arctic climates, and to demonstrate their use in the field.

Objectives

- 1) Conduct simulated laboratory tests at UAF for oil field niche applications of phosphate sealants.
- 2) Formulate and optimize the ceramic borehole cement for use in permafrost regions.
- 3) Collaborate with industrial partner (BJ Services), and conduct field tests.
- 4) Test the formulations for other applications in the infrastructure development of Alaska with additional industrial partner (Bindam Corporation).

Final Summary

Novel chemically bonded phosphate ceramic borehole sealant—Ceramicrete—has many advantages over conventionally used permafrost cement at the Alaska North Slope (ANS). However, in normal field practices when Ceramicrete is mixed with water in blenders, it has a chance of being contaminated with leftover Portland cement. In order to identify the effect of Portland cement contamination, tests were conducted at BJ Services in Tomball, Texas, as well as at UAF with Ceramicrete formulations proposed by the Argonne National Laboratory. The tests conducted at BJ Services with proposed Ceramicrete formulations and Portland cement contamination revealed significant drawbacks that caused these formulations to be rejected. However, the newly developed Ceramicrete formulation at UAF showed positive results, with Portland cement contamination as well as without Portland cement contamination, for its effective use in oilwell-cementing operations at the ANS.

[Link to final report](#)

Project Title:

Task 3.05.1 Evaluation of Wax Deposition and Its Control During Production of Alaska North Slope Oils

Program/Project Identification Number

DE-FC26-01NT41248 3.05.1

UAF PI Name and address

Tao Zhu
University of Alaska Fairbanks
411 Duckering Building
Fairbanks, AK 99775
(907) 474-5141 fftz@uaf.edu

External PI Name and address

Jack Walker
Conoco Phillips
(907) 265-6268
Jack.A.Walker@conocophillips.com

Abstract

Crude oil contains a wide variety of chemical compounds, including waxes. Given proper conditions of temperature and pressure, these waxes can deposit in wellbores, leading to reduced production and significant downtime while the waxes are removed. The problem is exacerbated by cold ambient temperatures on the Alaska North slope and by decreasing production volumes, which lead to lower temperatures in the wellbores. If the problem becomes severe, it is no longer economical to operate problem wells, and wells are shut down. However, wax production mechanisms vary from well to well, leading to difficulty in providing universal solutions. Solving this problem could significantly reduce the economic limit and spur development of smaller accumulations of oil on the North Slope.

Objectives

- 1) Evaluate the mechanisms and environments leading to wax deposition in candidate wells of selected Alaska North Slope oil fields.
- 2) Develop user-friendly models to predict wax deposition, and quantify its effects on oil production.
- 3) Design methods and techniques for preventing and controlling wax deposition.

Final Summary

The work completed during this study included measurement of density, molecular weight, viscosity, pour point, wax appearance temperature, wax content, rate of wax deposition using cold finger, compositional characterization of crude oil and wax obtained from wax content, gas-oil ratio, and phase behavior experiments, including constant composition expansion and differential liberation. Also, included in this study was the development of a thermodynamic model to predict wax precipitation. Comparison indicated that Pedersen's model gives better results, but the assumption of wax phase as an ideal solution is not realistic. Hence, Won's model was modified to consider different precipitation characteristics of the various constituents in the hydrocarbon fraction. The results obtained from the modified Won's model were compared with existing models, and it was found that predictions from the modified model are encouraging.

[Link to final report](#)

Project Title:

Task 3.05.2 Phase Behavior, Solid Organic Precipitation and Mobility Characterization Studies in Support of Enhanced Heavy Oil Recovery on the Alaska North Slope

Program/Project Identification Number

DE-FC26-01NT41248 3.05.2

UAF PI Name and address

Shirish Patil
University of Alaska Fairbanks
306 Tanana Drive, Room 415
Fairbanks, AK 99775
(907) 474-5127 ffslp@uaf.edu

External PI Name and address

Prasad Saripalli
PNNL

Abstract

The in-place resources of viscous oil on the Alaskan North Slope (ANS) are huge, estimated at between 20 and 25 billion barrels, as large as the nearby Prudhoe Bay oil fields. However, these viscous oils are cold and thick, difficult to produce and transport, and not economical to produce. Increasing world prices of oil and the decline in production of other ANS fields has led oil producers to focus more attention on this resource. Successful production of viscous oils requires an understanding of the complex phase behavior of these oils, especially in response to enhanced oil recovery (EOR) methods such as steamflooding, in-situ combustion, or miscible gas injection. This study is intended to evaluate these properties, and to share this information with ANS owners and producers.

Objectives

- 1) Conduct experimental and simulation studies designed to elucidate the PVT (pressure/volume/temperature) and fluid phase behavior of various representative ANS viscous oils in the presence of solvents, gases, heat, and precipitating phases.
- 2) Demonstrate the application of the above information in better understanding of production issues associated with viscous oils.

Final Summary

An experimental study was conducted to quantify the phase behavior and physical properties of viscous oils from the ANS oil field. The oil samples were compositionally characterized by the simulated distillation technique. Constant composition expansion and differential liberation tests were conducted on viscous oil samples. Experimental results for phase behavior and reservoir fluid properties were used to tune the Peng-Robinson equation of state and predict the phase behavior accurately. Based on the comprehensive phase behavior analysis of ANS crude oil, a reservoir simulation study was conducted to evaluate the performance of a gas injection EOR technique for the West Sak reservoir. It was found that a definite increase in viscous oil production could be obtained by selecting the proper injectant gas and by optimizing reservoir-operating parameters.

[Link to final report](#)

Project Title:

Task 3.05.3 Chemical and Microbial Characterization of North Slope Heavy Oils to Assess Viscosity Reduction and Enhanced Recovery with Microbial Methods

Program/Project Identification Number

DE-FC26-01NT41248 3.05.3

UAF PI Name and address

Shirish Patil
University of Alaska Fairbanks
306 Tanana Drive, Room 415
Fairbanks, AK 99775
(907) 474-5127 ffslp@uaf.edu

External PI Name and address

Harold J. Noyes
PNNL
(509) 528-5918
harry.noyes@pnl.gov

Abstract

Significant deposits of viscous oil have been identified on the Alaskan North Slope (ANS), but production of these reserves is limited by the difficulty in extracting this oil from the ground. While methods for extracting this type of oil are known, knowledge of the physical and microbiological properties of the oil is necessary to predict production rates and to optimize production strategies. This study will conduct careful measurements of the properties of a statistically and geographically significant ANS viscous oil target population to allow industry to develop effective recovery methods for this oil.

Objectives

- 1) Collect and characterize a representative population of ANS viscous crude oils and their substrates.
- 2) Determine if ANS viscous oils are amenable to viscosity reduction processes through natural or induced microbiological populations, or modifications to the molecular structure of the oil by chemical processes, or some combination of the two.

Final Summary

A microbial formulation containing a known biosurfactant-producing strain of *Bacillus licheniformis* was developed in order to simulate microbially enhanced oil recovery (MEOR). Coreflooding experiments were performed to simulate MEOR and quantify the incremental oil recovery. Properties like viscosity, density, and chemical composition of oil were monitored to propose a mechanism for oil recovery. The microbial formulation significantly increased incremental oil recovery, and molecular biological analyses indicated that the strain survived during the shut-in period.

[Link to final report](#)

Project Title:

Task 3.05.4 Operational Watershed Modeling Tools to Support North Slope Field Operations and Water Use

Program/Project Identification Number

DE-FC26-01NT41248 3.05.4

UAF PI Name and address

Dan White
University of Alaska Fairbanks
PO Box 755910
Fairbanks, AK 99775-5910
(907) 474-6222 fdmw@uaf.edu

External PI Name and address

Mike Lilly
GW Scientific
(907) 479-8891
mlilly@gwscientific.com

Abstract

Ice road construction is an important aspect of oil and gas exploration on the Alaska North Slope, as this allows access to undeveloped areas. Water for ice roads is taken from tundra lakes and ponds, as allowed by permit. However, the scientific basis for permitted water volumes is not well established, as rules have been created ad hoc, and this has become a trigger issue for those opposed to any development in the Arctic. This issue is becoming more important as exploration pushes out of the coastal areas, where ponds are common, into the National Petroleum Reserve, where lakes are less common and will be pumped harder. Starting in 2002, AETDL funded a study to look at the impacts of pumping on the physical and chemical characteristics of the lakes. One important parameter identified was the watershed recharge area, that is, the area of snow-covered tundra that provides spring meltwater to a lake to assure that sufficient flushing of concentrated ions takes place, and the lake returns to its natural state after pumping. This study continues work in this area.

Objectives

- 1) Work closely with industry to identify lakes of interest for this study.
- 2) Measure the water balance of lakes of interest, and monitor the changes in pond water volume and water chemistry.
- 3) Share this information with project participants, including the scientific community, regulatory agencies, the oil industry, and environmental groups.

Final Summary

The study found that the chemistry of tundra lakes varied due to natural processes, such as ice formation and exclusion of solutes from lake ice, but could not associate any changes in lake water chemistry to water use. All study lakes were observed to recharge during spring snowmelt. L9312 was recharged both by snowmelt from its contributing watershed and by overbank flooding from the adjacent Colville River in 2004, but was not flooded in 2005. The lake fully recharged by fall freeze-up, due to both spring snowmelt recharge and summer precipitation.

[Link to final report](#)

Project Title:

Task 3.08.1 Resource Characterization and Quantification of Natural Gas-Hydrate and Associated Free-Gas Accumulations in the Prudhoe Bay–Kuparuk River Area on the North Slope of Alaska

Program/Project Identification Number

DE-FC26-01NT41248 3.08.1

UAF PI Name and address

Shirish Patil

University of Alaska Fairbanks
306 Tanana Drive, Room 415
Fairbanks, AK 99775
(907) 474-5127 ffslp@uaf.edu

Abstract

Gas hydrates are considered an alternative energy resource of the future, as they exist in enormous quantities in permafrost and the offshore environment. One of the primary mechanisms involved in hydrate decomposition in porous media is the gas-water two-phase flow in the formations. Despite their importance, these functions are poorly known due to a lack of fundamental understanding of gas-water flows and the difficulty of direct measurements for hydrate systems.

Objectives

The objectives of this study are

- 1) to develop a laboratory method to form synthetic hydrates in field core samples for performing unsteady-state relative permeability displacement experiments; and
- 2) to measure relative permeability across hydrate-saturated core samples.

Final Summary

In February 2007, core samples were taken from the Mt. Elbert site, situated between the Prudhoe Bay and Kuparuk oil fields on the Alaska North Slope. Core plugs from those core samples were used as a platform to form hydrates and perform unsteady-steady-state displacement relative permeability experiments. The absolute permeability of Mt. Elbert core samples, determined by Omni Labs, was validated as part of this study. Data taken with experimental apparatuses at the University of Alaska Fairbanks, ConocoPhillips' laboratories at the Bartlesville Technology Center, and at the Arctic Slope Regional Corporation's facilities in Anchorage, Alaska, provided the basis for this study.

[Link to final report](#)

Project Title:

Task 3.08.2 DOE HARC Concept Study

Program/Project Identification Number

DE-FC26-01NT41248 3.08.2

UAF PI Name and address

Shirish Patil
University of Alaska Fairbanks
306 Tanana Drive, Room 415
Fairbanks, AK 99775
(907) 474-5127 fsjp@uaf.edu

External PI Name and address

Rich Haut
HARC

Abstract

The Alaska North Slope region presents one of the greatest opportunities the U.S. has to increase its domestic production of oil and gas; but this region also presents some of the world's most significant environmental and logistical challenges to oil and gas production. A number of studies have shown that weather patterns in this region are warming and that tundra is frozen fewer days each year. Operators are not allowed to explore until the tundra is sufficiently frozen, and then break-up forces rapid evacuation. Using the best available methods, exploration in remote arctic areas can take up to three years to identify a commercial discovery, and then it takes years to build the infrastructure for development and production. This makes exploration cost-prohibitive. New technologies are needed or oil and gas resources may never be developed outside limited exploration stepouts from existing infrastructure.

Objectives

Team collaboration is designed to reduce environmental concerns for ecologically sensitive areas currently open for extraction activities. The JIP addresses not only the engineering challenges that face the energy industry but also the considerable environmental concerns that face preserves and protected areas because of mineral extraction activities.

Final Summary

The team discussed various potential applications with industry, governmental agencies, and environmental organizations. The benefits and concerns associated with industry's use of technology were identified. In this discussion process, meetings were held with five operating companies (twenty-two people), including asset team leaders, drilling managers, HSE managers, and production and completion managers. Three other operating companies and two service companies were contacted by phone to discuss the project. A questionnaire was distributed and responses were provided, which are included in the final report. Meetings were also held with State of Alaska Department of Natural Resources officials and U.S. Bureau of Land Management regulators. Companies met with included ConocoPhillips, Chevron, Pioneer Natural Resources, Fairweather E&P, BP America, and the Alaska Oil and Gas Association.

[Link to final report](#)

Project Title:

Task 6.01.1 Administration

Program/Project Identification Number

DE-FC26-01NT41248 6.01.1

UAF PI Name and address

Dennis Witmer
University of Alaska Fairbanks
PO Box 755910
Fairbanks, AK 99775
(907) 474-7082 ffdew@uaf.edu

Abstract

The administration budget will be used for project management functions. These functions will include meetings with industry, regulatory agencies, and university faculty to facilitate team formation, address energy research needs, circulate RFPs for new projects, assemble and conduct panels for project reviews, develop the annual work plan, conduct annual conferences and workshops on both fossil energy and remote electrical energy, write quarterly reports to the DOE, maintain a database of contacts, travel to conferences and meetings, and maintain a web presence with the above information.

Objectives

- 1) Create dialog between the DOE, the University of Alaska, and industry to address energy issues in Alaska, through workshops, conferences, and individual meetings.
- 2) Find projects of high priority to Alaskan industry, and recommend these projects for funding.

Final Summary

This report represents the final summary of the project selection process, and a brief summary of each project undertaken. Final technical reports are attached.

Acknowledgments

This program would not have been possible without the dedicated efforts of many people in government, industry, and at the university. This project has proved to be especially challenging given the numerous parts to the entire contract—a challenge especially for those who had to step in at the middle of the process.

At the U.S. Department of Energy, special thanks to Mr. Brent Sheets of the Arctic Energy Office for his tireless work on behalf of this project. Thanks also to the contracting staff that assisted: Ray Johnson, Bonnie Dowdell, and Rich Rogus. The project also would like to thank the COTRs who participated: Arun Bose, James Hemsath, Perna Halder, Betty Felber, and Chandra Nautiyal. Several SAIC employees also helped on the DOE side, especially Charles Thomas and Bob Cheney.

Our industrial partners who so ably assisted with the project reviews also need to be thanked: Lee Schoen from Alyeska, Bill Streever from BP, John Tanigawa from Evergreen Gas Company, Michael Faust from Phillips Alaska, Kyle Monkeliën from MMS, Tom Gray from BP Exploration, Laura Silliphant from Conoco, Matt Cronin from LGL, Peter Crimp from AEA, David Lockard from AEA, Mark Bendersky from ASTF, Brent Petrie from AVEC, and Bob Chaney from ASTF.

At the University of Alaska Fairbanks, special thanks to Maggie Griscavage in our contracting department, and to Diane McLean, Juli Philibert, Kathy Petersen, and especially to Shannon Watson for their roles as administrative assistants during the course of the project. Thanks also for the assistance of Sandra Boatwright, Kala Hansen, and other staff at the INE proposal office. Thanks to Martha Stewart for watching over things in DC, and to President Mark Hamilton and Vice President for Research Craig Dorman for their interest in making sure that the funding for this important work was available.

Special thanks for the congressional support from Senator Ted Stevens, Frank Murkowski, and Lisa Murkowski.

Appendix A Request for Proposals

University of Alaska

Arctic Energy Technology Development Laboratory

The Arctic Energy Technology Development Laboratory (hereafter referred to as AETDL) at the University of Alaska requests pre-proposals to conduct projects to develop and deploy technologies for satisfying Alaska's unique energy needs. Proposals on electrical power generation technologies for rural and remote regions and fossil energy will be accepted.

AETDL's mission is to promote Research, Development and Deployment (RD&D) of energy technologies in Arctic regions by bringing together resources from the University of Alaska (UA) and Alaska's energy industry. Industry will be involved in defining areas of research, reviewing proposals, and evaluating the results of the research projects.

The U.S. Department of Energy (DOE) is providing financial assistance to the University of Alaska under Cooperative Agreement No. DE-FC26-01NT41248. UA will submit projects selected under this RFP as new research tasks under the Cooperative Agreement for DOE's consideration. The Cooperative Agreement may be viewed at <http://www.uaf.edu/ine/erc/home.html>.

Call for Proposals--FY 2003 and FY 2004 Funding Cycles

AETDL Technology Areas of Interest

Two broad areas of research will be funded:

1. Remote power generation technologies in arctic climates, including, but not limited to, fossil, wind, geothermal, fuel cells, and small hydroelectric facilities.

Within this area, based on the results of meetings with Alaskan industry, special consideration may be given to projects in the following sub-areas: economic analysis of the power cost equalization program, development of fossil energy sources for local consumption, and the development of an energy clearinghouse database.

2. Fossil energy areas including, but not limited to, enhanced oil recovery, heavy oil recovery, reinjection of carbon, and extended reach drilling technologies; gas-to-liquids technology and liquefied natural gas (including associated transportation systems); natural gas hydrates; coalbed methane; and shallow bed natural gas.

Within this area, based on the meetings with Alaskan industry, special consideration may be given to projects in the following sub-areas: coal technologies and coalbed methane projects, heavy oil recovery,

and developing scientific information useful for setting appropriate parameters for environmental permits.

ANTICIPATED SCHEDULE

ROUND 1

- December 23, 2002: Request for proposals published.
- January 31, 2003: One-page pre-proposals are due to the AETDL office by the close of business in electronic format (format below).
- February 17, 2003: Notification of results of preliminary round.
- February 28, 2003: Two-page proposals (format below) due in electronic format to AETDL office.
- March 11, 2003: Fossil Energy oral review panel meets in Anchorage.
- March 12, 2003: Remote Power Generation oral review panel meets in Anchorage.
- March 13, 2003: Notification of results from oral review panel distributed.
- April 11, 2003: Final proposals due from selected projects, in format listed below.

All pre-proposals and proposals must be submitted electronically to Juli Philibert at the AETDL office at fniap1@uaf.edu no later than close of business on the date due.

Project awards are dependent on available funding, and will be announced after the DOE review is completed, and the task is added to the AETDL cooperative agreement. Since AETDL has no guarantee of continued funding or any control over the timing of the DOE review and approval process, project funding start dates cannot be given.

ROUND 2

- May 30, 2003: Deadline for one-page pre-proposals for consideration in FY 2004 funding cycle
- June 13, 2003: Ranking completed. Projects selected for final review notified.
- June 28, 2003: Two-page proposals due in electronic format to AETDL office.
- July 9, 2003: Fossil Energy review panel meets in Fairbanks.
- July 10, 2003: Remote Power Generation review panel meets in Fairbanks.
- July 11, 2003: Notification of results from oral review panel distributed.
- August 9, 2003: Final proposals due from selected projects, in format listed below.

All pre-proposals and proposals must be submitted electronically to Juli Philibert at the AETDL office at fnjap1@uaf.edu no later than close of business on the date due.

Project awards are dependent on available funding, and will be announced after the DOE review is completed, and the task is added to the AETDL cooperative agreement. Since AETDL has no guarantee of continued funding or any control over the timing of the DOE review and approval process, project funding start dates cannot be given.

PROJECT REVIEW PROCESS

Project proposals are reviewed and evaluated at each stage of a three-stage process. Increasingly detailed proposals are required at each stage. Proposal submissions will be evaluated by advisory review panels composed primarily of representatives from Alaska's energy-related industries. Two review panels will be convened: one to evaluate fossil energy research proposals and one to evaluate remote power generation research proposals.

At each stage of the review process, the panels will evaluate submissions based on the following criteria:

- Relevance to the AETDL mission
- Relevance to industry
- Strength of the university/industry research partnership
- Uniqueness of approach
- Strength and viability of idea
- Impact to Alaska if project succeeds
- Leverage of funding
- Clarity of proposal, milestones, and objectives

Although AETDL will rely heavily on the panels' recommendations, the panels are advisory and their recommendations do not obligate AETDL to support any particular project. The final project review and approval will be conducted by DOE

PROPOSAL CONTENTS AND FORM

Technical Discussion

The technical discussion section of the proposal application shall provide technical information as follows:

The applicant shall provide a discussion that clearly delineates the scientific and technical merit of the technology to be developed in the proposed project. The application should address the following:

- (1) Statement of Problem/Project Objectives - How the proposed work relates to the "Research Objectives for This Solicitation" in either of the two AETDL Technical Areas of Interest and how it supports pertinent AETDL program missions and goals.
- (2) Statement of the Problem - Describe the problem the proposal seeks to solve or result in improvements to the current technological state-of-the art. Describe issues (identify current deficiencies) and how the intended results will overcome barrier (technical, economic, market, regulatory, environmental) issues, and the potential of a scientific or engineering breakthrough.
- (3) Statement of Work/Technical Approach - Describe the scientific and technical basis and merit of the proposed work. Describe the proposed technical strategy and rationale for choosing that strategy, i.e., a technical approach with a logical flow. A reviewer must be able to comprehend the rationale of the proposed work for achieving the intended results.
- (4) Impact to Alaska of a successful project - Anticipated benefits of the proposed work, such as performance improvements, cost savings, and environmental benefits. Suggest any crosscutting or technology spin-off benefits.
- (5) Proposed Products of R&D, - Describe the tangible products such as new knowledge bases, a new approach, etc. anticipated from the proposed project.
- (6) Dissemination of Project Results - Describe how new technologies and/or new knowledge resulting from the project will be disseminated to the public through commercialization or other means.
- (7) Additional background information the applicant wishes to include about the project.

Pre-Proposals

One-page pre-proposals should be submitted by filling out the Pre-proposal Application/Cover form, and attaching a one-page project description. This form is available on the AETDL web site at www.uaf.edu/AETDL. Please note that AETDL reserves the right to reject any pre-proposals that exceed the one-page limit.

Two-page Proposals

Applicants whose projects are selected for evaluation in the second phase will be required to submit a two-page proposal for evaluation by the review panel prior to the oral review. The format required will be the same as for the one-page document, but with two additional requirements: 1) cost share detail, including letters from industrial partners, and 2) a list of project milestones and deliverables.

Full Review Panel Process

Each applicant submitting a two-page proposal will be required to make a 15-minute presentation to an industry review panel. This presentation must be prepared in Power Point, and must be brought to the review session on CD. Following each presentation, panel members will have a five-minute discussion and question period. An additional five-minute period will follow for review panel members to complete their scorecards. After the presentations, panel members will discuss their combined scoring efforts and present their recommendations for funding to AETDL. In addition to numeric scores, reviewers will be encouraged to provide written comments concerning each research proposal. After the review process, AETDL will make copies of their respective scorecards available to each applicant. AETDL will submit the successful proposals as research tasks under the work plan as required by the Cooperative Agreement.

Final proposal format for inclusion in the AETDL Work Plan

The following additional information shall be required within 30 days of notification of being selected for review by DOE.

- Standard Form 424 - Application for Federal Assistance
- NEPA Environmental Questionnaire
- DOE F4600.4 - Federal Assistance Budget Information Form
- Supporting Cost Detail - Detailed budget including estimated unbigoted balances from the previous budget period (if applicable), identifying elements of cost for both the Government's and the third party's cost, their basis of estimate, and supporting documentation. See guidance below.
- Cost Share Commitment Letter - Must identify the composition and the source of cost share. (Cash, In-Kind) Cost share must be allowable costs under Federal Regulations. (See 10 CFR 600.123). Cost Share detail shall be provided for each budget period along with the Supporting Cost Detail information for each budget period.

All forms and instructions needed for preparation of the above referenced forms can be found on the NETL homepage at: <http://www.netl.doe.gov/business/faapiaf/main.html>. Instructions for completion of the forms are contained on the back of each form.

The SF424 and the NEPA Environmental Questionnaire can be found at the above website address in Volume I – Offer and Other Documents. The DOE 4600.4 form can be found in Volume III – Cost Application under Budget Forms. Guidance regarding Supporting Cost Detail can be found in Volume III under Supporting Cost Detail Requirements. An Excel Spreadsheet, V3-GUIDE.XLS may be used as a format in which to prepare this supporting cost detail. The format can be changed to reflect your company's specific cost elements.

Industry/University Collaboration and Cost Sharing

Joint proposals between industry and the University of Alaska are strongly encouraged. Projects demonstrating such a partnership will receive a scoring bonus used to rank the research proposals.

All applicants will be required to submit cost sharing at a minimum of 20% of the project total. In order to be recognized as allowable cost sharing, a cost must be included in the total project value, be necessary for completion of the proposed work effort, and be otherwise allowable in accordance with applicable Federal cost principles and DOE regulations governing cost sharing (See 10 CFR 600.123). Allowable cost sharing includes funds-in to UA or in-kind contributions. In-kind contributions can include donated equipment, labor costs for laboratory or fieldwork, or major work activities such as drilling.

Although not all-inclusive, provided below is a list of costs that are unallowable as project costs and, therefore, unallowable for cost sharing:

- Valuation for property sold, transferred, exchanged, or manipulated in anyway to acquire a new basis for depreciation purposes or to establish a fair use value in circumstances that would amount to a transaction for the purpose of the Cooperative Agreement.
- DOE will not share in both the direct cost and depreciation on the same item. Depreciation is not allowable for cost sharing on any item previously charged to the project as a direct cost. For example, DOE will cost share the direct cost on equipment or facilities purchased or constructed for the project, but will not also cost share the depreciation.
- Interest on borrowing (however represented) and other financial costs such as bond discounts, cost of financing and refinancing capital (net worth plus long-term liabilities), are unallowable project costs. This includes interest on funds borrowed for construction.
- Facilities capital cost of money shall be an unallowable cost on all real property or equipment acquired by or on behalf of the Participant in connection with the performance of the project.
- Previously expended research, development, or exploration costs, including existing data are unallowable.
- Forgone fees, forgone profits, or forgone revenues are unallowable. Business losses are unallowable.
- Allowable costs under past, present, or future Federal government contracts, grants or cooperative agreements may not be charged against the Cooperative Agreement. Likewise, the participant may not charge costs allowable under this project, including any portion of its cost share to the Federal government under any other contracts, grants, or cooperative agreements.

Funding Request Considerations

Participants are obliged to develop realistic budgets and schedules. The dollar size of individual AETDL projects is not fixed, but the goal is to fund multiple projects in each research area. As a general rule, individual proposals are suggested not to exceed \$350,000 per year from AETDL. Larger projects may be suitable for funding within other DOE funding streams, and submission to these programs will be encouraged where appropriate.

Depending on the availability of funding, and how a particular project is prioritized in the review, AETDL may recommend that a project be funded at less than the requested amount, provided that the project can proceed under a reduced scope-of-work, or an extended schedule.

Continuity, Completion, and Close-out of Projects

AETDL will endeavor to adequately fund each worthy project for a period of time sufficient to achieve success. However, there is no guarantee that a multi-year project, once started, will be funded at the requested level over the planned number of years. Beginning with the FY 2003 funding cycle, ongoing projects will be exempt from the one-page pre-proposal requirement, but must still participate in the Full Review Panel Process. While new proposals will be strictly limited to two pages, proposals for on-going projects will have a third page containing a

table showing the project funding history and accomplishments by year. Projects that extend beyond a single year are anticipated, but projects should be limited to three years.

Although not all-inclusive, possible reasons for the premature termination of a multi-year project include:

- The industry review panel assigns a low priority on the basis of relevance (e.g., the problem has been solved or is no longer important).
- Lack of funds available to AETDL.
- Programmatic considerations as judged by the AETDL program manager or DOE.
- Lack of performance or accomplishment of milestones (e.g., the investigators are not meeting their objectives).
- The principal investigator has left the project and there is no replacement.

For projects that are discontinued, the industry panel may recommend to AETDL “close-out” funding so that final reports can be prepared and steps to transfer the technology to industry can be made.

Funding of Projects

AETDL will use the recommendations of the review panels to create an annual work plan to be submitted to DOE for funding of the work. Applicants whose proposals are selected for funding will be required to submit a detailed report to AETDL showing the proposed use of DOE funds, the source of matching funds, and the schedule for deliverables, including quarterly progress reports.

REPORTING REQUIREMENTS: Those applicants whose projects are selected for funding will be required to submit the following reports:

Quarterly Project Status Reports - A format for this quarterly report will be posted on the AETDL web site. This report is a concise narrative describing the current status of the effort. The report allows Recipients to communicate developments, achievements, changes and problems. The award Recipient enters an abstract, along with a brief narrative discussion of the following topics: objectives, milestones, and highlights; approach changes, performance variances, accomplishments, or problems; open items; and status assessment and forecast. Each of these topics is addressed, as appropriate, and the report is submitted quarterly during the life of the project.

Topical Report - This is a final technical report, required in addition to the written quarterly report, which shall document and summarize all work performed over the duration of the project in a comprehensive manner. It shall also present findings and/or conclusions produced as a consequence of this work. This report shall not merely be a compilation of information contained in subsequent quarterly, or other technical reports, but shall present that information in an integrated fashion and shall be augmented with findings and conclusions drawn from the research as a whole. This final Topical Report will be due 30 days from the completion of the project.

In addition to the required written reports, projects will be required to participate quarterly in televideo conferences. These televideo conferences will be held bi-weekly, with two projects presenting in each session. Project PI's will be presented with a tentative schedule prior to the beginning of the quarter. Each project will be required to prepare a 15-minute Power Point presentation, and must be available for answering questions at the end of the presentation. The Power Point presentations will be posted to the AETDL web site.

Annual DOE Project Review

Under the terms of the Cooperative Agreement, AETDL, in coordination with DOE, will conduct annual reviews of each project's progress, problems, and accomplishments, and provide a forum for identifying and resolving significant problems (The review required under the Cooperative Agreement is separate and independent from the industry panel process used to select projects described above). Principal investigators will be responsible for preparing information packages, visual aids, and other data and providing such other assistance as may be necessary for efficient conduct of these reviews. Final date, place, agenda, and list of attendees for each such project review meeting will be coordinated between the principal investigators, AETDL and DOE.

Contact Information

For questions concerning this RFP, please contact Dennis Witmer at fdew@uaf.edu

The University of Alaska is an affirmative action/equal opportunity employer and educational institution.

Appendix B Enabling Legislation

114 STAT. 1654A–482 PUBLIC LAW 106–398—APPENDIX

SEC. 3197. OFFICE OF ARCTIC ENERGY.

(a) ESTABLISHMENT.—The Secretary of Energy may establish within the Department of Energy an Office of Arctic Energy.

(b) PURPOSES.—The purposes of such office shall be as follows:

(1) To promote research, development, and deployment of electric power technology that is cost-effective and especially well suited to meet the needs of rural and remote regions of the United States, especially where permafrost is present or located nearby.

(2) To promote research, development, and deployment in such regions of—

(A) enhanced oil recovery technology, including heavy oil recovery, reinjection of carbon, and extended reach drilling technologies;

(B) gas-to-liquids technology and liquified natural gas (including associated transportation systems);

(C) small hydroelectric facilities, river turbines, and tidal power;

(D) natural gas hydrates, coal bed methane, and shallow bed natural gas; and

(E) alternative energy, including wind, geothermal, and fuel cells.

(c) LOCATION.—The Secretary shall locate such office at a university with expertise and experience in the matters specified in subsection (b).

National Energy Technology Laboratory

626 Cochran Mill Road
P.O. Box 10940
Pittsburgh, PA 15236-0940

3610 Collins Ferry Road
P.O. Box 880
Morgantown, WV 26507-0880

One West Third Street, Suite 1400
Tulsa, OK 74103-3519

1450 Queen Avenue SW
Albany, OR 97321-2198

539 Duckering Bldg./UAF Campus
P.O. Box 750172
Fairbanks, AK 99775-0172

Visit the NETL website at:
www.netl.doe.gov

Customer Service:
1-800-553-7681



Energy Information Clearinghouse

Final report

Report start date: Sept 30, 2001

Report end date: Sept 30, 2002

Principal Author: Ron Johnson

Date of Issue: October 2003

DOE Award Number: DE-FC26-01N41248 Task 4.1

Submitting organization: University of Alaska Fairbanks
Institute of Northern Engineering
PO Box 755910, Fairbanks, AK
99775-5910

DISCLAIMER

“This report was prepared as an account of work sponsored by an agency of the United States Government. Neither the United States Government nor any agency thereof, nor any of their employees, makes any warranty, express or implied, or assumes any legal liability or responsibility for the accuracy, completeness, or usefulness of any information, apparatus, product, or process disclosed, or represents that its use would not infringe privately owned rights. Reference herein to any specific commercial product, process, or service by trade name, trademark, manufacturer, or otherwise does not necessarily constitute or imply its endorsement, recommendation, or favoring by the United States Government or any agency thereof. The views and opinions of authors expressed herein do not necessarily state or reflect those of the United States Government or any agency thereof.”

ABSTRACT

Alaska has spent billions of dollars on various energy-related activities over the past several decades, with projects ranging from smaller utilities used to produce heat and power in rural Alaska to huge endeavors relating to exported resources. To help provide information for end users, utilities, decision makers, and the general public, the Institute of Northern Engineering at UAF established an Energy Information Clearinghouse accessible through the worldwide web in 2002. This clearinghouse contains information on energy resources, end use technologies, policies, related environmental issues, emerging technologies, efficiency, storage, demand side management, and developments in Alaska.

TABLE OF CONTENTS

I.	Abstract.....	2
II.	Introduction.....	4
III.	Executive Summary	5
II.	Results and Discussion	7
III.	Conclusion	15
IV.	References.....	16

INTRODUCTION:

Alaska has spent billions of dollars on various energy related activities over the past several decades. Such projects range from smaller utilities used to produce heat and power in rural Alaska to huge projects relating to exported resources. Alaska has vast energy resources with petroleum, coal, and natural gas receiving the most attention to date. But there are also abundant renewable resources, including geothermal, wind, hydropower of various forms (including tidal, waves, and currents), and solar power for up to eight months of the year. With the high cost of heat and power -- especially in rural Alaska -- the state is eager to find ways of reducing state subsidies.

To help provide information for end users, utilities, decision makers, and the general public, the Institute of Northern Engineering at UAF submitted a proposal to AETDL in 2001 to develop an Energy Information Clearinghouse accessible through the worldwide web. This clearinghouse was established in 2002 and contains information on energy resources, end use technologies, policies, related environmental issues, emerging technologies, efficiency, demand side management, and developments in Alaska. This led to the development of a www page discussed below. Efforts to secure funding to maintain this site have not been successful to date.

EXPERIMENTAL: - not applicable for this project

EXECUTIVE SUMMARY:

To help provide information for end users, utilities, decision makers, and the general public, the Institute of Northern Engineering at UAF established an Energy Information Clearinghouse accessible through the worldwide web in 2002. This clearinghouse contains information on energy resources, end use technologies, policies, related environmental issues, emerging technologies, efficiency, demand side management, and developments in Alaska.

Energy resources discussed include oil, coal, and natural gas as fossil fuels; geothermal and nuclear power; and renewable resources, including hydropower, wind, wave and tidal, and solar electric as well as solar thermal. Conventional end use technologies discussed are steam, combustion, and hydraulic and wind turbines plus diesel electric generators for the production of electric power; and furnaces and boilers for the production of heat. Steam turbine plants generally have a history of achieving up to 95% availability and can operate for more than a year between shutdowns for maintenance and inspections. Their unplanned or forced outage rates are typically less than 2% or less than one week per year. This technology leads the others in total production of electric power in the US. Emerging technologies include fuel cells and thermoelectric generators. Energy storage via electrochemical batteries, flywheels, and hydrogen is also addressed.

Under environmental impacts, we address disposal of spent nuclear fuel, greenhouse gases, CO emissions in Alaska, fuel spills, and impacts of renewable technologies. As an example of a contentious national and global issue, the US DOE spent 14 years and \$4.5 billion on studies before recommending in January of 2002 that Yucca Mountain, a barren volcanic structure about 90 miles from Las Vegas, be used to bury thousands of tons of highly radioactive nuclear waste from power plants and nuclear weapons factories. The project faces substantial technical, legal and political challenges, and could be derailed by either house of Congress, the courts or engineering problems. In Alaska, the major ambient air quality issue associated with our use of fossil fuel resources is excessive levels of ambient CO in urban areas during the winter. This places Anchorage and Fairbanks in jeopardy of being sanctioned by the US EPA. Indoors, Alaska has the highest age-adjusted death rate from accidental CO poisoning in the nation.

“Energy conservation” refers to a variety of strategies employed to reduce the demand for energy. This can include adding extra insulation on building exteriors, setting building thermostats closer to ambient temperatures, or carpooling. Conservation is a different practice than increasing *energy efficiency*, which refers to increasing the useful output for a given energy input. This could involve replacing incandescent light bulbs with compact fluorescent ones, driving more fuel-efficient motor vehicles, and buying more efficient appliances.

With transportation accounting for roughly 25 percent of our nation's energy consumption, a key ingredient for future savings in energy is improving the corporate average fuel economy (CAFE) for motor vehicles. Other important components are use of more efficient lighting by homes and businesses, the use of more efficient electric

motors by industry, and increased use of solar energy for space and water heating. In Alaska, there is a large potential for fuel oil savings in villages by using heat captured from the jacket water of diesel - electric generators for space heating.

Alaska's electrical energy infrastructure differs from that of the rest of the United States in that most consumers in the Lower 48 states are linked to a huge, transcontinental electrical energy grid through transmission and distribution lines. In Alaska, there are at least 175 rural communities in the state that are not interconnected and must rely on their own power sources. These communities rely almost exclusively on diesel electric generators. In the central part of the state, from Fairbanks to the Kenai Peninsula south of Anchorage, (an area called the Railbelt), there is an interconnected grid. Natural gas is the primary fuel used in south central Alaska. Barrow, in far northern Alaska, also relies on natural gas. The largest hydroelectric plant is the state-owned 90 MW Bradley Lake Hydroelectric Project, near Homer, which provides approximately 10 percent of the electrical energy needs of the Railbelt. The Alaska Rural Electric Cooperative Association (**ARECA**) is the trade association for most electric utilities in Alaska. It provides advocacy and program services to help member utilities in their efforts to serve consumers with affordable, reliable electricity and improve the quality of life in Alaska's communities.

RESULTS AND DISCUSSION:

The opening page narrative plus a picture from the homepage appears below. This site is accessible over the www at http://www.uaf.edu/energyin/webpage/opening_page.htm.

Energy Information Clearinghouse University of Alaska Fairbanks

A guide to issues associated with the production of heat and electric power with an emphasis on northern applications. Additional information on [energy conservation](#), [environmental](#) issues and [energy storage](#).

Technologies for producing heat and electric power are central to modern civilization and are essential for well-being during much of the year in Alaska and other northern communities. Today, those most widely deployed in Alaska for electric power production include [gas](#) and [steam turbines](#) in urban areas, [diesel-electric generators](#) in rural regions, and [hydropower](#) in both rural and urban regions. The first three utilize [fossil fuels](#) while the latter together with [wind](#) and [solar](#) are examples of technologies based on renewable resources. [Nuclear power](#), although widely used worldwide, is not currently utilized in Alaska.

Heating is typically accomplished using [furnaces](#) and [boilers](#) fueled with oil or natural gas or [wood stoves](#). But dwellings and commercial buildings may also be heated by operating the electric power generators in a [cogeneration](#) mode.



Erection of wind turbine at Kotzebue Electric Association.

Energy storage is a critical issue for renewable-based technologies. The storage mechanism is elevated water in the case of hydropower while [electrochemical batteries](#) are commonly used to store electricity directly.

Other important issues include [energy conservation](#), [environmental impacts](#), [resources](#), [end uses](#), [demand side management](#) and [efficiencies](#).

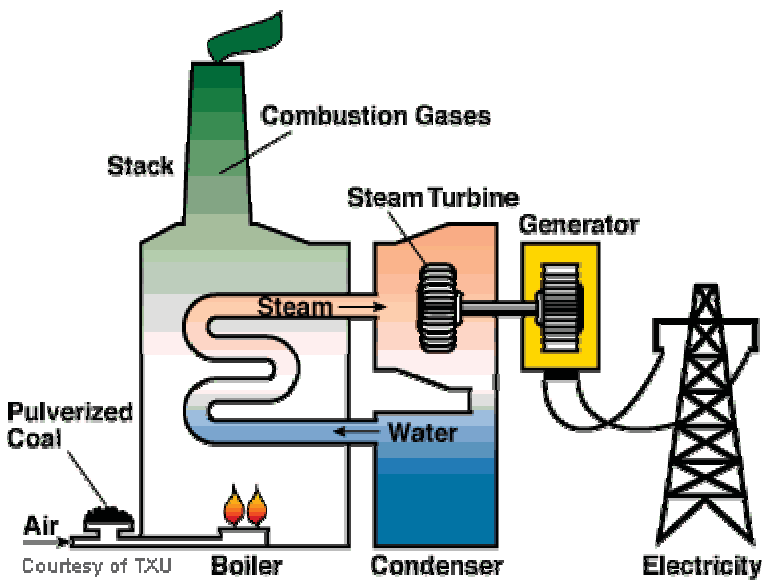
Examples of [emerging technologies](#) worth mentioning include [fuel cells](#), [thermoelectric generators](#), [flywheels](#), and [energy storage using hydrogen](#). These technologies are not now in widespread use.

The University of Alaska as well as various utilities and State and Federal agencies are currently pursuing [energy related activities](#) in Alaska.

As an example of one of the inside pages accessed from the opening page, see the below.

STEAM AND GAS TURBINE POWER PLANTS

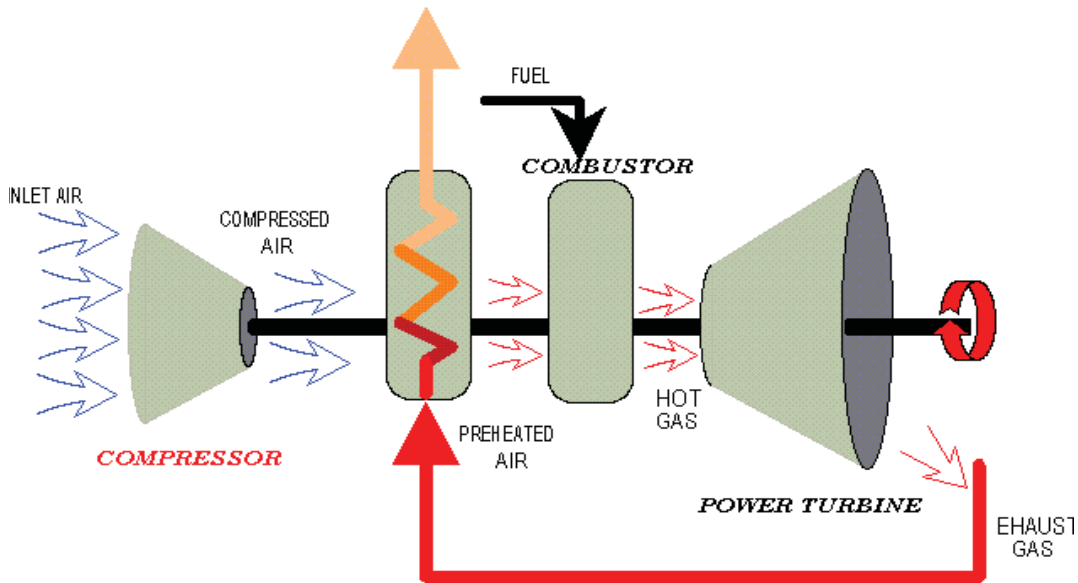
Fossil-fuel fired central station power plants world-wide normally use either steam or gas turbines to provide mechanical power to electrical generators. Pressurized high temperature steam or gas expands through various stages of a turbine, transferring energy to the rotating turbine blades. The turbine is mechanically coupled to a generator that produces electricity. Steam turbine power plants operate on a Rankine cycle, where the steam is created externally to the turbine in a boiler, where water under pressure passes through a series of tubes until it boils, eventually becoming superheated steam. The heat is provided by a furnace, normally burning coal, natural gas, or fuel oil. However, the heat could also be provided by biomass or solar or nuclear energy. Then, the plants wouldn't be fossil-fuel fired. After the steam exits the turbine, it is condensed in a condenser, pumped to boiler pressure, and reintroduced into the boiler. Heat is normally rejected from the condenser to a body of water such as a river.



Coal-fired Power Plant with Steam Turbine: courtesy of TXU.

A gas turbine plant uses a compressor to compress the inlet air upstream of a combustion chamber. Then, the fuel (normally natural gas) is introduced and ignited to produce high temperature combustion products (mostly nitrogen and uncombusted oxygen) which enter the turbine. The turbine powers the generator plus the compressor. The cycle efficiency can be increased by installing a recuperator after the turbine exhaust to preheat the inlet air after compression.

GAS-TURBINE WITH REGENERATION



Gas Turbine with Recuperation. Image by www.nyethermodynamics.com.

About 50% of Alaska's installed capacity is combustion turbines and 13 % steam turbines with 60% of the electricity produced using natural gas. Worldwide, 40 % of the electricity is produced from coal-fired steam turbines and 13 % from natural gas.

Modern large condensing steam turbine plants have efficiencies approaching 40-45%, with boiler/steam turbine installation costs between \$800-\$1000/kW or greater, depending on environmental requirements. The steam turbine itself is generally considered to have an availability at least 99 %, with longer than a year between shutdowns for maintenance and inspections.

Gas turbine development accelerated in the 1930's as a means of propulsion for jet aircraft. It was not until the early 1980's that the efficiency and reliability of gas turbines had progressed sufficiently to be widely adopted for stationary power applications. Gas turbines range in size from 30 kW (microturbines) to 250 MW (industrial frames). Industrial gas turbines have efficiencies approaching 40% and 60% for simple and combined cycles respectively.

The gas turbine share of the power generation market has climbed from 20 % to 40 % of capacity additions over the past twenty years, with this technology seeing increased use for baseload power. Much of this growth can be accredited to large (>50 MW) combined cycle plants that exhibit low capital cost (less than \$550/kW) and high thermal efficiency.

The capital cost of a gas turbine power plant can vary between \$300-\$900/kW, with the lower end applying to large industrial frame turbines in combined cycle. Availability when fueled with natural gas is in excess of 95%. In Canada, there have been 28 natural gas-fired combined cycle and cogeneration plants with an average efficiency of 48 %. The average power output was 236 MW and installed cost was around \$ 500/kW.

Pruden, D., 2001, Hydrogen system efficiency targets, pp 87 – 91 IN: McLean, G. (ed.), Proceedings of the 11th Canadian Hydrogen Conference, Victoria, B. C.

Review of Combined Heat and Power Technologies, 1999, ONSITE SYCOM Energy Corporation for the California Energy Commission under grant number 98R020974 with the U.S. Department of Energy, Office of Energy Efficiency and Renewable Energy.

Links on this page are:

Steam and Gas Links

Turbomotor Works
Dresser-Rand
How it Works: Small Gas
Turbine Engine
How Gas Turbines Work

And clicking on the second link leads to <http://www.dresser-rand.com/steam/default.asp>

One more section is presented below.



Photo courtesy of U.S. Department of Energy Geothermal Energy Program.
(<http://www.eren.doe.gov/geothermal/geobasics.html>)

Geothermal Energy

What is geothermal energy?

Geo, meaning (earth) and thermal meaning (heat) is a naturally occurring energy in the form of heat under the surface of the earth. This energy source can be only a few feet below the surface, in water that comes to the surface of the ground, in hot rocks miles below the surface, or even further down in molten rock called magma. This energy originates from radioactive decay deep within the earth's crust. The following websites give detailed information of geothermal energy.

How is geothermal energy a resource?

<http://www.iclei.org/efacts/geotherm.htm>
<http://solstice.crest.org/renewables/geothermal/grc/supply.html>
<http://www.eren.doe.gov/geothermal/geobasics.html>

What are the methods of harvesting this resource and how is it used?

<http://www.iclei.org/efacts/geotherm.htm>
<http://solstice.crest.org/renewables/geothermal/grc/supply.html>
<http://www.eren.doe.gov/geothermal/geobasics.html>

What is the potential for this resource?

<http://www.iclei.org/efacts/geotherm.htm>

<http://solstice.crest.org/renewables/geothermal/grc/supply.html>

<http://www.eren.doe.gov/geothermal/geobasics.html>

How does geothermal energy compare to other energy resources?

What is the electrical capacity of a geothermal power plant and how does this compare to other sources of energy? “The Geysers”, near San Francisco, having a generating capacity of 1360MW_e is the largest geothermal electric plant in the U.S. It is one of only two locations in the world where a high-temperature, dry steam is found that can be directly used to turn turbines and generate electricity (the other being Larderello, Italy). The Geysers is comparable to the hydroelectric Hoover dam project, which has a generating capacity of 1,345MW_e. Nuclear and coal-fired power plants may have generating capacities on the order of 1000MW_e.

<http://www.energy.ca.gov/geothermal/>

California's geothermal power plants produce about 40 percent of the world's geothermally generated electricity. U.S. geothermal power plants have a total generating capacity of 2,700 megawatts and produce electricity at 5¢ to 7.5¢ per kilowatt-hour. Iceland gets about one-third of its total energy from geothermal resources. (Ristinen, R and J. Kraushaar, 1999, Energy and the Environment).

http://www.nrel.gov/documents/geothermal_energy.html

What is the net positive environmental impact as compared to other energy sources?

Geothermal power plants have sulfur-emissions rates that average only a few percent of those from fossil-fuel alternatives. The newest generation of geothermal power plants emits only 0.3 lb of carbon (as CO₂) per MW-hr of electricity generated. This is 1000 times lower than that for a plant using natural gas (methane) and even more for a coal-fired plant. Nitrogen oxide emissions are much lower in geothermal power plants than in fossil power plants. Nitrogen-oxides combine with hydrocarbon vapors in the atmosphere to produce ground-level ozone, a gas that causes adverse health effects and crop losses as well as smog.

See - <http://solstice.crest.org/renewables/geothermal/grc/what-is.html>

What are some negative effects on the environment? Only hot water and natural steam reservoirs are being used today to create large amounts of electricity. Many of the hot water reservoirs, particularly those of higher temperature and salinity, pose the potential for contamination of the soil by salination if the extracted water is not re-injected into the ground. There is also the risk of aquifer disruption when large amounts of water are extracted from the ground. Gaseous air pollutants such as hydrogen sulfide can be liberated into the atmosphere by some hot water reservoirs and by natural steam. But again, this is often less than that emitted by other energy sources. Other possible environmental effects include induced seismic activity if water is injected into dry rock formations or if explosive fracturing techniques are used in normally impermeable rock formations (Ristinen, R and J. Kraushaar, 1999, Energy and the Environment).

Figure 30. Alaska has numerous geothermal springs, most of which issue from fractured intrusive igneous rocks or volcanic rocks.

Modified from:
 Muffler, L.P., ed., 1979, Assessment of geothermal resources of the United States, 1978: U.S. Geological Survey Circular 790, 163 p.
 Motyka, R.L., and Moorman, M.A., 1987, Geothermal resources of southeastern Alaska: Alaska Department of Natural Resources, Division of Geological and Geophysical Surveys Professional Report 93, 1 sheet, scale 1:1,000,000
 Lunis, B.C., 1990, Geopressured-geothermal direct use developments, in Geothermal Resources Council, International Symposium on Geothermal Energy: Davis, California, Transactions, v. 14, pt. I, p. 531-536
 Base modified from U.S. Geological Survey digital data.

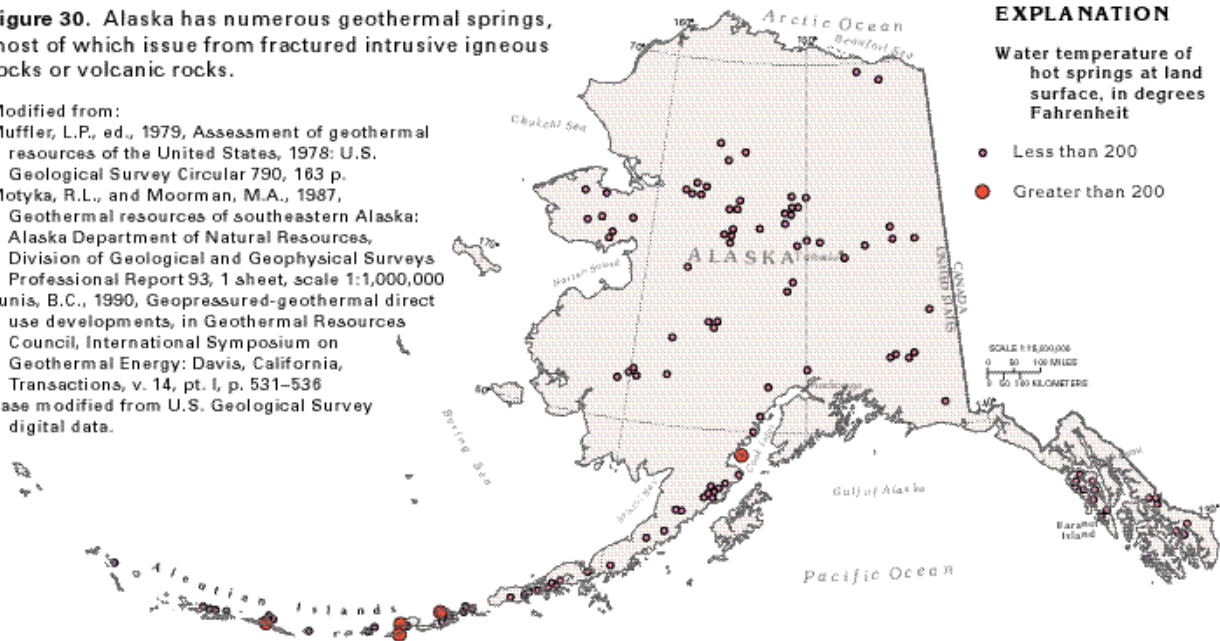


(Photo courtesy of U.S.G.S. <http://capp.water.usgs.gov/gwa/ch_n/N-AKtext4.html>)

What is the potential for this energy source in Alaska?

There are many geothermal sources in Alaska but only a few are available for producing good quality steam for direct use with a turbine, for producing electricity, and those that are available generally are not always in the place they are most needed. For use of steam directly from the source it is preferable the steam be well over 200°C, those at 200°C or lower will generally require the use of a binary cycle. A binary cycle plant is similar in construction to a direct-use-plant but the main difference is in the medium that goes through the turbine. Because steam that is lower than 200°C should not be sent through the turbine, a substance that vaporizes at much lower temperatures should be used as the medium through the turbine. The low temperature steam is sent through a heat exchanger in which the other substance, usually iso-butane, is on the other side of the heat exchanger and then this substance is sent through the turbine. The provided map shows some geothermal sources, in the form of surfacing water, in Alaska. The map reveals that the most productive sources for good quality steam at higher temperatures are on the Alaska Peninsula in the close proximity of volcanic activity. The closest source, over 200°C, to Alaska's largest city is across Cook Inlet from Anchorage and is well over 100 miles away. This is an obvious inconvenience since electric lines would need to be routed such a long distance and around such an obstacle as Cook Inlet. Most of the geothermal springs in Alaska are under 200°C and currently are being used to heat homes locally, for recreation at resorts, or are not being tapped. Low ground temperatures near the surface and permafrost limits the use of heat pumps. Because geothermal energy is associated with low emittance of SO₂, CO₂ and other pollutants and because there are many geothermal sources in the state, there is potential.

Information provided by the International Geothermal Association, last updated in 1999, indicates that there was a plan to build a 15MW_e plant at Unalaska, Alaska. With a population of over 4,300 and containing one of the United States' most productive fishing ports, Unalaska would be a great place to test geothermal electric generation in Alaska. Electricity currently costs \$0.24/kWh in Unalaska. State subsidized power cost equalization benefits provided for many remote villages in Alaska, including Unalaska, help to reduce electrical costs there because the cost of producing energy is so high. The current mode of electric generation at Unalaska is via diesel generators. One of the main obstacles to implementing a geothermal plant there is the difficult terrain that separates the source and the city. This would increase capital costs.

A third section follows

Environmental Impacts of Energy Use

The way we produce and consume heat and electricity can have profound effects on our environment. Such impacts can range from immediate consequences such as fuel oil spills or emission of carbon monoxide [CO] from motor vehicles to longer term issues such as safe disposal of radioactive wastes from nuclear power plants. In addition to the above direct impacts, there are also indirect or external consequences. These can include National security costs associated with safeguarding our infrastructure including power plants or rising sea levels due to global warming associated with greenhouse gases such as CO₂ (<http://www.aip.org/pt/vol-53/iss-11/p29.html>).

As an example of a contentious national and global issue, the US DOE spent 14 years and \$4.5 billion on studies before recommending in January of 2002 that Yucca Mountain, a barren volcanic structure about 150 km [90 miles] from Las Vegas, be used to bury thousands of tons of highly radioactive nuclear waste from power plants and nuclear weapons factories. The project faces substantial technical, legal and political challenges, and could be derailed by either house of Congress, the courts or engineering problems. Nevada officials and environmental groups have questioned the ability of engineers to reliably predict that it will not leak significantly for 10,000 years, as government rules require.

Those in favor of this recommendation cite the 103 operating power reactors in the US that are running out of storage space or spending money to extend their storage capacity plus the danger from terrorist attacks. Most of the spent fuel is stored in giant steel-lined pools, which were intended to hold only a few years of their reactors' outputs, but now have decades of fuel. They are built to withstand earthquake, tornado and other threats, but could overheat and spread large quantities of radiation if drained in a terrorist attack.

On the other hand, some opponents say that the waste would be even more at risk on trucks and trains en route to Nevada. The mayor of Las Vegas, Oscar B. Goodman, said he would oppose the use of Yucca by rallying the mayors of cities along the transportation routes. He said that there were 109 cities with populations of at least

100,000 on those routes, and 52 million people living within 0.8 km [half a mile] of the routes.

The federal effort to find a place to put wastes began in the 1960's. In 1982, Congress promised to have a repository open by January 1998, and the Energy Department signed contracts with the reactor owners to take their wastes, beginning at that time, in exchange for a payment of a tenth of a cent per kilowatt hour generated by nuclear power plants. Since then the government has collected about \$17 billion (<http://www.nytimes.com/2002/01/11/national/11NUKE.html>).

In the US, ambient air quality is guided by the National Ambient Air Quality Standards [NAAQS] which are part of the Clean Air Act last amended in 1990. This sets guidelines on allowable levels of CO, SO₂, NO_x, PM₁₀, Pb, and O₃. Electric power plants are major emitters of SO₂ and NO_x, with combustion processes having emitted 27 M tons in the US in 1997. These compounds are the precursors to acid rain and have adverse health impacts on humans and animals mainly by impacting respiration. Motor vehicles are the major source of carbon monoxide [CO] having emitted 67 M tons in 1997. [deNevers, 1999]. Ozone is a pollutant at sea level and is formed from hydrocarbons and NO_x catalyzed by sunlight. On the other hand, ozone is necessary in the stratosphere to filter our harmful UV rays.

Much attention has been devoted worldwide to climate change issues. The Third Assessment Report of Working Group I of the Intergovernmental Panel on Climate Change was prepared and reviewed by hundreds of scientists worldwide. It concludes that the global average surface temperature has increased by 0.6 ± 0.2 °C over the 20th century and that it is very likely the 1990s was the warmest decade since 1861. It also concluded that it was very likely the temperature increase in the Northern hemisphere was the largest of any century of the past 1000 years. Most of the warming over the past 50 years is likely to be caused by increases in greenhouse gas concentrations. Greenhouse gases such as CO₂ and CH₄ help trap the longer wavelength infrared radiation that is emitted from the earth's surface.

Suggestions for reducing emissions of greenhouse gases include: improved efficiencies of end use and energy conversion devices, shifting to lower carbon and renewable biomass fuels, zero emissions technologies, improved energy management, and reduction of process gas emissions (<http://www.ipcc.ch/>).

In Alaska, the major ambient air quality issue associated with our use of fossil fuel resources is excessive levels of ambient CO in urban areas during the winter. This places Anchorage and Fairbanks in jeopardy of being sanctioned by the US EPA. Indoors, Alaska has the highest age adjusted death rate from accidental CO poisoning in the nation with almost 10% of the homes in 5 villages studied having elevated levels (Howell et al, 1997). The most common cause was improperly ventilated hot water heaters.

A current issue in rural Alaska [and elsewhere] is the potential for ground water contamination resulting from bulk fuel oil storage. This has resulted in a major effort

funded by the [Denali Commission](#) to upgrade bulk fuel storage facilities. Besides leading to occasionally ambient air CO violations, transportation can also be associated with ground water contamination resulting from fuel spills of diesel fuel and gasoline at service stations.

Even renewable-based technologies can have adverse impacts such as noise and bird kills from [wind turbines](#) and fish migration issues associated with [hydropower](#). This leads to the saying "there is no free lunch". In deciding which technology to adopt, one must balance the pluses and minuses and look at total [life cycle costs](#) including environmental impacts.



Denver Temperature Inversion. Photo courtesy of NREL.

References:

- deNevers, N., 2000, Air Pollution Control Engineering, McGraw-Hill, NYC
Howell, J., M. Kieffer, and L. Berger, 1997, Carbon monoxide hazards in rural Alaskan homes, *Alaska Medicine*, 39, pp. 8-11.

[As this project ended over a year ago, the web pages have not been updated.](#)

CONCLUSION:

The Energy Information Clearinghouse is useful as one site that integrates a wide variety of information relating to energy issues both world-wide and within Alaska. The information is presented in such a way as to be intelligible to the general public as well as to provide details with links to relevant www sites for those with technical backgrounds.

REFERENCES*

These include

http://www.nrel.gov/lab/pao/biomass_energy.html
http://www.biomass.org/fact_sheet_2.htm
<http://www.eren.doe.gov/biopower/basics/index.htm>
(Ristinen, R. and J. Kraushaar, 1999, Energy and the Environment, John Wiley and Sons, NYC)
<http://www.sustainable.doe.gov/municipal/intro.shtml>
<http://bcn.boulder.co.us/environment/becc/>
<http://www.uaf.edu/coop-ext/publications/eehpubs.html>
<http://www.absn.com/index.html>
<http://www.eren.doe.gov/geothermal/geobasics.html>
<http://www.iclei.org/efacts/geotherm.htm>
<http://solstice.crest.org/renewables/geothermal/grc/supply.html>
<http://www.energy.ca.gov/geothermal/>
http://www.nrel.gov/documents/geothermal_energy.html
http://capp.water.usgs.gov/gwa/ch_n/N-AKtext4.html
<http://www.bchydro.com/business/etools/guides/EA-21.html>
<http://www.aceee.org/pubs/a984.htm>
http://www.thermopride.com/thermo_pride_oil_furnaces.htm

*A complete list of the citations may be found on the www site.

Report Title

**Small Scale Fuel Cell and Reformer Systems
for Remote Power**

Final Topical Report

October 1, 2001-September 30, 2002

Dennis Witmer

Report Issued December 2003

DOE Award Number DE-FG26-01NT41428

Task Number 1.1

Submitted by

University of Alaska Fairbanks
Institute of Northern Engineering
Arctic Energy Technology Development Laboratory
525 Duckering Building
Fairbanks, Alaska 99775

DISCLAIMER

This report was prepared as an account of work sponsored by an agency of the United States Government. Neither the United States Government nor any agency thereof, nor any of their employees, makes any warranty, express or implied, or assumes any legal liability or responsibility for the accuracy, completeness, or usefulness of any information, apparatus, product, or process disclosed, or represents that its use would not infringe privately owned rights. Reference herein to any specific commercial product, process, or service by trade name, trademark, manufacturer, or otherwise does not necessarily constitute or imply its endorsement, recommendation, or favoring by the United States Government or any agency thereof. The views and opinions of authors expressed herein do not necessarily state or reflect those of the United States Government or any agency thereof.

Abstract

New developments in fuel cell technologies offer the promise of clean, reliable affordable power, resulting in reduced environmental impacts and reduced dependence on foreign oil. These developments are of particular interest to the people of Alaska, where many residents live in remote villages, with no roads or electrical grids and a very high cost of energy, where small residential power systems could replace diesel generators.

Fuel cells require hydrogen for efficient electrical production, however. Hydrogen purchased through conventional compressed gas suppliers is very expensive and not a viable option for use in remote villages, so hydrogen production is a critical piece of making fuel cells work in these areas. While some have proposed generating hydrogen from renewable resources such as wind, this does not appear to be an economically viable alternative at this time. Hydrogen can also be produced from hydrocarbon feed stocks, in a process known as reforming. This program is interested in testing and evaluating currently available reformers using transportable fuels: methanol, propane, gasoline, and diesel fuels. Of these, diesel fuels are of most interest, since the existing energy infrastructure of rural Alaska is based primarily on diesel fuels, but this is also the most difficult fuel to reform, due to the propensity for coke formation, due to both the high vaporization temperature and to the high sulfur content in these fuels.

There are several competing fuel cell technologies being developed in industry today. Prior work at UAF focused on the use of PEM fuel cells and diesel reformers, with significant barriers identified to their use for power in remote areas, including stack lifetime, system efficiency, and cost. Solid Oxide Fuel Cells have demonstrated better stack lifetime and efficiency in demonstrations elsewhere (though cost still remains an issue), and procuring a system for testing was pursued.

The primary function of UAF in the fuel cell industry is in the role of third party independent testing. In order for tests to be conducted, hardware must be purchased and delivered. The fuel cell industry is still in a pre-commercial state, however. Commercial products are defined as having a fixed set of specifications, fixed price, fixed delivery date, and a warranty. Negotiations with fuel cell companies over these issues are often complex, and the results of these discussions often reveal much about the state of development of the technology. This work includes some of the results of these procurement experiments.

Fuel cells may one day replace heat engines as the source of electrical power in remote areas. However, the results of this program to date indicate that currently available hardware is not developed sufficiently for these environments, and that significant time and resources will need to be committed for this to occur.

Table of Contents

Abstract.....	3
Table of Contents.....	4
Introduction.....	5
Executive Summary	5
Experimental.....	6
Results and Discussion	12
Conclusions.....	12
References.....	13
List of Acronyms and Abbreviations.....	14

Introduction

The University of Alaska Fairbanks (UAF) Arctic Energy Technology Development Laboratory (AETDL) was formed with the mandate of evaluating new technologies for electrical production in remote areas. In the enabling legislation that created the office, fuel cells were specifically named as one technology of interest.

Fuel Cell work was begun at UAF several years prior to the formation of AETDL, in the Rural Alaska Power Program (RAPP), funded through the US DOE EE Hydrogen office. This work involved independent third party evaluation of PEM fuel cell technologies for residential stationary power. This report will discuss the results of that program, including the desire of AETDL to broaden the technology evaluation to include other fuel cell technologies, especially SOFC systems.

Executive Summary

Alaska's rural communities experience very high energy costs, especially for electrical power, due to the lack of electrical grids and roads, resulting in electricity production mostly using Diesel Electric Generators (DEGs). Electrical power costs in these communities ranges from \$.20 to \$.80 per kilo-Watt hour, which is a burden to both the residents and businesses of these communities. The high costs are from several factors, including the cost of transporting and storing diesel fuel, the cost of maintaining the generators in small communities where maintenance crews need to be flown in from outside to make necessary repairs, and the poor economies of scale from running a small utility.

Fuel cells designed for residential power offer several attractive benefits over the existing system. First, higher efficiency electrical power generation means less fuel would need to be transported to the village, reducing costs. Secondly, small, quiet units could be placed within individual residences, allowing efficient heat recovery, further reducing the fuel consumed by the village. High reliability would also result in significant cost savings, reducing the dependence on outside expertise for necessary repairs. Reliability of the system could also be improved, as a distributed network of units could provide back-up power for each other, much as larger grids improve reliability to all users by compensating for outages at individual plants.

While the benefits of these proposed fuel cell systems are quite apparent, the fuel cell hardware currently under development is still not readily available for use in remote villages in Alaska. Most fuel cell technology is still very much in the early product development stages, with manufacturers building prototypes for internal evaluation, or releasing hardware to carefully selected sites for evaluation. In 1998, UAF became involved in the Rural Alaska Power Program, intended to evaluate diesel fueled PEM fuel cell systems for residential power. This project was fueled by suppliers who claimed that they had beta test units capable of achieving 40% net electrical power out from diesel fuel, with system lifetimes of 40,000 hours, and that these units would be commercially available in 2001, with a project cost of \$3,500 for a 5 kW unit. The UAF role in the

project was to provide independent third party verification of this performance so that these units could be deployed in rural Alaska.

Unfortunately, the results of the project were not encouraging. First, the overall system efficiency of PEM fuel cell reformer systems was measured to be about 25%, which is lower than the current diesel generators operating in the field. Secondly, PEM fuel cell stacks failed in testing rapidly, and none of the systems tested in the program achieved more than a few hundred hours of run time operating on pure hydrogen. The diesel reformers provided to the program also experienced significant difficulties, with solid carbon formation, materials degradation, and balance of plant and control system issues contributing to the poor performance. Furthermore, costs remained high (well over \$10,000 per kW for units operating on natural gas), and no commercial production of these units occurred.

Based on these results, using diesel/PEM residential fuel cell systems in rural Alaska did not appear to be a viable alternative to diesel electric generators. However, Solid Oxide Fuel Cell (SOFC) technology appeared to be advancing rapidly. Preliminary discussions with SOFC suppliers indicated that higher system efficiencies (50% net AC out on large systems operating on natural gas) and longer stack lives (more than 69,000 hours in laboratory tests), as well as the onset of the SECA program, with aggressive price targets for this technology.

Fuel cells are still very much pre-commercial devices, with each of the technologies in the product development stage, with differing technical barriers to success. (Commercial product is defined by several characteristics: fixed product specifications, a fixed delivery date, a fixed delivery price, and a warranty.) Visiting web sites or booths at industry conferences may give the impression that commercial deployment is imminent, but the only way to determine the true state of product development is to purchase a fuel cell. This exercise can be thought of as an experiment, which in this work will be referred to as a "procurement experiment." Many times, these procurement experiments do not result in the delivery of a product to the purchaser, and can be thought of as failures, but, in fact, this null result contains much information about the state of technology development of the product.

Experimental

By the summer of 2001, experience with PEM fuel cell systems for distributed electrical power production indicated that suppliers of these systems had vastly overstated the capabilities of their product, and near term commercial deployment of these systems for use in rural Alaska was unlikely. Based on this conclusion, a decision was made to abandon further testing of this technology.

Procurement Experiment #1: The FCT Solid Oxide Fuel Cell

At a meeting in September 2000, a staff member of NETL stated in a meeting that a 5 kW SOFC operating on propane was scheduled for delivery to the Presidio Trust near San Francisco sometime in the next few months, and that the company that was supplying this unit was intending to market these units starting in late 2001 at a cost of \$5,000 per kW, or \$25,000 for a 5 kW unit.

Attempts to track down the source of this fuel cell were at first unsuccessful, but eventually it became clear that the supplier of this unit was a company called Fuel Cell Technologies, of Kingston Ontario. This company had entered into an agreement with Siemens Westinghouse for delivery of 5 kW fuel cell bundles, with FCT building the balance of plant and control systems. This agreement was announced in a press release found on the FCT web site. Also on the web site was an announcement on June 11, 2001 of the purchase order for the supply of the unit to the Presidio, as well as a second unit to the National Fuel Cell Research Center at the University of California.

Initial contact was made with FCT during the summer of 2001, when FCT indicated via e-mail on July 23, 2001 that they had “a limited number of field demonstration units available between July and December 2002. These initial units are available at a price of US \$5000 / kW, or \$25,000 per unit, FOB Kingston, Ontario, and excluding applicable taxes. This does not include any cost for installation. Scheduled maintenance cost will be low due to the very few moving parts in the system. We request a down payment of 20% with the purchase order.”

During the fall of 2001, UAF entered into an agreement with the USDOE through NETL to fund the Arctic Energy Technology Development Laboratory. Enabling legislation for this agreement included language indicating that the funds were to be used for research into improving the delivery of electrical power to rural communities in Alaska, with fuel cell technologies specifically named as a technology of interest. A project selection process was created using industry panels to review and select projects, and FCT elected to submit a proposal in this process, in cooperation with the staff at UAF.

During discussions with FCT in the early part of 2002, FCT indicated that the current price for the systems had risen to \$50,000 for new orders. However, we also discussed the fact that the University was interested in engaging in cooperative research, and would entertain a proposal in which development costs were included as part of the proposal. After a few weeks, FCT indicated that they would be interested in engaging in this kind of an arrangement, and proposed delivering and installing one of their first systems for a total contract value of \$170,000 from DOE, with additional cost share from FCT. This proposal was review and ranked highly by the industry panel, and so was selected as a project to be funded under AETDL. A subcontract was sent to FCT in July, 2002 for this work.

During the summer of 2002, UAF was told that the system would be delivered to Fairbanks in early fall of 2002, in keeping with the announced schedule of FCT. AETDL

sponsored a conference titled “Reliable and Affordable Energy for Rural Alaska” on September 17-19, 2002 in Fairbanks, and was hoping to have the fuel cell up and operating for that conference. However, shortly before this event, FCT called with the news that the stacks being supplied to them were failing in early tests, and were being sent back to the supplier. They felt it would be unwise on their part to ship a product they felt was not up to standards.

During the fall of 2002, discussions with FCT indicated that a stack delivered to them in late November was performing well, and that they expected delivery of the stack to FCT in early 2003, with delivery of the system to Fairbanks several weeks after they received it.

In February of 2003, a stack was to be shipped from the supplier to FCT for the UAF system. However, this stack was dropped and broken while being prepared for shipment at the supplier, and it was not clear when another stack would be ready for the system.

At this time, there was also discussion with regards to the fuel to be used in the system. Because our interest in Alaska is primarily to provide power to remote villages, our ultimate interest is to test units operating on fuels readily available in these places. For this reason, we indicated our interest in testing a unit operating on propane initially, followed later by a unit operating on diesel fuel. However, discussions with FCT indicated that they would be more comfortable shipping a unit designed to operate on natural gas. While this fuel is abundant in parts of Alaska (Anchorage and the North Slope, and parts of Fairbanks), it is not readily available in most rural communities. However, UAF was eager to test the operation of the fuel cell, and agreed to operate the unit on natural gas. A site at the Fairbanks Natural Gas Company in Fairbanks several miles from the university was located, and the cooperation of the site owners was obtained.

There were also several other issues that were raised with regards to the installation and operation of this fuel cell. First, the natural gas pressure needed was 40 psig, which is considerably higher than typical line pressure in most natural gas delivery systems. Fortunately, this pressure was available at the Fairbanks Natural Gas site, so we did not need to install a gas compressor to make the system work. The second issue was that the fuel cell needs to be heated before it can be started, and the heating in the alpha units is done electrically. The energy required for this heat-up is significant—about 12kW for a 24 hour period. Once again, since the unit was being installed in an industrial warehouse facility, this power was available, but this is an electrical load significantly higher than most residential loads. The third issue was the need for a 4% hydrogen / 96% nitrogen gas mix needed to maintain a reducing atmosphere in the unit during start-up. All of these changes in specifications--the sole use of natural gas, the pressure of the natural gas feed, the need for electrical power during start-up, and the need for the H₂/N₂ gas during start up—had an effect on the ability of this unit to meet the intended market needs in rural Alaska.

The good news is that the completed unit was shipped from FCT in late June, 2003, arrived in Fairbanks in mid-July, and was started up on August 1, 2003. The operation of this unit has been nearly flawless, and the project is a real success. The unit is producing both AC electrical power and usable heat, and is operating in a very stable manner. The results of the demonstration project will be covered in the report from that project, and will not be dealt with in detail here.

Procurement Experiment #2: The Diesel Reformer

Operating high efficiency fuel cells from diesel fuels is a high priority for military operations, where field deployments are often limited by fuel supply lines. Using logistical fuels for electric power generation would simplify field logistics (in the first Gulf war, small portable generators operating on gasoline were the only devices taken to the field that did not use diesel fuel, and carrying and tracking that fuel was a logistical problem for the soldiers). Use of fuel cells could also reduce noise and heat signatures from operations.

Diesel fuel is also the most common fuel used in rural Alaska, as this is the primary fuel for electrical generation in most remote villages and industrial sites. The high energy content, the relative safety with which the fuel can be handled (a match can be dropped in a bucket of diesel fuel without igniting), and the investment in current infrastructure are all reasons why the continued use of diesel fuel for operating high efficiency electrical generators is desirable. If fuel cells are to be used in these places, the development of a reformer technology for diesel fuel is critical.

In the RAPP program, two different diesel reformer technologies were tested. The first was a steam reformer, based on the design of a methanol reformer, with a palladium membrane to separate the hydrogen, providing pure hydrogen suitable for operation of a PEM fuel cell. However, the efficiency of this reformer (H₂ out/ Diesel fuel in) was at best about 35%, leading to an extremely poor overall efficiency. This reformer also experienced significant issues with materials degradation and coking. A second reformer from a different supplier used an Autothermal process to reform diesel. This unit demonstrated a higher efficiency (about 65%) but the gas stream produced was a hydrogen rich stream, also containing significant amounts of CO. This gas stream needed to be purified before a fuel cell could be connected to the system, and the gas purification system never operated properly. Other issues with the system included an unstable auxiliary burner, catalyst substrate breakdown, and oscillations in output.

Fundamental work being done in National Laboratories in the past few years has led to some understanding of the difficulties involved in the reformation of diesel fuels. This include the fact that all components of distillate fuels do not react in reformers at the same rate, with aromatic hydrocarbons breaking down at significantly slower rates than paraffins, and the role of sulfur in the nucleation of solid carbon (coking). Another issue has been the need to completely vaporize the fuel before the reaction begins (liquid droplets create local environments rich in fuel, which then thermodynamically favor the formation of solid carbon).

SOFC systems often permit internal reforming of natural gas. However, natural gas is considerably easier to reform than diesel fuel, since this has the most hydrogen per carbon, there are no aromatics in the fuel, and the fuel is a vapor at standard atmospheric conditions. The Siemens technology is designed to do reforming inside the fuel cell stack, taking advantage of the heat generated from the stack as the source of energy for the reformation process. However, heavier hydrocarbons require the presence of additional steam for the reformation to occur, and there is the increased risk of coke formation inside the stack. One possible way to deal with these issues is to separate the fuel cell and the reformer into two separate units. Doing this, however, changes dramatically the heat management of the fuel cell stack, as additional heat must be removed from the fuel cell, and (for steam reforming) supplied to the external reformer.

As part of this program, we attempted to purchase diesel reformers from several suppliers. Most reformer developers indicated to us that diesel reformers were not yet packaged for commercial deployment, and were more than happy to consider cooperative R&D projects in which small scale diesel reformers would be built and tested. However, these R&D projects are expensive, and success is not guaranteed.

One supplier did indicate, in the fall of 2002, that a diesel reformer was being packaged with a PEM fuel cell, and they were willing to provide units for testing for \$80,000. However, the longevity of these units was not very good, with a system lifetime of only a few hundred hours expected.

Another party, a reformer developer, indicated a willingness to partner on a R&D effort, using an Autothermal reformer being developed and tested for a Navy program. This reformer was intended to provide a hydrogen rich fuel stream for a 500 kW PEM fuel cell, but no 500 kW PEM fuel cell system is available for testing. The proposed plan was to use a slipstream from the reformer to operate a SOFC stack designed for natural gas. Two issues were identified, however: 1) The energy content of the hydrogen rich gas is 90 BTU/ft of gas, vs 1000 BTU/ft³ of natural gas, and 2) The heat generated in the fuel cell normally absorbed by the natural gas steam reformation needs to be removed from the system in some other way, most likely through an increase in airflow through the stack. Our original intention was to operate the FCT SOFC on this gas, but when we contacted FCT with this proposal, initial permission gradually gave way to a suggestion that we purchase an additional system engineered to handle the new gas stream.

Experiment #3: Methanol Fuel Reformer with PEM fuel cell

Methanol is a commonly available industrial substance, usually made in petrochemical refineries from natural gas, used for a variety of uses, most frequently for de-icing applications, including auto fuel tanks and airplane wings. Methanol was also a precursor to MTBE, an oxygenator added to gasoline to reduce air pollution. Due to environmental concerns associated with the rapid transport of MTBE in water tables from leaking fuel tanks, MTBE has been removed from the market, and refineries currently have excess capability for producing methanol.

Methanol is an ideal fuel for use in fuel cell applications due to the fact that it forms hydrogen at much lower temperatures than conventional hydrocarbons, at 350 C rather than at 800 C. This means that the heat required to drive a steam reformer is considerably lower, resulting in less energy loss due to heat leaving the system. Also, the lower temperatures enable the use of less costly materials in the construction of the reformer. Furthermore, since methanol and water are miscible, the fuel can be mixed with water to create a single feedstock, providing both a constant steam to carbon ratio, as well as a simplified mechanical system, since only a single pump is required for system operation. In Arctic applications, the fuel mix remains a liquid to -126 F, a temperature 38 degrees colder than the record recorded in Alaska.

Methanol also has significant disadvantages as a fuel. It has a much lower energy density per unit volume or weight (about half that of conventional liquid hydrocarbons), so is more expensive to transport to the final user. Creating a methanol/water premix for fuel only increases this disadvantage. Methanol is hazardous for human consumption, and the miscibility issue with MTBE is also an issue with methanol, where spills could contaminate large groundwater areas quickly. Also, since methanol is a product derived from natural gas, a “well to wheels” analysis of efficiency needs to be done if this fuel is proposed for a dominant fuel. Estimates of the efficiency of producing methanol (heating value of methanol/ heating value of natural gas) vary depending on the plant design where the fuel is produced, but estimates are typically about 65%.

After the difficulties experienced with diesel reformers in the RAPP program, this program investigated the feasibility of using PEM fuel cells operating on methanol for powering remote sites, especially applications such as remote communications repeaters. Idatech, from Bend, Oregon, is marketing methanol reformers, and integrated PEM systems. As part of the FY02 funding request, a project was started to create a system designed for Arctic environments using methanol/water premix as the fuel. The details of the performance of that system will be covered in the final report for that project.

The procurement experiment for the methanol/PEM system was quite interesting. First, the suppliers of both sides of the system admitted reliability issues. On the reformer side, the metering pumps used to supply the fuel premix were the weak link in the system, with the expected lifetime of these pumps only about 500 hours. This weakness has been remedied, with a new pump supplier located, with an expected lifetime of at least several thousand hours. (The cost of these pumps is an issue—currently the available price of the pump alone is comparable to the stated target price of the entire reformer.) On the Fuel Cell side, stack longevity remains an issue. While some progress is being made in understanding the failure mechanisms in membrane failure, currently stack life is extended mostly by reducing the maximum power extracted from the stack, limiting the maximum current density to no more than about half the maximum predicted from the polarization curve. While this may extend stack life, it de-rates the system power, thus increasing the cost per unit output of an already expensive system.

Phase 2 of the project, which was not funded, included funds for purchasing a second reformer. However, in the fall of 2002, Idatech announced the commercial launch of a methanol/PEM system based on a Ballard stack. Initial conversations indicated that the cost of these systems would be \$30,000 for a 1 kilo-Watt system, which was less than the \$40,000 in our budget for the purchase of a second methanol reformer. When UAF requested a formal quote for the system, however, the price had risen significantly, to \$45,500 for the base price, plus a charge of \$7,900 for spare parts and training. Cost share was listed as a 6 month parts and labor agreement, including a 500 hour warranty, parts, and labor, valued at \$14,500, for a total system value of \$67,900. This total is more than twice the initial price.

Experiment #4: The perfect procurement experiment

My clearest understanding of the level of development of the fuel cell industry came in a brief conversation with an individual who has been working on fuel cell development for more than a decade, in several companies. He announced that he was starting a new company and asked me if I was interested in buying a fuel cell. I said, “sure, but how much does it cost?”, and he replied “how much money do you have?”

Results and Discussion

Fuel Cells have been proposed as an ideal solution for providing efficient electrical power for remote villages in Alaska. However, successful deployment of this technology depends on affordable and reliable commercially available fuel cell hardware.

UAF has used the funding provided by DOE to attempt to purchase small scale fuel cells and reformers from a wide variety of suppliers. The performance of individual products is not covered in this paper, but the attempts to negotiate product delivery is documented.

The first obvious result of this investigation is that fuel cells for residential power are not commercially available. All product currently being produced is available only through cooperative R&D agreements intended as early demonstration projects, and most of the information generated is protected through non-disclosure agreements. No supplier currently meets the requirements of commercial product: fixed product specifications, fixed price, fixed delivery date, and a warrantee. In the Solid Oxide Fuel Cell industry, manufacturing of the cells and stacks in a timely and affordable manner appears to be the fundamental barrier. In the PEM industry, stack lifetime and low system efficiency are major barriers to successful use of this technology

The reforming of suitable fuels also remains problematic. Natural gas and methanol are easy to reform, but are not ideal for use in remote areas. Heavier hydrocarbons are more difficult to reform, and reliable reformers are not currently available.

Conclusions

Fuel Cells promise high efficiency, low emissions, high reliability, and low cost. However, these promises have yet to be fulfilled, as all fuel cell technologies are still very much in the product development stage.

Fuel cell developers are under tremendous pressure to produce commercial product from their investors, both private and public. Frequently, optimistic targets are set for product performance and release, and those who promise the most are rewarded with funding for product development.

Obtaining accurate information about the true state of product development is nearly impossible to obtain, unless one attempts to purchase product. This program has purchased several fuel cell systems for pre-commercial testing. While the original intent of these programs was to verify the performance of these fuel cells prior to deployment of these technologies in rural Alaska, the conclusion that we have reached is that none of the systems we have obtained are developed to the point where they would be likely to succeed in a field demonstration in remote areas.

References

Binder, Michael, "DOD Fuel Cell Residential Demonstration Program", Web Page http://www.dodfuelcell.com/res.site_performance.php3, 2003

Borup, Rod, J. Tafoya, M Inbody, D Buidry, W. Vigil, J. Parkinson, "Diesel and Gasoline Reforming for Fuel Cell Systems", 2003 Fuel Cell Seminar Abstracts, 2003

Feitelberg, A., "On the Efficiency of PEM Fuel Cell Systems and Fuel Processors", 2003 Fuel Cell Seminar Abstracts, 2003

Kreith, Frank, R. E. West, "Gauging Efficiency, Well to Wheel", Mechanical Engineering Power, 2003

Loffler, D. G., S. D. McDermott, and C. N. Renn, "Activity and Durability of Water-Gas Shift Catalysts Used for the Steam Reforming of Methanol", Journal of Power Sources, In Press 2003

Lutz, Andrew, Robert Bradshaw, Jay Keller, and Dennis Witmer, "Thermodynamic analysis of hydrogen production by steam reforming", International Journal of Hydrogen Energy, 2003

Rheume, J. M., M. S. Hsu, and Shih-Hung Chan, "Advancement of Solid Oxide Fuel Cell Systems and a Comparison with Polymer Electrolyte Fuel Cell Systems", Energy 2000 Conference, Las Vegas, 2000

Witmer, Dennis, Dan Morse, Thomas Johnson, Steve Guthrie, Ron Johnson, and Jay Keller, “Fuel Utilization Measurements of PEM Fuel Cells for Remote Power Applications, National Hydrogen Association Annual Meeting”, 1999

Witmer, Dennis, Jay Keller, and Ron Jonhson, “Remote Area Power Program for Alaskan Villages”, National Hydrogen Association Annual Meeting, 1999

List of Acronyms and Abbreviations

PEMFC-- Polymer Exchange Membrane Fuel Cell or Proton Exchange Membrane Fuel Cell (the two are different names for the same technology)

SOFC-- Solid Oxide Fuel Cell

RAPP-- Rural Alaska Power Program

UAF-- University of Alaska Fairbanks

DEG—Diesel Electric Generator

Note: SI is an abbreviation for “Le Systeme International d’Unites.”

Crack Growth Analysis of Solid Oxide Fuel cell Electrolytes

Final Topical Report

Jan 2002 – Sept 2002

Principal Authors:

Prof. S. Bandopadhyay

Dr. N. Nagabhushana

Re-Issued: October 2003

DOE Award # DE-FC26-01NT41248

**School of Mineral Engineering,
University of Alaska Fairbanks
Fairbanks, AK 99775**

DISCLAIMER

This report was prepared as an account of work sponsored by an agency of the United States Government. Neither the United States Government nor any agency thereof, nor any of their employees, makes any warranty, express or implied, or assumes any legal liability or responsibility for the accuracy, completeness, or usefulness of any information, apparatus, product, or process disclosed, or represents that its use would not infringe privately owned rights. Reference herein to any specific commercial product, process, or service by trade name, trademark, manufacturer, or otherwise does not necessarily constitute or imply its endorsement, recommendation, or favoring by the United States Government or any agency thereof. The views and opinions of authors expressed herein do not necessarily state or reflect those of the United States Government or any agency thereof

ABSTRACT

Defects and *Flaws* control the structural and functional property of ceramics. In determining the reliability and lifetime of ceramics structures it is very important to quantify the crack growth behavior of the ceramics. In addition, because of the high variability of the strength and the relatively low toughness of ceramics, a statistical design approach is necessary. The statistical nature of the strength of ceramics is currently well recognized, and is usually accounted for by utilizing Weibull or similar statistical distributions. Design tools such as CARES using a combination of strength measurements, stress analysis, and statistics are available and reasonably well developed. These design codes also incorporate material data such as elastic constants as well as flaw distributions and time-dependent properties. The fast fracture reliability for ceramics is often different from their time-dependent reliability. Further confounding the design complexity, the time-dependent reliability varies with the environment/temperature/stress combination. Therefore, it becomes important to be able to accurately determine the behavior of ceramics under simulated application conditions to provide a better prediction of the lifetime and reliability for a given component.

In the present study, Yttria stabilized Zirconia (YSZ) of 9.6 mol% Yttria composition was procured in the form of tubes of length 100 mm. The composition is of interest as tubular electrolytes for Solid Oxide Fuel Cells. Rings cut from the tubes were characterized for microstructure, phase stability, mechanical strength (Weibull modulus) and fracture mechanisms. The strength at operating condition of SOFCs (1000°C) decreased to 95 MPa as compared to room temperature strength of 230 MPa. However, the Weibull modulus remains relatively unchanged. Slow crack growth (SCG) parameter, $n = 17$ evaluated at room temperature in air was representative of well studied brittle materials. Based on the results, further work was planned to evaluate the strength degradation, modulus and failure in more representative environment of the SOFCs.

TABLE OF CONTENTS

EXECUTIVE SUMMARY	1
INTRODUCTION	2
TASK 1.2: Crack Growth Parameters	10
CONCLUSIONS	23

LIST OF GRAPHICAL MATERIALS

- Figure 1: a) Optical micrograph of the thermally etched YSZ indicating uniform grain size.
b) Higher magnification of a single grain of the thermally etched YSZ indicating closed porosity in the grain
- Figure 2: X-ray analysis of the YSZ tube indicating full stabilization of the cubic phase.
- Figure 3: C-ring test configuration for strength evaluation of YSZ tubes
- Figure 4: Weibull plot for strength evaluation of YSZ tubes at room temperature
- Figure 5: C-ring Fracture Strength-Stress Rate Diagram. a) Plot of strength vs. stress rate and b) Log (Fracture Strength) versus Log (Stress Rate)
- Figure 6 Fracture surfaces examined under SEM indicating transgranular fracture. At low stress rates (a and b), higher incidence of micro-cleavage in grains is visible. At higher stress rates (50MPa/s), grains are relatively smoother with reduced micro-cleavage planes.
- Fig. 7: Weibull plots of C-ring fracture strength at room temperature and at 1000°C in air.

Executive Summary

Increasing demand for clean fuel and raising global concerns on environmental issues in burning of fossil fuels has fuelled the search for alternate source of clean energy. Fuel cells represent an important opportunity to utilize fossil fuels in an efficient and environmentally friendly manner. Fuel cells produced in small expandable modules and manufactured cheaply by taking advantage of economies of production are well suited to meet a growing worldwide demand for energy. The modules produced could be made scalable allowing application of capital in smaller incremental amounts as electrical power demands increase.

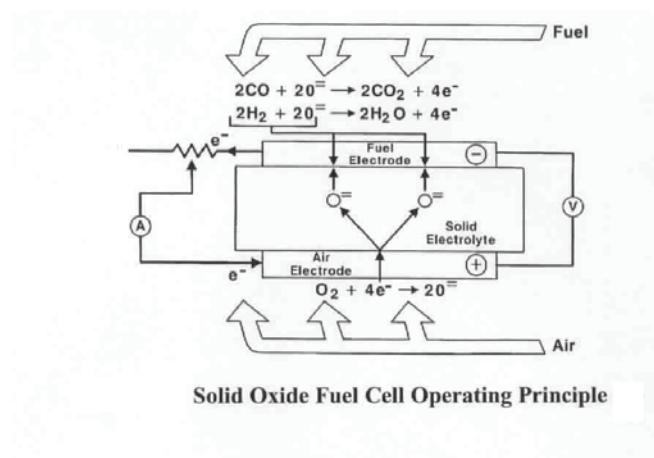
Solid Oxide Electrolyte Fuel Cells (SOFC) has been widely identified as one such possible source of clean energy. Although for these fuel cells, the preferred fuel is hydrogen, it has been shown that more commonly available fuels such as natural gas could also be used. Importantly, controlled oxidation of fuels such as natural gas can be carried out in the cell to produce chemical by-products to acts as feeders for the chemical industries.

Solid-oxide fuel cells were once considered the most technically challenging fuel cell type. However, many recent breakthroughs in ceramic materials, fuel cell design, and manufacturing technology have changed this view. Advances in ceramic thin film processes enabling the development of high power density electrode supported cells; compact fuel processing technology; and adoption of manufacturing methods developed in related industries such as the semiconductor industry are enabling the quick maturing of the technology and making the solid oxide fuel cells a viable option for mass applications in the future. A solid-oxide fuel cell is highly efficient. Even without cogeneration a solid-oxide fuel cell system can be twice as efficient as competing technologies due to the direct conversion of fuel to electrical power. With thermal recovery, system efficiency could reach as high as 85%. In addition, SOFC systems are clean. They generate no solid wastes, and due to the higher efficiency and the replacement of fossil fuel combustion with a lower temperature electrochemical conversion, fuel cells significantly lower emissions of nitrogen compounds and greenhouse gases.

One of the most common fuel cells presently in use is the Zirconia based cell. Fully stabilized and Ytria doped Zirconia (YSZ) ceramics, have been successfully used as fuel cell for about 10,000 hours. The fuel cells are typically in the form of thin walled tubes with fuel passing on one surface and air on the other. However, as all ceramics YSZ are by nature brittle and are prone to catastrophic failure. The high temperature and harsh environment make the ceramics more susceptible to slow crack growth and thus exhibit time-dependent failure. While this behavior is relatively simplistic (in reality it is complex) in bulk and regular bar test specimens, they tend to be more complex when irregular components (such as tubes) are involved. Predictions of, and improvements to, the reliability of components and systems are thus to be developed by combining the approaches of materials science and mathematical reliability analysis

Introduction

Fuel cells are electrochemical devices that convert the chemical energy of a reaction directly into electrical energy. The basic physical structure or building block of a fuel cell consists of an electrolyte layer in contact with a porous anode and cathode on either side. In a typical fuel cell, gaseous fuels are fed continuously to the anode (negative electrode) compartment and an oxidant (i.e., oxygen from air) is fed continuously to the cathode (positive electrode) compartment; the electrochemical reactions take place at the electrodes to produce an electric current. The fuel cell is thus an energy conversion device that theoretically has the capability of producing electrical energy for as long as the fuel and oxidant are supplied to the electrodes. In reality, degradation, primarily corrosion, or malfunction of components limits the practical operating life of fuel cells.

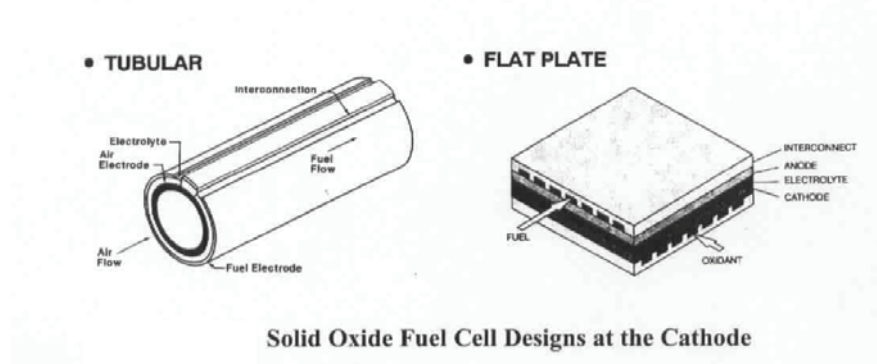


Solid Oxide Fuel Cells

Much of the recent effort in the development of fuel cell technology has been devoted to reducing the thickness of cell components while refining and improving the electrode structure and the electrolyte phase, with the aim of obtaining a higher and more stable electrochemical

performance while lowering cost. Of the various fuel cell being developed Solid Oxide Fuel Cell (SOFC) the tubular design has been with the longest continuous development period and has since grown in recognition as a viable high temperature fuel cell technology. The operating temperature of $\sim 800^{\circ}\text{C}$ allows internal reforming, promotes rapid kinetics with non-precious materials, and produces high quality byproduct heat for cogeneration or for use in a bottoming cycle. The high temperature of the SOFC, however, places stringent requirements on its materials. The development of suitable low cost materials and the low cost fabrication of ceramic structures are presently the key technical challenges facing SOFC's. However, since the electrolyte is solid, the cell can be cast into flexible shapes, such as tubular, planar, or monolith. The solid ceramic construction of the cell also alleviates any cell hardware corrosion problems characterized by the liquid electrolyte cells and has the advantage of being impervious to gas cross-over from one electrode to the other. The absence of liquid also eliminates the problem of electrolyte movement or flooding in the electrodes. At the temperature of presently operating SOFC's (1000°C) fuel can be reformed within the cell and some of the rejected heat used to preheat the incoming process air. The high temperature of the SOFC has its drawbacks. There are thermal expansion mismatches among materials, and sealing between cells is difficult. The high operating temperature places severe constraints on materials selection and results in difficult fabrication processes. The two major impediments to the widespread use of fuel cells are: 1) high initial cost and 2) high-temperature cell endurance operation. These two aspects are the major focus of manufacturer's technological efforts.

The solid-state character of all SOFC components means that, in principle, there is no restriction on the cell configuration and moreover, it is possible to shape the cell according to criteria such as overcoming design or application issues. Cells are presently being developed in different



configurations; however the flat plate and the tubular design are emerging as the most popular designs.

A brief description of the materials currently used in the various cell components of the more developed tubular SOFC, and those that were considered earlier is presented. Because of the high operating temperatures of present SOFC's (approximately 1000°C), the materials used in the cell components are limited by chemical stability in oxidizing and reducing environments, chemical stability of contacting materials, conductivity, and thermo-mechanical compatibility. These limitations have prompted investigations of developing cells with compositions of oxide and metals that operate at intermediate temperatures in the range of 650°C.

Present SOFC designs make use of thin film concepts where films of electrode, electrolyte, and interconnect material are deposited one on another and sintered, forming a cell structure. Often various thin layers of refractory oxides suitable for the electrolyte, anode, and interconnection are deposited. This procedure has also been used to fabricate the solid electrolyte Yttria

stabilized zirconia (YSZ). The anode consists of metallic Ni and an Y₂O₃ stabilized ZrO₂ skeleton. The latter serves to inhibit sintering of the metal particles and to provide a thermal expansion coefficient comparable to those of the other cell materials

Evolution of Cell Component Technology for Tubular Solid Oxide Fuel Cells

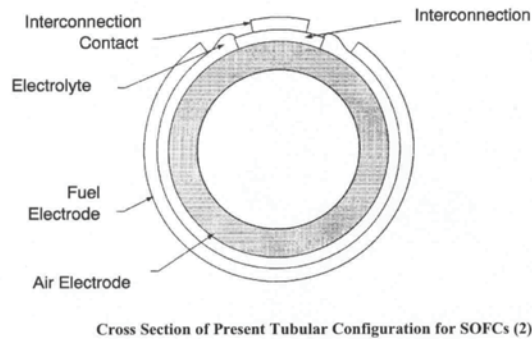
Component	Current Status
Anode	<ul style="list-style-type: none"> • Ni/ ZrO₂ cermet • Deposit slurry, EVD fixed • 12.5 x 10⁻⁶ cm/cm/°C • ~150 μm thickness • 20-40% porosity
Cathode	<ul style="list-style-type: none"> • Doped lanthanum manganite • Extrusion, sintering • ~2 mm thickness • 11 x 10⁻⁶ cm/cm/°C expansion from room temperature to 1000°C • 30-40% porosity
Electrolyte	<ul style="list-style-type: none"> • Yttria stabilized ZrO₂ (8 mol% Y₂O₃) • EVD d • 10.5 x 10⁻⁶ cm/cm °C expansion from RT-1000°C • 30-40μm thickness
Cell Interconnect	<ul style="list-style-type: none"> • Doped lanthanum Chromite • Plasma spray • 10 x 10⁻⁶ cm/cm °C • ~100μm thickness

The anode structure is fabricated with a porosity of 20 to 40% to facilitate mass transport of reactant and product gases. Doped lanthanum Magnetite is most commonly used for the cathode material. Similar to the anode, the cathode is a porous structure that must permit rapid mass transport of reactant and product gases. The cell interconnection material (doped lanthanum Chromite), however, must be impervious to fuel and oxidant gases and must possess good electronic conductivity. In addition, the cell interconnection is exposed to both the cathode and anode environments thus, it must be chemically stable under O₂ partial pressures of about ~1 to

10^{-18} atmospheres at 1000°C (1832°F). The solid oxide electrolyte must be free of porosity that permits gas to permeate from one side of the electrolyte layer to the other, and it should be thin to minimize ohmic loss. In addition, the electrolyte must have a transport number for O^- as close to unity as possible, and a transport and a transport number for electronic condition as close to zero as possible. Zirconia-based electrolytes are suitable for SOFC's because they exhibit pure anionic conductivity over a wide range of partial pressures (1 to 10^{-20} atmospheres). The other cell components should permit only electronic conduction, and inter-diffusion of ionic species in these components at 1000°C (1832°F) should not have a major effect on their electronic conductivity. Other severe restrictions placed on the cell components are that they must be stable to the gaseous environments in the cell and that they must be capable of withstanding thermal cycling. The materials listed above appear to have the properties for meeting these requirements.

As with the other cell types, it is necessary to stack SOFC's to increase the voltage and power being produced. Because there are no liquid components, the SOFC can be cast into flexible shapes. As a result, the cell configurations can respond to other design prerequisites. This feature has resulted in two major configurations and variations of them. The predominant oxide fuel cell configuration at this time is tubular. This tubular configuration (i.e., cylindrical design) adopted for SOFC's minimizes the use of seals, especially in the highest temperature parts of the cell. Overlapping components (i.e., electrodes, electrolyte, cell interconnection) in thin layers ($10\text{-}50\ \mu\text{m}$) are deposited on a porous support tube of Calcia-stabilized Zirconia. The very high efficiency cycle uses a configuration that requires seals at the high temperature parts of the cells. An early tubular design is illustrated in the schematic representation of the cross section of a SOFC stack. In this tubular design, individual fuel cells are arranged in bands along

the support tube and are connected in series by a ceramic interconnect material. The seal-less tubular design, however, is the most advanced among the several SOFC configuration concepts.



Seal-less Tubular Configuration: This approach results in eliminating seal problems between adjacent cells. A major advantage of this design over earlier designs is that relatively large single tubular cells can be constructed in which the successive active layers can be deposited without chemical or material interference with previously deposited layers. Materials and design approaches have been developed so that SOFC technology, particularly the tubular cell configuration, is technically feasible. However, the application of the materials used in the non-restrained tubular cell to the restrained alternative planar configurations results in excessive mechanical stresses. Moreover, the present approaches exhibit lower than desired performance (higher operating costs) and difficult designs and fabrication (higher capital costs). Cost reduction of cell components and simplification of the manufacturing are an important focus of ongoing development. The major issue for improving SOFC technology is to develop materials that sustain good performance while withstanding the high operating temperature presently used (1000°C), or to develop alternate cells with mixtures of ceramics and metals that operate at an

intermediate temperature of approximately 650°C. Two approaches are being pursued to alleviate the many materials and design concerns:

- 1) Research to address material and design improvements that allow operation within the high temperature environment (1000°C) of the existing state-of-the-art components
- 2) Lowering the operating temperature (600 to 800°C), so that metals could be substituted for ceramics, especially in the cathode and interconnect. A wider variety of materials could be used with lower temperature operation, with a subsequent reduction in cost.

High Temperature Cell Development (Present Operating Temperature, 1000°C)

Development work for cells operating at 1000°C is focused on increasing the mechanical toughness of the cell materials to alleviate the impact of thermal mismatch and to develop techniques that will decrease interfacial changes of the various material layers during thin film cell fabrication. Interfacial issues among cell components include diffusion, volatilization, and segregation of trace constituents. For example, $\text{La}_2\text{Zr}_2\text{O}_7$ and SrZrO_3 may form at the cathode/electrolyte interface, and Sr and Mn ions diffuse across the interface at temperatures as low as 800°C for up to 400 hours. Approaches to resolving the mismatch caused by different component materials' thermal expansion coefficient include increasing the fracture toughness of the electrolyte, controlling the electrolyte processing faults, varying the component thickness, and adding minor constituents to alter the anode properties. The electrolyte of choice at present is Yttria, fully stabilized ZrO_2 . Researchers are investigating partially stabilized ZrO_2 and adding Al_2O_3 to fully Yttria stabilized ZrO_2 to strengthen the electrolyte matrix. This increased strength is needed for self-supporting planar cells. An increase in bending strength of 1200 MPa was

observed in the TZP material compared to 300 MPa for cubic zirconia stabilized with > 7.5 mol% Y_2O_3 . The TZP was stabilized by taking advantage of fine particle technology and minor doping of Y_2O_3

Scientific Discussion

A broad program for resolution of the material and component issues prior to integration into a fuel cell require a research program to address various issues such as:

- 1) Magnitudes of ionic and electronic conduction,
- 2) Thermal expansion issues for compatibility with other cell components,
- 3) Phase stability in the fuel cell environment,
- 4) Mechanical strength,
- 5) Chemical interactions with the electrode materials, and
- 6) Stability of ionic conduction in reducing and oxidizing environments.

In addressing the structural issues of the cell it is essential to have a detailed knowledge of constitutive behavior of monolith and composite structures (ex: electrolyte materials over porous electrodes etc.). Along with functional aspects such as conductivity etc., issues such as mechanical integrity, long-term performance, and stability in a reducing environment, are of paramount importance. The various subtleties in the process conditions and its effect on the fuel cell materials structural properties are not entirely understood and have been a fertile area for research. There are also no definitive studies on the long term behavior of fuel cell materials at high temperatures and under severe reducing conditions/oxygen gradients. Specifically, it is important to be able to predict long-term behavior of fuel cells using short term and accelerated tests. However, experimental and reliable data on the materials behavior in the application environment are few or severely lacking. The results from the proposed study thus intend to provide important inputs for the design of fuel cell by characterization of material components in various environments.

Task 1.2.1 Determination of Crack Growth Parameters

A) YSZ characterization:

Yttria stabilized Zirconia (YSZ) of 9.6 mol% Yttria composition were procured in the form of tubes of length 100 mm. The tubes were processed by slip casting and are of the dimensions 9.6 O.D and wall thickness of ~ 1 -1.2 mm. Rings were cut from the tubes and characterized for microstructure, phase stability and mechanical strength.

Microstructure:

The YSZ rings were ground and polished to 0.25 μm finish. The polished sample were thermally etched at 1400°C for 2 hours and observed under an optical microscope.

Microstructural analysis indicated a dense and equi-axial grain size of $\approx 15 \mu\text{m}$. Isolated porosity were observed at triple grain boundary points. Micro pores in the grain were closed and did not contribute to the porosity.

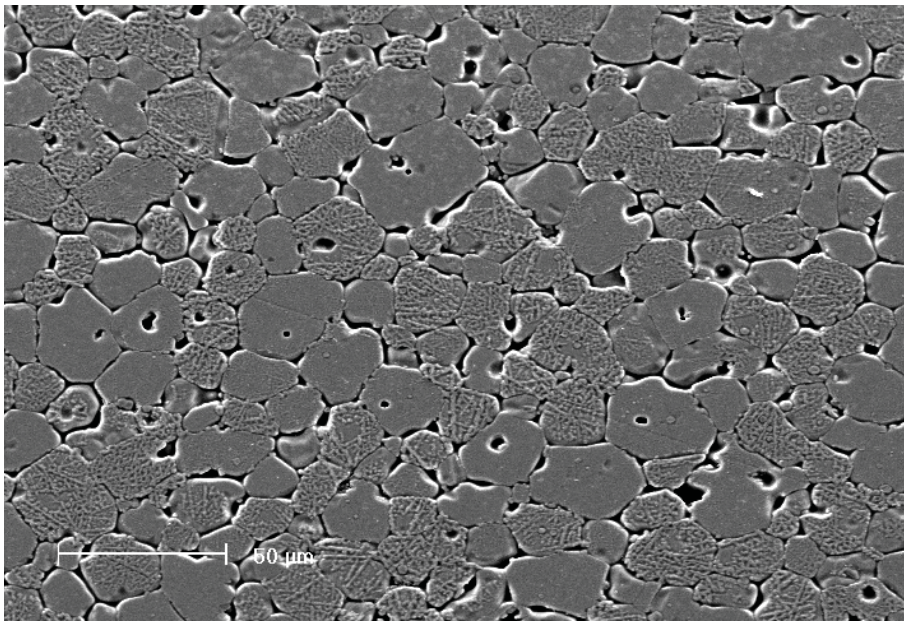


Figure 1: a) Optical micrograph of the thermally etched YSZ indicating uniform grain size.

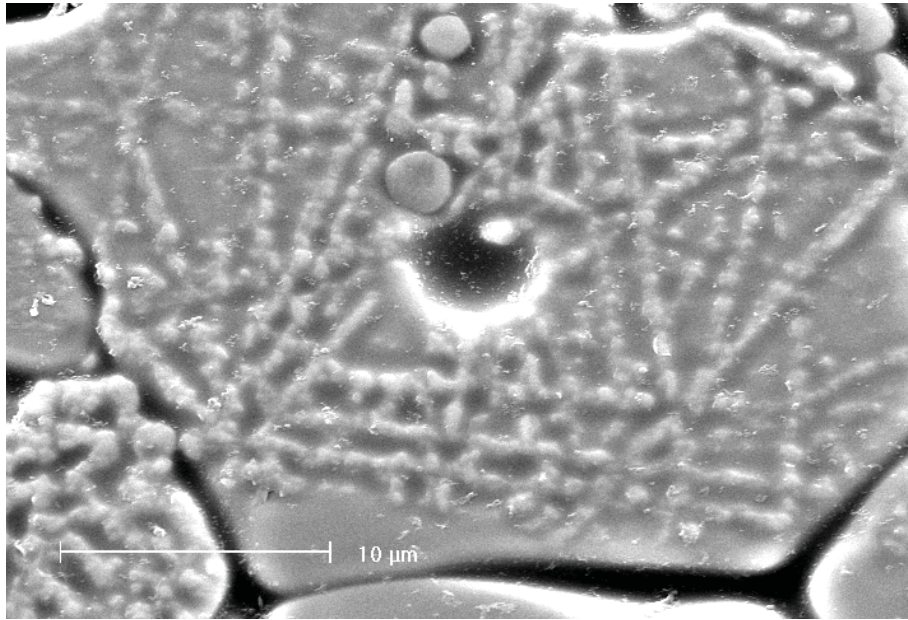


Figure 1: b) Higher magnification of a single grain of the thermally etched YSZ indicating closed porosity in the grain

The YSZ tubes were analysed for phase stability. The X-ray analysis as shown in figure 2, indicated full stabilization of the YSZ structure with the Ytria composition.

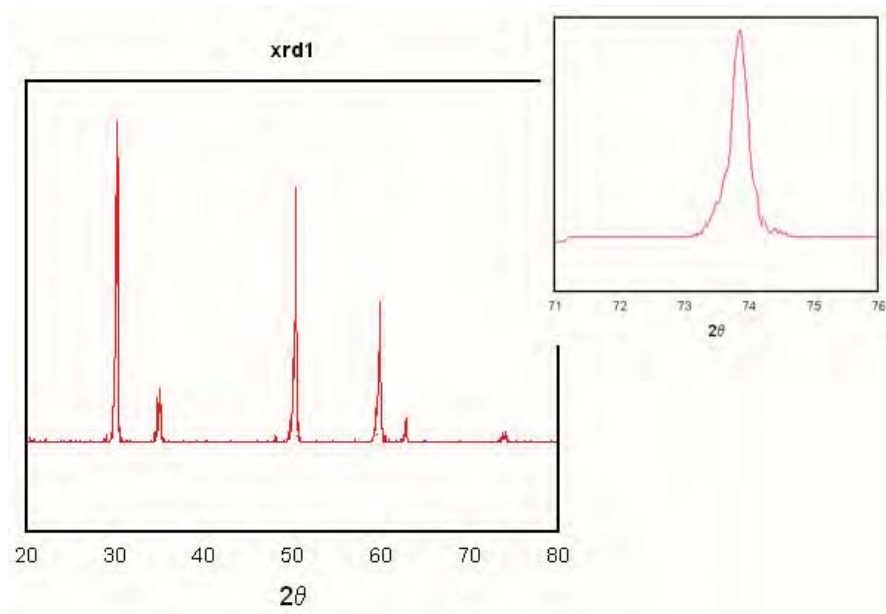


Figure 2: X-ray analysis of the YSZ tube indicating full stabilization of the cubic phase.

Mechanical Testing:

The YSZ tubes were sliced into rings and the strength of the rings was determined according to ASTM C 1323 - 96 (Standard test method for ultimate strength of advanced ceramics with diametrically compressed C-Ring specimens at ambient temperature). Rings of length ~ 4.4 mm were cut from the tubes in a low speed saw. The surfaces of the rings were ground and polished to a $1\mu\text{m}$ finish using successive grades of SiC paper and finally with a diamond compound. The edges of the rings were chamfered to minimize preferential failures from edge flaws and notched by a 0.5mm low speed saw to form a C-ring specimen. The C-rings were placed in an autoclave (to ensure uniform temperature and humidity) between two alumina platens in a hydraulic testing frame (MTS 858 MiniBionix II). Stabilized Zirconia cloth (0.5 mm) was used as pressure pads to reduce frictional stresses and to prevent slippage of the rings during testing (Fig. 1). All the tests were done by monotonically loading in plane strain diametral compression (induces a tensile field at the mid plane) to fracture at a constant crosshead speed of 1 mm./min. The maximum fracture strength of the C-Ring specimens were calculated from the equation

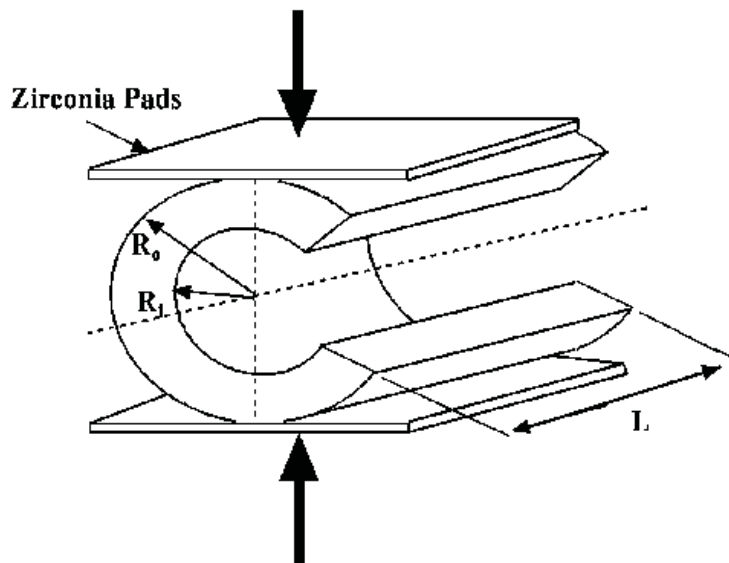


Figure 3: C-ring test configuration for strength evaluation of YSZ tubes

Where r_o - is the outer radius of the C-Ring, b – the width of the ring, t – thickness and P the fracture load. However, the actual fracture strength is calculated from the measure angle of fracture from the mid plane.

$$\sigma_{\theta_{\max}} = \frac{PR}{btr_o} \left[\frac{r_o - r_a}{r_a - R} \right] \quad \mathbf{1}$$

A total of 12 rings were evaluated and the results plotted as a Weibull graph. For this the sample were ranked in a ascending order of their measured strength. The failure probability was determined according to:

$$F = \frac{n - (\frac{1}{2})}{N} \quad \mathbf{2}$$

Where F is the failure probability, n is the order of ranking and N is the total number of samples tested.

The results were analyzed in a parameter Weibull distribution, where m is the modulus and σ_o is the characteristic strength. The parameter m in ceramics gives a measure of the strength distribution with a higher value denoting higher reliability.

$$F = 1 - e^{-\int (\frac{\sigma}{\sigma_o})^m dv} \quad \mathbf{3}$$

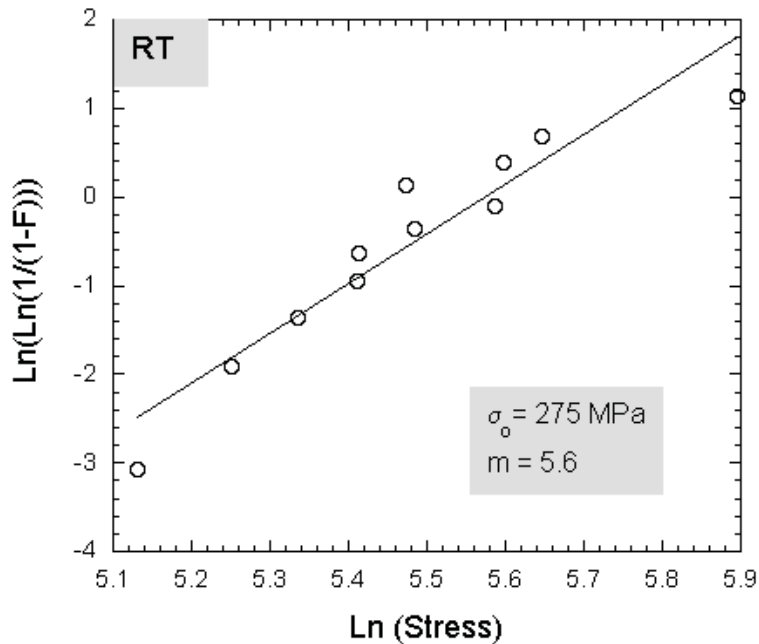


Figure 4: Weibull plot for strength evaluation of YSZ tubes at room temperature

The Weibull modulus for the YSZ tubes was determined as 5.6 and σ_0 as 275 MPa. A detailed examination of the fractured surfaces will be important in characterizing the flaws and fracture origins to complete the study at room temperature.

Slow Crack Growth Tests:

The YSZ tubes were sliced into rings and the strength of the rings was determined according to ASTM C 1323 - 96 (Standard test method for ultimate strength of advanced ceramics with diametrically compressed C-Ring specimens at ambient temperature). Rings of length ~ 4.4 mm were cut from the tubes in a low speed saw. The surfaces of the rings were ground and polished to a $1\mu\text{m}$ finish using successive grades of SiC paper and finally with a diamond compound. The edges of the rings were chamfered to minimize preferential failures from edge flaws and notched by a 0.5mm low speed saw to form a C-ring specimen. The C-rings were placed in an autoclave (to ensure uniform temperature and humidity) between two alumina platens in a hydraulic testing

frame (MTS 858 MiniBionix II). Stabilized Zirconia cloth (0.5 mm) was used as pressure pads to reduce frictional stresses and to prevent slippage of the rings during testing (Fig. 1). All the tests were done by monotonically loading in plane strain diametral compression (induces a tensile field at the mid plane) to fracture. Tests for evaluation of slow crack growth parameters were done in accordance with ASTM designation C 1368-97 and in plane strain conditions. The applied strain rates were calculated from the specimen geometry (ASTM C 1323-96) and the strength tests done in displacement control at a constant crosshead speed of 0.035, 0.3, 1 and 2.5 mm./min. according to the test standard, five samples were tested at each strain rate. The maximum fracture strength of the C-Ring specimens were calculated from the equation

$$\sigma_{\theta_{\max}} = \frac{PR}{btr_o} \left[\frac{r_o - r_a}{r_a - R} \right] \quad 4$$

In very low speed tests (0.035 mm/min), the time required for testing was minimized by applying a preload to the test specimen prior to testing. The preloads were approximately 0.5 times the fracture loads at that stress rate. The fracture strengths determined in this case was not observed to show any significant change.

Results of the strength tests at different crosshead speeds are reported in Table 1. The actual stress rates were calculated from the slope in the load vs. displacement curves of the individual strength tests in accordance with ASTM C 1368-97.

Table 1: Strength values of YSZ tubes at varying stress rates

Specimen No	Cross-head Speeds, mm/min	Stress Rates, MPa/s	Fracture strength, MPa
1	0.035	0.47604	181.92
2	0.035	0.41663	130.46
3	0.035	0.43918	194.06

4	0.035	0.43956	192.85
5	0.035	0.49566	170.21
6	0.3	4.9393	206.43
7	0.3	4.4950	197.04
8	0.3	4.3665	222.55
9	0.3	4.0640	166.03
10	0.3	4.4046	224.38
11	1	30.539	240.67
12	1	30.300	270.05
13	1	31.506	266.79
14	1	31.448	283.16
15	1	32.141	363.44
16	2.5	53.066	213.95
17	2.5	53.473	189.72
18	2.5	51.343	176.95
19	2.5	56.633	202.83
20	2.5	50.528	161.96

The strength values of the YSZ tubes decreased with decreased applied test rates. This behaviour is expected, as at lower stress rates, the strength is probably affected by sub-critical growth of cracks. The strength value at higher stress rates is however anomalous, since a drop in strength values were observed. This observed drop in strength could not be further verified as testing at higher stress rates were not possible in the present experimental set up. A detailed analysis of fracture surfaces could possibly provide clues to the observed effects.

The results of the strength tests as a function of stress rates are plotted in Fig 5. The plots are conventionally represented as a plot of Log (Fracture Strength) versus Log (Stress Rates) as shown in Fig 5b.

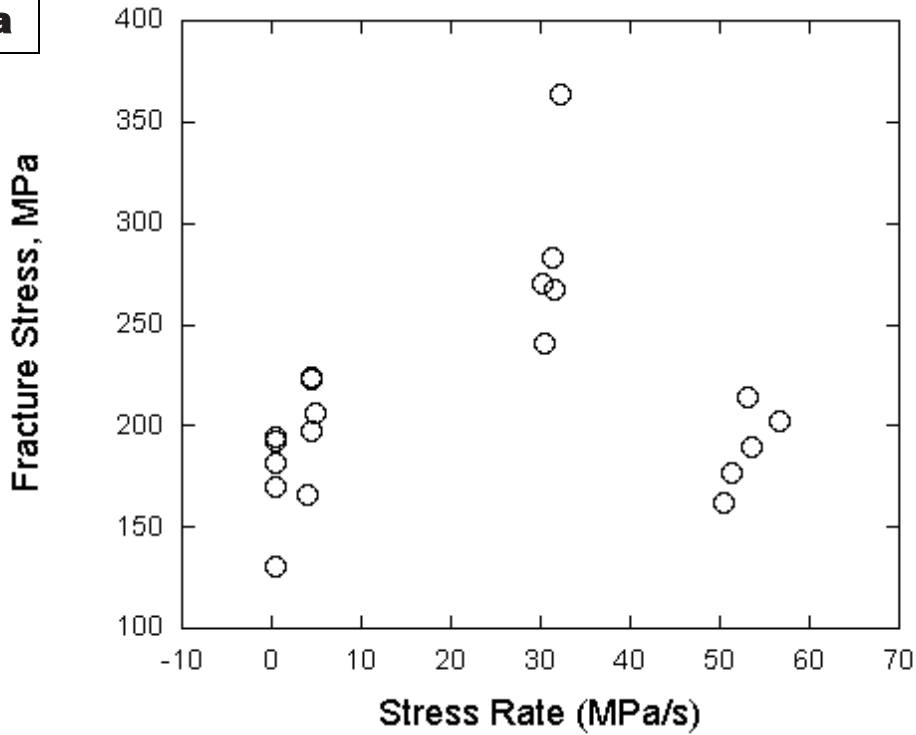
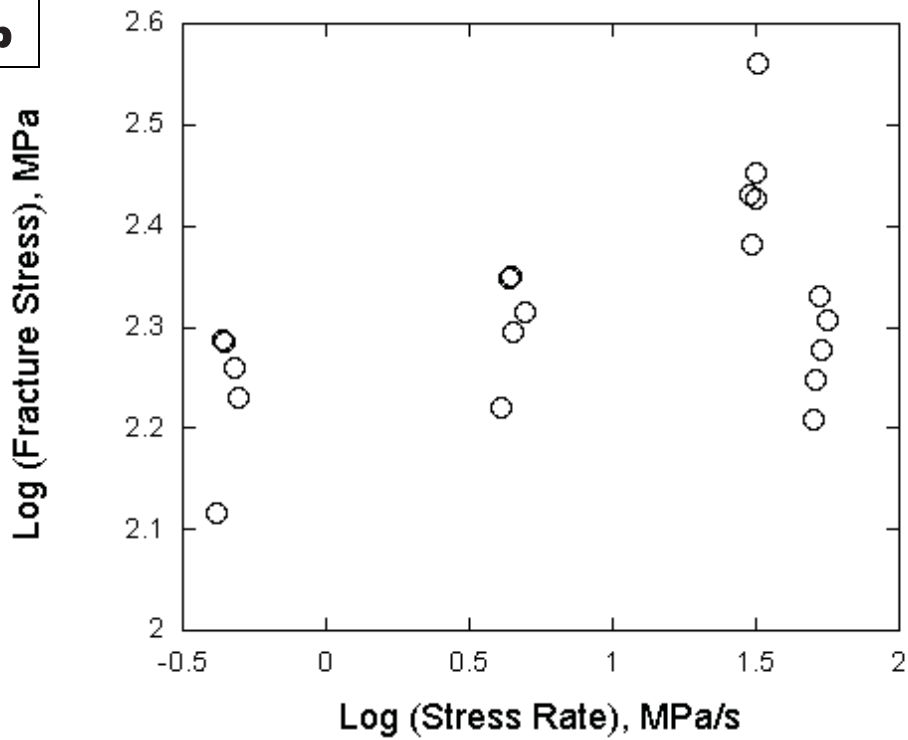
a**b**

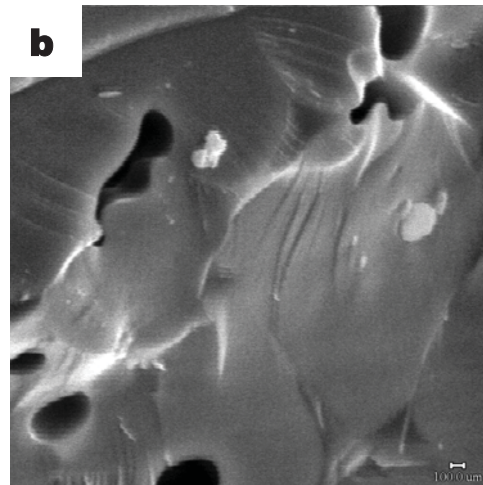
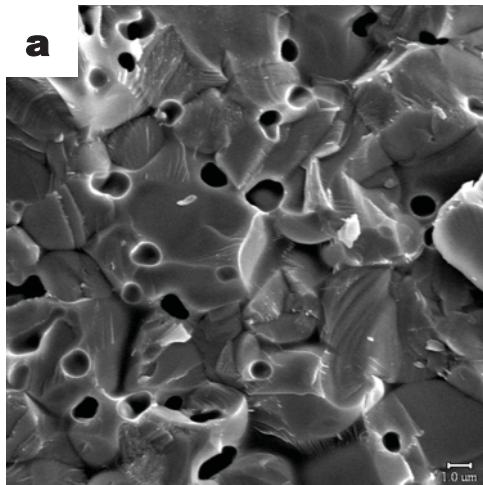
Fig. 5

C-ring Fracture Strength-Stress Rate Diagram. a) Plot of strength vs. stress rate and b) Log (Fracture Strength) versus Log (Stress Rate)

Fracture analysis:

The tested samples were sputtered with gold and observed in a SEM for study of fracture. Fracture was observed to be dominated from flaws originating from the surface. Although, volume pores were observed in the fractured surfaces, their contribution to the fracture processes was not significant.

Fracture in the YSZ material was by brittle trans-granular mode. The grains indicated presence of micro-cleavage planes. Micro-cleavage planes were significantly higher in specimens fracture at lower stress rates (Fig 2 a and b) indicating sub critical crack growth in the grains. At a stress rates of 30 MPa/s (Fig 2 c and d), the specimens indicated less roughness and reduced cleavage planes. Specimen fractured at higher stress rates are to analysed to study the reason for drop in strength.



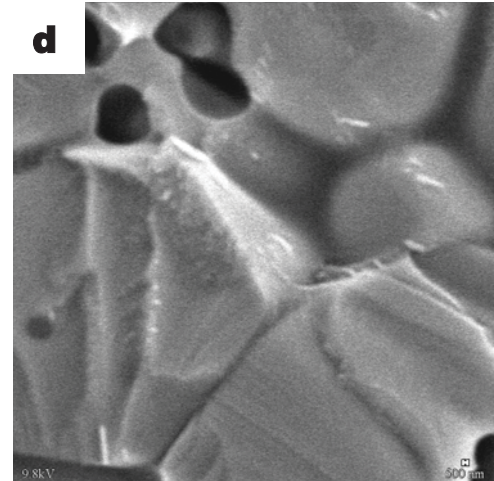
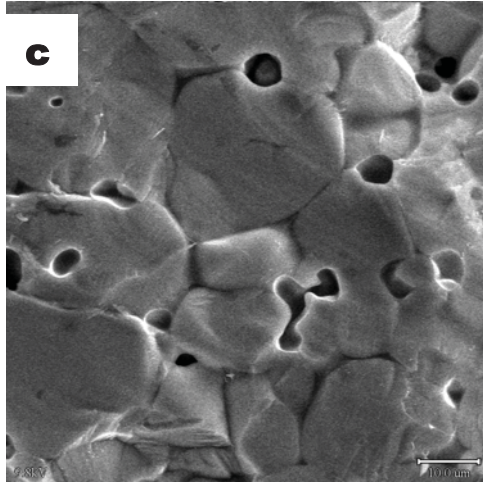


Fig. 6 Fracture surfaces examined under SEM indicating transgranular fracture. At low stress rates (a and b), higher incidence of micro-cleavage in grains is visible. At higher stress rates (50MPa/s), grains are relatively smoother with reduced micro-cleavage planes.

Slow Crack Growth Analysis

The ASTM test method C-1368, specifically deals with characterising ceramic materials with susceptibility to slow crack growth (SCG). SCG may be a product of both mechanical and chemical driving process. The present report is on the room temperature behaviour and the only consideration is the mechanical driving force. Latter studies will concentrate on the chemical driving forces (gas atmosphere and temperature).

The SCG parameters n and D can be determined by a linear regression analysis using log strength values over the complete range of individual log stress rates, based on the following equation.

$$\log \sigma_f = \frac{1}{n+1} \log \dot{\sigma} + \log D \quad 5$$

The slope of the linear regression line can be calculated as:

$$\alpha = \frac{K \sum_{j=1}^K \left(\log \dot{\sigma}_j \log \sigma_j \right) - \left(\sum_{j=1}^K \log \dot{\sigma}_j \sum_{j=1}^K \log \sigma_j \right)}{K \sum_{j=1}^K \left(\log \dot{\sigma}_j \right)^2 - \left(\sum_{j=1}^K \log \dot{\sigma}_j \right)^2} \quad 6$$

Where α = slope, K is the total number of specimens tested (=20), $\dot{\sigma}_j$ and σ_j is the stress rate and fracture strength of the individual test specimen respectively.

The SCG parameter n is calculated as

$$n = (1/\alpha) - 1 \quad 7$$

The intercept of the linear regression line is calculated as

$$\beta = \frac{\left(\sum_{j=1}^K \log \sigma_j \right) \sum_{j=1}^K \left(\log \dot{\sigma}_j \right)^2 - \left(\sum_{j=1}^K \log \dot{\sigma}_j \log \sigma_j \right) \left(\sum_{j=1}^K \log \dot{\sigma}_j \right)}{K \sum_{j=1}^K \left(\log \dot{\sigma}_j \right)^2 - \left(\sum_{j=1}^K \log \dot{\sigma}_j \right)^2} \quad 8$$

Where β is the intercept and the SCG parameter D is calculated as $D = 10^\beta$

From the above calculations, the SCG parameter for the YSZ tubes at room temperature under constant humidity was calculated as $n = 16.6$ and $D = 184.74$. Fitting these values in equation 2, it is possible to calculate the strength values at various loading rates, typically of static fatigue conditions.

The values of $n = 16.6$ implies a low susceptibility to SCG at room temperature. Typically, if a ceramic materials exhibits a high susceptibility the values of n would be lesser than 5.

Elevated Temperature studies:

AIR

Results of the strength tests at elevated temperature are reported in Table 1. As shown below, the strength of the YSZ tubes degraded significantly upon exposure to test condition of 1000°C in air. A maximum of 134 MPa corresponded to 37% of the strength observed at room temperature.

Table 2: Strength values of YSZ tube at 1000°C in air.

Test Condition	Air, RT	Air, 1000°C
No of Samples	11	11
Minimum Strength	97 MPa	73.4 MPa
Maximum Strength	363.4	134.3 MPa
Mean Strength	231.3	95.4 MPa

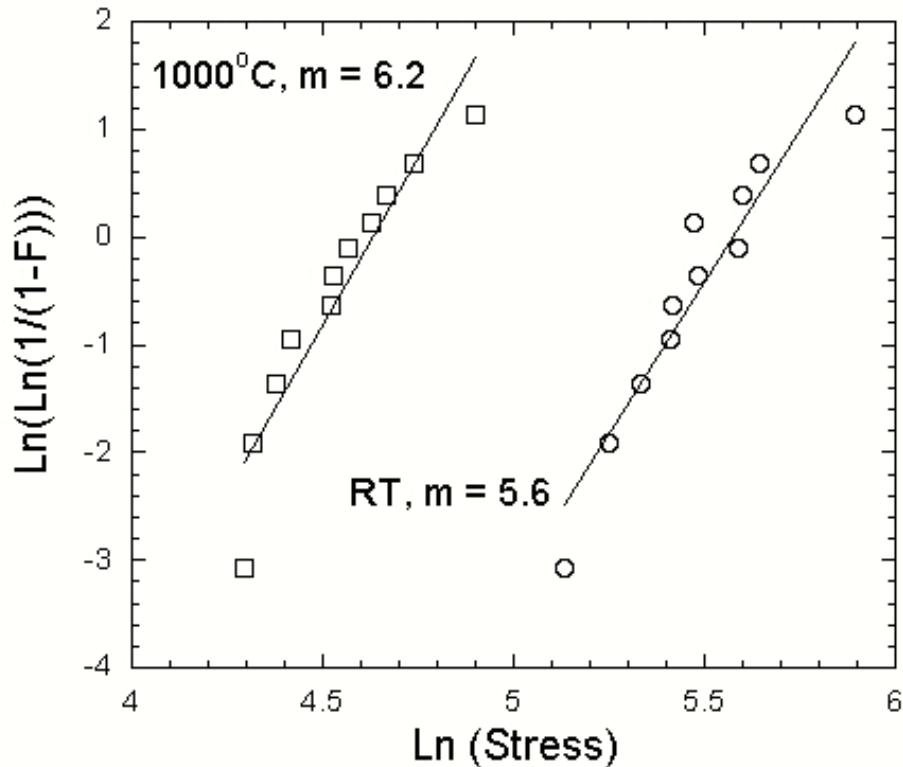


Fig. 7: Weibull plots of C-ring fracture strength at room temperature and at 1000°C in air.

The strength values plotted as Weibull distribution was similar to data of that of room temperature. However, a slight increase in Weibull modulus, m , from 5.6 to 6.2. Although, the change is not significant, there are possibilities of change in flaw distribution upon exposure to elevated temperature. Macroscopic observation indicated roughening of outer and fracture surfaces of the YSZ tubes. Microscopic and SEM studies should reveal more information on the strength controlling flaws and their influence on measured strength.

CONCLUSIONS

Yttria stabilized Zirconia with 9.6% mol composition of Yttria exhibited reasonable strength but with low Weibull Modulus 'm'. In air at 1000°C, the strength of the YSZ component was reduced to less 50%. However the Weibull modulus of the YSZ remains relatively unchanged. The SCG parameter for the YSZ tubes at room temperature under constant humidity was calculated as $n = 16.6$ and $D = 184.74$ and implied a low susceptibility to SCG at room temperature. SEM analysis of failed C-rings indicated flaws originating from the surface and crack progressing transgranularly as the primary mode of fracture as. At low stress rates higher incidence of micro-cleavage in grains is visible as compared to grains failing at higher stress rates (50MPa/s). The higher incidences of micro-cleavage planes are due to the slow crack growth in the YSZ specimens.

Low-Rank Coal Grinding Performance Versus Power Plant Performance

Final Report

10/01/2002–9/30/2008

Rajive Ganguli, PhD, PE
Associate Professor of Mining Engineering

Sukumar Bandopadhyay, PhD, PE
Professor of Mining Engineering

September 2008

DE-FC26-01NT41248
FY02 Task 1.6

Institute of Northern Engineering
University of Alaska Fairbanks
PO Box 755910
Fairbanks, Alaska 99775-5910

Disclaimer

This report was prepared as an account of work sponsored by an agency of the United States Government. Neither the United States Government nor any agency thereof, nor any of their employees, makes any warranty, express or implied, or assumes any legal liability or responsibility for the accuracy, completeness, or usefulness of any information, apparatus, product, or process disclosed, or represents that its use would not infringe privately owned rights. Reference herein to any specific commercial product, process, or service by trade name, trademark, manufacturer, or otherwise does not necessarily constitute or imply its endorsement, recommendation, or favoring by the United States Government or any agency thereof. The views and opinions of authors expressed herein do not necessarily state or reflect those of the United States Government or any agency thereof.

Abstract

The intent of this project was to demonstrate that Alaskan low-rank coal, which is high in volatile content, need not be ground as fine as bituminous coal (typically low in volatile content) for optimum combustion in power plants. The grind or particle size distribution (PSD), which is quantified by percentage of pulverized coal passing 74 microns (200 mesh), affects the pulverizer throughput in power plants. The finer the grind, the lower the throughput. For a power plant to maintain combustion levels, throughput needs to be high. The problem of particle size is compounded for Alaskan coal since it has a low Hardgrove grindability index (HGI); that is, it is difficult to grind. If the thesis of this project is demonstrated, then Alaskan coal need not be ground to the industry standard, thereby alleviating somewhat the low HGI issue (and, hopefully, furthering the salability of Alaskan coal).

This project studied the relationship between PSD and power plant efficiency, emissions, and mill power consumption for low-rank high-volatile-content Alaskan coal. The emissions studied were CO, CO₂, NO_x, SO₂, and Hg (only two tests). The tested PSD range was 42 to 81 percent passing 76 microns. Within the tested range, there was very little correlation between PSD and power plant efficiency, CO, NO_x, and SO₂. Hg emissions were very low and, therefore, did not allow comparison between grind sizes. Mill power consumption was lower for coarser grinds.

Table of Contents

Acknowledgments.....	2
2. Experimental.....	5
2.1 The Power Plant.....	5
2.1.1 Pulverizers.....	5
2.2 Overview of Tests.....	5
2.3 Sampling.....	8
2.3.1 Raw Coal Sampling.....	8
2.3.2 Pulverized Coal Sampling.....	9
2.3.3 Bottom Ash Sampling.....	15
2.3.4 Fly Ash Sampling.....	16
2.4 Reduction in the Number of Pulverized Coal Samples.....	17
3. Results and Discussion.....	19
3.1 Data from Tests.....	19
3.1.1 Feed (Raw) Coal.....	19
3.1.2 Pulverized Coal.....	20
3.1.3 Fly Ash Data.....	22
3.1.4 Bottom Ash Data.....	23
3.1.5 Emissions Data.....	24
3.1.6 Operational Data.....	25
3.2 Analysis.....	26
3.2.1 PSD Versus Power Plant Efficiency.....	26
3.2.2 PSD76 Versus SO ₂ , NO _x , CO, and CO ₂ Emissions.....	31
3.2.3 PSD76 Versus Hg.....	34
3.2.4 PSD76 Versus Mill Power Consumption.....	34
3.2.5 Other Relationships.....	37
3.2.5.1 Effect of Lower Weight Sample.....	37
3.2.5.2 PSD in Different Pipes.....	44
4. Conclusions and Recommendations.....	47
4.1 Conclusions.....	47
4.2 Conclusions: Implications.....	48
4.3 Recommendations.....	49
References.....	50
List of Acronyms and Abbreviations.....	51
Appendix I: Rosin-Rammler Plots.....	52

Acknowledgments

The authors would like to acknowledge the contribution of Mr. David Hoffman, Plant Superintendent of Golden Valley Electric Association's Healy Unit#1, and his staff. They were always willing to help us meet the objectives of the project. Thanks are also due to Dr. Terril Wilson, who helped start this project. Many students played a big role in the project. These include Mr. Dinesh Malav, Dr. Sridhar Dutta, Mr. Abhishek Choudhury and Ms. Rupali Panda.

The financial support from the United States Department of Energy, that made this project feasible, is gratefully acknowledged.

1. Executive Summary

The intent of this project was to demonstrate that Alaskan low-rank coal, which is high in volatile content, need not be ground as fine as bituminous coal (typically low in volatile content) for optimum combustion in power plants. The grind or particle size distribution (PSD) affects the pulverizer throughput in power plants. The finer the grind, the lower the throughput. For a power plant to maintain combustion levels, throughput needs to be high. The problem of particle size is compounded for Alaskan coal since it has a low Hardgrove grindability index (HGI); that is, it is difficult to grind. If the thesis of this project is validated, then Alaskan coal need not be ground to the industry standard, thereby alleviating somewhat the low HGI issue (and, hopefully, furthering the salability of Alaskan coal).

A total of 26 field tests were conducted at the Golden Valley Electric Association's (GVEA) Healy Unit #1 to study the relationship between the PSD of pulverized coal being burnt at a power plant and its impact on power plant performance. The PSD was quantified, as is commonly done in the power industry, as the percentage passing 76 microns (PSD76). Performance was measured through power plant efficiency (ratio of megawatt [MW] generated to MW burned as coal), mill power consumption, emissions (SO_2 , NO_x , CO, and CO_2) as measured by a continuous emissions monitoring system (CEMS), carbon content in fly ash and bottom ash, and Hg emissions in the stack. Other data collected included proximate analysis of raw coal, HGI of raw coal, and proximate analysis of pulverized coal. Operational data collected included mill amps, coal flow rate, air flow rate, and oxygen.

The project reached the following conclusions about low-rank high volatile Alaskan coal:

- For PSD in the tested range (40–80), there is very little correlation between the PSD of pulverized coal and power plant efficiency.
- There is very little correlation between PSD and SO_2 , NO_x , and CO.
- The data displayed a correlation between PSD and CO_2 , with finer grinds resulting in higher concentration of CO_2 . However, this correlation has been difficult to explain. It could be a new revelation or an artifact of measurement errors.
- Mill power consumption is greater when coal is ground more. Additionally, the HGI and coal flow rate impact mill power consumption. Harder coal was found to consume more power than softer coal, and power consumption went up as the coal flow rate increased.
 - If coal were to be burned at a PSD of 50 instead of 70, the 28 MW Healy Unit #1 would see a savings of over \$56,000 per year.
- Total Hg emissions are very low.

When the tests are split into two groups, one that averaged 50% passing 76 microns (the “coarse” group) and the other that averaged 73% passing 76 microns (the “fine” group), the following is observed:

- The coal burned in the fine group had more moisture (17.4%) and less heating value (18,774 kJ/kg or 8078 BTU) compared to the coarse group (15.2% and 19,337 kJ/kg or 8320 BTU). On a HGI basis, the coal was harder in the coarse group (HGI=34) than in the fine group (HGI=37.8). The fixed carbon content was higher in the coarse group (32.3%) than in the fine group (29.5%). There was no difference in the ash and volatile contents.
- The coarse group had higher unburned carbon in fly and bottom ash. However, this could be explained by its higher fixed carbon content.
- The fine group had an efficiency of 23.75% compared to 23.05% for the coarse group. Given that the fine group only had six data points, the observed difference could be due to the very low number of tests in the fine group or due to differences in the coal type.
- The coarse group had lower SO₂ emissions, though the two groups had similar sulfur contents.
- Observations not central to the project, but interesting nonetheless, included the following:
 - Pulverized coal samples that were underweight had PSDs similar to recommended weight samples.
 - PSD sometimes varied between pipes. The coal in pipe A1 was generally coarser than the coal in pipe A2.

2. Experimental

2.1 The Power Plant

A total of 26 field tests were conducted at Golden Valley Electric Association's 28 MW Healy Unit #1 power plant. The power plant, located on the banks of the Nenana River, is adjacent to the Usibelli Coal Mine (UCM). The mine provides low-rank high volatile coal to its customers, including GVEA.

The power plant (Figure 2.1a shows the system) has been described in detail in Malav (2005). It has two pulverizers (or mills), A and B, which feed the combustion chamber through four pipes: A1, A2 and B1, B2.

2.1.1 Pulverizers

Unit #1 has two Foster-Wheeler MBF-19.5 pulverizers, each with a capacity of approximately 10,800 kg (24,000 lb) per hour. These medium-speed pulverizers (Figure 2.1b) are air swept and have fixed rollers and vertical spindles. The plant is designed for a particle size of 65% passing 76 microns. The raw coal to the pulverizers is designed to be -32 mm (-1¼ in.) in size. The primary air, which comes to the pulverizers from the wind box, carries the pulverized coal to the classifiers. Particles that are finer than the desired size proceed through the classifiers to the combustion chamber, while the coarser particles continue to be retained in the pulverizer.

2.2 Overview of Tests

The basic goal of the project was to conduct the different tests at different PSDs (within operational limits) to examine how plant efficiency (ratio of MW, or MW generated to MW fed as coal) and emissions varied with PSD. However, since there is no direct way to "set" the PSD at a plant, tests were conducted by varying the primary air flow and classifier openings to achieve a target PSD. These two parameters affect the PSD of grind the most. The primary air flow through the pulverizer ensures that the coal remains in suspension. If the primary air flow is increased (without increasing the coal feed), coal does not reside in the pulverizer as long as before, resulting in coarser particles exiting the pulverizer. Similarly, the PSD is coarser when the classifiers are more open. The classifiers are simply vanes that direct the primary air to the outlet of the mill.

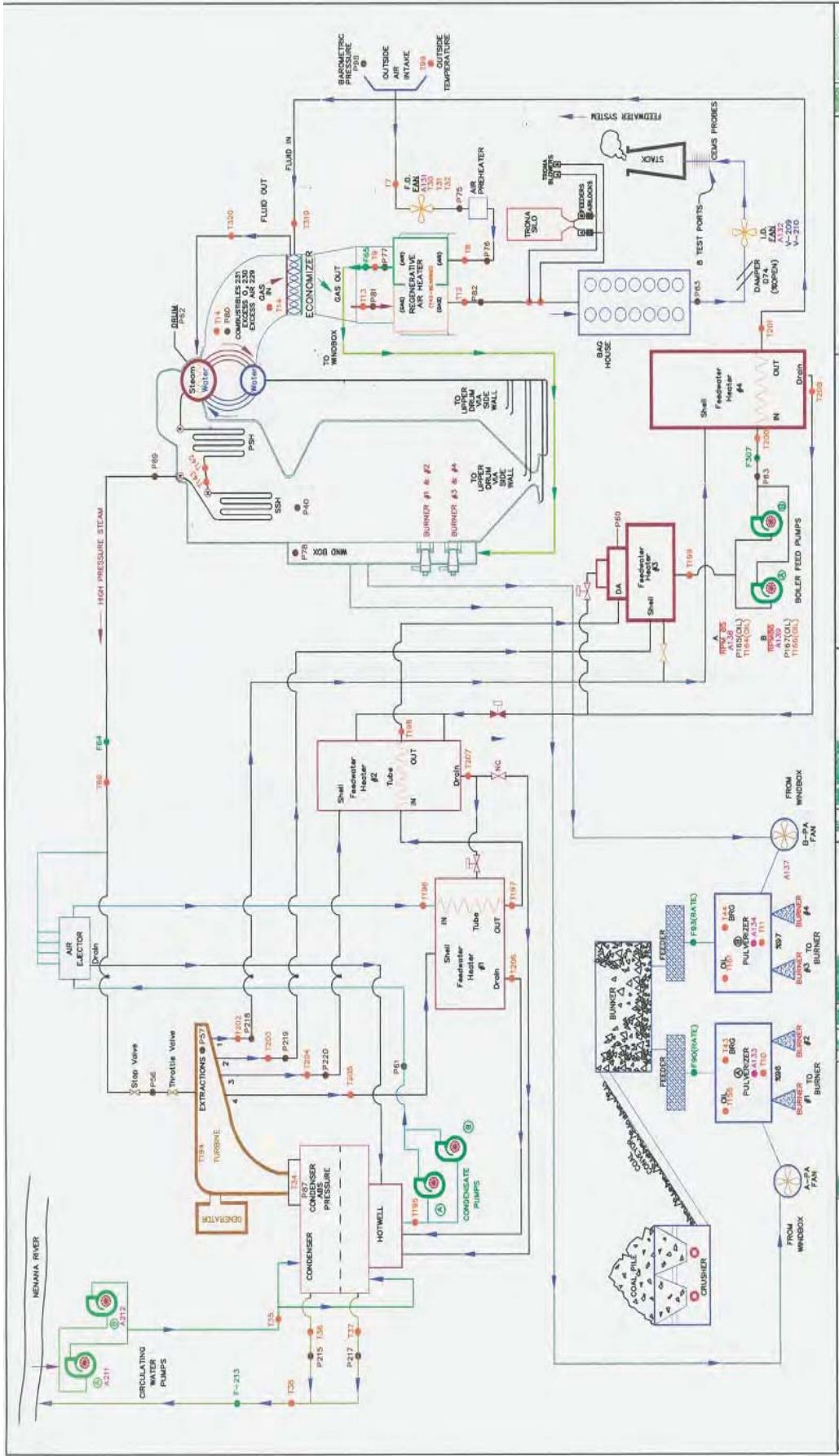


Figure 2.1.a. System layout of GVEA Healy Unit #1.

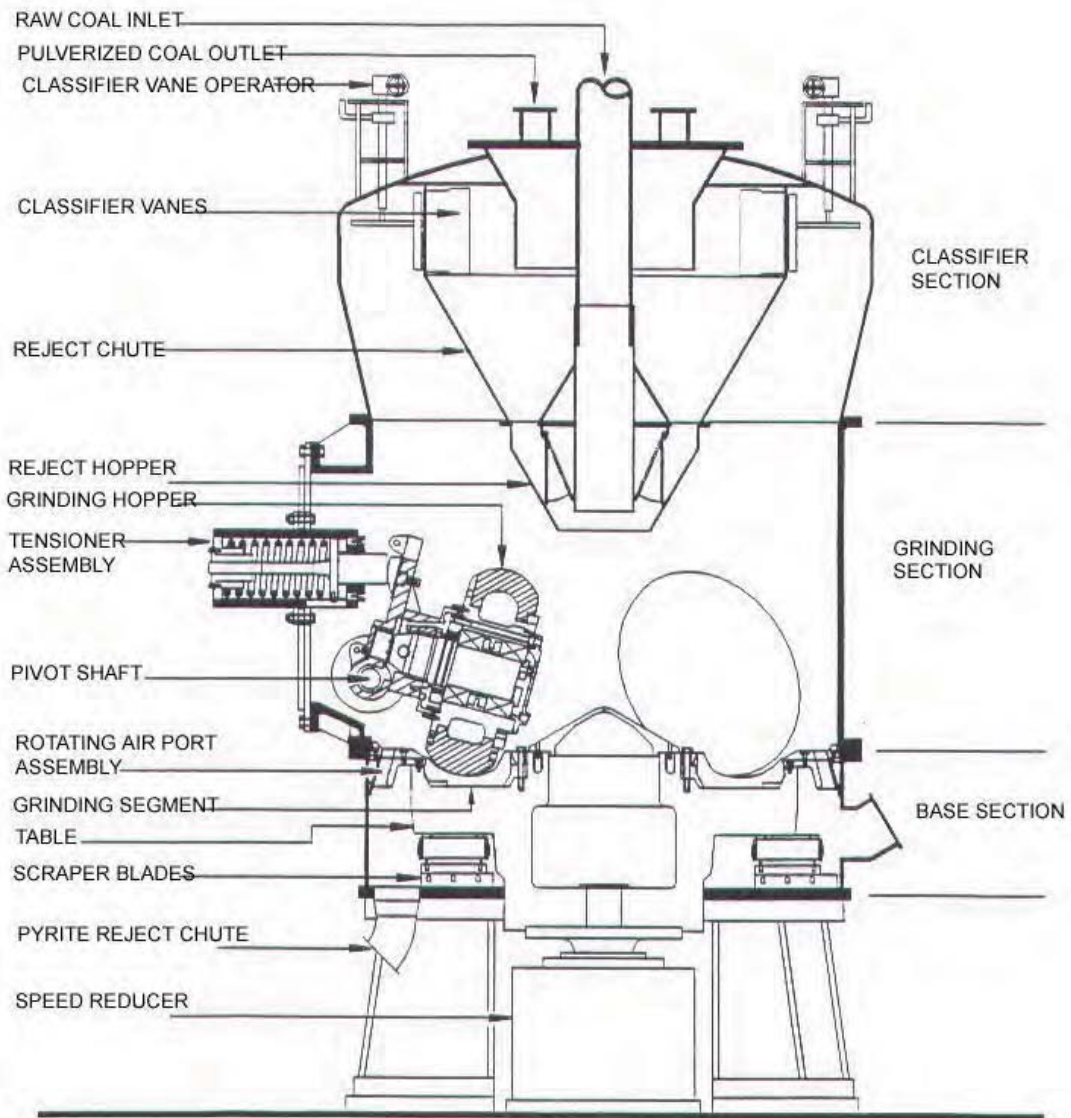


Figure 2.1b. The pulverizers (courtesy of GVEA).

Given that the PSD was never known at the time of testing (it was only known weeks after the test when the results returned from the lab), lab results often revealed that target PSD76 was not achieved for a given test. However, given the number of tests done, the required spectrum of PSD76 (from really coarse grind to really fine grind) was achieved.

Test duration was usually in the two- to three-hour range. It depended on the duration for which the power plant could maintain experiment conditions. Factors such as load response or classifier settings could affect the power plant’s ability to maintain stable experiment conditions.

The samples collected (and analysis done on them) during the tests are listed in Table 2.1.

Table 2.1. Samples collected during tests

Sample collected	Analysis done on samples
Raw coal feed	HGI
	Proximate analysis
Pulverized coal	PSD
	Proximate analysis
Bottom ash	Unburned carbon
Fly ash	Unburned carbon
Stack gas*	Hg

* Done only in two tests

The samples shown in Table 2.1 were sent to commercial labs (SGS or Intertek) for analysis. In addition, the automated continuous emissions monitoring system (CEMS) was used to obtain data on various emissions such as CO, CO₂, NO_x, and SO_x, and operational data such as mill amps, oxygen, coal flow rate, and primary air flow rate.

2.3 Sampling

2.3.1 Raw Coal Sampling

Raw coal samples were collected from a sampling port located just above the pulverizers. Each mill, A and B, had a port for collecting raw coal samples. During a test, two samples, each approximately 9.5 L (2.5 gal) in volume were collected from each port. The diameter of the sampling port was 38 mm (1.5 in.). The two samples from the same port were combined, ultimately resulting in just two raw coal samples per test. Figure 2.2 shows Dr. Terril Wilson and Mr. Abhishek Chowdhury (both with UAF) collecting the feed samples.



Figure 2.2. Raw (feed) coal sampling.

2.3.2 Pulverized Coal Sampling

Sampling of pulverized coal was by far the most challenging aspect of the project. ASTM standard D-197 was used as a guideline for this part for the first 22 tests, with the more stringent ISO 9931 standards used for the last 4 tests. See the next section for details on the number of pulverized coal samples that were taken during each test.

Figure 2.3 shows the layout of the plant relevant to pulverized coal sampling. Two pipes from each mill carry air-pulverized coal mixture to the combustion chamber. Each of these four pipes, A1, A2, B1, and B2, have sampling ports, with each pipe having two perpendicular ports.

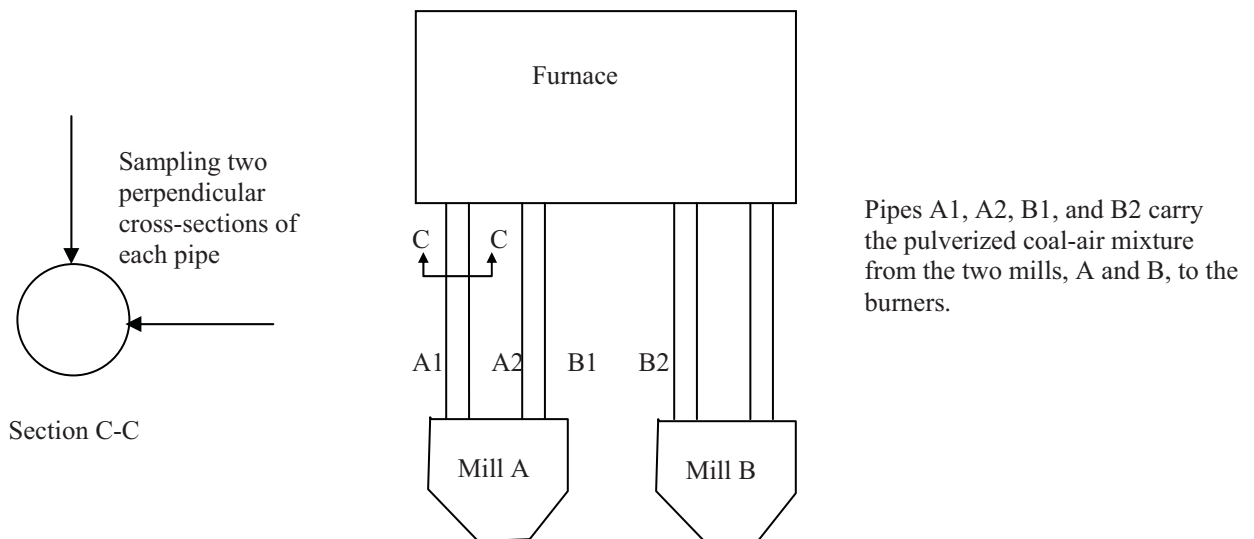


Figure 2.3. Schematic showing pulverized coal sampling (Malav et al., 2008).

ASTM D-197 Sampling Procedure

The ASTM D-197 sampling procedure is described in detail in ASTM manuals. For the sake of the reader, however, it is described briefly here.

The process requires two sampling ports (in the pipe being sampled) that are perpendicular to each other, with the intent being to sample the pipe in two perpendicular directions (Figure 2.4). The sampling device consists of a probe connected to a cyclone collector (Figure 2.5). It connects to the port through a dustless connection.



Figure 2.4. The perpendicular sampling ports.

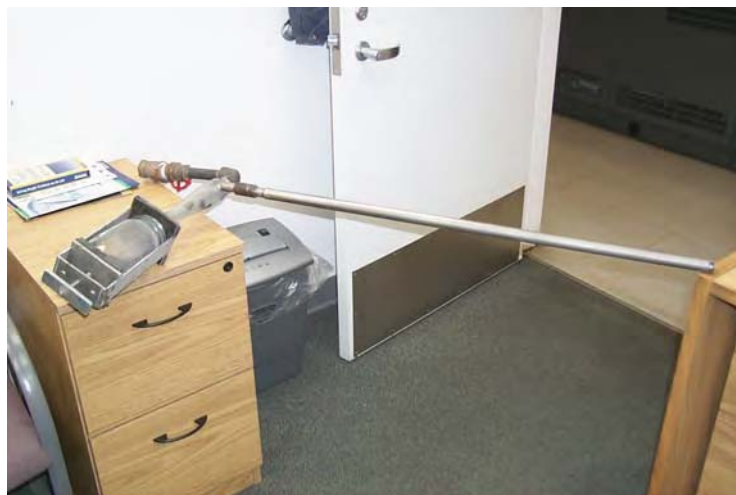


Figure 2.5. The sampling probe connected to the cyclone collector.

The procedure calls for isokinetic sampling of the air-coal mixture flowing through the pipe. The probe, which contained a sampling aperture of 197 sq. mm (0.305 sq. in.) near its tip, is inserted into the port. Over a period of 1 minute, it is slowly withdrawn from the pipe. During the withdrawal, the probe is stopped at 12 locations for about 5 seconds so that equal areas are sampled each time. This process is illustrated in Figure 2.6.

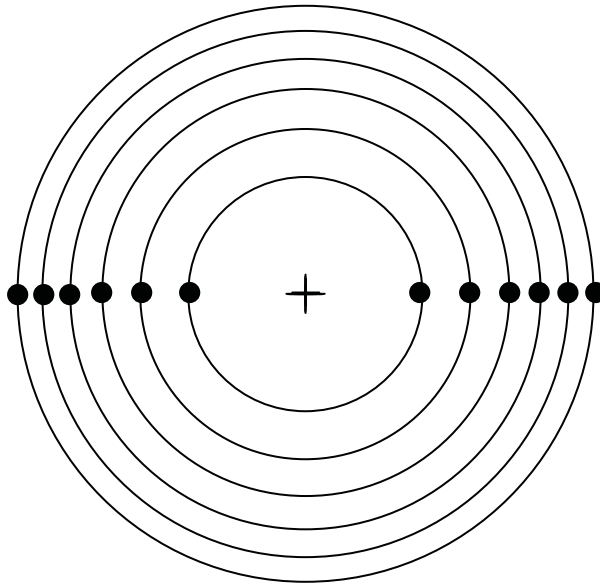


Figure 2.6. Equal area method of sampling. Each sampling “stop” shown by a dark circle.

The process is repeated at the other (perpendicular) port as well, resulting in a total sampling duration of two minutes per pipe. Due to limitations in the equipment, the sampling was not isokinetic. However, sample validity was verified using the Rosin-Rammler plot (as directed by the ASTM method).

Figure 2.7 shows the probe being set up for sampling.



Figure 2.7. From left to right, Srdhar Dutta, Dinesh Malav, and Rajive Ganguli (all with UAF) setting up the probe.

ISO 9931 Sampling Procedure

During the course of this investigation, the sampling probe for the ASTM method got damaged. Therefore, GE Energy, which uses the ISO 9931 isokinetic sampling procedure, was hired to obtain the pulverized coal samples. This process is described in detail in ISO's official manual¹. However, it is described here briefly for the benefit of the reader.

The method uses the Rotorprobe™, a GE Energy device certified for this method. The device (Figure 2.8) is similar to the ASTM method probe (shown in Figure 2.5), but with a major difference. The Rotorprobe has two sampling tips (each with two sampling apertures for a total of four apertures) that rotate on a vertical axis at the end of the probe. During sampling, the tips are rotated, resulting in the collection of samples from all around the pipe and not just from two perpendicular diameters.

¹ www.iso.org

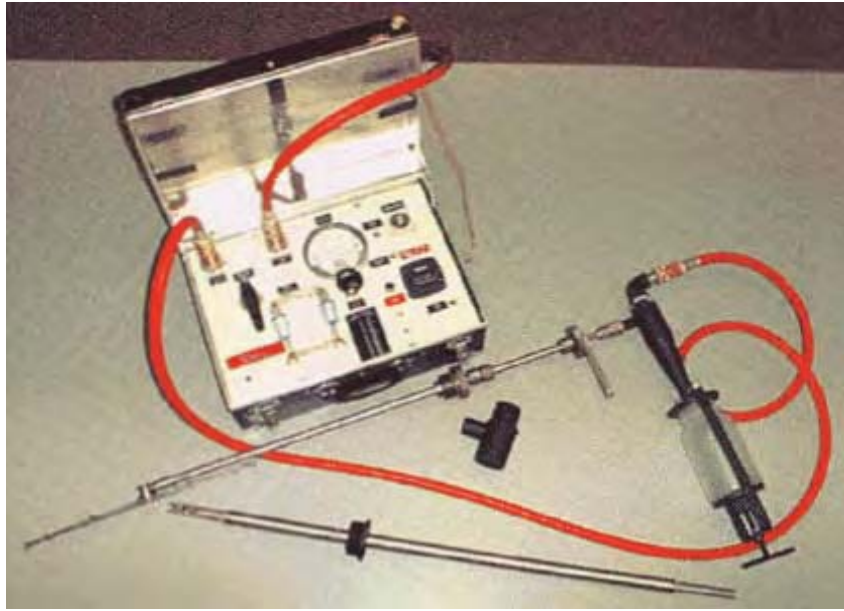


Figure 2.8. GE Rotorprobe and control box.

Figures 2.9 and 2.10 show sampling using the Rotorprobe procedure. A four-minute sample is collected from each pipe, during which time the tips are rotated twice (720°). During this rotation, however, the tips are paused for 15 seconds at 8 sampling points (similar to what is done in the previous method).



Figure 2.9. Dale Wilson, GE Energy, using the Rotorprobe.



Figure 2.10. Frank Coen (GE Energy) and Rupali Panda (UAF) operating the Rotorprobe control box.

Quantification of PSD

All pulverized coal samples were analyzed for PSD as percent passing 1180 microns, 600 microns, 300 microns, 150 microns, 76 microns, and 38 microns (16 mesh, 28 mesh, 48 mesh, 100 mesh, 200 mesh, and 400 mesh). This analysis was necessary for the Rosin-Rammler plots. However, in the power plant industry, it is common to quantify the PSD of grind as percent passing 76 microns (200 mesh). Therefore, the same nomenclature is used throughout the report. The “PSD76” of a test implies the percentage of samples that are smaller than 76 microns, while “PSD” implies the entire particle size distribution.

2.3.3 Bottom Ash Sampling

Prior to the start of each test, the bottom ash was flushed out of the combustion chamber by flooding the bottom with water. At the conclusion of the test, the process was repeated, though modified slightly, so that a sample could be collected during the flushing. There was no other way to sample the bottom ash. This was a tedious process and somewhat hazardous. If not done carefully, hot embers flew out of the chamber when the access door was opened. GVEA staff was required to help take the samples. Figure 2.11 shows the bottom ash sample being scooped up against the flaming red combustion chamber in the background. The wet sample was always air dried before being sent to the lab.



Figure 2.11. Dr. Terril Wilson (UAF) scoops up the bottom ash sample.

2.3.4 Fly Ash Sampling

GVEA Healy Unit #1 has a total of 12 fabric filters (bag houses), arranged in 2 columns, A and B, of 6 each. Figure 2.12 shows this arrangement.



Figure 2.12. The arrangement of fabric filters on either side of the aisle. Rupali Panda and Abhishek Choudhury are seen at a distance handling the samples.

The fabric filters were emptied prior to each test. Every fabric filter had a sampling port and required a probe to obtain the samples. Samples from the same two rows in each column were pooled to obtain a composite sample. Therefore, each test resulted in three fly ash samples. Figure 2.13 shows a fly ash sample being taken.



Figure 2.13. Abhishek Choudhury collecting a fly ash sample.

2.4 Reduction in the Number of Pulverized Coal Samples

When the project was started, it was decided to take as many pulverized coal samples as possible during a three-hour test. However, given how expensive the analysis was, the team decided to examine if indeed that many samples were needed.

Initially, the team took six cycles of pulverized coal samples in three hours. A cycle is described as samples from all four pipes. Thus, a test typically yielded 24 samples. To examine the possibility of reduction in the number of samples, the obtained PSD76 values from Test 1 were used in a statistical simulation, where “n” samples (out of 23 for Test 1) were randomly selected. Selection was such that a value was picked from every pipe (A1, A2, B1, and B2); that is, the selection was in complete cycles. Using the *t*-test, the selected group was compared to the entire sample group (size 23). This experiment was repeated 500 times for each “n.” The selected group was identical to the entire group over 95% of the time according to the *t*-test for all $n \geq 4$. Similar results were produced for Test 2 (24 samples total).

Thus, the simulation from the first two tests showed that four samples were sufficient to estimate the average PSD76 during the test. Also, according to the same simulation, there was no improvement in the standard deviation of the means after 12 samples per test. Therefore, it was decided that there was no need to take more than 12 samples per test.

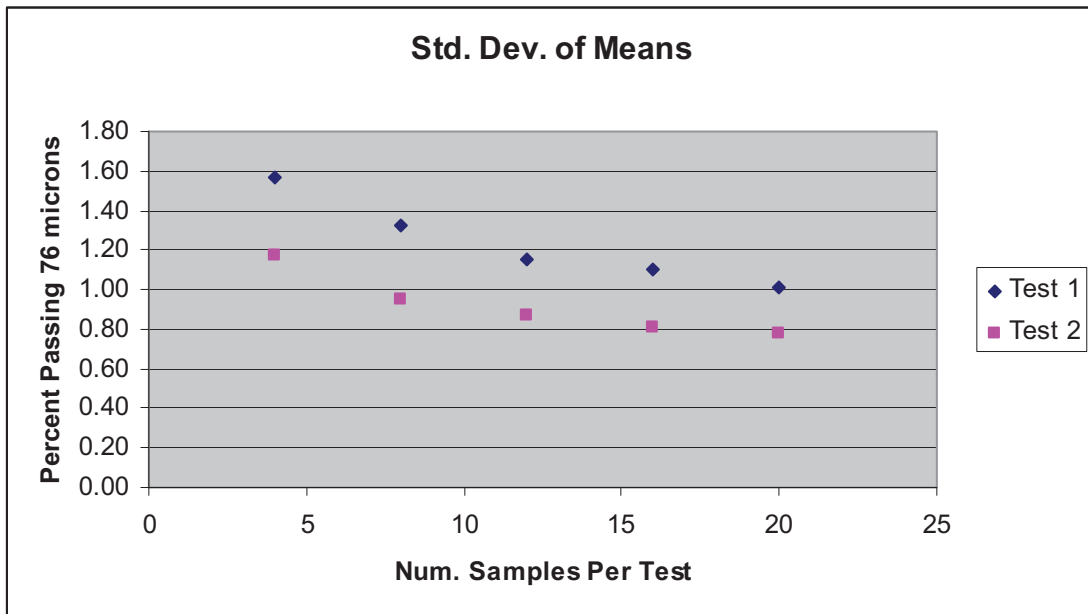


Figure 2.14. Lack of significant improvement of the standard deviation of means after 10–12 samples.

3. Results and Discussion

The data are first presented followed by analysis. Tests 1 and 2 were part of the initial seed grant project and, therefore, did not include coal quality analysis. The only sample analysis that was done in Tests 1 and 2 was PSD of pulverized coal.

3.1 Data from Tests

3.1.1 Feed (Raw) Coal

The data from raw coal that was fed into the pulverizers are shown in Table 3.1. The main goal of the raw coal analysis was determining the HGI. Other analyses (proximate) were done based on budget outlook. Note that proximate analysis was always done on pulverized coal.

Table 3.1. Raw coal quality data

	Ash	Moisture	Volatile	Sulfur	Fixed Carbon	kJ/kg (BTU/lb)	HGI
Test 3	11.7	27.2	34.3	0.21	26.9	16,907 (7275)	34
Test 4	10.2	28.7	34.3	0.19	26.8	16,865 (7257)	31
Test 5	11.9	25.2	35.2	0.22	27.7	17,309 (7448)	31
Test 6							32
Test 7							33
Test 8							31
Test 9	12.7	27.5	31.2	0.20	28.3	16,331 (7027)	37
Test 10	12.2	27.4	31.7	0.19	28.7	16,479 (7091)	34
Test 11	11.8	27.5	32.2	0.19	28.5	16,633 (7157)	36
Test 12	12.3	27.5	32.0	0.21	28.2	16,461 (7083)	36
Test 13	13.5	27.5	31.3	0.21	27.8	16,349 (7035)	36
Test 14	12.3	27.0	31.6	0.22	29.2	16,747 (7206)	34
Test 15	11.4	27.3	32.4	0.22	28.9	16,954 (7295)	32
Test 16	12.7	27.1	32.3	0.21	28.0	16,540 (7117)	33
Test 17	14.0	27.2	31.7	0.19	27.1		35
Test 18	13.9	27.2	32.3	0.19	26.7		35
Test 19	13.6	26.6	32.3	0.20	27.5		36
Test 20	12.3	26.1	33.1	0.18	28.5		36
Test 21	14.1	28.2	30.8	0.20	27.0		40
Test 22	12.8	28.3	31.2	0.20	27.7		40
Test 23	13.8	29.3	32.5	0.21	24.5		39
Test 24	13.3	31.3	31.8	0.20	23.6		37
Test 25	11.4	37.2	29.5	0.18	21.8		35
Test 26	13.4	29.0	33.2	0.20	24.4		36

NOTE: All values are as received (unless otherwise mentioned).

3.1.2 Pulverized Coal

The pulverized coal was sampled for proximate analysis and PSD analysis.

Table 3.2. Quality analysis of pulverized coal

	Ash	Moisture	Volatile	kJ/kg (BTU/lb)	Fixed Carbon	Sulfur
Test 1	15.8	14.1	38.7	19,094 (8216)	31.4	
Test 2	14.1	12.9	39.2	20,026 (8617)	33.9	
Test 3	13.8	15.6	40.0	19,329 (8317)	30.5	0.26
Test 4	12.9	16.7	40.0	19,324 (8315)	30.4	0.24
Test 5	13.0	16.0	40.4	19,552 (8413)	30.7	0.25
Test 6	11.1	19.9	37.6	18,838 (8106)	31.4	0.23
Test 7	11.6	18.4	37.7	19,096 (8217)	32.7	0.24
Test 8	10.3	18.5	37.9	19,296 (8303)	33.3	0.23
Test 9	13.6	17.5	36.3	18,564 (7988)	32.6	0.24
Test 10	14.3	13.3	38.8	19,640 (8451)	33.9	0.24
Test 11	14.1	13.1	38.0	19,856 (8544)	34.9	0.24
Test 12	14.2	12.5	38.2	20,038 (8622)	35.2	0.24
Test 13	15.5	15.5	36.7	18,941 (8150)	32.3	0.25
Test 14	14.9	15.3	37.4	19,236 (8277)	32.5	0.27
Test 15	14.5	15.0	37.6	19,310 (8309)	32.9	0.26
Test 16	16.1	15.2	37.0	18,766 (8075)	31.7	0.24
Test 17	15.6	15.1	39.9	19,868 (8162)	29.4	
Test 18	16.2	13.4	39.0	19,154 (8242)	31.4	
Test 19	15.6	12.9	39.3	19,459 (8373)	32.2	
Test 20	15.8	13.1	38.9	19,347 (8325)	32.2	
Test 21	15.1	17.9	37.4	18,357 (7899)	29.6	
Test 22	16.5	14.9	36.7	18,917 (8140)	31.9	
Test 23	13.9	17.9	39.0	19,029 (8188)	29.2	
Test 24	13.2	18.5	40.3	18,957 (8157)	28.1	
Test 25	14.9	18.0	38.1	18,671 (8034)	29.1	
Test 26	16.3	16.9	37.8	18,713 (8052)	29.0	

NOTE: All values are as received (unless otherwise mentioned)

Note (by comparing Tables 3.1 and 3.2) the seeming enrichment of the coal (in terms of heating value) by grinding. This occurs due to the loss of moisture during grinding.

The PSD76 data in the form of average percentage passing 76 microns (200 mesh) are given in Table 3.3.

Table 3.3. The average PSD76 (% passing 76 microns or 200 mesh) for the tests

	PSD76
Test 1	49
Test 2	42
Test 3	46
Test 4	48
Test 5	48
Test 6	50
Test 7	52
Test 8	46
Test 9	55
Test 10	54
Test 11	52
Test 12	46
Test 13	51
Test 14	52
Test 15	52
Test 16	51
Test 17	46
Test 18	49
Test 19	48
Test 20	50
Test 21	66
Test 22	70
Test 23	75
Test 24	67
Test 25	78
Test 26	81

The average *entire* PSD, or percentage passing 1180 microns, 600 microns, 300 microns, 150 microns, 76 microns, and 38 microns (or 16 mesh, 28 mesh, 48 mesh, 100 mesh, 200 mesh, and 400 mesh, respectively), is presented as Rosin-Rammler (RR) plots in Appendix I. This is because such data are best understood graphically. RR plots are a standard way to visualize pulverized coal PSD. Notice how very little coal is retained coarser than 300 microns; that is, the points to the right of 300 microns (50 mesh) are close to zero. Also, as should be expected, the 3 points at 300, 150, and 76 microns usually form a straight line.

3.1.3 Fly Ash Data

The fly ash samples were analyzed for ash; the carbon content in them was computed as *100 - percent ash_{dry basis}*. The unburned carbon in fly ash for the various tests is given in Table 3.4.

Table 3.4. The average unburned carbon in fly ash for the tests

	Carbon in fly ash (%)
Test 3	3.6
Test 4	3.1
Test 5	4.1
Test 6	3.1
Test 7	2.6
Test 8	2.7
Test 9	3.6
Test 10	3.7
Test 11	3.7
Test 12	4.2
Test 13	2.8
Test 14	3.0
Test 15	3.4
Test 16	3.2
Test 17	1.9
Test 18	1.9
Test 19	2.6
Test 20	2.6
Test 21	2.4
Test 22	2.5
Test 23	1.2
Test 24	1.3
Test 25	1.0
Test 26	0.8

3.1.4 Bottom Ash Data

The bottom ash samples were analyzed for ash; the carbon content in them was computed as *100 - percent ash_{dry basis}*. The unburned carbon in bottom ash for the various tests is given in Table 3.5.

Table 3.5. The average unburned carbon in bottom ash for the tests

	Carbon in bottom ash (%)
Test 3	18.1
Test 4	4.6
Test 5	22.6
Test 6	17.4
Test 7	22.3
Test 8	25.4
Test 9	5.0
Test 10	5.9
Test 11	3.5
Test 12	4.3
Test 13	6.9
Test 14	-
Test 15	3.4
Test 16	4.4
Test 17	3.6
Test 18	3.6
Test 19	5.8
Test 20	5.8
Test 21	1.9
Test 22	0.9
Test 23	4.3
Test 24	7.1
Test 25	3.2
Test 26	5.2

3.1.5 Emissions Data

Table 3.6 lists the total Hg (mercury) data (particle bound, oxidized, and elemental) on the stack gas samples taken for Tests 23 and 24. Note that Hg testing was added to the project at the very end. A contractor (Alaska Source Testing, Anchorage, AK) was hired to sample the stack gases and measure Hg emissions using the Ontario-Hydro method.

Table 3.6. Hg emissions through the stack

	Hg, kg/hr (lb/hr)	Hg type (percent of total)		
		Particle bound	Oxidized	Elemental
Test 23 (finer)	0.000408 (0.000760)	0.19	34.03	65.78
Test 24 (coarser)	0.000300 (0.000663)	0.66	14.02	85.31

The other emissions—SO₂, NO_x, CO, and CO₂—were measured using the automated CEMS. The data are presented in Table 3.7.

Table 3.7. Emissions data from continuous emissions monitoring system

	SO ₂ (ppm)	NO _x (ppm)	CO (ppm)	CO ₂ (%)
Test 3	113	164	817	11.3
Test 4	104	158	1423	11.2
Test 5	113	175	1474	10.6
Test 6	120	151	937	11.9
Test 7	119	150	918	11.9
Test 8	131	157	797	11.8
Test 9	121	147	1654	11.6
Test 10	107	145	2708	11.7
Test 11	115	149	1779	11.3
Test 12	121	150	1725	11.4
Test 13	120	153	1300	11.8
Test 14	129	156	2715	11.8
Test 15	107	165	561	11.3
Test 16	119	168	1990	11.7
Test 17	114	165	363	11.2
Test 18	115	166	411	11.3
Test 19	107	161	483	11.4
Test 20	144	164	549	11.5
Test 21	137	159	321	12.9
Test 22	135	153	718	12.5
Test 23	112	134	1096	12.3
Test 24	123	136	1489	12.4
Test 25	133	154	221	12.4
Test 26	136	156	201	12.5

3.1.6 Operational Data

The operational data from CEMS are given in Table 3.8.

Table 3.8. Operational data from CEMS

	Coal flow rate kg/hr	Oxygen	Mean MW generated	Mill amps
Test 3	22,615	2.60	28.12	83.5
Test 4	23,709	2.54	28.29	88.9
Test 5	22,828	2.96	27.92	87.4
Test 6	22,850	2.30	28.47	89.5
Test 7	23,780	2.37	28.24	90.0
Test 8	22,460	2.29	28.45	88.6
Test 9	22,778	3.18	28.28	80.9
Test 10	22,505	3.20	28.33	77.5
Test 11	22,377	3.66	28.26	75.3
Test 12	22,429	3.79	28.29	72.1
Test 13	23,346	2.29	28.11	90.3
Test 14	23,084	2.57	28.11	88.3
Test 15	22,729	2.76	28.07	85.8
Test 16	23,466	2.75	28.03	81.2
Test 17	22,635	2.75	28.14	74.6
Test 18	22,719	2.74	28.05	74.2
Test 19	22,279	2.49	28.04	74.1
Test 20	22,365	2.51	27.99	74.8
Test 21	22,761	2.75	28.41	91.1
Test 22	22,967	2.73	28.55	91.9
Test 23	22,663	2.00	27.88	93.7
Test 24	22,721	2.08	28.06	91.5
Test 25	22,465	2.33	28.07	93.7
Test 26	22,688	2.25	28.05	92.9

Note that the oxygen data are presented here to satisfy reader curiosity. The presented oxygen data are very difficult to use in any analysis since the plant setup (the path taken by the air and the location of the oxygen sensor) does not allow a direct relationship to be drawn between the oxygen and the nature of combustion.

3.2 Analysis

In this section, the important relationships are presented first, followed by other interesting observations.

3.2.1 PSD Versus Power Plant Efficiency

The efficiency of the power plant was computed as the ratio of energy burned as coal to energy generated as electricity. The energy burned as coal is computed from the coal flow rate (Table 3.8) during a test and the coal calorific value (Table 3.2), while the MW generated is directly obtained (Table 3.8).

Table 3.9 presents the efficiency of the tests.

Table 3.9. The average PSD76 (% passing 76 microns or 200 mesh) and power plant efficiency for the tests

	PSD76	Efficiency
Test 1	49	0.2299
Test 2	42	0.2305
Test 3	46	0.231
Test 4	48	0.222
Test 5	48	0.225
Test 6	50	0.238
Test 7	52	0.224
Test 8	46	0.236
Test 9	55	0.240
Test 10	54	0.230
Test 11	52	0.229
Test 12	46	0.226
Test 13	51	0.228
Test 14	52	0.228
Test 15	52	0.230
Test 16	51	0.229
Test 17	46	0.236
Test 18	49	0.232
Test 19	48	0.232
Test 20	50	0.233
Test 21	66	0.244
Test 22	70	0.236
Test 23	75	0.2323
Test 24	67	0.2342
Test 25	78	0.2406
Test 26	81	0.2377

The relationship between the PSD76 and efficiency is weak, as shown in Figure 3.1.

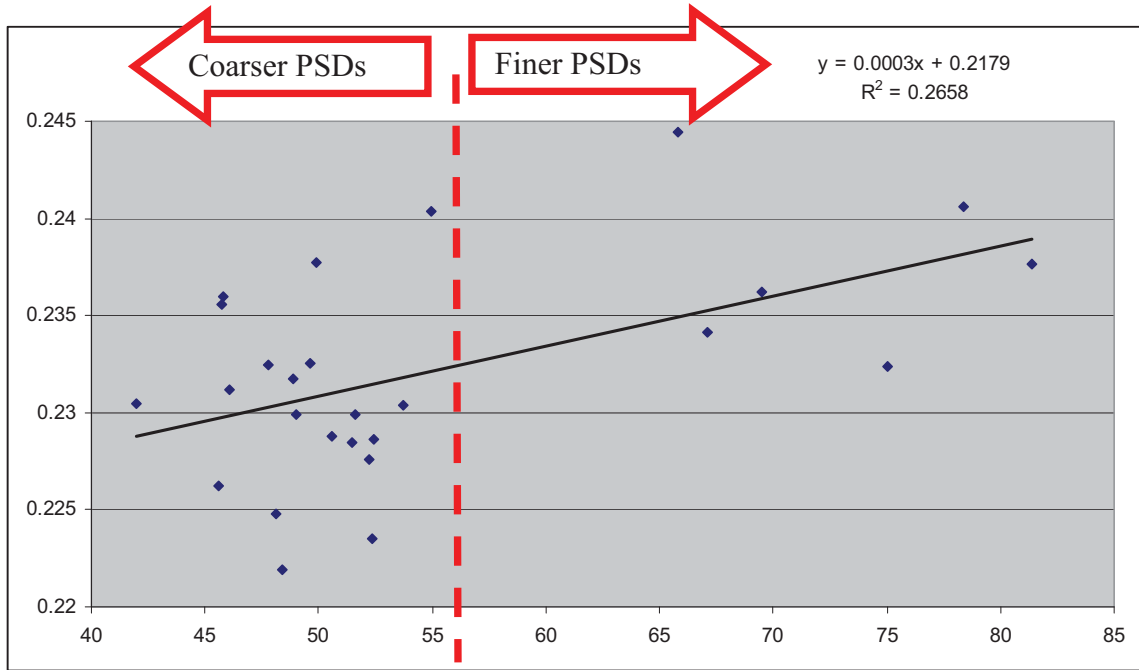


Figure 3.1. PSD of pulverized coal vs. plant efficiency.

The plot in Figure 3.1 makes the presence of two clusters of PSD76, one to the left of 60 (coarser PSD76) and the other to the right (finer PSD76), very evident. Therefore, it is tempting to compare the two clusters. The coarser PSD76 averaged 50% passing 76 microns, while the finer PSD76 averaged 73% passing 76 microns.

Table 3.10 presents the previous table (Table 3.9) as two separate clusters.

Table 3.10. The two separate groups of PSD76 tested in the project

Cluster 1: Coarse PSD76		
	PSD76	Efficiency
Test 2	42	0.2305
Test 3	46	0.231
Test 8	46	0.236
Test 12	46	0.226
Test 17	46	0.236
Test 4	48	0.222
Test 5	48	0.225
Test 19	48	0.232
Test 1	49	0.2299
Test 18	49	0.232
Test 6	50	0.238
Test 20	50	0.233
Test 13	51	0.228
Test 16	51	0.229
Test 7	52	0.224
Test 11	52	0.229
Test 14	52	0.228
Test 15	52	0.23
Test 10	54	0.23
Test 9	55	0.24

Cluster 2: Fine PSD76		
	PSD76	Efficiency
Test 21	66	0.244
Test 24	67	0.2342
Test 22	70	0.236
Test 23	75	0.2323
Test 25	78	0.2406
Test 26	81	0.2377

The average efficiencies of the two groups are 0.2305 and 0.2375, with the finer PSD76 having an efficiency about 3% higher than the coarser PSD76. However, the almost similar efficiencies are statistically different (*t-stat*: 3.44) when their means are compared by *t*-tests (assuming unequal variances). The *t*-test could be done since efficiency and PSD76 data in the two groups were normally distributed.

To explore if the difference in efficiency can be explained by factors other than PSD76, the coal quality (ash, volatile content, moisture, unburned carbon in fly ash and bottom ash, and oxygen) differences were studied. Note, however, that coal quality can only be used as a very broad guide when discussing combustion, since similar coals can often have very different combustion performance/characteristics while different coals have similar performance/characteristics (Carpenter et al., 2007).

Fuel Type Comparison

Table 3.11a summarizes the coal quality comparison. A comparison based on *t*-test was not done for any data group that failed the Anderson-Darling test for normality. Such groups are identified with an “N/A” under the *t*-stat column.

Table 3.11a. Comparison in the coal quality of the coal burned in coarser PSD76 tests and finer PSD76 tests (quality values are for pulverized coal unless mentioned otherwise)

	Average		t-stat	Significant* difference?
	Coarser	Finer		
Ash	14.15	14.98	1.28	No
Volatile content	38.43	38.22	0.37	No
Volatile content ^{RC}	32.5	31.5	1.66	No
Moisture	15.2	17.35	N/A	N/A
Moisture ^{RC}	27.1	30.6	MWT	Yes
Heat Val, kJ/kg (BTU)	19,337 (8320)	18,774 (8078)	4.1	Yes
Fixed carbon content	32.3	29.5	N/A	N/A
HGI	34	37.8	3.8	Yes

* at 95% confidence

RC: Raw Coal

MWT: Mann-Whitney Test

The ash and volatile contents are statistically similar for the two groups, with the pulverized coal volatile content being almost identical. However, there appears to be a difference in the moisture content, though the significance of the difference cannot be estimated for pulverized coal. The Mann-Whitney² test, which could be applied to the raw coal data (for moisture), implied that the moisture content was higher for finer PSD76. Higher moisture coals are more reactive, leading to more complete combustion and higher efficiencies. In this case, the finer grinds had over 14% more moisture than coarser PSD76. But higher moisture also means loss of heat in converting the moisture to steam, thereby lowering efficiency.

The fixed carbon content is higher in the coarser test coals. Since the fixed carbon data for the fine group were not normally distributed, a significance test could not be done to compare the two groups based on fixed carbon. Therefore, whether the difference is significant is unknown. When combined with their lower moisture contents, it is no surprise that they (coarser test coals) have higher heating values, though the heating value is impacted by more than just moisture and fixed carbon. Also, heating value is not an indicator of the quality and nature of combustion (Carpenter et al., 2007).

While the moisture content and fixed carbon probably help improve the efficiency of the coarser tests, their lower HGIs probably hurt their efficiencies. It is not possible to know, of course, if these two factors compensated for each other.

Unburned Carbon Comparison

² <http://faculty.vassar.edu/lowry/utest.html>

The unburned carbon (Table 3.11b) was also examined to understand the performance of the tests. The *t*-test was not applicable for bottom ash data, as the data for unburned carbon in bottom ash (coarse group) were not normally distributed.

Table 3.11b. Comparison of unburned carbon

	Average		t-stat	Significant difference*
	Coarser	Finer		
Unburned carbon (fly ash)	3.1	1.53	4.65	Yes
Unburned carbon (bottom ash)	9.56	3.77	N/A	N/A

*at 95% confidence

The unburned carbon in both fly ash and bottom ash are higher for coarser PSD76, which would suggest that there was loss of carbon when coal was burned coarser. This type of observation is standard in bituminous coal and could explain the lower efficiencies of coarser grind combustion. However, with Alaskan low-rank coal (according to US DOE researchers Freeman et al., 1996), almost complete burnout is typical even at significantly coarser grinds. Also, the higher unburned carbon contents can be very easily explained by the fixed carbon contents of the two groups. As presented earlier, the coarser tests had higher fixed carbon content than finer grinds, which could have resulted in higher unburned carbon. This is especially possible since the fixed carbon content percentage applies to the entire tonnage that is burned, while the unburned carbon percentage applies only to a small portion of the total tonnage.

An additional issue that prevents the aggressive use of unburned carbon values in differentiating the two groups would be the quality of bottom ash samples. As described in section 2.3.4, the bottom ash sampling was not ideal since samples had to be collected from whatever bottom ash washed out. Whether these samples are representative of the bottom ash is anybody's guess. As seen in Table 3.5, bottom ash values have had a wide range.

Coarse Versus Fine Efficiency Comparison: Summary

The aforementioned factors provide a fuzzy picture with regard to efficiency. One should also take into account that the finer grind group has only 6 data points compared with the coarse group, which has 18–20 data points. Since the difference in efficiency is small, a single high/low data point in the finer group (in a future test) could blur the differences. Also notable is that 7 out of the 20 tests in the coarse group have efficiency values that are within the fine group PSD76 range.

3.2.2 PSD76 Versus SO₂, NO_x, CO, and CO₂ Emissions

Figures 3.2 to 3.5 show the relationship between PSD76 and SO₂ (ppm), NO_x (ppm), CO (ppm), and CO₂ (%).

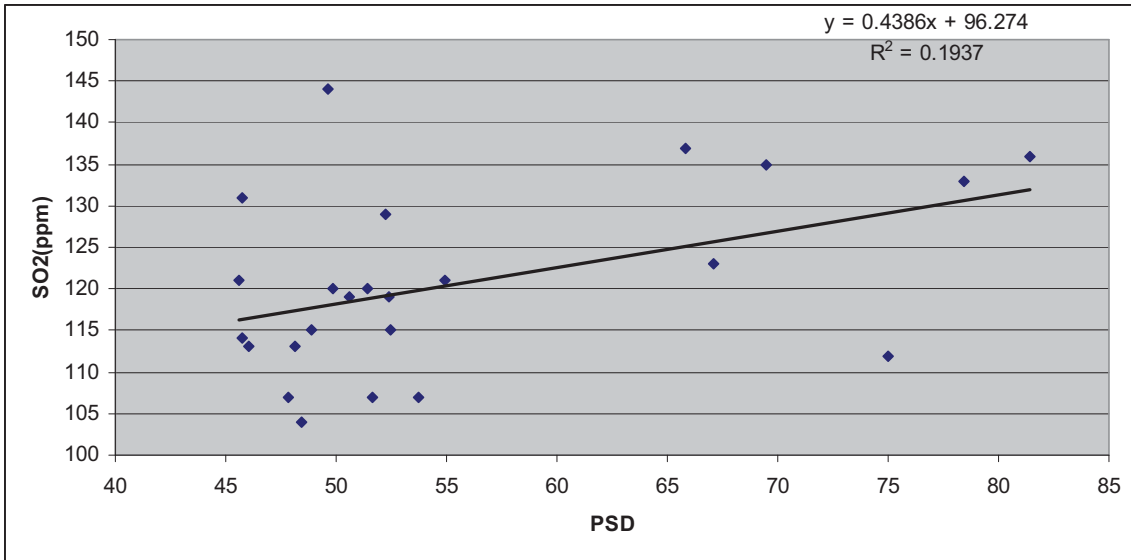


Figure 3.2. PSD76 vs. SO₂ (ppm).

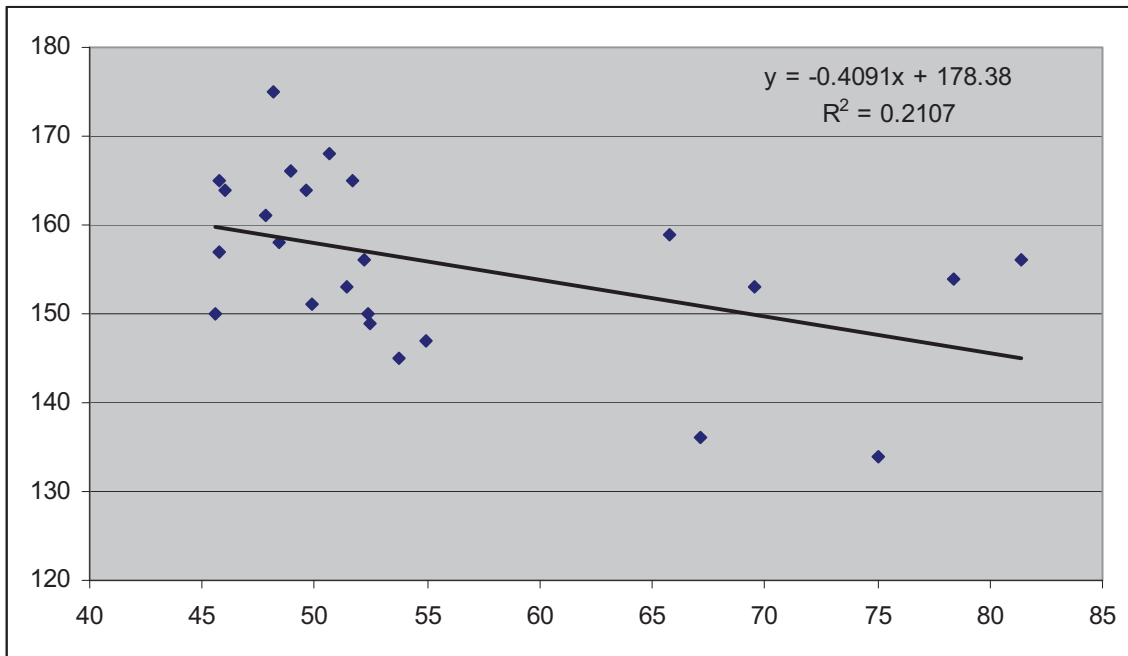


Figure 3.3. PSD76 vs. NO_x (ppm).

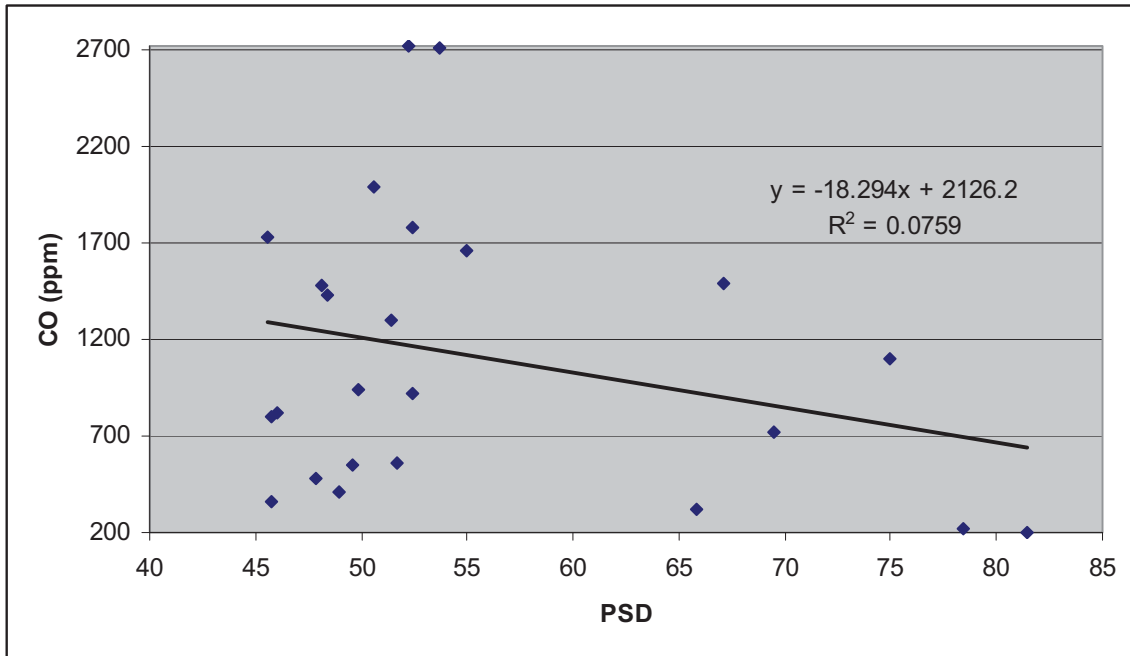


Figure 3.4. PSD76 vs. CO (ppm).

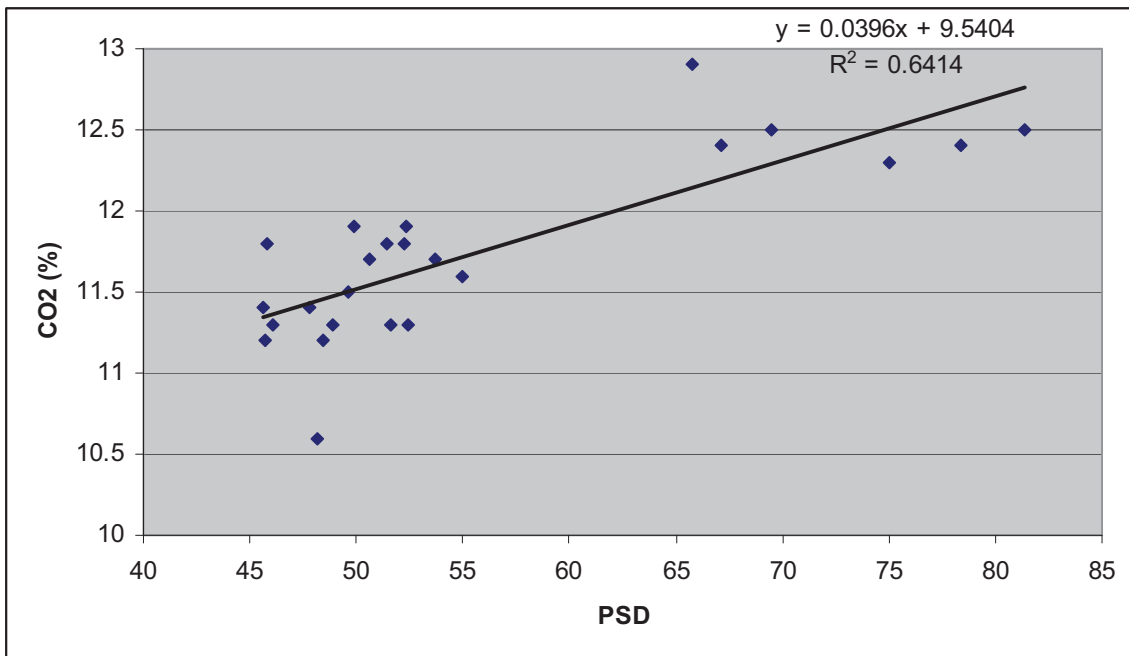


Figure 3.5. PSD76 vs. CO₂ (%).

Other than PSD76 versus CO₂, all the other relationships appear weak. As was done before, the tests were split into two groups: coarse (percent passing 76 microns at 55 and below) and fine.

Table 3.12. Comparison of emissions between coarser PSD76 tests and finer PSD76 tests

	Average		t-stat	Significant difference*
	Coarser	Finer		
SO ₂	118	129	2.5	Yes
NO _x	158	149	1.9	No
CO	1256	674	2.1	No
CO ₂	11.5	12.5	8.8	Yes

* at 95% confidence interval

SO₂ and CO₂ emissions seem to rise with finer grind. When sulfur (from Table 3.1) was explored as a possible reason for higher SO₂, it was found that there was no correlation (R² of 0.001) between the two (S and SO₂). The sulfur contents of the coarse group could not be compared to the fine group since the sulfur data of the fine group was not normally distributed.

As regards CO₂, fixed carbon was explored as a reason. As presented earlier, the fixed carbon contents of pulverized coal were higher for coarser grinds (mean: 32.3%) than for finer grinds (mean: 29.5%). Thus, the CO₂ emissions are contrary to what would be suggested by the fixed carbon contents. The finer tests did have higher moisture content, as seen in Table 3.11a. Higher moisture content could have increased CO₂ and SO₂ emissions, though a direct correlation between them (moisture content of pulverized coal and CO₂ and SO₂ concentration) shows negligible correlation (Figure 3.6).

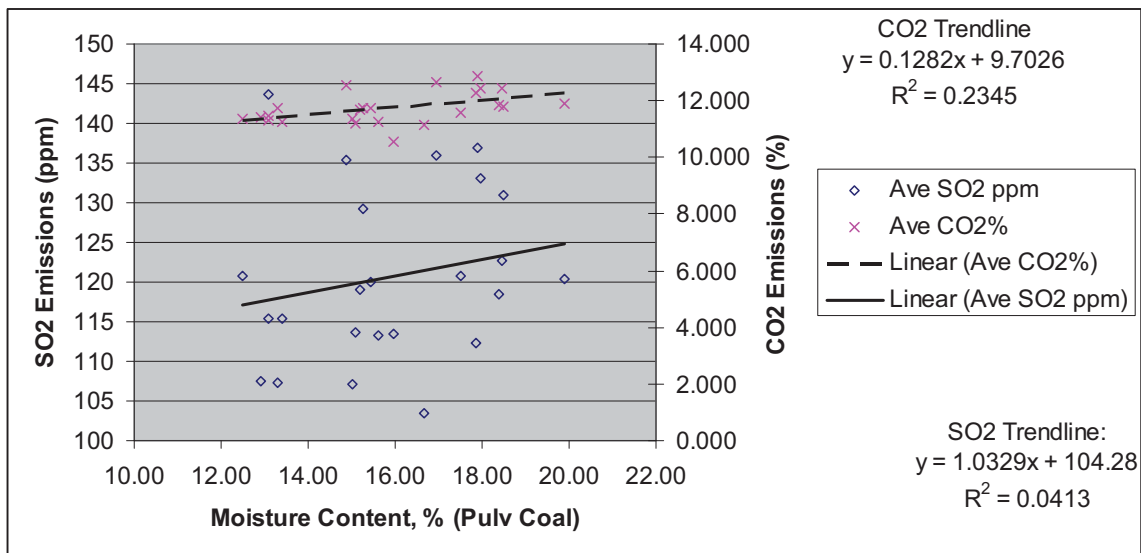


Figure 3.6. Negligible correlation between moisture content of coal and SO₂ and CO₂ emissions.

Note that higher moisture content (as for finer grinds) usually results in higher amounts of flue gases. Therefore, higher concentrations (in higher amounts of flue gases) of emissions are especially significant.

The CO₂ observation is critical in light of the current global sensitivity to CO₂ emissions. The implication of Figure 3.5 and Table 3.12 is that by burning low-rank Alaskan coal at a PSD76 of 50% instead of 70%, one could reduce the CO₂ emissions concentration by about 8% (the difference between 11.5% and 12.5% concentration), though reducing the *concentration* of emissions is not the same as reducing the *total quantity* of emissions. Unfortunately, total CO₂ emissions could not be studied, as neither the power plant nor the research was set up to conduct a carbon mass balance at the level necessary to conclude on CO₂ emissions. Additionally, it is difficult to explain the relationship. Measurement bias in the CEMS is a possibility since CO₂ data from 2005 (on days of the test but not during the test) reveal lower values of emitted CO₂ compared to 2006 and 2008. Since CO₂ tonnage values are based on many constants and assumptions, it is possible that a change was made to a factor that resulted in slightly higher values of CO₂. Note that this is only a suspicion and could not be verified.

Given the current importance of CO₂, PSD – CO₂ relationship may be worth examining.

3.2.3 PSD76 Versus Hg

Not much can be said about the relationship of PSD76 versus HG besides to note that Hg emissions through the stack are very small. These emissions are so close to detection limits that the difference evident in Table 3.6, where the coarser test had the lower Hg emissions, is negligible.

3.2.4 PSD76 Versus Mill Power Consumption

Ganguli and Bandopadhyay (2008) examined the relationship between mill power consumption and PSD76 based on data from Tests 3–22. A direct relationship between mill power consumption and PSD76 was not observed (Figure 3.7a).

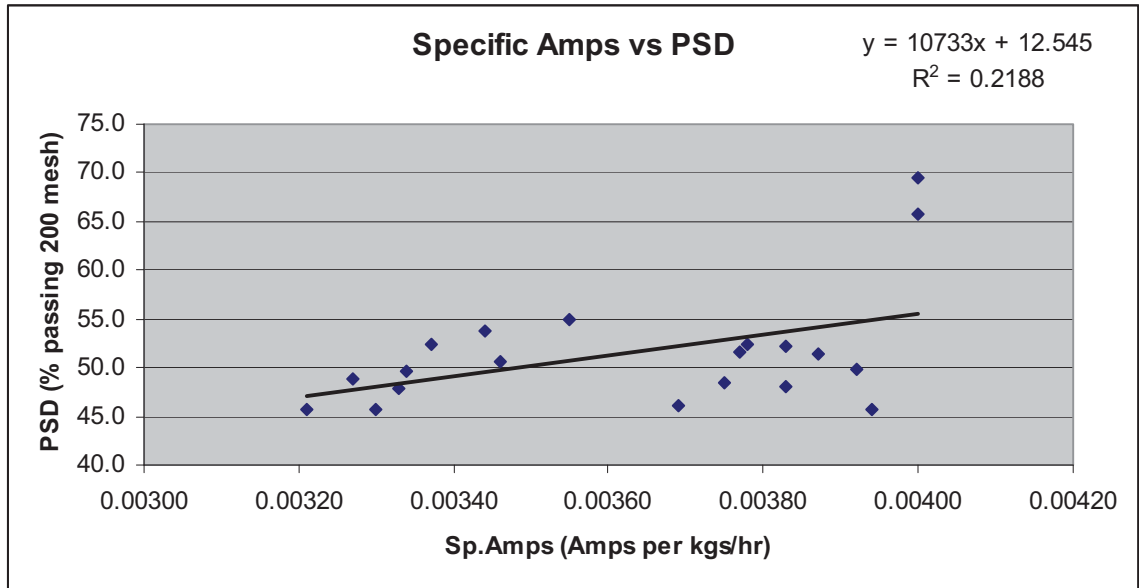


Figure 3.7a. Almost negligible relationship between PSD76 and specific mill amperage (Ganguli and Bandopadhyay, 2008).

When HGI and coal flow rates were factored in, the following relationship was observed:

$$\text{Amps} = -26.3113 + 0.908 \cdot \text{PSD76} - 1.652 \cdot \text{HGI} + 0.00523 \cdot \text{Flow} \quad (3.1)$$

where *Amps* is the combined amperage of the two mills and *Flow* is the coal flow rate in kg/hr.

The correlation coefficient for the relationship jumped from 0.22 (Figure 3.7a) to 0.64. Additionally, the coefficients for PSD76, HGI, and Flow were all significant, implying that these factors play a role in influencing *Amps*. Since PSD76 and Flow had positive coefficients, the relationship implies that as PSD76 and Flow go up, so do Amps, which makes sense.

When Figure 3.7a was updated with data from Tests 23–26, a direct correlation between PSD76 and power consumption appeared (Figure 3.7b).

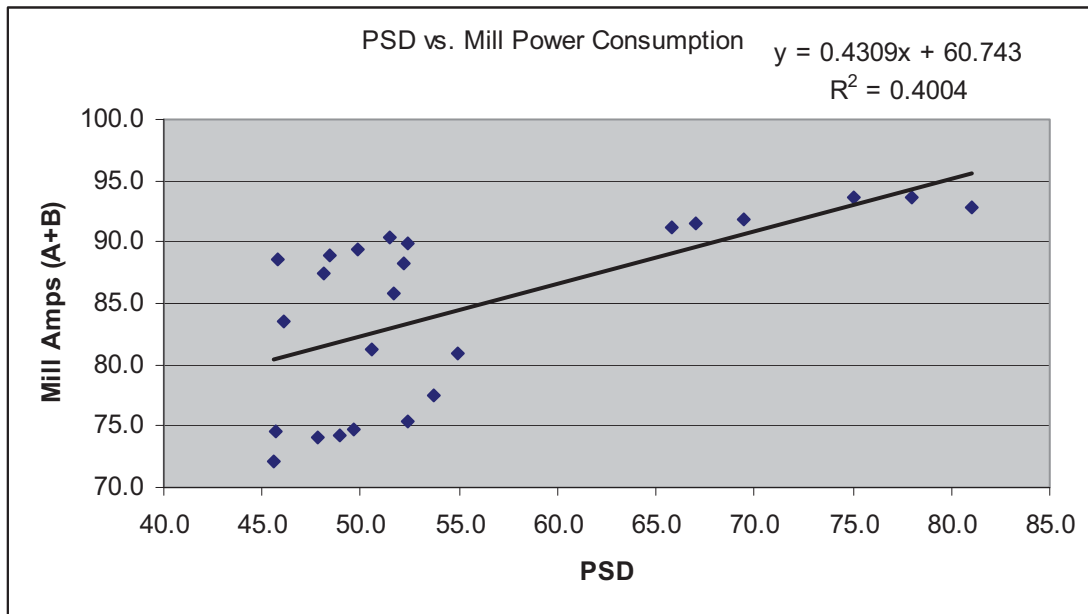


Figure 3.7b. Power consumption increases as PSD76 increases (becomes finer).

Equation (3.1) was updated also with the data from Tests 23–26:

$$\text{Amps} = -76.7 + 0.584 \cdot \text{PSD} - 0.942 \cdot \text{HGI} + 0.0071 \cdot \text{Flow} \quad (3.2)$$

The addition of the new data further improved the correlation coefficient to 0.68. The coefficients for PSD76, HGI, and Flow were all significant. The residuals from applying Equation (3.2) were centered at zero and passed the Anderson-Darling test for normality, thus validating Equation (3.2).

When the mill power consumption was studied on a coarse grind versus fine grind basis (Tables 3.8 and 3.10), the coarse grind tests consumed 13.34% less power (0.0036 amps per kg/hr) than the fine grind tests (0.0041 amps per kg/hr). The *t*-test was not applicable to the data; hence, no estimate of the significance of the difference is provided.

Equation (3.2) can be utilized to compute the savings in mill power consumption from coarse grinding. The electricity costs for the mill can be computed by the equation

$$\text{Amps} \cdot \text{Voltage} \cdot \sqrt{3} \cdot \text{power factor} \cdot \text{Hours} \cdot \text{Cost of saving electricity}$$

Since the mills are run at about 2.4 kV, 0.7 power factor, 365 days a year, with a 95% availability, the cost is (at 20 cents per kwh³ at Healy Unit #1)

$$\text{Cost} = \text{Amps} * 2.4 * 1.732 * 0.7 * (365 * 24) * 0.95 * 0.2 \quad (3.3)$$

If the power plant were to be run at 50% passing 76 microns instead of 70% passing 76 microns, the savings would be (from Equation [3.3])

$$(\text{Amps}_{70} - \text{Amps}_{50}) * 4843 \quad (3.4)$$

For the same HGI and Flow, applying Equations (3.2) to (3.4),

$$\begin{aligned} \text{Savings} &= 0.584 * (70 - 50) * 4843 \quad (3.5) \\ &= \$56,566 \end{aligned}$$

Ganguli and Bandopadhyay (2008) did not consider power factor, three-phase motors (which introduces the $\sqrt{3}$ in Equation [3.3]), and power source selection methodology in their computation.

3.2.5 Other Relationships

In this section, issues or relationships not directly related to project objectives are discussed/presented.

3.2.5.1 Effect of Lower Weight Sample

As evident from the previous sections, Alaskan low-rank coal is very moist, which makes sampling difficult. The moist pulverized coal had a tendency to run and clog the sampler. This often caused samples to be lower in weight than the recommended weight. Therefore, it was of interest to see if the lower-weight (LW) samples had a different PSD (and PSD76) than the recommended-weight samples.

The recommended weight is computed based on the coal flow, sampling aperture, and sampling duration as follows:

$$W = (a / A) * \text{Flow in Pipe/minute}$$

where W is the sample to be collected per minute, a is the area of the aperture in the sampling probe, A is the internal area of the pipe, and $\text{Flow in Pipe/minute}$ is self-explanatory. Since the sampling duration was 2 minutes for the first 22 tests, the computed sample weight was $2W$. The recommended weight, W_r , was

$$90\% \text{ of } 2W \leq W_r \leq 110\% \text{ of } 2W$$

³ The in-plant cost to generate electricity is 6.5¢/kwh. However, reduced mill power consumption makes more electricity available for the grid. Since the cheapest power source is always selected by the grid, more available power implies cutting down on electricity that is otherwise 20–25¢/kwh.

For example, in Test 1 the flow rate was 11,583 kg/hour for mill A, or 5791.5 kg/hr through pipes A1 and A2. The ratio of the areas was 0.001726, resulting in $W = 333.2$ grams. Therefore, the recommended weight was between 299.9 grams and 366.5 grams. Note that the above method does not apply to data from tests that used the ISO sampling method (Tests 23-26).

Tests 1 and 2 had samples that were either recommended weight or under weight. Therefore, they presented an excellent opportunity for comparison. WR is the ratio of the actual weight of the sample to the recommended weight. Since multiple samples were taken in each test, each sample usually being just minutes apart from the next one, this was an appropriate comparison. The comparison is done on a pipe basis as PSDs between pipes can and do vary (discussed later).

Tables 3.13a–3:13e present the results, while Figures 3.8–3.12 present the Rosin-Rammler (RR) plots. Note in the figures that the x-axis is labeled in SI units at the top and in US mesh sizes at the bottom, while the y-axis is percentage retained (and not percentage passing, as in the tables).

From the tables, it is apparent that particle sizes coarser than 150 microns are captured in identical proportions in samples of all sizes, while the RR plots and Figure 3.13 show that the PSD76 (the benchmark number since it was used in all analyses) is near-identical between lower-weight and recommended-weight samples in each case. In other words, the same line is a good fit no matter whether we fit the “red” dots or the “blue” dots. Table 3.13a. PSD76 (% passing) of lower-weight samples vs. recommended-weight samples for Pipe A1 in Test 1

Sample size	Lower weight				Recommended weight		
				Ave			Ave
WR	81.5	60.5	86.5	76.2	93.2	94.6	93.9
1180+	100	100	100	100.0	100	100	100
600 – 1180	100	100	100	100.0	100	100	100
300 – 600	100	100	100	100.0	100	100	100
150 – 300	98.9	100	98.9	99.3	98.7	100	99.4
76 – 150	83	87.21	87.5	85.9	84.3	86.9	85.6
38 – 76	44.5	57.0	52.4	51.3	49.1	50.0	49.6
0 – 38	19.9	27.7	25.0	24.2	23.1	20.3	21.7
PSD76				51.3			49.6

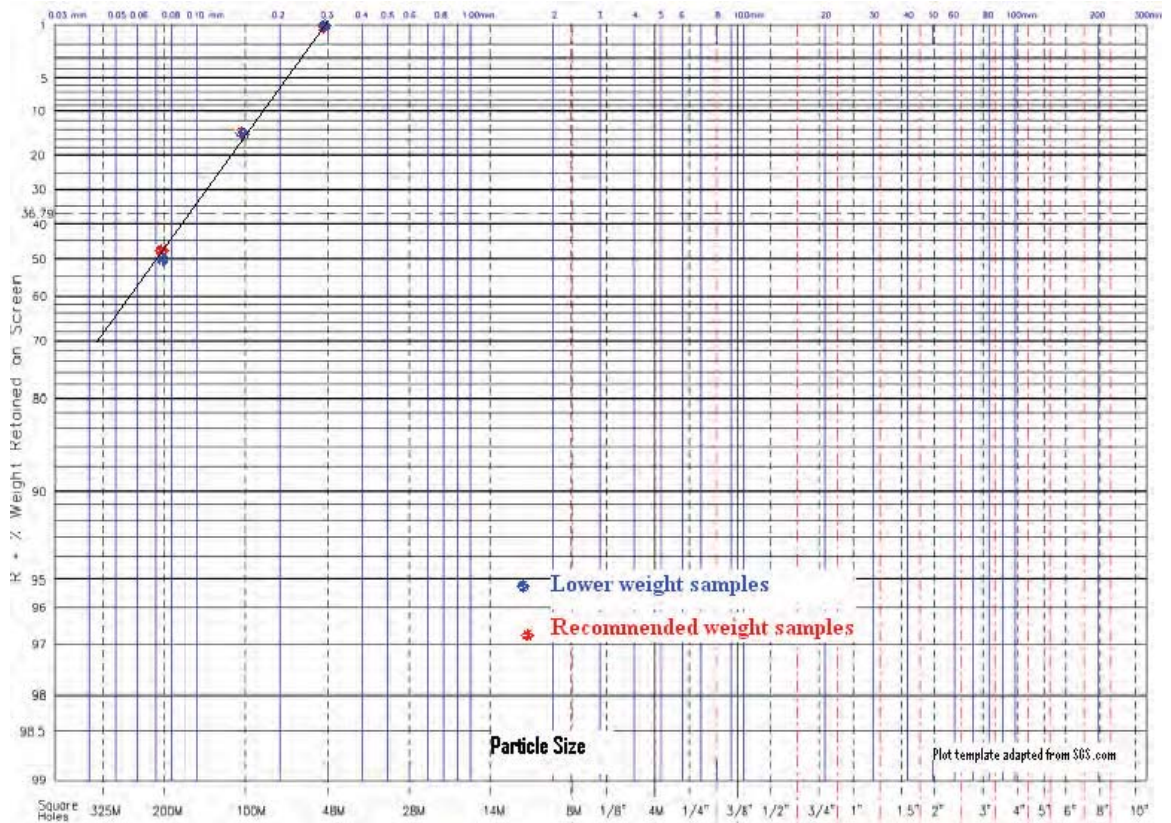


Figure 3.8. Rosin-Rammler plot of the average particle size distribution for the lower-weight samples and those of recommended weights (Pipe A1, Test 1).

Table 3.13b. PSD76 (% passing) of lower-weight samples vs. recommended-weight samples for Pipe A2 in Test 1

Sample size	Lower weight					Ave	Recommended weight
WR	77.1	88.7	48.3	58.5	68.2	105.0	
1180+	100	100	100	100.0	100.0	100.0	
600 – 1180	100	100	100	100.0	100.0	100.0	
300 – 600	100	100	100	100.0	100.0	100	
150 – 300	98.9	99.0	100	98.5	99.1	100	
76 – 150	85.4	84.8	89.1	80.4	84.9	85.7	
38 – 76	50.5	48.9	59.2	40.4	49.8	50.1	
0 – 38	22.1	22.3	29.3	18.3	23.0	23.2	
PSD76					49.8	50.1	

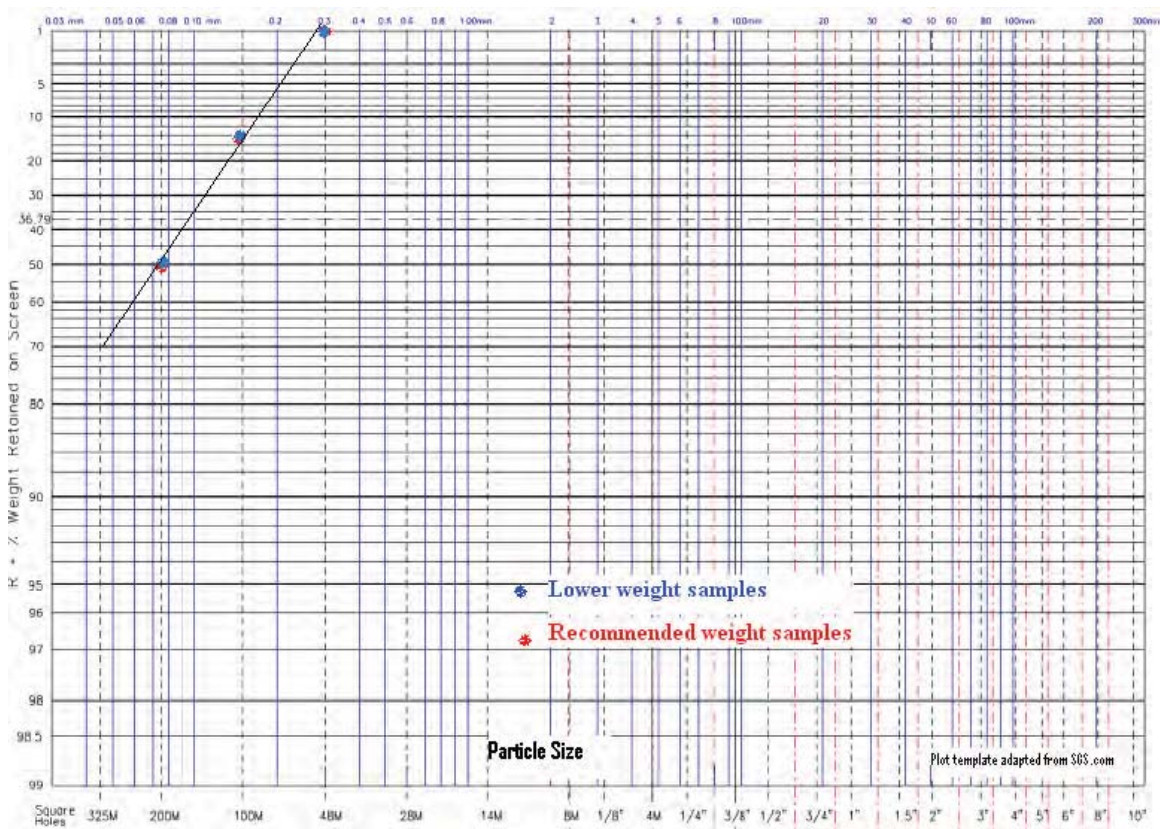


Figure 3.9. Rosin-Rammler plot of the average particle size distribution for the lower-weight samples and those of recommended weights (Pipe A2, Test 1).

Table 3.13c. PSD76 (% passing) of lower-weight samples vs. recommended-weight samples for Pipe A2 in Test 2

Sample size	Lower weight				Ave	Recommended weight		
								Ave
WR	55.6	73.8	86.6		72	103.9	91.2	97.55
1180+	100	100	100		100	100	100	100
600 – 1180	100	100	100		100	100	100	100
300 – 600	100	100	100		100	100	100	100
150 – 300	98.7	98.7	100.0		99.1	100	98.37	99.2
76 – 150	86.2	80.5	80.1		82.3	80.35	80.51	80.4
38 – 76	52.0	47.6	43.4		47.6	46.48	40.75	43.6
0 – 38	26.5	25.2	21.9		24.5	21.14	19.31	20.2
PSD76					47.6			43.6

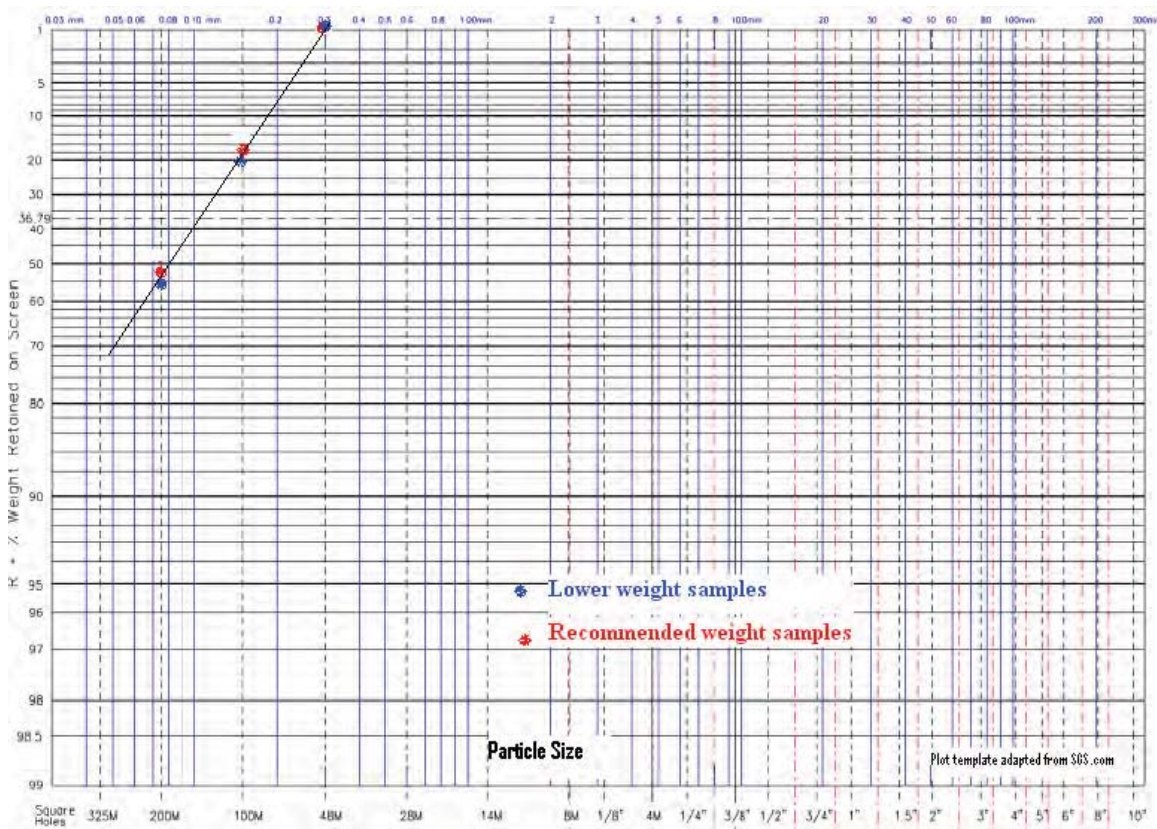


Figure 3.10. Rosin-Rammler plot of the average particle size distribution for the lower-weight samples and those of recommended weights (Pipe A2, Test 2).

Table 3.13d. PSD76 (% passing) of lower-weight samples vs. recommended-weight samples for Pipe B1 in Test 2

Sample size	Lower weight			Recommended weight			
			Ave				Ave
WR	88.5	82.0	85.3	92.1	104.2	97.1	97.8
1180+	100	100	100	100	100	100	100
600 – 1180	100	100	100	100	100	100	100
300 – 600	100	100	100	100	100	100	100
150 – 300	97.3	100	98.7	97.6	100	100	99.2
76 – 150	70.6	73.5	72.1	75.4	71.35	75.0	73.9
38 – 76	36.6	38.5	37.5	38.7	36.4	38.9	38.0
0 – 38	17.5	17.7	17.6	17.5	17.5	18.81	17.9
PSD76			37.5				38.0

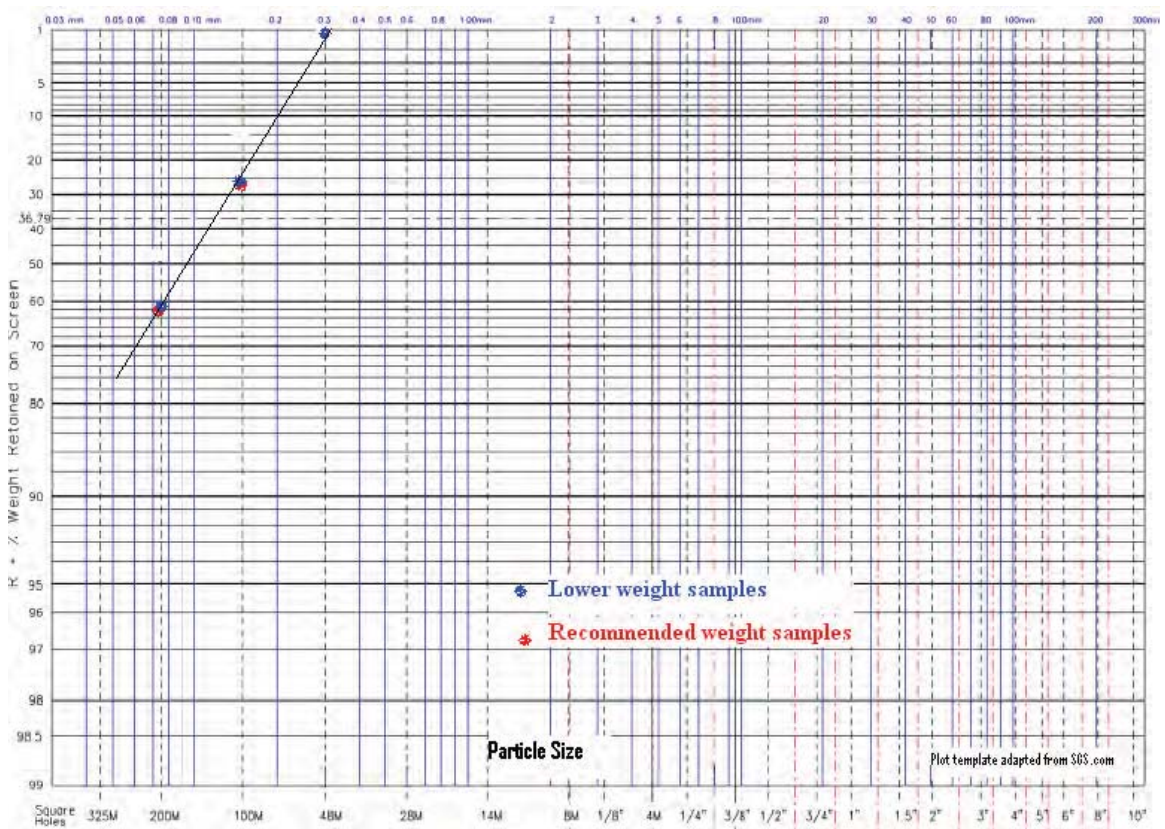


Figure 3.11. Rosin-Rammler plot of the average particle size distribution for the lower-weight samples and those of recommended weights (Pipe B1, Test 2).

Table 3.13e. PSD76 (% passing) of lower-weight samples vs. recommended-weight samples for Pipe B2 in Test 2

Sample size	Lower weight						Recommended weight
						Ave	
WR	86.3	77.4	70.9	54.5	54.8	68.78	92.1
1180+	100	100.0	100.0	100.0	100.0	100	100
600 – 1180	100	100.0	100.0	100.0	100.0	100	100
300 – 600	100	100.0	100.0	100.0	100.0	100	100
150 – 300	97.6	100.0	97.7	97.7	100.0	98.6	100
76 – 150	74.9	74.3	77.9	78.3	77.3	76.5	71.9
38 – 76	38.3	44.1	44.4	46.4	47.0	44.0	43.2
0 – 38	18.6	20.6	22.9	23.5	24.0	21.9	22
PSD76						44.0	43.2

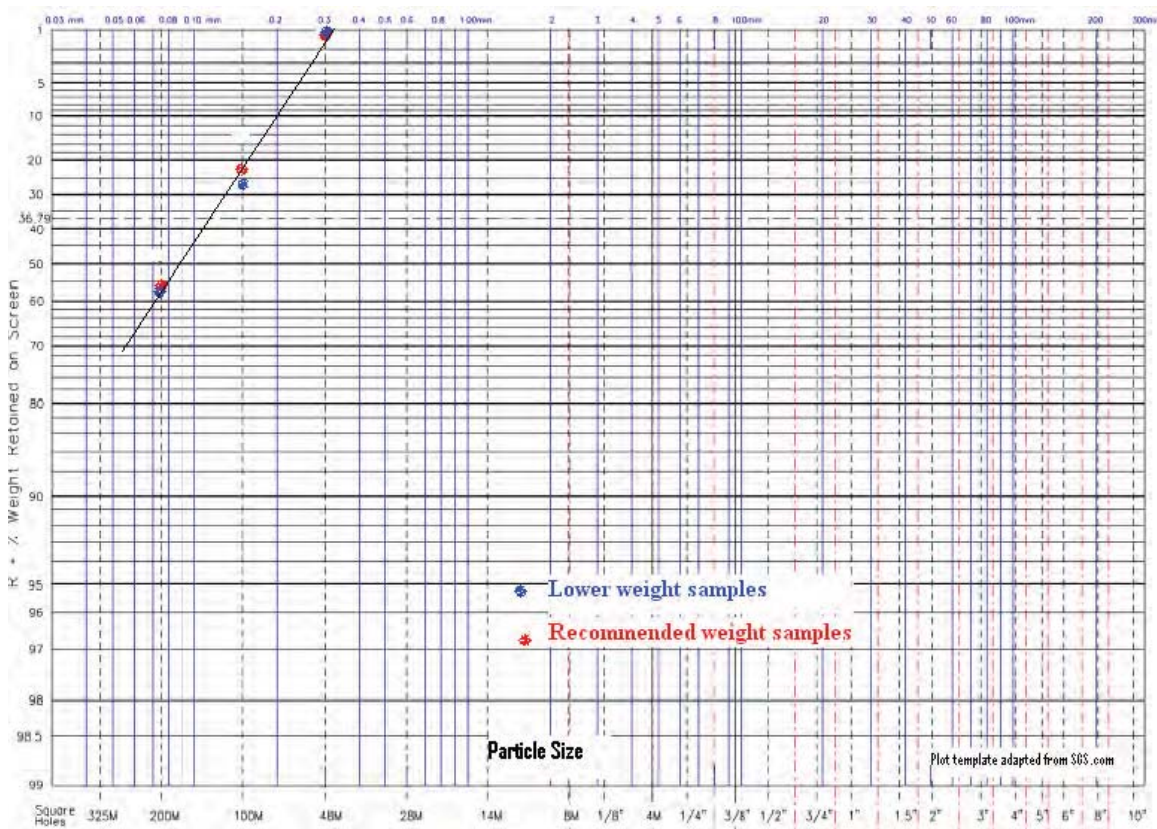


Figure 3.12. Rosin-Rammler plot of the average particle size distribution for the lower-weight samples and those of recommended weights (Pipe B2, Test 2).

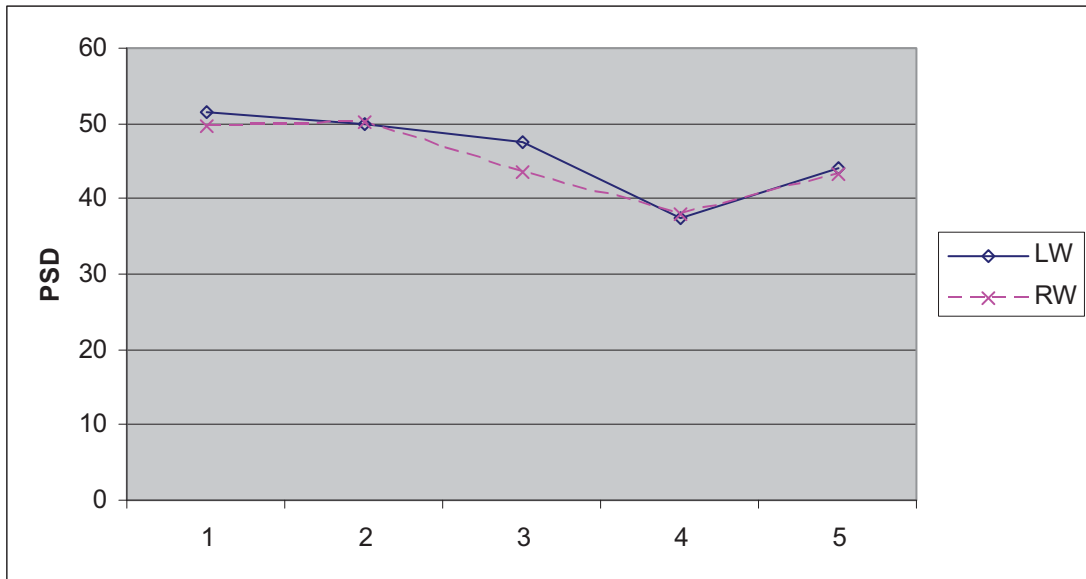


Figure 3.13. Comparing the PSD76 of the samples that are lower weight (LW) to those that are of recommended weight (RW).

The average PSD76 of the two sets were 46 and 45, respectively, for LW and RW.

In summary, it can be concluded that underweight samples were similar to the samples with the recommended weight.

3.2.5.2 PSD in Different Pipes

Table 3.14 presents the average PSD76 (percent passing 76 microns) in each of the four pipes for the various tests. Remember that A1 and A2 carry coal from mill A, while B1 and B2 carry coal from mill B. From Figures 3.14 and 3.15, it appears that while A1 and A2 seemed to have a consistent difference in their PSD76 (with A2 always being a bit finer), that was not the case for B1 and B2. However, the data demonstrate that in any particular test it was possible that the four pipes could have PSD76s that are different from each other. In other words, in any test, all four pipes should be sampled to determine the average PSD76 being burned.

Table 3.14. The average PSD76 in the four pipes for the tests

	A1	A2	B1	B2
Test 3	41.2	47.2	44.9	51.0
Test 4	40.3	42.8	56.2	54.2
Test 5	41.5	51.7	49.0	50.4
Test 6	48.4	54.9	48.9	47.3
Test 7	52.7	55.6	51.7	49.5
Test 8	46.7	50.1	40.3	46.0
Test 9	52.1	56.4	54.7	60.0
Test 10	43.2	58.9	55.2	57.6
Test 11	42.3	65.3	48.3	53.8
Test 12	33.2	46.5	55.7	47.6
Test 13	49.1	50.2	57.0	59.0
Test 14	40.3	56.5	55.2	54.6
Test 15	56.1	44.7	52.1	54.5
Test 16	40.9	54.0	61.5	46.0
Test 17	37.1	50.0	51.0	44.8
Test 18	38.8	47.5	64.5	44.7
Test 19	38.6	45.8	59.9	46.9
Test 20	39.9	49.7	58.4	50.4
Test 21	62.0	64.0	69.0	68.1
Test 22	64.6	66.3	72.9	74.2
Test 23	79.2	77.5	74.7	68.5
Test 24	66.8	68.6	66.2	63.4
Test 25	83.8	85.7	71.4	72.7
Test 26	84.8	86.8	77.9	76.1

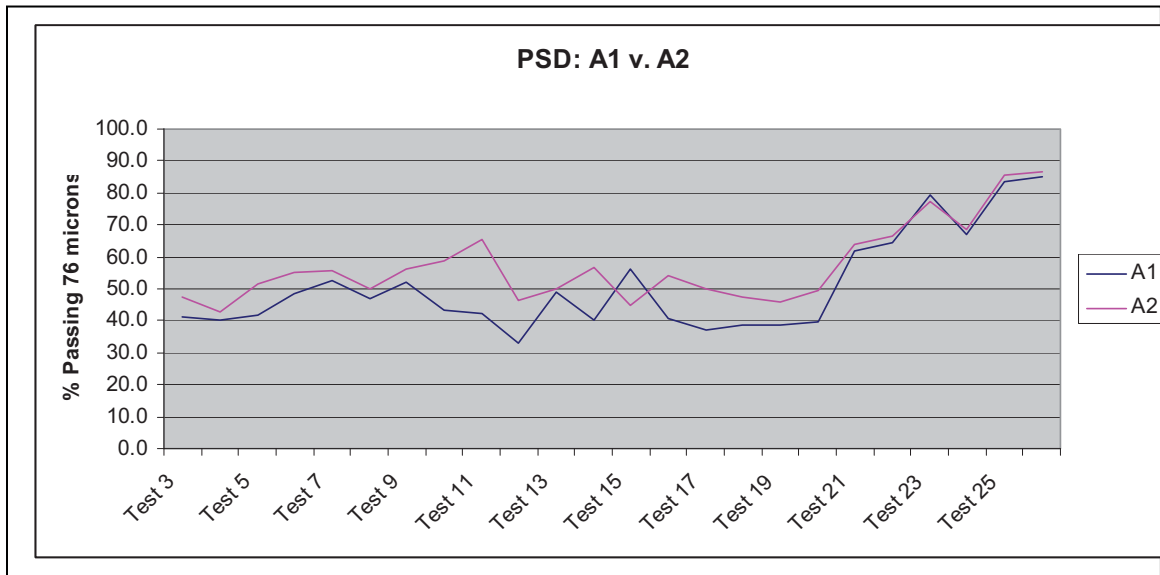


Figure 3.14. The coal in pipe A2 is usually finer than A1.

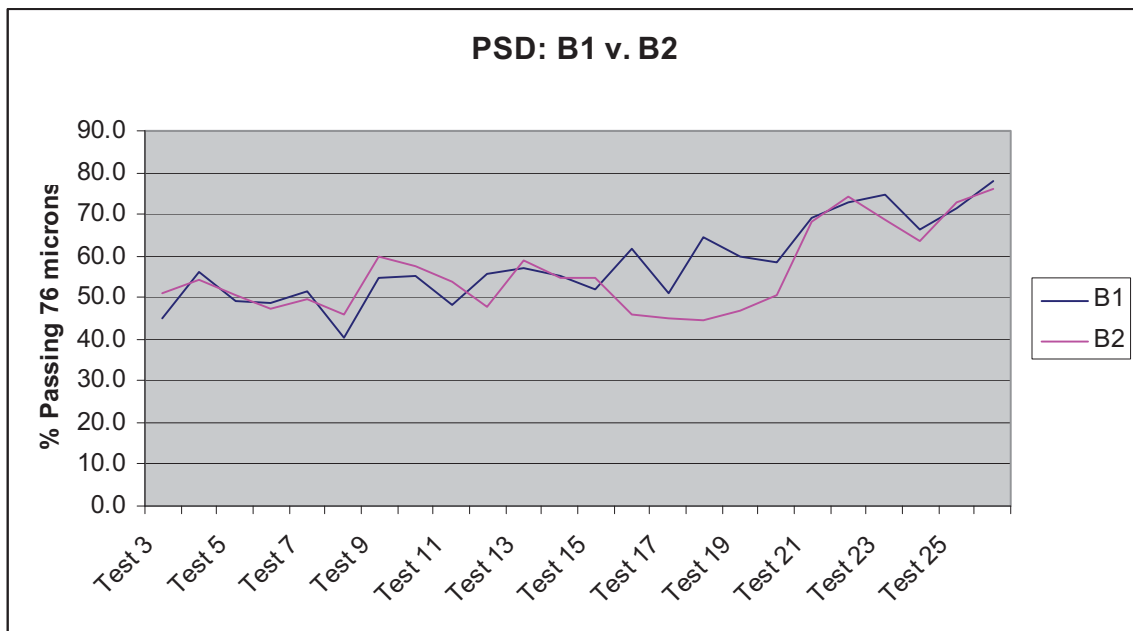


Figure 3.15. No consistent difference in the PSD76 between pipes B1 and B2.

4. Conclusions and Recommendations

4.1 Conclusions

Through a series of field tests at GVEA's Healy Unit #1, this project reached the following conclusions about low-rank high-volatile-content Alaskan coal:

- For PSD76 in the tested range (40–80), there is very little correlation between the PSD76 of pulverized coal and power plant efficiency.
- There is very little correlation between PSD76 and SO₂, NO_x, and CO.
- The data displayed a correlation between PSD and CO₂, with finer grinds resulting in higher concentration of CO₂. However, this correlation has been difficult to explain. It could be a new revelation or an artifact of measurement errors.
- Mill power consumption is greater when coal is ground more. Additionally, HGI and coal flow rate impact mill power consumption. Harder coal was found to consume more power than softer coal, and power consumption rose as the coal flow rate increased.
 - If coal were to be burned at a PSD76 of 50 instead of 70, the 28 MW Healy Unit #1 would see a savings of over \$56,000 per year.
- Total Hg emissions are very low.
- When the tests are split into two groups, one that averaged 50% passing 76 microns (the “coarse” group) and the other that averaged 73% passing 76 microns (the “fine” group), the following is observed:
 - There was a difference in the quality of coal in the two groups. The coal burned in the fine group had more moisture (17.4%) and less heating value (18,774 kJ/kg or 8078 BTU) compared with the coarse group (15.2% and 19,337 kJ/kg or 8320 BTU). On a HGI basis, the coal was harder in the coarse group (HGI=34) than in the fine group (HGI=37.8). The fixed carbon content was higher in the coarse group (32.3%) than in the fine group (29.5%). There was no difference in the ash and volatile contents.
 - The coarse group had higher unburned carbon in fly and bottom ash. However, this could be explained by its higher fixed carbon content.
 - The fine group had an efficiency of 23.75% compared with 23.05% for the coarse group. Given that the fine group only had six data points, the observed difference could be due to the very low number of tests in the fine group or due to differences in the coal type.
 - The coarse group had lower SO₂ emissions, though the two groups had similar sulfur contents.
- Observations not central to the project, but interesting nonetheless, include the following:
 - Pulverized coal samples that were underweight had PSD76 samples similar to recommended weight samples.
 - The PSD76 sometimes varied between pipes. The coal in pipe A1 was generally coarser than the coal in pipe A2.

4.2 Conclusions: Implications

This project has profound implications for the US coal and power industries, since a significant portion of the two industries involves coal (such as the Powder River Basin [PRB] coal) similar to the tested low-rank high-volatile-content Alaskan coal:

Help Sell Low-Rank Alaskan Coal

The primary conclusion of the project, that low-rank high volatile coal can be burned at a coarser particle size than the industry standard for bituminous coal, makes Alaskan coal attractive to utilities which otherwise are deterred by its hardness. This project implies that utilities can improve mill throughput simply by not grinding the coal as much. Alaska has had issues exporting its low-rank coal because of hardness concerns. This project will go a long way towards alleviating those concerns, and hopefully will help sell Alaskan coal to Pacific Rim and other nations, which would help the Alaskan economy.

Provide Significant Savings (\$\$\$) in Energy Costs

Another important implication is the cost savings with coarser grind, which, as the cost of energy rises, will become substantial. The savings for GVEA, which is a relatively small utility, is not insignificant (over \$56,000/year). The savings for larger utilities around the country would be substantially greater, though plants burning blends would see less in savings.

Reduce CO₂ Emissions

Though CO₂ emissions were specifically not the focus of this project, it may be that the most important, though currently dubious, conclusion of the project is that CO₂ emissions are related to the PSD of low-rank coal. In the near future, CO₂ emissions will prove very expensive to utilities. What the project data imply is that by simply burning low-rank high-volatile-content coal at a coarser grind, a utility could reduce its emissions by as much as 8% without incurring any cost or lowering plant efficiency. Power plants burning tested-type coal as part of a blend will not see the entire benefit. Still, given that PRB coals amount to approximately 40% of the coal-based electricity in the US⁴, the savings or prevented-cost is huge. According to the US DOE⁵, the cost of CO₂ removal is in the \$27/ton to \$70/ton range. An 8% reduction in CO₂ generation will result, therefore, in substantial prevented-cost.

Unfortunately, as mentioned before, the CO₂ projections from this project are just observations rather than phenomena explained by other data/observations. That is because this research project was never designed to conduct a carbon mass balance, something that would be essential to make firm conclusions on CO₂ emissions. However, given the importance of the issue and the fact that observed data cannot, and should not, be dismissed, this significant observation/conclusion needs more fundamental research for verification and explanation.

⁴ http://en.wikipedia.org/wiki/Powder_River_Basin

⁵ http://www.netl.doe.gov/technologies/carbon_seq/FAQs/benefits.html#

4.3 Recommendations

It is recommended that

- power plants that burn low-rank high-volatile-content coals examine the effect of burning their coals coarser. It is possible that power plants may stand to benefit from grinding the coal less.
- the US DOE initiates a research project examining the relationship between the PSD76 of low-rank high-volatile-content coal and CO₂ emissions.

References

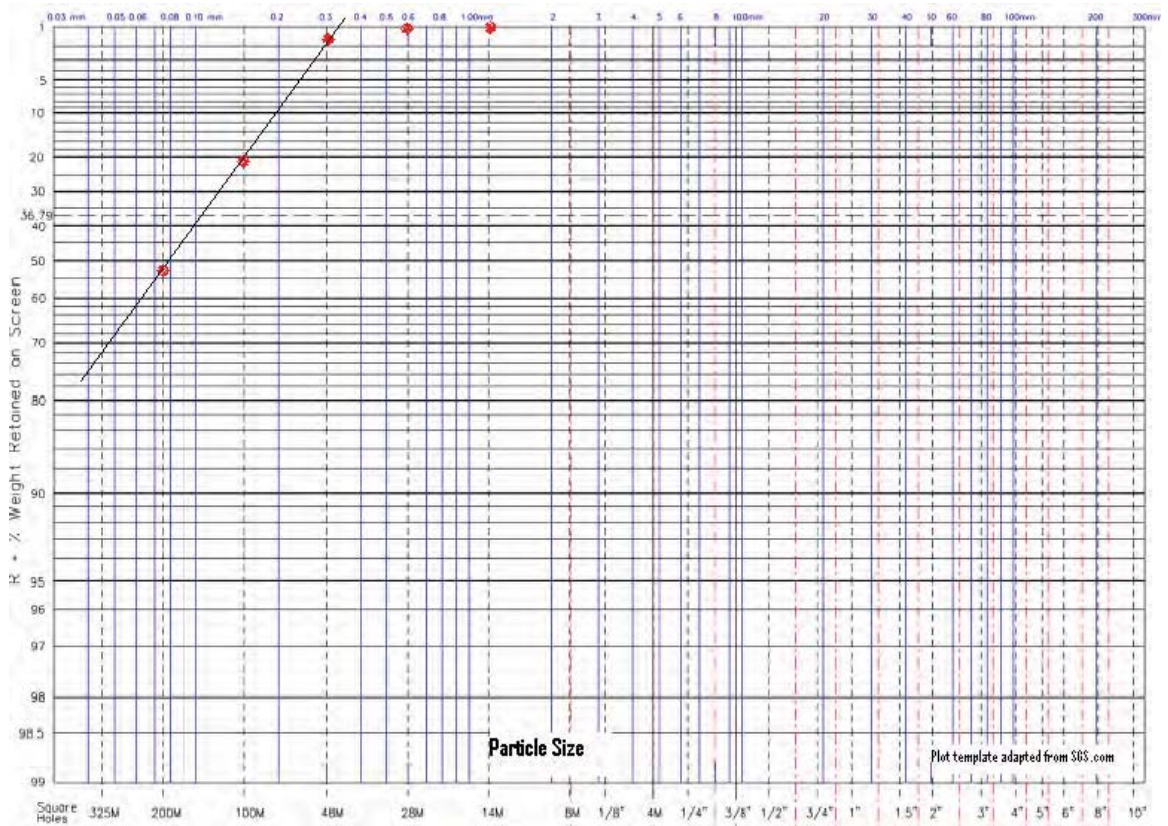
- Carpenter, A.M., Niksa, S., Scott, D.H., and Wu, Z. 2007. *Fundamentals of coal combustion*. IEA Clean Coal Centre 2007. Online publication (www.coalonline.org).
- Freeman, M., Smouse, S., and Walbert, G. 1996. *Preliminary Combustion Test Results of Alaskan/Russian Blends*. US Dept of Energy – National Energy Technological Laboratory.
- Ganguli, R., and Bandopadhyay, S. 2008. Field scale investigation of pulverized coal mill power consumption. *Minerals and Metallurgical Processing* 25(3):139–142.
- Malav, D. 2005. Low rank high volatile matter sub-bituminous coal grinding versus power plant performance. M.S. thesis, University of Alaska Fairbanks, Fairbanks, AK.
- Malav, D., Ganguli, R., Dutta, S., and Bandopadhyay, S. 2008. Non-impact of particle size distribution on power generation at a pulverized coal power plant burning low rank Alaska coal. *Journal of Fuel Processing Technology* 89(5):499–502.

List of Acronyms and Abbreviations

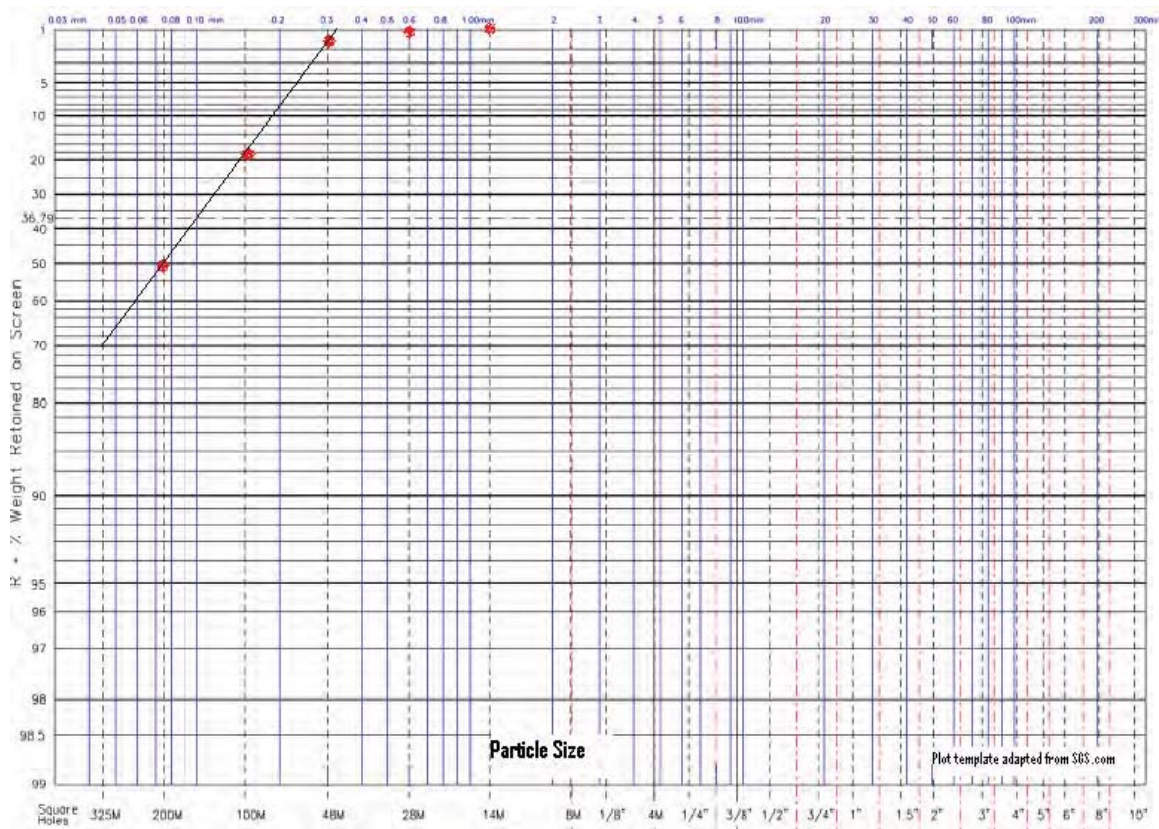
CEMS	Continuous emissions monitoring system
GVEA	Golden Valley Electric Association
HGI	Hardgrove grindability index
MW	Megawatt
MWT	Mann-Whitney Test
PSD	Particle size distribution
PSD76	A specific PSD: percentage passing 76 microns (200 mesh)
UAF	University of Alaska Fairbanks
UCM	Usibelli Coal Mine
US DOE	United States Department of Energy

Appendix I: Rosin-Rammler Plots

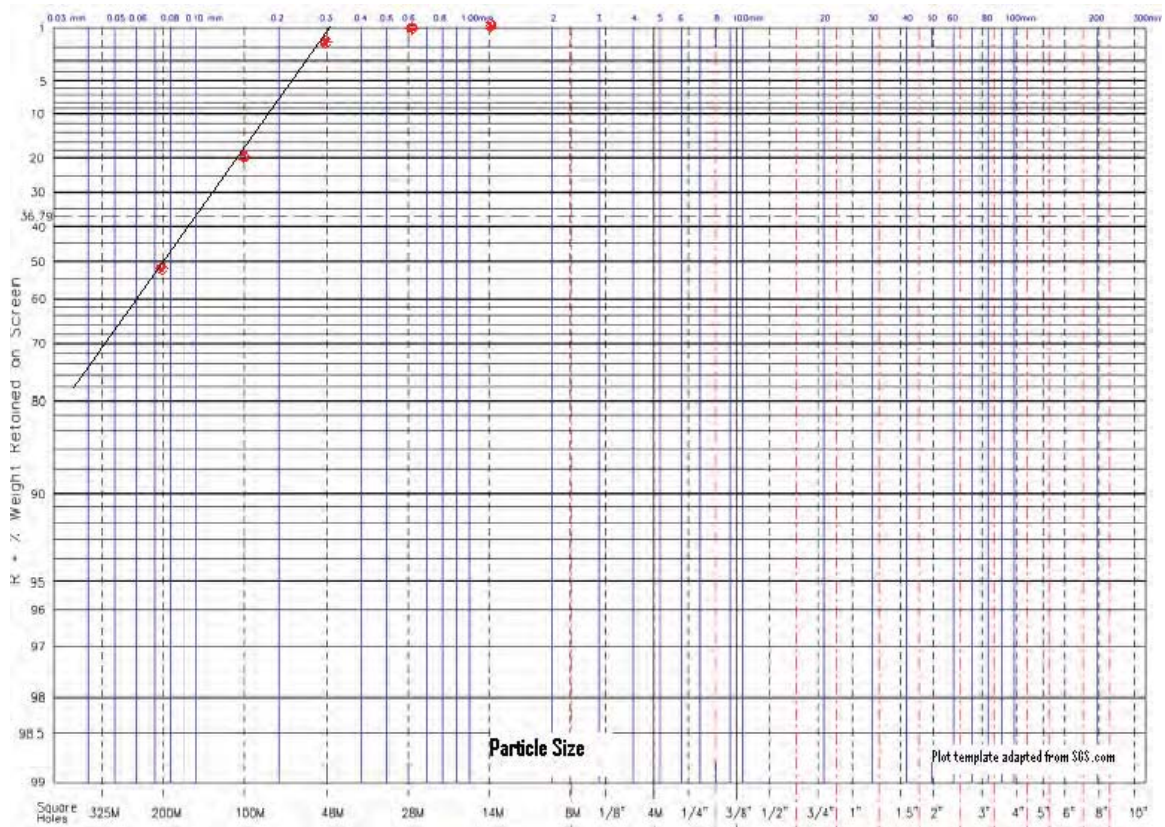
Test 3



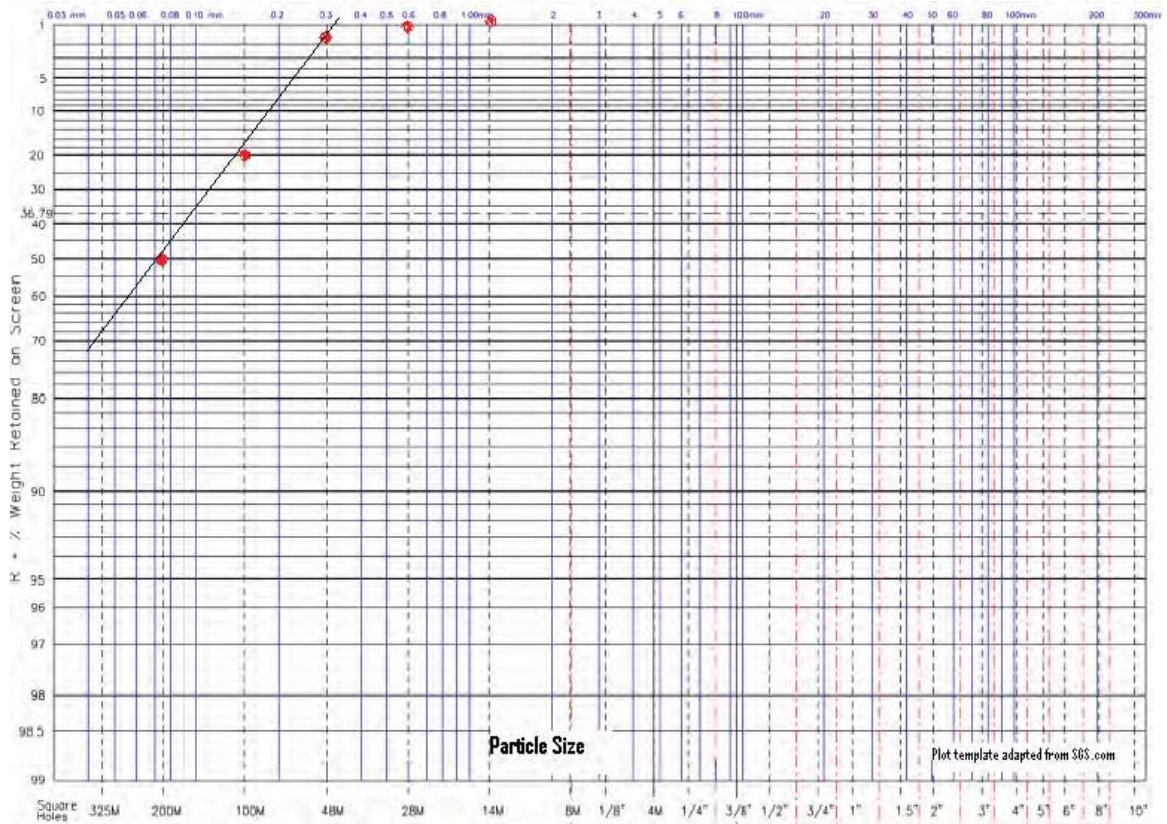
Test 4



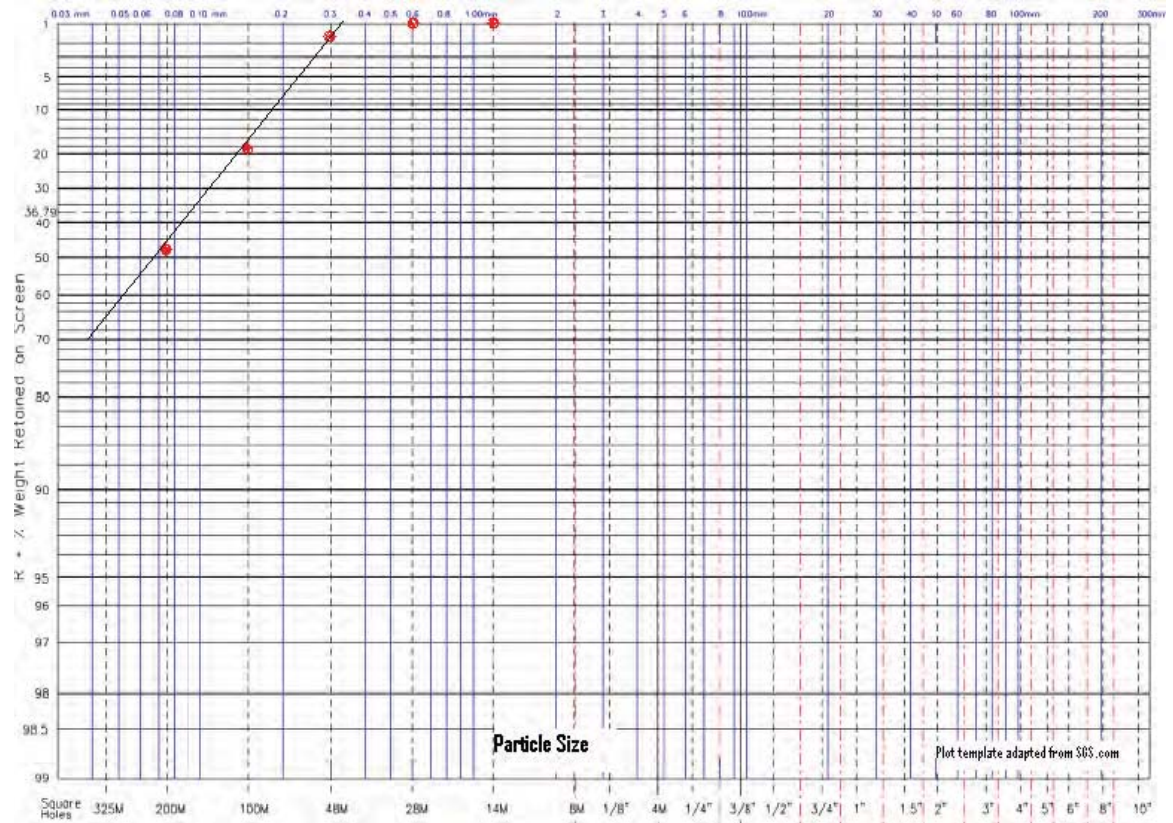
Test 5



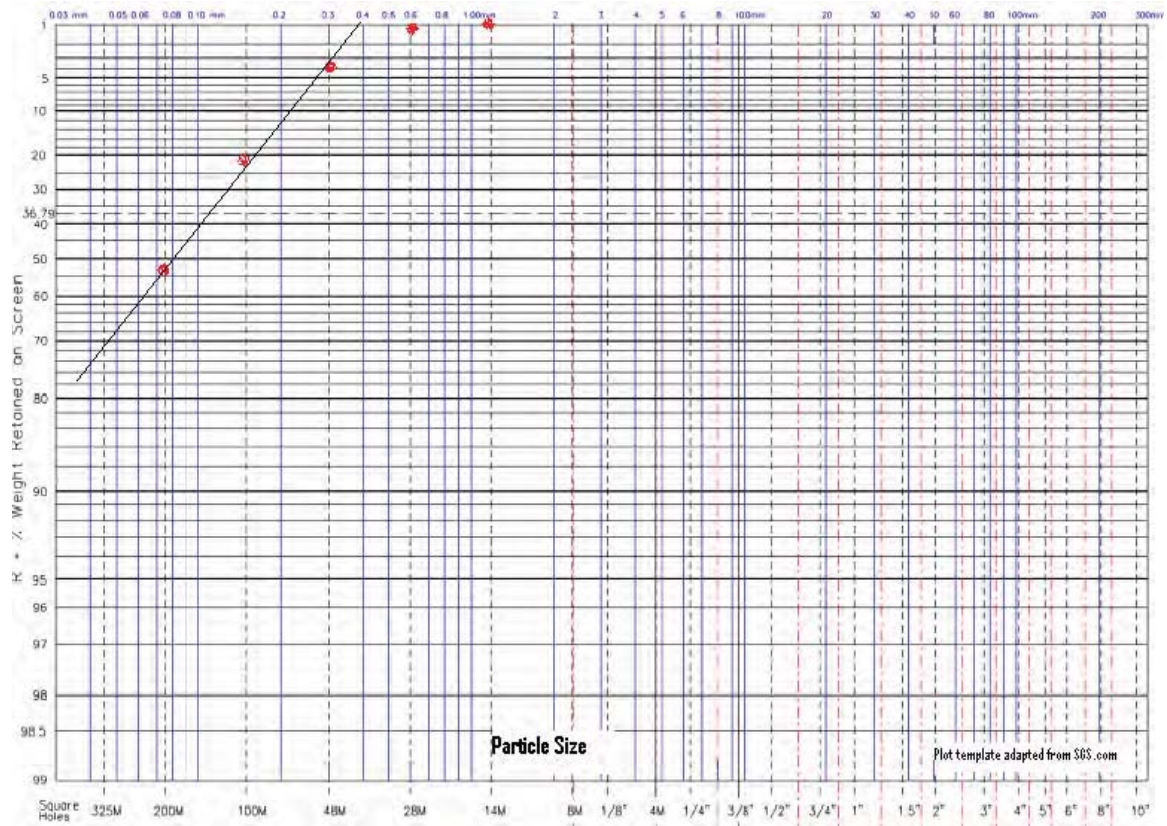
Test 6



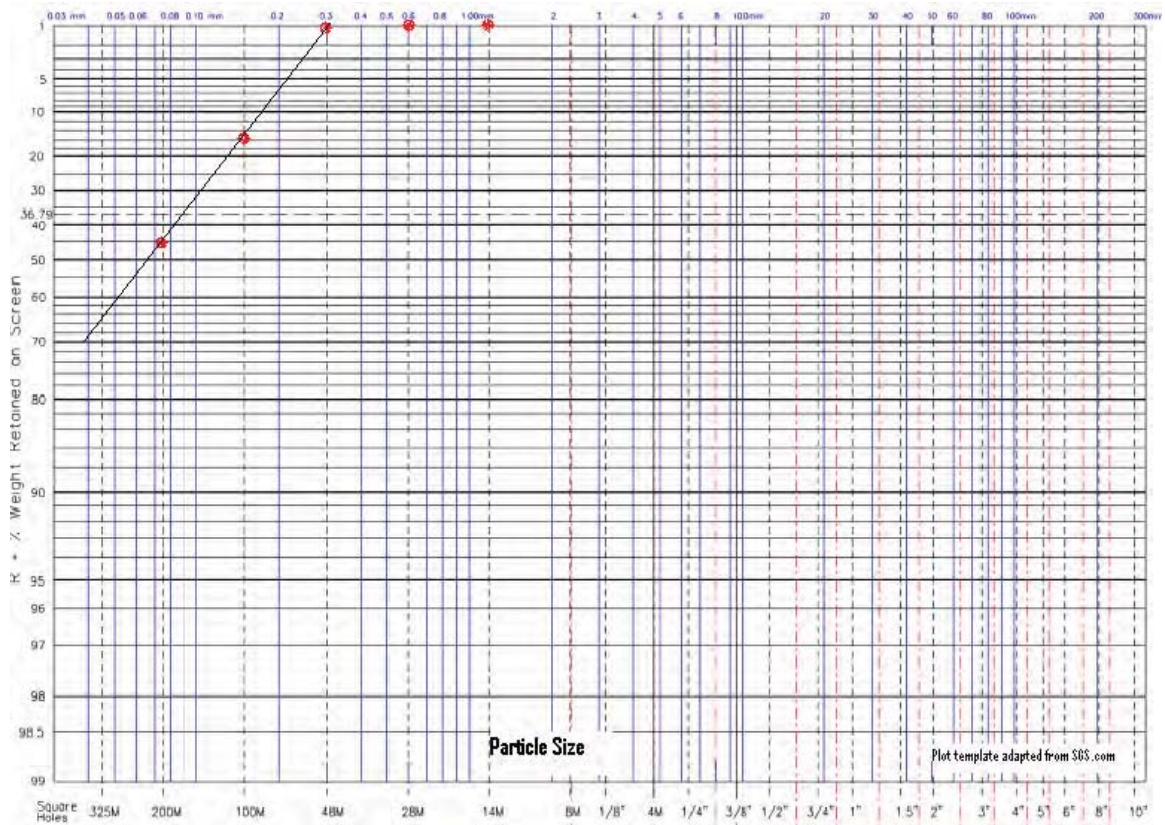
Test 7



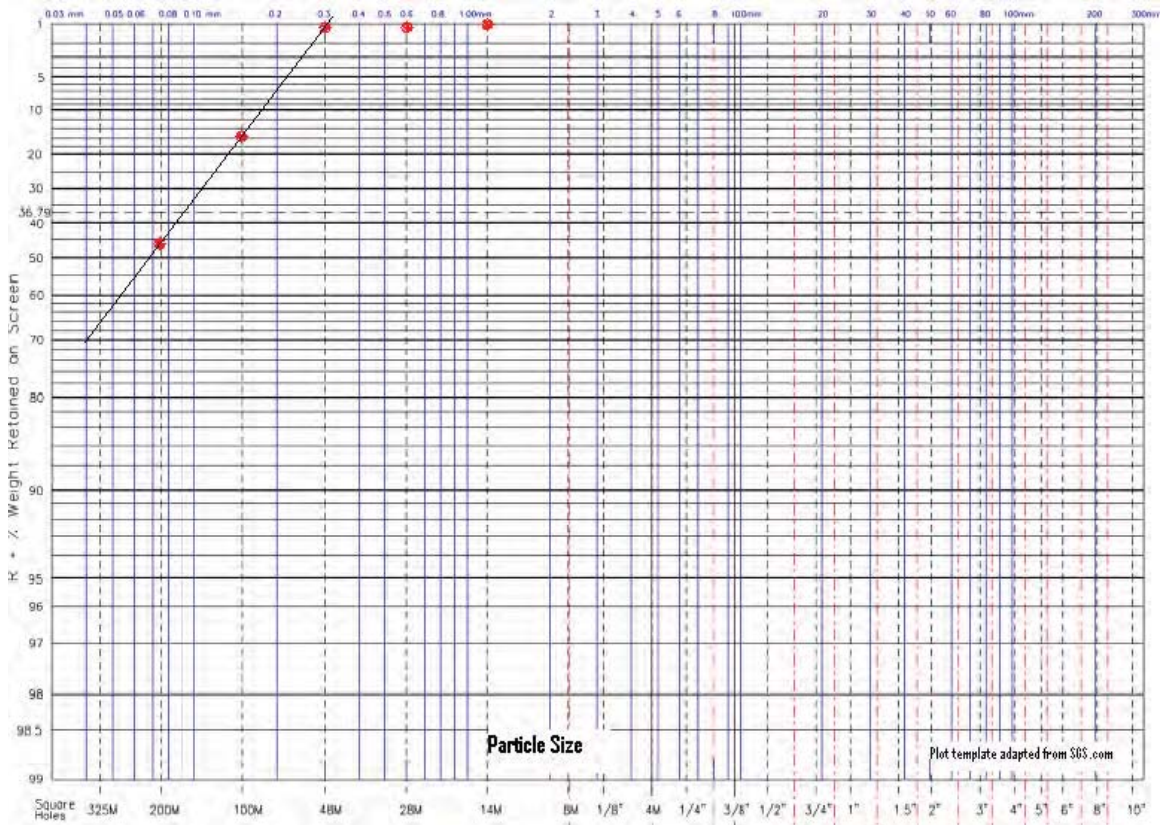
Test 8



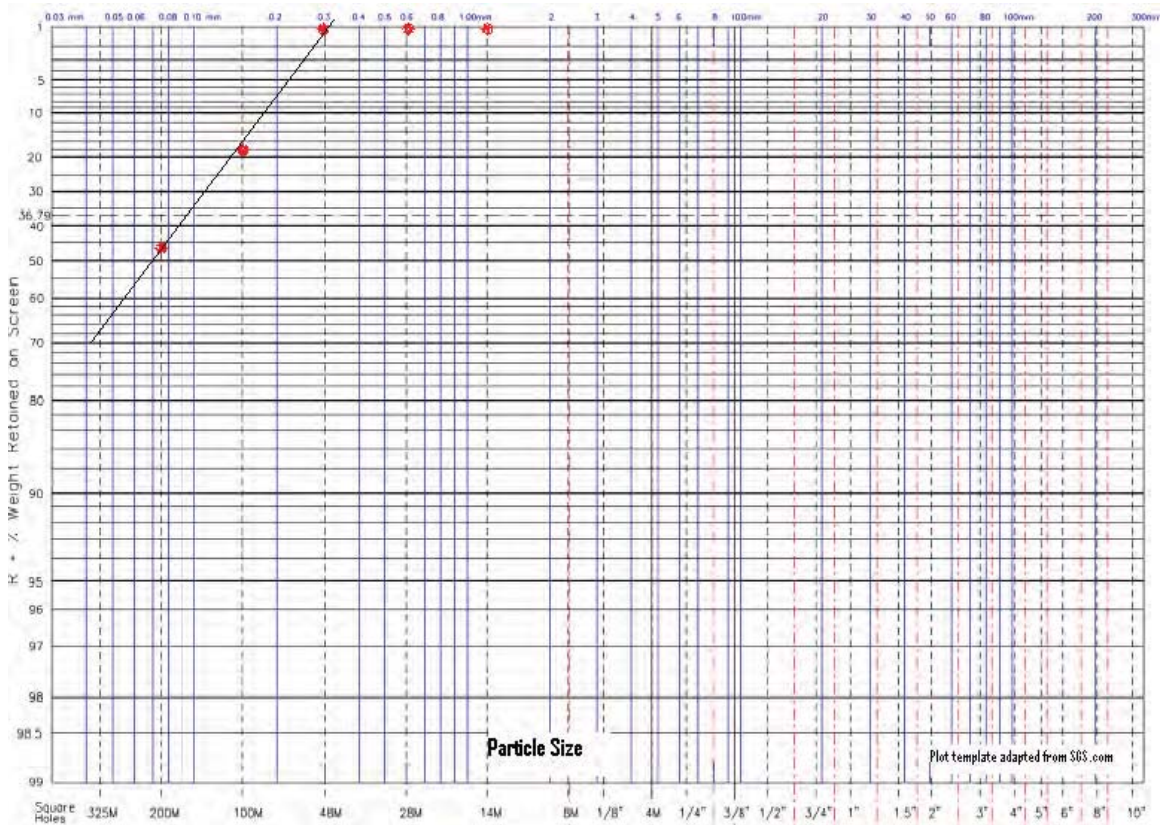
Test 9



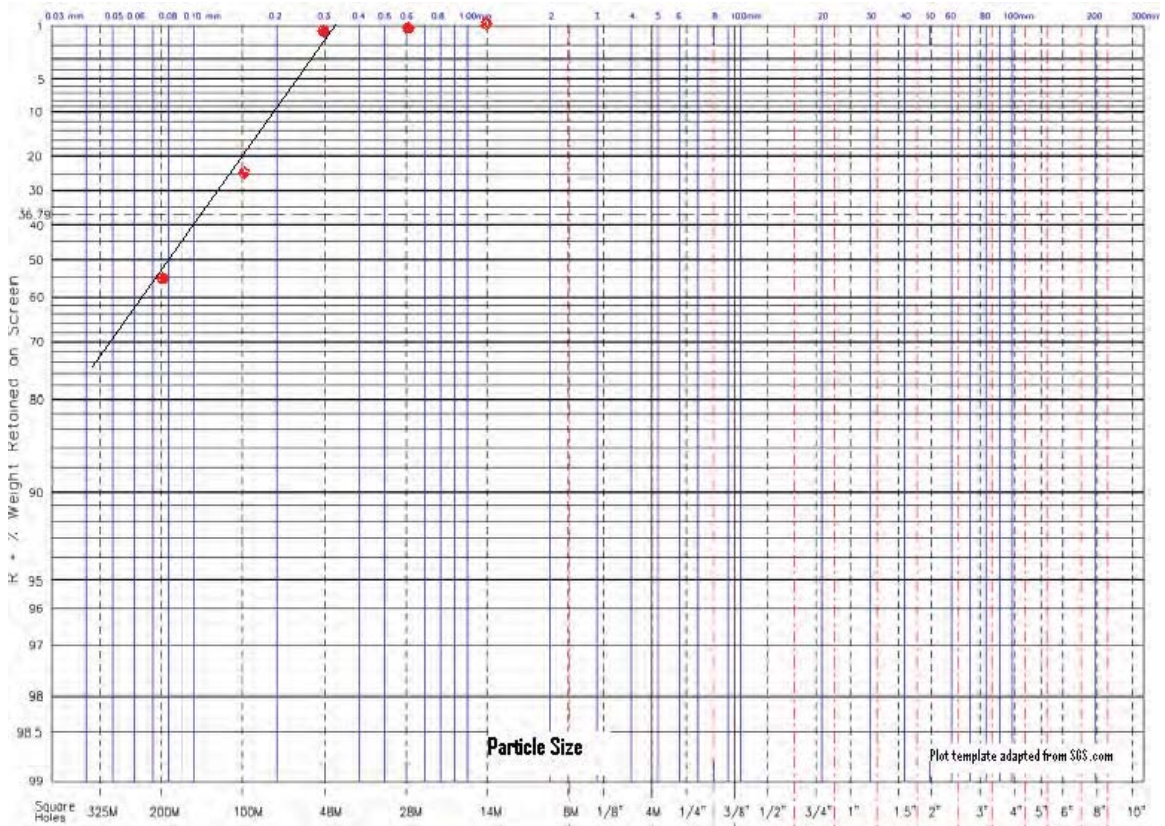
Test 10



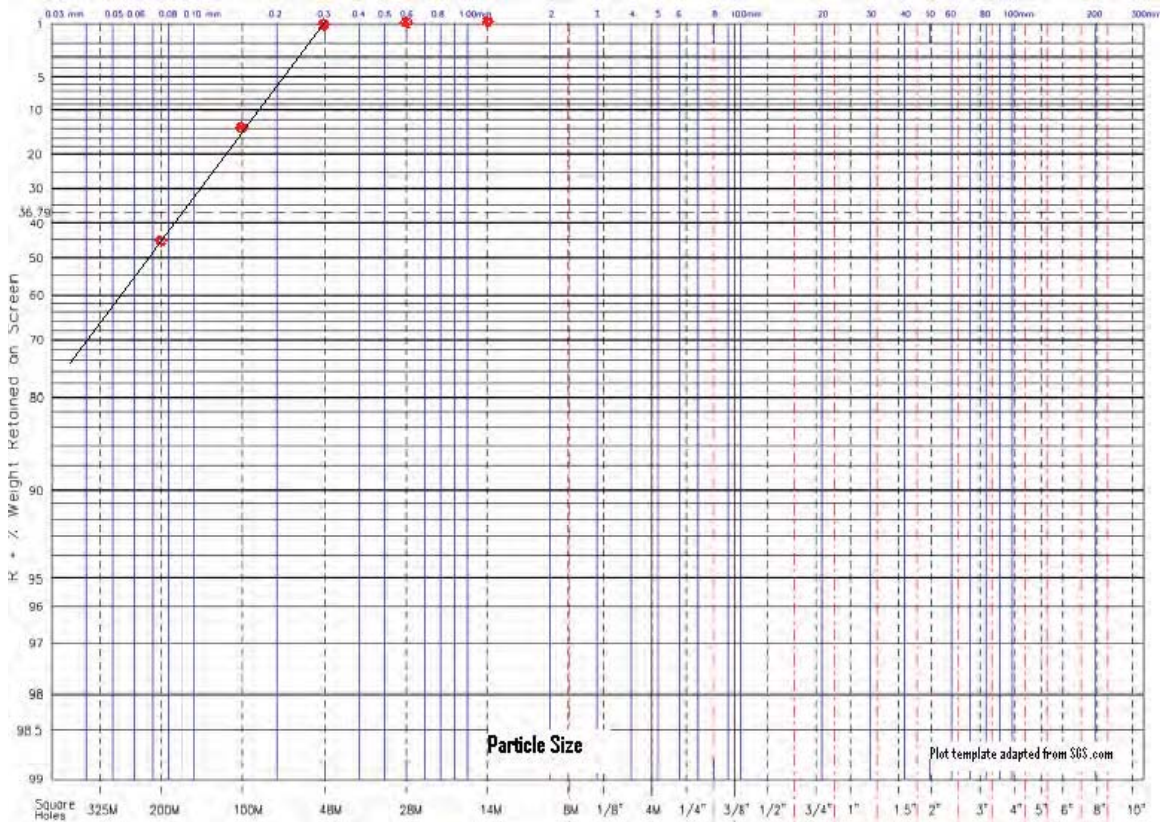
Test 11



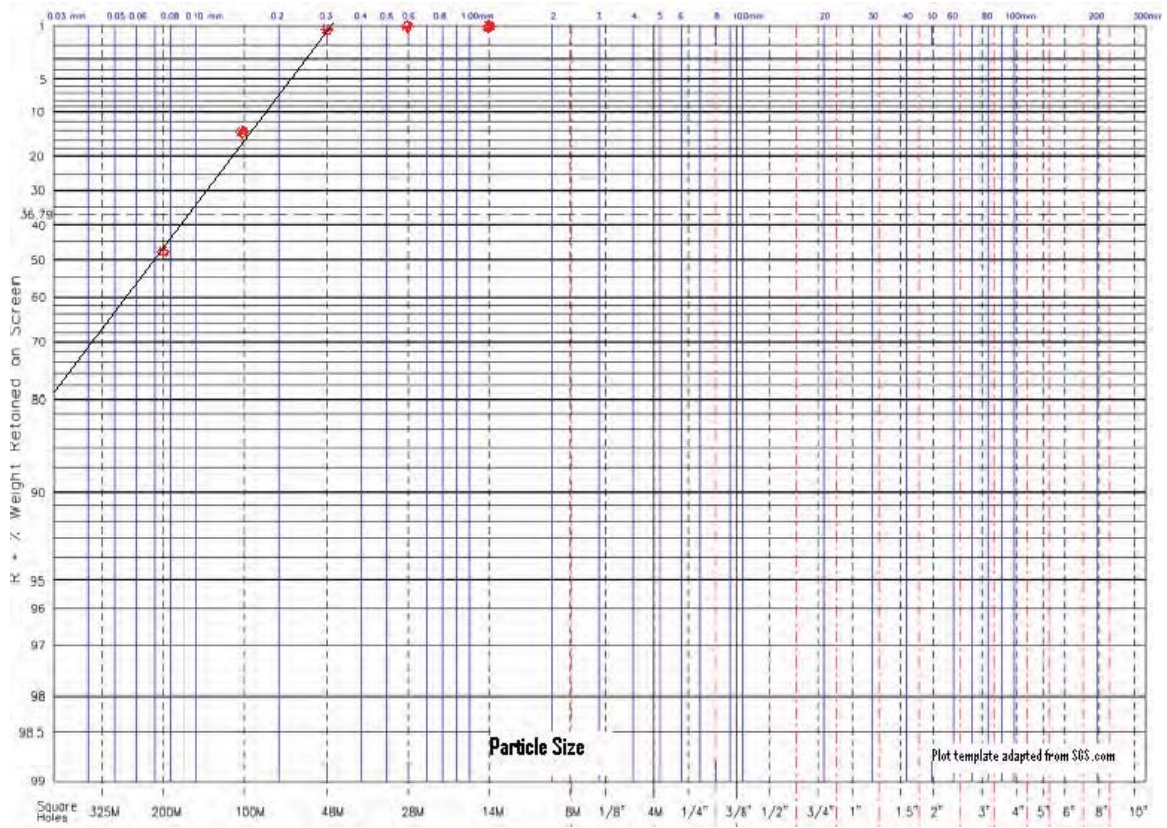
Test 12



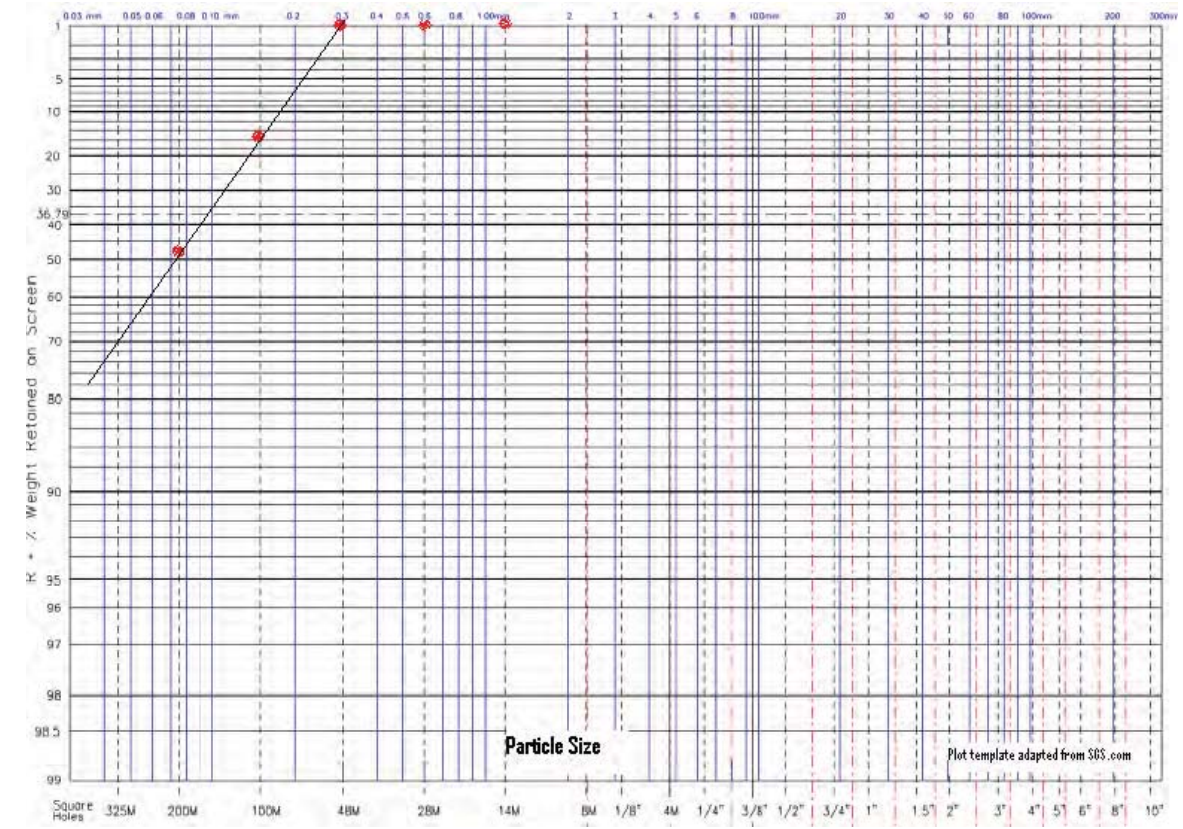
Test 13



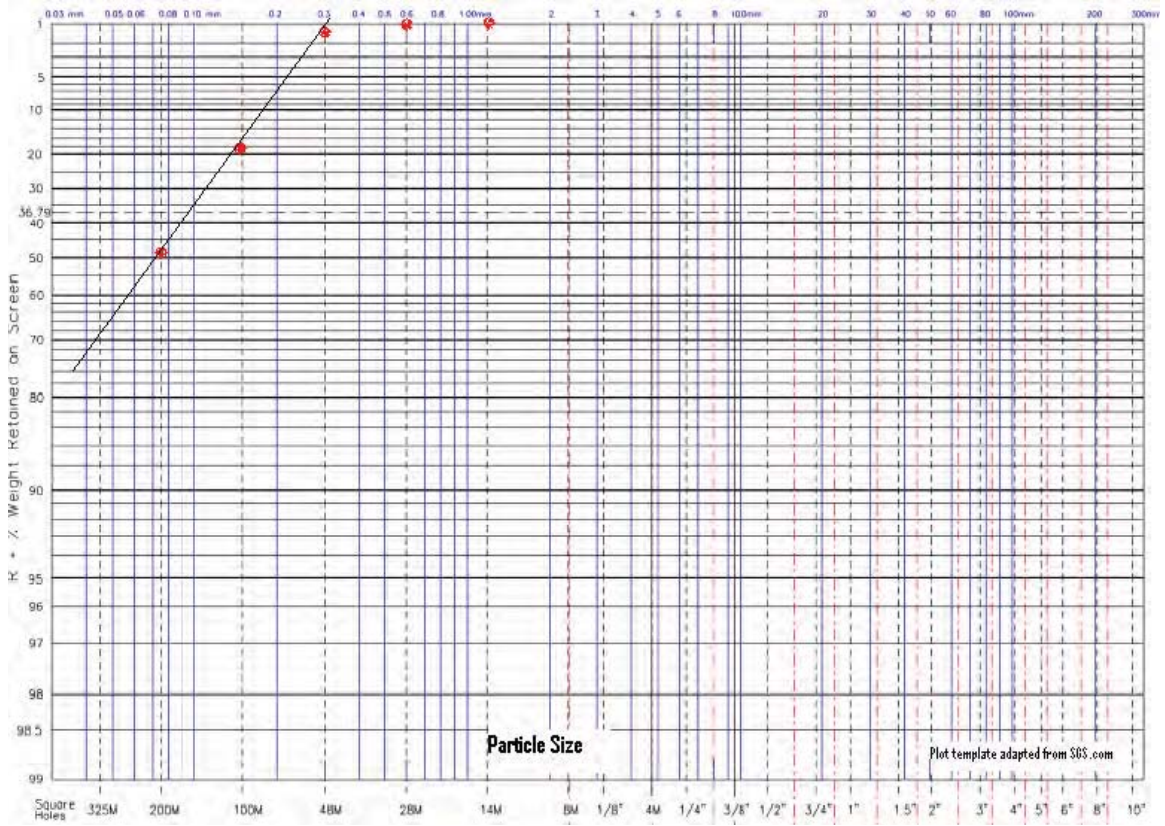
Test 14



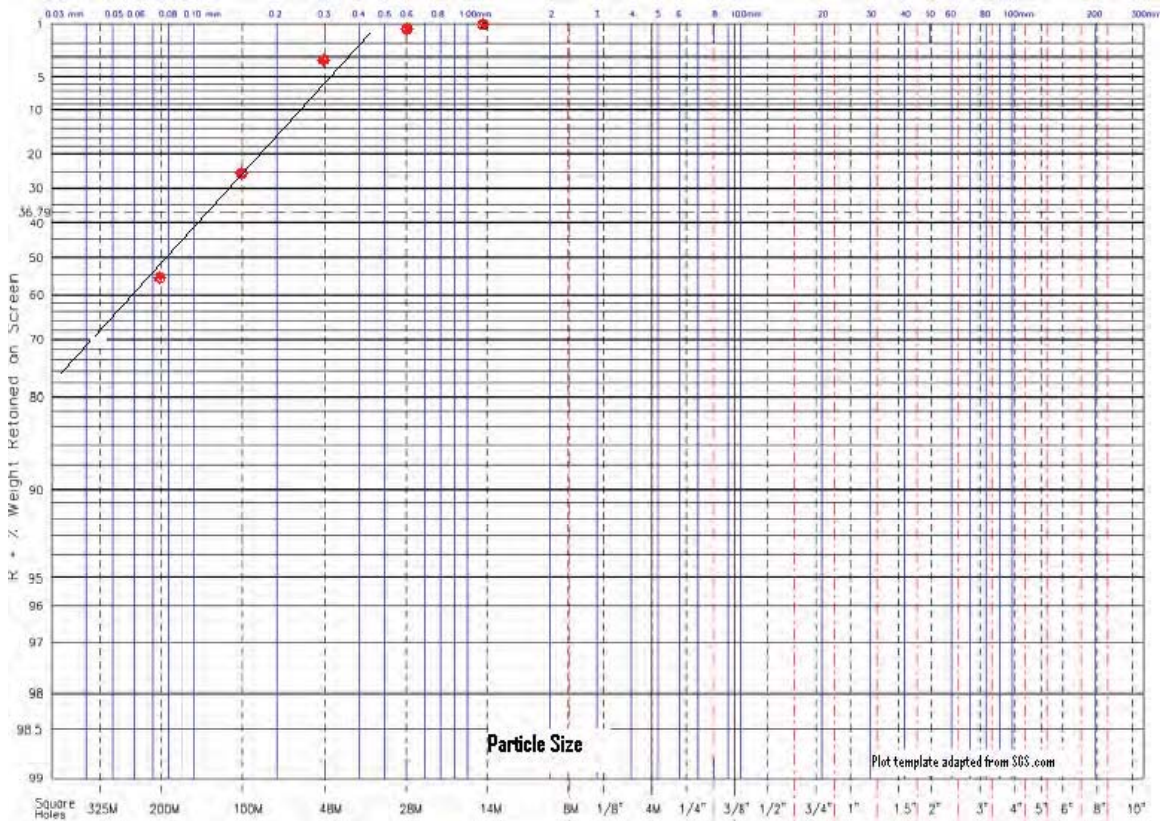
Test 15



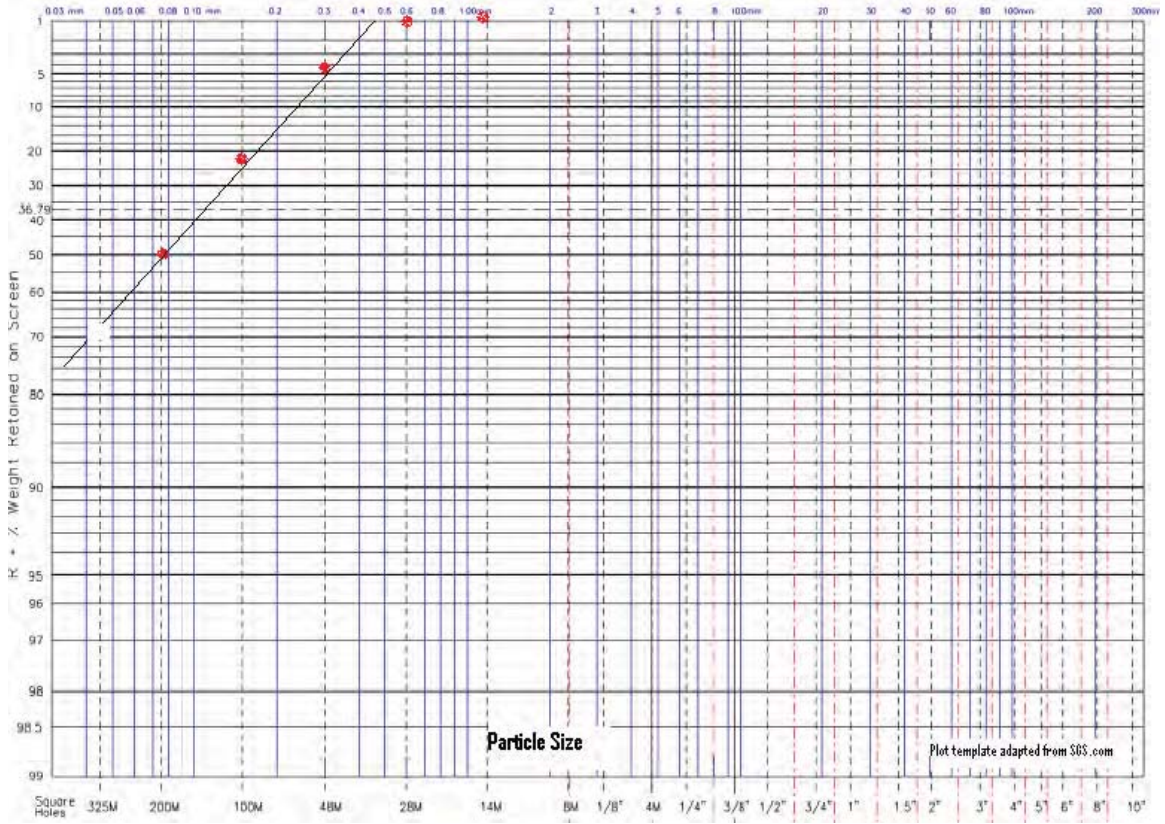
Test 16



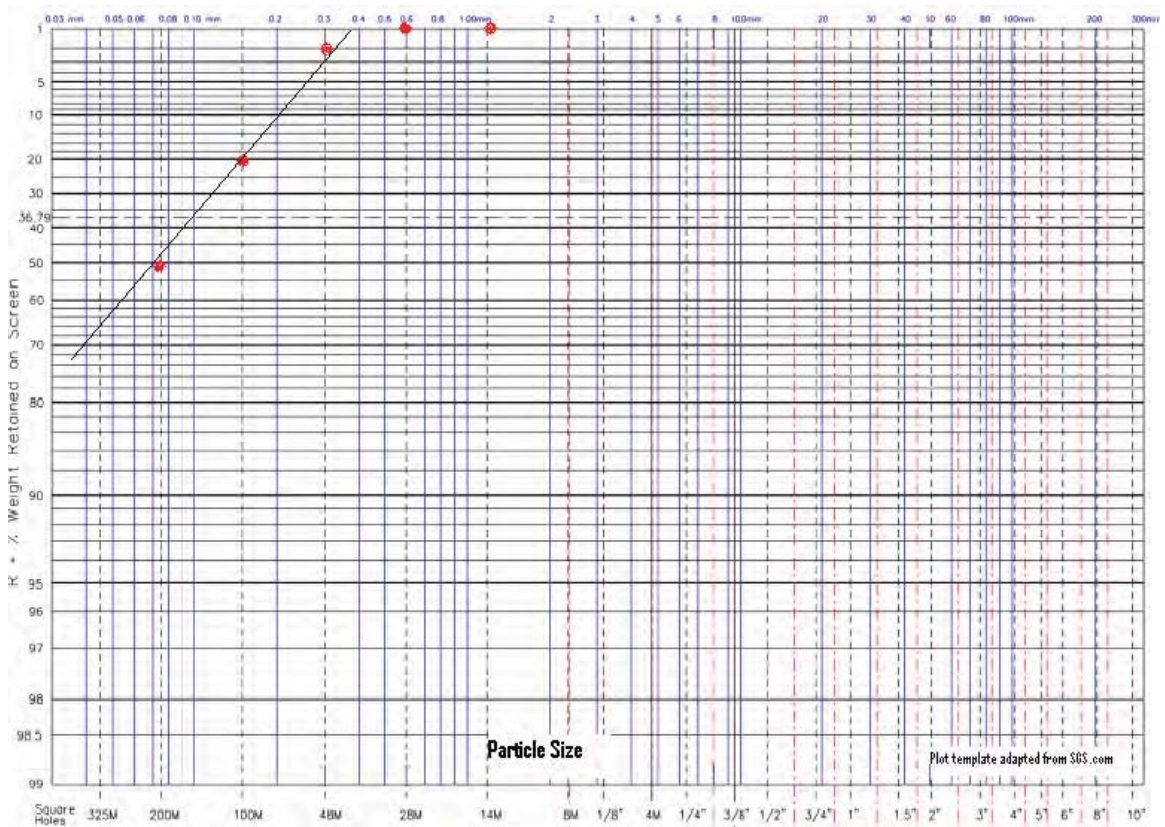
Test 17



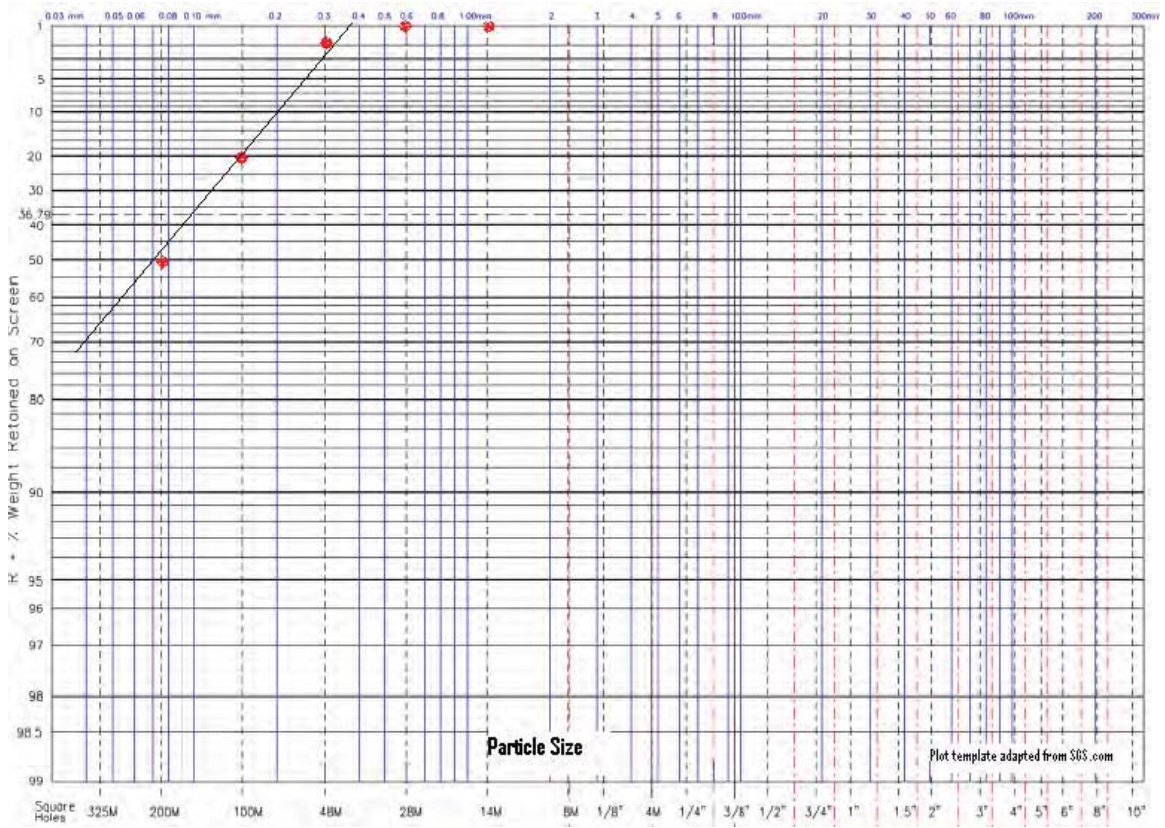
Test 18



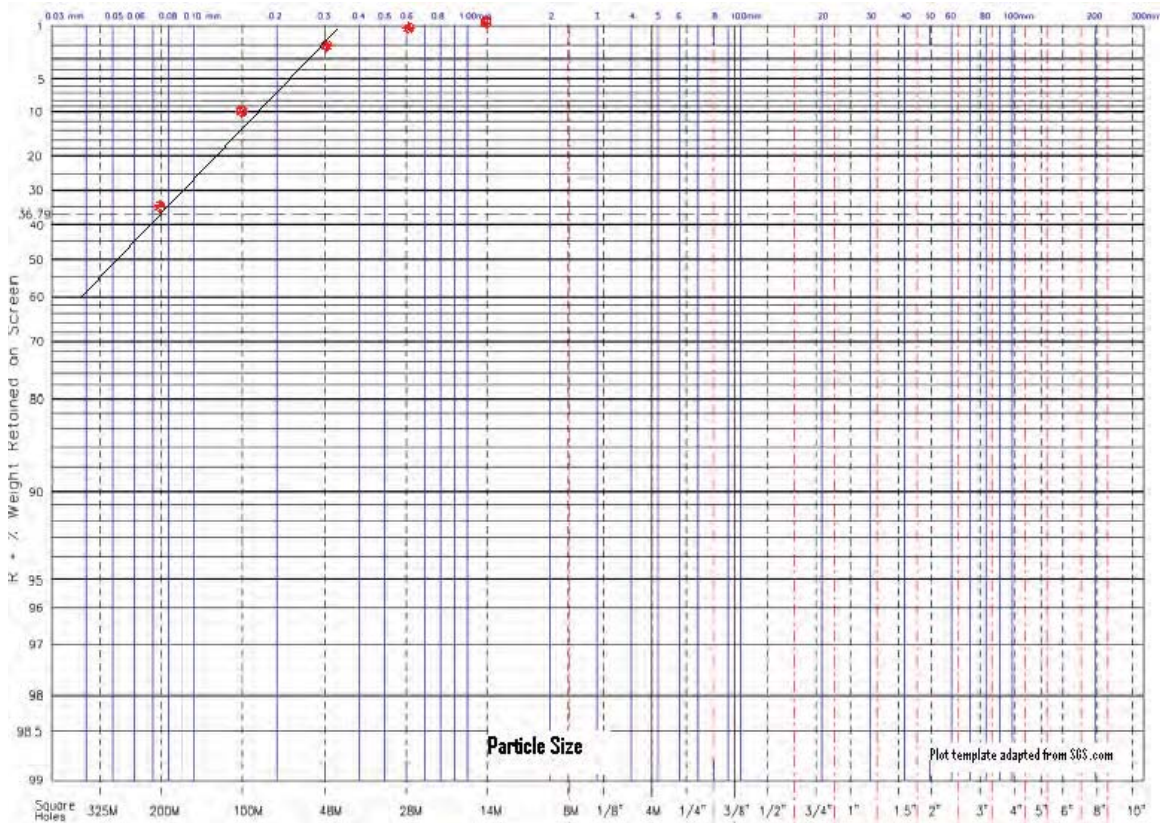
Test 19



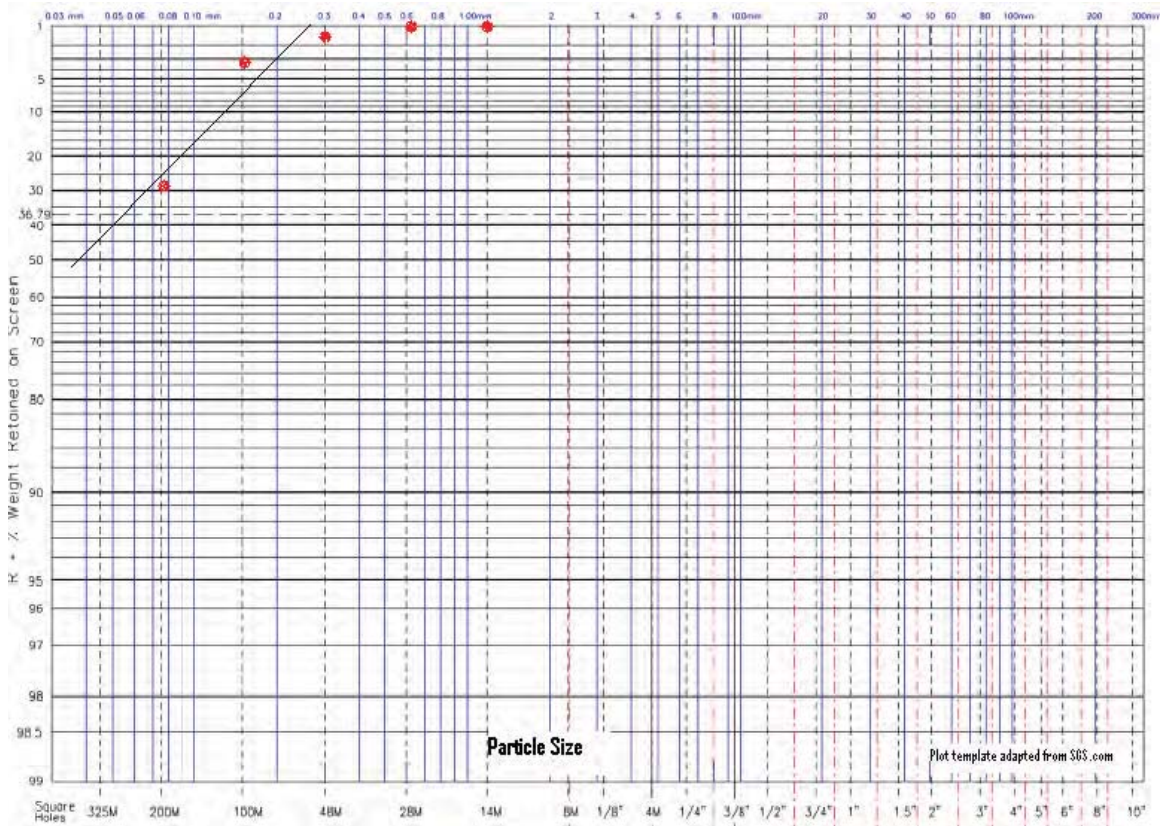
Test 20



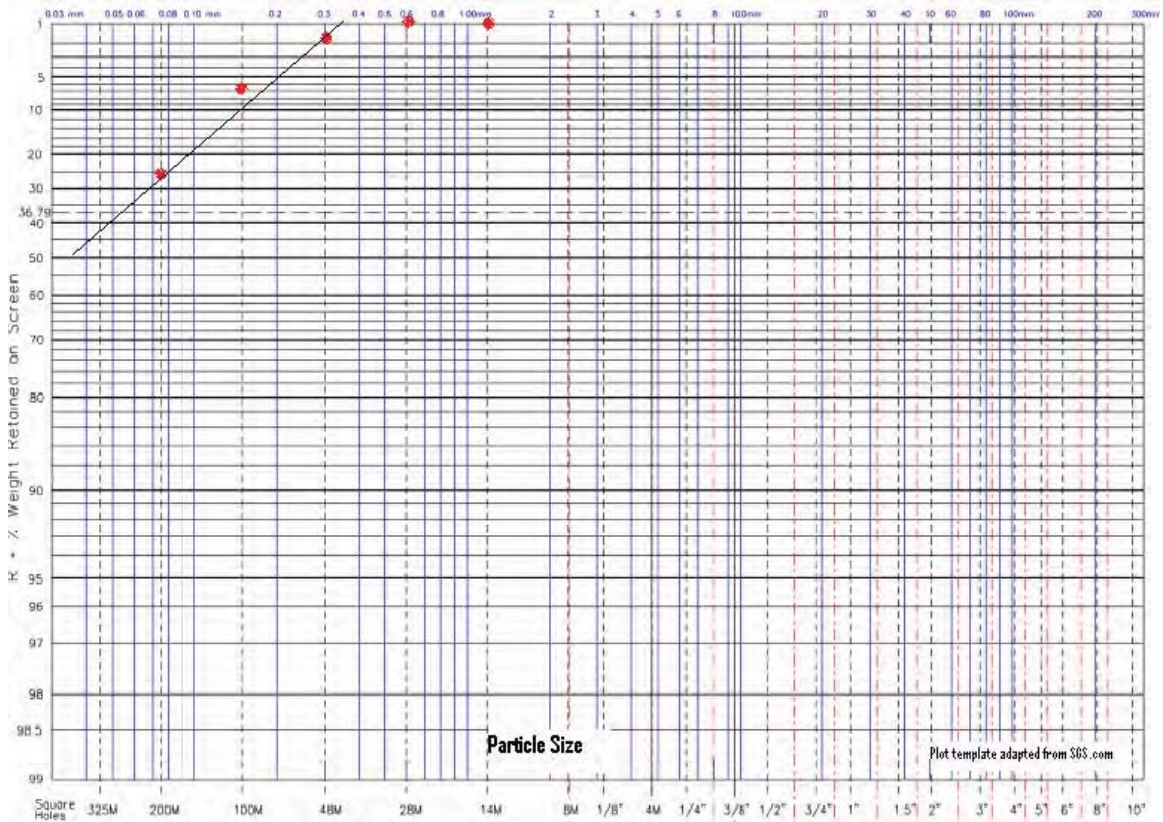
Test 21



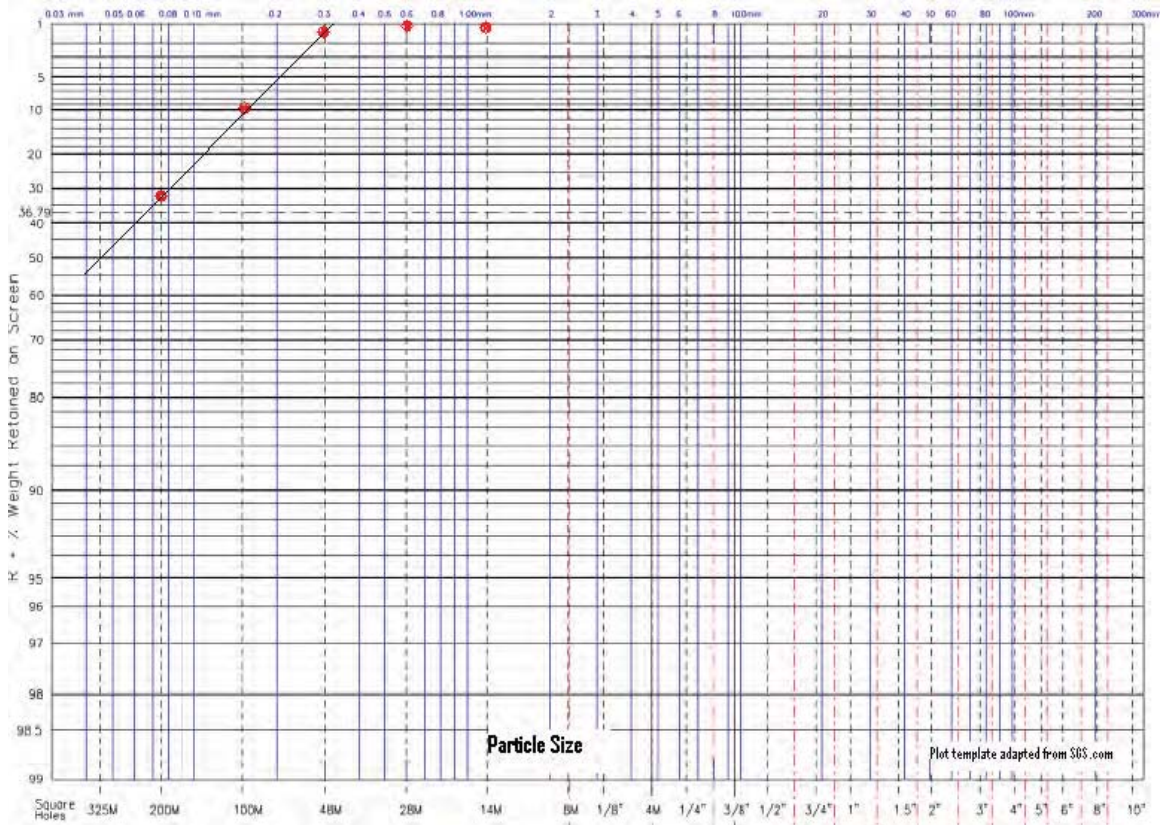
Test 22



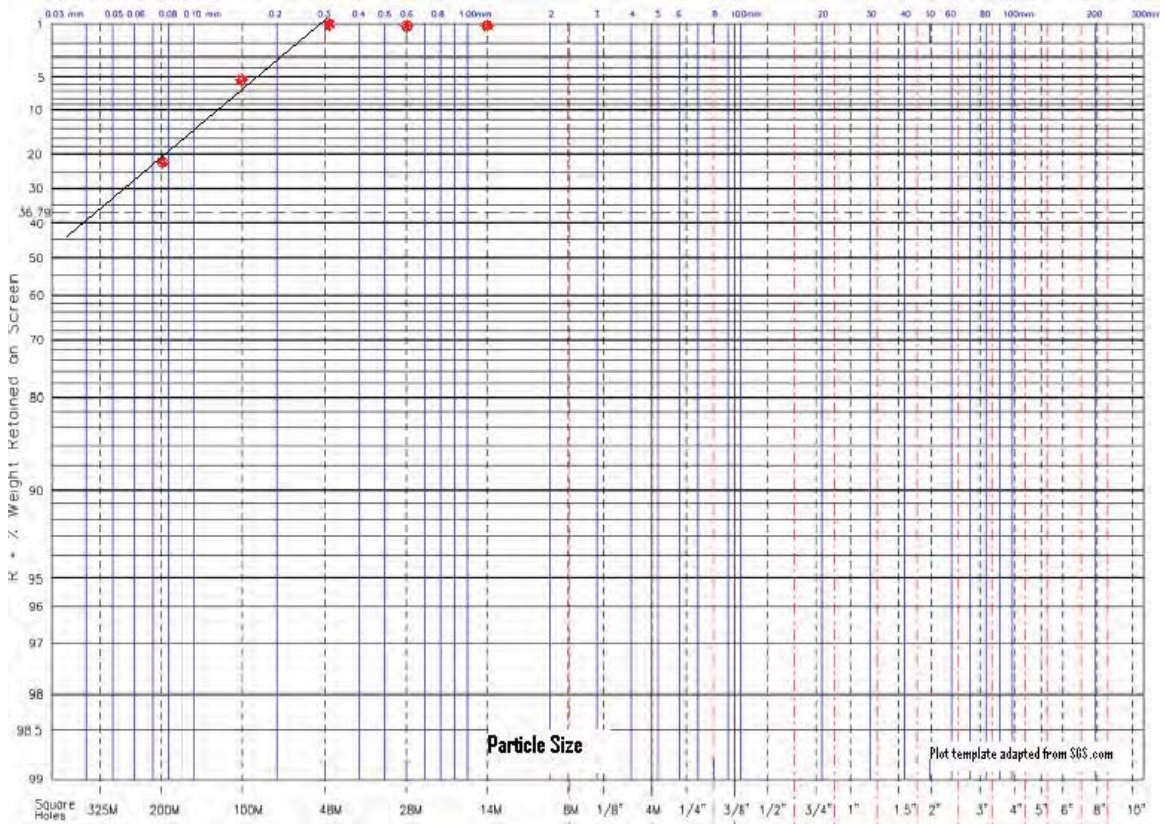
Test 23



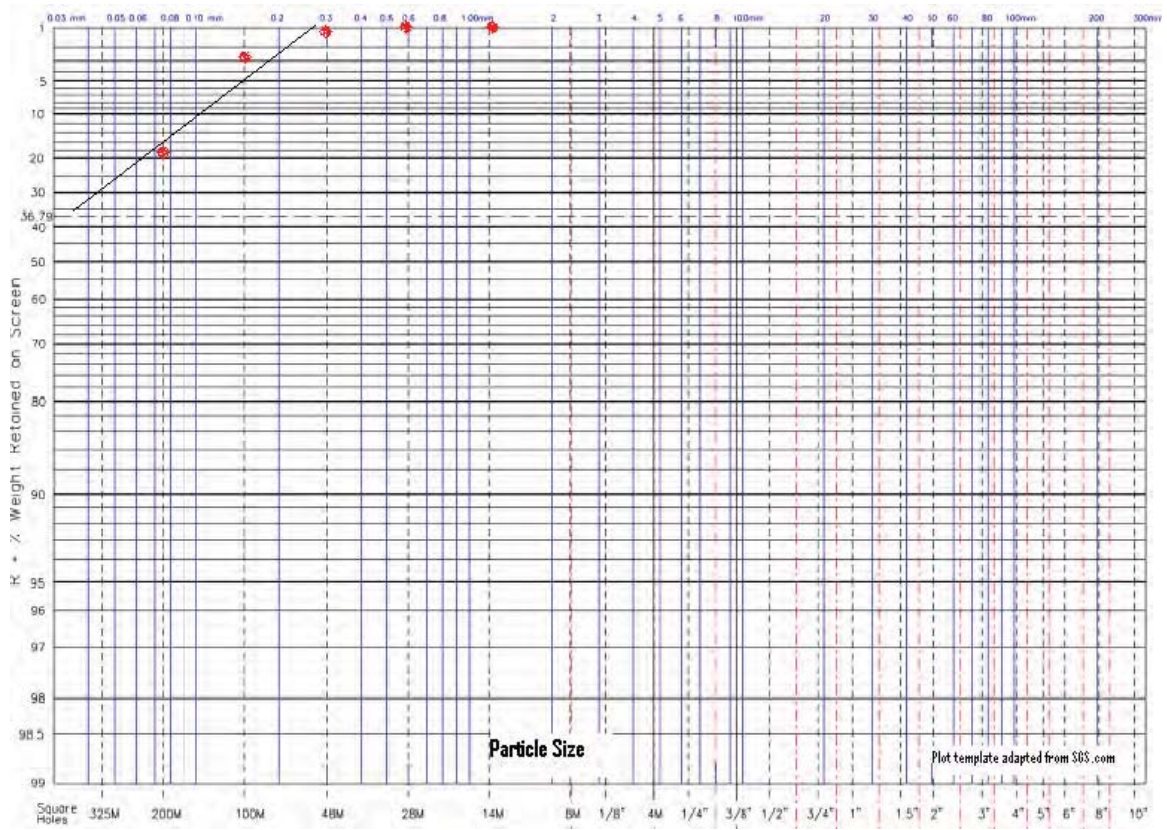
Test 24



Test 25



Test 26



Oil & Natural Gas Technology

DOE Award No.: DE-FC26-06NT41248

Final Report

Project Title

Submitted by:
Richard Wies, Ph.D.
University of Alaska Fairbanks
PO Box 755910
Fairbanks, AK 99775-5910

Prepared for:
United States Department of Energy
National Energy Technology Laboratory

December 17, 2008



Office of Fossil Energy



Effects of Village Power Quality on Fuel Consumption and Operating Expenses

Final Report

Report Period Start: 8/2002
Report Period End: 9/2008

Principal Author(s): Richard Wies and Ron Johnson

Issued: September 2008

DOE Award Number: DE-FC26-01NT41248
Task: 1.03.1

Submitting Organization and Subrecipient:

University of Alaska Fairbanks
Institute of Northern Engineering
Arctic Energy Technology and Development Laboratory
PO Box 755910
Fairbanks, AK 99775-5910

Alaska Energy Authority
813 West Northern Lights Blvd.
Anchorage, AK 99503

DISCLAIMER --

“This report was prepared as an account of work sponsored by an agency of the United States Government. Neither the United States Government nor any agency thereof, nor any of their employees, makes any warranty, express or implied, or assumes any legal liability or responsibility for the accuracy, completeness, or usefulness of any information, apparatus, product, or process disclosed, or represents that its use would not infringe privately owned rights. Reference herein to any specific commercial product, process, or service by trade name, trademark, manufacturer, or otherwise does not necessarily constitute or imply its endorsement, recommendation, or favoring by the United States Government or any agency thereof. The views and opinions of authors expressed herein do not necessarily state or reflect those of the United States Government or any agency thereof.”

Abstract

Alaska's rural village electric utilities are isolated from the Alaska railbelt electrical grid intertie and from each other. Different strategies have been developed for providing power to meet demand in each of these rural communities. Many of these communities rely on diesel electric generators (DEGs) for power. Some villages have also installed renewable power sources and automated generation systems for controlling the DEGs and other sources of power. For example, Lime Village has installed a diesel battery photovoltaic hybrid system, Kotzebue and Wales have wind-diesel hybrid systems, and McGrath has installed a highly automated system for controlling diesel generators. Poor power quality and diesel engine efficiency in village power systems increases the cost of meeting the load. Power quality problems may consist of poor power factor (PF) or waveform disturbances, while diesel engine efficiency depends primarily on loading, the fuel type, the engine temperature, and the use of waste heat for nearby buildings. These costs take the form of increased fuel use, increased generator maintenance, and decreased reliability. With the cost of bulk fuel in some villages approaching \$1.32/liter (\$5.00/gallon) a modest 5% decrease in fuel use can result in substantial savings with short payback periods depending on the village's load profile and the cost of corrective measures. This project over its five year history has investigated approaches to improving power quality and implementing fuel savings measures through the use of performance assessment software tools developed in MATLAB[®] Simulink[®] and the implementation of remote monitoring, automated generation control, and the addition of renewable energy sources in select villages. The results have shown how many of these communities would benefit from the use of automated generation control by implementing a simple economic dispatch scheme and the integration of renewable energy sources such as wind generation.

Table of Contents

Title Page.....	i
Disclaimer	ii
Abstract.....	iii
Table of Contents.....	iv
List of Figures	vi
List of Tables.....	viii
1: Introduction	1
2: Executive Summary	3
3: Experimental	5
3.1 Consortium of Alaska Rural Utilities.....	5
3.2 RTU, Temperature Sensor and Flow Meter Testing at UAF	5
3.2.1 RTU.....	6
3.2.2 Temperature Sensors	6
3.2.3 Coolant Flow Meters	7
3.2.3.1 Turbine Flow Meter	7
3.2.3.2 Magnetic Flow Meter.....	8
3.2.3.3 Ultrasonic Flow Meter	8
3.2.4 Instantaneous Fuel Flow.....	9
3.2.4.1 Fuel Flow Using Ultrasonic Flow Meter.....	9
3.2.4.2 Fuel Flow using Day Tank Volume	9
3.2.5 Exhaust Flow	10
3.2.6 Electrical Outputs.....	10
3.2.7 Energy Balance of DEG Plant	11
3.3 Village Power System Survey and Data Collection.....	12
3.4 Installation of Remote Monitoring Equipment	13
3.5 System Models	13
3.5.1 Hybrid Power System Models	13
3.5.1.1 Overall Hybrid Model	13
3.5.1.1.1 DEG Model	14
3.5.1.1.1.1 Optimization of DEG Model.....	17
3.5.1.1.1.2 Heat Exchanger Model.....	19
3.5.1.1.1.3 Boiler Model.....	21
3.5.1.1.1.4 WTG Model.....	21
3.5.1.1.1.5 PV Model	24
3.5.1.1.1.6 Battery Model.....	25
3.5.1.2 Economic Parameters Used in the Model.....	27
3.5.1.2.1 Investment Rate, Inflation Rate, and Discount Rate.....	27
3.5.1.2.2 Life Cycle	27
3.5.1.2.3 Net Present Value	27
3.5.1.2.4 Life Cycle Cost.....	27
3.5.1.2.5 Payback Period.....	28
3.5.1.3 Environmental Parameters in the Model.....	28
3.5.1.3.1 Carbon Dioxide (CO ₂).....	28

3.5.1.3.2 Nitrogen Oxide (NO _x).....	28
3.5.1.3.3 Particulate Matter (PM).....	29
3.5.1.3.4 Avoided Costs of Pollutants	29
3.5.2 DEG Model with Economic Dispatch	29
3.5.2.1 Overall DEG Model.....	29
3.5.2.2 DEG Thermodynamic Model Block	30
3.5.2.2.1 DEG Block: Exhaust Temperature Selection	32
3.5.2.2.2 DEG Block: E-Gen Efficiency & Input Power	33
3.5.2.2.2.1 Engine Efficiency Calculation Block: DengineE_Block.....	34
3.5.2.2.2.2 Adjustment Coefficient Table Construction.....	37
3.5.2.2.2.3 Generator Input/Output Power Calculation Block	40
3.5.2.2.2.4 AC Generator Efficiency Table.....	40
3.5.2.2.2.5 E-Gen Efficiency & Input Power: Inputs and Outputs	43
3.5.2.2.2.4 AC Generator Efficiency Table.....	40
3.5.2.2.3 DEG Block: Manufacturer's Fuel Curve	43
3.5.2.2.4 DEG Block: Value Integration Total Block	45
3.5.2.2.5 DEG Block: Diesel Electric Generator Overall Efficiency Block	46
3.5.2.2.6 DEG Block: Incoming Air Control Block	46
3.5.2.2.7 DEG Block: Heating Values for Diesel Fuel Block.....	47
3.5.2.2.7.1 Fuel Energy Component Development.....	47
3.5.2.2.7.2 Fuel Energy Component Testing	51
3.5.2.2.8 DEG Block: Fuel Use Conversion Block	51
3.5.2.3 Dispatch Techniques	51
3.5.2.4 Classical Economic Dispatch Algorithm.....	53
3.5.2.5 Unit Commitment Development	55
4: Results and Discussion.....	59
4.1 UAF Energy Center Diesel.....	59
4.1.1 Flow Meter Test Loop	59
4.1.2 Flow Meter and Temperature Sensor Tests on UAF DEG.....	60
4.2 Village Power Survey and Data Collection.....	65
4.3 Village Hybrid Power Performance Analysis.....	67
4.3.1 Performance Analysis for Kongiganak, Alaska	67
4.3.2 Performance Analysis for Wales Village, Alaska	73
4.3.3 Performance Analysis for Lime Village, Alaska.....	76
4.4 Economic Dispatch of Multi-DEG Systems	79
4.4.1 Economic Dispatch Feasibility for Buckland, Alaska.....	79
4.4.2 Economic Dispatch Feasibility for Kongiganak, Alaska	81
4.4.3 DEG Efficiency versus Ambient Air Temperature	83
5: Conclusion	84
References.....	85
Project Publications	88
List of Acronyms and Abbreviations.....	90

List of Figures

Figure 1.1: Alaska village hybrid power system.....	1
Figure 3.1: Diesel Electric Generator (125 kWe Detroit Diesel) at UAF Energy Center.....	5
Figure 3.2: Sample load profile for the UAF Energy Center DEG	6
Figure 3.3: Process of acquiring data from a thermocouple	7
Figure 3.4: Apparatus constructed to test flow meters.	7
Figure 3.5: Principle of operation of magnetic flow meter [11].....	8
Figure 3.6: Power distribution within a diesel generator	11
Figure 3.7: Overall PV-wind-diesel-battery hybrid power system model.	13
Figure 3.8: Electrical efficiency for a 21 kW Marathon electric generator [16]	14
Figure 3.10: Details of the electrical efficiency model block	15
Figure 3.11: Subsystem of the electrical efficiency model for the generator.....	16
Figure 3.12: Fuel consumption curve of a 24 kW John Deere DEG [17].....	16
Figure 3.13: Details of the engine model block.....	17
Figure 3.14: Subsystem for the engine model	17
Figure 3.15: Optimal point of operation for DEG 2	18
Figure 3.16: Details of the optimization model block	18
Figure 3.17: Subsystem for the optimization model.....	18
Figure 3.18: Subsystem for the heat exchanger model	19
Figure 3.19: Details of the heat exchanger model block.....	20
Figure 3.20: Details of the boiler model block.....	21
Figure 3.21: Subsystem for the boiler model	21
Figure 3.22: Power curve for 15/50 Atlantic Oriental Corporation WTG [19]	22
Figure 3.23: Details of the wind model block	23
Figure 3.24: Subsystem for the wind model.....	23
Figure 3.23: Details of the PV model block.....	24
Figure 3.26: Subsystem for the PV model	24
Figure 3.27: Details of the battery model block.....	26
Figure 3.28: Details of the temperature dependent available battery energy model.	25
Figure 3.29: Subsystem for the battery model.....	25
Figure 3.30: Overall Thermodynamic Model of DEG for Economic Dispatch.....	30
Figure 3.31: <i>DEG Model</i> internal diagram	31
Figure 3.32: Diagram of the <i>Exhaust Temperature Selection</i> block	33
Figure 3.33: CATERPILLAR® 175 kWe diesel generator fuel consumption efficiency in kWh/L [26].	34
Figure 3.34: Internal structure of <i>DEG Efficiency</i> block.....	34
Figure 3.35: Diesel Cycle P-v diagram [27]	35
Figure 3.36: Efficiency adjustment calculation simulation diagram	36
Figure 3.37: <i>Adj. Coefficient</i> block diagram calculating adjustment percentage for diesel thermal efficiency based on manufacturer's fuel consumption curves.	39
Figure 3.38: Electrical efficiency for a 21 kW Marathon electric generator [29]	41
Figure 3.39: UAF Energy Center diesel generator unit's AC generator efficiency curves [30].....	42
Figure 3.40: Block parameters screen for the <i>AC Gen Eff</i> block showing input data variables	43
Figure 3.41: Manufacturer's fuel curve for CATERPILLAR® 175 kWe and 455 kWe diesel electric generators [26] [28].	44
Figure 3.42: <i>Fuel Curve</i> table block parameter screen for manufacturer's fuel curve data variables.	45
Figure 3.43: Inner diagram of the <i>Total-lizer</i> block	44
Figure 3.44: Inner diagram of the <i>DEG Efficiency</i> block within the <i>DEG</i> block	46
Figure 3.45: <i>Incoming Air Control</i> block diagram.....	46
Figure 3.46: Simulink® model of the combustion equation (Eq. 3.53) for #1 diesel fuel.....	49
Figure 3.47: Simulink® model of the combustion equation (Eq. 3.54) for #2 diesel fuel.....	50
Figure 3.48: Diagram of <i>Fuel Use Conversion</i> block representing Eq. 3.55	51
Figure 3.49: PCC zoned manufacturer's fuel curves for the Kongiganak DEGs	52
Figure 3.50: ED zoned manufacturer's fuel curves for the Kongiganak DEGs.....	53

Figure 3.51: Two generator cost curves with both operating at different incremental costs [36], [37]	55
Figure 3.52: Forward dynamic programming flowchart recursive algorithm for unit commitment [37]	58
Figure 4.1: Magnetic and ultrasonic flow meter performance for high coolant flow rate	59
Figure 4.2: Magnetic and ultrasonic flow meter performance for low coolant flow rate	60
Figure 4.3: Ultrasonic fuel flow meter tests	60
Figure 4.4: Using pressure transducer data to find fuel consumption rate	61
Figure 4.5: Changing fuel consumption rate for UAF DEG	61
Figure 4.6: Magnetic and ultrasonic coolant flow meter comparison on UAF DEG	62
Figure 4.7: Exhaust system temperature and electrical power output over time for UAF DEG	62
Figure 4.8: Coolant temperature and electrical power output over time for UAF DEG	63
Figure 4.9: Effects of particle build-up in generator radiator	63
Figure 4.10: Energy output broken into individual forms	64
Figure 4.11: Energy balance input compared to energy balance output	65
Figure 4.12: Average energy outputs of UAF DEG operating near full load using a) data from tests and b) generator specifications	65
Figure 4.13: Map of select villages in AEAs service territory grouped by average load	66
Figure 4.14: Sample load profiles from five Alaska rural villages	67
Figure 4.15: Synthetic annual load profile for Kongiganak Village, Alaska	68
Figure 4.16: Synthetic annual wind speed profile for Kongiganak Village, Alaska	68
Figure 4.17: Annual solar flux for Kongiganak Village, Alaska	69
Figure 4.18: 20-year LCC analysis of the proposed Kongiganak hybrid power system	72
Figure 4.19: Sensitivity analysis of fuel cost and investment rate on the NPV for Kongiganak	72
Figure 4.20: Sensitivity analysis of fuel cost and investment rate on the COE for Kongiganak	73
Figure 4.21: Sensitivity analysis of fuel cost and investment rate on the payback period for Kongiganak	73
Figure 4.22: Annual load profile for Wales Village, Alaska	74
Figure 4.23: Annual wind speed profile for Wales Village, Alaska	74
Figure 4.24: Annual load profile for Lime Village, Alaska	76
Figure 4.25: Annual solar insolation profile for Lime Village, Alaska	77
Figure 4.26: CAT [®] Diesel Electric Generators at Buckland, Alaska (455 kWe on left and 175 kWe on right)	80
Figure 4.27: Manufacturer's fuel curves for CAT [®] 175 kWe and 455 kWe diesel electric generators	80
Figure 4.28: Kongiganak Load and Temperature Profiles for January 1, 2003 through January 1, 2004: (a) Load Profile (kW) (b) Ambient Temperature Profile (°C)	81
Figure 4.29: Ambient air temp vs. efficiency for 190 kWe John Deere [®] DEG at 80% rated output	83

List of Tables

Table 3.1: Comparison table of simulation heating values to referenced values.	51
Table 3.2: PCC control scheme for Kongiganak DEGs	53
Table 3.3: Example priority list for a three generating unit system [37].....	56
Table 4.1: Installation cost for different components for Kongiganak Village.	70
Table 4.2: Comparison of energy and economic analysis results for Kongiganak	70
Table 4.3: Comparison of results for two wind-diesel-battery hybrid power system	71
Table 4.4: Comparison of results for Wales Village with HOMER	75
Table 4.5: Avoided cost for different pollutants for Wales Village.....	76
Table 4.6: Component and installation costs for Lime Village	78
Table 4.7: Simulation results of Lime Village using HARPSim	78
Table 4.8: Comparison of results for Lime Village with HOMER	79
Table 4.9: Avoided cost of emissions for Lime Village..	79
Table 4.10: PCC and ED results for Kongiganak system using #1 diesel fuel.....	82
Table 4.11: Installation costs for two economic dispatch control schemes	82
Table 4.12: Payback periods for the PCC and ED control schemes at Kongiganak using #1 diesel.....	83

1. Introduction

Alaska's rural village electric utilities are standalone systems without connections to the main Alaska "Railbelt" electrical grid intertie. Of the approximately 5,646,290 MWh of electric power generated commercially in Alaska by power utilities in 2001, 24% of the generated power is distributed over unconnected grids [1]. Many of these rural communities rely solely on diesel electric generators (DEGs) for electric power and heat with electrical energy costs subsidized through the state's power cost equalization (PCE) program. A 2003 report by the Alaska Energy Authority (AEA) shows that 92% of the electrical production in Alaska communities not connected to the "Railbelt" electrical grid was produced by DEGs [2]. Based on a survey referenced in the *Screening Report for Alaska Rural Villages* (2001) most village utilities have a minimum of three DEGs within their systems [3]. For those communities that have installed hybrid power systems, such as wind turbine generators and solar photovoltaic arrays, DEGs are still required to make up the base load (see Figure 1.1). DEGs have the advantage of being able to generate the required electrical power when necessary. However, the use of DEGs comes with the high cost of supplying diesel fuel and the high cost of maintenance over their operational lifetime.

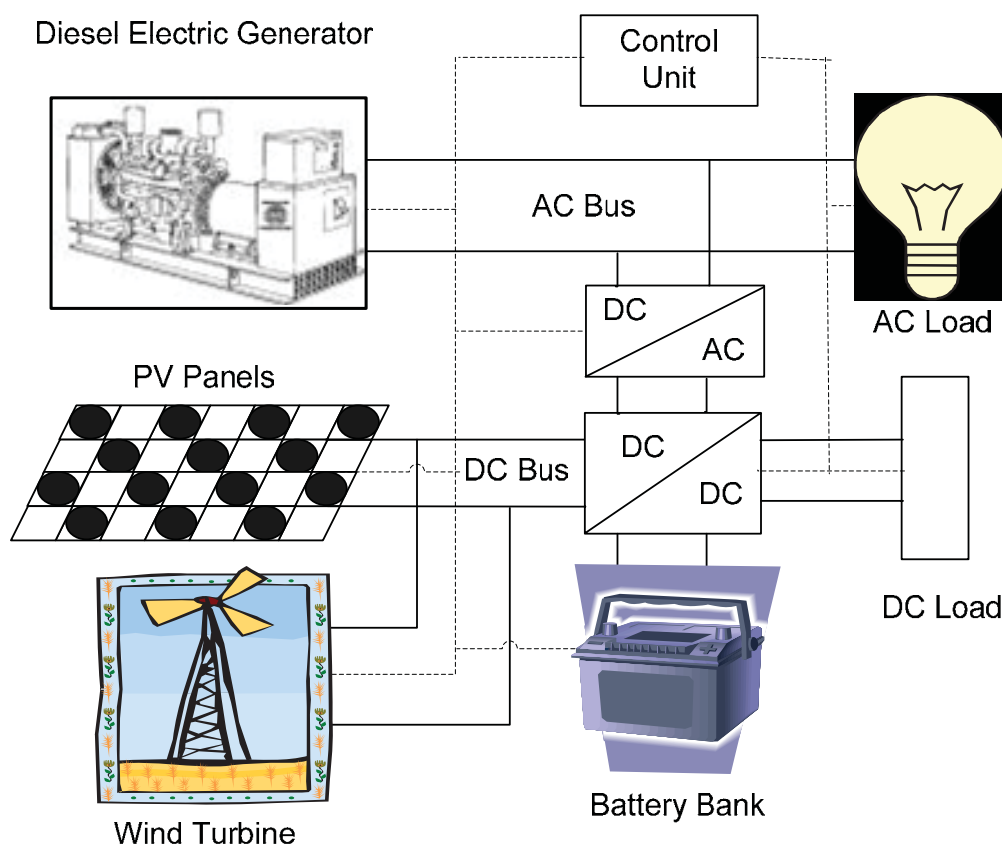


Figure 1.1: Alaska village hybrid power system.

The installation of renewable sources and automated generation control in some communities has helped to reduce fuel consumption. These fuel displacement and savings schemes are becoming more economically viable with shorter payback periods as the bulk fuel costs in some

communities approaches \$1.32/liter (\$5.00/gallon). On average rural communities spend significantly more for electrical energy than those communities connected to a large electrical infrastructure. For example, based on a 2001 study, villages that are a part of the Alaska Village Electric Cooperative (AVEC) on average pay \$0.42/kWh compared to \$0.11/kWh for those connected to the Railbelt electrical grid [1]. The rise in fuel prices has seen these average costs rise to \$0.52/kWh for AVEC villages and \$0.24/kWh for railbelt communities. As of June 1, 2008, residences tied to the interior railbelt system managed by Golden Valley Electric Association were paying about \$0.24/kWh because of the increase in the fuel surcharge. There is currently a proposal which would increase the minimum price for electric power in all Alaska villages to \$1.12/kWh for the power cost equalization (PCE) program which would likely put the average costs up around \$1.50/kWh. This indicates a need for the application of technologies to reduce the cost by improving the efficiency of the DEGs and utilizing renewable energy technologies which are dependent upon the available local resources. Methods of improving the efficiency of the DEGs such as economic dispatch of generation using control systems can be used in conjunction with renewable energy technologies.

The intent of this project was to assess the current operational state of standalone power systems in select rural communities in Alaska within Alaska Energy Authority's service territory by installing remote monitoring systems, developing a performance assessment method and providing recommendations for improvement of the efficiency of these DEG systems through analysis of data collected from existing and newly installed remote monitoring systems. The purpose of this research is to develop simulation models of the diesel-electric generation systems in rural communities using MATLAB[®] Simulink[®] for predicting the impact of using renewable energy sources and economic dispatch on the system efficiency and to determine if such system upgrades would be economically viable for these villages in terms of payback from displacement of fuel costs. The model also includes a simplified thermodynamic model of the DEGs to study the effects of ambient temperature on the generation efficiency. This power system simulation model is intended to help rural utility managers to investigate methods for: 1) increasing the diesel-electric generation efficiency, 2) decreasing the DEGs fuel consumption, 3) decreasing the maintenance costs, and 4) determining if the installation of renewable sources and automated generation control systems would be economical.

2. Executive Summary

Alaska's rural village electric utilities are isolated from the Alaska railbelt electrical grid intertie and from each other. Different strategies have been developed for providing power to meet demand in each of these rural communities. However, many of the communities in rural Alaska rely solely on diesel electric generators (DEGs) for power. The project was conducted in cooperation with the Alaska Energy Authority (AEA). The main goal of this project was to create a partnership with rural utilities and state energy organizations to coordinate the collection of energy system data in a representative set of rural Alaska communities in order to establish general performance assessments, and identify strengths and weaknesses of plant operations. These results will be used to improve system design and operation.

The project technical approach involved monitoring and analyzing the performance of a representative number of systems which reflect general operating conditions in Alaska village power systems served by the Alaska Energy Authority. The studies conducted in this project centered around five main tasks: 1) the development of a consortium of Alaska rural utilities, 2) the in-house (at UAF) testing of RTUs, flow meters and sensors for DEGs like those found in Alaska village communities, 3) survey of village power systems and data collection, 4) the deployment of remote monitoring systems in 25 villages in AEA's service territory, and 5) the development of system models in MATLAB[®] Simulink[®] to determine the optimal mix of DEGs and renewable sources of power as well as the feasibility of employing economic dispatch of power from these sources to serve the village loads.

A consortium of Alaska rural utilities and state energy organizations was developed as the project progressed for the collection and sharing of ideas for monitoring remote power systems. UAF PIs Richard Wies and Ron Johnson have been promoting the standardization of instrumentation and data collection systems in the villages since 2002. After setting up remote monitoring systems for large amounts of data in various formats with different sampling rates, AEA and the AVEC partnered to develop a standard instrumentation system for collecting and downloading the data.

A number of villages in AEA's service territory were surveyed and available data was collected from a number of villages in the AEA service territory. However, a lot of this data was found to have significant portions missing or consisted of only one or two days of recordings of the electric load at 15 minute intervals when maintenance personnel were on site. AEA was able to upgrade the switchgear in 25 villages which included remote monitoring as part of the package. A \$60k subcontract with AEA on this project helped in the purchase and install of some basic remote monitoring equipment in a couple of villages and a central server for collecting the large amounts of data from village monitoring systems. There is currently online access to real-time monitoring provided for about 25 villages in AEA's service territory <http://www.aidea.org/aea/aearemotemon.html> with limited data collection capabilities.

The UAF portion of the project consisted of three phases which resulted in one book, three peer-review journal publications, fifteen conference publications, one Ph. D. dissertation and three M. S. theses with work supervised by the PI Richard Wies and the co-PI Ron Johnson as outlined in the Project Publications section following the References section. Phase 1 (Aug 2003 - Dec 2004) consisted of testing and evaluation of a remote terminal unit, coolant flowmeters, fuel flow meters, and temperature and pressure sensors on the UAF Energy Center Diesel. Specific types of flow meters that were tested included the turbulent flow, ultrasonic, and

magnetic types. A magnetic flow meter was also tested independently in a small coolant flow loop in a UAF lab. Phase 2 (Aug 2003 - Aug 2006) overlapped phase 1 and consisted of the development of a hybrid power system model to investigate the economic feasibility of integrating renewable energy sources into existing rural village power plants. Phase 3 (Aug 2006 - Aug 2008) consisted of the development of an economic dispatch model for investigating the feasibility of integrating automated generation control to dispatch the most efficient generators to serve the load at the given operating point.

Results of testing a remote terminal unit, various types of fuel and coolant flow meters, and temperature and pressure sensors on the 125 kW Detroit DEG at UAF showed the importance of the proper selection of flow meters and sensors and remote metering. The energy balance calculated using the data collected in the RTU showed an overall error of about 2.5% using the manufacturer's specifications as a basis for comparison. A significant result occurred when fire ash in the summer of 2004 clogged the cooling system radiator and the operating temperature increased by 20 °C. In a village system without remote monitoring this situation might have led to a costly generator failure if left unchecked.

The hybrid power system model was used to evaluate the performance of power systems in Kongiganak, Lime Village, Stevens Village, and Wales Village and compared with results from the well known HOMER software developed at the National Renewable Energy Laboratory (NREL) with similar results. Our efforts were the first to include economic impacts of emissions from DEGs in Alaska rural villages in a simulation model. Results show economic feasibility through fuel savings of installing wind turbine generators in some villages. Puvarnaq Power which serves Kongiganak, AK received a Denali Commission grant for a new 3 wind-2 diesel system. A feasibility analysis using our model for the proposed system estimates the village will displace about 37,800 liters (10,000 gallons) of diesel fuel per wind turbine per year with a payback of about 3.5 years, while the contractor estimates about 45,360 liters (12,000 gallons) of diesel fuel per wind turbine per year with a payback of about 2.5 years.

A thermodynamic model of the DEG was also developed to investigate economic load dispatch incorporating ambient temperature variations. This was tested on load and ambient temperature data from Buckland, AK and Kongiganak, AK. Results of economic dispatch analysis show that Buckland, AK needs to turn off the less efficient 175 kW DEG and just operate the 455 kW DEG, so there is no real need for economic dispatch at this time. Results of an economic dispatch feasibility analysis show that Kongiganak, AK would reduce fuel consumption by about 9% by employing an economic dispatch system. Given their current cost of bulk fuel at \$0.93/liter (\$3.50/gallon) and the installed cost of a basic economic dispatch system at \$115k results in a payback of just under a year. With respect to our analysis regarding the impact of ambient temperature on performance, a 3 °C rise in temperature over the next 50 years would result in less than 0.2% change in DEG efficiency.

The results of this project have the following benefits: 1) The development of a centralized remote monitoring system for Alaska village power systems leading to efficiency and power quality improvements that have a direct impact on the reduction of fuel consumption and operating expenses, and 2) The development of energy, economic and environmental assessment tools for evaluating long term performance of remote village power systems in Alaska incorporating diesel electric generators as their main source of electric power and heat.

3. Experimental

The following sections provide a brief discussion of the project tasks and the procedures and equipment used to complete them. A more detailed discussion of the specific procedures used to obtain the results for the items in the two lists below are presented in the Ph. D. dissertation and three M. S. theses listed in the Project Publications section.

There were five main tasks which were completed on this project with procedures as discussed in sections 3.1-3.5.

3.1 Consortium of Alaska Rural Utilities

A partnership of village electric utilities and state energy organizations was created in order to coordinate the collection of energy system data in select rural communities in order to establish general performance assessments, and identify strengths and weaknesses of plant operations. An initial meeting was held in February 2002 at AEA to discuss the needs for remote monitoring of village power systems in Alaska. After that initial meeting the PI Richard Wies met with personnel from the village electric utilities and state energy organizations at the Alaska Rural Energy conferences in September 2002, April 2004, September 2005, and April 2007, and September 2008.

3.2 RTU, Flow Meter, and Temperature Sensor Testing at UAF

Remote monitoring systems, specifically remote terminal units (RTUs), temperature sensors and flow meters were tested and evaluated on the 125 kWe Detroit diesel electric generator at the University of Alaska Fairbanks (UAF) Energy Center as shown in Figure 3.1. The detailed procedures of these tests are presented by Tyler Chubb in a master's thesis, *Performance Analysis for Remote Power Systems in Rural Alaska*, under the direction of the project PIs (see MS Thesis 2 under Project Publications). Tests were conducted using an ElectroIndustries Nexus 1252 RTU, various temperature sensors, and three types of flow meters: 1) inline turbulent flow, 2) inline electromagnetic, and 3) ultrasonic. Data was collected and accessed through the Nexus 1252 RTU which was available online with password protection. The actual testing of the flow meters and temperature sensors on the 125 kWe Detroit diesel was conducted using all or parts of the load profile shown in Figure 3.2 below.



Figure 3.1: Diesel Electric Generator (125 kWe Detroit Diesel) at UAF Energy Center.

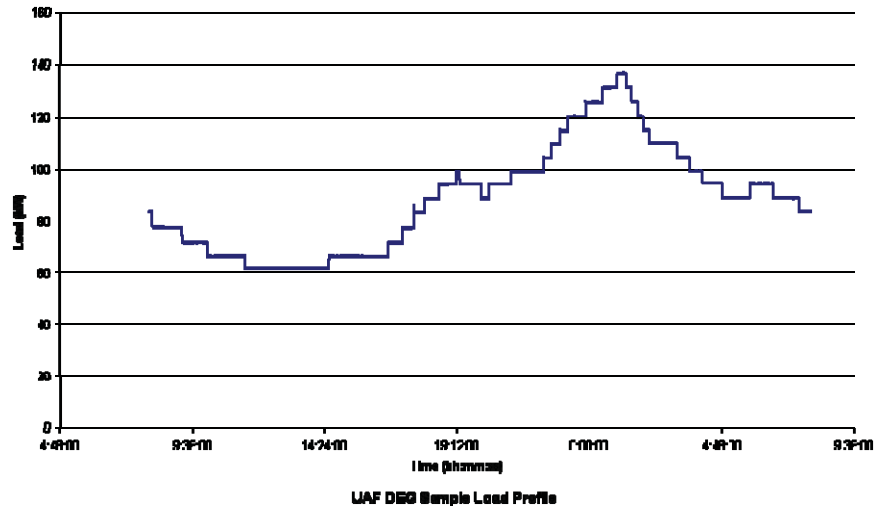


Figure 3.2: Sample load profile for the UAF Energy Center DEG.

3.2.1 RTU

Four different brands of RTU were considered for testing on the 125 kWe DEG. The first RTU that was evaluated was a National Instruments Fieldpoint 2015 [4]. The second RTU was an ION 7350 manufactured by Power Measurement Inc [5]. Much of the summer of 2003 was spent performing experiments with and programming settings into this RTU. PowerCorp, an Australian company attempting to expand into Alaska manufactures the Commander, the third brand of RTU that was considered [6]. The project did not have a chance to examine this device in as much detail as would have been sufficient to come to any conclusions about its usefulness to the project. A NEXUS 1252 series RTU manufactured by ElectroIndustries was the final device that was examined [7]. ElectroIndustries was very helpful and even loaned the project an RTU on a trial basis. Consequently, the Nexus RTU was chosen for this project.

3.2.2 Temperature Sensors

The monitoring system uses type K thermocouples to measure the temperature of different entities involved with the diesel generator. Thermocouples consist of wires made from two dissimilar metals touching at one end and left open at the other end. When the connected end is subjected to a different temperature than the open end, a voltage signal will be induced from the electron transfer caused by two different types of heated metals being in close proximity to each other. The magnitude of the generated voltage is mathematically related to the temperature difference between the open end and closed end of the thermocouple and can therefore be used to calculate the temperature at the open end. The different models of thermocouples (type D, F, K etc.) are referring to the types of metals used in the thermocouple design as this affects the magnitude of the induced voltage. The type K thermocouples utilized in this project are constructed of Nickel Chromium and Nickel Aluminum wires [8].

The relationship between voltage and temperature is highly nonlinear and the generated voltage must be conditioned as illustrated by the diagram in Figure 3.3 to produce a linear 4-20mA signal suitable for input into the NEXUS RTU. The signal conditioner digitizes the thermocouple voltage signal, applies it to the appropriate temperature conversion equation, and outputs a 4-20mA signal that is directly proportional to temperature at the closed end of the thermocouple.

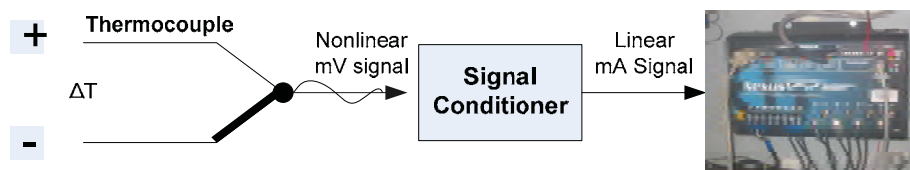


Figure 3.3: Process of acquiring data from a thermocouple.

Two Type K thermocouples are utilized to measure the input and output temperature of the glycol-water mixture used to cool the generator. The closed end of the thermocouple is inserted directly into the fluid using a “thermocouple well,” basically a compression fitting that allows the thermocouple insertion to pass through a hole in the pipe. Knowing the input and output temperature of the generator coolant allows the heat transfer rate of the system to be calculated. Additional thermocouples are used to measure the engine block temperature of the generator and ambient temperature of the generator container. Knowing the temperatures of these parameters is useful to gauge the amount of energy being lost as engine heat.

3.2.3 Coolant Flow Meters

Coolant flow meters were evaluated independently in a test loop in the Duckering building as shown in Figure 3.4. Three types of flow meters were tested including: 1) inline turbulent flow, 2) inline electromagnetic, and 3) ultrasonic. The system consists of two tanks (supply and fill) and a $\frac{3}{4}$ HP pump. A series of tests were conducted at various coolant flow rates to determine the range and accuracy of the three types of flow meters used in this DEG application.

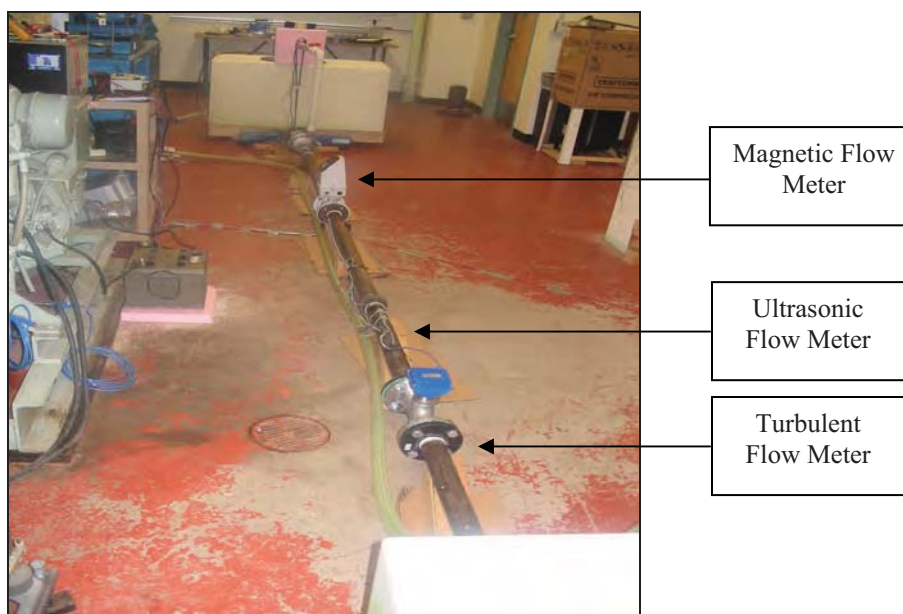


Figure 3.4: Apparatus constructed to test flow meters.

3.2.3.1 Turbine Flow Meter

The principle of operation of the turbine flow meter is quite straightforward. A probe is inserted directly into the coolant line through a tee section of pipe. The end of the probe is equipped with a small, plastic spinning wheel, better known as a turbine which is put into motion by the fluid flow through the pipe. There are magnets located at the end of four of the turbine blades and a

“high” voltage signal is emitted each time one of these magnets passes by a large magnet located at the end of the turbine shaft. The subsequent output of the meter is therefore a “pulse train” or a series of low and high voltage signals. The “K-factor” or conversion rate between the number of pulses and the volumetric flow rate is 60 pulses/gallon. The model of flow meter being used is the Omega FTB 720 [9].

The NEXUS RTU has the ability to count pulse signals and an attempt was made to utilize this feature. Recording the number of pulses over the time taken to create the pulses gives an accurate indication of flow rate. However, this attempt was unsuccessful and a signal conditioner had to be ordered that processed the pulse signal coming from the turbine meter and converted it to a 4-20 mA sign proportional to the flow rate. This signal could then be easily sent to the analog input module of the NEXUS RTU.

3.2.3.2 Magnetic Flow Meter

Magnetic flow meters, commonly known as electromagnetic flow meters, operate on the principle that fluids with charged particles moving at right angles to a magnetic field will induce an electric field or voltage. The voltage will be induced on a pair of electrodes mounted on the flow meter. There is a mathematical relationship between the magnitude of induced voltage and the velocity of the fluid. A fluid velocity is calculated by the microprocessor on the flow meter using the induced voltage and this relationship. A mass or volumetric flow rate can be calculated using the fluid velocity, density, and the cross sectional area of the fluid flow. A diagram showing the orientation of the magnetic fields used to operate the flow meter is shown in Figure 3.5. The model of flow meter used was the Siemens Magflo 7000 [10].

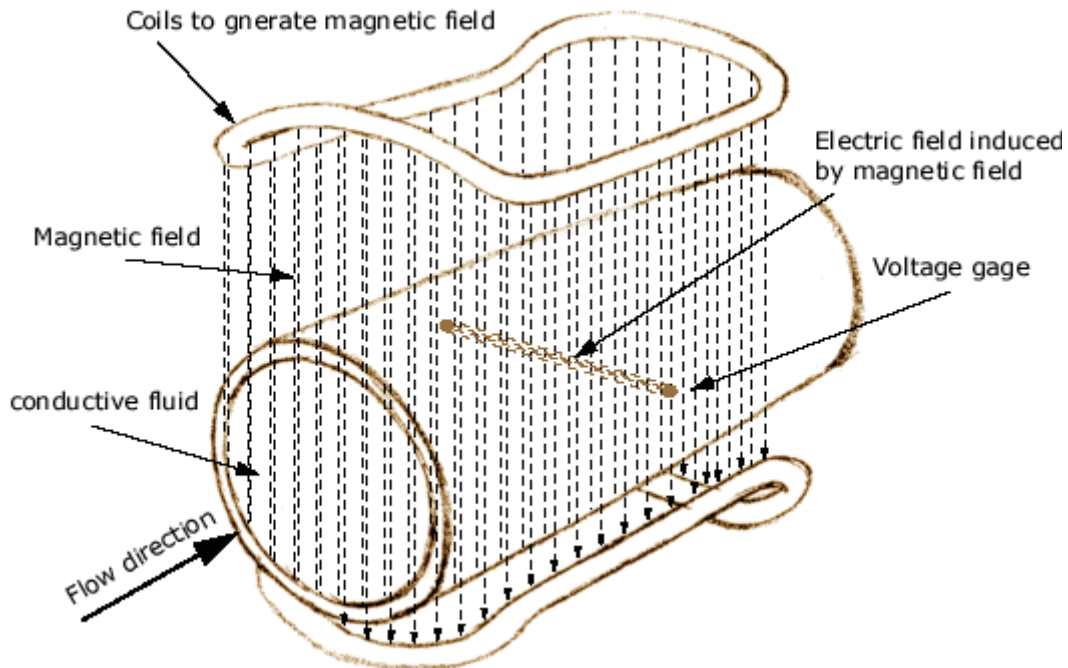


Figure 3.5: Principle of operation of magnetic flow meter [11].

3.2.3.3 Ultrasonic Flow Meter

The EESiFlo 5000 is an ultrasonic meter that is used to measure the coolant flow [12]. It consists of two sensors (upstream and downstream) that clamp around the coolant pipe for transmitting and receiving ultrasonic signals, therefore, it can be installed without cutting into the coolant loop. Ultrasonic flow meters present a distinct advantage over turbine or other in-line style meters as little time and effort is required for the installation process. The principle of the ultrasonic flow meter is centered on the apparent propagation velocity of the ultrasonic wave through a medium flowing through a pipe. If the medium is stationary and remains at a constant temperature and density, the time taken for an ultrasonic signal to be transmitted by one sensor, travel down the line a short distance, and then be received by another sensor will remain constant. However, if the medium is dynamic, the time taken for the transmitted signal to be received by a downstream sensor will be reduced proportional to the fluid speed. For the EESiFlo meters used in this project, the upstream sensor transmits an ultrasonic signal to a receiving sensor located approximately one to two inches downstream, the exact distance depending on the diameter of the pipe. The upstream sensor emits the testing signal 60 times per second, thus producing a very accurate profile of the fluid velocity. The microprocessor within the flow meter then compares the reception time for the dynamic fluid flow to the reception time if the fluid were static. This data provides sufficient information for the microprocessor to calculate the velocity and subsequent flow rate.

The EESiFlo 5000 meter is specifically designed to measure high volumetric fluid flows through pipes with a large cross sectional area. Due to the sizeable cross-sectional diameter of coolant line piping, the path of the ultrasonic signal will be distorted by a considerable amount as it travels through the medium. Therefore, a detailed set of information about the fluid parameters such as density and viscosity must be programmed into the flow meter. Also, the parameters regarding the pipe wall material, lining, and roughness are also very important for the meter to calculate appropriate correction factors and provide accurate flow rate data.

3.2.4 Instantaneous Fuel Flow

The amount of fuel consumed by the generator can be monitored in two ways: 1) on a real-time basis by using a flow meter to monitor the amount of fuel flowing through the supply and return fuel lines and 2) by measuring the known volume of fuel consumed from a day tank using a pressure transducer for timing. The momentary change in fuel consumption is useful to know as it allows the fuel consumption trend to be distinctly seen during times of changing electrical load on the generator.

3.2.4.1 Fuel Flow using Ultrasonic Flow Meter

The EESiFlo Inc. S-Series ultrasonic flow meter was used in this project to measure the flow of diesel fuel from a storage tank into the electric generator [13]. The operation of this ultrasonic flow meter for fuel is the same as that presented in section 3.2.3.3 for coolant except for one major difference. This particular EESiFlo ultrasonic meter is designed to measure fluid flow in small pipes with a diameter of three-quarters of an inch or less. Also, according to the manufacturer, the EESiFlo ultrasonic meters are advantageous over other ultrasonic meters because there are no requirements as to the mounting location on the pipe. The inner cross sectional area of the fuel line is programmed into the flow meter by the user and the meter performs the necessary calculations and outputs a 4-20 mA signal that is proportional to the volumetric flow rate of fluid through the line. In addition, the meter has an accumulator function that records the total amount of fuel that has passed through the line.

3.2.4.2 Fuel Flow using Day Tank Volume

The actual fuel flow rates were measured from the small day tank which fuels the DEG. The monitoring system contains two different sensors that are capable of measuring the volume of fuel in the day tank. These sensors include an ultrasonic rangefinder and a pressure transducer.

The ultrasonic rangefinder emits a 4-20mA analog signal proportional to the depth of fuel in the tank. The rangefinder transmits a 26 kHz signal from its base and then receives this signal after it is reflected off the medium. The microprocessor contained inside of the rangefinder measures the time between the signal transmission and reception and translates this into a distance between the bottom of the rangefinder and the medium below. Once the depth of the fuel in the tank is known, the volume of fuel can be easily calculated by factoring in the dimensions of the tank. Proper selection of the mounting location is the most important parameter that must be taken into consideration to ensure proper operation of the rangefinder. The device emits an 8 degree conical beam meaning that the larger the distance between the bottom of the rangefinder and the medium below, the larger the radius occupied by the ultrasonic signal. If a portion of this signal is obstructed by the wall of the fuel tank, a portion of it will be reflected prematurely and will cause erroneous calculations to be made by the microprocessor in the device.

The second method of measuring the fuel consumption is through the use of a pressure transducer located in the bottom of the day tank. The pressure transducer emits a 4-20mA signal proportional to the weight of the fuel in the tank. The pressure exerted on the transducer by the fluid is sufficient to distort a plastic diaphragm located within the transducer a small amount. The amount of distortion in the diaphragm is proportional to the pressure at the bottom of the fuel tank measured in lbs/in² (PSI) and a 4-20 mA signal proportional to the PSI is emitted. This signal can then be converted to volume by multiplying it by the surface area and the density. The change in volume over time can be used to calculate the fuel consumption rate of the generator.

3.2.5 Exhaust Flow

The mass flow rate of the exhaust is measured using a thermal anemometer. The primary component of a thermal anemometer is two temperature sensors that are inserted directly into the flowing exhaust gas. One sensor measures the ambient temperature and the other is heated 120 °F to 200 °F above ambient temperature. The motion of the exhaust gas passing by the heated sensor will cause a cooling process to occur. A feedback control system within the thermal anemometer will attempt to keep this heated sensor at a constant temperature by supplying more power to compensate for the temperature decrease. The corresponding increase in current due to the greater power draw will be related to the exhaust velocity.

A microprocessor within the meter records the current increase and combines this information with other settings to calculate a value for exhaust gas velocity. Applying the same concepts that were described in the description of the flow meters, a volumetric or mass flow rate value can be found from velocity. This value is then outputted from the meter as a 4-20 mA signal. The meter also has the ability to output the temperature of the exhaust gas as a 4-20 mA signal. This is advantageous as it negates the need for a thermocouple fixture to measure the exhaust temperature.

3.2.6 Electrical Outputs

Monitoring the electric power output of a generator is relatively simple; all that needs to be found are the voltage and current values of each phase between the generator and load. If the sampling rate is sufficiently high, all of the subsequent calculations that are needed to calculate power parameters can be found through manipulation of the current and voltage data. The primary equipment needed to monitor the level and trends of the electrical power produced by the generator are three current transformers situated on the wiring between the generator and load. The purpose of the current transformers is to step the current down to an acceptable level to be read and digitized by the data recorder. The current transformers used by this project are 500:5, meaning that 5 A will be sent to the NEXUS RTU for every 500 A of actual current flowing from the generator to the load. The size of the current transformer is programmed into the NEXUS RTU and enables the original current reading to be digitally reconstructed. Probes are connected at the load terminals to monitor the voltage being supplied to the load. The NEXUS RTU is equipped to measure up to 300V, enabling the voltage signal to be directly measured without the need for transformers to step the voltage down. Once the current and voltage signals have been sent to the RTU, the signals can be digitized and calculations can be performed to find all of the pertinent electrical information. The real power, power factor, and energy usage (kWh) are just a few of the parameters that the NEXUS can calculate once the current and voltage are known. The sampling rate of the NEXUS RTU pertaining to the electrical data (512 samples/cycle) is sufficient to perform in-depth calculations of the power quality parameters that may be used later in subsequent phases of the project.

3.2.7 Energy Balance of DEG Plant

Data from all the flow meter and sensor tests was then used to calculate the energy balance of the plant (see Figure 3.6) and compared to the energy balance calculated using the manufacturer's performance data for the DEG. The energy balance, the total amount of energy leaving the system in different forms compared to the total amount of energy entering the system as fuel, was calculated for the given load profile. The energy input for the DEG is the fuel while the energy outputs are the aftercooler, coolant loop, exhaust gas, electrical power, and miscellaneous losses in the engine and generator such as friction. The partial purpose of the energy balance calculations was to provide a means to verify the accuracy of the collected data. Also, viewing the energy balance provided a great deal of information in a concise format.

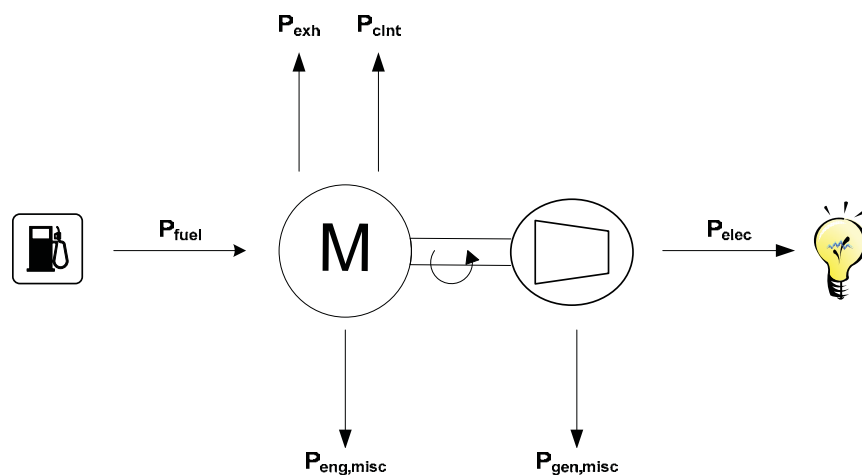


Figure 3.6: Power distribution within a diesel generator.

Sufficient data were recorded by the monitoring system to calculate the energy in the output coolant. The amount of energy being transported from the engine in the form of heated coolant, Q , can be found by the equation [14]:

$$Q = \dot{m} * C_p * \Delta T \quad (\text{Eq. 3.1})$$

The entities that need to be monitored to utilize this equation are \dot{m} , the flow rate of the coolant through the system, and ΔT , the temperature difference between the coolant before and after it has passed through a radiator or heat exchanger. C_p , the specific heat of the coolant, can be obtained through lookup tables. Using 0.81 BTU/lb °F for the specific heat of the 60/40 glycol-water mixture, the energy output through the generator coolant was calculated and equated to the amount of fuel lost due to the coolant.

The energy lost to the aftercooler and radiant heat along with the energy contained in the input fuel are the only items that remain to be found to complete the energy balance. Calculating the input fuel energy simply involved multiplying the heating value of the fuel by the instantaneous flow rate of the fuel into the engine. As the instantaneous fuel energy input was unknown due to the EESiFlo fuel flow meters malfunctioning, this information was obtained through sensors incorporated into the UAF Energy Center DEG.

Another element that needed to be calculated for the energy balance was the output energy from the aftercooler. The monitoring system built for this project did not have thermocouples in the necessary locations to perform this task and the data for these calculations had to be obtained from thermocouples that were installed as part of the Energy Center DEG. The energy output of the aftercooler was calculated by using Eq. 3.1 with 0.23 BTU/lb °F for the specific heat of air [15].

The final element that needed to be calculated for the energy balance was the radiant heat emitted by the generator. This was calculated by incorporating the engine block heat, T_b , with the temperature of the generator enclosure, T_{in} . This information was entered into Eq. 3.2 to calculate the amount of radiant heat.

$$\dot{Q} = \sigma A_b [T_b^4 - T_{in}^4] \quad (\text{Eq. 3.2})$$

The symbol σ is the Stefan-Boltzmann constant and has a value of $5.67 \times 10^{-8} \text{ W}/(\text{K}^4\text{m}^2)$. A_b is the surface area of the engine-generator set.

The energy output data from the aftercooler, the exhaust gas, electric generator, and coolant loop were all plotted and compared to the fuel input energy.

3.3 Village Power System Survey and Data Collection

Data was collected from a representative set of village power systems which have been instrumented with monitoring equipment by AEA. AEA provided the available power system data from a number of villages in its service territory. AEA also provided a plan of the current equipment used in some of the village power systems. Because of the variations in location,

population, and general village demographics, these villages were classified in terms of their average electric load requirement. This information was used to create a map which marks the location and average electrical load of each village represented in the survey.

3.4 Installation of Remote Monitoring Equipment

Remote monitoring equipment and switchgear upgrades were installed in 21 Alaska rural villages served by AEA using Denali Commission funding. Limited online access to the power systems including webcams in 16 of these villages was made available at ([URL:http://www.aidea.org/aea/aearemotemon.html](http://www.aidea.org/aea/aearemotemon.html)). A central server at AEA in Anchorage, Alaska and some basic remote monitoring equipment was installed in two more villages with the \$60k project subcontract.

3.5 System Models

Two system models were developed in MATLAB® Simulink®: 1) for long-term performance assessment of hybrid village power systems, and 2) for economic dispatch analysis of multi-DEG systems. Our efforts were the first to include economic impacts in a simulation model of emissions from DEGs in Alaska villages.

3.5.1 Hybrid Power System Model

Integrating other energy sources into power systems in Alaska rural villages could significantly reduce fuel consumption and operating costs for DEGs. A power system model was developed specifically for Alaska rural village power systems taking into account temperature effects, rising fuel costs, and plant emissions to investigate the feasibility of integrating renewable energy sources such as wind turbines and solar PV.

3.5.1.1 Overall Hybrid Model

An overall block diagram of the model developed in MATLAB® Simulink® is shown in Figure 3.7. The details of the hybrid power system model for Alaska rural villages is presented by Ashish Agrawal in a Ph. D dissertation, *Hybrid Electric Power Systems In Remote Arctic Villages: Economic And Environmental Analysis For Monitoring, Optimization, and Control*, under the direction of the project PIs (see Ph. D. dissertation 1 under Project Publications).

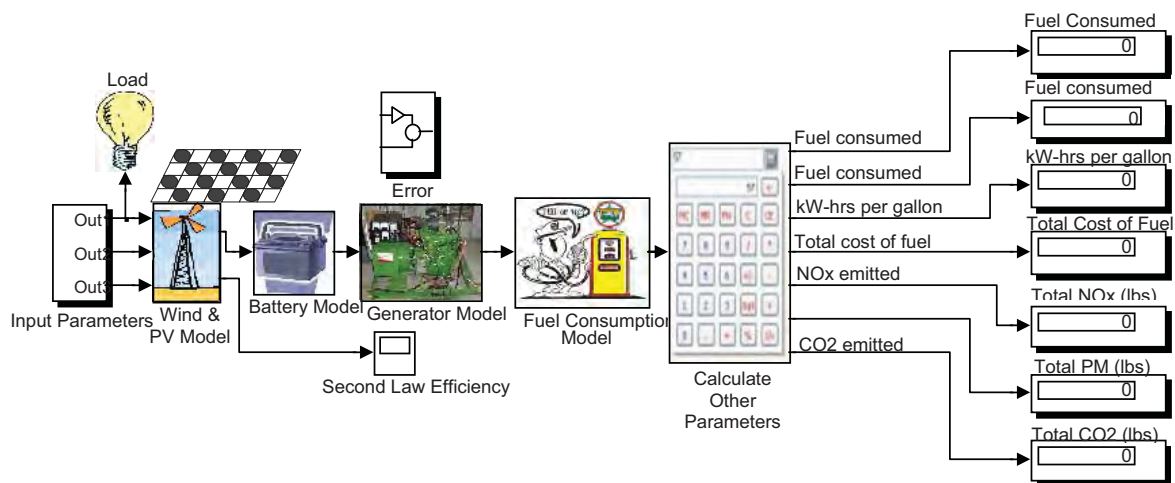


Figure 3.7: Overall PV-wind-diesel-battery hybrid power system model.

The model is used to perform an economic feasibility analysis for integrating renewable energy sources into existing DEG systems. Various hybrid power systems studied in this analysis include the diesel-battery system, the PV-diesel-battery system, the wind-diesel-battery system, and the PV-wind-diesel-battery system. Inputs to the model are the electrical load, wind, and solar profile for the village, and the manufacturer's performance curves for the DEGs, PV, wind turbines, and the battery bank. The outputs are the fuel consumption, efficiency (kW-hr/liter), total cost of fuel, and total emissions from CO₂, NO_x and PM₁₀. The life cycle costs (LCC) and sensitivity analysis of net present value (NPV), cost of energy (COE), and payback were also evaluated by porting data to Excel. The model was validated by comparing the results obtained from the Simulink[®] model, for supplying the annual load profile, with the available data obtained from the Hybrid Optimization Model for Energy Efficient Renewables (HOMER) software. At the time of this analysis HOMER was not set up to calculate payback period or NO_x and PM₁₀ emissions.

3.5.1.1.1 DEG Model

The DEG consists of two parts: the electric generator and the diesel engine. The electric generator model consists of the efficiency curve that describes the relationship between the electrical efficiency and the electrical load on the generator. Figure 3.8 shows a typical electrical efficiency curve for a 21 kW Marathon electric generator. The performance curve data were obtained from the manufacturer of the electric generator.

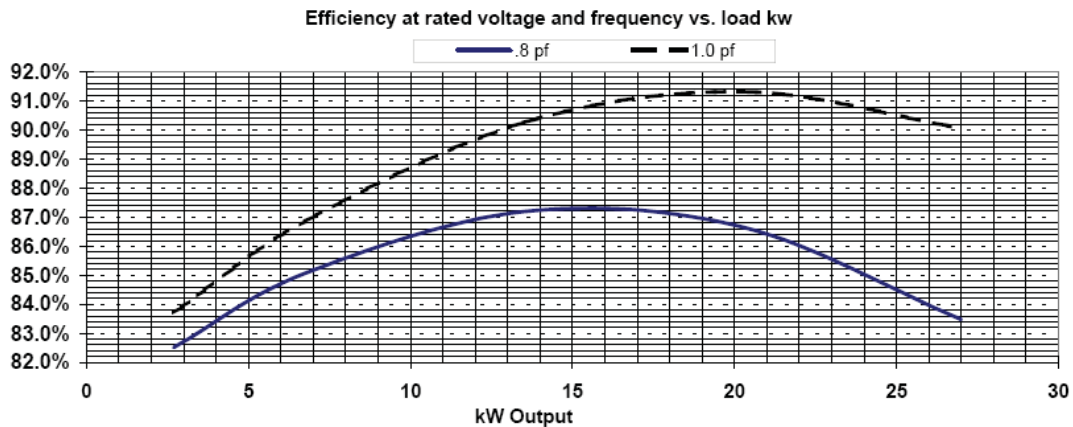


Figure 3.8: Electrical efficiency for a 21 kW Marathon electric generator [16].

A fourth order polynomial fit for the electrical efficiency curve at unity power factor and 0.8 power factor is given by Eq. 2-1 and Eq. 2-2, respectively,

$$\eta_{el1} = -6.953e-9 * L^4 + 2.932e-7 * L^3 - 9.858e-4 * L^2 + 0.201 * L + 81.372 \quad (\text{Eq. 3.3})$$

$$\eta_{el2} = 1.540e-7 * L^4 - 4.424e-5 * L^3 + 2.996e-3 * L^2 + 0.034 * L + 81.652 \quad (\text{Eq. 3.4})$$

where 'L' is the load on the electric generator (%). The actual load on the electric generator is converted to its percentage value by dividing the actual load with the rating of the electric generator as given by Eq. 3.5,

$$\text{percentage load} = \frac{\text{actual load}}{\text{generator rating}} * 100 . \quad (\text{Eq. 3.5})$$

This operation is performed so that the same efficiency equations are independent of the rating of the electric generators. The values from Eq. 3.3 and Eq. 3.4 are used to obtain the value for the electrical efficiency of the generator for any given power factor 'pf' by means of linear interpolation as follows:

$$\eta_{el} = \eta_{el2} + \left(\frac{(\eta_{el1} - \eta_{el2})}{0.2} * (\text{pf} - 0.8) \right) \quad (\text{Eq. 3.6})$$

where η_{el} is the electrical efficiency of the generator for a given power factor 'pf'.

The load on the diesel engine (the input to the electric generator) is obtained from the system load (the output of the electric generator) and the electrical efficiency of the generator as follows:

$$L_{eng} = \frac{L_{gen}}{\eta_{el}} \quad (\text{Eq. 3.7})$$

where ' L_{eng} ' is the load on the engine, ' L_{gen} ' is the load on the generator, and ' η_{el} ' is the electrical efficiency of the generator.

The block diagram representation of Eq. 3.3 through Eq. 3.7 as developed in Simulink® is shown in Figure 3.9, and the subsystem for the electric efficiency model for the generator is shown in Figure 3.10. Inputs to the model are the percentage load on the DEG and the power factor data, while outputs from the model are the electrical efficiency (%) of the generator and the engine load (% of rated).

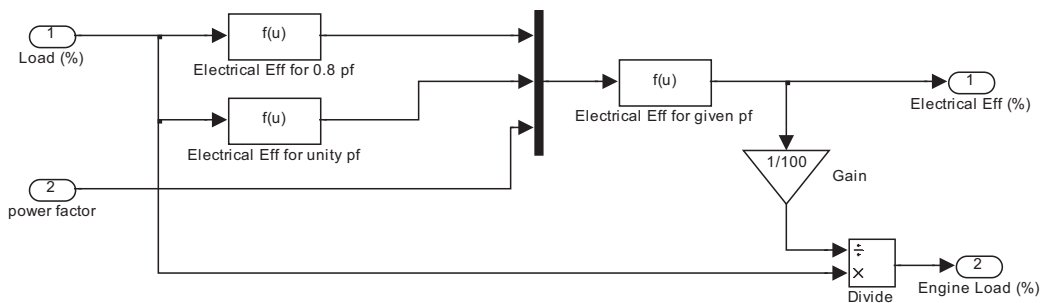


Figure 3.10: Details of the electrical efficiency model block.

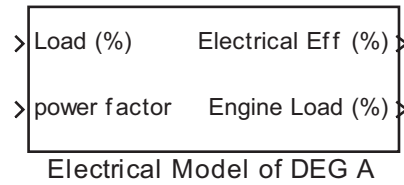


Figure 3.11: Subsystem of the electrical efficiency model for the generator.

The fuel curve for a diesel engine describes the amount of fuel consumed depending on the engine load. A typical engine fuel curve is a linear plot of load versus fuel consumption as shown in Figure 3.12 for the 24 kW John Deere DEG.

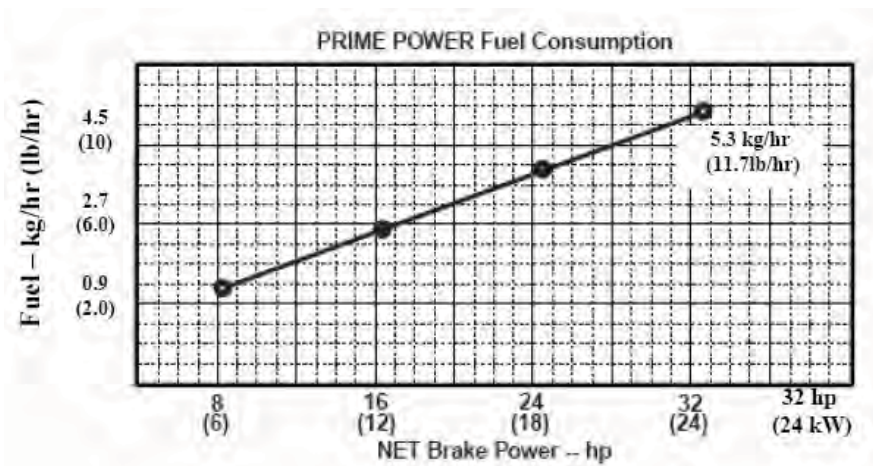


Figure 3.12: Fuel consumption curve of a 24 kW John Deere DEG [17].

The linear curve fit for the John Deere's engine fuel curve is given as:

$$\dot{F}_c = 0.5 * (L_{eng} * \frac{kW_A}{100}) - 0.44 \quad (\text{Eq. 3.8})$$

$$\text{Total } F_c = \int_0^T \dot{F}_c .dt \quad (\text{Eq. 3.9})$$

where ' \dot{F}_c ' is the fuel consumption rate in kg/hr (lbs/hr), ' L_{eng} ' is the percentage load on the engine, ' kW_A ' is the rating of the electric generator, ' F_c ' is the total fuel consumed in kg (lbs), ' dt ' is the simulation time-step, and ' T ' is the simulation period. The fuel consumed in kg (lbs) is obtained by multiplying the fuel consumption rate of kg/hr (lbs/hr) by the simulation time-step ' dt ' (given in hours), and the total fuel consumption in kg (lbs) is obtained by integrating the term ' $\dot{F}_c .dt$ ' over the period of the simulation.

The block diagram representation and the subsystem for the engine model block are shown in Figure 3.13 and Figure 3.14, respectively.

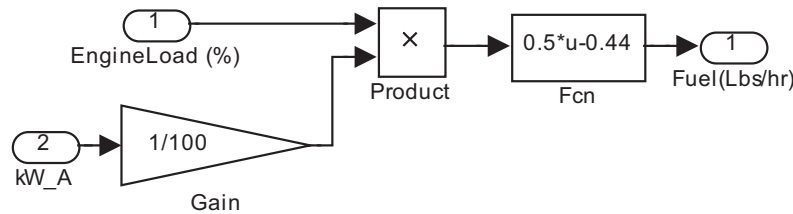


Figure 3.13: Details of the engine model block.

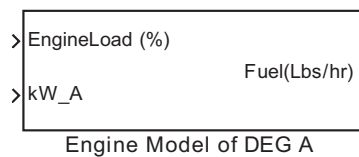


Figure 3.14: Subsystem for the engine model.

3.5.1.1.1 Optimization of DEG Model

When there are two DEGs to supply the load, it is important that DEGs operate optimally. In the Simulink® model, the data are supplied in such a way that DEG 1 is more efficient than DEG 2. The following steps are performed to find the optimal point of operation for DEG 2.

- 1) The electrical generator performance curve (Figure 3.8) and the diesel engine performance curve (Figure 3.12) are combined to obtain the overall fuel consumption for the given load profile.
- 2) The load on the DEGs is varied from 0 to 100%.
- 3) The fuel consumption for each DEG is noted at different load points.
- 4) The point of intersection of the two curves is the optimal point of operation for DEG 2. Beyond this point DEG 1 is more efficient than DEG 2.
- 5) If the two curves do not intersect, the optimal point is taken as 0. This situation implies that DEG 1 is efficient throughout the operating range of the load.

Figure 3.15 shows the overall fuel consumption curves for the two DEGs and the optimal point of operation for DEG 2. In order to avoid premature mechanical failures, it is important that DEGs operate above a particular load (generally 40% of rated). The long-term operation of DEGs on light loads leads to hydrocarbon built-up in the engine, resulting in high maintenance cost and reduced engine life [18]. In the Simulink® model, if the optimal point is less than 40% load, the optimal point is adjusted so that DEG 2 operates at or over 40% load.

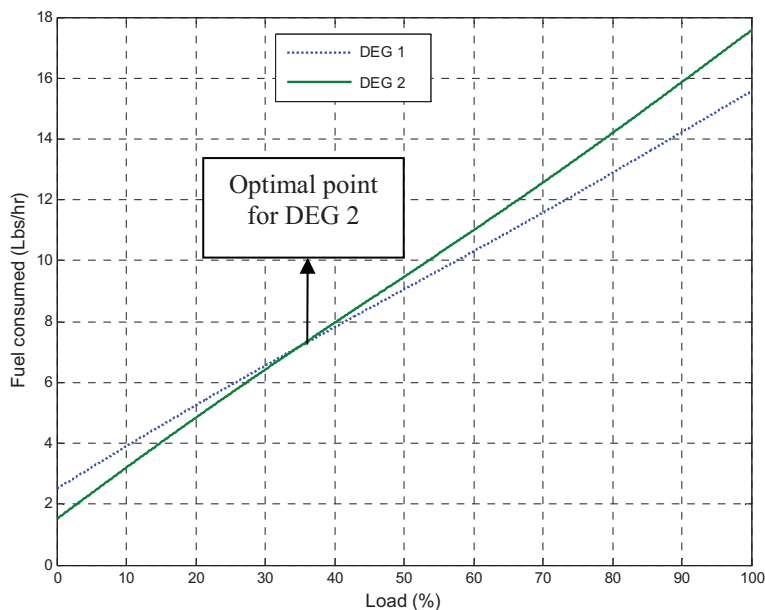


Figure 3.15: Optimal point of operation for DEG 2.

The block diagram representation and the subsystem for the optimization model are shown in Figure 3.16 and Figure 3.17, respectively. The 'DEG_Load' in Figure 3.17 is the s-function written in MATLAB[®] Simulink[®]. This s-function compares the load on two DEGs and divides the load based on the optimal point of operation.

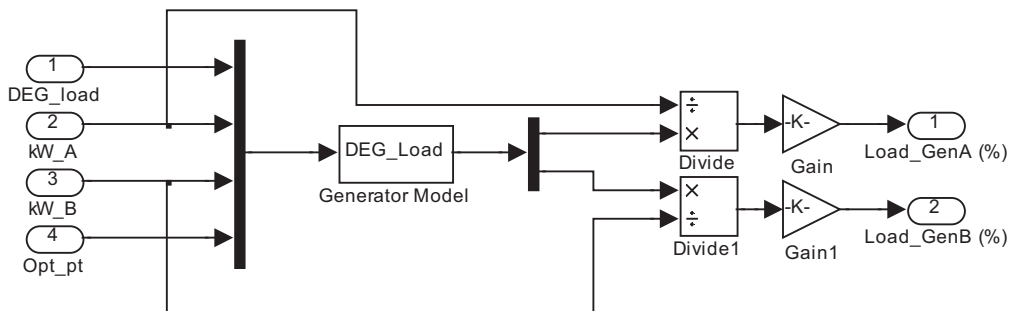


Figure 3.16: Details of the optimization model block.

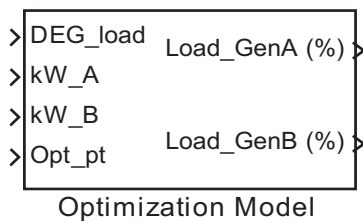


Figure 3.17: Subsystem for the optimization model

3.5.1.1.2 Heat Exchanger Model

The heat flux recovered from the jacket water of a DEG using a heat exchanger is calculated as follows [14]:

$$\dot{Q} = \eta_{HE} * \dot{m} * C_p * \Delta T \quad (\text{Eq. 3.10})$$

where ' \dot{Q} ' is the rate at which heat is transferred in Joules/sec (BTU/sec), ' η_{HE} ' (η_{HE} in

Figure 3.18 and Figure 3.19) is the efficiency of the heat exchanger, ' \dot{m} ' is the mass flow rate of the coolant in kg/sec (lbs/sec), ' C_p ' is the specific heat of the coolant in Joules/(kg °K) (BTU/(lb °F)), and ' ΔT ' is the temperature difference in °K (°F) of the coolant in and out of the jacket. The total heat recovered ' Q ' (kWh) is calculated by integrating the heat recovery rate over the entire time of the simulation and is calculated as follows:

$$Q = \int_0^T \dot{Q} . dt . \quad (\text{Eq. 3.11})$$

In addition to the total heat recovered, the heat exchanger model also calculates the total avoided pollutants including CO₂, PM₁₀, and NO_x. The method used to calculate the avoided pollutants is discussed in Section 3.5.1.3.4.

The subsystem and the block diagram representation for a heat exchanger model block are shown in Figure 3.18 and Figure 3.19, respectively.

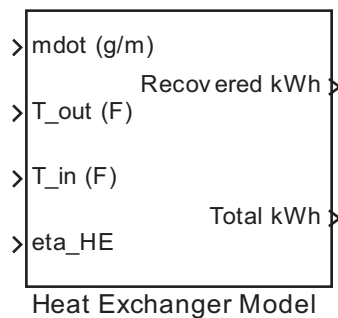


Figure 3.18: Subsystem for the heat exchanger model.

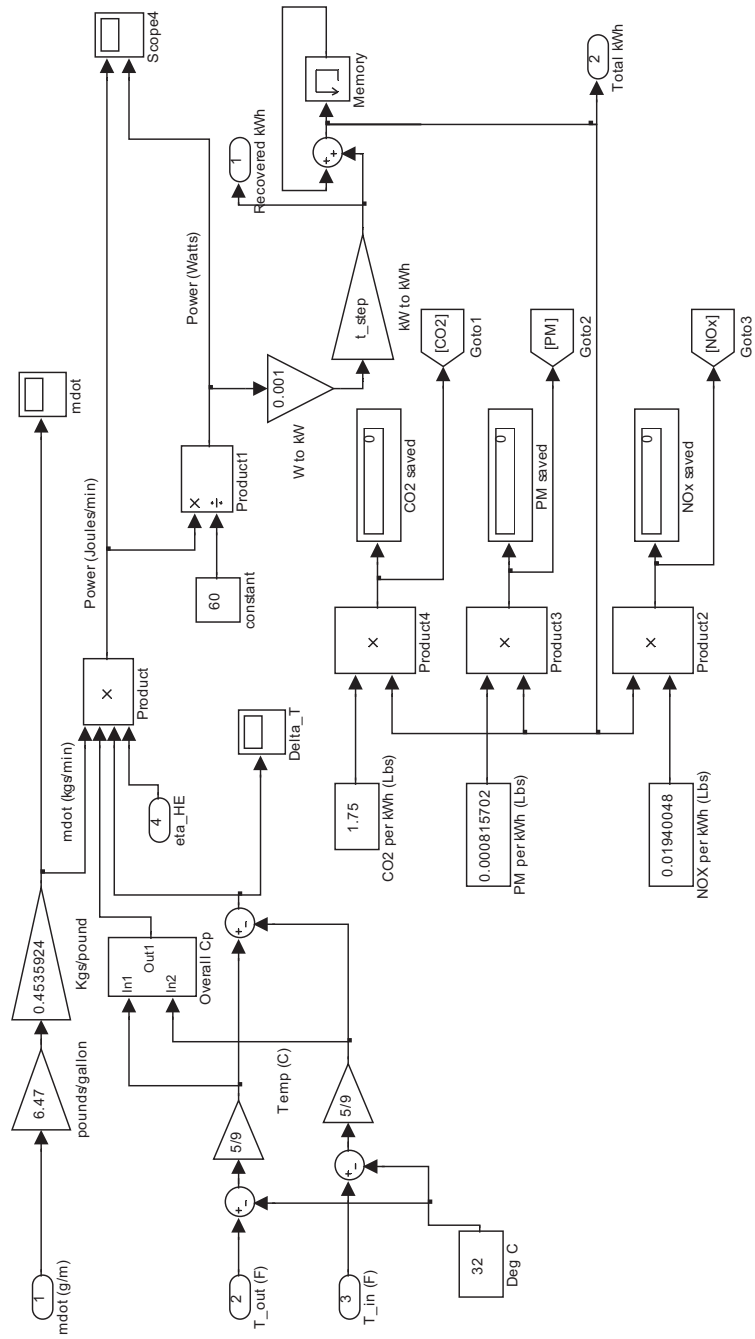


Figure 3.19: Details of the heat exchanger model block.

3.5.1.1.3 Boiler Model

The boiler model block calculates the fuel saved if the total heat recovered from the heat exchanger, given by Eq. 3.11, is supplied using a boiler. The total fuel saved is obtained using the following equation:

$$F_s = \frac{Q}{HV * \eta_b} \quad (\text{Eq. 3.12})$$

where 'Fs' in liters (gallons) is the total fuel saved due to the heat recovery, 'Q' is the total heat energy recovered (kWh), 'HV' is the heating value of the boiler fuel in kWh/liter (kWh/gallon), and ' η_b ' (eta_boiler in Figure 3.20 and Figure 3.21) is the efficiency of the boiler.

The block diagram representation and the subsystem for the boiler model block are shown in Figure 3.20 and Figure 3.21, respectively.

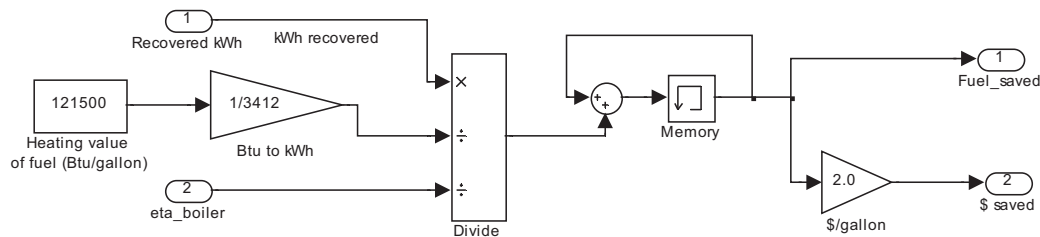


Figure 3.20: Details of the boiler model block.

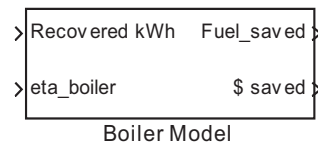


Figure 3.21: Subsystem for the boiler model.

3.5.1.1.4 WTG Model

The wind model block calculates the total power available from the wind turbines based on the power curve. The power curve gives the value of the electrical power based on the wind speed. Figure 3.22 shows the power curve for the 15/50 Atlantic Oriental Corporation (AOC) wind turbine generator [19].

The fifth order polynomial for the power curve is given as follows:

$$P_{WTG} = -4.12e - 6 * S^5 + 7.58e - 4 * S^4 - 5.22e - 2 * S^3 + 1.59 * S^2 - 17.8 * S + 63.12 \quad (\text{Eq. 3.13})$$

$$E_{WTG} = \int_0^T P_{WTG} dt \quad (\text{Eq. 3.14})$$

where ' P_{WTG} ' is the power output (kW) from the WTG, ' S ' is the wind speed in m/s (miles/hour), ' E_{WTG} ' is the energy obtained from the WTG (kWh), ' T ' is the simulation time (hours), and ' dt ' is the simulation time-step (hours).

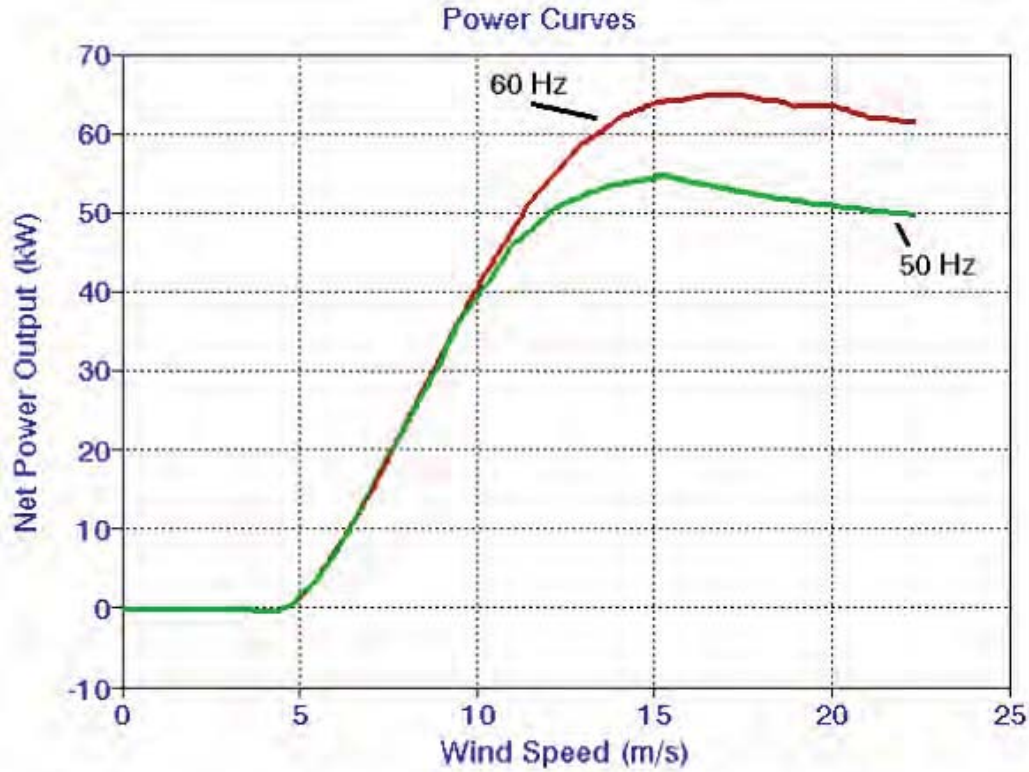


Figure 3.22: Power curve for 15/50 Atlantic Oriental Corporation WTG [[18]].

The wind model block also calculates the second law efficiency of the WTG. The second law efficiency of the WTG is given as follows:

$$\eta_{\text{second_law}} = \frac{\text{actual_power}}{\text{max_possible_power}} \quad (\text{Eq. 3.15})$$

where ' $\eta_{\text{second_law}}$ ' is the second law efficiency of the WTG, ' actual_power ' is the actual power output from the WTG and ' $\text{max_possible_power}$ ' is the maximum possible power output from the WTG.

The actual power of the wind turbine is obtained from the manufacturer's power curve given by Eq. 3.13 and the maximum possible power is obtained from the Betz formula described in [20] and given as follows:

$$P_{\text{max}} = \frac{1}{2} \rho \cdot A \cdot V^3 \cdot 0.59 \quad (\text{Eq. 3.16})$$

where ‘ P_{max} ’ is the maximum possible power, ‘ ρ ’ is the density of air taken as 1.225 kg/m^3 (0.076 lb/ft^3) at sea level, 1 atmospheric pressure i.e. 101.325 kPa (14.7 psi), and a temperature of 15.55°C (60°F), ‘ A ’ is the rotor swept area in m^2 (ft^2), ‘ V ’ is the velocity of wind in m/s (miles/hour), and the factor ‘ 0.59 ’ is the theoretical maximum value of power coefficient of the rotor (C_p) or theoretical maximum rotor efficiency which is the fraction of the upstream wind power that is captured by the rotor blade.

The air density ‘ ρ ’ can be corrected for the site specific temperature and pressure in accordance with the gas law and is given as follows:

$$\rho = \frac{p}{RT} \tag{Eq. 3.17}$$

where ‘ ρ ’ is the density of air, ‘ p ’ is the air pressure, ‘ R ’ is the gas constant, and ‘ T ’ is the temperature.

It should be noted from Eq. 3.16 that the wind power varies with the cube of the air velocity. Therefore, a slight change in wind speed results in a large change in the wind power.

The block diagram representation and the subsystem for the wind model are shown in Figure 3.23 and Figure 3.24, respectively.

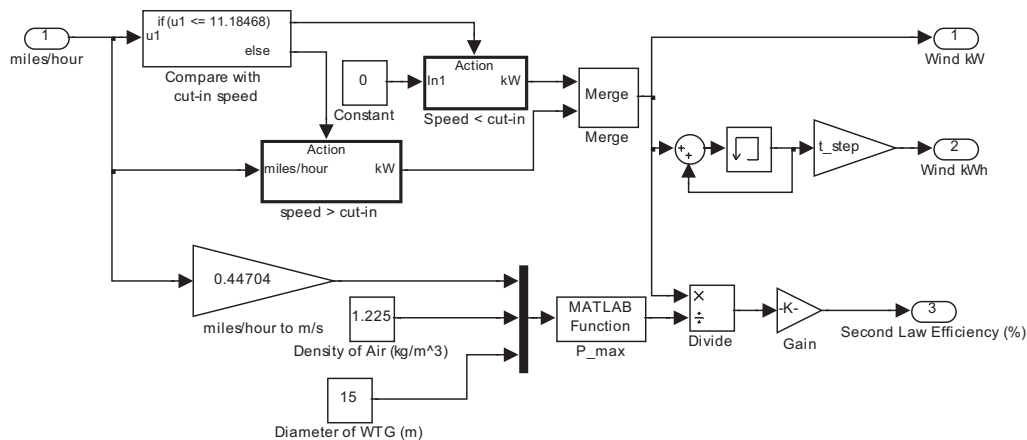


Figure 3.23: Details of the wind model block.

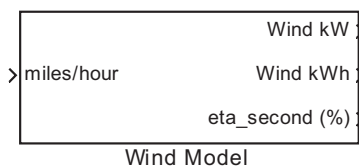


Figure 3.24: Subsystem for the wind model.

3.5.1.1.5 PV Model

The PV model block calculates the PV power (kW) and the total PV energy (kWh) supplied by the PV array using the following equations:

$$P_{PV} = \eta_{pv} * ins * A * PV \tag{Eq. 3.18}$$

$$E_{PV} = \int_0^T P_{PV} .dt \tag{Eq. 3.19}$$

where ‘P_{PV}’ is the power obtained from the PV array (kW), ‘η_{pv}’ is the efficiency of the solar collector, ‘ins’ is the solar insolation (kWh/m²/day), ‘A’ is the area of the solar collector/kW, ‘PV’ is the rating of the PV array (kW), and E_{PV} is the total energy obtained from the PV array.

The efficiency of the solar collector is obtained from the manufacturer. The solar insolation values are available from the site data or can be obtained by using the solar maps from the National Renewable Energy Laboratory website [21]. The area of the solar collector depends on the number of PV modules and the dimensions of each module. The number of PV modules depends on the installed capacity of the PV array and the dimensions of each PV module are obtained from the manufacturer’s data sheet.

The block diagram representation and the subsystem for the PV model block are shown in Figure 3.25 and Figure 3.26, respectively.

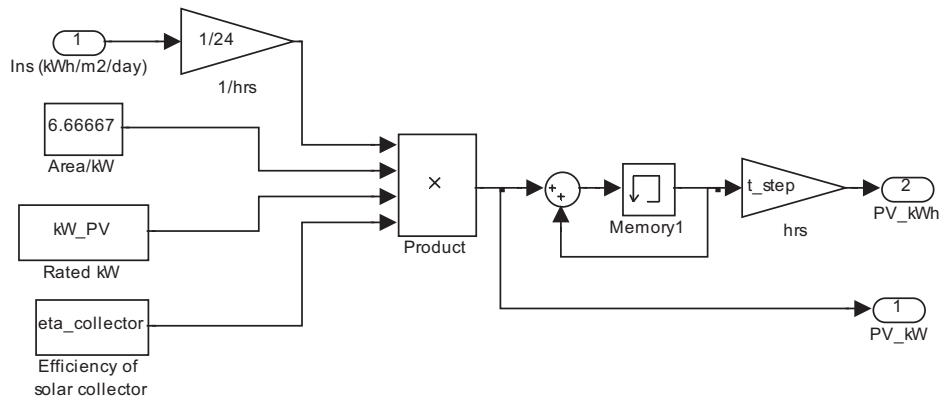


Figure 3.25: Details of the PV model block.

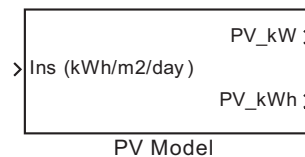


Figure 3.26: Subsystem for the PV model.

3.5.1.1.6 Battery Model

In the Simulink[®] model, the battery-bank is modeled so that the battery-bank acts as a source of power, rather than back-up power. The battery model block controls the flow of power to and from the battery bank. A roundtrip efficiency of 90% is assumed for the battery charge and discharge cycle. The battery model incorporates the effect of ambient temperature as described in [22] into the hybrid power system model. Therefore, the model can be used for cold region applications. The manufacturer's data sheet for the battery-bank is available in Appendix 5. The details of the battery model block are shown in Figure 3.27.

The details of the temperature dependent available battery energy model are shown in Figure 3.28 and the subsystem for the battery model is shown in Figure 3.29.

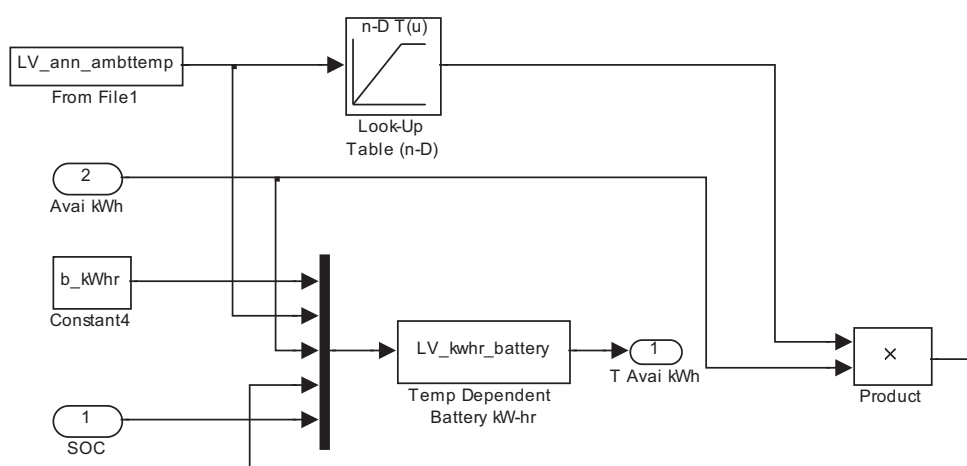


Figure 3.28: Details of the temperature dependent available battery energy model.

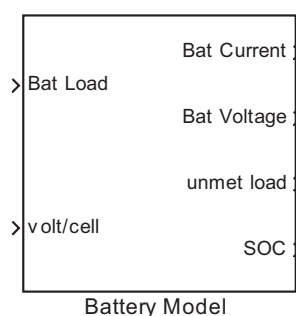


Figure 3.29: Subsystem for the battery model.

The life of the battery bank depends on the depth of discharge and the number of charge discharge cycles. In the Simulink[®] model the battery-bank is modeled so that it acts as a source of power rather than back-up power. Therefore, the depth of discharge of the battery-bank is assumed between 95% and 20% of the rated capacity. This higher depth of discharge reduces the number of battery operating cycles for the same energy output. It should be noted that the number of battery cycles plays a more significant role in the life of the battery-bank.

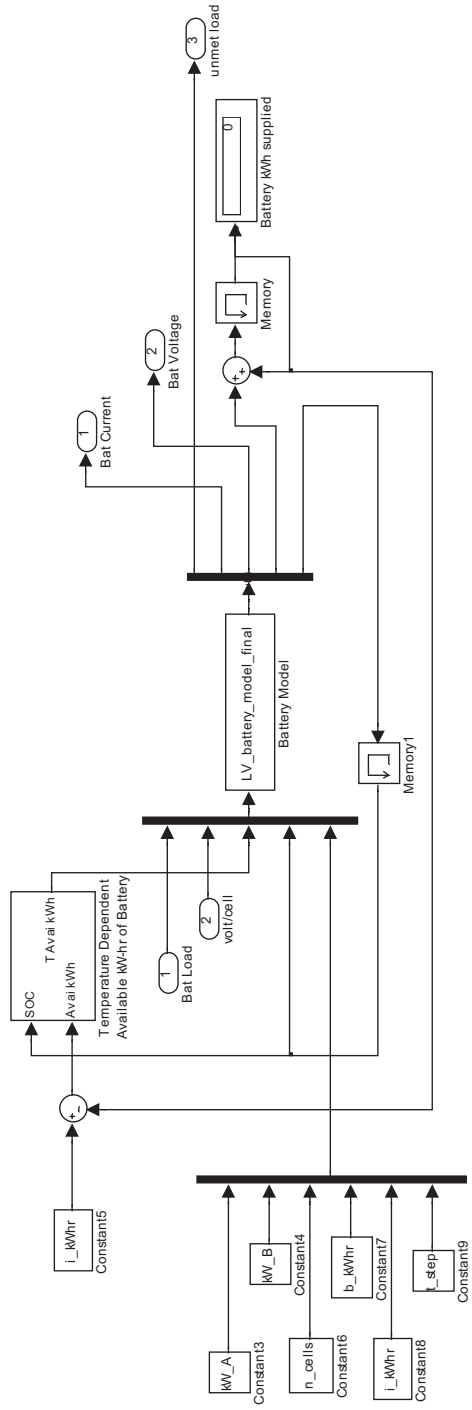


Figure 3.27: Details of the battery model block.

3.5.1.2 Economic Parameters Used in the Model

It is very important for the system designer to get acquainted with different economic parameters used in the modeling process of hybrid power systems. Economic parameters are used to calculate the COE, the payback period, and the life cycle cost of the system. The various economic parameters used in the hybrid power system model are discussed in the following sections [23].

3.5.1.2.1 Investment Rate, Inflation Rate, and Discount Rate

The investment rate is the percentage rate at which the value of money increases every year.

Inflation rate is the tendency of prices to rise over time. Inflation rate takes into account the future price rise in the project commodities including fuel and different power system components.

Discount rate is the difference between the investment rate and the inflation rate. Discount rate is generally used in life cycle cost analysis calculations.

$$\text{Discount rate} = \text{Investment rate} - \text{Inflation rate} . \quad (\text{Eq. 3.20})$$

3.5.1.2.2 Life Cycle

The life cycle is the life-time of the project. It is the time at the end of which the system components require replacement.

3.5.1.2.3 Net Present Value

The net present value (NPV) is the money that will be spent in the future discounted to today's money. The NPV plays an important role in deciding the type of the system to be installed. The NPV of a system is used to calculate the total spending on the installation, maintenance, replacement, and fuel cost for the type of system over the life-cycle of the project. Knowing the NPV of different systems, the user can install a system with minimum NPV. The different equations used in the calculation of NPVs are given as follows:

$$P = \frac{F}{(1+I)^N} \quad (\text{Eq. 3.21})$$

$$P = \frac{A[1 - (1+I)^{-N}]}{I} \quad (\text{Eq. 3.22})$$

where 'P' is the present worth, 'F' is the money that will be spent in the future, 'I' is the discount rate, 'N' is the year in which the money will be spent, and 'A' is the annual sum of money.

3.5.1.2.4 Life Cycle Cost

The life cycle cost (LCC) is the total cost of the system over the period of its life cycle including the cost of installation, operation, maintenance, replacement, and the fuel cost. The life cycle cost also includes the interest paid on the money borrowed from the bank or other financial institutes to start the project. The life cycle cost of the project can be calculated as follows:

$$\text{LCC} = C + M + E + R - S \quad (\text{Eq. 3.23})$$

where 'LCC' is the life cycle cost, 'C' is the installation cost (capital cost), 'M' is the overhead and maintenance cost, 'E' is the energy cost (fuel cost), 'R' is the replacement and repair costs, and 'S' is the salvage value of the project.

3.5.1.2.5 Payback Period

Payback period is the time in which the total extra money invested in a project is recovered and is given as,

$$\text{Payback Period} = \frac{\text{Extra Investment}}{\text{Rate of Return}} \quad (\text{Eq. 3.24})$$

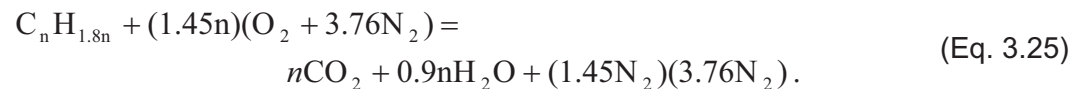
Payback period is the major deciding factor for the feasibility of the project. If the payback period of the system is less than the life cycle of the system, the project is economically feasible.

3.5.1.3 Environmental Parameters in the Model

The different environmental parameters in the analysis of the Simulink[®] model include carbon dioxide (CO₂), nitrogen oxide (NO_x), and particulate matter (PM₁₀). The environmental parameters are discussed in detail in the following sections.

3.5.1.3.1 Carbon Dioxide (CO₂)

CO₂ is released in the atmosphere due to the combustion of fossil fuels including coal, oil, natural gas, wood, and biomass. In the Simulink[®] model the total CO₂ was calculated based on the equation for the combustion of diesel fuel. For example, one empirical formula for light diesel C_nH_{1.8n} is given in [24]. For this empirical formula, with 0 % excess air the combustion reaction is given as follows:



For any n, the mass in kg (lb) of CO₂ per unit mass in kg (lb) of fuel = 44/(12 + 1.8) = 3.19. So, to get the emissions per unit electrical energy output, the above is combined with an engine efficiency of 3.17 kWh/liter (12 kWh/gallon) and a fuel density of 0.804 kg/liter (6.7 lb/gallon). Doing this results in specific CO₂ emissions of 3.1*(0.804/3.17) = 0.786 kg (1.73 lb) of CO₂ per kWh of electricity. This figure of 0.786 kg/kWh (1.73 lb/kWh) agrees closely with the data obtained from the manufacturer 0.794 kg/kWh (1.75 lb/kWh). The annual CO₂ amount was calculated from the lb CO₂/kWh and the annual kWh produced and is given as follows:

$$\text{Total pollutant in kg (lb)} = \frac{\text{pollutant}}{\text{kWh}} * \text{kWh}_{\text{Gen}} \quad (\text{Eq. 3.26})$$

where kWh_{Gen} is the total kWh supplied by the diesel generator during the simulation period.

3.5.1.3.2 Nitrogen Oxide

Nitrogen oxide (NO_x) is one pollutant responsible for acid rain and is the major source for the formation of ground ozone. In the Simulink[®] model, the total NO_x emitted is calculated based on

the value of 0.0088 kg (0.0194 lb) of NO_x per kWh of electricity produced, as obtained from the manufacturer. The annual NO_x was calculated using Eq. 3.26.

3.5.1.3.3 Particulate Matter

Particulate matter (PM) is the complex mixture of extremely small particles and liquid droplets. During the combustion of diesel fuel, PM may contain carbon particles and unburned hydrocarbons. In the Simulink[®] model, the total PM was calculated based on the value of 0.00037 kg (0.00082 lb) of PM₁₀ per kWh of electricity produced as obtained from the manufacturer. The annual PM₁₀ was calculated using Eq. 3.26.

3.5.1.3.4 Avoided Cost of Pollutants

Generally, a power plant incorporating renewable energy is more expensive than a non-renewable energy plant because of the high installation cost associated with the renewable energy systems. The avoided cost of pollutants is the extra cost associated with the low emissions power plant (the plant incorporating renewable energy sources) due to the use of renewable energy. The avoided cost of pollutants is given as follows [25]:

$$AC = \frac{COE_L - COE_H}{E_H - E_L} \quad (\text{Eq. 3.27})$$

where 'AC' is the avoided cost of pollutants in USD/metric ton (USD/US ton), 'COE_L' is the COE from the low emissions plant, 'COE_H' is the COE from the high emissions plant, 'E_H' is the amount of emissions from the high emissions plant in metric ton (US ton), and 'E_L' is the amount of emissions from the low emissions plant in metric ton (US ton).

3.5.2 DEG Model with Economic Dispatch

Rural utilities that do not have automated control and monitoring systems that perform economic dispatch (ED) must rely on operators to regulate system efficiency; however, an automated control system has the capability of accurately regulating system efficiency through economic dispatch and unit commitment [3]. In isolated villages with multiple generating units, the use of classical ED and normal unit commitment does not ensure a system is running at its most efficient point. In these villages where large fluctuations in load can occur, having the ability to bring units online or take units offline can help to ensure that the system is running efficiently. This type of automated control is a combination of economic dispatch and unit commitment running in real-time. An analysis tool was developed for economic load dispatch taking into account the fuel efficiency curves, the output power factor, and the thermodynamic model of each DEG.

3.5.2.1 Overall DEG Model

An overall block diagram of the thermodynamic model of the DEG developed in MATLAB[®] Simulink[®] is shown in Figure 3.30. This is a more detailed model than that presented in Section 3.5.1.1.1 for the hybrid power system model. The complete diesel generator model calculates the fuel consumed by a single diesel generator based on inlet air temperature, exhaust air temperature, diesel engine specifications, and the heating value of the fuel. The fuel consumed is also adjusted to meet manufacturer's fuel consumption data at standard operating temperatures. The details of the DEG model and the economic dispatch algorithm are presented by Larre Brouhard in a master's thesis, *Economic Dispatch and Control for Efficiency*

Improvements on Diesel Electric Power Systems in Alaska Rural Villages, under the direction of the project PIs (see MS Thesis 1 under Project Publications).

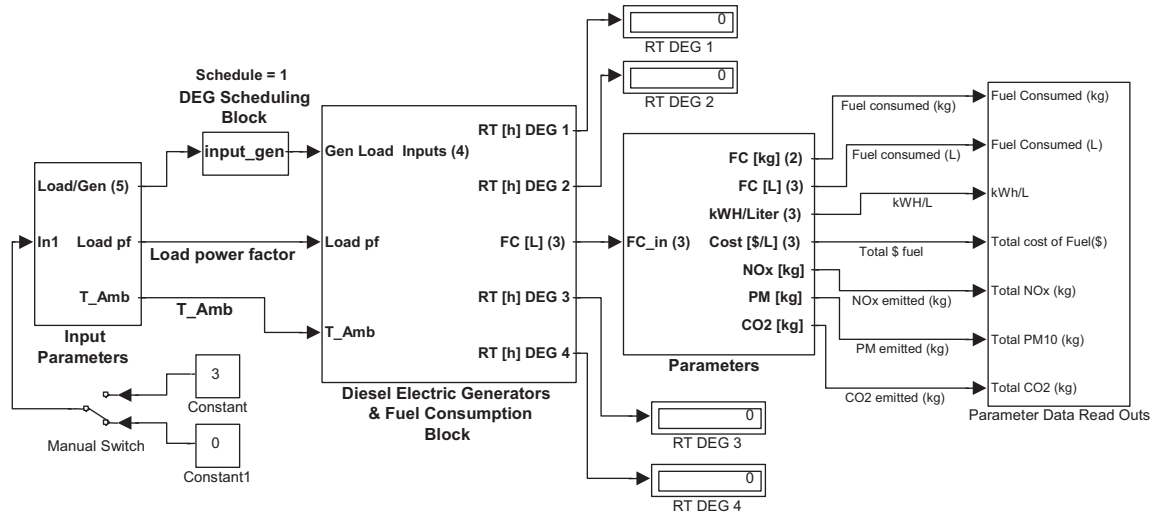


Figure 3.30: Overall Thermodynamic Model of DEG for Economic Dispatch

3.5.2.2 DEG Thermodynamic Model Block

The internal diagram and setup of the *DEG* block is illustrated in Figure 3.31. The *DEG* block consists of many sub-blocks which are described in detail in Chapter 4 of Larre Brouhard's M. S. thesis *Economic Dispatch and Control for Efficiency Improvements on Diesel Electric Power Systems in Alaska Rural Villages*. The inputs to the *DEG* blocks are data that come in from other blocks within the simulation or external data files.

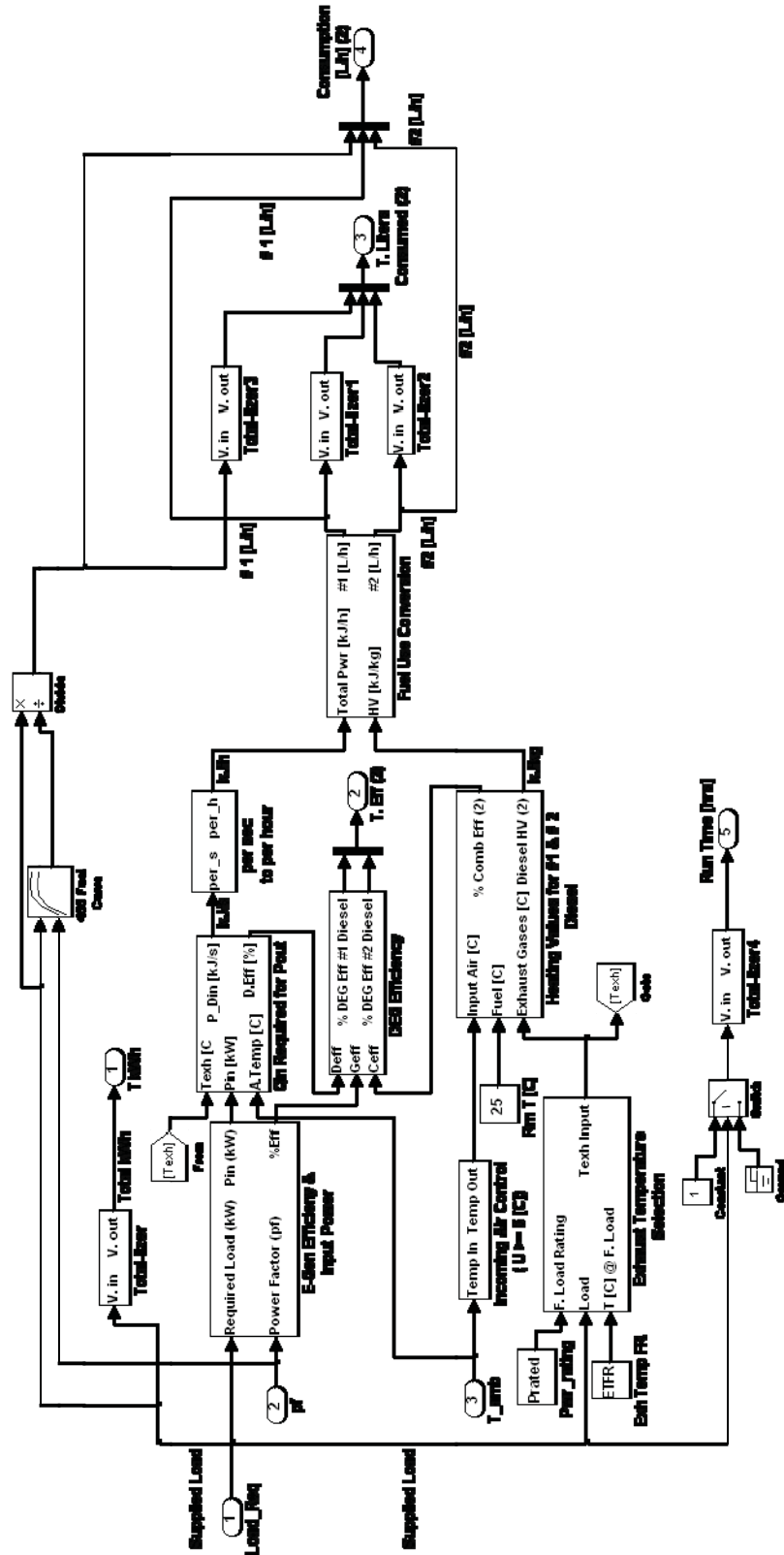


Figure 3.31: DEG Model internal diagram.

These other forms of input values are:

- Diesel Generator Power Rating [kW]
- Diesel Generator Power Factor Rating
- Diesel Engine Compression Factor – R_c
- Diesel Engine Exhaust Temp at Rated Power [C] – $ETFR$
- Fuel Rating: Temperature [C] – $Trated$
- DEG Performance Curves: Power Variables [Vector] – Eff_pwr_G
- DEG Performance Curves: Efficiency Variables [Vector] – Eff_eff_G
- DEG Performance Curves: Power Factor Variables [Vector] – Eff_pf_G
- Efficiency Adjustment Parameters for Power [Table Row] – $AdjEff_p$
- Efficiency Adjustment Parameters for Efficiency [Table Column] – $AdjEff$
- Fuel Curve Manufacturers Data: Power [kW] – $fulcrv_pwr$
- Fuel Curve Manufacturers Data: Power Factor – $fulcrv_pf$
- Fuel Curve Manufacturers Data: Fuel Efficiency[L/kWh] – $fulcrv_eff$

The input values above are either directly input or referenced by variables within a parameter window.

The outputs of the *DEG* block are $T kWh$ total power in (kW) produced per hour, $T.Eff$ overall efficiency for the generator, $T. Liters Consumed$ total fuel consumed by fuel type, $Consumption [L/h]$ fuel consumption rate of the generator by fuel type, $Run Time [hrs]$ the amount of time that the generator was in operation, and kWh/L efficiency of generator at each time step in energy (kWh) per liter of fuel.

3.5.2.2.1 DEG Block: Exhaust Temperature Selection

From examining data on the UAF Energy Center diesel generator as the load on the generator changes there is a corresponding change in the exhaust temperature. Therefore, to more accurately show how exhaust temperature may affect the efficiency of the diesel a sub-block to calculate changes in the exhaust temperature from the rated value was created. Figure 3.32 shows the diagram of the *Exhaust Temperature Selection* block.

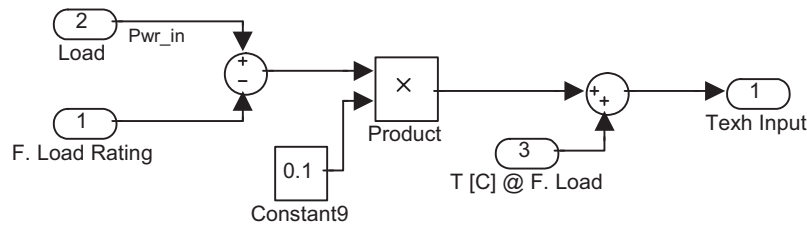


Figure 3.32: Diagram of the *Exhaust Temperature Selection* block.

The *Exhaust Temperature Selection* block subtracts the generators full load rating the full load exhaust temperature rating to establish a change in exhaust temperature with varying load requirements. Multiplying by $1/10^{\text{th}}$ was chosen due to the observation that the temperature for the UAF diesel's exhaust increased approximately one degree Celsius for every 10 kW. This value was based on an average change in temperature. The output of the *Exhaust Temperature Selection* block is then used by the *E-Gen Efficiency & Input Power* and *Heating Values For #1 & #2 Diesel* blocks.

3.5.2.2.2 DEG Block: E-Gen Efficiency & Input Power

Manufacturer's specification sheets contain information on the diesel engine and/or AC generator. This information usually includes the fuel consumption at various loads of the diesel generator as a set or on just the diesel engine. The fuel consumption data is often listed within a table. However, the fuel consumption data can also be given as a figure which requires conversion into a data set for implementation in this simulation model.

The fuel consumption of the diesel generator or diesel engine is usually based on steady state operating conditions at a specific temperature, pressure, and fuel type. The curve defined by this data, as seen in Figure 3.33, does not lend itself to calculation of fuel consumption with variable parameters such as intake air temperatures, fuel temperatures, and exhaust temperature. Since this simulation is to study the effects of how changing load and ambient temperature may affect the efficiency of the diesel generator set, an adaptation of the diesel cycle and diesel combustion formula is utilized for such analysis and is discussed in Section 3.5.2.2.2.1.

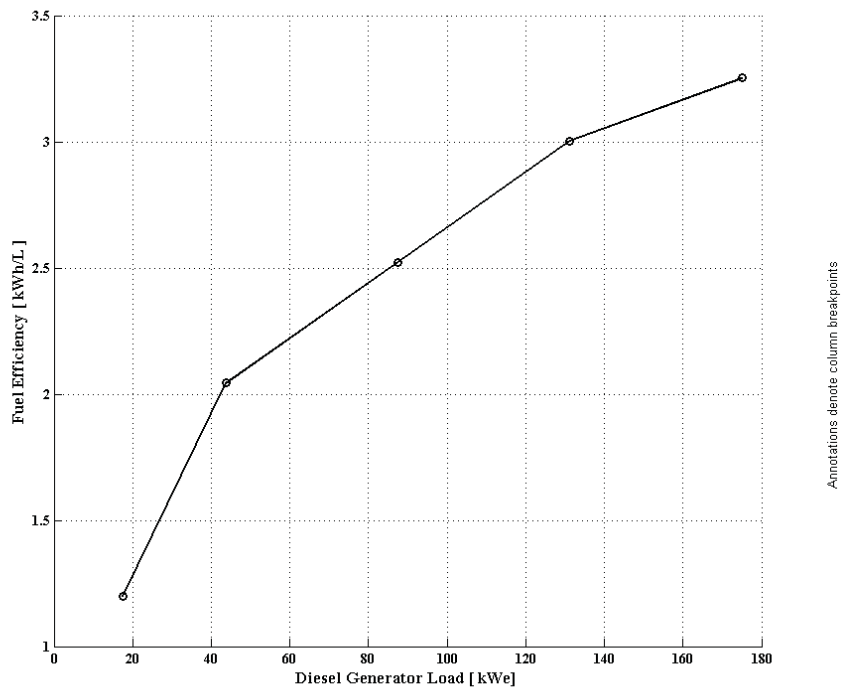


Figure 3.33: CATERPILLAR® 175 kWe diesel generator fuel consumption efficiency in kWh/L [26].

To analyze the temperature effects of both the inlet air and exhaust air on diesel efficiency, a model block of the diesel engine was necessary and is seen in Figure 3.34.

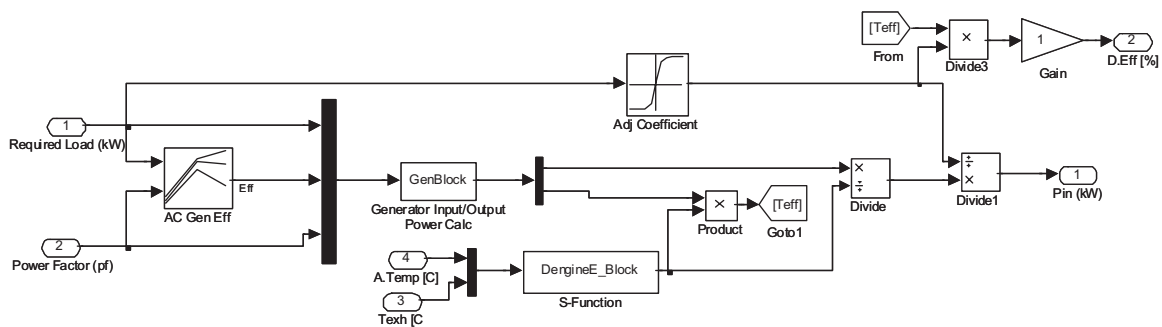


Figure 3.34: Internal structure of *DEG Efficiency* block.

3.5.2.2.1 Engine Efficiency Calculation Block: *DengineE_Block*

The model in Figure 3.34 utilizes the Diesel cycle to calculate the diesel engines efficiency. This calculation is programmed into the S-function *DengineE_Block*. Figure 3.35 illustrates the curves associated with the Diesel cycle.

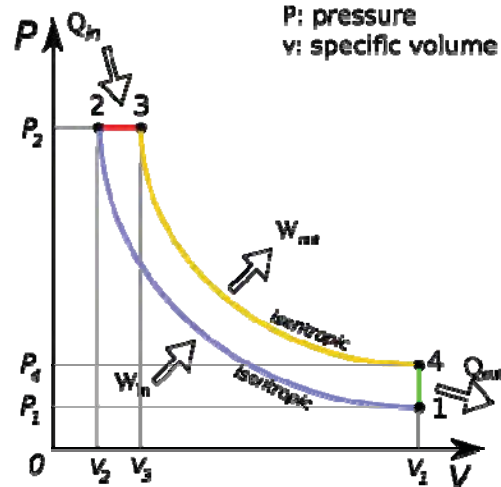


Figure 3.35: Diesel Cycle P-v diagram [27].

The equations that are derived from the Diesel cycle are as follows [24]:

$$r = \frac{V_1}{V_2}, \quad (\text{Eq. 3.28})$$

$$r_c = \frac{V_3}{V_2}, \quad (\text{Eq. 3.29})$$

$$V_4 = V_1, \quad (\text{Eq. 3.30})$$

where V_1 , V_2 , V_3 , and V_4 are the volumes of the piston at each point in the cycle. Eq. 3.28 shows that r (compression ratio) is a ratio of volumes at points 1 and 2 of the diesel cycle and r_c (exhaust ratio) is a ratio of volumes between points 2 and 3 of the Diesel cycle.

Process 1-2 is isentropic compression of an ideal gas given constant specific heats:

$$T_2 = T_1 \left(\frac{V_1}{V_2} \right)^{k-1}, \quad (\text{Eq. 3.31})$$

$$P_2 = P_1 \left(\frac{V_1}{V_2} \right)^k, \quad (\text{Eq. 3.32})$$

where T_1 is the inlet temperature, T_2 is the temperature of the working fluid after compression, P_1 and P_2 is the pressure within the cylinder at points 1 and 2, and k is the specific heat ratio value of air at room temperature.

Process 2-3 is constant pressure heat addition to an ideal gas:

$$P_3 = P_2, \quad (\text{Eq. 3.33})$$

$$\frac{P_2 V_2}{T_2} = \frac{P_3 V_3}{T_3} \rightarrow T_3 = T_2 \left(\frac{V_3}{V_2} \right), \quad (\text{Eq. 3.34})$$

where P_3 is the cylinder pressure and T_3 is the temperature at point 3.

Process 3-4 is isentropic expansion of an ideal gas given constant specific heats:

$$T_4 = T_3 \left(\frac{V_3}{V_4} \right)^{k-1}, \quad (\text{Eq. 3.35})$$

$$P_4 = P_3 \left(\frac{V_3}{V_4} \right)^k, \quad (\text{Eq. 3.36})$$

where P_4 (exhaust pressure) is the cylinder pressure and T_4 (exhaust temperature) is the temperature at point 4 of the Diesel cycle.

From the above equations diesel thermal efficiency can be calculated by the following equation:

$$\eta_{th,Diesel} = \frac{W_{net}}{q_{in}} = 1 - \frac{q_{out}}{q_{in}} = 1 - \frac{T_4 - T_1}{k(T_3 - T_2)}, \quad (\text{Eq. 3.37})$$

where $\eta_{th,Diesel}$ is the thermal efficiency of the ideal Diesel cycle, W_{net} is the net work of the cycle, q_{in} is the heat transferred into the working fluid, and q_{out} is the heat transferred out of the working fluid.

The variables that are given for calculation of efficiency are: T_1 , T_4 , and r . T_4 and r are given by the manufacturer's data sheet and T_1 is a variable determined by the ambient air temperature. Calculation of the diesel engine efficiency requires knowing T_2 and T_3 . T_2 is easily calculated using Eq. 3.31. The calculation of T_3 requires knowing r_c and the calculation of r_c can be accomplished by algebraic manipulation utilizing the relationships defined in Eqs. 3.28 - 3.30 as follows:

$$T_4 = T_3 \left(\frac{V_3}{V_4} \right)^{k-1} = T_3 \left(\frac{r_c V_2}{V_1} \right)^{k-1} = T_3 \left(\frac{r_c}{V_1} \left\{ \frac{V_1}{r} \right\} \right)^{k-1} = T_3 \left(\frac{r_c}{r} \right)^{k-1}. \quad (\text{Eq. 3.38})$$

Now, factoring the exponent and substituting the relationship between T_2 and T_3 we get:

$$T_4 = \frac{T_2 r_c (r_c)^{k-1}}{r^{k-1}} = \frac{T_2 r_c^k}{r^{k-1}}, \quad (\text{Eq. 3.39})$$

Solving for r_c ,

$$r_c = \left[\frac{T_4 (r^{k-1})}{T_2} \right]^{1/k} = \left(\frac{T_4}{T_1} \right)^{1/k}, \quad (\text{Eq. 3.40})$$

T_3 can then be calculated using r_c and the four temperatures can be input into Eq. 3.37 to find the diesel thermal efficiency based on inlet and outlet temperatures. Another method to calculate thermal efficiency is to use the values of r , r_c , and k directly into the thermal efficiency equation re-arranged as a function of r , r_c , and k as seen in Eq. 3.41 below.

$$\eta_{th, Diesel_c} = \frac{1}{r^{k-1}} \left[\frac{r_c^{k-1}}{k(r_c - 1)} \right], \quad (\text{Eq. 3.41})$$

However, it must be noted here that the value of r_c is calculated by using the exhaust temperature, T_4 rating of the DEG based on the manufacturer's data and an inlet temperature, T_1 at STP which is 25 °C. Since the values of T_1 and T_4 used in the calculation of r_c remain constant for a given diesel engine, r_c will remain constant for a given diesel electric generator. This means that the ratio T_4/T_1 must remain constant as well. This, combined with a constant r , results in a constant ideal cycle efficiency, since the efficiency becomes dependant only on r , r_c , and k seen in Eq. 3.41. For this thesis it is assumed that r and r_c are to remain constant. The changes in diesel generator efficiency that are seen in the simulation are not directly due to temperature effects on the diesel cycle, but are an effect of temperature on combustion discussed in a following section. However, if r_c was based on T_4 , an increase in efficiency would be seen for an increase in inlet temperature. The S-function *DengineE_Block* contains a program script for the calculation of diesel thermal efficiency.

3.5.2.2.2 Adjustment Coefficient Table Construction

The thermal efficiency of the diesel generator calculated by the model does not take into account thermal losses. Therefore, to more accurately define the efficiency of the diesel generator at standard operating conditions the curves of diesel thermal efficiency and the efficiency based on the manufacturer's curves *Fuel Curve* block are compared to create a table that defines the percentage of losses, this table is the *Adj Coefficient* block in Figure 3.36 and is determined by the *Adjustment Coefficient Simulation* seen in Figure 3.37. This allows the simulation when run at standard operating conditions for the generators to calculate fuel consumption equal to that of the manufacturer's curves. Now, when there is a change in operating temperatures the final efficiency will account for thermal and mechanical losses within the generator.

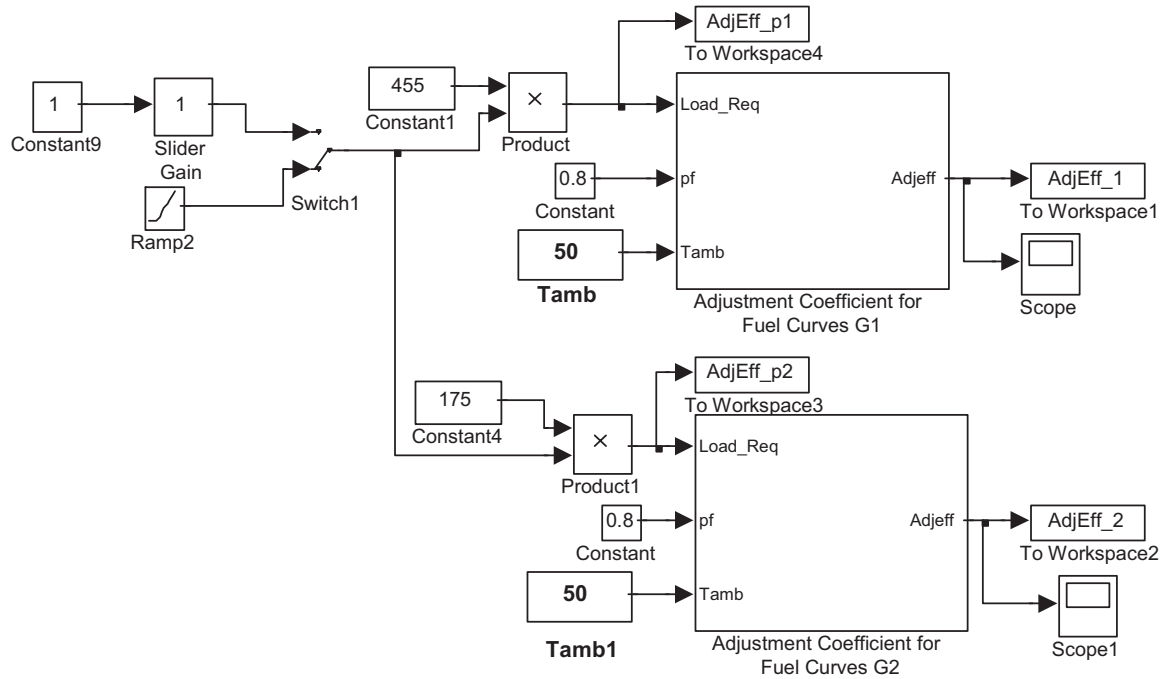


Figure 3.36: Efficiency adjustment calculation simulation diagram.

These thermal losses are affected by factors such as the difference between ambient room temperature and the generator's operating temperature. However, these factors affecting the thermal losses are not considered in this model for simplicity and computational time considerations. If we were to include these losses, we could say the convective heat loss rate from the engine to the surroundings decreases as T_{amb} increases. This is because this loss rate is proportional to $T_{eng} - T_{amb}$ which decreases as T_{amb} increases. Here, T_{eng} is the engine surface temperature and T_{amb} is the ambient temperature.

To calculate the diesel efficiency from the manufacturer's curves requires knowing what other parameters and conditions the data is based on. This information is included on the data sheets. For example, for the 445 kWe CATERPILLAR[®] diesel, the manufacturer's curves are based on steady state operating conditions of 25 °C and fuel rates based on #2 diesel fuel with a LHV of 42780 kJ/kg when used at 29 °C and weighing 0.08389 kg/L [28]. By taking this information and the fuel consumed for a value of output power in kWe, the overall percent efficiency between the fuel input and the electrical output for the diesel electric generator can be calculated based on manufacturer's data.

The following equation demonstrates these calculations and its representative Simulink[®] equivalent can be seen in the upper portion of Figure 3.34 showing the process diagram in the simulation.

$$\%Eff_{DEG} = Load \left(\frac{1}{Eff_{fuel}} \right) \rho_{fuel} LHV_{fuel} \left(\frac{h}{3600s} \right), \quad (\text{Eq. 3.42})$$

where $\%Eff_{DEG}$ is the diesel generator efficiency in percent, $Load$ is the load to be supplied by the generator in kW, $\%Eff_{fuel}$ is the efficiency of the generator supplied by the manufacturer's curve in (kWh/L), ρ_{fuel} is the density of the fuel, and LHV_{fuel} is the heating value of the fuel supplied on the manufacturer's specification sheet.

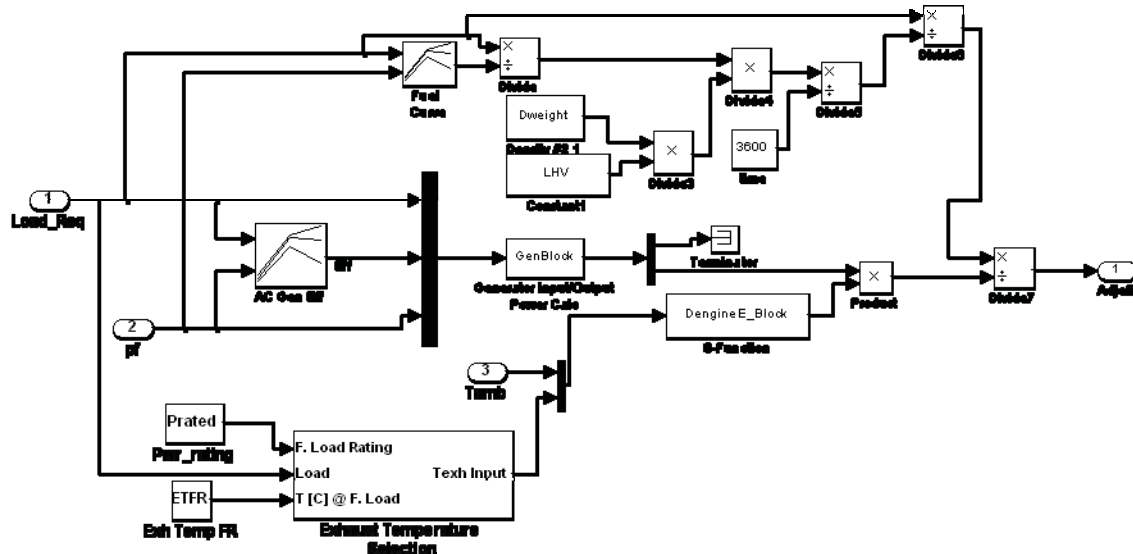


Figure 3.37: *Adj. Coefficient* block diagram calculating adjustment percentage for diesel thermal efficiency based on manufacturer's fuel consumption curves.

The following pieces of Figure 3.35 are identical to those found in the *E-Gen Efficiency & Input Power* block of the *Main System Simulation* and are discussed in Section 3.5.2.2.2.5:

- *Fuel Curve* Block
- *AC Gen Eff* Block
- S-Function *GenBlock*
- S-Function *DengineE_Block*
- Inputs & Constants:
 - *Prated*
 - *-C-*
 - *Load_Req*
 - *Tamb*

With the diesel generators calculated efficiency and the manufacturer's efficiency known then the manufacturer's efficiency can then be divided by the calculated efficiency to acquire an adjustment factor that can be used to create the adjustment *Adj Coefficient* block. To accomplish this, the *Adjustment Coefficient for Fuel Curves* block in Figure 3.36 which

represents the diesel generator has to be simulated at the standard operating condition given by the manufacturer's data sheet. The information of each generator was input manually at first, however, currently the information is transferred from the *Main System Simulation* to this *Adjustment Coefficient Simulation* prior to the main simulation running. The *Switch1* block seen in Figure 3.36 is normally set to route the *Ramp2* block output to the *Product* blocks. The range of values that the *Ramp2* block outputs is from 0 to 1 in steps of 0.1. This allows the *Adjustment Coefficient Simulation* to calculate the efficiency adjustment coefficient for any generator from zero load to full rated load. Upon completion of this pre-simulation the values for the adjustment coefficients for each generator are saved to the MATLAB® workspace for use in the *Adj Coefficient* block in the *E-Gen Efficiency & Input Power* block of the *Main System Simulation*.

3.5.2.2.2.3 Generator Input/Output Power Calculation Block

The *Generator Input/Output Power Calc* block located in the center of both Figures 3.34 and 3.35 is a MATLAB® S-Function block titled 'GenBlock'. The S-Function was originally written to allow for adjusting the AC generator curves of diesel generators that had their rotating speed reduced to 1,200-rpm from a rated speed of 1,800-rpm like the UAF Energy Center's generator. However, technological advancement in metallurgy, improved engine design, and better engine lubricants have narrowed the difference between 1,200-rpm and 1,800-rpm engines [3]. In addition, due to increasingly competitive markets in the size range of engines used in rural Alaska, the 1,800-rpm configuration provides more installed kW per dollar spent than the 1,200-rpm engine can provide. Therefore, it will be assumed that the approximately 23 percent of Alaska utilities having de-rated engines will in the future upgrade to 1,800-rpm engines. This will allow the program script in the S-function to be re-written to simplify the calculation and decrease computational time of the simulation. The new script is based on the following:

$$P_{in} = \frac{P_{sys}}{effr}, \quad (\text{Eq. 3.43})$$

where P_{sys} is the output power of the generator required to supply the load, $effr$ is the efficiency in percent of the AC generator at converting input power to output power as is a function of the required output power in kWe, and P_{in} is the input power from the diesel engine required to provide the required output power demanded by the load. This input power P_{in} in kW then goes to a *Product* block where it is multiplied by the engine efficiency. Due to the change in *Generator Input/Output Power Calc* block program script, the UAF diesel generators curves were adjusted prior to inclusion within the simulation.

3.5.2.2.2.4 AC Generator Efficiency Table

The *AC Gen Eff* block seen in Figures 3.34 and 3.36 are based on the manufacturer's specifications for the AC generator in the diesel generator unit. The manufacturer normally specifies the efficiency of the generator at a power factor (pf) of 0.8. After analyzing data from a number of villages, the power systems normally operate with a power factor that varies between 0.8 and close to 1.0. Therefore, to allow for the calculation of necessary input power with these higher power factors a 2.0 % increase in the data for the 0.8 pf was added to obtain the 1.0 pf curve. The 2.0 % increase was determined by taking the curves of an actual generator that provided curves for both 0.8 pf and 1.0 pf. Figure 3.38 shows the curves for a Marathon electric

generator. Four points have been labeled and are: point 1 (82.5%), point 2 (83.7%), point 3 (90.1%), and point 4 (83.4%).

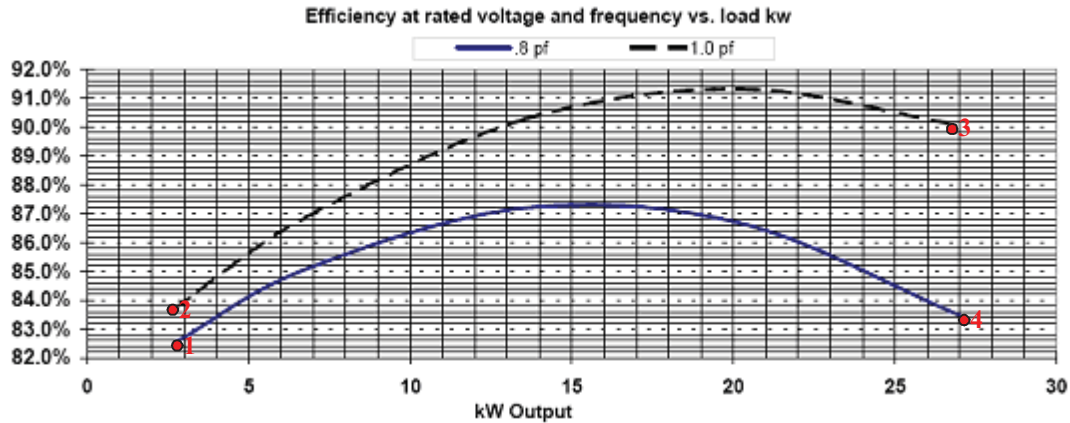


Figure 3.38: Electrical efficiency for a 21 kW Marathon electric generator [29].

$$Eff_{newavg} = \left[\frac{(pt2 - pt1) + (pt3 - pt4)}{2} \right] * 50\% = \left[\frac{(83.7 - 82.5) + (90.1 - 83.4)}{2} \right] * 50\% = 2.0\% , \quad (\text{Eq. 3.44})$$

The average difference between the points was calculated as illustrated in Eq. 4.24. The value was then multiplied by 50% to account for variations between different makes and models of generators. Figure 3.39 illustrates the AC generator efficiency curves at 0.8 pf and 1.0 pf for the UAF diesel generator.

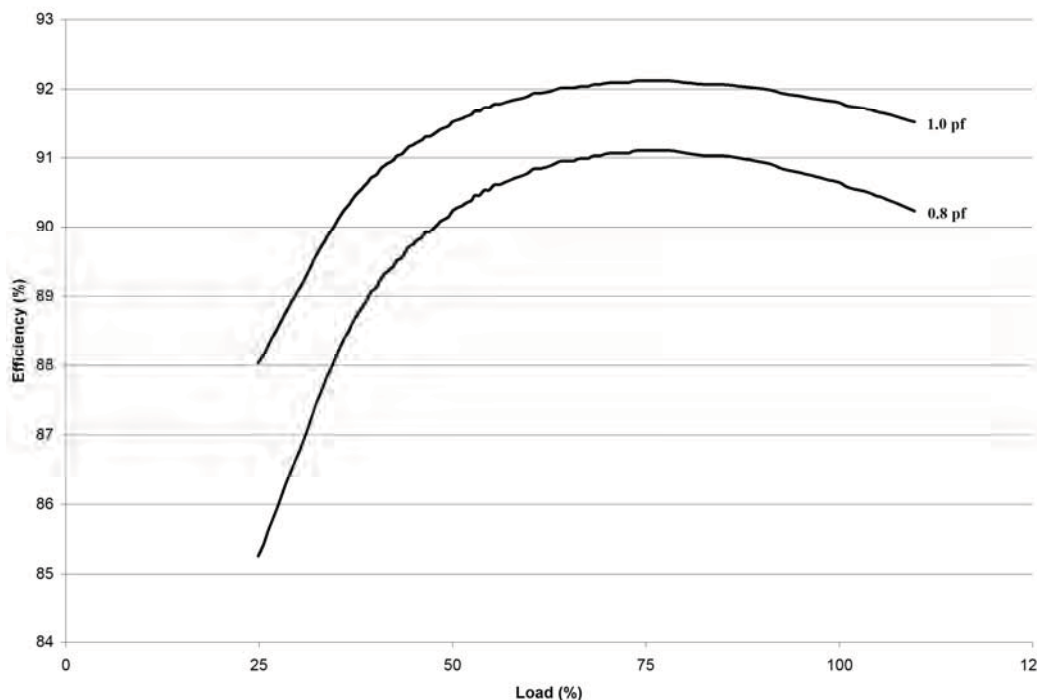


Figure 3.39: UAF Energy Center diesel generator unit's AC generator efficiency curves [30].

The UAF DEG curves in Figure 3.39 are in terms of percent load. These curves will be the basis for all other AC generators of DEGs used within the simulation. In addition, a 50% reduction was considered to be too conservative, therefore the 2% adjustment was applied to the 0.9 pf curve data and the base curve was readjusted. However, some of the manufacturers list the AC generator efficiencies only at rated power. Therefore, the data used to create the curves above are adjusted to match the specific AC generator efficiency at rated load. In addition, since the data pertaining to the curves in Figure 3.39 are in percent load, the percent load is multiplied by the generator's power rating to achieve a data set for the x-axis in kWe load. This process is repeated for all AC generators simulated in the system analysis and the data sets are utilized to create the table in the *AC Gen Eff* block. This data is then input into the *AC Gen Eff* block by use of the block parameters screen seen in Figure 3.40 where the load power data is the input to the block, the power factors are input in the column index, and the output values of efficiency are listed in the parameters output values as vectors.

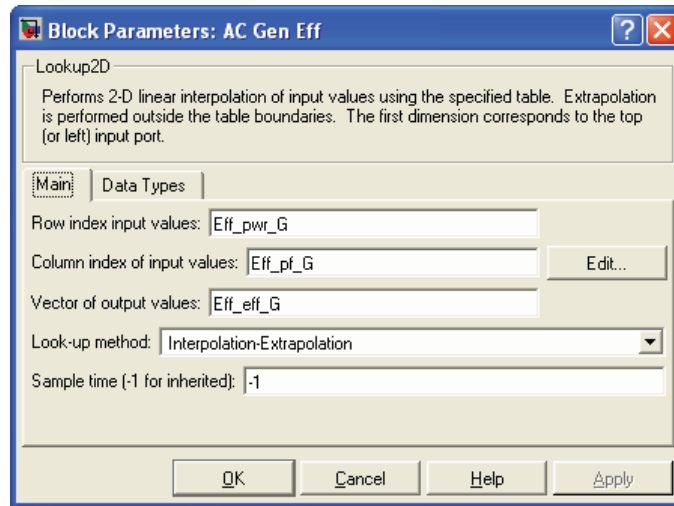


Figure 3.40: Block parameters screen for the *AC Gen Eff* block showing input data variables.

3.5.2.2.2.5 E-Gen Efficiency & Input Power: Inputs and Outputs

There are four direct inputs and two direct outputs to the *E-Gen Efficiency & Input Power* block, the inputs labeled *Required Load*, *Power Factor*, *A.Temp*, and *Texh* are tied to the direct inputs in the *DEG* blocks. *Required Load* is used as the input to the *AC Gen Eff* table block, the *Adj Coefficient* table block, and to the S-Function block *Generator Input/Output Power Calc* through a multiplexer block. *Power Factor* is only used as inputs to the *AC Gen Eff* table block and to the S-Function block *Generator Input/Output Power Calc* again through the multiplexer block. Both *A.Temp* and *Texh* inputs are directed through another multiplexer as inputs to the S-Function *DengineE_Block*.

The outputs of the *E-Gen Efficiency & Input Power* block are *D.Eff* and P_{in} which are inputs to other blocks within the *DEG* block. *D.Eff* is the total diesel generator efficiency after adjustment. It is the multiplication of the AC generator efficiency, the diesel engine efficiency, and the adjustment coefficient shown in Eq. 3.45.

$$D.Eff = AC\ Gen\ Eff(DengineE_Block\ Eff)(Adj\ Coefficient), \quad (\text{Eq. 3.45})$$

P_{in} is the total power in kW required as an input to achieve the desired output to meet the load. The value of P_{in} is calculated as

$$P_{in} = \frac{P_{sys}}{AC\ Gen\ Eff} \left(\frac{1}{DengineE_Block\ Eff} \right) \left(\frac{1}{Adj\ Coefficient} \right). \quad (\text{Eq. 3.46})$$

3.5.2.2.3 DEG Block: Manufacturer's Fuel Curve

The manufacturer's data on fuel consumption in kWh/L as a function of output load in kW as specified in the data sheets in graphical format is illustrated in Figure 3.41 for two diesel generators. As can be seen there is only one curve for each generator using #2 diesel with a 0.8 pf load. Higher power factor will lead to a higher efficiency, and therefore, lower fuel consumption. The fuel consumption efficiencies in kWh/L at higher power factors are calculated

by taking the data for the curves at 0.8 pf and adding approximately 0.2 kWh/L to the values for 0.8 pf to arrive at values for a 0.9 pf rating.

The 0.2 kWh/L was determined by using the 2% increase in the AC efficiency determined in a previous section, standard heating value (HV) of #2 diesel fuel (42780 kJ/kg), and the density of #2 diesel fuel (0.838 kg/L). First convert fuel HV from kJ/kg to kWh/L using fuel density and appropriate conversion factors, Eq. 3.47 illustrates this step.

$$HV = \frac{42780 \text{ kJ}}{\text{kg}} \frac{0.838 \text{ kg}}{\text{L}} \frac{\text{kW} \cdot \text{s}}{\text{kJ}} \frac{\text{h}}{3600 \text{ s}} = \frac{9.958 \text{ kWh}}{\text{L}} \quad (\text{Eq. 3.47})$$

Now, assuming an AC generator efficiency within the range of normal generators at 0.8 pf of 90% and now add 0.2% for an efficiency of 92% at 0.9 pf. Multiplying these two efficiencies with the value of the fuels HV converted above results in

$$\begin{aligned} 0.8 \text{ pf} : \frac{9.958 \text{ kWh}}{\text{L}} (0.90) &= \frac{8.962 \text{ kWh}}{\text{L}} \\ 0.9 \text{ pf} : \frac{9.958 \text{ kWh}}{\text{L}} (0.92) &= \frac{9.161 \text{ kWh}}{\text{L}} \end{aligned} \quad (\text{Eq. 3.48})$$

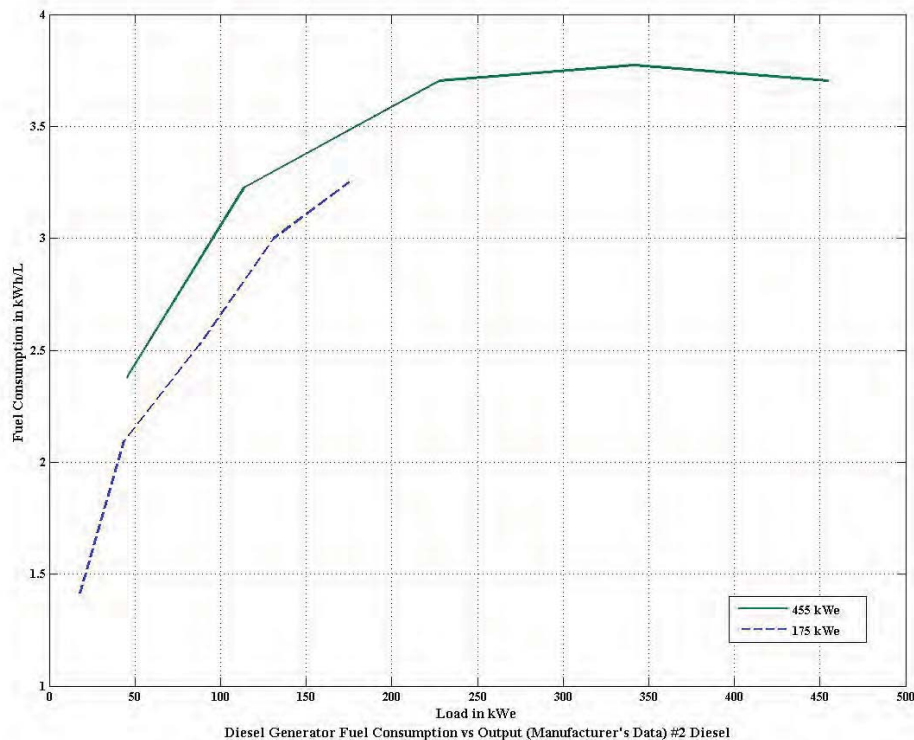


Figure 3.41: Manufacturer's fuel curve for CATERPILLAR® 175 kWe and 455 kWe diesel electric generators [26] [28].

Finally, the difference between the values above in Eq. 3.48 is 0.19936 kWh/L. This value is rounded up to 0.2 kWh/L and added to the value of efficiency at 0.8 pf to arrive at the value of fuel efficiency at 0.9 pf.

The data from the manufacturers is organized in vector form for input into the *Fuel Curve* table block parameter window in MATLAB® as seen in Figure 3.42 below. By listing this data as variables it allows multiple generators with their own fuel curves to be associated with just one *Fuel Curve* table block located within each *DEG* block.

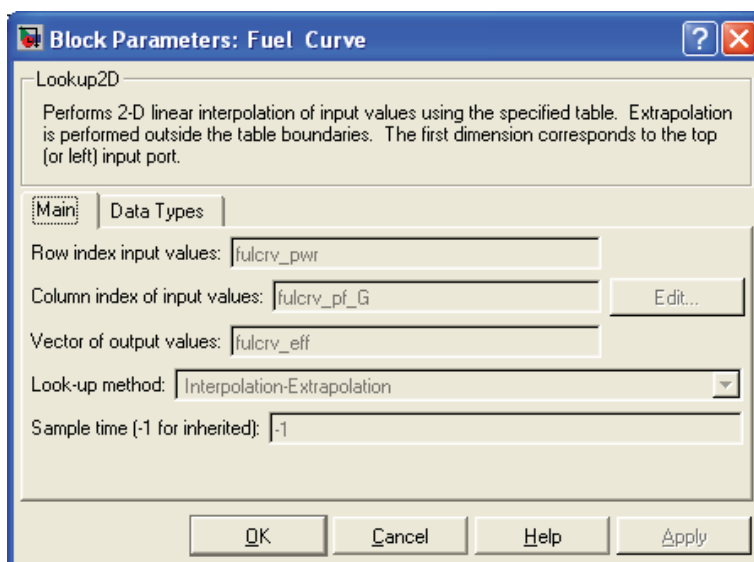


Figure 3.42: *Fuel Curve* table block parameter screen for manufacturer's fuel curve data variables.

3.5.2.2.4 DEG Block: Value Integration Total Block

The *Total-lizer* block shown in Figure 3.43, allows for the integration of a variable over time and is placed within the library for use throughout the *Main System Simulation* and the *Adjustment Coefficient Simulation*. The way the *Total-lizer* block works is that the *Memory* block stores the value output by the *sum* block for reuse as an input to the *sum* block on the next simulation time step. The *sum* block then adds the current value with the previous value and outputs the summed value to be held by the *Memory* block. The output of the *Memory* block is also multiplied by the simulation's sampling rate and the value 24 found within the *Gain* block. The value 24 represents 24 hours in a day, thereby converting the incoming hourly data into a daily value. The *Gain* block converts the current *Memory* block output value into a value based in hours.

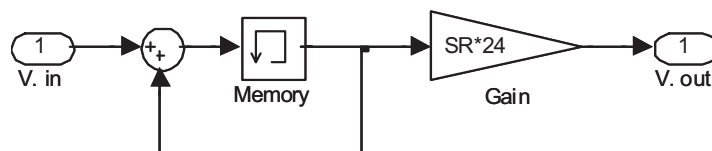


Figure 3.43: Inner diagram of the *Total-lizer* block.

3.5.2.2.5 DEG Block: Diesel Electric Generator Overall Efficiency Block

The *DEG Efficiency* block shown in Figure 3.44 multiplies the diesel generator units efficiency by the efficiency of the fuel which is based on the heating value of the fuel at the specified temperature divided by the heating value of the fuel at STP. The efficiency of the fuel is an output of the *Heating Values for Diesel* block. The outputs of the *DEG Efficiency* block are the diesel generator unit's efficiency and the diesel generator's overall efficiency for both fuel types.

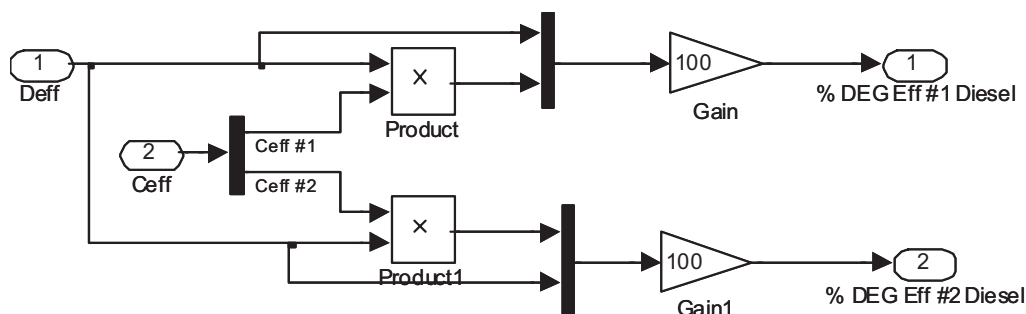


Figure 3.44: Inner diagram of the *DEG Efficiency* block within the *DEG* block.

3.5.2.2.6 DEG Block: Incoming Air Control Block

The *Incoming Air Control* block allows for the specification of the incoming air not to drop below a specific threshold. In Figure 3.45, the threshold specified is 5° C (41° F).

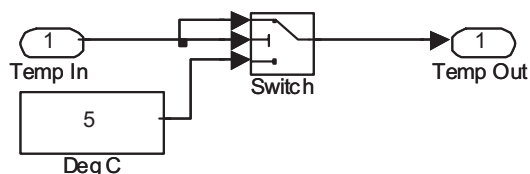


Figure 3.45: *Incoming Air Control* block diagram.

This value of the threshold will be maintained if the value of the incoming ambient air temperature is below the threshold value. The simulation is run at this value based on the following assumptions:

- Extreme cold temperature effects on diesel fuel combustion is difficult to model [31], [32].
- Optimal diesel engine efficiencies have been found to occur with inlet air temperatures above 5 °C.
- The model does not properly predict possible effects that icing and extreme cold air may have on the diesel engine internal components or on the combustion process, therefore in conjunction with the previous assumption a value of 5 °C was chosen.

3.5.2.2.7 DEG Block: Heating Values for Diesel Fuel Block

3.5.2.2.7.1 Fuel Energy Component Development

A combustion chamber typically has large amounts of heat output, and little or no heat input. In this case, the energy balance for a *typical steady-flow combustion process* becomes

$$Q_{out,comb} = \sum_r N_r \left(\bar{h}_f^\circ + \bar{h} - \bar{h}^\circ \right)_r - \sum_p N_p \left(\bar{h}_f^\circ + \bar{h} - \bar{h}^\circ \right)_p, \quad (\text{Eq. 3.49})$$

where $Q_{out,comb}$ is the heat output during combustion, N_r and N_p are the number of moles of the reactant r and the product p , respectively, per mole of fuel, and h_f° is the enthalpy of formation at the standard reference *state*. The reference *state* refers to the temperature in degrees Kelvin for the enthalpy in question. The N_r and N_p values are picked directly from the balanced combustion equations.

Eq. 3.49 expresses that the heat output or heating value of a fuel during the combustion process is simply the difference between the energy of the reactants entering and the energy of the products leaving the combustion chamber [24]. The heating value of a fuel is equal to the absolute value of enthalpy of combustion of the fuel. Therefore, in a reacting system the heating value of a fuel is represented by the difference between \bar{h} (sensible enthalpy at a specified *state*) and \bar{h}° (sensible enthalpy at the standard reference *state*) and is expressed in kJ/kmol (Btu/lbmol) of fuel. A simplified form of Eq. 3.49 is illustrated in Eq. 3.50 below:

$$Q_h = H_r - H_p, \quad (\text{Eq. 3.50})$$

where Q_h represents the energy input into the system by fuel combustion, H_r is the enthalpy of the reactant (intake air/fuel mixture), and H_p is the enthalpy of the product (exhaust gases). Examining Eq. 3.49 shows that, as the specified *state* changes so will the heating value. In simple terms efficiency is defined by the electrical work out produced W_{el} , divided by Q_h , Eq. 3.50. The simplified efficiency equation can be seen in Eq. 3.51.

$$\eta = \frac{W_{el}}{Q_h}, \quad (\text{Eq. 3.51})$$

Now, if the temperature of the reactants was to increase, enthalpy of those reactants would likewise increase, thereby increasing the energy input into the system from the combustion output of the fuel, Eq. 3.50. This would result in a decrease in efficiency, assuming that electrical work out does not increase proportionally. However, this is assuming that the enthalpy of the products does not increase with the increase in the reactants temperature. A change in inlet temperature affects the exhaust temperature. However, since it is expected that small changes in inlet air temperature will have little effect on efficiency and since many variables relate inlet air temp to exhaust temperature, changes in exhaust temperature maybe even

smaller. Therefore, we will not attempt to incorporate changes in exhaust temperature for this study. This effect is examined by simulation in the results section of this thesis.

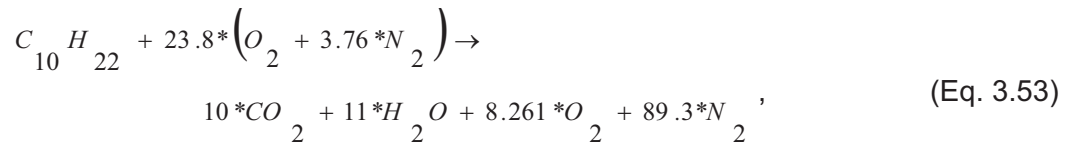
To examine the possible effects of temperature on fuel consumption and DEG efficiency, table blocks were developed in Simulink[®] that use NASA's 9-constants polynomials to calculate individual products and reactants change in sensible enthalpy over a range of temperatures, this calculation is represented by Eq. 3.52 [33-35].

$$\frac{H^\circ_T}{RT} = -a_1 T^{-2} + \frac{a_2 \ln T}{T} + a_3 + \frac{a_4 T}{2} + \frac{a_5 T^2}{3} + \frac{a_6 T^3}{4} + \frac{a_7 T^4}{5} + \frac{b_1}{T}, \quad (\text{Eq. 3.52})$$

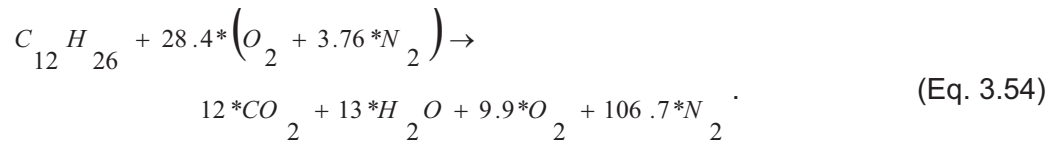
where $a_1, a_2, a_3, a_4, a_5, a_6, a_7,$ and b_1 are polynomial constants, T is the reference temperature, R is the gas constant, and H_T is the enthalpy of a component on a unit-mole basis.

Thermobuild an interactive tool which uses the NASA Glenn thermodynamic database was used to create a table of thermodynamic properties at specified temperatures that then could be input into the table blocks for use in the Simulink[®] model of Eq. 3.48 as shown in Figure 3.46 for # 1 diesel and Figure 3.47 for #2 diesel [24], [33]. The chemical formulas for #1 and # 2 diesel fuel chosen are $C_{10}H_{22}$ and $C_{12}H_{26}$, respectively.

Using the chemical formulas and the associated balance combustion, Eqs. 3.53 and 3.54, the molar units could be added to Eq. 3.48 as gain blocks in Figure 3.47.



and



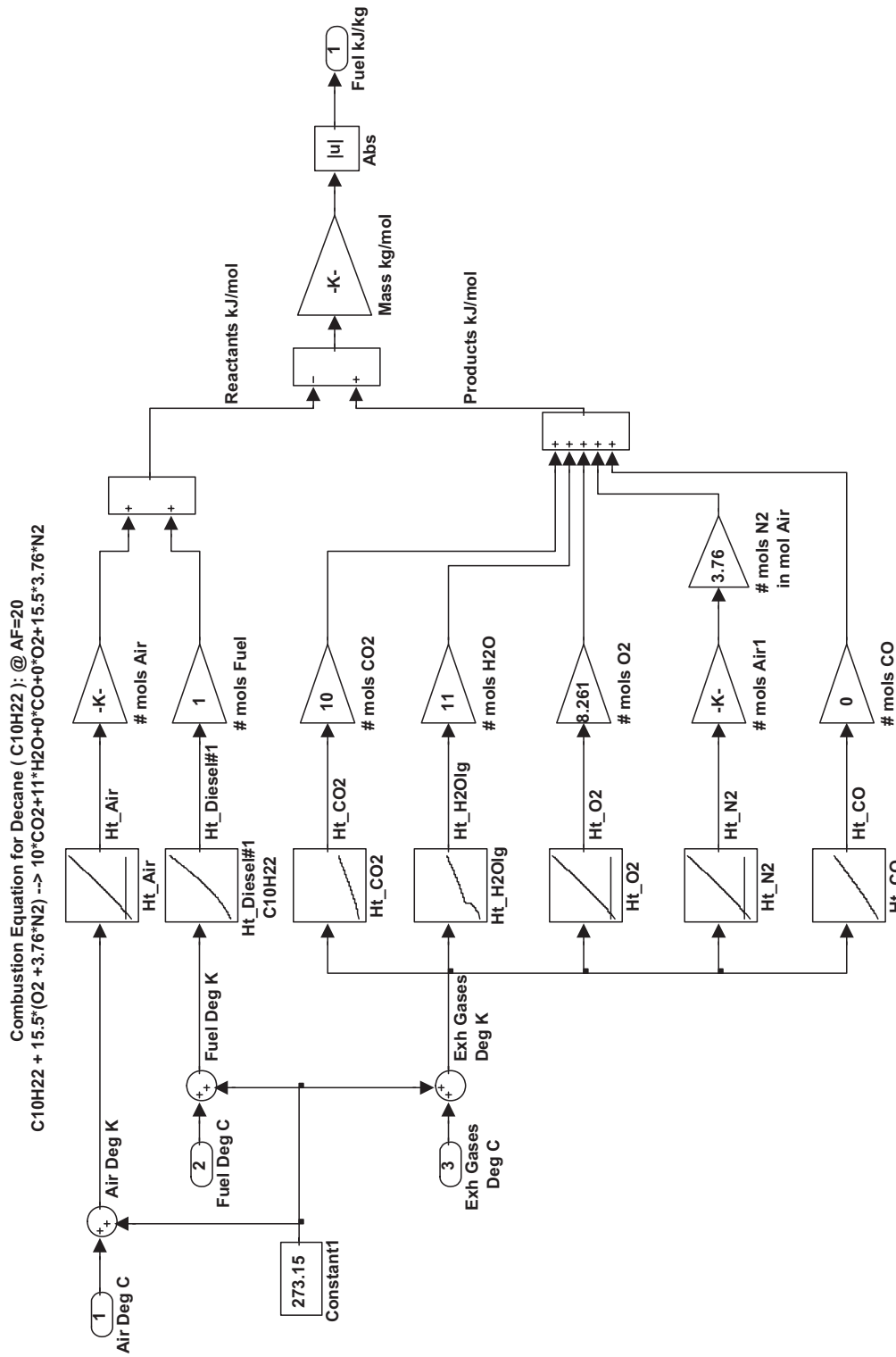


Figure 3.46: Simulink® model of the combustion equation (Eq. 3.53) for #1 diesel fuel.

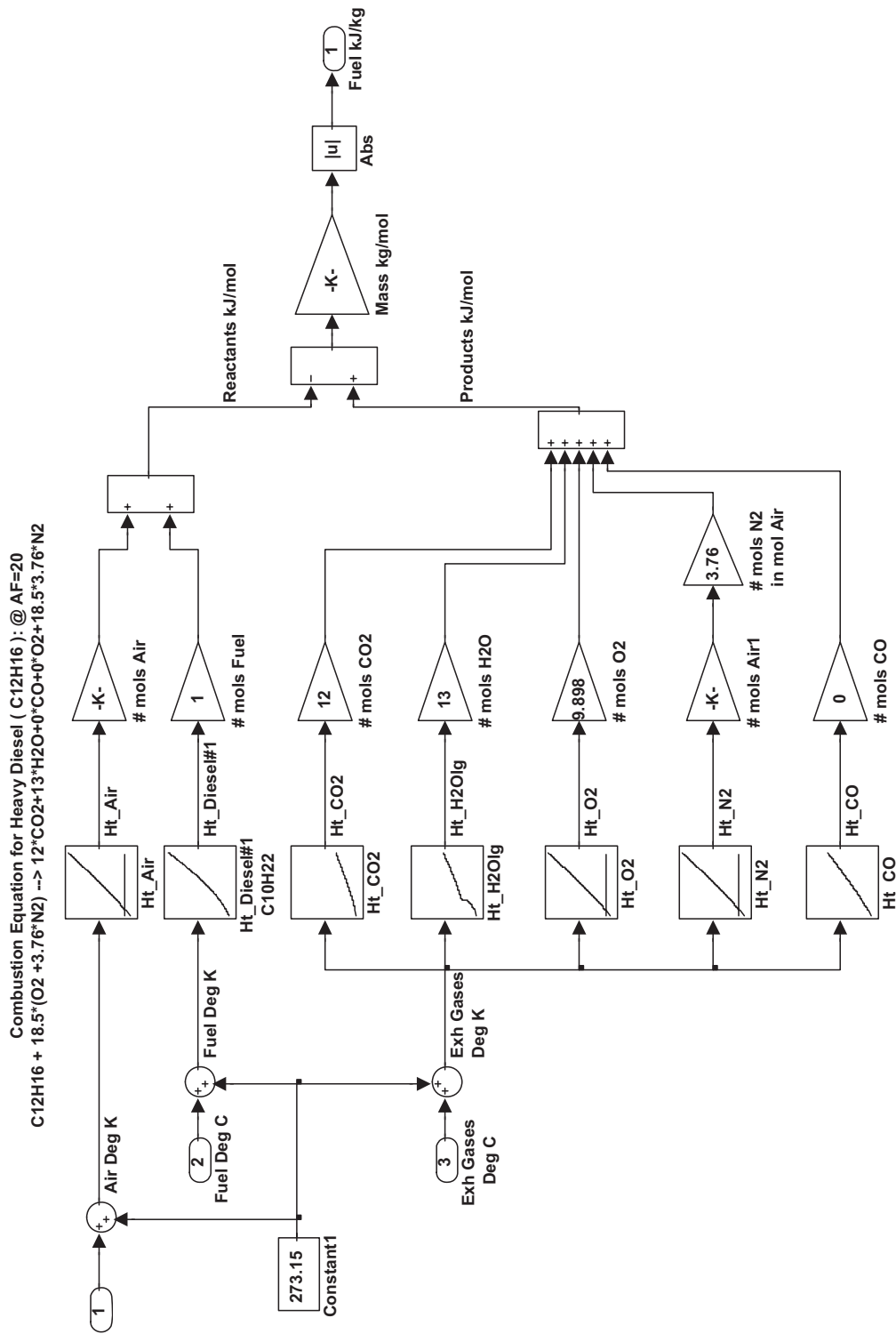


Figure 3.47: Simulink® model of the combustion equation (Eq. 3.54) for #2 diesel fuel.

3.5.2.2.7.2 Fuel Energy Component Testing

The systems in Figures 3.46 and 3.47 were simulated at STP to examine possible error between the simulated heating values for #1 and #2 diesel fuels. Table 3.1 shows the simulated values for both fuels at STP, compared to the higher heating value (HHV) and lower heating value (LHV) given in [24]. The simulated values for both diesel fuels are within the range of HHV and LHV from [24].

Table 3.1: Comparison table of simulation heating values to referenced values.

Parameter	Reference Heating Value kJ/kg (Btu/lbm) [13]		Simulated Heating Value (@ STP) kJ/kg (Btu/lbm)
	Higher	Lower	
# 1 Diesel	47640 (20490)	44240 (19020)	44580 (19166.2)
#2 Diesel	45500 (19600)	42800 (18400)	44450 (19109.3)

3.5.2.2.8 DEG Block: Fuel Use Conversion Block

The input energy divided by the fuel's heating value will result in the amount of fuel energy in (L/h) required to meet the load demand. This is illustrated by Eq. 3.55 and in the Simulink[®] version of the equation seen in Figure 3.48.

$$FuelConsumed \left[\frac{L}{h} \right] = \frac{Energy\ input \left[\frac{kJ}{h} \right]}{HV_{fuel} \left[\frac{kJ}{kg} \right] \left(Fuel\ Density \left[\frac{kg}{L} \right] \right)}, \quad (Eq. 3.55)$$

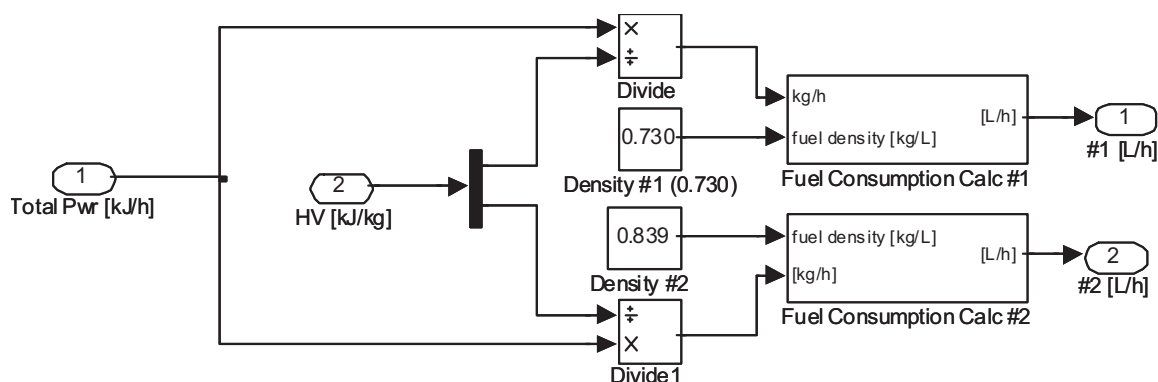


Figure 3.48: Diagram of Fuel Use Conversion block representing Eq. 3.55.

3.5.2.3 Dispatch Techniques

The model is used to perform an economic feasibility analysis for integrating economic dispatch control systems into existing DEG systems. Inputs to the model are the electrical load and power factor profile for the village, and the manufacturer's performance curves for the DEGs. The outputs are the fuel consumption, efficiency (kW-hr/liter), total cost of fuel, and total emissions of CO₂, NO_x and PM₁₀. The fuel efficiency curves for the DEGs in each system tested

were constructed from manufacturer's data and three different load dispatch schemes were implemented: 1) even load distribution (ELD) 2) pre-configured control (PCC) and 3) economic dispatch. ELD assumes all generators are operating to supply the load with the demand distributed evenly based on each DEGs capacity. PCC (see Figure 3.49 and Table 3.2 for Kongiganak, Alaska) turns on and off generators in order of their maximum rating to meet the total demand neglecting efficiency. In this case one of the 190 kW_e DEGs is used strictly as a back up. ED (see Figure 3.50 for Kongiganak, Alaska) finds the optimal operating point to satisfy the demand at the best possible efficiency. Although ELD is used as the base case, this is not necessarily the general operating condition in the village, as all generators would normally not be running unless there was a very high demand. So for comparison to ED, PCC was used to represent the closest possible scenario to the actual operating condition in the village where only the generators that need to be operated to supply the load are used.

This same economic dispatch program was also used to incorporate the effects of ambient temperature variations and was tested on ambient temperature and load data from Kongiganak, Alaska. A 3 °C rise in ambient air temperature over the next 50 years as predicted by scientist at the UAF Geophysical Institute's Alaska Climate Research Center was used in the model to determine the effect on DEG efficiency.

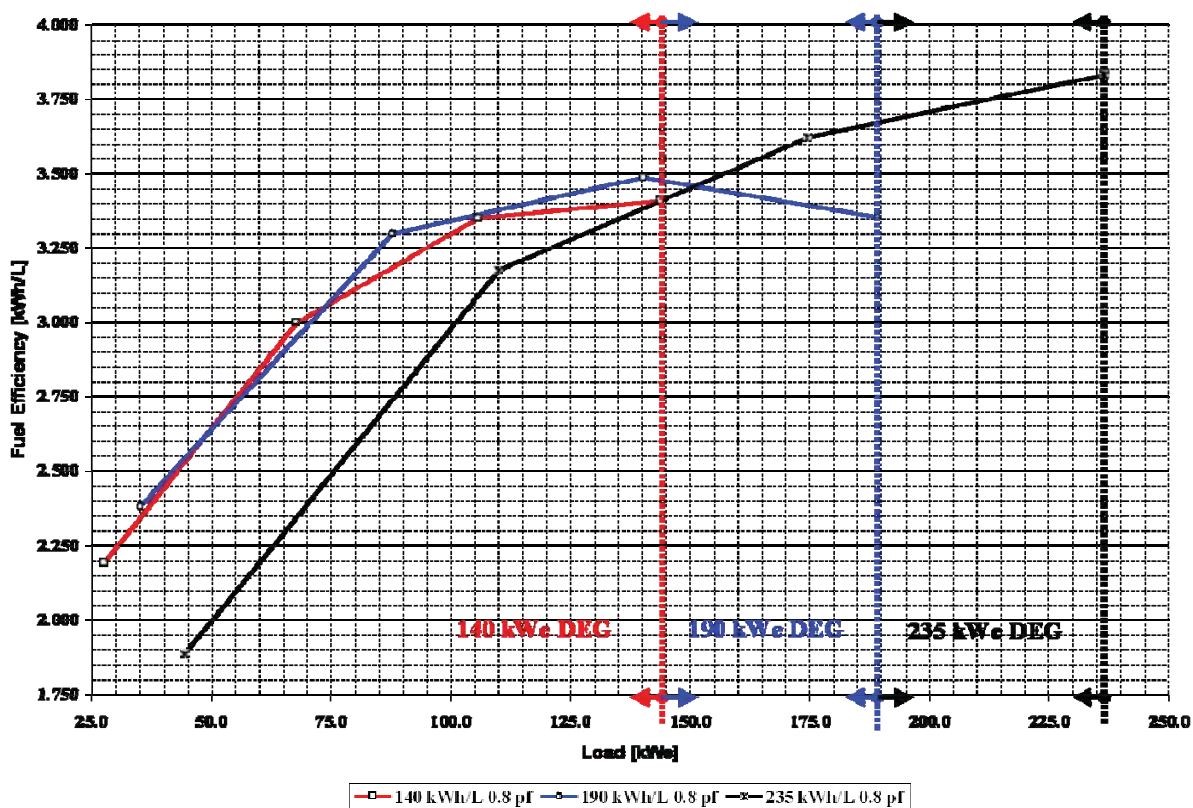


Figure 3.49: PCC zoned manufacturer's fuel curves for the Kongiganak DEGs.

Table 3.2: PCC control scheme for Kongiganak DEGs.

DEG	Load Demand (kWe)						
	< 140	140 – 190	190 – 235	235 – 375	375 – 425	425 - 565	565-755
235 kWe	Off-line	Off-line	On-line	On-line	On-line	ELD mode w/ All 3 DEGs	ELD mode w/ All 3 + Back-up DEGs
190 kWe (1)	Off-line	On-line	Off-line	Off-line	On-line		
140 kWe	On-line	Off-line	Off-line	On-line	Off-line		
190 kWe (2)	Back-up	Back-up	Back-up	Back-up	Back-up		

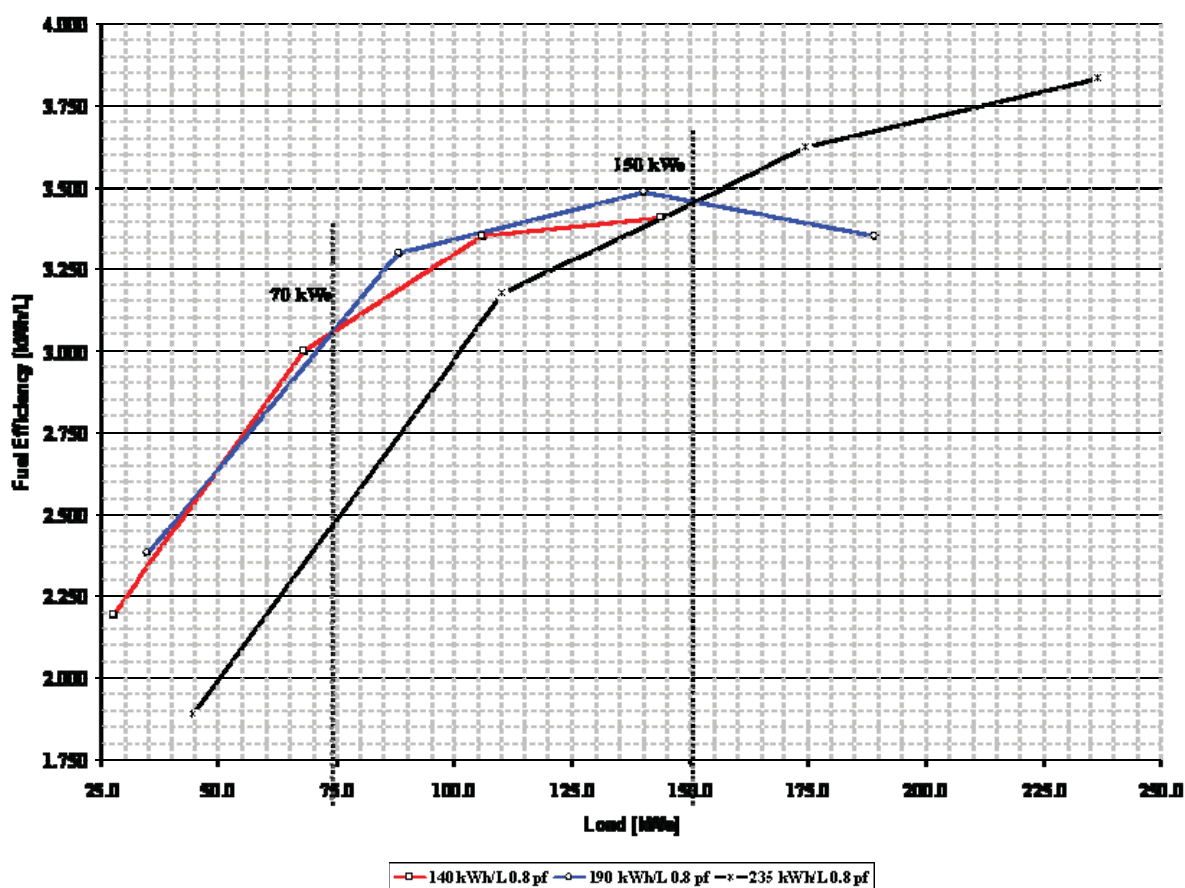


Figure 3.50: ED zoned manufacturer's fuel curves for the Kongiganak DEGs.

3.5.2.4 Classical Economic Dispatch Algorithm

The algorithm for classical economic dispatch is a minimized cost function for plant operation that includes all operating plants as follows in [36]. Given a system with m generators committed, pick the P_{Gi} to minimize the total cost

$$C_T = \sum_{i=1}^m C_i(P_{Gi}), \quad (\text{Eq. 3.56})$$

such that

$$\sum_{i=1}^m P_{Gi} = P_D, \quad (\text{Eq. 3.57})$$

and

$$P_{Gi}^{\min} \leq P_{Gi} \leq P_{Gi}^{\max} \quad i = 1, 2, \dots, m. \quad (\text{Eq. 3.58})$$

where power output is P_{Gi} , fuel cost as a function of power output is $C_i(P_{Gi})$ in the form

$$C_i(P_{Gi}) = \alpha + \beta P_G + \gamma P_G^2, \quad (\text{Eq. 3.59})$$

with positive coefficients, C_T is the total cost, P_D is the total load demand, P_{Gi}^{\min} is the minimum power capability of the generating unit, P_{Gi}^{\max} is the maximum power capability of the generating unit and m is the number of units committed [36].

Now, take the derivative of the fuel cost function with respect to power out to reach a solution in terms of *incremental costs (ICs)*

$$IC_i = \frac{dC_i(P_{Gi})}{dP_{Gi}} = \text{slope of fuel-cost curve}, \quad (\text{Eq. 3.60})$$

assuming the incremental cost curves are linear to arrive at

$$IC_i = \beta + \gamma P_G. \quad (\text{Eq. 3.61})$$

Now, apply the above equations to a known fuel-cost curve and a known total load to be supplied. Figure 3.51 shows an example of two generators with differing fuel-cost curves at different incremental costs. Assuming that the same incremental cost can be achieved by every generator, choose a value for IC_i , and solve for each P_{Gi} , check if Eq. 3.56 is satisfied. If not increase (decrease) IC_i until Eq. 3.56 is satisfied.

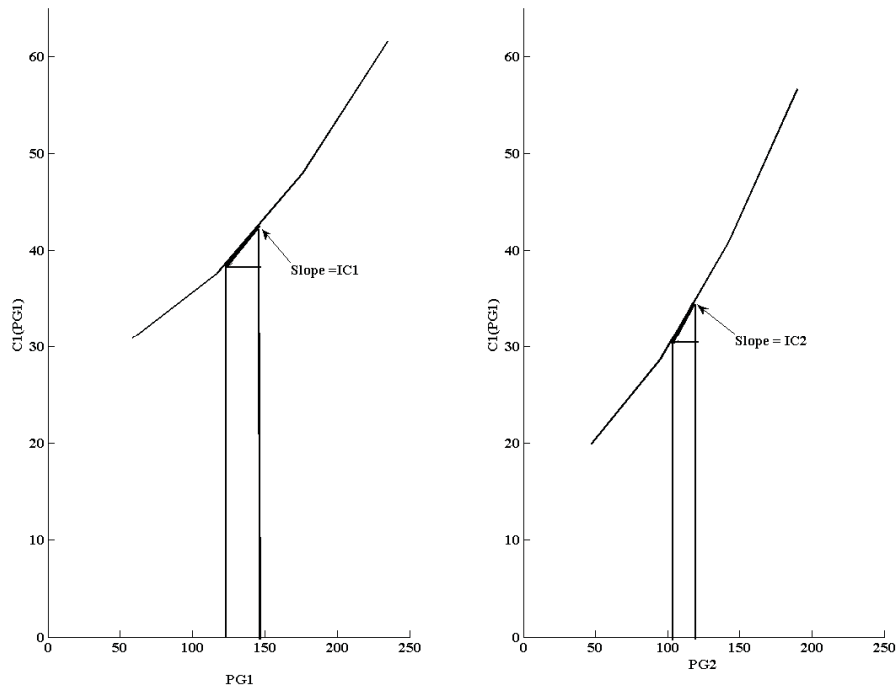


Figure 3.51: Two generator cost curves with both operating at different incremental costs [7], [8].

One significant difficulty in performing classical economic dispatch on any standalone DEG system in rural villages is the fact that not all DEGs are available to operate all the time. Therefore, unit commitment must be established before performing economic dispatch. In other words, the available units need to be determined and committed for operation before the economic dispatch problem can be solved and the program needs to allow for any DEG to go to the off state.

3.5.2.5 Unit Commitment Development

Unit commitment involves finding the combinations of DEGs that will most efficiently supply the given load using economic dispatch. Simply defined, a unit combination is feasible if it meets the following two criteria [37]:

- 1) The sum of all maximum power ratings (MW, kW, etc) for the units committed is greater than the load.
- 2) The sum of all minimum power ratings (MW, kW, etc) for the units committed is less than the load.

In equation format:

$$\sum_{i=1}^m P_{Gi}^{\min} \leq P_D \leq \sum_{i=1}^m P_{Gi}^{\max} \quad i = 1, 2, \dots, m. \quad (\text{Eq. 3.62})$$

Therefore, if the system is to be optimized, units must be shut down as the load goes down and then recommitted as the load goes back up.

The unit commitment problem can be very difficult as discussed in [37]. Very large numbers for enumerations can be required. This results in practical barriers in the optimized unit commitment problem with high dimensionality and a number of possible solutions. The following three techniques are the most commonly used to overcome the unit commitment problem:

- Priority-list schemes,
- Dynamic programming (DP),
- Lagrange relation.

However, after evaluating the three above techniques, the dynamic programming technique was utilized within the MATLAB[®] environment for modeling. Since the DP technique can create similar priority lists as a priority-list scheme, only the priority list and DP technique will be discussed here.

A simple shut-down rule or priority-list scheme could be obtained after an exhaustive enumeration of all unit combinations at each load level. However, a much simpler approach can be applied by noting the full-load average production cost of each unit, where the full-load average production is simply the net heat rate at full load multiplied by the fuel cost. Table 3.3 is an example of a simple priority list.

Table 3.3: Example priority list for a three generating unit system [37].

Unit Combination	Min kW from Combination	Max kW from Combination
2 + 1 + 3	300	1200
2 + 1	250	1000
2	100	400

A chief advantage of dynamic programming over the enumeration scheme is a reduction in the dimensionality of the problem [37]. For example suppose we have a system with four units and any combination of them could serve the load. There would be a maximum of $2^4 - 1 = 15$ combinations to test. However, if a strict priority order was imposed, there would only be four combinations to try:

- Priority 1 unit**
- Priority 1 unit + Priority 2 unit**
- Priority 1 unit + Priority 2 unit + Priority 3 unit**
- Priority 1 unit + Priority 2 unit + Priority 3 unit + Priority 4 unit**

Theoretically, a priority list arranged in order of the full-load average-cost rate would result in a correct dispatch and unit commitment only if [37]:

1. No load costs are zero.
2. Unit input-output characteristics are linear between zero output and full load.
3. There are no other restrictions.

4. Start-up costs are a fixed amount.

In the following approach, assume that:

- A *state* consists of an array of units with specified units operating and the rest off-line.
- The start-up cost for a unit is a fixed amount.
- There are no costs for shutting down a unit.
- There is a strict priority order, and in each interval a specified minimum amount of capacity must be operating.

A feasible state is one where the committed units can supply the required load and meet the minimum amount of capacity each period.

A forward dynamic programming algorithm is shown by the flowchart in Figure 3.52 [37]. The recursive algorithm to compute the minimum cost in hour K with combination I is as follows,

$$F_{\text{cost}}(K, I) = \min_{\{L\}} [P_{\text{cost}}(K, I) + S_{\text{cost}}(K-1, L: K, I) + F_{\text{cost}}(K-1, L)] \quad (\text{Eq. 3.63})$$

where

State (K, I) is the I^{th} combination in hour K ,

$F_{\text{cost}}(K, I)$ = least total cost to arrive at state (K, I) ,

$P_{\text{cost}}(K, I)$ = production cost for state (K, I) , and

$S_{\text{cost}}(K-1, L: K, I)$ = transition cost from state $S_{\text{cost}}(K-1, L: K, I)$ to state (K, I)

For the dynamic programming approach shown in Figure 3.52, a *strategy* is defined as the transition from one state at a given hour to a state at the next hour. In addition the two variables, X and N , in Figure 3.52 are as follows:

X = number of states to search each period

N = number of strategies to save at each step.

These variables allow control of the computational effort. For example, with a simple priority-list ordering, the upper bound on X is n , the number of generating units. Reducing the number of N means that the highest cost schedules at each time interval are discarded and only the lowest N strategies are saved. However, there is no reassurance that the theoretical optimal schedule will be found using a reduced number of strategies and search range (the X value); experimentation with a particular program is the only way of indicating any potential error associated with limiting the values of X and N .

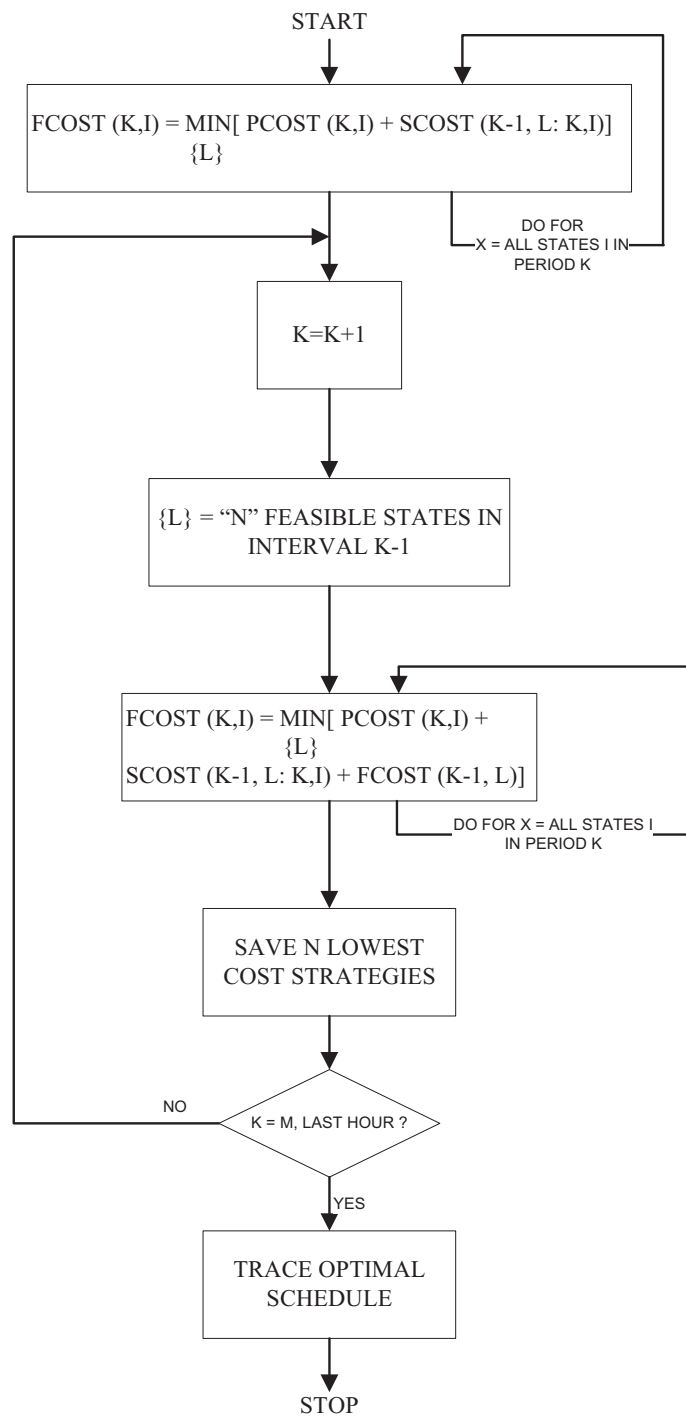


Figure 3.52: Forward dynamic programming flowchart recursive algorithm for unit commitment [37].

4. Results and Discussion

The results of studies conducted in this project have centered around the in-house (at UAF) testing of RTUs, flow meters and sensors for DEGs like those found in Alaska village communities, the development of a consortium of Alaska rural utilities, the deployment of remote monitoring systems in 25 villages in AEAs service territory, and the development of software programs and system models in MATLAB® Simulink® to determine the optimal mix of DEGs and renewable sources of power as well as the economic dispatch of power from these sources to serve the village loads.

4.1 UAF Energy Center Diesel

Results of testing a remote terminal unit, various types of fuel and coolant flow meters, and temperature and pressure sensors on the 125 kWe Detroit DEG at the UAF Energy Center showed the importance of remote metering and the proper selection of flow meters and sensors. The detailed results of these tests are presented by Tyler Chubb in a master's thesis, *Performance Analysis for Remote Power Systems in Rural Alaska*, under the direction of the project PIs (see MS Thesis 2 under Project Publications).

4.1.1 Flow Meter Test Loop

The results of the independent test on a magnetic and ultrasonic flow meter in a small coolant flow loop are illustrated in Figures 4.1 and 4.2 for a high and low flow rate, respectively. These results showed that electromagnetic flow meters are more accurate across the measurement range than the ultrasonic flow meters. The ultrasonic meter suffered from the effects of air within the coolant loop at lower flow rates which could be attributed to the pump and was also simply less accurate in this measurement range. Consequently, the range of flow rates to be measured is important in selecting the proper flow meter. In other words, if we know the coolant flow rate is nominally 45 liters/minute (12 gallons/minute) and varies by +/- 40 liters/minute during generator operation, then we would need to select a fuel flow meter that exhibits the highest degree of accuracy in the range from 5 to 85 liters/minute.

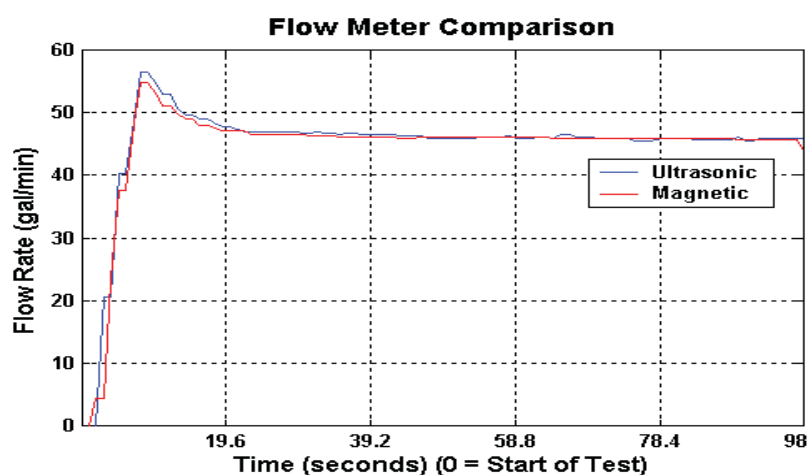


Figure 4.1: Magnetic and ultrasonic flow meter performance for high coolant flow rate.

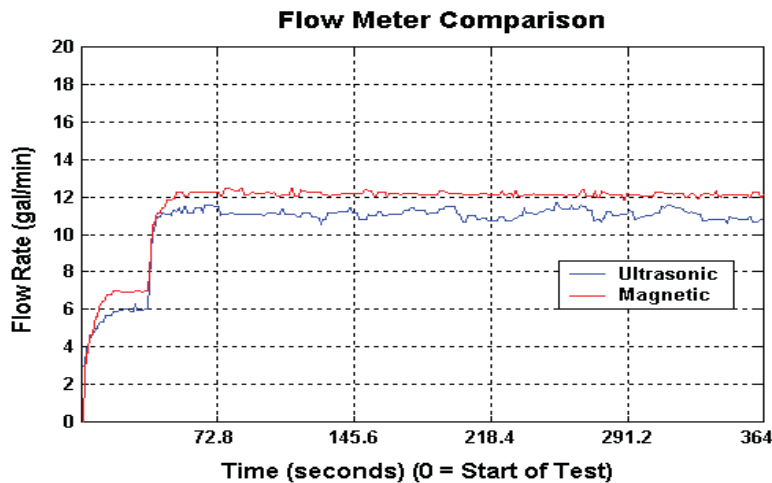


Figure 4.2: Magnetic and ultrasonic flow meter performance for low coolant flow rate.

4.1.2 Flow Meter and Temperature Sensor Tests on UAF DEG

A number of tests were conducted with flow meters on the UAF DEG coolant loop and fuel input line. The ultrasonic fuel flow meter that clamps around the fuel line was tested and found to be problematic because of generator vibration causing consistent errors with the fuel flow measurements as shown in Figure 4.3. The actual fuel flow rates were measured by timing the removal of fuel from a small day tank with a known volume using a pressure transducer and a level sensor as illustrated in Figure 4.4. An example of the increase in fuel flow rate with the increase in electrical load is shown in Figure 4.5.

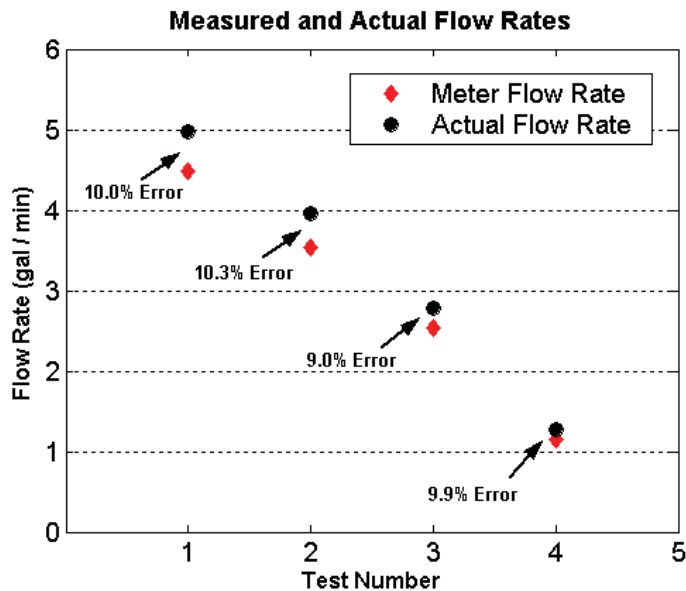


Figure 4.3: Ultrasonic fuel flow meter tests.

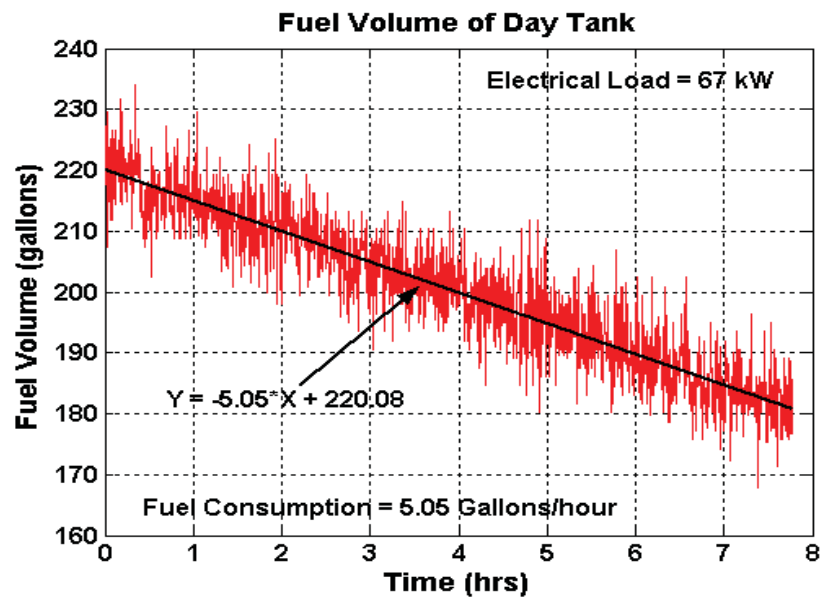


Figure 4.4: Using pressure transducer data to find fuel consumption rate.

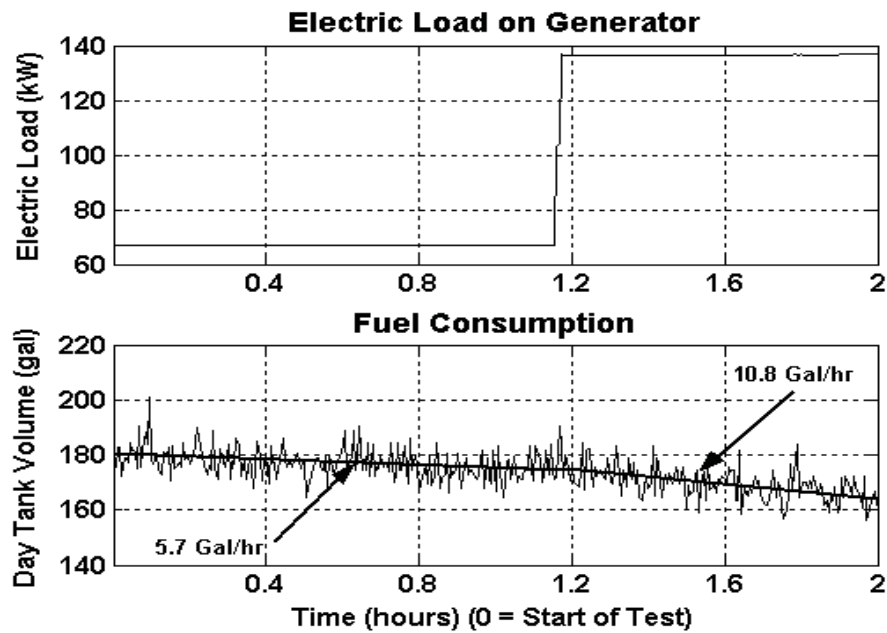


Figure 4.5: Changing fuel consumption rate for UAF DEG.

The magnetic and ultrasonic coolant flow meters were tested with the following results. Figure 4.6 shows the coolant flow rates (gal/min) for each meter and the electrical output (kWe) of the DEG over time. This illustrates that the coolant flow rate is directly proportional to electrical power output of the DEG. The ultrasonic flow meter suffers from high frequency noise (jitter) due to the generator vibration.

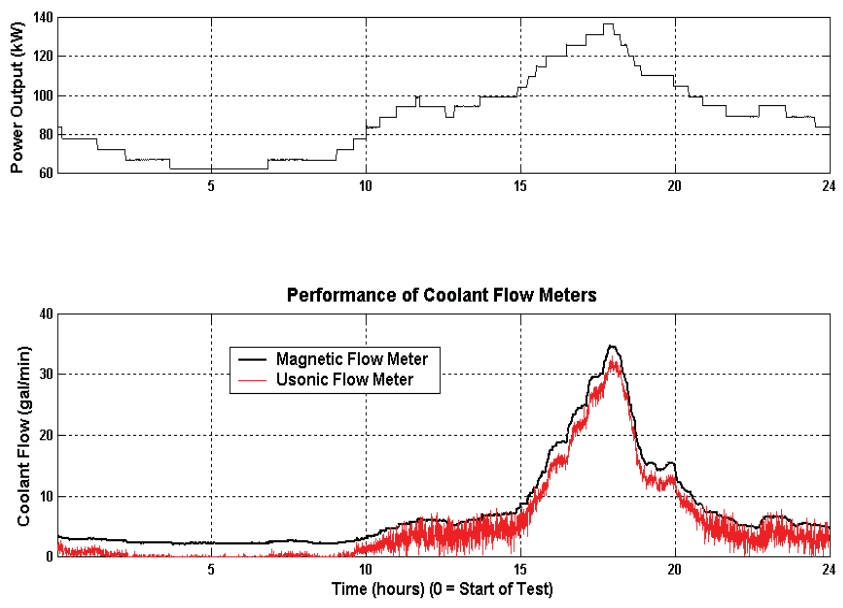


Figure 4.6: Magnetic and ultrasonic coolant flow meter comparison on UAF DEG.

Exhaust and coolant temperature sensors were also tested with the following results. Figure 4.7 shows the exhaust temperature (°F) and the electrical output of the DEG (kWe) over time. The exhaust temperature is directly proportional to the electrical power output of the DEG.

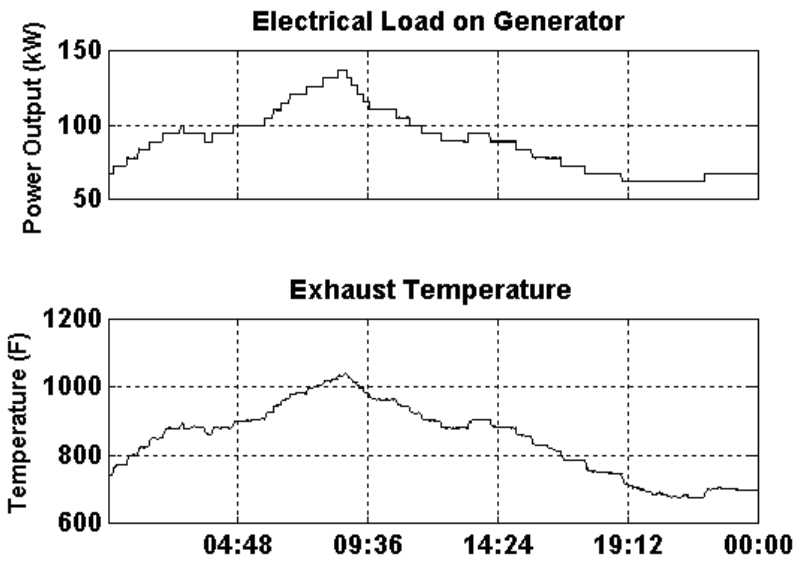


Figure 4.7: Exhaust system temperature and electrical power output over time for UAF DEG.

Figure 4.8 shows the coolant temperature ($^{\circ}\text{F}$) and the electrical output (kWe) of the DEG over time. The coolant temperature is directly proportional to the electrical power output of the DEG.

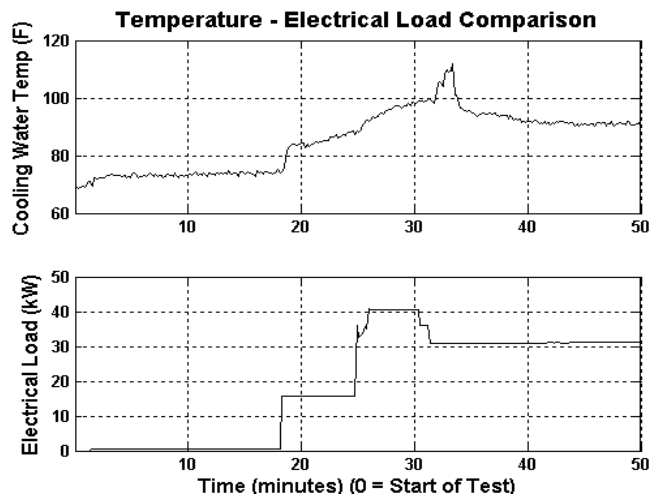


Figure 4.8: Coolant temperature and electrical power output over time for UAF DEG.

A significant result (see Figure 4.9) with regards to coolant temperature occurred when forest fire ash in the summer of 2004 clogged the cooling system radiator and the coolant operating temperature increased by 20°C . In a village system without remote monitoring this situation might have led to a costly generator failure if left unchecked.

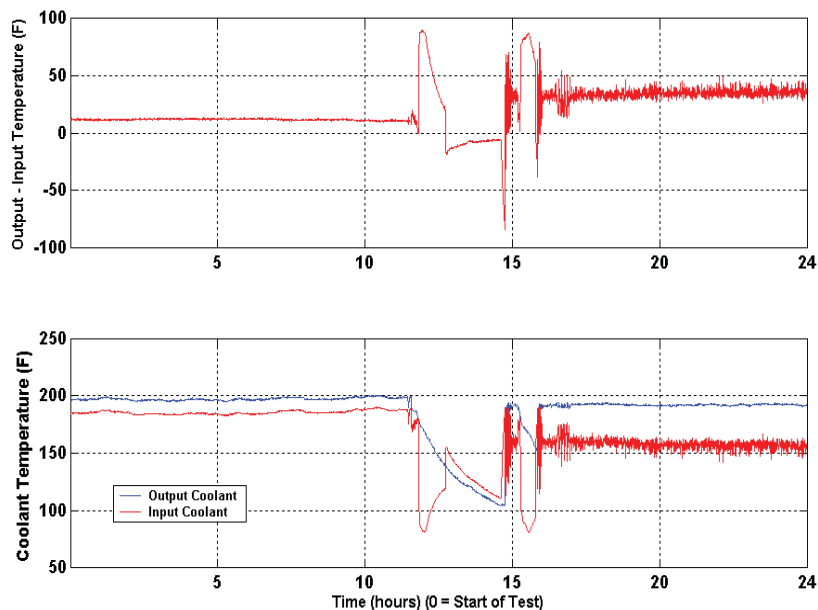


Figure 4.9: Effects of particle build-up in generator radiator.

The flow meter and temperature sensor measurements were used to develop the energy balance for the DEG plant. Using Eq. 3.1, the amount of energy contained in the coolant was calculated at 2,245,000 BTUs (658 kWh) over the course of the 24 hour load profile. Using the heating value of the Syntroleum fuel, 121,500 BTU/gallon [38] the lost energy in the coolant equates to 18.5 gallons of fuel per day. If a heat exchange system that were 80% efficient were utilized in this application, harnessing this wasted energy would be equivalent to saving 14.8 gallons of fuel per day or 5395 gallons of fuel over the course of a year. Using an estimated price for diesel fuel in rural Alaska, \$3.00/gallon, this is equivalent to \$16,185 over the course of a year in lost energy. Using Eq. 3.2, the average radiant heat emitted by the diesel engine was approximately 1.5 – 2.0 kW, or 2-3% of the input fuel energy. A value of 2.5% is used in the following energy balance calculations.

The overall energy balance plot is shown in Figure 4.10.

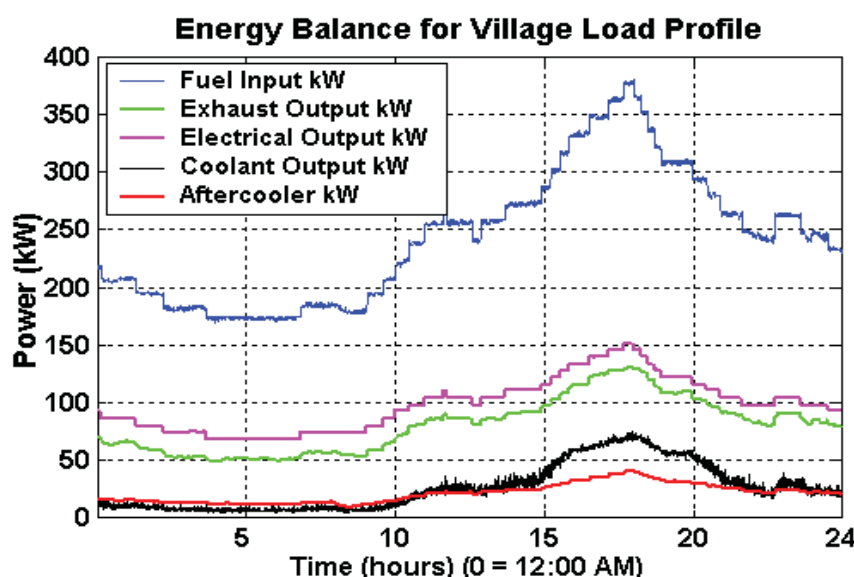


Figure 4.10: Energy output broken into individual forms.

Comparing the total output energy with the total input energy gives a means to verify the overall accuracy of the monitoring system as these two entities should ideally be equal. The comparison is shown in Figure 4.11. The accuracy of the energy balance was not perfect, but it must be taken into consideration that there were 11 sensors used to compile the information. Given that there was inaccuracy inherent with each sensor, an overall error of this magnitude should not be unexpected. At high electrical loads on the generator, the output energy exceeded the input energy by up to 30 kW (maximum 10% error) and at lower electrical load this situation was reversed by 35 kW (maximum 12% error). The output and input energies seemed to optimally correspond when the electrical load on the generator was 80 kW to 100 kW. It can be deduced from the energy balance that several of the sensors were in their optimal operating range when loads of 80 – 100 kW were placed on the generator.

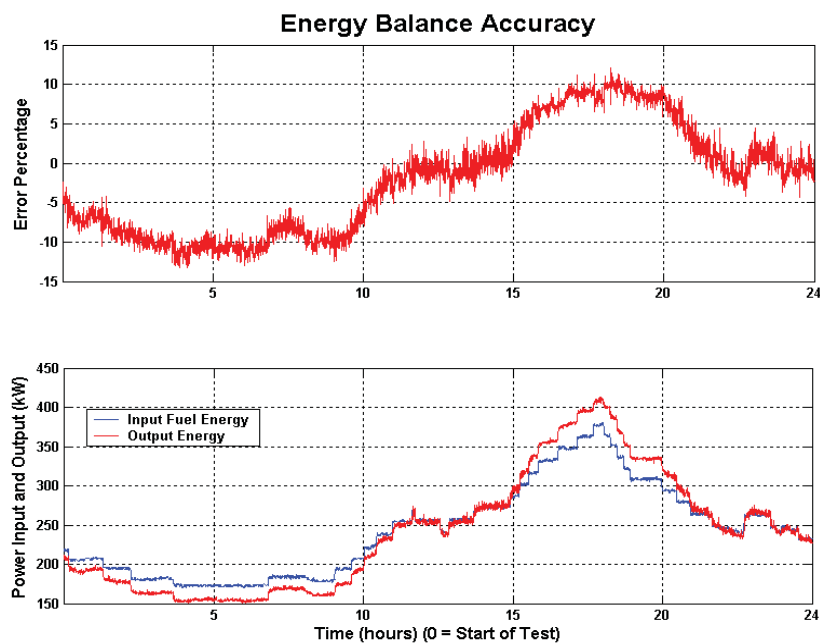


Figure 4.11: Energy balance input compared to energy balance output.

Figure 4.12 shows pie charts of the energy balance calculated for the DEG from the measured data (a) and generator specifications (b). A significant portion of the energy is lost in the exhaust and heated coolant. The heated coolant is used to heat buildings in the village by piping the heated coolant from the generator house to buildings in the village.

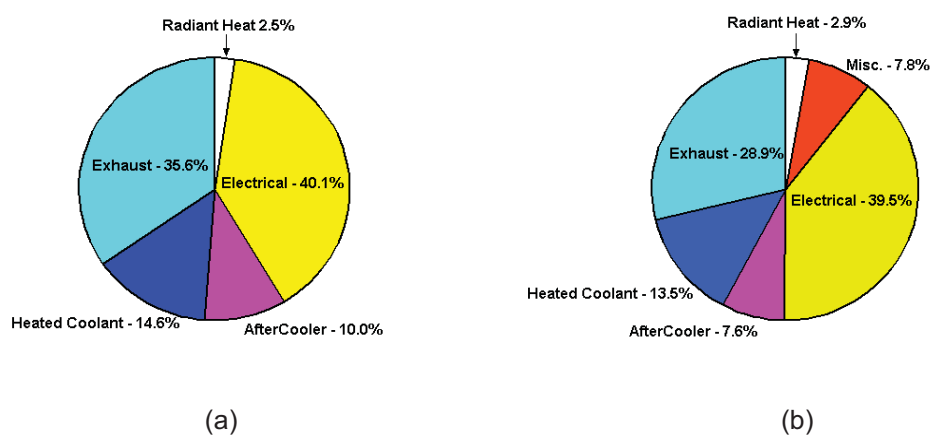


Figure 4.12: Average energy outputs of UAF DEG operating near full load using a) data from tests and b) generator specifications.

4.2 Village Power Survey and Data Collection

A number of villages in AEAs service territory were surveyed to collect current system information and existing data. These villages were classified in terms of their average electric load requirement as illustrated in Figure 4.13. However, much of the existing load data is of poor

quality, consisting of missing time windows, sampling errors, or only small time windows of data when service technicians were on site for a few days. An example plot of load profiles for five random villages in Figure 4.14 illustrates this point.

Both AEA and AVEC have partnered to install standard remote monitoring equipment in a number of villages in their service territories in order to work towards creating a standard data collection system. AEA currently has limited online access to real-time monitoring in many of its villages at <http://www.aidea.org/aea/aearemotemon.html>. The 21 villages included in this study are: Atka Diesel Powerhouse and Hydro Facility, Arctic Village, Buckland, Chefnak, Chuathbaluk, Crooked Creek, Diomede, Golovin, Hughes, Kongiganak, Koyukuk, Kwigillingok, Pedro Bay, Larsen Bay Hydro Facility, Manokotak, Nikolski, Ouzinkie Diesel Powerhouse and Hydro Facility, Sleetmute, Stevens Village, Stony River, and Takotna. This includes password access to the actual computer terminal in the village power house as well as video cameras in the power house. The problem has been collecting information from all of these communities in a standard format that can be stored and processed at a central server. Two more villages, Chitina and Chignak, in AEAs service territory received basic remote monitoring upgrades and were included in this study.

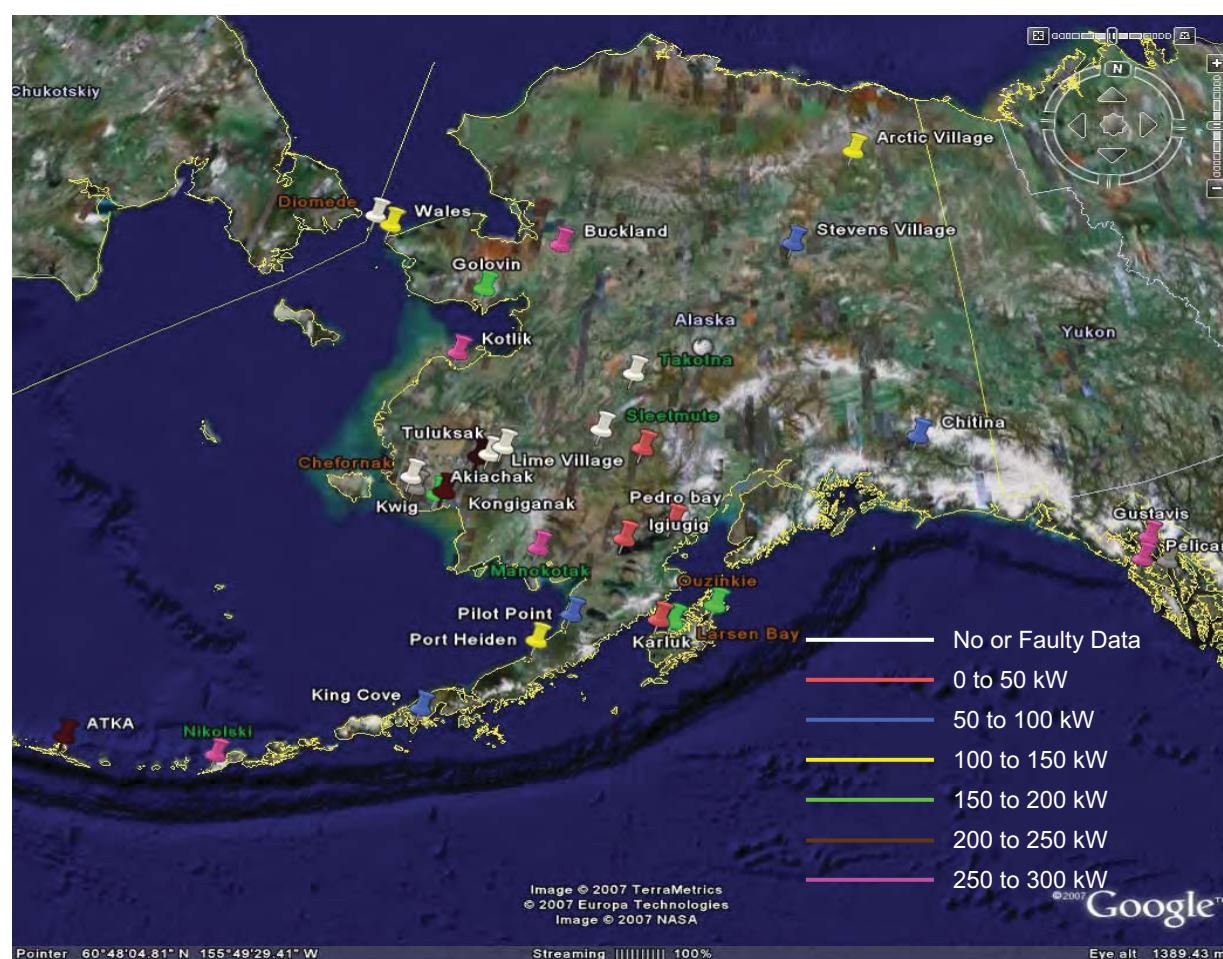


Figure 4.13: Map of select villages in AEA's service territory grouped by average load.

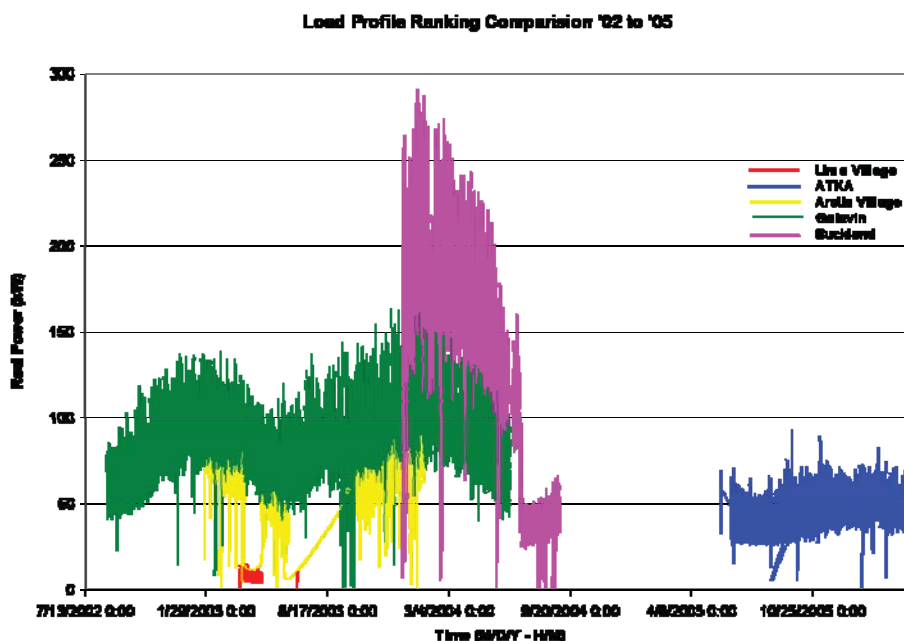


Figure 4.14: Sample load profiles from five Alaska rural villages.

4.3 Village Hybrid Power Performance Analysis

UAF evaluated the performance of systems at Kongiganak, Lime Village, Stevens Village, and Wales Village, Alaska using the hybrid power system model developed in MATLAB[®] Simulink[®] specifically for the Alaska rural village power systems. The model is used to perform an economic feasibility analysis for integrating renewable energy sources into existing DEG systems.

4.3.1 Performance Analysis for Kongiganak, Alaska

The hybrid power system model was used to study the performance of the system at Kongiganak, Alaska. Our model was used to study the feasibility of integrating a PV array, a WTG, and a battery bank with the existing DEGs to meet the village load demand. Currently, DEGs are the only source of power for the load demand. Load demand for the village of Kongiganak is supplied by Puvurnag Power Company which operates four diesel generator units: one 235 kWe John Deere[®] 6125AF, two 190 kWe John Deere[®] 6081AF, and one 140 kWe John Deere[®] 6081TF.

The annual synthetic load profile from January 1st, 2003 to December 31st, 2003 with one hour samples, the annual synthetic wind speed profile, and the annual solar flux profile used for analyzing the performance of the Kongiganak Village are shown in Figure 4.15, 4.16, and 4.17, respectively. The clearness index data for the solar insolation profile is obtained using the solar maps developed by the National Renewable Energy Laboratory (NREL) [39]. It can be observed from Figure 4.15 that the maximum load of the system is about 150 kW, the minimum load is about 45 kW and the average load is about 95 kW. From Figure 4.16 it can be observed that the annual average wind speed is about 7 m/s (15.66 miles/hr). From Figure 4.17 it can be observed that the village has low solar flux during winter months and high solar flux during summer months.

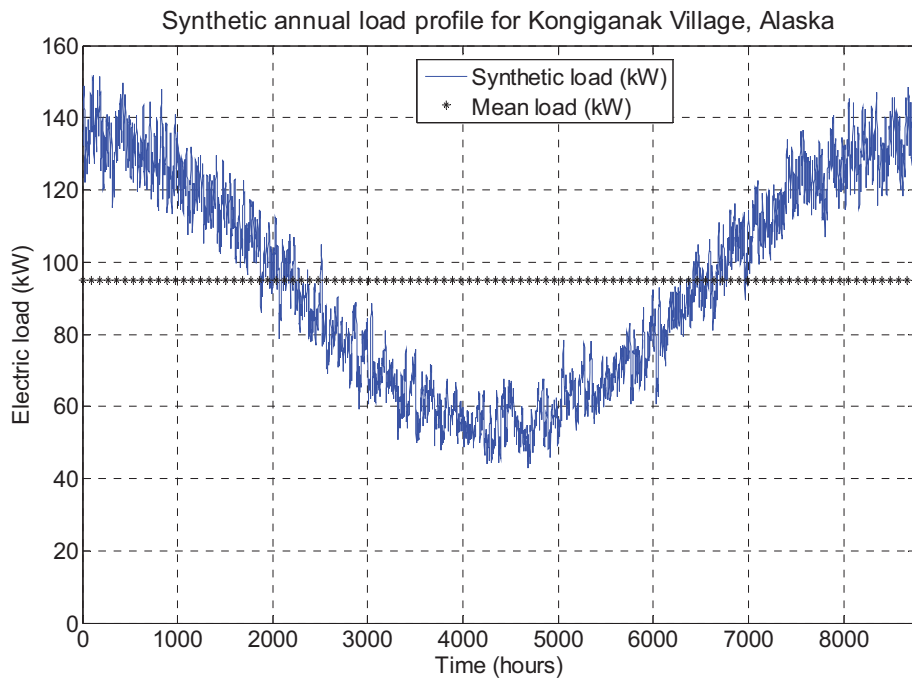


Figure 4.15: Synthetic annual load profile for Kongiganak Village, Alaska.

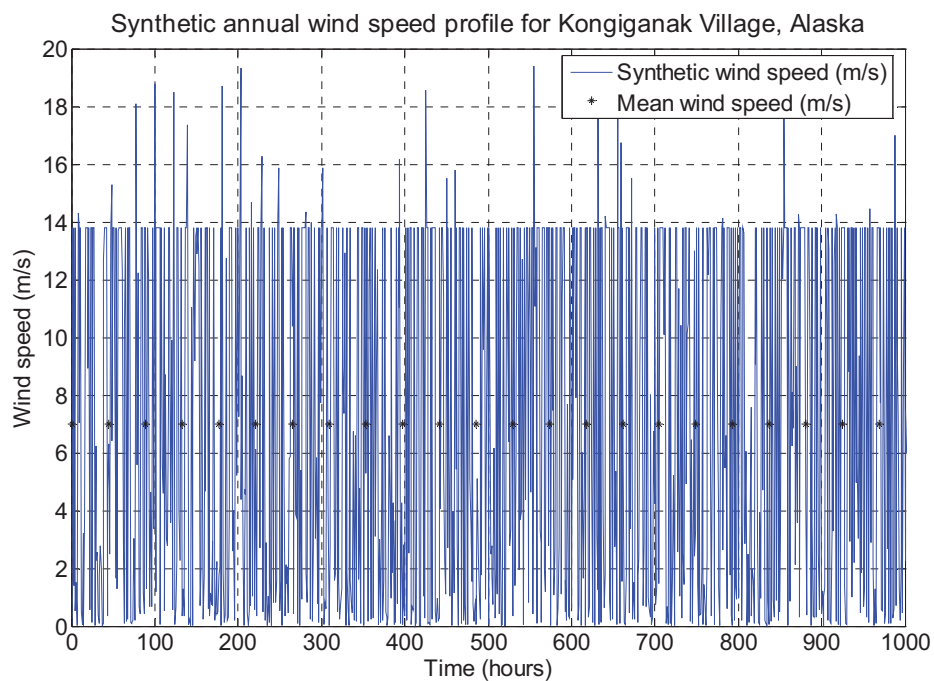


Figure 4.16: Synthetic annual wind speed profile for Kongiganak Village, Alaska.

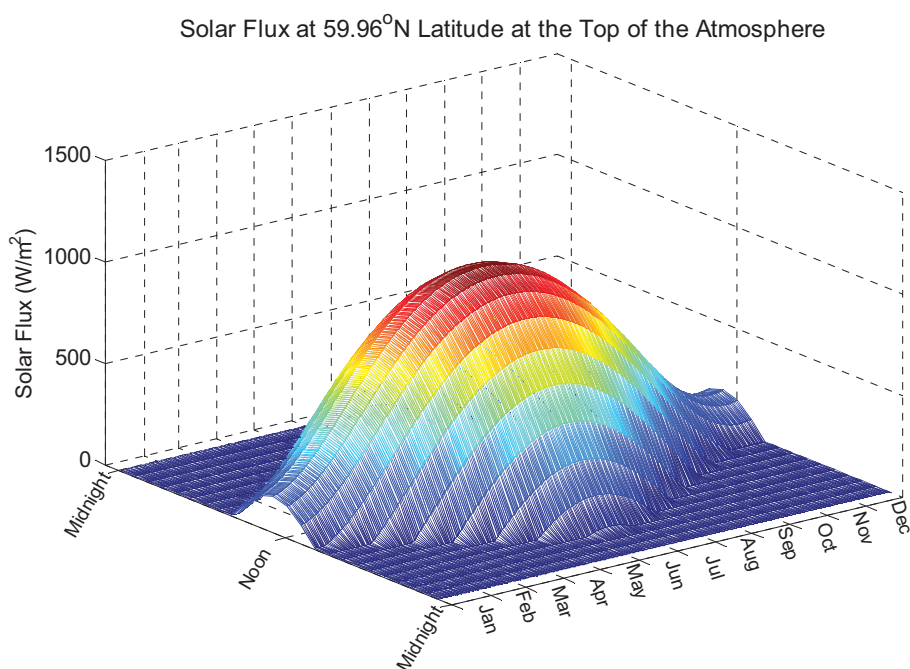


Figure 4.17: Annual solar flux for Kongiganak Village, Alaska.

Various hybrid power systems studied in this analysis include the diesel-battery system, the PV-diesel-battery system, the wind-diesel-battery system, and the PV-wind-diesel-battery system. Table 4.1 shows the installation cost (USD) for different components for the Kongiganak Village hybrid power system. The model was validated by comparing the results obtained from the Simulink[®] model, for supplying the annual load profile, with the available obtained from the HOMER software. The simulation results obtained from the HARPSim model were compared with those obtained from the HOMER software. Table 4.2 shows the comparison of results from the HARPSim model with HOMER for the Kongiganak Village hybrid power system. At the time of this analysis HOMER was not set up to calculate payback period or NO_x and PM₁₀ emissions. The LCC and sensitivity analysis of NPV, COE, and payback for Kongiganak were examined as shown in Figures 4.18-4.21.

Results of the performance analysis showed the economic feasibility and fuel savings of installing WTGs and PV arrays. The life cycle costs LCC and sensitivity analysis of fuel cost and investment rate showed that as the price of bulk fuel rises, the payback period of the WTG and the PV array decreases. The cost of energy COE and the net present value NPV increases linearly while the payback period decreases with the increase in the fuel price. However, the current economic feasibility analysis of integrating PV alone into Alaska rural village systems results in paybacks that are near or longer than the life cycle of the project because of the cost of the PV panels and the lack of light in the winter months. As fuel costs increase and the cost of PV panels decreases in the future, PV panels will become more economical in Alaska rural village power systems.

Table 4.1: Installation cost for different components for Kongiganak Village.

Item	Cost per unit (USD)	No of units	Diesel-only system (USD)	Diesel-battery system (USD)	PV-diesel-battery system (USD)	Wind-diesel-battery system (USD)	PV-wind-diesel-battery system (USD)	2 wind-diesel-battery system (USD)
140 kW diesel generator	40,000	1	40,000	40,000	40,000	40,000	40,000	40,000
190 kW diesel generator	45,000	1	45,000	45,000	45,000	45,000	45,000	45,000
Switch gear to automate control of the system	16,000	1	16,000	18,000	20,000	20,000	22,000	30,000
Rectification/Inversion	18,000	1	0	18,000	18,000	18,000	18,000	28,000
New Absolyte IIP 6-90A13 battery bank	2,143	16	0	34,288	34,288	34,288	34,288	68,576
AOC 15/50 wind turbine generator	55,000	1	0	0	0	55,000	55,000	110,000
Siemens M55 solar panels	262	180	0	0	47,160	0	47,160	0
Engineering		1	3,000	3,500	4,000	4,000	4,500	6,000
Commissioning, Installation, freight, travel, miscellaneous		1	13,000	14,000	16,000	18,000	20,000	30,000
		TOTAL	117,000	172,788	224,448	234,288	285,948	357,576

Table 4.2: Comparison of energy and economic analysis results for Kongiganak.

Item	Diesel-battery system		PV-diesel-battery system		Wind-diesel-battery system		PV-wind-diesel-battery system	
	HARPSim	HOMER	HARPSim	HOMER	HARPSim	HOMER	HARPSim	HOMER
System cost (USD)	172,788	172,788	224,448	224,450	234,288	234,288	285,948	285,950
Engine efficiency (%)	29.3	28.63	29.3	28.51	29.3	27.03	29.3	26.88
kWh/liter (kWh/gallon) for the engine	3.11 (11.75)	3.04 (11.48)	3.11 (11.75)	3.02 (11.43)	3.11 (11.75)	2.87 (10.84)	3.11 (11.75)	2.85 (10.78)
Fuel consumed in liters (gallons)	267,662 (70,810)	273,910 (72,463)	264,834 (70,062)	272,568 (72,108)	193,249 (51,124)	216,027 (57,150)	190,837 (50,486)	214,776 (56,819)
Total cost of fuel (USD)	212,429	217,390	210,185	216,325	153,373	171,451	151,458	170,456
Energy supplied								
(a) Diesel engine (kWh)	832,152	832,205	823,368	823,422	597,145	619,504	588,362	612,287
(b) WTG (kWh)	-	-	-	-	235,007	238,000	235,007	238,000
(c) PV array (kWh)	-	-	8,784	8,783	-	-	8,784	8,783
Energy supplied to load (kWh)	832,152	832,205	832,152	832,205	832,152	832,205	832,152	832,205
Operational life								
(a) Generator (years)	5	1.87	5	1.87	5	1.8	5	1.8
(b) Battery bank (years)	5	12	5.5	12	5.5	12	6	12
Net present value (USD) with $i = 7\%$ and $n = 20$ years	-	1,992,488	2,545,084	2,945,502	1,954,127	2,383,766	1,974,389	2,421,502
Cost of Electricity (USD/kWh)	0.301	22.6	0.304	0.334	0.237	0.27	0.24	0.275
Payback period for renewable (years)	-	-	Never	-	1.07	-	2.12	-
Emissions								
(a) CO ₂ in metric tons (US tons)	660 (728)	703 (775)	653 (720)	700 (772)	477 (526)	555 (612)	471 (519)	552 (608)
(b) NO _x in kg (lbs)	7,322 (16,143)	-	7,245 (15,972)	-	5,288 (11,657)	-	5,222 (11,512)	-
(c) PM ₁₀ in kg (lbs)	308 (679)	-	305 (672)	-	222 (490)	-	220 (484)	-

Since the wind-diesel-battery system was observed to be the most cost effective, further work was carried out to study the effect of installing another WTG into the wind-diesel-battery system. The addition of a second WTG required an increase in the capacity of the battery bank to accommodate more energy storage. Therefore, the battery bank capacity and the inverter rating were increased from 100 kW and 100 kVA to 200 kW and 200 kVA, respectively. Table 4.3 shows the comparison of results from the HARPSim model with HOMER for the two wind-diesel-battery hybrid power system for Kongiganak Village. It can be observed that the addition of the second WTG into the wind-diesel-battery hybrid power system resulted in the further reduction in the NPV and the COE, while the payback period with the two WTGs increased slightly. The WTG penetration level increases to 50% for this case. The payback period of the WTGs increased to 1.56 years due to the extra cost involved in the addition of the second WTG.

A new 3 WTG-2 DEG system for Kongiganak has been commissioned through a Denali Commission grant and is currently in the design and procurement phase. A feasibility analysis using our model for the proposed system estimates the village will displace about 37,800 liters (10,000 gallons) of diesel fuel per wind turbine per year with a payback of about 3.5 years, while the contractor estimates about 45,360 liters (12,000 gallons) of diesel fuel per wind turbine per year with a payback of about 2.5 years.

Table 4.3: Comparison of results for two wind-diesel-battery hybrid power system.

Item	Two wind-diesel-battery system	
	HARPSim	HOMER
System cost (USD)	357,576	357,576
Engine efficiency (%)	29.3	26.6
kWh/liter (kWh/gallon) for the engine	3.11 (11.75)	2.78 (10.53)
Fuel consumed in liters (gallons)	151,252 (39,961)	201,444 (53,222)
Total cost of fuel (USD)	119,883	159,876
Energy supplied		
(a) Diesel engine (kWh)	469,542	561,741
(b) WTG (kWh)	470,015	475,999
Energy supplied to load (kWh)	832,152	832,205
Operational life		
(a) Generator (years)	5	1.8
(b) Battery bank (years)	5.5	12
Net present value (USD) with $i = 7\%$ and $n = 20$ years	1,748,988	2,407,895
Cost of Electricity (USD/kWh)	0.22	0.273
Payback period for WTG (years)	1.56	-
Emissions		
(a) CO ₂ in metric tons (US ton)	367 (405)	517 (570)
(b) NO _x in kg (lbs)	4,068 (9,112)	-
(c) PM ₁₀ in kg (lbs)	171 (383)	-

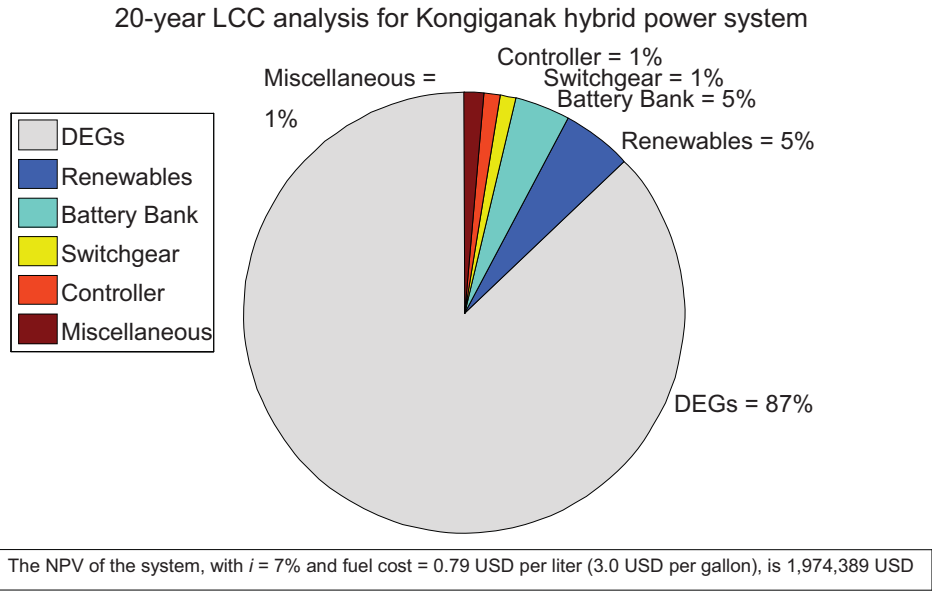


Figure 4.18: 20-year LCC analysis of the proposed Kongiganak hybrid power system.

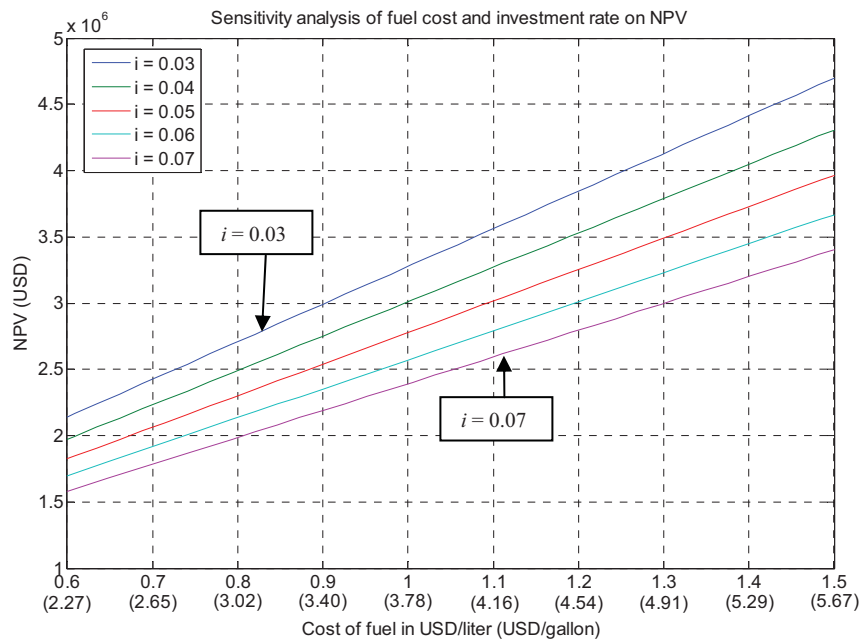


Figure 4.19: Sensitivity analysis of fuel cost and investment rate on the NPV for Kongiganak.

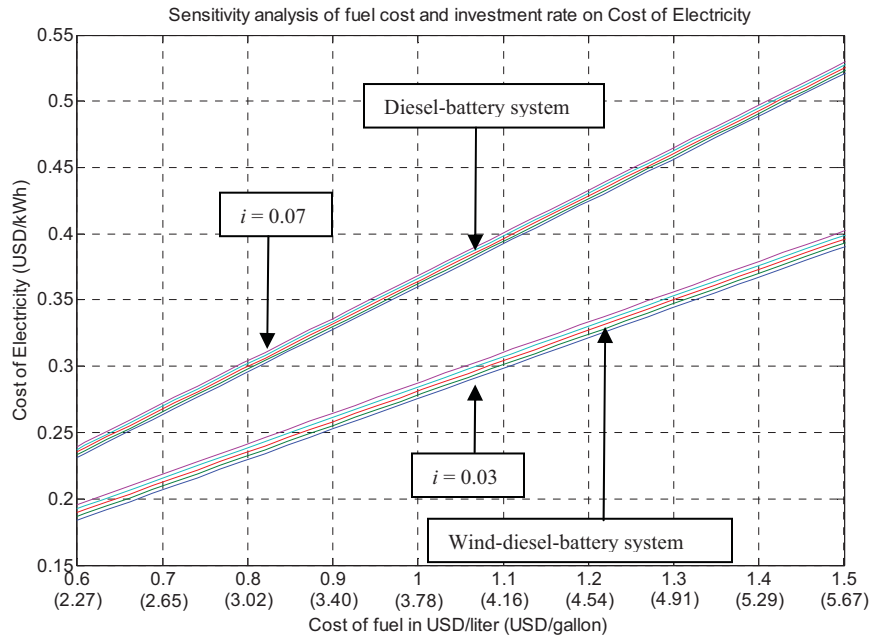


Figure 4.20: Sensitivity analysis of fuel cost and investment rate on the COE for Kongiganak.

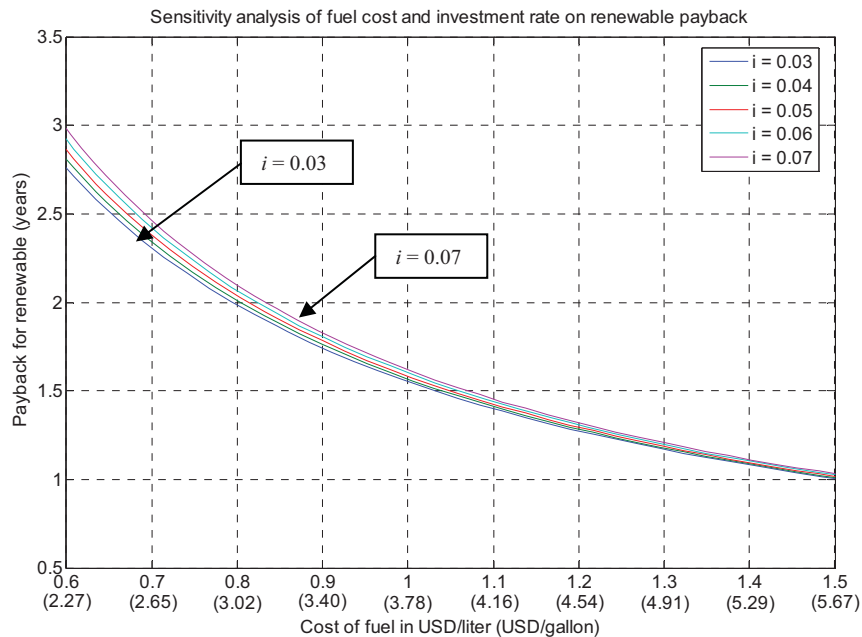


Figure 4.21: Sensitivity analysis of fuel cost and investment rate on the payback period for Kongiganak.

4.3.2 Performance Analysis for Wales Village, Alaska

The wind-diesel-battery hybrid power system of Wales Village has been in reliable operation since the summer of 2000. A Simulink[®] model for the hybrid power system was developed. The load and wind profiles shown in Figures 4.22 and 4.23 were input into the model. The annual

load data were recorded at Wales Village from August 1st, 1993 to July 31st, 1994 with the sampling period of 15 minutes. The average wind speed is about 8.4 m/s.

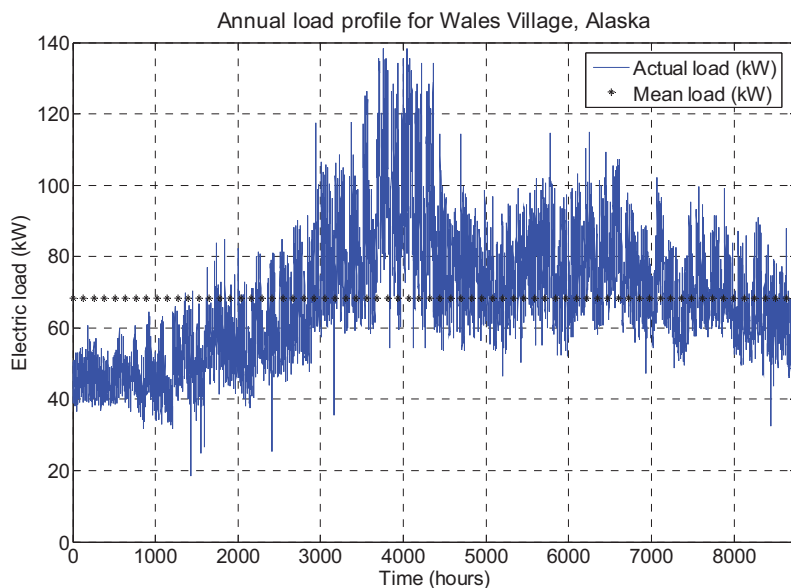


Figure 4.22: Annual load profile for Wales Village, Alaska.

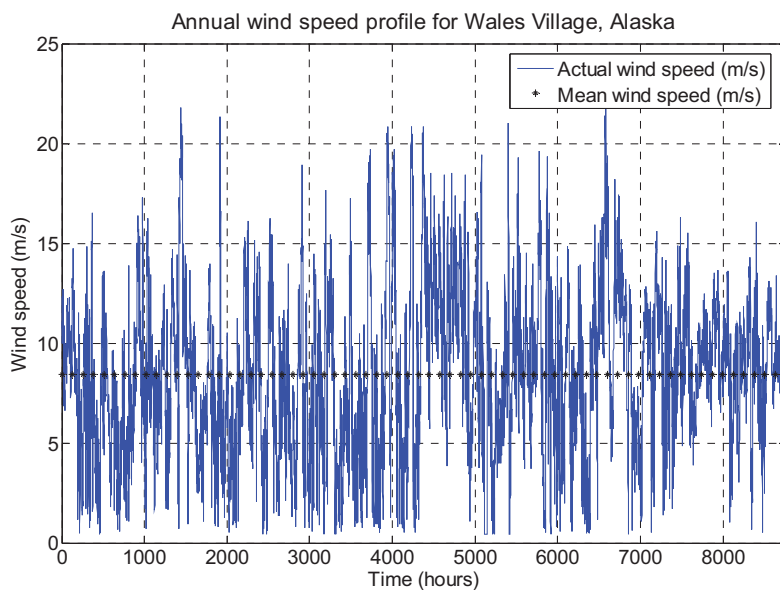


Figure 4.23: Annual wind speed profile for Wales Village, Alaska.

The model was validated by comparing the results obtained from the Simulink[®] model, for supplying an annual load profile, with those obtained from the HOMER software. Table 4.4 shows the overall comparison chart for the two models. It should be noted that the LCC analysis for 20 years with an investment rate of 7% is performed with the battery bank indoors. This is

Table 4.4: Comparison of results for Wales Village with HOMER.

Parameter	Simulink [®] Model			HOMER	
	Diesel-battery system	Wind-diesel-battery system		Diesel-battery system	Wind-diesel-battery system
	Battery Indoors (@ 20 °C)	Battery Indoors (@ 20 °C)	Battery Outdoors (Avg: -0.5 °C)	Battery Indoors (@ 20 °C)	Battery Indoors (@ 20 °C)
System cost (USD)	167,800	283,800	-	167,800	283,800
Engine efficiency (%)	29.55	29.55	29.55	29.4	29.55
kWh/liter (kWh/gallon) for the engine	3.13 (11.85)	3.13 (11.85)	3.13 (11.85)	3.09 (11.7)	3.13 (11.85)
Fuel consumed in liter (gallons)	199,890 (52,881)	155,762 (41,207)	185,020 (48,947)	196,621 (50,016)	156,653 (41,443)
Total cost of fuel (USD)	158,643	123,621	146,841	156,039	124,320
Energy generated					
(a) Diesel engine (kWh)	626,876	488,484	580,239	606,501	490,507
(b) WTG (kWh)	0	137,266	137,266	0	139,830
(c) Excess energy (kWh)	28,939	0	119,568	92.8	11,988
Energy supplied to load (kWh)	597,937	597,937	597,937	597,871	597,871
Operational life					
(a) Generator (years)	5.5	5.5	5.5	3.62	4.6
(b) Battery bank (years)	5.0	5.5	3.0	12	12
Net present value (USD) with $i = 7\%$ and $n = 20$ years	-	1,652,820	1,923,997	2,008,969	1,754,711
Cost of Electricity (USD/kWh)	0.32	0.28	0.32	0.32	0.28
Payback period for WTGs (years)	-	4.867	Never	-	-
Emissions					
(a) CO ₂ in metric tons (US tons)	498.65 (549.67)	388.57 (428.33)	461.55 (508.77)	497.10 (547.96)	*402.41 (443.58)
(b) NO _x in kg (Pounds)	5516.45 (12161.69)	4298.62 (9476.83)	5106.048 (11256.91)	-	-
(c) PM in kg (Pounds)	231.94 (511.34)	180.74 (398.49)	214.69 (473.3)	-	-

*Based on 88% carbon content in the diesel fuel

because in HOMER the battery bank is assumed to be kept at an optimal temperature. The results obtained with the battery bank kept outdoors are also presented in Table 4.4. The LCC and air emissions results of the Simulink[®] model were comparable with those obtained from the HOMER software. It was observed that the COE for the wind-diesel-battery hybrid power system is less than the COE for the diesel-battery system, thus making the wind-diesel-battery system more economical while emitting less pollution. The payback period of the WTG with a fuel cost of 0.793 USD per liter (3.00 USD per gallon) was less than 5 years and it decreases with the increase in the cost of fuel. The wind-diesel-battery hybrid power system will consume less fuel and emit less CO₂, NO_x, and PM₁₀. If the external costs associated with these

emissions are taken into account (see Table 4.5), the PV system payback period will decrease further, thus making these systems more viable and affordable.

Table 4.5: Avoided cost for different pollutants for Wales Village, Alaska.

Emission	Avoided costs
CO ₂	-194 USD/metric ton (176 USD/US ton)
PM ₁₀	-478 USD/kg (-217 USD/lb)
NO _x	-20 USD/kg (-9 USD/lb)

4.3.3 Performance Analysis for Lime Village, Alaska

The PV-diesel-battery hybrid power system of Lime Village has been in reliable operation since July 2001. A Simulink[®] model for the hybrid power system was developed. The load and wind profiles shown in Figures 4.24 and 4.25 were input into the model. Table 4.6 shows the costs of the different components installed at Lime Village. The costs of the different components were obtained from the various manufacturers. The engineering cost, commissioning, installation, freight and other miscellaneous costs were obtained from a report prepared by the Alaska Energy Authority (AEA) [40]. Due to the remoteness of the site, the cost for transporting and installing the various components is relatively high.

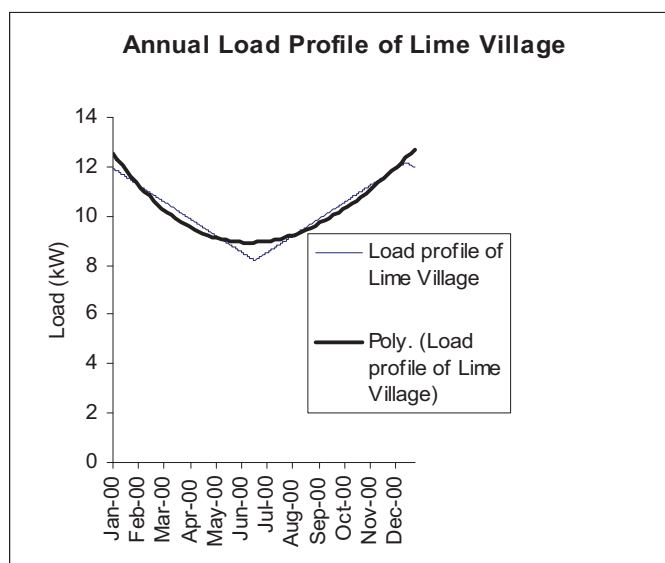


Figure 4.24: Annual load profile for Lime Village, Alaska.

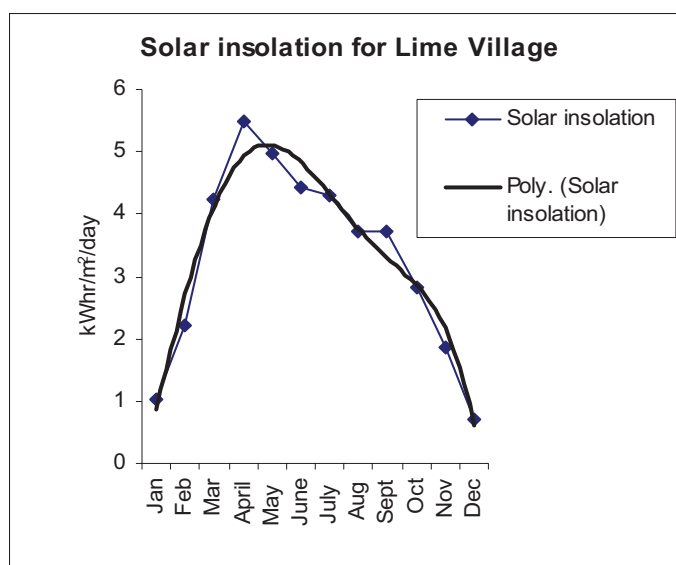


Figure 4.25: Annual solar insolation profile for Lime Village, Alaska.

The model was validated by comparing the results obtained from the Simulink[®] model, for supplying an annual load profile, with those obtained from the HOMER software. Table 4.7 shows the results obtained from the HARPSim model. In this model the roundtrip efficiency of the rectifier/inverter and the internal loss in the battery bank per cycle was considered as 90%. The collector efficiency for the PV array is assumed as 12%. As mentioned in HOMER, the heating value of fuel is assumed to be 48.5 MJ/kg (20,852 BTU/lb) and the density of fuel is assumed to be 840 kg/m³ (52.44 lb/ft³). The post-simulation analysis includes an economic and environmental component illustrating the simple payback and avoided cost of emissions using the PV array. The results obtained from HARPSim for the three systems shows that the addition of the battery bank and the PV array with the DEGs improves the system efficiency and reliability and decreases the fuel consumption and the environmental pollutants.

Table 4.8 shows the comparison of results from HARPSim with HOMER for the current Lime Village hybrid power system. The LCC and air emissions results of the Simulink[®] model were comparable to those obtained from the HOMER software. Although there is a significant capital investment to purchase a PV system for this application, the PV system may have acceptable 20-year life cycle costs for many remote locations. Furthermore, over its life cycle the PV-diesel-battery hybrid power system will consume less fuel and emit less CO₂, NO_x, and PM₁₀ than the diesel-battery system. If the external costs associated with these emissions are taken into account (see Table 4.9), the PV system payback period will decrease further, thus making these systems more viable and affordable. A simple payback period for the PV array of Lime Village with a fuel cost of 1.057 USD per liter (4.00 USD per gallon) was about 18 years and it decreases with the increase in the cost of fuel. The long payback period here is a direct result of the cost of the PV array and the lack of sunlight in the winter months.

Table 4.6: Component and installation costs for Lime Village.

Item	Cost per unit (USD)	No of units	Diesel-only system (USD)	Diesel-battery system (USD)	PV-diesel-battery system (USD)
35 kW diesel generator	28,000	1	28,000	28,000	28,000
21 kW diesel generator	18,500	1	18,500	18,500	18,500
Switch gear to automate control of both diesels	16,000	1	16,000	16,000	16,000
Rectification/Inversion	18,000	1	0	18,000	18,000
New Absolyte IIP 6-90A13 battery bank	2,143	16	0	34,288	34,288
BP275 Solar	329	105	0	0	34,545
Siemens M55 Solar	262	75	0	0	19,650
Engineering		1	3,000	3,500	4,000
Commissioning, Installation, freight, travel, miscellaneous		1	13,000	14,000	16,000
		TOTAL	78,500	132,288	188,983

Table 4.7: Simulation results of Lime Village using HARPSim.

Parameter	Diesel-only system	Diesel-battery system	PV-diesel-battery system
System cost (USD)	78,500	132,288	188,983
System efficiency (%)*	26.22%	29.94%	29.96%
kWh/liter (kWh/gallon)	2.81 (10.61)	3.20 (12.1)	3.20 (12.1)
Fuel consumed in liters (gallons)	31,789.80 (8410)	27,847.26 (7367)	24,883.74 (6583)
Total cost of fuel (USD)**	33,640	29,470	26,340
CO ₂ emitted in metric tons (US tons)	81.05 (89.34)	70.93 (78.19)	63.64 (70.15)
PM ₁₀ emitted in kg (lbs)	33.01 (72.77)	32.84 (72.4)	27.18 (59.92)
NO _x emitted in kg (lbs)	785.17 (1731)	784.71 (1730)	646.37 (1425)
System load (kWh)	89220	89220	89220
Energy supplied			
(a) DEG (kWh)	101900	100100	89500
(b) PV (kWh)	0	0	9445
Electrical efficiency of DEG (%)	87.56	89.13	90.17

*In this project System efficiency is the ratio of the total electrical energy supplied by the diesel generator to the total energy available from the fuel.

**Based on a diesel fuel price of 1.057 USD per liter (4.00 USD per gallon) for Lime Village, Alaska.

Table 4.8: Comparison of results for Lime Village with HOMER.

Parameter	HOMER	HARPSim
System cost (USD)	188,983	188,983
System efficiency (%)	29.9	29.96
kWh/liter (kWh/gallon)	3.13 (11.84)	3.20 (12.1)
Fuel consumed in liters (gallons)	25,768.26 (6,817)	24,883.74 (6,583)
Total cost of fuel (USD)	27,058	26,340
Energy generated		
(a) Diesel engine (kWh)	87,064	82,497
(b) PV (kWh)	9,444	9,445
Energy supplied to load (kWh)	89,224	89,220
Operational life		
(a) Generator (years)	4.62	5.4
(b) Battery bank (years)	6.07	5.4
Net present value (NPV) (USD)	581,350	557,154
Payback (Years)	-	18.11
Emissions		
(a) CO ₂ in metric tons (US tons)	*68.58 (75.60)	63.64 (70.15)
(b) NO _x in kg (lbs)	-	646.37 (1425)
(c) PM ₁₀ in kg (lbs)	-	27.18 (59.92)

*Based on 88% carbon content in the diesel fuel.

Table 4.9: Avoided cost of emissions for Lime Village.

Emission	Avoided costs
CO ₂	28.94 USD/metric ton (26.31 USD/US ton)
PM ₁₀	37.28 USD/kg (16.91 USD/pound)
NO _x	1.52 USD/kg (0.69 USD/pound)

4.4 Economic Dispatch Feasibility of Multi-DEG Systems

A software program was also developed for economic load dispatch for multi-DEG systems taking into account the fuel efficiency curves, the output power factor, and the thermodynamic model of each DEG.

4.4.1 Economic Dispatch Feasibility for Buckland, Alaska

For communities such as Buckland, Alaska, which operates a 175 kWe and a 455 kWe Caterpillar® (CAT®) diesel electric generator (see Figure 4.26), simply examining the manufacturer's fuel efficiency curves (see Figure 4.27) for the electric load range shows that they need to turn off the less efficient 175 kWe DEG and just operate the 455 kWe DEG, so there is no real need for an automated economic dispatch system at this time. In this case the 455 kWe DEG has a new CAT® fuel injection controller which provides for a flatter efficiency curve over a wider range of electric load (see Figure 4.27). Each of the DEGs specifications were obtained from the CAT® website.



Figure 4.26: CAT[®] Diesel Electric Generators at Buckland, AK (455 kWe on left and 175 kWe on right).

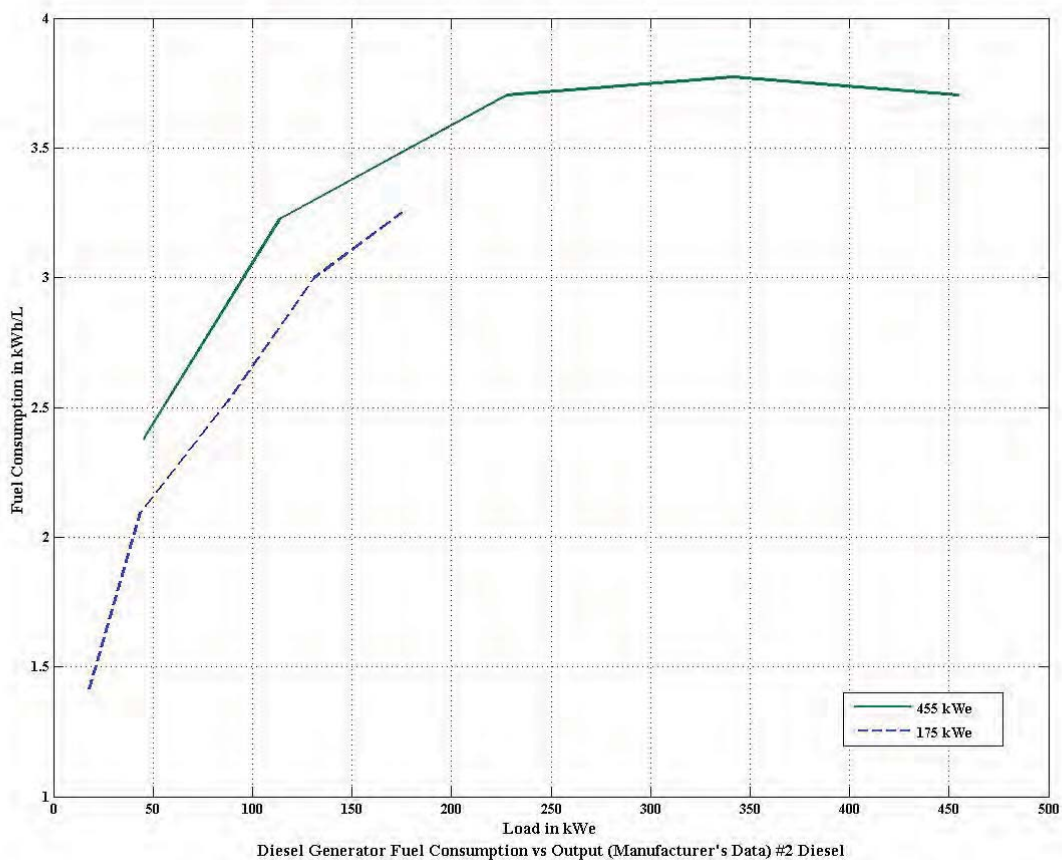


Figure 4.27: Manufacturer's fuel curves for CAT[®] 175 kWe and 455 kWe diesel electric generators.

4.4.2 Economic Dispatch Feasibility for Kongiganak, Alaska

Villages such as Kongiganak, Alaska would benefit from implementing an economic dispatch system. Power demand for the village of Kongiganak is supplied by Puvurnag Power Company which operates four diesel generator units: one 235 kWe John Deere® 6125AF, two 190 kWe John Deere® 6081AF, and one 140 kWe John Deere® 6081TF. With this information each of the DEGs specifications were obtained from the John Deere® website. The fuel efficiency curves for the three DEGs were constructed as shown in Figures 3.49 and 3.50 in Section 3.5.2.3 and three different load dispatch schemes were implemented: 1) even load distribution (ELD) 2) pre-configured control (PCC) and 3) economic dispatch.

Comparing economic dispatch ED where the load demand and the efficiency of each DEG is considered with PCC using #1 diesel fuel (see Table 4.10) shows a reduction in fuel consumption of about 9.5% by employing an economic dispatch system using the load and temperature profiles shown in Figure 4.28.

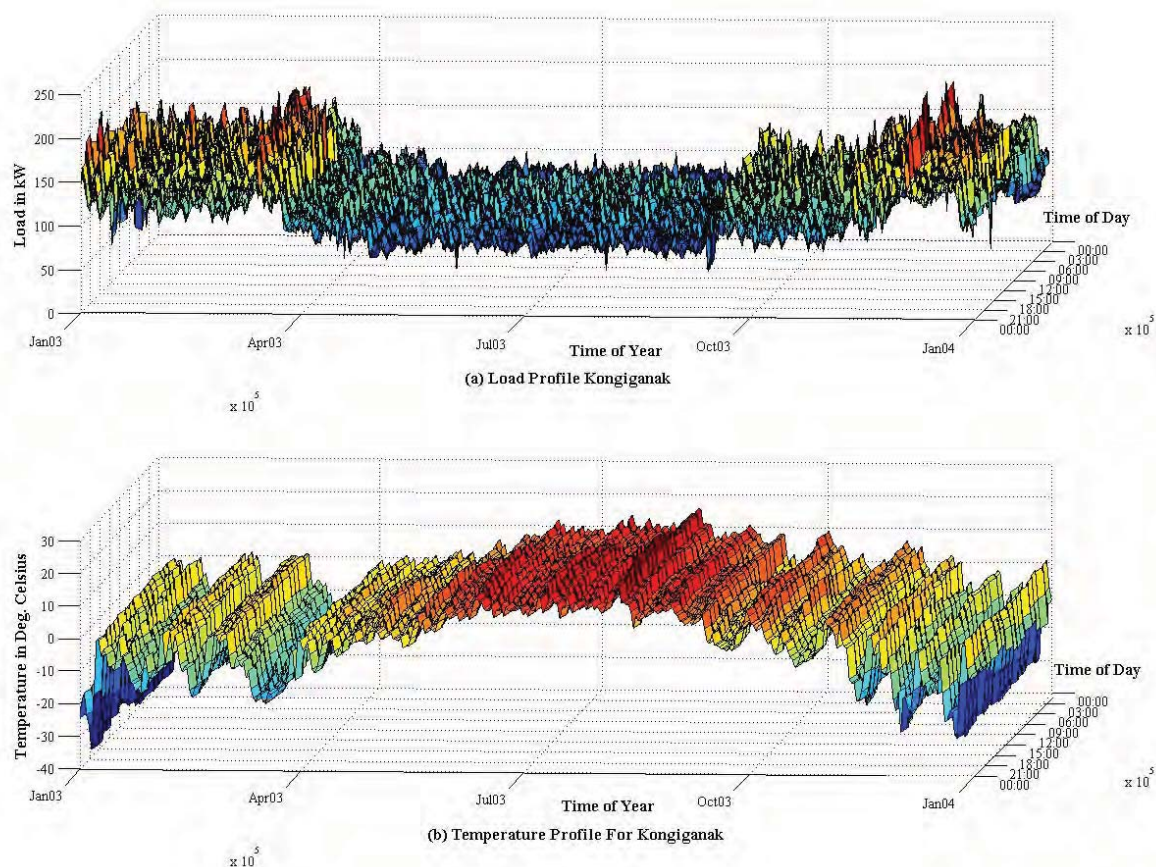


Figure 4.28: Kongiganak Load and Temperature Profiles for January 1, 2003 through January 1, 2004: (a) Load Profile (kW) (b) Ambient Temperature Profile (°C).

Given their current cost of bulk fuel at \$0.93/liter (\$3.50/gallon) for #1 diesel in Kongiganak and the installed cost of a basic economic dispatch system at \$114.2k (see Table 4.11b) offers a

payback of less than one year (see Table 4.12 below). Similar results are obtained for #2 diesel fuel. The two options in Table 4.11 are: 1) a basic system without security and 2) a more detailed system with security. Puvarnaq Power also received a Denali Commission grant for a new system with two DEGs and three WTGs so some of the cost for the economic dispatch system can be incorporated into this grant.

Table 4.10: PCC and ED results for Kongiganak system using #1 diesel fuel.

Parameter (for #1 Diesel)	Simulation / Scenario Data							
	PCC Control		Temperature Change Comparison	ED Control		Temperature Change Comparison	Control Scheme Comparison	
Ambient Temp Change in [°C]	0	3	-	0	3	-	0	3
Load energy- kWh	919433.5378	919433.5378	-	919433.5378	919433.5378	-	-	-
Fuel consumed- L (gal)	489808.0 (129,393.6)	490559.0 (129,591.9)	751.0 (198.4)	442987.0 (117,024.8)	443891.6 (117,263.7)	904.6 (239.0)	-46821.0 (-12,368.8)	-46667.3 (-12,328.2)
Efficiency of engine- kWh/l. (kWh/gal)	1.8771 (7.0956)	1.8743 (7.0847)	-0.0029 (-0.0109)	2.0755 (7.8455)	2.0713 (7.8295)	-0.0042 (-0.0160)	0.198 (0.750)	0.197 (0.745)
Total annual cost of fuel	0	0						
at \$1.082/L (\$3.50/gal)	\$529,972.2	\$530,784.8	\$812.6	\$479,311.9	\$480,290.7	\$978.8	-\$50,660.3	-\$50,494.1
at \$1.3209/L (\$5.00/gal)	\$646,987.4	\$647,979.3	\$992.0	\$585,141.5	\$586,336.4	\$1,194.9	-\$61,845.9	-\$61,642.9
NO _x emitted- ton _m (lbs)	12260.7 (27,030.2)	12279.5 (27,071.7)	18.80 (41.44)	11088.7 (24,446.4)	11111.4 (24,496.3)	22.64 (49.92)	-1172.01 (-2,583.8)	-1168.16 (-2,575.4)
PM ₁₀ emitted- kg (lbs)	92.2 (203.3)	92.4 (203.6)	0.14 (0.31)	83.4 (183.9)	83.6 (184.2)	0.17 (0.37)	-8.82 (-19.4)	-8.79 (-19.4)
CO ₂ emitted- kg (lbs)	1105963.9 (2,438,230.2)	1107659.6 (2,441,968.6)	1695.69 (3,738.34)	1000244.2 (2,205,158.5)	1002286.9 (2,209,661.7)	2042.65 (4,503.27)	-105719.70 (-233,071.8)	-105372.74 (-232,306.9)
Annual fuel savings			-0.153%			-0.204%	9.559%	9.513%

Table 4.11: Installation costs for two economic dispatch control schemes.

(a)Generator Control Automation Upgrade for a Three-Machine Plant (Buckland)

Item	Installed Cost (\$)	
	Option 1	Option 2
PLC/ Communications Hardware	26,625	33,571
PLC/ Communications Software	16,206	23,153
Plant Wiring	4,630	9,261
Transducer Installation	3,473	5,788
Setup and Commissioning	6,946	9,261
Total without RTED Software	\$57,880	\$81,034
RTED Software	27,783	27,783
Total with RTED Software	\$85,663	\$108,817

(b)Generator Control Automation Upgrade for a Four-Machine Plant (Kong)

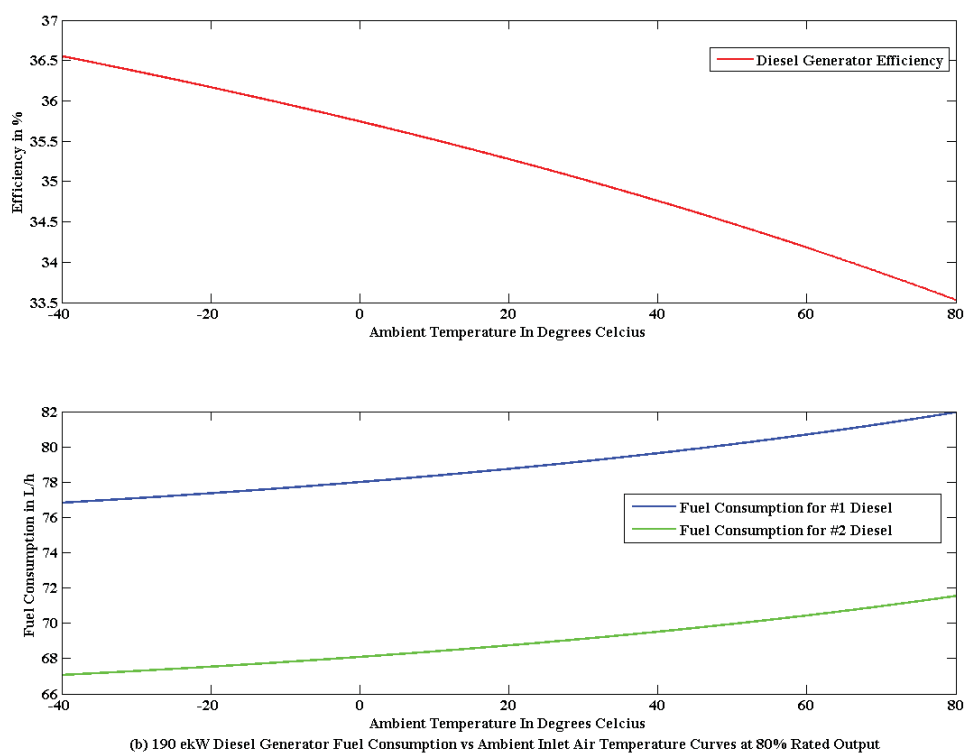
Item	Installed Cost (\$)	
	Option 1	Option 2
PLC/ Communications Hardware	35,501	44,762
PLC/ Communications Software	21,609	30,870
Plant Wiring	6,174	12,348
Transducer Installation	4,630	7,718
Setup and Commissioning	9,261	12,348
Total without RTED Software	\$77,175	\$108,046
RTED Software	37,044	37,044
Total with RTED Software	\$114,219	\$145,090

Table 4.12: Payback periods for the PCC and ED control schemes at Kongiganak using #1 diesel.

Variable	Payback Period at Different Average Fuel Costs Utilizing Control Schemes (yrs)			
	\$1.082/L (\$3.50/gal)		\$1.3029/L (\$5.00/gal)	
	PCC	ED	PCC	ED
Option 1				
Annual Fuel Savings (\$/yr)	150,301	50,660	183,487	61,846
Installation Cost (\$)	77,175	37,044	77,175	37,044
Payback Period (yrs)	0.51	0.73	0.42	0.60
Option 2				
Annual Fuel Savings (\$/yr)	150,301	50,660	183,487	61,846
Installation Cost (\$)	108,046	37,044	108,046	37,044
Payback Period (yrs)	0.72	0.73	0.59	0.60

4.4.4 DEG Efficiency versus Ambient Air Temperature

This same economic dispatch program was also used to incorporate ambient temperature variations and was tested for Kongiganak, Alaska as shown in Figure 4.28. The curves shown in Figure 4.29 below give the efficiency and fuel consumption of the 190 kW_e John Deere[®] DEG at Kongiganak as a function of ambient air temperature between -40 °C and 80 °C. The intake air temperature will be higher than the ambient air temperature due to heating of the incoming air by the building. An expected intake air temperature would likely be in the range from 4 °C to 20 °C. Given a 3 °C rise in ambient air temperature over the next 50 years as predicted by scientist at the UAF Geophysical Institute's Alaska Climate Research Center, there is approximately a 0.2% change in DEG efficiency which is negligible (see Table 4.11).

Figure 4.29: Ambient air temp vs. efficiency for 190 kW_e John Deere[®] DEG at 80% rated output.

5. Conclusion

Diesel electric power systems in Alaska rural villages are quite costly to operate given the price of bulk fuel to power the plants. The rising price of bulk fuel is motivating many rural utilities to investigate and implement renewable technologies for power generation in the villages and find ways of making the current DEG systems more efficient. The process used in this project included surveying the current state of Alaska village power systems, creating a consortium of rural utilities and state energy organizations with a vested interest in village energy, collecting available data, modeling village power systems for long term performance and feasibility analysis, and installing new remote monitoring systems in a select number of villages.

There has been a need to design remote monitoring systems for these villages in order to obtain reliable data for analysis to make recommendations for efficiency improvements in these plants. A survey of 25 villages in AEAs service territory revealed a number of issues with regards to power system data. There is simply either a lack of data or unreliable data in many cases either because a remote monitoring system was not in place or was not completely reliable due to equipment faults. Furthermore, the accuracy of the fuel and coolant flow meters and the intake, coolant and exhaust temperature sensors is critical in achieving reliable data as was demonstrated on the UAF Energy Center diesel. However, also of importance is the format in which the data is collected and stored with a number of villages to remotely monitor which is best served by using a central computer and server.

The analysis process used MATLAB[®] Simulink[®] to build a computer model of the DEG(s) to study the economic feasibility of integrating renewables such as WTGs and PV arrays into these stand-alone systems and economic dispatch control systems to improve system efficiency.

The results demonstrate that the integration of renewables such as WTGs and PV arrays into stand-alone hybrid power systems and the implementation of economic dispatch systems in Alaska rural villages improves system efficiency and reduces the operating costs and particulate matter emitted to the atmosphere. The results also demonstrate that while the integration of PV arrays into these systems has relatively long payback periods that exceed the life cycle of the project, the integration of WTGs results in much shorter payback periods in villages with a reliable wind resource. The implementation of economic dispatch control systems in villages with two or more DEGs results in even shorter payback periods making this an attractive first step for village utilities who are looking to cut the costs of electric power and do not have another reliable source of energy. The sensitivity analysis of fuel cost and investment rate showed that as the price of bulk fuel rises, the payback period of implementing the WTG, the PV array, and the economic dispatch system decreases. The cost of energy COE and the net present value NPV increases linearly with the increase in the fuel price.

In conclusion, this project served as a means of identifying the current state of power and energy in Alaska rural villages and suggests methods that are economically feasible for implementing more efficient standalone power systems which use DEGs as their main source of power and must operate in extreme climates like those found in Alaska. The assessment tools developed here which have been used to demonstrate the economic feasibility of integrating renewable energy sources and economic dispatch control systems into standalone village power systems using DEGs in Alaska are applicable to similar systems in other standalone applications such as remote oil platforms, remote sections of oil and gas pipelines, and remote mining.

References

- [1] Institute of Social and Economic Research, *Alaska electric power statistics (with Alaska energy balance)*, Report Prepared for Alaska Energy Authority, Regulatory Commission of Alaska, and Denali Commission, November 2003.
- [2] Alaska Energy Task Force, "NonRailbelt report findings and recommendations," Anchorage, Alaska, [Online]. Accessed February 18th, 2008. Available: <http://www.akenergyauthority.org/EnergyPolicyTaskForce/FinalNonRailbeltReport.pdf>
- [3] Northern Economics, *Screening report for Alaska rural energy plan*, Report Prepared for the Alaska Industrial Development and Export Authority, April 2006.
- [4] www.ni.com/pdf/manuals/322759c.pdf, National Instruments Fieldpoint 2015 Manual, accessed August 18th, 2008.
- [5] <http://www.powerlogic.com/products.cfm?id=64>, Powerlogic ION 7350 product information page, accessed August 18th, 2008.
- [6] http://www.pcorp.com.au/index.php?option=com_content&task=view&id=119&Itemid=171, Powercorp Commander information page, accessed August 18th, 2008.
- [7] <http://www.electroind.com/nexus1252.htm>, Electroindustries Nexus 1252 information, accessed August 18th, 2008.
- [8] National Instruments Application Note 043, pp. 1-35.
- [9] <http://omega.com/manuals/manualpdf/M1966.pdf>, Omega FTB 720 turbine flow meter manual, accessed August 18th, 2008.
- [10] http://www.lesman.com/unleashd/catalog/transmit/sitransfm_mag50006000blind_manED1.pdf, Magflo 7000 magnetic flow meter manual, accessed August 18th, 2008.
- [11] http://www.efunda.com/designstandards/sensors/flowmeters/flowmeter_mag.cfm, Magnetic Flow Meter Tutorial, accessed August 5th, 2004.
- [12] http://www.eesiflo.com/products/eesiflo_5000_series.pdf, Eesiflo 5000 ultrasonic flow meter product manual, accessed August 18th, 2008.
- [13] http://www.eesiflo.com/products/ultrasonic_flowmeter_portalok7s_01.html, Eesiflo S-Series ultrasonic flow meter product manual, accessed August 18th, 2008.
- [14] Sonntag, R. E., Borgnakke, C., and Wylen, G. J. V., "Fundamentals of Thermodynamics", *John Wiley & Sons, Inc.*, Fifth Edition, 1998.
- [15] <http://www.engineeringtoolbox.com>, Ethylene Glycol Heat – Transfer Fluid and Properties of Air, accessed Nov. 15th, 2004.
- [16] <http://www.marathonelectric.com/MGPS/standard.jsp>, Marathon Electric Generator main page, accessed August 18th, 2008.
- [17] http://www.deere.com/en_US/rg/productsequipment/productcatalog/gst/index.html?promo=jdps_home&bug=gendrive&tm=jdps, John Deere diesel engines for generators, accessed August 18th, 2008.
- [18] Malosh, J. A. and Johnson, R. A., "Part-Load Economy of Diesel-Electric Generators", a report prepared for Department of Transportation and Public Facilities, report # AK-RD-86-01, Jun 1985.
- [19] <http://www.aocwind.net/1550brochure.pdf>, Official Webpage for the Atlantic Orient Corporation, accessed Nov 2002.

- [20] M. Patel, "Wind and Solar Power Systems", *Florida: CRC Press LLC*, 1st Edition, 1999.
- [21] <http://www.nrel.gov/gis/solar.html>, Official Webpage of the National Renewable Energy, accessed Mar 22nd, 2006.
- [22] W. D. Winsor and K. A. Butt, "Selection of Battery Power Supplies for Cold Temperature Application", *Technical report, C-CORE Publication No. 78-13*, Sep 1978.
- [23] Sandia National Laboratories, "Stand-Alone Photovoltaic Systems - A Handbook of Recommended Design Practices", *a report prepared by Sandia National Laboratories*, report # SAND87-7023, Mar 1995.
- [24] Y. A. Cengel and M. A. Boles, "Engineering Thermodynamics", *McGraw Hill Publications*, 4th ed., 2002.
- [25] R. G. Narula, H. Wen, K. Himes, B. Power, "Incremental Cost of CO₂ Reduction in Power Plants", *ASME Turbo Expo*, 2002.
- [26] CATERPILLAR[®], "Diesel Generator Set 175 ekW," Document Num.: LEHE6275-03, April, 2007. [Online]. Accessed April, 2007. Available: www.CAT-ElectricPower.com
- [27] WikiPedia, "P-v diagram for the ideal diesel cycle," [Online]. Accessed February 18, 2008. Available: http://en.wikipedia.org/wiki/Diesel_cycle
- [28] CATERPILLAR[®], "Diesel Generator Set 455 ekW," Document Num.: LEHE1826-01, April, 2002. [Online]. Accessed April, 2007. Available: www.CAT-ElectricPower.com
- [29] A. N. Agrawal, *Modeling and optimization of hybrid electric power systems for remote locations in extreme northern climates*, M.S. Thesis, University of Alaska Fairbanks, August 2003. Fairbanks, Alaska.
- [30] T. Purtil and R. Robinson, "125 kWe Detroit Diesel AC Generator Curves," National Oilwell Varco, private communication, July 2007. Available: www.nov.com
- [31] K. Sastry, *Properties and performance evaluation of syntroleum synthetic diesel fuels*, M.S. Thesis, University of Alaska Fairbanks, December 2005. Fairbanks, Alaska.
- [32] Chevron Products Company, *Diesel fuels technical review (FTR-2)*, Chevron U.S.A. Inc, 1998.
- [33] A. Burcat and B. Ruscic, *Third millennium ideal gas and condensed phase thermochemical database for combustion with updates from active thermochemical tables*, Argonne National Laboratory, Chicago, Sept. 2005.
- [34] ThermoBuild, "Thermochemical Database," *Glenn Research Center, NASA*. [Online], accessed May 23rd, 2007. Available: <http://cea.grc.nasa.gov/>
- [35] M. J. Zehe, S. Gordon, and B. J. McBride, "CAP: A computer code for generating tabular thermodynamic functions from NASA Lewis coefficients," *Glenn Research Center, NASA*, Doc. NASA/TP—2001-210959, rev. 1, February 2002.
- [36] A. R. Bergen and V. Vittal, *Power systems analysis*, 2nd Ed., New Jersey: Prentice-Hall, 2000.
- [37] A. J. Wood and B. F. Wollenberg, *Power generation, operation, and control*, 2nd Ed., New York: John Wiley & Sons, Inc., 1996.
- [38] Syntroleum Corporation Technical Staff, *Syntroleum[®] S-2 Synthetic Diesel, Driving Clean-Fuel Innovation*, Syntroleum Corporation Publication, 2002.

- [39] <http://rredc.nrel.gov/solar>, Official Webpage of National Renewable Energy Laboratory, accessed Oct 2003.
- [40] D. Meiners, "Lime Village Power System Alternatives", *Alaska Energy Authority*, 2001.

Project Publications

As a result of research efforts on this project one book, three peer-review journal papers, fourteen conference proceedings, one Ph. D. dissertation and three M. S. theses have been published. Also, a portion of a book chapter which is currently in press contains some information with regards to village energy and environmental issues which is a direct result of efforts on this project.

Book:

- 1) A. N. Agrawal, R. W. Wies, and R. A. Johnson, *Hybrid Electric Power Systems: Modeling, Optimization, and Control*, VDM Verlag, 2007.

Journal Publications:

- 1) R. W. Wies, R. A. Johnson, and A. N. Agrawal, "Life Cycle Cost Analysis and Environmental Impacts of Integrating Wind-Turbine Generators (WTGs) into Standalone Hybrid Power Systems," *WSEAS Transactions on Systems*, iss. 9, vol. 4, pp. 1383-1393, 2005.
- 2) R. W. Wies, A. N. Agrawal, and T. J. Chubb, "Optimization of a PV with Diesel-Battery System for Remote Villages," *International Energy Journal*, vol. 6, no.1, part 3, pp. 107-118, 2005.
- 3) R. W. Wies, R. A. Johnson, A. N. Agrawal, and T. J. Chubb, "Simulink Model for Economic Analysis and Environmental Impacts of a PV with Diesel-Battery System for Remote Villages," *IEEE Transactions on Power Systems*, vol. 20, no. 2, pp. 692-700, 2005.

Conference Publications:

- 1) R. W. Wies, R. A. Johnson, and L. G. Brouhard, "Efficiency Improvements for Diesel Electric Generation Systems in Alaska Rural Villages through Economic Dispatch," *2008 Alaska Rural Energy Conference*, Girdwood (AK), 2008.
- 2) R. W. Wies, L. G. Brouhard, R. A. Johnson, and C. S. Lin, "Effects of Rising Electric Load and Ambient Air Temperature on Diesel Electric Generators in Alaska Rural Villages," *Proceedings of the 2007 Arctic Energy Summit*, Anchorage, AK, 2007.
- 3) R. W. Wies, R. A. Johnson, and A. N. Agrawal, "Life Cycle Cost, Efficiency and Environmental Impact Analysis for Integrating Renewable Energy Sources into Standalone Village Power Systems in Remote Arctic Climates," *Proceedings of the 2007 Arctic Energy Summit*, Anchorage, AK, 2007.
- 4) A. N. Agrawal, V. S. Sonwalkar, and R. W. Wies, "A Feasibility Analysis of Deploying Photovoltaic Array in a Remote Arctic Community," *Proceedings of the 2007 Arctic Energy Summit*, Anchorage, AK, 2007.
- 5) R. W. Wies and R. A. Johnson, "Village Metering and Power Study," *2007 Alaska Rural Energy Conference*, Session T5-C, Fairbanks (AK), 2007.
- 6) R. W. Wies, A. N. Agrawal, R. A. Johnson, and T. J. Chubb, "Implementation of a Remote Terminal Unit on a Diesel Electric Generator for Performance Analysis of Remote Power Systems in Rural Alaska," *2005 Alaska Rural Energy Conference*, Valdez (AK), 2005.
- 7) R. W. Wies, R. A. Johnson, and A. N. Agrawal, "Integration of Wind-Turbine Generators (WTGs) into Hybrid Distributed Generation Systems in Extreme Northern Climates," *2005 Alaska Rural Energy Conference*, Valdez (AK), 2005.
- 8) R. W. Wies, R. A. Johnson, and A. N. Agrawal, "Integration of Wind-Turbine Generators (WTGs) into Standalone Hybrid Power Systems in Extreme Northern Climates," *5th WSEAS International Conference on Power Systems and Electromagnetic Compatibility*, Corfu Island, Greece, 2005.
- 9) R. W. Wies, R. A. Johnson, A. N. Agrawal and T. J. Chubb, "Using HOMER and Simulink for Long-Term Performance Analysis of a Hybrid Electric Power System in a Remote Alaskan Village," *NREL World Renewable Energy Congress VIII*, Denver, CO, 2004.

- 10) R. W. Wies, R. A. Johnson, A. N. Agrawal, and T. J. Chubb, "Economic Analysis and Environmental Impacts of a PV with Diesel-Battery System for Remote Villages," *Proceedings of the 2004 IEEE Power Engineering Society General Meeting*, Denver, CO, 2004.
- 11) R. W. Wies, A. N. Agrawal, T. J. Chubb and R. A. Johnson, "Simulink Model for Economic Analysis & Environmental Impacts of a Photovoltaic with Diesel-Battery System for Remote Villages," *2004 Alaska Rural Energy Conference*, Talkeetna (AK), 2004.
- 12) R. W. Wies, A. N. Agrawal, and T. J. Chubb, "Electric Power Quality of Distributed Generation Systems in Rural Alaskan Villages," *2004 Alaska Rural Energy Conference*, Talkeetna (AK), 2004.
- 13) R. W. Wies, A. N. Agrawal, and T. J. Chubb, "Optimization of a PV with Diesel-Battery System for Remote Villages," *International Conference on Electric Supply Industry in Transition*, Asian Institute of Technology, Bangkok, Thailand, 2004.
- 14) R. W. Wies and A. N. Agrawal, "Integration of Wind-Turbine Generators (WTGs) into Hybrid Distributed Generation Systems in Extreme Northern Climates," *Proceedings of the 2003 International Yukon Wind Energy Conference: Cold Climate Opportunities*, 2003.
- 15) R. W. Wies and A. N. Agrawal, "Modeling and Optimization of Hybrid Electric Power Systems for Remote Locations in Extreme Climates," *Proceedings of the 2003 IASTED International Conference on Power and Energy Systems*, paper 379-190, pp. 241-246, 2003.

Ph. D. Dissertation:

- 1) A. N. Agrawal, *Hybrid Electric Power Systems In Remote Arctic Villages: Economic And Environmental Analysis For Monitoring, Optimization, and Control*, Ph. D. Dissertation, University of Alaska Fairbanks, August 2006. Fairbanks, Alaska.

M. S. Thesis:

- 1) L. G. Brouhard, *Economic Dispatch and Control for Efficiency Improvements on Diesel Electric Power Systems in Alaska Rural Villages*, M.S. Thesis, University of Alaska Fairbanks, August 2008. Fairbanks, Alaska.
- 2) T. Chubb, *Performance Analysis for Remote Power Systems in Rural Alaska*, M.S. Thesis, University of Alaska Fairbanks, May 2004. Fairbanks, Alaska.
- 3) A. N. Agrawal, *Modeling and optimization of hybrid electric power systems for remote locations in extreme northern climates*, M.S. Thesis, University of Alaska Fairbanks, August 2003. Fairbanks, Alaska.

List of Acronyms and Abbreviations

AEA – Alaska Energy Authority
AVEC – Alaska Village Electric Cooperative
CAT – Caterpillar®
COE – cost of energy
DEG – diesel electric generator
HARPSIM – Hybrid Arctic Remote Power Simulator
HOMER – Hybrid Optimization Model for Energy Efficient Renewables
kWe – kilowatt electric
kWh – kilowatt-hour
LCC – life cycle costs
MWh – megawatt-hour
NPV – net present value
NREL – National Renewable Energy Laboratory
PCE – power cost equalization
PF – power factor
PI – principal investigator
PV – photovoltaics
RTU – remote terminal unit
UAF – University of Alaska Fairbanks
WTG – wind turbine generator

National Energy Technology Laboratory

626 Cochrans Mill Road
P.O. Box 10940
Pittsburgh, PA 15236-0940

3610 Collins Ferry Road
P.O. Box 880
Morgantown, WV 26507-0880

One West Third Street, Suite 1400
Tulsa, OK 74103-3519

1450 Queen Avenue SW
Albany, OR 97321-2198

525 Duckering Bldg./UAF Campus
P.O. Box 755910
Fairbanks, AK 99775-5910

Visit the NETL website at:
www.netl.doe.gov

Customer Service:
1-800-553-7681



Methanol Reformer/PEM Fuel Cell Project

Final Report

Starting June 1, 2002
Ending September 30, 2006

Dennis Witmer,
University of Alaska Fairbanks
ffdew@uaf.edu
907-474-7082

Peter Lehman
Charles Chamberlin

Thomas Johnson
Jack Schmid
Tristan Kenny
UAF Energy Center

Report Issued September, 2006

DOE Award Number
DE-FC26-01NT41248
Task Number 1.03.4

Submitted by:
University of Alaska Fairbanks
Institute of Northern Engineering
Arctic Energy Technology Development Laboratory
437 Duckering Building
Fairbanks, AK 99775

Disclaimer

This report was prepared as an account of work sponsored by an agency of the United States Government. Neither the United States Government nor any agency thereof, nor any of their employees, makes any warranty, express or implied, or assumes any legal liability or responsibility for the accuracy, completeness, or usefulness of any information, apparatus, product, or process disclosed, or represents that its use would not infringe privately owned rights. Reference herein to any specific commercial product, process, or service by trade name, trademark, manufacturer, or otherwise does not necessarily constitute or imply its endorsement, recommendation, or favoring by the United States Government or any agency thereof. The views and opinions of authors expressed herein do not necessarily state or reflect those of the United States Government or any agency thereof.

Abstract

While grid connected electrical service is readily available in urban regions of the world, many places, including much of Alaska, are not serviced by this infrastructure. Diesel Electrical Generators provide power in many settings, but this solution becomes inefficient at loads under 100 kW. Very small loads (up to a few watts) can be serviced adequately by batteries, or batteries recharged by solar cells. However, at loads between 1 to 5 kW, these solutions are not cost effective, and small IC generators are typically used. However, these generators require frequent oil changes and other maintenance, and are designed for relatively short operating lives.

This project was designed to demonstrate an alternative to existing conventional technologies by developing an integrated power supply at 1 kW using a PEM fuel cell operated on methanol. During the course of this project, a methanol reformer was procured, and the efficiency of conversion of methanol to hydrogen was measured. This reformer was then integrated with a 1 kW PEM fuel cell, and the system efficiency measured using a 24 hour varying load profile.

Results indicate that methanol reformation is relatively efficient, approaching 80% (LHV, methanol fuel in/hydrogen out). PEM fuel cells operating on pure hydrogen have been demonstrated to operate at efficiencies of about 50% [1]. System efficiencies of greater than 30% were anticipated for the integrated system, but measured values were somewhat lower than this, due largely to a mismatch between reformer output and fuel cell size.

This project has successfully demonstrated the use of methanol as a fuel for powering a fuel cell, but was terminated before a field demonstration could be undertaken due to issues associated with the source of funds. However, significant issues remain with PEM fuel cells, including system costs and reliability, and further work is needed before these devices can be used for providing electrical power in remote areas of Alaska.

Table of Contents

Disclaimer	i
Abstract	ii
Table of Contents	iii
List of Figures	iv
Executive Summary	1
Introduction	3
Electrical supply for small remote loads	3
Methanol as a fuel	3
PEM Fuel Cell efficiencies	4
Systems Integration Issues	6
Experimental Methodology	6
Results and Discussion	10
Efficiency Measurements of the Methanol Reformer	10
System integration of Idatech Methanol Reformer with SERC PEM Fuel Cell	12
Discussion and Conclusions	16
References	19
List of Acronyms and Abbreviations	20
Appendices	21

List of Figures

Figure 1	Schematic of the mass and energy flows in a fuel cell and reformer system.....	9
Figure 2	Efficiency results of methanol reformer experiment.	10
Figure 3	Results for Idatech methanol reformer at lowest power setting.	11
Figure 4	Performance at highest setting.	11
Figure 5	Integrated Fuel Cell System at UAF.	13
Figure 6	Front view of integrated system.	13
Figure 7	AC load applied to integrated fuel cell system during the 48 hour test.	14
Figure 8	Stack Voltage during 48 hour test.	14
Figure 9	DC stack efficiency, and total system efficiency.	15

Executive Summary

Electrical power is one of the most useful forms of energy, but providing small amounts of electrical power (1-5kW) in areas not served by the electrical grid remains difficult. This project was intended to demonstrate a possible new solution to this issue: use of a PEM fuel cell operating on hydrogen provided by a reformer using a mixture of methanol and water. This fuel was of particular interest to arctic applications, given its low freezing point of -126°F.

Two partners were identified to work with the University of Alaska Fairbanks: the Schatz Energy Research Center (SERC) at Humboldt University in Arcata, California supplied the fuel cell and the balance of plant integration, while Idatech, of Bend, Oregon, supplied the methanol reformer. These partners were selected based on hardware delivered to UAF in a previous program.

The project was intended to be conducted in two phases, the first being assembly of a laboratory breadboard to verify thermodynamic efficiency and address system integration issues, the second being field demonstration of an integrated unit designed to address system lifetime issues. The degradation of reformer catalysts and fuel cell membranes was of particular interest. However, only the first phase of the project was complete due to a lack of available funding.

This project was selected in the FY 2002 RFP review process for AETDL, which was completed in early Spring, 2002. However, the project was not funded until early October 2002, when the subawards with the research partners were signed.

The first item delivered to the program was the Idatech methanol reformer, which arrived at UAF on December 20, 2002. This unit was packaged and integrated so that it started with a single push button, and could be controlled either by a set knob on the face of the unit, or by a voltage signal from an external source. Fuel was provided to the unit as a premixed liquid of methanol and de-ionized water. Testing was conducted at various hydrogen demand settings, and verified that efficiencies higher than 70% were achieved.

The methanol reformer was then shipped to the SERC laboratory for integration into the breadboard system. SERC build a PEM fuel cell stack, purchased the necessary blowers, pumps, and inverters for the balance of plant, and integrated the system together into a working system. The packaging was simple—a workbench was used for the mechanical support of the various sub-systems, with the fuel cell and air blower on top, and the reformer, control system electronics, inverter, and batteries mounted in the base. No covers were installed, so the basic subsystems were visible to the operator.

This demonstration unit was completed in the fall of 2003, and shipped to UAF for testing. In January of 2004, a 48 hour test was completed, with the load applied based on an average 500 watt load over a 24 hour period; the load peaked at about 1 kW for several brief periods. The unit performed very well, with no unexpected shutdowns or mechanical problems. The measured efficiency of the system was somewhat lower than the 30% goal, but this was due to a size mismatch between the reformer (most efficient at higher flow rates such as those needed by

3-5 kW stacks) and the fuel cell (providing a maximum of 1kW DC power). No change in performance was observed between the two cycles, though this is far too short a time to observe the expected degradation mechanisms.

This demonstration completed the first phase of the program, and the plan was to return the unit to SERC for additional work to make the unit field ready for the field demonstration. However, funding for phase 2 was not available, so the field demonstration phase could not be conducted as planned at an Alaskan location. SERC indicated that they had several possible demonstration sites in California, and a Memorandum of Understanding was created to return the unit to them in exchange for the ultimate lifetime operational data of the unit. It was expected that the unit would be deployed in the field, and that eventually the unit would fail.

However, at the time of this writing (September, 2006) SERC has not found a suitable field location for this demonstration, but indicated that the unit has found a home at the local high school, where it will be used in periodic short term demonstrations.

Idatech has also continued to develop methanol reformer systems, and currently advertises an integrated PEM fuel cell system on its web site. At several points during this program, an integrated unit was offered to this program for sale at about \$40,000, but never when funds were available. These units were observed operating at multiple fuel cell conferences over the years, and attract many interested observers.

This program successfully demonstrated that a methanol reformer can be made to provide a sufficient quantity of high purity hydrogen in a thermodynamically efficient way, and that a PEM fuel cell system can be designed to load follow a small load. However, significant barriers remain to the adoption of this technology in field applications, including cost and reliability.

Introduction

Electrical supply for small remote loads

While grid-connected electrical service is readily available in urban regions of the world, many places, including much of the land of Alaska, is not serviced by this infrastructure. Diesel Electrical Generators provide power in many settings, but this solution becomes very inefficient at loads under 100 kW. Very small loads (up to a few tens of watts) can be serviced adequately by batteries, or batteries recharged by solar cells. At loads between 1 to 5 kW, these solutions are not generally suitable due to the size of solar collectors needed and the cost (high) and lifetime (short) of the batteries, so small IC generators are typically used. However, these generators require frequent oil changes and other maintenance, and most are designed for relatively short operating lives (600 hours is typical).

Recent advances in fuel cell technology have given hope that this might be the appropriate technology for this application. High efficiencies have been demonstrated on fuel cells operating on hydrogen, and the lack of greenhouse gas emissions has caused considerable excitement. During the late 1990s, heavy investment in the industry led to the belief that commercialization of fuel cells was imminent. [2]

However, attempts to validate the claims of the fuel cell industry have revealed some problems with the current state of development. PEM fuel cells have not proved as reliable as initial claims indicated: stack lifetimes of 40,000 hours [1] indicated in industry product brochures have not yet been demonstrated (although stack lifetime is improving, and is currently about 5,000 hours). Hydrogen also is an issue: while abundant hydrogen is produced at petroleum refineries, hydrogen is not readily available as a fuel. This is due to several reasons: perceived safety issues (the Hindenburg effect); the lack of infrastructure to transport and store large amounts of hydrogen; and the physical properties of hydrogen, including the high cost of compression or liquefaction, the low volumetric energy density, and the decreased PV energy caused by the reduction in the number of molecules during combustion events. Using conventional hydrocarbons in on-board reforming, or in distributed reforming at fueling stations has been discussed, but these alternatives have also proved problematic, due in large part to the high temperatures (about 800°C) necessary to conduct this reaction.

Methanol as a fuel

Methanol has been suggested by some [3] as a better fuel for fuel cells as it is a liquid at normal ambient conditions, and can be readily reformed to create hydrogen. Unlike most hydrocarbon fuels which reform to hydrogen at 800°C [4], methanol can be reformed at 350°C, a range where conventional stainless steels can be used for fabricating reformer vessels. Heat management is also much easier at these lower temperatures, resulting in lower energy losses to the environment through radiation and sensible heat carried in the exhaust. (In the Idatech technology used in this

program, the temperature of reforming is also very close to the range needed for proper operation of the palladium membrane for hydrogen purification.)

Methanol is also a fuel readily available in the world market and in Alaska. Methanol is miscible with water, and has a very low freezing point, and as such can be used to de-ice fuels (and aircraft) at very low temperatures. Reforming hydrocarbons requires the addition of water, a problem for most hydrocarbon fuels where steam and fuel need to be added in precise ratios, but much easier for methanol, where the steam-to-carbon ratio can be controlled precisely in pre-mixing. Most methanol is produced from natural gas, and is priced at a point close to natural gas on a BTU basis. (Significant natural gas is considered “stranded” because it is not connected to the natural gas pipeline infrastructure, but these reserves can be converted on site to methanol, and shipped as a liquid.) Excess methanol production capacity is currently available in the US and the world due to the capacity built for MTBE production. Locally in Fairbanks, tanker loads of methanol pass through every day, destined for the North Slope oil fields, where it is used for de-icing gas handling pipes, and for de-icing aircraft throughout the state.

Methanol water mixtures for reforming typically are 63% methanol, 37% water by volume, a mixture with a freezing point of -88°C (-126°F). As such, it is an ideal fuel for arctic climates, where temperatures can typically dip to -45°C to -50°C (-50°F to -60°F). The record is about minus 68°C (-90°F). Most liquid hydrocarbon fuels exhibit problems at these temperatures: gasoline and propane stop vaporizing, and diesel fuels cloud and gel.

However, methanol does have some drawbacks as a fuel. From a pure thermodynamic point of view, methanol is partially oxidized methane, and carries less energy per molecule than other hydrocarbons. On a volumetric or mass basis, methanol has about half the energy content per unit as compared to other hydrocarbons. This problem is exacerbated if the fuel is pre-mixed with water, leading to a fuel with approximately 40,000 BTU per gallon. In remote locations, logistical costs of transporting fuels are often the most expensive component in energy costs, and so methanol is not a fuel typically used in those applications. There are some situations where methanol might be a suitable fuel, such as areas that are accessible by truck or by barge in the summer, but less accessible during the winter months.

In addition, there is one very significant disadvantage to methanol as a fuel: it is miscible in water. This means that fuel spilled accidentally can travel through soils to the water table, and then travel rapidly with the existing flow of ground water. This property has proved troublesome in MTBE (a chemical derived from methanol), where spilled fuel travels much faster through the underground water table with MTBE than without it.

PEM Fuel Cell efficiencies

PEM fuel cell efficiencies have been measured previously at UAF [1] and are approximately 50% when the fuel cell is operating on pure hydrogen, and system electrical parasitics are properly accounted for. In the intervening years, some small improvements have been made in fuel cell performance, but this number still serves as a good baseline for performance. PEM fuel cells also demonstrate very good load-following capabilities, being able to start from a cold state

in a few seconds, and respond to load changes rapidly, limited only by the ability of the air supply (usually a blower) to respond.

However, due to the difficulty and expense of using pure hydrogen, most stationary power users prefer to operate the fuel cell on some kind of hydrocarbon fuel. Since hydrocarbon reforming requires high temperatures, typically 600-800°C, there is a definite thermal response time associated with this process [4]. (A US DOE EE program for on-board gasoline reforming had a start-up requirement of less than 1 minute, but this program was abandoned in 2004 as being impractical.) Also, fuel cells can operate very efficiently at low power levels, but reformers need energy to maintain a hot standby state. This creates some systems issues that have not yet been adequately explored by the fuel cell industry.

Recent demonstrations by the US DoD residential fuel cell program [5] have solved this issue in another way, by operating the fuel cells at a constant power level. While this allows the demonstration projects to move forward, it does little to address the fundamental issue associated with transient response.

The addition of a hydrocarbon reformer and the associated heat required to drive the reactions also has a very negative impact on systems efficiency. Work on the RAPP at UAF in 2001 established a system efficiency based on steam reforming of hydrocarbons at approximately 24%. This number was not published in the open literature due to non-disclosure issues with the program participants, but this number has been verified on more than 100 PEM systems from multiple suppliers through the DoD Residential fuel cell program [5]. Results from these units can be viewed on line.

One other issue in PEM fuel cells is the issue of stack lifetime. Up until about 2002, PEM fuel cell stack lifetimes were short (exactly how short was a closely guarded industry secret), and failure mechanisms were not well understood. However, at some point it became apparent that stack lifetimes were very short if the fuel cell was operated at high power levels; that is, in excess of about 600 milli-watts per square centimeter. This is roughly half of the maximum power level advertised for PEM fuel cells. While exact failure mechanisms have not been published, some ideas floated in the industry involve hot spots developing on the membranes due to liquid water droplets forming, causing dead spots directly under the droplet, or hot spots along the perimeter, leading to membrane failure due to localized heating, forming pinholes. Other ideas include a mechanism associated with inhomogeneous compression of the stack, leading to fracture of the carbon fibers in the gas diffusion layer, leading to a local change in the wettability in that area, leading to water droplet formation, and failure by the mechanism described above.

The PEM industry has adjusted to the stack failure problem and resulting stack lifetime by conducting demonstrations where the stack is never exercised above the 50% power level. In the DoD demonstrations, stack lifetimes of several thousand hours have been achieved on some of the stacks using this rule, leading to the perception that the industry has this issue under control. However, the consequences of this solution are significant: PEM fuel cells are still significantly more expensive (by a factor of at least 100) than conventional technologies. Operating a PEM fuel cell at half power effectively doubles the capital cost, and halves the volumetric and mass power densities. Customers of the industry must feel like the purchaser of a fancy sports car

advertised to go like the wind, only to find that the dealer has installed a brick under the accelerator, with a note that the warrantee is voided if the brick is removed.

In this project demonstration, the fuel cell was sized so that the stack could operate safely below 600 milli-watts per square centimeter while delivering adequate power for a 1 kW peak load.

Recent work has also been focused on the damage that can be done to fuel cell stacks when left at open-circuit voltage for extended periods of time.[6] The high voltage conditions at open circuit results in chemical reactions that lead to rapid degradation of the fuel cell membrane—so it is important to keep the fuel cell under a minimum load to prevent this from occurring.

Systems Integration Issues

Fuel cells are advertised as being very simple devices that have no moving parts, and continue to provide electricity so long as fuel is supplied to them. This may be true for very small fuel cells, but systems designed for residential power require significant auxiliary systems for air supply, power management, and control. Batteries are also important for load leveling and start-up.

The addition of a fuel reformer to the system complicates the system even further. Fuel cells are most efficient at very low power levels, where the polarization losses are very low, while fuel reformers are most efficient at high power levels, where heat losses are minimized compared to the total energy of the system. PEM fuel cells operating on pure hydrogen can respond to rapid load changes, but reformers have significant thermal mass, and cannot respond as quickly to the change in load. The dynamic response of the system is a complicated issue, and systems integration strategies must address each of these issues.

Experimental Methodology

This project was proposed as a joint effort by Idatech Corporation of Bend, Oregon, and the Schatz Energy Research Center (SERC) at Humboldt State University, Arcata, California.

Idatech Corporation has been developing reformer systems to provide pure hydrogen to PEM fuel cells since 1997. Reforming reactions involve creating syngas, a mixture of CO, CO₂, H₂, H₂O, and CH₄. PEM fuel cells are particularly sensitive to the presence of CO, which acts as a poison and must be removed from the gas stream before it can be introduced into the fuel cell. Most reformer developers use a series of catalytic beds to condition the gas: a water/gas shift reactor to convert the bulk of the CO to CO₂ and H₂, and then a selective oxidizer to remove the last bit of CO, down to about 10 ppm, a level acceptable to the PEM fuel cell.

The Idatech reformer uses instead a palladium membrane separation technology to purify the hydrogen. Hydrogen is soluble in palladium, and diffuses quickly through the solid metal at temperatures of about 400°C, under the driving force of a pressure gradient. Idatech also uses

steam reforming, which can be easily done under pressure. Methanol is an ideal fuel for this process, as the liquid mixture of fuel and water can be pumped under pressure into the reforming region, and the resulting hydrogen pressure gradient is sufficient to allow pure hydrogen to be produced.

Idatech has been developing the methanol reformer for several years, and provided to this program a FPM20 unit capable of delivering 20 slm of hydrogen. This unit has a battery to allow independent start up, and also has a control system that allows a remote signal to control the hydrogen delivered. This unit is packaged as a commercial unit, though the price limits the likely market for the devices.

In the laboratory at UAF, researchers made efficiency measurements by establishing an energy balance for the methanol reformer. The most critical measurements in this energy balance are the fuel value in and the fuel value out. In this case, the fuel in is a low flow liquid mixture of methanol and water, and the fuel flow out is hydrogen. Other energy of concern is the flow of electrical energy in, and the heat losses associated with radiation and convection, as well as the sensible heat carried away in the exhaust.

In order to measure reformer efficiency, the fuel entering the reformer must be carefully measured. Previous experience has shown that commercially available flow meters are highly unreliable at the low flow (less than 10 ml/minute) rates that need to be measured to determine fuel flow in 1 kW systems. UAF has designed an optical flow meter using liquid levels and optical sensors in tubes to very accurately measure fuel transfer volumes, and used that system to determine the energy balance and efficiency. Hydrogen flow was measured using an MKS mass flow meter, but one concern was that impurities (water vapor or other gasses) might be flowing with the hydrogen. Mass measurements were made, but hydrogen purity could most easily be verified using the fuel cell stack, which would crash very quickly if carbon monoxide were leaking past the membrane.

Prior to receiving the FMP20 unit, Idatech provided us with some measurements they had made on their reformer. They claimed that they produced 27.2 slm H₂ at a feed rate of 33.0 ml/min fuel mix. The fuel is .69% methanol by volume, which gives a total of 33ml/min x .69 x 60/1000 = 1.366 l/hr methanol = .361 gal/hr. Using the heating value of methanol of 56,800 BTU/gal gives 20504 BTU/hr = 6.01 kW, which is the energy into the system in fuel. For the energy value of the hydrogen output, we have, based on the lower heating value of hydrogen, 1 slm = 179.9 W, so 27.2 slm = 4893 W = 4.893 kW. So $\eta = 4.893/6.01 = 81.4\%$, a rate which seemed very high.

A second data point provided by Idatech at 10 ml/min resulted in a H₂ flow of 7.7, which translates to .414 l/hr methanol = .1094 gallon/hr = 6213 BTU/hr = 1.82 kW methanol in, and 7.7 x 179.9 = 1.385 kW hydrogen out, or $\eta = 76.1\%$

After completing reformer testing at UAF, the reformer was shipped to SERC for integration into the fuel cell system. This task was somewhat delayed due to contract issues, but by late spring 2003 construction of the stack was underway. A "factory acceptance test" was conducted at the SERC facility in the fall of 2003, with special attention given to the power quality.

As part of the deliverable from SERC, a complete Operations and Maintenance manual was written, including specifications, schematics, photographic figures, and manuals from the major subsystems, including the reformer and inverter. The specifications and general system schematics are included in this report as Appendix A.

The unit was shipped from SERC to UAF in late fall, 2003, and additional instrumentation was added to the system for the purposes of establishing thermodynamic performance. In particular, the liquid optical flow meter used in previous experiments was used to instantaneously verify the flow meter calibration.

In January, 2004, a 48 hour test was conducted on the unit to measure the system's response to a typical daily cycle. A prescribed load was followed each day, based on an average load of 500W, with a peak of 1 kW during some periods. The load profile is show in Figure 2. The purpose of this experiment was to: 1) verify the ability of the system to load follow, 2) to measure the efficiency of the system at different loads, and 3) to verify the system stability over an extended test.

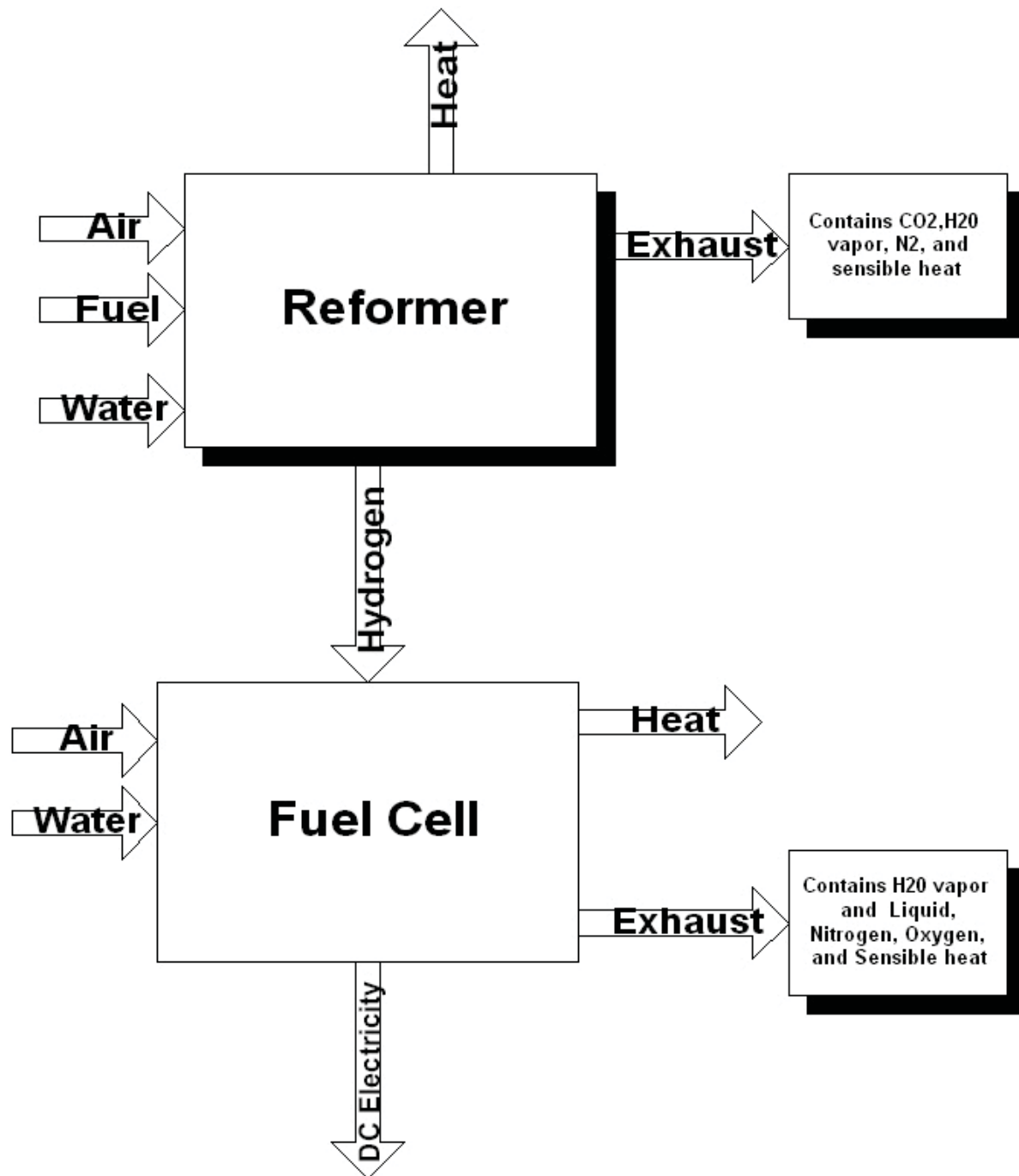


Figure 1 Schematic of the mass and energy flows in a fuel cell and reformer system.

Results and Discussion

Efficiency Measurements of the Methanol Reformer

Tests results are shown in Figures 2-7. For these tests, the demand setting on the reformer was varied, (the dial was labeled in percent, but it was more closely associated with the number of standard liters per minute) As can be seen in the figure, when the system was operating at maximum hydrogen output with no backpressure, the efficiency measured was just under 80%, which correlates well with the data given to us by Idatech. However, as expected, the efficiency of the reformer drops with reduced hydrogen output (some of the fuel energy must be used to maintain the system at temperature, so decreased output of product results in lower efficiency) and with backpressure (since the palladium membrane diffusion is proportional to partial pressure, increased back pressure results in less of the hydrogen in the syngas passing through the membrane). Also, it can be seen that response times are quite rapid, but thermal equilibrium is reached over a long period of time.

Output Level vs Efficiency for Various Backpressure Levels

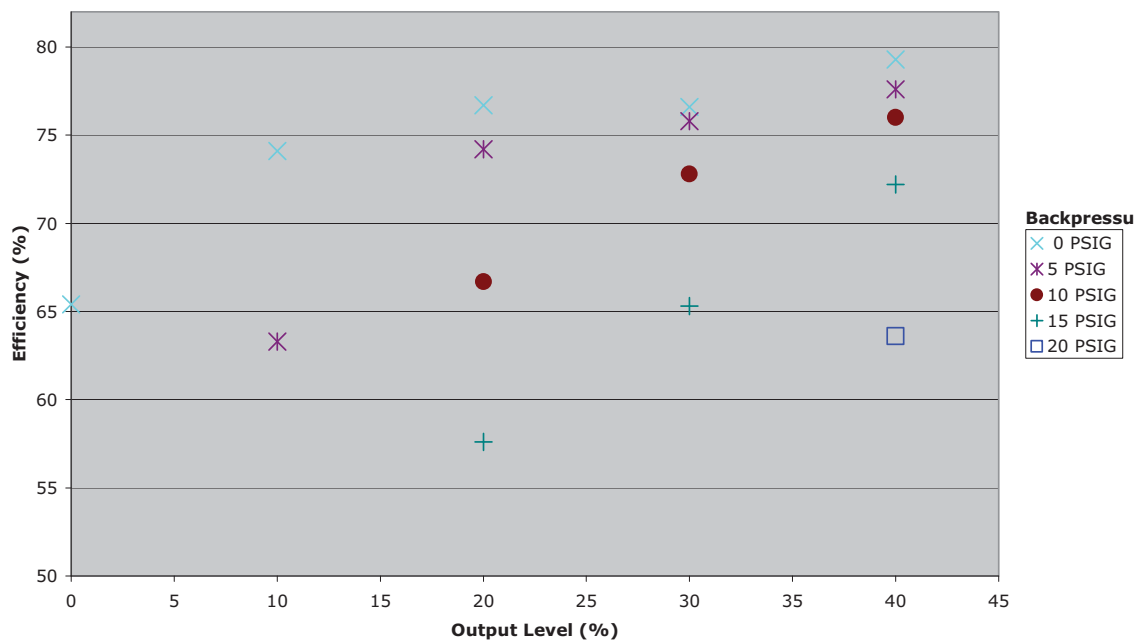


Figure 2 Efficiency results of methanol reformer experiment. Note that the power levels indicated on the x axis correspond to the settings provided on the Idatech unit, but that full power is at the 40% setting, which delivers approximately 27 slm of pure H₂.

Idatech Reformer 0% Output Setting

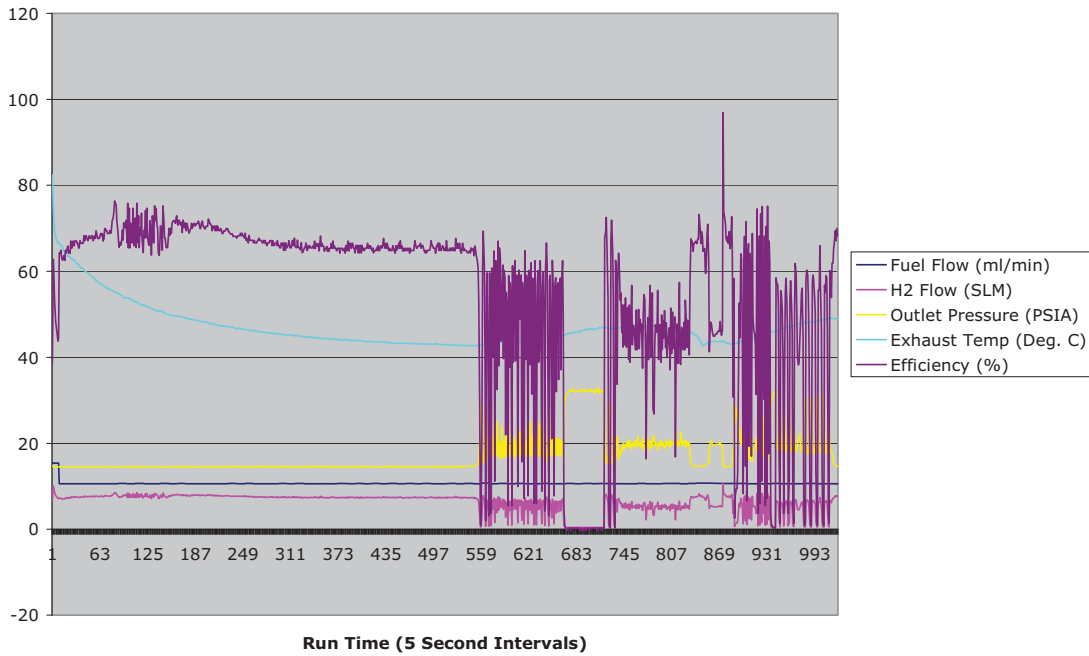


Figure 3 Results for Idatech methanol reformer at lowest power setting. Note that there is a fuel flow of about 10.5 ml/ min, corresponding to an energy input of about 1.9 kW, and a hydrogen flow of about 8slm under these conditions.

Reformer at 40% Setting

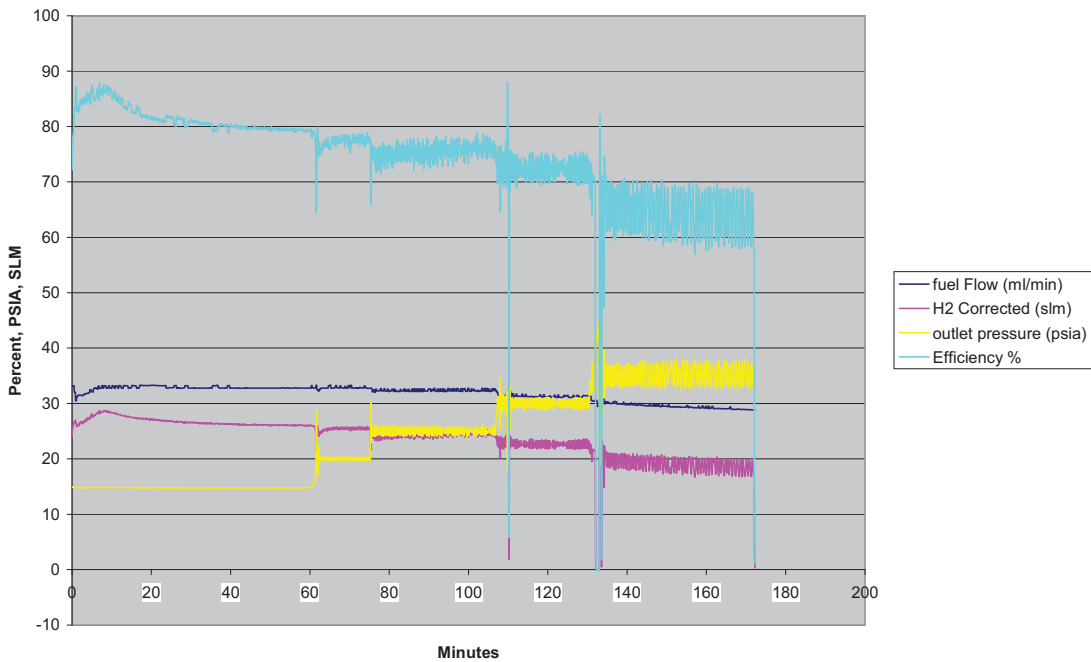


Figure 4 Performance at highest setting. Note stable performance, and decreasing efficiency at higher power levels.

As can be seen from the data collected during our testing, the FMP20 reformer performed as predicted by Idatech. In particular, our measurements verified the thermodynamic efficiency of the methanol reformer at over 70% (first law, lower heating value) over much of the performance range of the unit.

System integration of Idatech Methanol Reformer with SERC PEM Fuel Cell

At the end of the laboratory verification in January, 2003, the methanol reformer was shipped to SERC in Arcada, California for integration into the laboratory breadboard bench top unit. The system integration required developing a control system that allowed the unit to start with a single button, and provided power from that instant. The start-up of the methanol reformer required about 10 minutes, with a high electrical parasitic during that time, so batteries were sized to meet this initial load.

Much discussion about the design of this unit centered on the loads the system would be capable of supplying. In this demonstration, the fuel cell was sized so that the stack could operate safely below 600 milli-watts per square centimeter while delivering adequate power for a 1 kW peak load.

In this system, the responsibility for the systems integration and control system was delegated to the Schatz Energy Research Center, based on discussions with Idatech and UAF. It was determined that the dynamic issues could be addressed via energy storage in two forms: a ballast tank for leveling the hydrogen supply, and a battery bank for electrical load leveling.

Since the intent was to demonstrate this system for use in a remote residential application, a 24 hour load profile designed to give a peak load of 1 kW electrical, with an average load of 500W was devised. The basis for this profile is a residence in a rural village, where average loads are typically 500W average, but where loads peak during the day when people are active.

The controls for this system were also an issue. Previous systems built by SERC used PLC controls, but for this system, a Field point controller was used, based on programming in LabView. Control system logic is very important to assure not only that loads are met, but also that the fuel cell does not crash due to a lack of hydrogen.

This unit was built at SERC during the summer and fall of 2003, and was shipped to UAF in December, 2003. In early February, 2004, a 48 hour test was conducted to measure the unit performance. Photographs of the unit are shown below, as well as data summaries of the run. A complete operator's manual was written for the unit, and several pages from it are included in this report as appendices.

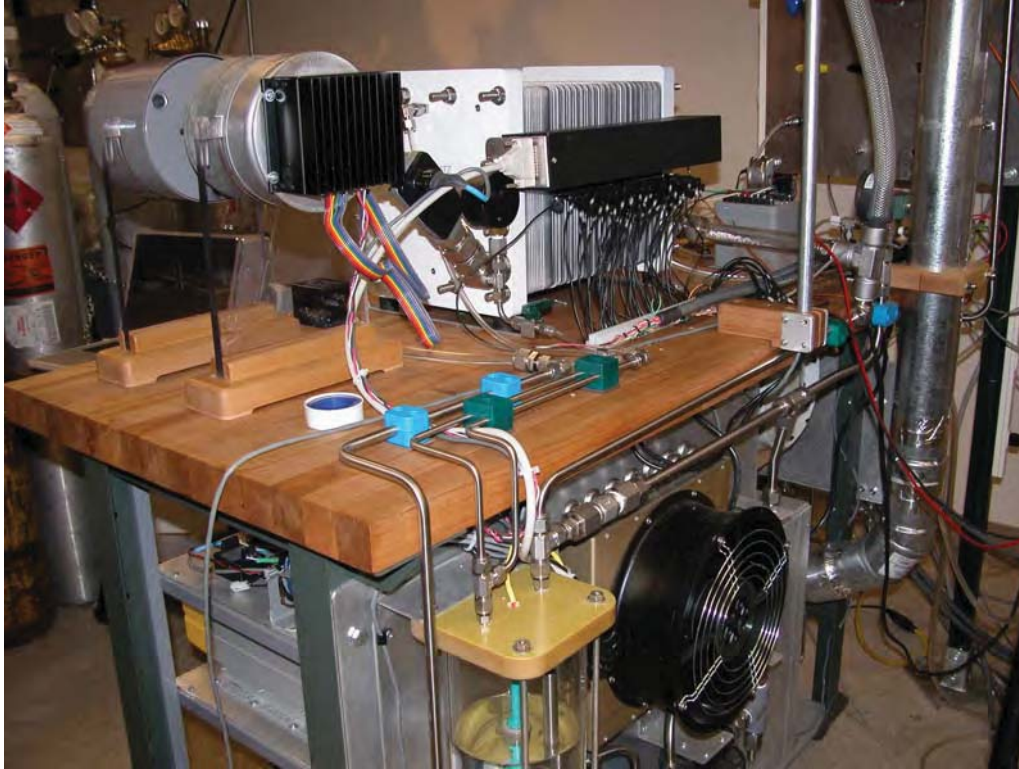


Figure 5 Integrated Fuel Cell System at UAF. Fuel Cell and blower are on the top, a blower for heat removal is visible on the bottom.



Figure 6 Front view of integrated system. Reformer, hydrogen ballast, batteries, inverter, safety system, and control system are visible.

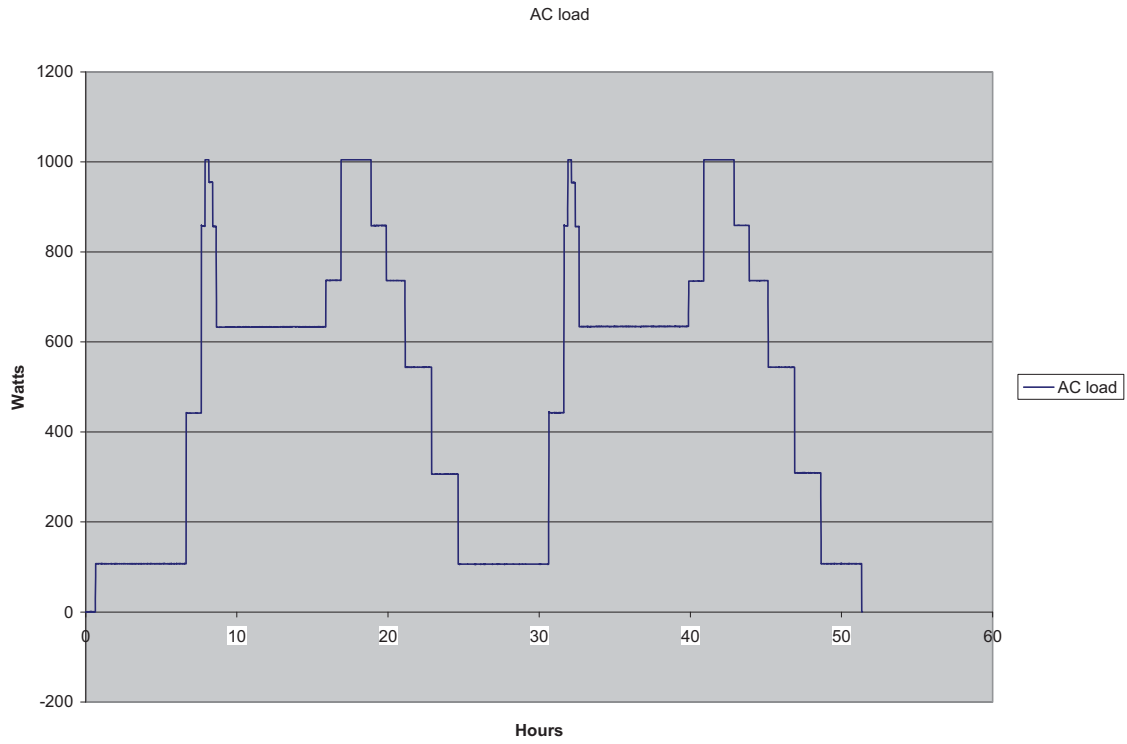


Figure 7 AC load applied to integrated fuel cell system during the 48 hour test. Load designed to peak at 1000 W, to average 500 W over a daily cycle, and to mimic household loads.

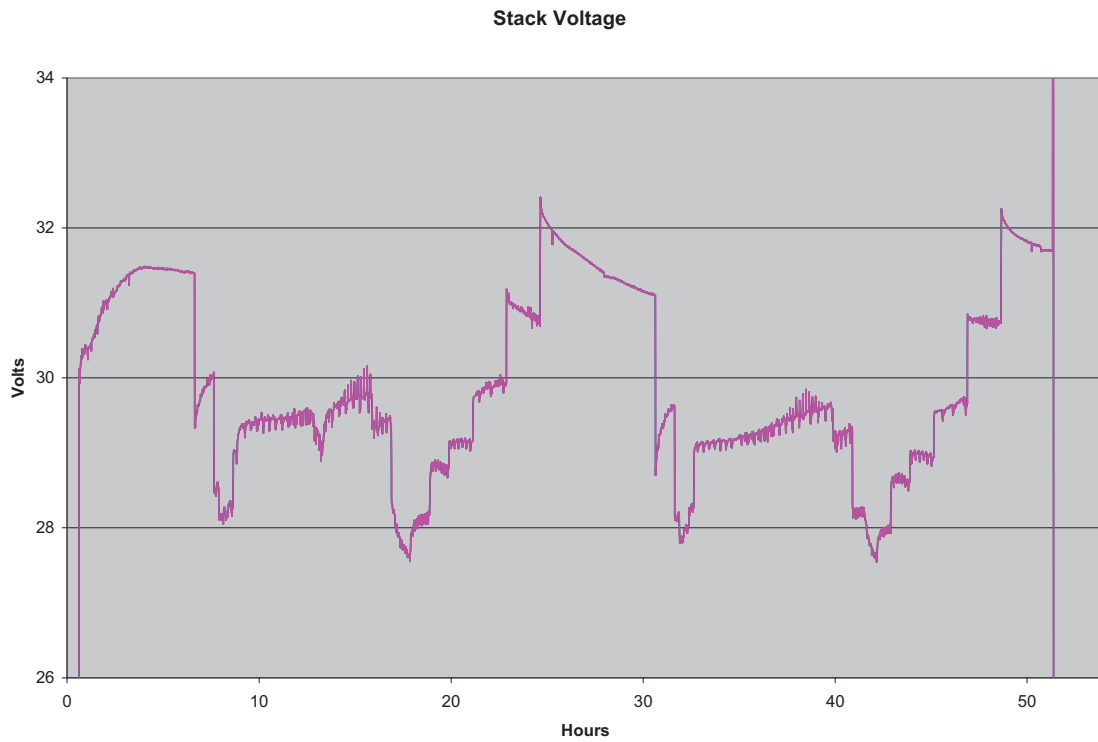


Figure 8 Stack Voltage during 48 hour test. Note the voltage lag due to battery charging effects.

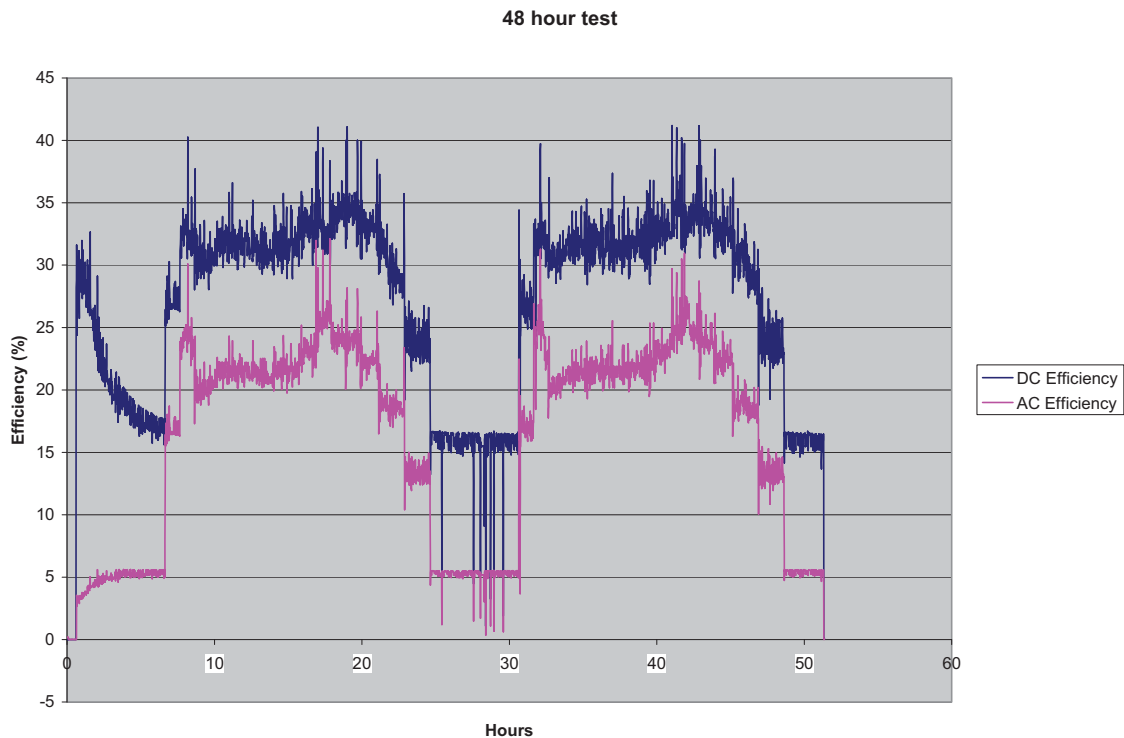


Figure 9 DC stack efficiency, and total system efficiency. Note the repeatable performance over the two cycles. Also note that the AC efficiency peaks at about 25%.

Originally this project included a Phase 2 packaging task, where the fuel cell and reformer were to be enclosed in a field-ready box, and the unit operated in some Alaskan field site. This would have provided data on the stack degradation rates, as well as information on the reliability of the balance of plant components. However, funding for Phase 2 was not available, so the unit could not be tested in a field demonstration.

The question arose as to what could be done with the hardware delivered to the program. SERC indicated that they had several possible field demonstration sites in California, and it was decided that the highest value use of this hardware would be to return it to SERC in exchange for operational data on the ultimate lifetime and failure modes of the unit. The most likely site appeared to be a remote radio repeater site in Northern California.

However, in a discussion with Peter Lehman, director of SERC, in the fall of 2006, no field test site was found to date, and the unit continues to sit at their laboratory unused. However, current plans with a local high school are to use the unit as an educational tool in high school science classes.

Discussion and Conclusions

The intent of this project was to design and demonstrate a PEM fuel cell system operating on methanol for a 1 kW peak load. Phase 1 was intended to be a laboratory demonstration, followed by a field demonstration in Phase 2. Due to funding issues, only Phase 1 was completed.

There are many successes to report in this project. The methanol reformer worked as advertised, providing pure hydrogen to the PEM fuel cell. Our 48 hour demonstration showed that the system was capable of starting and operating with methanol as the only energy input, and pressing the start button as the only operator interaction necessary. Also, the 48 hour demonstration completed two cycles, with the fuel cell and reformer operating in identical states during the two cycles, indicating that the system is operating in a repeatable manner, at least during a short laboratory test. This indicates that the hydrogen provided is free from any impurities that affect fuel cell performance.

Unfortunately, this demonstration also revealed some of the shortcomings with the current state of PEM fuel cell development. While the demonstration met most of the stated objectives, one of the most interesting lessons learned was what the program participants chose not to do. On the reformer side, very strong concern was raised with regards to the longevity of the fuel pump. While many pumps achieve the required pressure of 150 psi with a liquid fuel, there are few pumps capable of providing this pressure at low flow, while correctly metering the fuel into the reformer at a constant flow rate. During our initial conversations with Idatech, pump longevity was expected to be no more than 500 hours, with a rebuild required after that time. While this may be adequate for some applications, it is not sufficient for stationary power applications. By the end of our program, Idatech had found a replacement pump that they believed would operate for at least a few thousand hours.

The PEM fuel cell stack also still has longevity issues. Current state of the art shows that if stacks are operated only in low power conditions, stack lifetimes of several thousand hours are achievable. In automotive applications, engine lifetimes are only expected to be in this range, but stationary power stations are expected to have much longer lives.

While advocates of fuel cells cite high efficiencies as a prime reason for use of fuel cells, this demonstration did not achieve our stated goal of 30% while operating on methanol. One reason for this lower-than-expected efficiency came from the mismatch in output between the fuel cell and the reformer, as the reformer achieved its maximum efficiency of nearly 80% at full output with no back pressure, where it provided hydrogen sufficient for a 2.5 kW fuel cell, but our fuel cell was sized smaller than this. Also, the system was operated with a pressurized buffer between the fuel cell and reformer, which worked to reduce the overall efficiency.

There is also the issue of cost. In this program, \$40 K was paid for the methanol reformer, and \$120K paid for the fuel cell and system integration, for a total of \$160K. This is a considerable sum to pay for a 1 kW electrical generator, especially one expected to perform for only a few thousand hours at best. The argument can be made that fuel cells have not yet achieved the cost

reductions that come from mass production, but it must be noted that mass production is not likely to occur until users are convinced that fuel cells provide sufficient advantages over other technologies to justify mass production. Current stack lifetimes, sensitivity to impurities, the absence of a hydrogen infrastructure, and the cost of materials in PEM stacks all contribute to slow market development.

It should also be noted that fuel cells are attempting to compete in markets with mature conventional technologies, including batteries, solar panels, thermal electrics, and internal combustion engines. The internal combustion engine is particularly difficult to displace, as it possesses virtues that fuel cells can only dream of: a capital cost of about \$15 per kW (in auto engines), efficiencies of over 40% (in electronic injection diesel engines), use of widely distributed liquid fuels, improving emissions, and a widely trained work force to maintain these devices.

It is also worth considering the fundamental differences between combustion and the electrochemical reactions in fuel cells. Combustion is generally a homogenous, spontaneous gas phase reaction, occurring in three dimensions. Impurities introduced into a combustion reaction do not stop the reaction, but rather pass through the system and exit as exhaust products. While these products may be undesirable (think of sulfur contributing to acid rain), they do not affect the performance of the combustion reaction. The electrochemical reactions in a fuel cell are heterogeneous reactions, occurring at a gas-solid interface; they require the presence of a catalytic component, and also require a conduction path for the electrons to flow to an external circuit. Impurities introduced into the system typically lead to rapid degradation of the reaction, due to the blockage of catalytic sites, or to the corrosion of the metallic components in the electronic path. Removing impurities from the reactant streams remains a significant issue for all fuel cell systems, and adds considerable cost to the final electricity generated. In high temperature systems using hydrocarbons, sulfur is the most difficult contaminant; for PEM fuel cells it is CO.

In the system tested in this project, CO removal is accomplished by use of a palladium membrane, followed by a methanization catalyst to clean up any residual CO that may have slipped through pinholes in the membrane. This provides a very pure hydrogen stream, but depends on the mechanical integrity of a thin metal membrane. Large-scale applications have rejected the use of palladium membranes as being too unreliable, but this may be the ideal solution for small scale systems.

The issue of material cost is still very significant for PEM membranes. Currently, the Nafion used in the membrane costs more per ounce than the platinum used as a catalyst, and, unlike the platinum, is not recyclable. Bi-polar plates made of coated steel or stainless steel have been proposed, but the plates used in this demonstration were machined from high purity graphite. While this is a very stable material in highly corrosive environments, it is very expensive to purchase and to machine.

One recent industry insider also noted that fuel cells have proven to be very expensive to operate in field trials, noting that even if the purchase price of fuel cells were zero, the cost of produced

electricity would still be higher than grid-connected power. This is due partly to the current state of development in the field, but also due to the fundamental issue of reactant flow cleanup costs.

The value of electrical power in remote applications can be considerably higher than the value in grid connected environments. However, if fuel cells are to be competitive in this environment, they must prove highly efficient, reliable, and require only infrequent and predictable maintenance. This project did not provide confidence that PEM fuel cells operating on methanol have achieved that level of product development.

References

- [1] D. Witmer, Dan Morse, Thomas Johnson, Steve Guthrie, Ron Johnson, and Jay Keller, "Fuel Utilization Measurements of PEM Fuel Cells for Remote Power Applications," *National Hydrogen Association Annual Meeting*, 1999.
- [2] D. Witmer, Jay Keller, and Ron Johnson, "Remote Area Power Program for Alaskan Villages," *National Hydrogen Association Annual Meeting*, 1999.
- [3] U. Bossel, "The Future of the Hydrogen Economy: Bright or Bleak?," *sss.efct.com/reports*, pp. 1-39, 2003.
- [4] A. Lutz, Robert Bradshaw, Jay Keller, and Dennis Witmer, "Thermodynamic analysis of hydrogen production by steam reforming," *International Journal of Hydrogen Energy*, pp. 159-167, 2003.
- [5] E. C. W. s. DoD Fuel Cell Program, "Residential Demonstration Program," 2004.
- [6] D. Edlund, "Personal Communication," 2006.

List of Acronyms and Abbreviations

CH₄—Methane

CO—Carbon Monoxide

CO₂—Carbon Dioxide

H₂—Hydrogen

kW kilo-Watt

PEM—Polymer Electrode Membrane

SERC—Schatz Energy Research Center, at Humboldt State University, Arcata, CA

slm—standard liters per minute

Appendices

Operation and Maintenance Manual

Methanol-Fired Fuel Cell System for Remote Applications



September 2003

Prepared by
Schatz Energy Research Center
Humboldt State University
Arcata, California

© 2003
Schatz Energy Research Center

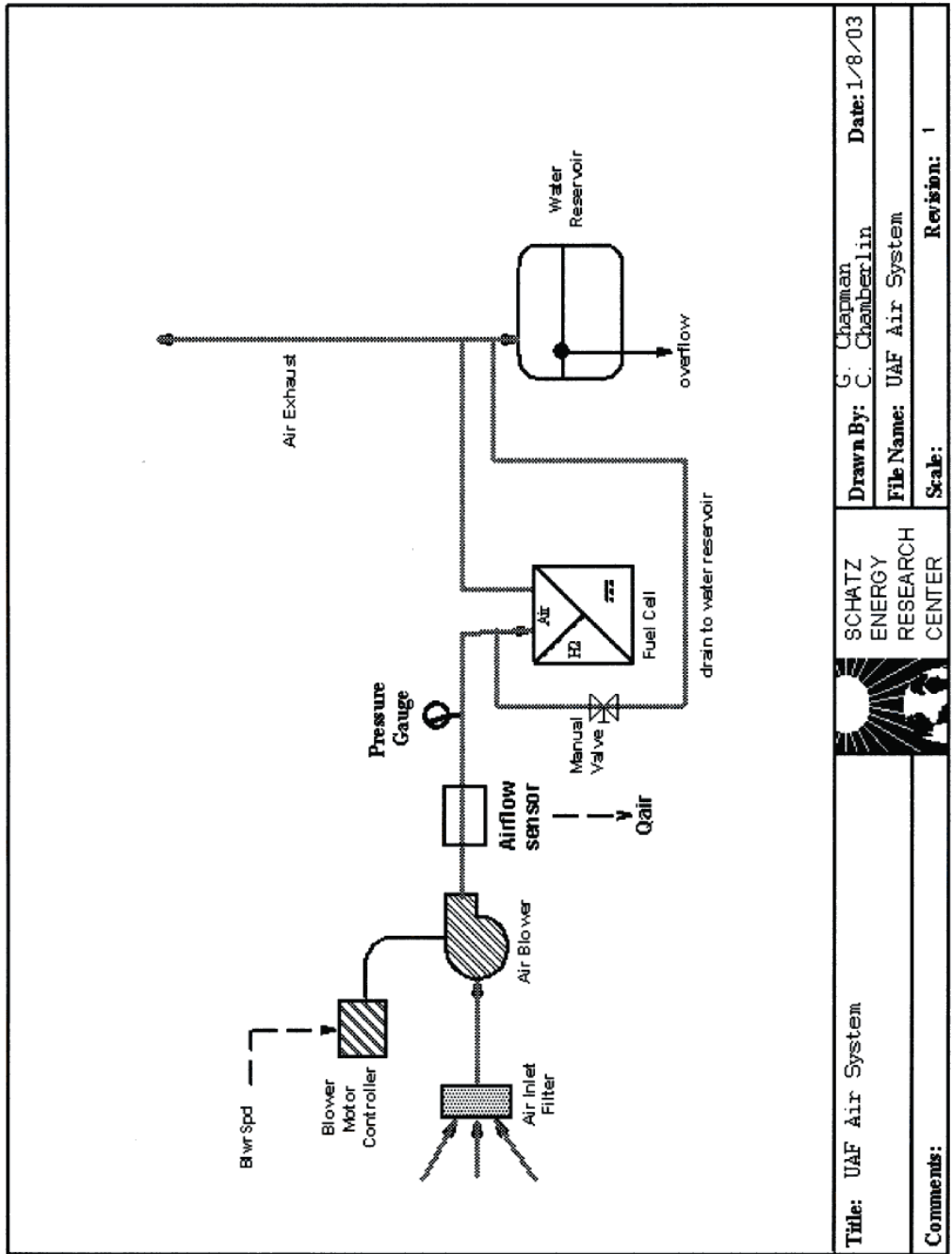


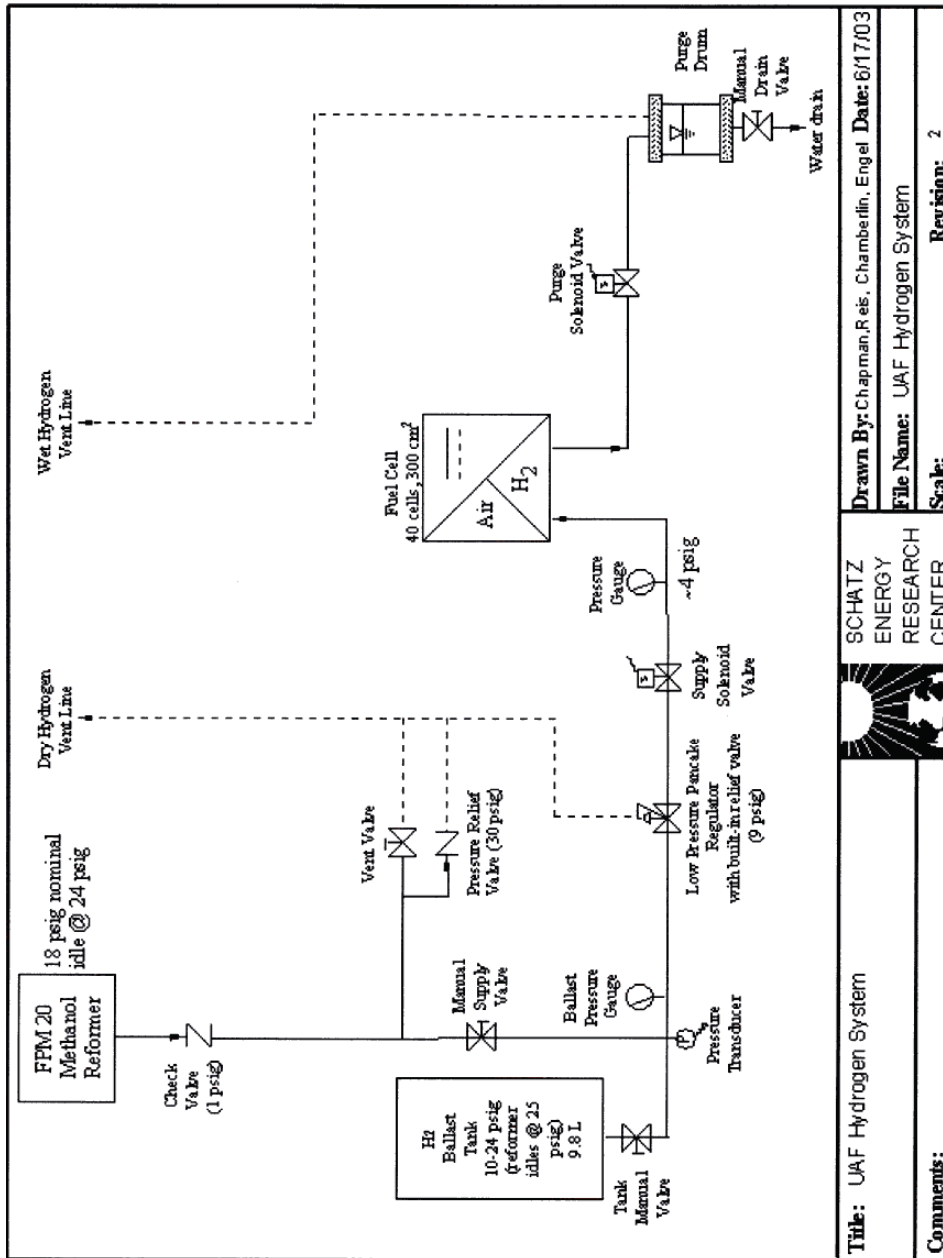
Appendix A: System Specifications and Drawings

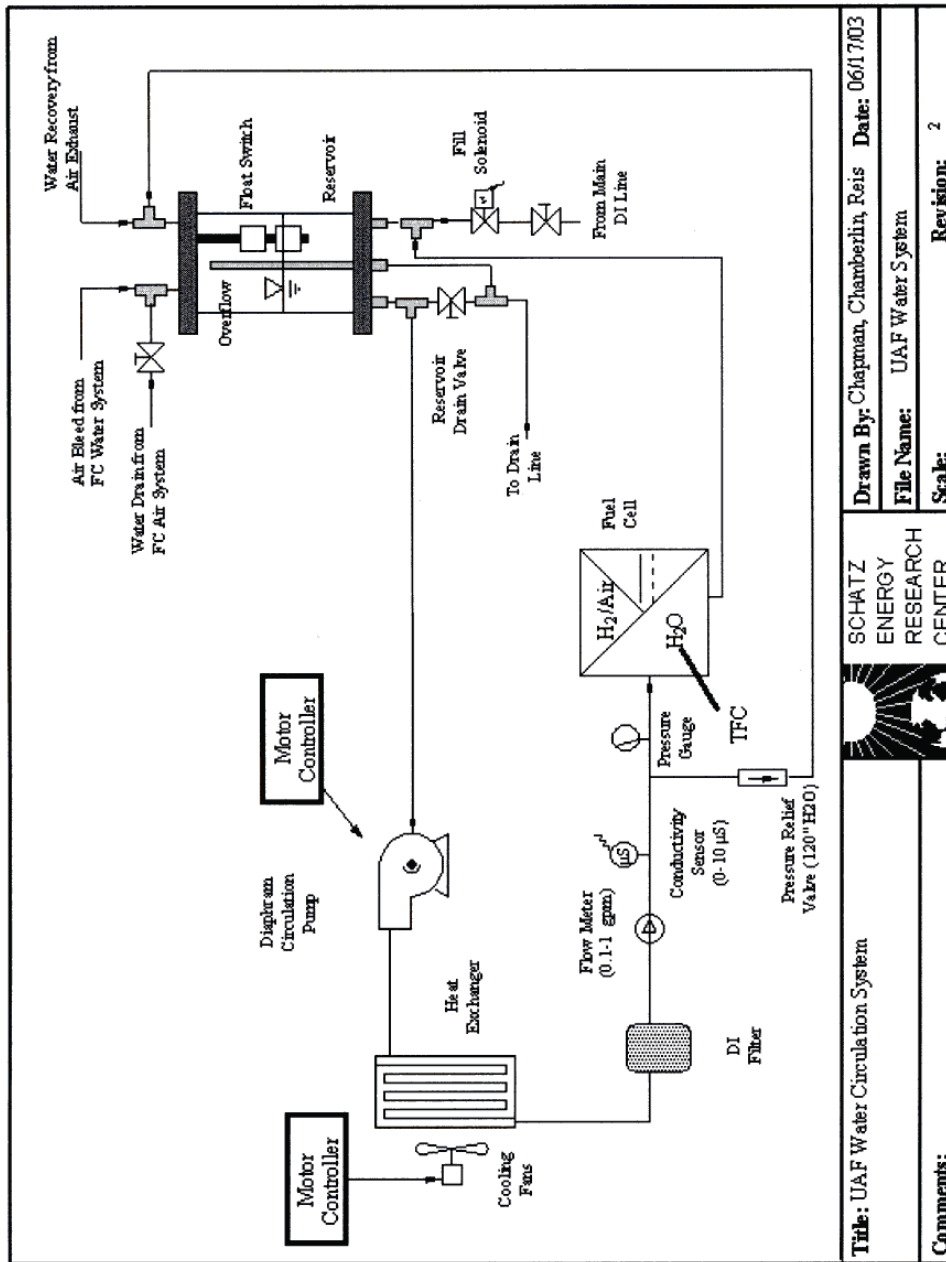
Fuel Cell System Specifications

Stack Specifications	
Number of Cells	40
Power Rating	2000 W DC(stack) 1000 W AC continuous (inverter) 1800 W AC peak (inverter)
Maximum Current	90 A
Fuel System Specifications	
Methanol Tank Capacity	10 liters (nominal)
Reformer Fuel Consumption Rate	at startup: 1 liter per hour maximum at rated output: 2 liters per hour maximum at idle: 0.210 liter per hour maximum
Reformer Hydrogen Output Rate	0 to 20 standard liters per minute
Reformer Hydrogen Output Pressure	normal = 18 psig max = 27 psig shutdown at 33 psig
Reformer Hydrogen Output Purity	>99.9%
Fuel Cell Delivery Pressure	3 to 4 psig
Air System Specifications	
Blower Airflow Range	0-200 slm
DI Water Cooling System Specifications	
Cooling Fan Airflow Rating	550 CFM
Heat Exchanger Heat Removal Capacity	2520 W @ $\Delta T = 30^{\circ} C$, flow = 1 GPM, $\Delta P = 2$ psi 5050 W @ $\Delta T = 50^{\circ} C$, flow = 2 GPM, $\Delta P = 5$ psi
Computer Control Specifications	
Software Safety Triggers	
Batt voltage < 22 V for longer than 5 seconds	
Batt voltage > 31 V	
Hydrogen ballast pressure >27 psig	
Fuel cell temperature >65° C	
Water conductivity >10 μS	
Fuel cell current > 90A	
Inverter current >70A for longer than 5 seconds	
Battery current >100A for longer than 5 seconds	
Safety circuit faults or not connecting	
Reformer fault	
No communication w/ reformer for longer than 10 seconds	
I/O not functioning properly for longer than 6 seconds	
Thermocouple disconnected	
Fuel cell voltage < 600 mv for any cell for longer than 5 seconds	

Hardware Safety Triggers	
safety circuit failure	
emergency stop button	
smoke detector	
H2 detector	
System Requirements	
Supply Water	<10 μ S conductivity
Methanol	1:1 molar mix, methanol and deionized water (62 to 64 percent methanol by weight, mixed with deionized water)
Air, Water and Hydrogen Vent Lines	vented directly to outdoors







Oil & Natural Gas Technology

DOE Award No.: DE-FC26-01NT41248

Final Report

Capture of Heat Energy from Diesel Engine Exhaust

Submitted by:
Arctic Energy Technology Development Laboratory
Institute of Northern Engineering
University of Alaska Fairbanks
PO Box 755910
525 Duckering Building
Fairbanks, AK 99775-5910

Prepared for:
United States Department of Energy
National Energy Technology Laboratory

November 2008



Office of Fossil Energy



Capture of Heat Energy from Diesel Engine Exhaust

Final Report

**Reporting Period:
September 2002 to September 2008**

**Principle Investigator:
Chuen-Sen Lin
(907) 474-5126, ffcl@uaf.edu**

**Report Issued:
November 2008**

**DOE Award Number:
DE-FC26-01NT41248
Task: 1.03.5**

**Submitted by:
Arctic Energy Technology Development Laboratory
Institute of Northern Engineering
University of Alaska Fairbanks
PO Box 755910
525 Duckering Building
Fairbanks, AK 99775-5910**

Disclaimer

This report was prepared as an account of work sponsored by an agency of the United States Government. Neither the United States Government nor any agency thereof, nor any of their employees, makes any warranty, express or implied, or assumes any legal liability or responsibility for the accuracy, completeness, or usefulness of any information, apparatus, product, or process disclosed, or represents that its use would not infringe privately owned rights. Reference herein to any specific commercial product, process, or service by trade name, trademark, manufacturer, or otherwise does not necessarily constitute or imply its endorsement, recommendation, or favoring by the United States Government or any agency thereof. The views and opinions of authors expressed herein do not necessarily state or reflect those of the United States Government or any agency thereof.

Abstract

Diesel generators produce waste heat as well as electrical power. About one-third of the fuel energy is released from the exhaust manifolds of the diesel engines and normally is not captured for useful applications. This project studied different waste heat applications that may effectively use the heat released from exhaust of Alaskan village diesel generators, selected the most desirable application, designed and fabricated a prototype for performance measurements, and evaluated the feasibility and economic impact of the selected application. Exhaust flow rate, composition, and temperature may affect the heat recovery system design and the amount of heat that is recoverable. In comparison with the other two parameters, the effect of exhaust composition may be less important due to the large air/fuel ratio for diesel engines. This project also compared heat content and qualities (i.e., temperatures) of exhaust for three types of fuel: conventional diesel, a synthetic diesel, and conventional diesel with a small amount of hydrogen. Another task of this project was the development of a computer-aided design tool for the economic analysis of selected exhaust heat recovery applications to any Alaskan village diesel generator set.

The exhaust heat recovery application selected from this study was for heating. An exhaust heat recovery system was fabricated, and 350 hours of testing was conducted. Based on testing data, the exhaust heat recovery heating system showed insignificant effects on engine performance and maintenance requirements. From measurements, it was determined that the amount of heat recovered from the system was about 50% of the heat energy contained in the exhaust (heat contained in exhaust was evaluated based on environment temperature). The estimated payback time for 100% use of recovered heat would be less than 3 years at a fuel price of \$3.50 per gallon, an interest rate of 10%, and an engine operation of 8 hours per day. Based on experimental data, the synthetic fuel contained slightly less heat energy and fewer emissions. Test results obtained from adding different levels of a small amount of hydrogen into the intake manifold of a diesel-operated engine showed no effect on exhaust heat content. In other words, both synthetic fuel and conventional diesel with a small amount of hydrogen may not have a significant enough effect on the amount of recoverable heat and its feasibility.

An economic analysis computer program was developed on Visual Basic for Application in Microsoft Excel. The program was developed to be user friendly, to accept different levels of input data, and to expand for other heat recovery applications (i.e., power, desalination, etc.) by adding into the program the simulation subroutines of the desired applications. The developed program has been validated using experimental data.

Table of Contents

Disclaimer	ii
Abstract	iii
List of Figures	vi
List of Tables	viii
Chapter 1 Introduction	1
Executive Summary	5
Chapter 2 Experimental	7
2.1 Background	7
2.1.1 Introduction	7
2.1.2 Literature Review of Exhaust Heat Recovery	7
2.1.3 Heat Exchanger Basics	12
2.1.4 Economic Study	13
2.1.5 Effect of Fuel Type on Heat Recovery	14
2.2 Design of an Exhaust Heat Recovery System	14
2.2.1 Introduction	14
2.2.2 Selection of Waste Heat	16
2.2.3 Selection of Heat Recovery Application	16
2.2.4 Experimental Site	16
2.2.5 Heat Recovery System Design	17
2.3 Installation and Instrumentation of the Heat Recovery System	26
2.3.1 Introduction	26
2.3.2 Heat Exchanger Section	31
2.3.3 Control System Section	32
2.3.4 Unit Heater Section	37
2.3.5 Flow Meter and Load Cell Calibration	38
2.3.6 Instrumentation of Exhaust Line Monitoring	40
2.3.7 Cost of the System	40
2.4 Experiment Setups for Exhaust Properties of Other Fuels	43
2.4.1 Synthetic Fuel	44
2.4.2 Conventional Diesel with a Small Amount of Hydrogen	44
Chapter 3 Results and Discussion	47
3.1 Introduction	47
3.2 Economic Analysis for Exhaust Heat Recovery for Heating	48
3.2.1 Design Verification	48
3.3 Feasibility and Performance	52
3.3.1 50-Hour Run	52
3.3.2 Forty Percent Propylene Glycol as Working Fluid	54
3.3.3 Efficiency	61
3.3.4 Soot Accumulation	61
3.4 Corrosion Experiment	63
3.5 Economic Analysis and Maintenance	67
3.6 Exhaust Emissions, Heat Content, and Temperatures of the Three Fuels	69
3.6.1 Conventional Diesel and Synthetic Fuel	69
3.6.2 Conventional Diesel and Conventional Diesel with a Small Amount of Hydrogen:	70

3.7	Economic Analysis Program for Exhaust Heat Recovery System	72
3.7.1	Results.....	73
Chapter 4	Conclusions.....	75
4.1	Experimental Economic Analysis of Exhaust Heat Recovery.....	75
4.1.1	Future Work.....	75
4.2	Evaluation of Exhaust Heat Contents and Temperatures for Different Fuels	76
4.2.1	Synthetic Diesel Versus Conventional Diesel	76
4.2.2	Diesel Fuel and Diesel Fuel with a Small Amount of Hydrogen	76
4.3	Economic Analysis Program for Exhaust Heat Recovery	76
4.3.1	Future Work.....	77
References	78
Appendix A	: Instruction Manual for Exhaust Heat Recovery System.....	80

List of Figures

Figure 1.1. Energy distribution of a diesel generator.....	2
Figure 2.1. Schematic diagram.	11
Figure 2.2. Alaskan household energy consumption [24].	15
Figure 2.3. Space allocated for the control system inside the ISO container.	22
Figure 2.4. Final design.	23
Figure 2.5. Owner’s manual – Bell and Gossett.	24
Figure 2.6. Block diagram showing the DAQ channels.	25
Figure 2.7. AutoCAD heat recovery design drawing.	27
Figure 2.8. Section 1 of the heat recovery system (on top of ISO container).....	28
Figure 2.9. Section 2 of heat recovery system (inside ISO container along west wall).	29
Figure 2.10. Section 3 of heat recovery system (sitting outside on the ground next to the west wall of the ISO container).....	30
Figure 2.11. Heat exchanger inlet/outlet pipe connections.	32
Figure 2.12. North half of the control system inside the ISO container on the west wall.	33
Figure 2.13. South half of the control system inside the ISO container on the west wall.	34
Figure 2.14. Expansion tank in the control system.....	34
Figure 2.15. Bypass line.....	35
Figure 2.16. Bypass line.....	36
Figure 2.17. Flow meter line.....	36
Figure 2.18. Unit heater inlet/outlet pipe connections.	37
Figure 2.19. Calibration curve for flow meter.	39
Figure 2.20. Calibration curve for load cell.	40
Figure 2.21. Thermocouples on the outlet of the heat exchanger.	41
Figure 2.22. Thermocouples on the core side.	41
Figure 2.23. Line diagram for hydrogen test.	45
Figure 3.1. Fluid flow distributions across the bypass and unit heater.....	49
Figure 3.2. Temperature on the fluid side across the heat exchanger.....	50
Figure 3.3. Flow distributions between the bypass and unit heater.	51
Figure 3.4. Energy balance with respect to the ambient temperature.	52
Figure 3.5. Enthalpy change in exhaust across the heat exchanger.	53
Figure 3.6. Heat flow rates of the exhaust entering and leaving the heat exchanger.....	54
Figure 3.7. Heat release versus heat absorption.....	55
Figure 3.8. Heat released by exhaust and heat absorbed by glycol fluid as outlet temperature to the heat exchanger on the fluid side is set to 87°C	56
Figure 3.9. Heat released by exhaust and heat absorbed by glycol fluid as outlet temperature to the heat exchanger on the fluid side is set to 77°C	57
Figure 3.10. Heat released by exhaust and heat absorbed by glycol fluid as outlet temperature to the heat exchanger on the fluid side is set to 65°C	58
Figure 3.11. Absorbed heat by propylene at 87°C, 77°, and 65°C as heat exchanger outlet temperature.	59
Figure 3.12. Percentage of heat extracted from the total exhaust heat during a 50-hour experimental run time.	60
Figure 3.13. Percentage of heat extracted from the total exhaust heat at different heat exchanger outlet temperatures on the fluid side.	61

Figure 3.14. Efficiency of the heat exchanger.	62
Figure 3.15. Shell side soot accumulation.	62
Figure 3.16. Soot accumulation on the fins.	63
Figure 3.17. Soot accumulation on the core side.	63
Figure 3.18. No exposure to air.	64
Figure 3.19. Exposure to air.	65
Figure 3.20. No exposure to air.	66
Figure 3.21. Exposure to air.	66
Figure 3.22. Payback time with respect to fuel price and interest rate.	68
Figure 3.23. Fuel sensitivity curve.	68
Figure 3.24. Comparison of exhaust gas emissions for different hydrogen flow rates.	71
Figure 3.25. Line diagram of exhaust heat recovery system (one heat exchanger).	72
Figure 3.26. Line diagram of exhaust heat recovery system (two heat exchangers).	73

List of Tables

Table 1.1. Generator Usage	1
Table 2.1. Percentage of waste heat.....	15
Table 2.2. Inlet/outlet temperatures with respect to the heat exchanger.....	18
Table 2.3. Quotation comparison.....	20
Table 2.4. DAQ channels.....	24
Table 2.5. Naming in the DAQ.....	25
Table 2.6. Component numbering	31
Table 2.7. Cost of the experimental system.....	42
Table 2.8. Estimated cost for the village recovery system	43
Table 3.1. Different cases with engine running on conventional diesel fuel.....	48
Table 3.2. Fluid side readings at different engine loads	50
Table 3.3. Load percentage against related kW	55
Table 3.4. Outlet temperature of 87°C on the fluid side of the heat exchanger.....	57
Table 3.5. Outlet temperature of 77°C on the fluid side of the heat exchanger.....	58
Table 3.6. Outlet temperature of 65°C on the fluid side of the heat exchanger.....	59
Table 3.7. pH value of exhaust condensate with the respective fuel burned.....	64
Table 3.8. Weight loss for C1010	65
Table 3.9. Estimated annual savings.....	67
Table 3.10. Emissions for diesel and synthetic fuel.....	69
Table 3.11. Exhaust property of conventional diesel fuel	70
Table 3.12. Exhaust property of synthetic fuel	70
Table 3.13. Comparison of exhaust property between conventional diesel fuel and synthetic fuel	70
Table 3.14. Heat in exhaust for different hydrogen flow rates.	71

Chapter 1 Introduction

In rural Alaska during 2007, approximately 180 villages consumed about 370,000,000 kWh [1] of electrical energy. During the process of producing electrical power, there is unused heat from the diesel engines. If the waste heat could be used, there would be a significant fuel savings. This project, which studied the selection of the most appropriate engine exhaust heat recovery application, is needed as part of village economic development.

There are many different heat recovery methods available for capturing engine waste heat, including thermal electric conversion; heat-to-power conversion (e.g., Sterling engines, Rankine cycle engines, gas turbines); direct heat application (e.g., space heating, waste water loop heating); heat for refrigeration and air conditioning; and heat for desalination. To optimize the benefit that heat recovery systems can bring to Alaskan villages, the engine performance characteristics and operational conditions that have important effects on the performance of heat recovery systems have to be understood. Important engine properties and operational conditions may include engine-generator load, engine fuel energy, soot produced by exhaust gas, and exhaust gas corrosivity. Engine load and fuel energy will affect the amount of heat that is recovered by the heat recovery system and the soot content in the exhaust. Corrosivity and soot content will affect the maintenance of the heat recovery system.

To understand the load condition of the village diesel generators, engine data sheets of annual generator usage were obtained from some of the Alaskan villages [2], including Ambler, Chevak, Noorvik, and Scammon Bay. These data show the load pattern of village electricity usage in June and December of 2002. Table 1.1 lists the month's load patterns according to the data sheets. The average load, based on this data, was about 65% of the engine rated load year-round. The load varied between 25% and 100% of the rated load.

Table 1.1. Generator Usage

Month	0% to 25% load	25% to 50% load	50% to 75% load	75% to 100% load
June	5%	34%	58%	3%
December	1%	4%	43%	52%

Based on engine specification sheets of similar diesel generators, a rough estimate of the fuel energy distribution is given in Figure 1.1. About half of the village generators have already been equipped with intercooler heat recovery systems, but intercooler heat recovery is not a part of this study. According to Figure 1.1, the heat energy contained in the exhaust was found to be 30% of the total fuel energy. If half of the heat contained in

the exhaust could be recovered for useful applications, the result would be a fuel savings of 15% in Alaskan village power generation.

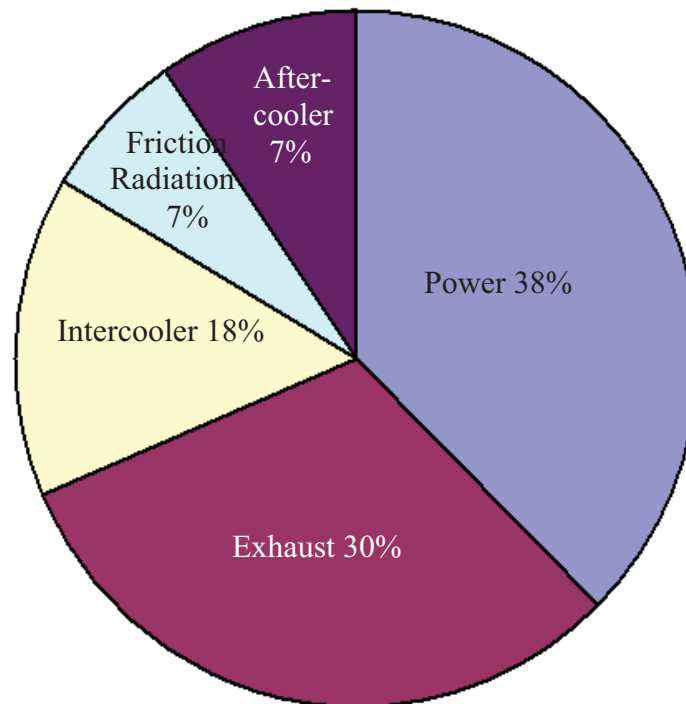


Figure 1.1. Energy distribution of a diesel generator.

The first task of this project studied the feasibility and economic effects of some of the most appropriate heat recovery applications for Alaskan village diesel generators. According to the cogeneration chapter of the “December 2002 Rural Alaska Energy Plan,” the proposed future cogeneration market segments included five different applications: community water loop temperature maintenance, public space heating using baseboard systems, public space heating using floor radiant systems, residential micro-cogeneration units, and school cogeneration units. The first three proposed applications are applicable to the existing village diesel generators, but the last two are not. Other heat recovery applications which were reviewed but rejected for further consideration included ice-making and refrigeration, desalination, thermal electricity generation, and steam engine electricity generation. Reasons for rejection included limited regions for adoption, limited economic benefit, limited amount of heat recoverable, high capital cost, and high frequency of maintenance requirement. This work was then converged to the feasibility study and economic analysis of an exhaust heat recovery system for heating.

Diesel engine exhaust contains soot and corrosive compounds which may cause performance deterioration, possibly resulting maintenance, and power outage problems with the heat recovery system and the engine exhaust system. No precise data describing the performance deterioration rate, corrosion rate, and maintenance frequency of exhaust heat recovery devices for general diesel engine applications were found in the literature.

According to a simplified experiment [3] of soot accumulation in a small bundle of tubes heated with combustion gas from controlled combustion, the deterioration rate reached the saturation point before the next maintenance was needed. Corrosion might not occur, provided that the exhaust temperature is kept appreciably higher than the dew point of sulfurous acid. Therefore, exhaust heat recovery systems may not cause serious problems that prevent it from being adopted for cogeneration. Soot- and corrosion-related feasibility is further discussed in later chapters of this report.

The objective of this experimental project was to conduct a feasibility and economic analysis of the heat recovery applications mentioned above. The experiment also included the design and installation of a heat recovery system for a given diesel generator for performance data collection, which then was used for analysis. The study results also provided a useful procedure which could be put into usable form for the end user, for designing an exhaust heat recovery system that would economically, reliably, and efficiently capture the unused heat from the village diesel engine generator sets. Considering the recent increase in fuel prices, this study is particularly important.

One recent consideration concerning fuels used in diesel engines has been introduced by the U.S. Environmental Protection Agency (EPA), which mandated a 95% reduction in the sulfur content of fuels used. Synthetic diesel matches the sulfur content requirement and may become an important fuel of the future. Since the fuel composition and combustion performance of synthetic fuels [4, 5] are known to be different from conventional diesel, the heat content and temperatures of the exhaust for these two fuels may be appreciably different, resulting in a difference in the amount of recoverable heat. An experiment to determine exhaust heat content and temperature (i.e., heat quality) was conducted on synthetic fuel and a conventional diesel. The results were then used to predict the advantages and disadvantages of these two fuels in exhaust heat recovery.

Recently, many individuals claimed the observation of significant engine efficiency improvement when using a hydrogen electrolyzer to generate a small amount of hydrogen and inject it into the intake manifold. A considerable change in engine efficiency may also mean a considerable change in exhaust property. This project conducted an experiment to measure the heat content and temperature of exhaust for conventional diesel with different levels of small amounts of hydrogen. The result was then used to estimate the effect of a small amount of hydrogen on exhaust heat recovery.

Since the performance and economic outcomes of installing an exhaust heat recovery system for heating are case-dependent and depend on many existing factors, a computer program which is able to help determine whether or not the installation is beneficial is important. The second task of this project was to develop a computer program for preliminary economic analysis of installing an exhaust heat recovery system in a village diesel generator set. The targeted users were the engineers and technicians of village power plants, who should be able to learn the program with a minimum amount of time and instruction. The program was developed on Virtual Basic for Application in Microsoft Excel, which is available on all personal computers. The program was designed to be user-friendly and able to accept different levels of input data (i.e., data obtained from measurements and manufacturers or data derived from analysis using

standard handbook procedures) of system and component properties, depending on the level of data available to the user. The program was also designed for continuing improvement and expansion, provided more design data and more effective methods become available.

Executive Summary

In rural Alaska, there are nearly 180 villages consuming more than 370,000 MWh of electrical energy annually from individual diesel generators. A similar amount of fuel energy is dissipated into the atmosphere from diesel exhaust. The purpose of this project was to evaluate the feasibility and economic impact of applying exhaust heat recovery on rural Alaska diesel generators. Two major tasks were included in this project. The first task was to conduct feasibility and economic analyses using the data obtained from a designed experiment. This task involved the selection of the best application of recoverable exhaust heat, design and fabricate an experiment setup, testing, and analysis. The second task was to develop a computer program for preliminary economic analysis of applying the selected exhaust heat recovery application to individual village diesel power generators.

Exhaust Heat Recovery System Design and Testing

Among several potential heat recovery applications (e.g. heating, electric power generation, desalination, and ice making), exhaust heat recovery for heating (EHRH) was selected for this project. The selection was based on need, availability, feasibility, and benefit that could be brought to rural Alaska.

An EHRH system was designed for a DD50 diesel engine located on UAF campus. The engine has a rated load of 125 kW and rated speed of 1200 rpm, is instrumented with a variety of sensors for engine performance monitoring, and is connected to a load bank for engine load control. The engine was not equipped with after treatment devices; therefore, the analysis results demonstrated the worst case scenario. The designed heat recovery system has 3 major parts, the exhaust to liquid heat exchanger for exhaust heat absorption, the unit heater for heat dissipation or heating load control, and the piping and control unit for temperatures and flow rate controls. Temperatures and flow rate controls made the system capable of simulating different heating methods at different loads for optimal heat absorption. The recommended working fluid was 40/60 mixture of Propylene glycol and water for cold weather in Alaska.

The designed heat recovery system was installed and instrumented. A National Instrument data acquisition system (DAQ) was used for experimental data collection and reduction and performance monitoring of the system and its components. Engine was running for 350 hours after installation. The system was operated under 25%, 50%, 75%, and 100% engine loads for three different heating operation conditions to simulate three different space heating methods possibly used in Alaskan villages. After the experimentation, the heat exchanger was dismantled for the observation and measurement of corrosion and soot accumulation for maintenance and feasibility study.

Engine performance and exhaust heat contents were also measured for two other fuels: the ultra-clean (synthetic) diesel and conventional diesel with complementary hydrogen (less than 1% by volume or 0.07% by mass). The purpose of the test was to evaluate the potential effects of different fuels on exhaust heat recovery performance.

Results derived from analysis of experimental data and observations on engine and heat recovery system performance led to the following findings. The performance of the exhaust heat exchanger was consistent and reliable. No noticeable difference was observed on engine performance before and after the installation of the heat recovery system. Corrosion and soot accumulation was not observed to be a problem in the laboratory test of 350 hours. For the 125 kW diesel generator used in this experiment, the rate of heat recovered from the exhaust was about 60 kW. Based on this heat recovery rate, the estimated payback time for a 100% use of recovered heat would be less than 3 years for a fuel price of \$3.5 per gallon (Village fuel price is considerably higher than that of cities) at an interest rate of 10% and an engine operation of 8 hours per day. Different types of fuels did not show noticeable effect on engine performance and exhaust heat content

An Economic Analysis Program for Exhaust Heat Recovery for Heating

Since the performance and economic outcomes of installing an EHRH system are case dependent and depend on many existing factors, a computer program, which is able to help determine whether or not the installation for a particular village diesel generator is beneficial, is important. The well known thermal science computation programs, which are not designed for economic analysis of EHRC problems in Rural Alaska, either not appropriate or not applicable, especially when the problems involve specific information about village infrastructure, power usage, heat usages, and local cost information.

The computer program developed for this task was based on the experience obtained from the first task of this project. The computer program is capable of doing preliminary design (if needed) and economic analysis for installing an exhaust heating system to any village diesel generators. This program was developed on Visual Basic for Application in Microsoft Excel, which is available on all personal computers. The targeted users of the program were engineers and/or technicians of the village power plants. The program was designed for user-friendly and being able to accept different levels of input, from measured data, manufactures' data, to data from analytical procedures, depending on the level of data available to the user.

The input of the computer program includes the power plant information, existing village heating system information, interest rate, and all other cost information. The output of the program includes predicted payback period and profits and also detailed information generated along the design and analysis process. The program can also provide a Microsoft Words document of all the significant data generated.

This program has been used to simulate the design and performance of the experiment conducted at UAF and to conduct the economic analysis based on data from simulation results. The results match well to that obtained using the experimental data. The program was also designed for continuation of improvement and expansion provided more design data and more effective analysis methods would become available. For example the program can be easily extended to economic analysis for other exhaust heat recovery applications (e.g. power, desalination) by adding into the computer program new subroutines of the desired applications.

Chapter 2 Experimental

2.1 Background

2.1.1 Introduction

The first task of this project included an experimental study of the feasibility and economic effects of exhaust heat recovery heating for Alaskan village diesel generators. This task involved the experimental procedure of design, procurement, installation, instrumentation, measurements, and data reduction. The first task also included the measurement of exhaust temperatures, flow rates, and emissions of an engine operated with conventional diesel, a synthetic fuel, and conventional diesel with different levels of a small amount of hydrogen. The measured data were used to estimate exhaust heat content and to evaluate the potential effects of different fuels on heat recovery performance. This project's second task was to develop a computer program for economic analysis of applying exhaust heat recovery to individual village diesel power plants. The second task did not involve an experiment.

2.1.2 Literature Review of Exhaust Heat Recovery

This subsection reviews the research that was being conducted in the field of recovery of rejected heat from diesel engines. During engine run time, there are different places in the engine's structure where significant amounts of heat are dissipated to the atmosphere. The rejected heat includes heat from the water jacket, the exhaust, and in more recent engines, the heat from the turbocharger aftercooler. This heat can be used for domestic or commercial purposes by using a recovery process, although this requires the addition of significant hardware which adds to the expense of the installation. In the past, fuel was cheap and it was very difficult to justify the cost of the heat recovery hardware. Furthermore, high sulfur fuel results in corrosive condensates, requiring either expensive alloys for heat recovery from exhaust systems or expensive replacements.

Previously, when the idea of heat recovery was not considered, the engine cooling system was used only for running the engines to prevent overheating. When fuel economy became important due to the energy crisis, especially in the early 1970s, different ways to recover an engine's unused heat for useful purposes became a practical research area. After the 1970s energy crisis eased, heat recovery research activities dropped accordingly, until the recent surge in fuel prices. From previous research, it was found that engine cooling systems and exhaust had abundant amounts of heat. The utilization of this energy would result in an increase in the efficiency of the system.

Experimental studies focused mainly on recovery of exhaust heat, which is one of the heat-carrying sources. The following sections provide the literature review for heat recovery from diesel engines.

Low-sulfur fuels: One recent consideration in fuels used in diesel engines has been the EPA-mandated reduction in sulfur content of fuels used for transportation. This reduction is anticipated to have several significant environmental benefits, including a direct reduction of sulfur oxides, a direct reduction in particulate matter (PM), and an

indirect reduction in other pollutants through the use of catalytic cleanup systems. For stationary diesel engine heat recovery systems, the reduction in sulfur and the reduction in PM mean that exhaust heat exchangers are likely to be more practical, as the exhaust will be less corrosive and form less soot, both of which have prevented economic heat recovery in the past.

Sulfur is an element that is naturally present in crude oil. Conventional diesel sold for transportation in the United States after 2001 contains a maximum of 500 ppm of sulfur [4,5]. This sulfur gets oxidized to sulfur dioxide (SO_2) or sulfur trioxide (SO_3) after combustion. These sulfur oxides play an important role in the corrosion process. The sulfur oxides dissolve in moisture to form sulfurous acid (H_2SO_3) or sulfuric acid vapor (H_2SO_4) [6].

The dew point of exhaust water vapor (37.78°C to 65.56°C) is considerably below typical exhaust temperatures. However, in boiler conditions, the formation of acid occurs at the dew point (115.56°C to 137.78°C), which is more likely to occur in combustion exhaust systems, especially when exhaust heat recovery is applied. The formation of these acids depends on the amount of air, moisture, and sulfur content [6].

The EPA proposed to decrease the sulfur content in the on-road diesel fuels to 15 ppm by 2006. These standards are scheduled to be extended to 2011 for off-road engines. One way of reducing sulfur is to use synthetic diesel (ULSD) created by Fischer–Tropsch, which has near-zero sulfur [4, 7]. This would largely reduce the problem of corrosion due to acids.

Soot formation: The major pollutants of fuel combustion are considered to be nitrogen oxides (NO_x) and PM. Particulate matter is a result of unburned hydrocarbons due to incomplete combustion, and is a major concern because it is a health hazard and impacts visibility. For our case, only PM was considered, as it is the source for soot in the heat exchanger. Soot is defined as a dark powdery deposit of unburned fuel residue mainly consisting of carbon. Significant accumulations of soot have a direct negative impact on the ability of a heat exchanger to extract usable heat from the exhaust.

The composition of PM by mass is as follows [8]:

Metal – 1.2%
Hydrogen – 2.6%
Nitrogen – 0.5%
Oxygen – 4.9%
Sulfur – 2.5%
Carbon – 88%

The soluble organic fraction in PM of a diesel engine varies from 5% to 40% by mass. The production of PM depends on the aromatic levels of the fuel. C_2 reacts with C_4 to generate aromatic structure [9], which comprises monocyclic and polycyclic aromatic hydrocarbons (PAH). Nanoparticles, which are formed during the engine cycle of the gas

phase PAH, grow to 2 nm and continue until growth vanishes. These smaller particles coagulate to 10 nm due to van der Waals forces [8].

Most soot ranges from 5 nm to 30 nm in diameter. Laser-induced incandescence (LII) was one of the techniques used to find particulate matter measurements. Primary soot particles (20 nm to 30 nm) absorb light radiation both in ultraviolet and visible regions.

Many experiments have been conducted to illustrate soot growth and coagulation. According to a study by Mathis, the primary soot particles of a diesel engine range from 17.5 nm to 32.5 nm, as determined by transmission electron microscopy (TEM) measurements [10]. This work demonstrated that primary soot particle diameter decreased from 25.9 nm to 17.5 nm at low loads and decreased from 28.4 nm to 21.6 nm at high loads during the start of ignition. Also noted was an effect due to injection pressure, as the primary soot particle diameter was reduced due to increase in injection pressure from 500 to 1100 bar at low loads. There was a small decrease in diameter of soot particle at high load when injection pressure was changed from 800 to 1400 bar.

In another study by Kitsopanidis in 2006, a rapid compression machine was adapted to replicate a diesel engine in which a line-of-sight (LOS) absorption method was used [11] to study soot growth. The volume concentration of soot grew depending on the fuel concentration of the compressed charge over a period of time, but an unexplained initial exponential growth was observed irrespective of the fuel concentrations.

Regarding the soot accumulation inside heat exchangers, a simulation experiment was conducted [3]. The experiment controlled the flow rate and pressure of combustion gas, which crossed a bundle of a small number of cooling pipes. The experiment was operated for an extended time for each of the combinations of selected flow rates and pressures. Soot accumulations were measured along with the experiment. According to the experiment results, the soot that accumulated on finned tubes for each case seemed to approach its plateau within a relatively short period of time.

Heat recovery applications: The idea of using waste heat from an engine to heat a space is not unique to this project, but there are fewer applications of heat recovery from diesel exhaust. During our literature search, we came across various projects that involved heat recovery in different aspects, but could not find any documents that are directly related to our project. Some of the heat recovery projects that were similar to our project were documented as case studies. Some of the most useful information related to diesel exhaust heat recovery in Alaska was obtained through personal communication with engineers working in Alaska.

Heat recovery for Eagle Community School in Eagle, Alaska: In the late 1970s a recovery system was built for the Eagle Community School in Eagle, Alaska, by Summit Logistics, a company owned by Dave Cramer. According to Mr. Cramer, the recovery of heat was done on a 350 kW Cummins diesel engine-generator set. The recovered heat was used to heat a water heating system using a gas-to-gas heat exchanger. "There was an awful effect due to soot on the heat exchanger components and also with the engine," said Mr. Cramer. He recollected that the engine manufacturer did

not recommend such systems. The heat exchanger was installed over the engine exhaust system, which was not appropriate for the given task. The system had an effect on the engine due to the increase in carbon deposits. Though the system was meant to work for 10 years, after a few hundred hours of running, it was observed that the recovery system did not work to Mr. Cramer's expectations, and it had to be removed within the first year of its installation.

"A constant temperature could not be maintained with the variation of loads," said Dave Cramer. The system required constant monitoring and maintenance four times a year to remove soot deposits. Lack of maintenance and observation might be a cause for the improper operation. Mr. Cramer stated that, for an engineer, the loads on the engine cannot be predicted on practical grounds. He estimated the entire system, with copper tubing of 2" to 1½", cost him about \$30K to \$40K.

Industrial waste heat recovery: During the 1970s, the Arab oil shocks convinced many energy users to attempt to reduce their energy consumption. Unfortunately, little effort was made in the recovery of waste heat during the initial stages, but after a few years, this idea was tested. A demonstration project was undertaken in 1976 by American Standard Corporation.

The demonstration project involved industrial waste heat recovery at a plant located in Louisville, Kentucky, that produced thermal energy. The combustion air was preheated electrically to 537.78°C for the coke-fired cupolas. Exhaust gases from iron foundry cupolas was close to 150,000 pounds per hour at a temperature of 760°C. A comprehensive study was performed in close cooperation with the staff of American Standard Corporation and with international experts. Economical and technical studies of heat recovery systems were made, and problems based on structure, space requirements, etc., were given close attention [12].

The new system that was installed included a gas-to-air heat exchanger to preheat the air to 537°C. Flue gas at 760°C was controlled to 676.67°C by a cooling tower to protect equipment and assure stable performance and efficient gas filtering. A wise decision to include air-operated soot blowers with the heat exchanger to remove dirty flue gases was considered. The gas and air tubes were filtered with damper valves to permit flexibility to the entire system.

Multiplying this experience by 10,000 industrial plants leads to an equivalent energy savings of 390,000 MBTU or 67,000 barrels of domestic heating oil for each hour.

Recovery of heat from the exhaust gas of a diesel engine: A large number of projects recover heat from natural gas-fired systems that would reduce carbon dioxide and nitrous oxide emissions, reducing the greenhouse effect. A recovery system described by Verneau was built in a Lucciana, Corsica, power plant on an 11 MW SEMT 18PC 3 diesel engine (much larger than the diesel engines used in Alaskan villages). The thermal power contained in the exhaust was of the same order as the shaft power (38%). The exhaust temperature was 390°C, but could not be cooled below 170°C because of corrosion effects. In this test, the experiments were conducted on a steam cycle and

organic fluid cycle, and the results were compared. Verneau states that better cycle and better expansion led to a net efficiency of 0.21 and 0.15 for organic fluid and steam. The cycle that was selected is shown in Figure 2.1.

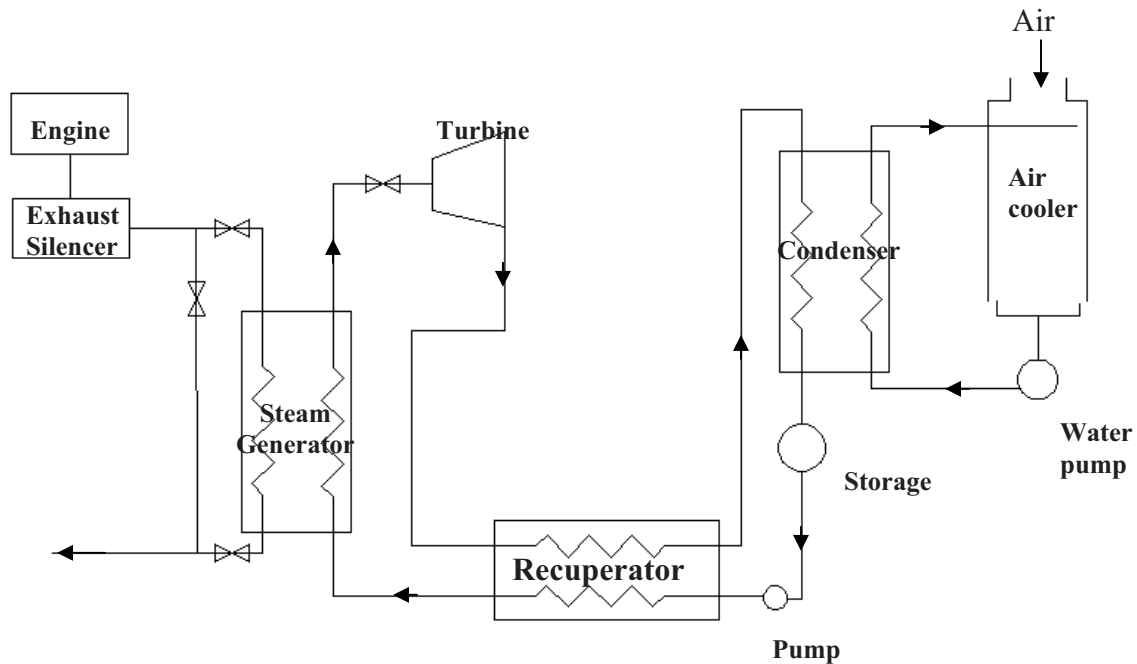


Figure 2.1. Schematic diagram.

The organic fluid required a larger heat exchange surface area and higher temperature, which was done by a recuperator. The recuperator increased the temperature of liquid going into the evaporator that avoided corrosion. The working fluid was a mixture of trifluoroethanol and water. The tests showed some corrosion on carbon steel and slightly alloyed steels [13]. However, the major disadvantage of these cycles is the high cost of both the recuperators and the turbines.

Exhaust heat recovery from midsize diesel engines for power generation:

Due to the recent surge in fuel prices, some research activities in exhaust heat recovery for power generation have been conducted with midsize diesel engines that are similar in size to most of the engines used in Alaskan villages. Most of the research activity in this area has focused on truck engines [14, 15, 16], and is still in the early stages. In general, the efficiencies of the prototypes developed are still much lower than exhaust heat recovery for heating applications. It is expected that the efficiency of exhaust for power will be improved and become competitive in the future.

Thermoelectric generators based on heat recovery: Exhaust heat can be used to produce electric power by means of thermoelectric generators (TEG). Several TEG were designed to fit the temperatures at various parts of the exhaust system [17, 18, 19]. TEG is easy to install and have few maintenance problems. There are no moving parts, so

there is less noise. Though the idea is relevant, the efficiency of the TEG is considered to be meager, peaking at about 4% under ideal conditions, and often much lower.

2.1.3 Heat Exchanger Basics

The inlet and outlet temperatures on the hot and cold side of a heat exchanger can be used to design a heat exchanger. The basic equations involved for a heat exchanger design are

$$Q = U_oAF(LMTD) \quad (2.1)$$

where

\dot{Q} = Heat transfer rate

U_o = Overall heat transfer coefficient

A = Heat transfer area

$LMTD$ = Logarithmic mean temperature difference

F = Correction factor

The size of a heat exchanger can be measured by means of number of transfer units (NTU). The equation for NTU is given in Equation 2.2.

$$NTU = \frac{AU}{\dot{C}} \quad (2.2)$$

where

U = Local overall heat transfer coefficient

A = Heat transfer area

\dot{C} = Product of mass flow rate and the coefficient of specific heat

In the absence of phase change, the NTU of a heat exchanger determines the performance in terms of effectiveness (E). Effectiveness is given by the ratio of actual heat transfer rate to the maximum heat transfer rate. The equation for effectiveness is given in Equation 2.3.

$$E = \frac{\dot{Q}}{\dot{Q}_{\max}} \quad (2.3)$$

where

\dot{Q} = Actual heat transfer rate

\dot{Q}_{\max} = Maximum heat transfer rate

There are many types of heat exchangers based upon their differences in temperature range, performance ratios, type of heat exchange carried out, efficiency, and working

condition [21, 22]. Based on ratio of heat transfer area and dimension of heat exchanger, heat exchangers can be categorized into shell and tube type and compact type. The compact type may include plate fin heat exchangers, tube fin heat exchangers, plate type heat exchangers, printed circuit heat exchangers, recuperators, and regenerators.

The main problems commonly faced when using compact heat exchangers are related to fouling due to accumulated solid materials or property changes on the walls of the heat exchanger. In our case, the fouling was high due to exhaust gases. Chemical cleaning, thermal baking and subsequent rising and wise design in maintenance and operation methods may help resolve these problems.

The following are different fouling mechanisms:

1. Crystallization/precipitation
2. Particulates
3. Chemical reactions
4. Corrosion
5. Biological effects
6. Freezing

The following are effects of fouling:

1. Increase in the capital costs
2. Increase in the maintenance costs
3. Loss of production
4. Increase in the energy losses

Compact heat exchangers are mostly the gas-to-gas type. Gas is harder to control than liquid. At the beginning of the project, most of the suppliers that we contacted provided compact heat exchangers, but either the temperature range or the material of construction did not match our project's needs. After further review and a literature search, it seemed that shell and tube type heat exchangers would be a better choice for this project.

Shell and tube heat exchangers are only limited by the materials of construction and have the additional advantage of being designed for special operating conditions, such as vibrations, heavy fouling, highly viscous fluids, erosion, corrosion, toxicity, radioactivity, and multicomponent mixtures. Shell and tube heat exchangers can be made from metal as well as non-metal, and their surface areas range from as little as 0.1 to 100,000 m². They have less surface area per unit volume than compact heat exchangers [21].

2.1.4 Economic Study

Heat recovery systems are not typically used in diesel engine generators due to cost issues. If the cost of purchasing a heat exchanger and installing it is high and the cost of diesel fuel is low, most users will elect to vent the hot exhaust and purchase additional fuel for the required heat loads. Only when the cost of fuel is high compared with the capital cost of heat recovery installation will this option make sense. The economic analysis is directly related to the cost of fuel and the cost of capital as given by the interest rate. These two considerations are discussed below.

Cost of fuel: In Alaska, small rural utilities have cooperated to purchase fuel in bulk quantities from the same vendor in order to reduce fuel costs. The fuel price depends on the crude oil cost, cost at the refinery, and transportation cost. Among these organizations were Alaska Native Industries Cooperative Association (ANICA) and Alaska Village Electric Cooperative (AVEC). ANICA purchases 2 to 3 million gallons of fuel each year to serve 25 communities. AVEC purchases about 6 million gallons of fuel each year to operate electric utilities for 51 rural villages [23].

Discounts of about 15% are available for a purchase of 100,000 gallons of fuel. Further reductions are given for purchases of more than 100,000 gallons of fuel. A reduction of 10 ¢/gal would result in \$2000 to \$4000 in fuel cost savings for a utility that consumes 100,000 gallons of fuel [23].

Interest rates: The interest rate determines the payback amount for money borrowed. Depending on the source of funds, the interest rates may vary from 0% to 12%. The 0% APR is in the case of grants allotted by the organizations that require repayment. The payback method differs from company to company. There are two methods of returning the borrowed money: The first method includes equal amounts to be paid each year. According to this method, the total amount will be calculated for a span of years with the interest rate, which needs to be repaid in equal amounts in equal intervals of time. In the second method, at a constant interest rate, the principle amount differs. The principle amount differs depending on the amount paid each year. The amount repaid by the end of each year will be deducted from the initial borrowed money, and the interest rate accounts for the current principle amount to be paid each year [25].

2.1.5 Effect of Fuel Type on Heat Recovery

Exhaust flow rate, composition, and temperature may affect the heat recovery system design and the amount of heat recoverable. In comparison with the other two properties, the effect of exhaust composition may be less important due to the large air/fuel ratio for diesel engine combustion. This part of the project was to measure the exhaust properties and to estimate the heat contents and heat qualities (i.e., temperatures) of exhausts obtained from diesel engine combustion of three different types of fuel: a synthetic fuel, the conventional diesel, and the conventional diesel with different levels of a small amount of hydrogen. The results were then used to predict the potential difference between the exhausts of the three types of fuel.

2.2 Design of an Exhaust Heat Recovery System

2.2.1 Introduction

In most parts of rural Alaska, diesel generators operate year-round to produce power to supply village residents and remote mining sites with electrical power. The power consumption determines the load pattern on the diesel engines. In most villages, the load in summer is less compared with that in winter due to the decreased demand for lighting and heating during the warm, bright summer months. In nearly all locations, heat was

unused and rejected to the atmosphere. The percentage of fuel heat left unused from the engine is shown in Table 2.1.

Table 2.1. Percentage of waste heat

Location of recoverable heat	Percentage of fuel energy
Exhaust	30
Turbocharged air	7
Jacket water	18

The average consumption of energy in rural Alaskan households is detailed in Figure 2.2.

	Rural Average	Anchorage	Fairbanks	Juneau
Median Household Income (MHI)	\$40,380 ¹⁵	\$55,546	\$40,577	\$62,034
Annual Electric Consumption	5040 kWh	7782 kWh	9048 kWh	10,428 kWh
Average Price ¹⁶ (After PCE)	\$0.20/kWh	\$0.095/kWh	\$0.089/kWh	\$0.102/kWh
Annual Amount	\$1080	\$739	\$805	\$1064
Electricity as Pct of MHI	2.7%	1.3%	2.0%	1.7%
Space Heating Consumption	700 gallons per year	2100 CCF per year	1500 gallons per year	1000 gallons per year
Average Price	\$2.00 per gallon ¹⁷	\$0.40 per CCF	\$0.75 per gallon	\$0.79 per gallon
Annual Amount	\$1400	\$890 ¹⁸	\$1125	\$790
Heating Consumption as Pct of MHI	3.5%	1.6%	2.8%	1.3%
Electric + Heating Consumption as Pct of MHI	6.2%	2.9%	4.8%	3.0%

Figure 2.2. Alaskan household energy consumption [24].

If this heat could be applied to useful applications such as heating, a savings in fuel consumption might result. Since it is difficult and expensive to move heat, one major issue is the need to have a heat sink close to the diesel generator. While most generators are located as far as possible from buildings for noise and emissions reasons, the recent spike in diesel fuel price means that the economics of these systems are changing.

The goal of this project was to design and test a system to utilize the waste heat from a small diesel generator through a recovery process that would be economical and cost efficient for Alaskan villages. A heat recovery system was designed and fabricated to implement the selected heat recovery application and determine the feasibility and

economic effect. To design and test the heat recovery application, a Detroit Diesel Series 50 engine with a 125 kW generator operated at 1200 rpm was used. The details of this approach and the design procedures are discussed in the following sections.

2.2.2 Selection of Waste Heat

The amount of heat present in the exhaust, the turbocharged air, and the jacket water are presented in Table 2.1. As seen in the table, the jacket water and turbocharged air have lower energy than the exhaust, which indicates that the exhaust waste heat is more prominent than the jacket water and the turbocharged air. The following are other reasons behind the selection of exhaust waste heat for this project:

1. Many of the diesel generators were already equipped with jacket water recovery systems, and recovery of this energy is well understood.
2. The temperature of the exhaust was much higher than the turbocharged air, while the mass flow was nearly the same. The heat recovery rate from the exhaust was also expected to be higher.
3. The introduction of new low sulfur fuels, which result in lower corrosivity and lower particulate matter generation, meant a reduction in the major technical barriers to heat recovery from the exhaust.
4. The recent increase in the cost of crude oil resulted in higher diesel and heating oil prices, making heat recovery more economically attractive.
5. A reduction in greenhouse gases would result from a reduction in the consumption of diesel fuel.

2.2.3 Selection of Heat Recovery Application

Several heat recovery applications had the potential to be economical and feasible for Alaskan villages, among which were space and water heating, desalination, ice making, and electric power generation. However, desalination does not appear to be locally useful. According to the Alaska Department of Environmental Conservation in March 2005 [29], the mineral content of groundwater for most Alaskan villages is well within acceptable ranges. Only a few villages in northern Alaska require purification of surface water for drinking, where the permafrost is very deep. Electric power generated from waste heat appears attractive, as it is a convenient form of energy. It was not selected, however, because of its low heat recovery rate—about 6% of fuel savings out of 30% of fuel energy contained in the exhaust—and because it is expensive. Ice making has been demonstrated in Kotzebue, but unless there is a large commercial user for ice in the summer (such as local fishing industry), the costs are not justified. However, heat is almost always needed in Alaska, so heating was considered to serve the purpose in this project. The recovered heat can be used either for space heating, domestic hot water, or warming municipal water supplies to prevent freezing.

2.2.4 Experimental Site

This experiment was conducted at the Arctic Energy Technology Development Laboratory at the University of Alaska Fairbanks, using a Detroit diesel engine-generator set. The rated speed of the generator is 1200 rpm with a rated electrical power of 125 kW. The generator was connected to an external load bank from Load Tech with a power of 250 kW. The engine has a rated speed of 1800 rpm with a power of 235 kW, so the engine was down rated and connected to the generator. The diesel generator set was placed inside an International Organization for Standardization (ISO) container with the load bank on the outside of the ISO container.

This engine and generator set were used for other experiments, including emissions experiments conducted in 2004 and 2005. The setup is discussed in more detail in Telang's master's thesis [4].

For the experiment's heat recovery system design and installation, the experimental site was considered a convenient substitute for a potential heat recovery application that mimics the diesel generators in rural Alaska. Heat was recovered from the exhaust, measured, and then rejected to the atmosphere through a dump load.

2.2.5 Heat Recovery System Design

The design of the heat recovery system involved determining the different functional parameters (e.g., exhaust backpressure, exhaust flow rate, total pressure drop, and temperatures) that needed to be considered. The parameters and the related components are discussed in detail below.

Heat exchanger: The exhaust heat exchanger was the first element to be considered in the design process. The specification sheet of our experimental engine was the primary information considered in coordination with the village data to get a brief idea for the selection of a heat exchanger. There were a few set points for the heat exchanger selection. Those set points include the following:

1. Amount of exhaust heat available
2. Corrosion of the exhaust system
3. Maximum exhaust backpressure permissible by engine
4. Dimensional constraints
5. Weight constraints
6. Maintainability

Given that electrical loads vary, the amount of recoverable heat also varies. In order to select a heat exchanger suitable for fluctuating exhaust heat energy, the heat exchanger needed to have some operational parameters adjustable with the varying engine load conditions and possibly with the heat requirements. Based on this consideration, the heat exchanger was designed for engine exhaust at engine-rated load conditions. At partial engine load conditions, the heat recovery system should be adjustable to the heat requirements. A major design concern for our work was the availability of space. As well, the following parameters needed attention:

1. Flow rate of the exhaust
2. Required heating temperatures
3. Exhaust temperature differential
4. Coolant temperature range

Another important consideration was atmospheric effect. As this project was designed for use in Alaska, the maximum ambient temperature differential in Alaska was considered. Any equipment selected must be capable of functioning in a wide range of ambient conditions.

For this project's design, a gas-to-liquid type heat exchanger was selected. The main reason behind this choice was to permit easy escape of the exhaust gases after passing through the heat exchanger without affecting engine exhaust backpressure. The heat exchanger acts as a muffler also. The design allowed the exhaust temperature to be above the water vapor dew point to reduce exhaust condensation and acid formation. (The issue of acid dew point was not discovered until the project was well underway, but fortunately, we seem to have avoided it.)

A shell and tube type heat exchanger was selected. In this design, exhaust gas passes through the shell, and liquid passes through the core side, that is, through the inner pipes. This design enables better exhaust escape to the atmosphere in a single pass without building much backpressure. This type of heat exchanger provides a relatively large area for heat transfer. For maintenance purposes, the liquid on the tube side and accessibility to remove the core were specified.

The parametric inputs considered for the heat exchanger design were

1. temperatures
2. heat transfer surface area
3. corrosion resistance

Temperature: Inlet and outlet temperatures of the liquid (Table 2.2) were based on a safety margin depending on the load conditions and weather conditions for convective space heating. The inlet temperature was the exhaust temperature of the engine at full load. The outlet temperature was selected based on the trade-off between cost and heat recovery. The possible reason for corrosive exhaust condensate formation was also considered for the outlet temperature selection; that is, the exhaust outlet temperature should be above the water dew point with a safety margin. (The acid dew point was not considered, but the temperatures seem fine for that issue also.) The liquid side temperatures were selected based on the feedwater temperature of 65°C, typical of boilers used for baseboard heating. Thus, a temperature of 77°C would be adequate for preheating the boiler feedwater.

Table 2.2. Inlet/outlet temperatures with respect to the heat exchanger

Gas/liquid	Inlet temperature (°C)	Outlet temperature (°C)
Exhaust	540	177
Liquid	77	87

Heat transfer surface area: Heat transfer surface area directly affects the heat exchange rate. The number of passes, the tube diameter, and the tube pattern affect the heat transfer surface area. The total area is constrained by the overall dimensions allowed for the heat exchanger.

The predesign calculation for the heat exchanger consisted of the overall heat transfer coefficient and the log mean temperature difference (LMTD). The correction factor was considered to be 1. The surface area required was calculated to be 8 m² (90.4 ft²) using the procedure given in [19]. The effectiveness was calculated to be 80%.

Based on the required temperature and surface area from the preliminary design calculations of the heat exchanger, 25 heat exchanger suppliers were contacted. Most of the heat exchanger manufacturers were unable to respond to our heat exchanger requirements for this project. The reasons were as follows:

1. High temperature on the gas side
2. Type of heat exchanger needed (shell and tube type)
3. Material of construction
4. Ease of maintenance

Two of the manufacturers were willing to fabricate the type of heat exchanger similar to the one that we needed in our project and they provided bids, summarized in Table 2.3.

Table 2.3. Quotation comparison

	Quotation 1	Quotation 2
Shell side	Gas	Liquid
Tube side	Liquid	Gas
Gas pressure drop	0.31 PSI	PSI
Maintenance	Removable core, 1 in. gap and straight tubes	U-tube for gas
Heat transfer area	87 ft ²	30 ft ²
Size	51 in. x 28 in. x 28 in. (with detailed drawings)	Shell Φ 6.625 in., Tube:72 in. (no details)
Weight	725 lb	350 lb
Material of construction	Tube: SS fin tube Shell: SS inner wall	Tube: Plain SS 316 Shell: CS
Insulation	Integrated insulation	No insulation included
Cost (\$)	9,800	7,979

After reviewing both of the quotations and designs, Quotation 1 was considered to be a better option for this project. The following were the main reasons for this choice:

1. Gas on the shell side and liquid on the tube side
2. Stainless steel material of construction
3. Less pressure drop
4. Inbuilt insulation
5. Easy maintenance due to straight tube structure

Even though the cost of Quotation 2 was less than Quotation 1, Quotation 1 was selected due to the insulation. Weight was not an important issue in this case.

Selection of unit heater: In any real system, the heat that is recovered from the heat exchanger needs to be used for a useful purpose. In order to replicate a real application, the recovered heat for space heating was simulated by the dispatched heat through the unit heater with controlled inlet and outlet temperatures and flow rate.

A unit heater is a simple radiator with an associated fan that dissipates the heat to the atmosphere; one can be purchased off the shelf. For this experimental setup, the heat recovered from the exhaust was dissipated to the atmosphere under different load conditions. The designed maximum capacity of heat recovered by the Cain Industries heat exchanger was 290,000 Btu/hr. The unit heater must be able to remove the same amount of heat, thus a unit heater (model S) built by Trane was selected.

Control system: The control system in this experiment used copper tubing that connected the heat exchanger to the unit heater in a closed loop. The components in the system contributed to desired functionality of the entire system. A three-way mixing valve was present in the control system connecting the bypass and the unit heater outlet pipe. The valve was controlled by a nickel immersion sensor and universal controller. The manual set temperatures in the universal controller helped in controlling the valve opening in the mixing valve in coordination with the nickel sensor to attain the required temperatures on the coolant inlet side of the heat exchanger. The major components considered for our heat recovery system were heat exchanger, pump, three-way valve, flow meter, and unit heater. The heat exchanger acted as a heat source to capture heat from the exhaust, while the unit heater acted as a heat sink to simulate the heat flow. The heat exchanger and the unit heater were connected in a closed loop. The purpose of the piping system was to transport the working fluid between the heat source (heat exchanger) and the heat sink (unit heater) to control the heat desired for practical applications in rural Alaska. The piping system needs to be operated in such a way that the inlet of the heat exchanger can be maintained at specific temperatures at variable load conditions. To obtain those temperatures, a three-way mixing valve with a nickel sensor was used.

The pipe design was iterated many times due to the unexpected real sizes of the components and space availability for system installation. The ISO container was preoccupied by the Detroit diesel engine-generator set and the day tanks. There was very limited space for the construction of the pipe system. This caused major changes in the preliminary pipe design. The total pressure drop of 10 psi in the pipe system remained almost the same after the changes in the design. The space that was allocated for building the control system inside the ISO container is shown in Figure 2.3.

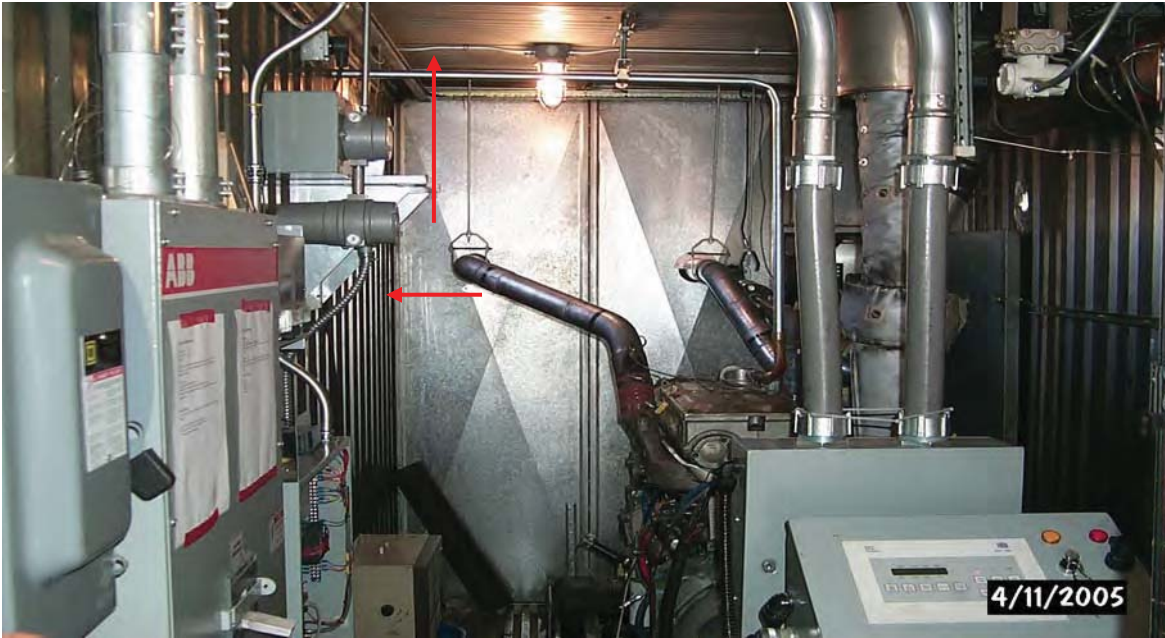


Figure 2.3. Space allocated for the control system inside the ISO container.

The final control system design is shown in Figure 2.4. A detailed description of the entire control system is discussed in Section 2.3.

Coolant side pressure drop calculations and pump selection: The pressure drop in the copper tubing decides the pump size. Pressure drop was estimated based on a procedure given in the ASHRAE handbook [20], which involved calculating the preliminary pressure drop. The total pressure drop was calculated to be 10 psi.

The pump was selected based on the calculated total pressure drop in the copper tubing with all components installed. The flow rate was taken from the selected heat exchanger's specifications. Figure 2.5 shows the pump curve used for selecting the pump. A margin of 5 gpm was added to the original flow rate for safety purposes. The calculated pressure drop was 23 ft of water. These two values correspond to a point that was marked in the graph. The graph shows a 1/3 HP pump that was suitable for our system.

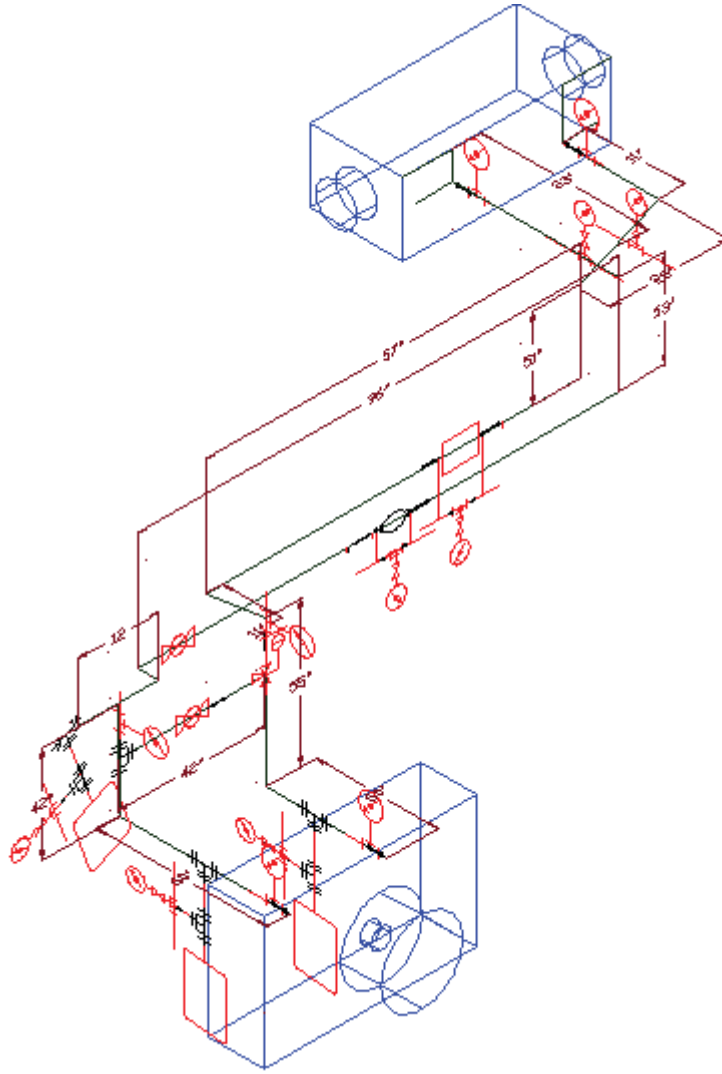


Figure 2.4. Final design.

Data acquisition (DAQ) system: A DAQ system was used to document the experimental readings. The different channels in the DAQ system are shown in Table 2.4. SCXI 1102 was used for all the thermocouples in the control system, and SCXI 1120 was used for the flow meter in the control system. The block diagram of all the channels to the DAQ system is shown in Figure 2.6. The naming is listed in Table 2.5.

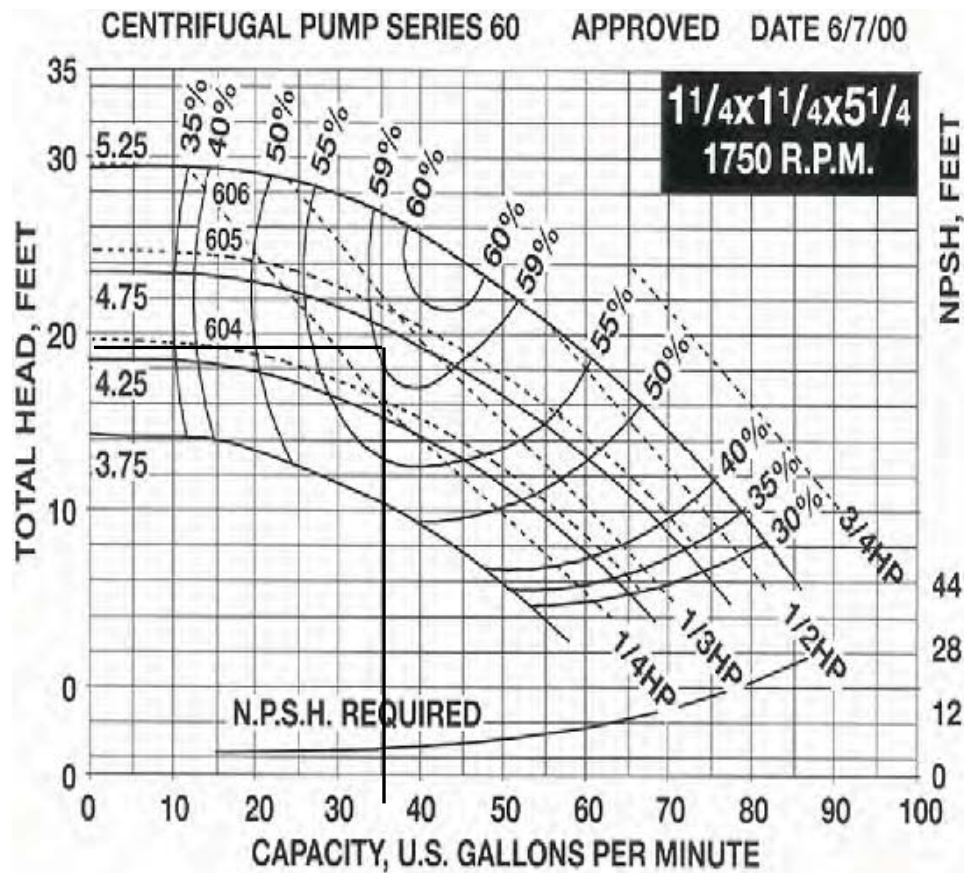


Figure 2.5. Owner's manual – Bell and Gossett.

Table 2.4. DAQ channels

Slot	Channel type	Purpose of the channel
1		- Empty -
2		- Empty -
3	SCXI 1120	8-channel isolation amplifier
4	SCXI 1180	Feed-through panel
5	SCXI 1120	8-channel isolation amplifier
6		- Empty -
7	SCXI 1120	8-channel isolation amplifier
8	SCXI 1121	4-channel isolation w/excitation
9		- Empty -
10		- Empty -
11	SCXI 1102	32-channel thermocouple amplifier - heat recovery
12	SCXI 1102	32-channel thermocouple amplifier

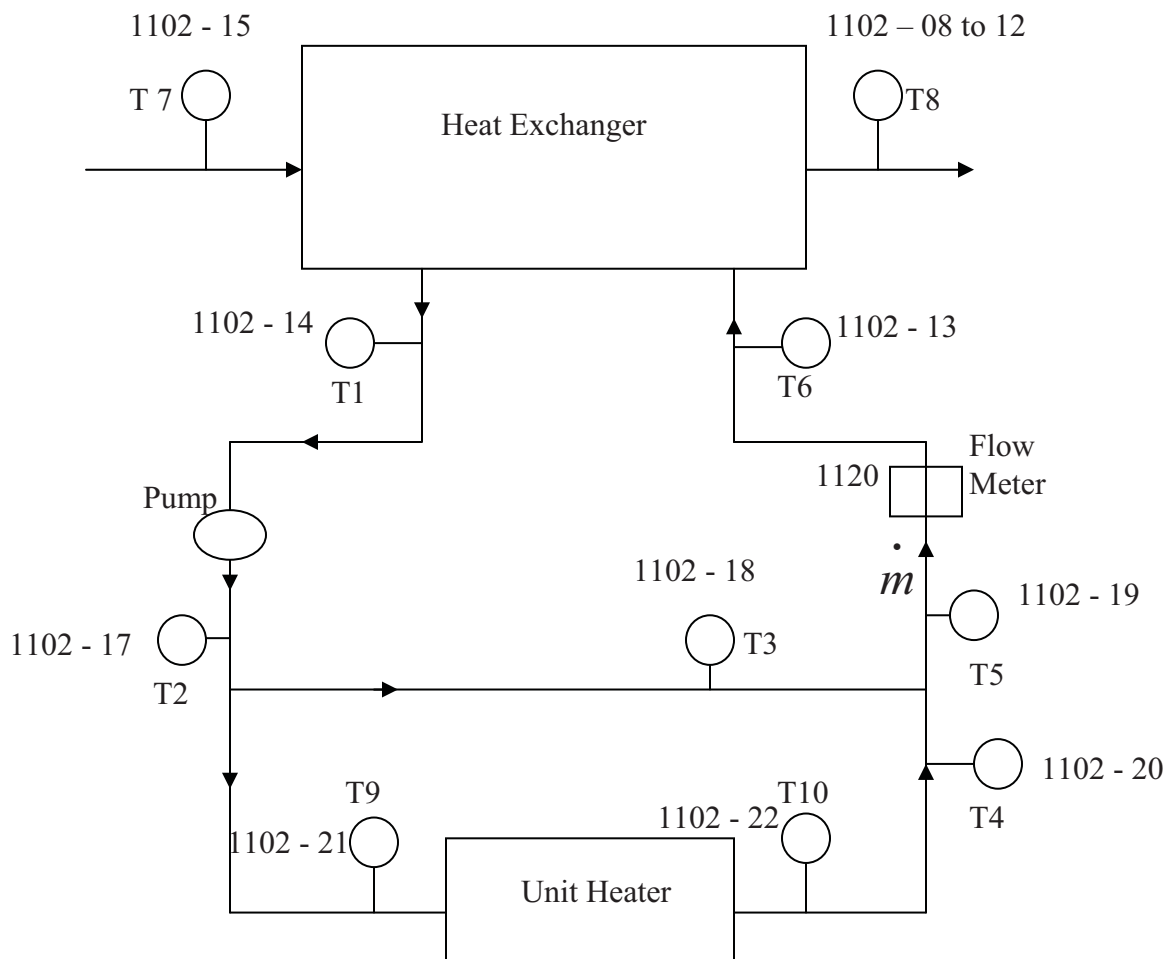


Figure 2.6. Block diagram showing the DAQ channels.

Table 2.5. Naming in the DAQ

Slot in SCXI 1102	Name in DAQ
8 to 12	Exhaust outlet temperature (T8)
13	Heat exchanger inlet temperature (T1)
14	Heat exchanger outlet temperature (T6)
15	Exhaust inlet temperature (T7)
17	Before bypass temperature (T2)
18	Bypass temperature (T3)
19	After 3-way valve temperature (T5)
20	Before 3-way valve temperature (T4)
21	Unit heater inlet temperature (T9)
22	Unit heater outlet temperature (T10)
SCXI 1120	Mass flow meter

2.3 Installation and Instrumentation of the Heat Recovery System

2.3.1 Introduction

This section of the report discusses installation, instrumentation, and calibration of different elements in the heat recovery system. The entire system can be divided into three sections: heat exchanger, unit heater, and control system.

The selected heat exchanger has gas on the shell side and liquid on the tube side, and its physical dimensions are 51 in. x 18 in. x 23 in. (LxWxH), with a heat transfer surface area of 87 ft². The heat exchanger weighs about 1000 lb and has 4 in. of inbuilt insulation.

The entire control system was designed to fit the ISO container design in this experimental project. The main aspect that needed to be considered during the heat recovery system design was our space allocation. The ISO container had two regions: (1) the water jacket radiator and (2) the engine, generator, day tanks, control unit, and DAQ. When the engine was running, the temperature in the engine section was maintained well above zero due to the heat radiated by the engine. The instruments and the engine needed to stay warm for normal operation, while the radiator section needed to be at a lower temperature, since the inlet manifold air temperature should be below 40°C.

For the convenience of connecting the heat exchanger to the exhaust pipe and because hot gases prefer to rise, the heat exchanger was installed on top of the ISO container. The size of the unit heater and the improved efficiency of using normal ambient air determined its installation outside the ISO container. For the sake of convenience, the unit heater was also installed on the west wall next to the control system, which was constructed inside the ISO container. Most of the control system needed to be maintained at room temperature for the specified operation of various sensors. For this project we used copper tubing, as it was (relatively) easy to make modifications when needed and is inexpensive.

The initial AutoCAD drawing of the whole system is shown in Figure 2.7. Details of the heat recovery system were split into three sections, based on their location. Figure 2.8 is section 1 showing the heat exchanger and its inlet/outlet pipe connections; Figure 2.9 is section 2, which includes major flow control elements; and Figure 2.10 is section 3, which shows the unit heater and its inlet/outlet pipe connections. Components of the control system are designated by numbers and are described in Table 2.6.

There were significant changes in the design of the control system due to space considerations. The final control system of this project is shown in Figures 2.8, 2.9, and 2.10, with brief descriptions added.

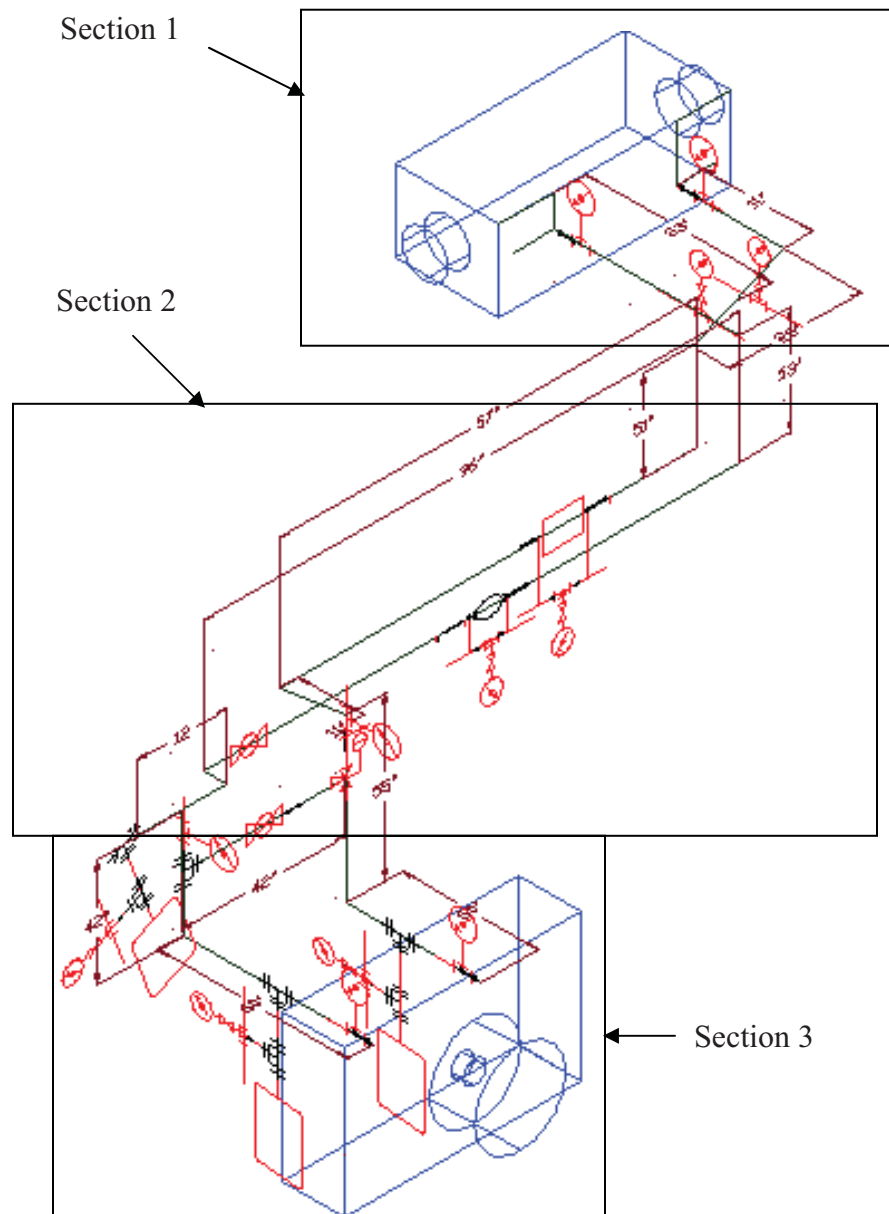
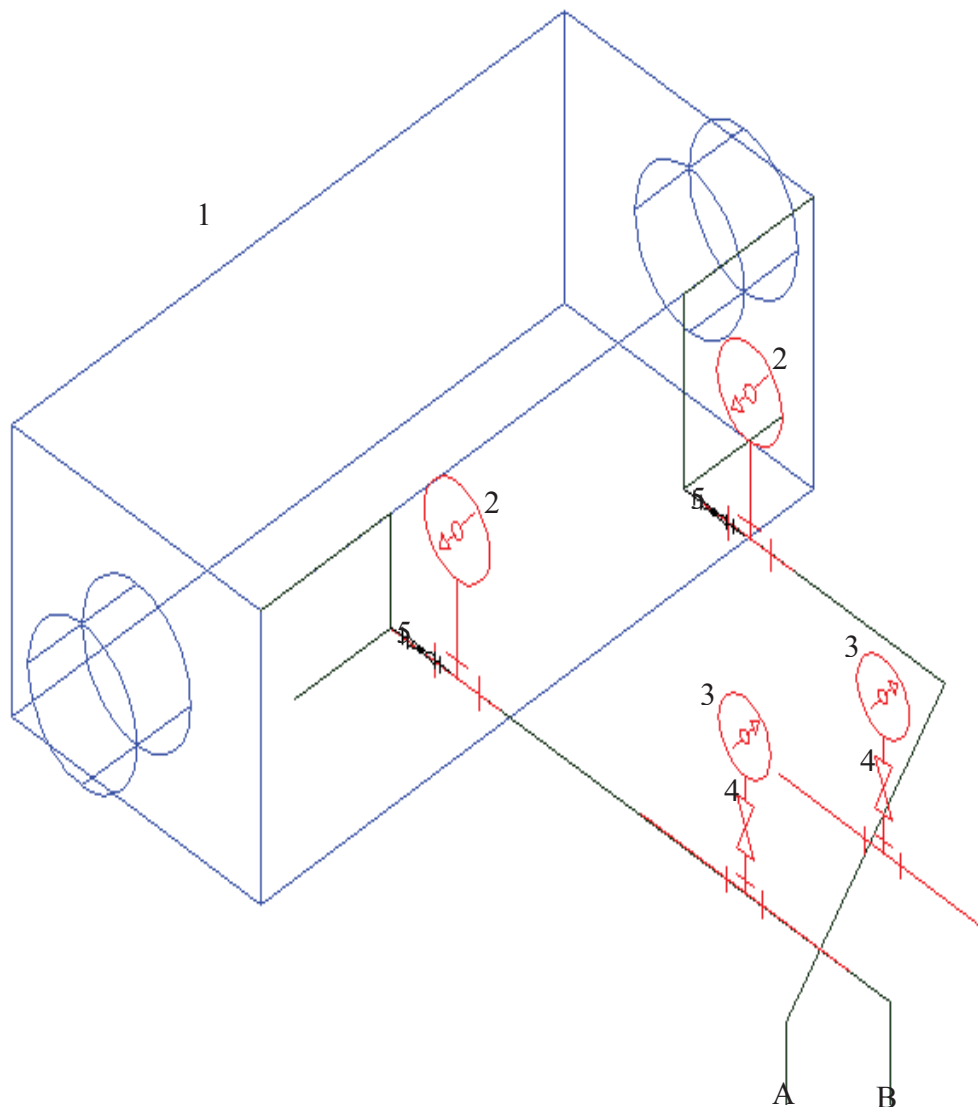


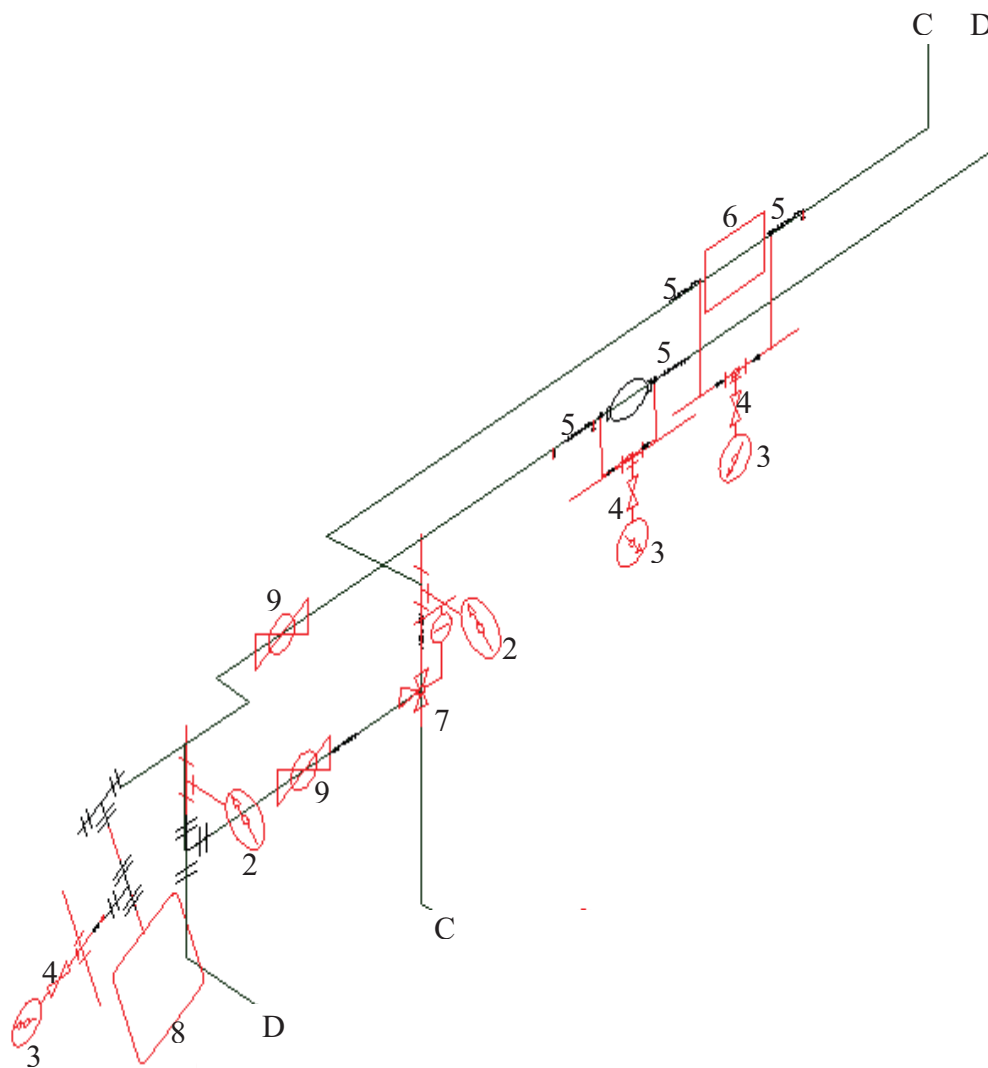
Figure 2.7. AutoCAD heat recovery design drawing.



Parts location and description:

1	Heat exchanger	5	Bronze ball valve
2	Temperature thermocouple	A	Inlet to the heat exchanger
3	Pressure gauge	B	Outlet from the heat exchanger
4	Snubber		

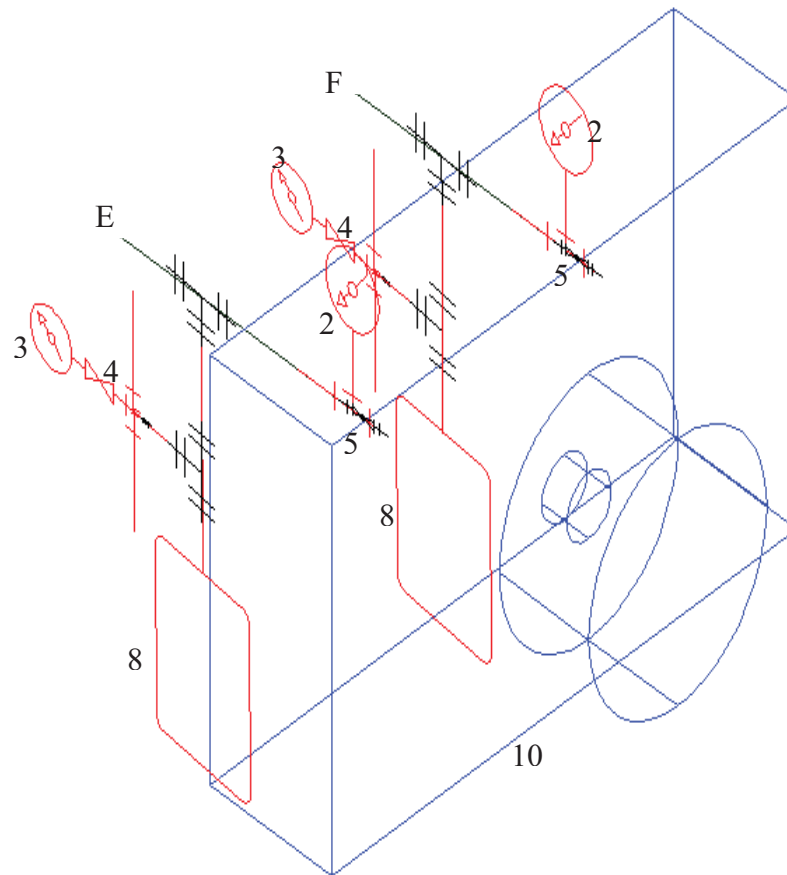
Figure 2.8. Section 1 of the heat recovery system (on top of ISO container).



Parts location and description:

3	Pressure gauge	8	Expansion tank
4	Snubber	9	Circuit setter
5	Bronze ball valve	C	Flow meter line
6	Flow meter	D	Pump line
7	3-way valve		

Figure 2.9. Section 2 of heat recovery system (inside ISO container along west wall).



Parts location and description:

2	Temperature thermocouple	8	Expansion tank
3	Pressure gauge	10	Unit heater
4	Snubber	E	Inlet to the unit heater
5	Bronze ball valve	F	Outlet from the unit heater

Figure 2.10. Section 3 of heat recovery system (sitting outside on the ground next to the west wall of the ISO container).

Table 2.6. Component numbering

1	Heat exchanger
2	Temperature thermocouple
3	Pressure gauge
4	Snubber
5	Bronze ball valve
6	Flow meter
7	3-way valve
8	Expansion tank
9	Circuit setter
10	Unit heater
A	Inlet to the heat exchanger
B	Outlet from the heat exchanger
C	Flow meter line
D	Pump line
E	Inlet to the unit heater
F	Outlet from the unit heater

2.3.2 Heat Exchanger Section

The heat exchanger section of the heat recovery system (see Figure 2.11) includes the heat exchanger, pipe components, and instruments connected to the heat exchanger located outside on top of the ISO container. The inlet and the outlet sides for the heat exchanger are indicated in the figure along with its associated components. For isolating the heat exchanger, bronze ball valves were installed along with the drain. During the experimental process, if there was any clogging due to scales or rust on the core side of the heat exchanger, the pressure would increase. In order to ascertain the presence of any clogging due to these kinds of obstacles, pressure gauges were installed on the inlet and the outlet side. A release valve (from Cain industries) was set on the inlet side of the heat exchanger to free excess pressure and prevent liquid from entering the heat exchanger. Temperature sensors (also from Cain industries) along with temperature thermocouples

were installed on the inlet and the outlet pipes, which help in calculating the heat that can be recovered. As these pipes were considered to be the highest points in the entire piping system, the air vents were installed on them.

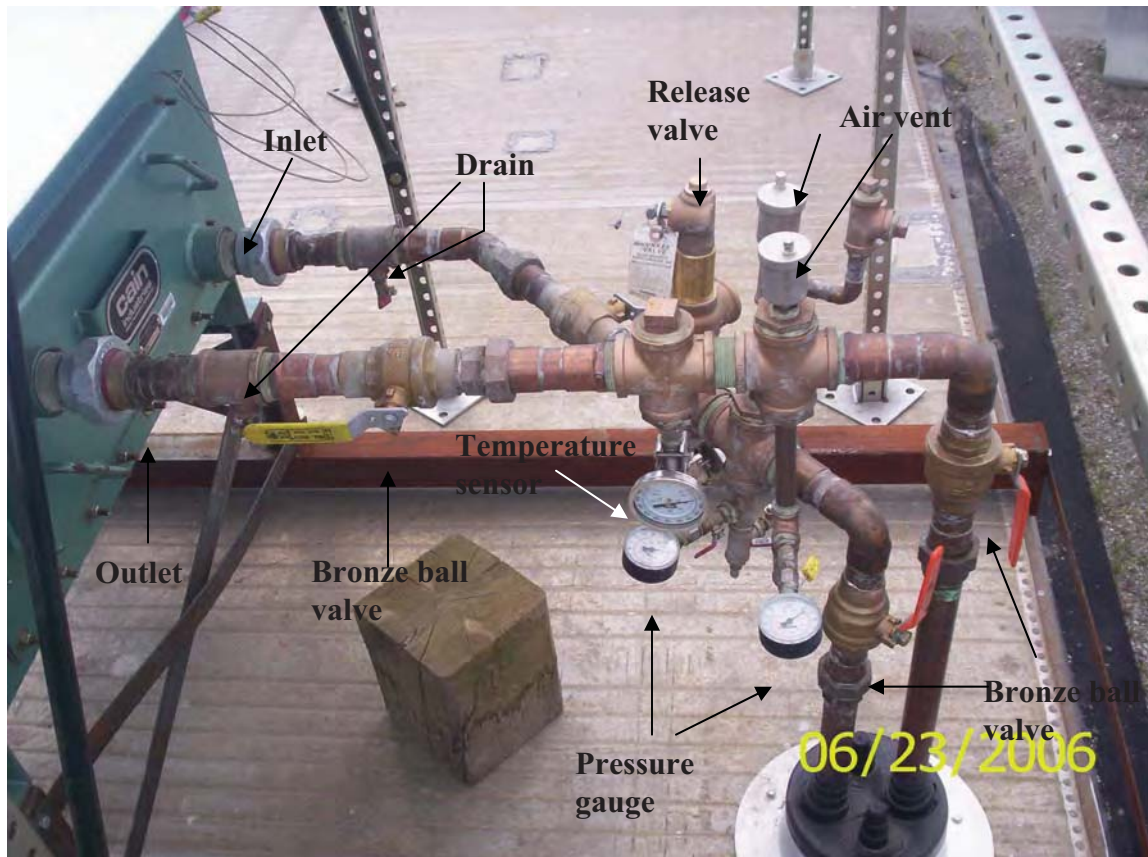


Figure 2.11. Heat exchanger inlet/outlet pipe connections.

2.3.3 Control System Section

The control system section of the heat recovery system (Figure 2.12 shows the north half and Figure 2.13 shows the south half) includes the pump and all pipes, fittings, components, and instruments installed inside the ISO container that are between the heat exchanger and the unit heater.

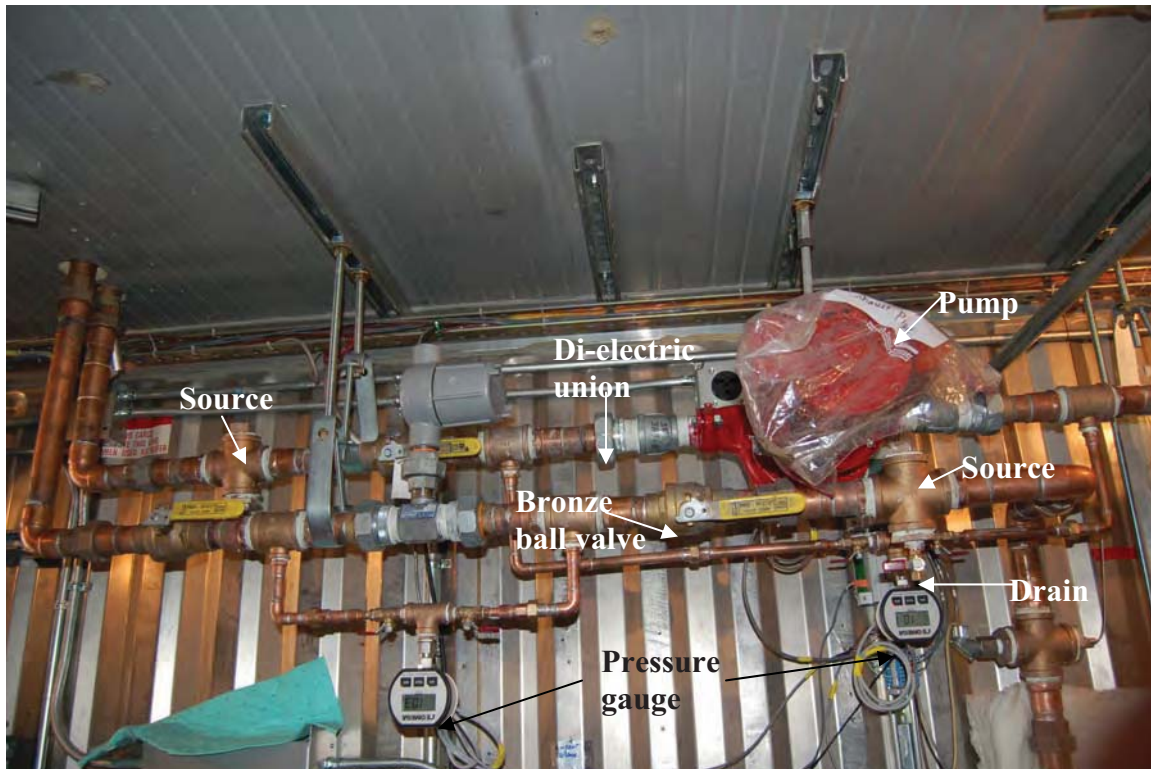


Figure 2.12. North half of the control system inside the ISO container on the west wall.

Pump system: The pump (18 kg) was supported from the roof in the middle of the control system. The support for the pump was fabricated to resist vibrations. A pressure sensor was installed across the pump for intermediate monitoring of its performance. The pump was connected to the copper pipe through dielectric unions which helped in avoiding the effects caused by the contact of two different materials and for the easy removal of the pump when isolated by the bronze ball valves when needed. A strainer was installed in the line to remove any metal residue in the coolant flow. The strainer can be placed anywhere in the control system, but due to space considerations, it was placed after the pump and before the expansion tank. This pipe came from the heat exchanger through the roof and ran along the roof of the ISO container, as that was the only place where it could be accommodated with enough space to walk around it.

Expansion tank in the control system: The expansion tank (Figure 2.14) was installed at a convenient location, and was provided with unions and bronze ball valves across it to isolate that section for maintenance. The expansion tank was fitted with a pressure gauge to note the pressure on the liquid side. This pressure was compared periodically with the initial pressure readings for maintenance purposes.

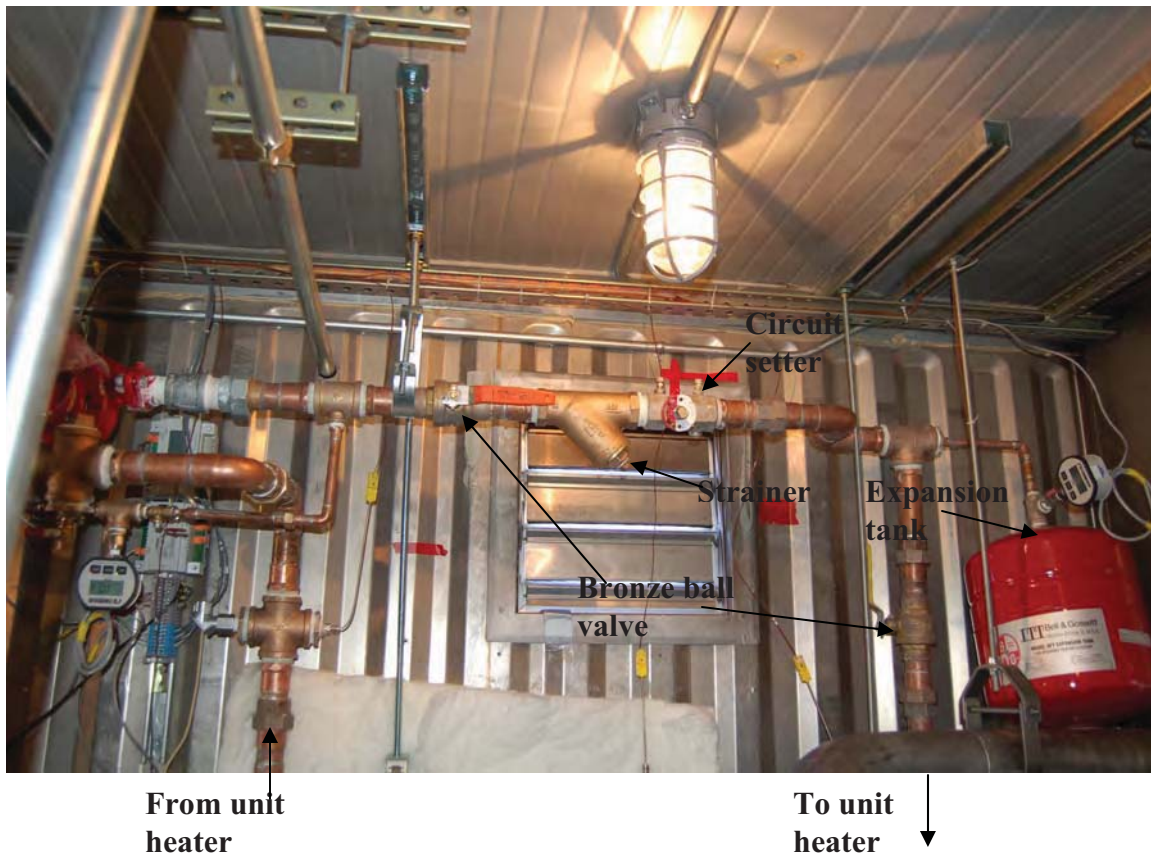


Figure 2.13. South half of the control system inside the ISO container on the west wall.



Figure 2.14. Expansion tank in the control system

Bypass looping: As noted in the control system discussion above, the unit heater was parallel to the bypass line (Figures 2.15 and 2.16) to maintain the outlet temperature of the parallel lines. The outlet temperature could be controlled to simulate different types of heat recovery applications, such as central floor heating, desalination, and ice making. A mixing valve with an actuator was installed in the end of the bypass, connecting the bypass line and outlet line from the unit heater. A temperature sensor was installed after the mixing valve, which controls the opening of the three-way valve with the help of a signal going to the actuator from the sensor. Thermocouple sensors were installed along and across the bypass for constant monitoring of the temperature difference taking place with the change of the engine load. A circuit setter was installed in the bypass to maintain the pressure and the flow rate.

Flow meter line: The flow meter line (Figure 2.17) was connected to the inlet of the heat exchanger. It was a turbine-type flow meter with bronze ball valves and dielectric unions on both ends. A pressure gauge was installed across the flow meter for intermediate monitoring of flow meter performance. The flow meter is an important component in a control system. The readings were recorded in the DAQ system.



Figure 2.15. Bypass line.



Figure 2.16. Bypass line.



Figure 2.17. Flow meter line.

2.3.4 Unit Heater Section

The unit heater section (Figure 2.18) includes the pipe, fittings, expansion tanks, and thermocouples. The inlet to the unit heater is the pipe coming from the pump. Strainers were attached across the unit heater to trap any possible metal pieces. Thermocouples were installed across the unit heater for monitoring the amount of heat extracted from the heat exchanger.

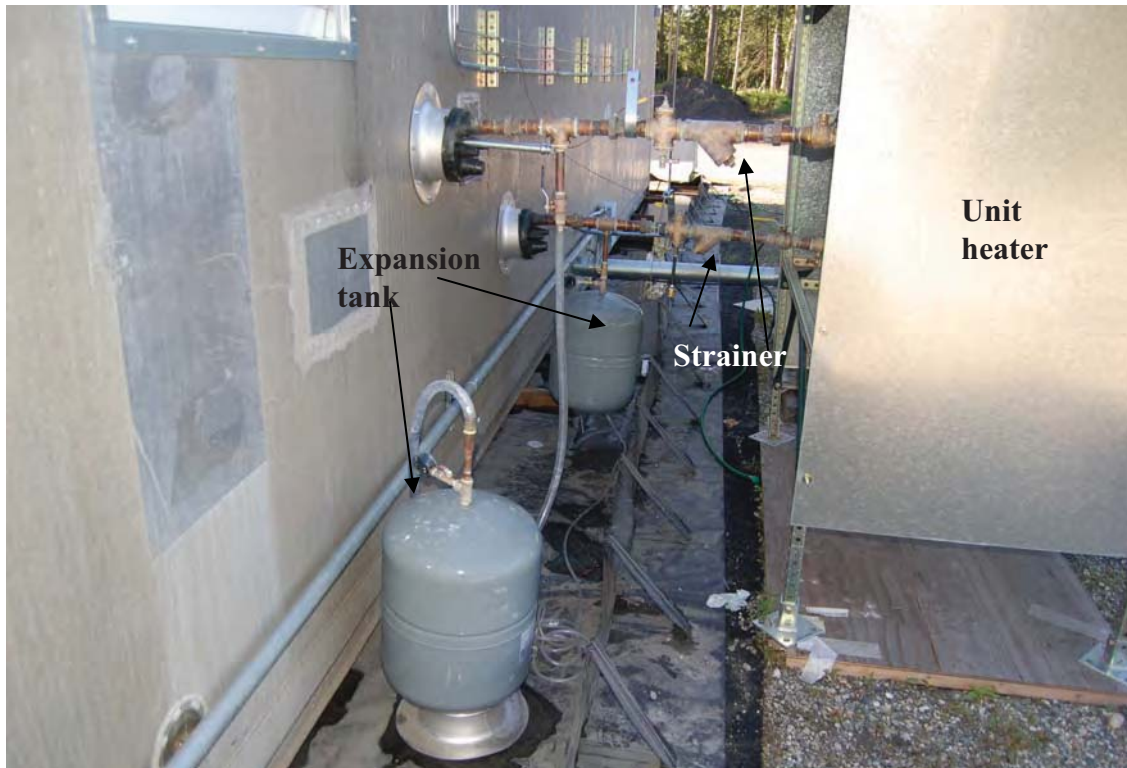


Figure 2.18. Unit heater inlet/outlet pipe connections.

Operation of control system: Once a control system is running, the pump moves the fluid in the pipe continuously, transferring the heat from the exhaust to the liquid passing through the tubes in the heat exchanger. The heat exchanger was designed for a maximum fluid flow rate of 30 gpm. The flow rate was maintained and monitored. The expected heat recovered was 290,000 Btu/hr with a built-in heat exchanger surface area of 87 ft². When the system was new, all the temperature, pressure, and flow measurements were recorded for reference purposes.

To begin with, liquid passes through the pump and expansion tank, and then enters into the unit heater or the bypass, depending on the three-way valve position. The three-way mixing valve opening was controlled by the temperature sensor attached to it. The temperature at which the mixing valve needs to be operated was set on the universal controller, which sends out a signal to the actuator attached to the mixing valve that

controls valve openings. The temperature on the universal controller was preset manually for the liquid entering the heat exchanger. If the sensor read less than the preset value, the bypass valve would open and distribute more fluid through the bypass instead of the unit heater. If the sensor read more than the preset value, the bypass valve would close, passing more fluid through the unit heater. For simulation of different heat recovery applications, different temperatures can be set accordingly.

Fluid enters the heat exchanger after passing through the flow meter. Pressure gauges were installed across the pump and the flow meter to monitor the inlet and discharge pressure of the pump and the flow meter. These pressure readings also helped in monitoring the performance of the pump and the flow meter.

All the thermocouples were connected to the DAQ system for continuous monitoring. The flow meter gave a 4-20 mA signal that was also connected to the DAQ system for monitoring.

2.3.5 Flow Meter and Load Cell Calibration

The flow meter calibration was calibrated gravimetrically. This involved measuring the weight of the fluid passing through the flow meter during a known time from a source to the sink. The flow meter calibration was set up onsite to carry out the calibration process. In this calibration process, two 15-gallon tanks that served as source and sink were used inside the ISO container. A load cell was fixed under one of the 15-gallon tanks (before the outlet of the heat exchanger) that acted as a sink. Before starting the calibration, the bronze ball valves across the unit heater were closed, allowing the fluid to pass only within the ISO container at room temperature. When the pump was run, the fluid from one tank was pumped to the other tank. The load cell would sense a change in the reading and record this in the DAQ system. The readings of the load cell and the flow meter are compared and graphed in Figure 2.19.

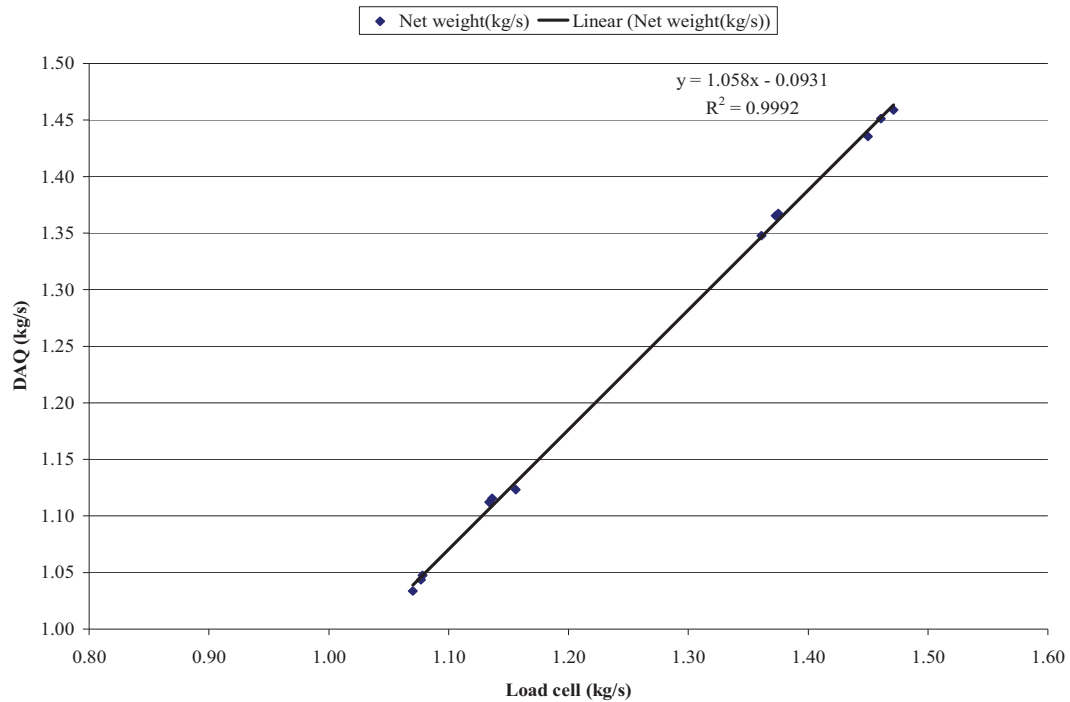


Figure 2.19. Calibration curve for flow meter.

The load cell was also calibrated by known weights. The load cell calibration curve is shown in Figure 2.20.

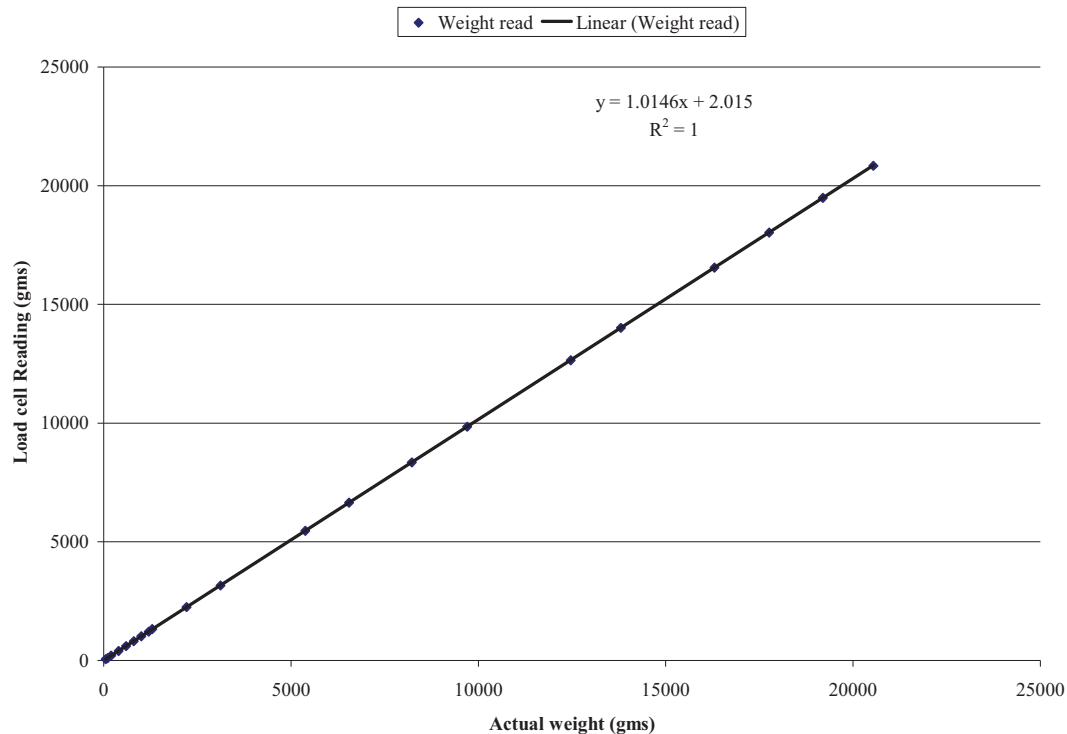


Figure 2.20. Calibration curve for load cell.

2.3.6 Instrumentation of Exhaust Line Monitoring

The purpose of instrumentation was to monitor the effects of the heat exchanger on engine performance and the exhaust system. The instruments included the thermocouples installed on the inlet and outlet of the heat exchanger on the shell side (Figure 2.21) and on the tube side (Figure 2.22). The thermocouples on the tube side gave the temperature drop across the heat exchanger.

2.3.7 Cost of the System

The total cost of the system includes all the components of the control system, the unit heater, and the heat exchanger. The cost of the experimental system is tabulated in Table 2.7. The total cost for the heat recovery system was \$30,000 (approximately). The estimated cost for the village heat recovery system is tabulated in Table 2.8.



Figure 2.21. Thermocouples on the outlet of the heat exchanger.



Figure 2.22. Thermocouples on the core side.

Table 2.7. Cost of the experimental system

Component	Qty	Unit Price (\$)	Total Price (\$)
Tristand pipe vise	1	319.00	319.00
Box beam 3"X3"X1/8" 20' bar	1	75.57	75.57
Flat stock 3"X3/16" 20' bar	1	24.31	24.31
Angle bar 2-1/2"X2-1/2"X3/16" 20' bar	1	33.22	33.22
Flat stock 1-1/2"X1/8" 20' bar	1	9.50	9.50
Flat stock 1"X1/8" 20' bar	1	6.57	6.57
Box beam 1-1/2"X3"X1/8" 20' bar	2	56.54	113.08
Box beam 1-1/4"X1-1/4"X1/8" 20' bar	2	32.02	64.04
Box beam 2"X2"X1/4" 20' bar	1	87.23	87.23
Flexible, insulated thermocouple probes with exposed junction	15	17.50	262.50
Slip-on flange, 150 psi, 5" pipe dia, 10" OD, 8-1/2" bolt	3	38.03	114.09
Great Stuff insulating foam sealant	6	8.49	50.94
Centrifugal pump 1/3 HP 30 GPM	1	672.00	672.00
Expansion tank	1	34.18	34.18
Heat exchanger	1	10,019.00	10,019.00
Fiberglass insulation - bag	1	61.79	61.79
Signal conditioner 0-5 V	1	524.00	524.00
Turbine flow meter, 4-60 linear range (GPM)	1	1,289.00	1,289.00
Pressure gauge, dc powered, dual alarms	3	375.00	1,125.00
Type K grounded thermocouple probe with dia 0.125"	10	25.90	259.00
Type K ungrounded thermocouple probe with dia 0.062	25	26.80	670.00
Type K ungrounded thermocouple probe with dia 0.062	10	27.60	276.00
Teflon insulated type K thermocouple wire	1	405.00	405.00
Miniature type K thermocouple connector pair	50	4.00	200.00
Type K grounded thermocouple probe with dia 0.062	10	24.00	240.00
Type K grounded thermocouple probe with dia 0.125	10	24.00	240.00
24-gauge galvanized metal (Size 63"X39")	1	78.00	78.00
24-gauge galvanized metal (Size 60"X40")	2	78.00	156.00
24-gauge galvanized metal (Size 66"X42")	1	100.00	100.00
Single-loop controller with two 0-10VDC analog outputs	1	100.45	100.45
1-1/4" 3W BR control valve UFxUF with 0-10VDC	1	292.77	292.77
Nickel immersion temperature sensor	1	35.02	35.02
30VA transformer for RWD controller	1	21.64	21.64
Hydronic unit heater, model S-Unit heater	1	1,655.00	1,655.00
Pipe components			6,303.90
Miscellaneous from warehouse			4,000.00
Total cost			\$29,917.80

Table 2.8. Estimated cost for the village recovery system

Component	Qty	Unit Price (\$)	Total Price (\$)
Box beam 3"X3"X1/8" 20' bar	1	75.57	75.57
Flat stock 3"X3/16" 20' bar	1	24.31	24.31
Angle bar 2-1/2"X2-1/2"X3/16" 20' bar	1	33.22	33.22
Flat stock 1-1/2"X1/8" 20' bar	1	9.50	9.50
Flat stock 1"X1/8" 20' bar	1	6.57	6.57
Box beam 1-1/2"X3"X1/8" 20' bar	2	56.54	113.08
Box beam 1-1/4"X1-1/4"X1/8" 20' bar	2	32.02	64.04
Box beam 2"X2"X1/4" 20' bar	1	87.23	87.23
Slip-on flange, 150 psi, 5" pipe dia, 10" OD, 8-1/2" bolt	2	38.03	76.06
Great Stuff insulating foam sealant	6	8.49	50.94
Centrifugal pump 1/3 HP 30 GPM	1	672.00	672.00
Expansion tank	1	34.18	34.18
Heat exchanger	1	10,019.00	10,019.00
Fiberglass insulation - bag	1	61.79	61.79
Type K ungrounded thermocouple probe	6	26.80	160.80
Teflon insulated type K thermocouple wire	1	405.00	405.00
Miniature type K thermocouple connector pair	50	4.00	200.00
Pressure gauge	3	10.00	30.00
24-gauge galvanized metal (Size 66"X42")	1	100.00	100.00
Single-loop controller with two 0-10VDC analog outputs	1	100.45	100.45
1-1/4" 3W BR control valve UFXUF with 0-10VDC	1	292.77	292.77
Nickel immersion temperature sensor	1	35.02	35.02
30VA transformer for RWD controller	1	21.64	21.64
Pipe components			6,303.90
Labor cost (hours)	80	75.00	6,000.00
Parts	1	400.00	400.00
Total cost			\$25,377.07

2.4 Experiment Setups for Exhaust Properties of Other Fuels

The engine used for this experiment was a 125 kW 4-cylinder DD50 diesel generator without exhaust gas recirculation and after-treatment devices. Engine load was controlled by a 250 kW resistive/reactive load bank. The interface between the engine and the load bank had customized generator load profiles. Exhaust heat content was estimated using exhaust temperatures and exhaust flow rates with specific heat data. The exhaust flow rate was estimated from the measured intake air flow rate and fuel consumption rate. Inlet air mass flow was measured using a laminar flow element manufactured by Mariam Instrument, coupled with a HART differential pressure transducer manufactured by ABB. Fuel flow-rate data were taken from the CANbus of the diesel generator, with appropriate

calibration using a gravimetric method. Exhaust temperature data were taken from the engine CANbus. All the measured data were processed via a National Instruments DAQ system and acquired at 10-second intervals.

2.4.1 Synthetic Fuel

Measurements in intake air flow rate, fuel consumption rate, and exhaust temperature for both synthetic diesel and conventional diesel were performed earlier while the synthetic fuel was available. The tests were conducted for 50% load and 100% load. Exhaust emissions had been measured in previous work [4] for NO_x, CO, and THC.

Testing procedure: The fuel tests performed during this study can be divided into two parts: the synthetic fuel test and the conventional diesel test. These tests were conducted on different days, and the synthetic fuel was tested first. The same procedure was used for both fuel tests. Tests for the synthetic fuel followed the procedure given below:

1. Before a test, the fuel line was emptied, and old filters were replaced with new ones.
2. The engine was then started with the synthetic diesel fuel and operated for 2 hours to purge all the residual conventional diesel fuel from the fuel line.
3. After this cleaning, the synthetic diesel fuel test was started, and data were collected.
4. The measured exhaust temperatures and flow rates were used to estimate the heat content in the exhaust.

2.4.2 Conventional Diesel with a Small Amount of Hydrogen

A small amount of hydrogen was introduced into the intake air stream of the diesel engine in flow rates of 0, 1, 2, 3, 4, 6, 8, 10, 12, 16, 30, 50, 100, and 150 liters per minute (lpm). Figure.2.23 shows the experimental setup for the test. The main components of the experiment were the diesel engine, compressed hydrogen tank, MKS mass flow controller, DAQ system, and exhaust gas analyzer.

The hydrogen tank was a commercially available compressed hydrogen tank used for industrial purposes. The hydrogen pipeline was connected to the inlet air stream of the diesel engine by the MKS mass flow controller. The MKS mass flow controller was connected in turn to the National Instruments DAQ system. The range of the MKS flow controller is 0 to 200 lpm. The DAQ system gives the signal to the mass flow controller for certain flow rates of hydrogen, and then the mass flow controller adjusts the flow of the hydrogen according to the signal received from the DAQ system. Data included exhaust temperature, ambient temperature, and fuel flow rate. The exhaust gases were analyzed by a Testo 350-S exhaust gas analyzer. A sample of exhaust gas was passed through the analyzer, and the data were analyzed for emissions. The analyzed data were stored in the DAQ system. The complete information collected by DAQ was stored in the

form of an Excel spread sheet. After the experiment was completed, the data in the spread sheet were analyzed. Engine load for this test was 56 kW.

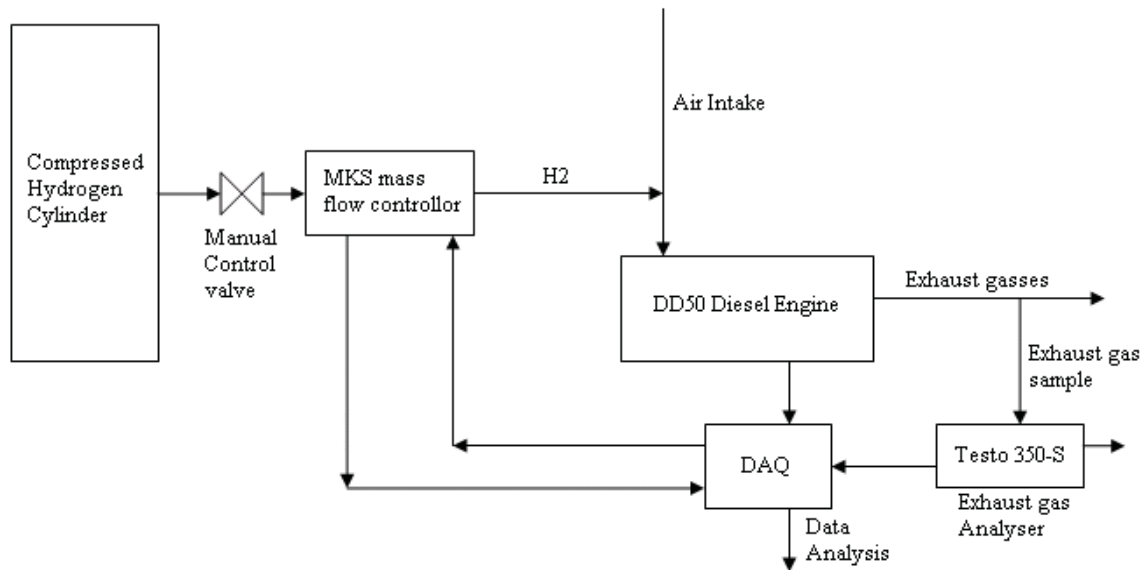


Figure 2.23. Line diagram for hydrogen test.

Testing procedure: An experiment was conducted to simulate the performance of a hydrogen electrolyzer (commercially available on the web) and to determine the effect of hydrogen on exhaust heat content and emissions. The difference between this experiment and one actually using an electrolyzer was that we used pure bottled hydrogen, while an electrolyzer decomposes water (H_2O) into hydrogen (H_2) and oxygen (O_2). In general, the mass flow rate of H_2 and O_2 generated by the electrolyzer is much lower than 1% of the intake air mass flow rate.

The following steps explain the test procedure:

Step 1: The diesel engine was started and ran for 3 h at 50 kW load to stabilize the temperatures surrounding the engine. This step ensures that the readings are being recorded at constant ambient temperatures. During this run, no hydrogen was supplied.

Step 2: The DAQ system collected data every 10 sec. The hydrogen was introduced into the intake air stream in regular intervals of 5 min; that is, the experiment was started with 0 lpm of hydrogen for the first 5 min, then hydrogen was introduced at 0.5 lpm to the intake air for the next 5 min, and then again the hydrogen flow was lowered to 0 lpm for the next 5 min and then at 1 lpm for the next 5 min. Likewise the hydrogen flow cycles of 0 lpm and designated flow (0.5, 1, 2, 3, up to 150 lpm) were introduced into the intake air stream. The DAQ collected nearly 30 data points for every hydrogen flow rate.

Step 3: The exhaust gas analyzer (Testo 350-S) is not a continuous measuring device. For every hydrogen flow rate of 5 min, the exhaust gas analyzer was switched “ON” for 3 min for taking the emissions data. Therefore, approximately 15 emissions data were available for averaging for every hydrogen flow rate.

Step 4: Exhaust emissions data for oxygen (O_2), carbon monoxide (CO), nitrous oxide (NO), nitrogen dioxide (NO_2), total nitrogen oxides (NO_x), and sulfur dioxide (SO_2) were collected. The exhaust gas analyzer gave the output of emissions in amperes. The exhaust gas temperatures and air flow rates were used to calculate the average heat content in the exhaust.

Chapter 3 Results and Discussion

3.1 Introduction

This chapter discusses the results obtained from our two tasks. The first task includes two parts. The first part discusses the measured results, performance, and economics of the designed heat recovery system. Discussions focus on verifying the match between the measured performance of the fabricated system and the desired performance of the original design, feasibility, and economic effect. The feasibility study includes the effect of the heat recovery system on engine performance, system efficiency, and reliability issues such as corrosion and soot accumulation. The second part of the first task discusses the heat energy contents in the exhaust from three different fuels. The results are used to compare the heat recovery potential of the exhaust from these three fuels. For the second task, this chapter discusses the structure of the developed economic analysis computer program and its performance. Discussions include the goal and structure of the program, validation of the program for its ability in heat recovery computation, and a demonstration of economic analysis result using an example.

Considering the economic analysis of exhaust heat recovery for heating, the heat recovery system was operated and monitored for nearly 350 hours after the completion of the system installation. The system was operated under generator-rated load conditions (125 kW) for most of the time. The system was also operated under different engine loads (25%, 50%, and 75%) for performance testing. For each load, the inlet or outlet coolant of the heat exchanger was controlled at various temperatures to simulate the requirements for different applications.

At the beginning of testing in the summer, water was used as a coolant for both ease of use and data analysis. However, data collection was not completed before the onset of cooler weather, so the coolant was changed from water to a mix of 40% propylene and 60% water at the 150th hour to avoid freezing. After 250 hours, one of the thermocouples (coolant inlet temperature to the heat exchanger) was recalibrated, and the time constant of the controller for the temperature control valve was adjusted to limit a large fluctuation in the temperature reading. In this chapter, data obtained between 250 and 300 hours were used for most of the analysis because the data are more accurate (Table 3.1).

Based on experimental data obtained, the upcoming sections discuss the verification of the heat recovery system, the consistency of the heat recovery system, the effect of heat recovery on engine performance, the feasibility and maintenance related issues, and the economic analysis.

The test for exhaust properties of the three fuels and their effect on exhaust heat recovery broke down to two parts. The first part involved the comparison of effects of the synthetic fuel and the conventional diesel on heat recovery performance; the second part concluded the effect of a small amount of hydrogen on exhaust heat recovery performance. The test for the synthetic fuel and the conventional diesel was conducted much earlier due to the time availability of the synthetic fuel. Comparison in exhaust emissions between the

synthetic fuel and the conventional diesel had been performed in a previous project; results were given in [4]. Because the tests of the two parts were carried out more than one year apart and the testing environment conditions were different, the results of the studies of the two parts were discussed separately.

Concerning the developed economic analysis computer program for exhaust heat recovery for heating, this chapter discusses the specific goals and desired features of the program, the platform chosen, program structure, input required, and output data and format. This chapter also discusses the links between different routines of the program, the data library, and the principles applied to design and analyses.

Table 3.1. Different cases with engine running on conventional diesel fuel

Heat exchanger outlet temperature	Working fluid	Case
50-hour run 87°C (190°F)	40% propylene glycol	Data analyzed at 100% load once every 10 hours
87°C (190°F)	40% propylene glycol	25%, 50%, 75%, and 100% engine loads
77°C (170°F)	40% propylene glycol	25%, 50%, 75%, and 100% engine loads
65°C (150°F)	40% propylene glycol	25%, 50%, 75%, and 100% engine loads

3.2 Economic Analysis for Exhaust Heat Recovery for Heating

3.2.1 Design Verification

The heat recovery system was tested to verify its design at different engine loads. The flow rate on the coolant side was observed to be constant throughout the experimental process. Figure 3.1 shows the flow rate distribution curve across the bypass and unit heater at different engine loads. There was a change in the flow rate at rated load. This can be explained as the change in the total pressure drop. When the engine is running at rated load, a higher percentage of coolant passes through the unit heater instead of the bypass, which increases the total pressure drop in the pipeline due to the higher flow resistance of the unit heater. This could be adjusted using the circuit setter. However, the flow rate was not adjusted due to very small changes, which might cause a small variation in the heat exchanger efficiency.

The inlet/outlet temperatures across the fluid side of the heat exchanger are shown in Figure 3.2. The temperature differentials at varying engine loads changed according to the heat present in the exhaust and the heat dissipation capacity of the unit heater, which depended on ambient temperature. At higher loads, as the exhaust heat was greater, the inlet temperature to the heat exchanger needed to be much lower in order to maintain the

required outlet temperatures and vice versa. At the same time, the unit heater needed to dissipate the absorbed heat by the coolant. In our case, the unit heater was smaller and could not dissipate enough heat at higher engine load conditions as it reached its maximum heat-dissipating capacity. This limitation resulted in the system being incapable of further lowering the heat exchanger inlet temperature which in turn increased the heat exchanger outlet temperature on the fluid side. Thus, the graph shows an increasing curve on the heat exchanger coolant outlet side and a decreasing curve on the coolant inlet side. However, the inlet temperatures of the heat exchanger on the fluid side matched the temperatures that were set on the temperature control valve, which confirms desired operation of the temperature-controlled three-way valve.

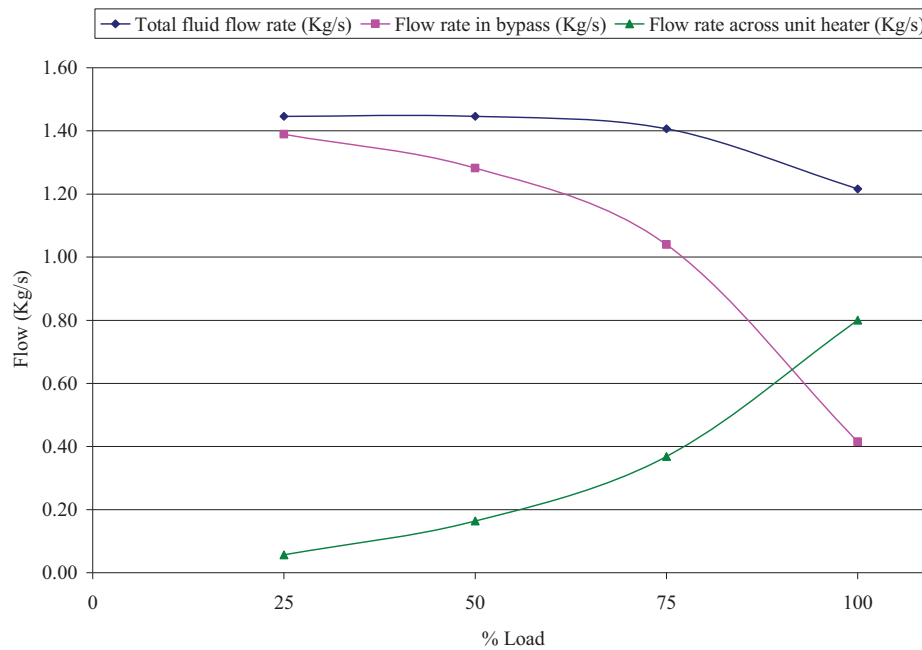


Figure 3.1. Fluid flow distributions across the bypass and unit heater.

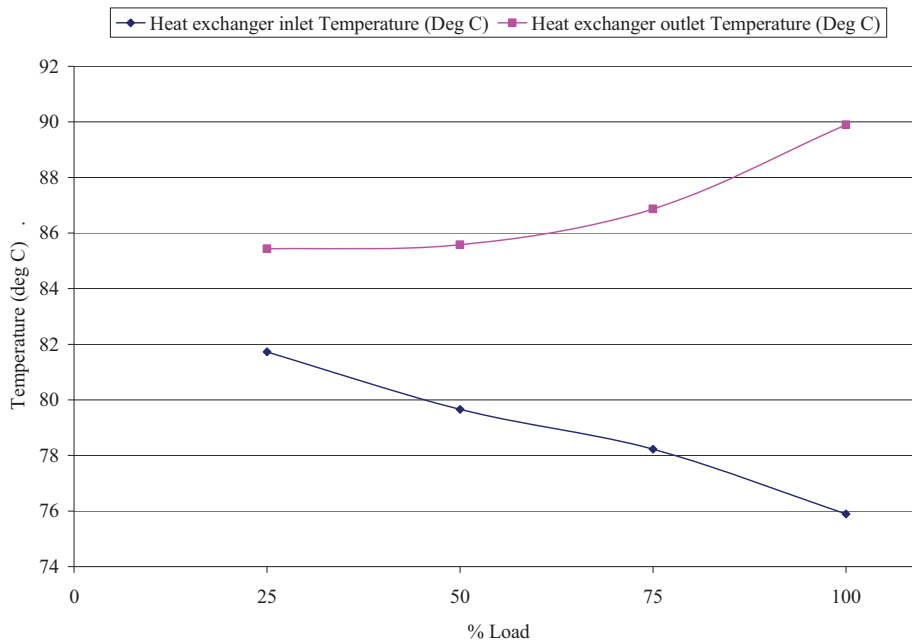


Figure 3.2. Temperature on the fluid side across the heat exchanger.

The unit heater was able to serve its purpose by dissipating the maximum amount of heat possible. In a real field situation, the system would be designed based on the heat requirements instead of using a unit heater to simulate the load required. Table 3.2 shows real values at different engine loads.

Table 3.2. Fluid side readings at different engine loads

Parameters	25% Load	50% Load	75% Load	100% Load
Heat exchanger inlet temperature (°C)	81.72	79.66	78.22	75.90
Heat exchanger outlet temperature (°C)	85.43	85.58	86.87	89.90
Total fluid flow rate (Kg/s)	1.45	1.45	1.41	1.22
Flow rate in bypass (Kg/s)	1.389	1.282	1.039	0.415
Flow rate across unit heater (Kg/s)	0.057	0.164	0.368	0.801
Exhaust inlet temperature	223.33	327.42	412.89	463.90
Exhaust outlet temperature	109.54	131.89	159.52	186.86

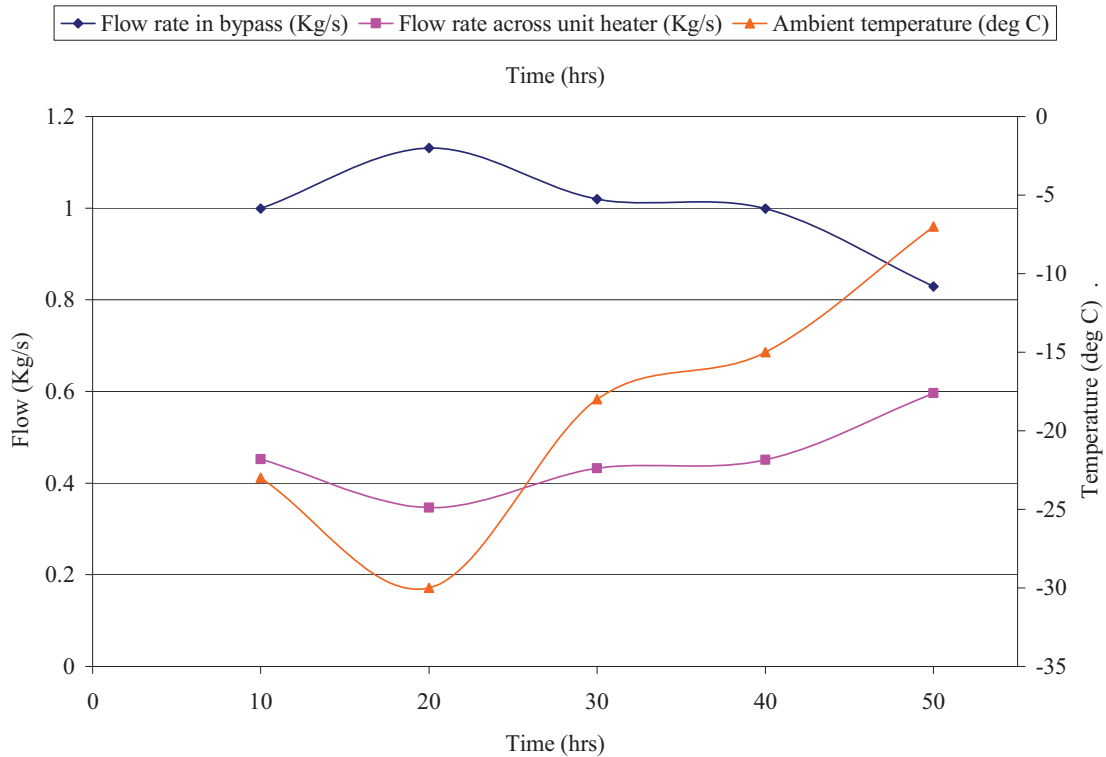


Figure 3.3. Flow distributions between the bypass and unit heater.

Effect of outside ambient temperature: As expected, the ambient temperature had a great impact on the flow distribution of the system between the bypass and the unit heater. The warmer the outdoor ambient temperature was, the more coolant was needed to pass through the unit heater.

Energy balance: Heat balance was checked between the heat absorbed from the exhaust side and the heat dissipated from the system, including heat loss from the unit heater and pipe. Figure 3.4 shows that the heat absorbed by coolant equals the sum of heat dissipations, as the laws of thermodynamics demand. The difference between the heat absorbed and dissipated by the coolant is less than 3%. Figure 3.4 also shows that the heat dissipated from the unit heater was higher for higher temperatures. This can be explained by the pipeline, at higher ambient temperatures, dissipating less heat which must be compensated for by increasing heat loss through the unit heater to maintain the inlet temperature of the heat exchanger.

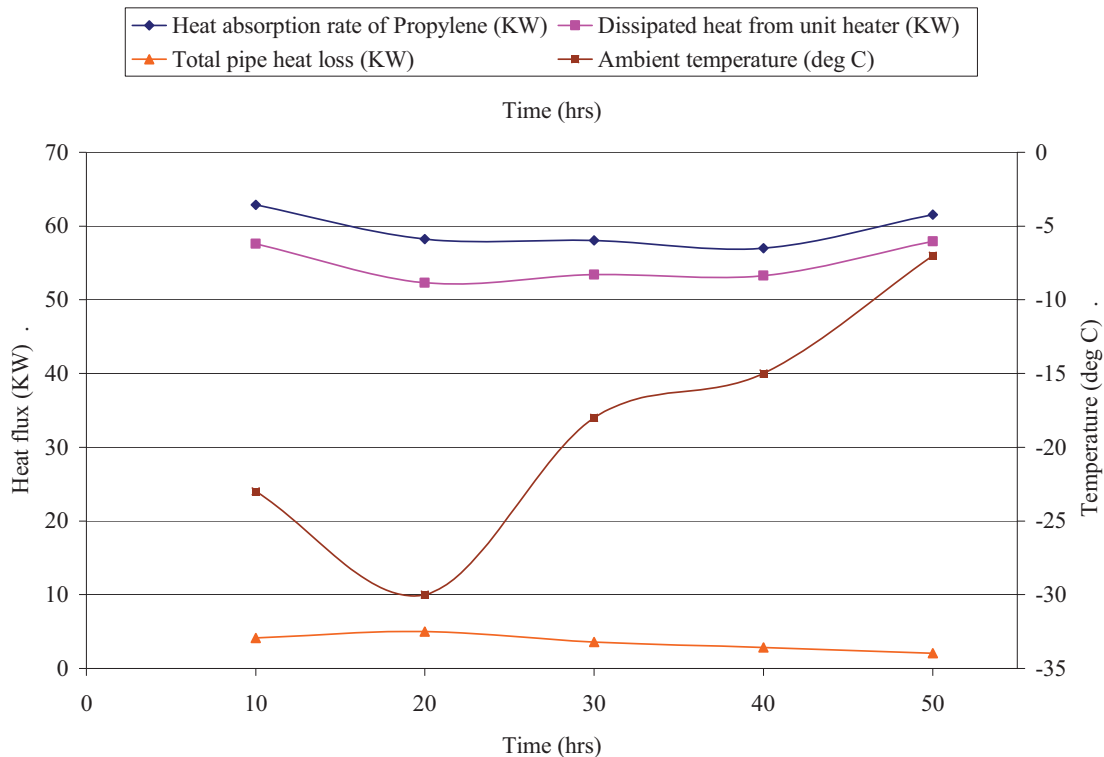


Figure 3.4. Energy balance with respect to the ambient temperature.

3.3 Feasibility and Performance

3.3.1 50-Hour Run

The heat recovery system was run for 350 hours to assess the maintenance that might be required for satisfactory system performance. There were two major concerns during this time: soot accumulation resulting in reduced heat flux, and corrosion due to condensation of sulfuric acid. During a 50-hour run, the heat exchanger efficiency was monitored, but no significant change was observed in either the efficiency or the system performance (temperature, pressure, and fluid flow rate) during this time. There was a small variation in the total enthalpy of the exhaust entering and leaving the heat exchanger. The variation followed a change in the conox temperature (graphed in Figure 3.5), and was found to be due to changes in ambient pressure, resulting in a slight change in mass flow. However, the efficiency of the system was seen to be almost constant, where the efficiency is the ratio of the amount of heat gained by the propylene to the amount of heat lost by the exhaust.

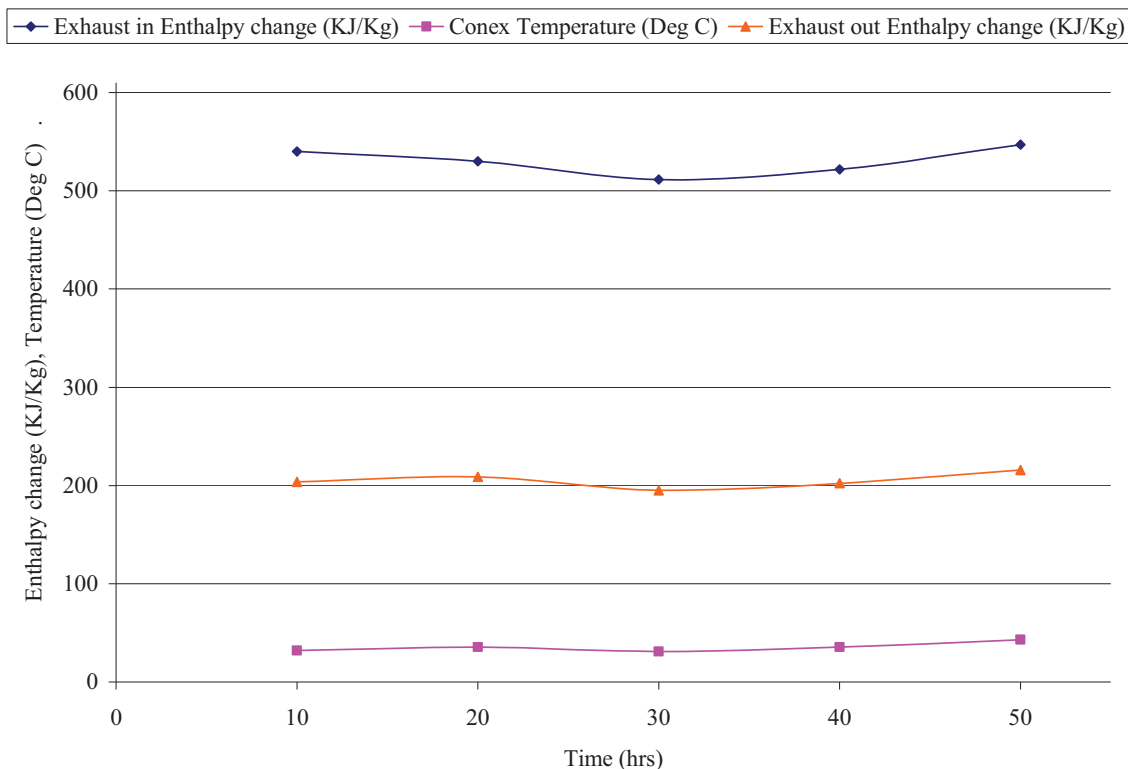


Figure 3.5. Enthalpy change in exhaust across the heat exchanger.

The exhaust mass flow rate was calculated using the sum of the engine manifold inlet air mass flow rate and fuel consumption rate. In order to determine the air mass flow rate, a laminar flow element and differential-pressure gage was used. The heat release rate of the exhaust across the heat exchanger is shown in Figure 3.6. The heat flux was calculated by the product of enthalpy change with respect to the standard conditions and flow rate of the exhaust. The enthalpy change was calculated based on the individual mass percentages of the exhaust components after combustion. In Figure 3.6, E_{in} and E_{out} represent, respectively, the total heat present in the exhaust before entering into and after passing through the heat exchanger.

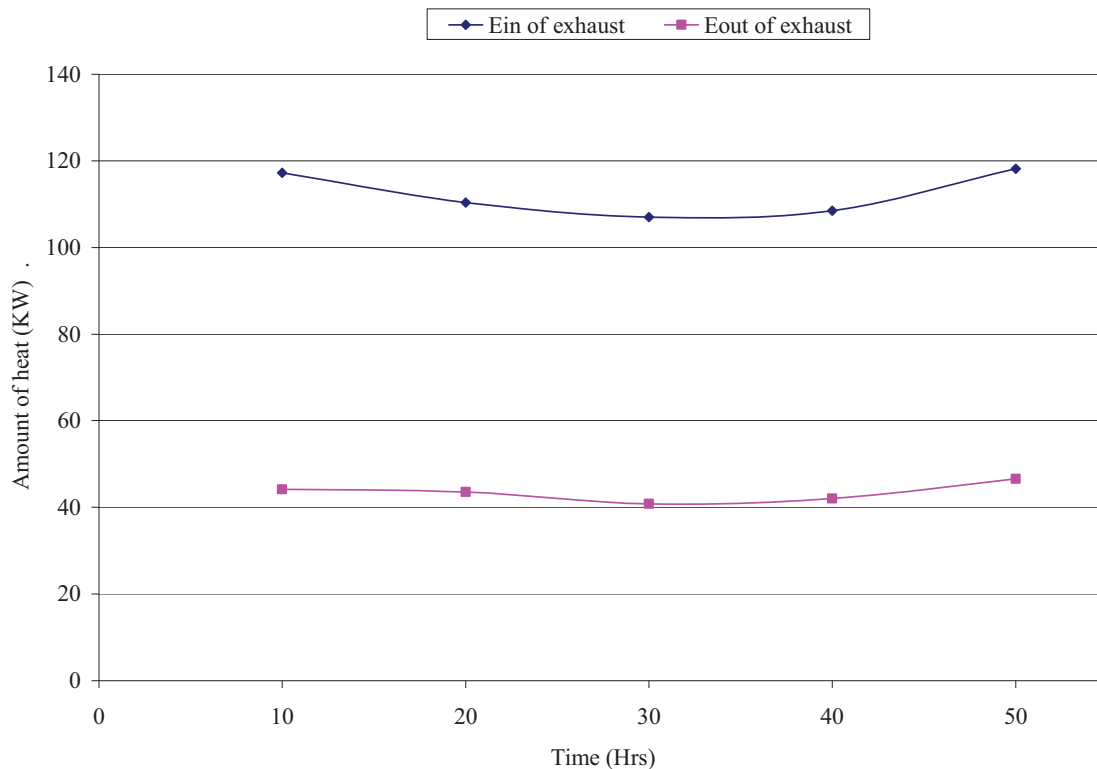


Figure 3.6. Heat flow rates of the exhaust entering and leaving the heat exchanger.

Figure 3.7 shows the heat release rate from the exhaust and the heat absorption rate of the glycol coolant. The heat absorption rate was evaluated using the coolant mass flow rate, the specific heat, and the temperature difference between the heat exchanger inlet and outlet flow. The amount of heat absorbed by the propylene glycol followed the same trend as the heat released from exhaust across the heat exchanger.

3.3.2 Forty Percent Propylene Glycol as Working Fluid

The working fluid was 40% propylene glycol and water mix. Propylene does not affect the environment negatively when spilled. This was the main reason behind its selection for this experiment. The freezing point of 40% propylene is -35°C . Corrosion inhibitors were added to the mix to avoid corrosion in the pipe. There were a few experiments using 40% propylene glycol as the working fluid to check the feasibility and performance of the heat recovery system. The different cases include variations in the heat exchanger outlet temperatures of around 87°C , 77°C , and 65°C , and variations in engine-rated load of 25%, 50%, 75%, and 100%.

This experiment was conducted at lower loads and higher loads. Lower loads were considered to be 25% and 50% loads, while higher loads were considered to be 75% and 100% loads. Table 3.3 shows related engine power to percentage of load. This table represents all cases in this project.

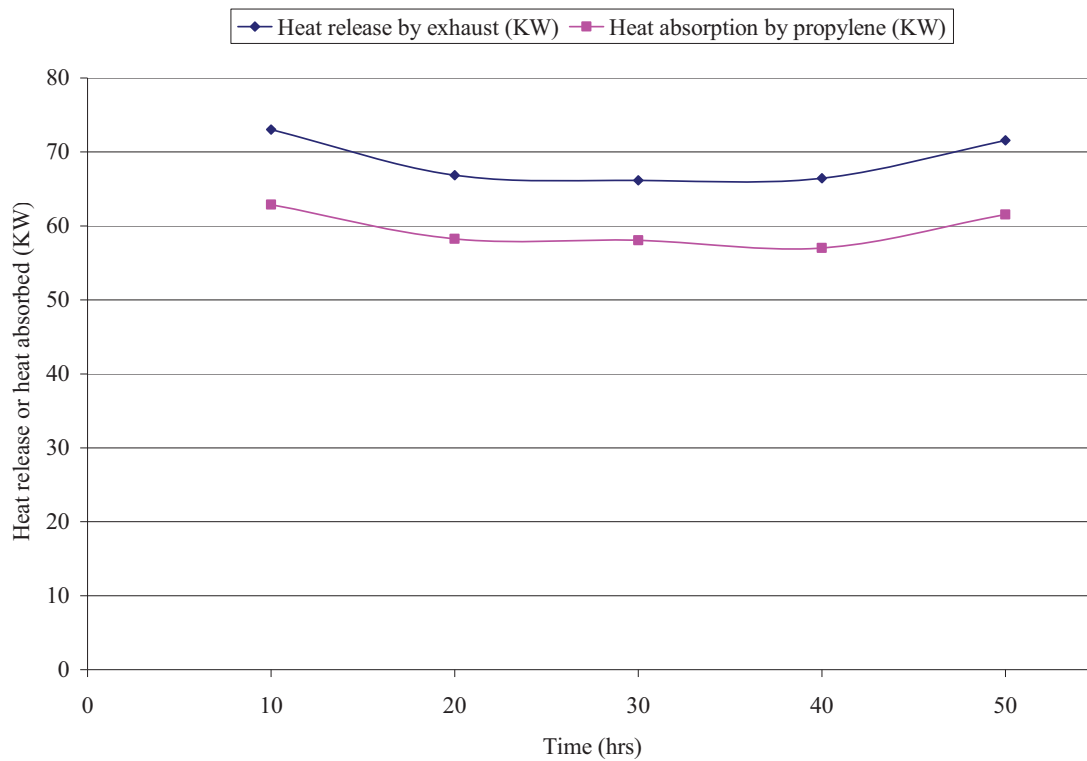


Figure 3.7. Heat release versus heat absorption.

Table 3.3. Load percentage against related kW

Loads	kW
25%	31
50%	62
75%	93
100%	128

The amount of heat that the fluid can recover depends on the heat present in the exhaust. Figure 3.8 shows the heat flow on the gas side of the heat exchanger at different loads.

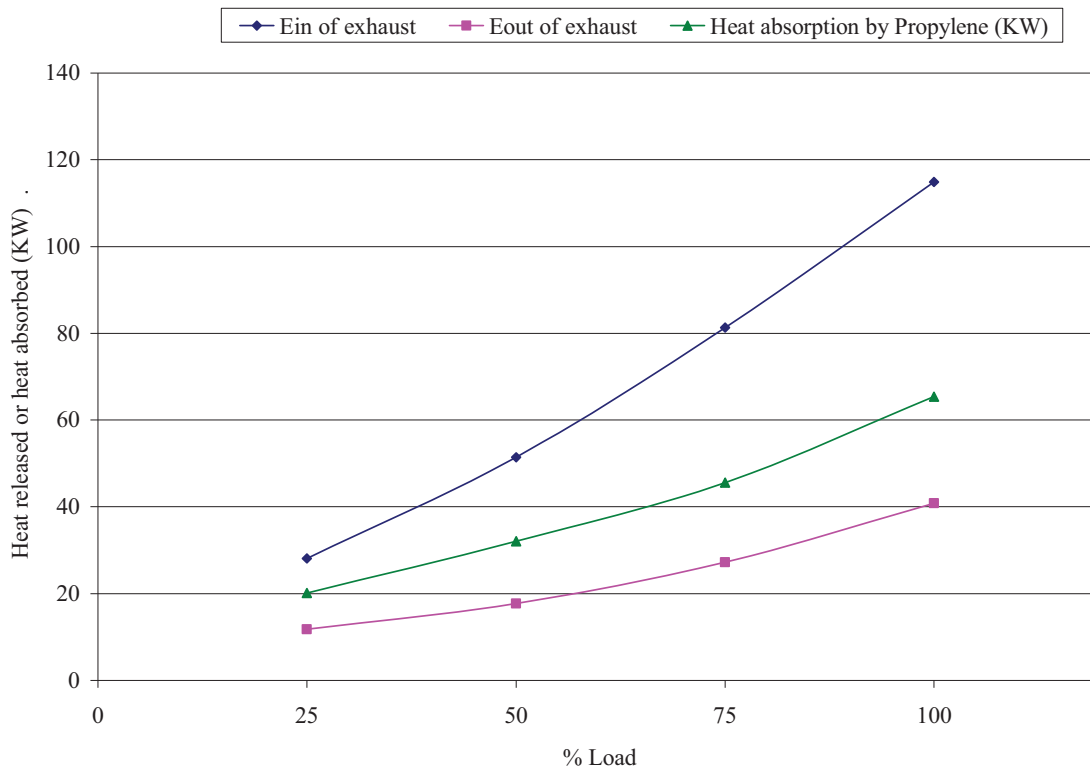


Figure 3.8. Heat released by exhaust and heat absorbed by glycol fluid as outlet temperature to the heat exchanger on the fluid side is set to 87°C

As predicted, the heat absorption rate varied at different loads. The heat absorption rate followed the same trend as the heat present in the exhaust shown in Figure 3.8. All the related temperature measurements and calculated values for the exhaust and fluid with 87°C as the outlet temperature on the fluid side of the heat exchanger are given in Table 3.4.

Similar system performances were observed for other cases. The related graphs are shown in Figure 3.9 and Figure 3.10.

All the related temperature measurements and calculated values for the cases of 77°C and 65°C as the outlet temperature on the fluid side of the heat exchanger are given in Table 3.5 and Table 3.6.

Table 3.4. Outlet temperature of 87°C on the fluid side of the heat exchanger

Temperature / calculations	25% Load	50% Load	75% Load	100% Load
Exhaust flow (Kg/s)	0.14	0.16	0.19	0.24
Exhaust outlet temperature (°C)	109.54	131.89	159.52	186.86
Heat exchanger inlet temperature (°C)	81.72	79.66	78.22	75.90
Heat exchanger outlet temperature (°C)	85.43	85.58	86.87	89.90
Exhaust inlet temperature (°C)	223.33	327.42	412.89	463.90
Total fluid flow rate (Kg/s)	1.45	1.45	1.41	1.22
Total absorbed heat by propylene (kW)	20.11	32.08	45.60	65.43
E_{in} of exhaust (kW)	28.06	51.43	81.28	114.86
E_{out} of exhaust (kW)	11.75	17.70	27.26	40.84

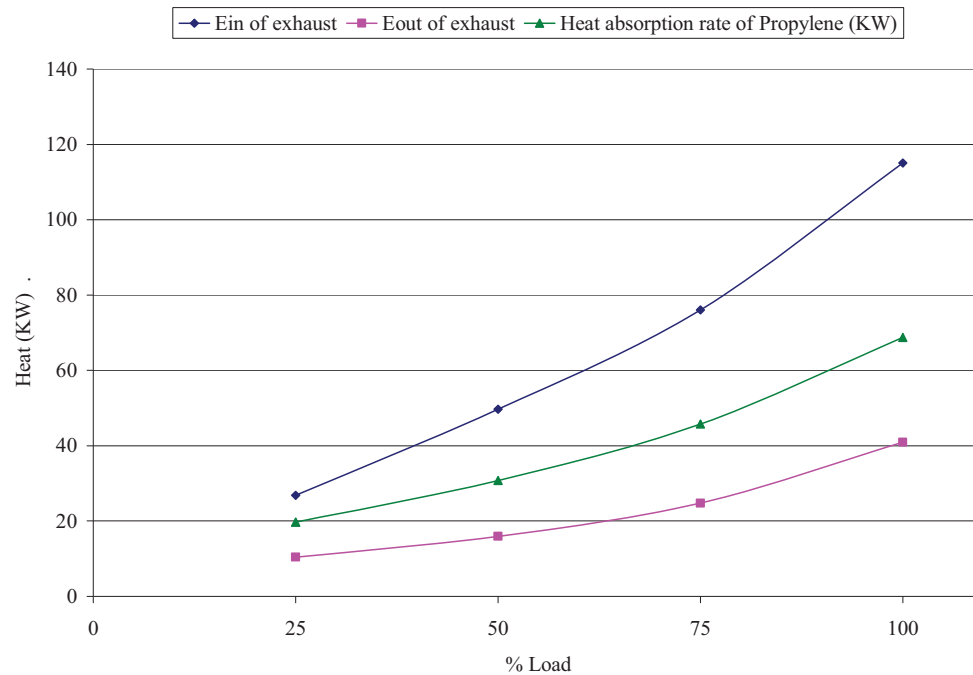


Figure 3.9. Heat released by exhaust and heat absorbed by glycol fluid as outlet temperature to the heat exchanger on the fluid side is set to 77°C

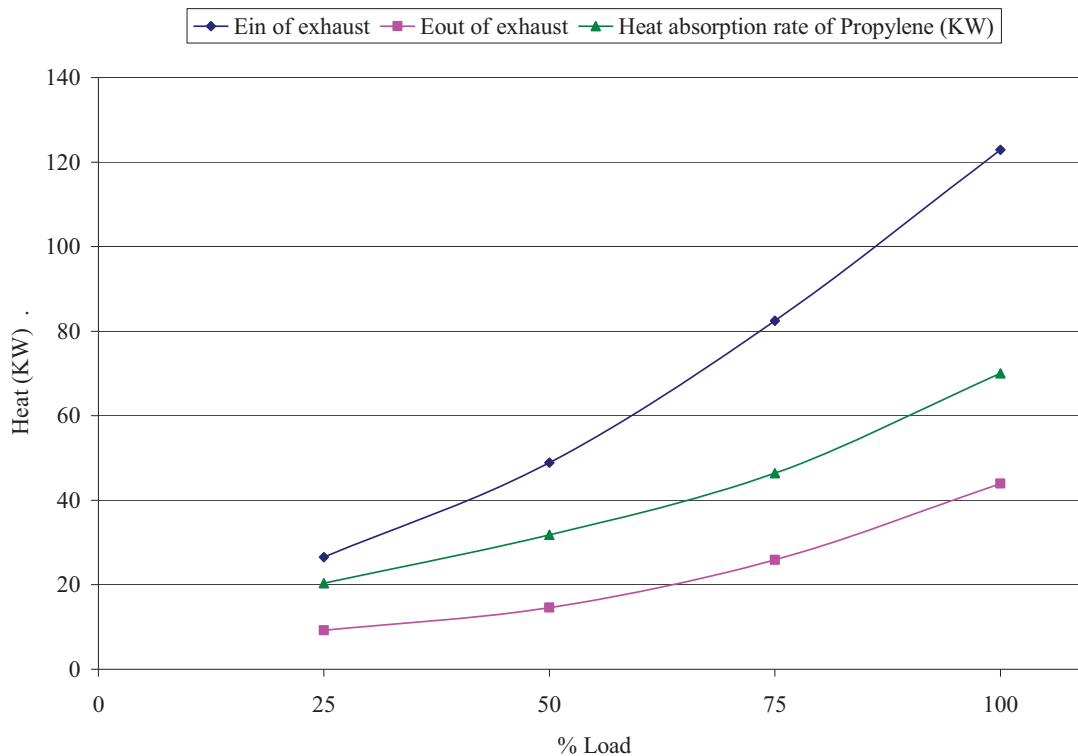


Figure 3.10. Heat released by exhaust and heat absorbed by glycol fluid as outlet temperature to the heat exchanger on the fluid side is set to 65°C

Table 3.5. Outlet temperature of 77°C on the fluid side of the heat exchanger

Temperature / calculations	25% Load	50% Load	75% Load	100% Load
Exhaust flow (Kg/s)	0.14	0.16	0.19	0.23
Exhaust outlet temperature (°C)	100.97	122.28	150.62	189.88
Heat exchanger inlet temperature (°C)	72.65	69.22	67.10	67.58
Heat exchanger outlet temperature (°C)	76.29	74.93	75.98	84.49
Exhaust inlet temperature (°C)	216.67	319.52	398.70	471.59
Total fluid flow rate (Kg/s)	1.45	1.44	1.38	1.08
Heat absorption rate of propylene (kW)	19.71	30.75	45.75	68.76
E_{in} of exhaust (kW)	26.87	49.65	76.08	115.04
E_{out} of exhaust (kW)	10.45	15.96	24.76	40.93

Table 3.6. Outlet temperature of 65°C on the fluid side of the heat exchanger

Temperature / calculations	25% Load	50% Load	75% Load	100% Load
Exhaust flow (Kg/s)	0.13	0.16	0.19	0.24
Exhaust outlet temperature (°C)	93.02	115.59	154.95	198.13
Heat exchanger inlet temperature (°C)	60.68	58.28	53.76	72.11
Heat exchanger outlet temperature (°C)	64.45	64.26	65.21	89.23
Exhaust inlet temperature (°C)	216.27	320.97	424.02	491.87
Total fluid flow rate (Kg/s)	1.44	1.42	1.08	1.09
Heat absorption rate of propylene (kW)	20.36	31.83	46.32	70.06
E_{in} of exhaust (kW)	26.49	48.92	82.46	122.97
E_{out} of exhaust (kW)	9.23	14.56	25.92	43.88

The total absorbed heat by the propylene with respect to each load and for each case is shown in Figure 3.11. According to Figure 3.11, the amounts of heat absorbed with respect to load for all cases followed the same trend with a difference of less than 4%. The difference may be due to the ambient conditions during the experimental run.

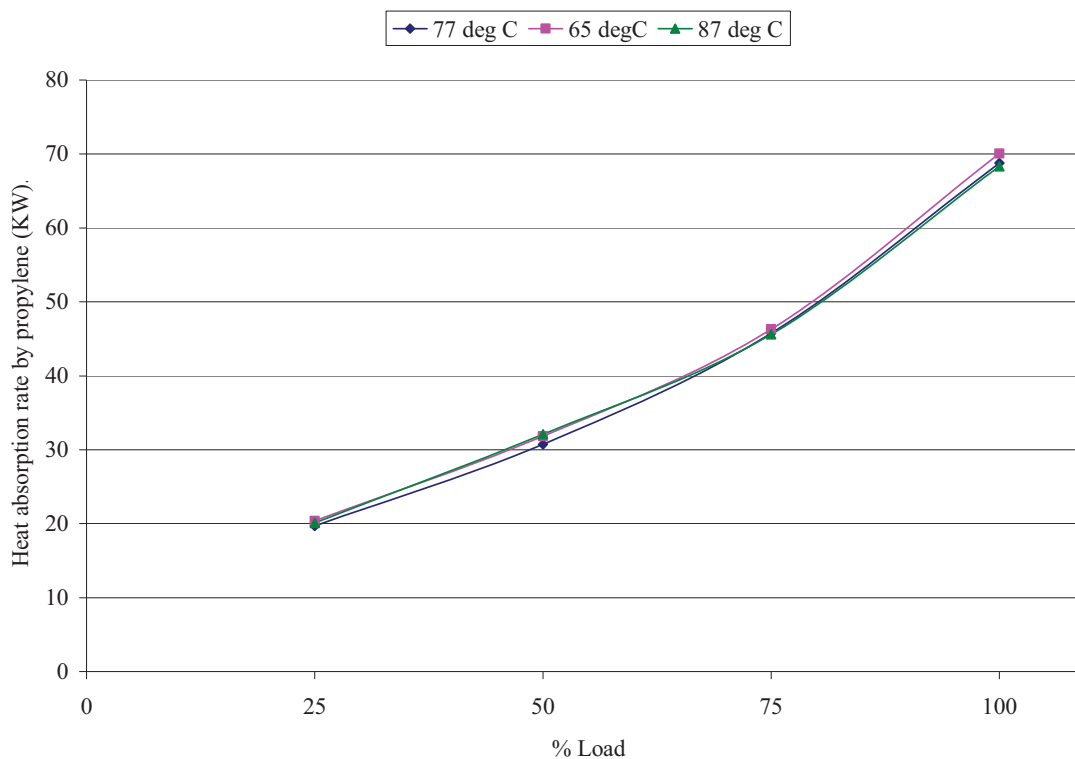


Figure 3.11. Absorbed heat by propylene at 87°C, 77°, and 65°C as heat exchanger outlet temperature.

Heat absorbed by propylene: The total heat present in the exhaust was calculated by assuming no heat exchanger attached to the engine exhaust pipe and allowing all the heat to be released to the atmosphere. For this case, the percentage of heat that can be recovered from exhaust was calculated by the ratio of heat absorbed by the propylene and total exhaust heat. The percentage of heat that can be recovered from the exhaust was observed to be constant for a 50-hour experimental run, which was about 52%. This is graphed in Figure 3.12.

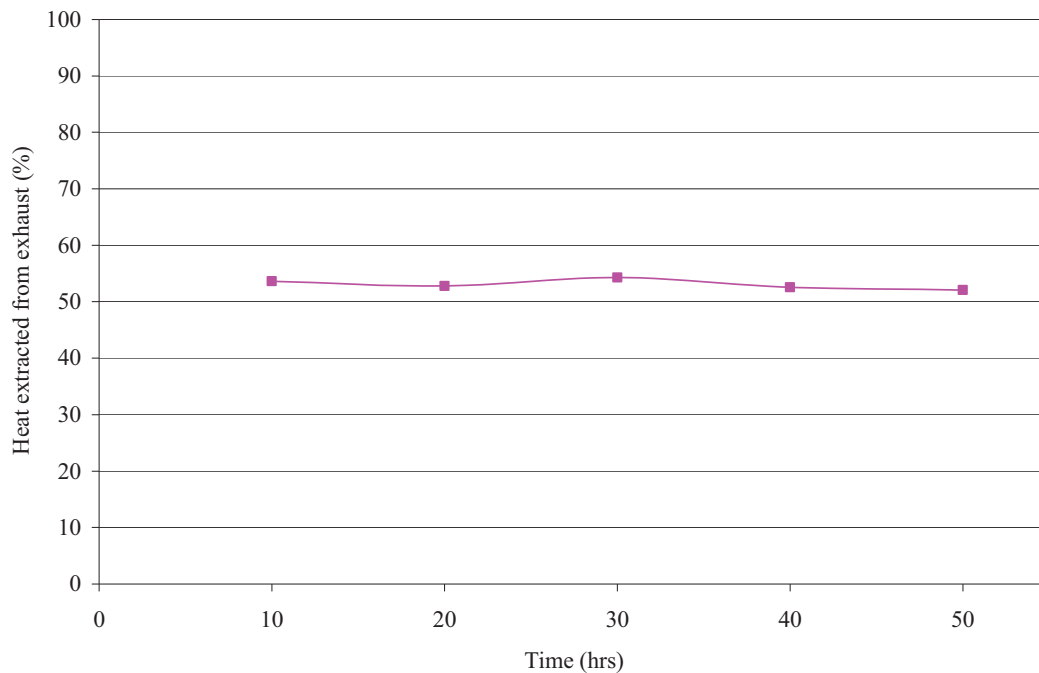


Figure 3.12. Percentage of heat extracted from the total exhaust heat during a 50-hour experimental run time.

At different heat exchanger outlet temperatures on the fluid side, the heat recovery rate followed the same trend. The recovery rate by the heat exchanger was seen to be higher at lower engine loads than at higher engine loads. This can be explained as: at low engine loads the heat content in the exhaust gas was less which the coolant was able to recover most part of it that would show a greater recovery rate by the heat exchanger and vice versa. At higher loads, however, the unit heater needed to be much larger to attain better recovery. For practical application, as we did not deal with the unit heater, the recovery rate remained constant. Figure 3.13 details the recovery rate in different cases. The decrease in the recovery rate in each case can be better explained now as the result of exhaust heat content and the dissipated heat capability of the unit heater. With a larger unit heater, the recovery rate will stabilize.

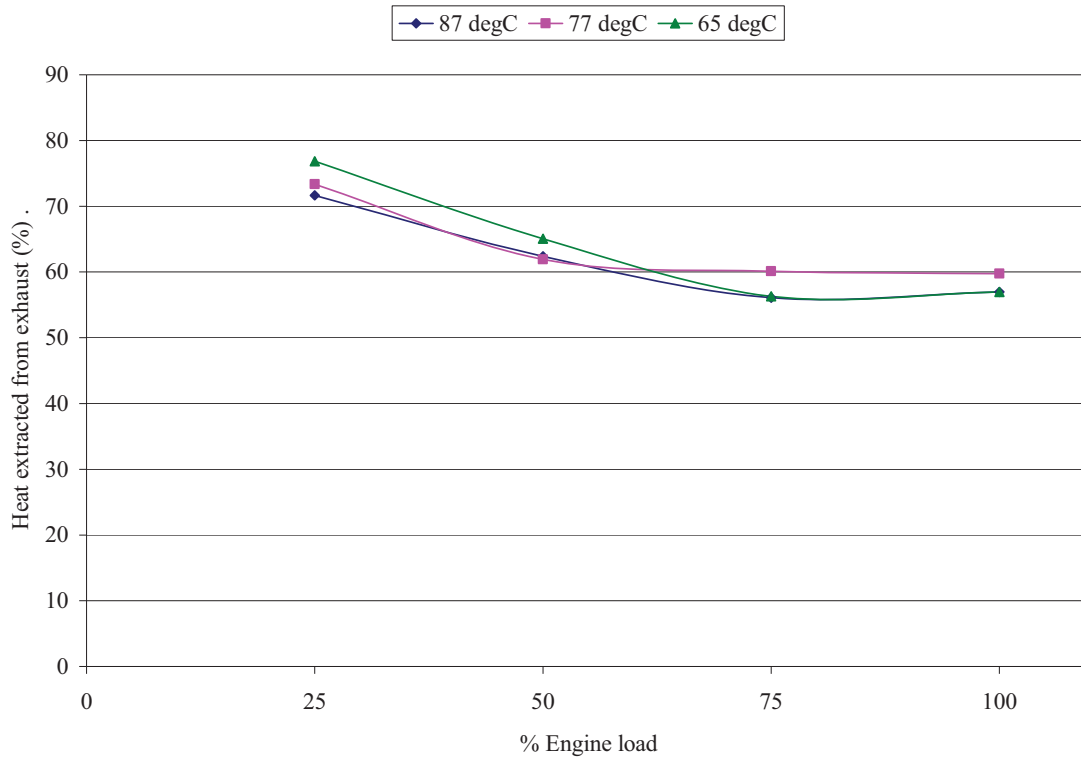


Figure 3.13. Percentage of heat extracted from the total exhaust heat at different heat exchanger outlet temperatures on the fluid side.

3.3.3 Efficiency

Efficiency is the percentage of the ratio of amount of heat gained by the propylene and the heat loss by the exhaust. The efficiency of the heat exchanger was constant throughout the experimental process. The efficiency of the heat exchanger was calculated to be 85%. The related graph is shown in Figure 3.14.

3.3.4 Soot Accumulation

The accumulation of soot in the heat exchanger was considered a critical performance parameter, as large accumulations of soot are known to have a strong negative effect on the performance of heat recovery systems. Over a span of 350 hours of run time, the total soot produced by the exhaust gas was expected to be 4000 to 6000 grams, as much of the PM passes through the heat exchanger.

After the experiments, the heat exchanger was dismantled. No significant amount of soot was seen deposited on the tube fins or on the shell side that would affect the heat transfer rate. Only a thin layer of soot was seen on the tube fins. The thickness of the soot was considered to be a few hundredths of a millimeter. On cleaning the heat exchanger, about 150 grams of soot was found to be accumulated, which is far less than the 6 Kg maximum expected. With this small amount of accumulated soot, the heat exchanger

would need maintenance not more than two times every year. Figure 3.15, Figure 3.16, and Figure 3.17 show the soot accumulation on the heat exchanger.

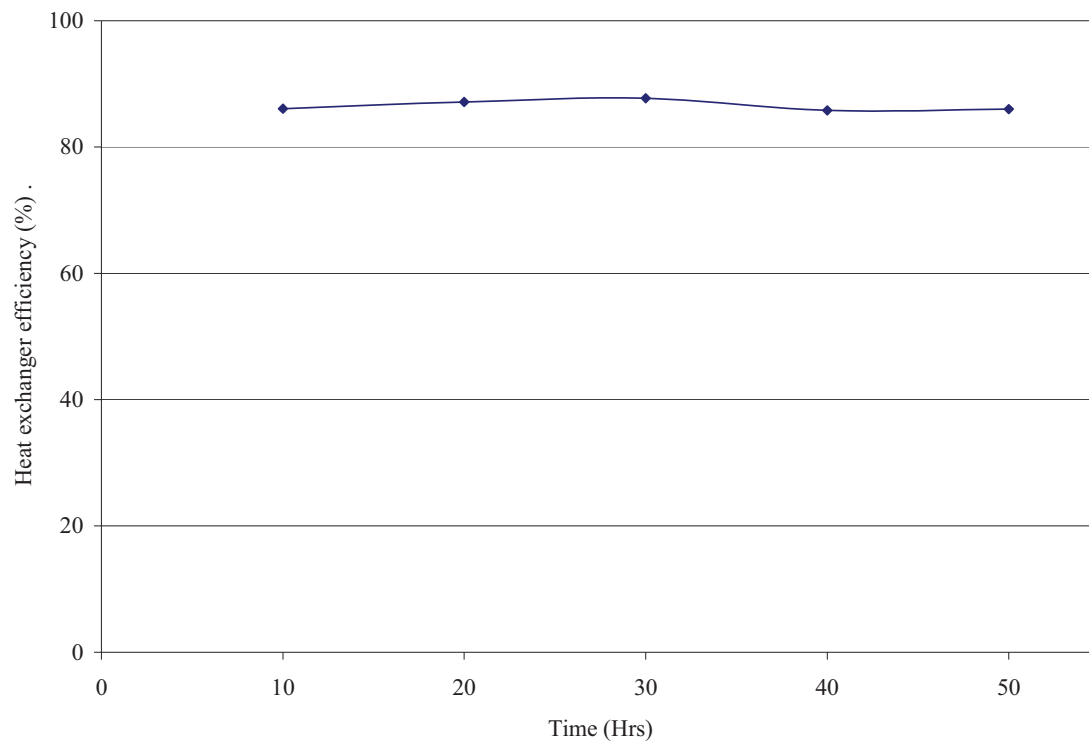


Figure 3.14. Efficiency of the heat exchanger.



Figure 3.15. Shell side soot accumulation.

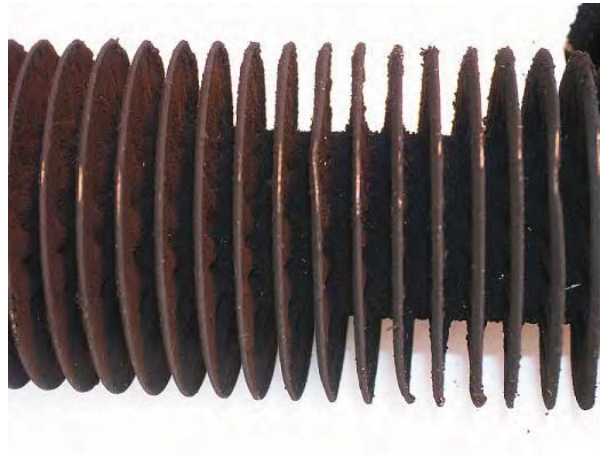


Figure 3.16. Soot accumulation on the fins.



Figure 3.17. Soot accumulation on the core side.

3.4 Corrosion Experiment

The corrosivity of the exhaust was evaluated by collecting condensate and evaluating both the pH and corrosion. In order to collect the condensate, the exhaust gas from the muffler was passed through a finned tube placed in a cold environment. The condensate was collected for different burning fuels. Stainless steel (SS316L) and mild steel (C1010) from Metal Samples were the corrosion coupons that were used in this experiment. The pH values of the condensates are tabulated in Table 3.7.

Table 3.7. pH value of exhaust condensate with the respective fuel burned

Fuel type	pH value
S1	3
S2	4
Conventional diesel	2
Blend*	3
Biodiesel	3

* Blend = 20% biodiesel + 80% conventional diesel

The exhaust condensate was then tested for its corrosive effect on different metals in two different cases:

Case 1: No exposure to air

Case 2: Exposure to air

The setup is shown in Figure 3.18 and Figure 3.19.

In both cases, the coupons were completely immersed in the exhaust condensate. In Case 1, the containers were airtight, while in Case 2, the containers were left to air without airtight caps.



Figure 3.18. No exposure to air.



Figure 3.19. Exposure to air.

The experiment was conducted for nearly four days for each coupon. In both cases, no corrosion was observed on the surface of SS316L coupons, but corrosion was observed on the surface of C1010 coupons. The corroded material was cleaned and checked for its weight. There was a weight loss in C1010 coupons. The changes in the actual weight of the C1010 coupons are tabulated in Table 3.8 for Case 1 and Case 2, and the respective bar graphs are shown in Figure 3.20 and Figure 3.21.

Table 3.8. Weight loss for C1010

	Conventional diesel	S1	S2	Blend
Case 1 (g)	0.0043	0.0013	0.0015	0.0046
Case 2 (g)	0.0067	0.004	0.0049	0.0048

When the heat exchanger was dismantled, the corrosive effect of exhaust gas on the heat exchanger was also investigated by examining the surface for the existence of corrosion spots on the tube and shell side. No trace of any such corrosion was observed. The reason seems to be that the exhaust temperature was always kept above the dew point of the acids and water vapor. This resulted in an absence of condensate in the heat exchanger throughout the run time. The construction material of the heat exchanger is SS316L because it reduces corrosion. This is of concern because even though the exhaust temperature was maintained above the dew point, there might be some acids formed during startup and shutdown that might cause corrosion.

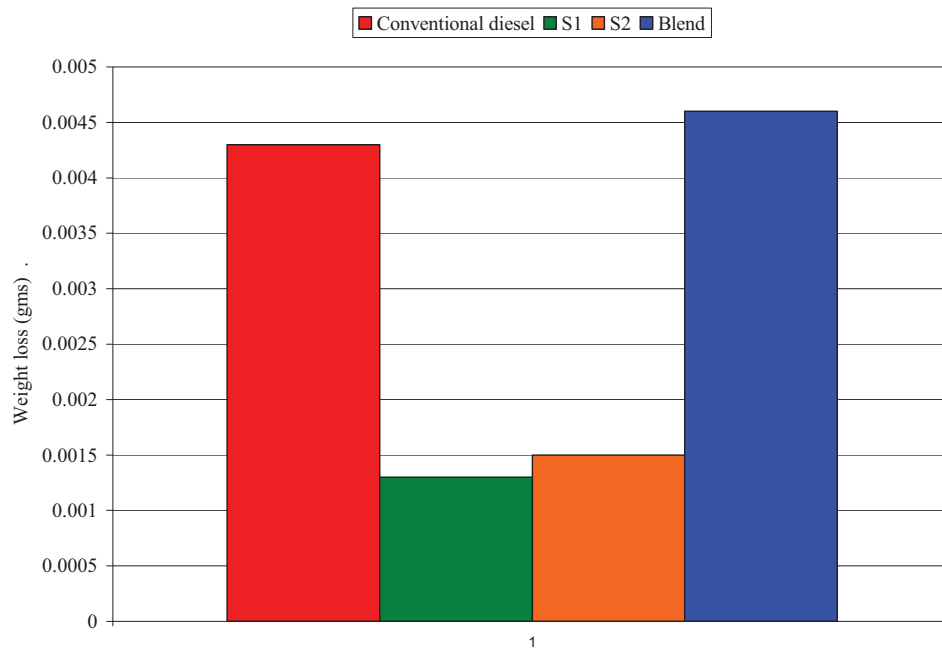


Figure 3.20. No exposure to air.

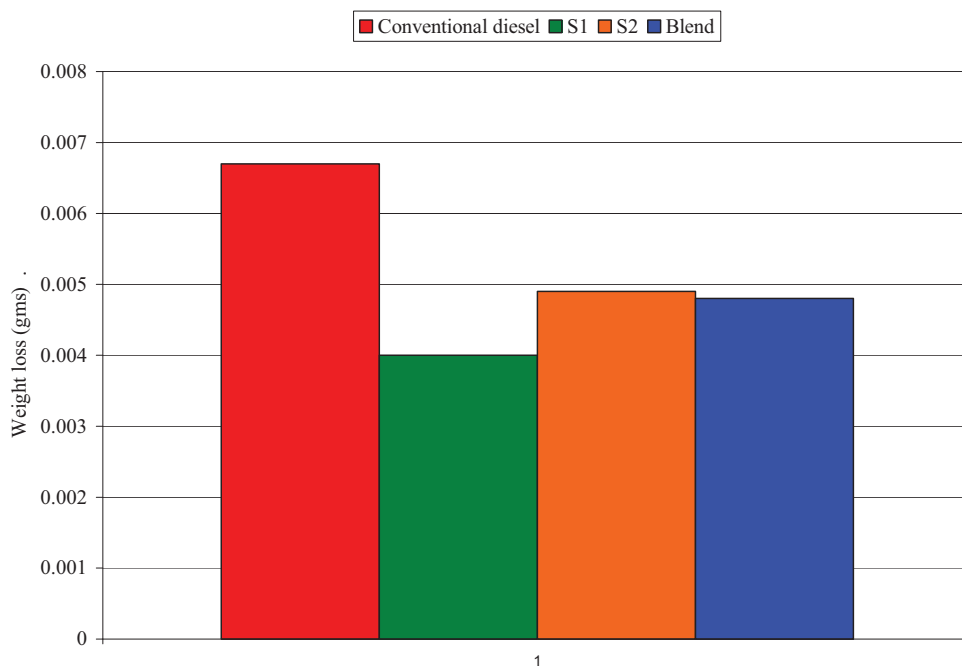


Figure 3.21. Exposure to air.

3.5 Economic Analysis and Maintenance

Economic analysis was based on the present heat recovery system of the test engine built at UAF, and it assumed 100% use of heat recovery. For further calculations, the heat recovery rate used was 60 kW at rated load 8 hours per day (Table 3.9).

The heating value for conventional fuel = 130,000 BTU/gal

The fuel flow rate at 100% load = 8 gal/hr

Initial cost of the recovery system = \$30,000

Installation cost = \$6,000 (\$75/hr x 8 hours x 10 days)

Airfare, lodging, meals = \$1,950 (600 RTAF + \$90/day x 15 days)

Total capital cost = \$37,950

Simple breakeven in terms of fuel cost savings = $\$37,950/\$11,461 = 3.3$ years

Table 3.9. Estimated annual savings

	Per hour	Per day	Per year
Heat recovery	204,728 BTU	1,637,824 BTU	597 MBTU
Fuel consumption savings	1.57 gal	12.56 gal	4584.4 gal
Fuel cost savings @ \$2.50/gal	\$3.90	\$31.40	\$11,461.00

Payback time: The payback time was calculated based on varying interest rates and increasing fuel prices. The graph in Figure 3.22 shows respective payback times with different interest rates and fuel prices, assuming 100% use of the recovered heat. The value of fuel savings increases with an increase in the fuel prices that would decrease the payback time. Therefore, the graph in Figure 3.22 shows a decreasing curve with increasing fuel prices.

Fuel Sensitivity: The value of fuel savings depends on the present fuel cost. As the fuel prices alter considerably over a span of years, a fuel sensitivity analysis was performed. The curve in Figure 3.23 shows the fuel savings over a period of 5 years against the fuel cost per gallon. If the fuel price is above \$2/gal, the principle amount for the project will be attained in less than 5 years in terms of fuel savings.

The heat recovery system maintenance cost was based on one day of labor (\$75/hr) and a flight ticket (\$600), which comes to \$1200 every visit. The maintenance costs also include additional money (\$300) every year for supplies. Maintenance is required every 6 months.

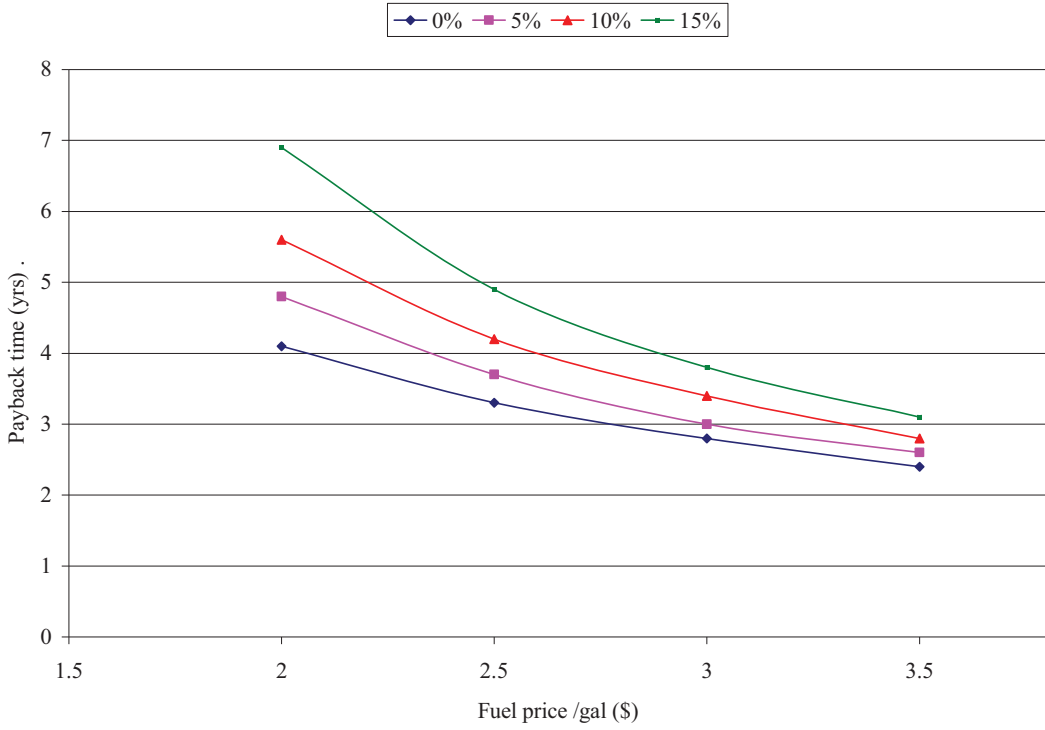


Figure 3.22. Payback time with respect to fuel price and interest rate.

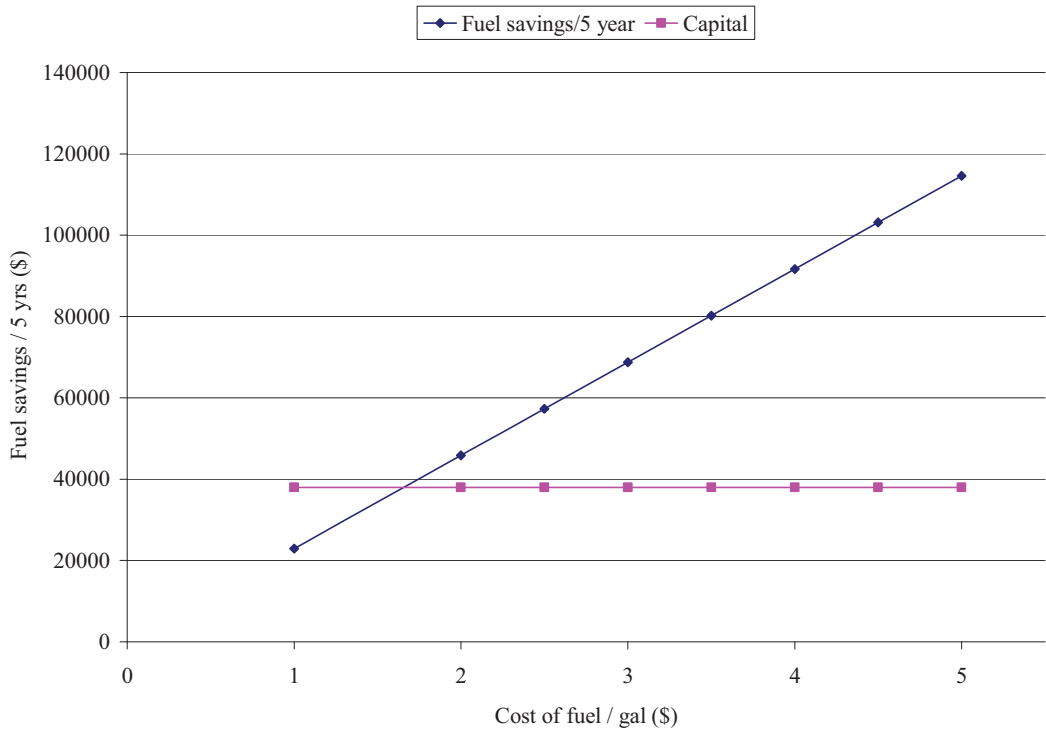


Figure 3.23. Fuel sensitivity curve.

3.6 Exhaust Emissions, Heat Content, and Temperatures of the Three Fuels

This section discusses the emissions, heat content, and temperatures of the exhausts obtained from an engine running on conventional diesel, synthetic fuel, and conventional diesel with different levels of a small amount of hydrogen. Heat content was estimated using exhaust mass flow rate, specific heat, and the temperature difference between the exhaust manifold and 170°C, which is the dew point of the sulfurous acid of exhaust. Exhaust flow rate was estimated using measured intake air flow rate and fuel consumption rate.

3.6.1 Conventional Diesel and Synthetic Fuel

Emissions: Table 3.10 shows the exhaust emissions for the two different fuels. It has been observed that the synthetic fuel performed better in every emission category.

- In comparison with conventional diesel, CO emission decreased by 40%, NO_x emission decreased by 9%, and THC emission decreased by 37%.

Table 3.10. Emissions for diesel and synthetic fuel

Test fuel	CO (g/kW-h)	NO _x (g/kW-h)	THC (g/kW-h)	Generator fuel efficiency (kW-h/gal)
Diesel	2.657	18.32	0.334	14.64
Synthetic	1.612	16.97	0.21	14.15

Heat Content and Temperatures: The properties of exhausts produced by different fuels at different engine loads are shown in Table 3.11, Table 3.12, and Table 3.13.

- For full load, the difference in specific heat between the exhausts of the two fuels was 0.6%, the difference in the exhaust mass flow rate was 3.6%, the difference in the exhaust temperature was 4% (or 20°C), and the difference in heat content was 9.9%.
- For 50% load, the difference in specific heat between the exhausts of the two fuels was 0.3%, the difference in the exhaust mass flow rate was 1.5%, the difference in the exhaust temperature was 2.4% (or 9°C), and the difference in heat content was 3.3%.

According to Table 3.13, the difference in calculated heat content between the exhausts of the two fuels was 9.9% for full load and 3.3% for 50% load. The estimated accumulated experiment uncertainty for heat content calculation, which involves at least 4 different measurements, is about $\pm 3\%$. In addition, environmental conditions can influence the heat content and temperature of exhaust. For 50% load, a 3.3% difference in heat content is within experiment uncertainty. For 100% load, a 9.9% difference in heat content resulted from a 20°C difference in exhaust temperature and a 3.6% difference in

heat flow rate. The heat content and temperature difference for full load may have some influence on the amount of heat recovered from the exhaust. However, the influence on the total heat recovered by a heat recovery system may be largely reduced when the engine load pattern (or average load about 70%), the design of the heat exchanger, and heat losses from the system (i.e., pipes, heat exchanger, etc.) are all taken into consideration. Table 3.10 shows that the emissions produced by synthetic fuel are less than conventional diesel. In addition, synthetic fuel is expected to have less PM emission [26, 27, 28] due to its zero aromatics and less corrosivity due to its zero sulfur content. Therefore, synthetic fuel is expected to have a slight disadvantage in amount of heat recovered and an advantage in maintenance, with less soot accumulation and corrosion.

Table 3.11. Exhaust property of conventional diesel fuel

% Load	Exhaust flow rate Kg/s	Overall Cp (J/gm-K)	Exhaust temp (T_{in} °C)	Exhaust temp (T_{out} °C)	Q (kW)
50	0.16	1.71	371.05	170.00	54.26
100	0.24	1.79	518.86	170.00	151.25

Table 3.12. Exhaust property of synthetic fuel

% Load	Exhaust flow rate Kg/s	Overall Cp (J/gm-K)	Exhaust temp (T_{in} °C)	Exhaust temp (T_{out} °C)	Q (kW)
50	0.16	1.70	362.09	170.00	52.46
100	0.23	1.78	498.25	170.00	136.31

Table 3.13. Comparison of exhaust property between conventional diesel fuel and synthetic fuel

% Load	% difference in exhaust mass flow rate	% difference in Cp	% difference in exhaust temperatures	% difference in exhaust heat
50	-1.50	0.29	2.42	3.31
100	3.60	0.64	3.97	9.87

3.6.2 Conventional Diesel and Conventional Diesel with a Small Amount of Hydrogen:

Emissions: Emissions data for different flow rates of hydrogen were plotted. Figure 3.24 shows the plot for hydrogen flow rate in lpm versus exhaust gas emissions in amps. The data were plotted for 0, 4, 10, 30, 50, 100, and 150 lpm of hydrogen and were compared with a 0 lpm hydrogen flow rate. The following results were observed:

- When compared with 0 lpm hydrogen, the amount of O₂, NO, NO_x, and SO₂ in the exhaust gases did not vary significantly with the hydrogen flow rate.

- The emission of nitrogen dioxide (NO₂) increased significantly—by 155% between 0 lpm and 150 lpm hydrogen—with the increase of hydrogen concentration.
- The emission of CO has no regular trend. When compared with 0 lpm hydrogen, the change in CO concentration is not significant.

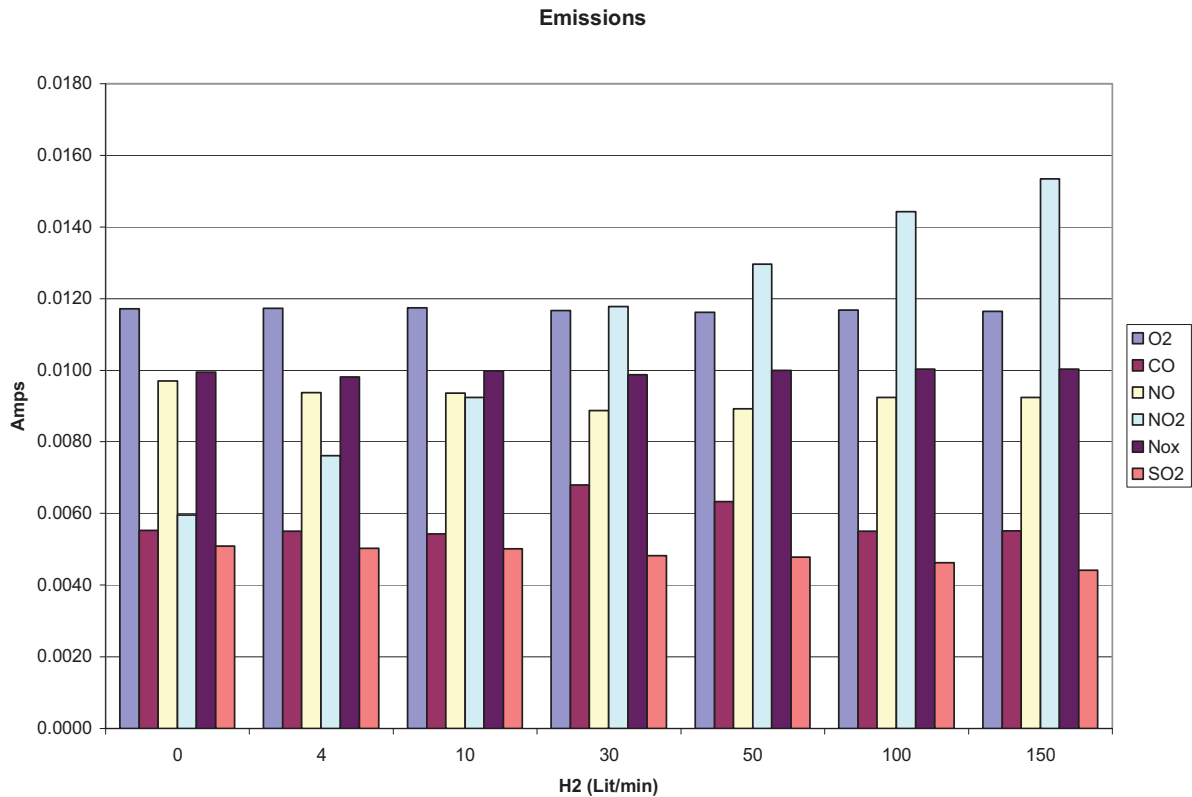


Figure 3.24. Comparison of exhaust gas emissions for different hydrogen flow rates.

Heat Content and Temperatures: The results for heat content and temperatures are given in Table 3.14, and discussed below.

Table 3.14. Heat in exhaust for different hydrogen flow rates.

H ₂ (lpm)	Exhaust flow rate Kg/s	Overall Cp (J/gm-K)	Exhaust temp (T _{in} °C)	Exhaust temp (T _{out} °C)	Q (kW)
0	0.153	1.72	395.15	170	59.07
10	0.152	1.72	395.02	170	58.86
50	0.152	1.72	402.53	170	61.01
150	0.148	1.72	404.94	170	60.11

- The exhaust gas mass flow rate, specific heat, and temperature did not vary significantly with the hydrogen flow rate.
- The calculated exhaust gas heat energy variation is within the experiment uncertainty range, so the variation in exhaust gas heat content is insignificant.

According to Table 3.14, the insertion of a small amount of hydrogen into the intake air stream has nearly no effect on the quantity and quality of exhaust heat and, therefore, has minimum effect on exhaust heat recovery and corresponding economics, as predicted.

3.7 Economic Analysis Program for Exhaust Heat Recovery System

A software program was developed for estimating the economic feasibility of installing an exhaust heat recovery system at any Alaskan village power plant for space heating and water loop temperature maintenance. This program was developed on Visual Basic for Application (VBA) in Microsoft Excel. The factors involved in the analysis include information about existing village community water loop and heating system infrastructure, existing heat recovery facility of power plant, engine size, power plant configuration, load pattern, and power plant location. The program uses given information to design the recovery system based on the trade-off between cost and amount of heat recovered. The designed system is analyzed for amount of heat recovery, energy requirement for operation, and maintenance requirements. Analyzed results are incorporated with capital cost, operation, and maintenance cost to evaluate the breakeven point and payback time.

In this program, two types of exhaust heat recovery systems can be designed and analyzed for any power plant. The first type uses only one gas-to-liquid (exhaust to coolant)—that is, shell and tube—heat exchanger, as shown in Figure 3.25. In this system the coolant from the community loop is pumped directly into the heat exchanger. The program calculates various physical parameters of the heat exchangers, such as heat transfer area required, overall heat transfer coefficient of heat exchanger, etc.

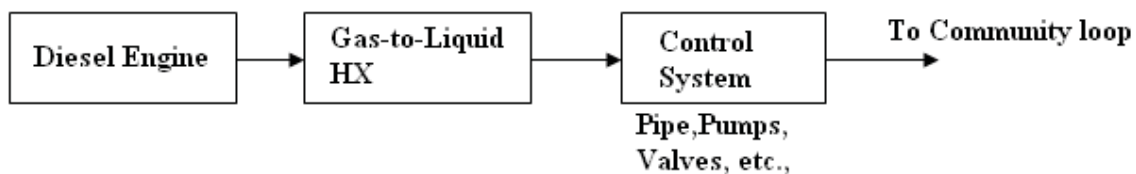


Figure 3.25. Line diagram of exhaust heat recovery system (one heat exchanger).

The program then goes to pressure-drop calculations in which the pressure drop in the pipe and piping components between the community loop and the heat exchanger (including the heat exchanger) is estimated. From the program library, the user can select various pipe components (such as valves, elbows, and strainers) which account for pressure drop in the system. Some of these selections are made by default, and the user can override them. Based on the pressure drop in the control system, the program suggests a pump size. The user can override the pump size and make another choice.

Then the program goes to cost estimates of the system in which capital investment cost and operation and maintenance costs are calculated. Capital costs include the cost of the heat exchanger, pipe components, pump, installation, etc. Operation and maintenance costs include operation of the system and frequency of maintenance, labor cost for maintenance, etc. Then the program goes to economic analysis, where the heat absorbed by the coolant, the capital costs and operation and maintenance costs (previously calculated), and the fuel costs and interest rates are utilized to do the economic feasibility study. The result of the economic analysis is represented as payback period, breakeven point, and profit gained for the given lifetime of the system. Finally, a copy of the all computations can be saved in the form of a Word document.

The second type of exhaust heat recovery system is one that uses two heat exchangers: a gas-to-liquid (exhaust to coolant)—that is, shell and tube heat exchanger—and a liquid-to-liquid (coolant to water) plate heat exchanger, as shown in Figure 3.26. The high temperature coolant, which is circulated between the gas-to-liquid heat exchanger and the liquid-to-liquid heat exchanger, takes heat from the exhaust in the shell and tube heat exchanger and gives off heat to the water in the plate heat exchanger. In this program, the design and analysis of both the shell and tube heat exchanger and the plate heat exchanger can be done at different loads. The program calculates the physical parameters of both heat exchangers, such as overall heat transfer coefficients, heat transfer area required for both heat exchangers, and amount of heat absorbed by both coolants.

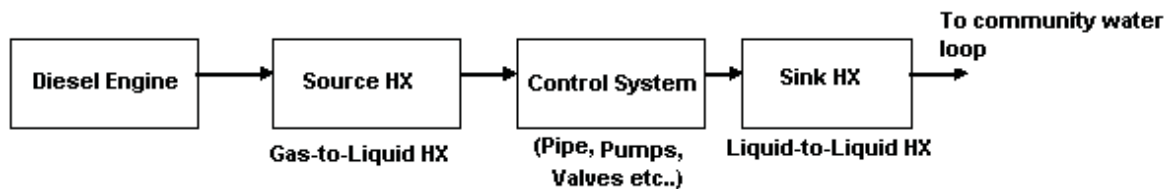


Figure 3.26. Line diagram of exhaust heat recovery system (two heat exchangers).

The program then goes to pressure-drop calculations in the control system, that is, pipe and pipe components (valves, strainers, etc.) between both heat exchangers (the shell and tube HX and the plate heat exchanger), including the heat exchangers. The pressure drop, cost estimations and economic analysis calculations, and the program outputs are similar to the first type of heat recovery system described above. At the end, all computations can be saved in the form of a Word document.

The following example explains in detail the program usage for the second type of heat recovery system in which two heat exchangers are used. In this example, the exhaust conditions of the UAF diesel engine at different loads are used for calculations.

3.7.1 Results

1. The computer program for the exhaust heat recovery system was developed on the Visual Basic for Application (VBA) platform in Microsoft Excel.

2. The program was validated with the experimental results of the exhaust heat recovery system (which is the first task of this project), and the outputs obtained in the program were within comparable range of the experimental results.
3. The program was evaluated for a midsize diesel engine (DD50) which has 125 kW rated power at 1200 rpm. Earlier, an exhaust heat recovery experiment was conducted on the same diesel engine. A comparison of the experimental results and the program outputs are presented below.
 - The heat exhaust heat exchanger surface area used was 8 m^2 , and the overall heat transfer coefficient of the exhaust heat exchanger was $46 \text{ W/m}^2\text{-K}$, which is close to 9 m^2 and $37 \text{ W/m}^2\text{-K}$ calculated by the program.
 - The heat absorbed by coolant in the exhaust heat exchanger at 100%, 75%, 50%, and 25% loads are 68.76 kW, 45.75 kW, 30.75 kW, and 19.71 kW, respectively, and the program calculated values are 76.54 kW, 55.6 kW, 37.8 kW, and 20 kW at respective loads, which are in close acceptance with experimental values.
 - The pressure drop used for selecting the pump in the experiment is 10 psig or 23 feet of water head. The program calculated the total pressure drop in the system to be 9 psig or 21 feet of water head.
 - The calculated payback period for the experimental setup was 2.9 years at a fuel price of \$3.50/gal and 10% interest rate, assuming 100% use of recovered heat which is taken as 60kW. The calculated value of the program for the same amount of heat recovery rate, fuel price of \$3.50/gal, and 10% interest rate was 2.6 years, which is close to the experimental value.
4. The program can do additional tasks, such as analysis of the system for different intermediate loads; can take into account the pressure drop in a liquid-to-liquid heat exchanger; and can accommodate village heating loop modification cost estimates.
5. The program was written in Microsoft Excel, which is available on almost all personal computers. The program instruction manual is given in the Appendix.

Chapter 4 Conclusions

4.1 Experimental Economic Analysis of Exhaust Heat Recovery

Experimental work was conducted using an experimental engine to check the feasibility and economic effect of recovering exhaust heat energy for useful applications. According to the analysis from the experimental data, the following conclusions are made:

1. A procedure of heat recovery system design and analysis was demonstrated. This procedure is applicable to exhaust heat recovery system designs for many Alaskan village diesel generator sets.
2. Performance and economic results will be different from one case to another. Analysis is recommended before the application of an exhaust heat recovery system to a village generator set.
3. The performance of an exhaust heat exchanger is reliable and consistent.
4. In our case, about half the exhaust heat was recovered, which kept the heat exchanger exhaust outlet temperature high enough to avoid major maintenance problems.
5. No effects were observed on engine maintenance frequency due to the heat recovery system.
6. According to the soot analysis, the estimated time for heat exchanger maintenance is about two days every year.
7. Corrosion was not observed to be a problem in the laboratory test of 350 hours.
8. Operation cost is largely case-dependent. Influential parameters would include diesel fuel cost, the electrical power pattern, the use of heat, the existing infrastructure of the community heating system, etc.
9. According to these experimental results, the payback time for 100% use of recovered heat would be less than 3 years at a fuel price of \$3.50 per gallon, an interest rate of 10%, and an engine operation of 8 hours per day. For 80% use of recovered heat, the payback time would be less than 4 years.

4.1.1 Future Work

The following is future work that can be done as an extension to the present work:

1. The present engine-generator set at UAF will allow testing of other fuels. Fuels such as extra low sulfur fuel and biodiesel can be used for testing (e.g., for soot property, soot accumulation, and corrosivity).
2. Field tests need to be done.
3. The control system could be improved.
4. Performance could be investigated by applying exhaust heat recovery for different heating applications such as power and desalination.

5. The current exhaust heating system could be modified to an exhaust Rankine cycle system for exhaust heat recovery for power.

4.2 Evaluation of Exhaust Heat Contents and Temperatures for Different Fuels

Heat content and average temperatures of exhaust from synthetic diesel, conventional diesel, and conventional diesel with different levels of a small amount of hydrogen were evaluated using experimental data. Based on the study results, conclusions about the expected effects of the exhausts of different fuels on heat recovery are derived.

4.2.1 Synthetic Diesel Versus Conventional Diesel

Based on the experimental data, the conclusions are as follows:

1. In comparison with conventional diesel, synthetic fuel has a slight disadvantage in amount of heat recovery.
2. In comparison with conventional diesel, synthetic fuel has an advantage in maintenance for exhaust heat recovery application.

Future work: Since the environmental condition may have a non-negligible effect on exhaust temperature and mass flow rate, more experimental data may be needed to improve the reliability of the conclusion.

4.2.2 Diesel Fuel and Diesel Fuel with a Small Amount of Hydrogen

The self-ignition concentration of hydrogen is 4% by volume in air. In this experiment, the maximum level of 150 lpm of hydrogen amounts to 1.5% by volume of hydrogen in the intake air, which may be an insignificant volume. Based on the experimental data, conclusions are as follows:

1. A significant variation in emissions and exhaust heat content were not observed at this volume.
2. Adding a small amount of hydrogen into the engine intake manifold causes no economic effect on exhaust heat recovery application.

Future work: More tests with a hydrogen concentration higher than 4% by volume is desired in the future. With the hydrogen concentration higher than the self-ignition concentration, significant changes in exhaust heat content, emissions, and engine performance may be observed.

4.3 Economic Analysis Program for Exhaust Heat Recovery

1. Results given in the previous chapter show that the economic analysis program works well for studying the economic feasibility of installing exhaust heat recovery systems on rural diesel generators, as validated by experimental results.
2. The program can be improved further for incorporating more design data, thus providing more accurate design and analysis and more capable design and analysis tools.

3. The program can be easily extended to other exhaust heat recovery applications such as electric power generation by organic Rankine cycle, desalination, etc.
4. The cost estimations and economic analysis part of the program can be used for studying the economic feasibility of other exhaust heat recovery system applications such as organic Rankine cycle, desalinations, etc.

4.3.1 Future Work

In comparison with heating applications, the application of electrical power is more flexible in implementation, more efficient in energy transmission, and applicable year-round in Alaska. In general, the efficiencies of the up-to-date prototypes developed for power applications are still much lower than those for exhaust heating applications. However, it is expected that the efficiency of exhaust for power will be improved and become competitive in the near future. To develop a computer module for heat-to-power conversion (e.g., organic Rankine cycle) and incorporate it with the current computer program would make the current program a more useful tool for both exhaust heat-to-power research and exhaust heat-to-power economic analysis.

References

1. *Alaska Electric Power Statistics*. 2003. Prepared by the Institute of Social and Economic Research, University of Alaska Anchorage, for the Alaska Energy Authority.
2. Logbook Information, 2002-2003. Alaska Village Electric Corporative, Inc.
3. Grillot, J., and Icart, G. 1988. Fouling of a cylindrical probe and a finned tube bundle in a diesel exhaust enviroment. *Experimental Thermal and Fluid Science*, 14(4), 442–454.
4. Telang, A.U. 2005. Testing of syntroleum fuels in diesel power plants suitable for Alaska. Master's thesis, University of Alaska Fairbanks.
5. Diesel Emissions Control: Sulfur Effects Project, Summer of Reports. National Renewable Energy Laboratory.
6. Ganapathe, V. Minimizing acid condensation concerns. <http://vganapathy.tripod.com/corros.html>.
7. Syntroleum S-2 Technical Bulletin. Syntroleum Corporation.
8. Vaglieco, B.M., Merola, S.S., Anna, A.D., and D'Alessio, A. 2002. Spectroscopic analysis and modeling of particulate formation in a diesel engine. *Journal of Quantitative Spectroscopy & Radioactive Transfer*, 73, 443–450.
9. Snelling, D.R., et al. 1999. Particulate matter measurements in a diesel engine exhaust by laser-induced incandescence and the standard gravimetric procedure. Society of Automotive Engineers, Inc.
10. Mathis, M.M., et al. 2005. Influence of diesel engine combustion parameters on primary soot particle diameter. American Chemical Society.
11. Kitsopanidis, I., and Cheng, W.K. 2006. Soot formation study in a rapid compression machine. *ASME*, 128.
12. Truedsson, G.R. 1980. Industrial waste heat recovery – A case in point. Plant Energy Conservation Council. H.W. Wilson Company.
13. Vernean, A. 1984. Recovery from exhaust gas on a diesel engine. VDI-Berichte 539, 501-513, VDI-Verlag, Dusseldorf.
14. Vuk, C.T. 2007. Electric turbo compounding technology update. Diesel Engine Efficiency and Emissions Research Conference.
15. Nelson, C.R. 2008. Cumins waste heat recovery. Diesel Engine Efficiency and Emissions Research Conference.
16. Patterson, D.J., and Kruiswyk, R.W. 2008. An engine system approach to exhaust waste heat recovery. Diesel Engine Efficiency and Emissions Research Conference.
17. Vazquez, J., et al. 2005. State of the art of thermoelectric generators based on heat recovery from exhaust gases of automobiles. 7th European Workshop on Thermoelectrics.
18. Haider, J.G., et al. 2001. Waste heat recovery from exhaust of low-power diesel engine using thermoelectric generators. 20th International Conference on Thermoelectrics, Beijing, China, 413–417.
19. Shock, H. 2008. Thermoelectric conversion of waste heat to electricity in an IC engine powered vehicle. Diesel Engine Efficiency and Emissions Research Conference.

20. Fundamentals. 1997. ASHRAE Handbook.
21. Kuppan, T. 2000. *Heat Exchanger Design Handbook*. Marcel Dekker.
22. Kreith, F. 2000. *The CRC Handbook of Thermal Engineering*. CRC Press.
23. Screening Report for Rural Energy Plan. 2001. Prepared for Alaska Industrial Development and Export Authority, Northern Economics, Inc.
24. Alaska Rural Energy Plan. 2004. Prepared for Alaska Energy Authority.
25. Leech, D.J. 1982. *Economic and Financial Studies for Engineers*. John Wiley & Son.
26. Code of Federal Regulations. Chapter 40, Part 80 and Part 86. United States Environmental Protection Agency.
27. Lange, W.W., et al. 1993. The influence of fuel properties on exhaust emissions from advanced Mercedes Benz diesel engine. *Society of Automotive Engineering*. Paper Number 932685.
28. Mitchell, K. 2000. Effects of fuel properties and source on emissions from five heavy duty diesel engines. *Society of Automotive Engineering*. Paper Number 2000-01-2890.
29. "Ground Water in Alaska," Alaska Department of Environmental Conservation, March 2005.

Appendix A: Instruction Manual for Exhaust Heat Recovery System

(Economic Analysis Program for Exhaust Heat Recovery System)

A software program was developed for estimating the economic feasibility of installing an exhaust heat recovery system at any Alaskan village power plant for space heating and water loop temperature maintenance. This program was developed on Visual Basic for Application (VBA) in Microsoft Excel. The factors involved in the analysis include information about existing village community water loop and heating system infrastructure, existing heat recovery facility of power plant, engine size, power plant configuration, load pattern, and power plant location. The program uses the given information to design the recovery system based on the trade-off between the cost and amount of heat recovered. The designed system is analyzed for amount of heat recovery, energy requirement for operation, and maintenance requirements. Analyzed results are incorporated with capital cost and operation and maintenance costs to evaluate the break-even point and payback time.

In this program two types of exhaust heat recovery systems can be designed and analyzed for any power plant. The first type uses only one gas-to-liquid (exhaust to coolant)—that is, shell and tube heat exchanger—as shown in Figure A.1. In this system the coolant from the community loop is pumped directly into the heat exchanger. The program calculates various physical parameters of the heat exchangers, such as heat transfer area required, overall heat transfer coefficient of heat exchanger, etc.

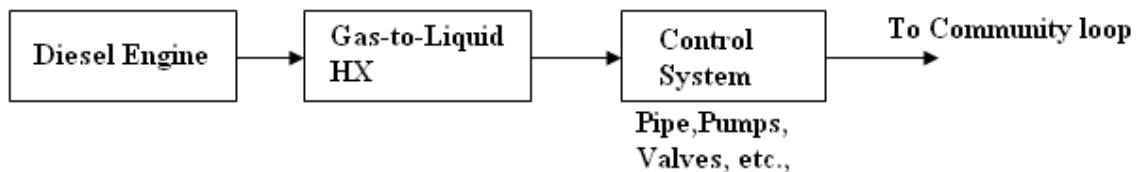


Figure A.1. Line diagram of exhaust heat recovery system (one heat exchanger).

The program then goes to pressure-drop calculations in which the pressure drop in the pipe and piping components between the community loop and the heat exchanger (including the heat exchanger) is estimated. From the program library, the user can select various pipe components (such as valves, elbows, and strainers), which account for pressure drop in the system. Some of these selections are made by default, and the user can override them. Based on the pressure drop in the control system the program suggests a pump size. The user can override the pump size and make another choice. Then the program goes to cost estimates of the system in which capital investment cost and operation and maintenance costs are calculated. Capital costs include the cost of the heat exchanger, pipe components, pump, installation, etc. Operation and maintenance costs include operation of the system and frequency of maintenance, labor cost for maintenance, etc. Then the program goes to economic analysis, where the heat absorbed by the coolant, the capital cost and operation and maintenance (previously calculated),

and the fuel costs and interest rates are utilized to do the economic feasibility study. The result of the economic analysis is represented as payback period, breakeven point, and profit gained for the given lifetime of the system. Finally, a copy of the all computations can be saved in the form of a Word document.

The second type of exhaust heat recovery system is one that uses two heat exchangers: a gas-to-liquid (exhaust to coolant)—that is, shell and tube heat exchanger—and a liquid-to-liquid (coolant to water) plate heat exchanger, as shown in Figure A.2. The high temperature coolant, which is circulated between the gas-to-liquid heat exchanger and the liquid-to-liquid heat exchanger, takes heat from the exhaust in the shell and tube heat exchanger and gives off heat to the water in the plate heat exchanger. In this program, the design and analysis of both the shell and tube heat exchanger and the plate heat exchanger can be done at different loads. The program calculates the physical parameters of both heat exchangers, such as overall heat transfer coefficients, heat transfer area required for both heat exchangers, and amount of heat absorbed by both coolants.

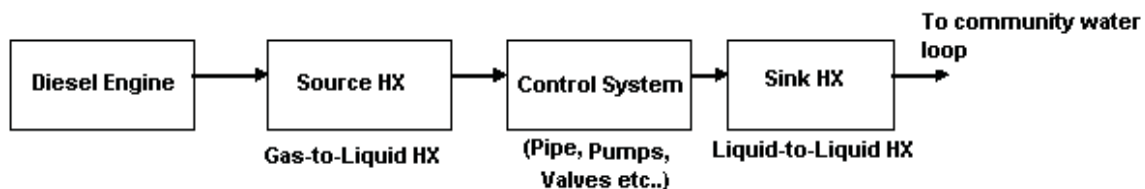


Figure A.2. Line diagram of exhaust heat recovery system (two heat exchangers).

The program then goes to pressure-drop calculations in the control system, that is, pipe and pipe components (valves, strainers, etc.) between both heat exchangers (the shell and tube HX and the plate heat exchanger), including the heat exchangers. The pressure drop, cost estimations and economic analysis calculations, and the program outputs are similar to the first type of heat recovery system described above. At the end, all computations can be saved in the form of a Word document.

The following example explains in detail the program usage for the second type of heat recovery system in which two heat exchangers are used. In this example, the exhaust conditions of the UAF diesel engine at different loads are used for calculations.

Usage of Exhaust Heat Recovery Program

1. An overview of economic analysis

The economic feasibility study for installing an exhaust heat recovery system is done based on expenditure and returns. Figure A.3 shows the flow chart for economic analysis. Expenditures include the total initial capital costs, which include component costs (such as for the heat exchanger, pipe, pipe components, etc.), installation costs (such as for labor, travel, etc.), interest rate on capital and operation and maintenance costs. On the other hand, we have returns in the form of amount of heat recovered, fuel costs, and fuel price escalation charges so that we can calculate the amount saved on fuel and payback period, breakeven point, and profit or loss for the given lifetime of a system.

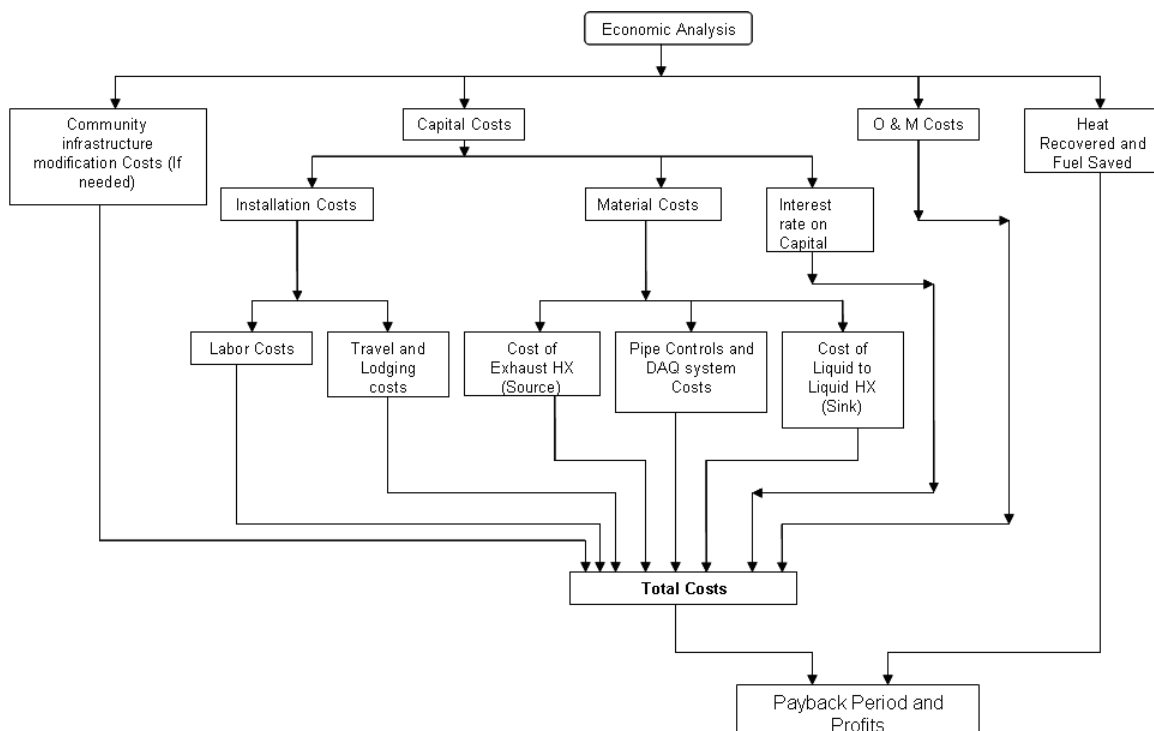


Figure A.3. Economic analysis flow chart.

2. Exhaust heat exchanger design and analysis

Figure A.4 shows the screen shot for calculating different physical parameters of an exhaust heat exchanger. This example is explained by using the exhaust parameters of a DD50 diesel engine located at the UAF campus. In the design of the exhaust heat exchanger (shell and tube heat exchanger), the exhaust conditions of the UAF diesel engine at 100% load are taken. To add the exhaust conditions of another diesel engine or any power plant, click on “Type of Diesel Engine” button. A window for the addition of a diesel engine appears on the screen as shown in Figure A.5. At this window in the fields provided enter the diesel engine or power plant name (to distinguish from others) and exhaust properties at different loads, and click “Add.” Select the diesel engine and click “OK.” The properties of exhaust at 100% load are automatically taken for the design.

Figure A.4. Exhaust heat exchanger design and analysis.

Next, go to selection of coolant and its properties. To select or to add a coolant from or into the program library click on “Select the Type of Coolant.” A window for addition or selection of coolant appears as shown in Figure A.6. For addition, enter the coolant type and its physical properties in the fields provided and click “Add.” Select a coolant type (high temperature coolant) that circulates between exhaust heat exchanger and liquid-to-liquid heat exchanger. From now on, the high temperature coolant (HT coolant) refers to the coolant circulating between the shell and tube heat exchanger and the liquid-to-liquid heat exchanger.

The design of the exhaust heat exchanger can be done based on the mass flow rate of the coolant or based on the coolant outlet temperature. In this example, it is done based on the coolant outlet temperature. Enter coolant inlet and outlet temperatures in degrees Kelvin in the fields provided

Select the type of Diesel Engine Data

Engine	Medot(kg/s)	Tein(in Kelvin)	Teout(in Kelvin)
<input checked="" type="radio"/> UAF Diesel Engine	0.2400	737.0000	460.0000
<input type="radio"/> DD60	0.3000	737.0000	460.0000
<input type="radio"/>			
<input type="radio"/>			
<input type="radio"/>			
<input type="radio"/>			
<input type="radio"/>			
<input type="radio"/>			

OK Delete Engine

Cancel

Add Engine Data

Engine type or Name

	Medot (kg/s)	Tein(Kelvin)	Teout(Kelvin)
100% Load	<input type="text"/>	<input type="text"/>	<input type="text"/>
75% Load	<input type="text"/>	<input type="text"/>	<input type="text"/>
50% Load	<input type="text"/>	<input type="text"/>	<input type="text"/>
25% Load	<input type="text"/>	<input type="text"/>	<input type="text"/>

Add

P.S. Engine Names should be different even if they are of same make (e.g. If you have two engines of DD60, then name them DD60-1 and DD60-2.)

Figure A.5. Adding a diesel engine and exhaust properties.

Select the type of Coolant

Coolant	Specific Heat (Cp in J/kg-K)	Density (kg/m3)	Dynamic Viscosity (Pa-s)	Thermal Conductivity (W/m-K)
<input checked="" type="radio"/> Water	4180.000	1000.000	3.5500E-04	0.600
<input type="radio"/> PropyleneGlycol	2481.000	1036.000	3.2200E-03	0.232
<input type="radio"/> PropyleneGlycol/Water 60/40	3800.000	1048.250	1.3500E-03	0.327
<input type="radio"/> PropyleneGlycol/Water 50/50	3532.000	1042.870	1.1200E-03	0.365
<input type="radio"/> EthyleneGlycol	2347.000	1113.000	2.1200E-03	0.276
<input type="radio"/> EthyleneGlycol 50/50	3281.000	1073.350	9.8000E-04	0.380
<input type="radio"/> EthyleneGlycol 60/40	3084.000	1086.270	1.1000E-03	0.349
<input type="radio"/>				

OK Delete Coolant Cancel

Add a Coolant

Coolant

Specific Heat (Cp in J/kg-K)

Density (Kg/m3)

Dynamic Viscosity (Pa-s)

Thermal Conductivity (W/m-K)

Add

P.S. Coolant Names should be different even if they have same composition (e.g. If you have two different property values for Propylene Glycol 50/50 then give Propylene Glycol 50/50-1 and Propylene Glycol 50/50-2.)

Figure A.6. Coolant selection and addition window.

Next, go to the specifications of the shell and tube heat exchanger. The heat exchanger specifications, such as the tube outer diameter, tube thickness, thermal conductivity of tube material, and fouling-factor specifications, are to be entered in respective fields. The film heat transfer coefficients of exhaust on the shell side and the coolant on the tube side can be input by the user, or the program can calculate the values using heat transfer principles.

The outputs of the exhaust heat exchanger design window are overall heat transfer coefficient of heat exchanger, heat transfer area requirement for heat exchanger, heat absorbed by HT coolant, and effectiveness and efficiency of heat exchanger. If the design is based on the coolant outlet temperature, then the coolant mass flow rate is output and vice versa.

Then, if wanted, the heat exchanger can be analyzed for different intermediate loads by going to analysis mode (click on “Analysis” tab) as shown in Figure A.7.

Diesel Engine data at different loads	
Medot (kg/s)	Tein(Kelvin)
100% Load	0.24, 737
75% Load	0.19, 686
50% Load	0.16, 601
25% Load	0.14, 497

Coolant Data	
Coolant Inlet Temperature (Tcin)	333 Kelvin
Mass Flowrate of Coolant (Mcdot)	1 kg/s, 15.1987 GPM
Coolant Outlet Temperature (Tcout)	Kelvin

Diesel Engine data used for calculations	
Percentage Load (in Percent)	80 %
Mass Flow of Exhaust (Medot)	0.2 kg/s
Exhaust inlet Temperature (Tein)	696.2 Kelvin

Calculations	
Overall Heat Transfer Coefficient of HX (Uo)	36.555 W/m2-K
Area of Exhaust HX (A)	8.907 m2
Mass flowrate of coolant (Mcdot)	kg/s, GPM
Coolant outlet temperature (Tcout)	350.41 Kelvin
Exhaust Outlet Temperature (Teout)	421.63 Kelvin
Heat absorbed by Coolant (Qc)	61492.12 W
Effectiveness of Heat Exchanger (Qactual/Qmax)	0.7558
Efficiency of Heat Exchanger	69.29 %

Figure A.7. Exhaust heat exchanger analysis window.

In the example shown in Figure A.7, the heat exchanger is analyzed at 80% load of engine by interpolating between 100% and 75%. The analysis is done based on mass flow rate of the coolant. In analysis the overall heat transfer coefficient of the heat exchanger and the area of the heat exchanger remain constant from the design mode. The results of the analysis mode are exhaust outlet temperature, heat absorbed by coolant, and effectiveness and efficiency of the heat exchanger. If the analysis is based on the coolant mass flow rate, then the coolant outlet temperature is output and vice versa.

3. Liquid-to-liquid heat exchanger design and analysis

Next, go to Liquid-to-Liquid Heat Exchanger (plate heat exchanger) Design and Analysis. The HT coolant temperature inlet-to-plate heat exchanger is taken to be equal to the HT coolant outlet temperature of the exhaust heat exchanger. If one clicked on “Go to Liquid-to-Liquid HX Design and Analysis” when in design mode, the mass flow rate of high temperature coolant and high temperature coolant inlet temperature for plate heat exchanger (i.e., coolant outlet temperature of shell and tube heat exchanger) are taken from the design calculations, and when in analysis mode, the values are taken from analysis calculations. Figure A.8 shows the design and analysis window for liquid-to-liquid heat exchanger (i.e., plate heat exchanger).

The screenshot shows the 'Liquid-to-Liquid Heat Exchanger Design and Analysis' software interface. It is divided into four main sections: Design, Analysis, Plate Heat Exchanger Specifications, and Calculations. The Design section includes input fields for high temperature coolant properties (type, specific heat, mass flow rate, inlet/outlet temperatures) and low temperature coolant properties (type, specific heat, density, thermal conductivity, dynamic viscosity, inlet/outlet temperatures, and mass flow rate). The Analysis section includes a 'Calculate' button. The Plate Heat Exchanger Specifications section includes input fields for plate thickness, gap between plates, thermal conductivity, convective heat transfer coefficients, and fouling resistances. The Calculations section displays results for overall heat transfer coefficient, area, mass flow rate, outlet temperature, heat absorbed, effectiveness, and efficiency. The bottom of the window features navigation buttons and the UAF logo.

Figure A.8. Plate heat exchanger design and analysis window.

The design and analysis of a liquid-to-liquid heat exchanger is very similar to that of an exhaust heat exchanger. The low temperature coolant can be selected from the library or can be entered manually. The type of heat application, such as space heating or community water loop temperature maintenance, can be selected from the options provided. The physical parameters (overall heat transfer coefficient, heat transfer area required, etc.) of a plate heat exchanger can be calculated based on low temperature coolant mass flow rate or low temperature coolant outlet temperature. In this example we selected based on coolant outlet temperature. The plate heat exchanger specifications can be entered in the next column. Specifications such as plate thickness, gap between plates, thermal conductivity of plate material, and fouling factor of high temperature coolant and low temperature coolant can be entered in respective fields. The convective heat transfer coefficients of high temperature coolant and low temperature coolant can be input by the user or the program can make the calculation. The results of the liquid-to-liquid heat

exchanger (i.e., plate heat exchanger) design are expressed as the overall heat transfer coefficient of the plate heat exchanger, heat transfer area required, heat absorbed by low temperature coolant, and effectiveness and efficiency of the heat exchanger. If the design is based on the low temperature coolant outlet temperature, then the coolant mass flow rate is output and vice versa.

After designing the plate heat exchanger (i.e., after calculating the overall heat transfer coefficient of the heat exchanger and heat transfer area required), an analysis of the plate heat exchanger can be done; that is, we can analyze the heat exchanger for different low temperature coolant outlet temperatures and mass flow rates by clicking on the “Analysis” tab. Figure A.9 shows the analysis window of the plate heat exchanger. In analysis, the overall heat transfer coefficient and the area of the plate heat exchanger remain constant from the design mode.

Liquid-to-Liquid Heat Exchanger Design and Analysis

Design Analysis

Coolant from Exhaust Heat Exchanger
 Mass Flowrate of High Temperature Coolant (M_{htc})
 0.7 kg/s
 High temperature Coolant inlet Temperature (T_{htcin})
 363 Kelvin

Low Temperature Coolant Inlet Temperature (T_{ltcin})
 288 Kelvin
 Mass flowrate of Low temperature Coolant (M_{ltc})
 1 kg/s | 15.8503 GPM
 Low Temperature Coolant outlet temperature (T_{ltcout})
 Kelvin

Calculate

Calculations

Overall Heat Transfer Coefficient of Plate HX (U_o)
 594.82 W/m²-K
 Area of Plate Heat Exchanger (A)
 1.71 m²
 Mass Flowrate of Low Temperature Coolant (M_{ltc})
 kg/s | GPM
 Low Temperature Coolant outlet temperature (T_{ltcout})
 301.72 Kelvin
 High Temperature Coolant outlet Temperature (T_{htcout})
 339.8 Kelvin
 Heat Absorbed by Low Temperature Coolant (Q_{ltc})
 57349.6 W
 Effectiveness of Plate heat exchanger (Q_{actual}/Q_{max})
 0.3093
 Efficiency of Plate Heat Exchanger (T_{htcout}=300K)
 36.82 %
 Efficiency of Plate Heat Exchanger (T_{htcout}=T_{ltcin})
 30.93 %

Go to Pipe Pressure Drop Calculations | Go back to Exhaust HX Design | Reset | Cancel

UAF
 UNIVERSITY OF ALASKA
 FAIRBANKS

Figure A.9. Liquid-to-liquid heat exchanger analysis window.

4. Pressure-Drop Calculations

After the design of both the shell and tube heat exchanger (exhaust heat exchanger) and the plate heat exchanger (liquid-to-liquid heat exchanger), the program goes to pressure-drop calculations in pipe and piping components (valves, strainers, elbows, etc.) forming the control system between the two heat exchangers (including the heat exchangers).

Figure A.10 shows the pressure-drop calculations window. The high temperature coolant, which is circulating between the exhaust heat exchanger and the liquid-to-liquid heat exchanger, and its mass flow rate and physical properties (i.e., density and viscosity) are automatically taken for the pressure-drop calculations, as shown in the Figure A.10. The pipe material and the pipe diameters can be selected from the program library. Length of pipe and elevation change (i.e., the elevation difference between the lowest and highest point in the piping system) are user inputs. The pressure drop in both heat exchangers can be entered in respective fields.

Pressure Drop Calculations in Pipes

Pipe Specifications

Mass Flow rate of Coolant: 0.7 Kg/s
 Density of Coolant: 1042.87 kg/m³
 Volume Flowrate of Coolant: 10.6391 GPM
 Dynamic Viscosity(μ): 0.00112 Pa-s
 Elevation Change (Z): 10 Feet(ft)
 Pipe Material: Copper
 Absolute Roughness: 0.000005 Feet(ft)
 Pipe Type and Nominal Diameter: copper Type L tubing, 1.50"
 Pipe Internal Diameter: 1.505 Inches
 Length of the Pipe: 46 Feet(ft)
 Pressure Drop in Exhaust Heat Exchanger (on Liquid Side): 1 PSIG
 Pressure Drop in Liquid-to-Liquid Heat Exchanger: 2 PSIG
 Total K-Factor for valves: 36.43
 Total Cost of Piping Components: \$ 6000

Pressure Drop Calculations

Velocity of Fluid flow: 1.9187 fps
 Reynolds Number: 20817.0852
 Friction Factor: 0.02568
 Total Pressure Drop: 8.706 PSI

Buttons: Calculate, Reset, Cancel, Go back to HX Design, Go to Cost Estimates

Figure A.10. Pressure-drop calculations window.

The piping components (i.e., valves, elbows, strainers, etc.) can be selected by clicking on “Select the Type of Valves and Calculate Their Total Cost.” Figure A.11 shows the screen shot for selection of piping components. For selecting a fitting, enter a value greater than zero in the quantity field. The K-factor for fittings is taken from the

manufacturer's catalog. The user can override the default values provided by the program. The total cost of the components can be calculated by entering the unit cost of each component in its respective field, or a total approximate cost can be entered in the "Total Cost of Piping Components" field provided in the pressure-drop calculations screen.

The results of the pressure-drop calculations are shown as fluid velocity in the piping system, Reynolds number, friction factor in the pipe, and total pressure drop in the system between the two heat exchangers (including the heat exchangers). The pressure drop can be calculated in psig (or) head of water in feet.

Fitting	L/D	Quantity	K-Factor	Unit Cost (\$)
Angle Valve	55	4	1.155	0
Angle Valve	150	0	3.15	0
Ball Valve	3	0	0.063	0
Butterfly Valve		0	0	0
Gate Valve	8	0	0.168	0
Globe Valve	340	0	7.14	0
Plug Valve Branch Flow	90	0	1.89	0
Plug Valve Straightway	18	0	0.378	0
Plug Valve 3-Way Thru-Flow	30	0	0.63	0

Other K-Factor: 0

Calculate Total K-Factor and Component Cost

Total K-Factor: 36.43

Total Cost of Pipe Components: \$ 0

Go to Pressure Drop Calculations Reset Cancel

Figure A.11. Piping components (i.e., valves, elbows, strainers, etc.) window which amount for pressure drop in control system.

5. Cost Estimations

After pressure-drop calculations in the piping system, the program goes to cost estimations of the system, where the total capital cost and operation and maintenance

costs can be calculated. The total capital cost includes the cost of heat exchangers, total cost of piping components, total cost of structural components which are used to build the system and do not account for pressure drop, and initial installation costs which include cost of labor, number of days for installation, freight charges, etc. Operation and maintenance costs include the cost for operating the system (electricity charges for running the pump, etc.) and maintenance costs such as labor, frequency of maintenance per year, number of days for maintenance per visit, freight charges, etc. Figure A.12 shows the screen shot for cost estimations.

Minimum components required for building the system are given in the first two tabs, labeled “Initial Capital Costs-1” and “Initial Capital Costs-2”. If the user has more components, there is an additional tab labeled “Other Initial Costs,” which is left blank so that the user can enter the component name, quantity, and unit cost, as shown in Figure A.13. Installation costs, which are added to total initial capital costs, can be calculated in the tab labeled “Initial Capital Costs-2,” as shown in Figure A.14. There, all costs add up to Total Initial Capital.

Cost Estimations

Initial Capital Costs-1 | Initial Capital Costs-2 | Operation and Maintenance Costs | Other Initial Costs

Component	Unit Cost(\$)	Quantity	Total Cost(\$)
Exhaust Heat Exchanger			10019
Liquid-to-Liquid Heat Exchanger			5000
Pump Cost	672	1	672
Pipe Cost	3 per foot	46 feet	138
Pipe Components Total Cost (Valves, Strainers, etc.,)			6000
Box Beam	62.84	6	377.04
Flat Stock	24.37	3	73.11
Angle Bar	33.22	1	33.22
Slip on Flange	38.3	2	76.6
Insulating Foam Sealant	8.49	6	50.94
Expansion Tank	34.18	1	34.18
Insulation	61.79	1	61.79

Continued in Next Tab....

Total initial Capital (Component Costs + Installation Costs) \$

Total Operation and Maintenance Costs \$

Figure A.12. Cost estimations screen shot.

The operation and maintenance screen shot is shown in Figure A.15. If the user has specific values for total installation costs and total operation maintenance costs, then the calculated values can be overridden. The total operation and maintenance costs are calculated for a year.

Cost Estimations ✖

Initial Capital Costs-1 | Initial Capital Costs-2 | Operation and Maintenance Costs | Other Initial Costs

Component	Unit Cost(\$)	Quantity	Total Cost(\$)
Parts	400	1	400
	0	0	0
	0	0	0
	0	0	0
	0	0	0
	0	0	0
	0	0	0
	0	0	0
	0	0	0
	0	0	0
	0	0	0
	0	0	0
	0	0	0
	0	0	0
	0	0	0
	0	0	0
	0	0	0
	0	0	0
	0	0	0

Total initial Capital (Component Costs + Installation Costs) \$
 Total Operation and Maintenance Costs \$

Figure A.13. Additional structural components window.

Cost Estimations

Initial Capital Costs-1 | Initial Capital Costs-2 | Operation and Maintenance Costs | Other Initial Costs

Component	Unit Cost(\$)	Quantity	Total Cost(\$)
Un-grounded Thermocouple Probes	26.8	6	160.8
Teflon insulated Thermocouple wire	405	1	405
Miniature Thermocouple connector pair	4	50	200
Pressure Gauge	10	3	30
24 gauge galvanized metal	100	1	100
Nickel immersion temperature sensor	35.02	1	35.02
30VA transformer for RWD controller	21.64	1	21.64

Installations Costs

Total number of days for installation: Days

Working hours per day: per Day

Labor required for installation:

Labor cost per hour: \$/hr

Round trip Total Airfare for all persons: \$

Lodging and meals cost per day per person: \$/Day

Total other installation costs: \$

Total Installation costs \$

Total initial Capital (Component Costs + Installation Costs) \$

Total Operation and Maintenance Costs \$

Go back to Pipe Pressure Drop Calculations | Calculate | Reset | Go to Economic Analysis | Cancel

Figure A.14. Installation costs window.

The screenshot shows a software window titled "Cost Estimations" with four tabs: "Initial Capital Costs-1", "Initial Capital Costs-2", "Operation and Maintenance Costs" (selected), and "Other Initial Costs".

Operation Costs

Number of hours engine is run per year	2920	hours
Electric power required to run the pump	0.33	hp
Cost of Electric power	2	per KWH
Other operation costs per year	0	\$
Total Operation Costs per year	1437.11	\$

Maintenance Costs

Number of maintenance visits required per year	2	
Total number of days for maintenance per visit	1	Days
Labor required for maintenance	1	
Cost of Labor per hour	75	\$/hr
Round trip Total Airfare for all persons per visit	600	\$
Lodging and meals cost per day per person	90	\$/Day
Other maintenance costs (supplies etc)	300	
Total Maintenance costs per	2880	\$

Summary

Total initial Capital (Component Costs + Installation Costs)	31388.34	\$	Total Operation and Maintenance Costs	4317.11	\$
---	----------	----	--	---------	----

Buttons at the bottom: "Go back to Pipe Pressure Drop Calculations", "Calculate", "Reset", "Go to Economic Analysis", "Cancel".

Figure A.15. Operation and maintenance costs screen shot.

6. Economic Analysis

After cost estimations of the system, the user goes to economic analysis of the system, where the total initial capital and operation and maintenance costs are taken from the previous cost estimations window. Figure A.16 shows the screen shot for economic analysis. In economic analysis, the heat recovered to the low temperature coolant is taken from the liquid-to-liquid heat exchanger window. The heating value of fuel, engine hours run per year, fuel price, and fuel price escalation rate are user inputs (program gives default values which the user can override). By default, the program gives 2920 hours (8 hr per day * 365 days) of engine run time per year.

The output of the economic analysis window has two types. Based on simple interest, the heat recovered per year and total savings on fuel, simple breakeven point and payback period are calculated. Based on compound interest and the lifetime of the system, the cost of capital per year (i.e., net present value), the total cost of heat recovery system per year (i.e., cost of capital per year + operation and maintenance costs per year), fuel savings for

the given lifetime of the system, and profit or loss made during the lifetime of the system are calculated.

Economic Analysis

Capital Costs and Operation & Maintenance Costs

Total Initial Capital Cost: 31388.34 \$

Total Operation and Maintenance Costs per year(B): 4317.11 \$

Interest rate on capital (Simple Interest for Payback Period): 10 %

Lifetime of System: 10 years

Interest rate on capital (Compound Interest for Capital cost per year): 6 %

Heat Recovered and Fuel Price

Heat Recovered from Exhaust: 57057 W

Engine hours per year: 2920 Hours

Heating value of Conventional Diesel Fuel per gallon: 130000 BTU/gal

Fuel price per gallon: 4.5 \$/gal

Percentage increase of fuel price per year: 2 %

Calculations

Heat Recovered per year: 568514866.351 BTU/year

Total savings on fuel per year: 19679.36 \$/year

Simple Breakeven (Capital/Savings on Fuel): 1.59 years

Payback period for given interest rate on capital: 2.37 years

Cost of Capital per year(A): 4264.67 \$

Total cost of Heat Recovery system per year (A+B): 8581.78 \$

Total investment for given Lifetime of system(C): 85817.8 \$

Fuel Savings for given lifetime of system(D): 215483.51 \$

Profit or Loss made during life time of system (D-C): 129665.71 \$

Go back to Cost Estimates Calculate Reset Cancel

Save as Word

Figure A.16. Economic analysis screen shot.

All the computations made—from the design of the exhaust heat exchanger to the economic analysis—can be saved as a Word document by clicking on “Save as Word.” Figure A.17 shows the screen shot for a Word document saved for this example.

At any point in the program computations, the user can go back to a previous window to check computations, make required changes in the inputs, and recalculate.

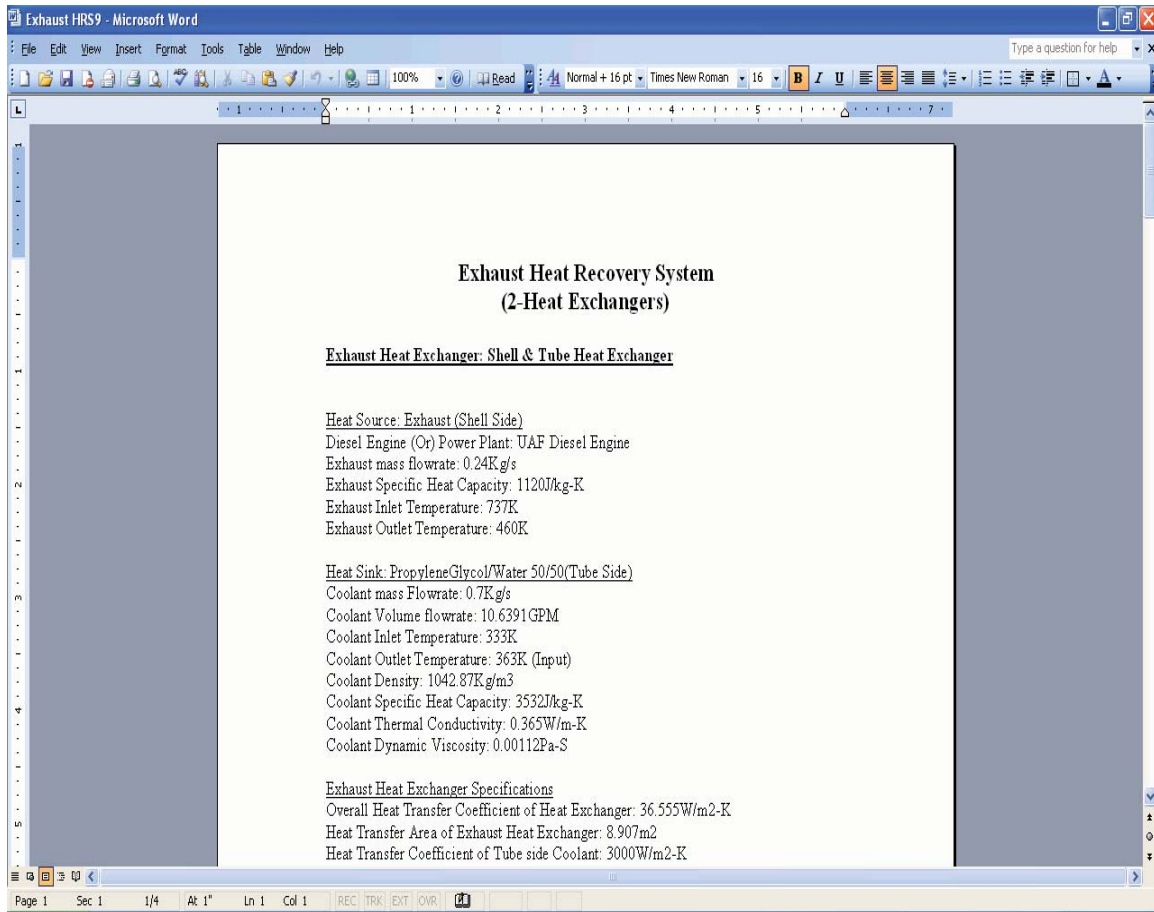


Figure A.17. Saved as Word document.

National Energy Technology Laboratory

626 Cochrans Mill Road
P.O. Box 10940
Pittsburgh, PA 15236-0940

3610 Collins Ferry Road
P.O. Box 880
Morgantown, WV 26507-0880

One West Third Street, Suite 1400
Tulsa, OK 74103-3519

1450 Queen Avenue SW
Albany, OR 97321-2198

539 Duckering Bldg./UAF Campus
P.O. Box 750172
Fairbanks, AK 99775-0172

Visit the NETL website at:
www.netl.doe.gov

Customer Service:
1-800-553-7681



Oil & Natural Gas Technology

DOE Award No.: DE-FC26-06NT41248

Final Report

Rural Energy Conference Project

Submitted by:
Dennis Witmer
Shannon Watson
University of Alaska Fairbanks

Prepared for:
United States Department of Energy
National Energy Technology Laboratory

December 31, 2008



Office of Fossil Energy



Rural Energy Conference Project

Final Report

Starting June 1, 2002
Ending Sept 30, 2008

Dennis Witmer
University of Alaska Fairbanks
ffdew@uaf.edu
907-474-7082

Shannon Watson

Report Issued December 2008
DOE Award Number
DE-FC26-01NT41248
Task Number 1.03.6

Submitted by:
University of Alaska Fairbanks
Institute of Northern Engineering
Arctic Energy Technology Development Laboratory
Building 814
Fairbanks, Alaska 99775

Disclaimer

This report was prepared as an account of work sponsored by an agency of the United States Government. Neither the United States Government nor any agency thereof, nor any of their employees, makes any warranty, express or implied, or assumes any legal liability or responsibility for the accuracy, completeness, or usefulness of any information, apparatus, product, or process disclosed, or represents that its use would not infringe privately owned rights. Reference herein to any specific commercial product, process, or service by trade name, trademark, manufacturer, or otherwise does not necessarily constitute or imply its endorsement, recommendation, or favoring by the United States Government or any agency thereof. The views and opinions of authors expressed herein do not necessarily state or reflect those of the United States Government or any agency thereof.

Abstract

Alaska remains, even at the beginning of the 21st century, a place with many widely scattered, small, remote communities, well beyond the end of both the road system and the power grid. These communities have the highest energy costs of any place in the United States, despite the best efforts of the utilities that service them. This is due to the widespread dependence on diesel electric generators, which require small capital investments, but recent increases in crude oil prices have resulted in dramatic increases in the cost of power.

In the enabling legislation for the Arctic Energy Office in 2001, specific inclusion was made for the study of ways of reducing the cost of electrical power in these remote communities. As part of this mandate, the University of Alaska has, in conjunction with the US Department of Energy, the Denali Commission and the Alaska Energy Authority, organized a series of rural energy conferences, held approximately every 18 months. The goal of these meeting was to bring together rural utility operators, rural community leaders, government agency representatives, equipment suppliers, and researchers from universities and national laboratories to discuss the current state of the art in rural power generation, to discuss current projects, including successes as well as near successes.

Many of the conference presenters were from industry and not accustomed to writing technical papers, so the typical method of organizing a conference by requesting abstracts and publishing proceedings was not considered viable. Instead, the organizing committee solicited presentations from appropriate individuals, and requested that (if they were comfortable with computers) prepare Power point presentations that were collected and posted on the web. This has become a repository of many presentations, and may be the best single source of information about current projects in the state of Alaska.

Contents

Rural Energy Conference Project

Final Report

Disclaimer 1

Abstract 2

Executive Summary 4

Background 4

Results 5

Acknowledgements 6

References 7

Attachments 7

Executive Summary

Alaska remains, even at the beginning of the 21st century, a place with many widely scattered, small, remote communities, well beyond the end of both the road system and the power grid. These communities have the highest energy costs of any place in the United States, despite the best efforts of the utilities that service them. This is due to the widespread dependence on diesel electric generators, which require small capital investments, but recent increases in crude oil prices have resulted in dramatic increases in the cost of power.

In the enabling legislation for the Arctic Energy Office in 2001, specific inclusion was made for the study of ways of reducing the cost of electrical power in these remote communities. As part of this mandate, the University of Alaska has, in conjunction with the US Department of Energy, the Denali Commission and the Alaska Energy Authority, organized a series of rural energy conferences, held approximately every 18 months. The goal of these meeting was to bring together rural utility operators, rural community leaders, government agency representatives, equipment suppliers, and researchers from universities and national laboratories to discuss the current state of the art in rural power generation, to discuss current projects, including successes as well as near successes.

Many of the conference presenters were from industry and not accustomed to writing technical papers, so the typical method of organizing a conference by requesting abstracts and publishing proceedings was not considered viable. Instead, the organizing committee solicited presentations from appropriate individuals, and requested that (if they were comfortable with computers) prepare Power point presentations that were collected and posted on the web. This has become a repository of many presentations, and may be the best single source of information about current projects in the state of Alaska.

The conference has been growing over the years, beginning with about 180 registrants at the first conference in 2002, expanding to 502 registrants at the most recent conference in September 2008.

Background

Most of the United States is serviced by electrical power generated in large central power plants and distributed to residences and businesses through the electrical grid. This allows power from many sources to be mixed, creating a system where the most cost effective power can find the largest markets, and where the redundancy of supply sources create inherent robustness to the system. More that 50% of the electrical market in the US is met by coal fired power plants, as coal is abundant and cheap. Other major sources are from natural gas (less attractive due to recent increases in fuel costs), nuclear, and hydro. Only a small fraction of the grid power is currently generated with wind, and almost none is from the most expensive form of energy, liquid fuels [1], which are used for transportation, but not for stationary power.

However, in Alaska, much of the land is still undeveloped, without roads or power grids, and most of the electrical power is generated using diesel electric generators [2]. The advantages of this form of power generation in remote communities should not be underestimated: diesel generators are inexpensive, transportable, and readily available, and the liquid fuels they use are easy to transport and store, and can be readily dispatched when power is needed. However, diesel fuel is expensive (current prices are \$2.50 per gallon in Fairbanks, and up to \$8.00 gallon in rural communities at the time of writing), resulting in fuel costs of \$.17 to \$.56 per kW-hr of generated electricity. At these prices, alternative energy from local resources such as small scale hydro, wind, fuel cells and hydrogen, solar, geothermal, wave and tidal currents, and small scale hydrokinetic devices might prove to be cost effective.

The issue with these forms of alternative power generation is that many of them have not been demonstrated adequately for utility managers to really know the cost of power from these sources. Small scale hydro is the best understood, but the high capital costs and small markets limit the number of communities where this is a viable solution. Most of the other alternatives have not been demonstrated at sufficient levels for defensible economic analysis to be done (although some of the economics are understood all too well—for example, a solar battery array in a small community proved so uneconomical that no one seemed willing to stand up in public and admit the costs...). When projects are done, however, it is important for this information to be disseminated to as wide an audience as possible.

The purpose for organizing this conference was to create a venue for the people who work in remote rural power to come together and discuss the current state of power generation in rural Alaska and ways of doing better. The rules for presentations were simple: only active Alaskan projects were presented, and proposers were expected to be honest about costs, operational issues, and their overall satisfaction with the process. Failures were to be discussed as well as successes. Industry promoters were not generally permitted to give oral presentations (the exception being a single session in which diesel manufacturers were encouraged to briefly discuss new developments in their product lines, but all brands were discussed in the same session). And sessions were held on every technology of interest. The goal is to find solutions, not to promote any given company or technology.

Results

A total of five conferences were held at approximately 18 month intervals. At each of these conferences, presenters were encouraged to prepare PowerPoint files, which were collected and then made public on the UAF AETDL Web site. This site itself has become the best record of the conference. This site is at:

<http://www.alaska.edu/uaf/cem/ine/aetdl/conferences/>

There are thousands of pages of information on this web site, on many topics. Given the uncertain longevity of web information, we are providing copies of all the information in electronic form as the documentation for this final report.

The conference is intended to attract people from a wide variety of backgrounds, and the diversity of participants can be seen thorough a scan of the attendee list. A summary of the number of participants from each category for the 2008 conference is shown in Figure 1.

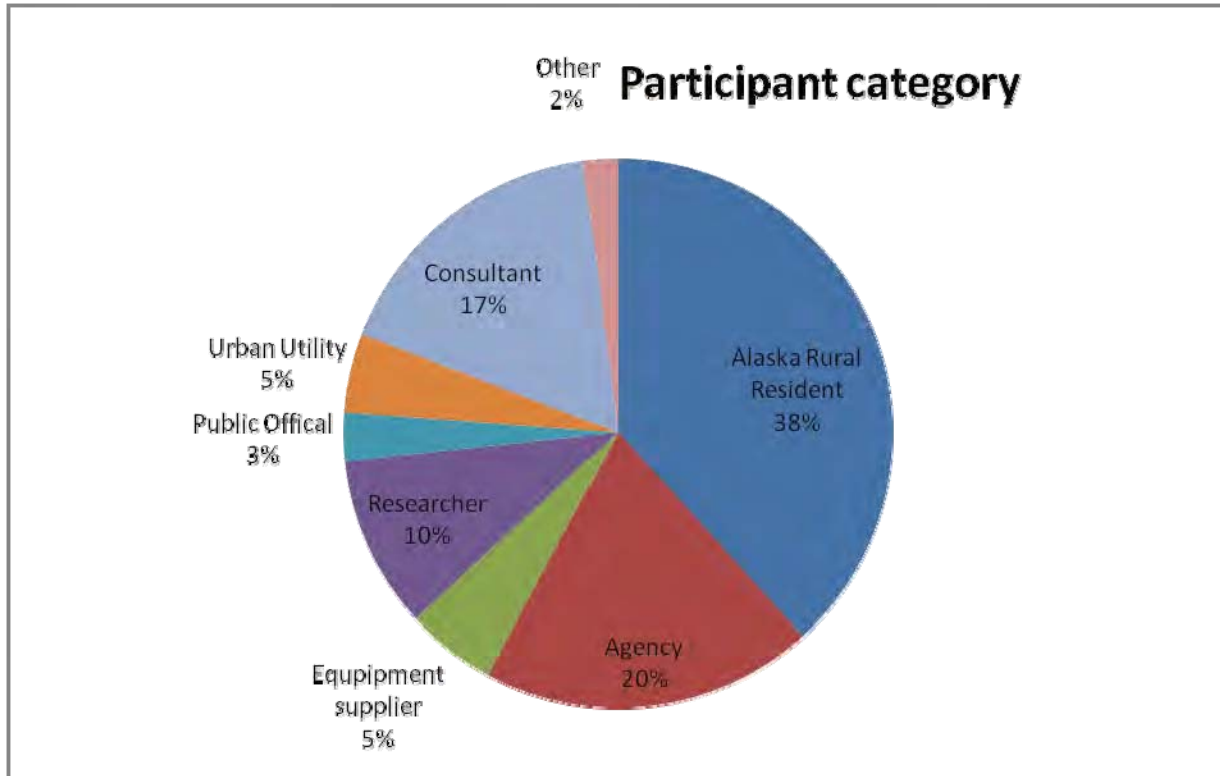


Figure 1 Participation in the 2008 Rural Energy Conference by category. Note the heavy participation by Alaska Rural Residents. The “Other” category includes participants from Conservation groups, oil companies, the press, and the Canadian consulate.

A complete list of attendees at each of the conferences can be found on the web site, or the attached CD.

Acknowledgements

In the absence of a formal structure responsible for the organization of the conference, this event occurs because of the willingness of individuals and their employers to participate. These individuals have included:

- Dennis Meiners, Alaska Energy Authority
- Rebecca Harper, Alaska Energy Authority
- Peter Crimp, Alaska Energy Authority
- David Lockard, Alaska Energy Authority
- Terri Harper, Alaska Energy Authority
- Mike Harper, Alaska Energy Authority

Shannon Watson, University of Alaska Fairbanks
Kathy Petersen, University of Alaska Fairbanks
Julie Philibert, University of Alaska Fairbanks
Dennis Witmer, University of Alaska Fairbanks

In addition to the generous funding from the US DOE, the following major supporters should be recognized:

The Alaska Energy Authority has been a major funder of this conference, especially through the use of their employees time and facilities.

The Denali Commission, for providing travel grants for residents of Alaskan Villages to attend the conference. The presence and participation of these rural residents is an important part of the tone of the conference, as their presence reminds all participants of the personal cost of high energy in these places.

Corporate sponsors have included many of Alaska's urban utility companies, equipment suppliers, and National Laboratories.

References

1. USDOE. *Energy Information Agency Web Site* 2008 [cited; Available from: <http://www.eia.doe.gov/>].
2. Colt, S., *Rural Hydro Screening Analysis*. 1997.

Attachments

CD containing the collected conference schedules, attendee lists, and presentations from the five conferences held in Alaska, 2002-2008.

National Energy Technology Laboratory

626 Cochrans Mill Road
P.O. Box 10940
Pittsburgh, PA 15236-0940

3610 Collins Ferry Road
P.O. Box 880
Morgantown, WV 26507-0880

One West Third Street, Suite 1400
Tulsa, OK 74103-3519

1450 Queen Avenue SW
Albany, OR 97321-2198

539 Duckering Bldg./UAF Campus
P.O. Box 750172
Fairbanks, AK 99775-0172

Visit the NETL website at:
www.netl.doe.gov

Customer Service:
1-800-553-7681



Galena Electric Power – a Situational Analysis



Robert E. Chaney, SAIC Corporation
Stephen G. Colt, University of Alaska Anchorage
Ronald A. Johnson, University of Alaska Fairbanks
Richard W. Wies, University of Alaska Fairbanks
Gregory J. White, Idaho National Engineering & Environmental Laboratory

DRAFT Final Report
December 15, 2004

Prepared for the U.S. Department of Energy
National Energy Technology Laboratory
Arctic Energy Office Contract
DE-AM26-99FT40575

DISCLAIMER

This report was prepared as an account of work sponsored by an agency of the United States Government. Neither the United States Government nor any agency thereof, nor any of their employees, makes any warranty, express or implied, or assumes *any* legal liability or responsibility for the accuracy, completeness, or usefulness of any information, apparatus, product or process disclosed, or represents that its use would not infringe privately owned rights. References herein to any specific commercial product, process, or service by trade name, trademark, manufacturer, or otherwise, does not necessarily constitute or imply its endorsement, recommendation, or favoring by the United States Government or any agency thereof. The views and opinions of authors expressed herein do not necessarily state or reflect those of the United States Government or any agency thereof.

Pre-Publication Draft – Subject to Change

EXECUTIVE SUMMARY

Purpose

The purpose of the investigation is to compare the economics of various electrical power generation options for the City of Galena. Options were assessed over a 30-year project period, beginning in 2010, and the final results were compared on the basis of residential customer electric rates (\$/kWh).

Galena's electric utility currently generates power using internal combustion diesel engines and generator sets. Nearby, there is an exposed coal seam, which might provide fuel for a power plant. Contributions to the energy mix might come from solar, municipal solid waste, or wood. The City has also been approached by Toshiba, Inc., as a demonstration site for a small (Model 4S) nuclear reactor power plant.¹ The Yukon River is possibly a site for in-river turbines for hydroelectric power. This report summarizes the comparative economics of various energy supply options.

This report covers:

- thermal and electric load profiles for Galena
- technologies and resources available to meet or exceed those loads
- uses for any extra power produced by these options
- environmental and permitting issues and then
- the overall economics of each of the primary energy options.

Loads

Currently, the city buildings, school, swimming pool, and health clinic space heating needs are met by capturing the heat rejected by the diesel electric generators (DEGs) and transferring the hot water to the buildings (all close to the power plant). We have assumed an existing average cogeneration load of 400 K Btu/hr for 8 months per year plus a 300 K Btu/hr [commercial/residential boiler load] for other buildings in town for eight months. This gives a total yearly cogeneration thermal load [CTLoad] projected for the future of about 4 B Btu. (Northern Resource Group, 2004). We have distributed these over a year using Fairbanks heating degree days [HDD] data. Analysis shows that allowing for expansion and additional customers for heat (the Air Station), the heat delivered annually could be about 8 B Btu in the future.

In **Figure ES.1**, we see the monthly electric energy generated. This results in an annual load slightly under 10 M kWh. The average monthly load was around 800 kW in July and over 1 MW in January.

¹ Subsequent to release of this report in draft form, Toshiba has offered clarifications to their proposal. First, due to current US regulations and fuel availability, the fuel would probably be manufactured and the reactor charged in a US nuclear facility (i.e. Argonne National Laboratory). Toshiba's assumption is that the reactor would be returned to that location for decommissioning. Second, the capital cost would be borne by a third party (to be determined) that would become the plant owner and responsible for decommissioning. Changes to the text have been made to reflect these assumptions.

Pre-Publication Draft – Subject to Change

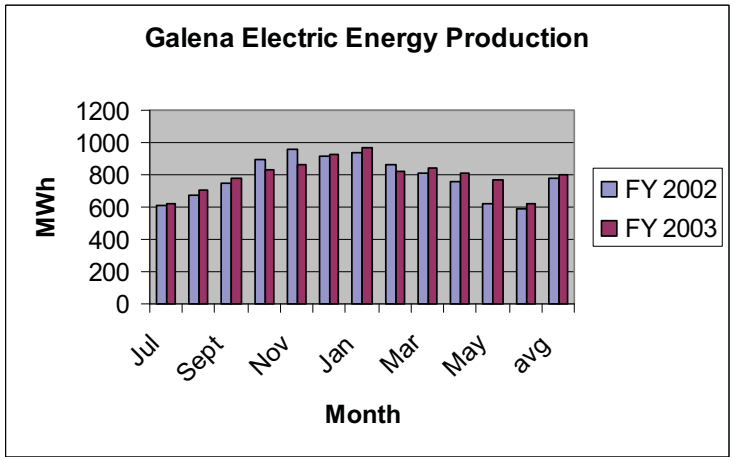


Figure ES.1. Monthly electric generation for Galena

Taking the equivalent projected heating loads and adding the electric loads over the year yields the load requirements displayed in **Figure ES.2.** for the year 2010.

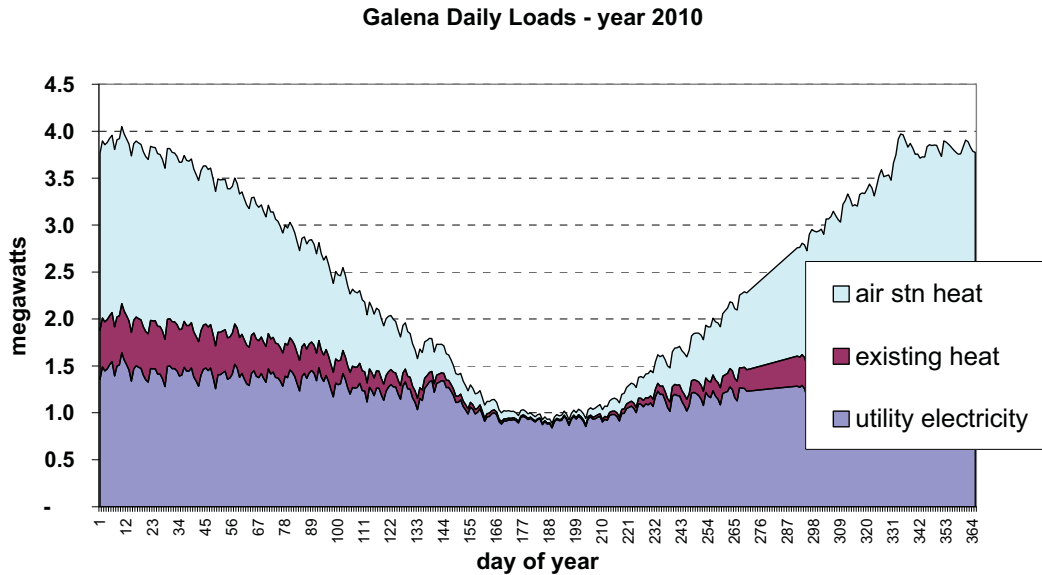


Figure ES.2. Combined heating and electrical loads based on current use in Galena

The various generation options available have different output capacities. For example, the Toshiba 4S system has a generation capacity of 10 MW. Thus, extra power would be available. If the rates were sufficiently low, residential space heating might be an option, as would commercial activities including greenhouses and aquaculture. **Figure ES.3.** illustrates a possible profile using the base loads from **Figure ES.2** with the addition of some of these options for the year 2039. The power requirements are about 8 MW. This would still leave extra power for other uses.

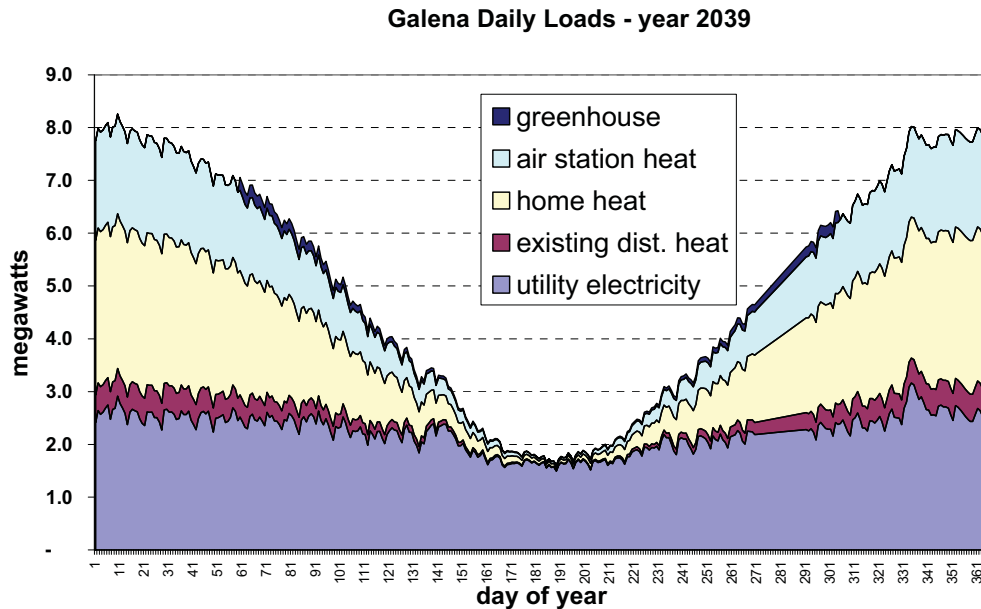


Figure ES.3. Projected combined loads for 2039 with residential space heating and one 2000 ft² greenhouse.

Power Generation Options

The three systems assessed in depth were enhanced diesel, coal (mine and power plant), and the Toshiba 4S nuclear reactor. In the later two cases, backup diesel generators were retained to provide power during any time the primary system was down for repairs or maintenance. All economic analyses included the cost of the backup diesel system.

Enhanced Diesel. According to the Rural Alaska Energy Plan (MAFAa, 2002), the most efficient village sized DEGs available today are capable of achieving peak efficiencies in the 15.8 kWh/gal range. With a fuel oil having a heating value of 135 K Btu/gal, this is equivalent to converting 40% of the energy in the fuel to electric power. For the past two years, the Galena average monthly electrical generation efficiency varied from about 13.2 to 14.8 kWh/gal and averaged 13.76 kWh/gal. For this analysis, we assumed that the units currently in use will continue to perform at 14 kWh/gal and any upgraded or new units will operate at 15 kWh/gal.

Coal (Mine & Power Plant). Exposed coal seams are about 18 road miles upriver from Galena near the Loudon town site. This deposit is not well-understood. Before much further analysis is attempted, the deposit must be explored to determine its size and very importantly its depth below the surface. Samples have been analyzed and have shown an estimated heating value averaging 9.4 K Btu/lb (18.6 M Btu/ton), sulfur content less than 0.5%, ash averaging 9 % [range 2 – 16 %], and moisture content averaging 19% [14 to 28%]. One exposed seam is about 9 feet high and 2,000 feet across. [Phillips and Denton, 1990]. If a 1-MW coal-fired plant were to operate with an efficiency of 25%, it would require about 0.68 tons/hr of coal or about 12,000 ft³/month. If a 100-foot width were taken from this 9-foot-high coal seam, 13 ft/month or 166 feet/yr

Pre-Publication Draft – Subject to Change

would have to be excavated. This coal might be delivered to Galena for an estimated \$100 to \$128/ton.

Atmospheric fluidized-bed combustion (AFBC) boilers are now well-established as a mature power generation technology with more than 620 AFBC units in operation worldwide in the size range 20 to 300 MW. Current operating experience shows that AFBC boilers meet high environmental standards and are commercially viable and economically attractive. For more information on AFBCs see <http://www.epri.com/journal/details.asp?id=627&doctype=features>

These plants burn a range of fuels, including bituminous and subbituminous coal, coal waste, lignite, petroleum coke, biomass, and a variety of waste fuels. In many instances, units are designed to fire several fuels (including biomass fuels), which emphasizes one of the technology's major advantages: its inherent fuel flexibility.

While no AFBC coal power plants in the small size range required at Galena have been built and operated at this time, small AFBC boilers have been used to provide heat for industrial processes. Adaptation to power production requires the addition of a steam turbine and ancillary equipment.

The U.S. Department of Energy (DOE) initiated a study in 1998 (Northern Economics, 2001) to investigate the capital and operating costs of small coal-fired power plants [600 kW to 2 MW]. The installed capital costs were estimated at from \$3.0K to \$4.3K/kW and an electricity cost of \$0.22 to \$0.77/kWh.

A 2003 feasibility study on a barge-mounted 5-MW AFBC power plant (Bonk, 2004) estimated capital costs from \$20M to \$25M and electricity costs of \$0.20/kWh minus a credit for heat delivered using Galena coal.

J.S. Strandberg (1997) did a feasibility analysis of an 800 kW AFBC coal plant in McGrath plus a 125 kW DEG. The analysis estimated a total project budget of about \$14 million, which included the power plant, coal mine development, haul road, and an expanded district heating system. The estimated electricity cost was \$0.176/kWh, which included a \$0.077/kWh credit for heat delivered. Over half the total cost was for coal and limestone. A major issue was the high parasitic power required [over 155 kW], and the estimate for it was increased as the study was completed.

Phillips and Denton (1900) calculated costs for a 483 kW coal-fired model cogeneration facility producing 6.8 M Btu/hr of heat. The costs of electricity ranged from \$0.11 to \$0.22/kWh for a base load plant to as much as \$0.80/kWh for a lightly loaded plant. Of the 21 M Btu/hr fuel input, 46% went to the production of electricity. Of the total capital cost of \$7.5 M, \$2.0 M was allocated to electrical and +\$5.5 M to heat. For a plant in Galena using Loudon coal, the electricity costs were estimated to range from \$0.26 to \$0.36/kWh.

A coal-fired plant should be a base-load plant sized to run near its capacity all of the time except for planned shutdowns for maintenance and repair.

Toshiba 4S Nuclear Plant. The 4S Model power plant concept is based on a design for a Small Innovative Reactor (SIR), which is a sealed unit. Unlike conventional

Pre-Publication Draft – Subject to Change

reactors, the 4S concept is for the sealed reactor to be delivered at the site, installed with the generator system, operated for the prescribed design life, removed, and replaced with the sealed assembly intact. Thus, there would be no emissions (other than steam), no release of radioactivity, and minimum chance of radiation exposure when the reactor assembly is buried. Toshiba has approached the City with a proposal to provide the reactor and power plant so that the 4S can have a reference site and gain operational experience. The capital cost would be borne by a third party to be identified. Some expense may be incurred by the City for site preparation and installation.

The 4S has no mechanical systems internal to the sealed assembly. Electromagnetic pumps move the cooling fluid. The reflecting shield that controls the reaction is also moved electromagnetically. This greatly reduces the potential for mechanical and equipment problems. Cooling and heat transfer is accomplished using liquid sodium metal. Heat is transferred to a steam generation loop and the resulting steam drives the turbine to generate electricity with rejected heat in the condensed water available for district heating or other uses. For district heating, the steam can be used directly. Problems that have occurred in sodium-cooled plants design have been in sections of the plant other than the reactor.

In this concept, the nuclear reactor is planned to be installed up to 100 feet below grade and capped with reinforced concrete. This provides a nearly impenetrable barrier that cannot be lifted by any heavy equipment available in Galena. The 4S also uses a nonproliferation fuel that cannot be used to produce a nuclear weapon without first undergoing isotopic enrichment, an extremely costly and technologically challenging process.

The projected 4S capital cost is projected to be \$2,500/kW for the 50-MW model when developed. If these assumption scales for a 10 MW unit, the capital cost would be \$25 million.² If fully utilized, electric power from the 50-MW unit is estimated by the vendor to be \$0.065/kWh. Our economic analysis proved to be highly sensitive to the number of plant personnel required. A reasonable number of operations personnel are required for efficiency and safety, but it is not known how many security personnel may be required. A detailed safety and security risk assessment, required by the Nuclear Regulatory Commission licensing process, will determine the necessary staffing levels. The time required for the NRC licensing process is not known at this time. It may add a significant period before the plant can be started, but for purposes of this analysis, we assumed a start date in 2010. The experience gained from the Galena project will be used to refine capital and installation cost estimates for future installations.

Other Generation Modules

Although, other options for power were considered, they were not viable for large-scale deployment by the utility. These include solar, wind, in-river turbines, biomass, fuels cells, and coal bed methane.

In-river Turbines. Prototype turbines have been developed but have not been demonstrated in arctic settings. Calculations of the power output from candidate models

² Toshiba presented this estimate with slides describing the 50-MW plant. We have used the cost per kW figure and applied it to the smaller size. Due to economies of scale, this approach may understate the cost of the smaller, 10-MW plant. However, we are unaware of a direct cost estimate for the 10-MW size.

Pre-Publication Draft – Subject to Change

indicate the output would be relatively low at Galena (22.5 kW for a unit with two 3m diameter turbines). For these reasons, we did not pursue or recommend installation of in-river turbines at this time.

Solar. Much of interior Alaska has a good solar resource for as much as eight months of the year, including the springtime when there is a large need for both heat and electricity. A downside to using solar energy is the intermittent nature of the resource. Hence, as with any intermittent resource, storage can be a key issue. Solar technologies take two forms, solar-electric (photovoltaic) and solar thermal. Photovoltaic devices convert sunlight directly to electricity at efficiencies as high as 25%, although 10% is typical. Installation of a 100 kW module in a Galena setting could cost \$2M. Solar thermal technologies use the heat in sunlight to produce hot water, heat for buildings, or electric power. In Galena, solar technology would best serve individual home or business owners. Its impact on the utility was determined to be limited.

Biomass. Biomass can be wood from trees as well as plant residue, animal waste, and the paper portion of municipal solid waste (MSW). The dispersed nature of this resource makes the energy and time involved in harvesting an important issue. We determined the contribution from this source to be too small for a stand-alone unit. However, MSW could be burned in the AFBC of the coal power plant.

Wind. Galena is located in a low wind resource region – Class 1. For wind turbines to work efficiently and contribute significantly to a utility, they must operate in a Class 5, 6, or 7 region. Thus, wind was not considered.

Fuel Cells. This technology is under intense development but has not been commercialized. While some demonstrations are underway, fuel cells are not available for utility applications at this time.

Coal Bed Methane. Gas has been produced commercially from coal beds in the lower 48. Development of resources in other parts of Alaska is in a preliminary stage. Because information to develop CBM in arctic conditions is insufficient, CBM cannot be considered for Galena. If considered for development, extensive work is required to delineate local reserves before development could occur.

Conservation

Conserving energy can reduce loads for utilities and reduce consumer power bills. Utilities have a role in providing information on conservation to their customers. This report discusses measures that can be taken by end-users to conserve.

Uses of Extra Power

Some power plant options have optimum sizes that would provide power over and above current and projected electrical consumption. For those cases, possible uses studied included district heating, residential electric baseboard heating, transmission to nearby villages, production of hydrogen, and horticulture/aquaculture. Use of all energy produced by generation options is essential to realize the full economic potential of generation systems.

Pre-Publication Draft – Subject to Change

District Heating/Heat Sales. Currently, DEGs provide heat to City buildings, the school, and swimming pool. This is assumed to continue in all of the scenarios considered. Some expansion is assumed. Also considered is the sale of heat through a hot water pipeline to the Air Station. To provide space heating, the Air Station consumes about the same volume of fuel oil each year as the electric utility. The value of the heat supplied is equivalent to the value of the displaced fuel oil.

Electric Space Heating to Residences. If electric rates can be lowered sufficiently, residents will begin to use more electricity in their homes. With sufficiently low rates, many will convert to electric baseboard heating systems. The only reasonable option here is the 4S nuclear plant. If this situation were to be realized, retrofitting the homes and upgrading the distribution system would result in economies of scale, increased convenience, and enhancement of in-door air quality. In considering the economics of the 4S option, the costs of retrofitting and installation were included in the capital cost to the utility.

Hydrogen Production. Projected electric and heat loads over the 30-year life of this analysis indicate that extra power will still be available. In considering other potential uses, we assessed the production of hydrogen for fuel. Transportation of hydrogen for sale outside the City was determined to not be economical. However, under certain conditions, converting City vehicles, school district buses, and Air Station heavy equipment may be economically feasible. It might also provide the City the opportunity to be a test-bed for production and use of hydrogen in remote arctic settings. Hydrogen production may be feasible but not economically viable without subsidies. No credit was taken for the oxygen that is coproduced, but it could be captured and compressed for local use.

Transmission to other villages. An analysis of estimated construction costs of transmission lines to the villages nearest to Galena revealed that the capital costs were several million dollars greater than the revenue that could be collected over the 30-year period. This option is therefore not considered feasible from an economic standpoint.

Greenhouses and Aquaculture. The extra heat produced by new power plants may give rise to private entrepreneurial activities. We briefly looked at the potential of greenhouses and aquaculture. Many other activities may be viable. If the cost for the heat (in the form of heated water) were low enough, these ventures appear to have merit.

Environmental Issues and Permitting

Issues related to permitting were surveyed for the generation options considered viable. The critical considerations are

- Air pollution control
- Water pollution control
- Waste management
- Disturbance of lands/habitat

After considering all issues and potential emissions, the 4S option appears to be the least problematic (this depends on the Nuclear Regulatory Commission) from the

Pre-Publication Draft – Subject to Change

standpoint of ease of gaining new permits. Opening a coal mine and building a coal-fired power plant appears to be the most difficult.

Economic Analyses

Estimating the cost of power to the consumer is the primary objective of this project. We considered the three options: improved diesel, coal (mine & power plant), and the Toshiba 4S nuclear power plant. In all cases, the base case was taken as the continuation and improvement of the diesel-based system now in place. The most critical parameters for each option are shown below.

In the base case, two extremes were taken. First, the continuation of diesel generation with a fuel cost of \$1.50/gal at a flat rate (no escalation). The second case took the cost of fuel at \$2.15/gal and escalated it at 2%/year. These cases were used to compare all the others. For the coal option, the delivered cost of the fuel and the conversion efficiency of the plant were the variables on which the power cost most depends. For the 4S option, the staffing levels (the plant operation staff was held constant, but the number of security personnel was varied) required were the most important.

Table ES.1. Most critical parameters for each option considered.

	units	low value	high value
Diesel fuel price in 2010	\$/gallon	1.50	2.15
Diesel fuel price increase (over and above general inflation)	% per year	0.0%	2.0%
Coal price (delivered to Galena)	\$/ton	100	125
Coal plant average efficiency		30%	40%
Nuclear plant security staff	positions	4	34

Numerous scenarios were run showing the effect of various assumptions. The power plant sizes, optimized for the various technologies, were taken with the load and energy uses, and the total project cost, as well as the electricity cost to the consumer, was calculated. The figures below show the results for various scenarios beginning in 2010. The coal and nuclear systems assumed that DEGs would be employed as back-up for maintenance and emergency shutdowns. Therefore, the price of diesel fuel affects the economics of those systems.

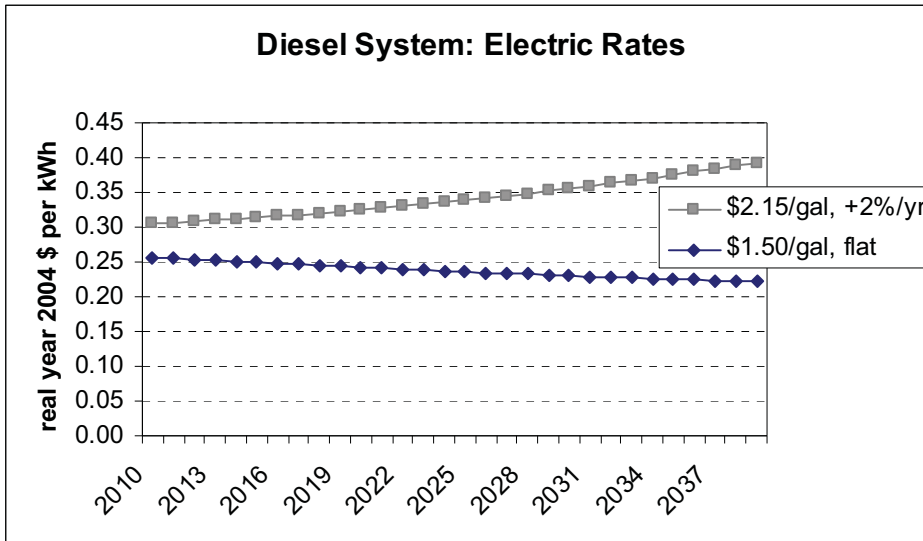


Figure ES.4. Projected future electric rates with a diesel system.

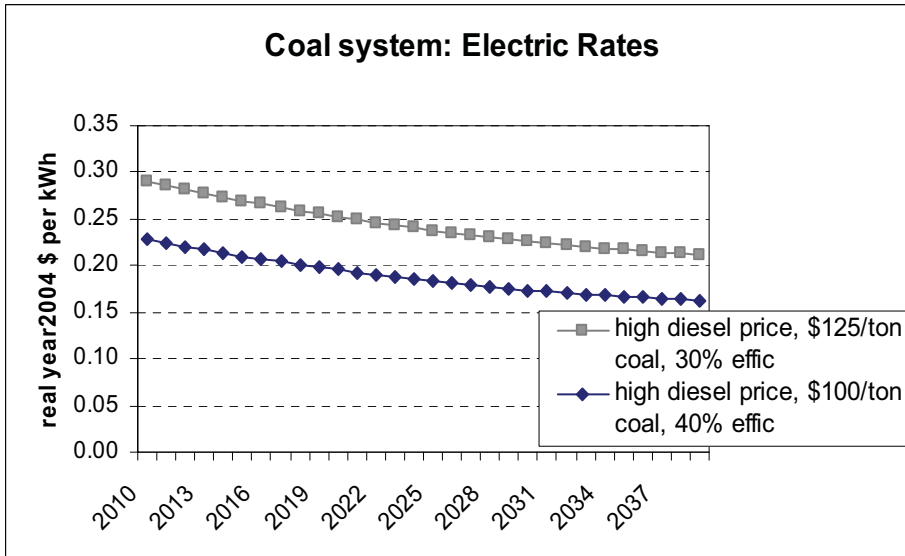


Figure ES.5. Projected future electric with rates with coal system.

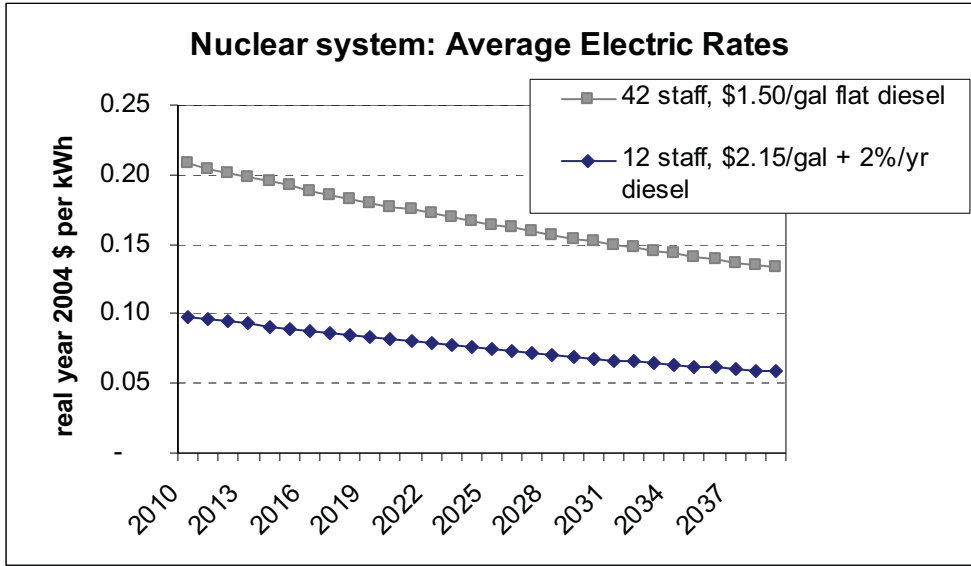


Figure ES.6. Projected future electric rates with nuclear system.

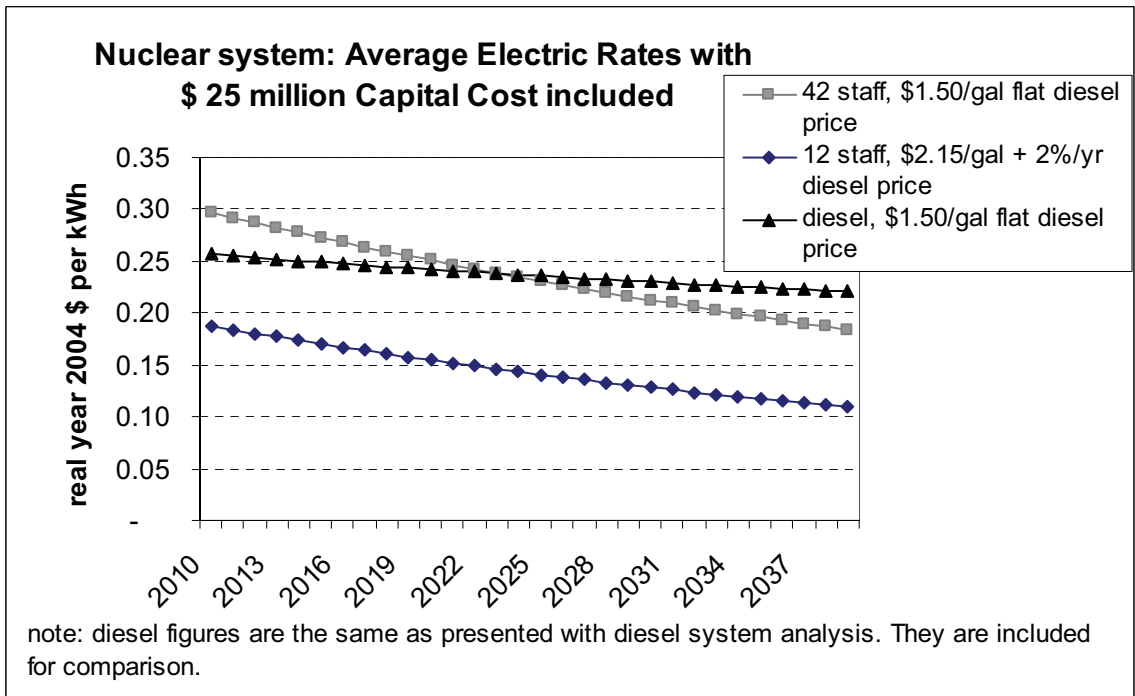


Figure ES.7. Projected future electric rates with nuclear capital costs included in rates.

ES.2. Summary of results of the economic evaluations

Pre-Publication Draft – Subject to Change

	Diesel	Nuclear	Coal
Loads served:			
utility electricity	X	X	X
existing district heat	X	X	X
residential electric space heat		X	
greenhouse		X	
air station district heat		X	[sometimes]
Life-cycle total cost (\$million)			
low value	38	(7)	23
high value	59	35	36
Net benefits compared to diesel (\$million)			
low value		3	3
high value		67	36
Average electric rate in 2010 (\$/kW h)			
low value	0.26	0.10	0.23
high value	0.30	0.21	0.29
Average electric rate in 2030 (\$/kW h)			
low value	0.23	0.07	0.17
high value	0.36	0.15	0.23

The economic evaluations included the costs of diesel backup generators for coal and nuclear.

In all cases, the nuclear system will provide the lowest cost power to the consumer. The coal option will beat the diesel option in some scenarios.

Conclusions and Recommendations

On the basis of environmental permitting, the nuclear plant appears to be a clear winner. Obtaining permits for the coal plant appears to be the most difficult. The validity of this conclusion depends on the process and length of time required to gain a license from the NRC. All assumptions regarding costs and timing require validation.

The economic analysis reveals that the 4S option will provide the lowest cost power if the assumptions hold. In the Galena case, the assumption is that capital cost will be borne by an outside party and that reasonable staffing levels will result from the licensing process. The coal option may be economic in some scenarios compared to enhanced diesel systems, so the coal option should not be entirely dismissed.

Even though installation of the 4S nuclear plant presents a potential long-term solution to Galena's critical energy issues from economic and environmental permitting standpoints, other aspects, such as safety analyses, remain to be performed as part of the licensing process. Ultimately, the selection of the best energy option must consider these analyses and other factors. Specifically, regarding the 4S nuclear plant option, safety relating to potential accidents involving the reactor core and the use of liquid sodium as a heat transfer medium must be adequately addressed. If this technology is successfully deployed in Galena, its economic viability in other Alaska villages and elsewhere depends on the actual life cycle costs yet to be quantified.

Pre-Publication Draft – Subject to Change

Benefits associated with adoption of one or more of the technologies discussed in this report go beyond their ability to meet Galena's thermal and electric energy loads.

We see the potential for Galena to serve as a training center for rural Alaskans interested in using similar technologies in their villages. We also see the potential for use of additional cogeneration leading to economic development such as the development of horticulture and aquaculture. Enhancement of local employment associated with these activities is another benefit. With today's uncertain energy situation, many communities are diversifying their energy options. This includes adding renewably based technologies to lessen dependence on fossil fuels. Adding a few tens of kW of PV arrays, for example, could help Galena insulate itself against fluctuations in the price and supply of diesel fuel.

Therefore, the recommendations are:

- ◆ Proceed with refining the 4S evaluation process in conjunction with the NRC
 - It may be advantageous for Galena to enlist an independent organization to estimate the time required for licensing and permitting
 - Toshiba and Galena should consider partnering with a U.S. organization or National Laboratory to assist in the process
- ◆ Retain the current diesel systems (with scheduled upgrades) until a decision is made regarding the installation of a replacement by about 2010.
- ◆ Retain the option of a coal mine and power plant until it is determined if the 4S system can be permitted and licensed. If the 4S cannot be realized, then the coal option appears feasible (with a favorable coal resource assessment result).

Pre-Publication Draft – Subject to Change

CONTENTS

GALENA ELECTRIC POWER – A SITUATIONAL ANALYSIS.....	ERROR!
BOOKMARK NOT DEFINED.	
EXECUTIVE SUMMARY	1
EXECUTIVE SUMMARY	1
TABLES	19
1. INTRODUCTION	22
1.1 Purpose	22
1.2 Setting.....	22
1.3 The Galena Situational Analysis Project	23
1.3.1 Scope.....	23
1.3.2 Limitations	23
1.4 Acknowledgements	24
1.5 Advisory Committee	24
1.6 Technical Contributors.....	25
2. POWER GENERATION OPTIONS	25
2.1 Loads	25
2.1.1 Heating Load for Cogenerated Heat.....	25
2.1.2 Electric Loading Profile.....	27
2.2 Enhanced Diesel	28
2.3 Coal (Mine & Power Plant).....	30
2.3.1 Coal Mine	30
2.3.2 Power Plant with AFBC and a Steam Turbine.....	30
2.3 Toshiba 4S Nuclear Power Plant	32
2.3.1 4S System Characteristics	32
2.3.2 Safety.....	35
2.3.3 Security	36
2.4 Other Power and Heat Generation Modules	37
2.4.1 Hydro In-river Turbines	37

Pre-Publication Draft – Subject to Change

2.4.2 Solar	38
2.4.2.1 <i>Solar-electric</i>	39
2.4.2.2 <i>Solar Thermal</i>	39
2.4.3 Biomass	39
2.4.4 Wind.....	39
2.4.5 Fuel Cells	40
2.5.6 Coal Bed Methane	41
3. ENERGY CONSERVATION.....	42
4. USES OF EXTRA POWER	42
4.1 District Heating – Sales to Air Station.....	43
4.2 Residential Electric Heating.....	43
4.3 Hydrogen Production	44
4.4 Transmission to Other villages.....	46
4.4 Greenhouses and Aquaculture.....	46
4.4.1 Greenhouses	47
4.4.2 Aquaculture	47
5. ENVIRONMENTAL ISSUES AND PERMITTING.....	48
5.1 Primary Environmental and Permitting Issues.....	48
5.1.1 Disturbance.....	49
5.1.2 Air Pollution.....	49
5.1.3 Water Pollution.....	49
5.1.4 Waste Management.....	50
5.2 Enhanced Diesel	50
5.2.1 Background and Assumptions.....	50
5.2.1.1 <i>Disturbance</i>	50
5.2.1.2 <i>Air Pollution</i>	51
5.2.1.3 <i>Water Pollution</i>	51
5.3 Coal	51
5.3.1 Background and Assumptions.....	51
5.3.1.1 <i>Coal Mining</i>	51
5.3.1.2 <i>Disturbance from Mining</i>	52
5.3.1.3 <i>Air Pollution for Coal Mining</i>	53
5.3.1.4 <i>Water Pollution for Coal Mining</i>	53
5.3.1.5 <i>Waste Management for Coal Mining</i>	54
5.3.2 Coal Preparation – Air Pollution.....	54
5.3.3 Coal – Transportation.....	55
5.3.3.1 <i>Federal</i>	55
5.3.3.2 <i>State of Alaska</i>	56
5.3.3.3 <i>Local</i>	56
5.3.4 Coal Power Generation.....	56

Pre-Publication Draft – Subject to Change

5.4 Toshiba 4S Nuclear Plant.....	56
5.4.1 Disturbance.....	57
5.4.2 Air Pollution.....	57
5.4.3 Water Pollution.....	57
5.4.4 Waste Management.....	57
5.5 Conclusions – Environmental Issues and Permitting	57
6. ECONOMIC ANALYSIS	58
6.1 Overview of Methodology	58
6.1.1 Example of Model Structure.....	58
6.1.2. Economic Model Limitations	59
6.2 Assumptions	60
6.2.1 Overview of Assumptions and their Use	60
6.2.2 Current Loads and System Costs	61
6.2.3 Assumptions about Future Loads.....	62
6.2.3 Assumptions about the Diesel System.....	64
6.2.4 Assumptions about the Coal System	65
6.2.5 Assumptions about the Nuclear System	65
6.3 Economic Analyses Results	66
6.3.1 Basic Results.....	66
6.3.1.1 <i>Diesel</i>	66
6.3.1.2 <i>Coal</i>	67
6.3.1.3 <i>Nuclear</i>	69
6.3.1.4 <i>Summary of Basic Results.</i>	70
6.3.2 Special Sensitivity Cases	71
6.3.2.1 <i>Cases with Nuclear Capital Costs Included</i>	71
6.3.2.2 <i>The Effect of Power Plant Location</i>	72
6.3.3 Transmission.....	73
6.3.4 Economics of hydrogen production	74
7. CONCLUSIONS	76
7.1 Economics Conclusions	76
7.2 Environmental Issues and Permitting Conclusions	78
8. RECOMMENDATIONS	78
APPENDIX A. Presentation by Yoshiaki Sakashita, Toshiba, at the 2004 Alaska Rural Energy Conference, April 27-29, 2004, Talkeetna, Alaska	81
APPENDIX B. Detailed Discussion of Hydropower, Solar, and Conservation	82
APPENDIX C. Summary of Nuclear Regulations.....	88

Pre-Publication Draft – Subject to Change

APPENDIX D. Economic Analysis Model.....94

FIGURES

Figure 2.1. Galena heating load for co-generation.	25
Figure 2.2. Monthly electric generation for Galena.	26
Figure 2.3. Hypothetical electric load for Galena for one year period.	27
Figure 2.4. Hypothetical electric load for Galena for Day 50.	27
Figure 2.5. Performance of DEG system at Galena.	28
Figure 2.6. Schematic of Nuclear Power Plant.	32
Figure 2.7. Schematic diagram of the 4S installation.	33
Figure 2.8. Solar insolation data for Fairbanks, Alaska.	37
Figure 2.9. Map of wind regimes in northern Alaska.	39
Figure 4.1. Energy Trapezoid.	41
Figure 4.2. Heat load for a greenhouse.	46
Figure 6.1. Current cost of electric service with diesel fuel at \$1.32/gal for 2003, the year of this data.	60
Figure 6.2. Projected future energy requirements.	61
Figure 6.3. Projected future electric rates with diesel system.	65
Figure 6.4. Coal plant capacity vs. daily loads for high diesel prices.	65
Figure 6.5. Projected future electric rates with coal system.	66
Figure 6.6. Daily loads vs. nuclear capacity, year 2039.	67
Figure 6.7. Projected future electric rates with nuclear system.	68
Figure 6.8. Projected future electric rates with nuclear capital costs included in rates.	69
Figure B.1. An active solar closed-loop water heating system.	82

Pre-Publication Draft – Subject to Change

TABLES

Table 2.1. Key parameters for four Alaska coal-power plant studies.	31
Table 4.1. Equivalent liquid hydrogen needed to displace local petroleum based fuels.	44
Table 4.2. Results of hydrogen economic analysis.	44
Table 4.3. Cost of installing a transmission line to serve near-by villages.	45
Table 5.1. Partial list of permitting requirements related to disturbance of lands and waters.	47
Table 5.2 Usibelli Coal Preparation Plant Source Inventory.	53
Table 6.1. Summary of critical assumptions.	59
Table 6.2. Galena electric utility statistics.	59
Table 6.3. Future energy requirements.	60
Table 6.4. Assumptions about heating loads.	62
Table 6.5. Assumptions about the diesel system.	62
Table 6.6. Assumptions about the coal system.	63
Table 6.7. Assumptions about the nuclear system.	64
Table 6.8. Summary of basic results.	68
Table 6.9. Economic costs and benefits of transmission lines.	71
Table 6.10. Hydrogen enterprise analysis.	72
Table 7.1. Summary of basic cases and sensitivity cases.	74
Table C.1. NRC Regulatory Guides - Environmental Siting (Division 4).	88
Table D.1. Parameters and Assumptions for Economic Analyses.	91
Table D.2. Diesel-Only Power Supply Economic Analysis.	93
Table D.3. Coal Power Supply Economic Analysis.	94
Table D.4. Nuclear Power Supply Economic Analysis.	96

Pre-Publication Draft – Subject to Change

ACRONYMS AND ABBREVIATIONS

ACMCRA	Alaska Surface Coal Mining Control and Reclamation Act
AFBC	atmospheric fluidized bed combustor
AVEC	Alaska Village Electric Cooperative
B	billion
Btu	British thermal unit
CGP	Construction General Permit
CFR	Code of Federal Regulations
CTLoad	cogeneration thermal load
DEG	Diesel Electric Generator
DEC	Alaska Department of Environmental Conservation
DOE	U.S. Department of Energy
DNR	Alaska Department of Natural Resources
DMLW	DNR Division of Mining, Land and Water Management
EPA	U.S. Environmental Protection Agency
Gal	gallon
GVEA	Golden Valley Electric Association
HDD	heating degree day
HDH	heating degree hour
HHL	hourly heat load
INEEL	Idaho National Engineering and Environmental Laboratory
K	thousand
kW	kilo-watt
kWh	kilo-watt hour
kWp	kilo-watt peak
M	million
MW	mega-watt
MWh	mega-watt hour
NRC	Nuclear Regulatory Commission
SIR	small innovative reactor
SMCRA	Surface Mining Control and Reclamation Act of 1977
NETL	National Energy Technology Laboratory
NPDES	National Pollutant Discharge Elimination Permit
NREL	National Renewable Energy Laboratory
MSW	municipal solid waste
PAFC	phosphoric acid fuel cell
PEM	proton exchange membrane
RCRA	Resource Conservation and Recovery Act
SMCRA	Surface Mining Control and Reclamation Act

Pre-Publication Draft – Subject to Change

1. INTRODUCTION

1.1 Purpose

The purpose of the investigation is to compare the future power generation options available to the City of Galena. The cost for power (\$/kWh) is the parameter used as the basis for this comparison.

Galena's electric utility currently generates power using internal combustion diesel engines and generator sets (DEG). An exposed coal seam nearby might provide fuel for a power plant. The City has been approached by Toshiba, Inc., as a demonstration site for a small 10-MW (Model 4S) nuclear reactor power plant. The Yukon River is possibly a site for in-river turbines for hydroelectric power. Additional contributions to the energy mix might come from solar, municipal solid waste, or wood. This report summarizes the comparative economics of various energy supply options.

This report will first discuss;

- thermal and electric load profiles for Galena
- technologies and resources available to meet or exceed those loads
- uses for any extra power produced by these options
- environmental and permitting issues and
- the overall economics of them.

The bottom-line conclusions will compare the consumer cost of power on a \$/kWh basis.

1.2 Setting

The City of Galena is a community of about 800 people situated on the north shore of the Yukon River in the interior of Alaska 270 air miles from Fairbanks. Galena experiences a cold continental climate with extreme temperature differences (-64 to 92 °F). Temperatures of -40° F are common during the winter. Annual precipitation is 12.7 inches, with 60 inches of snowfall. The River is ice-free from mid-May through mid-October. The climate is important to power use projections. For more information, see the State's community information web site for Galena; (www.dced.state.ak.us/dca/commdb/CB.cfm)

The City has three distinct districts: "Old Town," "New Town," and the Air Station. The community was formerly established in 1918 near an Athabaskan fish camp (Henry's Point) and became a supply and transshipment point for nearby lead mines. In 1920, Athabascans from the village of Loudon began moving to Galena to find employment selling wood to steam ships and hauling freight to the regional mines. The Galena airfield was established during World War II as a refueling point for planes being ferried to Russia as part of military operations (Lend-Lease Program). During the 1950s the military installations were expanded. Due to a severe flood in 1971, a new community site was developed 1 ½ miles east of the original town site. "New Town" is the site of the City offices, health clinic, schools, washeteria, store, and more than 150 homes. The Air Force Station was closed in 1993. It is maintained by the Chugach Development Corporation and is used as a backup Air National Guard facility. It is also

Pre-Publication Draft – Subject to Change

the site of Galena School District Boarding School and Vocational Training programs. (www.dced.state.ak.us/dca/commdb/CB.cfm).

Galena's current energy requirements are met by DEG-produced electricity, fuel oil-fired boilers, and oil- or wood-fired stoves. All economic analyses will compare considered options to those currently in widespread use.

1.3 The Galena Situational Analysis Project

1.3.1 Scope

The project scope is to assess the electric power generation/distribution options and compare their economics for the City of Galena. Conceptual plant designs from previous investigations were used. Current loads and projected uses for energy were considered in developing the projections. The final product is the comparison of consumer electric rates projected through a 30-year period (2010 through 2039).

Key issues to be addressed in choosing future energy options for any community include (1) available resources, (2) loads [electrical and thermal], (3) suitable technologies, (4) uses for extra power, (5) environmental and permitting issues and (6) economics. Uncertainties in the future price of imported fuel underlie all economic calculations. Additional considerations are possible linkages with neighboring villages and the potential for economic stimulation are presented in appropriate sections.

The Project Team visited the City twice. The first visit was April 1 and 2, 2004, to kick off the project, gather background information, and make presentations at both a town meeting and at the "Breakfast Club." During the second visit, June 15-16, presentations of our preliminary results were made to the City Council (in open meeting), at the "Breakfast Club," and to the staff of the Loudon Tribal Council. During these visits, options were discussed with many and we gained valuable insight and information.

1.3.2 Limitations

An investigation of this type has several constraints placed on it by time, resources, and the availability of data. Limitations specific to this project include:

- Coal resource data for the Loudon deposit is limited, therefore it was assumed to be sufficient to support the coal mine and power plant option. Detailed resource evaluation is needed.
- Detailed designs for power plants for the various fuel options, heat transfer systems, and extra power-use facilities were outside the scope of this project. Previous work cited was used for this analysis.
- The use of the Toshiba 4S reactor system will require extensive technical design, operations, safety, risk, and environmental analyses. The results of these analyses will determine the feasibility of the installation.
- The economic analysis is based on the comparison of scenarios for change occurring 30 years into the future. While scenario analysis is a useful tool for examining long-range feasibility, it does have several limitations.

Pre-Publication Draft – Subject to Change

- First, the validity of the analysis depends on the validity of the scenarios and the assumptions that are used to generate the scenarios.
- Second, the analytical model does not contain internal "feedbacks" such as an explicit link between higher electricity prices and reduced electricity consumption.
- Third, we have not attached probabilities to any of the assumptions or scenarios. Therefore the model cannot produce estimates of a single "most likely" or "best" estimate for any of the results.
- Finally, no attempt has been made to explicitly evaluate the degree to which any of the options may increase or decrease economic and financial risk. In summary, our scenario-based analysis requires readers of the report to make their own judgments about which scenarios and assumptions are more likely to occur. Although this can be viewed as a limitation of our method, it can also be viewed as a strength, since there is a clear link between assumptions and conclusions for each scenario examined.

Another uncertainty is the magnitude of any future carbon or other emissions taxes. Even a modest carbon tax such as that being proposed in some European countries can have a significant effect on the costs of using fossil fuels – in this study, the tax would have application in all options because either they are based on fossil fuels (coal and enhanced diesel) or employ diesel generation as a backup (coal and nuclear).

1.4 Acknowledgements

This study was conducted over a three-month period beginning in April 2004. Funding was provided by the U.S. Department of Energy's Arctic Energy Office. Assistance and support was received from many sources. Specifically, the authors thank: the members of the Advisory Committee (See Section 1.5) for input and guidance; the Galena City Council, City Manager, and "The Breakfast Club" for important background and operational information; the Loudon Tribal Council for insight into its perspective on development; the citizens of Galena for their hospitality; the Alaska Village Electric Cooperative (AVEC) for providing electric load data; and vendors of related systems and products for helping us understand system possibilities; and Ashish Agrawal of UAF for helping with the electric load calculations

1.5 Advisory Committee

An Advisory Committee was formed to review the project plans and progress through the study. The primary functions of the committee were to make sure the most critical issues were addressed and that reasonable assumptions were made. The Advisory Committee met on April 22, 2004, June 8, 2004, and July 21, 2004. The Committee members are

Peter Crimp, Alaska Energy Authority
Brent Petrie, AVEC
Kathy Prentki, Denali Commission
Tyg Skywatcher, Loudon Tribal Council

Pre-Publication Draft – Subject to Change

Marvin Yoder, City Manager, City of Galena

1.6 Technical Contributors

Robert E. Chaney, Project Manager, SAIC Corporation, Anchorage, Alaska

Stephen G. Colt, Assistant Professor, University of Alaska Anchorage, Anchorage, Alaska

Ronald A. Johnson, Professor, University of Alaska Fairbanks, Fairbanks, Alaska

Richard W. Wies, Assistant Professor, University of Alaska Fairbanks, Fairbanks, Alaska

Gregory J. White, Consulting Scientist, Idaho National Engineering & Environmental Laboratory, Idaho Falls, Idaho

2. POWER GENERATION OPTIONS

Essential in determining the most appropriate power generation options to consider is an understanding of the community's loads. After loads are assessed, then options are considered.

Note that for any system option, there is a requirement to provide for backup generation capacity, which is accomplished by retaining some level of diesel generation capacity.

2.1 Loads

2.1.1 Heating Load for Cogenerated Heat

Currently, the city buildings, school, swimming pool and health clinic space heating needs are met by capturing the heat rejected by the diesel electric generators (DEGs) and transferring the hot water to the buildings (all close to the power plant). We have assumed a existing average cogeneration load of 400,000 Btu/hr for eight months per year plus an 300,000 Btu/hr [commercial/residential boiler load] for other buildings in town for eight months. This gives a total yearly cogeneration thermal load [CTLoad] projected for the future of about 4 B Btu. The 400,000 and 300,000 Btu/hr were obtained from the 2004 Galena Energy Assessment (Northern Resource Group, 2004). These were distributed over a year using Fairbanks heating degree days [HDD] data. This gives a maximum heating load of 900,000 BTU/hr. However, in his response to the Denali Commission Screening Report (Northern Economics, 2001), city manager Marvin Yoder said the city uses 50% of DEGs BTUs in winter. With an average load of ~ 900 kW in winter, we can assume the heat rejected to the jacket water is ~900 kW. Using half of this results in 450 kW ~ 1.5 mm Btu/hr as the maximum cogenerated heat delivered. Allowing for expansion, the maximum cogenerated heat delivered is about 1.8 M Btu/hr. This results in the upper curve in the plot shown in **Figure 2.1** below and a

Pre-Publication Draft – Subject to Change

yearly total of about 8 B Btu.

These HDDs were found using 1958 to 1993 data for the average daily temperature in Fairbanks and noting that each English unit HDD is 24 hours with the average ambient temperature 1°F below 65°F. A curve fit for average daily temperature was used.

$$T = 27.5 + 36 \cdot \sin(\pi \cdot (d-96)/182) \quad \text{where day [d] 0 is on Jan 1.}$$

The minimum of this plot occurs on Jan 5.

Then $HDD = (65 - T)$ gives the distribution of HDD over the year. The corresponding equation for heating degree hours [HDH] is

$$HDH = 65 - T1 \quad \text{where}$$

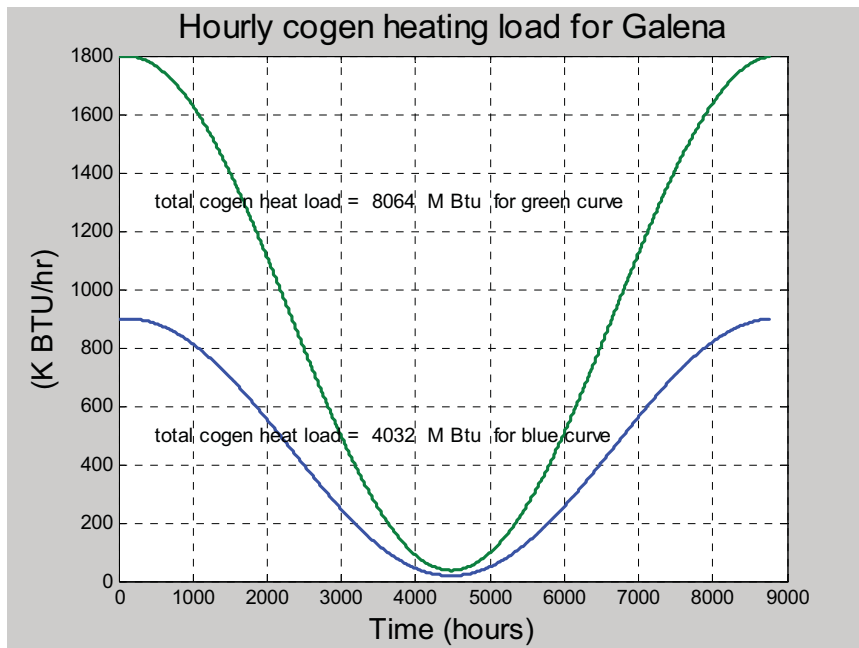
$$T1 = 27.5 + 36 \cdot \sin(\pi \cdot (hr/24-96)/182).$$

Using $HDH_{total} = \sum(HDH)$, one can calculate the hourly heat load (HHL),

$$HHL = CT_{Load} \cdot HDH / HDH_{total}$$

This results in curves shown in **Figure 2.1**, below. The yearly total HDD resulting from this curve fit is 13793, which is the average for the 35 years beginning in 1958.

Note: The Fairbanks average monthly minimum and maximum T over the 11-year period beginning with 1980 correlated with Tanana with an $R^2 > 0.99$. Since Tanana is 100 miles upriver from Galena, using Fairbanks temperature data to produce HDD is a good approximation for Galena.



Pre-Publication Draft – Subject to Change

Figure 2.1. Galena heating load for cogeneration

2.1.2 Electric Loading Profile.

To generate an electric load profile with data at 15-minute intervals for Galena, we started with the actual data for monthly kWh generated [Galena Energy Assessment, 2004], the data for winter and summer peaks from the Denali Commission Screening Report (Northern Economics, 2001) [1.6 MW and 0.9 MW], and used 15-minute load information from an interior Alaska Village Electric Cooperative (AVEC) village (Petrie, 2004) with a similar climate to provide profiles for diurnal and weekly variations for Galena. These 15-minute data were comparable with 1-hour data collected in Galena for the 1st quarter of 2004. In **Figure 2.2**, we see the monthly electric energy generated. This results in an annual load slightly under 10 M kWh. The average monthly load was about 800 kW in July and over 1 MW in January.

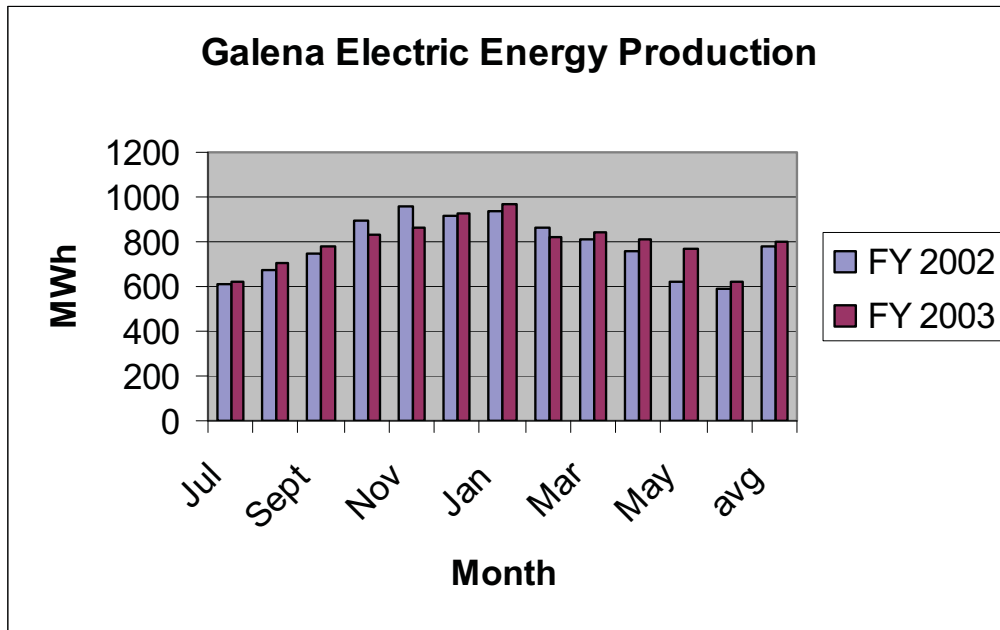


Figure 2.2. Monthly electric generation for Galena

By scaling the data for a northern AVEC village, we generated a map of yearly load excursions for Galena such that the yearly and monthly totals match the actual Galena data. The results are shown in **Figure 2.3**. Here, if we zoomed in on, for example, a 1- or 2-day time period, we would see the details of the loads for that particular period with the load being greater at 6 p.m. than 2 a.m. Such details can be extracted from the MATLAB™ program used to generate this plot and are shown in **Figure 2.4**.

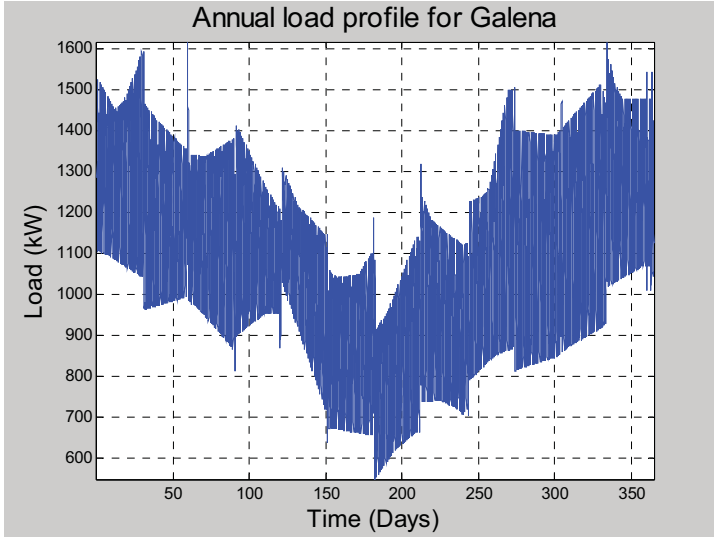


Figure 2.3. Hypothetical electric load for Galena for one-year period

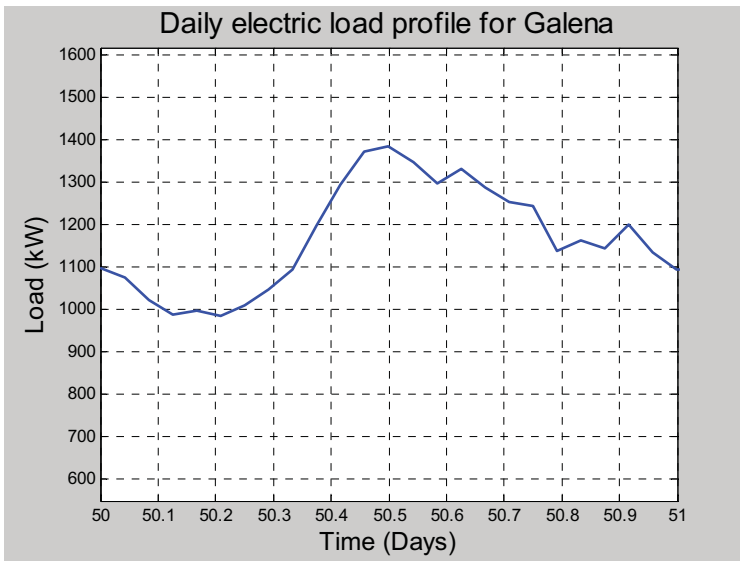


Figure 2.4. Hypothetical electric load for Galena for Day 50. The maximum is 1380 kW and the minimum is 990 kW.

2.2 Enhanced Diesel

According to the Rural Alaska Energy Plan (MAFA, 2002a), the most efficient village-sized DEGs available today are capable of achieving peak efficiencies in the 15.8 kWh/gal range. With a fuel oil having a heating value of 135 K Btu/gal, this is equivalent to converting 40% of the energy in the fuel to electric power. Technology improvements such as those associated with electronic fuel injection have reduced air pollution and noise due to more efficient combustion processes. The enhanced diesel scenario will assume an efficiency, for electric power production, of 15 kWh/gal as long as each

Pre-Publication Draft – Subject to Change

generator operating is at least 50% load. At the same time, we will assume that the captured heat from the jacket water and after-cooler [if applicable] is at least 50% of the electric power output.

We also estimate the cogenerated heat available in the jacket water is in the range of the electric power generated. Hence, the difference between these two will be proportional to the parasitic fan power needed for heat rejection when cogeneration is not sufficient for heat rejection requirements.

We can define three kinds of efficiency with

$$(1) \eta_{el} = W_{el}/Q_{dofh}$$

$$(2) \eta_{cogen} = [W_{el} + Q_{dotcogen}]/Q_{dofh}, \text{ and}$$

$$(3) \eta_{econ} = [W_{el} + \alpha Q_{dotcogen}]/Q_{dofh}$$

where W_{el} = the electric power produced (kW)
 Q_{dofh} = the rate of energy input in the fuel (kW)
 $Q_{dotcogen}$ = the heat recovery rate (kW), and
 α = an energy quality factor

α accounts for the lower quality of thermal compared with electric energy. An approximate figure for α may be 1/3.

Note: to convert heat rate into units associated with electric power, it is convenient to use 1 kW = 3,412 Btu/hr.

Figure 2.5 shows that the average monthly electrical generation efficiency varies from about 13.2 to 14.8 kWh/gal with an average of 13.76. If we assume the fuel has a heating value of 134K Btu/gal and uses 1 kWh = 3,412 Btu, the above corresponds to an actual Galena efficiency range of 33.5 to 37.6%. If we assume we can capture heat equivalent to one-half W_{el} , then each of these efficiencies increases by 50% according to Equation (2). From Equation (3), if $\alpha = 1/3$, each η increases by about 17%.

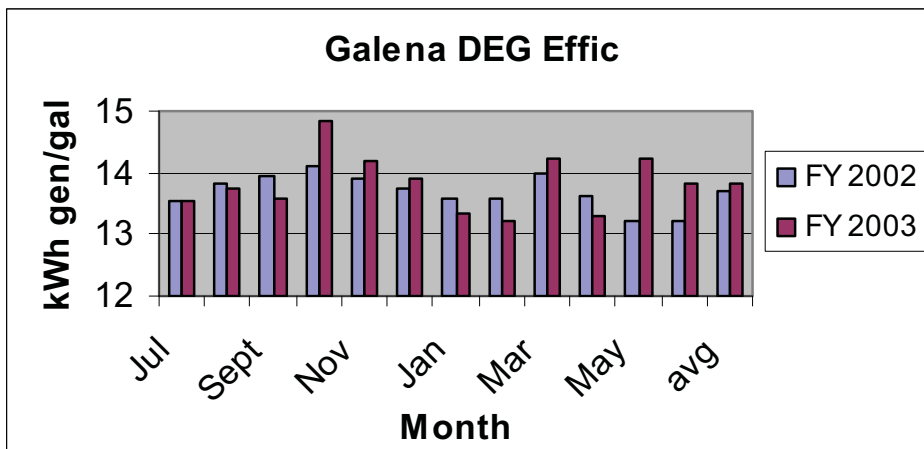


Figure 2.5. Performance of DEG system at Galena

Pre-Publication Draft – Subject to Change

By assuming enhanced utilization of cogenerated heat together with more efficient production of electric power, we can calculate the reduction in diesel fuel used annually compared with a baseline case. By amortizing the cost of buying new improved diesels and expanding district heating, we can calculate if the benefit cost ratio is greater than one.

2.3 Coal (Mine & Power Plant)

2.3.1 Coal Mine

An exposed coal seam about 18 road miles upriver from Galena has coal having an estimated heating value averaging 9.4 K Btu/lb (18.6 M Btu/ton). Its sulfur content is less than 0.5%, ash averages 9% [range 2 to 16%], and moisture content averages 19% [14 to 28%]. One exposed seam is about 9 feet high and 2,000 feet across. [Phillips and Denton, 1990]. If a 1-MW coal-fired plant were to operate with an efficiency of 25%, it would require 13.6 Btu/hr of fuel energy or about 0.68 tons/hr (6,000 tons/yr) of coal. At a density of ~ 80 lb/ft³, the required volume is about 17 ft³/hr or 12K ft³/month. If a 100-foot width were taken from this 9-foot-high coal seam and used, 13 ft/month or 166 feet/yr would have to be excavated.

The coal resource estimate was based only on the extent of the exposed seams. A detailed drilling program is required to delineate and define the magnitude of the coal resource contained in this bed.

A cost estimation for hauling 5K tons/yr of coal 10 miles is \$123/ton for a “model” mine with \$35 of this for hauling, \$35 for permitting and engineering, and \$25 for stripping (Phillips and Denton, 1990). This is slightly lower than the \$128/ton estimate for coal delivered from the Loudon prospect to Galena (Northern Economics, 2001).

2.3.2 Power Plant with AFBC and a Steam Turbine

Atmospheric fluidized-bed combustion (AFBC) boilers are now well-established as a mature power generation technology with more than 620 AFBC units in operation worldwide in the size range 20 to 300 megawatts (MW). Current operating experience shows that AFBC boilers meet high environmental standards and are commercially viable and economically attractive.

<http://www.epri.com/journal/details.asp?id=627&doctype=features>

Two commercial units are operating in Ohio at sizes < 5 MW. One (Johnson) unit has operated for about 20 years. A DOE-supported 8.5 M Btu/hr unit at Cedar Farms, Ohio, has completed four months of unattended computer operation of the combustor by April 2004. Furthermore, it received certification for long-term commercial operation from Ohio having met emissions requirements for sulfur and particulates. It provides hot water at 14 psia and 185°F for a commercial greenhouse operation. Since the greenhouse now operates with natural gas (NG) costing \$8.30/MBtu, the payback period is about four years accounting for combustor's the installed cost. This period is estimated to be six years if this unit were modified to produce electric power (Bonk, 2004). To do this, a turbine/generator, more heat transfer area, plus auxiliary equipment

Pre-Publication Draft – Subject to Change

must be added. The latter would include additional controls as well as transformers and a distribution system.

These plants burn a range of fuels, including bituminous and subbituminous coal, coal waste, lignite, petroleum coke, biomass, and a variety of waste fuels. In many instances, units are designed to fire several fuels, which emphasizes one of the technology's major advantages: its inherent fuel flexibility. AFBC boilers also can more readily handle fuels that are problematic in pulverized coal (PC) boilers (i.e., biomass and waste). The principle of operation involves tiny particles of combustible material such as coal being kept in suspension by upward flowing air. The bed of hot coals surrounds water-filled tubes to which heat is very efficiently transferred to make steam. The steam expands through a steam turbine that is coupled to an electric generator to produce electric power.

The U.S. DOE initiated a study in 1998 (Northern Economics, 2001) to investigate the capital and operating costs of small coal-fired power plants [600 kW to 2 MW]. For 50 and 85% load factors, fuel costs ranging from \$2.25 to \$12.00/MBtu, and efficiencies from 20 to 26 K Btu/kWh, the electricity costs ranged from \$0.22 to \$0.77/kWh. The installed costs ranged from \$3.0K to \$4.3K/kW and the total annual non-fuel costs ranged from \$1.0M to \$2.6M. Galena coal was mentioned to have a delivered cost of \$7.06/MBtu in that report. This is close to the \$6.15/M Btu derived from the 1990 study cited above. At the other end of the spectrum, the Royal Academy of Engineering (2004) calculated the electricity costs from large [>100 MW] coal-fired CFB power plants to be \$0.063/kWh with about 90% of that being approximately equally distributed among fuel, capital, and carbon emissions. These costs were slightly lower than those for plants using pulverized coal.

A 2003 feasibility study on a barge-mounted 5-MW AFBC power plant (Bonk, 2004) estimated capital costs from \$20M to \$25M and electricity costs of \$0.20/kWh minus a credit for heat delivered. This is for 11K Btu/lb coal delivered for \$100/ton [estimates for Galena]. These last two numbers are equivalent to \$4.54/MBtu delivered cost.

J.S. Strandberg (1997) did a feasibility analysis of an 800 kW AFBC coal plant in McGrath, Alaska, plus a 125 kW DEG. He estimated a total project budget of about \$14 million, which included the power plant, coal mine development, haul road, and an expanded district heating system. The coal had a heating value of about 6700 Btu/lb and was assumed to cost \$52/ton delivered. The district net output was 9 M Btu/hr and water was supplied at 240°F and 75 psig. The estimated electricity cost was \$0.176/kWh, which included a \$ 0.077/kWh credit for heat delivered. Over half of the total cost was for coal and limestone. A major issue was the system's high parasitic power required [over 155 kW], and the estimate for it was increased as the study was completed.

Phillips and Denton (1900) calculated costs for a 483 kW coal-fired model cogeneration facility producing 6.8 M Btu/hr of heat. The costs of electricity ranged from \$0.11 to \$0.22/kWh for a base load plant to as much as \$0.80/kWh for a lightly loaded plant. The corresponding heat costs ranged from \$16 - \$28/M Btu on the low end to as much as \$110 on the high. Of the 21 M Btu/hr fuel input, 46% went to the production of electricity. Of the total capital cost of \$7.5 M, \$2.0 M was allocated to electrical and

Pre-Publication Draft – Subject to Change

>\$5.5 M to heat. Almost half of the latter was for 12,000 feet of distribution piping at \$200/ft. For a plant in Galena using Louden coal, the electricity costs were estimated to range from \$0.26 to \$0.36/kWh and heat from \$24 to \$36/M Btu.

A comparison of the four Alaskan studies appears in **Table 2.1**.

Table 2.1. Key parameters for four Alaska coal-power plant studies

Study/Parameters	Size for We	Capital Cost	Est. Rate (\$/kWh)
Phillips & Denton, 1990	483 kW + 6.8 M Btu/hr heat	\$ 7.5 M [\$ 2M for elec. Rest for heat	0.11 to 0.80 [base load to lightly loaded
USDOE, 1998	600 kW to 2 MW	\$ 2.5 .. \$ 6M	0.22 to 0.77 [various fuel costs & loading]
Strandberg, 1997	800 kW + 9 M Btu/hr heat	\$ 14M [including coal mine + district heat]	0.18
Bonk, 2004	5 MW [barge mounted]	\$ 20 - \$25 M	0.20

For comparison, according to Colt et al. (2001), the true cost of rural electric utility service for 90% of rural Alaska villages runs less than \$0.45/kWh. The range is from \$0.17/kWh for larger regional center communities (Naknek) up to around \$1.80/kWh for small remote communities like Pedro Bay.

A coal fired-plant should be a base-load plant sized to run near its capacity all the time except for planned shutdowns for maintenance and repair.

2.3 Toshiba 4S Nuclear Power Plant

2.3.1 4S System Characteristics

This discussion of the proposed nuclear reactor is a summary and more details are enclosed in the Appendices. First, the characteristics of the design are presented. Then, sections are included describing the safety of the design and the security issues.

The nuclear reaction which occurs in the reactor core produces heat. This heat is conveyed by heat transfer fluids or coolants to the exterior of the reactor where the energy is used for electric power generation or for other purposes. Existing commercial plants in the United States employ water as the coolant and produce hot pressurized water from the energy released by radioactive decay in the nuclear core contained within a pressure vessel. This water, in turn, transfers heat to water in the secondary water system to vaporize it into steam. All this occurs within a thick concrete containment structure. The pressurized steam is transferred outside the containment vessel where it drives a steam turbine coupled to an electrical generator. Control rods in the core are used to moderate the reaction. Currently, the United States produces about 17% of its electricity from 109 nuclear power plants of up to 1000 MW capacity. Worldwide, there are over 400 nuclear plants; France generates 77% of its electricity from nuclear

Pre-Publication Draft – Subject to Change

reactors . There are no commercial nuclear power plants in Alaska (McKinney and Schoch, 1998)

Figure 2.6 shows the large containment structure in which the reactor and steam generator are housed. Note the parabolic-shaped cooling tower in which water is sprayed to allow heat to be rejected to the ambient air. This heat rejection provides a heat sink to condense the steam leaving the turbine. The pump feeding the working fluid to the steam generator requires water in the liquid form to work effectively. Hence, the steam must be condensed upstream of the pump. The pump pressurizes the water to allow proper operation of the pressurized water reactor.

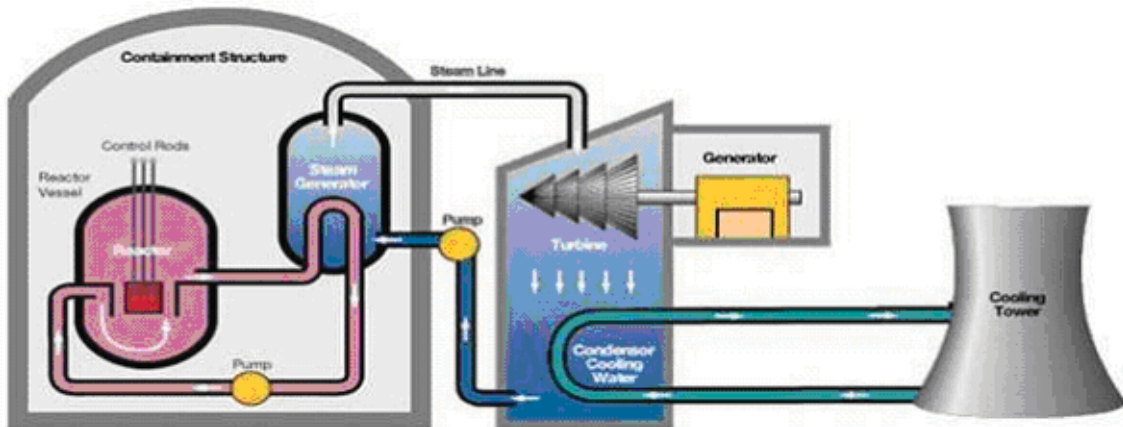


Figure 2.6. Schematic of Nuclear Power Plant: Photo courtesy of TVA

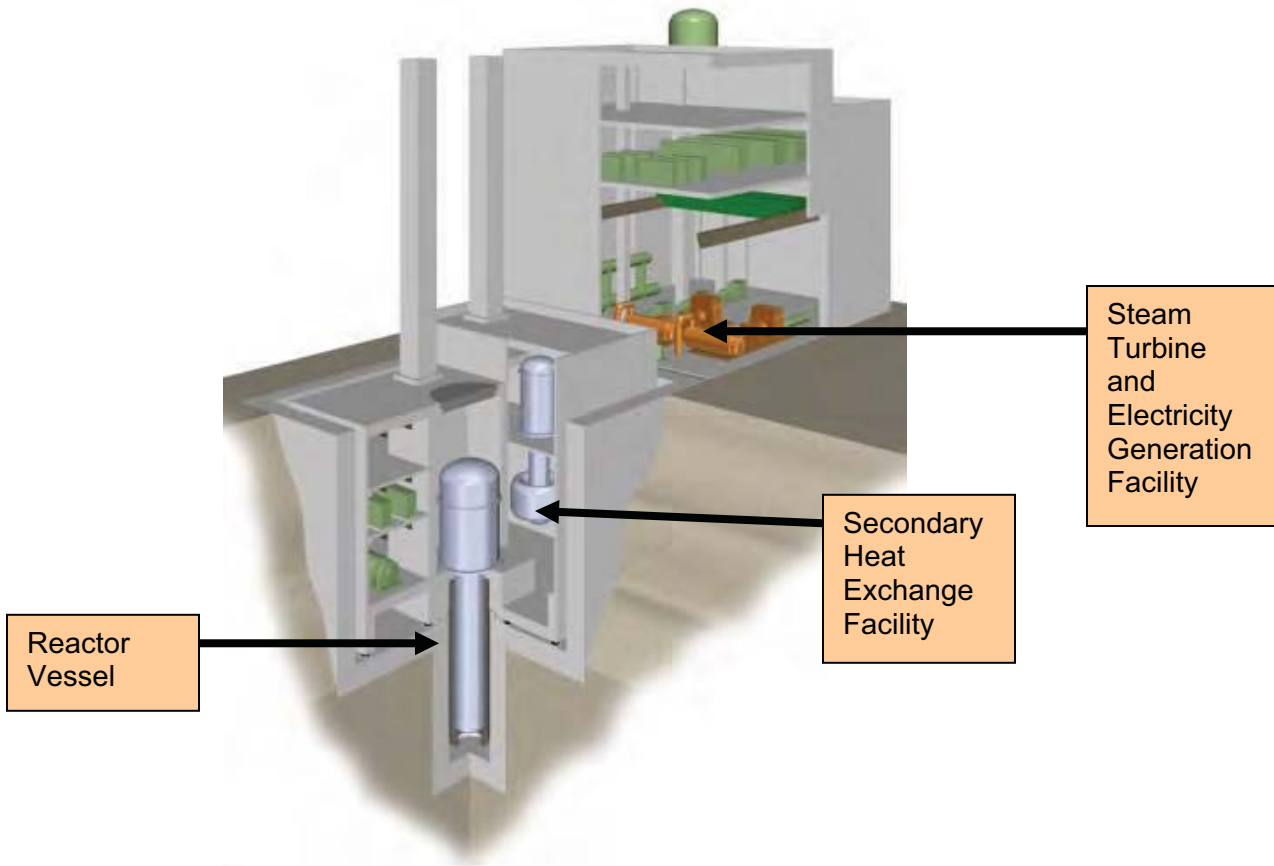
The 10 MW Toshiba 4 S nuclear power plant is an example of new small innovative reactor [SIR] designs that are under active development today. Most of the components of this system have been extensively tested and many have been licensed by the Nuclear Regulatory Commission (NRC). Toshiba currently is conducting engineering work to complete the reactor and plant designs. Therefore, if the first operational unit is installed at a site such as Galena, it would be considered a “reference” rather than a “prototype” or “demonstration” plant. Reactor development proceeds in several steps.

- *Experimental* reactors are the first stage to test the concept (research)
- *Demonstration* reactors use refined designs and test integrated systems (engineering)
- *Prototype* reactors are the first of several reactors of the fully engineered design
- *Reference* plants establish the design basis for licensing and serve as a model for the construction and licensing of additional commercial plants. (Rosinski, May 24, 2004, private communication)

The assumption that the 4S would be a reference plant is subject to some question by U.S. National Laboratory staff (Brown, 2004, Sackett, 2004). Further, caution should be taken in the estimated development time needed to bring this design to an operational state. In this study we assumed the plant would be ready in 2010, but it may require 3 to 5 years longer.

Pre-Publication Draft – Subject to Change

The 4S is schematically shown in **Figure 2.7**. These modular reactors are designed to require minimum field assembly and minimal maintenance by allowing spent or defective modules to be removed and repaired at a central facility. Unlike commercial power reactors, the 4S is designed as a totally enclosed unit. The core and the primary coolant loops are sealed in the cylindrical structure. The heat released by the fission process and radioactive decay in the core is transferred to a liquid metal [sodium] in a primary heating loop. This, in turn, heats sodium in a secondary loop that transfers heat to water to make steam in a second heat exchanger which in turn drives a steam generator. The sodium is maintained at about 1 atmosphere pressure and 500°C. There is no design capability to open the reactor vessel, for any purpose, other than at the factory. The coolant is circulated by electromagnetic pumps which have no moving parts. Coolant pumps and reservoirs are located above the core so that the structure design is kept long and narrow. This design also means that there are no emissions, except steam, throughout the lifetime of the plant.



Toshiba, Inc.

Figure 2.7. Schematic diagram of the 4S installation. Note that it is proposed that the Reactor Vessel be installed up to 100 feet below grade.

In the 4S design, the radioactive core is 2.0 m high and 0.7 m in diameter with the fuel composition of enriched uranium alloyed with zirconium. The fuel is less than 20% uranium. A cylindrical steel reflector shield rising from the bottom at a rate of around 5 cm/yr by means of an electromagnetic drive mechanism maintains the proper

Pre-Publication Draft – Subject to Change

reaction rate by reflecting neutrons back into the core. The reflectors are moving upward slowly in order to compensate the reactivity loss during 30 years burn-up. In the event of a shutdown for whatever reason, gravity will cause the shield to fall back down, slowing the reaction rate. Moreover, the reactivity temperature coefficient is negative, meaning that the reaction will slow down if the core temperature gets too high. If an accident occurred, power would be lost, the reflector would stop its ascent, and it would move down to make core sub-critical, terminating the fission reaction.

The projected design life of the sealed 4S reactor is 30 years. The intent is that refueling on site would not be necessary. The reactor is intended to be returned to the factory and a replacement unit installed at the end of the unit's life. For a first-of-a-kind installation in Galena, licensing requirements may include extensive analysis of the reactor after a short run-time (i.e. 1 to 5 years). In this case the reactor would be changed out at that interval and returned to Toshiba for analysis.³ Extensive technical design evaluations are underway at Argonne National Laboratory – West, in conjunction with Toshiba, to improve and refine features of the 4S, but the current design is a sound basic design with low technical risk. (Sackett, 2004)

Load following is achieved by controlling the water flow to the steam generator causing changes in the coolant temperature, which affects the core inlet temperature and hence alters the reaction rates in the core. Since the core reactivity has a negative temperature coefficient, the lower water flow rate [lower load] lowers the core thermal output [consistent with lower load] by raising the core temperature. This feature greatly simplifies operation of the 4S power plant. (USDOE, 2001)

A cost estimate provided by Toshiba in 2003 was a capital of \$2,500/kWe and electricity at \$0.05 to \$0.07/kWh assuming mass production of such plants. Experts may assert that this is a low value and does not include all of the development costs, as noted above. (Brown, 2004, Sackett, 2004)

Prior to the installation of any nuclear plant in the US, the Nuclear Regulatory Commission (NRC) conducts an extensive licensing process. This process includes extensive safety, security, and siting reviews. Detailed risk assessments are required; Safety and Security are critical elements of the process. The time required is not known precisely at this time.

2.3.2 Safety

The 4S is a pool type of reactor – not a breeder reactor- that has an “inherently” safe design so that it shuts itself down if coolant is lost. If that occurs, the reflector falls to the bottom of the reactor vessel, no longer performing its function, and the nuclear reaction slows down. This has been tested in the laboratory and will be verified as part of the Toshiba development work prior to NRC licensing and approval. The concept was also demonstrated at the Experimental Breeder Reactor II (EBR II) at the Argonne National Laboratory-West facility at the Idaho National Engineering Laboratory in 1988 when a large-scale reactor of this design was tested to failure, and the tests proved the reactor would shut down with no adverse effects.

³ According to Toshiba, this location would probably be the same as that for final reactor assembly.

Pre-Publication Draft – Subject to Change

The fact that there are no moving parts in the vessel adds to safety of the plant. The coolant is pumped using the electromagnetic properties of the sodium. Designed so that there is no refueling during its design-life, the 4S requires very low maintenance and reduces the risk of mechanical failure.

The possibility of sodium-water reactions is a serious consideration, and concerns about handling of sodium have resulted in extensive design consideration of the coolant loops in the 4S. Water and sodium react with the release of a large amount of energy, and the 4S is consequently designed with double-walled piping to contain the sodium and prevent leaks (Sakashita, 2004). Advanced leak detection systems sense the void between the walls of the pipe for sodium vapor. If detected at levels of 0.1 gram per second, the sodium circulation system is shut down. This contains the sodium within the piping, which is in turn contained inside the vessel or the secondary cooling loop housing. In the event of a leak, there are double and triple containment features. Leak detection systems monitor for sodium in each of the containment areas. This significantly reduces the risk of leaked sodium coming in contact with water.

Sodium cooled reactors throughout the world have been run for thousands of hours without incidents involving the reactor core. According to Neil Brown, a nuclear engineer at the Lawrence Livermore National Laboratory, there are 21 sodium-cooled fast reactors worldwide, including Japan's MONJU. This 280-MW plant operated for about one year starting in 1994 before being shut down after an accidental sodium leak and fire. No radioactivity leaked, but community concerns have kept MONJU shut down. (FDNM, 2004).

Another example of long-term operation is a 140-MW liquid metal reactor (JOYO), which has operated in Japan since 1977. It is a breeder reactor designed to produce more fuel than it consumes. It had operated for over 50,000 hours by the time it was shut down in 1994 and produced over 4,000,000 MWh of thermal energy.

http://www.iaea.org/inis/aws/fnss/fulltext/0791_4.pdf

During a period when the reactor was shut down, there was a fire lasting 3 hours in a maintenance facility 50m from the reactor in Oct. 2001. The fire may have been caused by spontaneous combustion of sodium on some of the equipment (Japan Times, Nov. 2, 2001).

In another example of long-term operation, the Experimental Breeder Reactor-II (EBR-II) generated over 2 B kWh of electricity while operating at Argonne National Laboratory from 1964 to 1994.

http://www.anlw.anl.gov/anlw_history/reactors/ebr_ii.html.

It successfully passed a series of safety tests including those involving loss of coolant flow. Even with the normal shutdown systems disabled, the reactor safely stopped operating without reaching excessive temperatures.

The 4S vessel is expected to be installed up to 100 feet below grade. With the nature of the vessel's walls, placing it in a concrete structure at this depth will help reduce safety issues.

2.3.3 Security

Pre-Publication Draft – Subject to Change

Since questions of security are foremost in our minds, the NRC-required risk assessment will consider this in depth. Installing the vessel deep underground with a large, heavy, reinforced concrete cap adds to the secure nature of the 4S installation. The core is designed so that the material is below the proliferation treaty limits. If it were to fall into the wrong hands, it cannot be easily converted or enriched to weapons-grade fuel.

No heavy equipment in Galena is capable of lifting/removing the cap. The cap would need to be broken and removed in pieces. Due to Galen's isolation, no group of insurgents could accomplish this without detection long before they could breach the vessel. Even if they did, the material in a core of this design would not be easily extracted.

In its economic analysis based on the current practices at large nuclear power plants in suburban areas of the lower 48 states and Japan, Toshiba conservatively estimated a security guard force of 34 would be required. Because of the design, isolation, and inaccessibility of the vessel or cooling loops, it is suggested that this level of surveillance may not be required. A detailed risk assessment will determine what level is needed. With remote monitoring from the City/State law enforcement offices, only one guard may be necessary on-site at all times. This would significantly reduce the manpower requirements and effect the economic assessment. Thus, in the economic section, we used four guards as a minimum and 34 guards as the upper level for security staffing.

2.4 Other Power and Heat Generation Modules

In addition to those technological options for electricity generation discussed above, others can be used and are briefly described below. It was determined that these options would not contribute a significant enough amount of affordable energy to the utility for the utility to justify a major investment in them. However, Galena may want to consider implementing these technologies on a pilot scale within the next 10 years. If they might be proven feasible or reduced in price in the future, these technologies can be added to the utility as modules. Included are in-river turbines, solar, biomass, fuel cells, and coal bed methane. Therefore, these options are briefly discussed below – further details for some are provided in the Appendices.

2.4.1 Hydro In-river Turbines

Galena is on the north bank of the Yukon River, one of the largest in the country. A tremendous amount of water passes the site each day – winter and summer - and it seems to be a logical place to install in-river turbines for electric power generation. However, compared to the load requirements of the City, this may not be a valid conclusion. From the discussion presented in Appendix 1, a variety of turbines are being developed, but none has been proven in arctic environments. The one apparently best suited to the Galena site is under development by UEK Corporation. It is proposed to be installed in rivers, anchored to the bottom, and operated year-around – even under ice. A project to demonstrate it at the village of Eagle on the upper Yukon River has been approved but is awaiting U.S. DOE funding. This turbine design has dual 3-meter diameter blades. To estimate the power output of such a unit at Galena, a look at the power density is in order.

Pre-Publication Draft – Subject to Change

The power density in a flowing fluid is

$$P_{\max} = 0.5\rho V^3$$

For water flowing at $V = 2$ m/sec (characteristic of the Yukon at Galena) and density $\rho = 1000$ kg/m³, this corresponds to 4 kW/m³. For reasons related to mass conservation and efficiency, one may only be able to capture 40% of this or less with a conventional turbine. For a water turbine with two 3-meter turbines or area of 14.1 m², this results in power generation of 22.5 kW – much less than that required by the City's load. Ten units would have to be installed to make even a marginal contribution and the cost may be too great for the benefit. UEK estimates \$1,000/kW capacity for a 10-MW plant yet to be built.

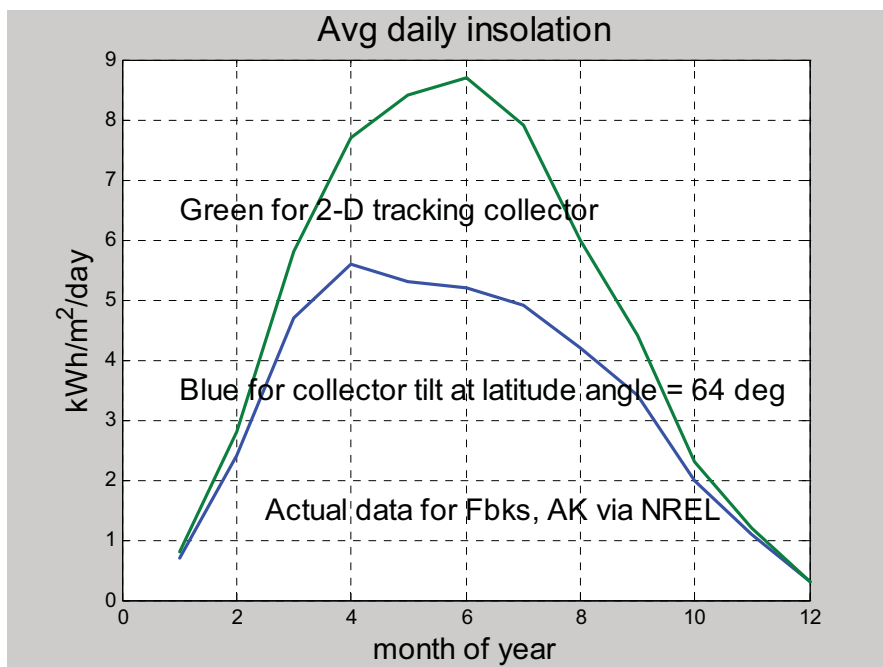
(<http://www.delawareonline.com/newsjournal/local/2003/09/06tidalpowerplant.html>)

On the other hand, an operational 300 kW tidal turbine in Norway costs \$23,000/kW capacity. (<http://www.eere.energy.gov/RE/ocean.html>)

2.4.2 Solar

Much of interior Alaska has a good solar resource for as much as eight months of the year. The National Renewable Energy Lab [NREL, 2004] has 30-year solar insolation data for hundreds of U.S. locations. Although there is no data for Galena, the plot shown in **Figure 2.8** below for Fairbanks probably provides a fair representation. Note, the data shows a substantial resource, even in the springtime, when both heat and electrical demands are high.

A downside to using solar energy is the intermittent nature of the resource. Hence, as with any intermittent resource, storage can be a key issue.



Pre-Publication Draft – Subject to Change

Figure 2.8. Solar insolation data for Fairbanks, Alaska

2.4.2.1 Solar-electric

Photovoltaic devices convert sunlight directly to electricity at efficiencies as high as 25%, although 10% is typical. Applications include residential both on and off grid, commercial buildings, remote systems for telecommunication, cathodic protection, pumping and irrigation, and land-based navigation aids. With output power densities around 125 W/m², a 1-square-meter panel may produce a kW-hr each 8-hour day. Brown (1999) estimated electric power can be produced for \$0.20/kW-hr. Obvious shortcomings in northern Alaskan applications are associated with the lack of solar input during the winter when the demand for electrical power is the greatest. But the solar resource is still significant for two-thirds of the year in much of the state.

According to a study done in Arizona (McChesney, 2003), the average installed system costs in Arizona varied from ~ \$6/peak watt for grid-tied facilities to over \$20/peak W (or \$20,000/kWp) for off grid systems. The latter would include battery storage. Installation of a 100 kW module in a Galena setting could cost \$2M.

2.4.2.2 Solar Thermal

Solar thermal technologies use the heat in sunlight to produce hot water, heat for buildings, or electric power. Solar thermal applications range from simple residential hot water systems to multimegawatt electricity generating stations. In Galena, discussions with the City Manager determined that this technology would more appropriately be installed by individual home or business owners. Its impact on the utility was determined to be limited. A more detailed discussion is presented in Appendix 2 and at the following web sites.

<http://solstice.crest.org/renewables/re-kiosk/solar/solar-thermal/index.shtml>

<http://www.eren.doe.gov/erec/factsheets/solrwafr.pdf>

<http://www.thermomax.com/>

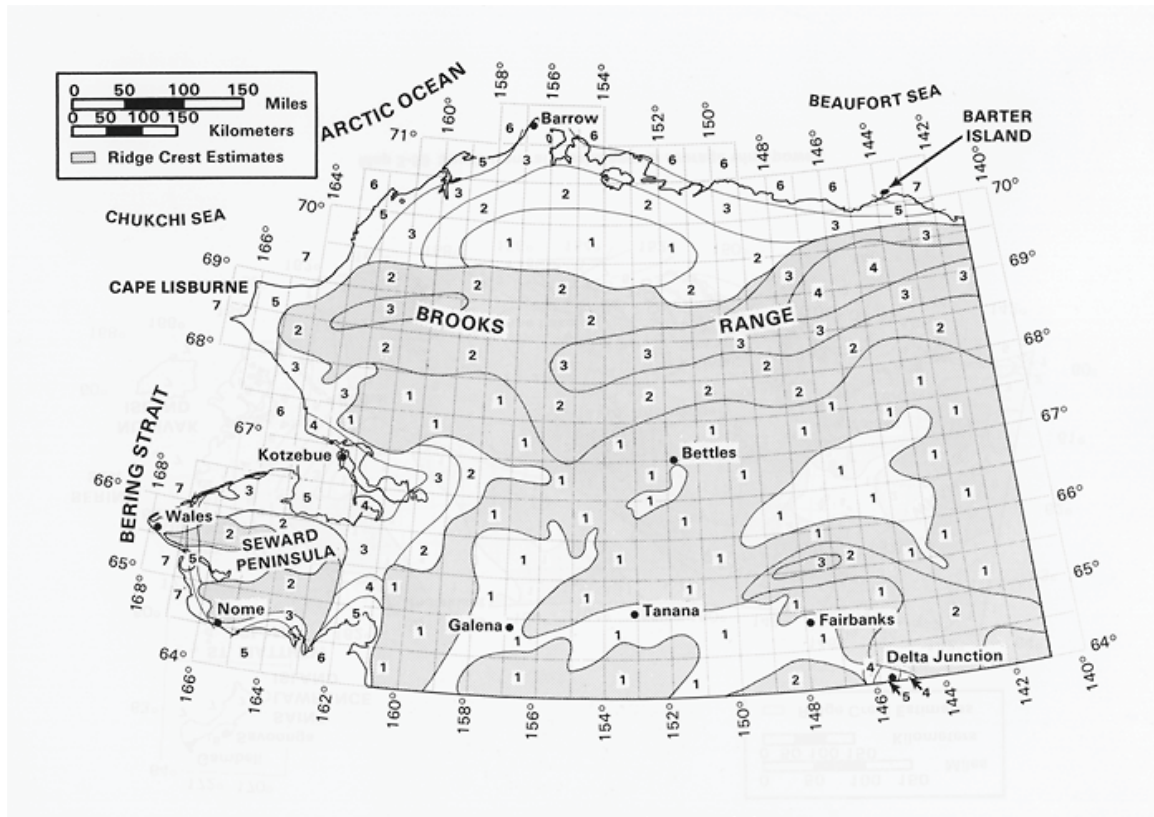
2.4.3 Biomass

Biomass can be wood from trees as well as plant residue, animal waste, and the paper portion of municipal solid waste (MSW). The dispersed nature of this resource makes the energy and time involved in harvesting an important issue. With a typical MSW generation of 4 lb/capita/day and an energy content of about 4 K Btu/lb, such wastes from a village of 700 people may have a heating value of 11 M Btu/day. If this could be converted to electricity with 20% efficiency, the power output may be about 34 kW – too small for a stand-alone unit. However, MSW could be burned in the AFBC of the coal power plant.

2.4.4 Wind

Pre-Publication Draft – Subject to Change

Wind generation is making in-roads into electricity production worldwide. However, at best wind turbines make up to 15 to 20% of the utility load. They are being employed successfully in Alaska in Kotzebue, Wales, and St. Paul. To be effective, a certain level of sustained wind resource is necessary. **Figure 2.9.** shows the wind regimes in Alaska. Average wind speed must be greater than about 16 miles/hr on average for wind generation to be effective (Class 5, 6, or 7). Galena is in a Wind Class 1 region with average speed much too low to be feasible. Therefore, wind generation was not assessed in detail for this investigation.



<http://rredc.nrel.gov>

Figure 2.9. Alaska, North, Wind Map. Map of wind regimes in northern Alaska. More information can be obtained on the web at www.bergey.com/Maps/Wind_classes.htm. Maps courtesy of U.S. DOE and NREL.

2.4.5 Fuel Cells

In fuel cells, hydrogen and oxygen are combined to produce water and release energy in the form of electricity. This reaction occurs in a thin layer on the surface of a membrane in the presence of a catalyst. Fuel cells convert the chemical energy of reactants (a fuel and an oxidant) into low voltage D.C. electricity via electrochemical reactions while generating almost no pollutants. Unlike conventional batteries, the fuel cell does not consume materials that are an integral part of its structure but rather acts as a converter. It will continue to operate as long as fuel and oxidant are supplied and reaction products are removed. Fuel cells require a minimum of maintenance, because

Pre-Publication Draft – Subject to Change

they have very few moving parts. The most mature technology is the phosphoric acid fuel cell (PAFC), which utilizes hydrogen for the fuel and produces water. This product is valuable, especially in Alaskan villages in the winter, where potable water can cost over 10 cents/gallon. Since the water is produced at temperatures approaching 200°F, it can be used for space heating. Current capital costs for a 200-kW device are around \$4500/kW, with efficiency for electrical production around 40%. A 1-MW PAFC plant consisting of 5-200 kW cells was installed at an Anchorage, Alaska airport post office complex. The project lasted for 5½ years and at the end, the cells were degraded to the point they needed to be replaced.

Other types of cells being actively developed include direct methanol (DMFC), molten carbonate (MCFC), and solid oxide (SOFC). The DMFC has the advantage of being fueled with a liquid fuel (methanol) which is more readily obtained than hydrogen. A disadvantage is crossover of some methanol from the anode to cathode side. The latter two offer the potential for internal reforming of conventional liquid and gaseous fossil fuel into hydrogen. Their higher operating temperatures also are more compatible with cogeneration. Disadvantages include the need for more expensive materials at these higher temperatures.

Since most fuel cell stacks under active development today require hydrogen as the fuel, reformers at the front end to convert fossil fuels to hydrogen are being developed. So far, cleaner fuels such as natural gas and methanol are easier candidates than "dirtier" fuels such as diesel and gasoline. Sulfur and CO in small concentrations can poison catalysts used in the stack membranes. It must be noted that when fossil fuels are used to produce hydrogen, CO₂ is released.

A second strategy is to use excess electrical generation capacity to generate hydrogen from water (electrolysis) and store the hydrogen for later use. This excess electrical power could come either from a renewable source, such as wind generation, or from excess capacity of existing diesel electric generators, using fuel cells in a load-leveling application.

The proton exchange membrane (PEM) fuel cell operates at around 60°C and has solid polymer membranes sandwiched between carbon cathodes and anodes. With a little less than one volt per cell, it takes about 18 cells in series to generate 12 volts. (Johnson et al., 2000). Multinational corporations such as Daimler Chrysler are spending billions of dollars developing this technology for transportation applications. Several corporations are also interested in this technology for stationary power.

Currently, this promising technology is not commercially available and thus was not considered for Galena deployment.

2.5.6 Coal Bed Methane

Gas has been produced commercially from coal beds in the lower 48 states. Development of resources in other parts of Alaska is in the preliminary stage. Insufficient information is available about how to develop CBM in arctic conditions to consider it for Galena. If considered for development, extensive work to delineate local reserves is required before development could occur.

3. ENERGY CONSERVATION

Important technologies and techniques, that impact the amount of electricity required of the utility, are available for energy conservation but implementation of them is end-user driven and best conducted by the users. Therefore, a discussion of conservation is included here for reference.

Energy conservation refers to a variety of strategies employed to reduce the demand for energy. This can include adding extra insulation on building exteriors, setting building thermostats closer to ambient temperatures, or carpooling. Conservation is different from increasing energy efficiency, which refers to increasing the useful output for a given energy input. This could involve replacing incandescent light bulbs with compact fluorescent ones, driving more fuel-efficient motor vehicles, and purchasing more efficient appliances. All of these practices are end-user initiatives. Even though end-use conservation is not the primary utility activity, utilities may help educate and encourage consumers. Utilities throughout the United States are engaged in energy conservation programs. For example, GVEA's Energy Conservation Program is outlined in Section 7.1 of the Administrative Manual. Some highlights of this program include

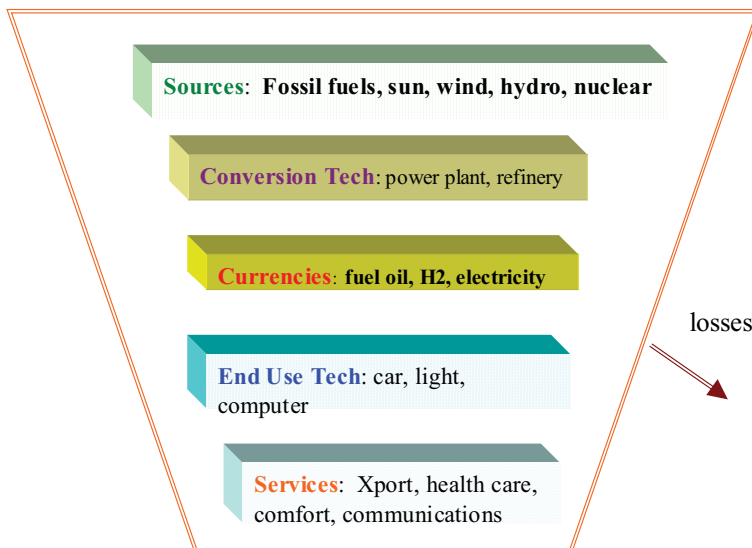
- (a) developing and maintaining an effective load-management program,
- (b) providing conservation information to the membership,
- (c) monitoring energy use in all aspects of operations including facility operation, facility construction, and use of vehicles, and
- (d) maintaining an active employee training program.

A detailed discussion of the options and benefits of conservation is given in the Appendix B.

4. USES OF EXTRA POWER

One unifying way to picture the flow of energy is by considering the below energy trapezoid as presented by Scott (2002) and others in **Figure 4.1**.

This study is focused on the top three items, sources and technologies and their ability to supply heat and electricity or other energy forms. The energy currencies of today are fossil fuels and electricity, but many believe hydrogen may be an important fuel in the future. What we want to provide are end services with several listed in the bottom part of the energy trapezoid.



Adapted from Scott(2001)

Figure 4.1. Energy Trapezoid

Some of the power plant enhancements being considered may provide electric power and heat at rates in excess of today's loads. Hence, one needs to consider growth in these loads such as that associated with population increases, new commercial enterprises, development of a regional grid, or tourism. In the future, if hydrogen becomes a vibrant energy currency, Galena could serve as a production center through water electrolysis powered by a coal or nuclear-fueled central power plant.

4.1 District Heating – Sales to Air Station

District heating currently serves the needs of the school, town offices, swimming pool, fire hall, and the power and water plants. Currently, the air station area gets space heat via oil-fired boilers that consume around 471,000 gals/yr of diesel fuel. This heat is delivered to individual buildings by utilidor. Part or all of this fuel could be displaced by district heating. If the power plant [nuclear, coal, or diesel] supplying this co-generated heat were located, say, 2 miles from the thermal load, a substantial capital expense would be required to construct the heat transmission line (\$200/ft). But, the losses in a well-insulated line would be substantially less than the heat delivered.

4.2 Residential Electric Heating

If electric rates to the homeowner can be sufficiently reduced, there is a strong possibility that many of the approximately 220 residences (and commercial/office buildings) would convert to electric baseboard heat as their primary method of heating. There are several reasons this may be attractive. If the cost is lower than the use of fuel oil, economics becomes a strong driver. Additionally, a clean heating source reduces contaminants in the air of the building thereby increasing the indoor air quality. Indoor air pollution is of particular concern during the long winter months when most people stay indoors much of the time. Convenience is also a strong incentive. Baseboard heat is even and automatic, reducing the need to bring fuel inside (as wood-fired stoves require) or fill/haul fuel tanks.

If it is assumed the 220 residences were converted to electric baseboard heat, the following summarizes the costs and requirements. Each home requires about 15 kW of heating capacity (50,000 Btu). Baseboard heaters cost \$50/kW and about \$25/kW for shipping and installation. Thus, each home would require an investment of \$1,125 to install the heating systems. Each home may also require up to \$1,000 investment to upgrade the service and wiring to handle the increase in load. This investment might be financed through the utility as an incentive for residents to convert. For this reason, the overall costs are included as part of the capital cost in assessing the economics of the 4S nuclear system. An estimated \$250,000 would be required to

Pre-Publication Draft – Subject to Change

upgrade the utility distribution system and purchase a replacement transformer. The following calculation yields \$717,500 as the total cost for conversion.

$$\frac{15 \text{ kW}}{\text{residence}} \times \frac{\$75}{1 \text{ kW}} = \frac{\$1125}{\text{residence}} \times 220 \text{ residences} = \$247,500$$
$$\$247,500 + \frac{\$1000}{\text{electric service upgrade}} \times 220 \text{ residences} = \$467,500$$
$$\$467,500 + \frac{\$250,000}{\text{distribution transformer \& feeders}} = \$717,500$$

Note that this cost estimate does not include the cost of electricity and is independent of the source. Supplying power for electric baseboard heaters from existing DEGs would result in operating costs much greater than for current forms of heating (oil furnaces and wood stoves). This option is discussed in more detail in the economics section.

4.3 Hydrogen Production

Many are projecting that hydrogen will be the fuel of the future. While there are some good reasons for this, significant issues that must be addressed. Hydrogen is the lightest element and thus has a very low density. It easily diffuses through many materials including some metals. One gallon of liquefied hydrogen weighs just 0.58 lbs (gasoline weighs over 6 lb/gal). It has a high energy content, but its low density means it has a low energy density (Btu/unit volume). Liquid hydrogen's energy density is about 22% of that for #2 diesel fuel. Thus, storage and containment are significant issues relative to hydrocarbon fuels.

Hydrogen is not a primary fuel as are conventional fuels such as natural gas, coal, and petroleum, but rather it is an energy carrier. Hydrogen does not occur in a free state in nature (because of its reactivity with oxygen to form water). Thus, hydrogen used as a transportation fuel must be made employing significant amounts of primary energy. Most hydrogen used is currently made from reforming of natural gas. It can be made by electrolysis of water – requiring large amounts of electricity. However it is made, more energy is used in its production than it contains. If produced from electricity from a 40% efficient coal-fired power plant, with a 75% efficient electrolyzer, the energy content of the hydrogen product would contain at most 30% of the energy of the coal used to produce it. Hydrogen is attractive as an alternative for transportation fuel because it burns very cleanly and has no by-products except water and perhaps some traces of nitrogen oxides. It produces no carbon dioxide. There is currently very little infrastructure for the production, storage, and distribution of hydrogen on a large scale anywhere in the world.

In Galena's setting, hydrogen would most efficiently be used locally in the community, because storage tanks are expensive. If it had to be shipped outside the City, tank storage would be required to store the production during the winter (about seven months) when the barges cannot use the river, adding significant capital cost. Shipping of the product might be envisioned using semi trailer mounted tanks that could be barged to Nenana and pulled to Fairbanks or Anchorage for sale to the military, railroad, or other users. Shipping in this manner would add more than \$0.90/gal to the

Pre-Publication Draft – Subject to Change

cost, making it prohibitively expensive.⁴ Therefore, it was concluded that any hydrogen enterprise should be sized to be used entirely in Galena.

For purposes of this study, it was assumed the venture would be a private enterprise and the economics were calculated as such. A modular plant was conceptualized and after several iterations, a plant based on the concept outlined by Air Products was used as a basis. It would use 1 MW as the input to the electrolyzer with a total power requirement of 1.5 MW. The output could be as large as 404,000 gallons per year of liquid hydrogen, matching well with the projected local demand. No provision was made to collect or market the coproduced oxygen. The economics were run assuming that the Air Station equipment was converted from diesel (50,000 gal/yr) and the school district buses and city vehicles were converted from gasoline (25,000 and 15,000 gal/yr, respectively).

Table 4.1. Equivalent liquid hydrogen needed to displace local petroleum based fuels

	Current Fuel Use	Equivalent Liq. Hydrogen
Air Station Vehicles	50,000 gal/yr diesel	229,000 gal/yr
School buses	25,000 gal/yr gasoline	94,000 gal/yr
City Vehicles	15,000 gal/yr gasoline	<u>56,000 gal/yr</u>
	TOTAL	379,000 gal/yr

Therefore, the local market could use about 94% of the production capacity.

Table 4.2. Results of hydrogen economic analysis

Capital	Power Cost	Production Cost	Target Price
\$6.2 million	-0-	\$46/M Btu	\$15-30/M Btu Diesel equivalent
-0-	\$0.015/kWh	\$17/M Btu	

Based on these assumptions, on a Btu comparative basis, hydrogen cannot compete with diesel and gasoline. However, if as a demonstration the capital equipment could be procured via a grant, with a low electrical power cost, the fuel can be produced at a rate comparable to diesel. Details are presented in the Economics Section.

Excess electricity could also be used to produce hydrogen via electrolysis of water. With a 70% efficient electrolyzer, each MW of electric power could produce hydrogen at an energy flux rate of 700 kW. An energy content of 141.8 MJ/kg = 39.4 kWh/kg results in an H₂ production rate of 17.8 kg/hr. Under 1 atmosphere pressure and 0°C, 2 kg of H₂ occupies 22.4 m³. If pressurized to 300 atmospheres [about 4500 psi], one day's production of H₂ would occupy about 16 m³. If stored for periods of weeks, the storage costs [amortization of the capital costs of the container] become significant. The

⁴ based upon barge shipping rate quotes, Inland Barge Service, Nenana, Alaska, May 2004

Pre-Publication Draft – Subject to Change

energy required for compression is a few percent of the energy contained in the hydrogen.

4.4 Transmission to Other villages

A regional grid could link five neighboring communities with transmission lines supplied by a central power plant in Galena. These five communities have a combined generation capacity of about 3 MW with the farthest (Kaltag) being 83 river miles away.

Table 4.3. Cost of installing a transmission line to serve near-by villages

Village/ Population	Distance			Cost (\$million)		Total for Segment
	From Galena	From Previous Village	Portion Along Roads	Road Portion @\$80K/mi	Overland Portion @\$200K/mi	
Down Stream						
Koyukuk/ 169	32**	32	5	0.4	5.4	5.8
Nulato/ 336	50**	18	4	0.32	2.8	3.1
Kaltag/ 230	83**	33	5	0.4	5.6	6
			TOTAL	1.1	13.8	14.8
Up Stream						
Ruby/ 169	42*		9	0.72	6.6	7.3
			TOTAL	1.8	20.4	22.2

* Used a direct route on north shore of Yukon River

** Used abandoned telegraph right-of-way to estimate

From Galena, Ruby is the closest village upstream on the Yukon. It is roughly 52 river miles away. If a transmission line was run along the north shore of the river cutting across some of the oxbows, the distance is estimated to be about 42 miles. Going downstream, a line could be run to pick up Koyukok (32 miles), Nulato (an additional 18 miles), and Kaltag (an additional 33 miles). **Table 4.3.** summarizes the cost for the lines. That portion of each leg, which can be constructed along a road is estimated to cost \$80,000/mile and overland the cost is \$200,000/mile, based on Galena and AVEC experience. Using these assumptions, a transmission line from Galena downstream to Koyukok, Nulato, and Kaltag covers about 85 miles along the river and would cost an estimated \$15 million. A line upstream to Ruby (population 169, generation capacity of 0.6 MW) would cost about \$7.3 million. Thus, for a total of about \$22.2 million, about 800 people with a load of 1.8 MW could be served. Details of the economic assessment of the Transmission Options are presented in the Economics Section.

4.4 Greenhouses and Aquaculture

Pre-Publication Draft – Subject to Change

With the copious amounts of low-grade heat produced in conjunction with power production, several opportunities for commercial enterprises exist, such as raising produce in greenhouses and fish farming. These ventures could supply Galena and surrounding villages with fresh and relatively low-cost produce. Fish raised in tanks could provide for local consumption or be marketed as fresh, frozen, and processed products. Besides providing fresh produce, new businesses such as this would provide employment opportunities.

4.4.1 Greenhouses

Galena has plenty of sunlight in the springtime and could readily grow various crops such as tomatoes, potatoes, squash, cabbage, carrots, etc. if the proper environment could be maintained. This includes the right temperature and an adequate supply of clean air. To illustrate, suppose one needed to keep a 100 x 20 x 10 ft greenhouse 80°F above ambient in which the shell had an R value of 2 ft² hr ° F/Btu, representing a day in March. **Figure 4.1** below illustrates how much heat would need to be supplied as a function of air changes per hour assuming a 50% efficient heat recovery ventilation system. This heat rate represents a small fraction of the rejected heat from a multimewatt power plant.

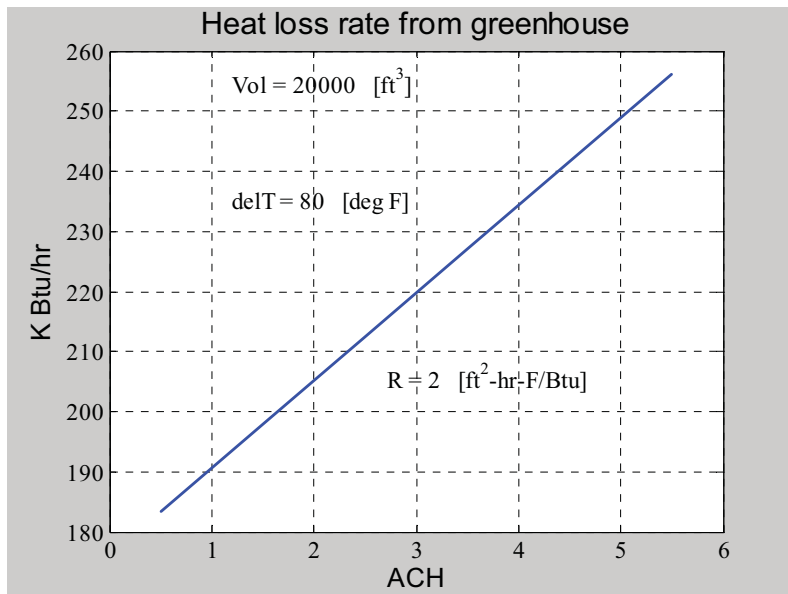


Figure 4.2. Heat load for a greenhouse

4.4.2 Aquaculture

Raising fish in tanks (farming) is often controversial, because of the concern of farmed fish escaping into local streams. However, if allowed and permitted by state and local processes, it is another avenue open for local entrepreneurs to use the heat produced by power plants of various types. Fish could be used locally or processed into frozen or value-added products for sale outside.

An example is trout production. Requirements include;

Pre-Publication Draft – Subject to Change

- Water temperatures of 8°C to 18°C are recommended
- Dissolved oxygen in excess of 5 mg/L
- 10-20 kg fish/cubic meter (22-44 lbs/264 gallons)
- Flow rates of recharge water = 510 L of water/sec/ton of fish (153 gallon/sec/ton)

Other species have less stringent water requirements. An economic comparison and assessment for various species would have to be conducted as part of the business planning process. (Gooley, 1997)

5. ENVIRONMENTAL ISSUES AND PERMITTING

5.1 Primary Environmental and Permitting Issues

All major aspects of power generation and distribution will carry with them some adverse environmental effects. There will be effects relating to the construction and operation of power plants, regardless of the means by which the power is generated. There will also be potential environmental effects from operating each type of power plant. Transportation of fuels and/or power plant components will also involve environmental impacts, especially if new power lines and/or roads are necessary. Each of the three primary energy options addressed in this report (diesel, coal, and nuclear) will also result in the emission of water and air pollutants and the generation of wastes of various types. In the case of coal, disturbance from mining must also be considered. Each of these potential threats to the environment are regulated by one or more agencies of the state or federal government.

The purpose of this portion of the Galena Energy Assessment is to (1) briefly summarize the key environmental issues associated with the primary energy options; (2) provide a short summary of the state and federal regulations that address these environmental issues; and (3) rank the primary energy options in terms of the effort and costs that will be associated with the various options. This section is **not** intended to provide a comprehensive assessment of environmental issues and permitting for energy development but is intended to provide a high-level summary of the key environmental issues relating to the potential diesel, coal, or nuclear power generation at Galena. Such a comprehensive assessment will be part of the overall permitting process, regardless of which option (or options) the City of Galena selects to pursue.

For the sake of convenience, environmental impacts associated with energy production and delivery can be placed into four general categories:

- (1) significant **disturbances** of land and surface water, and groundwater;
- (2) emission of **air pollutants**;
- (3) emission of **water pollutants**; and
- (4) management of various types of regulated **wastes**.

Pre-Publication Draft – Subject to Change

5.1.1 Disturbance

These issues are covered by a wide variety of permitting and licensing requirements from an equally wide variety of state and federal agencies. A partial list of issues and the agencies responsible for regulating those issues is provided in **Table 5.1**.

Permit requirement	Primary regulatory agency
NEPA Environmental Impact Statement	U.S. Environmental Protection Agency
Storm water Discharge Permit	U.S. Environmental Protection Agency
Threatened and Endangered Species and Critical Habitat Assessments	Alaska Department of Fish and Game
Wetlands Assessment	U.S. Army Corps of Engineers
Building Permits	Alaska Department of Public Safety
Wastewater and sewage permits	Alaska Department of Environmental Conservation

5.1.2 Air Pollution

Control of air emissions in the United States is regulated under the Clean Air Act as amended in 1990. At the national level, new air pollution point sources are regulated by the U.S. Environmental Protection Agency (EPA). However, as with most environmental regulations at the national level, the Clean Air Act provides states with the option to take over regulatory authority for air pollution sources within their boundaries. In Alaska, the Department of Environmental Conservation – Division of Air Quality is the primary regulatory agency with respect to air emissions. The State of Alaska therefore maintains primacy over air quality issues in the state through Title 44, Chapter 46, and Title 46, Chapter 3 and Chapter 14.

5.1.3 Water Pollution

Control of water pollution in the United States is also maintained by the EPA under authority of the Clean Water Act. In contrast to the situation with air emissions, however, the State of Alaska has not opted to take over regulatory authority from EPA. For this reason, any water pollution permitting must be through the EPA rather than through a state agency. Much of the general information on water pollution issues is taken directly from the EPA internet web sites.

<http://cfpub2.epa.gov/npdes/regs.cfm?program>

Although there are differences in water permitting needs for the three primary energy options discussed in this report, the primary permitting issue for each will be storm water permitting under the National Pollutant Discharge Elimination System

Pre-Publication Draft – Subject to Change

(NPDES). Administered by the EPA, the NPDES regulates point sources that discharge pollutants into waters of the United States. An NPDES permit is required for any construction activity that disturbs one acre or more of land, including construction of the power plant, roads, power lines, tank farms, mines, ore processing facilities, etc. On March 10, 2003, new regulations came into effect that extended coverage to construction sites that disturb one to five acres in size, including smaller sites that are part of a larger common plan of development or sale. Sites disturbing five acres or more were regulated previously.

Where the EPA is the permitting authority, the Construction General Permit (CGP) outlines a set of provisions construction operators must follow to comply with the requirements of the NPDES storm water regulations. The CGP covers any site one acre and above, including smaller sites that are part of a larger common plan of development or sale, and replaces and updates previous EPA permits. To be eligible for coverage under the Construction General Permit (CGP), you must assess the potential effects of storm water discharges and storm water discharge related activities on federally listed endangered and threatened species and any designated **critical habitat** that exists **on or near** the site. In making this determination, one will need to consider areas beyond the immediate footprint of the construction activity and beyond the property line, including those that could be affected directly or indirectly by storm water discharges.

5.1.4 Waste Management

Each of the three primary energy options will generate waste of various types. In Alaska, solid wastes (nonhazardous) are regulated by the Alaska Department of Environmental Conservation. Solid wastes will be a substantial issue with the coal option because coal mine overburden is classified as a solid waste. Each option will also generate some volume of wastes classified as hazardous. The primary authority for regulating hazardous wastes is the Resource Conservation and Recovery Act (RCRA), administered by the EPA. Regulatory authority for hazardous wastes in Alaska, however, is shared between EPA and the Alaska Department of Environmental Conservation.

Radioactive waste is unique in that it is regulated by the U.S. Nuclear Regulatory Commission (through a memorandum of understanding with the EPA) under authority of the Atomic Energy Act.

5.2 Enhanced Diesel

5.2.1 Background and Assumptions

It is assumed that a new diesel plant and related infrastructure will be located near the existing power plant, reducing the need for the construction of additional roads, power lines, and tank farms, thereby simplifying the environmental permitting process. It is also assumed that fuel will be transported to Galena in the same manner as at present, primarily by barge during the summer shipping season on the Yukon River. Although the permitting process for this option is probably the least restrictive, numerous permits will have to be obtained for the diesel option to be implemented.

5.2.1.1 Disturbance.

Pre-Publication Draft – Subject to Change

In comparison to the coal and nuclear power plant options, and based on the assumptions listed above, construction and operation of an enhanced diesel power plant will likely result in less disturbance of land and waters than the other primary options. However, a number of state and federal permits could be required, especially if additional roads and/or power lines are necessary.

5.2.1.2 Air Pollution.

The Alaska DEC Division of Air Quality has a general air quality operating permit for diesel electric generating facilities. This permit can be accessed through the DEC website (<http://www.state.ak.us/dec/air/ap/docs/gp1.pdf>). The general permit covers emissions of primary pollutants such as oxides of nitrogen and sulfur, respirable particulates (PM-10), volatile organic compounds, and carbon monoxide, all of which may be released from the power plant stack. There are also provisions for visible emissions (smoke) from the power plant, and for emissions from stored fuel.

5.2.1.3 Water Pollution.

A storm water permit through the EPA NPDES program will be required for any construction activity, including the new power plant, tank farm, roads, or power lines. Requirements for spill prevention and response may also be imposed.

5.3 Coal

5.3.1 Background and Assumptions

For coal to be a viable option as an energy source for the City of Galena, it has been assumed that a surface coal mine would be developed above old Loudon, and a coal-fired steam plant would then be built in or very near the City. All aspects of coal production and use must therefore be considered – from permitting the mine itself to the disposal of wastes generated by the power plant. All of the infrastructure required to extract the coal, transport the coal, and produce the power must therefore be considered. It is also assumed that coal generated would be used locally and not be shipped to market elsewhere.

Power generation using locally derived coal can be viewed as a five-step process: (1) mining; (2) preparation (primarily crushing); (3) transport; (4) power generation; and (5) waste management. Each of these basic steps in coal power generation has inherent environmental issues associated with it, and each is regulated by one or more state or federal agencies.

5.3.1.1 Coal Mining.

Much of the information in this section on coal mining environmental issues and permitting is taken directly from internet web sites of the Alaska Department of Natural Resources (DNR). Background information on Alaska's Coal Regulatory Program is taken largely (and often directly) from an Alaska Division of Mining, Land, and Water web site (<http://www.dnr.state.ak.us/mlw/mining/coal>). Permitting requirements for

Pre-Publication Draft – Subject to Change

surface coal mining are provided on a related DNR web site (<http://www.dnr.state.ak.us/mlw/mining/coal/coalreg.pdf>).

Although coal mines have operated in Alaska since 1855, only two mines are currently operating in Alaska: the Gold Run Pass Mine and the Poker Flats Mine. Both mines are owned and operated by Usibelli Coal Mine, Inc., and both are located within six miles of each other east of Healy. Usibelli has been mining coal in the Healy area since 1948. Production therefore began before the current federal and state regulatory programs were put into effect, so not all of the standards that would be applied to a new mine are actually in effect at the two Usibelli mines. Also, coal mining is regulated in a manner that is entirely different from that of other types of mines. Points of comparison for environmental compliance for any new mine near Galena or elsewhere in Alaska are therefore generally lacking.

At the federal level, coal mining is regulated primarily by the Surface Mining Control and Reclamation Act (SMCRA) of 1977. This Act substantially increased the environmental oversight applied to coal mining nationwide. As with many federal environmental regulations, SMCRA also provided individual states with the opportunity to assume primacy over the federal program by developing a state regulatory program for coal in a manner which complies with federal SMCRA standards. Alaska opted to develop its own program consistent with SMCRA, enacting the Alaska Surface Coal Mining Control and Reclamation Act (ACMCRA) in 1983.

ACMCRA is administered by the Alaska Division of Mining, Land and Water Management (DMLW), a division of the Department of Natural Resources. The Act comprehensively regulates almost all aspects of coal mining activity from exploration through final reclamation. Some of the more important parts of the program include the following (<http://www.dnr.state.ak.us/mlw/mining/coal/>):

- Exploration permit: Permitting is required before any coal exploration activity occurs on any land ownership (federal, state, municipal, or private lands).
- Review Process: Any new mine proposal must undergo extensive review before any permit is approved. The review includes at least two separate public notice periods and is highly prescribed by regulation.
- Performance Standards: 65 separate performance standards are set for various coal mining activities, everything from the placement of signs to statistical requirements for measuring revegetation success.
- Inspection: DMLW personnel must inspect each operating coal mine an average of once each month.
- Penalties: Criminal and civil penalties are enforced for violations of ACMCRA.

5.3.1.2 Disturbance from Mining

It is impossible to mine coal without disturbing large areas of the land surface. This is especially the case with surface mines, although land disturbance from subsurface, tunnel mines may also be substantial. Disturbance of the environment due to mining is generally covered by reclamation requirements, and one of the primary goals of ACMCRA (and SMCRA) is to ensure that reclamation is performed in an effective and timely manner. Toward that end, the State of Alaska's coal mining

Pre-Publication Draft – Subject to Change

regulations contain a variety of reclamation requirements. To ensure that reclamation is accomplished adequately, the operator must submit a reclamation bond before mining begins. This bond must be sufficiently large to allow the state to reclaim the site if the operator fails to do so. The Usibelli Coal Mine, Inc. has pledged a collateral bond of approximately \$3 million for the reclamation at its two mines. Once the area is reclaimed, the state can incrementally release the bond. Alaska's coal program regulations require that final bond release not occur until at least 10 years after the mine site is graded and initial vegetation established. The 10-year period is intended to provide time to determine whether revegetation is successful. The Usibelli Coal Mine, Inc., has a full-time reclamation engineer on staff, as well as seasonal reclamation work crews. Each year, the company seeds and fertilizes land being reclaimed. In 1997, they planted several thousand birch, willow, alder, and spruce seedlings on the two mines. Reclamation requirements may be found on the Alaska DNR internet web site (<http://www.dnr.state.ak.us/mlw/mining/coal/coalreg.pdf>).

DMLW recently approved a new mine permit for the Two Bull Ridge Mine. Some of the important reclamation provisions of the permit were the following:

- **Topsoil:** An extensive pre-mining soil inventory was conducted, and all soils removed were required to be saved except those that are unsuitable for reclamation use and those on steep slopes. All of these salvaged soils will ultimately be placed back onto reclaimed areas. As the active mining area moves through the 832-acre area of the mine, grading will be completed and topsoil will be replaced within approximately 800 feet of the actively mined area.
- **Post-Mining Land Use:** The mining area will ultimately be reclaimed for wildlife habitat, which was the predominant pre-mining land use.
- **Revegetation:** Usibelli's Revegetation Plan has two parts. First, the area will be seeded with native grasses to quickly establish a ground cover that will control erosion. Second, although they expect natural regeneration to provide the larger woody plants, this natural regeneration process will be accelerated by planting 100 plants per acre using naturally occurring woody plants such as willow, alder, or spruce.

5.3.1.3 Air Pollution for Coal Mining

For coal mining, the primary air pollution issues include the generation of fugitive dust and the potential release of methane. These emissions will be controlled under a permit by the Alaska Division of Air Quality.

5.3.1.4 Water Pollution for Coal Mining

Aside from standard storm water discharge issues, coal mining is a water pollution concern primarily because of acid mine drainage. Requirements of the EPA will restrict or eliminate the potential for acid mine drainage. The greatest water pollution regulatory burden for coal mining will be the NPDES permitting, which has been cited as "the greatest obstacle to timely development of mines in Alaska" (Report of the 2004 Alaska Minerals Commission).

Pre-Publication Draft – Subject to Change

5.3.1.5 Waste Management for Coal Mining

A solid waste disposal permit will be required from the Alaska Department of Environmental Conservation. The most recent solid waste disposal permit approved in Alaska was a renewal of a solid waste disposal permit for the Usibelli mine. This permit (<http://info.dec.state.ak.us/decpermit/eh/sw/0031-ba002.pdf>) is for the continued operation of “an inert waste monofill for construction and demolition debris, shop wastes, and coal ash, located at the Usibelli Coal Mine “... in accordance with AS 46, 18 AAC 15, and 18 AAC 60.” The permit was issued in April 2000, and extends for a five-year period, after which it must be renewed again. The Usibelli permit allows for the disposal of these specific nonhazardous waste types “within the boundaries of the Poker Flats and Two Bull Ridge mining areas at Usibelli Coal Mine.”

5.3.2 Coal Preparation – Air Pollution

In April 2003, the Alaska Department of Environmental Conservation, under the authority of AS 46.14 and 18 AAC 50, issued Air Quality Operating Permit No. 317TVP01 to the Usibelli Coal Mine, Inc., for the operation of the Usibelli Coal Preparation Plant. This permit is in force until the expiration date of May 13, 2008. The Usibelli permit included provisions limiting emissions of regulated air contaminants including particulate matter (PM-10), Sulfur Oxides (SO_x), Nitrogen Oxides (NO_x), Carbon Monoxide, and Volatile Organic Compounds (VOCs), and requires the permittee to submit assessable emission estimates no later than March 31 of each year. The submittal is required to include all of the assumptions and calculations used to estimate the assessable emissions in sufficient detail so they can be verified. A list is provided below of sources at the Usibelli mine site that have specific permit stipulations for monitoring, record keeping, or reporting conditions. From **Table 5.2** (below) each source has stipulations associated in the permit. Many of these involve record keeping.

Table 5.2 Usibelli Coal Preparation Plant Source Inventory

Pre-Publication Draft – Subject to Change

ID	Source Name	Source Description	Rating/size	Install Date
1	CRU1-Primary Crusher	Stamler Feeder Breaker-12465	1,400 Tph	1986
2	CRU2-Secondary Crusher	McNally 34 x 38	1,000 Tph	1982
3	CRU3-Secondary Crusher	Gundlach	500 Tph	1997
4	SCR1 Screener	Rippleflow Screener	500 Tph	1997
5	SCR2 Screener	Rippleflow Screener	500 Tph	1997
6	TRA1	Transfer point #1	500 Tph	1997
7	TRA2	West Tipple Transfer	400 Tph	1997
8	FIN1	Fine coal Loadout	1,400 Tph	1982
9	DUM-1	Truck Dump	1,400 Tph	1990
10	TRN1	Train loadout	2,500 Tph	1992
11	TRK1	West Tipple Truck Loadout	200 Tph	1996
12	STK1	Coal Stockpile Loadout	20,000 tpy – loadout	1992
13	Boiler 1	Kewanee Coal fired	7.22 M Btu/hr	1982
14	Boiler 2	Ferrar & Trefts 578 Coal fired	7.69 M Btu/hr	1977
15	Boiler 3	Hastins 55A Diesel fuel	1.0 M Btu/hr	1996
16	Boiler 4	Kewanee 4430 Waste Oil	5.0 M Btu/hr	1996
17	Tank 1	Diesel Fuel	24,000 gal	1993
18	Tank 2	Diesel Fuel	24,000 gal	1993

5.3.3 Coal – Transportation

A new coal mine, even if “local,” will require that some new roads be built. For Galena, the type and distance of these roads will depend on a number of factors, including (1) how close the mine and coal processing facilities are located from the power plant; and (2) whether coal will be produced to be shipped for use elsewhere. Construction of new roads in Alaska require a number of permits, the most substantive of which are summarized below:

5.3.3.1 Federal

U.S. Army Corps of Engineers: Disturbance of any lands containing wetlands requires a permit (or waiver) from the Army Corps of Engineers before any dredged or fill material is placed in wetlands. The Corps is responsible for determining whether an area is wetland for permit purposes and issues permits for dredging, filling, or placing structures in tidal waters, streams, lakes, and wetlands. For additional information, or for a wetlands determination, contact the U.S. Army Corps of Engineers, Regulatory Branch, PO Box 898, Anchorage, AK 99506-0898 (1-800-478-2712).

U.S. Environmental Protection Agency: As described in previous sections, the EPA manages NPDES storm water permits required for all construction projects that disturb over 5 acres of land. Contact information: U.S. Environmental Protection Agency, Region 10, Office of Water, 1200 Sixth Avenue, Seattle WA 98101 or

Pre-Publication Draft – Subject to Change

1-800-424-4372 x6650. Permits available at <http://www.epa.gov.r10earth/stormwater.htm>

5.3.3.2 State of Alaska

Department of Fish and Game: The Alaska Department of Fish and Game is responsible for issuing permits for any activities or projects which impact waters that support salmon and high value resident fish species as well as for activities within Critical Habitat Areas, State Game Refuges and State Game Sanctuaries. Contact the Alaska Department of Fish & Game, Habitat & Restoration Division, 333 Raspberry, Anchorage, AK 99518. (907) 267-2285.

Department of Public Safety: A State building permit is required for all commercial buildings for any location in the State. The State Fire Marshal issues permits after appropriate plans and specifications are submitted and approved. Information and application are available at: State Fire Marshal, 5700 East (907) 269-5604, Tudor Road, Anchorage, AK 99507

Department of Environmental Conservation: The Alaska Department of Environmental Conservation (ADEC) provides and enforces standards for water quality and waste disposal, as described in earlier sections. For information specific to domestic water wells and septic systems, contact the state or local ADEC office.

5.3.3.3 Local

There may also be additional permits required relating to construction, zoning, easements, covenants, waste disposal, flood plain development, critical habitat, etc.

5.3.4 Coal Power Generation

Construction of a coal-fired power plant in Galena will require a number of construction, air pollution, water pollution, and waste management permits. Air permits will deal with emissions for sulfur and nitrogen oxides, particulates, and carbon monoxide, and may also restrict visible emissions. For water, an NPDES permit will be required for the power plant, and thermal loading to waters may also be restricted. Waste management will include disposal of ash and other materials.

5.4 Toshiba 4S Nuclear Plant

The U.S. Nuclear Regulatory Commission (NRC) regulates the construction and operation of all new commercial nuclear power facilities that produce electricity in the United States. The NRC is responsible for issuing standard design certifications, early site permits, construction permits, operating licenses, and combined licenses for commercial nuclear power facilities. NRC regulates reactor siting, construction, operation, and decommissioning through a combination of regulatory requirements, licensing, and oversight, including inspection. Recently, the NRC has been making minor revisions in its policies to help make new licensing reviews more effective and efficient and to reduce unnecessary regulatory burden on future applicants. NRC's Regulations

Pre-Publication Draft – Subject to Change

are found in Chapter I of Title 10, "Energy," of the Code of Federal Regulations (CFR). These are summarized in Appendix 3.

5.4.1 Disturbance

As with the other energy options discussed, construction of the Toshiba 4S reactor in Galena would require a storm water permit under EPA's NPDES program. Depending on the area of land disturbed (including security fences, etc.), additional disturbance-related regulations may be invoked, including those listed in Table 4-1 for Coal Mining.

5.4.2 Air Pollution

The Toshiba 4S power plant is an entirely closed system. As such, no atmospheric emissions are anticipated under normal operating conditions. Any air permitting issues associated with the 4S plant will likely be routine nonradioactive emissions permits through the Alaska Division of Air Quality.

5.4.3 Water Pollution

As with air pollution, the closed system design of the 4S plant will likely limit water pollution permitting to the construction storm water permits described above under "disturbance."

5.4.4 Waste Management

Operation of the 4S reactor will generate small volumes of solid waste (trash) and potentially some small volumes of hazardous (nonradioactive) wastes. Both classifications will be permitted as described for the other energy options listed above. Under the assumptions provided by Toshiba, the 4S plant will not generate any radioactive waste except the reactor core itself, which will be returned to Japan following the decommissioning of the plant.

5.5 Conclusions – Environmental Issues and Permitting

Given the assumptions stated throughout this report, and strictly from an environmental permitting standpoint for the City of Galena, evaluation of the permitting requirements for each of the three primary energy options yields a clear loser (coal) and an apparent winner (nuclear). Two key assumptions that play heavily into this result. The first is that coal will be generated locally. This represents a distinct disadvantage from a permitting standpoint in that permitting for the mine site must be considered for this option, but not the others. The second assumption is that all of the information provided to us by Toshiba proves to be accurate and is accepted by the NRC. Specifically, (1) if the 4S reactor truly generates no air or water emissions; (2) the reactor is returned to the final assembly point the end of its useful lifetime (thereby eliminating

Pre-Publication Draft – Subject to Change

nuclear waste issues in Alaska), and (3) Toshiba⁵ bears all (or most) of the licensing costs, then the permitting “cost” to Galena is reduced to the point that the nuclear power option becomes the clear preference. Before a final decision is made, it is imperative that these assumptions be verified.

6. ECONOMIC ANALYSIS

6.1 Overview of Methodology

The economic analysis model calculates the total cost of providing electric power to the Galena utility distribution system (the “busbar cost”). The analysis runs for 30 years, from 2010 to 2039. In all cases, the existing electric and district heat loads are served as firm loads. In some cases, additional heating loads are also served, and the delivered energy is valued at the avoided cost of displaced fuel. Electric space heating of residences is treated as a firm load, which must be met by the utility with diesel backup, while the air station heating load is treated as a nonfirm or “economy energy” load.

The model computes and considers the relevant electric and heat loads one day at a time to determine how much energy can be delivered that day by the primary generation source (diesel, coal, or nuclear) and how much must be delivered from diesel as a peaking and/or backup resource. Nonfirm energy sales are counted as a credit against total energy production cost to determine the net cost of serving the firm load. The model calculates the net present value of all annual costs to determine the total system life-cycle cost of power generation to the City of Galena Electric Department. It also computes the approximate average electric rate necessary to cover each year’s annual cost of providing electric service. The average electric rate also includes estimated distribution and administration costs.

To deal with uncertainty, we employ low and high values for some critical parameters. These are discussed below. We also employ sensitivity analysis to determine the effect of changing some specific assumptions.

6.1.1 Example of Model Structure

The following highly simplified example illustrates the basic steps in the analysis. More details on the model structure are presented in Appendix D. The full model is available from the authors as an Excel spreadsheet.

Suppose the total firm load to be served on January 1, 2010, is one megawatt (1 MW) of electricity (measured at the busbar) and the primary generation resource is diesel.

The busbar energy requirement for that day is
 $1 \text{ MW} \times 24 \text{ hours} = 24 \text{ megawatt-hours (MWh)},$

The amount of diesel required is
 $24,000 \text{ kWh} / (14 \text{ kWh/gallon}) = 1,714 \text{ gallons/day}.$

where 14 kWh/gallon is the assumed efficiency of the diesel generators.

⁵ Toshiba or the third party owner

Pre-Publication Draft – Subject to Change

The cost of this fuel is

$$1,714 \text{ gallons times } \$2.50 / \text{gallon} = \$3,685/\text{day}$$

Additional variable operating costs (such as lube and overhauls) are

$$24,000 \text{ kWh} \times \$0.02/\text{kWh} = \$480/\text{day}$$

The total variable cost of generation for this one day is

$$480 + 3,685 = \$4,165/\text{day}$$

The total variable cost for other days differs because more or less electricity is produced. The model adds all of these daily variable costs together; the total variable cost for one year might therefore be about \$1.2 million.

The annual fixed cost is

$$\$300,000 \text{ (for labor)} + \$200,000 \text{ (for generation equipment)} = \$500,000$$

Therefore the total annual cost of generation for the year 2010 is \$1.7 million. If the total cost of the distribution system and utility administration is \$500,000 per year, then the total cost of electric service for the year is \$2.2 million.

Total electric sales are projected to be

$$9,440 \text{ MWh} \times 0.9 = 8,496 \text{ MWh,}$$

where the factor 0.9 accounts for 10% losses between the point of generation and the customers' meters.

To cover the total cost of generation, the average rate must be

$$\$2,200,000 / 8,496,000 \text{ kWh} = \$.26/ \text{kWh}$$

Of this, 18 cents per kWh is for generation and the remaining 8 cents per kWh is for distribution and administration. In this simple example, the entire load is a firm load. In subsequent years, the load grows and costs increase. The required electric rate may go up or down over time. The life-cycle cost of electric service is the discounted present value of all annual costs.

This simplified example does not consider the economics of serving additional heat loads. Sales of additional heat or electricity beyond the current utility requirements would be counted as a credit against the total cost of the energy system. The details of how this analysis plays out are considered below, in the results section.

6.1.2. Economic Model Limitations

The economic analysis is based on the comparison of scenarios for change occurring 30 years into the future. While scenario analysis is a useful tool for examining long-range feasibility, it does have several limitations.

Pre-Publication Draft – Subject to Change

1. the validity of the analysis depends on the validity of the scenarios and the assumptions that are used to generate them.
2. the analytical model does not contain internal "feedbacks" such as an explicit link between higher electricity prices and reduced electricity consumption.
3. we have not attached probabilities to any of the assumptions or scenarios. Therefore the model cannot produce estimates of a single "most likely" or "best" estimate for any of the results.
4. finally, no attempt has been made to explicitly evaluate the degree to which any of the options may increase or decrease economic and financial risk.

In summary, our scenario-based analysis requires the reader of the report to make their own judgments about which scenarios and assumptions are more likely to occur. Although this can be viewed as a limitation of our method, it can also be viewed as a strength, since there is a clear link between assumptions and conclusions for each scenario examined.

6.2 Assumptions

6.2.1 Overview of Assumptions and their Use

The analysis period runs for 30 years, starting in 2010. This is the first year in which the nuclear or coal systems could plausibly be put in place. All dollar values are "real" dollars with today's (year 2004) purchasing power. The discount rate for computing the net present value of future dollar amounts is assumed to be 4% over and above inflation. This is consistent with interest rates for public-sector borrowers such as the City of Galena.

Numerous assumptions drive the analysis. Some are more important than others, and some are more uncertain than others. Some assumptions are both very important and fundamentally uncertain. We have designated these as *critical assumptions*. The five critical assumptions for this analysis are

- 1) the initial price of diesel in 2010,
- 2) the future increase in the price of diesel,
- 3) the price of coal,
- 4) the efficiency of the coal plant, and
- 5) the number of security staff needed at the nuclear plant.

Each critical assumption has a low value and a high value, which are presented below and summarized in **Table 6.1**. Combinations of low and high values for the five critical assumptions jointly determine the basic range of results. We have made no attempt to choose a "most likely" value or an "average value" for any of the critical assumptions.

Pre-Publication Draft – Subject to Change

Table 6.1. Summary of critical assumptions

	units	low value	high value
Diesel fuel price in 2010	\$/gallon	1.50	2.15
Diesel fuel price increase (over and above general inflation)	% per year	0.0%	2.0%
Coal price (delivered to Galena)	\$/ton	100	125
Coal plant average efficiency		30%	40%
Nuclear plant security staff	positions	4	34

For all other assumptions, we have adopted single values for the basic analysis. These are presented and discussed in the following sections. Sensitivity cases explore some variation in these other assumptions, which are discussed in the results section, below.

6.2.2 Current Loads and System Costs

Galena electric energy requirements have been growing at about 2% per year, reaching about 9.5 MWh in 2003. Generation efficiency has also increased and is now close to 14 kWh per gallon. The current cost of providing electric service is about 26 cents per kWh, as shown in **Figure 6.1**. As this figure shows, about one-third of the total cost is for distribution and administration. To be competitive with diesel, an alternative generation system must deliver electricity to the distribution system for about 18 cents per kWh.

Table 6.2. Galena electric utility statistics.

	units	FY00	FY01	FY02	FY03	Average annual growth
Electricity generated	MWh/yr	9,026	9,141	9,408	9,578	2.0%
Electricity sold	MWh/yr	8,038	8,531	8,342	8,103	0.3%
Diesel fuel used	gallons	667,815	662,908	686,104	692,932	1.2%
Peak load	MW				1.6	
kWh generated per gallon		13.5	13.8	13.7	13.8	0.8%
Electric losses		10.9%	6.7%	11.3%	15.4%	
District heating load	B Btu/yr				8.0	

source: City of Galena

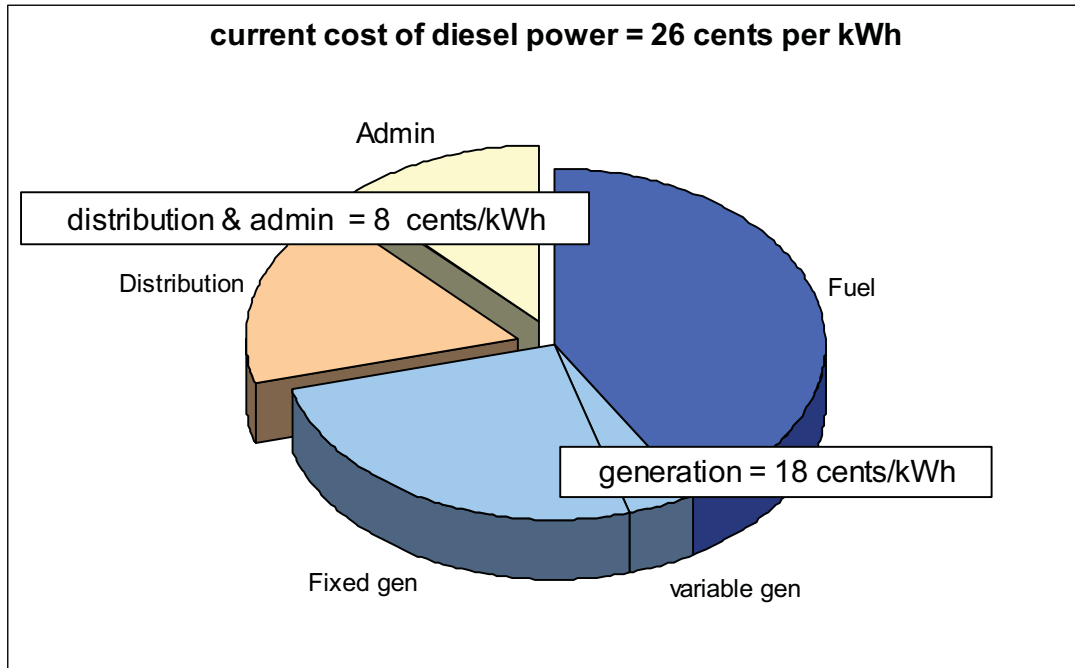


Figure 6.1. Current cost of electric service with diesel fuel at \$1.32/gal for 2003, the year of this data.

6.2.3 Assumptions about Future Loads

Table 6.3 and Figure 6.2 summarize our projections of future energy requirements. We assume that current utility electricity requirements will continue to grow at 2% per year. The existing district heating load remains constant and is treated as a firm load. Both the coal and nuclear systems must serve this load.

Table 6.3. Future energy requirements.

source of load	type	units	2010	2039
Utility electricity	firm	MW h	11,002	19,539
Existing city heating loop	firm	MW h	2,344	2,344
Residential space heating	firm	MW h	7,413	13,164
Air station heat	non-firm	MW h-equiv	8,464	8,464
Greenhouse	firm	MW h	570	570
Total energy requirements at power plant		MW h	29,794	44,081

note: MW h-equiv denotes the amount of electricity that could be generated by passing the heat load in question through a turbine/generator.

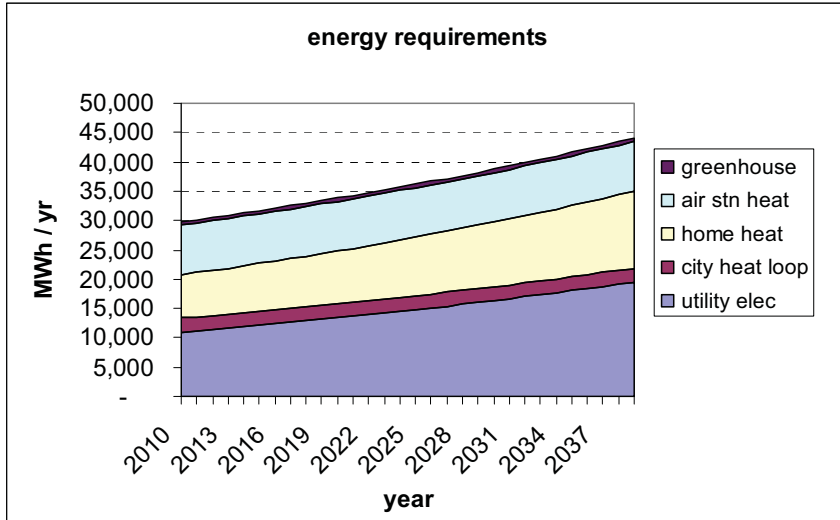


Figure 6.2. Projected future energy requirements.

Table 6.4. shows additional assumptions about the residential space heating load and the air station district heat load. We have estimated the home space heating load to be about 7.4 MWh in 2010, based on 220 houses each using the equivalent of 1,000 gallons of stove oil per year. This home space heating load is also treated as a firm load. However, our analysis revealed that it does not make economic sense to try to serve any of this load with electricity generated from diesel or coal. Therefore, home electric space heating is only provided by the nuclear system. It is valued at the avoided cost of stove oil, which we assume costs 75 cents more per gallon than utility diesel. Partially offsetting these savings are the costs of upgrading the distribution system and installing electric baseboard heating in all existing homes.

The air station heat load is assumed to remain constant at 52 billion Btu per year (B Btu/yr). To analyze this load in the context of the electric system, we have expressed this load in terms of how much electricity could be produced with the heat energy.⁶ The air station heat load is nonfirm. The nonfirm heat sales are treated as economy energy sales of steam or hot water metered at the power plant. In the model, these sales are not backed up with diesel power when the coal or nuclear systems are down. The coal or nuclear power plant is assumed to be sited near the current power plant, resulting in a 2-mile distance to the air station. The capital cost of installing this heat distribution pipe is deducted from the fuel savings measured at the air station when calculating the benefits of providing this heat.

⁶ We assume a 50% conversion efficiency in the turbine/generator system. A 52 billion Btu/yr thermal load can also be expressed as 15,235 MWh of heat energy. This heat energy could be converted at 50% to 7,618 MWh of electric energy. Adjusting this figure for 10% heat losses in the heat delivery pipe, we arrive at a figure of 8,464 MWh-equivalent. It takes the same fuel resources to provide 52 billion Btu to the distant end of a heating pipe as it does to produce 8,464 MWh of electricity at the busbar.

Pre-Publication Draft – Subject to Change

Table 6.4. Assumptions about heating loads.

Residential Space Heat		
number of houses, year 2010		220
annual growth in number of houses		2.0%
stove oil consumption per house	gallons/yr	1,000
residential furnace efficiency		75%
residential fuel price premium (delivery c	\$/gallon	0.75
Utility line upgrades capital cost	\$	800,000
customer premises upgrade cost	\$/house	3,000
electric dist'n loss from busbar to house		10.0%
District Heat		
Current district heat load	B Btu/yr	8.0
Cost of bulk distribution pipe	\$/foot	200
Air station boiler efficiency		80%
Distance from power plant to air station	miles	2.0
district heat loss in pipes		10.0%
Heat load factor (based on HDD data)		0.51
Heat sales tariff as % of net avoided cost		75%

6.2.3 Assumptions about the Diesel System

Table 6.5 summarizes our assumptions about the diesel system. The main technical assumption is that starting in 2010 new units will be rotated into the system such that the overall generation efficiency is 15 kWh per gallon. We assume that this figure then remains constant throughout the analysis. This is a simplification of what would actually be a gradual improvement in efficiency over time.

The main economic assumption underlying the cost of diesel generation is the price of fuel. The low projection for diesel fuel prices is constant (in real dollars) at \$1.50 per gallon. Historically, utility diesel prices have actually been constant or declining for significant periods during the past 30 years when measured in real dollars. The high assumption is that diesel fuel prices start at \$2.15 per gallon (in today's dollars) in year 2010, then increase at 2% per year over and above inflation. Since the cost of crude oil represents only about 30% of the cost of delivered diesel fuel, this assumption of 2% diesel price growth corresponds to a 7% annual growth in real crude oil prices. Crude oil prices could rise to over \$300 per barrel (in today's dollars) by 2039 and still be consistent with this scenario. Of course, numerous other factors -- such as carbon taxes or increasing costs of tank farm storage -- could also contribute to increased prices.

Table 6.5. Assumptions about the diesel system.

	units	selected value (yr 1)	low value	high value
Diesel capital cost (replace engines)	\$/kW	400		
Diesel Fuel				
Utility fuel initial price	\$/gallon	1.50	1.50	2.15
Annual real escalation	% per yr	0.0%	0.0%	2.0%
Utility initial fuel efficiency	kWh/gal	14		
kWh measured at busbar				
Efficiency of New Units	kWh/gal	15		
Nonfuel diesel O&M				
Diesel generation labor	\$/year	305,157		
Variable O&M (includes overhauls)	\$/kWh	0.017		

Pre-Publication Draft – Subject to Change

If the diesel system is run as the primary generation source, we assume that capital replacements would be required such that every seven years new capacity equal to the current peak load for that year is added to the system to replace old units and to expand overall capacity consistent with load growth. Engine overhaul costs are subsumed into the assumed variable O&M cost of 1.7 cents per kWh. The capital cost of possible incremental fuel storage is not considered. The maintenance cost of fuel storage is included in the variable O&M cost.

Note that for all systems considered, a diesel generation capability is retained to serve as backup for times when the primary production facility is down for maintenance or emergencies.

6.2.4 Assumptions about the Coal System

Table 6.6 summarizes our assumptions about the coal system. It is important to recognize at the outset that all of these assumptions are very uncertain. Very few AFBC units have been built at the scale contemplated here (between 1 and 5 MW). The Galena coal resource has not been delineated. Detailed designs that would match the thermal and electrical output of the coal plant to these loads have not been developed. To address this uncertainty, we have designated the coal plant electric generation efficiency and the delivered price of coal as critical assumptions with low and high values.

Table 6.6. Assumptions about the coal system.

	units	selected value (yr 1)	low value	high value
Coal plant capital cost	\$/kW	3,000	3,000	not used
Coal plant availability		91%		
Coal plant efficiency (electric output/coal input)		40%	30%	40%
Coal or nuclear "heat to electric" efficiency		50%		
Coal fuel				
Energy content	M Btu/ton	20		
Delivered price of coal	\$/ton	100	100	125
Ash disposal cost	\$/ton	20		
Nonfuel coal O&M				
Coal labor	people	6		
cost per operator	\$/yr	53,200		
variable O&M and consumables	\$/kWh	0.01		

The size of the coal plant is not predetermined. For each set of critical assumptions, we used the model to determine the optimal size for the coal plant. We also determined whether or not it was economic to serve the air station heat load with coal-fired district heat.

6.2.5 Assumptions about the Nuclear System

Table 6.7 presents our assumptions about the nuclear system. In all basic cases, the assumed capital cost to the City of Galena and to ratepayers is zero. For

Pre-Publication Draft – Subject to Change

the purposes of sensitivity analysis, the assumed capital cost for the 10-MW plant is \$25 million, based the 50MW capital cost assumption of \$2,500 per kW.

Annual supplies and expenses are in addition to labor. Toshiba estimates about \$1 million for this line item for their 50-MW plant. Since the reactor is sealed, these expenses probably relate almost exclusively to the steam piping and turbine/generator systems. Although the components would be smaller, it does not seem plausible that consumables costs for a 10-MW plant could drop to one-fifth of those for 50 MW. Some of these costs probably do not change at all. Lacking specific data on this point, we have assumed that annual supplies and expenses are one-half the amount estimated by Toshiba for the 50-MW design.

Decommissioning costs are not considered in the analysis, under the assumption that they would be borne by the plant owner or some other party.

Table 6.7. Assumptions about the nuclear system.

	units	selected value (yr 1)	low value	high value
Nuclear capacity	MW	10.0		
Nuclear capital cost	\$	0		
Nuclear security staff	people	34	4	34
Nuclear operator staff	people	8		
Nuclear availability		95%		
Nuclear annual supplies and expenses	\$/yr	500,000		

6.3 Economic Analyses Results

6.3.1 Basic Results

The basic results presented in this section come from varying only the five critical assumptions. Additional sensitivity cases are discussed in the following section.

6.3.1.1 Diesel

The total life-cycle cost of power generation with diesel ranges from \$38 million to \$59 million. This range results solely from variation in the future price of diesel fuel. **Figure 6.3** shows that electric rates (in inflation-adjusted dollars) could go down if fuel prices stay flat, or they could rise significantly under the high fuel price assumption. The projected electric rates are determined by adding estimated distribution and administration costs to the cost of power generation. Total distribution costs are assumed to increase with the number of households (2% per year) while total administration costs are assumed to remain constant. Electric rates go down slightly under the assumption of low and flat diesel prices because the constant total cost of administration gets spread over more and more kilowatt-hours.

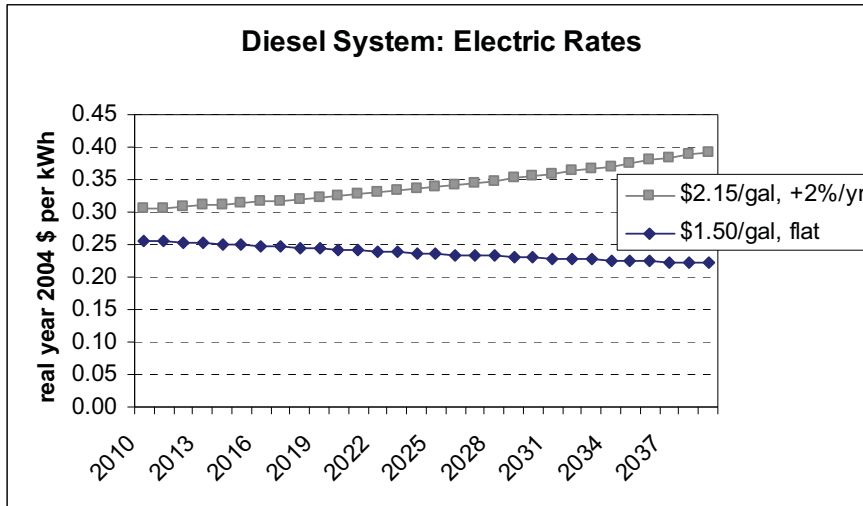


Figure 6.3. Projected future electric rates with diesel system.

6.3.1.2 Coal

The total life-cycle cost of power generation with coal ranges from \$23 million to \$35 million. The low cost of \$23 million results from a combination of high diesel fuel prices, low coal prices (\$100/ton), and high (40%) coal plant efficiency. Under these conditions, it is economic to serve the air station heat load with district heat. Almost \$20 million worth of fuel oil costs can be avoided, which more than justifies a \$2 million capital expenditure to build a distribution pipe from the power plant to the air station. The optimal size of the coal plant under these assumptions is 4.0 MW, which is sufficient to meet all peak loads in 2010, as shown in **Figure 6.4**.

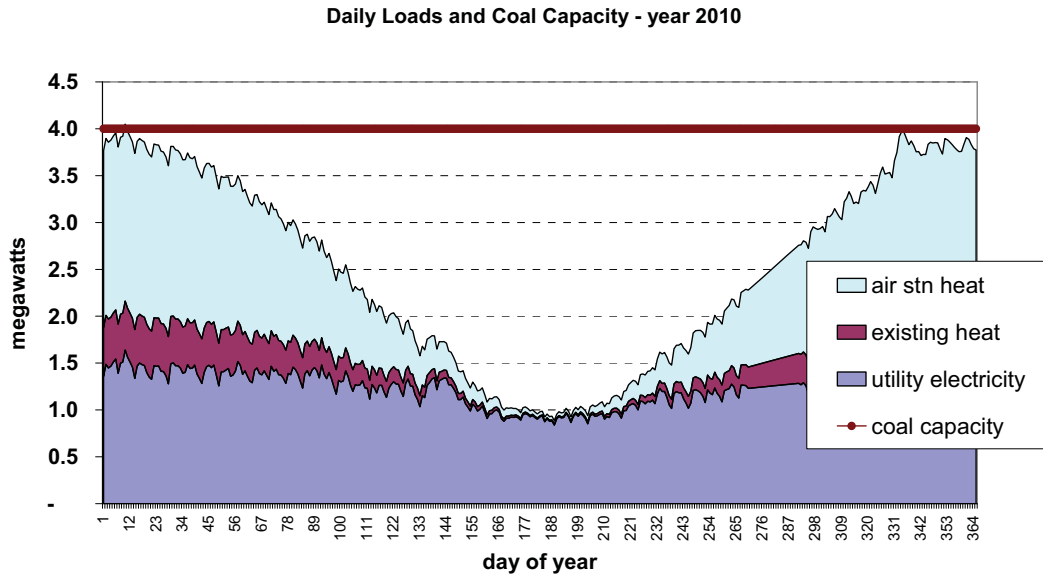
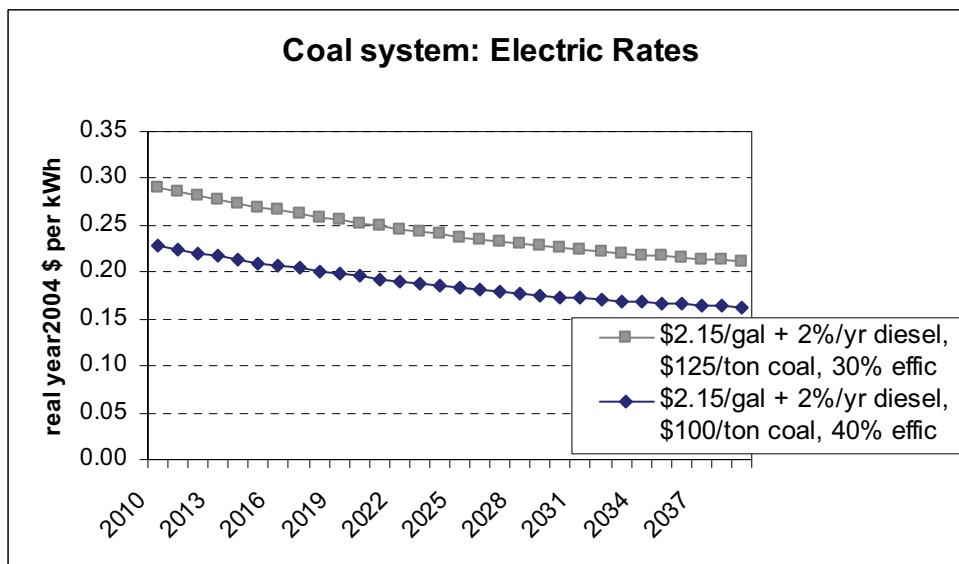


Figure 6.4. Coal plant capacity vs. daily loads for high diesel prices.

The net cost of power generation from a coal system is highest when diesel prices are high, coal prices are high (\$125/ton), and coal plant efficiency is low (30%). Under these conditions, it is still economic to serve the air station heating load and the optimal size of the coal plant drops only slightly, to 3.8 MW. However, the higher cost of coal drives up the overall cost of power. Figure 6.6 shows projected electric rates corresponding to the two scenarios just discussed.



Pre-Publication Draft – Subject to Change

Figure 6.5. Projected future electric rates with coal system

Although the absolute cost of the coal system varies by only \$12 million, it is important to note that the net benefits from coal relative to diesel vary by much more. When diesel prices are high and coal prices are low, the coal system costs \$36 million less than diesel. When diesel prices are low and coal prices are high, the coal system costs only \$3 million less than diesel. However, in all cases, the coal system costs less than diesel under the assumptions used here.

6.3.1.3 Nuclear

Inspection of the projected daily load curves shows sufficient nuclear capacity to meet all the potential electric and heating loads at all times during all years. (Some diesel power is still required during times of unavailability.) This is demonstrated in **Figure 6.7**, which compares daily loads to nuclear system capacity for the year 2039, when loads are highest. This figure also shows the large amount of heat energy that can be provided in a way that displaces expensive diesel fuel and generates revenue for the utility. Revenue from heat sales can be applied against the total cost of all utility service to drive down consumer electric rates.

The total life-cycle cost of providing power with the assumed nuclear system ranges from *minus* \$7 million to [plus] \$35 million. The low figure occurs when diesel prices are high and the required security staff is low (4 people). The total cost of electric generation at the busbar is negative because the avoided cost value of heat sales to the air station and to residential customers is more than enough to pay for the total cost of serving *all* loads. Therefore the remaining cost to be allocated to the provision of nonheat electricity is negative.

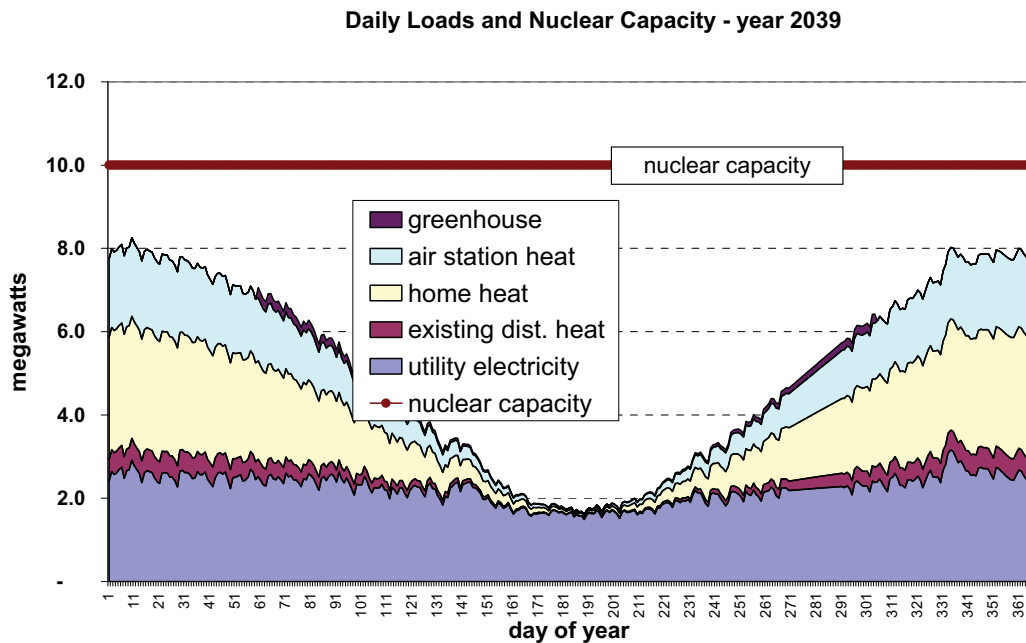


Figure 6.6. Daily loads vs. nuclear capacity, year 2039.

Pre-Publication Draft – Subject to Change

This result does not mean that electric rates can be negative. There are two reasons for this. First, even if the total cost of electricity generation was minus \$7 million, there is also a total life-cycle cost of about \$14 million for distribution and administration. This would yield a net life-cycle revenue requirement of \$7 million that would have to be covered by rates. Second, actual sales of electric space heat and air station district heat are unlikely to take place at a price equal to the buyer's avoided cost. The actual price will surely "split the savings" between the utility and the heat customers. In calculating projected electric rates, we have assumed that air station heat will be sold, on average, for about 75% of its avoided cost value. For both of these reasons, the projected average electric rate when nuclear costs are lowest declines over time from 10 cents per kWh to 6 cents per kWh.

The life-cycle cost of power generation from nuclear is highest, at \$34 million, when diesel prices are low and when the required number of security staff is high (34 people). This cost is still \$3 million below the comparable cost of diesel power. Under these conditions, the avoided cost value of electric heat and district heat is much lower and the absolute cost of running the nuclear plant is much higher due to labor costs. The projected average electric rates decline over time from 21 cents per kWh to 13 cents per kWh. In this case, it would be necessary to offer a special rate for electric heat, since with low diesel prices the avoided cost of oil heating would equate to only about 7.5 cents per kWh. Even with special rates for electric heat, it is important to remember that customers would pay less for their core (nonheat) electricity than they would with diesel.

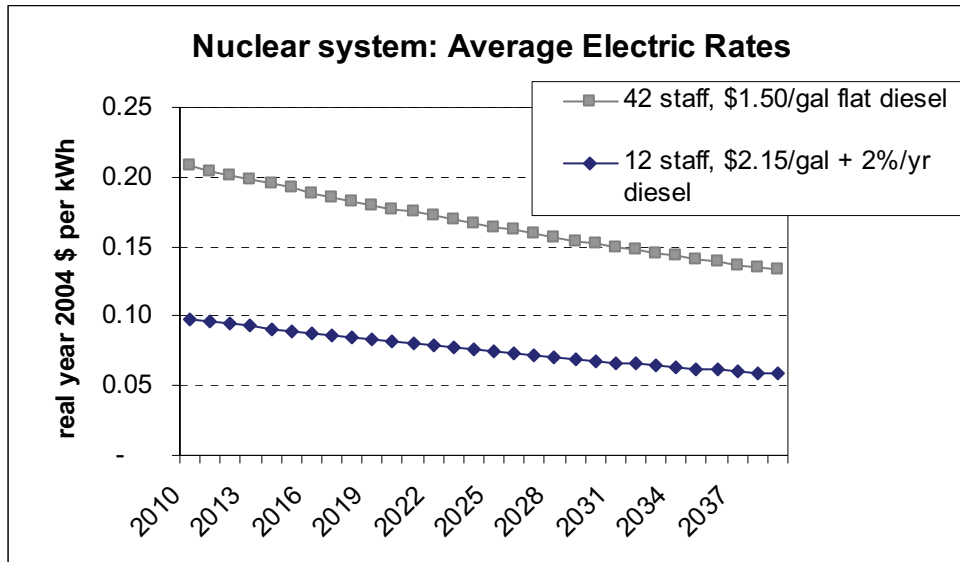


Figure 6.7. Projected future electric rates with nuclear system.

6.3.1.4 Summary of Basic Results.

Table 6.8 summarizes the results described above. The ranges shown for costs and rates come from varying only the five critical assumptions.

Pre-Publication Draft – Subject to Change

Table 6.8. Summary of basic results.

	Diesel	Nuclear	Coal
Loads served:			
utility electricity	X	X	X
existing district heat	X	X	X
residential electric space heat		X	
greenhouse		X	
air station district heat		X	[sometimes]
Life-cycle total cost (\$million)			
low value	38	(7)	23
high value	59	35	36
Net benefits compared to diesel (\$million)			
low value		3	3
high value		67	36
Average electric rate in 2010 (\$/kW h)			
low value	0.26	0.10	0.23
high value	0.30	0.21	0.29
Average electric rate in 2030 (\$/kW h)			
low value	0.23	0.07	0.17
high value	0.36	0.15	0.23

6.3.2 Special Sensitivity Cases

In this section, we report the results of several sensitivity cases. These cases address two questions that are a natural outgrowth of the basic analysis. The first question is, how does the analysis change if nuclear capital costs are included? The second question is, how does the analysis change if the nuclear or coal plants were sited 7 miles from the air station rather than 2 miles away.

6.3.2.1 Cases with Nuclear Capital Costs Included

Toshiba estimates that the capital cost of its 4S system is \$2,500 per kW, or \$25 million for the 10 MW plant.⁷ Using this figure, the life-cycle costs of the nuclear system would increase in all cases by exactly \$25 million. They would range from \$18 million to \$60 million. The impact on average rates is to increase them all by about 9 cents per kWh.

If diesel prices stay low and flat, as in our low critical assumption, then diesel power generation is less expensive than nuclear by \$22 million (life-cycle cost). **Figure 6.8.** shows that with low diesel prices, average electric rates would be comparable between nuclear and diesel. However, as discussed above, lower rates would be needed for electric heat and rates for nonheat electricity would be higher than this average. Ratepayers would clearly be better off with diesel if diesel prices stay flat and nuclear capital is included in rates and a large security staff is required.

⁷ Toshiba presented this estimate with slides describing the 50-MW plant. We have used the cost per kW figure and applied it to the smaller size. Due to economies of scale, this approach may understate the cost of the smaller, 10-MW plant. However, we are unaware of a direct cost estimate for the 10-MW size.

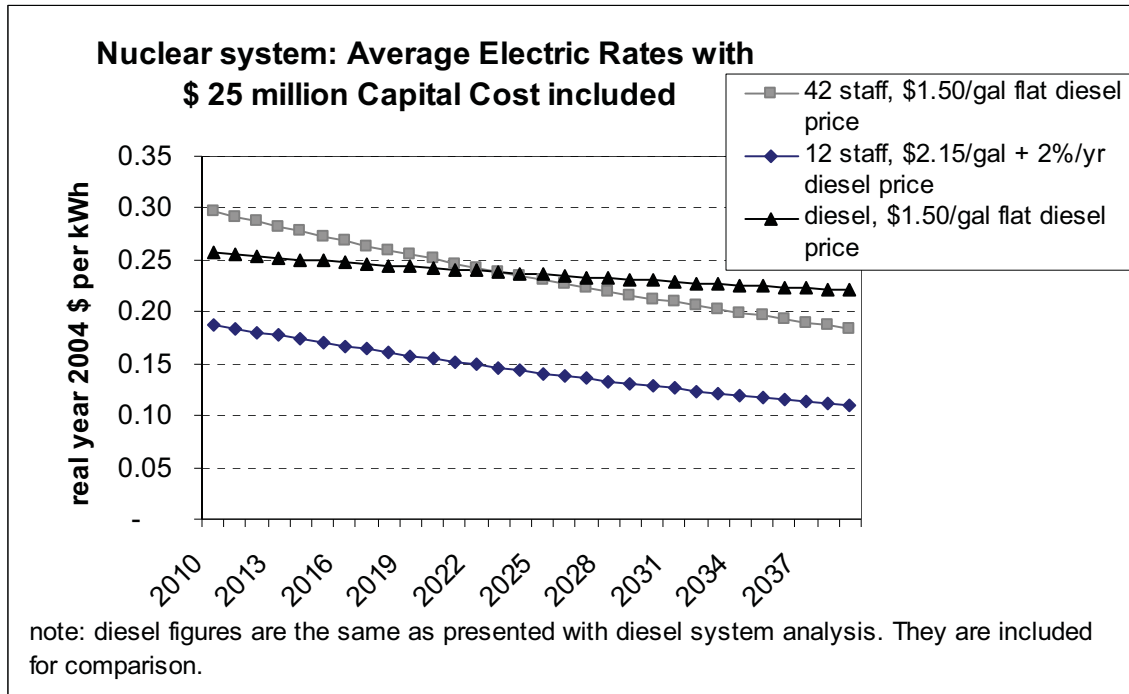


Figure 6.8. Projected future electric rates with nuclear capital costs included in rates.

If diesel prices are high, rising at 2% per year from a base of \$2.15 per gallon, and if the nuclear plant requires only a small security staff, then the life-cycle cost of power generation from nuclear would be \$41 million lower than the cost of diesel and electric rates would be dramatically lower.

These sensitivity cases demonstrate that if a \$25 million capital cost is included in the analysis, the nuclear system is not always a clear winner. There are many combinations of slowly rising diesel prices and high staffing requirements that would make nuclear more expensive than diesel or coal. If the analysis were being done for another community, the rankings would also depend strongly on the size and nature of the electric and heating loads in that place.

6.3.2.2 The Effect of Power Plant Location

The basic analysis assumes that the nuclear or coal plant would be sited near the current Galena power plant, resulting in the need for a 2-mile pipe to transport district heat to the air station. If this distance were increased to 7 miles, the capital cost of a heat distribution pipe costing \$200 per foot would increase by \$5.3 million.⁸ Under our methodology, this increased capital cost of the pipe would increase the life-cycle cost of power generation by exactly the same amount - \$5.3 million – in all cases where the air station heat load is served.

⁸ We recognize that there would also be additional costs in the form of higher heat losses, but for simplicity these are not treated explicitly, since this case is only illustrative. Adding a specific allowance for higher heat losses would be analytically equivalent to postulating an even longer distance with the same losses.

Pre-Publication Draft – Subject to Change

This increase would not affect the economic attractiveness of the nuclear or coal systems if diesel prices take on the high trajectory, although average rates would increase by about 1 cent per kWh. In particular, with high diesel prices it would still make economic sense for the coal plant to serve the air station. If diesel prices are low and flat, however, and if the nuclear staff is large, then the increased capital cost of heat pipe makes the nuclear system slightly more expensive than diesel. Adding 5 miles of extra distance to the heat pipe is economically equivalent to adding about 6 security staff to the required nuclear labor force.

These sensitivity cases demonstrate that distance from the coal or nuclear power plant matters, but only in a moderate way. Adding distance becomes critical to the economic conclusion only if diesel prices are low and flat. If diesel prices are high and rising, even a 7-mile heat transmission line still makes good economic sense at a \$200/foot construction cost.

6.3.3 Transmission

Since the nuclear plant is capable of producing large amounts of electricity in excess of current Galena electric loads, it is natural to consider the economics of building a transmission line to send the excess electricity to neighboring communities. We considered two possible transmission lines. Line A would run from Galena to Koyukuk, Nulato, and Kaltag. The total distance is 83 miles, and the transmitted electricity could displace about 172,000 gallons of diesel per year. We assume that the line could be built for \$80,000 per roadside mile plus \$200,000 per overland mile. The total cost would be \$14.9 million and the net present value of the avoided fuel costs would be \$8.1 million under our high diesel price assumption. Thus, this line would have a net economic cost of \$6.8 million.

The second line we considered was from Galena to Ruby. The distance is 42 miles and the transmitted power could displace 59,000 gallons of diesel per year. The total cost of \$7.3 million would far exceed the avoided fuel costs of \$2.8 million. **Table 6.9** summarizes the transmission analysis.

Pre-Publication Draft – Subject to Change

Table 6.9. Economic costs and benefits of transmission lines.

from	to	segment avoidable diesel gal/yr	segment road miles	segment overland miles	segment cost
Line A:					
Galena	Koyukuk	23,279	5	27	5,800,000
Koyukuk	Nulato	89,448	4	14	3,120,000
Nulato	Kaltag	58,929	5	28	6,000,000
Total line A		171,656	14	69	14,920,000
Present value of avoided costs (assumes high diesel price)					8,147,440
Net economic benefit of line (with free power at Galena)					(6,772,560)
Line B:					
Galena	Ruby	59,180	9	33	7,320,000
Total line B		59,180	9	33	7,320,000
Present value of avoided costs (assumes high diesel price)					2,808,906
Net economic benefit of line (with free power at Galena)					(4,511,094)

6.3.4 Economics of hydrogen production

Another potential use for the power generated by the nuclear plant in excess of existing needs is the production of hydrogen. We considered hydrogen production from the point of view of a potential private business enterprise. The enterprise would obtain power from the Galena electric utility and bear the responsibility for all aspects of the hydrogen production process. **Table 6.10** summarizes our analysis of this option.

The potential hydrogen enterprise is assumed to have a higher required rate of return – 7% above inflation. The analysis begins by assuming that electricity is a free input to the production process. There appears to be sufficient local demand for vehicle fuel to fully utilize one hydrogen production module (about 1 MW of electricity input). However, the production cost of hydrogen to meet this demand is extremely capital intensive. Using current costs of commercially available equipment, we estimate that it would cost at least \$6.2 million to construct one production module producing 404,000 gallons of liquid hydrogen per year with an energy content of about 12 billion Btu (Keenan, 2004). When modest operating costs are added, the total annual cost of energy is about \$46 per million Btu, which far exceeds the target cost of diesel or gasoline for vehicle and equipment use. This target cost is about \$17 per million Btu under the high diesel price assumption, rising over time to about \$30 per million Btu. This conclusion is based on almost full utilization of the capital equipment to serve local demands. In other words, there is no “excess capacity,” and it would not make sense to produce additional hydrogen and ship it by barge to a community like Fairbanks that has lower fuel costs.

Pre-Publication Draft – Subject to Change

Table 6.10. Hydrogen enterprise analysis.

Variable	Unit cost, or # of units, or units	present value cost	Year	
			1 2010	30 2039
Real discount rate for enterprise venture	7.0%			
Capital Cost:				
H2 generator (900 kW e input, 150Nm ³ /hr output))		1,500,000		
H2 liquefier (150 Nm ³ and 175 kW e input)		2,000,000		
Storage tanks unit cost, per 50,000	500,000			
Number of storage tanks	1			
Storage tanks capital cost		500,000		
Shipping tnks unit cost 17k gal ea	450,000			
Number of shipping tanks	1			
Shipping tanks capital cost		450,000		
Nitrogen liquefier		700,000		
Filling station equipment, contingency		1,000,000		
Total Capital per Gasifier		6,150,000		
Electricity	0.000 \$/kWh		-	-
O&M on gasifier & liquefier	\$/yr	\$153,682		85,000
Labor on gasifier, liquefier, and storage	\$/yr	\$620,452	50,000	50,000
Total liquid H2 production	gal/yr		404,000	404,000
Energy content of liquid H2 Btu/gal	30,000			
Total Energy in liquid H2 form	billion Btu		12.12	12.12
Local demands and export availability	gallons	Btu/gal	billion Btu	
City vehicle demand	15,000	114,100	1.7	3.0
Schools vehicle demand	25,000	114,100	2.9	5.1
Military vehicle demand	50,000	138,000	6.9	6.9
Total local demand	billion Btu		11.5	15.0
Total local demand	gal H2		382,133	500,165
Supply to local market	gal H2		382,133	404,000
Available for Export	gal H2		21,867	-
Amortized production cost				
Amortized capital including return			495,606	495,606
Amortized (smoothed) O&M			12,385	12,385
Labor			50,000	50,000
Electricity			-	-
Total amortized cost			557,991	557,991
Amortized cost per gallon H2 of local demand			1.46	1.38
Amortized cost per million Btu			48.67	46.04
Target cost per million Btu			12.00	12.00

Nearly the entire cost of hydrogen production is the cost of capital equipment. If this capital could be secured with a grant or other external funding source, the operating cost of producing hydrogen would likely be low. A sensitivity case shows that with zero capital cost, a hydrogen enterprise could afford to pay about 1.5 cents per kWh for electricity and still produce hydrogen at a cost per million Btu comparable to diesel or gasoline.

7. CONCLUSIONS

7.1 Economics Conclusions

Under the assumptions presented above, the nuclear system is the clear economic winner when compared to diesel, even when diesel prices are low and nuclear security staff requirements are high. This result is due to the ability of the 10-MW nuclear plant to serve the entire residential heat load (about 8,000 MWh/yr and 2.3 MW peak) and the entire air station heat load (52 B Btu/yr). We have used a daily dispatch model to verify that nuclear capacity is always adequate to meet daily energy requirements for both of these large loads. When the nuclear plant is unavailable, the air base can back up its own heat load and the Galena diesel system can almost surely back up the Galena residential heat load.

The nuclear system also beats coal on economic grounds in every basic case except one. If diesel prices are low *and* coal prices are low *and* coal efficiency is high *and* the total required nuclear staff is 42 people (8 operators plus 34 security), then the coal system has a life-cycle cost that is \$7 million below that of nuclear.

Coal is attractive relative to diesel in all of the basic cases. It must be stressed that the critical assumptions about coal prices and coal plant capital costs, fuel costs, and efficiency are perhaps the most uncertain, and they all matter. Having said that, when diesel prices are high and rising, the coal system is very likely to produce less expensive power for Galena customers than diesel.

Sensitivity cases show that if a \$25 million capital cost is included in the analysis, the nuclear system is not always a clear winner. When capital charges are included, many combinations of slowly rising diesel prices and high nuclear staffing requirements would make nuclear more expensive than diesel or coal. The amount of potential electricity demand would also be a critical factor in system economics if the nuclear system were to be considered for a community other than Galena. Siting the nuclear or coal plants farther from the air station heat load has a similar but smaller direct effect on system costs. For Galena, this variation in distance is only important if diesel prices remain low.

Table 5.11 supports these conclusions with a comprehensive summary of all cases considered in this analysis. The first six cases are the basic results that come from varying only the critical assumptions. The second six cases report the same results, but include an additional \$25 million capital cost for the nuclear system. The final four cases document the effect of siting the nuclear or coal plants 7 miles from the air station.

Pre-Publication Draft – Subject to Change

Table 7.1. Summary of basic cases and sensitivity cases.

case code	diesel price	coal price	coal average efficiency	coal capacity MW	nuclear capital charges	nuclear staff	total present value cost \$ million		
	\$/gal	\$/ton					diesel	nuclear	coal
basic cases (varying the critical assumptions)									
lhllh	1.50	125	30%	1.3	0.0	42	37.8	34.6	35.2
llhh	1.50	100	40%	2.1	0.0	42	37.8	34.6	27.5
llhll	1.50	100	40%	2.1	0.0	12	37.8	7.0	27.5
hhllh	2.15	125	30%	3.8	0.0	42	59.3	20.2	35.5
hlhll	2.15	100	40%	4.0	0.0	42	59.3	20.2	23.1
hllhl	2.15	100	40%	4.0	0.0	12	59.3	(7.4)	23.1
sensitivity cases - nuclear capital included									
lhllh	1.50	125	30%	1.3	25.0	42	37.8	59.6	35.2
llhhh	1.50	100	40%	2.1	25.0	42	37.8	59.6	27.5
llhhl	1.50	100	40%	2.1	25.0	12	37.8	32.0	27.5
hhllh	2.15	125	30%	3.8	25.0	42	59.3	45.2	35.5
hlhhh	2.15	100	40%	4.0	25.0	42	59.3	45.2	23.1
hllhl	2.15	100	40%	4.0	25.0	12	59.3	17.6	23.1
sensitivity - nuclear and coal sited 7 miles rather than 2 miles from air station									
llhh	1.50	100	40%	2.1	0.0	42	37.8	39.9	27.5
llhll	1.50	100	40%	2.1	0.0	12	37.8	12.3	27.5
hlhll	2.15	100	40%	4.0	0.0	42	59.3	25.4	28.4
hllhl	2.15	100	40%	4.0	0.0	12	59.3	(2.1)	28.4

NOTE: shaded cells highlight changes in assumptions and results relative to the previous case

Even though installation of the 4S nuclear plant presents a potential long-term solution to Galena’s critical energy issues, one must caution that, as with any non-commercialized technology, there is no guarantee. In our view, the most critical issue associated with the adoption of this technology is the difficulty of utilizing liquid sodium as a heat transfer medium. With any nuclear power plant, long-term disposal of radioactive waste is also an issue. If this technology is successfully deployed in Galena, its economic viability in other Alaska villages and elsewhere depends on the actual life-cycle costs yet to be quantified, as well as the actual energy demands in these places.

Benefits associated with adoption of one or more of the technologies discussed in this report go beyond their ability to meet Galena’s thermal and electric energy loads. We see the potential for Galena to serve as a training center for rural Alaskans interested in utilizing similar technologies in their villages. We also see the potential for use of additional cogeneration leading to economic development such as the development of horticulture and aquaculture. The enhancement of local employment by these activities is another benefit. With today’s uncertain energy situation, many communities are diversifying their energy options. This includes adding renewably based technologies to lessen dependence on fossil fuels. Adding a few tens of kW of PV arrays, for example, could help Galena insulate itself against fluctuations in the price and supply of diesel fuel.

Pre-Publication Draft – Subject to Change

7.2 Environmental Issues and Permitting Conclusions

Given the assumptions stated throughout this report, and strictly from an environmental permitting standpoint for the City of Galena, evaluation of the permitting requirements for each of the three primary energy options yields a clear loser (coal) and an apparent winner (nuclear). Two key assumptions play heavily into this result. The first is that coal will be generated locally. This represents a distinct disadvantage from a permitting standpoint in that permitting for the mine site must be considered for this option, but not the others. The second assumption is that all of the information provided to us by Toshiba proves to be accurate and is accepted by the NRC. Specifically, (1) if the 4S reactor truly generates no air or water emissions; (2) the reactor is returned to the final assembly point at the end of its useful lifetime (thereby eliminating nuclear waste issues in Alaska), and (3) Toshiba (or some other party) bears all (or most) of the licensing costs, then the permitting “cost” to Galena is reduced to the point that the nuclear power option becomes the clear preference. Before a final decision is made, it is imperative that these assumptions be verified.

8. RECOMMENDATIONS

On the basis of environmental permitting, the nuclear plant appears to be a clear winner. The coal mine and power plant option appears to be the most difficult for which to obtain permits. This conclusion is stated with the caveat that this will be determined by the process of gaining a design certification and a license from the NRC.

The economic analysis reveals that the 4S option will provide the lowest cost power if the assumptions hold. In the Galena case, the assumption is that capital cost will be borne by an outside party and that reasonable staffing levels will result from the licensing process. The coal option may be economic in some scenarios compared to enhanced diesel systems, so the coal option should not be entirely discounted.

Therefore, the recommendations are:

- ◆ Proceed with refining the 4S evaluation process in conjunction with the NRC
 - It may be advantageous for Galena to enlist an independent organization to estimate the time required for licensing and permitting
 - Toshiba and Galena should consider partnering with a U.S. organization or National Laboratory to assist in the process
- ◆ Retain the current diesel systems (with scheduled upgrades) until a decision is made regarding the installation of a replacement by about 2010.
- ◆ Retain the option of a coal mine and power plant until it is determined if the 4S system can be permitted and licensed. If the 4S cannot be realized, then the coal option appears feasible (with a favorable coal resource assessment result).

Pre-Publication Draft – Subject to Change

REFERENCES

- Bonk, D, US DOE, 2004, Personal communication
- Brown, Neil, Lawrence Livermore National Laboratory, Oct. 4, 2004, private communication
- Brown, K, 1999, Bright Future - or Brief Flare - for Renewable Energy, *Science*, 285, pp. 678-680
- Colt, S., S. Goldsmith, A. Witta, and M. Foster, 2001, Sustainable Utilities in Rural Alaska, prepared for USDA Rural Development.
- Gooley, G.J, Trout, December 1997, The New Rural Industries – A Handbook for Farmers and Investors, Australian Rural Industries R&D Corp.
- Johnson, R., D. Das, D. Witmer, H. Bretas Rueter, 2000, The Creation and Design of an Energy Center, *Jl. of Cold Regions Engineering*, Vol. 14, pp. 13 – 23.
- Keenan, Gregory, June 8, 2004, Air Products Corp., Personal Communication,
- MAFAa, 2002, Rural Alaska Energy Plan, Diesel Efficiency Chapter, prepared for AEA and AIDEA, December 2002
- MAFAb, 2002, Rural Alaska Energy Plan, Cogeneration Chapter, prepared for AEA and AIDEA, December 2002
- MAFAc, 2002, Rural Alaska Energy Plan, End Use Efficiency Chapter, prepared for AEA and AIDEA, December 2002
- McChesney, C, 2003, Arizona PV costs, Environmental Portfolio Standard Cost Evaluation Working Group Cost Committee, UPEX 2003, APS.
- McKinney, M., and R. Schoch, 1998, *Environmental Science*, Jones and Bartlett, Boston, MA.
- NREL, 2004, Solar Radiation Data Manual, <http://www.nrel.gov/>
- Northern Economics, April 2001, Screening Report for Alaska Rural Energy Plan, prepared for AIEDA.

Pre-Publication Draft – Subject to Change

Northern Resource Group, January 26, 2004, Galena Energy Assessment, Fairbanks, AK.

Petrie, B, 2004, Manager, Special Projects, Alaska Village Electrical Cooperative, Inc, Personal communication.

Phillips, N. and S. Denton, October 1990, Coal Resource and Utilization Survey on Doyon, Lmted. Lands.

Prindle, W. et al, 2003, Energy Efficiency's Next Generation: Innovation at the State Level, Report E 031, <http://aceee.com>.

Ristinen, R and J. Kraushaar, 1999, Energy and the Environment, John Wiley and Sons, NYC.

Royal Academy of Engineering, March 2004, The Cost of Generating Electricity, London, G.B. www.raeng.org.uk.

Rosinski, Douglas, May 24, 2004, Shaw Pittman, private communication.

Sackett, John, October 21, 2004, Argonne National Laboratory – West, private communication

Sakashita, Yoshiaki, 2004, Specialist, Advanced Reactor System Engineering Group, Toshiba Corp., Yokohama, Japan, Personal communication.

Scott, D., 2002, Hydrogen System Development – Status and Drivers, 11th Canadian Hydrogen Conference, June 17 – 20, Victoria, B.C.

J.S. Strandberg Consulting Engineers Inc., June 1997, A feasibility analysis of a proposed coal fired thermal power station for McGrath, Alaska. Prepared for MTNT Lmted and McGrath Light and Power,

Triton Consultants, 2002, Green Energy Study for BC, Tidal Current Energy, prepared for BC Hydro.

US Department of Energy, May 2001, Office of Nuclear Energy, Science and Technology, Report to Congress on Small Modular Nuclear Reactors.

Yoder, M, 2004, City Manager, Galena, Alaska, Personal communication,

APPENDICES

APPENDIX A. Presentation by Yoshiaki Sakashita, Toshiba, at the 2004 Alaska Rural Energy Conference, April 27-29, 2004, Talkeetna, Alaska

4S Current Status

4S: *Super Safe, Small & Simple*

2004 Alaska Rural Energy Conference
Talkeetna, Alaska
April 27-29, 2004

TOSHIBA Corporation
Industrial and Power Systems & Services Company

Contents

1. 4S Overview

Features, Plant outline, Target cost,
Expected schedule, R&Ds

2. 4S applications

Fresh water

Hydrogen & oxygen

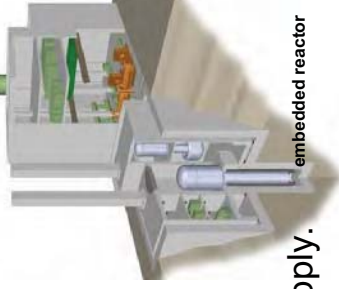
What is 4S ?

4S Major Features

- (1) No refueling,
- (2) Passive safety,
- (3) Transportability,
- (4) Reasonable cost for distributed power supply.

4S power station

Turbine building



What is no refueling ?

No refueling means

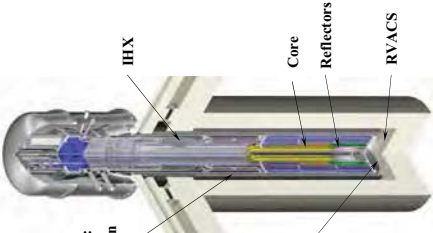
- (1) Reducing a load of fuel transportation,
- (2) Lower maintenance requirements,
- (3) Non proliferation,
- (4) Design simplification, ex., no refueling device,
- (5) Zero emission during plant lifetime.

4S Core

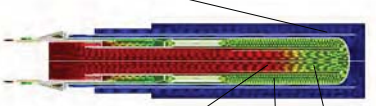
- Fuel material: U-Zr (metallic)
 - Coolant material: sodium
 - Core lifetime: 30 years
 - Core height: 2.5 m (50MWe)
2.0m (10MWe)
 - Core diameter: 1.2m (50MWe)
0.9m (10MWe)
 - Reactivity temperature coefficient: negative
- 
- Center SA: Ultimate shutdown rod (neutron absorber as back up)
 - Fuel subassemblies (18 SAs)
 - Reflectors are moving upward and surrounding the core slowly(*) in order to compensate the reactivity loss during 30 years burn-up. If an accident occurred, reflector would fall down to make core subcritical.

(*) average velocity: 1mm/week approximately

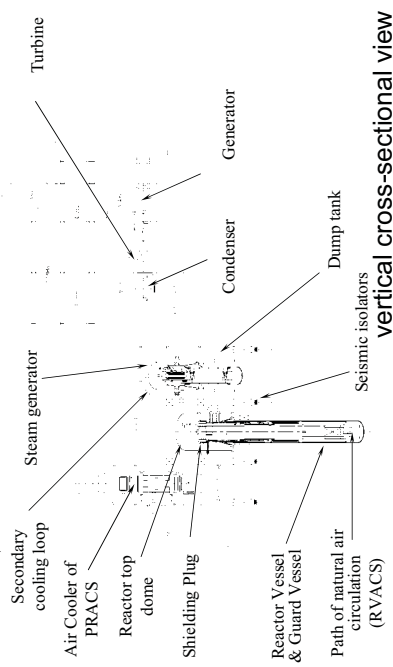
4S Reactor

- Output: 10MWe (30MWt),
50MWe (135MWt)
 - Coolant: sodium
 - Coolant temp: 510 / 355 deg.C
 - Reactivity control: movable reflectors
 - RV type: integral type
 - EM Pumps: annular type
 - Core position: bottom in the RV
 - RVACS: natural air circulation (Reactor Vessel Auxiliary Cooling System)
 - GV: second boundary for sodium (Guard Vessel)
- 
- EM Pumps: two pumps in series
 - IHX
 - Core
 - Reflectors
 - RVACS
 - Double boundary: RV & GV

4S Primary Cooling System

- Primary Coolant**
Sodium coolant flows inside the reactor vessel by static (EM) pumps.
 - Outer region:**
downward flow
 - Inner region:**
upward flow
 - RVACS**
Natural air circulation around the reactor vessel for decay heat removal
- 
- Temperature scale: 540.1, 412.6, 285.1, 157.5, 30.0

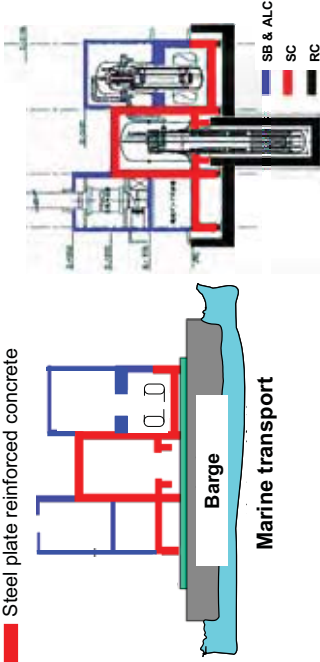
4S Plant Arrangement (50MWe)



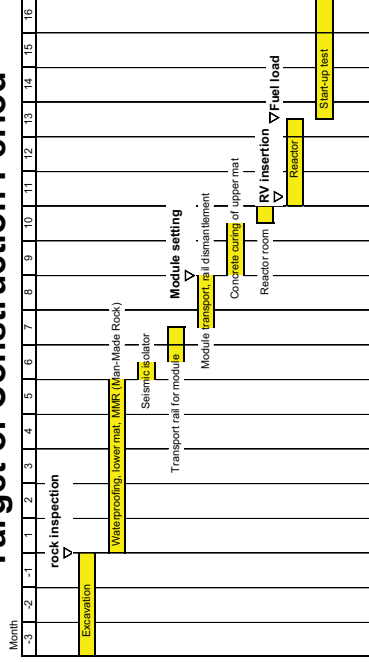
Transportation

Design for shop fabrication, lightweight, and mass production

- Steel beam and autoclaved lightweight concrete
- Steel plate reinforced concrete



Target of Construction Period

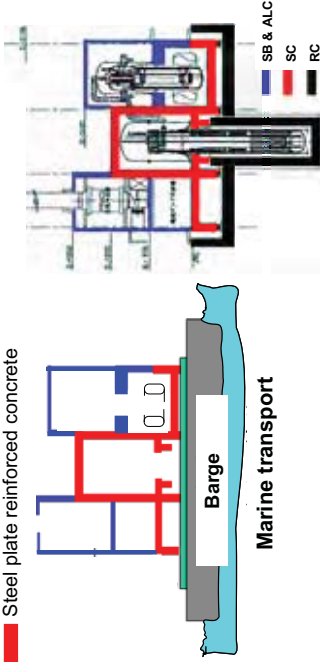


Construction periods for laying underground in frozen-soil site should be optimized.

Safeguard & Security

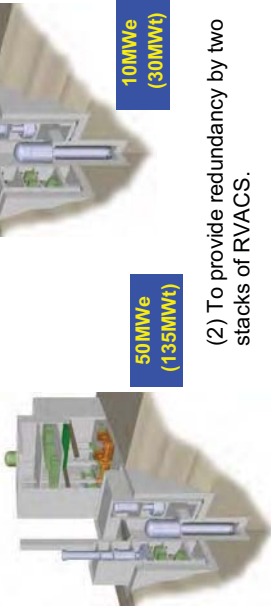
For safeguard and security

- (1) To minimize unauthorized accessibility to the reactor including fuels by earth-sheltered reactor building.
- (2) To provide redundancy by two stacks of RVACS.



After 30 years

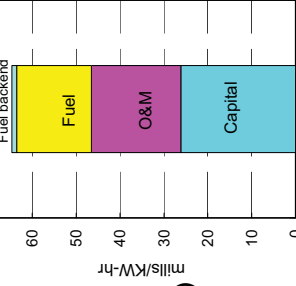
- (1) Fuel
- Long-term geologic repository in Yucca Mountain site.
- (2) Reactor
- Transport and disposition in accordance with US experience, e.g., Hanford site (Trojan reactor, etc.)
- (3) Sodium, buildings & substructure
- Reutilized for next 4S installation.



4S Preliminary Cost Estimation

50MWe (135MWt) :

Commercial plant (mass production phase)



- Plant Construction:

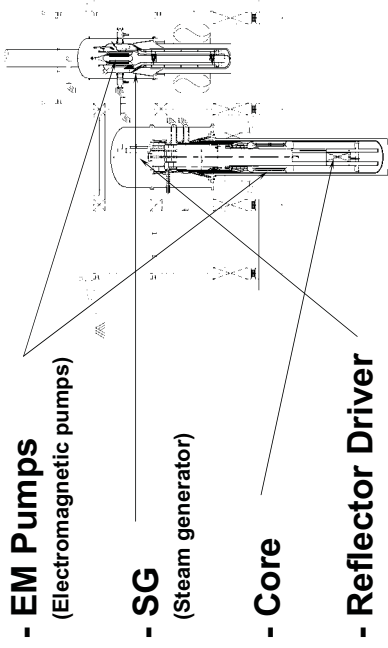
\$ 2,500/KWe

- Busbar Cost:

65 mills/KW-hr^(*1)

(*1) 8% house load factor is assumed.

R&D status for 4S



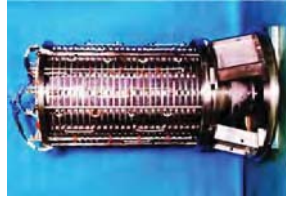
EM Pumps

Capacity for 4S:

50m³/min (50MWe)

Sodium Test Facility:

ETEC, U.S.



40 m³/min^{*1}

160 m³/min^{*2}

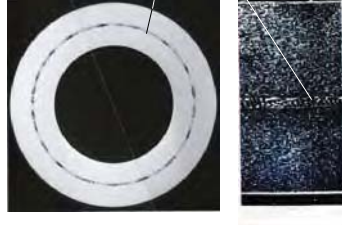


^{*2}) These R&Ds have been performed as a part of joint R&D projects under sponsorship of the nine Japanese electric power companies, Electric Power Development Co., Ltd., the Japan Atomic Power Company (JAPC) and the U.S. Department of Energy (DOE).

^{*3}) These R&Ds have been performed as a part of joint R&D projects under sponsorship of the nine Japanese electric power companies, Electric Power Development Co., Ltd., and JAPC.

SG

Double wall tube with leakage detection system for both inner and outer tubes to prevent a reaction between secondary sodium and water



Inner tube

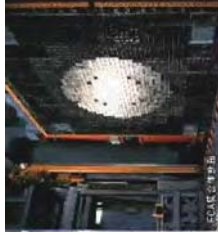
Outer tube

^{*2}) These R&Ds have been performed as a part of joint R&D projects under sponsorship of the nine Japanese electric power companies, Electric Power Development Co., Ltd., the Japan Atomic Power Company (JAPC) and the U.S. Department of Energy (DOE).

Core: Critical experiment for 4S

FCA: 2004 (JAERI)^{*1}

NCA: finished (TOSHIBA)



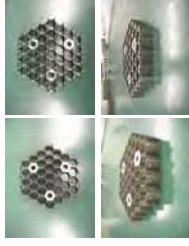
Toshiba and CEPCO^{*2}

JAERI, Toshiba, CRIEPI, Osaka Univ.

^{*1}) These R&Ds have been performed as a part of "Innovative Nuclear Energy System Technology (INEST) Development Projects" under sponsorship of MEXT (JAPAN).
 CRIEPI: Central Research Institute of Electric Power Industry, JAERI: Japan Atomic Energy Research Institute.
^{*2}) CEPCO: Chubu Electric Power Co., Inc.

Fuel subassembly

Hydraulic Experiments for high fuel-volume fraction subassembly^{*1}



CRIEPI and Toshiba

Basic tests: finished,

Full-scale mockup: 2003-04

^{*1}) These R&Ds have been performed as a part of "Innovative Nuclear Energy System Technology (INEST) Development Projects" under sponsorship of MEXT (JAPAN).

Reflectors

(EMI: Electromagnetic Impulsive force drive)

Fundamental test: finished 1/3 model test: 2004-05^{*1}



Photo: EMI pre-test module^{*1}; finished

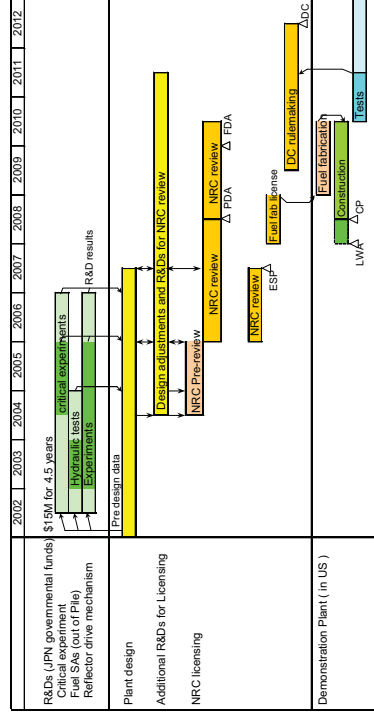


Toshiba and CEPCO^{*2}

Toshiba, Univ. of Tokyo, and CRIEPI

^{*1}) These R&Ds have been performed as a part of "Innovative Nuclear Energy System Technology (INEST) Development Projects" under sponsorship of MEXT (JAPAN).
^{*2}) CEPCO: Chubu Electric Power Co., Inc.

Expected 4S developing schedule



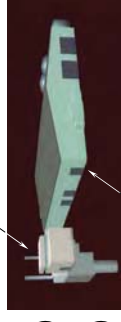
2. 4S applications

4S applications (1)

Sea water desalination

Single 4S Plant

- Two stage reverse osmosis system
- Water production:
 - 34,000 m³/day (10MWe)
 - 170,000 m³/day (50MWe)



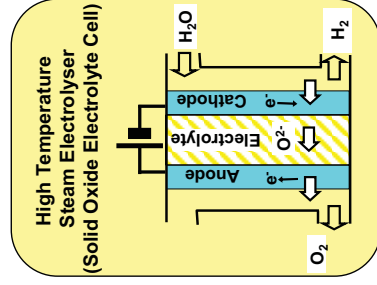
Desalination plant

4S applications (2)

Hydrogen production

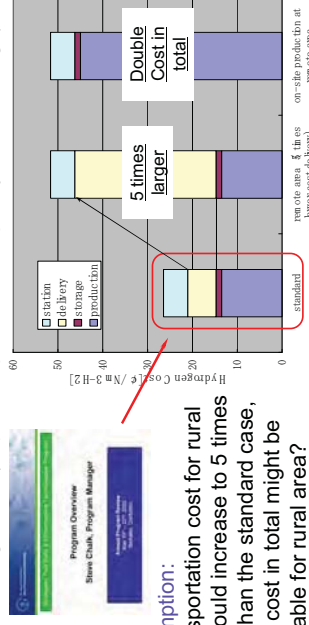
Single 4S Plant

- High temperature steam electrolyser,
- No CO₂ emission.
- Hydrogen production:
 - 3,000 Nm³/h (10MWe)
 - 15,000 Nm³/h (50MWe)



Discussion: Acceptable cost of hydrogen in rural area.

- *Point 1: Transportation cost would increase along the distance from production site to user area.
- *Point 2: Production cost in rural area tends to increase because of scaling-effect (requested production capacity is not so large).



*Assumption:
If transportation cost for rural area would increase to 5 times larger than the standard case, double cost in total might be acceptable for rural area?

Summary

4S is a sodium cooled, metallic fuelled small fast reactor with long core lifetime.

4S has a proper features for distributed energy station in rural areas, such as

- No refueling,
- Passive safety,
- Lower maintenance requirements,
- Transportability on construction,
- Reasonable cost.

Pre-Publication Draft – Subject to Change

APPENDIX B. Detailed Discussion of Hydropower, Solar, and Conservation

Presented below are detailed discussions of the Hydropower, Solar, and Conservation topics. These technologies are available to be applied in Galena, but their nature or capacity is not suited to make large impacts on operation of the electric utility. They can be used in conjunction with the utility (as add-on modules) or by end-users (utility customers) to reduce their energy use.

Hydro - In-river Turbines

Galena is on the north bank of the Yukon River, one of the largest in the country. A tremendous amount of water passes the site each day – winter and summer and seems to be a logical place to install in-river turbines for electric power generation. However, compared to the load requirements of the City, this may not be a valid conclusion. A variety of turbines are being developed. The one apparently most suited to the Galena site is under development by UEK Corporation. It is proposed to be installed in rivers, anchored to the bottom, and operated year around – even under ice. A project to demonstrate it at village Eagle on the upper Yukon River has been approved but is awaiting U.S. DOE funding. This turbine design has dual 3-meter diameter blades. To estimate the power output of a similar unit at Galena, a look at the power density is in order.

The power density in a flowing fluid is

$$P_{max} = 0.5\rho V^3$$

For water flowing at $V = 2$ m/sec (characteristic of the Yukon at Galena) and density $\rho = 1000$ kg/m³ corresponding to 4 kW/m³. For reasons related to mass conservation and efficiency, one may only be able to capture 40% of this or less with a conventional turbine. For a water turbine with two 3-meter turbines or an area of 14.1 m², this results in power generation of 22.5 kW – much less than that required by the City's load. Ten units would have to be installed to make even a marginal contribution and the cost would be too great for the benefit. UEK estimates \$ 1,000/kW capacity for a 10-MW plant yet to be built.

(<http://www.delawareonline.com/newsjournal/local/2003/09/06tidalpowerplant.html>)

On the other hand, an operational 300kW tidal turbine in Norway, costs \$23,000/kW capacity. (<http://www.eere.energy.gov/RE/ocean.html>)

Operational issues include turbine blade erosion [and maybe even destruction] caused by solid objects in the river, impacts on aquatic life, and hazards to navigation. For rivers that are ice-covered at least part of the year, one must also deal with potential damage to submersed structures associated with breakup.

On the plus side, the Yukon River flows year round so the hydro resource is a continuous one.

Pre-Publication Draft – Subject to Change

Water turbines

Several firms worldwide have developed in-stream water turbines with applications to typically capture the power from tidal currents. UEK Corporation has estimated the capital cost for 56 machines generating 10.8 MW in a 7-knot current to be \$10M. It is a buoyant turbine/generator suspended like a kite in a tidal stream (Tricon Consultants, 2002). At the present time, the standard UEK machine consists of twin turbines, each 3 m in diameter. This produces 90 kW in 5-knot currents and weighs approximately 3 tons without the anchorage harness and shore equipment. UEK plans to have a 6.7 m twin turbine system available in the future and has plans for a 1-MW system.

Blue Energy Canada is developing Darrieus [vertical axis] turbines and Marine Current Turbines Ltd [MCT] incorporates two axial flow rotors, each 15 to 20 m in diameter mounted on a vertical tower set in the seabed. Each turbine could develop up to 1 MW.

Limited cost data are available for the MCT units and for smaller UEK units. The lack of detailed cost data from other tidal current companies makes it impossible to compare the proposed technologies on the basis of cost efficiency. For two 15.9-m diameter variable-pitch rotors with a combined power output of 1 MW at a rated velocity of 2.3 m/s, estimated units costs of electricity at two different sites on the Canadian west coast were \$0.11 [800 MW cap] and \$ 0.26/kWh. [43 MW]

For these studies, the energy output was estimated assuming a rotor efficiency of 45% (based on wind power experience), gearbox and generator efficiencies of 94% and 92%, respectively, and a reliability of 95%. A discount rate of 8% was assumed with the scheme being decommissioned after 25 years of production.

A 300-kW unit [\$7M] in Norway operating in a 1.8 m/sec current has $D = 20$ m blades. It can rotate to keep the turbine facing the current and is 12% efficient. This tidal power plant in Kvalsundet was made by Hammerfest Strø.

<http://www.eere.energy.gov/RE/ocean.html>

Solar

Solar-electric

Vendors of PV components in Fairbanks include ABS Alaskan [907-452-2002] and Arctic Technical Services [907-452-8368]. Major US manufacturers include BP Solar [<http://www.bpsolar.com>], and Kyocera Solar Inc. [<http://www.kyocerasolar.com>].

In one specific example, the BP 3160B photovoltaic module has 72 cells in series and produces 160 watts [4.5 A at 35 V] of nominal maximum power [at 1 sun]. It has a footprint of 159 x 70 cm [1.11 m²]. It weighs 35 lbs and has a 25-yr power output warrantee. The temperature cycling range is – 40 to 185°F, and the allowable wind and snow loadings are 50 and 113 psi, respectively. The temperature coefficient [Tcoef] for power is – 0.5%/°C with a nominal panel $T = 47^{\circ}\text{C}$ at $T_a = 20^{\circ}\text{C}$, $e_s = 0.8 \text{ kW/m}^2$, and $V_w = 1 \text{ m/sec}$. The negative Tcoef is good news for Alaska. For example, if the panel $T = 5^{\circ}\text{C}$ instead of a nominal 25°C , the output power will be 10% higher.

Pre-Publication Draft – Subject to Change

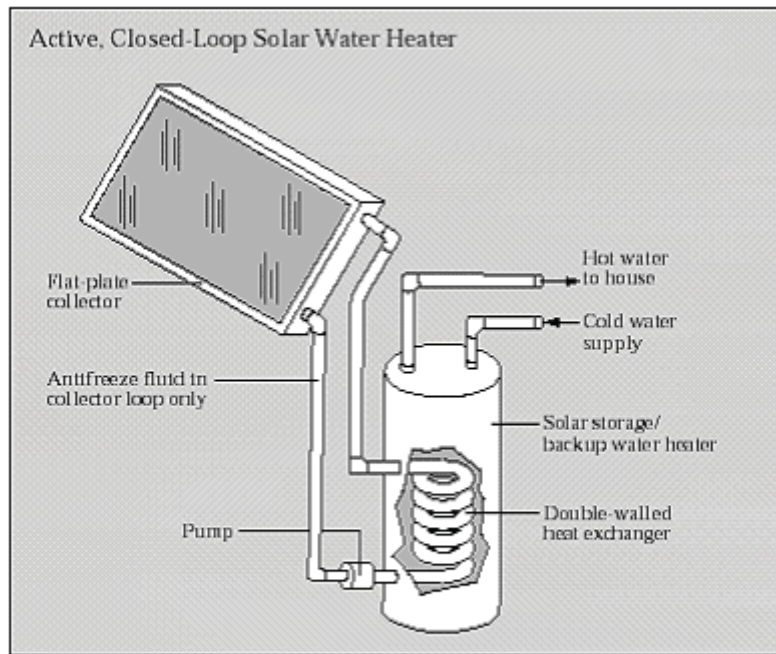
As an example, **Figure 2.8**, indicates average daily insolation in Fairbanks [approximating that for Galena] from March – July of about 5 kWh/m^2 or about 5.5 kWh incident on the BP 3160B daily for a tilt angle of 64° . This panel produces 160 W for each 1000 W/m^2 incident or 160 Wh for each kWh/m^2 incident. Hence, its nominal daily output at 25°C is $5[160] = 800 \text{ Wh}$. This can be increased by ambient temperatures colder than 25°C and decreased by system losses. If the solar generated electricity is worth about $\$0.28/\text{kWh}$, then over the aforementioned 5-month period, the approximately $150[0.8] = 120 \text{ kWh}$ would be worth about $\$33$. If one assumes an installed cost of $\$10/W_p$, then the initial capital outlay would be $\$1,600$. For the nine months [March through November], the insolation for a collector at latitude tilt of about 1131 kWh/m^2 . This corresponds to a daily average of about 4.2 kWh/m^2 . So, the PV module would output $1131[0.16] = 180 \text{ kWh}$ worth approximately $\$51$, making a very long payback period.

Solar Thermal

Solar thermal technologies use the heat in sunlight to produce hot water, heat for buildings, or electric power. Solar thermal applications range from simple residential hot water systems to multimegawatt electricity generating stations.

Throughout history, humans have used the heat from sunlight directly to cook food and heat water and homes. Today, solar collectors can gather solar thermal energy in almost any climate to provide a reliable, low-cost source of energy for many applications including hot water for homes, residential heating, and hot water for industries such as laundry and food processing. In recent years, utilities have begun to use solar thermal energy to generate electricity by boiling water and using the steam to drive a turbine which generates electrical power.

Millions of solar thermal systems are in place around the world today with many used for hot water heating. The three types of collectors are flat-plate, evacuated-tube, and concentrating. The most common, the flat-plate type, consists of an insulated, weatherproofed box containing a dark absorber plate at the bottom with the side closest to the sun covered with a transmitting material such as glass. The fluid being heated flows through tubes placed on the black surface and can be warmed by tens of degrees C as it passes through the collector. If the fluid is pure water, it must be drained if the temperature is predicted to fall below freezing. The water can be forced through the collector by a pump or can flow because of thermal siphon effects. The latter relies on the fact that warm water is less dense than cold and hence tends to rise. The active system shown in **Figure B.1** below relies on a double-walled heat exchanger to prevent the antifreeze solution on the hot side from contaminating the domestic water on the cold side. Not shown are sensors and controls to protect the system from excessive temperatures or pressures. This control loop would, for example, only turn the pump on to circulate water through the collector when the water temperature about to leave the collector exceeded a preset amount such as 90°F . It could cause a pressure relief valve to release fluid if the pressure exceeded a set point.



An active, closed-loop system heats a heat-transfer fluid (such as water or antifreeze) in the collector and uses a heat exchanger to transfer the heat to the household water.

Figure B.1 An active solar closed-loop water heating system. Courtesy of U.S. DOE

<http://www.eren.doe.gov/erec/factsheets/solrwatr.pdf>

In addition to collectors, the complete system needs an insulated storage tank, and sensors and controls to prevent overheating. Cold water flows from the bottom of the insulated storage tank to the bottom of the collector, and then returns to the storage tank when warmed. Active systems use electric pumps, valves, and controllers to circulate water or other heat-transfer fluids through the collectors and range in price from about \$2,000 to \$4,000 installed for residences. Storage tank sizes can range from 50 gals for 1 to 3 people up to 120 gals for 4 to 6 people. For sizing collector area, allow about 40 ft² for 2 people with another 8 ft² for each additional person in the Sun Belt. These numbers should be around 60% larger for the northern United States.

<http://solstice.crest.org/renewables/re-kiosk/solar/solar-thermal/index.shtml>

<http://www.eren.doe.gov/erec/factsheets/solrwatr.pdf>

One example of a technology applicable for northern climates, Thermomax Evacuated Heat Pipe Solar Collectors, consists of copper heat pipes inside vacuum sealed tubes.

As the sun shines on the black surface of fins mounted on the heat pipes, the alcohol within the heat pipes is heated and the hot vapor created rises to the tops of the pipes. Water, or glycol, flows through a manifold at the top of the tube bank and picks up

Pre-Publication Draft – Subject to Change

the heat from the tubes. The heated liquid circulates through another heat exchanger and gives off its heat to water stored in a solar storage tank.

A 20-tube array is 60" by 80" by 6 " and gives a maximum of ~ 25K Btu/day ~ 8 kWh/day

The A ~ 3 m² [not all of this area filled with tubes] and, with a peak insolation ~ 5.6 kWh/m²/day, we expect ~ 16.5 kWh in. Hence, the system efficiency $\epsilon_p \sim 50\%$.

<http://www.thermomax.com/>

Energy Conservation

Energy conservation refers to a variety of strategies employed to reduce the demand for energy. This can include adding extra insulation on building exteriors, setting building thermostats closer to ambient temperatures, or carpooling. Conservation is different from increasing energy efficiency, which refers to increasing the useful output for a given energy input. This could involve replacing incandescent light bulbs with compact fluorescent ones, driving more fuel-efficient motor vehicles, and buying more efficient appliances.

Projections made in early 1970s indicated the United States would be using energy at the rate of 160 Q by 2000 (Ristinen and Kraushaar, 1999). In actuality, our use today is less than 100 Q. Here, $Q = 10^{15}$ Btu where a Btu is the energy required to heat 1 lb of water by one degree Fahrenheit. A typical home in Alaska today might require 100 million Btu annually for space heating. Reasons that our energy use today is less than predicted include a rising cost of energy, the adoption of many federally and state sponsored energy conservation programs, and the use of more efficient technologies.

In Alaska, there is a large potential for fuel oil savings in villages by using heat captured from the jacket water of diesel-electric generators for space heating.

Ideas for lowering energy use in homes include lowering the water heater thermostat temperature to 120°F, insulating the water tank and hot water piping, replacing incandescent light bulbs with compact fluorescent ones, installing better weather stripping, increasing the thickness of insulation, and installing air to air heat exchangers. The latter preheat outside air by capturing heat from the inside air before it exits to the outdoors. Their use can save hundreds of dollars annually in fuel bills in a residence in Alaska. As much as 30 percent of a home's heating and cooling energy is lost through leaky ductwork. In the United States, that totals \$5 billion in wasted energy each year. A good site for energy conservation issues in homes including heat loss from ducts is

<http://www.southface.org/home/sfpubs/miscpubs.html>

A 15-watt compact fluorescent light bulb costing about \$5 and lasting 10,000 hours provides the same illumination as a 60-watt incandescent bulb costing about \$0.50 and lasting 1000 hours. Hence, over 10,000 hours of use, the total capital outlay for each is the same, \$5.00. But, the compact fluorescent will use $[60-15][10] = 450$ kWh less electrical energy and save \$45 in energy bills at \$0.10/kWh. Replacing

Pre-Publication Draft – Subject to Change

the higher use light bulbs in a home with compact fluorescent light bulbs can easily save hundreds of dollars in energy bills over a several year period.

As an example of a federal program encouraging energy conservation, the U.S. Department of Energy (DOE) has established a [Center Of Excellence For Sustainable Development](#). This center assists communities across the United States in establishing programs on community conservation, industrial efficiency, building efficiency, community renewable energy, and demand-side management (DSM).

The [Energy Efficiency And Renewable Energy Network of the U.S. Department of Energy](#) has a web site dedicated to helping homeowners save energy. The site covers topics such as weatherization, water heating, lighting, and appliances. It has a special section on the use of windows in cold climates, encouraging the use of double pane windows with low emissivity coatings. With appliances representing about 20% of a household's energy consumption, buying energy efficient refrigerators can save up to \$1000 over a 15-year lifetime compared with a model designed 15 years ago. In fact, the cumulative energy saved by adopting energy efficient refrigerators starting around 1974 represents \$17 billion annually in the United States. This energy savings represents the value of all electricity produced by nuclear power plants.

The American Council for an Energy Efficient Economy (Prindle, 2003) found a typical U.S. household could save \$500 annually by adopting more efficient appliances and lights.

According to MAFAc (2002), aggregate household electrical energy use could improve from roughly 6.7kWh/ft²/yr to around 4.5kWh/ft²/yr if rural households adopted a number of the end-use energy efficiency measures including switching from electrical hot water heaters to efficient oil-fired water heaters. Heating energy use could improve from roughly 1.14 to around 1.0 gal/ft²/yr if rural households switched to high efficiency direct vent heaters for space and water heating.

The benefits of new high efficiency lighting and electric water heater replacement programs appear to far outweigh the cost, including the potential for “free riders,” short-term declines in utility energy demand and efficiency and market uncertainty.

Rural Alaska schools consume roughly 49,200,000 kWh/yr electric energy and 5 M gal/yr of fuel oil. According to MAFAb (2002), these could each be reduced by 50% by end-use efficiency improvements. Some of this is being realized every year as schools periodically replace existing inefficient lighting, appliances, fixtures, and HVAC equipment with new, more efficient ones.

Pre-Publication Draft – Subject to Change

APPENDIX C. Summary of Nuclear Regulations

Chapter I of Title 10, "Energy," of the Code of Federal Regulations (CFR) guide licensing of nuclear power plants. .

Among the most important for permitting are the following Parts:

Chapter 1 Title 10, "Energy," of the Code of Federal Regulations (CFR)

10 CFR Part 2. Governs all proceedings, other than export and import licensing proceedings, under the Atomic Energy Act of 1954, as amended, and the Energy

Reorganization Act of 1974, for --

(a) Granting, suspending, revoking, amending, or taking other action with respect to any license, construction permit, or application to transfer a license;

(b) Issuing orders and demands for information to persons subject to the Commission's jurisdiction, including licensees and persons not licensed by the Commission;

(c) Imposing civil penalties under section 234 of the Act; and

(d) Public rulemaking.

10 CFR Part 50. Domestic Licensing of Production and Utilization Facilities: Provide for the licensing of production and utilization facilities pursuant to the Atomic Energy Act of 1954, as amended (68 Stat. 919), and Title II of the Energy Reorganization Act of 1974 (88 Stat. 1242). This part also gives notice to all persons who knowingly provide to any licensee, applicant, contractor, or subcontractor, components, equipment, materials, or other goods or services, that relate to a licensee's or applicant's activities subject to this part, that they may be individually subject to NRC enforcement action for violation of § 50.5.

10 CFR Part 51. Environmental Protection Regulations for Domestic Licensing and Related Functions: Contains environmental protection regulations applicable to NRC's domestic licensing and related regulatory functions. Subject to these limitations, the regulations in this part implement Section 102(2) of the National Environmental Policy Act of 1969, as amended.

10 CFR Part 52. Early Site Permits, Standard Design Certifications, and Combined Licenses for Nuclear Power Plants: This part governs the issuance of early site permits, standard design certifications, and combined licenses for nuclear power facilities licensed under Section 103 or 104b of the Atomic Energy Act of 1954, as amended (68 Stat. 919), and Title II of the Energy Reorganization Act of 1974 (88 Stat. 1242). This part also gives notice to all persons who knowingly provide to any holder of or applicant for an early site permit, standard design certification, or combined license, or to a contractor, subcontractor, or consultant of any of them, components, equipment,

Pre-Publication Draft – Subject to Change

materials, or other goods or services, that relate to the activities of a holder of or applicant for an early site permit, standard design certification, or combined license, subject to this part, that they may be individually subject to NRC enforcement action for violation of § 52.9.

As used in this part,

(a) Combined license (COL) means a combined construction permit and operating license with conditions for a nuclear power facility issued pursuant to subpart C of this part. A COL authorizes construction and conditional operation of a nuclear power facility. An application for a COL may, but need not, reference a standard design certification issued under Subpart B of 10 CFR Part 52 or an ESP issued under Subpart A of 10 CFR Part 52, or both.

(b) Early site permit means an NRC approval for a site or sites for one or more nuclear power facilities. The NRC can issue an ESP for approval of one or more sites for one or more nuclear power facilities separate from the filing of an application for a construction permit or combined license in accordance with 10 CFR Part 52. An ESP is a partial construction permit and is, therefore, subject to all procedural requirements in 10 CFR Part 2 that are applicable to construction permits. Applications for ESPs will be reviewed according to the applicable standards set out in 10 CFR Parts 50 and 100 as they apply to applications for construction permits for nuclear power plants. Early site permits are good for 10 to 20 years and can be renewed for an additional 10 to 20 years. ESPs address site safety issues, environmental protection issues, and plans for coping with emergencies, independent of the review of a specific nuclear plant design.

(c) Standard design means a design which is sufficiently detailed and complete to support certification in accordance with subpart B of this part, and which is usable for a multiple number of units or at a multiple number of sites without reopening or repeating the review.

(d) Standard design certification, design certification, or certification means a Commission approval, issued pursuant to subpart B of this part, of a standard design for a nuclear power facility. A design so approved may be referred to as a certified standard design.

10 CFR Part 100. Reactor Site Criteria: The siting requirements contained in this part apply to applications for site approval for the purpose of constructing and operating stationary power and testing reactors pursuant to the provisions of part 50 or part 52 of this chapter.

Reactor Decommissioning

NRC continues to regulate nuclear reactors after they are permanently shut down and begin decommissioning. Decommissioning is defined in NRC regulations as "to remove a facility or site safely from service and reduce residual radioactivity to a level that permits (1) release of the property for unrestricted use and termination of the license; or (2) release of the property under restricted conditions and termination of the license." The NRC maintains a series of internet web sites to provide information on

Pre-Publication Draft – Subject to Change

reactor decommissioning (see <http://www.nrc.gov/reactors/decommissioning/regs-guides-comm.html>)

During the operating life of a reactor, plant components can become radioactive, either through contamination or as a result of activation caused by the fission reaction. Therefore, special care is needed in the decontamination and dismantlement of the facility. Contaminated materials are shipped to a low-level radioactive waste disposal site for burial. The NRC has adopted extensive regulations for dealing with the technical and financial issues associated with decommissioning.

During the reactor decommissioning process, NRC conducts inspections, processes license amendments (including approval of the License Termination Plan), and monitors the status of activities. This monitoring ensures that safety requirements are being met throughout the process.

All decommissioning associated with the 4S reactor is assumed will be the responsibility of Toshiba, the plant owner, or some other party, which will remove the entire reactor module at the end of the 30-year operating life. They will therefore be responsible for all wastes, spent fuel, etc. associated with the 4S plant. The NRC license will stipulate details as to how and when this removal will occur. NRC may also require some form of financial guarantee that the decommissioning occur according to the license granted. Because the entire reactor module will be removed, and will remain sealed until returned to the point of assembly, it is assumed that many of the standard NRC decommissioning requirements will not be applicable to the 4S reactor. However, once the power plant is removed, the demolition of the buildings and infrastructure are assumed to be the responsibility of Galena. This may include a requirement to monitor the remaining buildings and infrastructure for radioactivity prior to release for unrestricted use.

NRC regulations that are most applicable to reactor decommissioning include:

- 10 CFR Part 20, Standards for Protection Against Radiation
- 10 CFR Part 30, Rules of General Applicability to Domestic Licensing of Byproduct Material
- 10 CFR Part 40, Domestic Licensing of Source Material
- 10 CFR Part 50, Domestic Licensing of Production and Utilization Facilities
- 10 CFR Part 51, Environmental Protection Regulations for Domestic Licensing and Related Regulatory Functions
- 10 CFR Part 70, Domestic Licensing of Special Nuclear Material
- 10 CFR Part 72, Licensing Requirements for the Independent Storage of Spent Nuclear Fuel and High-Level Radioactive Waste
- 10 CFR Part 73, Physical Protection of Plants and Materials

Regulatory guides are issued in 10 divisions and are intended to aide licensees in implementing regulations. The guides most applicable to reactor decommissioning are in:

Pre-Publication Draft – Subject to Change

Division 1, Power Reactors (<http://www.nrc.gov/reading-rm/doc-collections/reg-guides/power-reactors/active/>)

Division 4, Environmental and Siting (<http://www.nrc.gov/reading-rm/doc-collections/reg-guides/environmental-siting/active/>). The list of environmental and siting Reg Guides is provided below.

Division 8, Occupational Health (<http://www.nrc.gov/reading-rm/doc-collections/reg-guides/occupational-health/active/>)

Monitoring and Emergency Preparedness: NRC permits will likely involve some routine monitoring as well as some emergency preparedness activities. How involved each of these activities will be is not known at this time.




NRC Regulatory Guides - Environmental and Siting (Division 4)

This page lists the title, date issued, revisions, and some ADAMS accession numbers for each regulatory guide in Division 4, Environmental and Siting.

Table C.1. NRC Regulatory Guides - Environmental Siting (Division 4)

Guide Number	Title	Rev.	Publish Date
4.1	Programs for Monitoring Radioactivity in the Environs of Nuclear Power Plants (Rev. 1, ML003739496)	--	01/1973
		1	04/1975
4.2	Preparation of Environmental Reports for Nuclear Power Stations (Rev. 2, ML003739519)	--	03/1973
		1	01/1975
		2	07/1976
4.2S1	Supplement 1 to Regulatory Guide 4.2, Preparation of Supplemental Environmental Reports for Applications To Renew Nuclear Power Plant Operating Licenses (ML003710495) (Proposed Supplement 1, DG-4002, published 8/91; second Proposed Supplement 1, DG-4005, published 7/98)		09/2000
4.3	(Withdrawn--See 41 FR 53870, 12/199/1976)	--	--
4.4	Reporting Procedure for Mathematical Models Selected To Predict Heated Effluent Dispersion in Natural Water Bodies (ML003739535)	--	05/1974
4.5	Measurements of Radionuclides in the Environment--Sampling and Analysis of Plutonium in Soil (ML003739541)	--	05/1974

Pre-Publication Draft – Subject to Change

4.6	Measurements of Radionuclides in the Environment-- Strontium-89 and Strontium-90 Analyses (ML003739544)	--	05/1974
4.7	General Site Suitability Criteria for Nuclear Power Stations (Revision 2, ML003739894) (DG-4003, Proposed Revision 2, published 11/1992) (DG-4004, Second Proposed Revision 2, published 2/1995)	--	09/1974
		1	11/1975
		2	04/1998
4.8	Environmental Technical Specifications for Nuclear Power Plants (for Comment) (ML003739900)	--	12/1975
4.9	Preparation of Environmental Reports for Commercial Uranium Enrichment Facilities (Rev. 1, ML003739926)	--	12/1974
		1	10/1975
4.10	(Withdrawn--See 42 FR 59436, 11/17/1977)	--	--
4.11	Terrestrial Environmental Studies for Nuclear Power Stations (Rev. 1, ML003739935)	--	07/1976
		1	08/1977
4.12	(Not published)	--	--
4.13			
1	Performance, Testing, and Procedural Specifications for Thermoluminescence Dosimetry: Environmental Applications (Rev. 1, ML003739935)	--	11/1976
		07/1977	
4.14  (1.1M)	Radiological Effluent and Environmental Monitoring at Uranium Mills (Rev. 1, ML003739941)	--	06/1977
		1	04/1980
4.15 	Quality Assurance for Radiological Monitoring Programs (Normal Operations) -- Effluent Streams and the Environment (Rev. 1, ML003739945)	--	12/1977
		1	02/1979
4.16 	Monitoring and Reporting Radioactivity in Releases of Radioactive Materials in Liquid and Gaseous Effluents from Nuclear Fuel Processing and Fabrication Plants and Uranium Hexafluoride Production Plants (Rev. 1, ML003739950) (Draft CE 401-4, Proposed Revision 1, published 9/1984) (Errata published 8/1986)	--	03/1978
		1	12/1985
4.17		--	07/1982

Pre-Publication Draft – Subject to Change

	Standard Format and Content of Site Characterization Plans for High-Level-Waste Geologic Repositories (Rev. 1, ML003739963) (Draft GS 027-4 published 4/1981) (Draft WM 404-4, Proposed Revision 1, published 2/1985)	1	03/1987
4.18	Standard Format and Content of Environmental Reports for Near-Surface Disposal of Radioactive Waste (ML003739515) (Draft WM 013-4 published 4/1982)	--	06/1983
4.19	Guidance for Selecting Sites for Near-Surface Disposal of Low-Level Radioactive Waste (ML003739520) (Draft WM 408-4 published 3/1987)	--	08/1988
4.20	Constraint on Releases of Airborne Radioactive Materials to the Environment for Licensees other than Power Reactors (ML003739525) (Draft DG-8016 published 12/1995)	--	12/1996

A number of other useful guidance documents are available, including:

- Responses to Frequently Asked Questions Concerning Decommissioning of Nuclear Power Reactors (NUREG-1628)
- Standard Review Plan for Evaluating Nuclear Power Reactor License Termination (NUREG-1700)
- Residual Radioactive Contamination From Decommissioning Parameter Analysis (NUREG/CR-5512)
- Standard Review Plan on Power Reactor Licensee Financial Qualifications and Decommissioning Funding Assurance (NUREG-1577)
- Technical Study of Spent Fuel Pool Accident Risk at Decommissioning Nuclear Power Plants (NUREG-1738)
- Multi-Agency Radiation Survey and Site Investigation Manual (MARSSIM) (NUREG-1575)
- NMSS Decommissioning Standard Review Plan (NUREG-1727)
- Report on Waste Burial Charges: Changes in Decommissioning Waste Disposal Costs at Low-Level Waste Burial Facilities (NUREG-1307)
- Decommissioning of Nuclear Power Reactors (Regulatory Guide 1.184)
- Standard Format and Content for Post-Shutdown Decommissioning Activities Report (Regulatory Guide 1.185)
- Fire Protection Program for Nuclear Power Plants During Decommissioning and Permanent Shutdown (Regulatory Guide 1.191)
- Final Generic Environmental Impact Statement on Decommissioning of Nuclear Facilities (NUREG-0586)

APPENDIX D. Economic Analysis Model

This appendix provides sample output from the economic analysis model. The sample output illustrates some of the calculations and provides a sense of how the assumptions are translated into results. Some sections of the model, such as the daily dispatch algorithms, are too voluminous to present here. Others, such as the analysis of transmission lines, have already been presented in the text. Interested readers may obtain the full Microsoft Excel spreadsheet model from the authors.

The sample output is organized as follows:

- Parameters and Assumptions
- Diesel system cost
- Coal system cost
- Nuclear system costs

Table D.1. Parameters and Assumptions for Economic Analyses

Pre-Publication Draft – Subject to Change

Parameters and Assumptions

	units	selected value (yr 1)	low value	high value
Overall Parameters				
Start Year		2010		
Real discount rate	%	4.0%		

Loads and Common Parameters

Utility Electric Load

Initial load at busbar	MWh/yr	11,002		
Annual load growth	% per yr	2.0%		
Peak Load	MW	1.8		

	units	value		
Residential Space Heat				
number of houses, year 2010		220		
annual growth in number of houses		2.0%		
stove oil consumption per house	gallons/yr	1,000		
residential furnace efficiency		75%		
residential fuel price premium (delivery c	\$/gallon	0.75		
Utility line upgrades capital cost	\$	800,000		
customer premises upgrade cost	\$/house	3,000		
electric dist'n loss from busbar to house		10.0%		
District Heat				
Current district heat load	B Btu/yr	8.0		
Cost of bulk distribution pipe	\$/foot	200		
Air station boiler efficiency		80%		
Distance from power plant to air station	miles	2.0		
district heat loss in pipes		10.0%		
Heat load factor (based on HDD data)		0.51		
Heat sales tariff as % of net avoided cost		75%		

Pre-Publication Draft – Subject to Change

Table D.1. Parameters and Assumptions for Economic Analyses - continued

Diesel

	units	selected value (yr 1)	low value	high value
Diesel capital cost (replace engines)	\$/kW	400		
Diesel Fuel				
Utility fuel initial price	\$/gallon	2.15	1.50	2.15
Annual real escalation	% per yr	2.0%	0.0%	2.0%
Utility initial fuel efficiency kWh measured at busbar	kWh/gal	14		
Efficiency of New Units	kWh/gal	15		
Nonfuel diesel O&M				
Diesel generation labor	\$/year	305,157		
Variable O&M (includes overhauls)	\$/kWh	0.017		

Coal

	units	selected value (yr 1)	low value	high value
Coal plant capital cost	\$/kW	3,000		
Coal plant availability		95%		
Coal plant efficiency (electric output/coal input)		40%	30%	40%
Coal or nuclear "heat to electric" efficiency		50%		
Coal fuel				
Energy content	M Btu/ton	20		
Delivered price of coal	\$/ton	100	100	125
Ash disposal cost	\$/ton	20		
Nonfuel coal O&M				
Coal labor	people	6		
cost per operator	\$/yr	53,200		
variable O&M and consumables	\$/kWh	0.01		

Nuclear

	units	selected value (yr 1)	low value	high value
Nuclear capacity	MW	10.0		
Nuclear capital cost	\$	0		
Nuclear security staff	people	34	4	34
Nuclear operator staff	people	8		
Nuclear availability		95%		
Nuclear annual supplies and expenses	\$/yr	500,000		

Pre-Publication Draft – Subject to Change

Table D.2. Diesel-Only Power Supply Economic Analysis

Diesel-Only Power Supply Economic Analysis					
				Year	
				1	30
Variable		Units	Present Value	2010	2039
Busbar Energy Requirements		MW h		11,002	19,539
Peak Demand		MW		1.8	3.2
Diesel Fuel Use by Unit					
	kWh/gal				
1	15.0 New	gal		733,497	1,302,576
2	15.0 New	gal			
3	14.0	gal			
4	14.0	gal			
5	14.0	gal			
6	14.0	gal			
Total Diesel Fuel Used		gal		733,497	1,302,576
Diesel Fuel Price		\$/gal		2.15	3.82
Total Diesel Fuel Cost		\$	\$45,745,507	1,577,018	4,973,321
Labor			\$5,276,785	305,157	305,157
Other Diesel System Variable Costs					
Major Overhauls ** included in O&M					
O&M (includes overhauls)		\$	\$4,129,163	187,042	332,157
Total nonfuel variable cost		\$	\$4,129,163	187,042	332,157
Diesel Avoidable Capacity Cost		\$	\$4,147,366	711,886	
amortized				239,843	239,843
Total Cost of Busbar Diesel Electricity		\$	\$59,298,821	2,309,059	5,850,478
Rate Impacts				2010	2039
Total sales		MW h		9,902	17,585
avoidable busbar cost		\$/kW h		0.23	0.33
distribution, general, and admin		\$/kW h		0.07	0.06
Average cost of electric service		\$/kW h		0.30	0.39

Pre-Publication Draft – Subject to Change

Table D.3. Coal Power Supply Economic Analysis

Coal						
Power Supply Economic Analysis						
				Year		
				1	30	
Variable		Units	in- clude?	Present Value	2010	2039
Busbar Energy Requirements						
Utility electricity		MW h	1		11,002	19,539
Existing city heating loop		MW h	1		2,344	2,344
Residential heating		MW h	0		-	-
Air station heating		MW h-equiv	1		8,464	8,464
Greenhouse		MW h	0		-	-
Total Energy Requirements at power plant		MW h			21,811	30,347
Total Energy Output Capacity (electric equ		MW			4.0	4.0
Availability		%			95%	95%
Energy from Coal and from diesel						
firm energy from coal		MW h			12,679	20,788
firm energy from diesel		MW h			667	1,094
non-firm energy for Air Station		MW h-equivalent			8,040	5,816
Total Energy generated by coal		MW h-equivalent			20,719	26,605
Coal Fuel						
Coal requirements		tons			8,839	11,350
Cost per ton		\$/ton			100	100
Total coal fuel cost		\$		17,035,458	883,920	1,135,027
Coal Capital				12,000,000	693,961	693,961
Coal labor				5,519,617	319,200	319,200
Diesel peaking and backup variable cost (from below)				2,614,234	96,746	267,259
Other coal system variable costs						
consumables and variable O&M				3,993,075	207,189	266,048
Ash disposal @ \$20/ton				3,407,092	176,784	227,005
Total nonfuel variable cost				7,400,167	383,973	493,053
Total busbar cost of coal system				40,576,400	2,170,610	2,642,453
less: net value of heat sent to air station				(17,483,703)	(839,746)	(1,113,613)
equals: net busbar cost of coal system				23,092,697	3,010,357	3,756,066

Pre-Publication Draft – Subject to Change

Table D.3. Coal Power Supply Economic Analysis – continued

Avoided cost from heat used by Air Station				
Air station end-use heat demand	B Btu		52.0	52.0
Coal heat energy delivered to station	B Btu		49.4	35.7
avoided diesel fuel	gallons		447,388	323,659
avoided diesel price	\$/gallon		2.15	3.82
avoided diesel cost	\$	19,595,703	961,884	1,235,750
less: capital cost of pipe upgrade		(2,112,000)	(122,137)	(122,137)
equals: Net value (fuel savings only) of heat		17,483,703	839,746	1,113,613
Net value per M Btu delivered at plant	\$/M Btu		15.30	28.05
Rate Impacts				
			2010	2039
Total cost of coal system			2,170,610	2,642,453
prospective tariff for heat (metered at plant)	\$/M Btu		11.48	21.04
amount of heat sold (metered at plant)	B Btu		54.9	39.7
sales revenue from base heat sales	\$	13,112,777	629,810	835,210
net cost of generation			1,540,801	1,807,243
distribution, general, and admin			710,728	1,054,748
Utility revenue requirement from rates			2,251,529	2,861,991
utility non-heat electricity sales	MWh		9,902	17,585
Electric heat sales to homes	MWh		0	0
Average cost of electric service	\$/kWh		0.23	0.16
avoidable busbar cost	\$/kWh		0.16	0.10
distribution, general, and admin	\$/kWh		0.07	0.06

Pre-Publication Draft – Subject to Change

Table D.4. Nuclear Power Supply Economic Analysis

Nuclear					
Power Supply Economic Analysis					
				Year	
				1	30
			Present		
	Variable	Units	Value	2010	2039
Busbar energy requirements		MW h		11,002	19,539
Peak demand		MW		1.8	3.2
Power output		MW		10.0	10.0
Availability		%		95%	95%
Available energy output		MW h		83,220	83,220
	Firm energy requirements	MW h		21,330	35,617
	Firm energy supplied	MW h		20,263	33,836
	to utility electricity	MW h		10,452	18,562
	to district heat	MW h		2,227	2,227
	to home space heating	MW h		7,042	12,506
	to greenhouse	MW h		542	542
	Surplus energy available for H2 production	MW h		62,957	49,384
Diesel energy to cover unavailability		MW h		1,066	1,781
Nuclear capital paid by utility			0	0	0
	Nuclear decommissioning		[not considered in this model]		
Labor					
	plant operators	persons		8	8
	cost per operator	\$/yr		82,460	82,460
	Operator Labor			659,680	659,680
	security staff	persons		34	34
	cost per security staff	\$/yr		53,200	53,200
	Security Labor			1,808,800	1,808,800
Total nuclear labor			42,685,038	2,468,480	2,468,480
Nuclear annual O&M			8,646,017	500,000	500,000
Diesel backup variable cost (from below)			4,984,179	181,911	515,947
Total busbar cost of nuclear energy production			56,315,234	3,150,391	3,484,427
less:	Avoided cost from using residential electric heat (below)		(15,903,166)	(553,568)	(1,700,247)
less:	Avoided cost of heat for air base, at power plant		(20,243,434)	(890,513)	(1,676,172)
equals: Net busbar cost of electric service			20,168,634	1,706,310	108,008
	Surplus energy for hydrogen production	MW h		62,957	49,384

Pre-Publication Draft – Subject to Change

Table D.4. Nuclear Power Supply Economic Analysis – continued

Savings from sales of heat to air base					
	Air station end-use heat demand	B Btu		52.0	52.0
	less: unserved energy at peak times	B Btu		0.0	0.0
	equals: heat energy delivered to base	B Btu		52.0	52.0
	avoided diesel fuel	gallons		471,000	471,000
	avoided diesel price	\$/gallon		2.15	3.82
	avoided diesel cost	\$	22,355,434	1,012,650	1,798,309
less:	capital cost of pipe upgrade	\$	(2,112,000)	(122,137)	(122,137)
	Net value (fuel savings only) of heat at power plant		20,243,434	890,513	1,676,172
	Net value per M Btu of heat at power plant			15.41	29.01
Rate Impacts					
	Total cost of nuclear system		56,315,234	3,150,391	3,484,427
	prospective tariff for heat (metered at plant)	\$/M Btu		11.56	21.76
	amount of heat sold (metered at plant)	B Btu		57.8	57.8
	sales revenue from air station heat sales	\$	15,182,576	667,885	1,257,129
	net cost of generation		41,132,659	2,482,507	2,227,298
	distribution, general, and admin		14,299,453	710,395	1,037,214
	Utility revenue requirement from rates		55,432,111	3,192,901	3,264,511
	non-heat electricity sales	MW h		9,895	17,193
	Electric heat sales to homes	MW h		6,338	11,255
	Average cost of electric service	\$/kW h		0.20	0.11
	Check savings to homes:				
	per household cost of diesel			2,900	4,568
	per household cost of electric heat			5,667	3,306
Required Diesel generation					
		MW h		1,066	1,781
Diesel Fuel Use by Unit					
	kW h/gal				
1	14.0 Unit 1	gal		76,177	127,204
2	14.0 Unit 2	gal			
3	14.0 Unit 3	gal			
4	14.0 Unit 4	gal			
5	14.0 Unit 5	gal			
6	14.0 Unit 6	gal			
	Total Diesel Fuel Used	gal		76,177	127,204
	Diesel Fuel Price	\$/gal		2.15	3.82
	Total Diesel Fuel Cost	\$	\$4,595,785	163,781	485,672
Other Diesel System Variable Costs					
	Major Overhauls				
	Other Energy-related O&M	\$	\$388,394	18,130	30,274
	Total Nonfuel Variable Cost	\$	\$388,394	18,130	30,274
	Diesel Avoidable Capacity Cost	\$	\$0		
	Total Identifiable Cost of [backup] Diesel	\$	4,984,179	181,911	515,947

**Development and Assessment of Options for
Potential CO₂ Sequestration in Alaska**

Final Report

Reporting Period:

August 1, 2004–December 31, 2006

Prepared by:

**Shirish Patil, Principal Investigator
Abhijit Dandekar, Co-Principal Investigator**

September 2007

**DOE Award No.:
DE-FC26-01NT41248**

**Petroleum Development Laboratory
Arctic Energy Technology Development Laboratory
Institute of Northern Engineering
University of Alaska Fairbanks
425 Duckering Building
P.O. Box 755880
Fairbanks, AK 99775-5880**

Disclaimer

This report was prepared as an account of work sponsored by an agency of the United States Government. Neither the United States Government nor any agency thereof, nor any of their employees, makes any warranty, express or implied, or assumes any legal liability or responsibility for the accuracy, completeness, or usefulness of any information, apparatus, product, or process disclosed, or represents that its use would not infringe privately owned rights. Reference herein to any specific commercial product, process, or service by trade name, trademark, manufacturer, or otherwise does not necessarily constitute or imply its endorsement, recommendation, or favoring by the United States Government or any agency thereof. The views and opinions of authors expressed herein do not necessarily state or reflect those of the United States Government or any agency thereof.

Abstract

Carbon dioxide (CO₂), the main component of greenhouse gases, is released into the atmosphere primarily by combustion of fossil fuels like coal and oil. Some areas of the oil industry could employ CO₂ sequestration, the capture of CO₂ for storage or other uses, as a way to mitigate CO₂ release and simultaneously improve extraction methods for some oil fields. Very little study of CO₂ sequestration has addressed the Alaskan North Slope (ANS) area, although such study could open new avenues for CO₂ disposal options, such as in viscous oil reservoirs and coal seams on the ANS, particularly if a natural gas pipeline presently under consideration is constructed. This study investigated CO₂ storage options by screening ANS oil pools amenable to enhanced oil recovery (EOR), by evaluating the phase behavior of viscous oil and CO₂ mixtures, and by simulating EOR through CO₂ flooding and migration of CO₂ in a saline aquifer.

Phase-behavior studies revealed that CO₂ gas was partially miscible with West Sak viscous oil at a pressure close to the reservoir pressure. Compositional simulation of CO₂ flooding for a five-spot West Sak reservoir pattern showed an increase in percent recovery with an increase in pore volume (PV) injected, but at the expense of an early breakthrough. A sensitivity analysis of this CO₂ flooding project was found to be strongly dependent on such variables as oil price and discount rate. Investigation of supercritical CO₂ injection in a saline formation did not indicate an increase in temperature in this permafrost-heavy region.

Table of Contents

	<u>Page</u>
Title Page	i
Disclaimer	ii
Abstract	iii
Table of Contents	iv
List of Figures	vi
List of Tables	ix
Chapter 1 – Introduction	1
1.1 Overview	1
1.2 Objectives	5
Executive Summary	7
Chapter 2 – Characterization of CO ₂ Sinks and Sources	9
2.1 Alaskan North Slope Oil Pools: Methodology of Parametric Screening	10
2.2 Ranking of ANS Oil Pools Based on Screening Criteria	14
2.3 Characterization Using the GIS and Shortest-Path Analysis Model	16
2.3.1 Input for Shortest-Distance Model	16
Chapter 3 – Phase Behavior Study of West Sak Oil and CO ₂ System	20
3.1 Description of EOS	20
3.2 Characterization of West Sak Oil and Phase Behavior with CO ₂	22
3.3 Phase Behavior of West Sak Oil with CO ₂	24
Chapter 4 – CO ₂ -EOR Study	29
4.1 Description of West Sak Reservoir	29
4.2 Theory, Field, and Simulation Review	30
4.3 Simulation of CO ₂ Injection for Enhanced West Sak Oil Recovery	39
4.3.1 Grid System and Petrophysical Properties	39

	<u>Page</u>
4.3.2 Relative Permeability Data	42
4.4 Simulation Results for Enhanced Viscous Oil Recovery by CO ₂	48
Chapter 5 – Economic Analysis of CO ₂ -EOR	58
5.1 Review of Economic Analysis Study	58
5.2 Method for Economic Feasibility of CO ₂ Sequestration with EOR	63
5.3 Economic Benefits and Incremental NPV of CO ₂ -EOR	66
Chapter 6 – CO ₂ Sequestration in a Saline Aquifer	71
6.1 CO ₂ Sequestration in a Saline Aquifer using STOMP [®] -WCSE	74
6.2 Effect of CO ₂ Storage on a Saline Aquifer	76
Chapter 7 – Conclusions and Recommendations	81
7.1 Conclusions	81
7.2 Recommendations	81
Acknowledgment	83
References	84
Appendix A	90

List of Figures

	<u>Page</u>
Figure 1.1. Carbon dioxide sources with and without major gas sales along with oil pools on the Alaska North Slope. Figure courtesy of British Petroleum.	2
Figure 1.2. A typical CO ₂ sequestration scheme (after Research Institute of Innovative Technology for the Earth, 2004).	4
Figure 2.1. Location of sedimentary basins and their thickness on the Alaska North Slope.	17
Figure 2.2. Location of coal resource and available road infrastructure on the Alaska North Slope for development of CO ₂ sequestration project.	18
Figure 2.3. A typical shortest distance scheme in ArcGIS.	19
Figure 2.4. Shortest path analysis for CO ₂ sink and source system on the Alaska North Slope.	19
Figure 3.1. Percentage liquid volume before and after regression.	25
Figure 3.2. Relative oil volume before and after regression.	26
Figure 3.3. (a–d) Pseudo-ternary diagrams for West Sak crude + CO ₂ system.	27
Figure 4.1. Three-dimensional view of the grid system.	41
Figure 4.2. Five-spot CO ₂ injection pattern.	41
Figure 4.3. Water-oil relative permeability of West Sak upper sand #1 (modified after Bakshi, 1991).	43
Figure 4.4. Water-oil relative permeability of West Sak upper sand #2 (modified after Bakshi, 1991).	44
Figure 4.5. Water-oil relative permeability of West Sak lower sands (modified after Bakshi, 1991).	45

	<u>Page</u>
Figure 4.6. Gas-oil relative permeability of West Sak upper sand #1 (modified after Bakshi, 1991).	46
Figure 4.7. Gas-oil relative permeability of West Sak upper sand #2 (modified after Bakshi, 1991).	47
Figure 4.8. Gas-oil relative permeability of West Sak lower sand #2 (modified after Bakshi, 1991).	48
Figure 4.9. Changes in oil and CO ₂ rate for 10% pore volume.	51
Figure 4.10. Changes in oil and CO ₂ rate for 20% pore volume.	52
Figure 4.11. Changes in oil and CO ₂ rate for 30% pore volume.	53
Figure 4.12. Changes in oil and CO ₂ rate for 50% pore volume.	54
Figure 4.13. Percent oil recovery versus injected pore volume.	55
Figure 4.14. (a–d) Oil saturation profile for 10% pore volume injection.	56
Figure 5.1. Probability distribution of capital cost of CO ₂ storage project (modified after Allinson & Nguyen, 2002).	59
Figure 5.2. Net present value (NPV) with and without CO ₂ credits.	67
Figure 5.3. Sensitivity chart of input variables affecting net present value (NPV).	68
Figure 5.4. Probability distribution of net present value.	69
Figure 5.5. Net present value of the CO ₂ -EOR project for increasing oil prices with changing discount rate.	70
Figure 6.1. Two-dimensional cylindrical model used in Subsurface Transport Over Multiple Phases [®] -Water-CO ₂ -NaCl-Energy (STOMP [®] -WCSE).	76
Figure 6.2. Gas saturation at a horizontal distance of 280 ft from an injection well.	78
Figure 6.3. CO ₂ aqueous fraction at a horizontal distance of 280 ft from an injection well.	79

Figure 6.4. Temperature profile at a horizontal distance of 280 ft from an injection well.

List of Tables

	<u>Page</u>
Table 2.1. Optimum reservoir parameters with respective weights (modified after Rivas, Embid, & Bollvar, 1992).	13
Table 2.2. Worst parameters from the Alaska North Slope oil pool database.	13
Table 2.3. Parametric ranking of oil pools on the Alaska North Slope with respect to optimum reservoir parameters.	15
Table 3.1. West Sak oil composition (after Bhandari, 1988).	23
Table 4.1. Average layer properties of West Sak for 40-acre injection pattern (after Bakshi, Ogbe, Kamath, & Hatzignatiou, 1992).	40
Table 4.2. Percentage recovery and CO ₂ storage ratio at different pore volumes (PV).	50
Table 5.1. Overview of carbon capture and storage project costs and cost drivers (modified after Senior, Adams, Espie, & Wright, 2004).	61
Table 5.2. Assumed values of parameters for net present value (NPV) calculation.	65
Table 5.3. Assumed distribution and parameter values of variables for sensitivity analysis.	66
Table 6.1. CO ₂ and water properties at 45 °C (modified after Oostrom, Meck, & White, 2003).	72

Chapter 1

Introduction

1.1 Overview

Carbon dioxide is predominantly released into the atmosphere by burning fossil fuels. According to the Energy Information Administration (2005), in 2004 the United States' estimated emissions of greenhouse gases totaled 7,122 MMTCO₂e (million metric tons CO₂ equivalent); of this amount, the majority—5973 MMT—was CO₂.

In 2001, Alaska alone emitted around 43.20 MMTCO₂e from sundry sources such as transportation, industry, municipal electric power generation, and commercial and residential activities (EIA, 2001). Currently, the bulk of the natural gas produced during drilling for fossil fuels on the ANS is re-injected into the reservoir. This process helps maintain pressure in the reservoir, enhancing oil extraction, and it serves as a way to store the natural gas. In the future, when appropriate infrastructure has been built, the gas can be re-extracted and transported to market. At this point, if all the natural gas produced were sold to a ready market (in the literature, this is often termed *after major gas sales*), approximately 8 million tons of CO₂ would be released into the atmosphere (see Figure1.1, courtesy of British Petroleum).

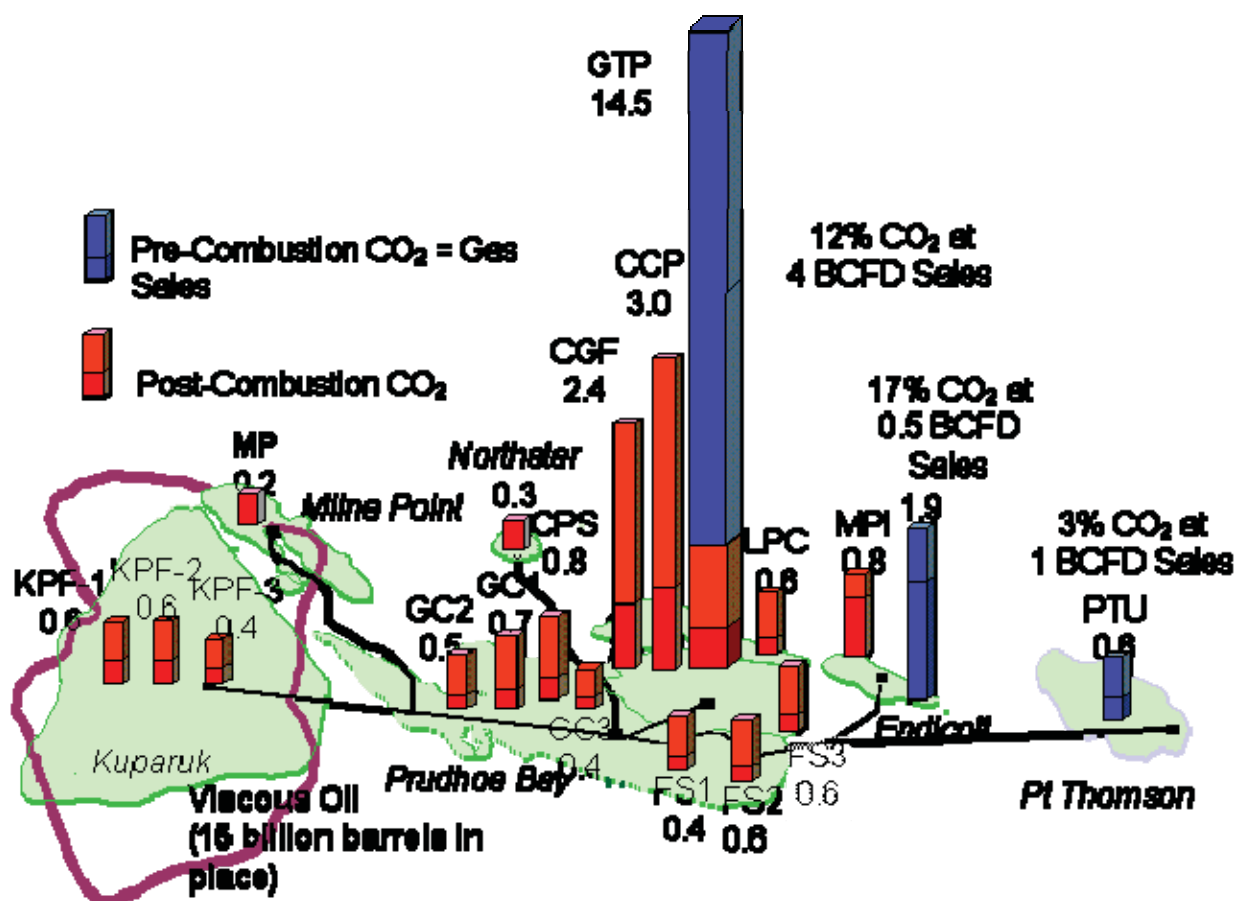


Figure 1.1. Carbon dioxide sources with and without major gas sales along with oil pools on the Alaska North Slope. Figure courtesy of BP.

The impact of global warming on the arctic environment is widely discussed both in scientific and public literature. Key interactions between global warming and the arctic environment can be summarized as follows:

- Released CO₂ can result in more heat trapped in the atmosphere, which may increase average winter temperatures.

- Higher average temperatures can cause reduction in the extent of the Arctic Ocean's summer ice pack.
- Either of the above-mentioned changes could further accelerate warming.
- Changes in temperature could substantially reduce the winter drilling window on the ANS, thus threatening oil and gas developmental drilling and related activities.

CO₂ storage in geological formations is an important sequestration option in decreasing or limiting concentration of CO₂ in the environment. Other synergies such as recovery of viscous oil by CO₂ flooding could also be very attractive and economical. Bachu and Shaw (2003) defined geological sequestration of CO₂ as capturing CO₂ from anthropogenic sources and disposing of it in geological media. A typical CO₂ sequestration project includes (a) CO₂ capture from point sources like power plants and natural gas production and sales, using chemical techniques such as amine absorption; (b) gas compression; (c) transportation through a corrosion-resistant pipeline or tanker; and (d) storage in potential geological sinks. Figure 1.2 represents a typical CO₂ sequestration scheme.

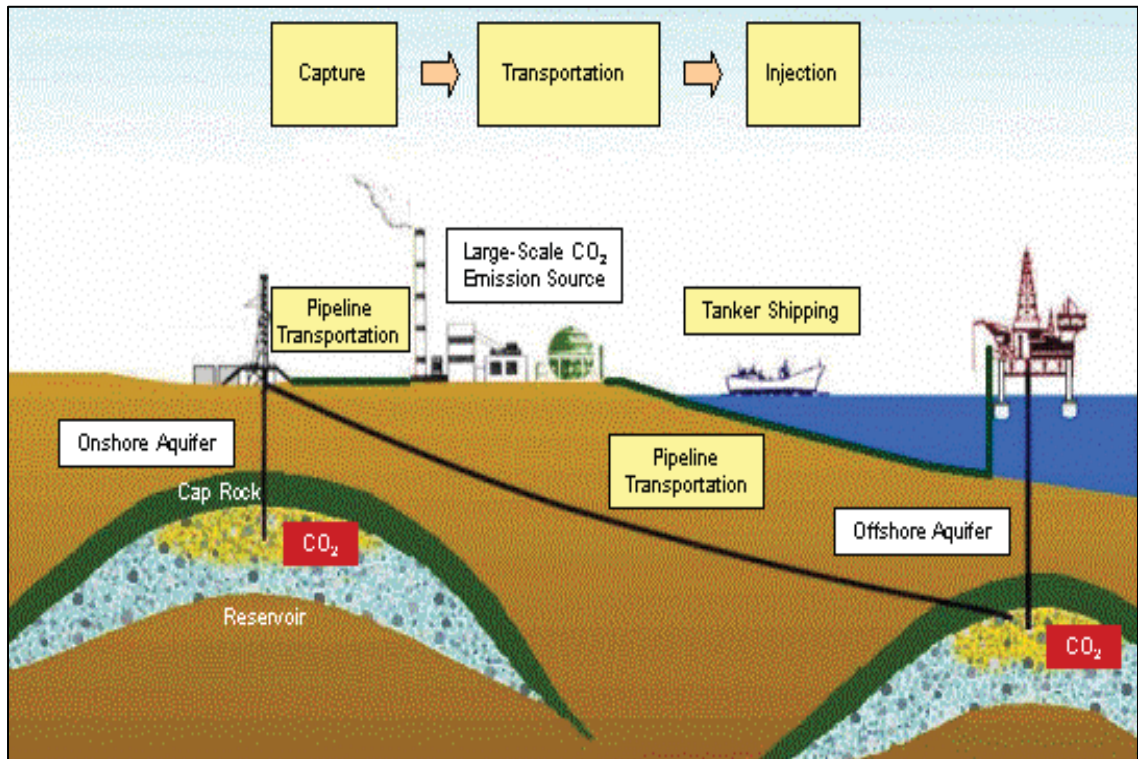


Figure 1.2. A typical CO₂ sequestration scheme (after Research Institute of Innovative Technology for the Earth, 2004).

In addition to sequestering CO₂ for EOR, CO₂ can also be sequestered in (a) depleted oil and gas reservoirs, (b) deep coal beds through replacing methane with CO₂, and (c) deep saline aquifers (Bachu & Stewart, 2002). There are three important mechanisms by which CO₂ is geologically sequestered: hydrodynamic trapping, solubility trapping, and mineral trapping (Kovscek, 2002).

With a ready collection system, CO₂ can be injected in the ANS to produce viscous oil (immiscible/miscible displacement) and coal bed methane, leading to increased oil and gas production, respectively, and helping producers meet energy demands by taking advantage of existing production infrastructure on the ANS. For example, West Sak and

Ugnu sands are amenable to CO₂ flooding due to the viscous nature of the oil there. Carbon dioxide sequestration in this area could reduce oil viscosity, enhance oil swelling, and in some cases, support immiscible or miscible displacement. These methods for enhancing oil recovery can start after a secondary recovery process or at any time during the productive life of an oil reservoir to improve fluid displacement. In this report, the term *EOR* is used in conjunction with “improved viscous oil recovery by CO₂ injection.”

A gas pipeline is essential to establishing a ready source of CO₂ on the ANS. If Alaska’s existing production and transportation infrastructure can economically and feasibly support the operations necessary for building a new gas pipeline, then the ANS will be a highly suitable site for CO₂ geological storage. Moreover, successful sequestration on the ANS will require advances in drilling technology; well bores must be engineered to avoid communication between injected CO₂ and producer wells. Successful CO₂ sequestration on the ANS could provide value-added oil production, an essential element of Alaska’s continued economic growth. Additionally:

- EOR by CO₂ injection can support control of greenhouse gas emissions in conjunction with fossil fuel production; and
- CO₂ sequestration projects can provide a key to unlocking ANS viscous oil reserves as well as furthering development of such options such as saline aquifers and using depleted oil and gas reservoirs.

1.2 Objectives

The objectives of this study were to investigate different sequestration options and their specific feasibility for the Alaska North Slope. Objectives were:

- (1) To characterize oil pools amenable to CO₂-EOR by using a screening technique and the Geographic Information System (GIS).
- (2) To perform a phase-behavior study of viscous oil and CO₂.

- (3) To predict viscous oil production levels made possible by CO₂ injection,
- (4) To calculate the time value of the CO₂-EOR project.
- (5) To simulate injection of supercritical CO₂ into a saline aquifer.

The University of Alaska Fairbanks strongly encourages its students to take an active role in research projects, and subsequent chapters in this report are the result of work by a graduate student (Patil, 2006) in the Petroleum Department, College of Engineering and Mines.

Executive Summary

Signs of global warming tend to be more pronounced in the Arctic than in any other place in the world, and the ANS is no exception. The past few decades have shown changes in winter freeze-up and spring break-up, and impacts include a narrower window for transporting goods and equipment across the tundra, which can directly affect ANS infrastructure and operations for the commercial oil fields. If the gas pipeline currently under discussion is built, CO₂ mitigation will become a much larger concern for oil field operations. Some sources suggest that the ANS could produce around 22 million tons of CO₂ per annum from power plant operation and gas sales. Some options for CO₂ sequestration, such as recovering vast viscous oil reserves (> 25 billion barrels) by CO₂-EOR and geological storage, could be crucial to the ongoing economic success of ANS-based projects.

This study focused on characterization of CO₂ point sources and sinks, a simulation study for EOR of viscous oil and CO₂ storage in a saline aquifer, and an economic analysis of CO₂-EOR. Our approach used a parametric screening technique to examine reservoir parameters such as porosity, permeability, depth, and temperature of the ANS oil pools, comparing these properties to both worst and optimum parameters. The West Sak pool, with oil of 12–20°API gravity, is located in the Kuparuk oil field on the ANS. Using Computer Modeling Group's WinProp[®] simulator, researchers performed regression analysis of pressure, volume, and temperature (PVT) data of West Sak oil to tune an equation of state (EOS). Using a tuned EOS, pseudo-ternary diagrams showed that, at the current West Sak reservoir pressure, partial miscibility is a possible mechanism for recovery. Then researchers carried out compositional simulation of CO₂ flooding using a GEM[®] simulator. To explore the injection of CO₂ into a saline aquifer, a superheated CO₂ injection into a 4-layer model (sand-shale-sand-permafrost) system (NaCl salt fraction = 0.05) for a 10-year period was simulated using Subsurface Transport Over Multiple Phases (STOMP[®]).

In summary, performing a technical feasibility study of CO₂-EOR by parametric screening of the oil pools is essential for ranking those pools amenable to EOR. A phase-behavior study of a West Sak crude and CO₂ system predicted the presence of partial miscibility at a pressure of around 1600 psia. Composition simulation work predicted an increase in the percent of West Sak oil recovery as the amount of injected CO₂ is increased (for 10%–50% PV injection), but at the expense of early gas breakthrough. Sequestration of CO₂ in saline aquifers on the ANS can provide additional storage. CO₂ is sequestered in both gas and aqueous phases when injected in a saline aquifer. Simulation via the STOMP[®] simulator showed that injecting the CO₂ in the bottommost layer of sand is advantageous, since the overlying shale layer can act as a barrier to prevent any future gas leakage. Moreover, this model indicated no temperature increase in the permafrost region.

Chapter 2

Characterization of the CO₂ Sinks and Sources

The design of any EOR project involves such steps as data gathering, economic and technical feasibility studies, and reservoir simulation and sensitivity analysis, followed by pilot project studies. The simulation study by Bossie-Cordreanu and Gallo (2004), based on a synthetic reservoir, quantified uncertainties due to reservoir parameters in order to establish a set of guidelines to determine the most suitable depleted reservoirs for sequestration. In their work, Bossie-Cordreanu and Gallo studied influencing parameters such as API gravity, heterogeneity (Dykstra-Parson coefficient), and cap rock integrity. Sequestration capacity was estimated through the sequestration factor for different reservoirs.

According to Klins (1984), the major task of screening potential reservoirs for EOR is accomplished by binary evaluation and project evaluation criteria. In the case of binary evaluation criteria, Klins carried out a comparison of important parameters with observed parameters of technically and economically successful EOR projects. The limited number of projects and publicly available data, however, hinders the use of screening as the sole criterion. Nevertheless, thanks to its less cumbersome application, binary evaluation is a popular preliminary screening tool.

Rivas, Embid, and Bollvar (1992) developed a new screening tool to account for synergistic effects on process performance, which the binary evaluation criterion fails to do. The study examined reservoir parameters such as porosity, permeability, temperature, API gravity, oil saturation, and net pay thickness. The optimum parameters—those leading to the best average production rate—were obtained from simulation studies by using fully compositional, black-oil, and semi-analytical models. An arbitrary heuristic, exponentially varying function was employed to rank different reservoirs. The value of that function depended on the difference between the properties characteristic of the reservoir and the

optimum values of the simulation studies. This screening technique was successfully used by Shaw and Bachu (2002) to rank the oil reservoirs in the Western Canada Sedimentary Basin. The optimum properties for the CO₂ injection project were found to be an API gravity of 37°, a temperature of 160 °F, permeability of 300 md, oil saturation of 60%, and porosity of 20%.

There are an estimated 20 to 25 billion barrels of original-oil-in-place (OOIP) medium and heavy oil deposits on the ANS (McGuire, Redman, Jhaveri, Yancey, & Ning, 2005). Figure 1.1 shows the oil reservoirs on the ANS, along with CO₂ sources such as potential gas sales and other emissions. In the current study, screening of oil reservoirs on the ANS for their CO₂-EOR potential was based on the work of Rivas et al. (1992).

2.1 Alaskan North Slope Oil Pools: Methodology of Parametric Screening

Oil reservoir ranking with respect to CO₂-EOR potential and technical feasibility was performed by comparing parameters such as oil gravity (°API), porosity (Φ), permeability (k), temperature (T), pay zone thickness (h), oil saturation (S_o), and minimum miscibility pressure (MMP) with the optimum reservoir parameters (see Table 3.1, Chapter 3). All the parameters except MMP were obtained from the oil pool database of the Alaska Oil and Gas Conservation Commission (2003). The step-by-step procedure for ranking is detailed below:

(a) MMP Estimation

The calculations of MMP for oil and a pure CO₂ system rely on the proper characterization of oil, particularly the C₅₊ component. To circumvent the tedious and time-consuming nature of collecting oil composition for each oil pool on the ANS, this study used a simpler method first reported by the National Petroleum Council (Ahmed, 1997) to predict MMP based on API gravity and temperature of the system. Using this method for API gravity less than 27°, MMP is 4000 psia; as the API gravity increases, MMP is found to decrease

with a reservoir temperature correction. A description of this method can be obtained from Ahmed (1997).

(b) Parameter Normalization

The normalized parameter ($X_{i,j}$) is given by:

$$X_{i,j} = \frac{|P_{i,j} - P_{o,j}|}{|P_{w,j} - P_{o,j}|} \quad (2.1)$$

Where $P_{o,j}$ is the magnitude of parameter (j) in an optimum reservoir, which results in optimum CO₂ flooding; these optimum parameters were obtained from the studies by Rivas et al. (1992). The optimum properties for the most favorable reservoir were determined by performing a numerical simulation, which optimized the reservoir response to gas flooding. $P_{w,j}$ is the magnitude of the parameter for a reservoir least favorable to CO₂-EOR, which was determined based on the data bank of reservoirs to be screened. For each reservoir parameter, the value farthest from the optimum value was then selected as the worst value of that parameter. $P_{i,j}$ is a parameter under consideration for the i^{th} reservoir.

(c) Transformation to Exponential Function

Since exponential function is more adequate than linear function for comparing different elements in the same set, $X_{i,j}$ was transformed into an exponentially varying function ($A_{i,j}$) as given below:

$$A_{i,j} = 100 \times e^{(4.6X_{i,j}^2)} \quad (2.2)$$

(d) Generation of Weighted Grading Matrix

To account for the relative importance of each reservoir parameter, a weighted grading matrix, W_{ij} was determined as follows:

$$W_{ij} = A_{ij} \times w_j \quad (2.3)$$

Where w_j is the weight of each reservoir parameter. Table 2.1 gives optimum values with respective weights assigned to each parameter, while worst values for each parameter for oil pools on the ANS are given in Table 2.2.

(e) Rank of Reservoir (R_i)

Ranking of the reservoir is given as:

$$R_i = 100 \times \frac{\sum_{j=1}^j M_{i,j}}{\sum_{j=1}^j M_{1,j}} \quad (2.4)$$

Where M_{ij} is the product of W_{ij} and its transpose, $W_{j,i}$. $M_{1,j}$ represents the values corresponding to the optimum reservoir.

Table 2.1

Optimum Reservoir Parameters with Respective Weights (modified after Rivas, Embid, & Bollvar, 1992)

Parameter	Optimum	Weight
API Gravity	37	0.24
Oil saturation, %	60	0.2
Pressure/ MMP	1.3	0.19
Temperature, °F	160	0.14
Net thickness, ft	50	0.11
Permeability, md	300	0.07
Porosity, %	20	0.02

Table 2.2

Worst Parameters from Alaska North Slope Oil Pool Database

Parameter	Upper Limit	Lower Limit
API Gravity	44	17.5
Oil saturation, %	90	50
Pressure/ MMP	4.11	0.4
Temperature, °F	254	75
Net thickness, ft	290	20
Permeability, md	1007.5	1.5
Porosity, %	30	10

2.2 Ranking of ANS Oil Pools Based on Screening Criteria

Parametric screening of ANS oil pools, which is based on the optimum parameters and assigned weights to each parameter, is an advantageous approach to selecting potential pools for CO₂-EOR. The values of gravity for various oils from the ANS oil database generally delineate the suitability of an oil pool for CO₂-EOR. Table 2.3 lists the petrophysical properties of a few ANS oil pools, while the last column gives the rank of oil pools, according to the study by Rivas et al. (1992). Table 2.3 shows the screening of 14 ANS oil pools (14 = least suitable for CO₂-EOR; 1 = most suitable). It is evident that oil pools with lower gravity (viscous oil) have been placed lower in the ranks, while this is not entirely true for the light oil (oil with higher API gravity). Ivishak pool would be the last chosen for CO₂-EOR if such a selection of ANS oil pools were performed. Thus, Ivishak is a good example of how parameters other than oil gravity play a role in screening; in this case, its low porosity (15%) has hampered its suitability. The abundant West Sak pool, despite its rank of 11, has been selected for future phase behavior and simulation studies for CO₂ flooding because conventional EOR processes like waterflooding are cost-prohibitive.

Table 2.3

Parametric Ranking of Oil Pools on the Alaska North Slope with Respect to Optimum Reservoir Parameters

Pool	°API	Φ, %	P/ MMP	T, °F	h, ft	k, md	S _o , %	R _i
Pt. McIntyre	27	22	1.27	180	156	200	60	1
Meltwater	36	20	1.5	140	95	10	60	2
Lisburne	27	10	1.03	183	125	1.5	70	3
Tarn	37	20	1.64	142	40	9	60	4
Prudhoe	28	22	0.94	200	222	265	70	5
Alpine	40	19	1.81	160	48	15	80	6
Kuparuk -Milne	24	20	0.79	160	100	150	90	7
Kuparuk River	22	23	0.76	165	35	40	70	8
Sag River	37	18	1.86	234	30	4	60	9
North Prudhoe	35	20	2.07	206	20	590	60	10
West Sak	19	30	0.41	75	70	1007	70	11
Schrader Bluff	17.5	28	0.4	80	70	505	70	12
Hemlock	33.1	10.5	2.34	180	290	53	70	13
Ivishak	44	15	4.11	254	125	200	50	14

Note. All parameter values but MMP were obtained from the oil pool database of the Alaska Oil and Gas Conservation Commission (2003). For MMP calculation, see Section 2.1 (a) above.

2.3 Characterization Using the GIS Shortest-Path Analysis Model

Figures 2.1 and 2.2 present GIS maps depicting, respectively, sedimentary basins along with oil and gas pools, and coal beds, along with available road infrastructure, on the ANS.

A determination of the least-cost path is crucial to minimizing the costs of CO₂ transportation, given constant compression and injection costs. The “shortest path” travels from the destination to the CO₂ source via the cheapest route (depending on the cost raster defined by the user). The shortest-path analysis can be employed to locate the least-cost paths for any CO₂ sink and source pair. Section 2.3.1 gives the input data that were used in the shortest-distance model in ArcGIS (Geographical Information Systems Software). Figure 2.3 represents a typical shortest-distance analysis flowchart for CO₂ sequestration. Two different shortest paths are found to be favorable for the pipeline from the gas source (Pt. Thomson) to the coal bed and a viscous oil reservoir (such as West Sak), as shown in Figure 2.4.

2.3.1 Input for Shortest-Distance Model

- Source dataset-CO₂ gas sale location
- Sink dataset-coal bed, sedimentary basins, CO₂-EOR sites
- Cost raster: Elevation (mountainous area) and land/ecosystem type converted to grid cells and assignment of weight
- Use of cost distance with direction to find the least-cost path to the sink (destination)

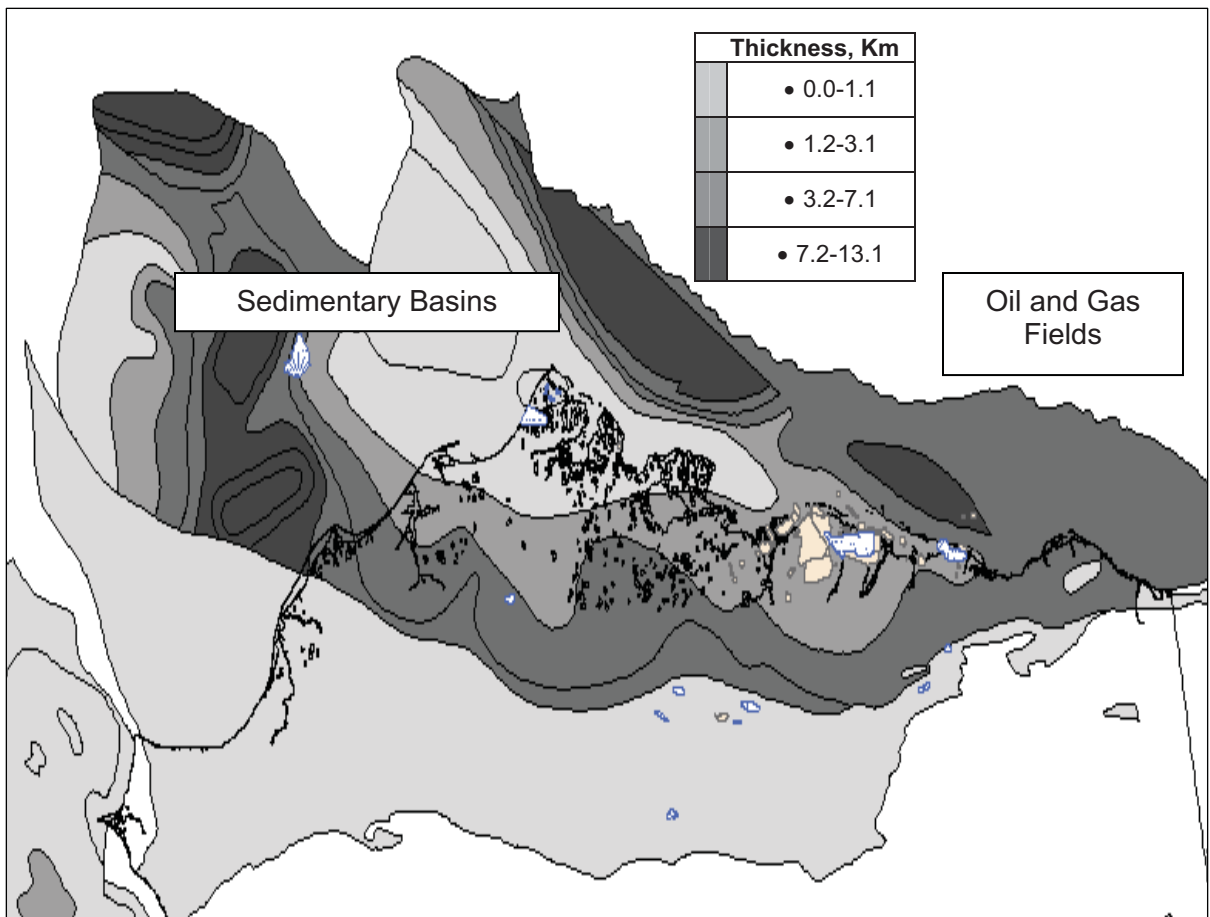


Figure 2.1: Location of sedimentary basins and their thickness on the Alaska North Slope.

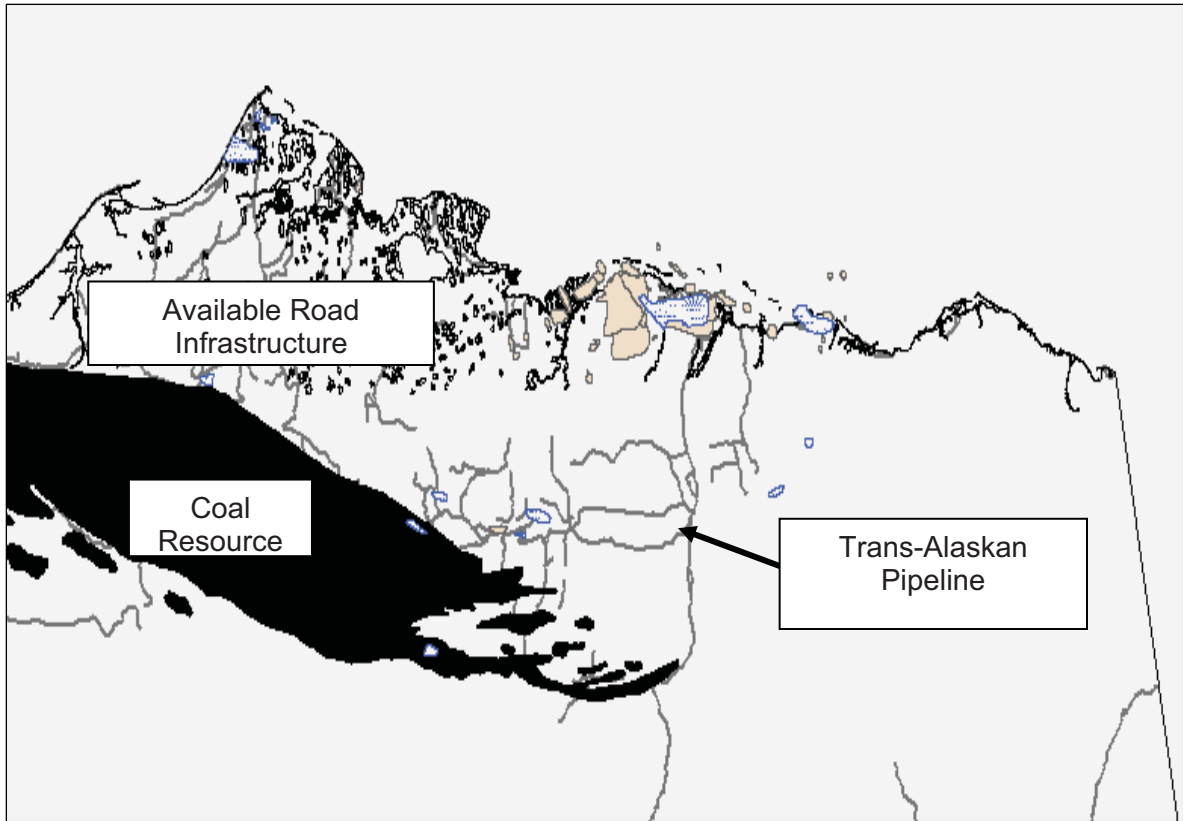


Figure 2.2. Location of coal resource and available road infrastructure on the Alaska North Slope for development of CO₂ sequestration project.

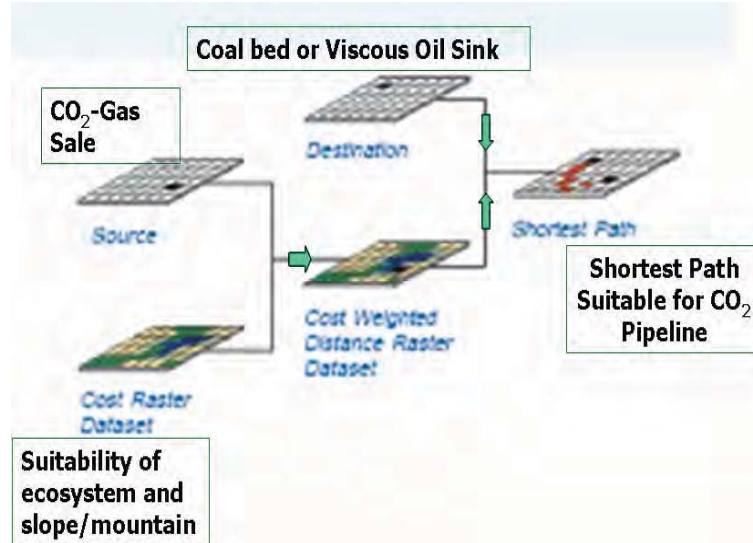


Figure 2.3. A typical shortest-distance scheme in ArcGIS.

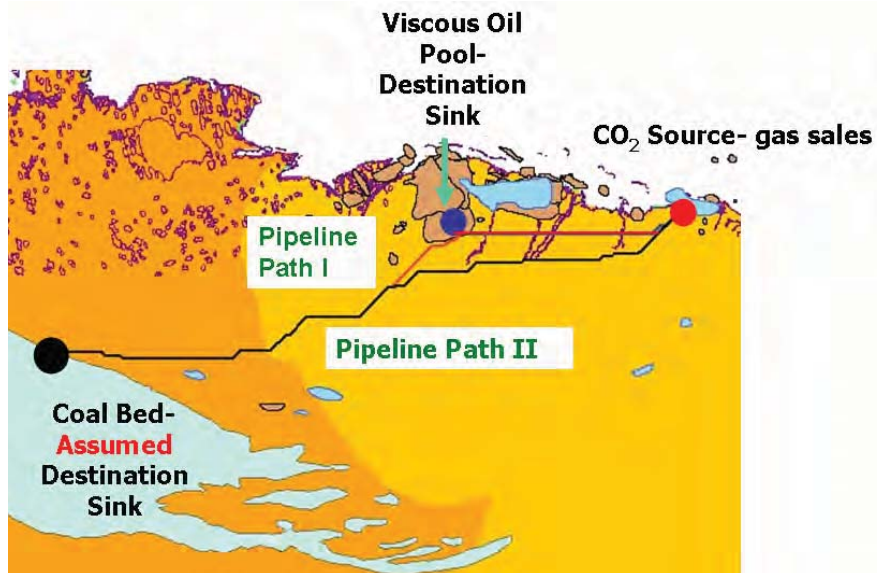


Figure 2.4. Shortest-path analysis for CO₂ sink and source system on the Alaska North Slope.

Chapter 3

Phase-Behavior Study of West Sak Oil and CO₂ System

3.1 Description of EOS

Minimum miscibility pressure (MMP) is the pressure at which injected gas and oil become miscible by multiple-contact displacement. There are various generalized methods to evaluate MMP for pure and impure CO₂. Ahmed (1997) briefly described various methods for determination of MMP. These methods primarily depend on the molecular weight of C₅₊, temperature, and a weighted-composition parameter (based on partition coefficients of C₂ through C₃₇ fractions).

The phase behavior of oil in CO₂ injection processes consists mainly of mass transfer and composition changes. The importance of tuning EOS for prediction of phase behavior of complex processes with a compositional simulator was recognized by Coats and Smart (1986) and Abrishami, Hatamian, and Dawe (1997). Cubic EOS like Peng-Robinson (1976) are widely used for convenient and flexible calculation of the complex phase behavior of reservoir fluids (Peng & Robinson, 1976). Equation 3.1 gives the original Peng-Robinson equation of state (PR-EOS). This equation can indicate the relationship among pressure (P), temperature (T), and mole volume (V) of components:

$$P = \frac{RT}{V - b} - \frac{a}{V(V + b) + b(V - b)} \quad (3.1)$$

The correction factor (α) in Equation 3.2 is dependent on the reduced temperature and quadratic function based on the acentric factor. Robinson and Peng (1978) recommended a modification to the acentric factor function to account for the heavier components; this modification will be referred as PR-EOS (1978).

$$a = \frac{\Omega_a R^2 T_c^2}{P_c} \alpha \text{ and } b = \frac{\Omega_b RT_c}{P_c} \quad (3.2)$$

Where a and b coefficients account for mixing in the case of multi-component mixtures, and Ω_a and Ω_b are the constants.

EOS parameters are interdependent on the binary interaction coefficient (BIC), which represents the intermolecular forces between molecules. In spite of suitability of PR-EOS to predict phase behavior of many components, it is a far-fetched endeavor to use PR-EOS for all components present in a fluid mixture. The need to incorporate any EOS for hydrocarbon mixtures to realize its suitability should always be weighed against the degree of inaccuracy, which is inherently expected due to the presence of heavy components. To overcome the deficiencies of EOS to predict the phase behavior of a fluid, tuning of EOS has been found to be an important practice, wherein laboratory PVT study acts as a basis for comparison to alter a and b coefficients by changing their parameters. Acentric factors and critical properties, primarily of the plus fraction, are changed in the tuning process. Based on the consideration of methane as a dominant component and the inadequacy related to heavy fraction characterization, Abrishami et al. (1997) reported different regression variables that can be chosen in the tuning process: (a) critical properties, such as P_c and T_c of heavy components since in many cases, there may not be a proper characterization of heavy fractions available; (b) Ω_a and Ω_b values of methane; (c) Ω_a and Ω_b values of heavy fractions; and (d) BIC.

Setting of Ω_a and Ω_b and critical properties of heavy fractions such as regression variables can lead to altering a and b coefficients. While Danesh (1998) stated that the selection of BIC as a regression parameter should be dealt with by acknowledging its role as

a fitting parameter rather than a physical property, it can also act effectively in changing the results predicted by tuned EOS. It should, however, be recognized that a tuned EOS is only applicable and valid for the same system at same temperature and pressure conditions. For CO₂ gas injection in oil, the adaptation to the compositional changes necessitates the modifications of the tuned EOS. According to Danesh (1998), all reliable experimental data must be used in the tuning process.

3.2 Characterization of West Sak Oil and Phase Behavior with CO₂

West Sak live oil is characterized by 23 components (Table 3.1), with the molecular weight of a heavy component (C₂₁₊) as 455 lb/lbmole (Bhandari, 1988). Experimental data on constant compositional expansion and differential liberation experiments on West Sak oil provided the values of relative-oil volume, percentage of liquid volume, and oil viscosity, gas-oil ratio, and specific gravity of gas at different pressures, as reported by Roper (1989). A compositional PVT simulator (WinProp[®]), developed by Computer Modeling Group (CMG), was used for this study. It minimizes the sum of squares of the relative errors by using regression technique for PR-EOS (1978) tuning, and calculates the values of different properties before and after EOS tuning. Furthermore, C₇₊ components of the West Sak oil were regrouped into five components by the equality-of-mole-fractions method to save the time required for the compositional simulation study. Tuning of the regression parameter was carried out by setting up variables such as critical properties and acentric factors of components C₇ through C₂₁₊. In addition to that, omega A and B parameters for methane and C₂₁₊, viscosity parameters, and interaction coefficients were used as regression variables (Danesh, 1998). The step-by-step procedure of lumping components and tuning EOS is given in Appendix A. Tuned EOS was implemented in the compositional simulation study of CO₂ injection for EOR.

For simplicity, the ternary phase-behavior diagram can be defined as a representation of three different components at constant pressure and temperature. Pseudo-ternary diagrams are used for multi-component mixtures by combining several components into three groups, representing three apexes on the ternary diagrams. Tuned PR-EOS (1978) was then used as the new EOS for West Sak oil and 100% CO₂ system. The PVT simulation of CO₂ injection into the oil was carried out to generate pseudo-ternary diagrams. This simulation resulted in the formation of two different phases from the mixture. The initial pressure of 1600 psia was increased in a step-wise manner to observe the miscibility condition for West Sak oil and CO₂.

Table 3.1

West Sak Oil Composition (after Bhandari, 1988)

Component	Mole %	Component	Mole %
CO ₂	0.016	C ₁₁	1.72
N ₂	0.032	C ₁₂	1.346
C ₁	38.333	C ₁₃	1.496
C ₂	0.857	C ₁₄	1.795
C ₃	0.359	C ₁₅	1.944
C ₄	0.179	C ₁₆	1.795
C ₅	0.064	C ₁₇	1.57
C ₆	0.2	C ₁₈	1.795
C ₇	0.016	C ₁₉	2.468
C ₈	0.008	C ₂₀	2.841
C ₉	0.823	C ₂₁₊	39.037
C ₁₀	1.496		

3.3 Phase Behavior of West Sak Oil with CO₂

The performance of untuned and tuned PR-EOS for prediction of the percentage of liquid volume and relative oil volume are shown respectively in Figures 3.1 and 3.2. Clearly, these figures demonstrate the importance of the tuning process, which would help in reliably predicting the phase behavior of the West Sak oil under CO₂ injection at various pressure values.

In pseudo-ternary diagrams (Figure 3.3), CO₂ was lumped with the intermediate components (C₂-C₆) to form an intermediate fraction. At lower pressures, closer to West Sak reservoir pressure, the vapor phase consists of intermediate and light components (Figure 3.3 [a]). At the lower pressure, partial miscibility of CO₂ with West Sak oil fluid is present. As the pressure of the system increases, the heavy and light components were found to be present in either vapor or liquid phase, while the intermediate components were present mainly in the vapor phase (Figure 3.3 [b]). At pressure 3600 psia and more, the nature of shrinking ternary plots remained unchanged, which was contrary to most of the miscibility conditions observed in the vaporizing or condensing drive. In the case of CO₂ injection, vaporizing of intermediate oil components by CO₂ is a dominant displacement drive mechanism. So as to represent the vaporizing drive on the ternary diagram, the tie line at a critical point should pass through the reservoir fluid; but this phenomenon was clearly absent in the diagrams at higher pressures, as can be seen in Figure 3.3. In the description of displacement mechanisms by Zick (1986) and Stalkup (1987), it was observed that a combination of condensing and vaporizing drive led to displacement of the oil in the case of enriched gas injection. By applying the same logic in this study, for CO₂ injection at a pressure of 3600 psia and higher, as injected CO₂ came into contact with the West Sak oil, the intermediate components were vaporized into CO₂ gas which resulted in a richer injection gas. As this heavier gas moved further into fresh oil, its capacity to vaporize intermediate components would diminish after a few contacts. Lighter fractions of the

intermediate components from heavier injection gas started condensing into oil, which resembles the condensing mechanism of enriched gas injection. Hence the combination of vaporizing and condensing mechanisms was observed in this study. The gas in the vaporizing/condensing mechanism never becomes rich enough to be miscible with the original oil. This apparent miscibility can explain the nature of ternary plots, wherein injected gas and oil are apparently miscible but not miscible.

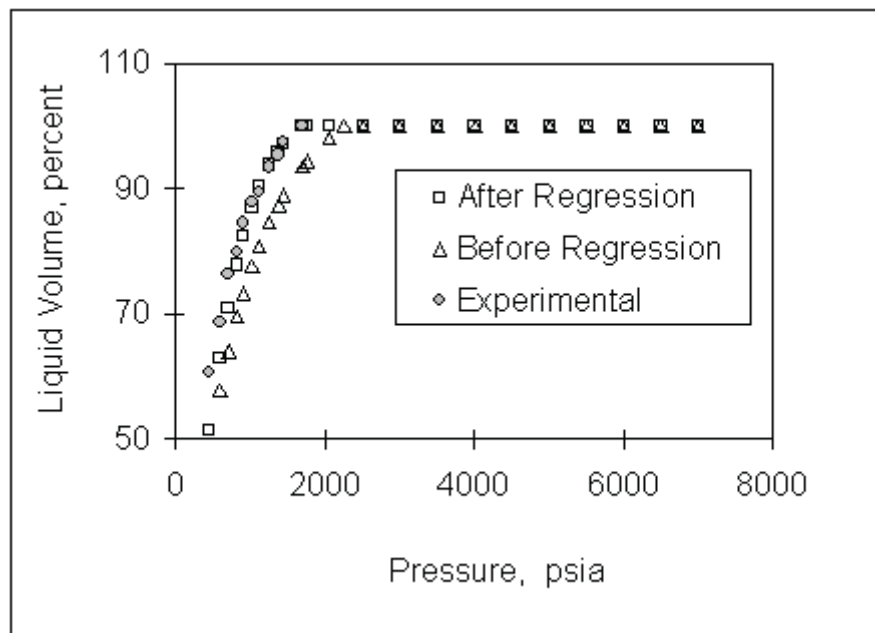


Figure 3.2. Percentage of liquid volume before and after regression.

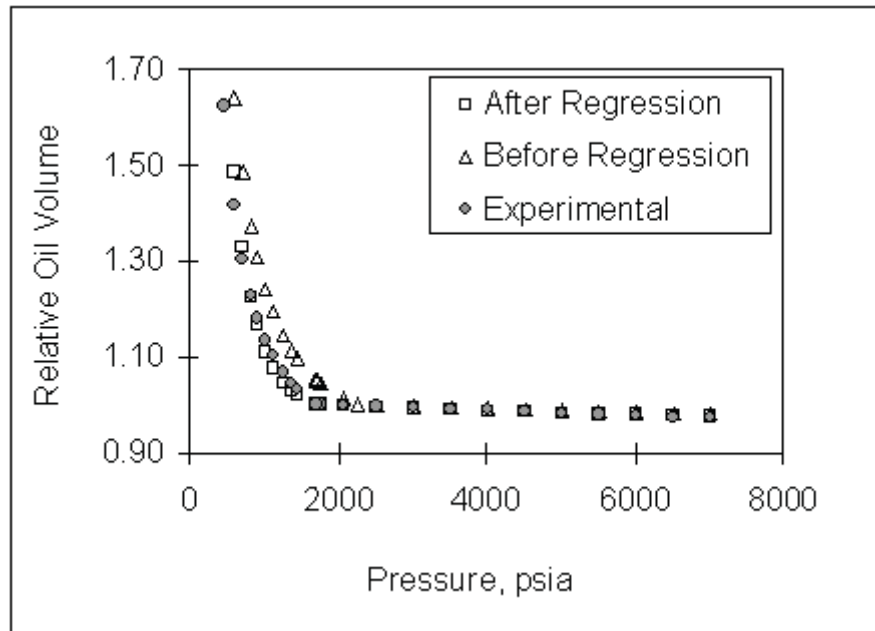
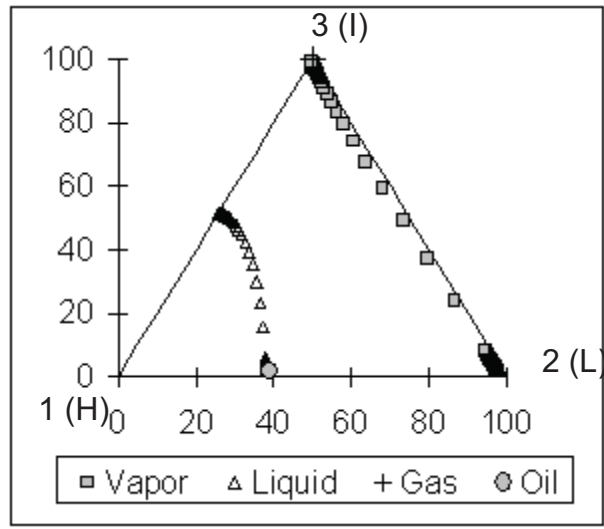
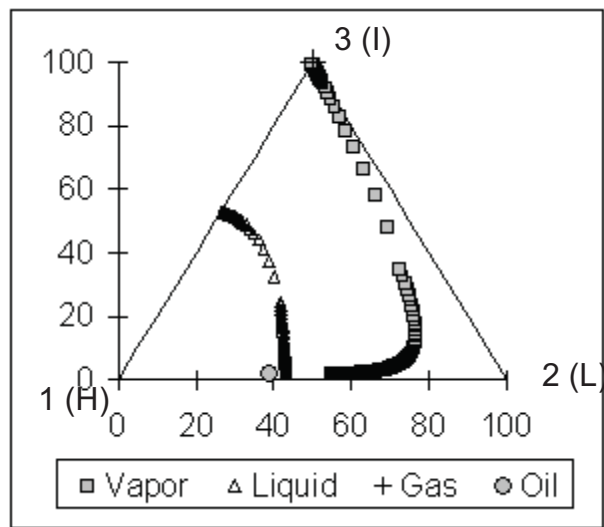


Figure 3.2. Relative oil volume before and after regression.

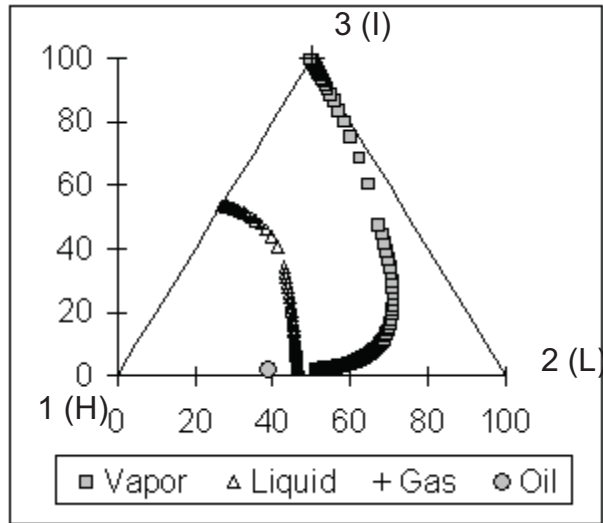


(a) 1600 psia

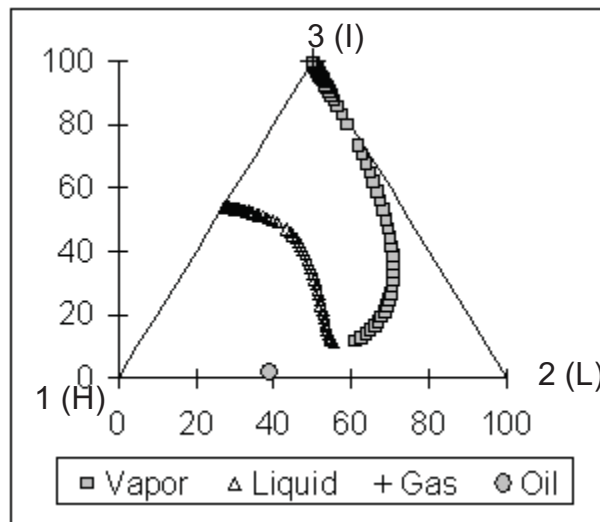


(b) 2600 psia

Figure 3.3 (a–b). Pseudo-ternary diagrams for West Sak crude + CO₂ system, where component 1: C₇₊ as the heavy fraction (H), component 2: N₂, C₁ as the light fraction (L), and component 3: C₂, C₃, C₄, C₅, C₆, and CO₂ as the intermediate fraction (I).



(c) 3600 psia



(d) 6600 psia

Figure 3.3 (c–d). Pseudo-ternary diagrams for West Sak crude + CO₂ system, where component 1: C₇₊ as the heavy fraction (H), component 2: N₂,C₁ as the light fraction (L), and component 3: C₂,C₃,C₄,C₅,C₆, and CO₂ as the intermediate fraction (I).

Chapter 4

CO₂-EOR Study

4.1 Description of West Sak Reservoir

Werner (1987) discussed in detail the low-gravity oil zones—i.e., West Sak and Ugnu sands—of the Kuparuk River Unit (KRU), Alaskan North Slope. According to Werner, the Chevron Kavearak Point No.1 (drilled in 1969) was the first well to encounter low-gravity oil in shallow zones of the Kuparuk River area. The depth of these shallow zones, later referred to as shallow sands, was less than 4500 ft. The regional setting of all of the shallow oil zones is a monocline with a gentle dip of 1°–2° degrees (130 ft/mi), which runs from northwest to northeast. Most of the oil was found in two zones: West Sak sands and the overlying Ugnu sands.

The gravity of oil in the late Cretaceous and early Tertiary marine-aged West Sak reservoir was from 16° to 22° API. The West Sak sands are very fine and unconsolidated with inter-bedded siltstones and mudstone, and have an areal extent of 30 mi north to south and 20 mi east to west from the western area of the Prudhoe Bay Field across the Kuparuk River Field. West Sak oil-bearing sands, similar to the Schrader Bluff Formation, are present from 3742 to 4040 ft when measured at the ARCO West Sak No.1 well. Geochemically, the sand grains are made up of quartz, lithic rock fragments, and feldspar with small amount of mica and glauconite.

West Sak is a highly stratified reservoir. The average stratigraphic interval thickness of the West Sak sands is 300 ft in the southwest and 200 ft in the northeast. The sands are divided into upper and lower members. The lower-member sands are thin-bedded, ranging from 0.2–5 ft in thickness with, in part, amalgamated sand-rich units up to 10 ft in thickness. Lower-member sands can be laterally continuous for three to five miles. The upper member consists of 2 laterally distinct sands—upper sand #1 and upper sand #2—with an average thickness of 30 and 20 ft, respectively. The top of the West Sak sands ranges from 2400 ft

true vertical subsea depth on the western edge of the Kuparuk region, to 3800 ft on the eastern edge.

The primary control on regional distribution of oil in the West Sak oil pool is north-south and east-west trending faults. The temperature in West Sak oil varies from 40 °F to 100 °F (Panda, Zhang, Ogbe, Kamath, & Sharma, 1989) due to overlaying permafrost, while pressure ranges from 1000 psi to 1800 psi due to there being shallow sands. Core data indicate that the horizontal air permeability is between 10 and 800 milidarcy, with an average permeability value of 140 milidarcy; porosity can be as high as 0.38.

The West Sak oil pool contains around 7–9 billion barrels of OOIP (McGuire et al., 2005). According to the Alaska Oil and Gas Conservation Commission (2003), the West Sak oil pool has produced continuously since December 1997. Oil production increased from a monthly average of 19 barrels of oil per day (BOPD) to 9300 BOPD during the first 8 months of 2004. After bringing several new wells into production in September 2004, West Sak oil production increased to its current rate of 17,000 BOPD. By December 2004, the average oil production from the 31 wells of the West Sak pool averaged 17,072 BOPD.

4.2 Theory, Field, and Simulation Review

Gas injection is one of the important tertiary injection processes that play a crucial role in EOR. Because of its large production, non-toxic nature, role in global warming, and tendency to vaporize intermediate components, CO₂ gas acts as an important injectant for EOR.

For many CO₂ flooding projects, approximately 5 to 10 Mscf (gross utilization) of CO₂ are required to recover an additional barrel of stock tank oil by miscible CO₂ displacement (Stalkup, 1987). On reaching maturity in the early 1970s, the Permian Basin oil reservoirs were thought to be potential candidates for tertiary oil recovery with CO₂ obtained from natural gas produced in nearby fields (Holtz, Nance, & Finley, 1999). Shaw and Bachu

(2002) stated that there are 76 sites worldwide that are commercially proven, of which 67 are in the U.S. Carbon dioxide flooding is attracting attention today because it can lead to additional oil production while providing a disposal site (sink) for industrial CO₂ emissions. Proximity to a large, high-purity source of industrial CO₂ emissions is an essential criterion for a feasible CO₂ flooding project, since the extraction of enough CO₂ from low-purity sources is an economically unfavorable scenario. High-purity (minimum of 80%) CO₂ can be transported to the oil field via a pipeline. Proximity of a CO₂ source to the oil reservoir is essential for economic feasibility, since it reduces the capital and operating costs of the pipeline.

The injected gas contacts reservoir oil which causes changes in the phase behavior as well as the equilibrium conditions. Taber et al. (1997) classified the EOR by oil displacement mechanism. For CO₂ flooding, miscible and immiscible processes fall under vaporizing/condensing and viscosity-reduction mechanisms, respectively. Miscible CO₂ injection results in higher recovery when compared with immiscible options (Srivastava et al., 1995). Immiscible CO₂ flooding, which occurs in low-pressure (below 1000 psia) reservoirs, can aid oil production by oil swelling, viscosity reduction, or solution gas drive as CO₂ gas dissolves in oil and carbonates it (solubility of CO₂ in oil is a pressure-dependent phenomenon), thus increasing oil volume and reducing its viscosity. Normally, during an immiscible-displacement regime, the presence of partial miscibility is essential for oil displacement by swelling and viscosity reduction. In the case of miscible flooding, the interfacial tension between the displacing phase and the displaced phase is minimized, and consequently, the reduction in drag forces for fluid flow in porous media acts as a favorable condition for miscible flooding. Different types of mechanisms initiate the oil displacement by CO₂; nevertheless injected CO₂ may lead to a miscible front, which may be similar to the rich-gas injection process. Essentially, extraction of intermediate to heavier components (C₅ to C₃₀) from oil by CO₂ can generate a favorable miscible condition.

When CO₂ is injected into oil reservoirs to increase oil recoveries, it can develop first-contact miscibility or multiple-contact miscibility if the system pressure is higher than minimum-miscibility pressure. If the injected CO₂ mixes with reservoir oil in all proportions on first contact, it is called first-contact miscibility. With multiple-contact miscible fluids, in situ mass transfer of components occurs between injected and reservoir fluids, and all compositions within the transition zone of these phases become miscible (Stalkup, 1984). For oil viscosities of 100 to 1000 cp, however, if CO₂ is not miscible with reservoir oil, the CO₂-EOR may be achieved by swelling the oil to sweep the reservoir and by decreasing the effective mobility ratio due a large reduction in oil viscosities (Klins, 1984). Thus immiscible CO₂ can prove to be superior to waterflooding. Due to the similar viscosity range of West Sak oil, immiscible CO₂ flooding can be an effective way to increase incremental oil production.

CO₂ injection can be useful in viscous oil reservoirs where thermal methods fail to perform efficiently and CO₂-saturated oil exhibits moderate swelling, in turn reducing oil viscosities and affecting the mobility ratio. Klins (1984) enumerates different advantages of injecting CO₂ into oil reservoirs along with its obvious disadvantages. The following are the advantages and disadvantages of the CO₂ injection process for EOR:

Advantages:

1. CO₂ can achieve dynamic miscibility at lower-pressure values than methane (Stalkup, 1984).
2. In the case of CO₂ miscible flooding, the displacement efficiency is high.
3. Overall oil recovery is also increased by solution gas drive.
4. CO₂ injection can be applicable for a wider range of crude oils than other hydrocarbon injection.

Disadvantages:

1. CO₂ is expensive to capture from sources and to transport to field locations for EOR.
2. Poor sweep efficiency and gravity segregation are problematic for certain conditions.
3. CO₂ is very corrosive when it is in carbonic acid form.

Displacing oil by CO₂ injection essentially depends on the number of mechanisms that are inherently linked to the phase behavior of CO₂-oil mixtures (Klins, 1984). Attainment of miscibility or immiscibility during CO₂ injection is a function of reservoir temperature, pressure, and oil composition; hence the dominant displacement mechanisms fall into one of four following cases:

- (a) Low-pressure scenario
- (b) Intermediate-pressure and high-temperature scenario
- (c) Intermediate-pressure and low-temperature scenario
- (d) High-pressure scenarios

At pressures below 1000 psia (case [a]), the injected CO₂ dissolves in the oil and thereby reduces the viscosity of the oil, swells the oil, contributes to the solution gas drive mechanism, and aids increased injectivity. Mainly, this low-pressure scenario can be observed in shallow, viscous oil fields.

For intermediate-pressure (> 1000 psia) and high-temperature (> 122 °F) applications (case [b]), not only does the CO₂ injection increase the reservoir pressure and lead to oil swelling, but also some of the hydrocarbons may be vaporized into the gas phase. At miscible pressure, the oil starts losing its intermediate components into a CO₂-rich gas phase (vaporizing gas drive). Mead-Strawn oil swelled to 40% of its original volume on injection of CO₂ up until 1400 psia. Above 1400 psia, however, the oil phase started shrinking due to hydrocarbon extraction by the CO₂-rich phase (Klins, 1984).

At intermediate pressure but low temperatures (< 122 °F) (case [c]), rather than vaporizing oil, CO₂ extracts the lower ends of the oil to form CO₂-rich liquid mixtures. The presence of two liquid phases with (lower pressure) or without (higher pressure) gas phase does not prohibit high oil recoveries. For the high-pressure miscible scenario (case [d] at pressures of 2000 to 3000 psia), injected CO₂ would be able to vaporize significant volumes of oil by generating multiple-contact miscibility in a short period of time and over a very short distance in the reservoir.

Apart from the benefits of immiscible or miscible oil displacement mechanisms by CO₂ flooding, many factors should be considered while designing any CO₂-EOR project (Holm, 1987). Proximity of the CO₂ source and available infrastructure may be a limiting factor for many CO₂-EOR flooding projects. Project designers should be wary of the fact that not all the reservoirs can be candidates for a CO₂-EOR project. Reservoir conditions such as temperature, pressure, permeability, and oil saturation, and anomalies, such as fractures, can affect the efficiency of the project. Whether slug injection (and size of slug) of CO₂ followed by water or continuous injection of CO₂ can yield favorable oil recovery is a crucial decision to make, and it determines incremental recovery of the project. Adverse mobility ratio of CO₂ injection can also hamper success of an EOR project. As well, the acidic nature of CO₂ in the presence of water should be given due consideration to alleviate future problems of corruptions in the wells.

Saner and Patton (1983) reported on a pilot test of the continuous CO₂ immiscible-drive oil-recovery process (due to shallow depth of the tar zone) conducted in the Wilmington Field Tar Zone of the Los Angeles basin. In the early 1960s, primary production from the field was supplemented by waterflooding (secondary recovery). Tertiary oil recovery by immiscible CO₂ flooding was studied over a 50-month injection period in a large-scale (1700 acre-ft) pilot. Laboratory experiments were performed to evaluate the process by understanding swelling of the oil-phase and viscosity reduction. It was found that the

amount of CO₂ dissolved, and in turn, that an increase in oil swelling by 105% of original volume is proportional to an increase in pressure. It was observed that the viscosity of the oil was dramatically altered by CO₂ dissolution; viscosity of Tar Zone oil was reduced from 283 to 18 cp at a CO₂ pressure of 1080 psig.

A second series of experiments to test the feasibility of CO₂ flooding involved huff-and-puff stimulation tests of a single-producing well. Four tests were conducted with liquid CO₂ to measure, in situ, the effect of the crude oil/CO₂ interaction on oil and water mobility. The results from these tests showed that each well exhibited strong stimulation in oil production and a large decrease in water production. Initial stimulation ratios were about two- to three-fold for oil rates, and a more than tenfold magnitude reduction occurred in the flow rate of water.

To increase chances of a successful EOR project, prediction of oil production by reservoir simulation is a way to optimize outcome of a CO₂-EOR project. Reservoir simulation is the most important predictive tool available to the reservoir engineer in comparison with other reservoir production-prediction techniques. Black oil and compositional are two reservoir simulation models that are widely used. Black-oil models are capable of simulating water, oil, and gas phases with negligible dispersion. Phase transfers between the gas and water and the gas and oil are accounted for in the black-oil model, whereas the compositional model takes the transfer of oil and injection fluid components into account. A simulator based on the compositional model offers an advantage over the black-oil model for immiscible or near-miscible displacement when compositionally-dependent mechanisms (such as condensation, vaporization, and oil swelling) are essential to understanding those displacement processes influenced by the compositional dependence of viscosities and densities (Stalkup, 1987). But limitations like (a) requirement of a large number of components for accurate prediction of phase behavior, (b) numerical dispersion leading to erroneous prediction of oil production, and (c) inability to model accurate viscous

fingering observed in the CO₂ flooding process are common to a compositional simulator. In compositional models, it is assumed that the water component is not soluble in the hydrocarbon phase, and the water phase contains only water as a component. This assumption is valid, as solubility of water into oil is negligible, but this assumption has a flaw when a significant amount of injected CO₂ dissolves into water.

The flow and pressure equations in either simulation model cannot be solved by analytical techniques, so numerical solutions are used to solve these equations. The numerical method, known as *implicit in pressure and explicit in saturation*, is used to solve the flow and pressure equations numerically.

Bakshi, Ogbe, Kamath, and Hatzignatiou (1992) carried out a numerical simulation study of the CO₂ stimulation process for the West Sak field using a three-dimensional, three-phase, black-oil simulator. In that study, parameters such as bottom-hole pressure, soak period, CO₂ slug size, and number of cycles were evaluated for the West Sak field. The CO₂ stimulation involved the injection of a slug of CO₂ into the well, followed by a shut-in for several days (soak period). During the soak period, CO₂ travels several hundred feet into the reservoir while displacing mobile water surrounding the well and is absorbed by the oil, reducing its viscosity. After the soak period, the well was allowed to produce. The CO₂ stimulation process can be applicable to viscous oil reservoirs where absence of miscibility conditions between oil and CO₂ can make the viscous oil reservoir a potential candidate for the stimulation. At the end of a soak period, the region surrounding the well bore area contains mostly low-viscosity mobile oil, free CO₂ gas, and immobile water. The maximum oil production rate for a stimulated well was found to be 2.5 to 3 times the maximum oil production rate for unstimulated wells.

Application of immiscible CO₂ injection into the Avile Reservoir, Puesto Hernandez Field, Argentina, was found to be economical, technically feasible, and promising (Brush, Davitt, Aimar, Jorge Arguello, & Whiteside, 2000). The field's high permeability and low

apparent heterogeneity led to high-sweep efficiency. First, a five-component PR-EOS was developed by a regression technique to match laboratory data and swelling and viscosity data with the values estimated by tuned EOS. The swelling of oil was 35% of its original volume and viscosity was reduced by a factor of 4 through immiscible CO₂ injection. A series of unsteady-state CO₂ core flooding experiments were carried out to determine residual oil saturation to waterflooding and to CO₂ flooding with respect to changes in pressure. Furthermore, the core flood tests were simulated with a tuned 5-component EOS model in a 1-dimensional, 180-grid-block model, representing a 1-foot composite core. A simulation study predicted oil recovery by CO₂ injection within 1% of laboratory core-flood recovery. A pilot area simulation model was generated with log, core, fluid, and production data, spanning 30 years. A black-oil model was used for prediction of production due to primary depletion and waterflooding, and then a compositional model was employed to predict oil production during CO₂ flooding.

Klins and Farouq Ali (1981) conducted a simulation study of immiscible CO₂ flooding with a three-phase, two-dimensional simulator. It was observed that the oil recovery by CO₂ flooding is dependent on initial oil saturation for oil viscosities equal to 100 cp and 1000 cp. For 100-cp oil, recovery increased from 3% to 29% as the oil saturation was increased from 40% to 70%, respectively. CO₂ flooding was found to be superior to other processes such as natural depletion, nitrogen flooding, and conventional waterflooding for the oil (> 70 cp). In the case of 1000-cp oil, the oil recoveries of less than 1%, 16%, and 25% were observed for the natural depletion, waterflooding, and CO₂ flooding, respectively.

Doleschall, S., Szittar, A. and Udvardi, G. (1992) performed a simulation study, using a 10-component, 3-phase mathematical model of pure CO₂ and partially miscible, carbonated natural gas flooding in the western region of the Budafa Oil Field, Hungary. Laboratory PVT studies showed that gas containing 81 mole % CO₂ could be used for EOR.

At probable optimal CO₂ slug size of 20% PV, additional oil recovery was estimated to be 12%–16% of the OOIP.

Prototype reservoir models of a Weyburn unit, which is located in the southeastern part of Saskatchewan, Canada, were developed by Malik and Islam (2000) by using geological and petrophysical data. After successful history matching with previous production data, the models were able to optimize secondary and tertiary recovery schemes. The controlling parameters, such as injection in bottom zones and presence of impurities in the CO₂, which influence the miscible CO₂ flooding process (tertiary recovery), were studied. Presence of contaminants in the injected CO₂ gas lowered the solubility and diffusivity of CO₂ into reservoir oil, which reduced swelling of oil by CO₂. The low cumulative oil production due to an injection of impure CO₂ gas stream into bottom water was attributed to an inefficient transfer of CO₂ from the water phase to the oil phase. Horizontal injection of CO₂ in the reservoir was an effective way to increase anthropogenic CO₂ storage while reaping the benefit of optimized incremental oil production by reducing gravity segregation due to an unfavorable mobility ratio.

In another numerical simulation study, Domitrović, Šunjerga, and Jelić-Belta (2004) planned a tertiary CO₂ injection at Ivanić Oil Field in Croatia. A numerical model was built with previously acquired seismic data. The black-oil model was used to match the history of 40 years of production by changing transmissibility of faults. Regression-matched PR-EOS, along with snapshots of the state of the black-oil model, initiated the compositional model to simulate three different CO₂ and water slug-size scenarios. Repressurizing by waterflooding proved to be important to increasing reservoir pressure to reach miscibility conditions of CO₂ injection. The incremental oil recovery was more than 88.29 million ft³ in the scenario that involved repressurizing the reservoir.

Different types of flood pattern are used for EOR projects. Takur and Sattar (1998) summarized the five-spot, seven-spot, and nine-spot injection patterns for waterflooding

projects. Oil companies use similar patterns for CO₂ flooding projects. In the case of a 5-spot injection pattern, the typical area of the project is 40 acres. One production well is situated in the center, while 4 injection wells occupy the corners of a square 40-acre area.

4.3 Simulation of CO₂ Injection for Enhanced West Sak Oil Recovery

Generalized Equation-of-State Model (GEM[®]), developed by the Computer Modeling Group, is an efficient and multidimensional compositional simulator. This simulator was used to conduct CO₂ displacement studies by taking into account gas injection processes like vaporization and swelling of oil, condensation of gas, viscosity and interfacial tension reduction, and solubility of CO₂ in water.

The explicit mode for solving forward-difference formulation, which evaluates interblock-flow equations, suffers from restrictions on the time-step size due to conditional stability of the procedure. GEM's adaptive-implicit formulation, however, uses implicit formulation (unconditional stability is achieved but it is time consuming) of the flow equation, choosing at every time-step which grid blocks should be solved either in implicit mode or explicit mode, thus saving time required for a simulation run. The adaptive-implicit mode is beneficial for applications involving high flow rates at injection wells, pressure gradients near wells, and flow through very thin layers (as in the case of the West Sak reservoir).

4.3.1 Grid System and Petrophysical Properties

A three-dimensional Cartesian grid system was adopted for this study. A total of 5625 grid blocks were divided as 25, 25, and 9 grids in X, Y, and Z direction, respectively (Figure 4.1). Due to the vast nature of the West Sak reservoir, a 5-spot injection pattern (40 acres) was considered in the current simulation work. The distance between the adjacent injection wells was 1320 ft, and the distance between the injection and production well was 933 ft. All injection wells were on the corners of the square area, while the production well

was set in the center at the midpoint of bisectors. Figure 3.2 shows the 40-acre pattern. Continuous CO₂ was injected for 25 years in the injection wells so that the total injected CO₂ was 10%, 20%, 30%, and 50% of the PV of the reservoir.

Each porous and permeable bed was considered as one layer of productive sand with average porosity, thickness, and water saturation. A layer of shale, which acts as an impermeable layer (inactive) with zero porosity, separated the sand layers. The average values of the important petrophysical properties for the five sand layers are given in Table 4.1. During production and injection, reduction in internal pressure can lead to a decrease in porosity, especially above bubble-point pressure. A constant rock compressibility of 5×10^{-6} per psi was assumed for this simulation study (Bakshi, 1991).

Table 4.1

Average Layer Properties of West Sak for 40-Acre Injection Pattern (after Bakshi, Ogbé, Kamath, & Hatzignatiou, 1992)

Layer No.	Sand	Interval (ft)	Avg. Porosity (%)	Avg. water saturation, (%)	Net pay (ft)
9-topmost	Upper 1	3544-3584	30	24	30
7	Upper 2	3614-3640	31	31	21
5	Lower1	3660-3686	23	45	3
3	Lower2	3695-3760	25	47	3
1-bottommost	Lower3	3776-3814	27	41	17

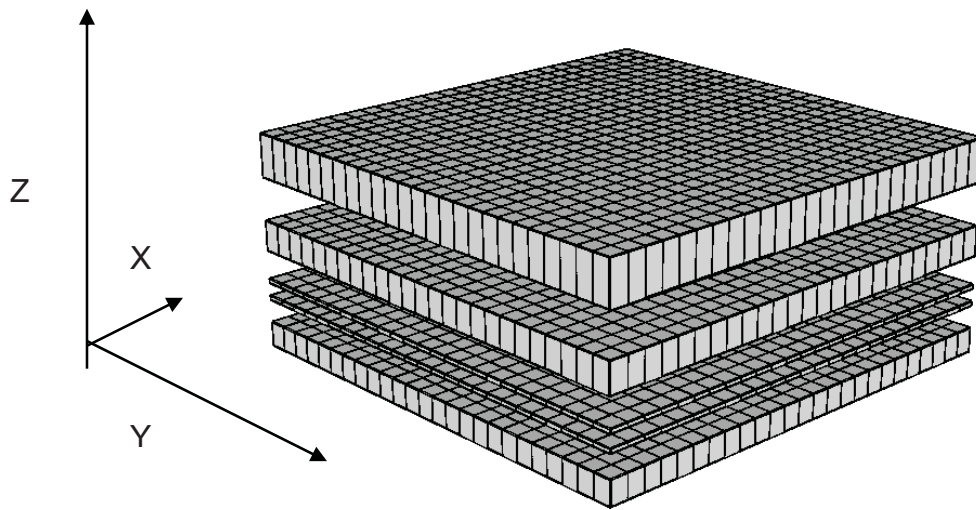


Figure 4.1. Three-dimensional view of the grid system.

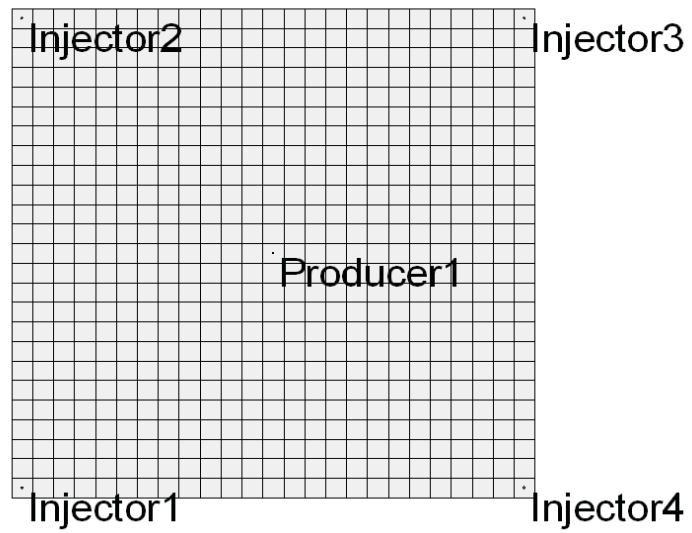


Figure 4.2. Five-spot CO₂ injection pattern.

4.3.2 Relative Permeability Data

From a previous study by Bakshi (1991), the water-oil relative permeability and gas-oil relative permeability data were acquired. A West Sak operator had provided the data on relative permeability. The water-oil relative permeability curves for the West Sak upper sand #1, upper sand #2, and lower sands are given in Figures 4.3, 4.4, and 4.5, respectively. Figures 4.6, 4.7, and 4.8 are the graphical representation of the gas-oil relative permeability for upper sand #1, upper sand #2, and lower sands, respectively. These relative permeability (K) curves were digitized for use in this simulation study. The subscripts o , w and g represent oil, water, and gas phases, respectively.

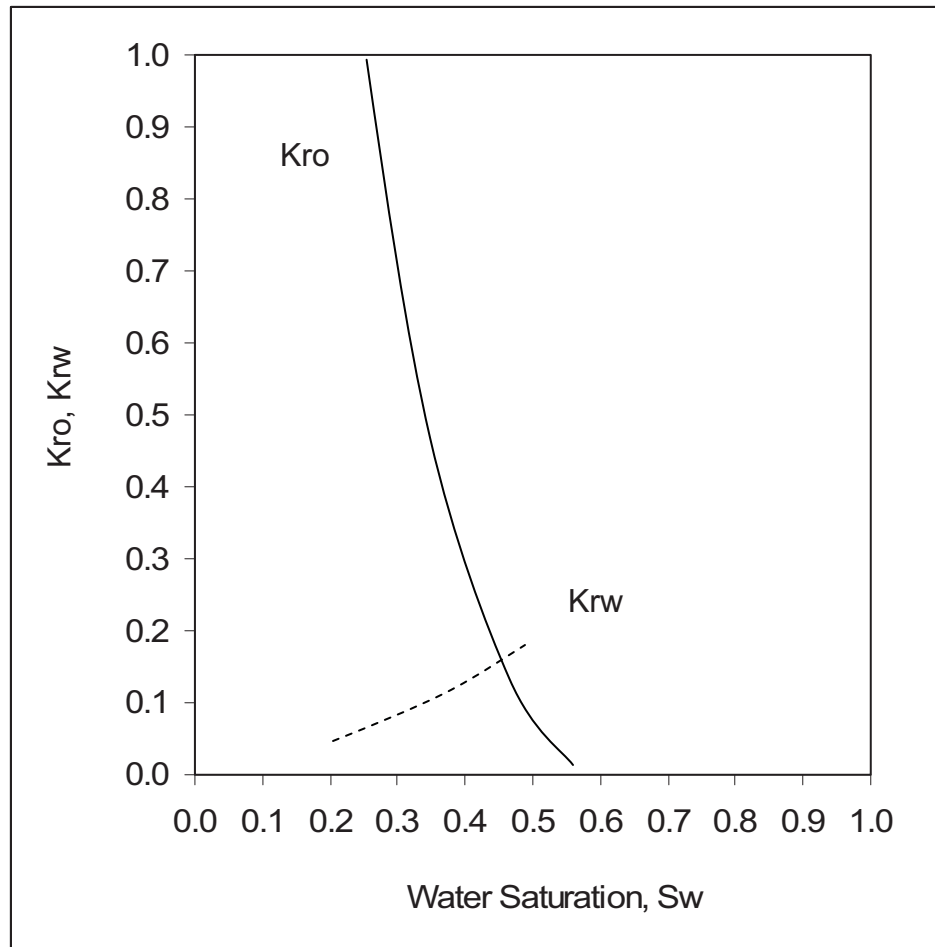


Figure 4.3. Water-oil relative permeability of West Sak upper sand #1 (modified after Bakshi, 1991).

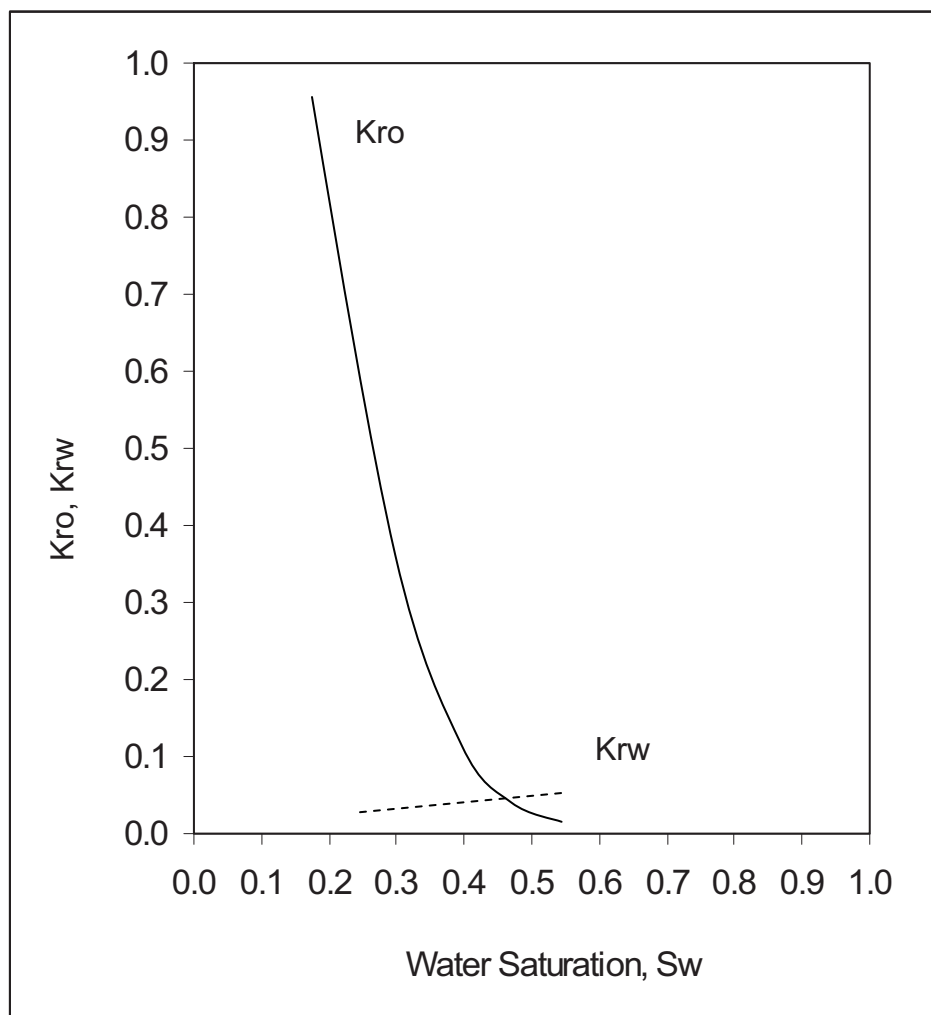


Figure 4.4. Water-oil relative permeability of West Sak upper sand #2 (modified after Bakshi, 1991).

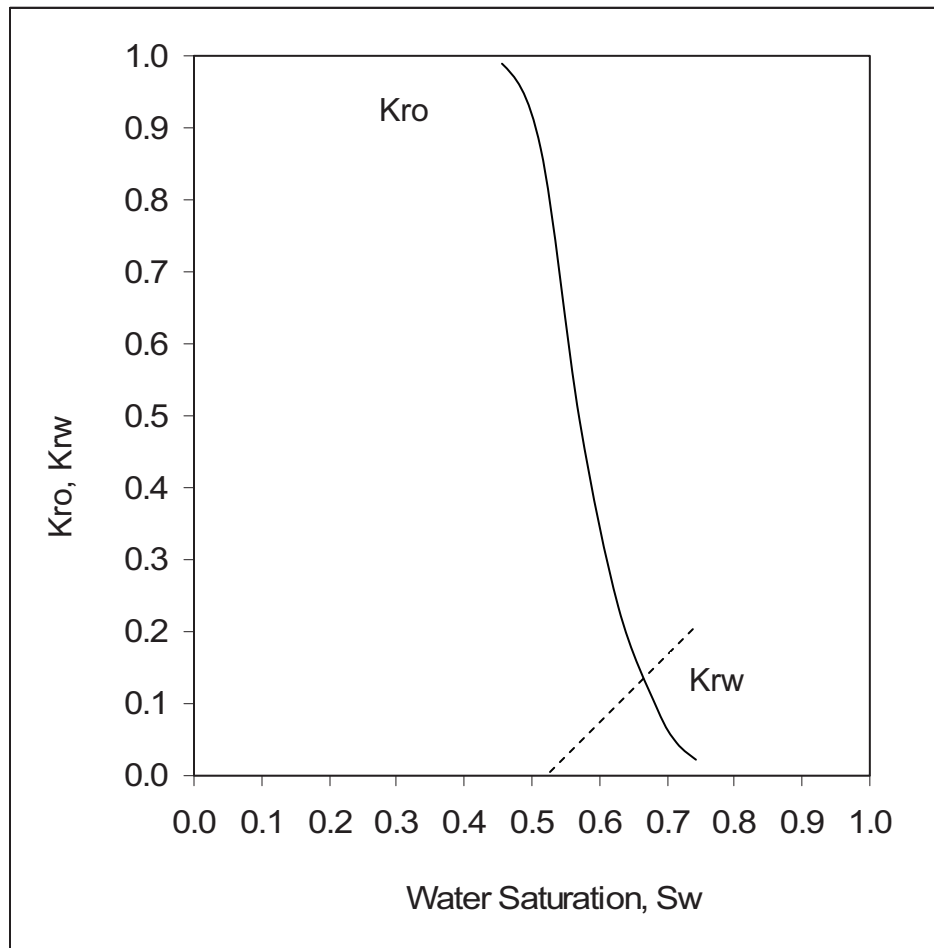


Figure 4.5. Water-oil relative permeability of West Sak lower sands (modified after Bakshi, 1991).

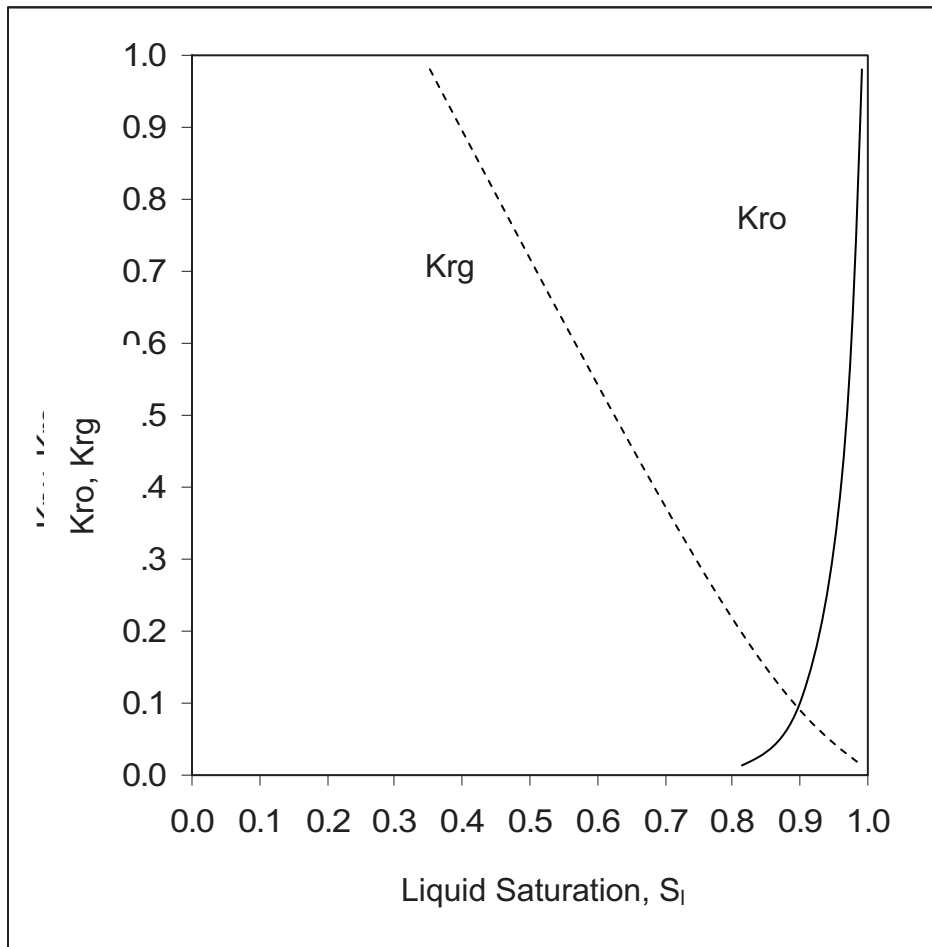


Figure 4.6. Gas-oil relative permeability of West Sak upper sand #1 (modified after Bakshi, 1991).

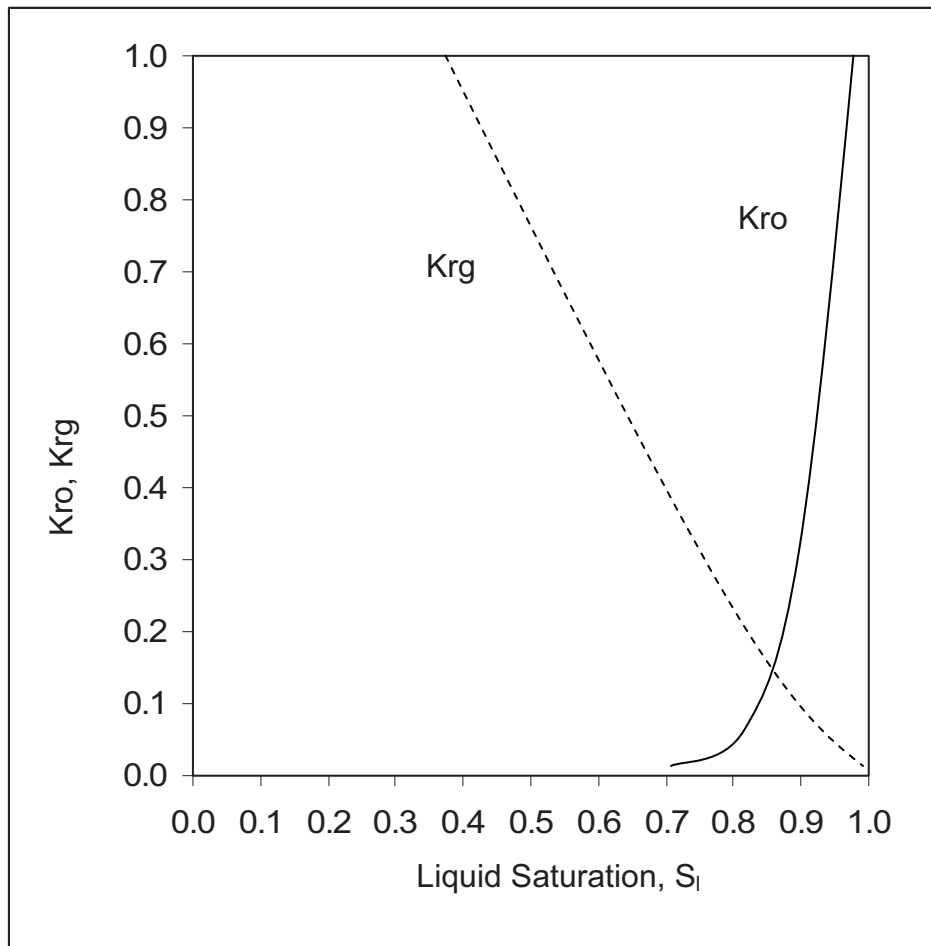


Figure 4.7. Gas-oil relative permeability of West Sak upper sand #2 (modified after Bakshi, 1991).

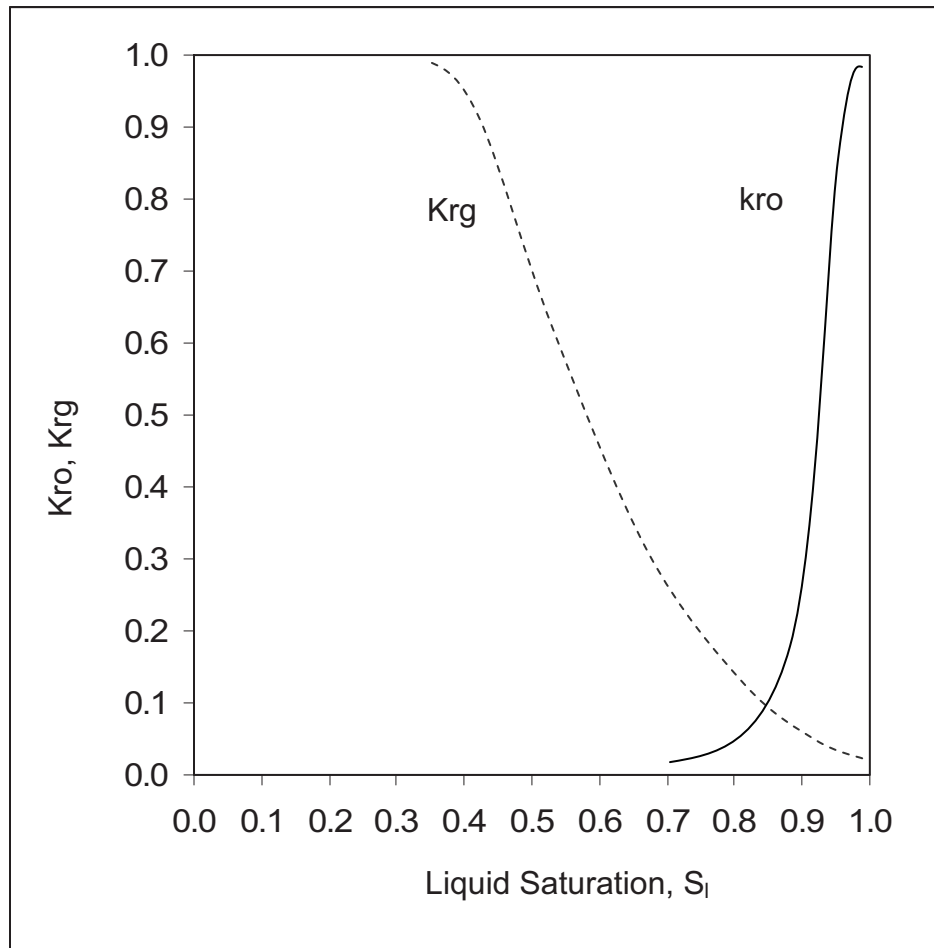


Figure 4.8. Gas-oil relative permeability of West Sak lower sands (modified after Bakshi, 1991).

4.4 Simulation Results for Enhanced Viscous Oil Recovery by CO₂

On injection of pure CO₂ in the 40-acre 5-spot injection pattern for 25 years, the oil rate in terms of stock tank barrel (STB)/day was observed for each year. The OOIP for each PV injection case was 4.015 million STB. The occurrence of CO₂ breakthrough phenomenon for 10%, 20%, 30%, and 50% of PV can be seen in Figures 4.9, 4.10, 4.11, and 4.12, respectively. The decrease in oil rate and increase in CO₂ flow rate clearly show the onset of

a breakthrough pattern in each PV injection scenario. For 50% PV injection, the gas breakthrough occurred after around 4.5 years into injection, which can be seen in Figure 4.12 as the beginning of a decrease in oil rate and increase in CO₂ rate. Similarly, Figure 4.11 shows the breakthrough after 6 years into injection. Figures 4.9 and 4.10 show a delayed occurrence of breakthrough for 10% and 20% PV. Table 4.2 lists the volume of CO₂ injected and produced for a 25-year injection period at surface conditions of 60 °F and 14.7 psia. The percentage recovery of OOIP increases as the amount of CO₂ injected increases, as can be seen in Table 4.2 and Figure 4.13, but along with an increase in percent recovery, storage ratio decreased. Gross utilization of CO₂, which is total CO₂ injected per barrel of oil produced for 50% PV of CO₂ injection, was found to be 9.709 Mscf/STB of oil produced. Additionally, increase in percent recovery will reach its plateau, where further increase in PV injected will not affect recovery, as can be observed in Figure 4.13.

Figures 4.10–4.12 show the sudden dip in the CO₂ flow rate after the breakthrough of CO₂. This could be attributed to an increase in the reservoir pressure due to continuous injection of CO₂, which could have led to the development of partial miscibility of incoming CO₂ with the West Sak oil. The incoming CO₂ tries to vaporize remaining heavier intermediate components due to increased reservoir pressure. This phenomenon could be observed as a small increase in the oil rate after the breakthrough.

Table 4.2

Percentage Recovery and CO₂ Storage Ratio at Different Pore Volumes (PV)

% PV	% Recovery	CO ₂ Injected, million standard cubic ft	CO ₂ Produced, million standard cubic ft	CO ₂ Storage Ratio
10	11.40	1.598	0.075	0.95
20	14.93	3.196	1.009	0.68
30	16.82	4.841	2.327	0.52
50	20.62	8.040	4.981	0.38

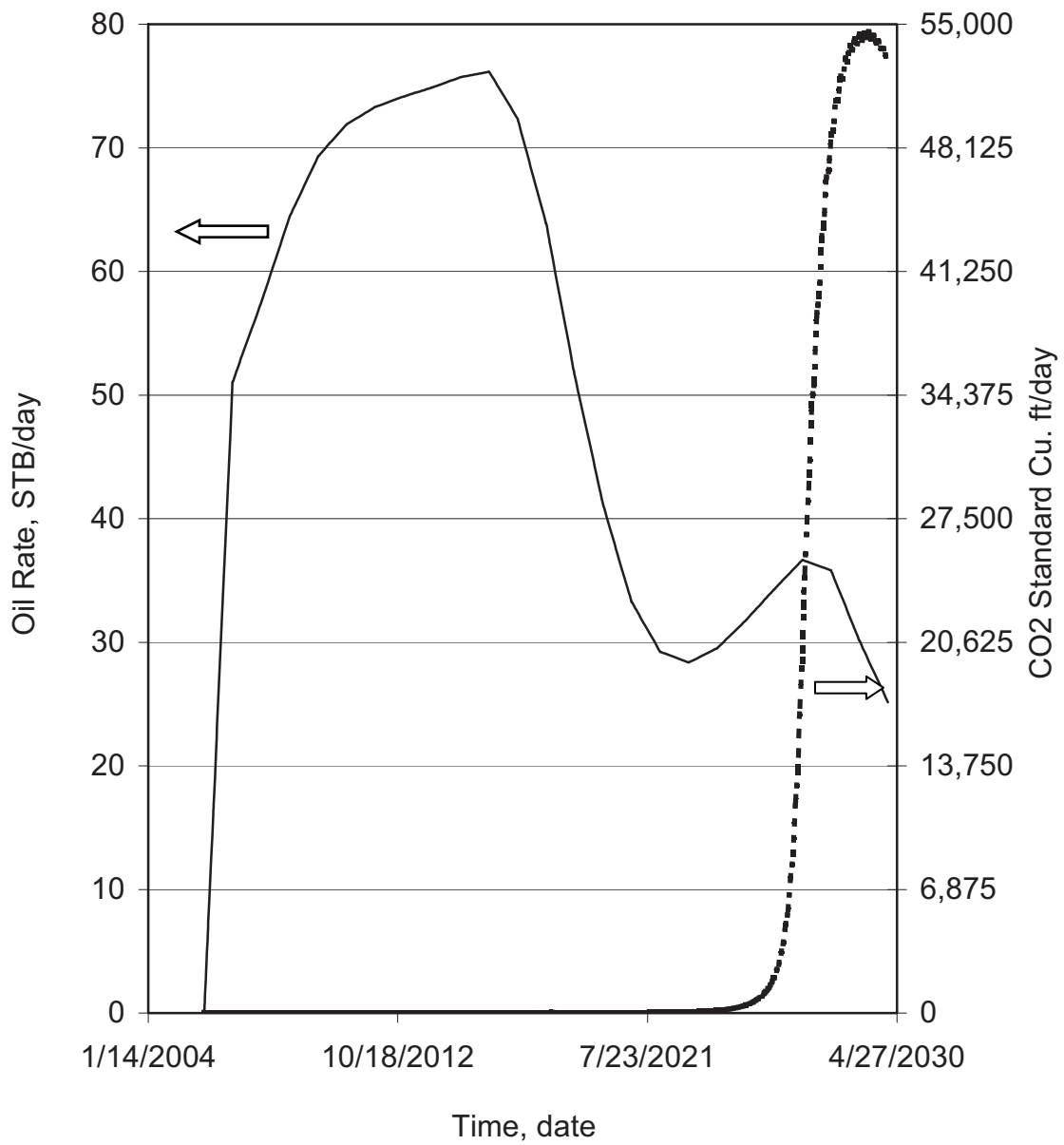


Figure 4.9. Changes in oil and CO₂ rate for 10% pore volume.

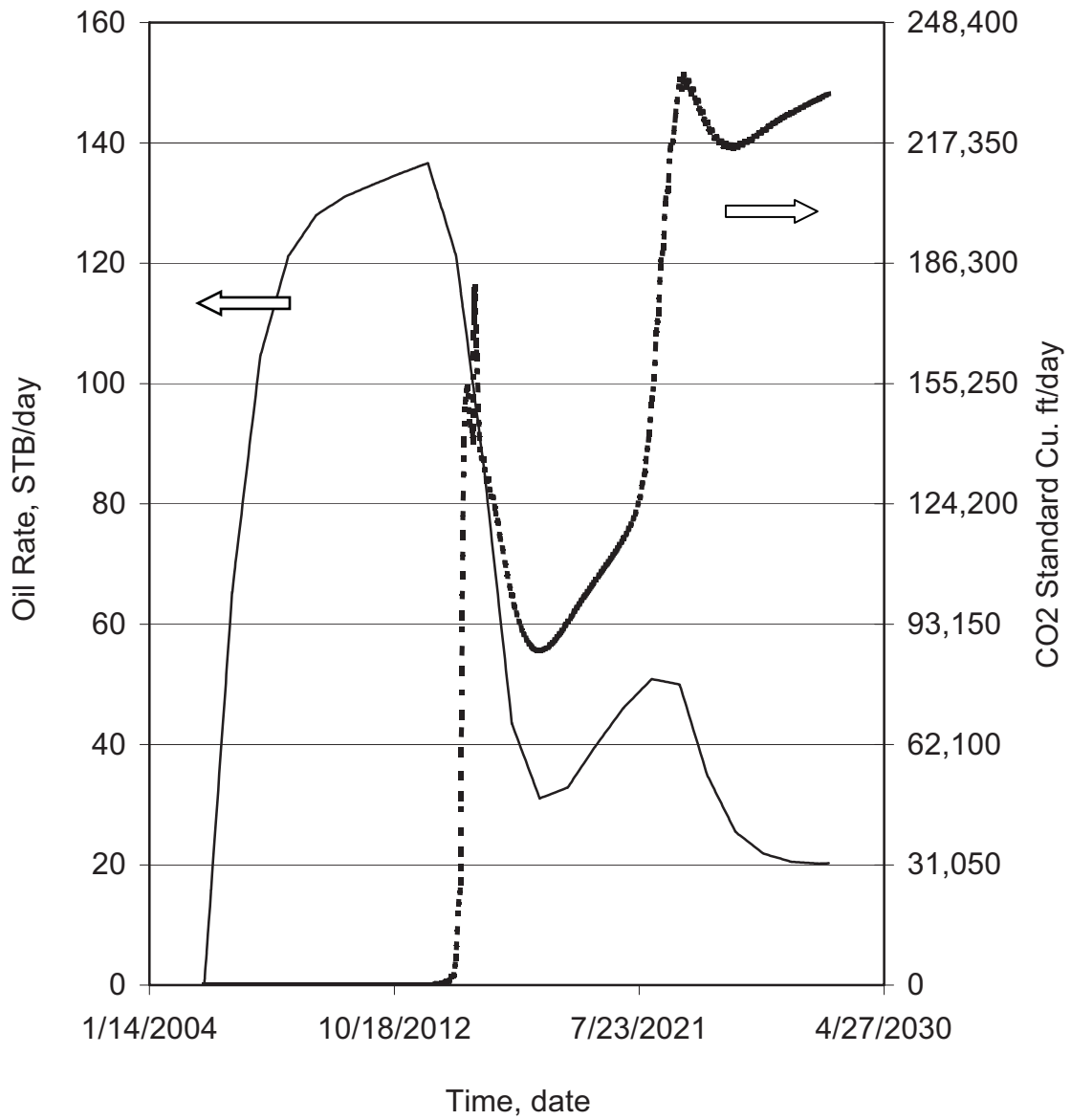


Figure 4.10. Changes in oil and CO₂ rate for 20% pore volume.

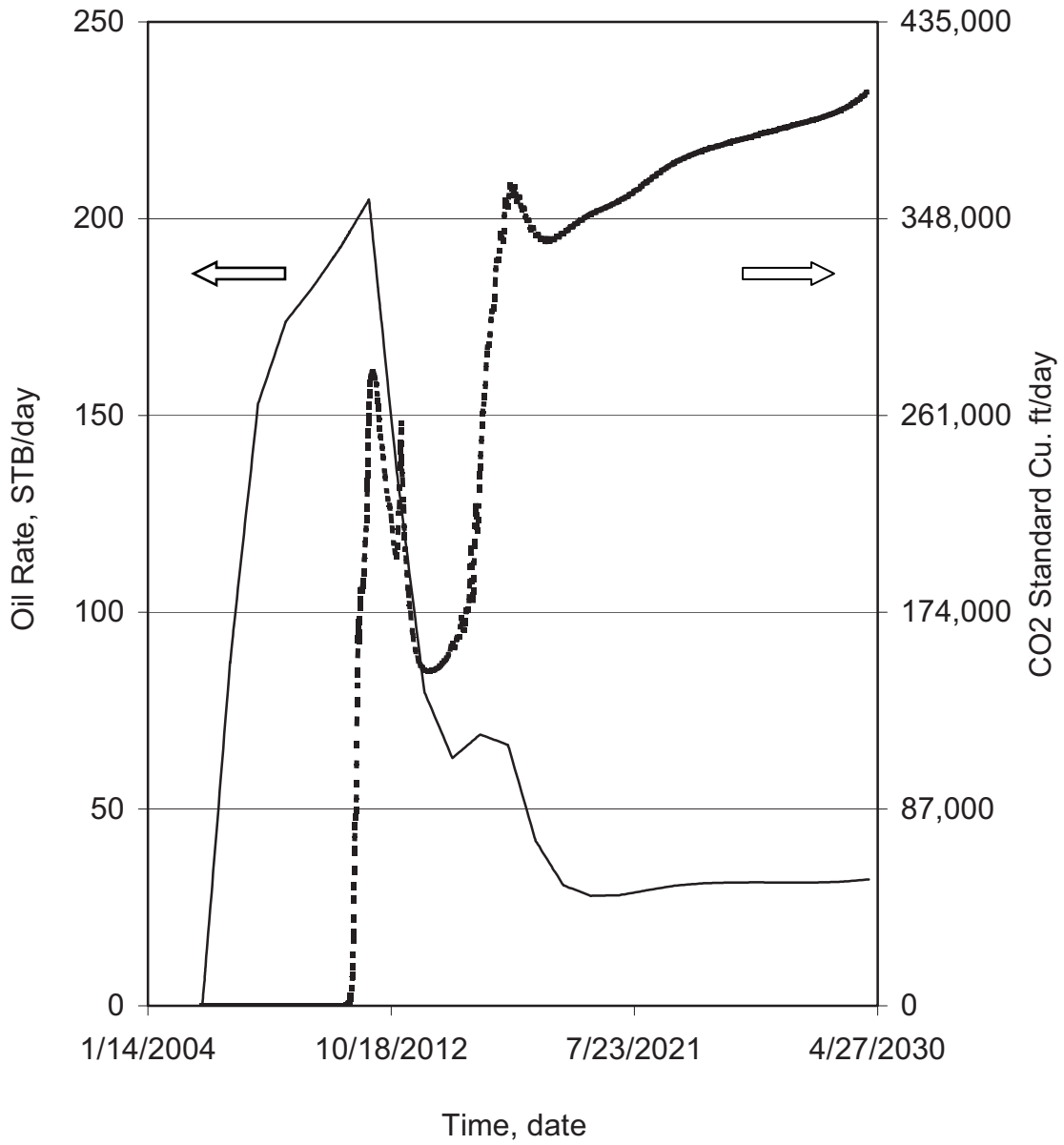


Figure 4.11. Changes in oil and CO₂ rate for 30% pore volume.

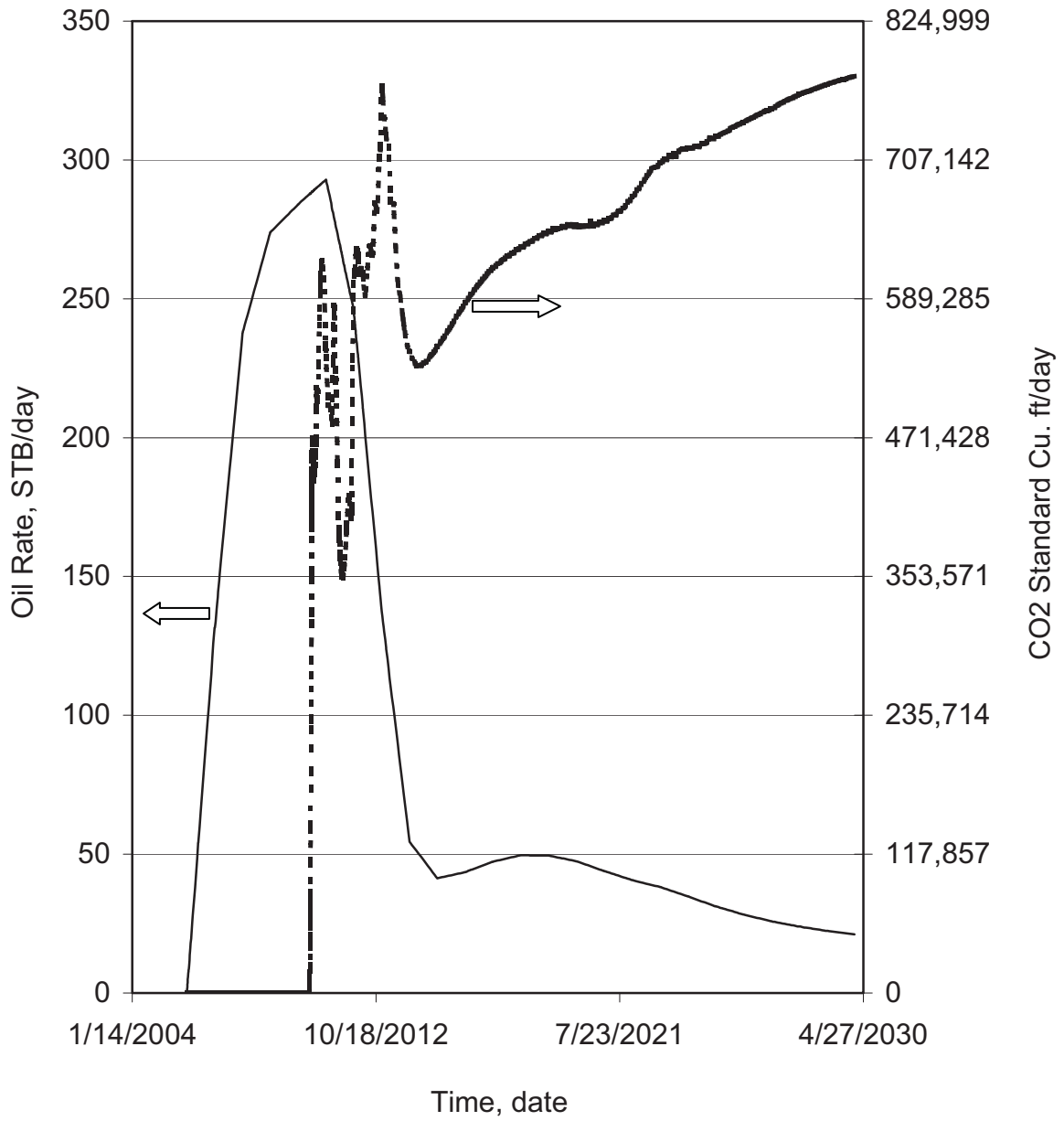


Figure 4.12. Changes in oil and CO₂ rate for 50% pore volume.

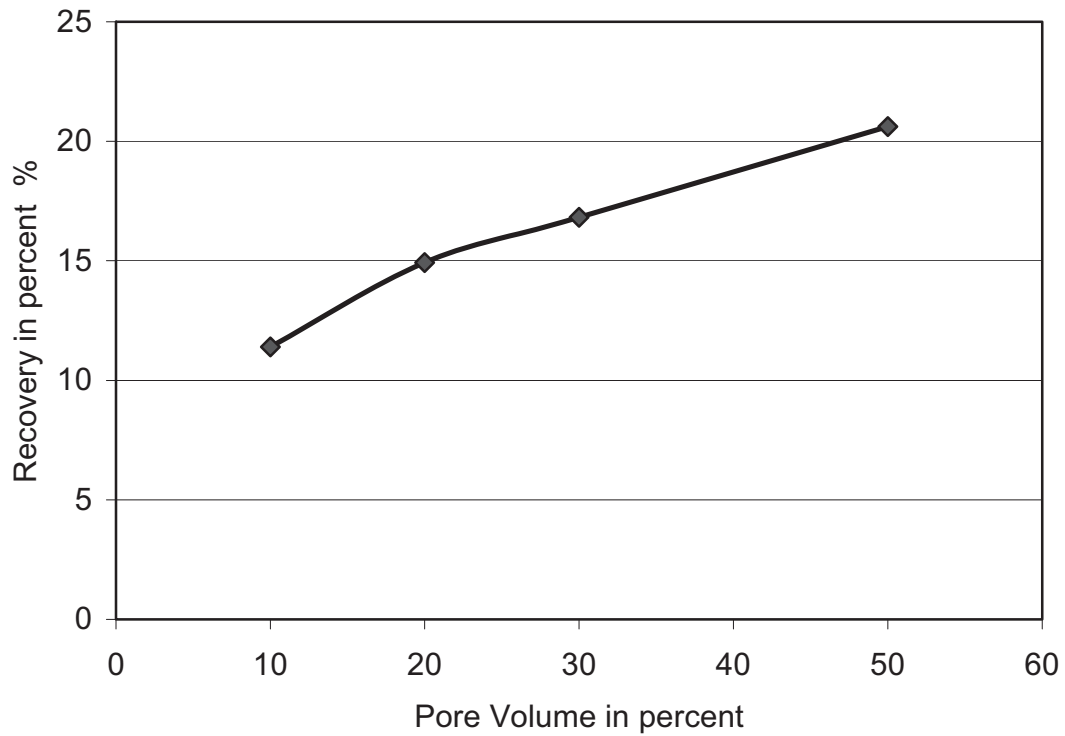
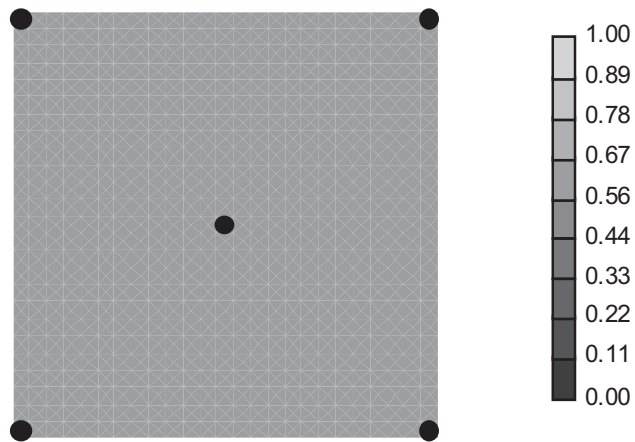
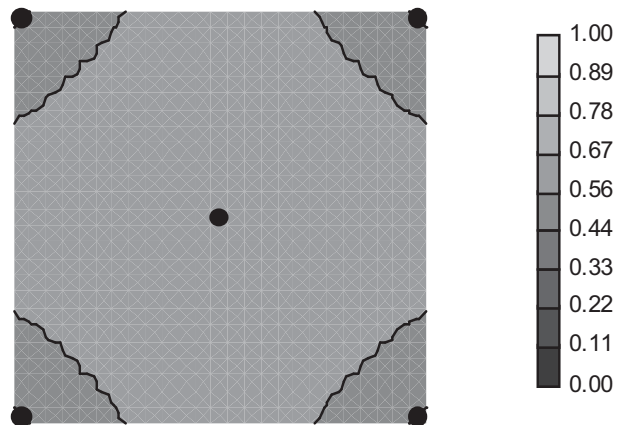


Figure 4.13. Percent of oil recovery versus injected pore volume.

Figure 4.14 (a–d) illustrates the oil saturation profile for the 10% PV injection case at different time (t) intervals. Due to the size of the grid in this case, the oil saturation profile fails to show the viscous fingering phenomenon, which is observed when the viscous phase is displaced by a lighter phase. Since the length of the viscous finger is smaller than the grid size of the model, the oil and CO₂ gas are assumed to mix instantly in each coarse grid block. The viscous fingering can be seen if the finer size grid system is selected, but it substantially increases the time and, in turn, the cost of simulation.

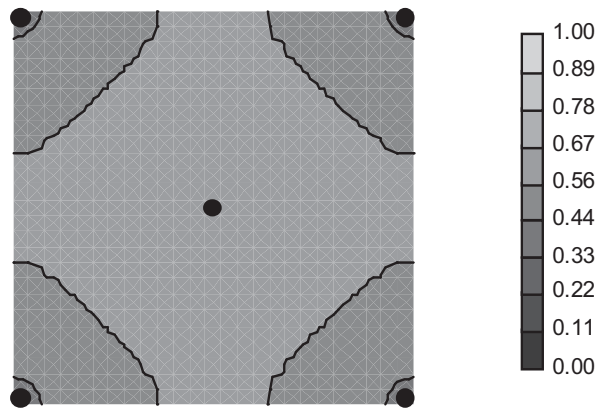


(a) $t = 0$ years

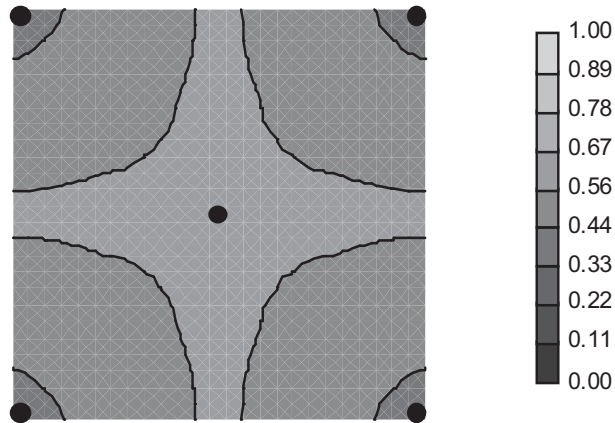


(b) $t = 4$ years

Figure 4.14 (a–b). Oil saturation profile for 10% pore volume injection.



(c) $t = 8$ years



(d) $t = 18$ years

Figure 4.14 (c–d). Oil saturation profile for 10% pore volume injection.

Chapter 5

Economic Analysis of CO₂-EOR

5.1 Review of Economic Analysis Study

Borchiellini, Massardo, and Santarelli (2002) carried out economic analysis and optimization of three existing power plants in Italy by considering effects of CO₂ sequestration versus carbon tax. In this study, the Environomics technique was used to create the thermoeconomic (i.e., thermodynamics and economics) objective function in which classic thermoeconomic arguments were extended to include the economic aspect of environmental pollution. Various components of the objective function included capital cost, cost of the fuel, cost of the CO₂ pollution abatement components, cost of the resources used for the abatement (such as water, limestone, and ammonia), and cost of environmental pollution resulting from the cost of operation. Non-linear programming was used to minimize the objective function to optimize the field of energy system. Since the cost of CO₂ disposal and compression as well as CO₂ tax are difficult to estimate, each of these costs was considered as a parameter. For CO₂ sequestration, a parametric cost analysis based on capital cost was considered in the objective function. This approach is overly complicated, as it involves non-linear programming.

As part of the Australian Petroleum Cooperative Research Centre's GEODISC project, Allinson and Nguyen (2002), performed an economic evaluation of CO₂ storage in underground reservoirs by taking into account various uncertainties linked to the costs of storing CO₂. This evaluation, based on the uncertain nature of influencing parameters, was found to be sensitive to market prices of equipment and services, physical properties of the underground reservoirs, and CO₂ flow rates. Sensitivity analysis of each parameter was carried out, followed by the Monte Carlo simulation technique, to determine probability distribution of the CO₂ storage costs with respect to the variations in each input parameter. One hypothetical 22-year CO₂ storage project example was formulated to illustrate the

sensitivity of present value of costs in US\$/ton of CO₂ injected to changes in engineering and economic inputs.

Figure 5.1, generated by Monte Carlo analyses, shows the capital cost of CO₂ storage of the hypothetical project could fluctuate between US \$412 million with more than 90% confidence and US \$734 million with 10% confidence and more. The same study for other gases (N₂, CH₄, NO_x, SO_x, and H₂S) showed that storage economics was also a function of composition of the gases that were being stored.

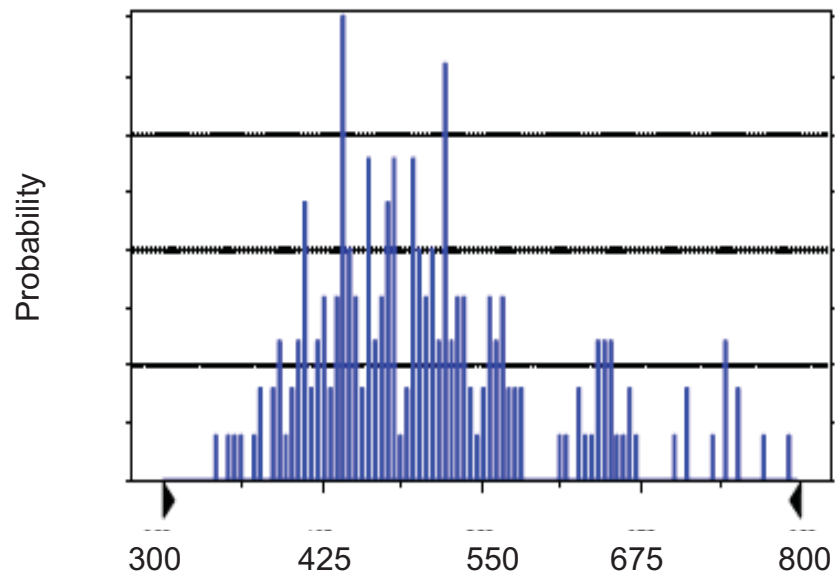


Figure 5.1. Probability distribution of capital cost of CO₂ storage project (modified after Allinson & Nguyen, 2002).

Transportation cost of any CO₂ pipeline is a useful parameter, as this cost will always be part of the CO₂ sequestration project. This cost is mainly influenced by the terrain. For example, a pipeline built on mountainous terrain would be costlier than on flat terrain. For such conditions, the shortest-distance analysis method in GIS could assist the project designer to decide which path should be chosen for gas transport. Removing any water

content present in the gas should minimize corrosion of pipelines due to CO₂, hence reducing operating costs of the transportation. Skovholt (1993) performed a screening study to understand transportation of CO₂ over large distances with a reasonable unit cost. The unit cost of the pipeline could be minimized by properly controlling aspects such as transportation conditions, flow capacity, and pipeline construction methods.

Work by Rubin and Rao (2003) reviewed the key determinates of the CO₂ control-cost estimates by defining system boundary, technology, time frame, unreported assumptions to calculate capital cost, and operating costs of a carbon capture and storage (CCS) project. Assumptions for the capacity factor of the capture plant and efficiency of the power plant should be transparent to avoid any misunderstanding of CCS economics. Furthermore, in a case study of a new pulverized plant with an amine-based CO₂ capture unit, Rubin and Rao (2003) illustrated the effect of the uncertainties on CO₂ control cost by using a computer model developed by the U.S. Department of Energy.

Senior, Adams, Espie, and Wright (2004) analyzed the capital investment requirements for a large-scale CCS project, along with the emission reductions, to evaluate when and how CCS should be deployed in the power sector. The authors overviewed costs and cost drivers for capture, transportation, and storage, as given in Table 5.1, which could act as the basis for any CCS project.

Table 5.1

Overview of Carbon Capture and Storage Project Costs and Cost Drivers (modified after Senior, Adams, Espie, & Wright, 2004)

Segment	Costs, \$/ton of CO ₂	Common Cost Drivers	Specific Cost Drivers
Capture	5-90	Volume of CO ₂ Location Onshore/Offshore	Type of Sources Retrofit
Transportation	0-20		Distance from sink Existing infrastructure Ship vs. pipeline
Storage	2-12		Existing infrastructure Size of storage field Monitoring requirements

Similarly, Pike (2006) provided the cost of a carbon sequestration project with or without CO₂ capture for geological storage and EOR projects for natural gas combined cycle, pulverized coal, and integrated gasification combined types of power plants. For a natural gas combined power plant with geological storage, the cost of CCS would be US \$0.04–\$0.08 per kWh of energy produced, while the cost of CCS combined with EOR would be US \$0.04–\$0.07 per kWh. The CCS costs were the highest for a pulverized-coal type power plant. Thus selection of type of new power plant, closer to the deemed sequestration site, is important for any future CCS project.

In 1991, British Coal began a program to develop fossil fuel power generation and integral CO₂ removal and disposal. In this study, a range of different options were studied, such as CO₂ disposal options, options for power plants, and CO₂ separation process and disposal route options. Summerfield, Goldthorpe, Williams, and Sheikh (1993) showed that the cost of CO₂ disposal contributed to a large portion of the cost of a low-CO₂ generation

system. The cost of CO₂ transport and removal ranged from around £18-£108 per ton (US \$33-\$203/ ton) of CO₂ emission avoided, depending on the type of power plant, and the CO₂ separation and disposal options.

The price of oil always determines the present value of any CCS project with EOR. Morgan (2005) performed stochastic modeling as a prediction of future Canadian oil prices. It has inherent flaws due to its dependency on fluctuating supply and demand. In the stochastic model, changes in oil price are set as a function of difference between the current spot price and mean-reversion price, reversion rate, and price volatility. Such stochastic modeling of oil prices is essential in predicting the future trend of oil-price fluctuation, which is essential for decision makers when deciding the fate of a CO₂-EOR project. Similar future studies could be useful in understanding fluctuation in oil prices in the US.

Net present value (NPV) is considered to be the most accepted economic index in the oil industry. Cash flows, lifetime of the project, and time value of the money are included in the calculation of NPV. NPV is a measure of profit, and thus, yields a direct measure of the success of a project. To determine economic feasibility, a study based on the NPV and sensitivity analysis of the CO₂-EOR project in a small mature Brazilian oil field was carried out by Gasper, Suslick, Ferreira, and Lima (2005). NPV of the project was calculated by taking into account the capital expenditures, operating expenditures, price of oil, CO₂ credits, and taxes, and the capture, transport, and storage costs of the CO₂ injection in a cash-flow model. Initial investment arising from the capture from a fertilizer plant, compression, and storage and transport of CO₂ gas was included as capital expenditure of the project. The NPV of the project, at a discount rate of 12%, was calculated to be \$3.2 million, which is significant for the small field.

On the other hand, GIS-based carbon management can also be used to select economically feasible EOR projects. One such study by Dahowski, Dooley, Brown, and

Stephan (2001) developed a GIS-based carbon management strategy to economically screen oil reservoirs amendable to EOR.

Though the United States does not provide incentives like CO₂ credits to the industries for abatement of CO₂ emissions, introduction of such CO₂ credits in the near future is highly possible due to increased public concern over global warming. Once such credits are started for CO₂ abatement, net carbon flow calculations must be performed to deduct the amount of sequestered CO₂ that otherwise would be released into the atmosphere.

5.2 Method for Economic Feasibility of CO₂ Sequestration with EOR

In this part of the study, an economical analysis of the CO₂-EOR project was carried out to evaluate the feasibility of CO₂ sequestration with EOR. A cost for each stage of CO₂-EOR project includes:

- a. Capital Expenditures (CAPEX) that include initial investments for transportation, capture, compression, and storage of CO₂
- b. Operating Expenditures (OPEX), which include labor and maintenance costs for transportation, capture, compression, and storage of CO₂

Apart from the CAPEX and OPEX, the economics of the CO₂-EOR project are also influenced by market prices of equipment and services, life of the project, fiscal regime, price of the oil, and all the sundry costs related to the recompletion of wells and drilling. According to Gasper et al. (2005), the annual net cash flow (NCF) of a CO₂-EOR project can be calculated as follows:

$$\begin{aligned}
\text{NCF} = & [\text{Gross revenue from oil production} + \text{CO}_2 \text{ credits} - \\
& \text{Royalty} - \text{OPEX} - \text{Annual drilling or completion cost (if} \\
& \text{any)} - \text{Rental cost} - \text{Depreciation}] \times (1 - \text{Corporate} \\
& \text{tax}) + \text{Depreciation} - \text{CAPEX}
\end{aligned}
\tag{5.1}$$

In Equation 5.1, the gross revenue is the product of the oil price and production rates. The credits of CO₂ are incorporated as an additional gain by keeping in mind that the implementation of CO₂ credits in the future is inevitable by providing incentives to industries for reducing CO₂ emission by sequestration.

Simulation results were obtained from the 40-acre injection pattern of West Sak oil by using 50% PV of CO₂ injection, and multiplying the area by 75 (3000 acres) to justify the initial investment in CO₂ capture, compression, transportation, and storage. It was assumed that there were 75 five-spot injection patterns. The NPV of the 3000-acre CO₂-EOR project was calculated from the following assumptions, based on the study of Brazilian oil fields; hence assumptions were according to the Brazilian fiscal regime, as reported by Gasper et al. (2005) and illustrated in Table 5.2. The values of corporate tax, royalty, and rent were changed as per the Alaskan fiscal regime. Carbon dioxide credits in Equation 5.1 were determined by multiplying total injected CO₂ with credit-per-ton of CO₂ and storage ratio, values of which were assumed to be US \$10/ton and 0.38, respectively. The storage ratio was calculated as given in Equation 5.2:

$$\text{Storage Ratio} = \frac{\text{Quantity of CO}_2 \text{ stored}}{\text{Total quantity of CO}_2 \text{ injected}}
\tag{5.2}$$

To investigate the impact on NPV of variables such as oil price, discount rate, OPEX costs, and CO₂ credits, sensitivity analysis was performed. Values of variables and assumed

distribution are given in Table 5.3. Additionally, the Monte Carlo simulation technique in Crystal Ball[®] software was used to show the probability distribution of NPV by overcoming problems associated with a limited range of input variables. The Monte Carlo simulation technique randomly and repeatedly generates values for uncertain variables to simulate a model, and thus considers full range of uncertainty for a variable.

Table 5.2

Assumed Values of Parameters for Net Present Value Calculation

Parameter	Assumed Value for NPV
Oil Price (US \$/bbl)	50
Project Life (years)	25
Royalty	12.50%
Corporate Tax	35%
Discount Rate	12%
Rent	\$12/acre
Storage Ratio	38 %
CO ₂ Credits (US \$/ton CO ₂)	10
Capture Cost (US \$/ton CO ₂)	3
Compression Cost (US \$/tonCO ₂)	7.5
Transportation Cost (US \$/ton CO ₂)	8
Storage Cost (US \$/ton CO ₂)	3

Table 5.3

Assumed Distribution and Parameter Values of Variables for Sensitivity Analysis

Variable	Distribution	Parameter Values
Discount Rate	lognormal	mean = 12%; standard deviation = 4%
Oil Price	lognormal	mean = 50; standard deviation =10
CO ₂ Credits	lognormal	Mean =10;standard deviation = 5
Storage Cost	triangular	1.5; 3; 4.5
Capture Cost	triangular	1.5; 3; 4.5
Compression Cost	triangular	6; 7.5; 9
Storage ratio	normal	mean = 38%; standard deviation = 10%
Transportation Cost	triangular	6; 8; 10

5.3 Economic Benefits and Incremental NPV of CO₂-EOR

Time value of the project by calculating NPV was used to evaluate the economical feasibility of CO₂-EOR. Comparison of NPV of CO₂-EOR with and without CO₂ credits was essential to understanding how important the introduction of CO₂ credits is to making CO₂ flooding projects economically successful. Figure 5.2 shows the comparison of NPV of the CO₂-EOR project with and without CO₂ credits. It was found that for 3000 acres CO₂-EOR, 1.37 million tons (average) of CO₂ per annum was injected, and 38% of that injected CO₂ was stored in the reservoir formation. If the operating oil company were awarded US \$10 for each ton of CO₂ stored, then for a 25-year project life with CO₂ credits, NPV would be US \$26.90 million higher than a project without CO₂ credits.

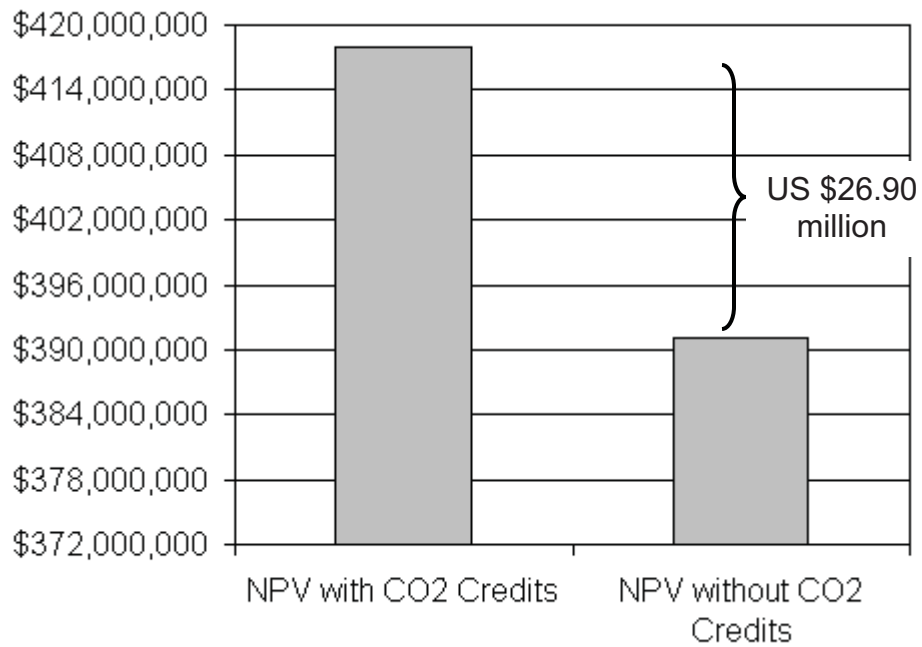


Figure 5.2. Net present value (NPV) with and without CO₂ credits.

Sensitivity analysis of variables that influence NPV of the CO₂-EOR project is given in Figure 5.3, which shows that an increase in market price of oil by US \$1 could increase NPV by 45.5%, while an increase in the discount rate would decrease NPV by 52.3%. The CO₂ credits are the third influencing parameter after discount rate and oil price. Even though the impact of CO₂ credits on NPV is smaller, it can greatly increase NPV if higher CO₂ credits (more than US \$10/ton of CO₂) are considered. Probability distribution (Figure 5.4) shows that the mean of NPV would be around US \$0.44 billion. Figure 5.5 is plotted to demonstrate how the NPV would be affected if the oil price were increased from US \$50 to \$90 in \$10 increments at discount rates ranging from 8% to 15%. As the value of the discount rate increases, the NPV of a CO₂-EOR project declines for each assumed oil price.

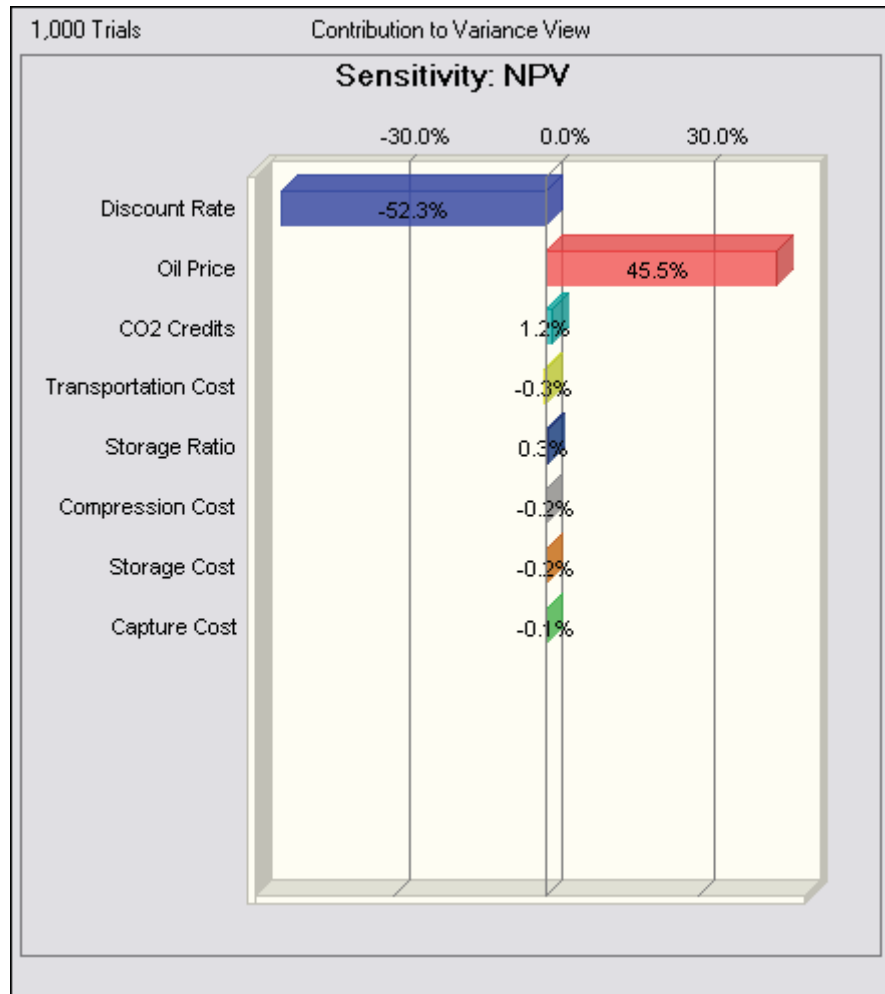


Figure 5.3. Sensitivity chart of input variables affecting net present value (NPV).

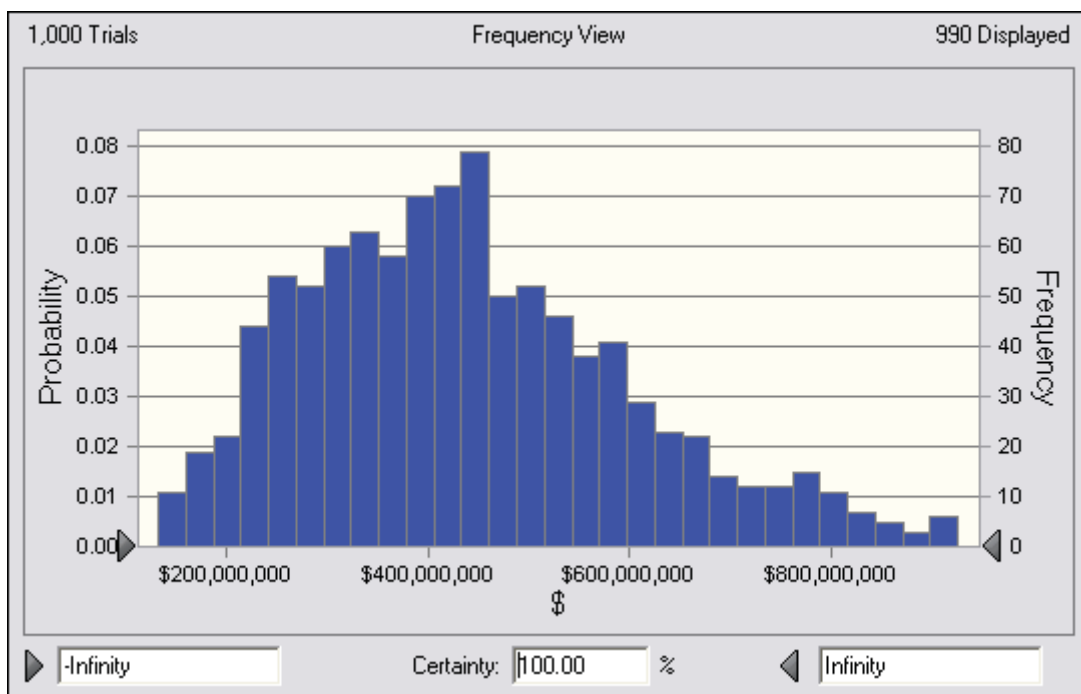


Figure 5.4. Probability distribution of net present value.

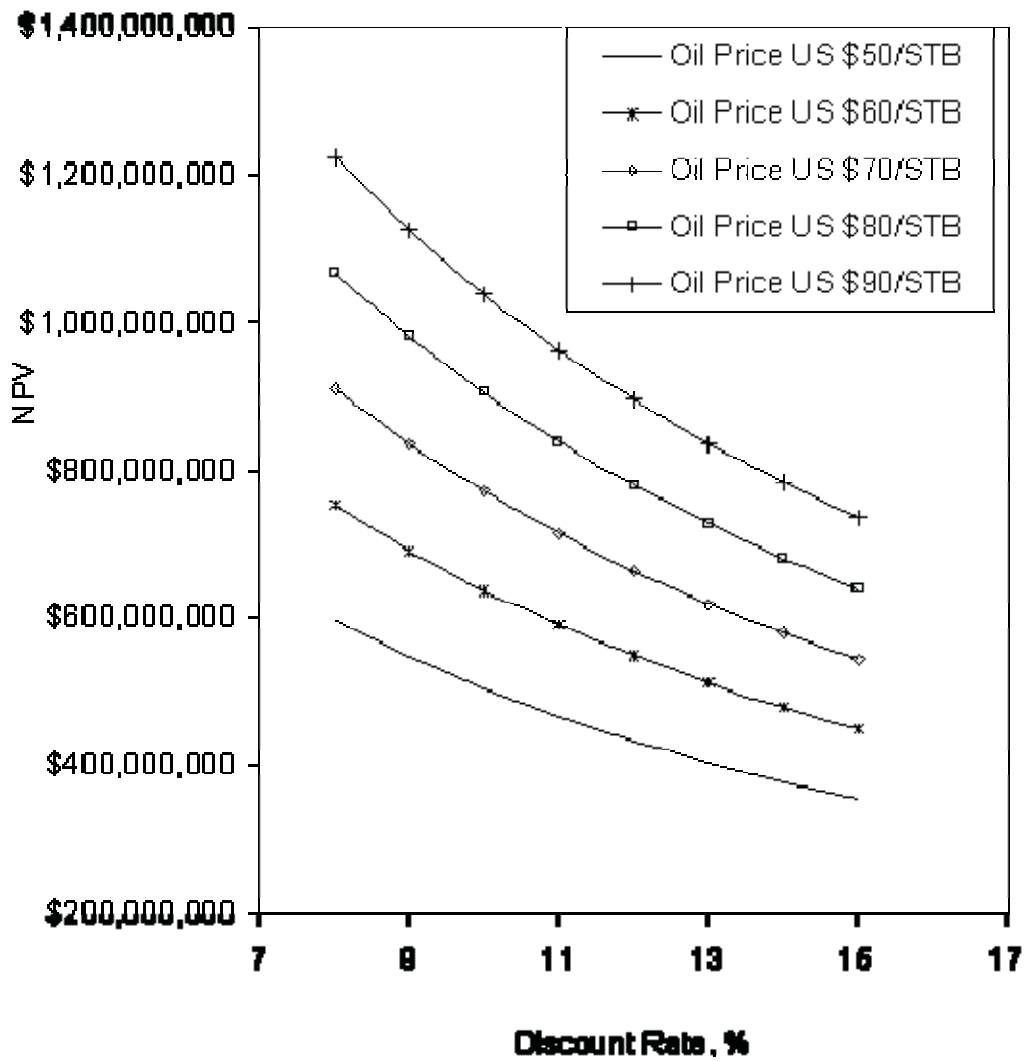


Figure 5.5. Net present value (NPV) of the CO₂-EOR project for increasing oil prices with changing discount rate.

Chapter 6

CO₂ Sequestration in a Saline Aquifer

Thick, highly permeable and porous saline aquifers with impermeable cap rock are the ideal formation targets for CO₂ sequestration. Deep and laterally extensive aquifer formations are essential for the slow flow of CO₂ gas bubbles to the top of the formation. Injected CO₂ is always less dense than the saline formation water and may migrate to the top of the formation (Benson, 2003).

The mineralogy of aquifer-formation rock dictates the geochemical binding of the CO₂ molecule to rock mineral in the form of various carbonates (Pruess, Xu, Apps, & Garcia, 2003; Sass, Gupta, Sminchal, & Bergman, 1998). Predominately, the injected CO₂ occupies the free gaseous phase in the available pore space, and some fraction of CO₂ dissolves into water. Solubility of CO₂ takes place according to Henry's Law, which is a relation between partial pressure of the dissolving gas and its concentration in the aqueous form. An increase in temperature and salinity of water decreases the solubility of gases in the aqueous phase, while an increase in pressure of the system increases solubility of gas in the water.

Whether the injected CO₂ is found in liquid, gas, or a supercritical fluid state depends on pressure and temperature. The effect of pressure at 45 °C on density and viscosity of a CO₂ + water system is given in Table 6.1 (Oostrom, Meck, & White, 2003). At 2352 psia, the density of the supercritical CO₂ (critical temperature of 31.1 °C and critical pressure of 1071.63 psia) is higher than that of 1764 psia. It is worth noting that the difference between the density of pure water and CO₂ gas decreases from 336.2 kg/m³ at 1764 psia to 235.4 kg/m³ at 2352 psia, which is important to reduce the buoyancy effect due to the large density difference.

Table 6.1

CO₂ and Water Properties at 45 °C (modified after Oostrom, Meck, & White, 2003)

Fluid Phase		1764 psia	2352 psia
Pure water	Density (kg/m ³)	994.768	996.292
	Viscosity (Pa s)	5.9778 x 10 ⁻⁴	5.98341 x 10 ⁻⁴
Water with CO ₂	Density (kg/m ³)	994.768	996.292
	Viscosity (Pa s)	5.9778 x 10 ⁻⁴	5.98341 x 10 ⁻⁴
	CO ₂ mass fraction	5.22541 x 10 ⁻²	5.70921 x 10 ⁻²
Gas	Density (kg/m ³)	658.574	760.891
	Viscosity (Pa s)	5.16820 x 10 ⁻⁵	6.56320 x 10 ⁻⁵
	Water mass fraction	9.93985 x 10 ⁻⁵	8.60323 x 10 ⁻⁵

Van der Meer (1996) studied commercial capabilities of reservoir simulators based on the Darcy flow to predict the effects of CO₂ injection in an aquifer; he compared the results with previous studies based on the user-defined equilibrium ratio value and gas-solution ratio approach. The author used the gas-water option of the SIMBEST II SSI simulator for this study. It was observed that local grid refinements, displacement front tracking methods, and inclusion of a function to describe dependency of solubility on time and salt concentration could improve simulation results.

Shan and Pruess (2004) developed an improved model over the previous TOUGH2 model, in which Henry's Law and gas diffusivity coefficients were considered constant by introducing temperature dependence of the coefficients. The importance of this study is the inclusion of temperature-dependent diffusivity and Henry's Law constant terms, which many of the gas displacement algorithms do not incorporate in their codes. This thermodynamic reliance of the coefficients is useful when there are significant variations in temperature and pressure, but it should not be used when temperature is in the range of 10 °C–20 °C; for example in the case of examining ground water problems. The new model can be used to

study CO₂ sequestration in saline aquifers, where temperature and pressure of the system vary due to the injection of CO₂.

At Lawrence Berkeley National Laboratory, Pruess et al. (2003) carried out a detailed numerical modeling study of CO₂ disposal into brackish (saline) aquifers. At the beginning of their study, the sequestration capacities using volumetric estimates were calculated. The numerical simulation showed the effect of gravity overriding because of water bypassing the CO₂-rich gas-like phase. The gravity-overriding phenomenon, due to the density difference between the water and gas phase, led to an increase in gas saturation in the vertical direction, thus decreasing the contact volume of the aquifer by CO₂ gas. For the 30-year injection of CO₂ gas in the aquifer, a CO₂ plume formed approximating a 38.61-mile² area, and the aquifer pressure increased by 14.7 psia over the 956.26-mile² area. Changes in morphology of the rock matrix and reduction in porosity due to the formation of secondary carbonates are important factors also and must be included in designing any numerical code.

A mathematical model for the CO₂ displacement studies is a set of differential equations for each grid cell, describing the conservation of mass and the superficial velocity for water, gas and oil, if present. To study simulation of CO₂ displacement and long-term storage in underground formation in general, deep saline aquifers in particular, require algorithms with multi-fluid capabilities to predict phase transitions (Oostrom et al., 2003). Modeling of CO₂ dissolution in saline aquifers should be able to take into account buoyancy-driven flow due to density difference, Rayleigh instability fingering arising from viscosities of displacing and displaced phases, aqueous dissolution, molecular diffusion, hydrodynamic dispersion, and phase transitions.

In a study by Saripalli, McGrail, and White (2003), a semi-analytical model was developed that would simulate sequestration of CO₂ in deep geological formations. Since phase-behavioral properties (e.g., density) do not change drastically with changes in

temperature, isothermal conditions were assumed in the semi-analytical model. It was concluded that the semi-analytical model could effectively simulate injection of water-immiscible, gaseous, or supercritical CO₂ into confined formations. However, semi-analytical model assumptions such as uniform formation properties and instantaneous dissolution of CO₂ in the formation water are not real-life situations. Laminar flow (low Reynold's number) of the formation water can slow the dissolution of CO₂, making the dissolution process rate limiting in the sequestration. Pacific Northwest National Laboratory's (PNNL) STOMP[®]-*Water-CO₂-NaCl* (WCS) numerical model is an advanced numerical model used to adequately simulate the dissolution non-equilibrium. STOMP[®]-WCS can simulate changes in hydrological properties, especially porosity and relative permeability. But temperature changes in the geothermal gradient of the formation due to injection of supercritical CO₂, which is necessary in the permafrost regions of the Alaskan North Slope, are needed to simulate and observe a possible increase in temperature. By including energy equations in the WCS operational mode of STOMP[®], another simulator model, represented as *Water-CO₂-NaCl-Energy* (WCSE), was generated by PNNL. In the present study, STOMP[®]-WCSE was used to simulate sequestration of CO₂ in a deep saline aquifer.

6.1 CO₂ Sequestration in a Saline Aquifer using STOMP[®]-WCSE

Advantages of injection of supercritical CO₂ (2352 psia and 45 °C) are discussed in Chapter 2. However, injection of supercritical CO₂ in the saline aquifer could be detrimental to the permafrost region when the injected heat travels through the formation by conduction or convection, possibly causing a temperature increase in the permafrost region. Deep saline aquifers with low vertical permeability should be chosen for CO₂ injection in order to minimize any heat conduction due to fluid movement.

A 2-dimensional cylindrical model (42 grids in horizontal direction and 28 grids in vertical direction) was formulated for STOMP[®]-WCSE simulation runs. Figure 6.1 illustrates

the two-dimensional model, representing four different layers. Total formation depth was 4780 ft from the top, and the model spans 5280 ft (1 mile) horizontally. According to the STOMP[®] user guide (White and Oostrom, 2003), an input file was written to include relative permeability functions, thermal properties of the formation, and permeability and porosity values of each layer. An injection of 4.40 lb/sec of supercritical CO₂ in layer #1, having a porosity of 30% and a constant permeability value of 1 darcy in both the horizontal and vertical direction, was simulated. The injection well was assumed to be perforated 100 ft in layer #1. The permeability of layers #2 and #3 was 1×10^{-6} and 0.1 darcy, respectively. At the beginning of simulation, the pressure and the temperature in the bottommost grid were 2055 psia and 39 °C, respectively. The geothermal gradient of 0.0127 °C/ft was set for layers #1, #2, #3 and water body, while the permafrost gradient was set to 0.0015 °C/ft. The geothermal gradients were calculated so that the temperature at the bottom of the permafrost region was 4 °C and the top was 0 °C. Sodium chloride mass fraction for layers 1, 2 and 3 was assumed to be 0.05, while that for permafrost and water body was set to zero. At the rate of 4.40 lb/sec, a total of 1.39×10^9 lb of CO₂ was injected in the 10-year injection period. Changes in CO₂ gas saturation and its aqueous mass fraction and temperature profile were observed for 20 years.

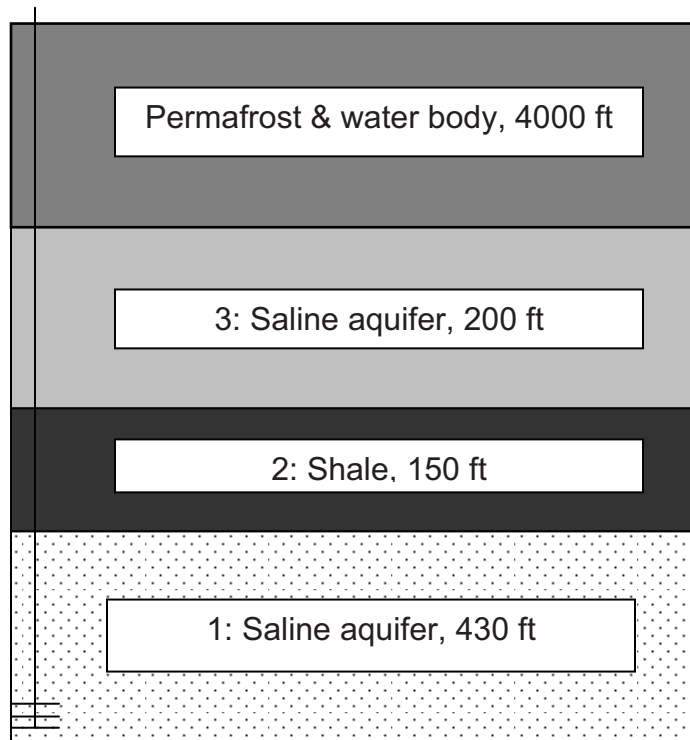


Figure 6.1. Two-dimensional cylindrical model used in Subsurface Transport Over Multiple Phases[®]-Water- CO₂-NaCl-Energy (STOMP[®]-WCSE).

6.2 Effect of CO₂ Storage on a Saline Aquifer

To observe the effect of CO₂ injection on a saline aquifer, a simulation study was carried out in STOMP[®]; 4.40 lb/sec of CO₂ were injected for a 10-year period. After simulating injection of CO₂ in a saline aquifer with STOMP[®]-WCSE, with assumed NaCl mass fraction of 0.05 at a pressure of 2352 psia and 45 °C (supercritical condition) in a 2-dimensional radial model, the changes in variables such as gas saturation, aqueous mass fraction, and temperature along the vertical distance were observed. Figures 6.2, 6.3, and 6.4 are plotted with above-mentioned variables on abscissa and vertical distance on ordinate at a radial distance of 280 ft from the injection point. Legends show the changes in

variables at different time intervals for equal permeability values in the horizontal and vertical direction.

Figure 6.2 shows the CO₂ gas saturation at time intervals of 500, 1000, 3650, and 7300 days. Up until the end of the injection period, i.e., 3650 days, the gas saturation is increasing with increase in time, which is expected, as injected gas moves along the radial distance. Ten years after the discontinuation of CO₂ injection, the gas saturation front starts receding as CO₂ gas moves vertically upward in the aquifer until it reaches a less permeable shale layer and gets trapped.

Dissolution of CO₂ gas, according to Henry's Law, can be found as an aqueous mass fraction in Figure 6.3. In Figure 6.3, the mass fraction of CO₂ in saline water follows the same trend as gas saturation for 500 and 1000 days into injection, but as the time progresses, the concentration of CO₂ in aqueous form increases in vertical direction as gas moves and gets dissolved in the upper layer. It is worth mentioning that leakage of CO₂ from layer #1 was zero; thus overlaying a less-permeable layer provides a seal against upwardly migrating CO₂.

Figure 6.4 illustrates the temperature profile for the same CO₂ injection scenario. Due to the supercritical nature of injected CO₂, the heat of the injection is transferred in a radial direction only along with movement of a supercritical gas, as can be seen in Figure 6.4, which represents the changes in the temperature profile in the saline aquifer region of the model. The geothermal temperature gradient in the permafrost region (from 0 °C to 4 °C) remains the same at all time intervals.

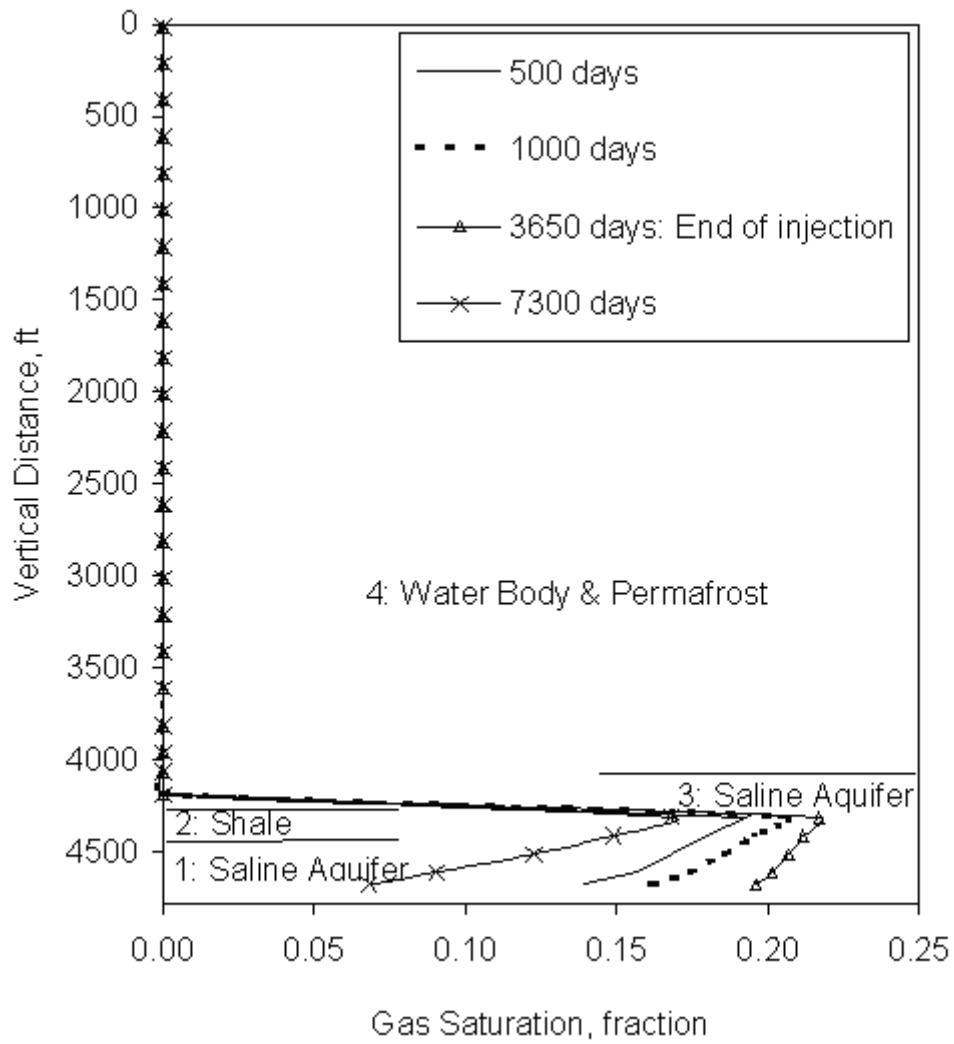


Figure 6.2. Gas saturation at a horizontal distance of 280 ft from the injection well.

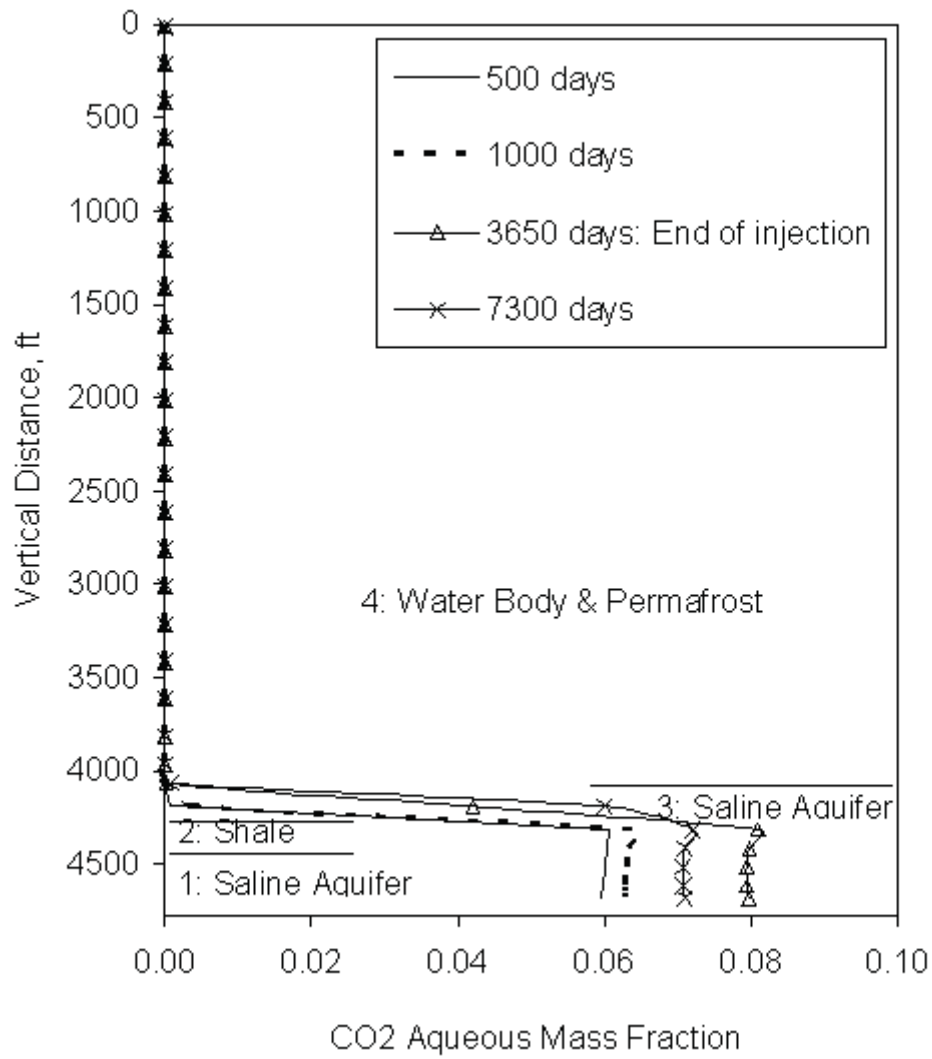


Figure 6.3. CO₂ aqueous fraction at a horizontal distance of 280 ft from an injection well.

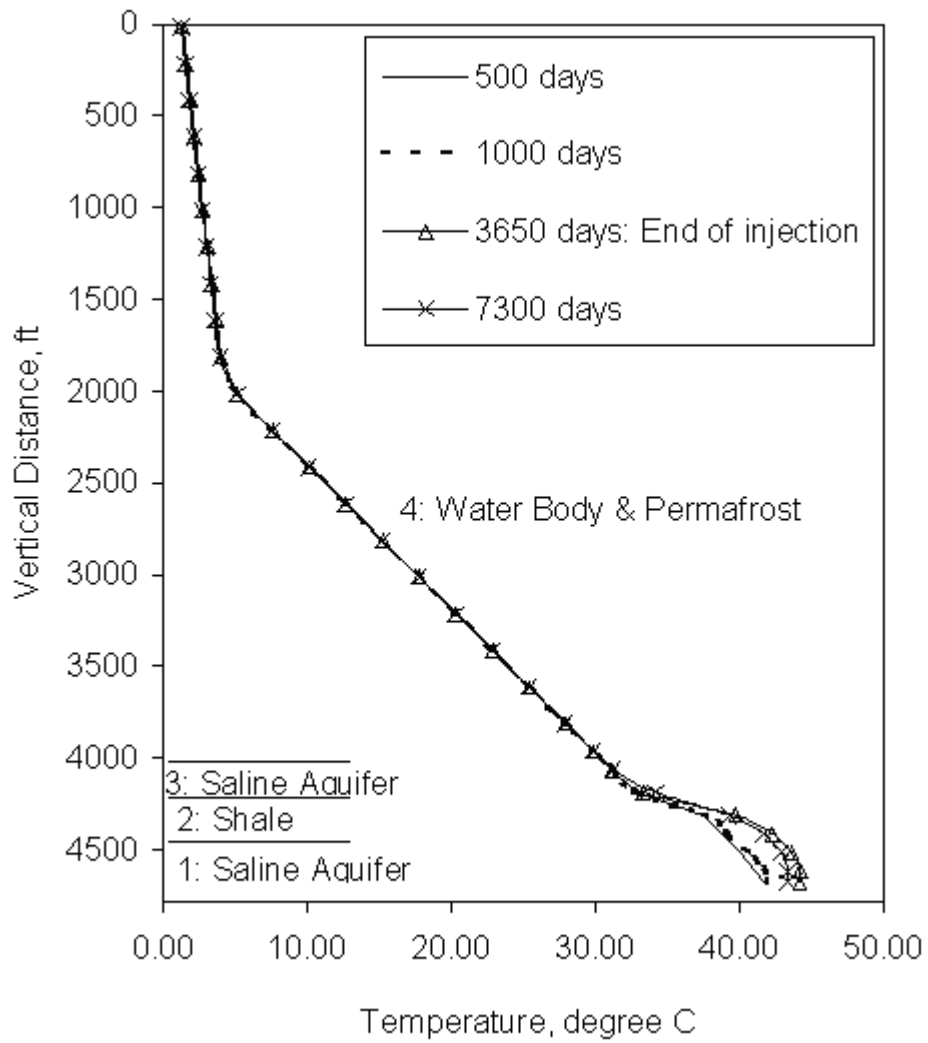


Figure 6.4. Temperature profile at a horizontal distance of 280 ft from an injection well.

Chapter 7

Conclusions and Recommendations

The conclusions derived from this study are contained in Section 7.1. Recommendations for future work are given in Section 7.2.

7.1 Conclusions

- Weight-assigned parameters such as temperature, pressure, and average petrophysical properties of the oil pools are important in carrying out rudimentary screening of potential oil pools on the ANS with respect to their amenability to CO₂-EOR.
- At the reservoir pressures typical of the West Sak oil pool, the presence of partial miscibility can be determined through phase-behavior study.
- Oil recovery by continuous CO₂ injection for 25 years predicted 20.62% oil recovery when 50% PV of CO₂ was injected. An increase in PV led to a decrease in CO₂ storage ratio.
- Economical analysis of CO₂-EOR proved to be important in estimating the time value of the project. The NPV of the project with CO₂ credits was found to be higher by US \$26.90 million than NPV without CO₂ credits.
- At a rate of 4.40 lb/sec, a saline aquifer can successfully sequester CO₂ with no leakage. Changes in the temperature profile were negligible when supercritical CO₂ was injected in a saline formation with a NaCl mass fraction of 0.05.

7.2 Recommendations

Characterization studies of all Alaskan coal beds, depleted oil, and gas pools could be performed to estimate the sequestration capacity and to screen out potential geological storage sites.

Complete characterization of the live West Sak oil could be helpful in describing a miscibility condition accurately. Due to the vast nature of the West Sak reservoir, a small pilot area for which the production history is available could be selected to perform compositional simulation and history matching.

There are many disposal wells on the ANS in which to inject generated waste into saline formation. The locations of these wells should be chosen in such a way that there is no migration of fluids due to structural traps and faults. The formation of physical properties of a saline aquifer would be important in using STOMP[®] to simulate true migration of CO₂ gas and observe temperature changes. Geochemical binding of CO₂ with rock could be predicted by developing a module in STOMP[®], as chemical uptake of CO₂ over the long-term is also crucial for sequestration studies.

Acknowledgment

The material was prepared with financial support from the Arctic Energy Office, National Energy Technology Laboratory, U.S. Department of Energy. Their support is highly appreciated.

References

- Abrishami, Y., Hatamian, H., & Dawe, R. A. (1997). Tuning of Peng-Robinson equation of state for simulation of compositional change in flue gas injection processes. *Fluid Phase Equilibria*, 139(1), 219-254.
- Ahmed, T. H. (1997). A generalized methodology for minimum miscibility pressure. *Proceedings of the SPE Latin American and Caribbean Petroleum Engineering Conference*, SPE paper 39034.
- Alaska Oil and Gas Conservation Commission (AOGCC). (2003). *Annual Report*. (Revised June 8, 2004). Retrieved February 26, 2006, from <http://www.state.ak.us/admin/ogc/annual/2003/2003annindex.htm>.
- Allinson, G., & Nguyen, V. (2002). CO₂ geological storage economics. *Proceedings of the Sixth International Conference on Greenhouse Gas Control Technologies*, 615-620.
- Bachu, S., & Shaw, J. (2003). Evaluation of the CO₂ sequestration capacity in Alberta's oil and gas reservoirs at depletion and the effect of underlying aquifers. *Journal of Canadian Petroleum Technology*, 42(9), 51-61.
- Bachu, S., & Stewart, S. (2002). Geological sequestration of anthropogenic carbon dioxide in the Western Canada sedimentary basin: Suitability analysis. *Journal of Canadian Petroleum Technology*, 41(2), 32-40.
- Bakshi, A. K. (1991). *Computer modeling of CO₂ stimulation in West Sak reservoir*. Unpublished master's thesis, University of Alaska Fairbanks, Fairbanks, AK.
- Bakshi, A. K., Ogbe, D. O., Kamath, V. A., & Hatzignatiou, D. G. (1992). Feasibility study of CO₂ stimulation in the West Sak field, Alaska. *Proceedings of the SPE Western Regional Meeting*, SPE paper 24038.
- Benson, S. (2003). *Geologic sequestration of carbon dioxide*. Retrieved July 12, 2006, from <http://www.nap.edu/openbook/0309089212/html/29.html>.

- Bhandari, R. (1988). *Prediction of phase behavior and miscibility conditions for West Sak crude-solvent mixtures*. Unpublished master's thesis, University of Alaska Fairbanks, Fairbanks, AK.
- Borchiellini, R., Massardo, A. F., & Santarelli, M. (2002). Carbon Tax vs. CO₂ effects on environmental analysis of existing power plants. *Energy Conversion and Management*, 43(9-12), 1425-1443.
- Bossie-Cordreanu, D., & Gallo, Y. L. (2004). A simulation method for the rapid screening potential depleted oil reservoirs for CO₂ sequestration. *Energy*, 29(9-10), 1347-1359.
- Brush, R. M., Davitt, H. J., Aimar, O. B., Jorge Arguello, S. A., & Whiteside, J. M. (2000). Immiscible CO₂ flooding for increased oil recovery and reduced emissions. *Proceedings of the SPE/DOE Improved Oil Recovery Symposium*, SPE paper 59328-MS.
- Coats, K. H., & Smart, G. T. (1986). Application of a regression-based EOS PVT program to laboratory data. *SPE Reservoir Engineering* 1(3), SPE paper 11197, 277-299.
- Dahowski, R. T., Dooley, J. J., Brown, D. R., & Stephan, A. J. (2001). Economic screening of geologic sequestration options in the United States with a carbon management Geographic Information System. *Proceedings of the Eighteenth Annual International Pittsburgh Coal Conference*.
- Danesh, A. (1998). *PVT and phase behavior of petroleum reservoir fluids (developments in petroleum science)*. Elsevier Science.
- Doleschall, S., Szittar, A. and Udvardi, G. (1992). Review of the 30 years experience of the CO₂ imported oil recovery projects in Hungary. *Proceedings of the SPE International Meeting in Beijing, China*, SPE paper 22362.
- Domitrović, D., Šunjerga, S., & Jelić-Belta, J. (2004). Numerical solution of tertiary CO₂ injection at Ivanić oil field, Croatia. *Proceedings of the SPE/DPE Fourteenth Symposium on Improved Oil Recovery*, SPE paper 89361.

- Energy Information Administration (EIA). (2005). *Emissions of Greenhouse Gases in the United States 2004* (DOE/EIA-0573, 2004).
- Energy Information Administration (EIA). (2001). *State energy-related carbon dioxide emissions by energy sectors*. Retrieved June 30, 2006, from http://www.eia.doe.gov/oiaf/1605/ggrpt/pdf/appc_tbl2.pdf.
- Gaspar, A. T. F. S., Suslick, S. B., Ferreira, D. F., & Lima, G. A. C. (2005). Economic evaluation of oil production project with EOR: CO₂ sequestration in depleted oil fields. *Proceedings of the SPE Latin American and Caribbean Petroleum Engineering Conference*, SPE paper 94922.
- Holm, W. L. (1987). Evolution of the carbon dioxide flooding processes. *Journal of Petroleum Technology*, 39(11), 1337-1342.
- Holtz, M. H., Nance, P. K., & Finley, R.J. (1999). *Reduction of greenhouse gas emissions through underground CO₂ sequestration in Texas oil and gas reservoirs*. Retrieved February 26, 2006 from <http://www.beg.utexas.edu/enviro/qly/abndnhydrores/co2text.pdf>.
- Klins, M. A. (1984). Carbon dioxide flooding: Basic mechanisms and project design. *International Human Resources Development Corporation*.
- Klins, M. A., & Farouq Ali, S. M. (1981). Oil Production in shallow reservoirs by carbon dioxide injection. *Proceedings of the Eastern Regional Meeting of the Society of Petroleum Engineers of AIME*, paper 10374.
- Kovscek, A. R. (2002). Screening criteria for CO₂ storage in oil reservoirs. *Petroleum Science and Technology* 24(7-8), 841-866.
- Malik, Q. M., & Islam, M. R. (2000). CO₂ injection in the Weyburn field of Canada: optimization of enhanced oil recovery and greenhouse gas storage with horizontal wells. *Proceedings of the SPE/DOE Improved Oil Recovery Symposium*, SPE paper 59327.

- McGuire, P. L., Redman, R. S., Jhaveri, B. S. Yancey, K. E., & Ning, S. X. (2005). Viscosity reduction WAG: An effective EOR process for North Slope viscous oils. *Proceedings of the SPE Western Regional Meeting*, SPE paper 93914.
- Morgan, M. D. (2005). A model of Canadian oil and gas price fluctuations. *Journal of Canadian Petroleum Technology*, 44(7), 48-54.
- Oostrom, M., Meck, D. H., & White, M. D. (2003). *STOMP: Subsurface Transport Over Multiple Phases [Version 3.0], an introductory short course*. Prepared for the U.S. Department of Energy under Contract DE-AC06-76RL01830, Pacific National Laboratory.
- Panda, M. N., Zhang, M., Ogbe, D. O., Kamath, V. A., & Sharma, G. D. (1989). Reservoir description of West Sak sands using well logs. *Proceedings of the SPE California Regional Meeting*, SPE paper 18759.
- Patil, S. B. (2006). Investigation of CO₂ sequestration options for Alaskan North Slope with emphasis on oil recovery. Unpublished master's thesis, University of Alaska Fairbanks, Fairbanks, AK.
- Peng, D. Y., & Robinson, D. B. (1976). A new two-constant equation of state. *Ind. Eng. Chem. Fundam.*, 15, 59-64.
- Pike, R. (2006). Technology tomorrow: The chemistry of carbon capture and storage. *Journal of Petroleum Technology*, 58(6), Editorial.
- Pruess K., Xu, T., Apps, J., & Garcia, J. (2003). Numerical modeling of aquifer disposal of CO₂. *Proceedings of the SPE/EPA/DOE Exploration & Production Environment Conference*, SPE paper 83695.
- Research Institute of Innovative Technology for the Earth (RITE). (2004). *Overview of the CO₂ geological sequestration system*. Retrieved January 26, 2006 from <http://www.rite.or.jp/English/lab/geological/geological.html>.

- Rivas, O., Embid, S., & Bollvar, F. (1992). Ranking reservoirs for carbon dioxide flooding processes. *SPE Advanced Technology Series 2(1)*, SPE paper 23641.
- Robinson, D. B., & Peng, D. Y. (1978). The characterization of the heptanes and heavier fractions. *Research Report 28, Gas Producers Association*. Tulsa, Oklahoma.
- Roper, M. (1989). An experimental study of CO₂ /West-Sak-crude-oil phase behavior. Unpublished master's thesis, University of Alaska Fairbanks, Fairbanks, AK.
- Rubin, E. S., & Rao, A. B. (2003). Uncertainties in CO₂ capture and sequestration costs. *Proceedings of the Seventh International Conference on Greenhouse Gas Control Technologies*, 3, 1119-1124.
- Saner, W. B. and Patton, J. T. (1983). CO₂ recovery of heavy oil: Wilmington field test. *Proceedings of the SPE Annual Technical Conference and Exhibition*, October 5-8, 1983, San Francisco, CA, SPE 12082.
- Saripalli, P. K., McGrail, B. P., & White, M. D. (2003). *Modeling the sequestration of CO₂ in deep geological formations*. Prepared for the U.S. Department of Energy under Contract DE-AC06-76RL01830, Pacific National Laboratory.
- Sass, B., Gupta, N., Sminchal, J., & Bergman, P. (1998). Geochemical modeling to assess the capacity of a Midwestern United States geological formation for CO₂ sequestration. *Greenhouse Gas Control Technologies*, 1079-1086.
- Senior, B., Adams, J., Espie, T., & Wright, I. (2004). Investigation of capture and storage could evolve as a large scale CO₂ mitigation option. *Proceedings of the Seventh International Conference on Greenhouse Gas Control Technologies*.
- Shan, C., & Pruess, K. (2004). EOSN-a new TOUGH2 module for simulating transport of noble gases in the subsurface. *Geothermics*, 33, 521-529.
- Shaw, J. and Bachu, S. (2002). Screening, evaluation and ranking of oil reservoirs suitable for CO₂ flood EOR and carbon dioxide sequestration. *Journal of Canadian Petroleum Technology*, 41 (9), 51-61.

- Skovholt, O. (1993). CO₂ Transportation System. *Energy Conversion and Management*, 34(9-11), 1095-1103.
- Srivastava, R. K., Huang, S. S., Dyer, S. B. and Mourits, F. M. (1995). Quantification of asphaltene flocculation during miscible CO₂ flooding in the Weyburn reservoir. *Journal of Canadian Petroleum Technology*, 34, 31-42
- Stalkup, F. I. (1987). Displacement behavior of the condensing/vaporizing gas drive process. *Proceedings of the SPE Annual Technical Conference and Exhibition*, SPE paper 16715.
- Summerfield, I. R., Goldthorpe, S. H., Williams, N., & Sheikh, A. (1993). Costs of disposal options. *Energy Conversion and Management*, 34(9-11), 1105-1112.
- Taber, J. J., Martin, F. D. and Seright, R. S. (1997). EOR screening criteria revisited – Part 1: Introduction to screening criteria and enhanced recovery projects field projects. *SPE Reservoir Engineering*, 12 (3), 189-198.
- Takur, G. C., & Sattar, A.(1998). *Integrated waterflood asset management*. Tulsa, OK: Penn Well Publishing Company.
- Van der Meer, L. G. H. (1996). Computer modeling of underground CO₂ storage. *Energy Convers. Mgmt.*, 37(6-8), 1155-1160.
- Werner, M. R. (1987). West Sak and Ugnu Sands: Low gravity oil zones on the Kuparuk River area, Alaskan North Slope. *Alaskan North Slope Geology*, 1, 109-118.
- White, M. D., & Oostrom, M. (2003). *STOMP-Subsurface Transport Over Multiple Phases*. Prepared for the US Department of Energy under Contract DE-AC06-76RLO 1830.
- Zick, A. (1986). A combined condensing/vaporizing mechanism in the displacement of oil by enriched gases. *Proceedings of the SPE Annual Technical Conference and Exhibition*, SPE paper 15493.

Appendix A

Lumping of Components and Tuning of EOS in CMG-WinProp[®]

The step-by-step procedure for lumping oil components, followed by tuning of EOS, in CMG-WinProp is given below with an example of the West Sak oil.

1. On launching WinProp[®] in CMG, in titles/EOS/units section, first the EOS is chosen from four available EOS models. The four EOS models are Peng-Robinson (1978), Peng-Robinson (1976), and Soave-Redlich-Kwong (SRK) with proposed constant by Graboski and Daubert and original SRK. For the phase-behavior study of West Sak oil, Peng-Robinson (1978) was selected, which is referred as PR-EOS (1978) in this study. The units and pressure of the system were set to psia, and the temperature was set to degree F, with component composition set to mole.
2. In the component-selection section, components and their properties can either be manually entered or selected from the hydrocarbon-nonhydrocarbon-component library, which can be performed by selecting **Insert Library Component** from the **Options** of the **Component Definition** window. For the single-carbon-number hydrocarbons, for example C₆-C₂₀, components **FC₆- FC₂₀** can be selected from the component library. In the case of West Sak oil, 23 components (Bhandari, 1988) were selected from the library. Properties of heavy components (molecular weight of C₂₁₊ for West Sak oil) could be changed as per the available experimental values.
3. For West Sak oil, molar compositions of 23 components were entered in the composition section.
4. To group components according to the requirements of the study, the **Component Lumping** option available from **Characterization** of the menu is invoked. In the lumping scheme window, 23 components of the West Sak oil were transformed into 8-component oil. CO₂ was set as a single group by assigning it Number 1 in the scheme column, and combining methane and nitrogen as a second group, assigning each component

Number 2 in the scheme column. Similarly, C₂-C₆ components were lumped as a third group, and then C₇₊ fractions were grouped into five pseudo-components. By clicking on **OK**, the components are lumped together. In the **File** option from the menu, the properties of the components should be updated after lumping (Using **Update Component Properties**). This must be followed by deleting the lumping option from the main window before starting the tuning of EOS by regression.

5. The advantage of using lumping in this study was that it allowed more flexibility in the selection of regression parameters for tuning EOS and in reducing the compositional simulation run time in GEM[®].
6. To tune EOS, the regression feature of WinProp[®] can be used. The experimental data are matched with values predicted by EOS by selecting regression parameters, which are properties of the component and interaction coefficients. First, the **Regression** option from the menu is invoked to begin selection of the regression parameters. To tune PR-EOS (1978) for West Sak oil, the critical properties and acentric factors of components C₇ through C₂₁₊, omega A and B parameters for methane and C₂₁₊, viscosity parameters, and interaction coefficients are used as regression parameters. These parameters are selected by clicking on the respective grids of the properties of components.
7. Experiments for EOS tuning are entered by invoking **Lab** options of the menu. Constant composition expansion and differential libration experimental data, obtained from Roper (1989), were used to tune PR-EOS (1978). Weights are assigned according to importance and reliability of the experimental data to the tuning. For example, the saturation pressure was assigned a weight of 50, while the volumetric analysis and viscosity of the oil were given weights of 7 and 40, respectively.
8. Once the experimental data are entered, end of regression should be invoked by selecting **End of Regression** from **Regression** on the menu. Then the regression

scenario is run to obtain tuned parameters of EOS. Subsequently, the tuned EOS is used for performing other phase-behavior calculations.

Oil & Natural Gas Technology

DOE Award No.: DE-FC26-06NT41248

Final Report

A Compilation and Review of Alaska Energy Projects Task 1.04.3

Submitted by:

Arlon Tussing
Institute of the North

Steve Colt
Institute of Social and Economic Research
University of Alaska Anchorage

Prepared for:
United States Department of Energy
National Energy Technology Laboratory

December 31, 2008



Office of Fossil Energy



A Compilation and Review of Alaska Energy Projects

Final Report

Starting June 1, 2004
Ending December 30, 2006

Arlon Tussing
Institute of the North

Steve Colt
Institute of Social and Economic Research
University of Alaska Anchorage

Report Issued December 2008
DOE Award Number
DE-FC26-01NT41248
Task Number 1.04.3

Submitted by:
University of Alaska Fairbanks
Institute of Northern Engineering
Arctic Energy Technology Development Laboratory
Building 814
Fairbanks, Alaska 99775

Disclaimer

This report was prepared as an account of work sponsored by an agency of the United States Government. Neither the United States Government nor any agency thereof, nor any of their employees, makes any warranty, express or implied, or assumes any legal liability or responsibility for the accuracy, completeness, or usefulness of any information, apparatus, product, or process disclosed, or represents that its use would not infringe privately owned rights. Reference herein to any specific commercial product, process, or service by trade name, trademark, manufacturer, or otherwise does not necessarily constitute or imply its endorsement, recommendation, or favoring by the United States Government or any agency thereof. The views and opinions of authors expressed herein do not necessarily state or reflect those of the United States Government or any agency thereof.

Abstract

There have been many energy projects proposed in Alaska over the past several decades, from large scale hydro projects that have never been built to small scale village power projects to use local alternative energy sources, many of which have also not been built.

This project was initially intended to review these rejected projects to evaluate the economic feasibility of these ideas in the light of current economics. This review included contacting the agencies responsible for reviewing and funding these projects in Alaska, including the Alaska Energy Authority, the Denali Commission, and the Arctic Energy Technology Development Laboratory, obtaining available information about these projects, and analyzing the economic data.

Unfortunately, the most apparent result of this effort was that the data associated with these projects was not collected in a systematic way that allowed this information to be analyzed.

Contents

A Compilation and Review of Alaska Energy Projects.....	1
Final Report	1
Disclaimer	2
Abstract.....	3
Executive Summary:.....	5
AGENCY STATUS & MISSIONS	5
AIDEA / AEA	5
Institutional History.....	5
Results:.....	8
Re: Contract between Institute of the North [ION] and Arctic Energy Office of the United States Department of Energy [DOE]: Final Report	8
Original Project “Plan A”	8
“Plan B”	10
“Plan C”	10
“Plan D”	11
Topic D-1: A new long-term primary energy supply for Barrow, in light of rapid maturation and decline of the Barrow gas field.	11
Topic D-2: The long-term place of Alaska in the world market for liquefied natural gas [LNG]. Considerations include	12
Appendix: List of Unfunded or Failed Projects.....	13

Executive Summary:

There have been many energy projects proposed in Alaska over the past several decades, from large scale hydro projects that have never been built to small scale village power projects to use local alternative energy sources, many of which have also not been built.

This project was initially intended to review these rejected projects to evaluate the economic feasibility of these ideas in the light of current economics. This review included contacting the agencies responsible for reviewing and funding these projects in Alaska, including the Alaska Energy Authority, the Denali Commission, and the Arctic Energy Technology Development Laboratory, obtaining available information about these projects, and analyzing the economic data.

Unfortunately, the most apparent result of this effort was that the data associated with these projects was not collected in a systematic way that allowed this information to be analyzed.

AGENCY STATUS & MISSIONS

AIDEA / AEA

Institutional History

In 1976, the Alaska legislature created the Alaska Power Authority (APA) for the primary purpose of constructing and operating power projects that would reduce consumer costs and encourage economic growth. APA was empowered to incur debt in carrying out its mission, and was required by statute to comply with an extensive reconnaissance and feasibility study process for any proposed project before authorizing its construction. Many such studies were conducted although no projects built by APA were financed by debt alone. State general fund grants were appropriated to fund, in whole or in part, such projects as the Four Dam Pool, the Bradley Lake hydroelectric project, and the Anchorage-Fairbanks intertie.

Because APA's statutes allowed the agency to construct energy projects other than electric power system components – for example, waste heat recovery and distribution projects, energy conservation projects – its name was changed in 1989 to the Alaska Energy Authority (AEA) in order to reflect this wider scope of project possibilities.

In 1993, the legislature restructured AEA as follows:

- AEA's authority to incur debt and construct projects was removed. Since AEA could no longer build new projects, the statutory requirements for conducting reconnaissance and feasibility studies were also removed. As a result, the last major project feasibility study undertaken by AEA was completed in 1994. The study evaluated a proposed transmission line be-

- tween Sutton and Glennallen, which was intended to connect the Railbelt grid with the Copper Valley electric system serving Glennallen and Valdez.
- What remained of AEA – its ownership and operation of several major projects – was merged with the Alaska Industrial Development and Export Authority (AIDEA). AEA ceased to have its own separate Board of Directors. From that time forward, the AIDEA Board served also as the AEA Board.
 - AEA’s rural energy functions were transferred to a new Division of Energy within the State Department of Community and Regional Affairs. For the next several years, the Division of Energy managed and/or funded the construction of rural bulk fuel storage systems, the replacement or upgrade of diesel power plants, and the construction of small hydroelectric projects. It operated other programs as well, including but not limited to the Power Cost Equalization rate subsidy program, the Power Project loan program, and the circuit rider maintenance program offering emergency response and preventive maintenance services to rural electric utilities.

In 1999, the Department of Community and Regional Affairs was abolished and its functions were parceled out to other agencies. At that time, the rural energy programs and associated personnel from the Division of Energy were merged back into the Alaska Energy Authority.

Assistance Programs and Methods of Evaluation

- Power Project Fund loan program (AS 42.45.010). Loans are available to electric utilities, municipalities, regional and village corporations, village councils, and independent power producers for reconnaissance and feasibility studies, constructing or equipping power generation projects of less than 10 MW, power transmission and distribution lines, bulk fuel storage facilities, energy conservation measures, and other purposes. AEA must determine that the project is technically, economically, and financially feasible before a loan can be approved. Interest rates are set at the average municipal revenue bond rate on 30-year bonds over the previous 12 months (currently about 5.1 percent). Interest rates can be reduced to as low as zero if such reduction is needed for the project to meet financial feasibility criteria. Loans in excess of \$1.0 million are unusual.
- Bulk Fuel Revolving Loan program (AS 42.45.250). Loans are available to “communities” and to electric utilities for the purchase of bulk fuel supplies, provided the community to be served has a population of 2,000 or less. Loans may not exceed \$300,000 and must be repaid within one year. The interest rate is typically zero the first year, 5.0 percent the second year, and the same as the Power Project Fund rate after that.

The applicant's credit history is the primary evaluation criterion. Loan applications are typically considered on a first-come, first-served basis. In the past, AEA has approved less than the full amount requested by each applicant if AEA anticipates that the aggregate demand for loans will exceed the amount available to lend.

- Rural Bulk Fuel Storage – New Facilities and Upgrades: Most recently, funding for this program has come primarily from the Denali Commission. Statutory authority is derived from the legislature's approval of AEA's capital budget submission, which states what AEA intends to build and how it intends to build it.
Several years ago, AEA created a database on the condition of each bulk fuel tank farm in rural Alaska. These condition assessments were quantified and ranked. The initial project selection criterion is the condition of the tank farm – the worst facility is at the top of the list. However, the tank farm owner must demonstrate that an effective maintenance plan and business plan is in place before funds will be released for upgrade or replacement of the facility. In other words, the owner must show that the new project will be sustainable. Since the tank farms that are in the worst condition typically have seen the poorest maintenance in the past, these two criteria tend to conflict.
- Rural Power System Upgrades: Virtually the same description provided above for the rural bulk fuel storage program applies also to the rural power system upgrade program, including: the Denali Commission has recently provided most of the funds, statutory authority is derived from AEA's capital budget submission, a comprehensive data base on the condition of electric utility systems in rural Alaska was created, these condition assessments were quantified and system conditions were ranked, and the project selection criteria were based on the system condition and consequent need for assistance coupled with a requirement for an effective maintenance and business plan needed for project sustainability.
- Energy Cost Reduction Program: This program was developed jointly by AEA and the Denali Commission, with AEA providing program management and the Denali Commission providing most of the funds. For several years, AEA solicited proposals from rural electric utilities and other eligible applicants for projects that would reduce energy costs through improved efficiencies. Each proposal determined to be technically feasible was analyzed and ranked by its expected economic benefit – cost ratio. Projects passing the economic test were further analyzed to determine the maximum amount of debt financing the project could support. Each of these project applicants was expected to provide, from its own sources or from borrowed funds,

- ½percent of this maximum level of debt financing, and grant funding was offered for the remainder of project cost
- AIDEA itself has several programs that can provide financing assistance for energy projects. Under its Development Finance program, AIDEA can participate in projects (including energy projects) for which tax exempt financing is dependent in part on project ownership by a public entity such as AIDEA. The primary example of such a project is the 50 MW Healy “Clean Coal” plant that is now sitting idle near GVEA’s Healy 1 plant. The project was built with a combination of federal grants, state grants, and tax exempt bonds issued by AIDEA. To be considered for such assistance, project proposals must meet extensive criteria for technical, economic, and financial feasibility as well as contribute to economic growth. Other financing assistance, either in the form of loan participation or conduit revenue bond financing, can be offered for energy projects that meet similar feasibility criteria.

Results:

Re: Contract between Institute of the North [ION] and Arctic Energy Office of the United States Department of Energy [DOE]: Final Report

Original Project “Plan A”

This study as originally planned was to be based on to a careful examination and quantitative (statistical and financial) analysis of a representative sample of proposals for financial or technical assistance, generated by or submitted to certain State and Federal funding agencies¹ in Alaska since 1990. The premise of this plan

¹ The agencies or data sources whose records were examined included the Denali Commission (a joint state-federal institution), the Alaska Industrial Development and Export Administration [AIDEA] and the Alaska Energy Authority, two state agencies that have been merged into one operating under the single acronym AIDEA-AEA, the Arctic Energy Technology and Development Laboratory [AETDL], an entity of the University of Alaska Fairbanks whose functions include administrations of grants and contracts on behalf of the Arctic Energy Office of the US Department of Energy, and the Alaska Resources Library and Information Service [ARLIS], a records-and-data management entity serving several agencies, most but not all of them units of the US Department of Interior.

was that such an examination might disclose classes of project proposals (1) intended to improve the accessibility or cost of energy to specific enterprises, industrial sectors, or communities, (2) that were not implemented in the past, but (3) which the researchers recommended revisiting in the light of intervening changes in prices, demand, technology, or public policy.

On April 18, 2005, we concluded and reported orally to the Institute of the North and to the study's sponsoring agency, the DOE Arctic Energy Office, that the established work plan for the study, based upon a survey of agency records, had proved unproductive, and that a further examination of project proposals from earlier years at the listed agencies would be a waste of effort.² We accordingly re-

Accompanying this memorandum is a document not previously submitted, which was produced under Work Unit 2, entitled "Agency Status and Missions", which summarizes the institutional history of AIEDA/AEA and the Denali Commission.

² The following are excerpts from our memorandum of the above date, relating to the incompatibility of the proposed method to the actual information base:

"Firstly, the time intervals for which records exist, were preserved, or made available to the researchers vary profoundly among the agencies surveyed, diminishing our ability to register the impact of project evaluation of changing costs, prices or technology . . .

"[The] Alaska Energy Authority underwent several pronounced changes in its location within the structure of State government (sometimes along with its name), its source(s) and magnitude of funding, and its statutory authority and mission.

"The Denali Commission, a significant "wholesale" source of energy funding in Alaska, commenced operation only in 1999, while AETDL, a creature of the US Department of Energy, is now in only its fifth Fiscal Year.

"The total number of individual 'project proposals' that our researchers encountered at these agency archives numbered more than one thousand, and varied in format and content in myriad directions. None of the funding agencies seems to have required a standard application questionnaire, or in many cases, a business plan of any type.

"Out of the thousand or so records encountered, less than seventy seemed to contain or allude to any quantitative estimate of intended or expected financial benefits. In all of their efforts, project researchers encountered NO proposal that was (1) sufficiently specific, (2) based on sufficiently credible information or assumptions, and (2) on its face economically promising or socially necessary.

"None of [the foregoing] observations is intended to fault either the assistance programs or the record-keeping policies [of the various entities]. What our efforts revealed as flawed is, rather, the assumption that the large number of Alaska project proposals . . . was inherently a workable data base for economic analysis."

quested that ION deem Work Unit 2 as it is described in previous reports to be complete, and indicated our intention to suspend all further effort under the contract, pending possible approval of an alternative objective and plan of work by the Alaska Energy Office.

On behalf of the research team, I hereby report that no mutually acceptable alternative plan is in prospect that is congruent with the existing contract. Accordingly, we have no objection to the Institute of the North executing termination at this time. On that assumption, this communication should be regarded as our final report.

“Plan B”

After the April meeting, project researchers subsequently conferred with the representative of the Alaska Energy Office, and officers of relevant agencies, electric utilities and industry bodies, regarding alternative ways of reexamining significant project or programmatic proposals over the last 15 years, that were (1) investigated but not executed, (2) executed in part but not completed, or (3) completed but failed. Our first proposal for an alternative approach, here tagged “Plan B”, centered on a series of structured interviews with managers of the respective agencies, utilities, and trade associations regarding their recollections and recommendations.

While some of the candidate interviewees related strong (and sometimes persuasive) opinions about specific proposals involving their own organizations, including projects which that were either implemented, rejected, or “orphaned,” we found no consensus as to what methodology or standards should be adopted for any new survey, and indeed, as to whether the Arctic Energy Office ought to be supporting such an inquiry or whether our research team should conduct it.

“Plan C”

Our third approach was to suggest a list of potential issues and initiatives worth revisiting, based primarily on the personal experience and knowledge of members of the research team, augmented by insights obtained in discussions of the Plan B approach. Our draft of such an issue list was not greeted with enthusiasm by members of our informal panel of industry discussants, or by the Arctic Energy Office representative, and we have accordingly not proposed it as the core of any revised study plan. Because we nevertheless believe that this draft might contain useful information for future researchers or for the public, it is nevertheless appended to this report as Plan C.

“Plan D”

Notwithstanding our agreement to termination of the contract based on infeasibility of the original work plan, and lack of agreement regarding any alternative approach congruent with the existing contract, the project’s professional staff (Tussing, Tichotsky, and Emerman) would be interested in devoting the remaining unexpended resources in an exploration, on behalf of the Arctic Energy Office, of one of the two following topics, including but not limited to the subtopics shown below.

These are topics of a kind about which we have special expertise and demonstrated insight and foresight, and on which there are major stakeholder groups and/or sections of the public that would support our inquiry because they have a particular confidence or interest in our findings or opinions. Our contributions on these topics typically involve “linking the dots” of market or technical information that is outside public awareness, perhaps because they are “hidden outside in plain view.”

Topic D-1: A new long-term primary energy supply for Barrow, in light of rapid maturation and decline of the Barrow gas field.

Barrow, Alaska (population in Census of 2000, about 4,500 persons, 64 percent of whom are Alaska Native) is one of the few North American communities in its size class that is effectively self-sufficient in energy, and as far as we know, the only such settlement anywhere in Alaska or the Arctic. In particular, Barrow may be the only “off-net” settlement anywhere in the Circumpolar North that does not depend primarily upon distillate fuel (diesel), but has been able to rely upon locally produced natural gas for the generation of electricity and for other stationary energy needs.

Barrow’s source of natural gas initially consisted of two small pools of about 4 and 5 bcf respectively in the Barrow field, which the US Navy discovered in 1949 and developed in 1952 to supply heat and power for Federal facilities. The Barrow field was then also authorized to supply civilian uses through a municipal utility operated by the North Slope Borough (NSB, the county-level government). Incident to a substantial shrinkage of Navy activities, the Federal government in 1984 transferred ownership and operation the now largely depleted field and production facilities to the NSB.

The Borough subsequently developed another gas field at Walapka, 20 miles SW of Barrow, and built a pipeline connecting it to the town. This field, whose initial

reserves were about 25 bcf, commenced production in 1992. Together with residual producing capacity in the Barrow field, Walapka has since then been meeting typically annual loads on the order of 1.3 to 1.5 bcf—a level which, however, it cannot long sustain. Barrow’s ability to rely on local natural gas, and its corresponding freedom from dependence on imported diesel oil or LPG—which have been signal economic, lifestyle and environmental advantages for almost half a century—now threaten to become a major handicap to the community.

We would be willing and able to make an initial pre-feasibility reconnaissance of and comparison of alternative courses of action available to the Borough for replacing Barrow’s existing gas supply.

Topic D-2: The long-term place of Alaska in the world market for liquefied natural gas [LNG]. Considerations include . . .

- Implications of the early-21st Century reversal of terms of trade in LNG between Asia and North America, which create a powerful drive to install LNG import facilities in the Lower 48 and Canada and, indeed, suggest that Cook Inlet and the Railbelt are likely to become an importer of LNG from, rather than an exporter to, the Pacific Basin.
- The preconditions for, likelihood, and likely timing of, an impending emergence of a Pacific Basin commodity (“spot”) market in LNG, and a with it a single global market for natural gas comparable to the existing world crude-oil market.
- Implications of large-scale LNG imports to North America for economics and viability of the contemplated overland natural-gas pipeline, the wellhead value of ANS gas, and the delivered cost of gas in the Alaska Railbelt.

Appendix: List of Unfunded or Failed Projects

PDF attachment.

APPENDIX II: SAMPLE OF UNFUNDED, UNFINISHED OR FAILED PROJECTS

A	B	C	D	E	F	G	H
	Project Type	Project / Proposal / Study	Year	Sponsor	Cost	Why Unsuccessful	Obstacle Type
2	Transmission (Rural)	Study: Comprehensive survey of proposed transmission lines in rural Alaska. Intent to consolidate all published information on rural intertie options and conduct economic screening to identify cost-effective proposals. 173 intertie proposals listed, none selected. Data base of results available at www.aieea.org/AEEEPublications.htm	1997	Division of Energy (now AEA)	Aggregate cost of all proposed lines not provided	Economic screening not conducted because: cost data not reliable and prospects for savings considered poor.	Poor Cost Data. Uncertain economics.
3	Transmission (Rural)	Proposal: Build transmission line from Bethel to villages of Kwethluk, Akiachak, Akiak and Tuluksak. Initially replace remote diesel power in villages with power imported from Bethel. Project expansion would follow.	1992	Callista Corporation	\$10 million for "single wire ground return" line	SWGR does not meet NESC standard which would cost \$30 million. Econ OK for \$10 million but not for \$30 million.	High cost to meet NESC. SWGR is controversial.
4	Transmission (Rural)	Proposal: Transmission line from Petersburg to Kake. Petersburg served by Tye Lake hydro which has surplus available. Kake served by diesel. Concept to supplant diesel with surplus hydro.	1996	Division of Energy (now AEA)	\$15 million	Intertie cost exceeded diesel savings.	Economic feasibility.
5	Transmission (Rural)	AVEC evidently plans to build some transmission lines. Informally states that, in general, villages must be 10 miles apart or closer to realize economic benefit.	current	AVEC	??	[NEED TO ACQUIRE INFO ON THIS AND OTHER INTERTIE PROPOSALS]	
6	Transmission (SE AK)	Studies: AEA study in 1980s on comprehensive SE AK transmission grid. Southeast Conference published more recent study. Congress authorized \$435 million for project but appropriated very little. Most segments of the proposed grid fail economic test. Studies identified 2 most promising segments described below.	1980s and forward	AEA, then Southeast Conference	\$435 million	Economic feasibility lacking for overall grid. High gov't subsidy needed but has not been provided.	Economic and financial feasibility
7	Transmission (SE AK / Tye-Swan)	Proposal: Build transmission line linking Swan Lake and Tye Lake hydro projects. Ketchikan served by Swan Lake but must supplement with diesel. Concept is to displace Ketchikan diesel with surplus Tye Lake hydro.	1992, + updates	AEA, + Ketchikan Public Utilities	\$73.2 million (\$ 1998)	Despite >\$25 million in gov't grants, limited early year savings cause financing problem. Also, competing Native hydro proposal.	Financial feasibility. Political issues.
8	Transmission (SE AK / Juneau-Greens Crk)	Proposal: Build transmission line linking Juneau with Greens Creek mine. Concept is to displace Greens Creek diesel generation with surplus hydro from Snettisham. Preliminary economics were favorable, and both Kennicott and Juneau utility were interested.	1993	AEA, Kennicott Mining Co.	??	[NEED TO FIND OUT WHAT HAPPENED]	
9	Transmission (Railbelt / Anch-Kenai)	Proposal: Build second line between Anchorage and Kenai Peninsula. Route under Turnagain Arm. Intent is to reduce costs and improve reliability.	1989, + updates	AEA, + Rbit Utilities	Approx. \$100 million (need update)	Most studies, including 2004 update, show costs exceed benefits. Also environmental hurdles.	Economic feasibility.
10	Transmission (Sutton-Glennallen)	Proposal: Build 135 mile line north of Glenn Highway to link Copper Valley system (Valdez and Glennallen) with Railbelt. Supplant Glennallen diesels with gas-fired electricity from Anchorage area. Allison Lake hydro in Valdez might win economic test but hydro cost data only preliminary. Inertie project wins econ test vs. diesel.	1994	AEA, + Copper Valley Elec Utility	Approx. \$55 million (??)	Financial feasibility and environmental opposition were the main problems.	Financial feasibility. Environmental opposition.
11	Electric End-Use Conservation (Railbelt)	Proposal: AEA defined the 3 most promising electric end-use conservation programs and compared them with other Railbelt power alternatives. The conservation programs won the econ test. Budget proposal to implement was submitted to AEA Board, which turned it down. [REBATE PROGRAMS - GET SPECIFIC INFO]	1989	AEA	?? \$50 million over 5 years ?? [get info]	AEA Board uneasy about complex program to influence 000s of consumer decisions, and also about political reaction to request.	Complex to implement. Anticipated influence 000s of consumer decisions, and also about political reaction.
12	End-Use Conservation (Rural)	Proposal: Recent study estimates about half of rural households have hot water heaters, and 40% of those are electric. High B/C ratios estimated for replacing with oil-fired heaters. Although the study recommends govt expenditure of \$7.5 million over 4 years on this, it provides no hint on how the program should be structured.	2004	AEA	\$7.5 million	Hasn't "failed" yet but there seems to be no clear idea how to implement the recommendation.	Implementation plan has not been designed

APPENDIX II: SAMPLE OF UNFUNDED, UNFINISHED OR FAILED PROJECTS

A	B	C			D	E	F	G	H
	Project Type	Project / Proposal / Study			Year	Sponsor	Cost	Why Unsuccessful	Obstacle Type
2	Natural Gas / Coal Bed Methane	Study: Technical and economic potential of substituting natural gas or coal bed methane for diesel fuel in rural Alaska. Conclusion - given expected costs of exploration and development, typical size and density of rural communities, and assertion that capital costs are much less for diesel generators than for gas-fired generators, economic prospects for domestic use of natural gas in rural Alaska are poor. Study is available at www.aidea.org/AEEPpublications.htm .			1997	AEA	Study includes cost estimates of rural gas exploration and development	Study results were re-examined and reaffirmed in 2001 "Screening Report for Alaska Rural Energy Plan," available on Denali Commission web site.	Economic feasibility.
14	Natural Gas / Coal Bed Methane	Study: Aerial magnetic survey of Lower Kuskokwim basin conducted to determine likelihood of finding natural gas or coal bed methane. Ak Dept. of Natural Resources concluded that accumulations of these resources in the area were unlikely.			1995	AEA / DNR Calista	No cost data	Study results argue against exploration investment in this region.	Physical conditions in the region.
15	Natural Gas / Coal Bed Methane	Study: Naknek Electric utility retained geological consultant to study potential for natural gas to displace diesel. Based on subsurface geology, conclusion was that the closest prospect for "commercial quantities" was at least 30 miles from Naknek. Costs of pipeline or transmission line over this distance likely too high.			1988	Naknek Electric Assoc.	[DETAILS IN STUDY]	Assumed that transmission or pipeline costs, on top of exploration and dev. costs, would not meet economic feasibility requirements.	Physical conditions, economic feasibility
16	Natural Gas / Coal Bed Methane	[NEED TO ACQUIRE ADDITIONAL INFO FROM DNR, ENSTAR, AND PERHAPS OTHERS -- Fort Yukon? Chignik Lagoon? Homer? Other locations?]							
17	Natural Gas / Coal Bed Methane	Proposal: Deliver natural gas (as LNG or CNG) from southcentral Alaska to SE Alaska communities, which now rely on electricity and oil for space and water heat. One recent proposal asked AIDEA to finance \$50 million for pipeline distribution while the private owners would finance the rest. Distribution pipelines in place provide very little security for loan repayment in case the venture is unsuccessful - a major reason why AIDEA declined.			2001 (and before)	Private consortium proposal to AIDEA	\$66 million (\$50 million of which was for pipeline distribution)	AIDEA declined due to inadequate security for loan. No public feasibility study released for review. Unsure of project economics.	Financial feasibility. Economics uncertain.
18	Geothermal	Proposal: Develop Unalaska geothermal resource (Makushin volcano) to supply power primarily to fish processors in Dutch Harbor. 1995 cost estimate (including well field development and all other project costs) was \$90 million. It was estimated that a \$45 million govt grant would be needed to break even with diesel.			1995	AEA	\$90 million	Low probability of acquiring \$45 million govt grant. Also, fish processors unwilling to sign long-term "take or pay" agreements needed to secure bond financing.	Economic and financial feasibility
19	Geothermal	Proposal: Develop geothermal resource at Pilgrim Hot Springs on Seward Peninsula, 60 road miles from Nome. \$1.7 million estimate for local development, but project economics per AEA loan analysis require transmission line to Nome estimated to cost at least \$5 million.			1995	Pilgrim Springs Ltd.	\$6.7 million	Project economics require power sales to Nome but cannot survive inclusion of Nome transmission costs.	Economic and financial feasibility
20	Geothermal	Study: Consultant to State examined prospect of developing geothermal resource at Lake Chakachamna on the west side of Cook Inlet as a potential source of power for the Railbelt. [NEED TO REVIEW INFO]			1980s	Office of Governor	??	??	??
21	Coal (Rural)	Proposal: A small coal-fired power plant was proposed for McGrath. Coal was to be supplied from a proposed coal mine 90 miles away over a winter road. High fixed costs of coal plant (capital and fixed O&M) are difficult to overcome when built on a small scale for a small load. Small coal plant economics have also been studied for Galena and Tok (Northern Economics) and for Unalaska (Financial Engineering Co.). In each case diesel was found to be less costly. A small coal plant was also proposed for Bethel by Bettine - feasibility numbers unknown but proposal was not successful.			1997	Doyon Ltd (McGrath)	??	Not economically feasible, despite advances in technology and cost for small-scale coal plants.	Economic feasibility.
22									

APPENDIX II: SAMPLE OF UNFUNDED, UNFINISHED OR FAILED PROJECTS

A	B	C			D	E	F	G	H
	Project Type	Project / Proposal / Study			Year	Sponsor	Cost	Why Unsuccessful	Obstacle Type
2	Coal (Railbelt)	Study: A comprehensive study of Railbelt power alternatives included detailed cost estimate and economic analysis for conventional coal-fired power plant in Healy area (prior to Healy Clean Coal proposal). Of all the alternatives, the economics of building a conventional coal plant (with no consideration of govt subsidy) were the least favorable.			1989	AEA	[NEED TO OBTAIN]	Not economically feasible. Life-cycle costs exceeded all other alternatives and scenarios.	Economic feasibility.
23	Coal (Railbelt)	Proposal: Usibelli Coal Mine recently proposed to construct and operate the "Emma Creek Coal Project," a 200 MW coal-fired power plant at Healy. A 2004 study by R.W. Beck for the Railbelt utilities concluded that Emma Creek was not economically feasible (though it appears to be close). However, Beck also concluded that "generic" 150 MW coal plants in southcentral and in the interior have favorable economics in 2015 if coal can be provided at the same price it is sold to Golden Valley for its existing coal plant at Healy. Unclear at this point how these conclusions are compatible.			2004	Usibelli proposal, R.W. Beck analysis	??	[NEEDS CAREFUL REVIEW OF BECK STUDY]	??
24	Coal (Cordova)	Proposal: Cordova Electric Coop issued an RFP for power supply in 1994. 3 proposals were submitted, including 1 by a private group offering to build a small-scale coal-fired power plant that would incorporate used equipment and burn coal from the Matanuska Valley. Cordova decided that lower costs would be realized by developing the Power Creek hydro project proposed by another developer.			1994	Bettine et al	[NEED TO OBTAIN]	Proposals were evaluated by a consultant. Economics was one factor. There may have been other concerns about the coal proposal.	Economic feasibility.
25	Biomass (electricity)	Study: 1994 feasibility study of building a power plant fueled by municipal solid waste (MSW) in Thorne Bay concluded that it might be cost-effective. However, the idea went no further as Thorne Bay elected instead to tie into the Alaska Power Co. (APC) grid and to purchase power from APC. Most of that power is generated by hydro. The new transmission connection to Thorne Bay was largely subsidized by federal grants.			1994	AEA (study by ISER)	[NEED TO OBTAIN]	One factor was federal subsidy for competing alternative.	
26	Biomass (electricity)	Study: 2001 "Screening Report for Alaska Rural Energy Plan" considered power plants fueled by biomass (wood, wood waste, MSW). It found that biomass power plants are similar to coal plants in that capital and operating costs are high relative to diesel and natural gas -- possibly higher due to heat content and quality of fuel. Conclusion was that, at least for plants scaled for rural Alaska, no amount of fuel cost savings was likely to make up for the capital and O&M cost penalty.			2001	AEA study by Northern Economics	Various	Economic feasibility	Economic feasibility.
27	Biomass (space heat systems)	Study: "Rural Alaska Heat Conservation and Fuel Substitution Assessment" examined, among other things, wood fuel substitution for fuel oil in space heat boilers in several rural communities, including McGrath, Tanana, Elm, Grayling, and Dot Lake. Annual fuel cost and labor favored wood but not enough to recover capital cost penalty within 20 year planning horizon.			1996	AEA (study by USKH)	Various	Economic feasibility	Economic feasibility.
28	Biomass (space heat systems)	Proposal: A biomass heat demonstration project was proposed for McGrath in 1999. A govt grant subsidy of \$1.6 million (out of a total capital cost of \$1.8 million) would have been needed for financial feasibility (Strandberg 1999). An update by MBA Consulting Engineers in 2000 concluded that a 30-year horizon and a favorable assumption of the cost of wood would be needed for economic feasibility.			1999	Studies by Strandberg and MBA Consulting Engineers	\$1.8 million	Economic and financial feasibility	Economic and financial feasibility
29									

APPENDIX II: SAMPLE OF UNFUNDED, UNFINISHED OR FAILED PROJECTS

A	B	C	D	E	F	G	H
	Project Typ	Project / Proposal / Study	Year	Sponsor	Cost	Why Unsuccessful	Obstacle Type
2	Wind (Rural)	Study: ISER study in 2001 for AIDEA evaluated Kotzebue wind project and concluded that, without subsidy, the project would have resulted in a net economic loss to local consumers. The main reason identified by ISER is insufficient wind resource. Kotzebue also purchases diesel fuel for a lower price than many smaller rural communities. Study summary can be found in the "Screening Report for Alaska Rural Energy Plan" on Denali Commission web site.	2001	ISER	Cost Details estimated in study	Study suggests that wind projects at sites with stronger wind resource and higher diesel prices could be economically feasible.	
30	Wind (Rural)	Study: A rural energy plan prepared in 2004 for AEA identifies 30 rural communities in which wind power development may, upon confirmation of wind resource and other variables, provide economic benefit. (Study available at www.aidea.org/aeaRuralEnergyPlan.htm). See p. 3-3 for list. The plan proposes govt expenditure of \$29.1 million over 5 years - including \$1.6 million for site-specific wind recon and final feasibility studies, and \$27.5 million for construction financing.	2004	AEA (Energy Plan by Mark Foster & Assoc)	\$29.1 million	Study suggests possible economic benefits from wind development.	
31	Wind (Rural)	[AVEC CURRENTLY INSTALLING WIND IN SEVERAL LOCATIONS. NEED INFO ON AVEC WIND EXPERIENCE, FEASIBILITY ANALYSIS AND PLANS]					
32	Wind (Railbelt)	Proposal: Chugach Electric is considering a possible wind project on Fire Island. The 2004 Railbelt study by R.W. Beck modeled this as a 50 MW project and concluded in its "base case" that it would produce economic benefit, though the result is close to breakeven. (Beck study is available at www.aidea.org/EnergyTaskForce.htm). Look under proceedings on 12/2/03.	2003	Chugach Electric (study by Beck)	??	Marginal economic benefit	
33	Solar	Study: See "Screening Report..." on Denali Commission web site for brief analysis of solar energy costs and issues (p. 5-24). A 12 kW solar system with battery storage was installed in Lime Village in the 1990s -- current status unknown. Study concludes that solar is not cost competitive with diesel in rural Alaska.	2001	AEA study by Northern Economics	??	Economic feasibility	Economic feasibility.
34	Tidal	Study: See "Screening Report..." on Denali Commission web site for brief analysis of tidal energy costs and issues (p. 5-26). Tidal Electric of Alaska, Inc. conducted a feasibility study of a tidal power system in Cordova, and estimated a \$14 million capital cost for a 5 MW system. (Study available at www.aidea.org/AEEPPublications.htm). Cordova utility proceeded with hydro construction (Power Creek) and Tidal Energy moved on to consider alternative sites. Screening report concludes that tidal energy not cost-effective for rural Alaska.	2001	AEA study by Northern Economics	??	Economic feasibility	Economic feasibility.
35	Waste Heat Distribution	Studies: AEA conducted feasibility studies in 30 rural communities in 1988-90 and, using state grants, constructed extensive systems in the 10 locations considered most cost-effective. (The systems capture excess heat from the jacket water of diesel engines and distribute that heat via insulated pipe to buildings in the area.) Unless there is one or more large heating load near the powerhouse, the systems tend to be uneconomic in rural villages due to the small size and low density of most local structures. Currently, both AEA and AVEC install waste heat systems when replacing diesel powerplants to the extent that significant heating loads are located nearby.	1988-90	AEA	Various	Economic feasibility. Technical problems with early systems [NEED UPDATE]. Also a "hassle factor" for customers -- now a hybrid rather than a simple boiler operation.	Economic feasibility.
36							

APPENDIX II: SAMPLE OF UNFUNDED, UNFINISHED OR FAILED PROJECTS

A	B	C	D	E	F	G	H
	Project Typ	Project / Proposal / Study	Year	Sponsor	Cost	Why Unsuccessful	Obstacle Type
2	Waste Heat Distribution	Proposal: Copper Valley Electric requested a loan from AEA in 1998 for a system to supply waste heat from the Glennallen diesel generators to the nearby Glennallen school facility. If the school paid 70% of its avoided fuel cost, the utility could pay for the system and realize modest returns, according to the AEA analysis. Due to marginal financial feasibility, AEA offered the loan at 1% interest. [NEED TO DETERMINE IF CVEA BUILT THE SYSTEM OR NOT]	1998	Copper Valley Electric Assoc	\$406,000	[NEED FOLLOWUP INFO]	
35	Waste Heat Distribution	Study: The 2004 Alaska Rural Energy Plan proposes \$3.1 million be spent over the next 5 years to help implement waste heat projects in additional rural communities. 27% of rural diesel plants now include a waste heat component. The study suggests that waste heat in some configuration should be cost-effective in 70% of rural communities. Primary customers would be schools and water systems. Obstacles to address include standardized contracts, informing customers on design and operating issues, and developing standardized system designs.	2004	AEA (Energy Plan by Mark Foster & Assoc)	\$3.1 million		
36	Waste Heat Distribution						
37	Hydroelectric	Study: AEA (Div. of Energy) published a data base on existing and proposed hydroelectric projects in rural Alaska, along with an economic screening analysis to determine which, if any, potential projects appeared cost-effective on a preliminary basis. (Report available at www.aidea.org/AEEEPublications.htm). Projects in 10 communities were identified as promising candidates based on preliminary information, 4 of which were under development at the time. At least 1 of those 4 has now stalled [REASON?], while another project not on the list (South Fork on Prince of Wales island) is nearing completion.	1997	AEA (Study by Locher Interests and ISER)	N/A	[ADDITIONAL REVIEW NEEDED TO IDENTIFY OBSTACLES TO DEVELOPMENT FOR INDIVIDUAL HYDRO PROSPECTS]	
38	Rural Bulk Fuel Storage Facilities	Study: AEA compiled a comprehensive data base on the configuration and condition of all bulk fuel storage facilities in rural Alaska, based entirely on site visits to each facility. This has served as the primary basis for estimating the cost to bring these facilities into regulatory compliance and for prioritizing project funding requests to the Denali Commission. Estimated that \$200-\$300 million is needed to complete the replacement or rehabilitation of these facilities. The data base has not been updated in over 5 years, and there has been no systematic follow-up on completed replacement projects to determine how they are holding up. Data base is available on the Denali Commission web site.	late 1990s	AEA	Up to \$400 million initially estimated to bring rural fuel storage into regulatory compliance		
39	Rural Diesel Power Plant Upgrades	Study: AEA compiled a comprehensive data base on the configuration and condition of all rural electric utilities (with some exclusions such as AVEC), based entirely on site visits to each facility. As with bulk fuel storage, this has served as the primary basis for estimating the cost to bring each system into compliance with accepted utility standards and to prioritize funding requests to the Denali Commission. Estimated that >\$100 million (?) still needed to complete the job. Again, this data base has not been updated in over 5 years, and there has been no systematic follow-up on upgrade projects to determine how they are holding up. Data base is available on the Denali Commission web site.	late 1990s	AEA	[NEED TO REVIEW THE MATERIAL]		
40							
41							

APPENDIX II: SAMPLE OF UNFUNDED, UNFINISHED OR FAILED PROJECTS

A	B	C	D	E	F	G	H
	Project Typ	Project / Proposal / Study	Year	Sponsor	Cost	Why Unsuccessful	Obstacle Type
2	Intertie, hydro, bulk fuel storage, and rural electric data bases	Issue: It would be useful to update these data bases to gain a current grasp on existing projects, existing conditions, and needed or potentially beneficial projects or improvements.					
40							
42	Package Power Plants and Fuel Storage (Rural)	"Utilitymaster" systems: During the 1990s, a now defunct company named Alaska Power Systems (APS) developed a packaged utility system intended for rural villages. Major system components included a new powerplant, bulk fuel storage tanks mounted on skids, pre-pay metering systems, plus certain O&M, management, and admin services. The Alaska Science and Technology Foundation (ASTF) provided funds for APS to develop a form of automated control for the power plant, which would be monitored and, possibly, controlled remotely from Anchorage by APS. AEA provided funds to help install 3 demonstration projects. APS asked for funds to help expand to at least 20 more villages. The 3 projects ended in failure.	mid-1990s	Alaska Power Systems, AEA, ASTF	various	Contributing factors: technical problems with Perkins diesel engines (incl spare parts); fuel storage tanks not code compliant, contracts between APS and villages unclear on service and equipment to be provided, poor service from APS, inadequate pmtis from villages, APS folded.	Many problems. An evaluation report exists (possibly in AEA library).
43							
44	Diesel Powerplant Efficiencies	Study: 2004 Alaska Rural Energy Plan proposes govt expenditure of \$20 million over 5 years for diesel efficiencies, 1/3 of which is for metering and SCADA systems to help locate inefficiencies and identify corresponding efficiency upgrades. These could include upgraded control systems, diesel generator replacements, distribution system upgrades, and/or O&M protocols.	2004	AEA (Energy Plan by Mark Foster & Assoc)	\$20 million over 5 years		
45	Diesel Powerplant Efficiencies	Proposals: Over the last several years, AVEC has submitted funding requests to AEA both for diesel engine replacements and for automated switchgear, many of which have been funded. System efficiencies have been improving for years, documented in PCE statistical reports that show annual kWh sold per gallon. [NEED ADDTL RESEARCH ON WHAT AVEC, AEA, and APC HAVE BEEN DOING TO UPGRADE DIESEL EFFICIENCY]	on-going	AVEC			
46	Energy Resource Development Projects						

National Energy Technology Laboratory

626 Cochrans Mill Road
P.O. Box 10940
Pittsburgh, PA 15236-0940

3610 Collins Ferry Road
P.O. Box 880
Morgantown, WV 26507-0880

One West Third Street, Suite 1400
Tulsa, OK 74103-3519

1450 Queen Avenue SW
Albany, OR 97321-2198

525 Duckering Bldg./UAF Campus
P.O. Box 750172
Fairbanks, AK 99775-0172

Visit the NETL website at:
www.netl.doe.gov

Customer Service:
1-800-553-7681



Oil & Natural Gas Technology

DOE Award No.: DE-FC26-06NT41248

Final Report

Beluga Coal Gasification – ISER

Submitted by:
Steve Colt, Ph.D.
Institute of Social and Economic Research
University of Alaska Anchorage
3211 Providence Dr
Anchorage AK 99508

Prepared for:
United States Department of Energy
National Energy Technology Laboratory

December 31, 2008



Office of Fossil Energy



Beluga Coal Gasification – ISER

Final Report

December 2008

DOE Award Number: DE-FC26-01NT41248

Submitted and Prepared by:

Steve Colt, Ph.D.
Institute of Social and Economic Research
University of Alaska Anchorage
3211 Providence Dr
Anchorage AK 99508

Disclaimer

This report was prepared as an account of work sponsored by an agency of the United States Government. Neither the United States Government nor any agency thereof, nor any of their employees, makes any warranty, express or implied, or assumes any legal liability or responsibility for the accuracy, completeness, or usefulness of any information, apparatus, product, or process disclosed, or represents that its use would not infringe privately owned rights. Reference herein to any specific commercial product, process, or service by trade name, trademark, manufacturer, or otherwise does not necessarily constitute or imply its endorsement, recommendation, or favoring by the United States Government or any agency thereof. The views and opinions of authors expressed herein do not necessarily state or reflect those of the United States Government or any agency thereof.

Abstract

ISER was requested to conduct an economic analysis of a possible “Cook Inlet Syngas Pipeline.” The economic analysis was incorporated as section 7.4 of the larger report titled: “Beluga Coal Gasification Feasibility Study, DOE/NETL-2006/1248, Phase 2 Final Report, October 2006, for Subtask 41817.333.01.01”. The pipeline would carry CO₂ and N₂-H₂ from a synthetic gas plant on the western side of Cook Inlet to Agrium’s facility. The economic analysis determined that the net present value of the total capital and operating lifecycle costs for the pipeline ranges from \$318 to \$588 million. The greatest contributor to this spread is the cost of electricity, which ranges from \$0.05 to \$0.10/kWh in this analysis. The financial analysis shows that the delivery cost of gas may range from \$0.33 to \$0.55/Mcf in the first year depending primarily on the price for electricity.

Table of Contents

Abstract	ii
Introduction	1
Executive Summary	1
Experimental Methods.....	2
Results and Discussion.....	4
Conclusion	5
References.....	5

List of Figures and Tables

Table ES-1. Annual SynGas Pipeline Cost of Service.....	2
Table 1. Capital Cost Assumptions	3
Table 2. Summary of O&M Costs.....	4
Table 3. Present Value of Total Project Lifecycle Cost.....	4
Figure ES-1. Annual Cost of Service for 20 Years	2
Figure 1. Range of Total Project Capital Costs	3
Figure 2. Components of Lifecycle Cost	5

Introduction

ISER was asked to prepare an economic analysis of a possible “Cook Inlet Syngas Pipeline” for inclusion in phase 2 of the “Beluga Coal Gasification Feasibility Study, DOE/NETL-2006/1248.”

The pipeline chosen for analysis was described in section 7.1 of the *Phase 2 Report* as follows:

“The concept includes two pipelines to transport CO₂ and N₂/H₂, which will be fed into the Agrium plant and used as synthesis gas. This study assumes a coal gasification plant location within a one mile radius of the village of Tyonek. The presently planned plant configuration could be modified to take Carbon Dioxide (CO₂) and Hydrogen (H₂) from the stream produced by the Syngas gasifier prior to the introduction of those gases into the F-T reactor. Nitrogen (N₂) would come from the oxygen plant that is planned in conjunction with the F-T plant process and is a byproduct of the oxygen production. The H₂ and N₂ are then combined in a mole ratio of 3:1 into one product stream and the CO₂ is delivered as a second product stream. Each stream is to be transported in a separate pipeline.”¹

Executive Summary

ISER was asked to prepare an economic analysis of a possible “Cook Inlet Syngas Pipeline” for inclusion in Phase 2 of the “Beluga Coal Gasification Feasibility Study, DOE/NETL-2006/1248.” The request was made the principal author of the Phase 2 study, Robert Chaney. Dr. Steve Colt of ISER performed the economic analysis using pipeline cost data provided by other project contributors.

The analysis determined that the net present value of the total capital and operating lifecycle costs for the pipeline ranges from \$318 to \$588 million. The greatest contributor to this spread is the cost of electricity, which ranges from \$0.05 to \$0.10/kWh in this analysis. The financial analysis shows that the delivery cost of gas may range from \$0.33 to \$0.55/Mcf in the first year depending primarily on the price paid for electricity to power the pipeline compressors.

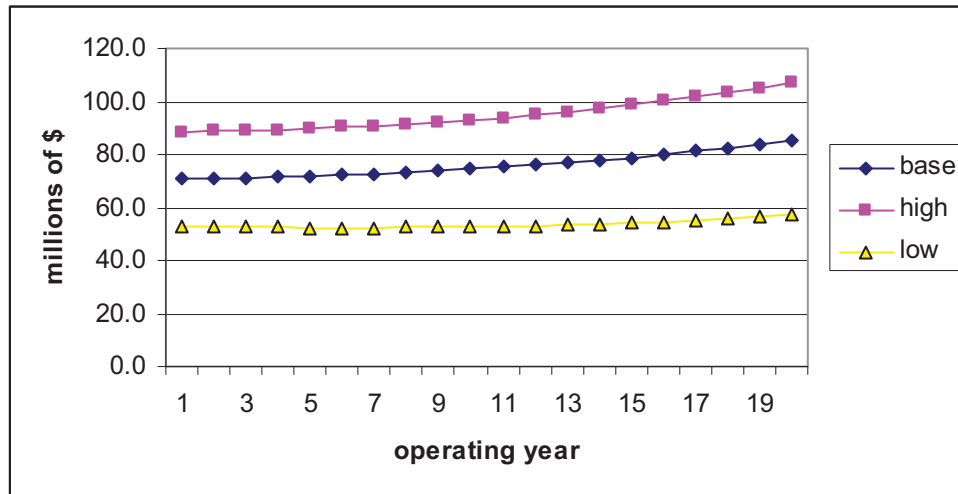
¹ Chaney, et. al. “Beluga Coal Gasification Feasibility Study, DOE/NETL-2006/1248, Phase 2 Final Report, October 2006 for Subtask 41817.333.01.01” Section 7.1.

Table ES-1. Annual SynGas Pipeline Cost of Service

		BASE	HIGH	LOW
COST COMPONENTS, Year 1				
	O&M	35,839,800	44,799,750	23,072,850
	Capital charges	35,100,287	43,875,359	29,835,244
TOTAL COST of SERVICE, YEAR 1		70,940,087	88,675,109	52,908,094
	Total volume of gas from both pipelines (Mcf)	161,030,200	161,030,200	161,030,200
	Cost per Mcf	0.44	0.55	0.33
TOTAL COST of SERVICE, YEAR 20				
	Total volume of gas from both pipelines (Mcf)	161,030,200	161,030,200	161,030,200
	Cost per Mcf	0.53	0.66	0.36

The following chart shows the range and trajectories of the total annualized cost of service for the syngas pipeline.

Figure ES-1. Annual Cost of Service for 20 Years



Experimental Methods

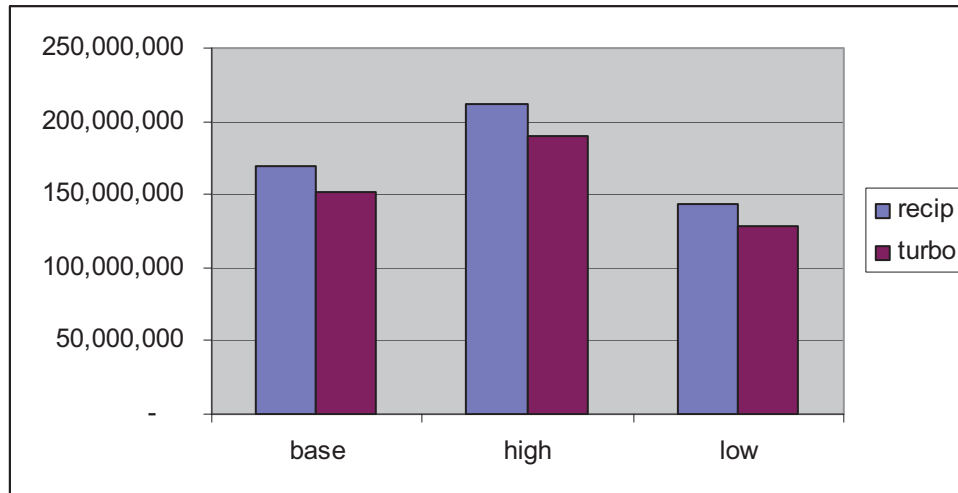
The analysis was conducted using scenario methods combined with net present value discounted cash flows and levelized cost-of-service methods commonly used in utility and regulatory economics. Table 1 shows the scenarios for pipeline capital cost. Turbo compressors were deemed a possible option for reducing capital cost.

Table 1. Capital Cost Assumptions

PROJECT COMPONENT	Capital Cost Amount		
	BASE	HIGH (+25%)	LOW (-15%)
CO2 Land portion			
Compressors (recip)	15,520,400	19,400,500	13,192,340
Material	7,007,000	8,758,750	5,955,950
Construction	3,915,000	4,893,750	3,327,750
Other	5,560,933	6,951,166	4,726,793
Total CO2 land	32,003,333	40,004,166	27,202,833
N2H2 Land Portion			
Compressors (recip)	33,426,000	41,782,500	28,412,100
Material	13,923,000	17,403,750	11,834,550
Construction	8,187,976	10,234,970	6,959,780
Other	10,184,486	12,730,608	8,656,813
Total N2H2 land	65,721,462	82,151,828	55,863,243
Submarine portion	71,307,000	89,133,750	60,610,950
TOTAL PROJECT COST	169,031,795	211,289,744	143,677,026

Possible Savings from Turbo Compressors			
	BASE	HIGH (+25%)	LOW (-15%)
CO2 pipeline savings	(4,700,000)	(5,875,000)	(3,995,000)
N2H2 pipeline savings	(12,800,000)	(16,000,000)	(10,880,000)
TOTAL PROJECT WITH TURBO COMPRESSORS	151,531,795	189,414,744	128,802,026

Figure 1. Range of Total Project Capital Costs



The timing of capital expenditures is assumed to follow a four-year pattern with annual fractions of 15-30-30-25 percent expenditure. The assumed weighted cost of capital is 12.0 percent (base case), leading to additional capitalized interest of about 12% of the overnight cost. This capitalized interest is incorporated when determining annualized total costs below.

The following table summarizes the O&M cost assumptions used in the economic model.

Table 2. Summary of O&M Costs

COST COMPONENT	O&M Cost Amount		
	BASE	HIGH	LOW
Electricity			
Electricity quantity (million kWh)	410.6	410.6	410.6
Electricity price in 2011 (\$/kWh)	0.08	0.10	0.05
Electricity cost in 2011 (\$)	32,848,800	41,061,000	20,530,500
Labor	995,000	1,243,750	845,750
Other	1,996,000	2,495,000	1,696,600
TOTAL O&M COST	35,839,800	44,799,750	23,072,850
note: High and Low electricity prices are author judgment. High and Low labor and other are +25% and -15%			

Results and Discussion

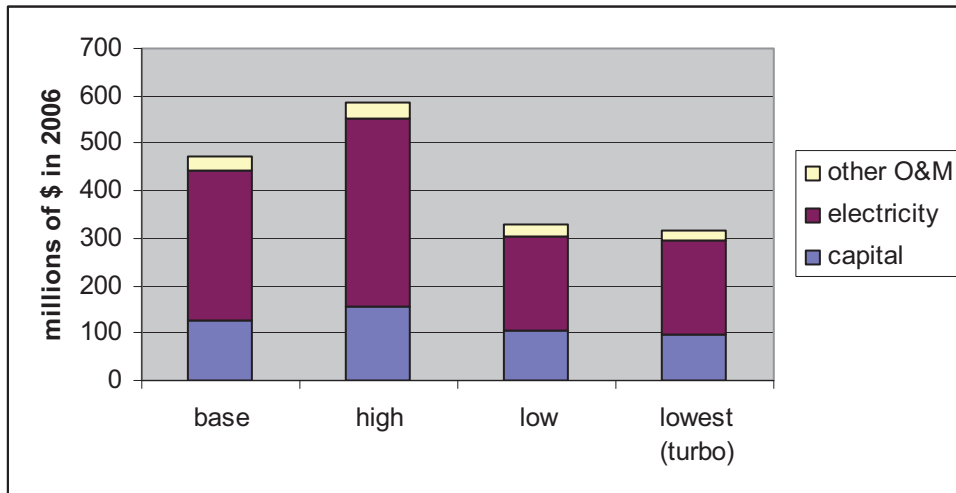
One way to view the overall cost of the syngas pipeline is to combine capital and operating costs into a single net present value (NPV) of future costs. The following table summarizes these NPV cost results assuming a 12% weighted cost of capital as the discount rate and the year 2006 as the decision year or base year for discounting. A 20-year operating life is assumed running from 2011 to 2030.

Table 3. Present Value of Total Project Lifecycle Cost

COST COMPONENT	Net Present Value of all Costs, as of 2006		
	BASE	HIGH	LOW
NPV of Capital Cost (recip compressors)	126,013,259	157,516,573	107,111,270
NPV of O&M Costs, based on:			
annual electricity price escalation	4.0%	4.0%	4.0%
annual escalation all other O&M	3.0%	3.0%	3.0%
NPV of Electricity cost (2011-2030)	317,341,315	396,676,644	198,338,322
NPV of all other O&M costs	27,010,933	33,763,666	22,959,293
NPV of Total O&M	344,352,248	430,440,310	221,297,615
NPV of TOTAL PROJECT COST (2011-2030)	470,365,507	587,956,883	328,408,885
Item: NPV using Low Capital Costs with Turbo Compressors:			317,319,567

Two conclusions are noteworthy from the NPV numbers. First, the range from lowest to highest NPV is \$271 million, with the highest NPV almost twice the level of the lowest. Second, almost \$200 million, or 77%, of this range is due to the range of possible electricity costs that results from a price range of \$0.05 to \$0.10/kWh. In the base case electricity costs constitute 67% of the NPV of all costs. The following chart summarizes these conclusions by showing the components of total NPV for each case. The “lowest” case is based on the low case but with the additional deduction for turbo compressors.

Figure 2. Components of Lifecycle Cost



A second way to view the cost of this project is to annualize the capital cost and calculate an annualized total cost of service. The following estimates are based on a 20 year straight-line depreciation procedure and a depreciated original cost methodology, as would be used if a separate entity operated the pipeline as a regulated utility.

The total annualized cost of service in year 1 (2011) ranges from \$53 million to \$89 million. Roughly half of this year 1 cost is O&M and half is capital charges. By year 20 the cost rises somewhat in nominal dollars, but would actually fall in real dollar terms after factoring out general inflation. By year 20 almost all of the annualized cost is for O&M. On a volumetric basis, using a total gas volume of 161,030,200 Mcf, the annualized cost in year 1 ranges from \$0.33/Mcf to \$0.55/Mcf.

Conclusion

Two major conclusions are apparent from this analysis. First, the range of capital costs for the pipeline depends on the feasibility of turbocharged compressors. Additional technical research might be able to determine whether such technology was feasible and at what incremental capital cost. Second, and most important, although the subsea pipeline is capital-intensive, it would be the ongoing cost of electricity that largely determines the cost of service for the pipeline and hence the project's economic viability.

References

Chaney, Robert, et al. Beluga Coal Gasification Feasibility Study, DOE/NETL-2006/1248, Phase 2 Final Report, October 2006 for Subtask 41817.333.01.01

National Energy Technology Laboratory

626 Cochrans Mill Road
P.O. Box 10940
Pittsburgh, PA 15236-0940

3610 Collins Ferry Road
P.O. Box 880
Morgantown, WV 26507-0880

One West Third Street, Suite 1400
Tulsa, OK 74103-3519

1450 Queen Avenue SW
Albany, OR 97321-2198

539 Duckering Bldg./UAF Campus
P.O. Box 750172
Fairbanks, AK 99775-0172

Visit the NETL website at:
www.netl.doe.gov

Customer Service:
1-800-553-7681



**TRANSPORTATION ISSUES IN THE DELIVERY OF GTL PRODUCTS FROM
ALASKAN NORTH SLOPE TO MARKET**

FINAL REPORT

(Reporting Period: 10/1/2001 to 9/30/2002)

Principal Author: Godwin A. Chukwu, Ph.D., P.E.

January, 2004

Work Performed under Cooperative Agreement No. DE-FC26-01NT41248

Submitted by:

Petroleum Development Laboratory
University of Alaska Fairbanks
P.O. Box 755880
Fairbanks, AK 99775-5880

Prepared for:

The US Department of Energy
National Energy Technology Laboratory
P.O. Box 880
Morgantown WV 26507-0880

TRANSPORTATION ISSUES IN THE DELIVERY OF GTL PRODUCTS FROM ALASKA NORTH SLOPE TO MARKET

DISCLAIMER

This report was prepared as an account of work sponsored by an agency of the United States Government. Neither the United States Government nor any agency thereof, nor any of their employees, makes any warranty, express or implied, or assumes any legal liability or responsibility for the accuracy, completeness, or usefulness of any information, apparatus, product, or process disclosed, or represents that its use would not infringe privately owned rights. Reference herein to any specific commercial product, process, or service by trade name, trademark, manufacturer, or otherwise does not necessarily constitute or imply its endorsement, recommendation, or favoring by the United States Government, or any agency thereof. The views and opinions of authors expressed herein do not necessarily state or reflect those of the United States Government or any agency thereof.

TRANSPORTATION ISSUES IN THE DELIVERY OF GTL PRODUCTS FROM ALASKA NORTH SLOPE TO MARKET

ABSTRACT

The Alaskan North Slope (ANS) is one of the largest hydrocarbon reserves in the United States where Gas-to-Liquids (GTL) technology can be successfully implemented. The proven and recoverable reserves of conventional natural gas in the developed and undeveloped fields in the Alaskan North Slope (ANS) are estimated to be 38 trillion standard cubic feet (TCF) and estimates of additional undiscovered gas reserves in the Arctic field range from 64 TCF to 142 TCF. Because the domestic gas market in the continental United States is located thousands of miles from the ANS, transportation of the natural gas from the remote ANS to the market is the key issue in effective utilization of this valuable and abundant resource. The focus of this project is to study the operational challenges involved in transporting the gas in converted liquid (GTL) form through the existing Trans Alaska Pipeline System (TAPS).

A three-year, comprehensive research program was undertaken by the Petroleum Development Laboratory, University of Alaska Fairbanks, under cooperative agreement No. DE-FC26-98FT40016 to study the feasibility of transporting GTL products through TAPS. Cold restart of TAPS following an extended winter shutdown and solids deposition in the pipeline were identified as the main transportation issues in moving GTL products through the pipeline. The scope of work in the current project (Cooperative Agreement No. DE-FC26-01NT41248) included preparation of fluid samples for the experiments to be conducted to augment the comprehensive research program.

TABLE OF CONTENTS

CHAPTER		PAGE
	Abstract	3
	Executive Summary	5
1	Experimental	6
2	Results and Discussion	7
3	Conclusion	8
	References	9

TRANSPORTATION ISSUES IN THE DELIVERY OF GTL PRODUCTS FROM ALASKA NORTH SLOPE TO MARKET

EXECUTIVE SUMMARY

The Alaskan North Slope is one of the largest hydrocarbon reserves in the United States where Gas-to-Liquids (GTL) technology can be successfully implemented. Gas-to-liquids (GTL) conversion technology, where natural gas is chemically converted to transportable liquid products, is an emerging technology that is expected to reach commercialization within the next decade. The proven and recoverable reserves of conventional natural gas in the developed and undeveloped fields in the Alaskan North Slope (ANS) are estimated to be 38 trillion standard cubic feet (TCF). Currently, only a small portion of the produced natural gas of the North Slope of Alaska is used in the oil-field operation, such as gas lift and power generation, and in local sales. The unused portion is injected back into the reservoir for pressure maintenance and oil production. It is expected that as crude oil production on the North Slope continues to decline, approximately 26 TCF of ANS natural gas will become available for gas sales, transportation and/ or conversion to GTL products. This equates to over 4 billion barrels of oil equivalent.

Transportation of the natural gas from the remote ANS is the key issue in effective utilization of this valuable and abundant resource. The throughput of oil through the Trans Alaska Pipeline System (TAPS) has been on the decline and is expected to continue to decline in future. It is projected that by the year 2015, ANS crude oil production will decline to such a level that there will be a critical need for pumping additional liquid from GTL process to provide an adequate volume for economic operation of TAPS.

A three-year, comprehensive research program was undertaken by the Petroleum Development Laboratory, University of Alaska Fairbanks, under cooperative agreement No. DE-FC26-98FT40016 to address the transportation issues involved in moving GTL products through TAPS. A material testing program for GTL and GTL/Crude oil blends was designed following discussions with John Hackworth (UAF consultant on GTL studies) and Alyeska Pipeline Service Company, the TAPS operator. The main objective of the current project (Cooperative Agreement No. DE-FC26-01NT41248) was to augment the comprehensive research program through preparation of additional fluid samples for the material testing program.

CHAPTER 1

EXPERIMENTAL

This project addresses the study of GTL product transportation through the existing Trans Alaska Pipeline System (TAPS). One of the objectives of this project is to select tests and evaluate samples of GTL products and GTL-crude oil blends in order to assess the feasibility of transporting such materials through TAPS. Density and viscosity measurements as functions of temperature are necessary for calculating horsepower requirements. Experimental data on density and viscosity of naturally occurring hydrocarbon mixtures are not well documented. However, measurements on true boiling point (TBP) fractions of various Arab (Amin and Beg 1994) and North Sea Crudes (Dandekar et. al., 1998), Alberta bitumen (Miadoyne et al., 1994) and Saskatchewan oils (Singh et al., 1994) have been reported. Additionally, the predictive capabilities of various viscosity correlations still remain a weak link. Therefore, the need for accurately measured experimental data is indispensable for evaluating the feasibility of transporting GTL products through the TAPS.

Another important GTL testing parameter is the gel strength, which is one of the most important properties necessary to evaluate the feasibility of cold restart of TAPS. The measurement of gel strength gives an indication of the so-called ‘cold restart pressure’ at which the liquid in the pipeline can yield under the given arctic conditions in Alaska. Thus, bearing in mind the significance of this parameter, gel strengths of various GTL and GTL-ANSC blends need to be determined by the rotating vane technique at different temperatures.

There still exists an uncertainty as to exactly which particular type of GTL product will be the potential candidate for flow through TAPS. A number of GTL product matrix possibilities exist, which are dependent on GTL process options such as catalyst used, process employed, operating conditions and type of GTL product upgrading, and other factors such as gas quality, Alaskan North Slope (ANS) logistics etc. In this study, a GTL sample product was obtained from the US Department of Energy and different fractions of the sample material were used to simulate variation of GTL product types. Thus, we were able to represent a wide range of GTL material that could potentially be produced from a North Slope GTL plant.

CHAPTER 2

RESULTS AND DISCUSSION

Fluid samples for the experiments planned in the comprehensive research project were prepared to represent a wide range of possible GTL output from the proposed GTL plant in the Alaskan North Slope. Fischer Tropsch synthesis for GTL production results in a highly variable liquid composition depending on the exact process used. Therefore, multiple distillate fractions (e.g. 90%, 80%, 70% etc.) of the available GTL sample were prepared and blended with ANS crude oil for the material testing program. In addition, the paraffin wax (heavier alkanes) was separated from the wax sample by a modified ASTM-1160 Vacuum Distillation process to produce only a 20% overhead fraction. This wax fraction was then gravimetrically mixed with the light hydrocarbon GTL liquid in the proportions of 25% wax distillate + 75 % light GTL and 50 % wax distillate + 50 % light GTL. Thus, twenty-four samples were gravimetrically prepared for the material testing program as per the ratios listed below:

- (a) 25 % wax distillate + 75 % light hydrocarbon (LH) GTL
- (b) 50 % wax distillate + 50 % light hydrocarbon GTL
- (i) sample (a) + crude oil (1:4)
- (ii) sample (a) + crude oil (1:3)
- (iii) sample (b) + crude oil (1:4)
- (iv) sample (b) + crude oil (1:3)
- (v) LH sample + crude oil (1:4)
- (vi) LH sample + crude oil (1:3)

In the GTL:crude oil blend ratios, smaller proportions of GTL were used because GTL production in the North Slope is expected to be far less than crude oil production in the foreseeable future. Thus, blends containing lower proportions of GTL are likely to flow through TAPS.

CHAPTER 3

CONCLUSION

The scope of work for this project included preparation of GTL and GTL-crude oil blend samples to be used in the material testing program of the comprehensive research project. Two graduate students, Mr. Aaron White and Mr. Jason Westervelt, were funded through this project. Samples of GTL and GTL-crude oil blends were prepared with varying wax content to simulate a wide range of possible product streams generated by a futuristic GTL plant on the Alaskan North Slope. This was a necessary and crucial step in the overall research program because the exact composition of GTL to be produced on the North Slope is not known at this time.

REFERENCES

- Amin, M. B.; Beg, S. A. Generalized Kinematic Viscosity-Temperature Correlation for Undefined Petroleum Fractions of IBP-95 °C to 455 °C⁺ Boiling Ranges. *Fuels Science & Technology International* 1994, 12, 97-129.
- Dandekar, A., Andersen, S.I.A. and Stenby, E. Measurement of Viscosity of Hydrocarbon Liquids Using a Microviscometer. 1998. *J. Chem. Eng. Data*, 43 (4): 551.
- Malone, R.D. and Komar, C.A. (Eds.): "Natural Gas to Liquids" Technology Status Report, Morgantown Energy Technology Center, US DOE, DOE/METC-89/0265, Jan. 1989.
- Miadoyne, A.; Singh, B.; Puttagunta, V. R. Modelling the Viscosity-Temperature Relationship of Alberta Bitumen. *Fuels Science & Technology International* 1994, 12, 335-350.
- Robertson, E.P., Thomas, C.P. and Avellanet, R.A.: "Economics of Alaska North Slope Gas Utilization Options," paper presented at the SPE Western Regional Meeting, Anchorage, Alaska, May 1996.
- Sharma, G.D., Kamath, V.A., Patil, S.L. and Godbole, S.P.: "The Potential of Natural Gas in the Alaskan Arctic," paper SPE 17456, Proceedings of the SPE California Regional Meeting, Long Beach, CA, March 1988, pp. 515-523.
- Singh, B.; Miadoyne, A.; Huang, S. S.; Srivastava, R.; Puttagunta, V. R. Estimating Temperature and Pressure Effects on Viscosity of Saskatchewan Heavy Oils. *Fuels Science & Technology International*. 1994, 12, 693-704.

Oil & Natural Gas Technology

DOE Award No.: DE-FC26-06NT41248

Final Report

Five Kilowatt Fuel Cell Demonstration for Remote Power Applications Task 2.02.1

Submitted by:

Dennis Witmer
Tom Johnson
Jack Schmid

UAF Energy Center / University of Alaska Fairbanks
Institute of Northern Engineering Arctic Energy Technology Development Laboratory
306 Tanana Loop, 525 Duckering
Fairbanks, Alaska 99775

Prepared for:

United States Department of Energy
National Energy Technology Laboratory

December 31, 2008



Office of Fossil Energy



Five Kilowatt Fuel Cell Demonstration for Remote Power Applications

Final Report

Starting June 1, 2002
Ending Sept 30, 2007

Dennis Witmer
University of Alaska Fairbanks
[@uaf.edu](mailto:dwitmer@uaf.edu)
907-474-7082

Tom Johnson
Jack Schmid
UAF Energy Center

Report Issued December 2008
DOE Award Number
DE-FC26-01NT41248
Task Number 2.02.1

Submitted by:
University of Alaska Fairbanks
Institute of Northern Engineering
Arctic Energy Technology Development Laboratory
Building 814
Fairbanks, Alaska 99775

Disclaimer

This report was prepared as an account of work sponsored by an agency of the United States Government. Neither the United States Government nor any agency thereof, nor any of their employees, makes any warranty, express or implied, or assumes any legal liability or responsibility for the accuracy, completeness, or usefulness of any information, apparatus, product, or process disclosed, or represents that its use would not infringe privately owned rights. Reference herein to any specific commercial product, process, or service by trade name, trademark, manufacturer, or otherwise does not necessarily constitute or imply its endorsement, recommendation, or favoring by the United States Government or any agency thereof. The views and opinions of authors expressed herein do not necessarily state or reflect those of the United States Government or any agency thereof.

Abstract

While most areas of the US are serviced by inexpensive, dependable grid connected electrical power, many areas of Alaska are not. In these areas, electrical power is provided with Diesel Electric Generators (DEGs), at much higher cost than in grid connected areas. The reasons for the high cost of power are many, including the high relative cost of diesel fuel delivered to the villages, the high operational effort required to maintain DEGs, and the reverse benefits of scale for small utilities.

Recent progress in fuel cell technologies have lead to the hope that the DEGs could be replaced with a more efficient, reliable, environmentally friendly source of power in the form of fuel cells. To this end, the University of Alaska Fairbanks has been engaged in testing early fuel cell systems since 1998. Early tests were conducted on PEM fuel cells, but since 2001, the focus has been on Solid Oxide Fuel Cells.

In this work, a 5 kW fuel cell was delivered to UAF from Fuel Cell Technologies of Kingston, Ontario. The cell stack is of a tubular design, and was built by Siemens Westinghouse Fuel Cell division. This stack achieved a run of more than 1 year while delivering grid quality electricity from natural gas with virtually no degradation and at an electrical efficiency of nearly 40%. The project was ended after two control system failures resulted in system damage.

While this demonstration was successful, considerable additional product development is required before this technology is able to provide electrical energy in remote Alaska. The major issue is cost, and the largest component of system cost currently is the fuel cell stack cost, although the cost of the balance of plant is not insignificant. While several manufactures are working on schemes for significant cost reduction, these systems do not as yet provide the same level of performance and reliability as the larger scale Siemens systems, or levels that would justify commercial deployment.

Table of Contents

Five Kilowatt Fuel Cell Demonstration for Remote Power Applications	1
Final Report	1
Abstract	3
Executive summary.....	5
Background.....	6
Experiment.....	9
Results.....	12
Table 1 Run log for FCT Unit at UAF.....	12
Discussion and Conclusions	14

Executive summary

While most areas of the US are serviced by inexpensive, dependable grid connected power, many areas of Alaska are not. In these areas, electrical power is provided with Diesel Electric Generators (DEGs), at much higher cost than in grid connected areas. The reasons for the high cost of power are many, including the high relative cost of diesel fuel delivered to the villages, the high operational effort required to maintain DEGs, and the reverse benefits of scale for small utilities. This problem has been exacerbated by the recent price spike in diesel fuel, resulting in cost of electrical power to levels several times that of urban areas.

Recent progress in fuel cell technologies have lead to the hope that the DEGs could be replaced with a more efficient, reliable, environmentally friendly source of power in the form of fuel cells. To this end, the University of Alaska Fairbanks has been engaged in testing early fuel cell systems since 1998. Early tests were conducted on PEM fuel cells, but these proved expensive, unreliable, and thermodynamically less efficient than existing technology [1]. In particular, the energy required to reform hydrocarbon fuels needed to come from the incoming fuel [2], given the low temperature heat generated by the fuel cell, resulting in a system efficiency of about 25%, which is less than the 35% efficiency typical of a new diesel generator. These results have been verified by the DoD residential fuel cell program [3].

Since 2001, the focus at UAF has been on Solid Oxide Fuel Cells (SOFC), which are capable of higher system efficiencies due to the high operating temperatures, which provide heat of sufficient quality to drive the reformation reaction. This results in a much higher system efficiency, which can approach 50% for large systems operating on natural gas. [4].

Small scale SOFCs are being developed as part of the US DOE SECA program [5], which are of the proper size (a few kilowatts) for distributed residential applications [6]. The major effort of the SECA program focuses on the development of small planar SOFC stacks, while most SOFC demonstrations to date have used tubular cells. Most of the SECA participant teams are currently still in the laboratory stack development stage, and that program is not currently advocating the deployment of these systems in the field.

However, SOFCs are still very much in the pre-commercial development stage, typified by initial unique prototypes requiring significant assembly effort. This also means that the cost of these units is very high, significantly more than any commercial market could bear. First units to leave the factory are typically sent to “safe” locations, where technical support is available, and failure is not public. UAF has played this role for several fuel cell companies, receiving first units shipped, testing them in private, providing technical support, and reporting successes when they occur.

In this program, a cooperative agreement was created between the UAF AETDL (funded by NETL) and Fuel Cell Technologies, of Kingston, Ontario, to demonstrate an “alpha” pre-commercial prototype 5 kW SOFC intended for residential use with combined heat and power. This project was proposed in February, 2002 with an intended delivery of the fuel cell in late 2002. However, delays in the delivery of the stack resulted in a delivery date to Fairbanks of August 1, 2003.

In summary, this demonstration achieved significant technical milestones in demonstrating a small scale SOFC operating on natural gas, with an efficiency of nearly 40%, and stable operation for more than a year in a field location. However, significant additional development needs to occur before small scale SOFCs are ready for large scale commercial deployment.

Background

Electrical grids are capable of providing large amounts of electrical power to consumers and industry at reasonable rates, using large scale coal, natural gas, nuclear, and hydro plants, typically at about 6-10 cents per kW-hr. However, in areas not served by electrical grids, other means need to be found to provide electricity. The most common form generating small amounts of power (1 kW to 2.5 MW) is the diesel electric generator. However, a reasonably efficient DEG can provide about 13 kW hours of electricity per gallon of fuel consumed, a diesel cost of \$1.00 per gallon gives a fuel cost alone of 7 cents per kW-hr. Recent fuel costs have gone much higher, with proportional increases in the cost of power. Typical diesel generators require frequent oil changes, and the high number of moving parts result in significant maintenance costs. While capital costs for DEGs are relatively low compared to other forms of power of generation, the system lifetime is only about 5 years, as opposed to 20-50 years for larger power plants. All of these factors contribute to the high cost of electricity produced from DEGs. Typically, in Alaska, these rates are 20 cents per kW-hr, or higher. These rates are also directly related to the cost of diesel fuel, which has recently increased due to the rising price of crude oil.

Fuel cells have been proposed as a more efficient, environmentally friendly, reliable, and cost effective source of electricity in these remote areas of Alaska. However, justification for many of these claims are based on projected performance and system costs based on estimates provided by the US Department of Energy and fuel cell suppliers. Typically these projections assume efficiencies of near 50% AC out based on the lower heating value of natural gas, system lifetimes of 40,000 hours (5 years) or longer, and stack costs of \$400 per kW, and total system costs of under \$1500 per kW. If systems could be developed that meet these specifications, fuel cells would likely find a large market and displace diesel generators in Alaska. However, the industry still needs to demonstrate that these performance objectives can be met in mass produced commercial devices.

Fuel cells have been in existence for a long time, having been first invented by Grove in 1839. Attempts to generate electricity directly from coal were made in the early 1900's, but the first notable success of fuel cells came during the space program in the 1960s. Fuel cells operating on pure hydrogen and oxygen were introduced during the Gemini program, and continue to be used on current shuttle missions. Fuel cells are ideal for space applications, as the produced water, the waste heat, and the electricity are all useful products, the power to weight ratio is higher than for batteries, and the spacecraft have an ample supply of liquid hydrogen and oxygen already on board for propulsion. However, these fuel cells operate for only short mission lifetimes (less than 1000 hours) in an environment where high performance is valued much higher than the cost of electricity. One additional issue is that the fuel cells used in the space program are alkaline fuel cells, and operate well on pure oxygen, but are contaminated by the carbon dioxide found in the earth's atmosphere.

Fuel cells for terrestrial applications need to be competitive with conventional methods of generating electrical power, which are typically based on combustion to provide the energy for operation of a heat engine. Combustion is a three dimensional gas phase reaction that scales with volume, and is relatively insensitive to impurities. Fuel cells are open system electrochemical devices, and electricity is produced at the solid gas interface. This interface scales with surface area, and is very sensitive to impurities in the system. This requires the use of filters on the reactant flow streams, especially the fuel stream, where the naturally occurring sulfur compounds must be removed. Some fuel cells are sensitive to impurities in the air, such as PEM sensitivity to hydrocarbons. Low temperature fuel cells are also contaminated by CO in the fuel stream.

High temperature Solid Oxide Fuel Cells (SOFCs) use a solid ceramic material as the electrolyte, and use oxygen ions as the ionic transport medium. However, at the operating temperatures required to provide the oxygen mobility, other ions can also move in the structure. This means that impurities in the oxide are mobile, and can form new phases, which can block ionic transport. SOFCs are therefore also sensitive to impurities and interface effects in the materials of construction.

Previous demonstrations of solid oxide fuel cell systems have shown that high efficiency, low degradation, and long lifetimes are achievable. In particular, the Siemens Westinghouse web site indicates that one stack operated for 69,000 hours with little noticeable stack degradation. [4] Conversation with those close to that experiment, however, reveal that that particular system was a stack of only 4 cells constructed with high purity oxide materials, operated inside a tube furnace on pure hydrogen. Achieving this same level of operation on a large stack (a 200 kW stack has about 2300 tubes) using a real fuel (natural gas) has not yet been demonstrated.[7] Field demonstrations have been for 35,000 hours or less, and the hybrid system at Irvine operated for only 3400 hours.

One issue for Siemens Westinghouse has been the need to reduce manufacturing costs for their fuel cell systems. During the 1990's fuel cell tubes were manufactured using an Electro Vapor Deposition (EVD) process which provides a very uniform and consistent

electrolyte layer, but the equipment necessary to do this process is both expensive and slow. A new technique called plasma spray was developed, but switching between these two processes resulted in inconsistent product, and a significant delay in shipping completed stacks to customers. However, as of this writing (February, 2008) it appears that the cost reduction strategies have not been as successful as hoped.

The University of Alaska Fairbanks has been involved in independent third party testing of fuel cells for nearly a decade. The role of an independent test site is to answer several basic questions

1. What does the fuel cell supplier promise: delivery date, specifications, performance? How closely does the fuel cell company meet its own specifications?
2. How long does the fuel cell run, and how much attention does it require to keep it running?
3. What is the cause of shutdowns? Are they scheduled or unscheduled?
4. What is the efficiency of the unit, and how does this compare to other ways of generating power?
5. What is the cost of power from the fuel cell?
6. Is the unit ready for further field demonstrations?

The History of FCT

The fuel cell tested in this project was provided by Fuel Cell Technologies (FCT) of Kingston, Ontario. FCT began in the early 1990s as a company to provide power supplies for unmanned underwater vehicles. These power supplies used aluminum as the energy storage media, and were much like fuel cells in terms of operation and control. In this business activity, FCT developed expertise in Balance of Plant (BOP) and control systems for small power systems in conditions that demanded extremely high reliability, a skill set which they determined to be transferable to the new, growing field of fuel cells. By 2000, FCT's business plans called for development of integrated fuel cells for commercial sale based on the purchase of SOFC stacks from other sources. This strategy took advantage of FCT's expertise in Balance of Plant (BOP) designs from previous products.

In June of 2000, FCT signed an agreement with Siemens Westinghouse Power Corporation to study SOFC systems for residential and remote applications [8]. The agreement was followed by a more formal Joint Development Agreement in November 2000, which indicated that Siemens was responsible for the design and testing of the fuel cell stack, while FCT would design, build, and test the Balance of Plant (BOP), carry out system integration and performance testing, and have demonstration units operating and available in mid-2002. The agreement allowed FCT to market fuel cells under 50kW, while Siemens focused on larger units.

FCT began attempting to market their 5 kW units in the summer of 2001. At that point in time, they were offering units to be shipped between July and December of 2002 at a cost

of \$5,000 per kW, or \$25,000 per unit. This unit was described in a brochure printed for potential customers and investors. FCT contacted UAF for the first time in July, 2001 [9]. By fall, the price had risen to \$50,000 for a 5 kW unit.

At that time, UAF recommended that FCT prepare a proposal for consideration by the newly formed Arctic Energy Technology Development Laboratory (AETDL) at UAF. A proposal package was prepared for the 2002 RFP, which closed at the end of February, 2002. However, part of the discussion leading up to the proposal was the fact that the funding was intended for cooperative R&D efforts, and the total support requested by FCT was for \$169,000, to include engineering support for the design and building of the unit. Additional funds were requested by UAF for support of the demonstration phase. The project was selected by the review panel as one to be recommended for funding.

FCT was also taking orders for other demonstration units at \$50,000 each, and at one time had at least 18 standing orders. However, by late 2002, it was apparent that there was a problem with the supply of fuel cell stacks from Siemens. Instead of a delivery of 25 stacks that FCT anticipated in 2002, only 4 stacks were actually delivered, and those much later than anticipated, in the spring of 2003. FCT was placed in the unfortunate position of needing to cancel contracts, and elected to do so in a way that prioritized delivery of systems to their highest value customers. Because the contract we negotiated with FCT provided additional funding for support of engineering efforts, FCT decided that the UAF contract would be honored.

The initial delivery date given in the February 2002 proposal was for the end of year in 2002. However, due to the delay in stack delivery noted above, the unit was not delivered to Fairbanks until July, 2003, and start-up of the unit was not done until August 1, 2003.

Experiment

Description of this project

In this work, a 5 kW fuel cell was delivered to UAF from Fuel Cell Technologies (FCT) of Kingston, Ontario. The cell stack is of a tubular design, and was built by Siemens Westinghouse Fuel Cell division. The cells were of a 70 cm length, unlike the 150 cm cells typically used in Siemens' larger stacks. A total of 88 tubes were assembled in two bundles to form the total stack.

A brochure from FCT printed in February, 2002 lists the performance characteristics of the SOFC system anticipated. These parameters are listed in Table 1, and compared to the properties of the unit actually delivered to the program. It should be noted in fairness to FCT that the brochure described the anticipated performance of a high volume commercial unit, which, at the time of this writing, has yet to be achieved.

The unit shipped to this program was described as an “apha” unit, meaning that there were several features of the unit that were considered to be unacceptable for commercial field units. These features were: 1) the need for a purge gas of 4% hydrogen in nitrogen for start-up and shut-down (to be replaced with a methanol and water system), 2) electrical heaters of 15 kW for unit pre-heating (to be replaced by a combustor), 3) the need for 40 psig natural gas (to be reduced to 1 psig for commercial units), 4) an inverter capable of only discrete power outputs (commercial units need to load follow), 5) and weight and volume of the unit were above intended specifications. The expectation was that each of these problems could be solved through engineering solutions, though some of the problems were more difficult than others.

The need for 40 psig gas was particularly troublesome, as in most locations this requires both a gas compressor and a special dispensation from the local fire marshal, but the requirement was driven by the need to re-circulate anode tail gas as a source of steam for the reformation of natural gas. In commercial units, this could be accomplished by use of a high temperature fan, but these devices are not common commercial hardware.

The role of the UAF Arctic Energy Technology Development Laboratory in this project was to act as a first customer for this technology.

The first decision that needed to be made was the location for the demonstration. The natural gas infrastructure in Fairbanks is still limited, as there are no local natural gas fields or major pipelines currently passing through the town (though many residents are hoping this changes soon.) However, Fairbanks Natural Gas was founded in 1998 and delivers natural gas to commercial and residential customers. The gas supply currently comes from Cook Inlet, and is liquefied in Wasilla, and trucked to Fairbanks, where it is vaporized and sent through the local pipeline system. The University had no natural gas service at the time of the beginning of the project, and installation of the fuel cell in the laboratories there would have required the extension of the local pipeline by about two miles, at a cost of approximately \$350,000. This was beyond the installation budget of this project.

During the assessment of the cost of bringing gas to the university, it became apparent that Fairbanks Natural Gas was very interested in fuel cell technology, so discussions were held to see if FNG would have a suitable site for the demonstration. One advantage in using the FNG site was that while all residential and commercial customers provided with gas at 2psig for safety reasons, as the natural gas utility, FNG had both access to and permission to deliver gas at higher pressure into their facilities, at 35 psig, eliminating the need for a gas compressor. A second benefit was that the FNG site was capable of absorbing the entire electrical output of the fuel cell at all times, with the produced power simply offsetting the power that needed to be purchased from the local utility. FNG was willing to provide the natural gas at no charge in exchange for the generated power (about a break-even proposition for them, given the retail value of the gas in Fairbanks). Additional considerations were that the unit was physically larger than a typical residential doorway, and heavy (2700 pounds).

A suitable spot was identified in the FNG warehouse to place the fuel cell, and installation was undertaken, with the assistance of Mr. Jim Buckley, from Energy Alternatives, who was acting as the field representative for FCT. This site was close to a large overhead door, had a robust poured concrete floor, a nearby unit heater capable of using the produced heat, and was available for use. In addition, the site was not open to the public, and access to the warehouse was controlled, and visitors monitored through a sign-in sheet at the reception area.

The site preparation required mechanical hookups for 1) Natural Gas at 35 psig, 2) Nitrogen 4% Hydrogen mix at 50 psig, 3) Three phase electrical service for 15 kW (to operate the start-up heaters), 4) plumbing for the heat recovery glycol loop, 5) plumbing for the summer heat dump load, outside the building, 5) an exhaust line for removal of the combustion products, and 6) a high speed data port for data acquisition and control. Supply air for the unit was from the existing heated space. In addition, utility grade gas meters and electrical meters were installed for measurement of the overall efficiency measurements.

The site preparation was somewhat more complicated than a typical home boiler installation, and the costs were significant—about \$15,000 for materials and labor for all the electrical, mechanical, and communications lines. While this number probably overstates the costs that would be associated with the installation of a SOFC system in a residential application in the future, it must be noted that most residential mechanical rooms are separate from the electrical service to the home, and that some modification to homes or home design would be required to minimize the additional cost that installation of these units might cost.

There were many delays in the initial schedule, which called for delivery and start-up of the unit by the end of 2002. FCT's plan called for deployment of 4 field units in 2002, and an additional 50 units in 2003. However, the stack supplier was unable to fabricate fuel cell bundles as quickly as anticipated. This unit was completed at the factory in Kingston, Ontario in May of 2003, and shipped to Fairbanks in July, 2003. Start-up occurred on August 1, 2003.

Results

Table 1 Run log for FCT Unit at UAF

	Date	Meter Hours	Cum Hours
Factory Start-up	6/3/2003	384	
Fairbanks Start-up	8/1/2003	0	384
E-Stop (1)	9/8/2003	921	1305
Restart	9/17/2003	921	1305
Stop (2)	3/19/2004	5342	5726
Start	4/1/2004	5342	5726
E-stop	7/20/2004	7971	8355
Start (70% power)	7/31/2004	7971	8355
E-stop (4)	9/23/2004	9267	9651

(1) Unit faulted due to backpressure on exhaust line. Blower installed in exhaust line, and several other repairs made, including data transfer protocols to store data

(2) Unit shut down deliberately to change de-sulphurizer bed material.

(3) Control system failure occurred, uncontrolled shutdown, some damage to stack occurred. Problem traced to "housekeeping" records in software that were not deleted from buffer, eventually filled available memory, and system failed.

(4) Second control system failure, traced to error in fix for problem (3) above. Second uncontrolled shutdown caused crack of one tube, and a field repair was not attempted.

The unit performed quite well during the testing period, with a steady run of 921 hours before the first shutdown occurred, to allow the correction of several minor installation issues. This was followed by a continuous run of approximately 4421 hours, when a shutdown was scheduled to replace the desulfurizer bed. The unit was then restarted and ran for 2629 hours until an emergency stop occurred. This was determined to be due to a control system issue, as the computer controlling the system was creating daily buffer files, which were exported off the machine and deleted, but each record also resulted in a software "housekeeping" record which was inadvertently not deleted, and eventually filled all available memory. When the memory filled, the operating system crashed, resulting in an uncontrolled shutdown, with some damage to the stack occurring. The unit was restarted, but operated at about 70% of the original power level. The unit failed again on September 23, 2004, once again due to a software failure in the control system, this time due to a small error in the repair done to correct the initial problem. This second uncontrolled shutdown resulted in additional damage to the stack, and restart attempts were not successful. And inspection of the stack revealed that at least one tube had been cracked. There was some discussion about plugging the cell and jumping

around it, but it was decided that this was not practical. The unit had achieved approximately 9267 hours in the field, and the stack had reached 9651 hours when the time at the factory was included. During the field demonstration, this represents an availability (time producing power divided by total time) of 92.2%, which is very good considering that much of the down time was due to the time needed to schedule a restart rather than any difficulty in repair.

The efficiency of the unit can be measured in several ways, and the internal instruments on the fuel cell indicated a first law efficiency of about 40%, as claimed by FCT. However, UAF also installed utility meters to measure the natural gas consumed by the unit and the net AC power produced by it, and these measurements indicated a slightly lower efficiency of 37%, with the discrepancy between the two numbers due to differences in the fuel consumption value.

Stack degradation was anticipated, but measurements taken did not indicate a statistically significant (more than .5%) change in stack performance over the life of the test. This is due in part to the fact that the system was operated at a single set point for several months, then changed to a different static set point, making changes somewhat difficult to observe, but also indicates that the stack was not experiencing rapid degradation.

Based on the long system run, the excellent efficiencies achieved, and the absence of degradation, this demonstration was quite successful. These results were shared with the fuel cell community in a press release, and in a paper presented at the 2004 Fuel Cell Seminar in San Antonio in November 2004.

However, there were several issues that remain to be addressed before SOFC's can be considered for most field applications. Some of these issues are specific to this unit, and can be solved through better product development, while others are perhaps a bit more difficult to address.

The specific issues identified with this unit include:

1. The need to provide significant amounts of electrical power to the system during start-up (15 kW for about 24 hours).
2. The need to provide purge gas during start-up and shutdown.
3. The system size and weight (2700 pounds).
4. Operation on natural gas (usually available only in urban/suburban areas, where grid connected electricity is also available).
5. Requirement that natural gas be provided at 40 psig rather than at the 1-2 psig typical of utility natural gas.
6. The lack of load following ability due to the inverter selection.

The more general issues for all small scale SOFCs include:

1. The cost of producing SOFC stacks
2. The intolerance of SOFC systems to thermal shock and thermal cycling
3. System degradation

In fairness, it must be noted that the issues identified on this list are being addressed by the SOFC industry. In particular, FCT was aware of the issues identified, and was attempting to create a fleet of “beta” units for testing that addressed most of the issues on the first list. The US DOE SECA program is intended to address the broader issues of the SOFC industry, and significant progress is being made on issues on the second list.

Parameter	FCT 2002 Brochure	FCT Hardware Achieved
Dimensions	24x31x67	32X36X76
Weight	350 lbs	2700 lbs
Output (Electrical)	0-5kW load following	2.8 and 3.2 kW fixed
Efficiency (Electrical)	47%	38%
Efficiency (overall)	90%	69%
Fuels	Utility natural gas, propane, hydrogen	Natural Gas @ 40psig
Operating life	16 years	1 year
Operating conditions	-40C to 50 C	0 C to 30 C
Service Interval	6 months	6 months
Cost	\$1000 per kW in high volume	\$52,000 per kW in Alpha unit

Table 2 Comparison of specifications to delivered unit.

Discussion and Conclusions

By many measures, this project was a significant success:

- A 5 kW SOFC was delivered to a field site.
- The unit started as expected.
- After correcting minor installation problems, the unit ran flawlessly for a year.
- The unit delivered three phase grid quality power to a commercial building.
- Stack degradation was negligible during the run.

- The system balance of plant was very robust.
- The system efficiency (AC electricity out/ Natural Gas energy in) was 37%.
- The project was ended by two control system failures (not stack issues).

The project also revealed that there is considerable need for improvement in these SOFC systems before they will be commercially viable. These issues include:

- Requirement of high pressure natural gas (40PSIG) for operation
- Requirement of significant electrical power for start up (15 kW needed for heaters)
- Requirement for bottled purge gas for start-up and shut down
- Improvements needed in electrical deliver system to allow load following

Several issues were also noted with the economics of this unit. These include:

- The rising price of natural gas means that producing electricity from this fuel is not competitive with other forms of power generation.
- Fuel cell system prices in general, and SOFC prices in particular need to fall dramatically before these systems can compete with conventional power generation. In this study, the price of the fuel cell system rose over the project (from \$25,000 to \$50,000 to \$169,000 to \$300,000 for a 5 kW system).
- The expectation was that as time passes, mass manufacturing techniques would increase the availability of fuel cell stacks, and lower the cost. During the period of 2001 to 2007, this did not occur.

The economic issues identified above led to the end of FCT as a company in October, 2006. While the authors of this report were not privy to the details of this business failure, perhaps some general observations could be made. First, FCT decided that its strength was in the production of the balance of plant for fuel cells, and created a business plan based on their strength. As a small company, FCT wisely decided that it could not compete effectively in the development of the fuel cell stacks, and left this task to others. The quality of the systems they developed, the engineering, component selection, control software, and field support, were excellent. However, they depended on other fuel cell developers to supply stacks to them, and negotiated contracts for these to be supplied to them. These contracts were not fulfilled, leaving FCT with no product to ship, unhappy customers, rising costs, and, ultimately, failure of the company.

However, FCT is not alone in its failure, as currently there are no companies delivering a commercial small scale fuel cell product to the market. While the DOE SECA program is still investing in this technology, commercial products still are at least several years away.

What this project did show, however, is that producing a small scale, efficient, robust, reliable solid oxide fuel cell is possible—there are no barriers in terms of science. However, the engineering questions—producing these systems in sufficient volume to meet market demands, improving the product to operate in field conditions, increasing

the robustness of the control system, and, especially, reducing the cost to provide real value to the customers—remain open. It is not clear if the potential markets will justify the investments needed to make these systems real.

References

1. Witmer, D., Ronald Johnson, Tristian Kenny, Chris Morgan, Baskar Neogi, Jose Reuter, Jack Schmid, Andy Lutz Dan Morse, Thomas Johnson, Steve Guthrie, Ron Johnson, and Jay Keller, *Rural Area Power Program (RAPP) Final Report*, in *University of Alaska Fairbanks*. 2002. p. 352.
2. Lutz, A., Robert Bradshaw, Jay Keller, and Dennis Witmer, *Thermodynamic analysis of hydrogen production by steam refoming*. International Journal of Hydrogen Energy, 2003: p. 159-167.
3. DoD Fuel Cell Program, E.C.W.s., *Residential Demonstration Program*. 2004.
4. Siemens. *Siemens Power Systems Web Site*. 2006 12/18/2006 [cited; Available from:
[://www.powergeneration.siemens.com/en/fuelcells/history/milestones/index.cfm](http://www.powergeneration.siemens.com/en/fuelcells/history/milestones/index.cfm).
5. SECA. *SECA Web Page*. 2006 [cited; Available from:
[://www.netl.doe.gov/technologies/coalpower/fuelcells/seca/](http://www.netl.doe.gov/technologies/coalpower/fuelcells/seca/).
6. Witmer, D., Jay Keller, and Ron Jonhson, *Remote Area Power Program for Alaskan Villages*. National Hydrogen Association Annual Meeting, 1999.
7. Singhal, S., *Discussion of Siemens Web site* 2002.
8. FCT, *Press releases from fct.ca*. 2003.
9. Allen, G., *Personal communication (e-mail)*.

National Energy Technology Laboratory

626 Cochrans Mill Road
P.O. Box 10940
Pittsburgh, PA 15236-0940

3610 Collins Ferry Road
P.O. Box 880
Morgantown, WV 26507-0880

One West Third Street, Suite 1400
Tulsa, OK 74103-3519

1450 Queen Avenue SW
Albany, OR 97321-2198

525 Duckering Bldg./UAF Campus
P.O. Box 750172
Fairbanks, AK 99775-0172

Visit the NETL website at:
www.netl.doe.gov

Customer Service:
1-800-553-7681



**Using Carbon Dioxide to Enhance
Recovery of Methane from Gas Hydrate
Reservoirs: Final Summary Report**

B. P. McGrail
H. T. Schaefer
M. D. White
T. Zhu
A. S. Kulkarni
R. B. Hunter
S. L. Patil
A. T. Owen
P. F. Martin

September 2007

Prepared for
the U.S. Department of Energy
under Contract DE-AC06-76RLO 1830



DISCLAIMER

This report was prepared as an account of work sponsored by an agency of the United States Government. Neither the United States Government nor any agency thereof, nor Battelle Memorial Institute, nor any of their employees, makes **any warranty, expressed or implied, or assumes any legal liability or responsibility for the accuracy, completeness, or usefulness of any information, apparatus, product, or process disclosed, or represents that its use would not infringe privately owned rights.** Reference herein to any specific commercial product, process, or service by trade name, trademark, manufacturer, or otherwise does not necessarily constitute or imply its endorsement, recommendation, or favoring by the United States Government or any agency thereof, or Battelle Memorial Institute. The views and opinions of authors expressed herein do not necessarily state or reflect those of the United States Government or any agency thereof.

PACIFIC NORTHWEST NATIONAL LABORATORY
Operated by
BATTELLE MEMORIAL INSTITUTE
for the
UNITED STATES DEPARTMENT OF ENERGY
under Contract DE-AC06-76RLO 1830

Printed in the United States of America

**Available to DOE and DOE contractors from the
Office of Scientific and Technical Information, P.O. Box 62, Oak Ridge,
TN 37831;
prices available from (615) 576-8401.**

**Available to the public from the National Technical Information Service,
U.S. Department of Commerce, 5285 Port Royal Rd., Springfield, VA 22161**

U.S. Department of Commerce, 5285 Port Royal Rd., Springfield, VA 22161



This document was printed on recycled paper.

Executive Summary

Although recent estimates (MILKOV et al., 2003) put the global accumulations of natural gas hydrate at 3,000 to 5,000 trillion cubic meters (TCM), compared against 440 TCM estimated (COLLETT, 2004) for conventional natural gas accumulations, how much gas could be produced from these vast natural gas hydrate deposits remains speculative. What is needed to convert these gas-hydrate accumulations to recoverable reserves are technological innovations, sparked through sustained scientific research and development. As with other unconventional energy resources, the challenge is to first understand the resource, its coupled thermodynamic and transport properties, and then address production challenges.

Carbon dioxide sequestration coupled with hydrocarbon resource recovery is often economically attractive. Use of CO₂ for enhanced recovery of oil, conventional natural gas, and coal-bed methane are in various stages of common practice. In this report, we discuss a new technique utilizing CO₂ for enhanced recovery of natural gas hydrate. We have focused our attention on the Alaska North Slope where approximately 640 Tcf of natural gas reserves in the form of gas hydrate have been identified. Alaska is also unique in that potential future CO₂ sources are nearby, and petroleum infrastructure exists or is being planned that could bring the produced gas to market or for use locally.

The EGHR (Enhanced Gas Hydrate Recovery) concept discussed in this report takes advantage of the physical and thermodynamic properties of mixtures in the H₂O-CO₂ system combined with controlled multiphase flow, heat, and mass transport processes in hydrate-bearing porous media. A chemical-free method is used to deliver a L_{CO₂}-L_w microemulsion into the gas hydrate bearing porous medium. The microemulsion is injected at a temperature higher than the stability point of methane hydrate, which upon contacting the methane hydrate decomposes its crystalline lattice and releases the enclathrated gas. Conversion of the microemulsion to CO₂ hydrate occurs over time as controlled by heat transfer, diffusion, and the intrinsic kinetics of CO₂ hydrate formation. Sensible heat of the emulsion and heat of formation of the CO₂ hydrate provide a low grade heat source for further dissociation of methane hydrate away from the injectate plume. Process control is afforded by variation in the temperature of the emulsion, ratio of CO₂ and water, and droplet size of the discrete CO₂ phase. Small scale column experiments show injection of the emulsion into a methane hydrate rich sand results in the release of CH₄ gas and the formation of CO₂ hydrate. The experimental results were verified with computer modeling using the STOMP-HYD simulator, which showed over 3X enhancement in production rate using the EGHR technique when compared with warm water injection alone.

The gas exchange technology (including EHGR) releases methane by replacing it with a more thermodynamic molecule (e.g., carbon dioxide). This technology has four advantageous: 1) it sequesters a greenhouse gas (CO₂), 2) it releases energy via an exothermic reaction, and 3) it retains the mechanical stability of the hydrate reservoir, and 4) produced water can be used to form the emulsion and recycled into the reservoir thus eliminating a disposal problem in arctic settings.

Page intentionally left blank

CONTENTS

1.0	Introduction.....	1
1.1	Gas Hydrate Occurrence.....	1
1.2	Production of methane from Gas Hydrate Reservoirs.....	1
1.2.1	Thermal Stimulation.....	2
1.2.2	Depressurization.....	2
1.2.3	Inhibitor Injection.....	3
1.2.4	Gas Exchange.....	3
2.0	Experimental.....	7
2.1	Gas Phase Exchange Experiments.....	7
2.2	Single-Phase Injection Experiments.....	8
2.3	L _{CO2} -L _w Emulsion Injection Experiments.....	9
2.4	Continuous Microemulsion Injection Experiments.....	12
2.4.1	Microemulsion injector.....	12
2.4.2	Microemulsion Injection Experiments.....	13
3.0	Modeling.....	19
3.1	Mathematical Model.....	19
3.1.1	Governing Equations.....	19
3.1.2	Phase Saturations.....	20
3.2	Numerical Solution.....	21
3.2.1	Discretization and Linearization.....	21
3.2.2	Primary Variable Switching.....	22
3.3	Application.....	23
3.3.1	Pure Water Injection.....	25
3.3.2	Liquid-CO ₂ Microemulsion Injectant.....	26
4.0	Discussion.....	29
5.0	Conclusion.....	31
6.0	References.....	33

FIGURES

1.	Distribution of gas hydrates on the North Slope of Alaska (MORIDIS et al., 2004).....	1
2.	Carbon dioxide exchange in bulk CH ₄ hydrate as function of time at three different temperatures (0°, 2.5°, and 4°C).....	7
3.	Schematic showing injection path of CO ₂ saturated water into a sand packed HYDEX® 301 column.....	8
4.	Temperature profile as a function of time after injection of CO ₂ saturated water into a sand packed HYDEX® 301 column	9
5.	Density of liquid water and CO ₂ as a Function of Pressure at 15°C.....	9
6.	Schematic showing injection path of L _{CO2} -L _w into a CH ₄ rich hydrate sand packed HYDEX® 301 column.....	10
7.	View through quartz window into magnetically stirred pressure cell containing liquid CO ₂ and water at 15°C and 1000 psig	10
8.	Temperature of sand packed column as a function of time, following injection of L _{CO2} -L _w emulsion	11
9.	Schematic of microemulsion injector	12
10.	High speed photograph (500 fps) of L _{CO2} -L _w microemulsion created inside a sapphire high pressure column (2.54 cm OD).	13
11.	Schematic showing the high pressure sapphire cell equipped with a multi-port thermocouple probe	14
12.	Schematic showing the redesigned high pressure sapphire cell equipped with a bypass port and cooling shroud.....	14
13.	Raman spectra of CH ₄ as vapor, aqueous dissolved, and gas hydrate (porous media).....	15
14.	Raman spectra of CO ₂ as vapor, liquid, aqueous dissolved, and gas hydrate (porous media)	15
15.	Microemulsion injection valving schematic	16
16.	Temperature profile of HYDEX® 301 pressure cell during the formation of CH ₄ hydrate, injection of CO ₂ microemulsion, followed by the formation of CO ₂ hydrate as a function of time	16
17.	Temperature profile of sapphire high pressure cell during the formation of CH ₄ hydrate, injection of L _{CO2} -L _w microemulsion, followed by the formation of CO ₂ hydrate as a function of time	17
18.	Gas analysis data collected during L _{CO2} -L _w microemulsion injection experiments	18
19.	CO ₂ hydrate rich sand extracted from a column injected with L _{CO2} -L _w microemulsion.	18
20.	Hydrate saturation histories for 15°C pure-water injectant	25
21.	Hydrate saturation histories for 50°C pure-water injectant	26

22. Hydrate saturation histories for 15°C, 50% volume liquid-CO ₂ microemulsion injectant...	27
23. Hydrate saturation histories for 25°C, 50% volume liquid-CO ₂ microemulsion injectant...	27
24. ANS well log temperature data shown as shaded area (after Collett 1993).	29
25. Schematic of down borehole injection tool.....	30

TABLES

3.1. Conceptual Phase Conditions and Primary Variable Sets	22
3.2. Implemented Phase Conditions and Primary Variable Sets.....	23
3.3. Hydrologic Parameters and Initial Conditions.....	24
3.4. Hydrate Production Scenarios.....	24
3.5. Liquid-CO ₂ Microemulsion Injectant Simulation Results	26

NOMENCLATURE

- \mathbf{D}_{h_γ} phase hydraulic dispersion coefficient, m^2/s
- D_γ^i diffusion coefficient of component i in phase γ , m^2/s
- g acceleration of gravity, m/s^2
- h_g^i, h_γ gas of component i , phase enthalpy, J/kg
- \mathbf{J}_γ^i diffusive flux of component i in phase γ , $\text{kg}/\text{m}^2 \text{ s}$
- \mathbf{k} intrinsic permeability, m^2
- \mathbf{k}_e equivalent thermal conductivity, $\text{W}/\text{m K}$
- $k_{r\gamma}$ phase relative permeability
- L_w liquid water
- L_{CO_2} liquid CO_2
- \dot{m}_γ phase mass source rate, kg/s
- M^i, M_γ component, phase molecular weight, kg/kmol
- $P_g, P_h, P_i, P_l, P_n, P_\gamma$ gas, hydrate, ice, aqueous, liquid- CO_2 , phase pressure, Pa
- P_g^a, P_g^o, P_g^w $\text{CO}_2, \text{CH}_4, \text{H}_2\text{O}$ vapor partial pressure
- P_{nc} liquid- CO_2 critical pressure
- P_{sat}^a saturated CO_2 vapor pressure
- \dot{q} energy source rate, W
- r_{hl}, r_{il} hydrate-aqueous, ice-aqueous radius, m
- $s_g, s_h, s_i, s_l, s_n, s_t$ gas, hydrate, ice, aqueous, liquid- CO_2 , total-liquid saturation
- $\bar{s}_g, \bar{s}_h, \bar{s}_i, \bar{s}_l, \bar{s}_n, \bar{s}_t$ effective gas, hydrate, ice, aqueous, liquid- CO_2 , total-liquid saturation
- $\bar{s}_{hl}, \bar{s}_{il}$ effective hydrate-aqueous, ice-aqueous saturation
- $\bar{\bar{s}}_l, \bar{\bar{s}}_t$ apparent aqueous, total-liquid saturation
- s_{lr} residual aqueous saturation
- s_γ phase saturation
- t time, s
- T temperature, K
- T_{eq}^{ex}, T_{fp}^{ex} ex-situ hydrate equilibrium, ice freezing point temperature, K
- u_l, u_s, u_γ aqueous, precipitated salt, phase internal energy, J/kg
- \mathbf{V}_γ phase volumetric flux, m/s
- \mathbf{z}_g gravitational unit vector
- β_{gl}, β_{gn} gas-aqueous, gas-liquid CO_2 scaling factor
- $\beta_{hl}, \beta_{il}, \beta_{nl}$ hydrate-aqueous, ice-aqueous, liquid CO_2 -aqueous scaling factor
- θ_{gn}, θ_{nl} gas-liquid CO_2 , liquid CO_2 -aqueous contact angle, radian

μ_γ phase viscosity, Pa s

ζ_l^s total salt aqueous mass fraction

$\rho_l, \rho_s, \rho_\gamma$ aqueous, precipitated-salt, phase density, kg/m³

σ^{ref} reference interfacial tension, dynes/cm

σ_{gl}, σ_{gn} gas-aqueous, gas-liquid CO₂ interfacial tension, dynes/cm

$\sigma_{hl}, \sigma_{il}, \sigma_{nl}$ hydrate-aqu., ice-aqueous, liquid CO₂-aqueous interfacial tension, dynes/cm

τ_γ phase tortuosity factor

ϕ_D, ϕ_T diffusive, total porosity

χ_γ^i mole fraction of component i in phase γ

ψ entry pressure, Pa

ω_γ^i mass fraction of component i in phase γ

1.0 INTRODUCTION

1.1 GAS HYDRATE OCCURRENCE

Clathrate hydrates are solid crystalline “inclusion” compounds, which form when water (the host) is contacted with small hydrophobic molecules (the guest) such as methane, ethane, H₂S, and CO₂ (ENGLEZOS, 1993; SLOAN, 1998) under certain pressure and temperature conditions. When the guest molecule is a constituent of natural gas, clathrate hydrates are also referred to as gas hydrates (SLOAN, 1998). Solid gas hydrates occur generally in two types of geologic settings: 1) on land in permafrost regions where cold temperatures persist in shallow sediments, and 2) beneath the ocean floor at water depths greater than about 500 meters where high pressures dominate (KVENVOLDEN et al., 1993). Although estimates of the amount of in situ hydrates vary considerably, even the most conservative estimate puts the amount of gas present as gas hydrates in the earth at 10¹⁵ m³ (KVENVOLDEN, 1995). This amount far exceeds all conventional energy reserves by as much as a factor of two and could provide for the energy demands of the planet well into the next century.

In 1995, the U.S. Geological Survey (USGS) conducted a study to assess the quantity of natural gas hydrate resources in the United States and found that the estimated quantity exceeded known conventional domestic gas resources (COLLETT, 2004). Recovery of natural gas from these hydrate-bearing deposits has the potential for being economically viable (COLLETT, 2004; MORIDIS et al., 2004; CIRCONE et al., 2005), but there remain significant technical challenges in converting these natural deposits into useable reserves (COLLETT, 2004).

The occurrence of gas hydrates on the Alaska North Slope was confirmed in 1972 in the northwest part of the PBU field (Collett; 1993, Thomas; 2001) and the North Slope now is known to contain several well-characterized gas hydrate deposits. The methane hydrate stability zone extends beneath most of the coastal plain province and has thicknesses >1000 m in the Prudhoe Bay area. Figure 1 depicts the distribution of the Eileen and Tarn gas hydrate accumulations in the area of the Prudhoe Bay, Kuparuk River, and Milne Point oil fields on the North Slope of Alaska. The estimated amount of gas within these gas hydrate accumulations is approximately 37 to 44 Tcf which is equivalent to twice the volume of conventional gas in the Prudhoe Bay field (Collett; 1993).

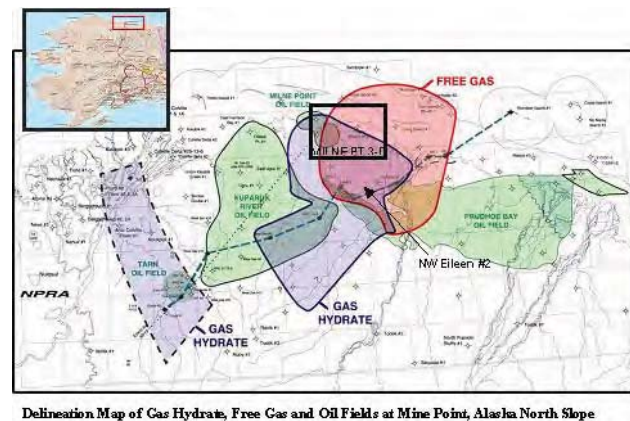


Figure 1. Distribution of gas hydrates on the North Slope of Alaska (MORIDIS et al., 2004)

1.2 PRODUCTION OF METHANE FROM GAS HYDRATE RESERVOIRS

In conventional gas reservoirs, natural gas migrates to the recovery point via pressure gradients. For these reservoirs, the recovery rate is a function of the formation permeability and pressure gradients established between the reservoir and extraction well(s). Natural gas recovery

from hydrate-bearing deposits requires additional energy to dissociate the crystalline water lattice that forms the gas hydrate structure. A variety of methods have been proposed for producing natural gas from hydrate deposits: 1) thermal stimulation, where the temperature is increased above the hydrate stability region; 2) depressurization, where the pressure is decreased below the hydrate stability region; 3) chemical injection of inhibitors, where the temperature and pressure conditions for hydrate stability are shifted; and 4) CO₂ or mixed CO₂ and N₂ exchange, where CO₂ and N₂ replace CH₄ in the hydrate structure. Each of these methods is briefly reviewed in the sections that follow.

1.2.1 Thermal Stimulation

Gas hydrate production via thermal stimulation recently has been investigated experimentally (TANG et al., 2005) and numerically (TSYPKIN, 2000; MORIDIS, 2003, 2004; MORIDIS et al., 2004; POOLADI-DARVISH, 2004). Technologies for implementing thermal stimulation include hot brine injection, steam injection, cyclic steam injection, fire flooding, and electromagnetic heating. Steam injection, cyclic steam injection and fire flooding suffer from high heat losses and the by-products of fire flooding can dilute the produced natural gas. Hot brine injection involves the injection of a saline aqueous solution at an elevated temperature into a gas hydrate bearing geologic reservoir. In general, brine injection yields a heating process that is dominated by advection of sensible heat carried by the brine. The dissolved salt lowers the gas hydrate dissociation temperature. Visual experiments of the dissociation process (TOHIDI et al., 2001) in glass micro-models indicate that during the dissociation process, the hydrate becomes colloidal and migrates advectively with the injected brine. Production experiments of Tang et al. (2005) indicate that the efficiency of the hot brine injection production methodology is dependent on the inlet brine temperature, injection rate, and initial hydrate saturation; where the measure of efficiency is the energy ratio, defined as the ratio of combustion heat of the produced gas over the heat input to the brine. Tang et al. (2005) concluded that lower temperatures and injection rates yield higher recovery energy ratios, as did higher initial hydrate saturations.

The downside of higher energy ratios realized through lower inlet temperatures and injection rates, however, are the lower production rates. Energy ratios for moderate to high temperatures and injection rates are on the order of 2.0, which means 50% of the recovered energy would be used to heat the injected brine. Another class of thermal stimulation technologies involves the injection of two fluids that react exothermally when mixed, such as the acidic- and basic-liquid approach proposed by Chatterji and Griffith (1998). The reaction of these two aqueous solutions would yield a hot salt solution.

1.2.2 Depressurization

Gas hydrate production via depressurization is considered to be the most economically promising technology (COLLETT, 2004). The Messoyakha field in northern Russia is a natural gas accumulation, containing both free gas and hydrate-bearing formations, which has been produced by simple depressurization. The sustained production of natural gas from this field is due to the dissociation of gas hydrate into an underlying free-gas formation, and has demonstrated that gas hydrates are immediately producible using conventional methods. However, production rates are ultimately controlled by heat transfer toward the hydrate dissociation region. Gas production using depressurization at the Mallik site was numerically simulated (MORIDIS et al., 2004) as part of a study to analyze various production methods. A geothermal gradient of 0.03 °C/m across

the hydrate-bearing formation was assumed. The simulation results for a single vertical production well show temperatures dropping in response to depressurization of the formation and hydrate dissociation. The temperature decrease, however, is reversed as deeper warmer water is drawn to the well, providing the needed energy to sustain hydrate dissociation in the depressurized system. When augmented with either steam or hot methane (CH₄) gas injection from a second well, natural gas production is superior in terms of the ratios of produced gas to water and fraction of produced hydrate CH₄.

Numerical depressurization studies for a one-dimensional radial confined reservoir with a central well were conducted using a linearization model (Ji et al., 2001). These studies and others (HONG and POOLADI-DARVISH, 2005; SUN et al., 2005) represent depressurization in its most basic configuration. As expected, simulation results indicate that hydrate dissociation rates and associated gas production rates are controlled by the far-field reservoir pressure and temperature, via energy supplied by natural gas advected from the far field to the dissociation front. Laboratory experimental studies of gas hydrate production via depressurization (LIU et al., 2002; SUNG et al., 2003) have been limited in number and scope. Because of the thermal self-regulation of gas hydrates, pure depressurization is a viable option for natural accumulations of gas hydrates, but may suffer from slow production rates. Sustained production using depressurization additionally requires a heat source. At the Messoyakha field, that energy source is likely heat transfer into the dissociation zone via thermal conduction and advection, which ultimately controls the production rate.

1.2.3 Inhibitor Injection

Thermodynamic inhibitors lower the hydrate formation temperature, which can result in hydrate dissociation when injected into a gas-hydrate-bearing formation (SUNG et al., 2002). The most common thermodynamic organic inhibitors are methanol, monoethylene glycol (MEG) and di-ethylene glycol (DEG) commonly referred to as glycol. Dissolved salts (e.g., NaCl, CaCl₂, KCl, NaBr) can also be inhibitors. Whereas gas hydrate inhibitors are an effective methodology for preventing hydrate formation in engineering applications, their use in the production of natural gas hydrates is prohibitive from three perspectives: 1) environmental impact, 2) economic costs, and 3) thermal self regulation of gas hydrates.

1.2.4 Gas Exchange

Ohgaki et al. (1994; 1996) first advanced the concept of exchanging CO₂ with CH₄, through experiments that showed CO₂ to be preferentially clathrated over CH₄ in the hydrate phase and demonstrated the possibility of producing CH₄ gas by injecting CO₂ gas. During the exchange process, Ohgaki et al. (1996) observed that the mole fraction of CO₂ in the hydrate phase was greater than that in the gas phase. Seo et al. (2001; 2001) quantified this effect by noting that gas phase mole fractions of the hydrate formers (i.e., CH₄ and CO₂) above 40% CO₂ yielded hydrate phase mole fractions of CO₂ in the hydrate phase greater than 90%. Pure CH₄ and CO₂ form structure I (sI) type hydrates (SLOAN, 1998) and their mixtures also form sI type hydrates (LEE et al., 2003). In forming mixed CH₄ and CO₂ hydrates, the CH₄ molecules occupy both the large and small cages of type sI hydrates, whereas the CO₂ molecules only occupy the large cages. Without hydrate dissociation, there is an upper limit to the substitution of CO₂ for CH₄ in hydrates. Lee et al. (2003) estimated that approximately 64% of the CH₄ could be released via exchange with CO₂. In addition to equilibrium considerations, the heat of CO₂ hydrate formation

(-57.9 kJ/mol) is greater than the heat of dissociation of CH₄ hydrate (54.5 kJ/mol), which is favorable for the natural exchange of CO₂ with CH₄ hydrate, because the exchange process is exothermic (SMITH et al., 2001). Although there are a considerable number of open literature publications on the CO₂-CH₄ gas exchange concept, U.S. patent applications with very similar ideas have recently been filed.^{a,b}

Neither Ohgaki et al. (1996) or Nakano et al. (1998) addressed the important issue of the kinetics of the gas exchange reaction. The first attempt to do so was performed by Uchida et al. (2001). Using a Raman spectroscopic method, they confirmed the swapping reaction at the hydrate-gas interface. Although the authors did not directly address the issue in their paper, their results suggested that the exchange mechanism was slow with induction times requiring several days. They did not address the more difficult question of the rate of CO₂ gas penetration further into bulk hydrate, beyond the first few hundred nanometers at the interface.

Multiphase exchange of CO₂ for CH₄ was proposed by Hirohama et al. (1996). Essentially, the method is identical to that proposed by Ohgaki et al. (1996) except extending to higher pressures such that CO₂ was in the liquid state instead of gaseous. The authors reported slow conversion kinetics with liquid CO₂ and in fact had much more rapid CH₄ recovery using gaseous N₂ instead. For liquid CO₂ injection, thermodynamic conditions can either favor CO₂ or CH₄ cage occupation. This transition occurs where the pure CO₂ and CH₄ temperature-versus-pressure equilibrium functions cross with increasing pressure above the gas-liquid CO₂ phase boundary.

Hydrate formation in geologic media that have a distribution of pore sizes will begin in the largest pore spaces and then continue into smaller pore spaces until the *in-situ* equilibrium condition is reached for a particular pore radius (CLENNELL et al., 1999). In addition to the equilibrium condition, porous media may affect other thermodynamic properties of hydrates. For example, in Goel's (2006) review of CH₄ production with CO₂ sequestration, a number of contrasting observations were revealed concerning the *in-situ* enthalpy of dissociation of CO₂ and CH₄ hydrates. Some research indicated that there was an increase in the heat of dissociation between *in-situ* and *ex-situ* conditions; whereas, other research indicated the opposite. Another example is the value of the lower quadruple point (ice-water-hydrate-gas) temperature and pressure for CH₄ and CO₂, and the upper quadruple point (water-hydrate-gas-liquid CO₂) for CO₂ hydrate between *in-situ* and *ex-situ* conditions; where, the *in-situ* conditions were determined for a porous media of limited pore-size distribution. In geologic media that have distribution of pore sizes, hydrates would form and dissociate over a range of temperatures and pressures according to the distribution of pore radii and accounting for the impact of salts in the residual pore water (MCGRAIL et al., 2007). The critical conclusion from Goel's (2006) review with respect to hy-

^aSivaraman, A. 2005. "Process to Sequester CO₂ in Natural Gas Hydrate Fields and Simultaneously Recover Methane." Gas Technology Institute, U.S. Patent Application No. 20050121200.

^bGraue; A. 2006. "Production of Free Gas by Gas Hydrate Conversion." ConocoPhillips Company, U.S. Patent Application No. 20060060356.

drates in porous media is that to understand the gas exchange technology there is a need for quantitative estimates of formation and dissociation processes in geologic media core samples.

In the following section, we describe a set of laboratory experiments that were performed leading to a new approach for execution of the CO₂-CH₄ exchange process in gas hydrate reservoirs that we call the Enhanced Gas Hydrate Recovery (EGHR) process.

2.0 EXPERIMENTAL

A series of laboratory experiments designed to investigate the feasibility of releasing CH₄ from natural gas hydrates by injecting a CO₂ rich fluid into a gas hydrate rich sediment is described below. Different forms of CO₂ (vapor, aqueous dissolved, and L_{CO2}-L_w) were tested and evaluated.

2.1 GAS PHASE EXCHANGE EXPERIMENTS

Although swapping CO₂(g) for CH₄(g) in bulk CH₄ hydrates is thermodynamically favorable, important factors such as kinetics of the reaction had not been fully investigated. Experiments were designed to measure the rate of CO₂ replacement in bulk CH₄ hydrate using a high pressure cell equipped with quartz viewing windows. Raman spectroscopy was used to monitor the CO₂(g) penetration rate as a function of time at the solid-gas interface and into the bulk gas hydrate. No porous medium was used in these experiments.

Measurements for the rate of CO₂ replacement were determined by swapping out the head-space gas in a chilled, high-pressure cell containing bulk CH₄ hydrate and collecting Raman spectra at discrete time intervals and depth. Production of bulk CH₄ hydrate was achieved simply by pressurizing a measured amount of water in the Paar cell up to 1400 psig with methane and chilling in a freezer while a magnetic stir bar vigorously agitated the water. The identifying peak wavelengths for CO₂ hydrate were used to determine the mass transfer of CO₂(g) into the bulk CH₄ hydrate. Depth of penetration verses time was determined by establishing peak intensity to baseline noise criteria.

A number of experiments were conducted at different temperatures under constant pressure (500 psig). An example of measured CO₂ penetration rates into bulk CH₄ hydrate at three different temperatures (0°, 2.5°, 4.5°C) is shown in Figure 2. As the temperature of the cell increases, the exchange rate of CO₂ for CH₄ in the bulk CH₄ hydrate increases. The maximum rate of penetration was 9 mm after 6 hours at 4.5°C. For this particular experiment, a duplicate run was conducted for 2.5°C and appeared to produce similar results (Figure 2). The calculated rate of CO₂ exchange is approximately 0.25 mm/h at 0°C. Increasing the temperature to 4.5°C increases the CO₂ rate of exchange to approximately 1.3 mm/h.

The gas exchange rate data show that penetration of CO₂ into bulk methane hydrate is a slow process and would be ineffective as a production method unless a means was employed to mix the CO₂ into the zone where the methane gas hydrates were present. Because of the low intrinsic permeability of gas hydrate bearing porous media, achieving such intimate mixing appears to be difficult without implementing some means to either stimulate the formation or induce bulk methane gas hydrate dissociation. As such, the

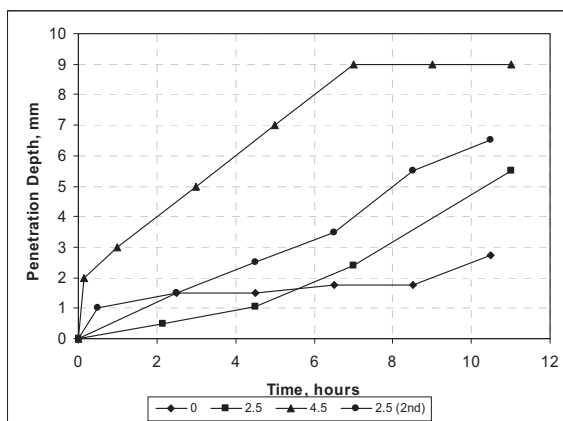


Figure 2. Carbon dioxide exchange in bulk CH₄ hydrate as function of time at three different temperatures (0°, 2.5°, and 4°C)

author's conclude that a strictly gas exchange method does not appear to be practical for gas hydrate production in the absence of other stimulation methods.

2.2 SINGLE-PHASE INJECTION EXPERIMENTS

The next set of experiments consisted of injecting a CO₂ rich fluid into a gas-hydrate bearing sand column. Extensive laboratory experimentation utilizing custom designed and fabricated equipment was used throughout this phase of the project.

All experiments were conducted in custom high-pressure columns constructed from a rigid polyurethane resin HYDEX® 301 (Dow Chemical Company). The five inch long, 37-ml volume columns consisted of one input port in the bottom and one outflow port in the top. Approximately 35g of 20/30 mesh Accusand (Unimin Corporation, Le Sueur, Minnesota) was used to fill the column before each experiment. A small piece of Spectra Mesh fluorocarbon filter was attached to the top inside area of the column to prevent sand from migrating out of the column. Pressurized water was supplied through ISCO syringe pumps. Column temperature was controlled by 3.05 m of 0.30 cm (outer diameter) copper tubing coiled around the cylinder portion of the column and connected to a Thermo Neslab (model RTE7) Digital One circulating water bath. For added temperature stability, a thermal blanket was placed on top and around the HYDEX® 301 column and copper tubing coil. Internal column temperature was monitored by two type T-thermocouples positioned in opposite ends of the column and connected to an Omega HH509R digital meter.

Gas volume measurements were conducted with a “J” tube type manometer assembly. After completion of the experiment, the HYDEX® 301 column was connected to a series of three calibrated tubes, with the last two tubes containing H₂O. As the CO₂-saturated H₂O exited the HYDEX® 301 column, the H₂O was trapped in the first tube (later weighed) and the evolved CO₂ gas displaced H₂O from the second column into a third column. The displaced volume was used to calculate the amount of CO₂ present in the HYDEX® 301 column. The mass of water evolved during column depressurization was added to the residual mass of water in the column, which was determined by subtracting the known initial dry weight of the column.

Single-phase injections (CO₂-saturated water) occurred in the experimental setup shown in Figure 3. At first, the Parr high-pressure reactor containing water was pressurized with CO₂ to 1040 psi, chilled to 15°C, and allowed to equilibrate over night. A line attaching the HYDEX® 301 column (sand packed) to a dip tube in the Parr reactor delivered CO₂ saturated water into the column.

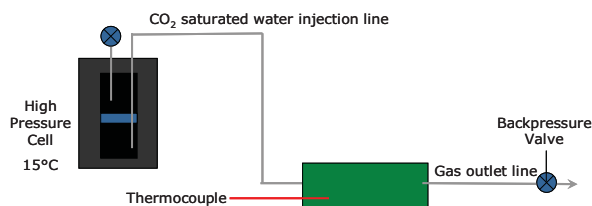


Figure 3. Schematic showing injection path of CO₂ saturated water into a sand packed HYDEX® 301 column

As shown in Figure 4, following the injection of CO₂-saturated water, the column temperature steadily declines toward the water bath temperature of 2°C. Pressure on the column was maintained at 1040 psi. After 30 minutes, a significant thermal spike occurred, indicating the formation of CO₂ hydrate. This example, a temperature increase of 4°C above baseline, is typical of results obtained during these single-phase injection experiments.

For this particular experiment, the total amount of CO₂ and water in the HYDEX® 301 column was determined to be 0.53g and 6.8g respectively, giving a hydration number of 30. The ideal hydration number for sl gas hydrate is 5.75 mol-H₂O per mol gas. However, complete filling of the gas hydrate cages is never achieved in practice and natural gas hydrates typically have hydration numbers of approximately 6 to 6.5. The very high measured ratio of 30 reflects the fact that CO₂-saturated water contains insufficient total CO₂ to achieve complete conversion of the available water to gas hydrate. However, the experiment did prove the feasibility of injecting CO₂ rich fluid into a porous sand, dissociating the methane hydrate in the process. To obtain higher CO₂ hydrate saturations and thus improve process efficiency, a means to increase the amount of CO₂ available for conversion to gas hydrate is required. Our approach to achieving that objective is provided in the next section.

2.3 L_{CO2}-L_w EMULSION INJECTION EXPERIMENTS

Figure 5 shows the change in fluid density of CO₂ and water at 15°C as pressure increases. At sufficiently high pressure, CO₂ becomes a liquid and the density difference between water and liquid CO₂ is reduced to just a few percent. In contrast, the equilibrium pressure to form CO₂ hydrate at 15°C is approximately 43 MPa (6200 psia). Consequently mixtures of liquid CO₂ and water can be formed at 15°C to very high pressures and remain well outside the stability region where a CO₂ hydrate can form. Exploiting these unique physical properties of the CO₂-H₂O system is the fundamental idea behind our Enhanced Gas Hydrate Recovery method. Our concept is to utilize the small density contrast between liquid CO₂ and water to form a transiently stable microemulsion that could be injected into a porous medium containing gas hydrate. The emulsion can be formed with the proper ratio of CO₂ and water to ensure

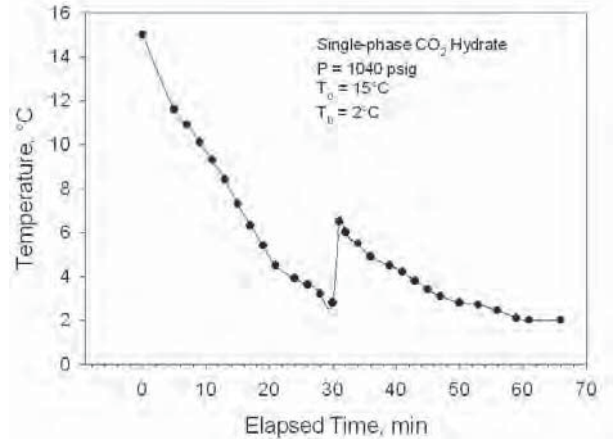


Figure 4. Temperature profile as a function of time after injection of CO₂ saturated water into a sand packed HYDEX® 301 column

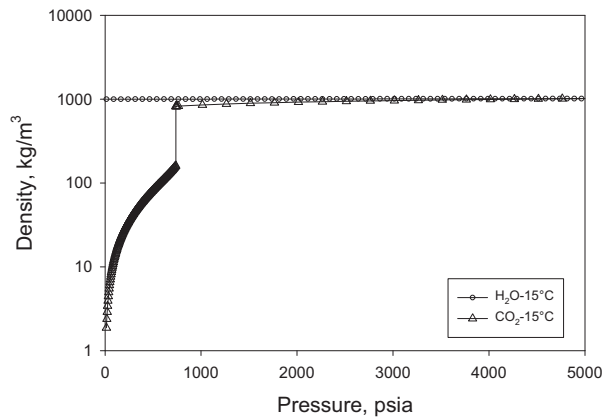


Figure 5. Density of liquid water and CO₂ as a function of pressure at 15°C

optimum conversion of the water to gas hydrate upon cooling into the stability region. The idea of injecting emulsions into porous media is not new; emulsions are used in a variety of subsurface applications including bioremediation, surfactant-enhanced remediation, and enhanced oil-recovery (YAN et al., 2006; CORTIS and GHEZZEHEI, 2007). However, we are unaware of any prior attempt to use high pressure liquid CO₂-H₂O emulsions to produce gas hydrates.

Our first attempt at injecting a two phase mixture of L_{CO₂} and L_w was accomplished using the experimental setup shown in Figure 6. The high pressure Parr reactor containing 750 ml of deionized water was pressurized to 1000 psig with CO₂ and chilled to 15°C while being vigorously stirred. The HYDEX® 301 column packed with moist sand was pressurized with CH₄ to 1000 psig and chilled to -2.5°C, forming CH₄ hydrate rich sand. After overnight equilibration, the HYDEX® 301 column was connected to a 0.30 cm (outside diameter) stainless steel dip tube inserted into the Parr reactor with approximately 10.16 cm of tubing. The outflow (top) of the HYDEX® 301 column remained connected to an ISCO pump.

The L_{CO₂}-L_w emulsion shown in Figure 7 was delivered to the inlet of the HYDEX® 301 column by extraction through the dip tube. Pressure on the HYDEX® 301 was maintained at 980 psig (ISCO pump), which was 20 psi lower than the Parr reactor. Upon opening the sampling valve on the Parr reactor, the L_{CO₂}-L_w emulsion flowed at a maximum rate of 75 mL/min from the Parr reactor through the HYDEX® 301 column and through the back-pressure valve into an ISCO pump. Approximately 75 ml of emulsion was pumped through the sand before the outflow valve on the HYDEX® 301 column was closed. Pressure of 1000 psig was maintained on the HYDEX® 301 column by maintaining pressure in the Parr reactor with the ISCO pump.

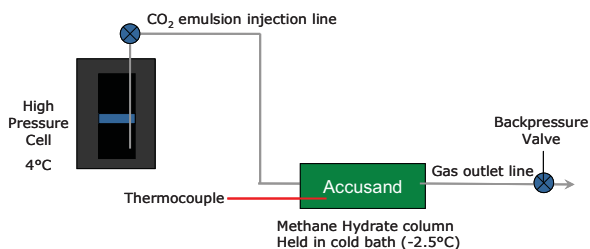


Figure 6. Schematic showing injection path of L_{CO₂}-L_w into a CH₄ rich hydrate sand packed HYDEX® 301 column



Figure 7. View through quartz window into magnetically stirred pressure cell containing liquid CO₂ and water at 15°C and 1000 psig

Temperature changes occurring inside the HYDEX® 301 column after injection of emulsion were recorded for approximately four hours. Figure 8 shows the difference in temperature between the top and bottom of the HYDEX® 301 column over a period of 250 minutes. The cooling profiles show significant deviations from the expected parabolic cooling profile indicating hydrate formation within the column. The total amount of CO₂ and water in the sand was measured to be 2.72 g CO₂ and 6.80 g-H₂O for a hydration number of 6.1. Hence, the injection method produced an almost ideal stoichiometric quantity of CO₂ and water for conversion to hydrate.

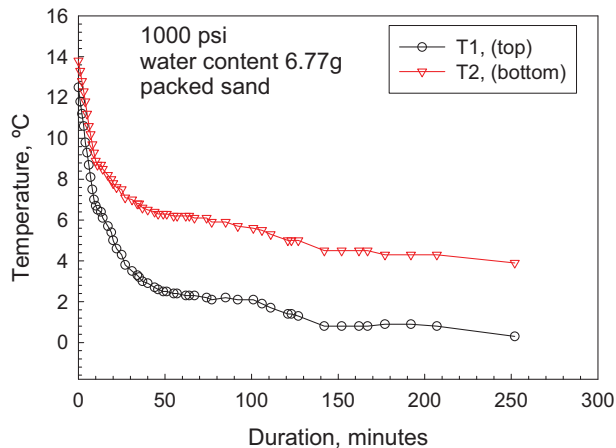


Figure 8. Temperature of sand packed column as a function of time, following injection of L_{CO2}-L_w emulsion

We also performed an experiment injecting a three phase fluid containing L_w-L_{CO2}-H. For this series experiment, the objective was to examine impacts of having preformed CO₂-hydrate nuclei present in the injectate on the rate of CO₂-hydrate formation post-injection. Consequently, CO₂-hydrate was grown in the stirred Parr pressure vessel the day before injection and hydrate formation was confirmed using scanning laser Raman analysis. Utilizing the same experimental setup as described in Figure 6, a series of CO₂ hydrate injections was conducted.

Initially a known amount of distilled water was injected into the HYDEX® 301 column near the inlet thermocouple port to bring the volumetric water content in the cell such that 70% of the pore space was occupied with water. Weight measurements were recorded to accurately know the water content of the column. Methane gas was then injected into the column bringing the pressure of the cell up to 700 psig. The HYDEX® 301 column was then placed into a cooling bath held at room temperature and allowed to equilibrate for 2 hours. After this time, the cooling bath was set to -10°C and temperature recordings were made every 15 seconds. This temperature was maintained overnight to allow maximum equilibration for the methane-water/ice system. After a 20 hour time period elapsed, the cooling bath temperature was raised to -2.5°C and stabilized for 2 hours. Methane was then allowed to flow through the column and the resulting pressure differential was recorded. When gas flow between the outlets was induced, pressure drop across the column increased significantly because of the reduction in porosity upon hydrate formation. The system was allowed to flow until a constant pressure differential was maintained. After this process, flow was stopped and the column pressure was raised to roughly 600 psig.

Just prior to injection, the Parr reactor containing CO₂ hydrate was removed from the freezer and allowed to warm under ambient conditions. Mechanical stirring was started so as the solid hydrate mass broke up, CO₂ hydrate particulates formed that could enter the pore space. Once the aqueous phase was highly turbid with these nucleated CO₂-hydrate particles (occurred at a temperature of 4°C), injection of a known amount of liquid was carried out through 0.63 cm tubing. The tubing connected the Parr reactor directly to the column containing methane hydrate. Water bath temperature where the column was immersed was maintained at -2.5°C. The volume

of tubing was also measured and used in the calculation for the total amount of injectant added to the column.

Shortly after injection of the turbid fluid, the column temperature in the cooling bath spiked to 8°C. This large heat gain could only occur from the heat released from formation of CO₂-hydrate. Gas samples were also obtained from the outlet port of the column and analyzed by gas chromatography. Gas chromatography was used to analyze a sample taken 30 minutes after injection. Peak area analysis reveals no CO₂ vapor contained in the extracted gas phase, only methane. Hence, this experiment provides conclusive proof that multiphase CO₂ injection can be performed successfully in CH₄ hydrate bearing sediments, the free methane gas can be recovered, and the injected CO₂ retained as a gas hydrate in the sediment. However, we elected not to pursue this method further because the technique would be very difficult to implement in a field setting and injection of particulates was considered likely to lead to pore plugging.

2.4 CONTINUOUS MICROEMULSION INJECTION EXPERIMENTS

The injection experiments discussed in Section 2.3 were far from optimal in that use of pressure vessel inherently limits the volume of the two phase mixture that can be delivered and as is apparent from Figure 7, the droplet size of the liquid CO₂ spans a considerable range, much of which is far too large to pass through pore throats in typical sandy sediments. Consequently, a device was developed to supply a continuous stream of liquid CO₂ droplets suspended in water that is formed immediately before injection into a porous medium.

2.4.1 Microemulsion injector

Requirements for a microemulsion injector included combining liquid CO₂ and H₂O to form an emulsion without using chemicals or additives. Multiple injector designs were tested. Initially the injector was placed up into the column, but sealing problems proved difficult to overcome. Mature designs positioned the injector inside the base of the pressure cells, eliminating o-rings and potential fluid leakage. The resulting product, shown in Figure 9, was fabricated from 304 stainless steel. The base measures 7.62 cm x 5.08 cm x 2.54 cm and has an inlet for CO₂, H₂O, and an outlet for the L_{CO₂-L_w} microemulsion. The bypass positioned on the side of the injector (Figure 9) is used to direct the emulsion away from the column, which is used in the initial stages of the injection experiments. Details on the internal configuration of the injector used to form micrometer size droplets of liquid CO₂ are not disclosed in this report due to intellectual property considerations.



Figure 9. Schematic of microemulsion injector

Testing of the microemulsion injector was conducted through a number of experiments by changing the ratio of H₂O to CO₂ as well as both the CO₂ and H₂O injection rates. Each time, the microemulsion formed as expected. Figure 10 shows an example of the resulting microemulsion jets exiting the injector that were captured with high speed photography. The digital video images were captured by a Photron 1280 PCI high-speed digital camera equipped with a 105-mm lens. In all testing conducted, the camera was operated at 500 frame-per-second with a resolution of 1,280 by 1,024 pixels or at 1,000 frame-per-second with a resolution 1,280 by 512 pixels. The microemulsion is formed inside the injector before exiting the microemulsion outlet (Figure 10). At 500 fps, the individual discrete particles of CO₂ were too small to distinguish. Additional images were collected at 1000 fps, which also showed no discernible detail of the emulsion structure. The large L_{CO2} droplets apparent in Figure 10 result from droplet coalescence and collisions in the pressure cell long after exiting the injector.

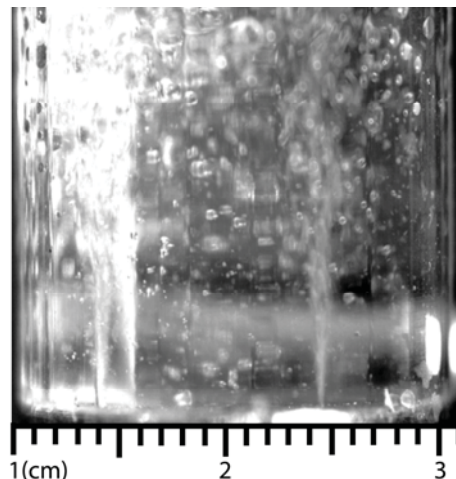


Figure 10. High speed photograph (500 fps) of L_{CO2}-L_w microemulsion created inside a sapphire high pressure column (2.54 cm OD).

2.4.2 Microemulsion Injection Experiments

Originally, L_{CO2}-L_w microemulsion experiments were conducted in pressure cells constructed of HYDEX® 301, which had been commercially polished to appear transparent. Cell temperature was controlled by a Plexiglas shroud wrapped around the cell through which chilled fluid (antifreeze) was distributed by a bench top chiller. This experimental cell worked well for observing the formation of gas hydrates in porous sand. The material is robust and capable of withstanding multiple assemblies and unexpected pressure spikes without creating safety concerns. Additionally, the material is cost effective and has a long history of use as construction material for pressure cells. However, there were some disadvantages associated with using this type of resin. Characterization and confirmation of the formation of hydrates in a porous media were limited to thermal signatures, with no direct verification of the presence of gas hydrate via optical spectroscopic methods. The polished surface of the cell also reacted with CO₂ and turned cloudy. Therefore, an alternate type of reactor material was required.

A thin walled high-pressure sapphire tube rated for 1300 psig was procured and integrated into the current cell design (Figure 11). The sapphire tube, measuring 15.24 cm long and 1.11 cm in diameter, allowed ex situ characterization by Raman spectroscopy of interstitial pore fluids and gas hydrates formed in porous media such as sand. As can be seen in Figure 12, the pressure cell is equipped with the microemulsion injector and a multi-channel thermocouple capable of monitoring internal cell temperature at six different locations. The cell temperature was controlled either by submersing in a water bath or by wrapping a coil of copper tubing around the cell and using chilled fluids as a heat transfer source. Preliminary experiments indicated problems with moisture condensation on the outside of the cell while collecting Raman spectra, which caused undesirable specular reflections. Also during these experiments, it was found that some startup time with the high pressure pumps was required before a consistent microemulsion could be generated for injection.

The base of the pressure cell was modified to include a small port for pre-injection fluids to bypass the column (Figure 12). At the start of the injection, H₂O flow is required to reach a desired level before liquid CO₂ is introduced to create the emulsion. Directing this fluid out the bypass rather than through the porous media and out the top of the column is necessary to achieve optimal ratios of water and CO₂ in the column.

Once the desired flow for both H₂O and liquid CO₂ are sufficient to generate the L_{CO₂}-L_w microemulsion, the bypass is closed and the emulsion is directed up through the CH₄ hydrate rich sand. Additionally, a vortex tube was incorporated into the cell design to control the cell temperature. This device uses ordinary compressed air to generate a stream of cooled air to -46°C. The stream of air is directed into a Plexiglas shroud surrounding the sapphire cell (Figure 12). This technique was very effective in cooling the column and eliminated interference with moisture condensation. Preliminary tests were conducted without sand in the column allowing for a visual confirmation that the injector produced a microemulsion at appropriate pressures and flow rates.

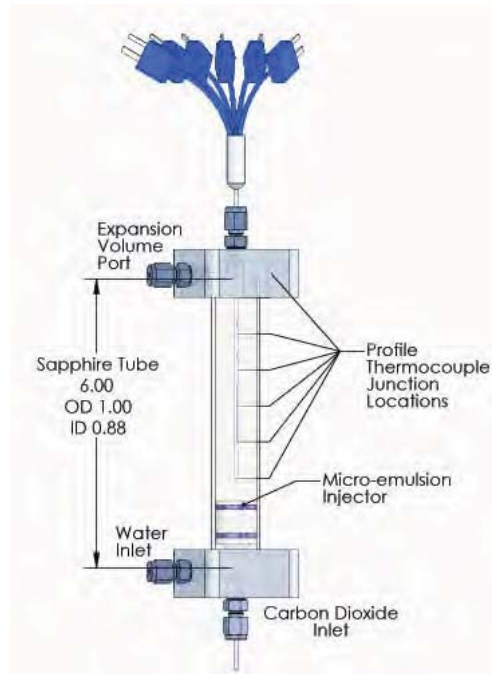


Figure 11. Schematic showing the high pressure sapphire cell equipped with a multi-port thermocouple probe

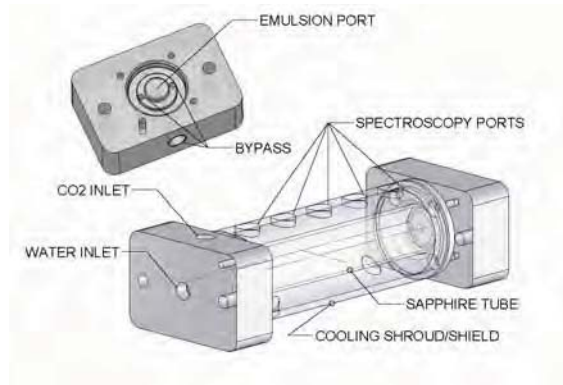


Figure 12. Schematic showing the redesigned high pressure sapphire cell equipped with a bypass port and cooling shroud

Methane hydrate rich sand was produced by packing the sapphire cell with 20/30 mesh Accusand, vacuum saturating with water to 80% pore volume, and then thermally cooling to 2°C. Following pressurization with CH₄ gas to 1300 psig, CH₄ hydrate formed spontaneously and the crystal formation could easily be observed visually. Generally, CH₄ gas hydrate initially appeared as a small white spot in the porous sand and then rapidly grew in all directions until complete coverage.

Figure 13 shows the Raman spectra taken of the white precipitate which produced a peak at 2906.8 cm⁻¹, the main symmetrical band of CH₄ hydrate (SUM et al., 1997).

Also evident in Figure 13 is the shift in frequency between the vibrational band for free vapor CH₄ (2917.6 cm⁻¹) and CH₄ hydrate (2906.8 cm⁻¹). For reference, Raman spectra of bulk CH₄ hydrate, aqueous dissolved CH₄, and CH₄ vapor as formed in a large mixing cell are provided in Figure 13.

Another important aspect of the experiment was to accurately identify the formation of CO₂ hydrate in sand. Accomplishing this task involved identifying each of the four phases of CO₂ (vapor, liquid, aqueous dissolved, and hydrate) by Raman spectroscopy in situ. Carbon dioxide vapor gives rise to Raman shifts at 1392.1 cm⁻¹ and 1288.6 cm⁻¹. Examination of liquid CO₂ shows the Raman shifts at a slightly lower wavelength, 1390.0 and 1286.2 cm⁻¹, respectively (Figure 14). As the CO₂ converts to gas hydrate, Raman peaks were observed at 1384.9 and 1281.1 cm⁻¹, while for the dissolved CO₂,

1387.3 and 1281.1 cm⁻¹, respectively. As can be seen from Figure 14 the Raman shifts of the CO₂ molecule in the hydrate phase are very close to the CO₂ molecule in the dissolved phase, making the distinction of the two phases by Raman spectroscopy difficult (NAKANO et al., 1998).

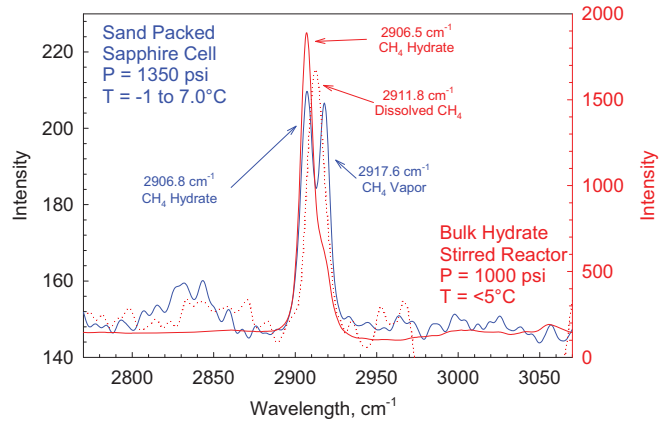


Figure 13. Raman spectra of CH₄ as vapor, aqueous dissolved, and gas hydrate (porous media)

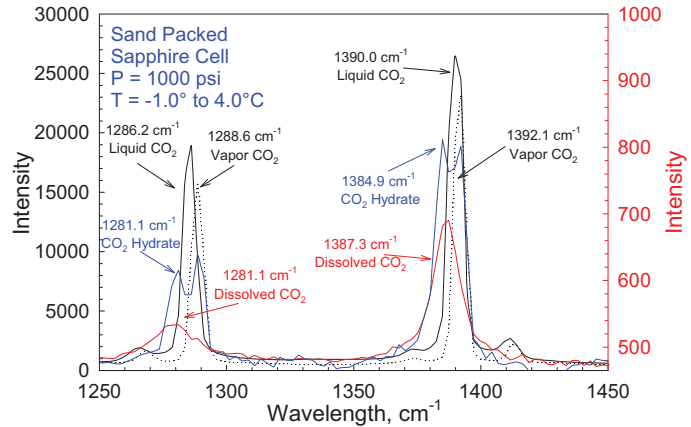


Figure 14. Raman spectra of CO₂ as vapor, liquid, aqueous dissolved, and gas hydrate (porous media)

Establishing identification parameters for each phase of CH₄ and CO₂ (gas, liquid, dissolved, and gas hydrate) by Raman spectroscopy allowed for the next phase of the injection experiment to start. After the formation of CH₄ hydrate, injection of the two phase L_{CO2}-L_w microemulsion fluid was initiated. A schematic diagram of the valving for the microemulsion experimental setup is shown in Figure 15. Both H₂O and CO₂ are delivered by ISCO syringe pumps into the take up ISCO pump during the first segment of the injection. Bypassing the injector and packed sand column is critical while pressurizing the system with liquid CO₂ and H₂O.

After achieving the desired flow rates and pressure, the separate fluids (H₂O & liquid CO₂) are diverted into the injector (Figure 15), located in the bottom of the cell, to form the L_{CO2}-L_w microemulsion. At first, the microemulsion is diverted out the side of the column, allowing time for the system to stabilize (Figure 15). After the L_{CO2}-L_w microemulsion is created, usually less than 15 seconds, the bypass valve is closed, diverting the microemulsion upwards through the sand packed column. As the relatively warm microemulsion fluid front (21°C) penetrates and moves through the porous CH₄ hydrate rich sand column being held initially at 2°C, CH₄ hydrate is seen to “dissociate” leaving behind pores filled with L_{CO2}-L_w microemulsion. During injection, the temperature of the column reaches 21°C and upon termination is allowed to return to the pre-injection temperature of 2°C. Cell pressure is maintained by the ISCO H₂O pump. Conversion of CO₂ microemulsion into CO₂ hydrate was found to occur anywhere between 10 to 500 minutes, depending on the rate of cooling.

Experiments conducted in the HYDEX® 301 columns produced exothermic thermal signatures, an indication of hydrate formation, several degrees above the cell cooling profile. For example, Figure 16 shows an experiment conducted with moist sand packed into a HYDEX® 301 column. Following pressurization with CH₄ to 1000 psig and subsequent lowering of the temperature from 27°C to near 0°C, a significant temperature spike is observed after 18 minutes. The largest change in temperature occurs in the bottom third of the cell with a delta temperature

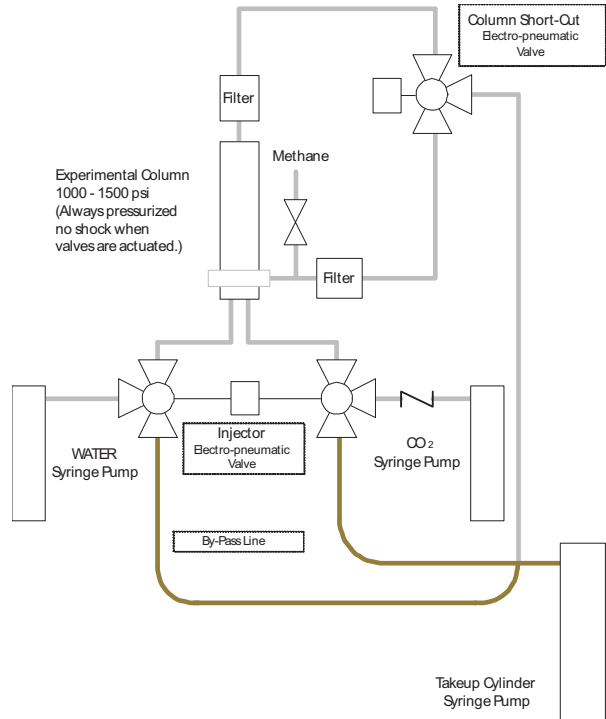


Figure 15. Microemulsion injection valving schematic

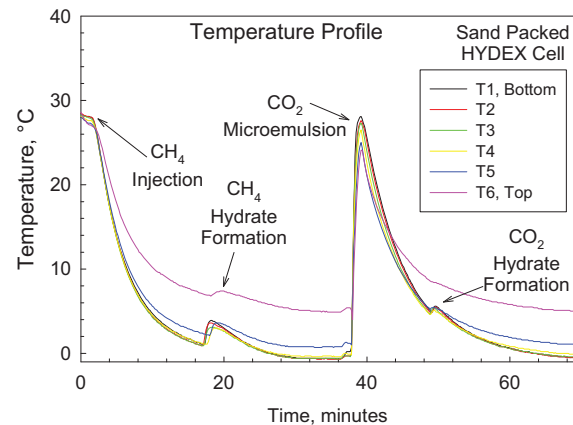


Figure 16. Temperature profile of HYDEX® 301 pressure cell during the formation of CH₄ hydrate, injection of CO₂ microemulsion, followed by the formation of CO₂ hydrate as a function of time

of over 1°C. The large temperature differential between the top of the cell (T6) and the bottom (T1) is directly related to the probe positioning. Thermocouple T6 is actually in the cap of the cell and is not embedded into the hydrated sand.

Growth of the hydrate was also evident from the white color change in the pore spaces and along the walls of the cell. Often, extra H₂O from the moist sand collected near the bottom of the cell. Initial pressurization with CH₄ (through bottom of cell, Figure 15) caused free water to move upward and concentrate in an area resulting in reduced porosity. These areas typically contained dense CH₄ hydrate, but often caused problems in the second phase of the experiment, the L_{CO2}-L_w microemulsion injection. Precautions were taken to prevent excessive areas of water from forming during the CH₄ pressurization. A number of these experiments were conducted using different ratios of H₂O and CO₂, with the majority of tests being conducted with a ratio of 2:1. Fluid injection rates were typically kept at 40 and 20 ml/minute. Although the ISCO pumps are capable of delivering fluid at 200 ml/minute, the slower flow rates allowed more time to observe the warm fluid front move up through the column. Very similar results were observed in each experiment with the HYDEX® 301 columns.

Experiments conducted with a sapphire pressure cell followed the same injection process as described above. A typical thermal profile of an injection experiment is shown in Figure 17. As described earlier, similar exothermic signatures representing CH₄ hydrate and CO₂ hydrate formation within the sand packed column at distinct times were captured (Figure 17). For this experiment, the H₂O and CO₂ volumetric ratio was maintained at 2:1. The maximum change in temperature (5°C) during CH₄ hydrate formation was measured in the upper portion of the cell 70 minutes after pressurization with CH₄ gas. Following the microemulsion injection, CO₂ hydrate began forming in the cell, which was visible as white pore filling material (Figure 17). Coinciding with formation of the pore filling white precipitate was a slight increase in cell temperature (0.3°C), confirmed by the measurements taken by the six port thermocouple. This exothermic event occurred 170 minutes into the experiment, following the H₂O-CO₂ microemulsion injection by 32 minutes.

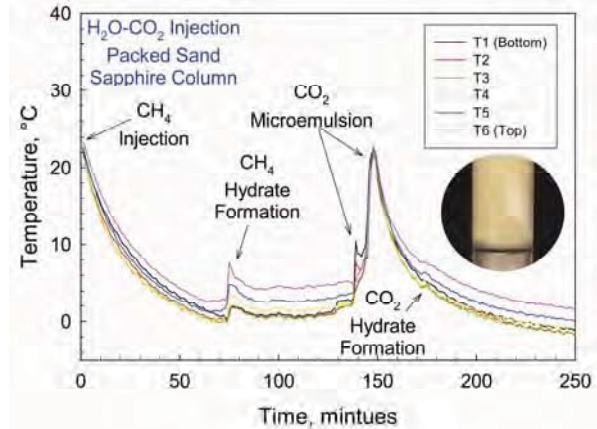


Figure 17. Temperature profile of sapphire high pressure cell during the formation of CH₄ hydrate, injection of L_{CO2}-L_w microemulsion, followed by the formation of CO₂ hydrate as a function of time

Five small diameter sampling tubes with valves were placed between the pressure cell and backup pump (Figure 15), allowing for the collection of discrete gas samples. A series of gas samples were collected during various stages of H₂O-CO₂ microemulsion experiments, usually lasting 30 to 45 seconds. Each sample was subsequently analyzed on a residual gas analyzer (RGA). Monitoring masses 16 amu (CH₄) and 44 amu (CO₂) provided evidence of breakthrough of the injected CO₂. Shown in Figure 18 are a few results taken from the HYDEX® 301 column experiments. The ratio of CH₄ to CO₂ is shown as a function of sample collection, which was typically 5 seconds apart from start to finish. For example, during experimental run 1 (Figure 18), five samples were collected in less than 45 seconds. Breakthrough clearly occurs when approximately 1 pore volume of the emulsion had been injected. Some CH₄ was still detected in Run 1 after 1 pore volume of injection indicating that some methane hydrate was still dissociating in addition to gas mixing at the leading edge of the emulsion front as would be expected. However, Runs #2 and #3 show that most of the CH₄ has been recovered by the time more than 1 pore volume of fluid has passed through the cell, verifying the efficiency of the L_{CO2}-L_w microemulsion in removing CH₄ hydrate.

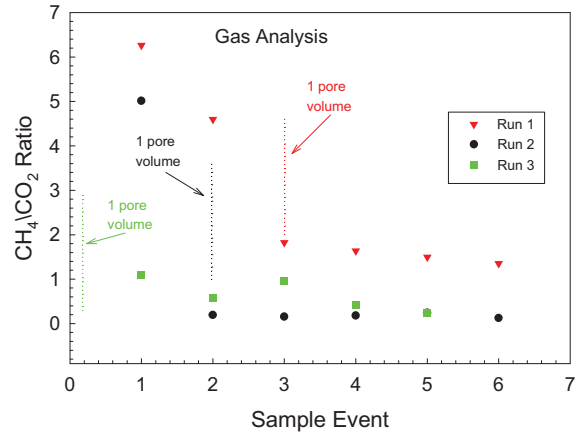


Figure 18. Gas analysis data collected during L_{CO2}-L_w microemulsion injection experiments

Post characterization of the CO₂ hydrated sand was conducted to evaluate pore space filling and condition of CO₂ hydrate. Determining if the L_{CO2}-L_w microemulsion remained stable in discrete particles and converted to CO₂ hydrate was essential to determine. Therefore, after completion of an injection experiment, a HYDEX® 301 column was chilled to -10°C and quickly depressurized to release any liquid CO₂ present in the column that had not converted to gas hydrate. The column was then submerged in liquid nitrogen and mechanically split to reveal the sand. Characterization of the sand aggregates was accomplished by optical light microscopy while samples were held partially immersed in LN₂. An example of CO₂ hydrated sand is shown in Figure 19. No void areas where free liquid CO₂ would have existed were observed in the CO₂ hydrate rich sand. Figure 19 illustrates the complete filling of the porosity by CO₂ hydrate, suggesting complete saturation of the pores with the microemulsion fluid.



Figure 19. CO₂ hydrate rich sand extracted from a column injected with L_{CO2}-L_w microemulsion.

3.0 MODELING

The objective of the modeling work conducted in this investigation has been the development of a numerical simulation tool for analyzing the production of natural gas hydrates using conventional technologies, but also with the capabilities for considering the gas exchange technology. In the gas exchange production technology, clathrated methane is released when a more thermodynamically favorable molecule (e.g., carbon dioxide) replaces it in the hydrate. The outcome of this work has been a new operational mode for the STOMP simulator (WHITE and OOSTROM, 2006), which will be commonly referred to as STOMP-HYD. This operational mode of the simulator solves the governing conservation equations for heat, H₂O mass, CH₄ mass, CO₂ mass, and NaCl (inhibitor mass) that describe the flow and transport of the conserved quantities through multifluid filled geologic media. The flow and transport equations are solved fully coupled, considering three mobile phases: 1) aqueous, 2) gas, and 3) liquid CO₂; three immobile phases: 1) hydrate, 2) ice, and 3) precipitated salt, and the geologic media.

3.1 MATHEMATICAL MODEL

The mathematical model for the STOMP-HYD simulator comprises governing conservation equations and associated constitutive equations that describe the flow and transport of heat and components through multiphase geologic media. In general the solved flow and transport equations are identical across the community of numerical simulators for methane hydrate production. STOMP-HYD, however, differs from hydrate production simulators in its use of capillary pressure functions to calculate phase saturations. This section describes the governing conservation equations and the calculation approach for the mobile and immobile phases.

3.1.1 Governing Equations

The STOMP-HYD simulator solves five conservation equations, which can be expressed in two forms: 1) conservation of heat and 2) conservation of component mass (i.e., H₂O, CH₄, CO₂, and NaCl). The conservation of heat equation, expressed in differential form, states that the time rate of change of internal energy equals the net transport of heat into the system, according to:

$$\begin{aligned} \frac{\partial}{\partial t} \left[\sum_{\gamma=l,n,g,h,i,p} (\phi_D \rho_\gamma s_\gamma u_\gamma) + (1-\phi_T) \rho_s s_s u_s + (\phi_T - \phi_D) \rho_l u_l \right] = \\ - \sum_{\gamma=l,n,g} \nabla (\rho_\gamma h_\gamma \mathbf{V}_\gamma) - \sum_{i=w,a,o} \nabla (h_g^i \mathbf{J}_g^i) + \nabla (\mathbf{k}_e \nabla T) + \sum_{\gamma=l,n,g} (h_\gamma \dot{m}_\gamma) + \dot{q} \end{aligned} \quad (1)$$

where the phase flux is computed via Darcy's law according to:

$$\mathbf{V}_\gamma = - \frac{k_{r\gamma} \mathbf{k}}{\mu_\gamma} (\nabla P_\gamma + \rho_\gamma \mathbf{g} \mathbf{z}_g) \quad (2)$$

and component diffusion is computed from molar gradients, considering molecular diffusion and hydraulic dispersion, according to:

$$\mathbf{J}_\gamma^i = -\phi_D \rho_\gamma s_\gamma \frac{M^i}{M_\gamma} (\tau_\gamma D_\gamma^i + \mathbf{D}_{h_\gamma}) \nabla \chi_\gamma^i. \quad (3)$$

Only the contribution of gas phase diffusion-dispersion is considered for the conservation of heat equation.

The conservation of component-mass equation, expressed in differential form, states that the time rate of change of component mass equals the net transport of component mass into the system, as given by:

$$\begin{aligned} \frac{\partial}{\partial t} \left[\sum_{\gamma=l,n,g,h,i,p} (\phi_D \omega_\gamma^i \rho_\gamma s_\gamma u_\gamma) \right] = & - \sum_{\gamma=l,n,g} \nabla (\omega_\gamma^i \rho_\gamma \mathbf{V}_\gamma) \\ & - \sum_{\gamma=l,n,g} \nabla (\mathbf{J}_\gamma^i) + \sum_{\gamma=l,n,g} \omega_\gamma^i \dot{m}_\gamma \text{ for } i = w, a, o \end{aligned} \quad (4)$$

where, for mass transport, diffusion through all mobile phases is considered. Hydraulic dispersion is considered only for the transport of NaCl.

3.1.2 Phase Saturations

The conceptual pore-space model for the STOMP-HYD simulator includes five potential phases: aqueous, gas, liquid CO₂, hydrate and ice. Hydrate and ice phases are assumed to be immobile and completely occluded by the aqueous phase. The mobile phases are assumed to decrease in wettability from aqueous to liquid CO₂ to gas phases. To reduce the number of phase conditions associated with the numerical solution, STOMP-HYD uses interfacial-tension-scale saturation versus capillary pressures to calculate phase saturations from the phase pressure primary unknowns. For conditions without liquid CO₂, the aqueous saturation is calculated as a function of the scaled gas-aqueous capillary pressure, and for conditions with liquid CO₂, the aqueous saturation is calculated as a function of the scaled liquid CO₂-aqueous capillary pressure:

$$\bar{s}_l = \frac{s_l + s_h + s_i - s_{lr}}{1 - s_{lr}} = \text{func}(\beta_{gl} [P_g - P_l]) \text{ or } = \text{func}(\beta_{nl} [P_n - P_l]) \quad (5)$$

where, the scaling factors are computed as:

$$\beta_{gl} = \frac{\sigma^{ref}}{\sigma_{gl}}; \beta_{nl} = \frac{\sigma^{ref}}{\sigma_{nl} \cos(\theta_{nl})}; \beta_{gn} = \frac{\sigma^{ref}}{\sigma_{gn} \cos(\theta_{gn})}; \frac{1}{\beta_{gl}} = \frac{1}{\beta_{gn}} + \frac{1}{\beta_{nl}} \quad (6)$$

The functional forms shown in Equation (5) are generally those of van Genuchten (1980) or Brooks and Corey (1964). The closing Equation (6) provides continuity in the functions as liquid-CO₂ appears or disappears. The liquid-CO₂ saturation is computed indirectly from the total-liquid and aqueous saturations; where the total liquid saturation is computed as a function of the gas-liquid CO₂ capillary pressure:

$$s_n = s_l - (s_l + s_h + s_i); \bar{s}_l = \frac{s_l + s_h + s_i + s_n - s_{lr}}{1 - s_{lr}} = \text{func}(\beta_{gn} [P_g - P_n]) \quad (7)$$

For continuity in liquid-CO₂ transitions, the liquid-CO₂ pressure, as shown in Equation (8) is set to a critical pressure, whenever liquid-CO₂ is absent from the system:

$$P_n = \frac{\beta_{nl} P_l + \beta_{gn} P_g}{\beta_{nl} + \beta_{gn}}; \bar{s}_l = \frac{s_l - s_{lr}}{1 - s_{lr}}; \bar{s}_g = \frac{1 - \bar{s}_l}{1 - s_{lr}}; \bar{s}_n = \frac{s_n}{1 - s_{lr}} \quad (8)$$

The hydrate and ice saturations are computed indirectly from the hydrate-aqueous and the ice-aqueous capillary pressures, as shown in Equation (9), where ice saturation only occurs whenever the ice-aqueous interfacial saturation is less than the hydrate-aqueous interfacial saturation:

$$\begin{aligned} \bar{s}_h &= \bar{s}_l - \bar{s}_{hl}; \bar{s}_{hl} = \text{func}(\beta_{hl} [P_h - P_l]) \\ \bar{s}_i &= \bar{s}_l - \bar{s}_h - \bar{s}_{il}; \bar{s}_{il} = \text{func}(\beta_{il} [P_i - P_l]) \end{aligned} \quad (9)$$

The hydrate- and ice-aqueous capillary pressures are computed from the hydrate- and ice-aqueous interfacial tensions and radii of curvature, respectively:

$$P_h - P_l = \frac{2 \sigma_{hl}}{r_{hl}}; P_i - P_l = \frac{2 \sigma_{il}}{r_{il}} \quad (10)$$

where the hydrate-aqueous radius of curvature is computed from the difference in ex-situ hydrate equilibrium temperature and the system temperature, and the ice-aqueous radius of curvature is computed from the difference in freezing point temperature and system temperature (JIANG et al., 2001) given by:

$$r_{hl} = r_c \left[1 + \frac{(1 - \alpha)}{\log\left(\frac{T}{T_{eq}^{ex}}\right)} \right]; r_{il} = r_c \left[1 + \frac{(1 - \alpha)}{\log\left(\frac{T}{T_{fp}^{ex}}\right)} \right]; r_c = 3.6 \times 10^{-9} \text{ m}; \alpha = 1.66. \quad (11)$$

3.2 NUMERICAL SOLUTION

The governing conservation equations in the STOMP-HYD simulator are solved using integral volume differencing for spatial discretization on structured grids and a backward-Euler temporal discretization. These discretizations transform the governing equations to algebraic form; however, the resulting algebraic equations are nonlinear. Nonlinearities are resolved using multivariate Newton-Raphson iteration. This general numerical solution approach of spatial and temporal discretization and Newton-Raphson linearization is followed by the community of hydrate production simulators. STOMP-HYD differs in the selection of primary variable sets and the number of phase conditions. The use of capillary pressure functions to calculate hydrate and ice phase saturations greatly reduces the number of primary variable sets.

3.2.1 Discretization and Linearization

STOMP-HYD solves algebraic forms of the five governing conservation equations, Equations (1) through (5), that result from their discretization using the integral volume differencing technique on structured orthogonal grids, including boundary-fitted curvilinear grids. The backward-

Euler temporal discretization yields an implicit scheme, which requires the coupled solution of five nonlinear equations at each grid cell. Newton-Raphson iteration transforms the five nonlinear equations into a linear system of equations, but does not alter the requirement for a coupled solution of five unknowns at each grid cell (e.g., a problem involving 10K active grid cells requires a linear-system solve of order 50K). Partial derivatives required in the Jacobian matrix of the Newton-Raphson scheme are computed numerically, which greatly simplifies code development and also improves convergence performance during phase transitions. The linear-system solve yields corrections to the five primary variables, which are then used to calculate secondary variables and reconstruct the Jacobian matrix. For closure on the system of equations, all secondary variables must be calculated from the set of five primary variables.

3.2.2 Primary Variable Switching

As described above, STOMP-HYD solves for five unknowns or primary variables at each grid cell. One distinguishing feature of the simulator from others for methane hydrate production is that primary variable sets are principally phase pressure and vapor pressure as opposed to phase saturation and component mole fractions. By assuming that the aqueous phase never disappears the number of possible phase conditions (ignoring precipitated salt) is 16, where the saturation combinations are:

$$s_l = 1 \text{ or } s_l < 1; s_n = 0 \text{ or } s_n > 0; s_h = 0 \text{ or } s_h > 0; s_i = 0 \text{ or } s_i > 0 \quad (12)$$

With the hydrate and ice saturations defined through capillary pressure functions, the number of active phase conditions reduces to 4, where the saturation combinations are:

$$s_l = 1 \text{ or } s_l < 1; s_n = 0 \text{ or } s_n > 0 \quad (13)$$

The primary variable sets for the 4 active phase conditions can be further reduced to 2 by appropriately defining the gas and liquid CO₂ phase pressures, shown in Table 3.1.

Table 3.1. Conceptual Phase Conditions and Primary Variable Sets

Phase Condition	Energy	H ₂ O Mass	CH ₄ Mass	CO ₂ Mass	NaCl Mass	P_g, P_g^o	P_n, P_g^a
$s_l = 1$ $s_n = 0$	T	P_l	P_g^o	P_g^a	ζ_l^s	$P_g = P_l + \frac{\beta_{gl}}{\psi}$	$P_n = P_{nc}$
$s_l < 1$ $s_n = 0$	T	P_l	P_g	P_g^a	ζ_l^s	$P_g^o = P_g - P_g^a - P_g^w$	$P_n = P_{nc}$
$s_l = 1$ $s_n > 0$	T	P_l	P_g^o	P_n	ζ_l^s	$P_g = P_l + \frac{\beta_{gl}}{\psi}$	$P_g^a = P_{sat}^a$
$s_l < 1$ $s_n > 0$	T	P_l	P_g^o	P_n	ζ_l^s	$P_g = P_g^a + P_g^o + P_g^w$	$P_g^a = P_{sat}^a$

The primary variable sets shown in Table 3.1 functionally allow for the solution of the governing equations for each phase condition. Application of the simulator to a variety of problems, however, has shown that the implementation of the primary variable set could be improved for cer-

tain phase transitions. Low liquid-CO₂ saturation conditions (i.e., less than 0.001) are difficult to resolve using the liquid-CO₂ pressure as the primary unknown. Including two additional phase conditions for low liquid-CO₂ saturations yields improved convergence and increased time steps. Low concentrations of CO₂ or CH₄ for unsaturated conditions are resolved more efficiently if the lower vapor partial pressure is used as the unknown, rather than using only the CO₂ vapor pressure. Therefore, the unsaturated phase condition without liquid CO₂ was split into two phase conditions. The resulting phase condition and primary variable set scheme, implemented into the code, is shown in Table 3.2.

Table 3.2. Implemented Phase Conditions and Primary Variable Sets

Phase Condition	Energy	H ₂ O Mass	CH ₄ Mass	CO ₂ Mass	NaCl Mass	P_g, P_g^a, P_g^o	P_n, P_g^a
$s_l = 1$ $s_n = 0$	T	P_l	P_g^o	P_g^a	ζ_l^s	$P_g = P_l + \frac{\beta_{gl}}{\psi}$	$P_n = P_{nc}$
$s_l < 1$ $s_n = 0$	T	P_l	P_g^o	P_g	ζ_l^s	$P_g^a = P_g - P_g^o - P_g^w$	$P_n = P_{nc}$
$s_l < 1$ $s_n = 0$	T	P_l	P_g	P_g^a	ζ_l^s	$P_g^o = P_g - P_g^a - P_g^w$	$P_n = P_{nc}$
$s_l = 1$ $s_n > 0$	T	P_l	P_g^o	P_n	ζ_l^s	$P_g = P_l + \frac{\beta_{gl}}{\psi}$	$P_g^a = P_{sat}^a$
$s_l < 1$ $s_n > 0$	T	P_l	P_g^o	P_n	ζ_l^s	$P_g = P_g^a + P_g^o + P_g^w$	$P_g^a = P_{sat}^a$
$s_l = 1$ $0 < s_n < 0.001$	T	P_l	P_g^o	s_n	ζ_l^s	$P_g = P_l + \frac{\beta_{gl}}{\psi}$	$P_g^a = P_{sat}^a$
$s_l = 1$ $0 < s_n < 0.001$	T	P_l	P_g^o	s_n	ζ_l^s	$P_g = P_g^a + P_g^o + P_g^w$	$P_g^a = P_{sat}^a$

3.3 APPLICATION

To demonstrate STOMP-HYD, the simulator has been applied to series of hydrate production scenarios involving idealized injection and extraction wells across a one-dimensional horizontal column of porous media. The horizontal domain is 20-m long, discretized into 20 grid cells with a cross-sectional area of 1 m². Injection of liquid water with microemulsions of gaseous or liquid CO₂ occur at the left-hand boundary at a fixed pressure of 7 MPa, whereas, the right-hand boundary is maintained at 4.5 MPa and 3°C. The domain porous media is a 1-Darcy sandstone with an initial porosity of 0.3. Initially the domain is set to a pressure of 6 MPa, a temperature of 3°C and a CH₄-hydrate saturation of 0.5. The complete list of hydrologic properties and initial conditions are shown in Table 3.1.

Table 3.3. Hydrologic Parameters and Initial Conditions

Parameter	Value
Porosity	0.3
Compressibility	0.093×10^{-5} 1/psi
Intrinsic Permeability	1 Darcy
Grain Thermal Conductivity	2.0 W/m K
Grain Specific Heat	700 J/kg K
Saturation-Capillary Pressure Model	van Genuchten (1980)
van Genuchten α Parameter	0.132 m^{-1}
van Genuchten n Parameter	2.823
Residual Aqueous Saturation	0.0
Gas-Aqueous Scaling Parameter	1.0
Liquid CO ₂ -Aqueous Scaling Parameter	3.0
Gas-Liquid CO ₂ Scaling Parameter	1.5
Hydrate-Aqueous Scaling Parameter	2.697
Ice-Aqueous Scaling Parameter	2.697
Aqueous Relative Permeability Model	Mualem (1976)
Gas Relative Permeability Model	Mualem (1976)
Liquid-CO ₂ Relative Permeability Model	Mualem (1976)
Initial Pressure	6.0 MPa
Initial Temperature	3°C
Initial CH ₄ Fraction of Hydrate Formers	1.0
Initial Hydrate Saturation	0.5
Initial Aqueous Saturation	0.5
Initial Dissolved Salt Concentration	0.0 kg/m^3
Initial Dissolved CO ₂ Concentration	0.0 kg/m^3

A series of simulations was executed with STOMP-HYD that differed in the inlet boundary conditions. Microemulsions of liquid CO₂ and water were executed that varied in temperature and volumetric ratios, including pure water injections. Table 3.4 summarizes the suite of production scenarios.

Table 3.4. Hydrate Production Scenarios

Temperature	Microemulsion Volume Percent	Microemulsion State
15°C	0%	N/A
15°C	40%	Liquid CO ₂
15°C	50%	Liquid CO ₂
15°C	60%	Liquid CO ₂
20°C	50%	Liquid CO ₂
50°C	0%	N/A

3.3.1 Pure Water Injection

Two pure water injection simulations were executed at 15°C and 50°C. After injecting for 700 hr, the 15°C injectant produced 13.4% and the 50°C injectant produced 57.5% of the CH₄ mass through dissociation. To produce 75% of the CH₄ mass in the system through dissociation required 1254 hrs for the 15°C injectant, and 748.4 hrs for the 50°C injectant. As shown by the simulation results, CH₄ production rates for the pure water injectants are characteristically related to the inlet temperature, as the dissociation reaction is endothermic. Secondary hydrates form downstream from the dissociation front in both scenarios, with the 15°C injectant yield maximum secondary hydrate saturations of 0.55 and the 50°C injectant yield values of 0.61. Plots showing the hydrate saturations at points along the domain over time are shown in Figure 20 and Figure 21, respectively, for the 15 and 50°C injectant.

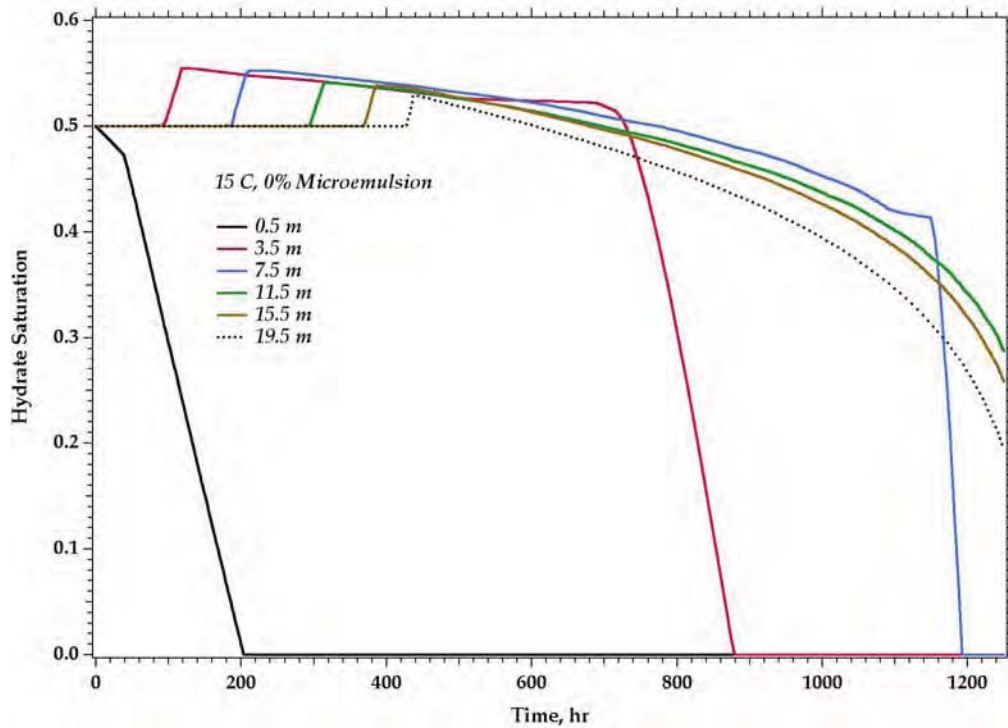


Figure 20. Hydrate saturation histories for 15°C pure-water injectant

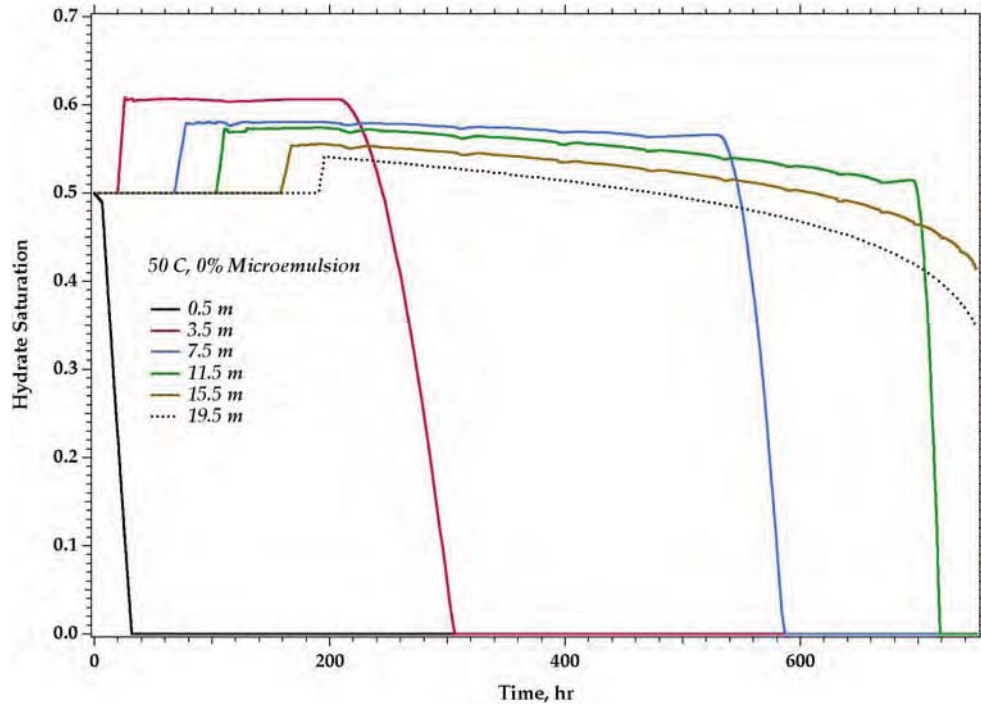


Figure 21. Hydrate saturation histories for 50°C pure-water injectant

3.3.2 Liquid-CO₂ Microemulsion Injectant

The saturation temperature for 7 MPa for CO₂ is 28.7°C, which means the CO₂ in microemulsion form will be in supersaturated liquid conditions for the 15 and 20°C injectant temperatures. The CH₄ hydrate production method for liquid CO₂ microemulsion involves principally exchange of CO₂ with CH₄ with some dissociation. Production continues until CO₂ breakthrough occurs at the domain outlet (i.e., producing well). Breakthrough was considered to have occurred when the mass fraction of CO₂ in the exiting gas phase reached 0.01. Breakthrough times, production percents at breakthrough, and maximum secondary hydrate saturations are shown in Table 3.5 for the liquid-CO₂ microemulsion injectant scenarios. Simulation results indicate that volumetric ratios of CO₂/water have the greatest impact on breakthrough times, but generally no effect on production or maximum secondary hydrate saturations. Production times are considerably faster compared against the pure water injectant at 15°C, but production is limited by the breakthrough of CO₂ in the gas phase. Increasing the injectant temperature yields slightly faster breakthrough times and higher production. Plots showing the hydrate saturations at points along the domain over time are shown in Figure 22 and Figure 23, respectively, for the 15°C, 50% volume and 20°C, 50% volume liquid-CO₂ microemulsion injectant.

Table 3.5. Liquid-CO₂ Microemulsion Injectant Simulation Results

Injectant Conditions	Breakthrough Time	Production Percent at Breakthrough	Max. Secondary Hydrate Saturation
15°C, 40% Volume	272.1 hr	55.3%	0.72
15°C, 50% Volume	202.2 hr	55.5%	0.72
15°C, 60% Volume	149.2 hr	55.6%	0.72
20°C, 50% Volume	197.1 hr	56.0%	0.69

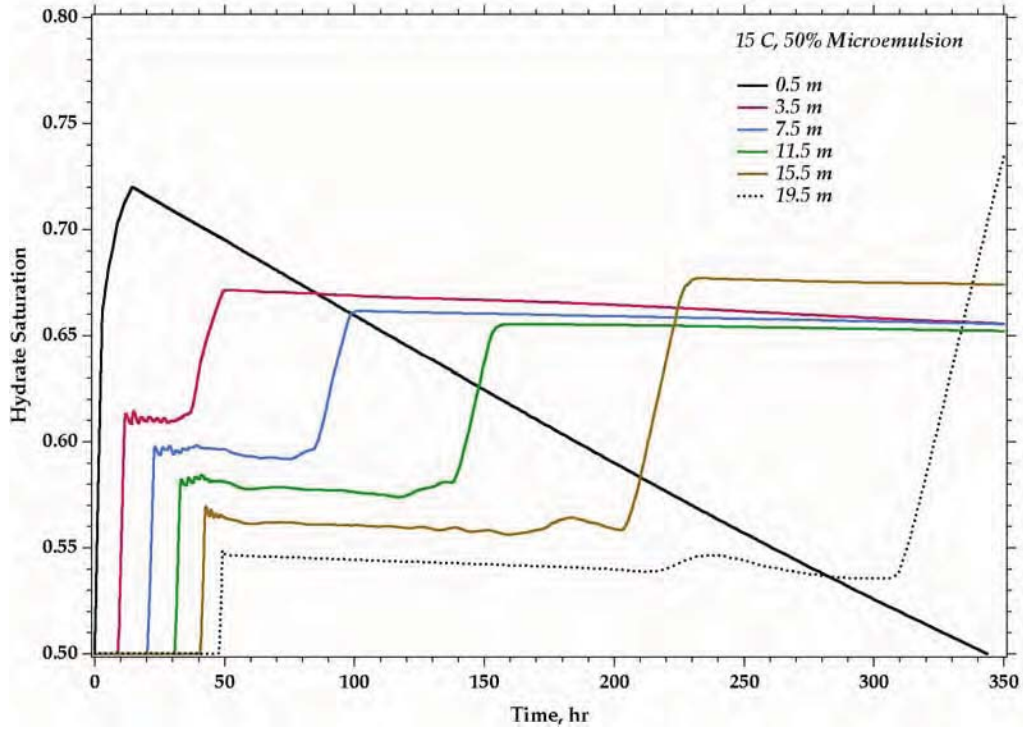


Figure 22. Hydrate saturation histories for 15°C, 50% volume liquid-CO₂ microemulsion injectant

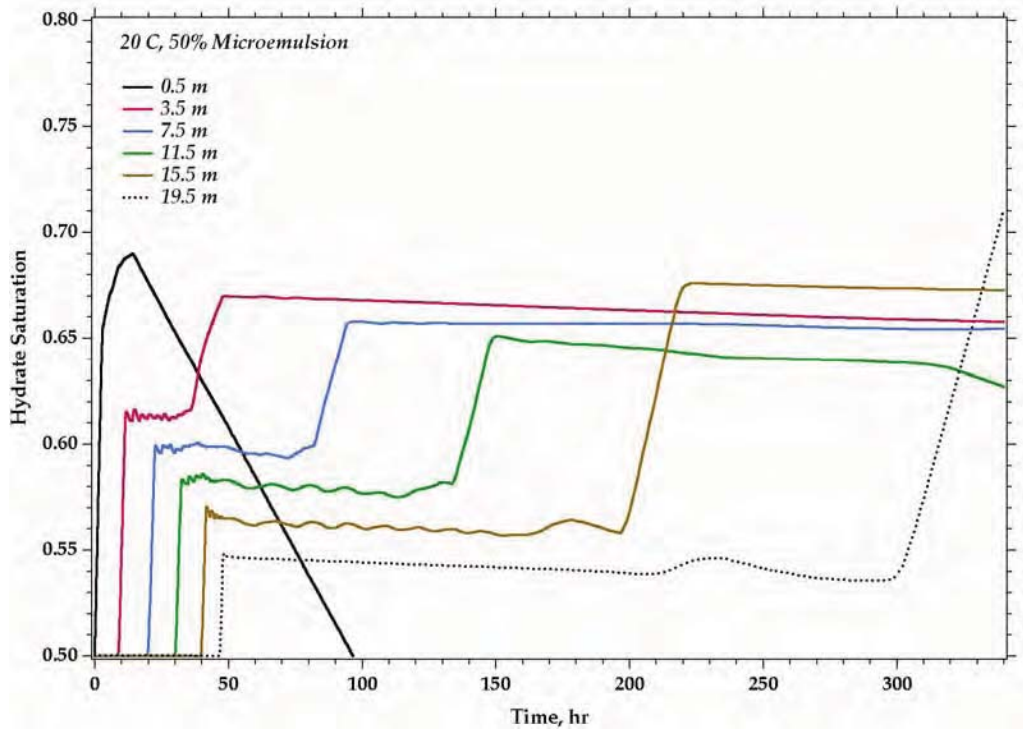


Figure 23. Hydrate saturation histories for 25°C, 50% volume liquid-CO₂ microemulsion injectant

4.0 DISCUSSION

The laboratory experiments presented in this report suggest that a strict gas exchange of CO₂ for CH₄ in bulk CH₄ hydrate is too slow by several orders of magnitude to be considered an effective method of gas hydrate production. In contrast, both laboratory experiments and numerical modeling indicate that an EGHR process based on injecting a two phase emulsion of liquid CO₂ and water at the proper volumetric ratio, can considerably enhance (3X and higher) production rate over injecting cool water (15°C) alone.

An important consideration in the EGHR technique is the range of reservoir conditions where the method might be applied. Figure 24 shows a compilation of well log temperature data reported by Collett (1993) for the Alaska North Slope. The vapor-liquid equilibrium line for CO₂ is plotted on the same graph. The data suggest that the EGHR method could be implemented over a large fraction of the ANS, wherever deeper gas hydrate deposits exist. Typical ANS reservoir conditions would inject liquid CO₂ with a density approximately 82% to 94% of the water phase. Note that CO₂ hydrate would be stable under almost any conditions on the ANS short of very near the ground surface.

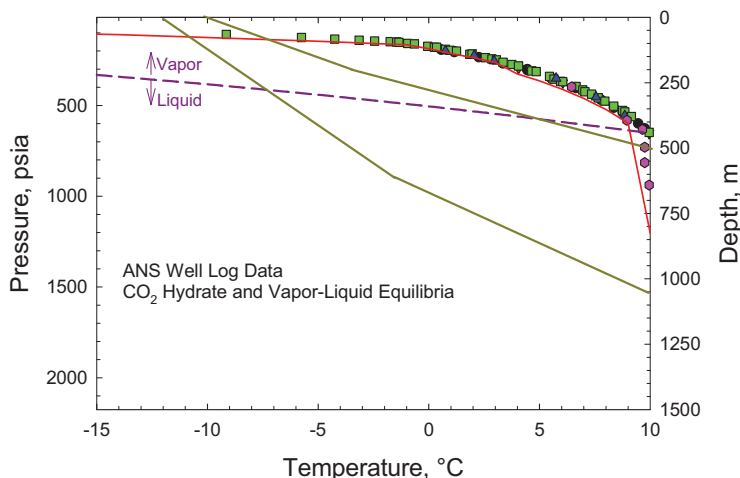


Figure 24. ANS well log temperature data shown as shaded area (after Collett 1993). Carbon dioxide hydrate and vapor-liquid equilibria are also plotted.

A number of other questions regarding application of the EGHR technique remain to be addressed. The bench scale experiments conducted in this project show no signs of coagulation into macrodroplets as the emulsion moves away from the injector. However, it remains to be investigated whether coagulation can be avoided at reservoir scale. Recent advances in modeling emulsion behavior in porous media (CORTIS and GHEZZEHEI, 2007) could help explore this issue. Additionally, an important restriction is that temperature of the water-CO₂ emulsion remains above the equilibrium point where CO₂ hydrate could form in the wellbore or near-wellbore. Interruption of the supply of the emulsion fluid during production for an extended period could result in the premature formation of CO₂ hydrate and plugging. Provisions for temporary introduction of heat may be needed to allow for flow interruptions, such as for well maintenance.

Although we have demonstrated a method for *continuous* production of a suitable L_{CO₂}-L_w emulsion, the device has only been tested at laboratory bench scale and is configured for injection into an essentially 1-D columnar domain. Development of a suitable downhole tool will be needed to supply the volumes of fluids required for a field trial. The injector tool design should be compatible with downhole conditions typical of gas hydrate formations. Wellbore completion requirements such as open hole, uncased, or perforated casing influence design parameters of the injector tool. Injection of the L_{CO₂}-L_w emulsion directly into the target formation is the most

important requirement. For example, the gas hydrate production research well, Mallik 5L-38, was cased and perforated at several different hydrate bearing zones (TAKAHASHI et al., 2005). Each zone was isolated with packers prior to testing. A similar approach could be used with a suitable downhole tool.

Redesigning the injector to deliver the microemulsion radially into the formation of interest is likely a priority. This might be accomplished by repositioning the emulsion outlets from the top of the injection tool to the sides as shown by the schematic in Figure 25. Surface warmed L_w and L_{CO_2} can then be directed into the injector from the high pressure lines. Use of produced water to form the emulsion would eliminate issues associated with disposal of these fluids in arctic conditions. Both rate and distance of formation penetration can be controlled from the surface by adjusting the L_{CO_2} and L_w pumps.

There are several parameters associated with injecting a L_{CO_2} - L_w microemulsion into a porous hydrate rich formation that are still unknown. Placement of recovery wells including distance from the injection site, and spacing to maximize recovery of CH_4 gas are a few of the important issues still unanswered. Identification and delivery logistics of an economical supply of CO_2 are also essential factors in selecting an appropriate field site for demonstration. Additional numerical studies of the EGHR method are needed to address these questions and to guide design of an effective downhole tool.

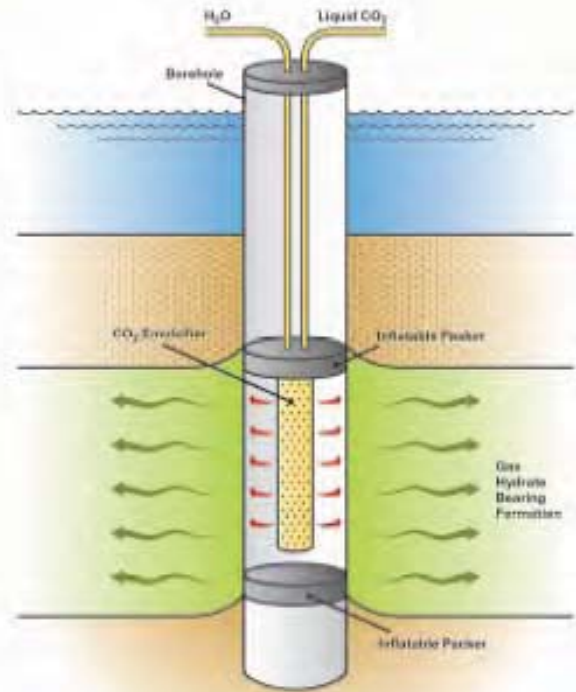


Figure 25. Schematic of down borehole injection tool

5.0 CONCLUSION

Through a proprietary method, a microemulsion injector was designed and tested to enhance production of methane hydrate-bearing porous media. A number of experiments were performed where a two-phase microemulsion (L_{CO_2} - L_w) was injected into a CH_4 hydrate bearing sand packed column, a technique we call Enhanced Gas Hydrate Recovery (EGHR). The two-phase emulsion formed micrometer size droplets of liquid CO_2 in the water phase at a ratio of approximately 44 g of CO_2 per 103 g of water. This ratio was chosen to optimize filling of the small and large cages of the sI hydrate formed with CO_2 . The temperature of the injectate was set significantly higher than the stability point of methane hydrate causing destruction of the gas hydrate crystalline lattice and release of enclathrated gas. The freed gas was displaced ahead of the microemulsion injection front and collected. After injection was stopped, the emulsion-containing sand was cooled into the stability region for CO_2 hydrate. In every case, CO_2 hydrate was observed to form visually, was monitored by an increase in temperature, and verified by Raman spectroscopy.

A numerical simulator, STOMP-HYD, was developed to investigate the feasibility of producing CH_4 hydrate from geologic reservoirs beneath the permafrost and in deep ocean sediments. The simulator is capable of modeling CH_4 hydrate production using the conventional technologies of thermal stimulation, depressurization and inhibitor injection, but additionally able to model the unconventional CO_2 exchange approach. The principal objective in developing the simulator was to explore gas hydrate production using a combination of conventional and unconventional technologies using numerical simulation prior to testing the approaches in the field. Although the solved governing equations and constitutive equations are nearly identical to those of other methane hydrate production simulators, STOMP-HYD differs in use of capillary pressure functions to calculate hydrate and ice saturations. This approach considers the effect of porous media on the hydrate equilibrium function and ice freezing point (i.e., the hydrate and ice saturations are functions of the difference in system temperature and *ex-situ* hydrate equilibrium temperature and *ex-situ* ice freezing point). Simple 1-D simulations comparing injection of cool water ($15^\circ C$) alone with injection of a microemulsion (also at $15^\circ C$), showed much higher ($>3X$) production of $CH_4(g)$ using the EGHR technique.

The EGHR concept described in this report clearly has potential for use in converting a portion of natural gas hydrate reservoirs into a usable energy source. There are several advantages to the EGHR process, including: 1) Replacing CH_4 with CO_2 in gas hydrated sediment is thermodynamically favorable and heat generated from formation of CO_2 hydrate is approximately 20% greater than heat consumed from the dissociation of CH_4 , resulting in a low grade heat source to facilitate further dissociation of gas hydrate, 2) Once the CH_4 is extracted and CO_2 rich fluid fills pore space voids, the subsequent formation of CO_2 hydrate would mechanically stabilize the formation eliminating subsidence concerns in some production situations, and 3) the process is carbon neutral in terms of replacing methane with CO_2 , which is permanently sequestered in situ as a crystalline gas hydrate. Produced water could also be used to form the emulsion, eliminating a problematic disposal issue in arctic settings.

6.0 REFERENCES

- Brooks, R. H. and A. T. Corey. 1964. *Hydraulic Properties of Porous Media*. Hydrology Papers 3, Colorado State University, Fort Collins, Colorado.
- Chatterji, J. and J. E. Griffith. 1998. *Methods of Decomposing Gas Hydrates*. Patent No. 5,713,416, USA.
- Circone, S., S. H. Kirby, and L. A. Stern. 2005. "Thermal Regulation of Methane Hydrate Dissociation: Implications for Gas Production Models." *Energy Fuels* **19**(6):2357-2363.
- Clennell, M. B., M. Hovland, J. S. Booth, P. Henry, and W. J. Winters. 1999. "Formation of Natural Gas Hydrates in Marine Sediments 1. Conceptual Model of Gas Hydrate Growth Conditioned by Host Sediment Properties." *J. Geophys. Res.* **104**(B10):22985-23003.
- Collett, T. S., K. J. Bird, and L. B. Magoon. 1993. "Subsurface Temperatures and Geothermal Gradients on the North Slope of Alaska." *Cold Reg. Sci. Tech.* **21**(3):275-293.
- Collett, T. S. 2004. "Gas Hydrates as a Future Energy Resource." *Geotimes* **49**(11):24-27.
- Cortis, A. and T. A. Ghezzehei. 2007. "On the Transport of Emulsions in Porous Media." *J. Colloid Interface Sci.* **313**(1):1-4.
- Englezos, P. 1993. "Clathrate Hydrates." *Ind. Eng. Chem. Res.* **32**(7):1251-1274.
- Goel, N. 2006. "In Situ Methane Hydrate Dissociation with Carbon Dioxide Sequestration: Current Knowledge and Issues." *J. Pet. Sci. Eng.* **51**(3-4):169-184.
- Hirohama, S., Y. Shimoyama, A. Wakabayashi, S. Tatsuta, and N. Nishida. 1996. "Conversion of CH₄-Hydrate to CO₂-Hydrate in Liquid CO₂." *J. Chem. Eng. Japan* **29**(6):1014-1020.
- Hong, H. and M. Pooladi-Darvish. 2005. "Simulation of Depressurization for Gas Production from Gas Hydrate Reservoirs." *J. Canadian Petrol. Tech.* **44**(11):39-46.
- Ji, C., G. Ahmadi, and D. H. Smith. 2001. "Natural Gas Production from Hydrate Decomposition by Depressurization." *Chem. Eng. Sci.* **56**(20):5801-5814.
- Jiang, Q., L. H. Liang, and M. Zhao. 2001. "Modelling of the Melting Temperature of Nano-Ice in Mcm-41 Pores." *J. Phys. Condens. Matter* **13**(20):L397-L401.
- Kvenvolden, K. A., G. D. Ginsburg, and V. A. Soloviev. 1993. "Worldwide Distribution of Subaquatic Gas Hydrates." *Geo-Marine Letters* **13**(1):32-40.
- Kvenvolden, K. A. 1995. "Natural-Gas Hydrate Occurrence and Issues." *Sea Tech.* **36**(9):69-74.

- Lee, H., Y. Seo, Y. T. Seo, I. L. Moudrakovski, and J. A. Ripmeester. 2003. "Recovering Methane from Solid Methane Hydrate with Carbon Dioxide." *Angewandte Chemie-International Edition* **42**(41):5048-5051.
- Liu, J., L. J. Yan, G. J. Cheng, and T. M. Guo. 2002. "Kinetics of Methane Hydrate Dissociation in Active Carbon." *Acta Chimica Sinica* **60**(8):1385-1389.
- McGrail, B. P., S. Ahmed, H. T. Schaefer, A. T. Owen, P. F. Martin, and T. Zhu. 2007. "Gas Hydrate Property Measurements in Porous Sediments with Resonant Ultrasound Spectroscopy." *J. Geophys. Res.* **112**(B05202), doi:10.1029/2005JB004084.
- Milkov, A. V., G. E. Claypool, Y. J. Lee, W. Y. Xu, G. R. Dickens, and W. S. Borowski. 2003. "In Situ Methane Concentrations, at Hydrate Ridge, Offshore Oregon: New Constraints on the Global Gas Hydrate Inventory from an Active Margin." *Geology* **31**(10):833-836.
- Moridis, G. J. 2003. "Numerical Studies of Gas Production from Methane Hydrates." *SPE Journal* **8**(4):359-370.
- Moridis, G. J., T. S. Collett, S. R. Dallimore, T. Satoh, S. Hancock, and B. Weatherill. 2004. "Numerical Studies of Gas Production from Several CH₄ Hydrate Zones at the Mallik Site, Mackenzie Delta, Canada." *J. Pet. Sci. Eng.* **43**(3-4):219-238.
- Moridis, G. J. 2004. "Numerical Studies of Gas Production from Class 2 and Class 3 Hydrate Accumulations at the Mallik Site, Mackenzie Delta, Canada." *SPE Reservoir Eval. Eng.* **7**(3):175-183.
- Mualem, Y. 1976. "A New Model for Predicting the Hydraulic Conductivity of Unsaturated Porous Media." *Water Resour. Res.* **12**:513-522.
- Nakano, S., K. Yamamoto, and K. Ohgaki. 1998. "Natural Gas Exploitation by Carbon Dioxide from Gas Hydrate Fields - High-Pressure Phase Equilibrium for an Ethane Hydrate System." *Proceedings of the Institution of Mechanical Engineers* **212**:159-163.
- Ohgaki, K., K. Takano, and M. Moritoki. 1994. "Exploitation of CH₄ Hydrates under the Nankai Trough in Combination with CO₂ Storage." *Kagaku Kogaku Ronbunshu* **20**:121-123.
- Ohgaki, K., K. Takano, H. Sangawa, T. Matsubara, and S. Nakano. 1996. "Methane Exploitation by Carbon Dioxide from Gas Hydrates - Phase Equilibria for CO₂-CH₄ Mixed Hydrate System." *J. Chem. Eng. Japan* **29**(3):478-483.
- Pooladi-Darvish, M. 2004. "Gas Production from Hydrate Reservoirs and Its Modeling." *J. Petrol. Tech.* **56**(6):65-71.
- Seo, Y. T. and H. Lee. 2001. "Multiple-Phase Hydrate Equilibria of the Ternary Carbon Dioxide, Methane, and Water Mixtures." *J. Phys. Chem. B* **105**(41):10084-10090.
- Seo, Y. T., H. Lee, and J. H. Yoon. 2001. "Hydrate Phase Equilibria of the Carbon Dioxide, Methane, and Water System." *J. Chem. Eng. Data* **46**(2):381-384.

- Sloan, E. D., Jr. 1998. *Clathrate Hydrates of Natural Gases*. Marcel Dekker, Inc.
- Smith, D. H., K. Seshadri, and J. W. Wilder. 2001. "Assessing the Thermodynamic Feasibility of the Conversion of Methane Hydrate into Carbon Dioxide Hydrate in Porous Media." *First National Conference on Carbon Sequestration*, National Energy Technology Laboratory, Proceedings available at <http://www.netl.doe.gov/events/01conferences/carbseq/carbseq01.html>.
- Sum, A. K., R. C. Burruss, and E. D. Sloan. 1997. "Measurement of Clathrate Hydrates Via Raman Spectroscopy." *J. Phys. Chem. B* **101**(38):7371-7377.
- Sun, X., N. Nanchary, and K. K. Mohanty. 2005. "1-D Modeling of Hydrate Depressurization in Porous Media." *Transport in Porous Media* **58**(3):315-338.
- Sung, W. M., H. Lee, and C. Lee. 2002. "Numerical Study for Production Performances of a Methane Hydrate Reservoir Stimulated by Inhibitor Injection." *Energy Sources* **24**(6):499-512.
- Sung, W. M., H. Lee, S. Kim, and H. Kang. 2003. "Experimental Investigation of Production Behaviors of Methane Hydrate Saturated in Porous Rock." *Energy Sources* **25**(8):845-856.
- Takahashi, H., E. Fercho, and S. R. Dallimore. 2005. Drilling and Operations Overview of the Mallik 2002 Production Research Well Program. In *Scientific Results from Mallik 2002 Gas Hydrate Production Research Well Program, Mackenzie Delta, Northwest Territories, Canada*, Vol. Bulletin 585 (ed. S. R. Dallimore and T. S. Collett). Geological Survey of Canada, Vancouver, British Columbia.
- Tang, L. G., R. Xiao, C. Huang, Z. P. Feng, and S. S. Fan. 2005. "Experimental Investigation of Production Behavior of Gas Hydrate under Thermal Stimulation in Unconsolidated Sediment." *Energy Fuels* **19**(6):2402-2407.
- Tohidi, B., R. Anderson, M. B. Clennell, R. W. Burgass, and A. B. Biderkab. 2001. "Visual Observation of Gas-Hydrate Formation and Dissociation in Synthetic Porous Media by Means of Glass Micromodels." *Geology* **29**(9):867-870.
- Tsyppkin, G. G. 2000. Mathematical Models of Gas Hydrates Dissociation in Porous Media. In *Gas Hydrates: Challenges for the Future*, Vol. 912, pp. 428-436.
- Uchida, T., S. Takeya, T. Ebinuma, and H. Narita. 2001. Replacing Methane with CO₂ in Clathrate Hydrate: Observations Using Raman Spectroscopy. In *Proceedings of the Fifth International Conference on Greenhouse Gas Control Technologies* (ed. D. J. Williams, R. A. Durie, P. McMullan, C. A. J. Paulson, and A. Y. Smith), pp. 523-527. CSIRO Publishing, Collingwood, Australia.
- van Genuchten, M. T. 1980. "A Closed-Form Equation for Predicting the Hydraulic Conductivity of Unsaturated Soils." *Soil Sci. Soc. Am. J.* **44**:892-898.
- White, M. D. and M. Oostrom. 2006. *STOMP: Subsurface Transport over Multiple Phases, Version 4.0, User's Guide*. PNNL-15782, Pacific Northwest National Laboratory, Richland, Washington.

Yan, L., K. E. Thompson, and K. T. Valsaraj. 2006. "A Numerical Study on the Coalescence of Emulsion Droplets in a Constricted Capillary Tube." *J. Colloid Interface Sci.* **298**(2):832-844.

Distribution

**No. of
Copies**

OFFSITE

- 2 Robert Hunter
ASRC Energy Services
3900 C. Street, Suite 702
Anchorage, AK 99503
- 2 Tao Zhu
University of Alaska Fairbanks
425 Duckering Building
P.O. Box 755880
Fairbanks, AK 99775-5880
- 1 Ray Boswell
Strategic Center for Natural Gas & Oil
U.S. Department of Energy
National Energy Technology Laboratory
3610 Collins Ferry Road
P.O. Box 880
Mail stop C02
Morgantown, WV 26507-0880
- 1 E. Dendy Sloan, Jr.
426 Alderson Hall
Chemical Engineering Department
Colorado School of Mines
Golden, CO 804011
- 1 Timothy S. Collett
US Geological Survey
Denver Federal Center, MS-939
Box 25046
Denver, CO 80225 USA

- 1 Robert Vagnetti
Strategic Center for Natural Gas & Oil
U.S. Department of Energy
National Energy Technology Laboratory
3610 Collins Ferry Road
P.O. Box 880
Mail stop C02
Morgantown, WV 26507-0880
- 1 Brent Sheets
Arctic Energy Office
U.S. Department of Energy
P.O. Box 755910
Fairbanks, AK 99775-5910

**No. of
Copies**

ONSITE

- 6 **Pacific Northwest National Laboratory**
- | | |
|---------------|-------|
| B. P. McGrail | K6-81 |
| H. T. Schaeff | K6-81 |
| M. D. White | K6-81 |
| A. T. Owen | K6-81 |
| P. L. Martin | K6-81 |
| P. E. Long | K9-33 |

Final Report

DE-FC26-01NT41248

Rural Alaska Coal bed Methane: Application of New Technologies to Explore and Produce Energy

Work Performed During Period: June 1, 2003 – June 30, 2005

For

**National Energy Technology Laboratory
Arctic Energy Office
US Department of Energy**

Through

**Arctic Energy Technology Development Laboratory
University of Alaska Fairbanks
Fairbanks, Alaska 99775**

Prepared by:

Principal Investigator: David O. Ogbe, Ph.D., P.E.

Co-Principal Investigator: Shirish L. Patil

Participating Scientist: Doug Reynolds

Petroleum Development Laboratory

University of Alaska Fairbanks

425 Duckering Building, P.O. Box 755880

Fairbanks, Alaska 99775-5880

Telephone: (907) 474-7734 FAX: (907) 474-5912

Email: ffslp@uaf.edu

Principal Investigator: James G. Clough

Alaska Department of Natural Resources

Division of Geological and Geophysical Surveys

3354 College Road Fairbanks, AK 99709-3707

Phone: (907) 451-5030 Fax: (907) 451-5050

Email: jim_clough@dnr.state.ak.us

December 2006

DISCLAIMER

This report was prepared as an account of work sponsored by an agency of the United States Government. Neither the United States Government nor any agency thereof, nor any of their employees, makes any warranty, express or implied, or assumes any legal liability or responsibility for the accuracy, completeness, or usefulness of any information, apparatus, product, or process disclosed, or represents that its use would not infringe privately owned rights. Reference herein to any specific commercial product, process, or service by trade name, trademark, manufacturer, or otherwise does not necessarily constitute or imply its endorsement, recommendation, or favoring by the United States Government or any agency thereof. The views and opinions of authors expressed herein do not necessarily state or reflect those of the United States Government or any agency thereof.

ACKNOWLEDGEMENTS

The Petroleum Development Laboratory, University of Alaska Fairbanks prepared this report. The US Department of Energy NETL sponsored this project through the Arctic Energy Technology Development Laboratory (AETDL) of the University of Alaska Fairbanks. The financial support of the AETDL is gratefully acknowledged. We also acknowledge the co-operation from the other investigators, including James G. Clough of the State of Alaska Department of Natural Resources, Division of Geological and Geophysical Surveys; Art Clark, Charles Barker and Ed Weeks of the USGS; Beth Mclean and Robert Fisk of the Bureau of Land Management. James Ferguson and David Ogbe carried out the pre-drilling economic analysis, and Doug Reynolds conducted post drilling economic analysis. We also acknowledge the support received from Eric Opstad of Elko International, LLC; Anchorage, Alaska who provided a comprehensive AFE (Authorization for Expenditure) for pilot well drilling and completion at Fort Yukon. This report was prepared by David Ogbe, Shirish Patil, Doug Reynolds, and Santanu Khataniar of the University of Alaska Fairbanks, and James Clough of the Alaska Division of Geological and Geophysical Survey. The following research assistants, Kanhaiyalal Patel, Amy Rodman, and Michael Olaniran worked on this project.

TABLE OF CONTENTS

DISCLAIMER	ii
ACKNOWLEDGEMENTS	iii
EXECUTIVE SUMMARY	1
NOMENCLATURE	4
CHAPTER 1: INTRODUCTION	5
1.1 Objectives	6
1.2 Tasks	6
1.2.1 First Year: June 1, 2003 to June 1, 2004	8
1.2.2 Second Year: June 1, 2004 to June 1, 2005	9
1.2.3 Third Year: June 1, 2005 to June 1, 2006	10
CHAPTER 2: GAS CONTENT DETERMINATION	12
2.1 Coring Operations	14
2.1.1 Upper coal zone	15
2.1.2 Lower coal zone	17
2.2 Core Analysis	18
2.2.1 Desorption method	18
2.2.2 Desorption temperature during lost gas estimate	19
2.2.3 Analysis of desorption data	21
2.3 Results	21
2.3.1 Desorption	21
2.3.2 Coal bed saturation from isotherms	21
CHAPTER 3: COAL BED PROPERTIES	29
3.1 Laboratory Measurement of Permeability	29
3.1.1 Experimental set up	29
3.1.2 Core plug and sample preparation	30
3.1.3 Experimental procedure	31
3.1.4 Results	32

3.2 Well Log Analysis	33
3.2.1 Log-derived properties	38
CHAPTER 4: RESERVOIR MODELING	40
4.1 Reservoir Modeling Results	41
CHAPTER 5: ECONOMIC ANALYSIS	49
5.1 Objectives of Economic Analysis	52
5.2 Methodology	53
5.3 Assumptions	54
5.3.1 CBM field modeled	54
5.3.2 Scale and duration	54
5.3.3 Ramp up	55
5.3.4 Energy demand	55
5.3.5 Costs	55
5.4 Results	64
CHAPTER 6: USE OF DRILLING WASTE	67
6.1 Beneficial Use of Drilling Waste as Sealant	67
CHAPTER 7: CONCLUSIONS AND RECOMMENDATIONS	72
7.1 Conclusions	72
7.2 Recommendations	73
APPENDIX A: Tables and Figures from Economic Analysis	75

ATTACHMENT:

Stratigraphy and Depositional Settings of the Nonmarine Tertiary (Miocene)
Sedimentary Succession in the 2004 Lower Drill Core, Fort Yukon, Alaska

LIST OF FIGURES

Figure 2.1	Location of 2004 slim hole drilling operations	13
Figure 2.2	Well completion scheme at Fort Yukon, Alaska	14
Figure 2.3	Photograph of lower Fort Yukon core	18
Figure 2.4	Methane adsorption isotherm for Canister 104-5	22
Figure 2.5	Methane adsorption isotherm for Canister 104-33	23
Figure 3.1	Schematic diagram of experimental set up	30
Figure 3.2	Trace plot for Fort Yukon well DOI-04-1A	35
Figure 3.3	Density response for Fort Yukon well DOI-04-1A	36
Figure 3.4	Clay volume interactive plot for Fort Yukon well DOI-04-1A	37
Figure 4.1	Impact of permeability on coal gas recovery	40
Figure 4.2	Gas in place (FGIP) vs. time	42
Figure 4.3	Coalbed gas content from Fort Yukon and continental US	43
Figure 4.4	Gas production rate (MSCF/D) vs. time (Years)	44
Figure 4.5	Cumulative gas produced (MSCF) vs. time (Years)	45
Figure 4.6	Water production rate (STB/D) vs. time (Years)	46
Figure 4.7	Effect of coal permeability on gas production rate	47
Figure 5.1	Pie chart of costs for wells and capital	61
Figure 6.1	Fort Yukon's old landfill near airport	69
Figure 6.2	Plan for sealing part of old landfill at Fort Yukon	70
Figure 6.3	Successful use of drilling waste as sealant for landfill	71

LIST OF TABLES

Table 2.1	Summary of canister desorption results, upper coal zone	25
Table 2.2	Summary of canister desorption results, lower coal zone	27
Table 3.1	Measurement of horizontal permeability	32
Table 3.2	Petrophysical properties of Fort Yukon well DOI-04-1A	38
Table 5.1	Summary of current Fort Yukon area fuel usage	50
Table 5.2	Coal bed methane well costs for site #1: Fort Yukon	56
Table 5.3	Capital costs of surface facilities/pipeline to relocated power utility	59
Table 5.4	Fuel gas distribution system	60
Table 5.5	Gas power utility conversion costs	61
Table 5.6	Operating costs	62
Table 5.7	Taxes	64
Table 5.8	Economic model results	64

Rural Alaska Coal Bed Methane: Application of New Technologies to Explore and Produce Energy

EXECUTIVE SUMMARY

The conventional method of power generation in the remote and rural areas of Alaska involves use of diesel powered electric generators. Use of diesel for power generation in remote areas is very expensive because of high diesel price and additional transportation costs to remote locations. A possible alternative for power generation in the remote areas of Alaska is use of natural gas associated with coal deposits, known as coal bed methane (CBM). Alaska has the largest coal deposit in the entire US. The CBM potential in Alaska has been estimated to be 1000 trillion cubic feet (TCF) methane in place. The Alaska Division of Geological and Geophysical Survey has determined that over 37 remote villages are situated on or are immediately adjacent to coal deposits. Therefore, Alaska's vast coal reserve could potentially provide clean and low cost power to the rural areas if the CBM could be harnessed.

The objective of this project was to investigate the feasibility of CBM production in rural Alaska for the purpose of power generation for local use. The project would evaluate producibility of methane from low rank coals using slim hole drilling techniques that are essential to greatly reducing mobilization and drilling costs in remote areas. During the first year of the project, an initial core hole would be drilled to collect reservoir and geologic data, to determine well spacing, and to identify potential water injection zones in the largest identified rural village, Fort Yukon. In the later part of the project,

methodology of small scale production would be tested by drilling a five spot pattern at a more accessible and affordable location in the Matanuska-Susitna valley. Reservoir modeling to forecast production rate and economic analysis would be performed to determine feasibility of overall CBM production scheme for power generation.

The project was initiated by re-entering a core hole drilled in 1994 by USGS at Fort Yukon. The well was deepened to 2287 ft and coal samples were retrieved from two different zones. The coal samples were analyzed for gas (CBM) content by desorption experiments. Petrophysical analysis of coal samples was also carried out to generate input data for reservoir modeling. An economic analysis of a typical CBM power generation project for a remote Alaskan village like Fort Yukon was conducted using technical and economic data obtained from the Fort Yukon well.

The results from coal desorption study showed that the Fort Yukon CBM content was 3.5 and 19 SCF/ton for the upper and the lower coal zones, respectively. This level of gas content is extremely low compared to gas content of the coal deposits in the Lower 48 states. The permeability of the coal samples was also determined to be very low, of the order of 1 to 2 millidarcy (md). Reservoir modeling studies to predict gas production rate showed the maximum possible production rates to be less than 10 MSCF/D, even with well spacing as close as 20 acres. The economic analysis including the costs of drilling, maintenance and dewatering indicated that the cost of electricity generated at Fort Yukon from CBM would be in the range of 35 to 50 cents per kWh. However, in order to fulfill

the energy needs of Fort Yukon, the gas requirements were estimated at 220 MSCF/D, which was far in excess of the gas production rate possible from Fort Yukon coal beds.

Conclusions

From the results summarized above, it was concluded that Fort Yukon coal deposit has neither an adequate gas content, nor sufficient permeability to supply the amount of gas required to meet the energy needs of Fort Yukon village. Even if the required amount of methane could be produced, the cost of electricity may not be competitive with the current method of power generation using diesel. However, the project did show that slim hole drilling with lightweight, portable rigs is a technically feasible method for CBM gas production in remote areas.

An initially unanticipated outcome of the project was that drilling waste generated in the project could be successfully used as a sealant in landfill areas without any significant environmental risk. This provides for a method to dispose of drilling waste in remote areas at reduced cost.

NOMENCLATURE

ATORR	= After-tax rate of return
BTROR	= Before-tax rate of return
BTU	= British thermal unit, an English standard unit of energy. It is the amount of thermal energy required to raise the temperature of one pound of water by one degree Fahrenheit. One BTU is equivalent to approximately 1055 joule (or 1055 watt-seconds)
CBM	= Coal bed methane
ID	= Inner diameter of pipe
MAOP	= Maximum allowable operating pressure
MMBTU	= Million BTU
MSCF	= Thousands standard cubic foot of gas at 14.7 psia and 60°F
MSCFD	= Gas flow rate in thousands standard cubic foot of gas per day
MMSCF	= Million standard cubic foot of gas at 14.7 psia and 60°F
OD	= Outer diameter of pipe
O&M	= Operations and maintenance
ROR	= Rate of return
TD	= Total depth
USAF	= United States Air Force

CHAPTER 1

INTRODUCTION

At a high cost to the state and to the people of Alaska, diesel is used for power generation in the remote and rural areas of the state. Alaska has the largest coal deposits in US. Natural gas is often associated with coal deposits. This associated gas, known as coal bed methane (CBM), can potentially be produced to replace diesel as energy source in remote areas. The Alaska Division of Geological & Geophysical Surveys (DGGS) investigated CBM potential in rural Alaska and reported over 37 rural villages are situated on or are immediately adjacent to coals. This vast potential resource, that has been estimated to be 1,000 trillion cubic feet of methane in-place, could provide low cost and relatively clean energy to rural Alaska for generations to come. However, compared to the lower 48 states, coal bed methane production in Alaska poses some unique challenges as listed below.

1. Alaska's coals are young and low-rank. Production of natural gas from these coals can be difficult, depending on gas content and permeability of the coal.
2. Exploration drilling costs are 10 times higher than equivalent wells in the continental US.
3. Produced water management in rural arctic to sub-arctic environments poses a problem.
4. Ability to produce gas, saturated with water, at low temperatures well below freezing.

1.1 OBJECTIVES

The objective of this study is to investigate the technical and economic feasibility of producing natural gas from Alaska's low rank coals for the purpose of power generation in remote areas of the state. The project will involve drilling test wells in Fort Yukon and in the Matanuska-Susitna valley for producing coal bed methane. These wells will test the producibility of low-rank coals using slim-hole drilling techniques that are essential to greatly reduce mobilization and drilling costs, especially in remote locations. During year one of the program, an initial core hole will be drilled to collect reservoir and geologic data, to determine well spacing, and to identify potential water injection zones in the largest identified rural village, Ft. Yukon. If this study demonstrates success of closely spaced slim hole drilling plan for producing coal bed methane from Alaska's low rank coals, then clean and low cost energy can be made available in remote areas of Alaska on a sustained, long term basis.

1.2 TASKS

The proposed research program is to design, drill, and test six pilot slim-holes to collect reservoir and geologic data, evaluate producibility of low-rank coals, and utilize slim-hole drilling techniques in CBM well production and dewatering. Of all the places in Alaska to conduct our research, Fort Yukon is the best logical location to base this pilot study because it is the largest remote village near a coal bed identified in the DGGs study. Fort Yukon is a community of about 600 people without any road access, located along the Yukon River. Based on village demographics, geological setting and presence of potentially gassy coal beneath the community (Tyler et al., 2000), Fort Yukon was

determined as a priority site for testing CBM gas production potential. Currently, diesel fuel is barged into the village during summer months when the river is ice-free. The diesel is used in power generators which provide residential and commercial electricity. The cost of diesel at Fort Yukon can be as much as \$4 per gallon (as of 2003), which translates to the cost of electricity being about 45 cents per kWh. Because of such high energy costs, it is necessary to evaluate the potential of producing CBM from local coal deposits for the purpose of power generation at lower cost. From past research, the following are known:

- (1) There is gas in the coals (indicated by well drilled in 1994), and
- (2) Coals are laterally continuous over a large area (seismic survey in 2001).

The proposed work encompasses three consecutive years, with each year gathering additional data needed for the next step. During year one, the well drilled by the USGS at Fort Yukon in 1994 will be re-entered to collect coal gas content, continuous stratigraphic, water quality and geophysical data. While continuing the project at Fort Yukon would be optimal, logistical costs associated with a production test are prohibitive. Therefore, during years two and three, the project will relocate to the Matanuska-Susitna Valley, close to Evergreen Resources Alaska's operations. Here, a closely spaced five-spot well consisting of four dewatering holes surrounding a central gas producer will be drilled, completed and production tested. Results from this production test will then be combined with geologic and hydrologic data from the Fort Yukon well to develop a comprehensive CBM exploration-to-production model. The following specific tasks are envisioned in this project.

1.2.1 First Year: June 1, 2003 to June 1, 2004

Task 1: Pre-Field Evaluation

This task is designed to resolve the challenging logistics of working in rural Alaska. Major sub-tasks are: Define overall project work plan for Fort Yukon pilot hole designed to gather baseline geologic and hydrologic data; Identify geophysical logging methods and site preparation requirements; Acquire necessary permits and hold public meetings to educate local groups; and Contract drilling equipment and services or outright purchase necessary drilling equipment and transport materials and project personnel to Fort Yukon. Conduct an economic analysis to define the fuel gas requirements and the surface facility conceptual design to meet energy needs in a medium-sized village based on Fort Yukon example (approximately 650 people). This information is needed to plan well spacing, identify number of wells to be drilled and forecast production rates necessary to meet village energy needs.

Task 2: Drilling and development of first test well at Fort Yukon

Following the pre-field tasks, we propose to locate and re-enter the existing test-hole drilled by the US Geological Survey (USGS) in 1994. We will utilize a helicopter-portable coring rig to drill and core a slim-hole to approximately 2500 ft, collect open-hole geophysical logs, analyze core data, determine hydraulic properties, collect reservoir and water quality data in targeted coal beds, and identify possible zones for re-injection of produced water. Data from the test hole will be analyzed to support future CBM exploration programs in Fort Yukon and other areas in rural Alaska.

1.2.2 Second Year: June 1, 2004 to June 1, 2005

Task 3: Drill and complete the first three-well set in Matanuska-Susitna

In the second year, the project will focus on testing and proving methodology of small-scale production techniques in a more accessible and affordable location near Houston, Alaska. The pilot slim-holes will be drilled near Evergreen Resource's Houston leases to share water disposal facilities and to considerably reduce costs. This task will include the following:

- Design the work plan for the first three-well set. Secure permits to drill, test and produce pilot holes in the northern Cook Inlet.
- Drill, case and cement three wells – one producer and two dewatering wells to a depth of about 900 feet. Obtain suites of well logs.
- Complete both dewatering wells by perforating, & slightly stimulating with a water fracture treatment.

Task 4: Pilot production, system monitoring and coal seam evaluations

We plan to pump and produce gas and water from the pilot holes. Water production requirements versus gas recovery from the coal beds will be used to specify hole size, casing design, details of cementing and production, testing, perforating and other operations necessary to put the well on production. Well design will include facilities to execute post-drilling remedial services inside the wellbore, stimulation and water production operations. The wells will be instrumented to monitor water and gas production until completion of the project. The production data will be evaluated and related to coal seam properties, and used to develop gas well deliverability models (predictive tools) for future applications of this technology.

Water production is an essential companion to coal bed gas production. The technological challenge is to produce gas from a central slim-hole with well drawdown interference from surrounding dewatering wells rather than co-production in single wells. Surface and underground water disposal systems will be evaluated. Will evaluate downhole produced water injection systems and gas stream dehydration systems as this is likely what permafrost production will require. Produced water will be reinjected in the Evergreen water disposal well.

1.2.3 Third Year: June 1, 2005 to June 1, 2006

Task 5: Drill and complete the final two dewatering well set in Matanuska-Susitna Valley

Design work plan for two additional dewatering wells. Obtain permits for drilling, production and testing. Drill, case, cement and complete two dewatering wells in the same manner as the year two wells.

Task 6-Pilot production, system monitoring, analyses and model northern Cook Inlet exploration-to-production data

Assemble a database of information on gas and water flow rates, gas content, coal seam properties, well drilling, completion and stimulation techniques, pumping and injection systems for dewatering and water management. The data will be analyzed to model the economics of coal bed methane production in rural Alaska.

Reference

Tyler, R., Scott, A.R., and Clough, J.G., 2000, "Coalbed methane potential and exploration targets for rural Alaska communities", Alaska Division of Geological & Geophysical Surveys, Preliminary Interpretative Report 2000-2, 169 p., 1 sheet.

CHAPTER 2

GAS CONTENT DETERMINATION

The gas content study for Fort Yukon coal was done by reentering a 1994 USGS core hole to sample lignite coal found in Tertiary strata of the Yukon Flats Basin (Ager, 1994). The 1994 well cut a coal bed at 1253 ft and drilled into it for 28 ft when coring stopped at 1281 ft, still in coal. In 1994, it was noted that gas was bubbling from the core but desorption testing of the coal was not possible at that time. Consequently, the reentry of the 1994 well, now officially named DOI-04-1A, was designed to test the methane content of the Miocene age coal (Ager, 1994). The DOI-04-1A well (API No. 50-091-20001) is located at latitude 66.55949° N and longitude 145.20616° W, on the southeast end of the community site. A topographic map and areal view of Fort Yukon area indicating drill site location is shown in Figure 2.1. In 2001, high resolution shallow seismic reflection data was acquired to estimate the thickness and lateral extent of the coal seam encountered in 1994 coring operation (Miller et al., 2002). After reentry in 2004, the well was drilled to total depth (TD) of 2287 feet. Figure 2.2 shows construction and completion scheme of the well. The strata encountered was about 100 ft of River Gravel, followed by Pliocene to Miocene lake beds some 1.5 to 15 million years old (Ager, 1994). Permafrost was encountered in the well from just below the surface to about 300 ft depth. The well cut three major coal beds in two coal zones: the shallowest coal zone has two major coal beds from 1257 to 1315 ft (from gamma log picks) and at 1340 to 1345 ft. The second coal zone was at 1875 to 1920 ft with a major coal bed at 1900 to 1920 ft. The net coal thickness for the major coal beds in the two coal zones was

83 ft. Thin or muddy coals at 1875-1880 ft, 2030 ft, 2039 ft, 2057 ft. and 2067 ft were not sampled for desorption. The following sections describe the coring operations at the reentry well and the desorption method used to determine gas content of the coal from core samples.

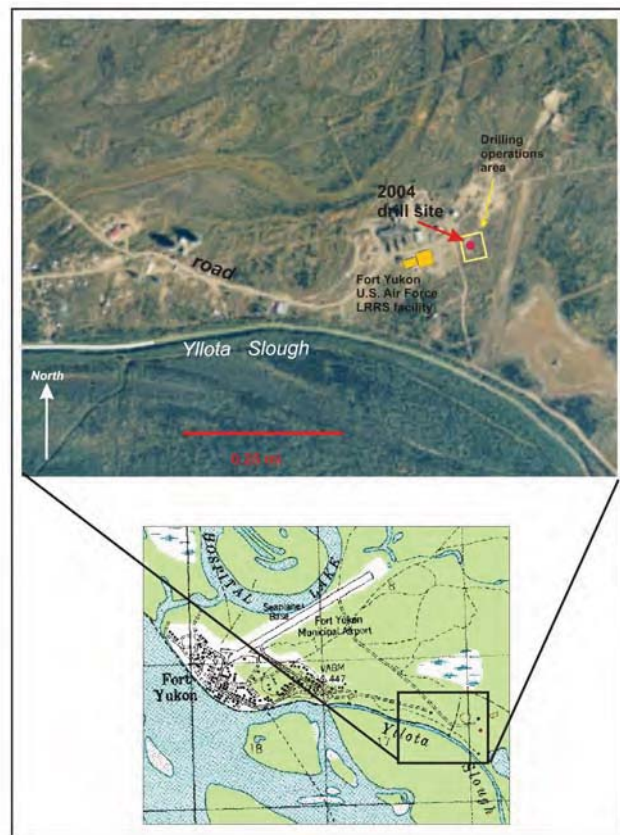


Figure 2.1 Location of 2004 slim hole drilling operations area (yellow box) and drill hole location (shown as red circle) to the southeast of the community of Fort Yukon

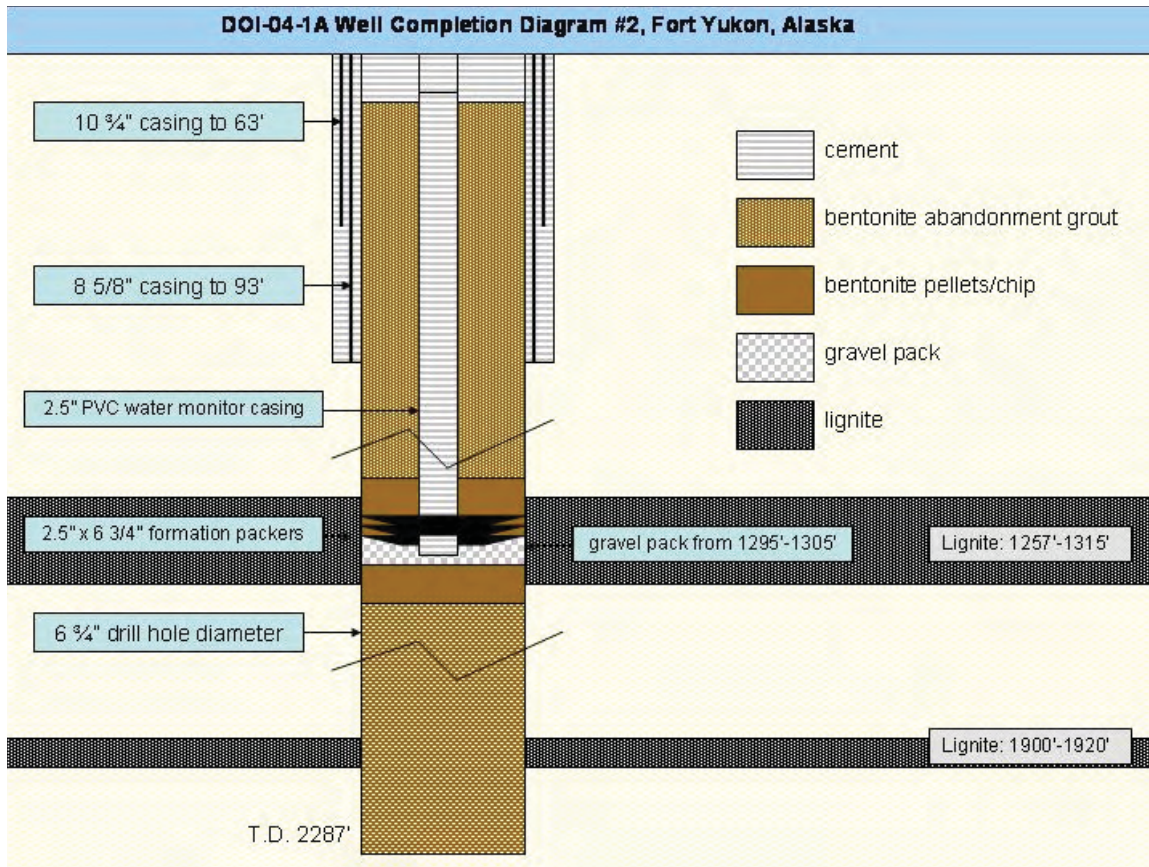


Figure 2.2 Well completion scheme at Fort Yukon, Alaska

2.1 CORING OPERATIONS

The 2004 reentry well, DOI-04-1A was spudded on August 21, 2004 by drilling out a cement and completion bentonite plug in an existing 120 ft of casing left from the 1994 USGS well. The drillers expected that the new well would soon divert away from the strata disturbed by the 1994 well and enable us to core the entire coal rather than

missing the first 28 feet that had been cored in 1994. Open-hole drilling was used to reach the core point at 1200 ft. A Christensen CS 1000 P6L portable rig was used in drilling (re-entering) the well. The drilling rig specifications are listed below.

Christensen CS 1000 P6L specifications

Lightweight, helicopter portable

Fly-in Total Wt: 8,605 LB (3,904 kg)

Power Unit: Cummins Model: 6BTA 5.9 LITER 6 CYLINDER

Power: 175 HP (131 KW), RPM: 2,500

Engine Type: DIESEL TURBOCHARGED/AFTER COOLED

Cooling: Water

Capable of drilling/coring 2.5 inch diameter core to depths up to 3000 ft.

Capable of making single-stroke 10 ft. core runs

Capable of drilling (advancing) 4 5/8 inch OD casing through surficial (glacial, alluvial, colluvial) deposits

Using lightweight HCT composite drill rod (57 lbs/10' section)

depth capacity of the CS 1000 P6L rig is increased to 3000' taking a 2.5" core

2.1.1 Upper Coal Zone

The core point at 1200 ft is some 53 ft above the upper coal zone, the open-hole drill string was tripped out of the well to put in the slim-hole diamond wireline coring system. Tripping in the core string proceeded normally until the core string was dropped early in the morning of August 25. Drill string recovery operations ("fishing") ensued and the string was recovered to the surface during the evening of August 25. Given the depth of top of the lost core string and its known length, it appears that the core string had accessed the existing 1994 hole and the core bit had settled to within 4 feet of the original 1994 core well TD (total depth) at 1281 ft.

When the core string was recovered, the base of the core string was plugged with about 12-15 inches of what appeared to be solid coal rather than coal cuttings. This coal plug was interpreted as further evidence that the base of the drill string had penetrated the coal at the base of the existing 1994 hole. Given the evidence, the decision was made to ream out the hole to within a few feet of the original 1994 TD and start coring from there. Monitoring of drill cuttings during reaming confirmed that a thick section of coal was now found above the base of the well. Addition of the 12 to 15 inches of coal found in the base of the recovered drill string to the original 28 feet cored in 1994 means that approximately first 30 feet of the coal seam were not cored in DOI-04-1A. However, as the coal bed was reamed in preparation for coring, we recovered three drill cuttings samples from the interval 1251 – 1281 ft and placed them in canisters for desorption (canister sample cuttings 104-1, -2, -3 in Table 2.1).

The first core run, intentionally cut short to test the coring system and recovery, was retrieved at about 19:30 on August 26, 2004 and consisted of 18 inches of brown coal (lignite) that were placed in canisters 104-1 and 104-2. To ensure that we had enough desorption data, we placed all coal core in canisters for the first ten feet of recovered coal. After we had about 10 canisters filled with coal, we started desorbing every other foot of coal. Some coal core was lost during coring and core retrieval as well. Among the other vagaries of coring in general, the recovery problems are thought to be caused by sticky clay partings in the coal zone that clogged the carbide core catcher leading to some core slipping out of the core barrel during retrieval. In some cases, the lost coal cores were recovered on the next core run and placed in canisters (see can 104-9 spreadsheet notes)

since they should have retained their gas by staying at the hydrostatic pressure at the bottom of the well. Coring in mostly coal continued to about 1345 ft when the last approximately 4 ft thick coal was recovered from the coal zone. Thus, the major Fort Yukon coal zone lies from about 1257 to 1345 ft (drillers depths corrected using gamma log picks).

2.1.2 Lower Coal Zone

A lower coal zone was intersected at about 1900 ft (driller depths are herein corrected to gamma log depths) and was inadvertently drilled into for about 10 ft before the open hole drilling was stopped. Coal cuttings were recovered from 1905 – 1910 ft in placed in canisters 104-31 and 104-32. Coring commenced at 1909 ft and continued to 1919 ft. A total of 10 ft of coal core was recovered and all of this core was placed in canisters 104-33 to 104-42. Figure 2.3 shows the photograph of a core sample retrieved from the lower coal zone. Core samples from the upper and the lower coal zones were studied for methane content using a canister desorption method, as well as for lithology, depositional settings and fluid flow properties.



Figure 2.3 Photograph of lower Fort Yukon core removed from core barrel

2.2 CORE ANALYSIS

2.2.1 Desorption Method

Coal desorption followed a modified US Bureau of Mines (USBM) canister desorption method as described by Diamond and Levine (1981), Close and Erwin (1989), Ryan and Dawson (1993), McLennan et al. (1994), Mavor and Nelson (1997) and Diamond and Schatzel (1998) as adapted and modified by Barker et al. (1991, 2002) for the use of PVC canisters.

A major modification of the USBM technique in this study was the use of zero-headspace canisters (Barker and Dallegge, 2005). Canisters were filled with distilled water instead

of helium gas as described in Barker et al. (2002). Distilled water was pre-chilled to about 45 to 50 °F in the chilled water tanks to speed up equilibration of the can and the coal core to the lost gas temperature.

Also we used a different desorption log form in the Barker et al. (2002) modified for zero headspace canisters. In zero headspace canisters, it is not necessary to measure internal can temperature for a subsequent headspace correction (Barker and Dallegge, 2005). All canisters were pressure tested for leaks at 6 psi over a period of at least 24 hours before use.

2.2.2 Desorption Temperature during Lost Gas Estimate

Lost gas is the unmeasured gas desorbed from coal core from the time it is cut by the drill bit to the time the sample is sealed within the canister. Lost gas is controlled by the coal diffusivity and the length of time required to retrieve a sample. Lost gas is estimated by measuring the apparent rate of gas desorption from the sample sealed in the canister. This rate is used to extrapolate back to time zero, the time of the onset of sample desorption during retrieval.

During the lost gas period, we desorb at ambient mud temperature as discussed further in Barker et al. (2002). This is because mud temperature has been found at DOI-04-1a and wells in several other basins, such as the Maverick basin in Texas; the Nenana and Cook Inlet basins in Alaska to be close to the temperature measured at the center of a freshly opened core face (unpublished USGS data). We imply that because the gas is lost during core retrieval, as pressure decreases, that the mud temperature that the core is bathed in and has equilibrated to, rather than the in-situ coalbed temperature, is the relevant

temperature to estimating diffusion of gas out of the coal matrix and therefore, lost gas.

We calculated a formation temperature in the coal zone by using a subsurface temperature of 32 °F at the base of the permafrost at about 300 ft and a geothermal gradient range of 1 to 2 °F/100 ft. Thus, 950 ft below the base of the permafrost at about 1250 ft, a temperature of 41.5 to 51 °F is estimated for the undisturbed equilibrium rock temperature. The drilling operations may warm the mud in the well somewhat above this temperature range. Infrared thermometers were used to check drilling mud, tank and core-face temperature.

Actual mud temperature measurements varied on a roughly diurnal cycle with highs of about 48 to 52 °F reached during the day and lows of about 42-45 °F reached at night. Depending on the time of the core run, the tank temperatures were adjusted to the mud temperature. Confirmation of the use of mud temperature is made by measuring the temperature at the center of core faces freshly broken open immediately after the core is extruded from the core barrel into the tray. These measurements are typically very close to mud temperature if mud circulation through the well has been maintained for enough time for a thermal stability to be established.

After desorption during the lost gas period was nearly completed, tank temperature was allowed to rise to room temperature to prepare the canisters for transport from the drill site to the laboratory.

2.2.3 Analysis of Desorption Data

The method used for correction of the data to standard pressure and preparation of a lost gas estimate uses a spreadsheet described in Barker et al (2002). The data from this analysis are presented in Table 2.1 (for the upper coal bed) and Table 2.2 (for the lower coal bed)

2.3 RESULTS

2.3.1 Desorption

The upper coal zone cores gas contents average 13.1 scf/ton with a standard deviation of 3.5 scf/ton for 21 samples. The lower coal zone cores gas contents average 19.1 scf/ton with a standard deviation of 4.0 scf/ton for 10 samples.

2.3.2 Coalbed Saturation from Isotherms.

Methane adsorption isotherms are measured by reintroducing methane to a coal and measuring the equilibrium gas content at a given pressure and at a constant temperature. The resulting curves (Figures 2.4 and 2.5) can be used with measured gas content from canister desorption (Tables 2.1 and 2.2) to estimate several parameters. Two of these parameters, degree of saturation and the reduction in reservoir pressure needed to saturate the coal, are significant in resource assessment.

The degree of saturation for the upper coal zone is calculated to be 31%. The reduction of reservoir pressure to saturate the coal bed with methane is 435 psi. The degree of saturation for the lower coal zone is calculated to be 41%. The reduction of reservoir

pressure to saturate the coal bed with methane is 600 psi. This is a relatively low degree of saturation in both coal zones. The low saturation is reflected in the relatively high reduction in reservoir pressure required to saturate the coals in either coal zone. Because a coal bed must reach saturation for desorption to occur, the large indicated pressure reduction required to reach saturation suggests that a large volume of water would have to be pumped out of the coal beds before gas production by desorption would occur. Based on this analysis, the cost for pumping out the coal bed water and disposing of the produced water would appear to be a major factor in determining if gas production is cost effective at Fort Yukon.

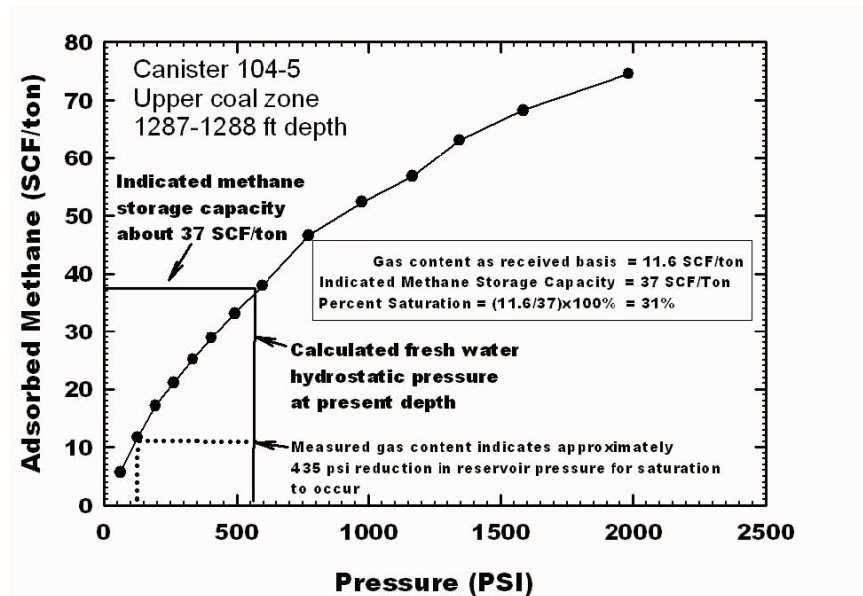


Figure 2.4 Methane adsorption isotherm for Canister 104-5 at 1287 to 1288 ft depth in the upper coal zone, DOI-04-1A well, Fort Yukon, AK. Isotherm conditions were: 15 °C, coal at equilibrium moisture. Adsorbed methane values reported on an as received basis. Coal zone pressures calculated using a fresh water hydrostatic gradient projected to the sample depth.

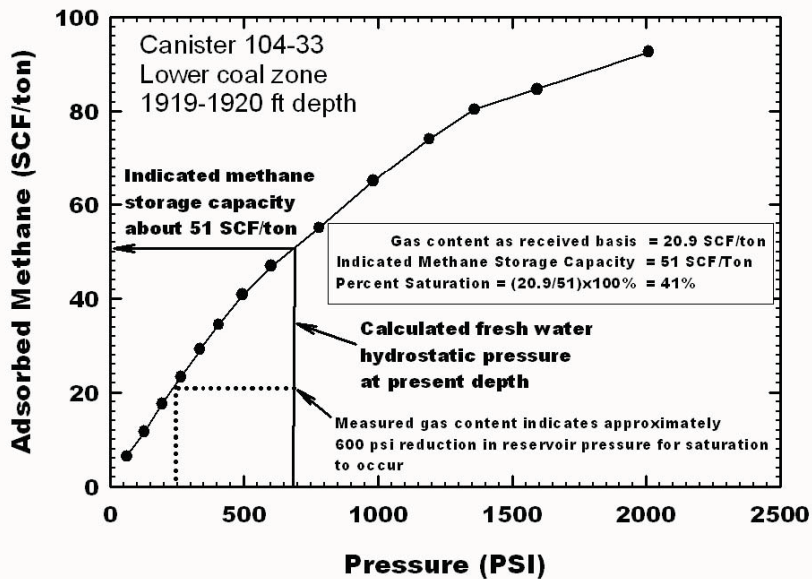


Figure 2.5 Methane adsorption isotherm for Canister 104-33 at 1919 to 1920 ft depth in the lower coal zone, DOI-04-1A well, Fort Yukon, AK. Isotherm conditions were: 15 °C, coal at equilibrium moisture. Adsorbed methane values reported on an as received basis. Coal zone pressures calculated using a fresh water hydrostatic gradient projected to the sample depth.

Conclusion

From the canister desorption study and methane adsorption isotherms, gas content of the tertiary age Fort Yukon coal was found to be very low.

References

Ager, T., 1994, The U.S. Geological Survey Global Change Drilling Project at Fort Yukon, Alaska, 1994: USGS Administrative Report, 36 p.

Barker, C.E., R.C. Johnson, B.L. Crysedale, and A.C. Clark, 1991, A field and laboratory procedure for desorbing coal gases: USGS Open-File Report OF-91-0563, 14 p.

Barker, C.E., Dallegge, T.A. and A.C. Clark, 2002, USGS Coal Desorption Equipment and a Spreadsheet for Analysis of Lost and Total Gas from Canister Desorption Measurements: USGS Open-File Report OF-2002-496. 13 p. plus spreadsheet.

Barker, C.E. and T.A. Dallegge, 2005, Zero-headspace coal-core gas desorption canister, revised desorption data analysis spreadsheets and a dry canister heating system: USGS Open-File Report OF-2005-1177

Close, J.C., and T.M. Erwin, 1989, Significance and determination of gas content data as related to coalbed methane reservoir evaluation and production implications: Proceedings of the 1989 Coalbed Methane Symposium, paper 8922, p. 37-55.

Diamond, W.P., and J.R. Levine, 1981, Direct method determination of the gas content of coal: procedures and results: U.S. Bureau of Mines Report of Investigations 8515, 36 p.

Diamond, W.P., and S.J. Schatzel, 1998, Measuring the gas content of coal: a review, in R.M. Flores, ed., Coalbed methane: from coal-mine outbursts to a gas resource: International Journal of Coal Geology, v. 35, p. 311-331

Mavor, M. and Nelson, C.R., 1997, Coalbed reservoir gas-in-place analysis: Gas Research Institute Report no. GRI-97/0263, 134 p.

McLennan, J.D., P.S. Schafer, and T.J. Pratt, 1994, A guide to determining coalbed gas content: Gas Research Institute, variously paginated.

Miller, R.D., Davis, J.C., Olea, R., Tapie, C., Laflen, D.R., Fiedler, M., 2002, Delineation of Coalbed Methane Prospects Using High-Resolution Seismic Reflections at Fort Yukon, Alaska, Kansas Geological Survey, Open-file Report No. 2002-16, 47 p., 83 figs.

Ryan, B.D. and Dawson, F.M., 1993, Coalbed methane canister desorption techniques; in Geological fieldwork 1993, B.C. Ministry of Energy, Mines and Petroleum Resources, Paper 1994-1, pages 245-256.

Table 2.1 Summary of Canister Desorption Results, Upper Coal Zone

Canister Number	Depth Interval		Canister Sample Lithology	Raw coal mass	Lost Gas Estimate	Total Raw Gas Content
	From gamma ray log (drillers depth)					
Upper Coal Zone	Top	Bottom				(as-received basis)
	(feet)	(feet)	% coal	(g)		(scf/ton)
CORE						
104-1	(1283)	(1284)	100	1056	60	14.1
104-2	(1284)	(1284.5)	50	490	40	13.5
104-3	(1285)	(1286)	100	907	85	10.8
104-4	(1286)	(1287)	100	905	80	9.8
104-5	(1287)	(1288)	100	951	80	11.6
104-6	(1288)	(1289)	100	1009	115	21.1
104-7	(1289)	(1290)	100	1149	85	7.0
104-8	(1290)	(1290.7)	70	471	85	14.5
104-9	(1295)	(1296)	100	961	85	13.4
104-10	(1304.5)	(1305.5)	100	1087	110	13.8
104-11	(1306.5)	(1307.5)	100	1193	95	12.1
104-12	(1308.5)	(1309.5)	100	1115	130	13.6
104-13	(1310.5)	(1311.5)	100	1132	130	13.9
104-14	(1312.5)	(1313.5)	100	842	80	11.0
104-15	(1315)	(1316)	100	1038	80	12.9
104-16	(1319)	(1320)	100	1171	85	8.6
104-17	(1324)	(1325)	100	1518	100	9.0
104-18	(1339.7)	(1340.7)	100	1082	100	18.7

104-19	1342 (1343)	1343 (1344)	100	749	100	19.5
104-20	1343 (1346)	1344 (1347)	100	1028	110	15.2
104-21	1344 (1349.25)	1345 (1350.25)	100	1098	100	10.9
Statistics:				Sample	Mean	13.1
				Standard	Deviation	3.5
CUTTINGS						
Cuttings-1	1265*	1270*	80	575	45	7.7
Cuttings-2	1270*	1275*	80	609	20	4.6
Cuttings-3	1275*	1280*	80	886	20	2.0
Statistics:				Sample	Mean	4.8
				Standard	Deviation	2.9

* = depth interval estimated from lag time. These cuttings were not screened and the coal fines lose their gas quickly thought to lead to the spuriously low raw gas content.

Table 2.2 Summary of Canister Desorption Results, Lower Coal Zone

Canister Number	Depth Interval		Canister Sample Lithology*	Raw coal mass	Lost Gas Estimate	Total Raw Gas
	From gamma ray log (drillers depth)					
Lower Coal Zone	Top	Bottom				Content (as-received basis)
	(feet)	(feet)	% coal	(g)		(cc/g)
CORE						
104-33	1909 (1919)	1910 (1920)	n.r. 100?	1006	120	20.9
104-34	1910 (1920)	1911 (1921)	n.r. 100?	1037	100	22.5
104-35	1911 (1921)	1912 (1922.1)	n.r. 100?	1105	100	19.4
104-36	1912 (1922.1)	1913 (1923.1)	n.r. 100?	994	120	20.4
104-37	1913 (1923.1)	1914 (1924.1)	n.r. 100?	996	120	20.9
104-38	1914 (1924.1)	1915 (1925.0)	n.r. 100?	1239	120	12.8
104-39	1915 (1925.0)	1916 (1926.0)	n.r. 100?	1118	120	17.8
104-40	1916 (1926.0)	1917 (1927.0)	n.r. 100?	1115	125	21.7
104-41	1917 (1927.0)	1918 (1928.0)	n.r. 100?	993	85	23.1

104-42	1918 (1928.0)	1919 (1929.0)	n.r. 100?	1233	85	11.2
					Mean	19.1
					Standard Deviation	4.0

Abbreviations: n.r. = not reported.

*Lithology about 100% coal from gamma log interpretation

CHAPTER 3

COAL BED PROPERTIES

This chapter describes the geological and reservoir properties measured from the Fort Yukon Pilot hole. The drill cores collected during the 2004 operations at Fort Yukon were studied for general lithology, characteristics, depositional settings and flow properties. The results in this chapter include data obtained from core analysis and well log analysis.

3.1 LABORATORY MEASUREMENT OF PERMEABILITY

The results of the permeability measurements are presented in this section. It is noted that the results may not be quite representative as it was not possible to replicate the reservoir conditions in the laboratory.

3.1.1 Experimental Set Up

The experimental set up used in the permeability measurements is shown in the schematic diagram (Figure 3.1). The set up consists essentially of a pump to circulate fluid (water) through a series of flow lines and across the face of core plug and to a flow meter. The flow rate is controlled from a digital controller attached to the pump. The core holder is a standard Hassler-sleeve core holder. It can hold cores of 1 inch to 2 inch diameter, with a length of 2 to 10 inches. The core holder has ports for applying confining pressure of up to 2000 psi. The pressure measurements and flow rates are recorded automatically using a data acquisition system with interface from the digital pump controller.

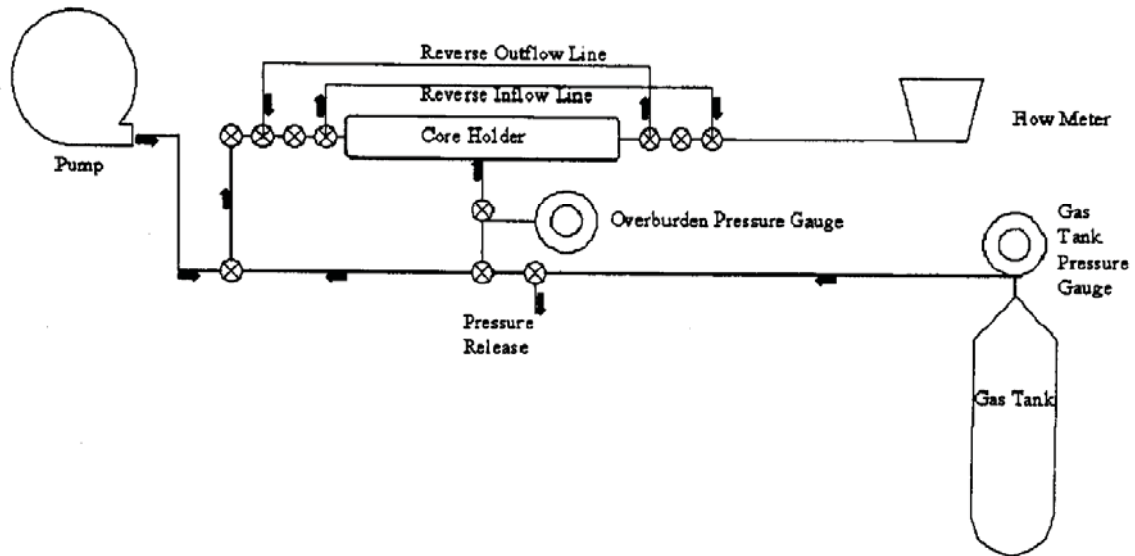


Figure 3.1 Schematic diagram of experimental set up

3.1.2 Core Plug and Sample Preparation

The core plug samples used were obtained from Fort Yukon. Two core plug samples, one extracted from depth intervals ranging from 1307.5 to 1308.5 ft and other from 1810.3 to 1820.7 ft, were used. The core plug samples were kept under freezing conditions to preserve the initial characteristics prior to the tests. The permeability was measured at an average room temperature of 71°F. The nitrogen gas was used to provide the overburden pressure. Overburden pressure of 300 psi was applied for both samples.

The core plug samples were very unconsolidated. The cross-sectional area of the core plugs was reduced using core-cutting tool to fit into the core sleeve of the equipment used. The lengths of the samples were also trimmed to obtain even cross-sectional area at both ends. Water was used as injection fluid in a single-phase flow determination of the initial permeability. The average viscosity of water used was 1 centipoise.

3.1.3 Experimental Procedure

The procedure for performing the permeability measurements is detailed as follows. There were two core plug samples. Each one was removed from the preserved condition in a freezer. Detailed information about the core plug (mainly depth interval, and physical dimensions) was recorded. The laboratory temperature condition was also recorded. In all cases, the original diameter of the core plug was wider than the core sleeve used. The core plug was then trimmed to obtain an average diameter of 1.5 inches using a 1.5 inch diameter diamond core bit in a water-lubricated drill press. Significant portions of the core samples were lost to the trimming process due to brittle nature of the core samples. The core plug was also trimmed at both ends to obtain even cross-sectional areas. The core length and the diameter were then recorded. The flow lines between the various units of the equipment setup were pressure-checked to circumvent leakages. The core was inserted into the core sleeve and loaded into the core holder. An overburden pressure of 300 psi was applied to the rubber sleeve of the core holder by injecting the nitrogen gas. The water was then allowed to flow through the core samples at a constant flow rate. The pressure drop was recorded for that particular flow rate. The water flow rate was then

changed and again the pressure drop was recorded. The experiment was repeated a number of times by varying the flow rate.

3.1.4 Results

The results obtained from the experiments are summarized in this section. Table 3.1 lists the permeabilities measured from the core samples obtained from the upper coal seam.

Measurement of Horizontal Permeability:

Sample: Coal Seam

Depth Interval Sampled: 1307.5 – 1308.5 ft

Length of core sample, L: 1.46 cm

Diameter of core sample, D: 3.6 cm

Cross section area of core, A: 10.18 cm²

Viscosity of water, μ : 1 cp

Table 3.1 Measurement of Horizontal Permeability

Flow rate	Pressure drop (Δp)	k
(ml/min)	(psia)	(md)
5	196	0.896058
10	225	1.561133
15	235	2.242052
20	248	2.8327

The results show permeability values between 0.9 and 2.8 md. These permeabilities are relatively high compared to those obtained from the hydrologic test. It is observed that the core samples were quite unconsolidated and the experimental conditions (in-situ stresses, gas saturations) do not represent the in-situ reservoir conditions. Coal

permeability at reservoir conditions is expected to be lower than the laboratory measured permeabilities.

3.2 WELL LOG ANALYSIS

The major objectives of well log analysis of Fort Yukon well (DOI-04-1A) were to identify the hydrocarbon bearing zones and to determine the petrophysical properties of these zones, such as porosity, water saturation, and clay contents. Well log analysis is the process by which the reservoir rock and fluid properties are obtained from the interpretation of the responses of various logging tools. Analysis was performed using a computer software package Interactive Petrophysics (IP) developed by PGL (Production Geoscience Ltd.) in Banchory, Scotland. The technical support for Interactive Petrophysics (IP) is provided by Schlumberger GeoQuest. The original well log data used were obtained from U. S. Geological Survey (USGS). The first step was to generate a trace plot which displayed the various log responses versus depth (see Figure 3.2). From the trace plot, the zones of interest were identified. These zones include: hydrocarbon bearing zones, the 100% water saturation zone, clean sands and shale zone. From the trace plot it can be observed that for the intervals 1258 ft-1317 ft (zone 2); 1340 ft-1348 ft (zone 4) and 1900 ft- 1920 ft (zone 6), the gamma ray response is very low and the resistivity response is high, indicating the presence of hydrocarbon bearing zones. Also for these zones the density response is very low (see Figure 3.3).

The basic log analysis module is useful for making a quick basic log interpretation. Clay volume is calculated using the gamma ray (GR), SP, Neutron, and Resistivity responses,

which allow us to compare the results obtained from different indicators. But for Fort Yukon well we had only GR and resistivity responses for calculation of clay volume (see Figure 3.4). Porosity is calculated either from the density or sonic tool. Water saturations are calculated from the electrical resistivity curves using the basic Archie equation.

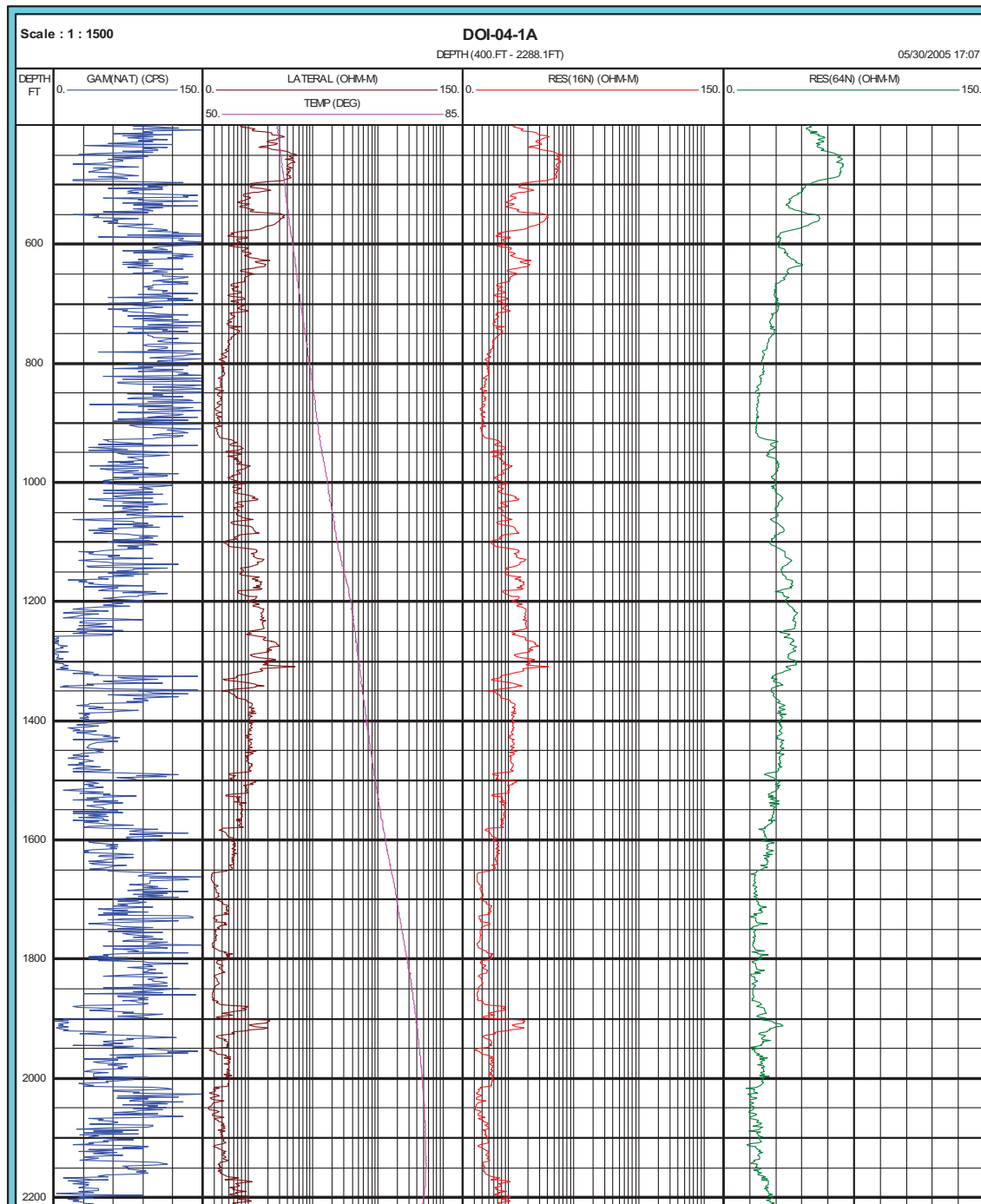


Figure 3.2 Trace plot for Fort Yukon well (DOI-04-1A)

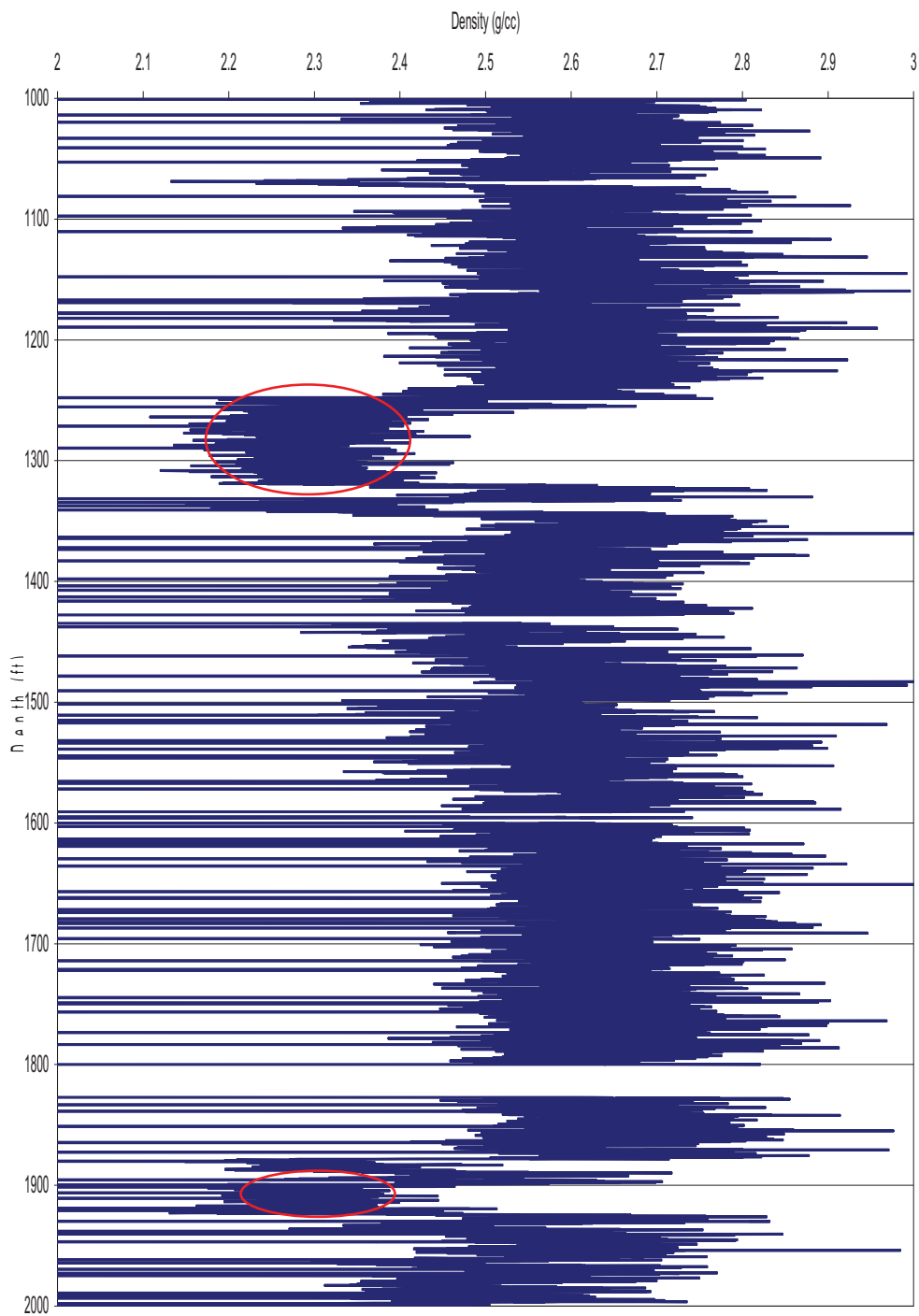


Figure 3.3 Density response for Fort Yukon well (DOI-04-1A)

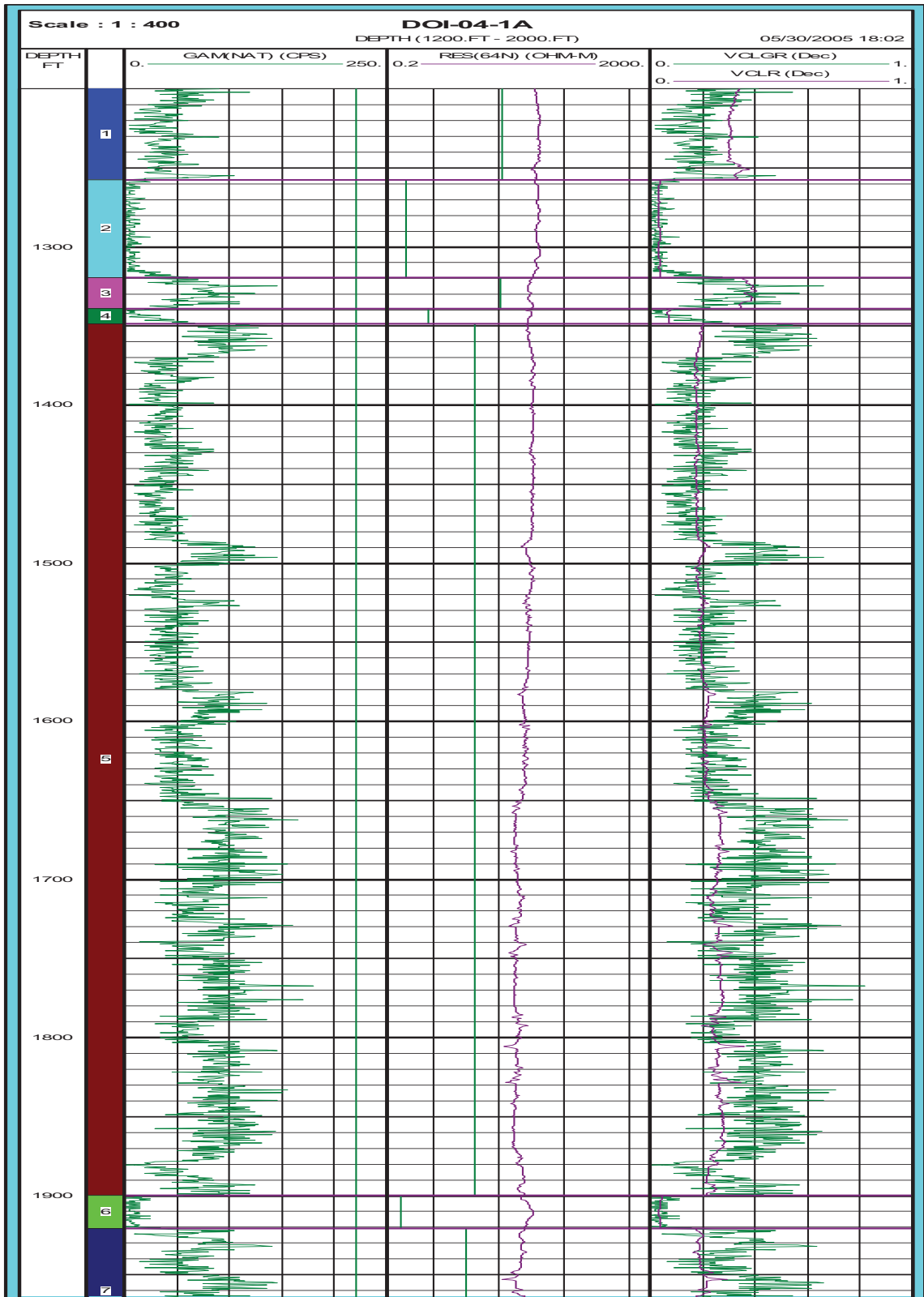


Figure 3.4 Clay volume interactive plot for Fort Yukon well (DOI-04-1A)

3.2.1 Log-Derived Properties

The average petrophysical properties (porosity, water saturation, and clay volume) obtained from well logs of the Fort Yukon well (DOI-04-1A) are summarized in Table 3.2 as shown below.

Table 3.2 Petrophysical Properties of Fort Yukon well (DOI-04-1A)

Productive zone	Depth Interval (ft)	Porosity (%)	Water Saturation (%)	Clay Volume (%)
2	1258-1317	16.41	36.87	3.37
4	1340-1348	15.3	43.66	9.55
6	1900-1920	17.4	39.23	4.576

The relatively high water saturations indicate presence of mobile water in the coal beds. Mobile water contributes to water production.

Conclusions

Low coal permeability observed in the laboratory experiments indicates that permeability of Fort Yukon coal in-situ will be even lower. The well logs indicate that these coals also have significant water saturation, which may prolong the dewatering process.

References

Production Geoscience Ltd.: “Interactive Petrophysics (IP) Help Manual, Version 3.0.0.13”, Banchory, Scotland, 2003.

Schlumberger Ltd.: “Log Interpretation Principles/Applications,” Schlumberger Educational Service, Houston, Texas, 1987

CHAPTER 4
RESERVOIR MODELING

A numerical reservoir simulation study was conducted to forecast CBM production rates in the Fort Yukon area. Gas production rate and cumulative recovery depend on gas content of the coal, coal bed permeability and well spacing. A previous study by Olsen et al. (2004) showed that gas recovery may decrease significantly in coal beds with permeability less than 10 md (Figure 4.1). In this study, Fort Yukon reservoir data were used to forecast gas production rates and gas recovery from coal beds using five-spot injection pattern.

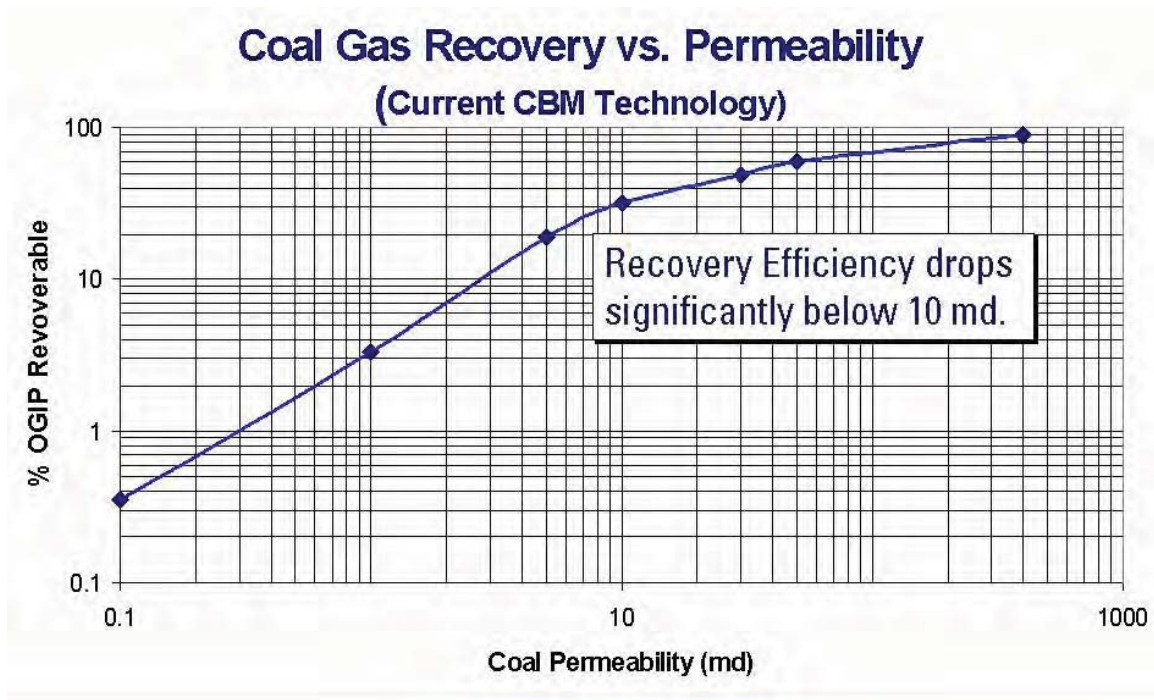


Figure 4.1 Impact of Permeability on Coal Gas Recovery (Source: Olsen et al., 2004)

4.1 Reservoir Modeling Results

The results from this simulation study are shown in Figures 4.2 through 4.7. Figure 4.2 shows gas in place as a function of time with three different production scenarios, where well spacing is varied from 80 acres to 20 acres. With 80 acre spacing, no significant decline in gas in place is seen even after 30 years of production. This shows that large well spacing may not be suitable for recovering CBM from Alaska's low rank coals. With 20 and 40 acre well spacings, significant decline in gas in place is seen after 10 to 15 years of production.

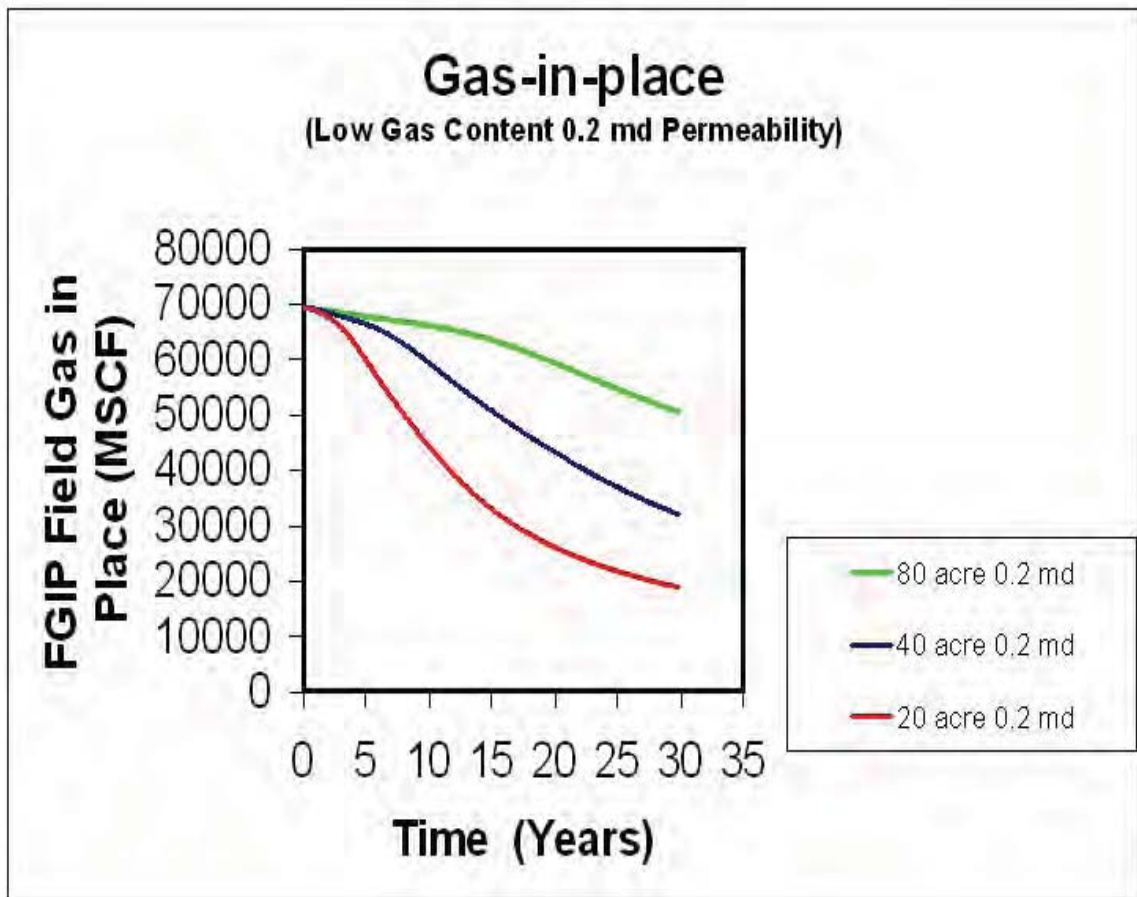


Figure 4.2 Gas in place (FGIP Field Gas in Place) vs. Time

The gas content of Fort Yukon coal, as determined from the canister desorption experiments, is shown in Figure 4.3. For comparison, the average gas content of coal from the lower 48 states is also plotted on the same graph. It is clear that Fort Yukon coal is very low in gas content. At 1000 psi, Fort Yukon coal’s gas content is less than one sixth that of the lower 48 coal. The low gas content makes it difficult to produce CBM from Fort Yukon coal at significant rates. Figure 4.4 shows that even with well spacing as close as 20 acres, the maximum daily gas production rate is less than 10

MSCF/D. Such a low production rate is not adequate to provide enough gas for power generation. Cumulative gas recovery as a function of time is shown in Figure 4.5. The cumulative recovery declines sharply with increasing well spacing.

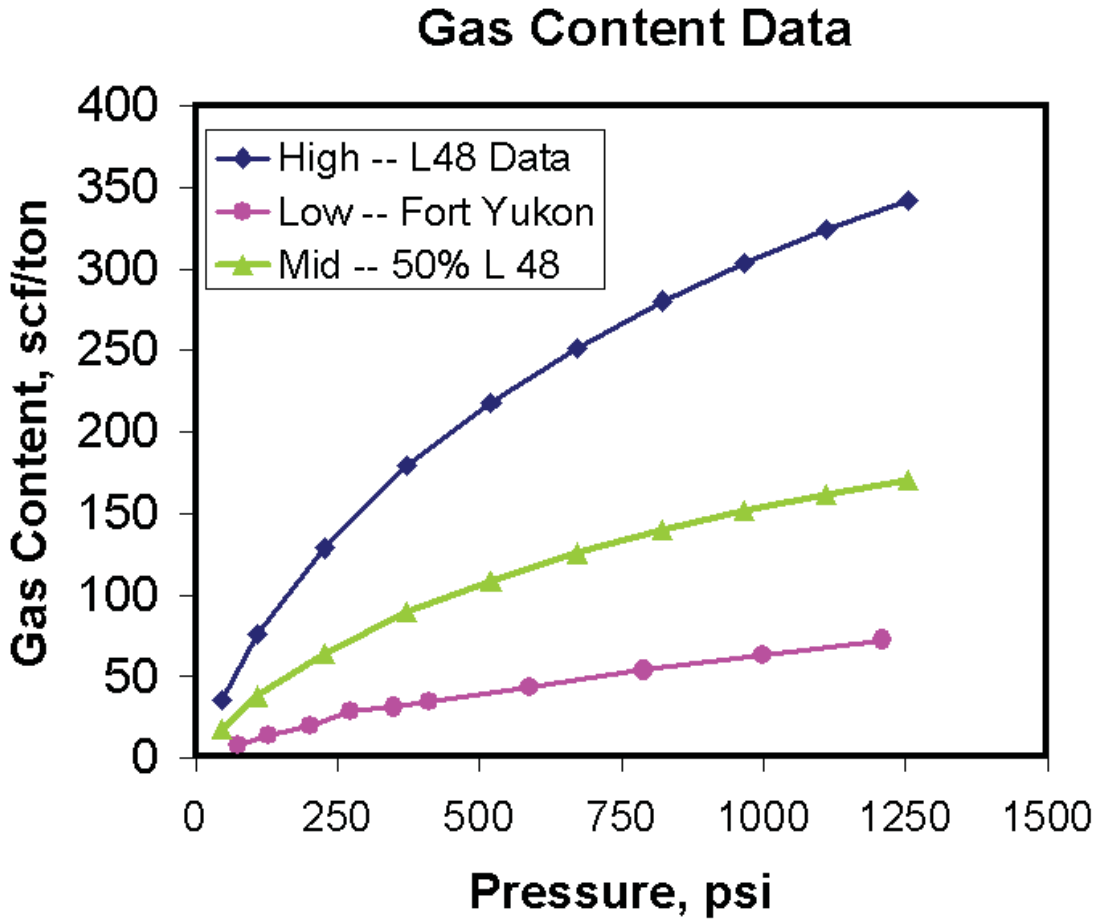


Figure 4.3 Coalbed Gas Content from Fort Yukon and Continental US

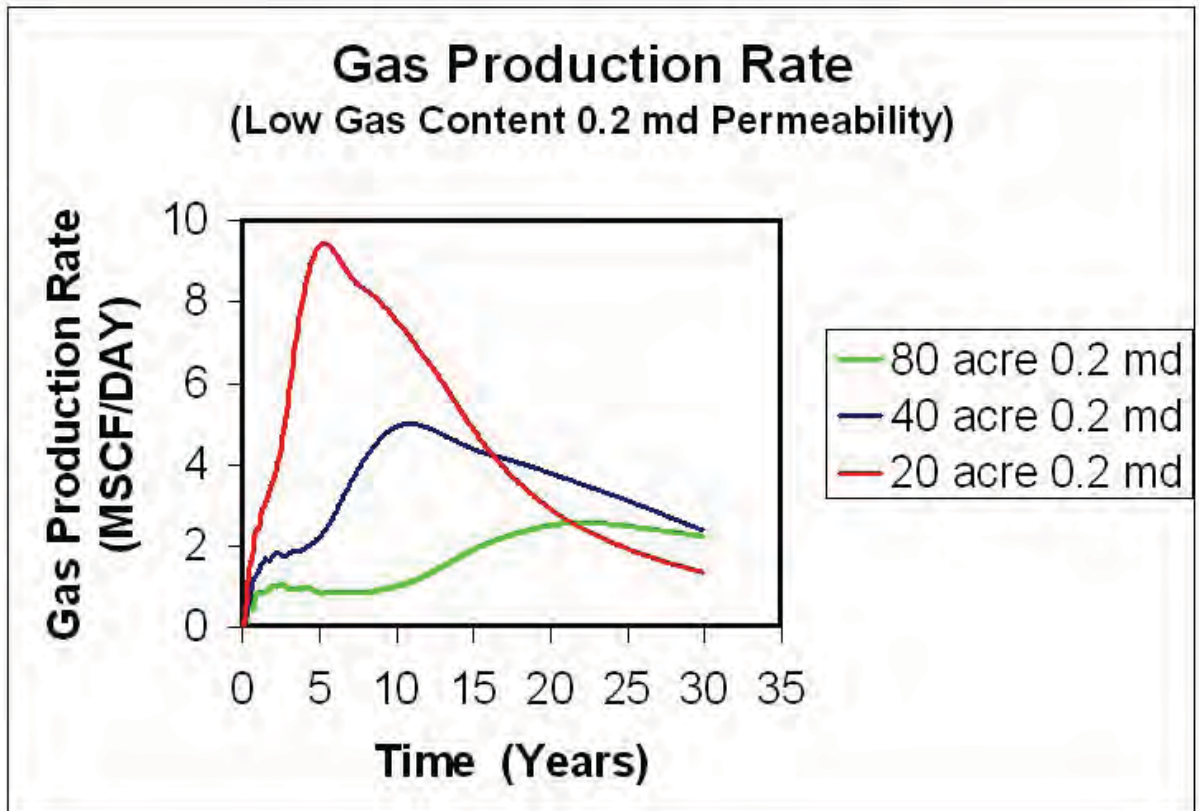


Figure 4.4 Gas Production Rate (MSCF/D) vs. Time (Years)

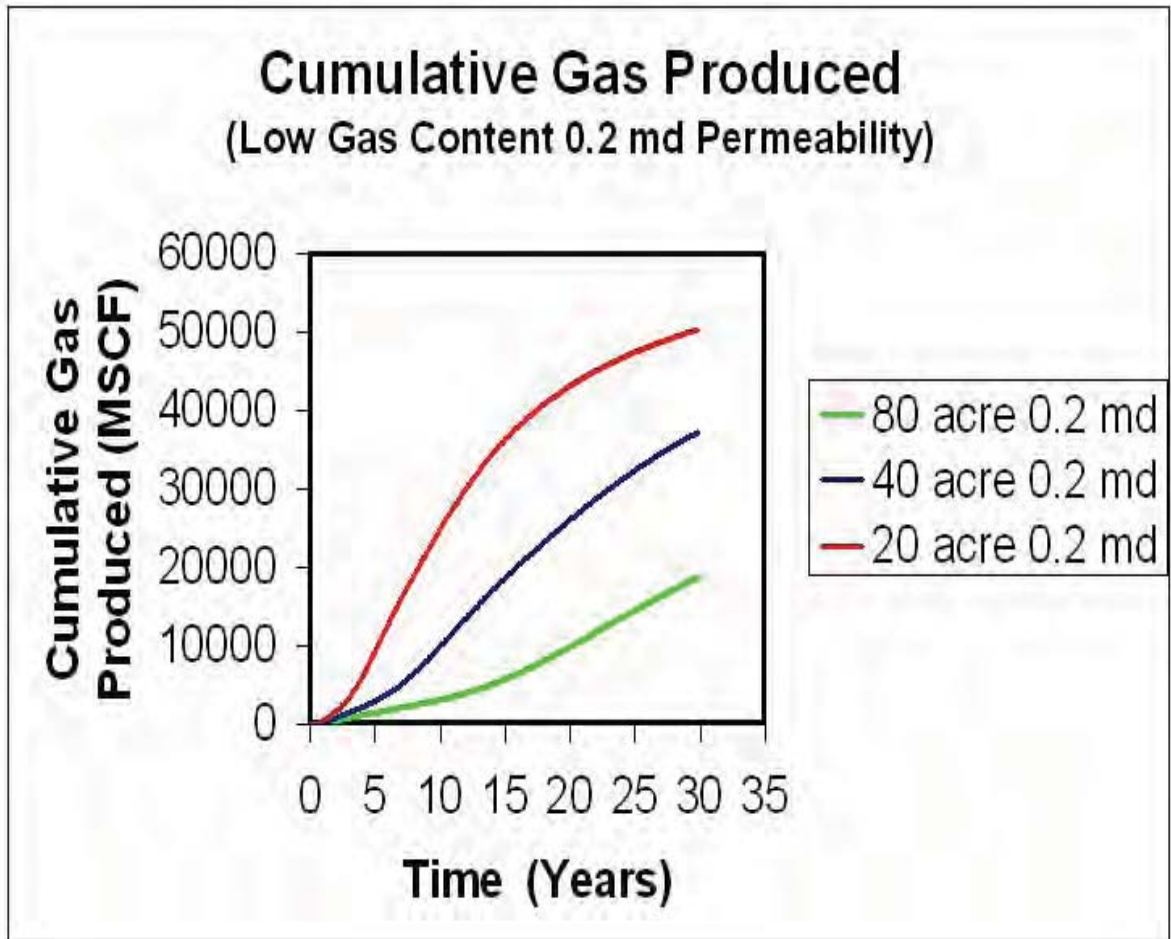


Figure 4.5 Cumulative Gas Produced (MSCF) vs. Time (Years)

Another issue associated with CBM production is disposal of produced water. The 20 acre well spacing results in the highest amount of produced water as shown in Figure 4.6. Disposal of produced water adds to the overall cost of CBM production. A sensitivity study of the effect of coal bed permeability on gas production rate is shown in Figure 4.7. The gas production rate increased from 10 to 25 MSCF/D when coal permeability was increased from 0.2 to 2 md, however, further increase in coal permeability did not

increase the gas production rate. Clearly, at permeabilities above 2 md, gas production rate becomes constrained by low gas content of the coal.

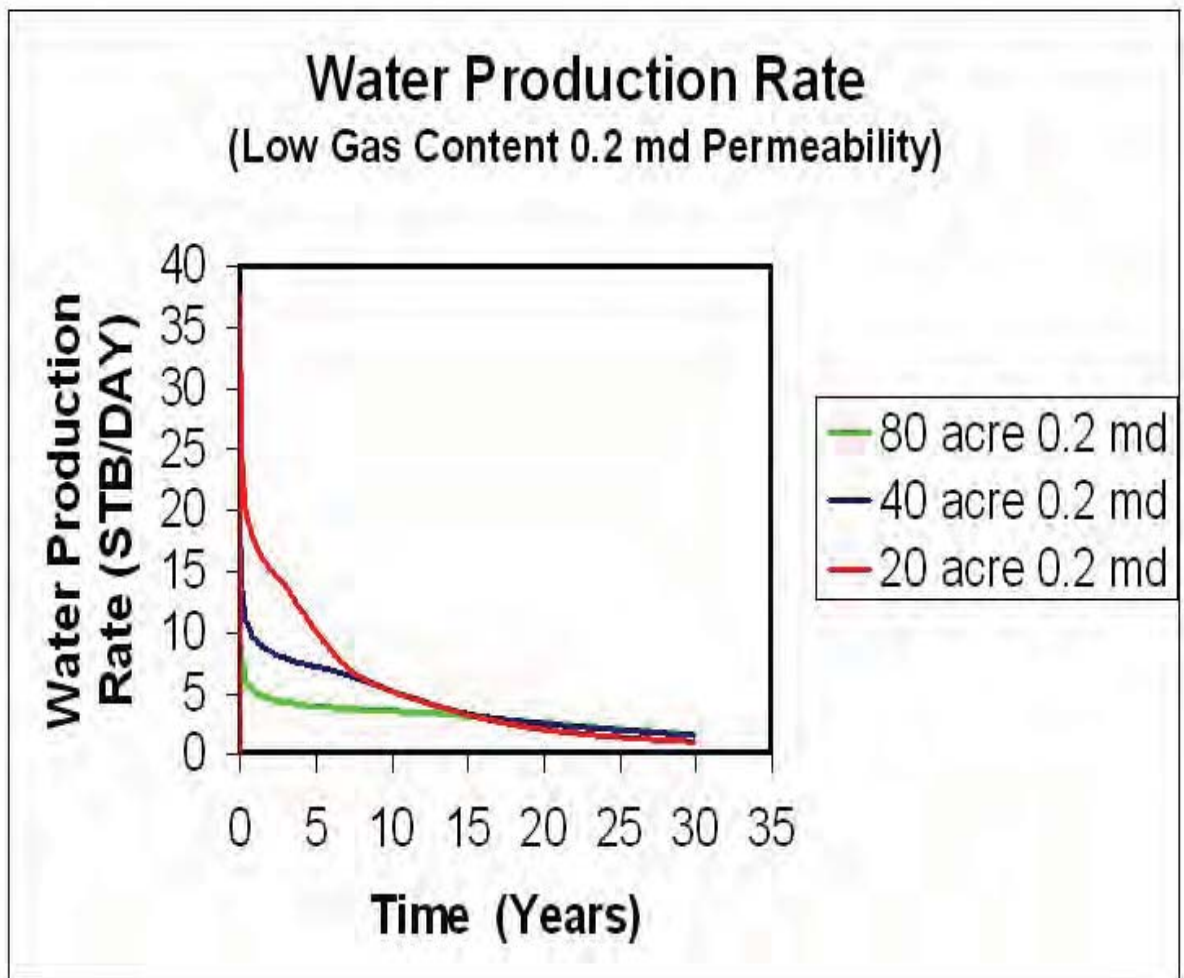


Figure 4.6 Water Production Rate (STB/D) vs. Time (Years)

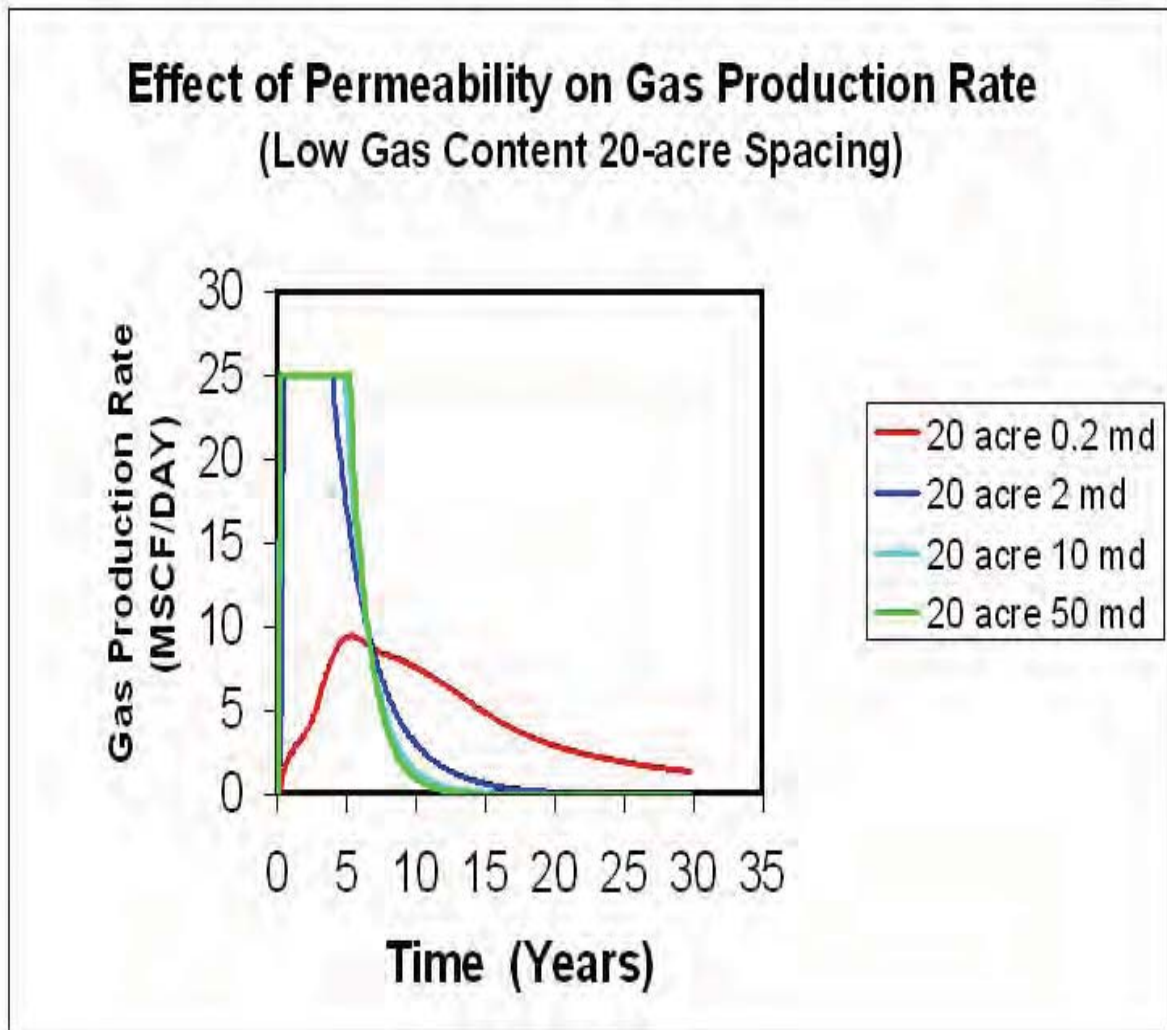


Figure 4.7 Effect of Coal Permeability on Gas Production Rate

Conclusions

In conclusion, the simulation study indicated that CBM gas production from the Fort Yukon coal beds would not result in significant gas production, even if close well spacing were used, because of low gas content and low permeability of the Fort Yukon coal beds.

The simulation study also showed that low gas content, rather than low permeability, is the primary cause of the lack of significant gas production from these coal beds.

Reference

T. Olsen, G.Brenize and T. Frenzel: "Improvement Processes for Coalbed Natural Gas Completion and Stimulation," ICMS 2004

CHAPTER 5

ECONOMIC ANALYSIS

The first step in evaluating the viability of coal bed gas as an alternative source of energy is to correctly define the equivalent fuel gas usage rates, surface facility specifications and design requirements for this community. In an earlier study (Ferguson and Ogbe, 2003), the surface facility design requirements, approximate costs for using treated coal bed gas as the primary energy source were estimated and used to establish “rough order of magnitude” costs for developing total system for production of CBM. The study gathered data on the volumes of fuel consumed in Fort Yukon area and performed a preliminary economic analysis of CBM production using a conceptual surface production and distribution facility. Table 5.1 summarizes the fuel gas utilization data for Fort Yukon area. Equivalent CBM fuel gas rate requirements were determined based on the current liquid fuel heating values and expected heating values of future coal bed gas. The conceptual production facility design was based on peak anticipated fuel gas needs through the year 2015. The cost estimate utilized typical factors for similar equipment installed in remote arctic environments such as the Alaskan North Slope oil fields.

The key findings of this pre-drilling economic study are as follows:

1. The total equivalent fuel gas usage needs for the Ft. Yukon area were determined to be 250 MSCFD based on current electric and heating needs (as of 2003). This includes both the local community and the adjacent USAF military facility.

Table 5.1 Summary of Current Fort Yukon Area Fuel Usage

(Source: Ferguson and Ogbe, 2003)

Consumer	Current Fuel Usage (Gallons/ Year)	Project Fuel Gas Needs (MSCF / Day)
GZ Power Utility	186,000	74
USAF Power Utility	109,000	43
Local Grocery Store	35,000	14
Other/Contingency (10%)	32,000	13
Total Electric	362,000	143
Yukon Flats School District	27,000	11
Water Treatment and Supply	31,000	12
Municipal/Tribal Gov't	30,000	12
Residential housing	150,000	59
Other/Contingency (10%)	23,000	9
Total Heating	261,000	103
<i>Grand Total</i>	623,000	247

2. Including the effects of peak winter month consumption swings and the projected future needs through the year 2015, a peak fuel gas need of 460 MSCFD was projected.
3. The total capital costs for the subsurface and surface equipment to supply coalbed gas for Fort Yukon's energy needs were estimated at \$5.06 to \$7.06 million for a range of potential well development costs to provide the necessary gas rate. This assumes the current plan to relocate the GZ Power Utility proceeds. We also estimated the incremental cost to convert from diesel to gas fired generators.
4. The current total electric and heating fuel cost to the Fort Yukon community is approximately \$1.2 million per year. The energy cost for the average commercial and residential consumer in the Fort Yukon area is approximately \$14.40/ MMBTU. Assuming a fuel gas value of \$8/MSCF (\$8.89/MMBTU), the total energy cost to all commercial and residential consumers in the community would be reduced to approximately \$700,000 per year resulting in a savings of approximately \$500,000 per year. The average residential household savings were estimated to be \$700 to \$1,500 per year depending on the Power Cost Equalization (PCE) subsidy assumed in the calculations.

The Fort Yukon well drilled in 2004 as a part of this project determined that the coal beds in this area cannot produce adequate amount of CBM to meet the energy needs of the village. However, the cost data from the trial can be used to perform a realistic economic analysis of a Fort Yukon project for developing and producing CBM, and the data may

also be useful for studying similar developments in other remote Alaskan villages. In this chapter, the Fort Yukon drilling costs and fuel usage rates are entered into an economic model to determine the final CBM based energy prices for the area. The cost of delivery of CBM gas determined from this study can be compared to the current energy costs as well as other alternative sources of energy. The following sections describe the specific objectives, methodology, and results from the economic analysis.

5.1 OBJECTIVES OF ECONOMIC ANALYSIS

The Fort Yukon CBM project conducted a trial drilling in a Fort Yukon coal bed in order to determine the costs and physical potential of fully developing a reservoir. Data on costs for building and constructing surface facilities to handle gas processing and gas distribution to end users in the community was also gathered. The cost data is evaluated using an economic model to determine the feasibility of CBM for rural Alaskan communities. While the trial drill hole in Fort Yukon came up dry, the cost data from the trial was sufficient to determine the feasibility of a CBM project in other locations.

Specific goals of the economic analysis are as follows.

1. To assemble a database of information. The data base will include the estimated fuel gas required to meet current energy usage/consumption in Fort Yukon, the reservoir characteristics, the number of wells required to deliver gas, and the water production rates. The previous trial drill established the costs of drilling, completing, and maintaining the wells down to a depth of 3,000 ft. sub-sea.

2. To develop an economic model to show the feasibility of developing a CBM project for Fort Yukon. The model is general enough to use for other rural Alaska areas.
3. To give results from the model to show how feasible a CBM project is in Fort Yukon or in a comparable rural Alaskan village.
4. To prepare the data and results in a format that can be used as a model for implementing the use of CBM gas in other rural Alaska communities.

5.2 METHODOLOGY

Oil and gas companies use economic models of projects to determine whether a project is economically feasible and to compare the economics of various projects. They also use the models to conduct “sensitivity analyses,” that is to answer questions like how will the project’s economics change if the price of oil increases by ten percent or there are cost overruns of twenty percent. Governments use economic models to determine the appropriateness of fiscal systems and the effect of various incentives on private investment and government revenues.

All models are evaluated using the project return on investment (ROI). The ROI indicates which project may prove the better investment. The ROI is used to compare project scenarios that have different patterns of costs and expenditures and evaluate them all on a common basis. Generally, better projects have higher returns on investments. The ROI, however, must be high enough to make the project feasible. The point at which a project becomes feasible is called the hurdle rate.

In this analysis, a specific hurdle rate is fixed and the economic model is used to determine a price for heat and electricity for the village based on that specific hurdle rate. Cost data obtained from the trial drilling and other sources are included in the model. In addition, a sensitivity analysis is carried out. Since costs to run a CBM project in a rural Alaskan village are expected to be higher than some of the cost estimates included, the economic model was run over different cost scenarios. Specifically a cost overrun multiplier was created at 50%, 100%, 150%, and 200% above the base case data to determine how such a cost overrun will affect the final price of heat. The model runs given in the appendixes show the relationships between the final price of energy and the cost overrun multiplier.

5.3 ASSUMPTIONS

5.3.1. CBM Field Modeled

The model assumes that the project occurs in Fort Yukon. The field is in the vicinity of the site where an exploratory well was drilled in 2004.

5.3.2. Scale and Duration

The economic model is constructed at the pod level, where a series of CBM wells from a contiguous field tie into a single pod. The node feeds its gas into higher-pressured pipelines. The produced gas is transported to Gwichyaa Zhee (GZ) Corporation power utility plant for electrical power generation and also distributed to end users (homes) for heating. The FY-CBM (Fort Yukon CBM) model assumes that the entire system

operates for 15 years. Costs, revenues, and profits are calculated as if the entire system from wellhead to burner tip and electrical appliance were one system.

5.3.3. Ramp Up

The model includes three scenarios for the ramp up of the system. Usually coal-bed methane fields take one to three years to dewater before the methane becomes available for sale. Since dewatering represents a significant cost and since it causes revenues to be delayed, it will have a significant impact on the economics of such a project. In this study, a one year, two year, and three year ramp up are considered.

5.3.4. Energy Demand

Energy demand includes the demand for CBM gas delivered to the GZ power utility plant in Fort Yukon as well as gas delivered to the town for heating. Another energy user is the U.S. Air Force's Power House that is on location near Fort Yukon. The consumption quantities were estimated from earlier studies for Fort Yukon. The demand also includes fuel use for powering the compressors that transport the gas through the pipeline. The demand is adjusted for differences in the BTU content and the impurities of the FY-CBM gas, as measured against natural gas standards. The demand for Fort Yukon is shown in the Appendix A.

5.3.5. Costs

Costs are broken down as follows. Tables 5.2 to 5.7 give specific estimates. These include the costs of CBM production and dewatering well construction, water disposal

well, fuel gas distribution system, utility conversion costs, operating costs, taxes and other costs.

A.) CBM production and dewatering wells

Based on project specifications, five wells will be used to create a single pod. This one pod will normally be enough to produce the required methane consumption. Slim hole wells were used in the analysis. The tangible and intangible costs for each well drilled are \$853,000. These capital costs of constructing the pod include drilling and completing the five wells. Each well will be used to dewater and to produce CBM gas. Detailed cost estimates of CBM production and dewatering wells at Fort Yukon are shown in Table 5.2.

**Table 5.2 Coal Bed Methane Well Costs for Site #1: Fort Yukon
(Cost of Constructing Five Wells for Producing CBM gas and Dewatering)**

Itemized Project Expenses	Drill, Test & Completion Summary Costs	<i>Sources and Comments</i>
Tangible Costs:		
Tubular Equipment	---	
Wellhead Equipment	---	
Completion Equipment	---	
Dewatering Equipment	---	
Total Tangible Costs:	\$150,000	Based on Petroleum News Article

Intangible Costs:		
Project preparation including equipment repair, parts, and supplies	\$112,000	Based on 2004 Drilling Costs
USGS Headquarters Assessment	\$96,000	"
Drilling charges	\$175,000	"
Expendable items (bits, mud, casing, grout, cement etc)	\$81,000	"
Other USGS personnel charges (logging, GW, QW) and data analysis	\$13,000	"
Shipping and transportation related expenses	\$143,000	"
Pack equipment and prepare for barge	\$15,000	"
Transportation of equipment from Denver to Nenana	\$30,000	"
Transportation of equipment from Nenana to Fort Yukon	\$35,000	"
Total Intangible Expenses	\$702,000	
Tangible and Intangible	\$853,000	
Open Hole Costs	\$853,000	Per well
Total Site Costs	<u>\$4,264,000</u>	5 wells for dewatering and producing CBM gas

B.) Water disposal well

There are two options for water disposal. One option is shallow re-injection, and the other is deep re-injection. The options are governed by finding a competent formation to contain the produced water. An important consideration is to avoid contaminating water tables in the vicinity of the formation. Such formations could be 3000 feet (shallow well) or deeper (deep well). Since a deep well is not going to cost much more than a shallow well, we assume a typical well cost similar to the CBM wells as listed in Table 5.2 above. This would include the costs of constructing the surface water re-injection facilities.

C.) Well peripherals

Capital costs of constructing surface facilities for gas processing include water removal, gas treatment, and a pipeline to the relocated power utility. The following items are expected as part of the water removal and gas treatment bundles: insulated housing for meters, filters and separators to prevent freezing, water flow lines, water meters, PVC line to water treatment pits, vacuum breakers to prevent a vacuum lock from stopping water flow in the line, gas meters, gas dehydrator, compressor, gas scrubber. Table 5.3 provides details of these costs.

Table 5.3 Capital Costs of Surface Facilities/Pipeline to Relocated Power Utility

	Process Equipment Cost	Fort Yukon Installed Module Cost
Water Removal		
Two-phase Separator -Water KO Drum (2' OD *6'H)	\$2,100	\$11,000
Water Re-injection Pump (400BWPD, 1000psi, 10HP)	\$5,250	\$26,000
Total:		\$37,000
Gas Treatment		
Mole Sieve incl. Regeneration	\$52,500	\$263,000
Total Processing Building		\$299,000
Pipeline to Relocated Power Utility		\$184,000
(Nominal 3.5" line ~ 1 mile from well locations)		
Total:		<u>\$483,000</u>

D.) Fuel gas distribution system

This is the system of pipelines which will carry the methane to individual houses and businesses for heating needs. The costs associated with constructing the distribution system are shown in Table 5.4.

Table 5.4 Fuel Gas Distribution System

Components	Anchorage Installed cost	Fort Yukon Installed Cost	Total Costs
2" Main trunk line through town (3 miles)	\$5.25/ft	\$10.5/ft	\$166,000
1" Lateral lines to buildings (30 miles)	\$1.05/ft	\$2.1/ft	\$333,000
Pressure regulatory station			\$26,000
Building tie-in/metering (300 @ \$525/building)			\$158,000
<i>Total:</i>			<u>\$683,000</u>

E.) Utility conversion costs

The power generation facilities need to be converted to burn methane. These costs include additional modules for gas-fired plant, an additional footprint, and the conversion of existing diesel power generators (Table 5.5).

The capital costs described in A.) through E.) are summarized in Figure 5.1.

Table 5.5 Gas Power Utility Conversion Costs

Modules	Costs
Additional modules for gas fired plant (additional footprint)	\$856,000
Conversion of existing diesel power generators	\$1,628,000
<i>Total:</i>	<u>\$2,483,000</u>

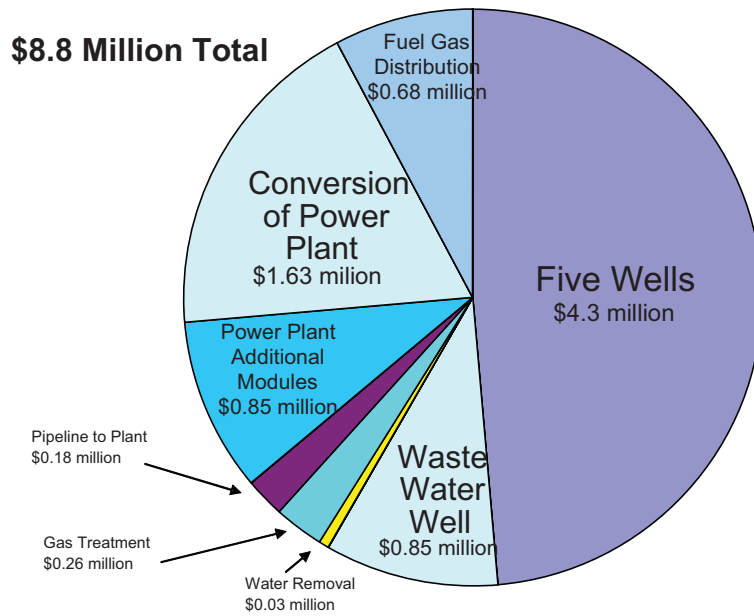


Figure 5.1: Pie Chart of Costs for Wells and Capital

F.) Power plant move (optional)

Costs include the relocation of the existing power plant. The plant is scheduled to be moved due to flood plain considerations. Therefore, this is not a typical expense when comparing a Fort Yukon project to other villages. However, one model run was done with this expense included. The cost is projected at over \$7.1 million, which would almost double the costs of a Fort Yukon project.

G.) Operating costs

Operating costs comprise the costs of operating the node and surface facilities as well as the costs of operating water re-injection facilities. This is based on direct annual operating costs for CBM production in Powder River Basin in Montana and Wyoming. Here, there are 10 wells dewatering from 1,000 ft. Since the FY-CBM project is first of its kind in Alaska, no operating cost estimates for remote Alaskan location are available. Thus, data from Montana and Wyoming, which are somewhat similar to Alaska in terms of rural nature and population density, was used. The operating cost estimates are listed in Table 5.6.

Table 5.6 Operating Costs

Expenses:	Yearly Costs
Supervision and Overhead	\$5,300
Labor (pumper)	\$8,100
Auto Usage	\$2,400
Chemicals	\$0
Fuel, Power & Water	\$23,600

Operative Supplies	\$1,900
Subtotal	\$41,300
Surface Maintenance, Repair & Services:	
Labor (roustabout)	\$11,600
Supplies & Services	\$7,300
Equipment Usage	\$4,100
Subtotal	\$23,000
Subsurface Maintenance, Repair & Services:	
Well Servicing	\$25,100
Remedial Services	\$5,700
Equipment Repair	\$11,800
Subtotal	\$42,600
Total	<u>\$106,900</u>

H.) Cost multiplier

It is expected that costs for a village CBM project will be higher than the estimates above because of Alaska's extreme remoteness and weather. Therefore, the economic model includes a multiplier that will run the costs at multiples of the base case of 1, 1.5, 2, 2.5, and 3. This will take into account the higher costs of a commercial project in Alaska. Experience from other projects in Alaskan villages suggests that rural Alaska's total project costs will end up being in the 1.5 to 2.5 cost multiplier range.

i) Taxes

Taxes are determined assuming the final value of natural gas at the burner tip and of electricity at the transformer. Tables 5.7 gives specific taxes.

Table 5.7 Taxes

Taxes	Rates
Federal Income Tax	35%
State Income Tax	9.4%
Severance	10%
Royalty	6%
Depreciation	
MACRS	7 years for well costs
MACRS	15 years for utility and gas distribution

5.4 RESULTS

Table 5.8 summarizes the results from the base case economic model runs. Detailed plots for the different economic scenarios are shown in Appendix A.

Table 5.8 Economic Model Results

Base Case Costs (with no cost overruns)	\$/MSCF	\$/kWH
3 year ramp up to dewater		
5% ROI	\$14	14¢
10% ROI	\$24	24¢

15% ROI	\$35	35¢
2 year ramp up to dewater		
5% ROI	\$14	14¢
10% ROI	\$21	21¢
15% ROI	\$31	31¢
1 year ramp up to dewater		
5% ROI	\$13	13¢
10% ROI	\$19	19¢
15% ROI	\$26	26¢

Conclusions

The equivalent total fuel consumption for both electrical and heating needs in the Fort Yukon community has been estimated by this study to be 220 MSCF/D with a projected slow increase in demand for fifteen years. The cost for initial capital and wells is estimated at \$8.8 million with an initial operating and maintenance cost of \$107,000 per year that will increase with inflation. These costs and consumption figures were used in the economic model to estimate fuel prices for a given return on investment (ROI). Based on current energy costs for liquid fuels (\$29/MMBTU), there is the potential for significant savings to the consumer converting this alternate energy source. The final price for electricity generated from CBM gas will be between 35¢ and 50¢ per kWh assuming a 10% ROI and a three year start up. This price is comparable, but not competitive with the price of electricity (45 cents/kWh) generated using diesel, based on a diesel price of \$4 per gallon at the time of this analysis. However, power generation from CBM is likely to be more environmentally friendly than using diesel.

References

Ferguson, J.C. and Ogbe, D.O.: “Fuel gas utilization and economic study: Application to Fort Yukon, Alaska”, Final Report, October 2003.

City of Fort Yukon: Comprehensive Plan: Report from City Hall, 1996

Cuthbert, Don (2003): Personal Communication, July 2003

Hall, Tim (2003): Personal Communication, July 2003

Hirschberg, Gary (2003): Personal Communication, July 2003

Luper, Deborah (2003): Personal Communication, July 2003

RSA (October,1996): Project Analysis Report for the GZ Utilities Ft. Yukon Power Plant

RSA (May, 2003): Project Analysis Report for the GZ Utilities Ft. Yukon Power Plant

Tanigawa, John (2003): Personal Communication, July 2003

Titus, Dave (2003): Personal Communication, July 2003

CHAPTER 6

USE OF DRILLING WASTE

An unanticipated and positive outcome of the drilling process at Fort Yukon was innovative use of drilling waste as sealant for landfill site. This was neither part of the initial project objectives nor the anticipated tasks. The use of drilling waste as a sealant is described below.

6.1 Beneficial Use of Drilling Waste as a Sealant for Old Landfill Site

Drilling waste, predominately bentonite, that was generated by the project was used as a sealant for an old landfill site southwest of Fort Yukon's airport runway (Figure 6.1). It was determined that surface disposal of the solid waste would not present a threat to the public health, safety, or welfare, or to the environment, but rather would provide a beneficial seal to an old problem that existed in the Fort Yukon area. This opportunity provided for convenient disposal of the product and would help to protect the water table and Yukon River from possible contaminants from the old landfill. The State of Alaska, Div. of Geological & Geophysical Surveys in a July 9, 2004, memorandum from the project team, DGGS, U.S. Geological Survey (USGS), University of Alaska Fairbanks and Bureau of Land Management, to The State of Alaska Department of Environmental Conservation (ADEC), Div. of Environmental Health, requested approval to manage drilling waste to help seal an old landfill site, known as the Old City Garbage Dump, at Fort Yukon near the barge landing site. The location of this site is in the SE $\frac{1}{4}$, SE $\frac{1}{4}$ of Section 12, T20N, R11E Fairbanks Meridian. Fannie Carroll, City Manager of Fort Yukon submitted a letter to ADEC (dated June 27, 2004) requesting this beneficial use of

the drilling mud at the Old City Garbage Dump. The plan for sealing the old Fort Yukon landfill using drilling waste is shown schematically in Figure 6.2.

The drilling waste that was generated by this exploration project consisted of bentonite clay, drill cuttings, water, and cellulose polymer-quick-gel high yield bentonite (used for hole stability, circulation control, clay-shale control); Aqua-gel bentonite (hole stability, circulation control, mud weight); Pac-L powdered cellulose polymer (clay-shale control); EZ mud liquid polymer (clay-shale control); and Pennetrol liquid detergent (to prevent clay balling around drill bit). Art Clark, U.S. Geological Survey in Denver, CO supervised the landfill seal operations. Drilling activities were anticipated to produce 10,000 to 20,000 gallons (1,336-2,673 cubic feet) of drill mud/additives/cuttings that would dehydrate to approximately half its original volume leaving a total of approximately 750-1250 cubic feet of dry product. 1250 cubic feet will then cover a 100' X 50' area to a depth of 3 inches. A vacuum-truck was rented from the City of Fort Yukon to collect the mud and cuttings from the drill site's ADEC-permitted temporary containment pit during drilling operations and driven to the old landfill site. The drilling mud waste was then sprayed through a hose evenly across the old landfill site. The disposal covered up to ½ of the old landfill site, or approximately 100 feet long by 50 feet wide. The wet mud subsequently generated about 15 cubic feet of dry product once dehydrated and provided between 2 to 4 inches of seal. When the bentonite and cuttings dried out, the area was covered with about 2 inches of soil/gravel seal. Figure 6.3 shows a sample photograph of the landfill area after it was successfully sealed with drilling waste.

1993 aerial photograph of Fort Yukon area. Enlargement of area with old landfill site and boxed in red shown below



Topographic map of Fort Yukon area



Figure 6.1 Fort Yukon's old landfill near airport

2004 drilling mud seal plan at old Fort Yukon landfill site for 2004

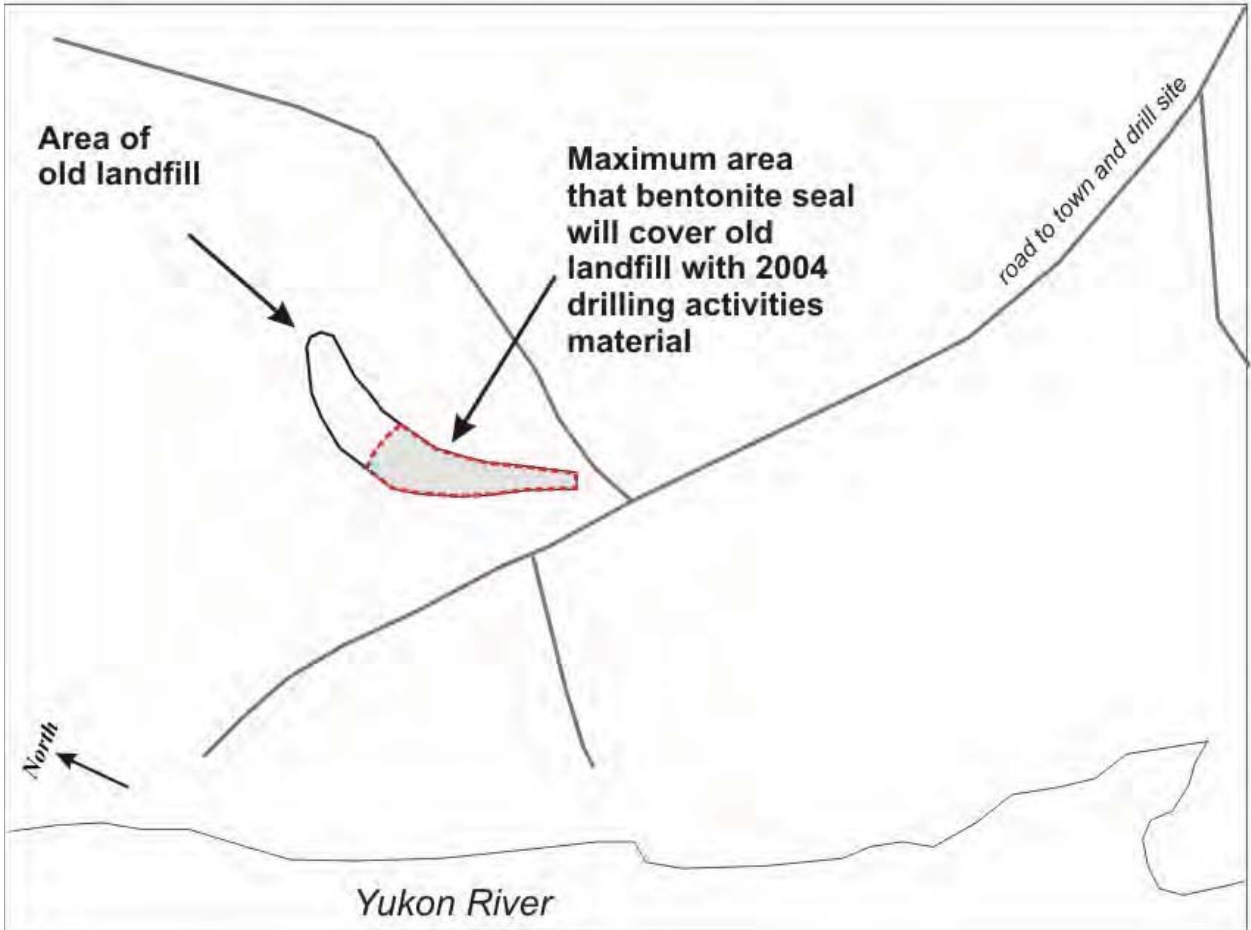


Figure 6.2 Plan for sealing part of old landfill at Fort Yukon



Figure 6.3 Successful use of drilling waste as sealant for landfill

Conclusion

Drilling waste generated from a water-based drilling fluid system, drilling through non-oil bearing zones, can be successfully used as sealant for landfill areas without any significant environmental risks.

CHAPTER 7

CONCLUSIONS AND RECOMMENDATIONS

7.1 CONCLUSIONS

The re-entry well DOI-04-1A at Fort Yukon drilled in 2004 using a lightweight, portable rig cut through two coal zones of tertiary age. Core samples of coal from both zones were recovered and analyzed for geological and petrophysical properties, and methane gas content. Reservoir simulation for gas production rate forecast and economic analysis of power generation from CBM gas at Fort Yukon using actual drilling cost data were performed. The following conclusions are drawn from this study.

1. The project demonstrated that use of lightweight, portable drilling rigs is a viable way for drilling slim holes for CBM production and dewatering in remote locations of Alaska.
2. Production of CBM gas in sufficient quantity to meet the energy needs of Fort Yukon is not feasible because of very low gas content and very low permeability of the coal beds. Even with close well spacing, CBM production rate at Fort Yukon would fall far short of the amount of gas needed.
3. Economic analysis of power generation from CBM at Fort Yukon, using actual drilling cost data, shows that the cost of electricity generated via CBM is comparable, but competitive with the cost of electricity generated traditionally using diesel. This conclusion is based on the prevailing price of diesel at the time of analysis. If the price of diesel goes up significantly, power generation from CBM may become economically attractive. On the other hand, power generation

by using CBM, a clean fuel, always has intangible benefits in the form of reducing environmental damage.

4. Drilling waste generated in a drilling process using water-based drilling fluid system and drilling through non-oil bearing zones can be successfully used as sealant for landfill areas without any significant environmental risks. This is likely to help reduce drilling waste disposal costs in remote areas.

7.2 RECOMMENDATIONS

Additional work should investigate the synergy of combining the GZ Power Utility with the U.S. Air Force Power House to reduce overall relocation and gas conversion costs. RSA Engineering considered some of these options for a diesel plant. More detailed analysis is needed to explore gas-fired generator conversion costs for the existing utilities. In addition, investigations should analyze the potential to utilize waste heat recovery to enhance energy efficiency and reduce heating fuel needs.

Further work must focus on the response of variations in reservoir rock permeability and the drainage area of each well (acreage). Also it would be wise to analyze how produced water can be processed for significant amounts of drinking-quality water. Finally for the Fort Yukon Coal-Bed Methane Economic Model (FY-CBM-EM) to provide even better results, we need additional industry cost estimates which are difficult to obtain because these are proprietary.

The cost for residents and commercial buildings to convert to gas heating systems will vary for each consumer. A future study should be performed to determine the best options available to the primary commercial consumers (i.e., Yukon Flats School District,

Water Supply and Treatment, and other key municipal/tribal government facilities) as well as to the various residential consumers. This will help establish the upper limit of the gas price that the overall project investor(s) can reasonably expect to charge for his product.

If a similar project is done for another Alaskan village, detailed work needs to be done to ascertain design requirements and costs of all the elements of such a project. The largest area of uncertainty is the number of wells and the costs to meet the projected gas supply and demand. Future well gas rates and deliverability will be critical to calculation of the well costs. The associated water rates will also represent a key design and cost factor. The best site for the coal-bed methane wells and processing facilities must be determined. The associated pipeline routing and gas distribution network should be included in a site evaluation. The impact of soil conditions on the pipeline route and on the gas distribution network needs to be investigated to better establish design requirements and project costs.

APPENDIX A

Tables and Figures from Economic Analysis

Appendix A includes fuel demand table, and results from specific economic model runs based on different cost options.

**Table A.1 Fort Yukon Diesel Fuel Demand Projection
and its Equivalent Gas Requirement**

Year	Total Gallons Of Diesel Fuel	Gas Equivalent (MSCF/D)
2004	527,337	209
2005	534,039	211
2006	541,038	214
2007	548,093	217
2008	555,205	220
2009	562,375	223
2010	569,602	225
2011	576,888	228
2012	584,232	231
2013	591,635	234
2014	599,098	237
2015	606,620	240
2016	614,203	243
2017	621,846	246
2018	629,551	249
2019	637,317	252
2020	645,145	255

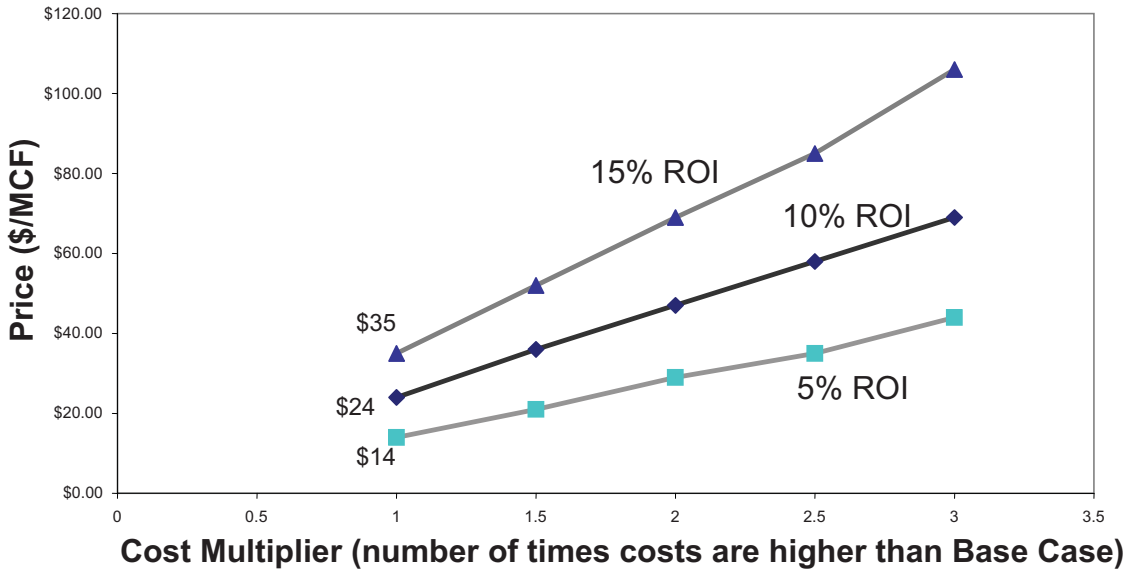


**Figure A.1 Price to cost Multiplier Relationship with no Plant Relocation Cost
(Start in 3rd year-price/MCF)**

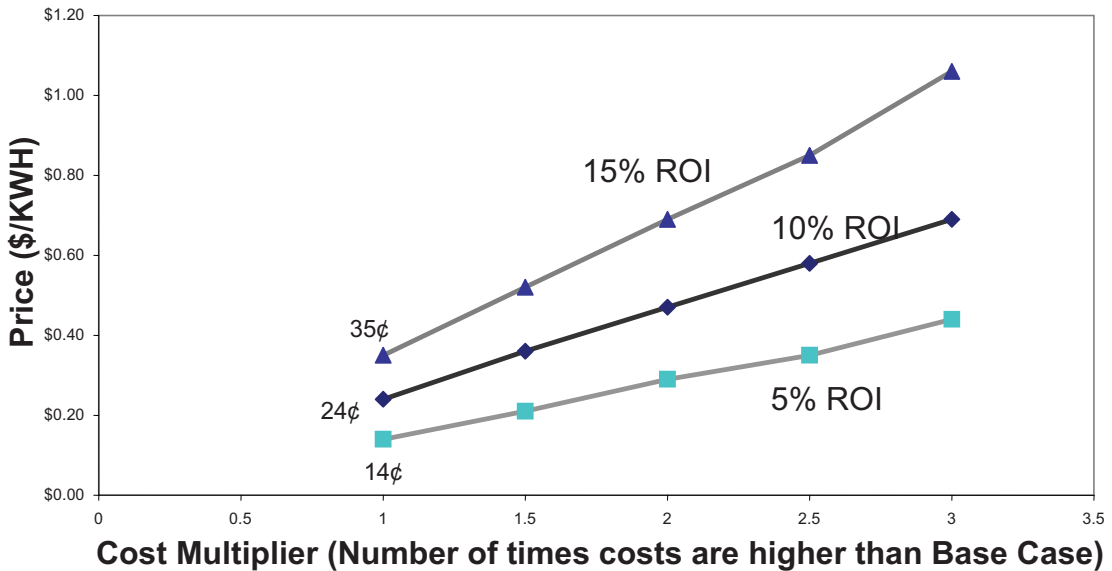


**Figure A.2 Price to Cost Multiplier Relationship with No Plant Relocation Costs
(Start in 3rd Year-price/kWH)**

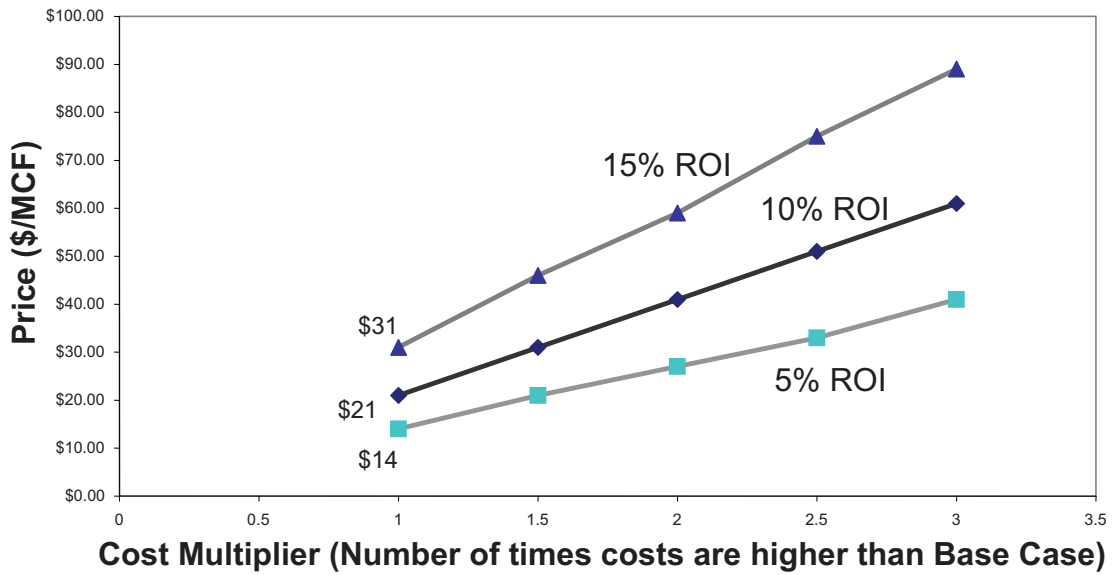


**Figure A.3 Price to Cost Multiplier Relationship with No Plant Relocation
Costs(Start in 2nd Year-Price/MCF)**

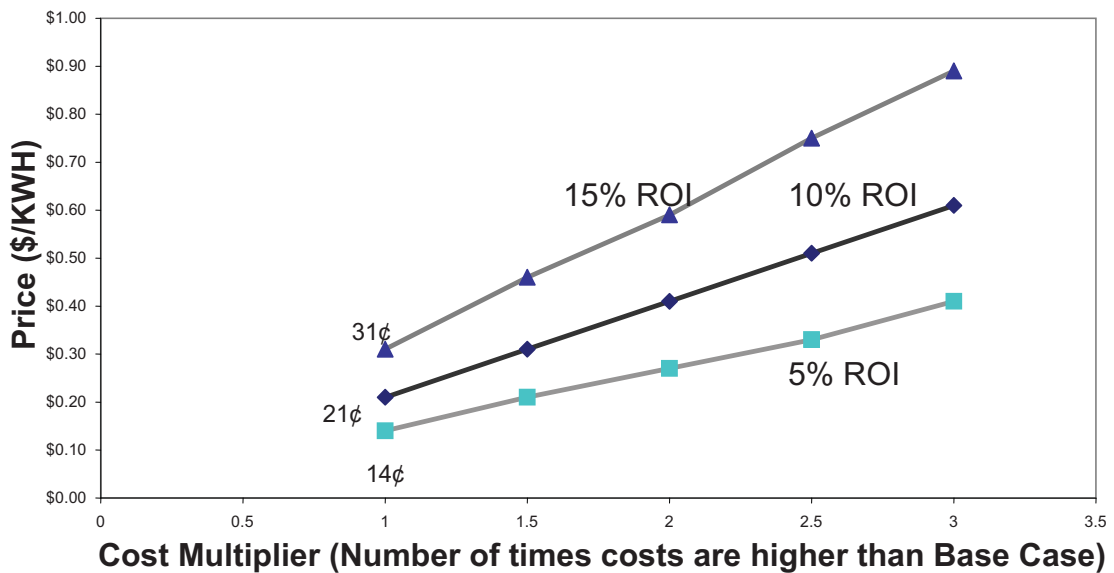


**Figure A.4 Price to Cost Multiplier Relationship with No Plant Relocation
Costs(Start In 2nd Year-Price/kWH)**

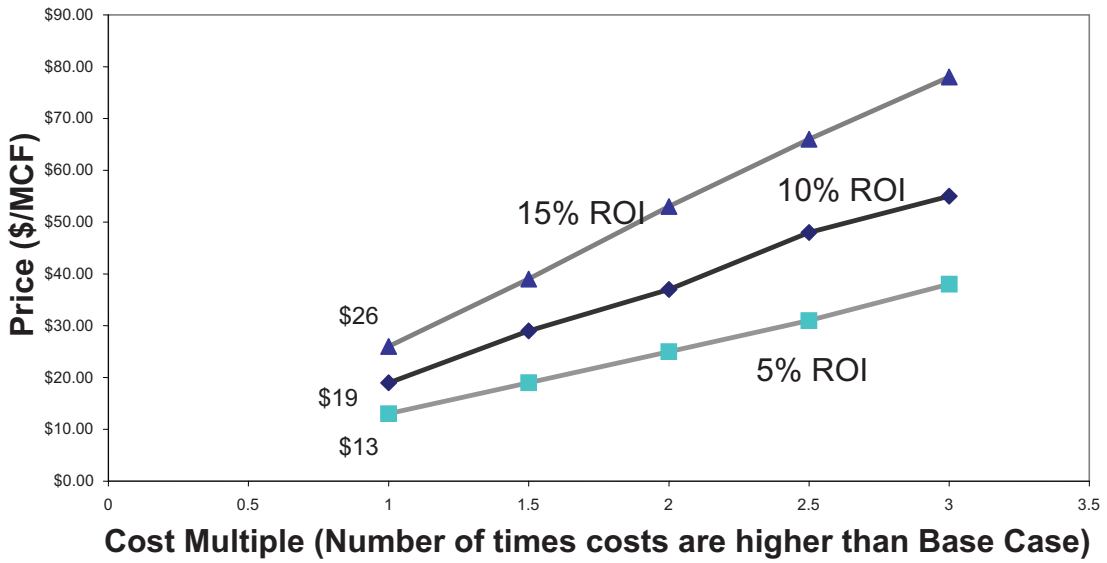


Figure A.5 Price to Cost multiplier relationship with no Plant Relocation Costs(Start In 1st Year-Price/MCF)

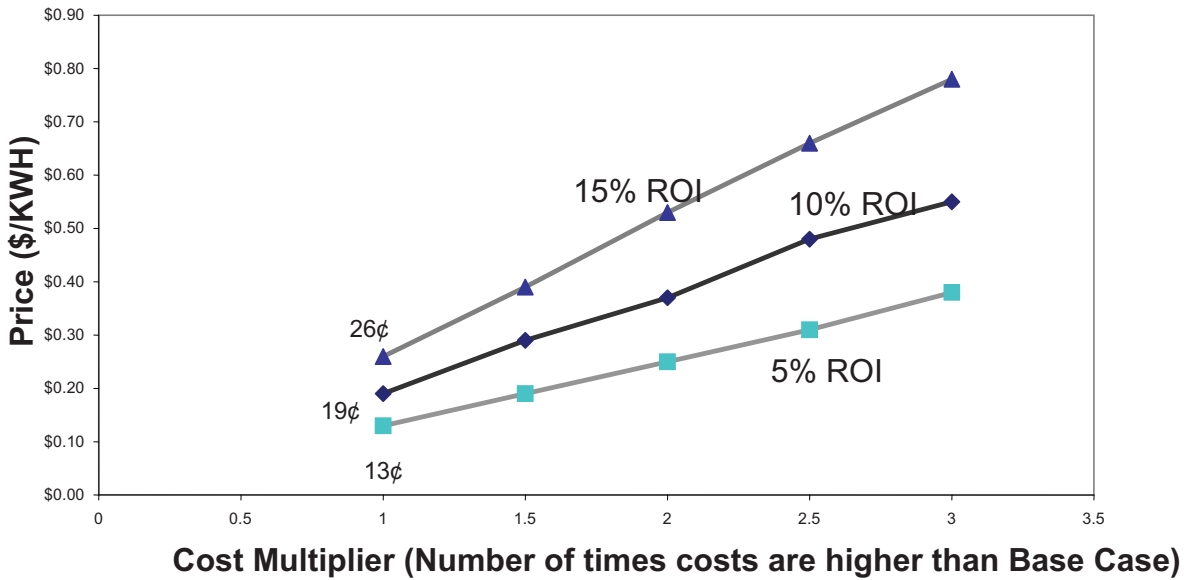


Figure A.6 Price to Cost Multiplier Relationship with No plant Relocation Costs (Start In 1st Year-Price/kWH)

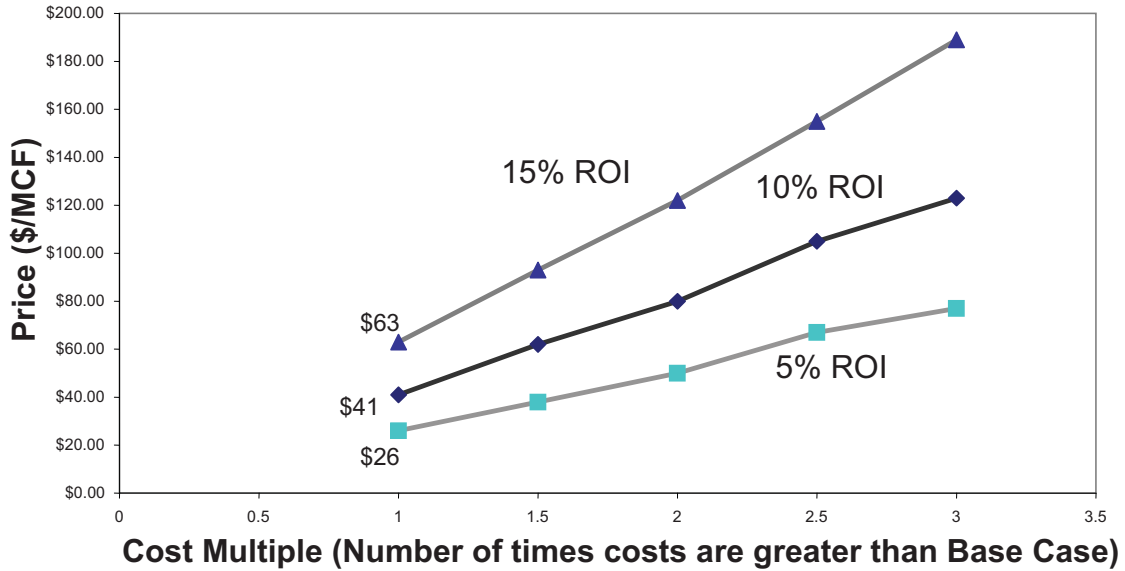


Figure A.7 Price to Cost Multiplier Relationship with Plant Relocation Costs (Start in 3rd Year-Price/MCF)

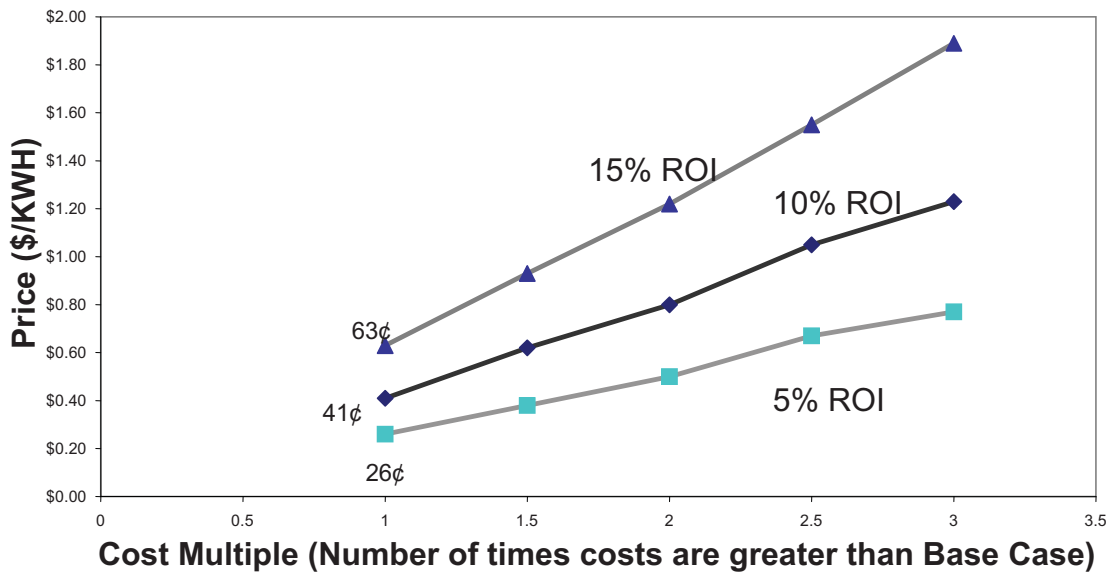


Figure A.8 Price to Cost Multiplier Relationship with Plant Relocation Costs (Start in 3rd Year-Price/kWH)

**Stratigraphy and Depositional Setting of the Nonmarine Tertiary
(Miocene) Sedimentary Succession in the 2004 Lower Drill Core,
Fort Yukon, Alaska**

Final Report

for

**Arctic Energy Office
Fairbanks, Alaska
National Energy Technology Lab
US Department of Energy**

Through

**Arctic Energy Technology Development Laboratory
University of Alaska Fairbanks
Fairbanks, Alaska 99775**

For grant DE-FC26-01NT41248

Prepared by

James G. Clough¹, Arthur C. Banet, Jr.², Jesse G. White¹, and Rocky R. Reifentstahl¹

¹Alaska Division of Geological & Geophysical Surveys, 3354 College Road, Fairbanks, AK
99709-3707

²Bureau of Land Management-Alaska, Energy and Minerals Division, 3801 Centerpoint Drive,
Anchorage, Alaska 99503

Stratigraphy and Depositional Setting of the Nonmarine Tertiary (Miocene) Sedimentary Succession in the 2004 Lower Drill Core, Fort Yukon, Alaska

James G. Clough¹, Arthur C. Banet, Jr.², Jesse G. White¹, and Rocky R. Reifentstuhl¹

¹Alaska Division of Geological & Geophysical Surveys, 3354 College Road,
Fairbanks, AK 99709-3707

²Bureau of Land Management-Alaska, Energy and Minerals Division,
3801 Centerpoint Drive, Anchorage, Alaska 99503

ABSTRACT

Tertiary non-marine sedimentary rocks beneath Fort Yukon, Alaska were drilled and cored in 2004 as part of a joint effort between the Alaska Division of Geological & Geophysical Surveys, U.S. Geological Survey, U.S. Bureau of Land Management-Alaska, University of Alaska Fairbanks, and U.S. Department of Energy-Arctic Energy Office to evaluate the shallow gas potential of lignite seams beneath Fort Yukon. This effort reentered a 1994 U.S. Geological Survey drill hole that was originally drilled and cored to 1,283 feet to study Tertiary paleoclimates. The 2004 drilling operations drilled to a total depth of 2,287 feet and recovered about 650 feet of core from core drilling, and cuttings were collected from about 330 feet of rotary drilling. We studied the lower Fort Yukon 2004 core in order to describe its stratigraphy and interpret its depositional settings.

The 1994 and 2004 drilling combined encountered two major coal zones, an upper coal zone about 58 feet thick (from 1,257 to 1,315 feet) and a lower 45-ft-thick coal zone (from 1,875 to 1,920 feet). The upper coal zone is middle Miocene in age (16-18 Ma) and the age of the lower coal zone is likely Miocene in age as well (T. Ager, USGS, personal communication). Lithologies within the Fort Yukon core are organized into eight general lithofacies that are: coal (lignite), carbonaceous shale, claystone, silty claystone, siltstone, silty sandstone, sandstone, and pebble sand. Grain types within the silty claystone to sandstone include polycrystalline and monocrystalline quartz, chert, white mica, lithic clasts, and traces of plagioclase. Beginning at ~2,170 feet are pebbly sand interbeds of unknown thickness that coincide with a prominent reflector recognized in a 2001 shallow seismic study of Fort Yukon.

Generally, the lower Fort Yukon core consists of stacked sequences of sandstone, siltstone and claystone, ±carbonaceous shale and/or coal. We interpret these sediments to represent a meandering river to lacustrine and sometimes poorly drained swamp system. The fluvial settings fine upwards from sand- to silt-dominated facies into eventual lake and sometimes a poorly-drained swamp environment above, represented by carbonaceous shale or lignite. Parallel laminations in some claystone horizons suggest varved lake deposits representing seasonal variations in sedimentation.

INTRODUCTION

Drill core collected during 2004 operations at Fort Yukon, Alaska (figs. 1 and 2) to test the methane content of Tertiary-age lignite was studied for general lithology, characteristics and depositional settings. Fort Yukon, Alaska was determined to be a priority site for testing the potential for shallow coalbed gas as a rural energy source based on village demographics, geologic setting, and the presence of potentially gassy coal beneath the community (Tyler and others, 2000). The drilling operations and coal desorption are described in Clark (in press), Barker and others (in press), along with an aquifer test assessment (Weeks and Clark, in press). The 2004 project reentered a 1994 U.S. Geological Survey (USGS) climate study drill hole located at the U.S. Air Force Fort Yukon Long Ranger Radar Site (LRRS) that was initially drilled to a depth of 1283 feet. The drill hole, now named DOI-1a-04 well (API no. 50-091-20001) is located at latitude 66.55949° N and longitude 145.20616° W on the southeast end of the community site (fig. 1). In 2001, high-resolution shallow seismic reflection data was acquired to determine the thickness of the coal seam encountered in the 1994 coring operations and its lateral extent (Miller and others, 2002). Hereafter we refer to the 2004 core study as the “lower Fort Yukon core”.

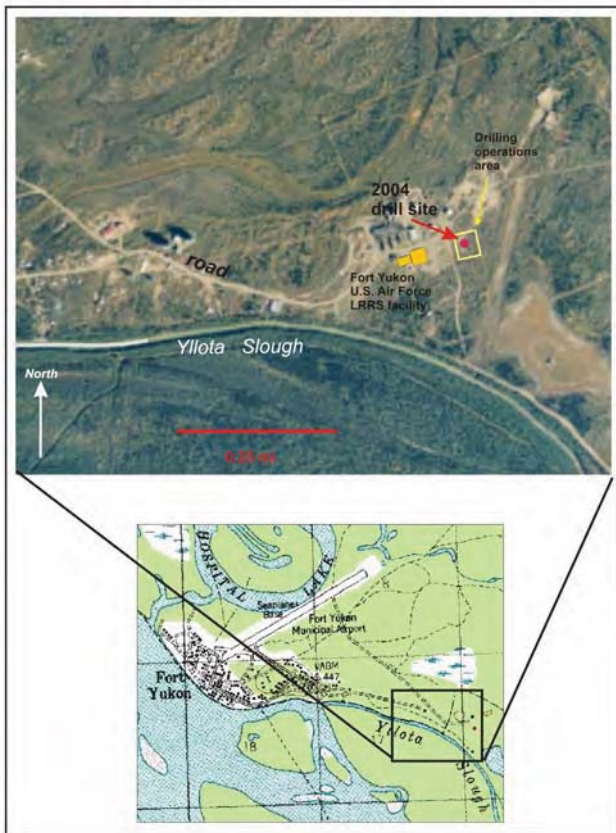


Figure 1. Location of 2004 slim-hole drill coring operations area (yellow box) and drill hole location (shown as red circle) to the southeast of the community of Fort Yukon.



Figure 2. Photograph of lower Fort Yukon core removed from core barrel.

GEOLOGIC SETTING

The community of Fort Yukon, is situated approximately in the northeast center of the Yukon Flats basin (fig. 3), an alluvial and marshy, lake-dotted lowland of more than 13,600 mi², that is confined by the arcuate Tintina-Kaltag fault system to the south, to the west by the Kokrine-Hodzana highlands, to the east by the Kandik thrust belt, and the southern foothills of the Brooks Range to the north. On the basis of gravity modeling, it is suspected that the Yukon Flats basin may have almost 2 mi of Cenozoic fill, with portions along the Yukon River as thick as 2.8 mi (Hite and Nagayama, 1980) (30-50 mgal gravity lows, fig. 3). The metamorphic basement in the Yukon Flats basin consists of two main terranes, the Tozitna and Porcupine terranes. The Porcupine terrane contains Precambrian metamorphic rocks and Cambrian-Devonian to Pennsylvanian-Permian structurally complex marine and non-marine sedimentary strata (Kirchner, 1994).

Structurally, the Yukon Flats basin has been interpreted as an extensional graben complex indicated by topography representing normal faults and divergent magnetic patterns are observed beneath the Tertiary fill (Kirchner, 1994). Till and others (2004) cite geophysical evidence of major crustal-scale splays of the Tintina system that cut through the entire thickness of the crust. Using new apatite fission track data, they have documented uplift events that correlate with similar eastern Brooks Range events that suggest a continental-scale linkage of crustal deformation during the Tertiary (Till and others, 2004).

Three cycles of Tertiary sediments of nonmarine affinity are exposed around the perimeter of the Yukon Flats and within the Tintina trench. Tertiary coal outcrops at several localities (fig. 3) including the Mudbank on the Hodzana River (See fig. 4), Drew Mine near Rampart, Schieffelin Creek, and Coal Creek. Reifenstuhl (2006) reports a few hundred feet of Eocene to Oligocene fluvial sandstone, pebbly sandstone with lesser conglomerate, and minor coal are exposed at Schieffelin Creek. The first sedimentary cycle is represented by latest Cretaceous-early Tertiary strongly folded conglomerate, sandstone, shale, and minor coals in the Tintina trench (Brabb and Churkin, 1969). In mid-Tertiary time, Miocene coal bearing formations exposed at Coal and Mudbank Creeks, outcrops in the Tintina trench, and northeast of Fort Yukon are evident typically consisting of conglomerate, sandstone, coal bearing siltstone-shale, and fine grained lacustrine sediments. The final Tertiary sedimentary cycle is composed of sand and gravel deposits that may extend into the Quaternary (Brosgé and others, 1973).

Farmer and others (2003) suggests that the Paleocene-early Eocene strata deposited in the southwest perimeter of the Yukon Flats basin, notably near Rampart, may be the result of extension related to early Tertiary strike-slip displacement on the Tintina fault. During this stage of basin development, regional tectonic subsidence led to the development of poorly organized, internally drained watersheds with intermittent ponding of water within the basin (Farmer and others, 2003).

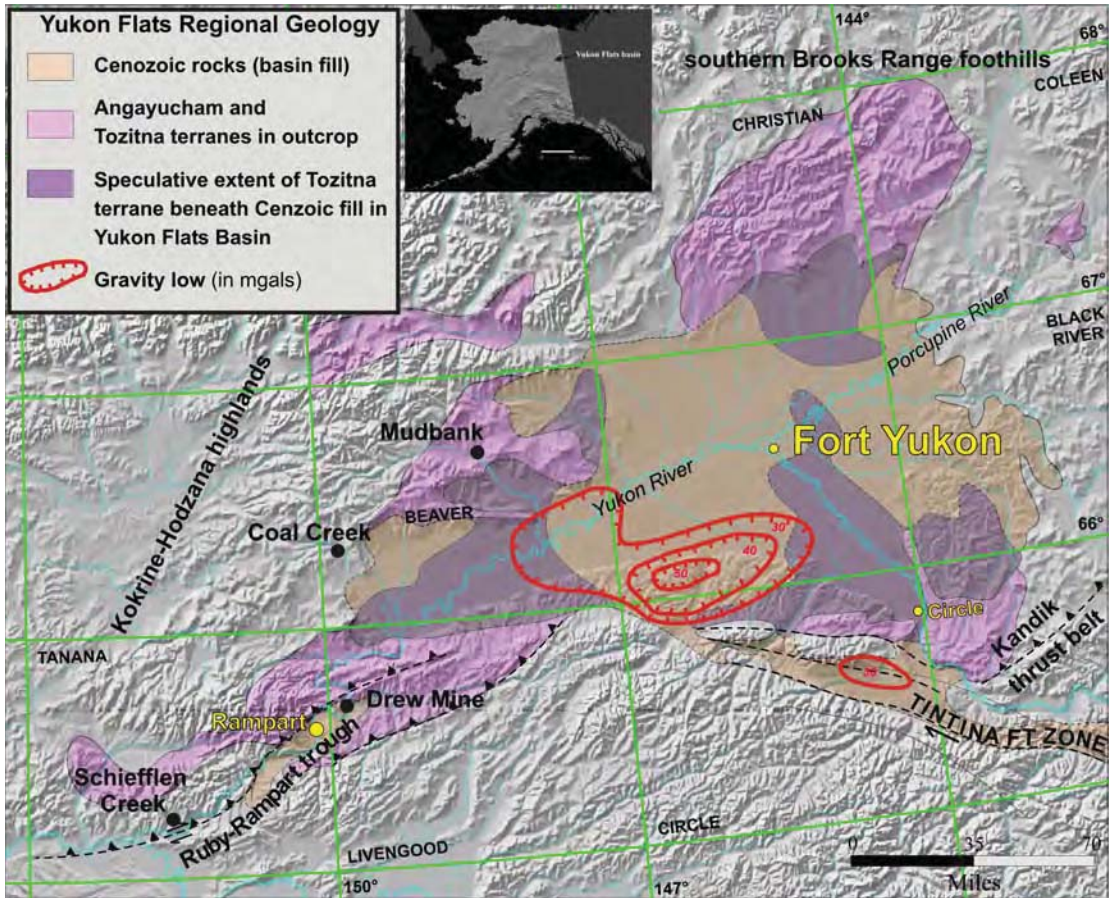


Figure 3. Regional geology of the Yukon Flats basin. Green lines delineate 1:250,000-scale quadrangles. Geology modified from Kirchner (1994) and Troutman and Stanley (2003).

Thickness of the Tertiary section beneath Fort Yukon is likely on the order of 6000-7000 feet based on a recent gravity inversion (J.D. Phillips, U.S. Geological Survey, unpublished data). The lithology and depth of basement rocks beneath Fort Yukon are uncertain. Aeromagnetic and gravity data, together with regional geologic relationships, suggest that the basement at Fort Yukon consists of Devonian to Jurassic oceanic rocks related to the Tozitna and Angayucham terranes (Saltus and others, 2004). On the basis of gravity modeling, it is suspected that the Yukon Flats basin may have almost 2 mi of Cenozoic fill, with portions along the Yukon River as thick as 2.8 mi (Hite and Nagayama, 1980).



Figure 4. Photograph of Tertiary outcrop containing thin lignite seams at the “Mudbank” on the Hodzana River, a tributary to the Yukon River. Approximately 80 air miles from Fort Yukon.

CORE DESCRIPTION PROCEDURE

Continuous 2.4 inch diameter core was collected from 1283 to 1835 feet during drilling operations. Rotary drilling only was conducted from 1835 to 1900 feet where a deeper, significant lignite was encountered and the rig returned to continuous coring from 1900 to 1965 feet. Rotary drilling operations resumed from 1965 to the final depth of 2287 feet. For the non-core intervals, cuttings that were collected during drilling operations were utilized for this study. Art Clark, USGS-Denver, provided preliminary interpretations of the gamma ray log which conveyed additional information on the lithology of the non-cored intervals. The core and cuttings were stored in 10-foot cardboard core boxes (fig. 5) and subsequently shipped to Anchorage, Alaska.

The approximately 650 feet of core (2.4 inch diameter) collected from the 2004 drilling operations was processed and described in detail during May and June, 2005 at the USGS storage facility in Anchorage. Processing of the core included removal of residual drilling mud where necessary to show representative sedimentary features, lithologic mineralogy and grain size variations. Detailed descriptions of the core lithologies were recorded, starting from the base to the top of the core. In addition to detailed lithologic descriptions, the core was photographed (under sunlight) at core box-, sedimentary contact- and macro-scales to illustrate the various depositional environments. Representative samples of the pertinent lithologies were collected for thin section study and photomicrographs. The foot-by-foot descriptions and subsequent thin section descriptions are provided in Appendix A. Lithologies, brief core descriptions, interpreted depositional settings, and relevant thin section photographs are in figures 7 to 18. Future core studies may include porosity and permeability measurements, palynological, and geochemical analyses.

Figure 5. Composite photograph of lower Fort Yukon core boxes with drill core and cuttings from 2004 drilling operations at Fort Yukon, Alaska.



Figure 6. Generalized 2004 lower Fort Yukon core (left) and Key to Lithologic Columns (right) shown in figures 7 to 16.

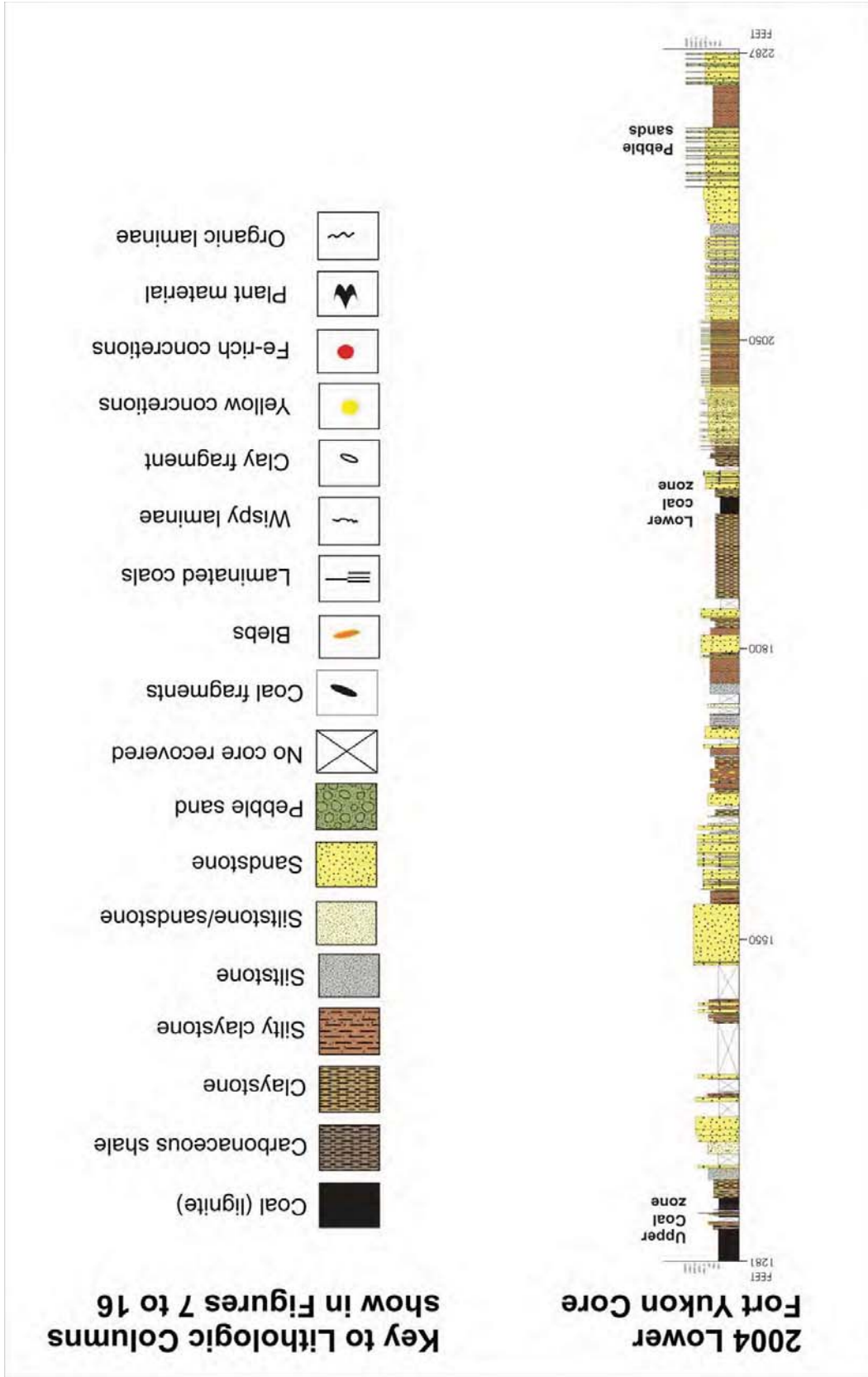


Figure 7. Graphic representation of lower Fort Yukon core and depositional settings for fining-upward cycle A, 2225 to 2287 feet below surface. See Fig. 6 for lithologic legend.

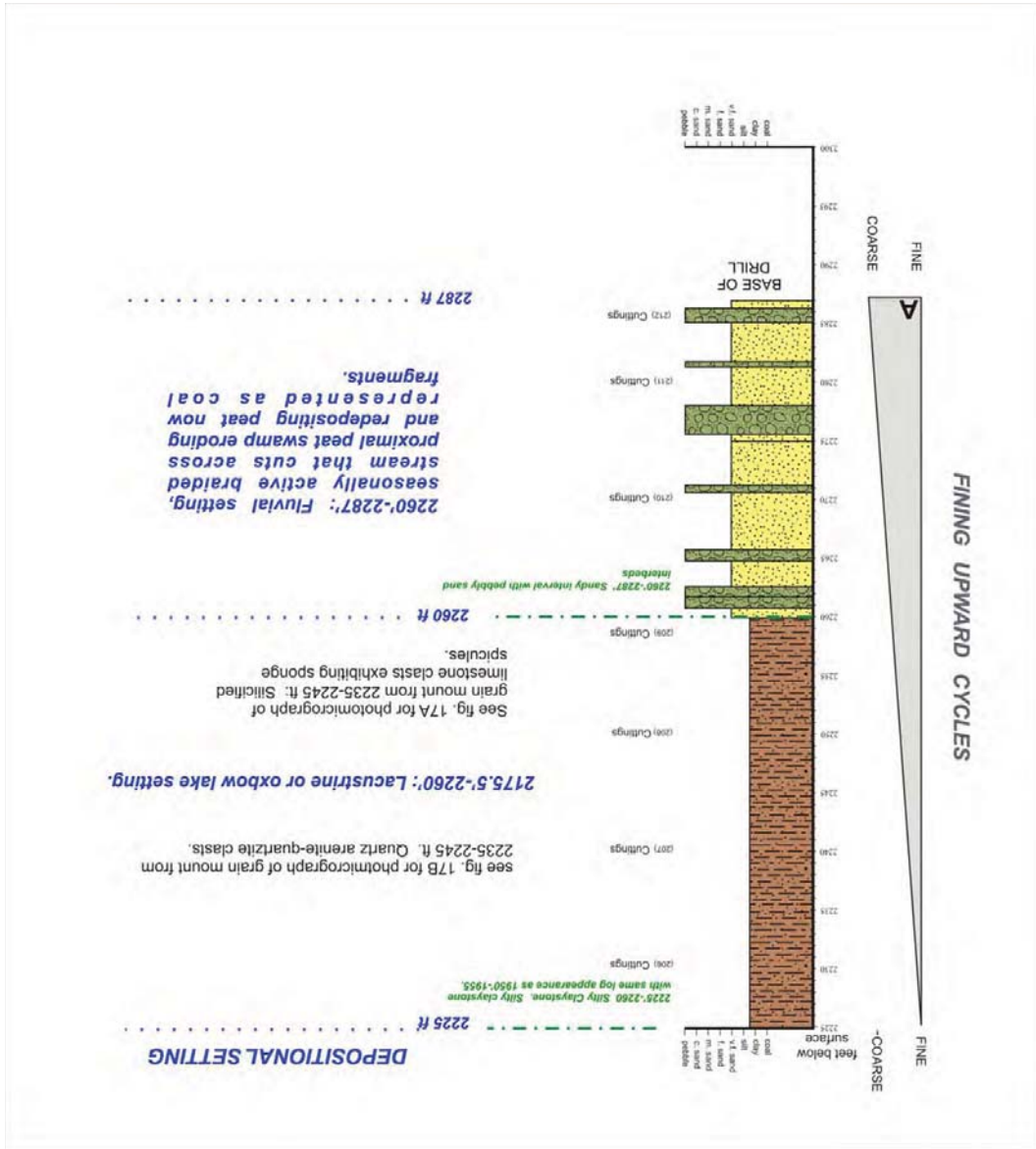


Figure 8. Graphic representation of lower Fort Yukon core and depositional settings for fining-upward cycle B, 2135 to 2225 feet below surface. See Fig. 6 for lithologic legend.

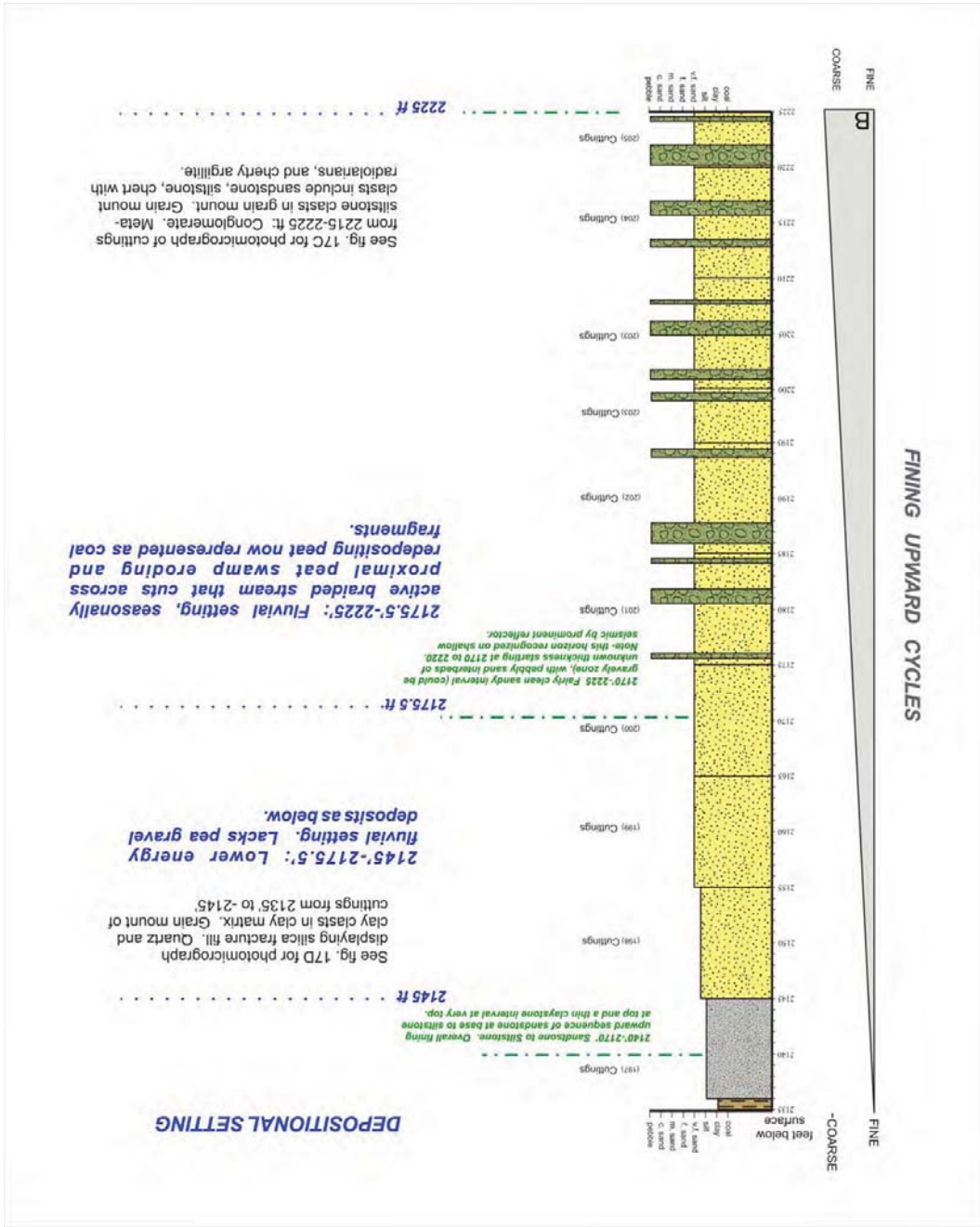


Figure 9. Graphic representation of lower Fort Yukon core and depositional settings for fining-upward cycle C, 2010 to 2135 feet below surface. See Fig. 6 for lithologic legend.

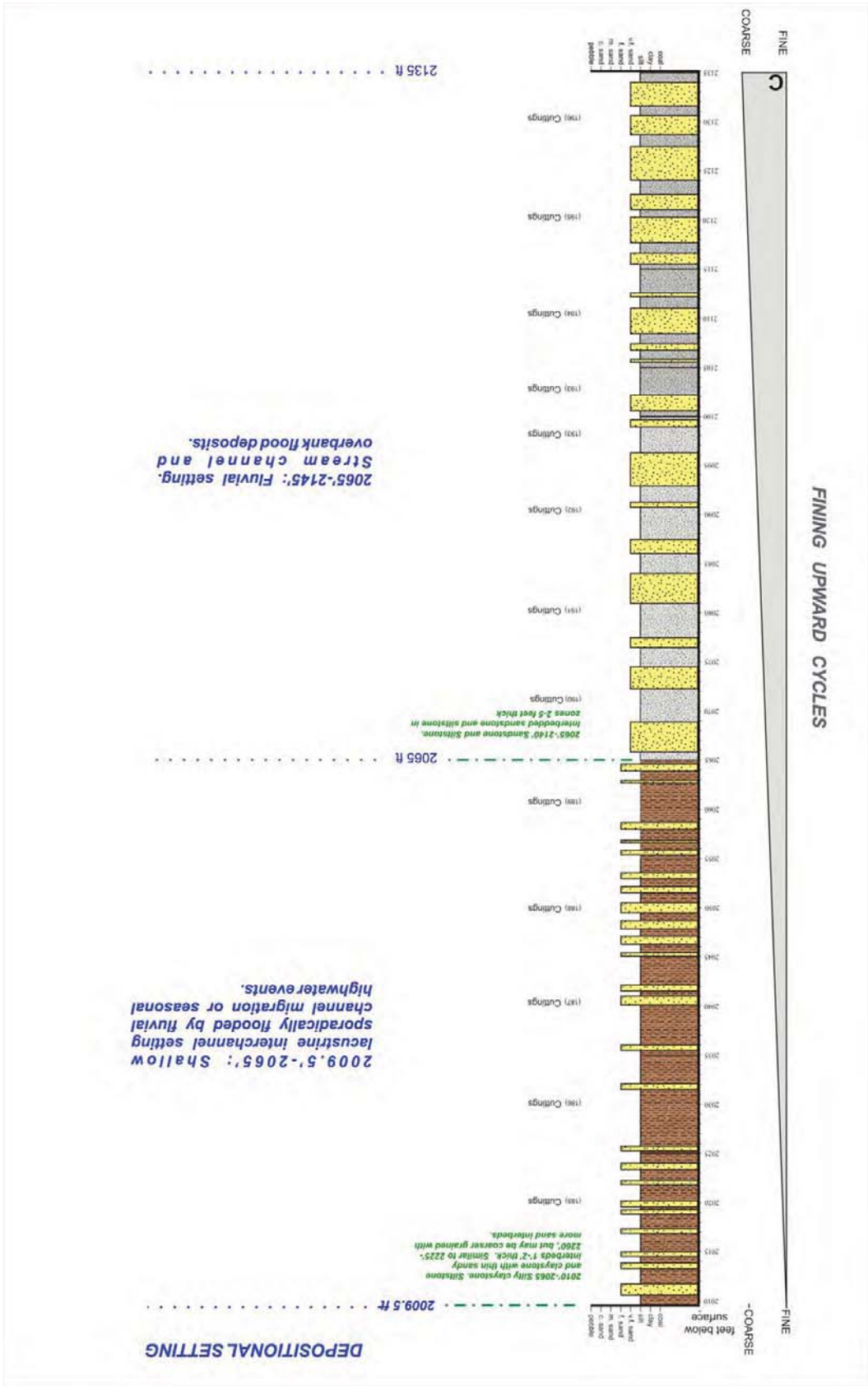
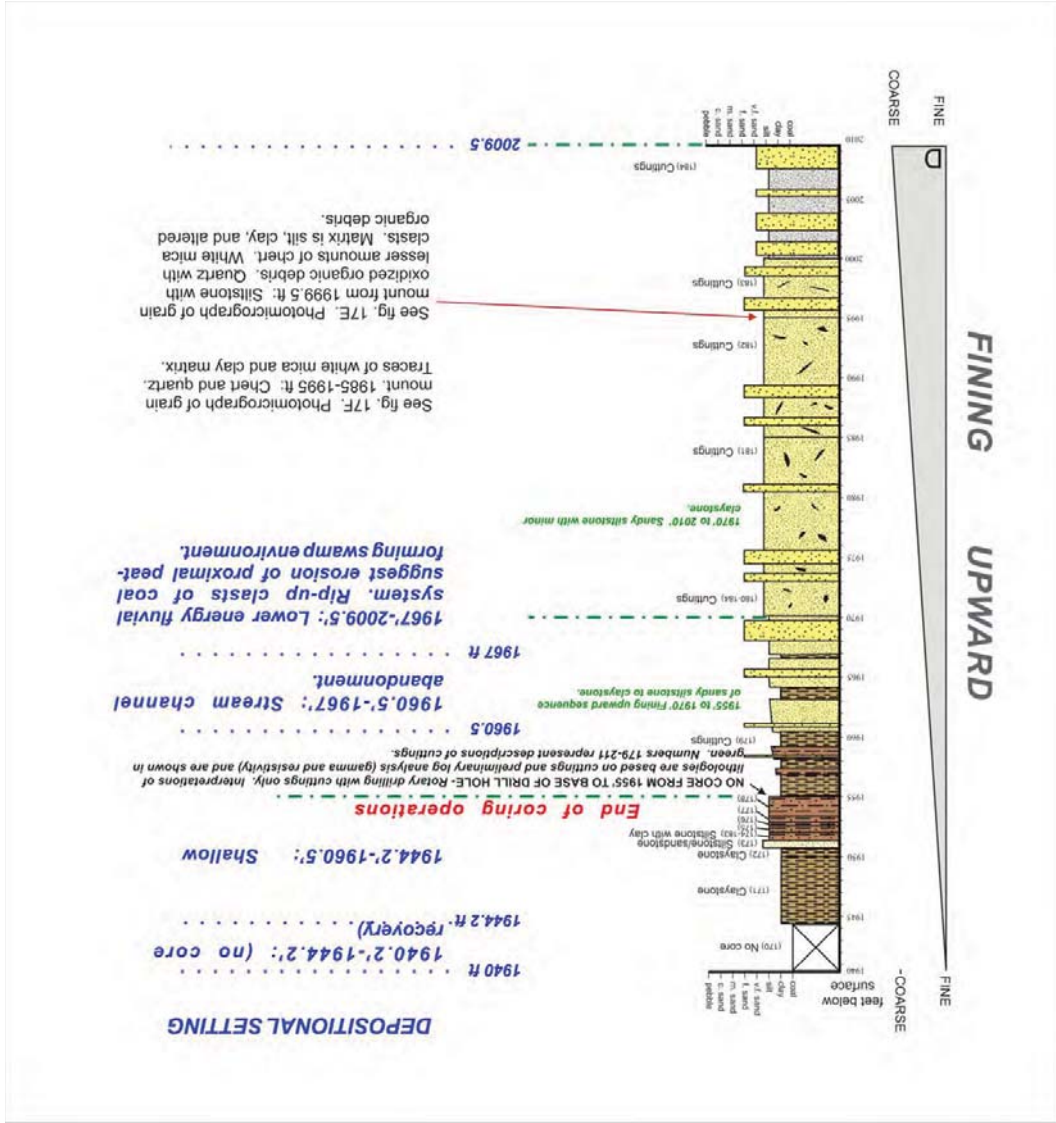


Figure 10. Graphic representation of lower Fort Yukon core and depositional settings for fining-upward cycle D, 1940 to 2010 feet below surface. See fig. 6 for lithologic legend.



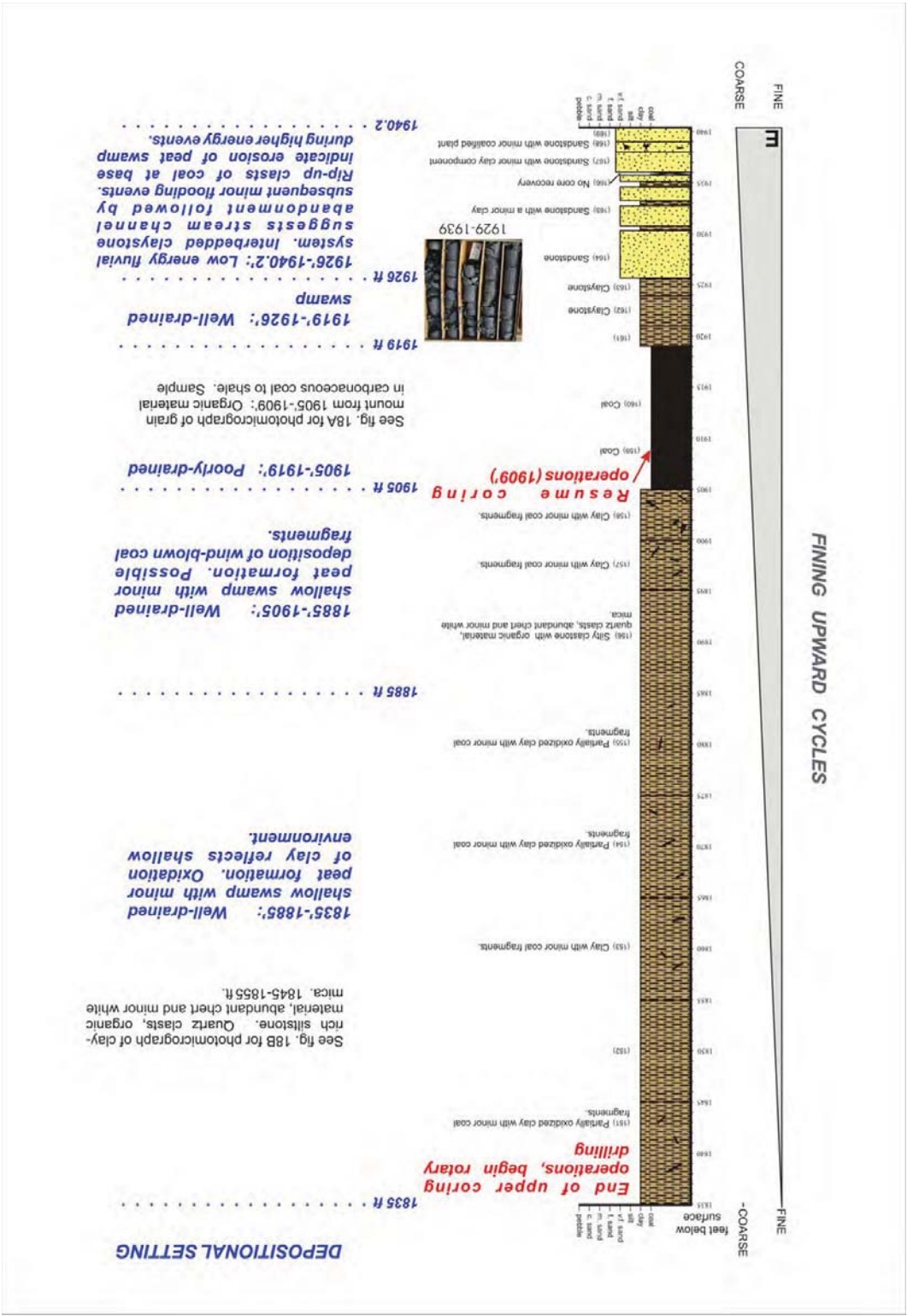


Figure 1. Graphic representation of lower Fort Yukon core and depositional settings for fining-upward cycle E, 1835 to 1940 feet below surface. See Fig. 6 for lithologic legend.

Figure 12. Graphic representation of lower Fort Yukon core and depositional settings for fining-upward cycles F, G and H, 1730 to 1835 feet below surface. See fig. 6 for lithologic legend.

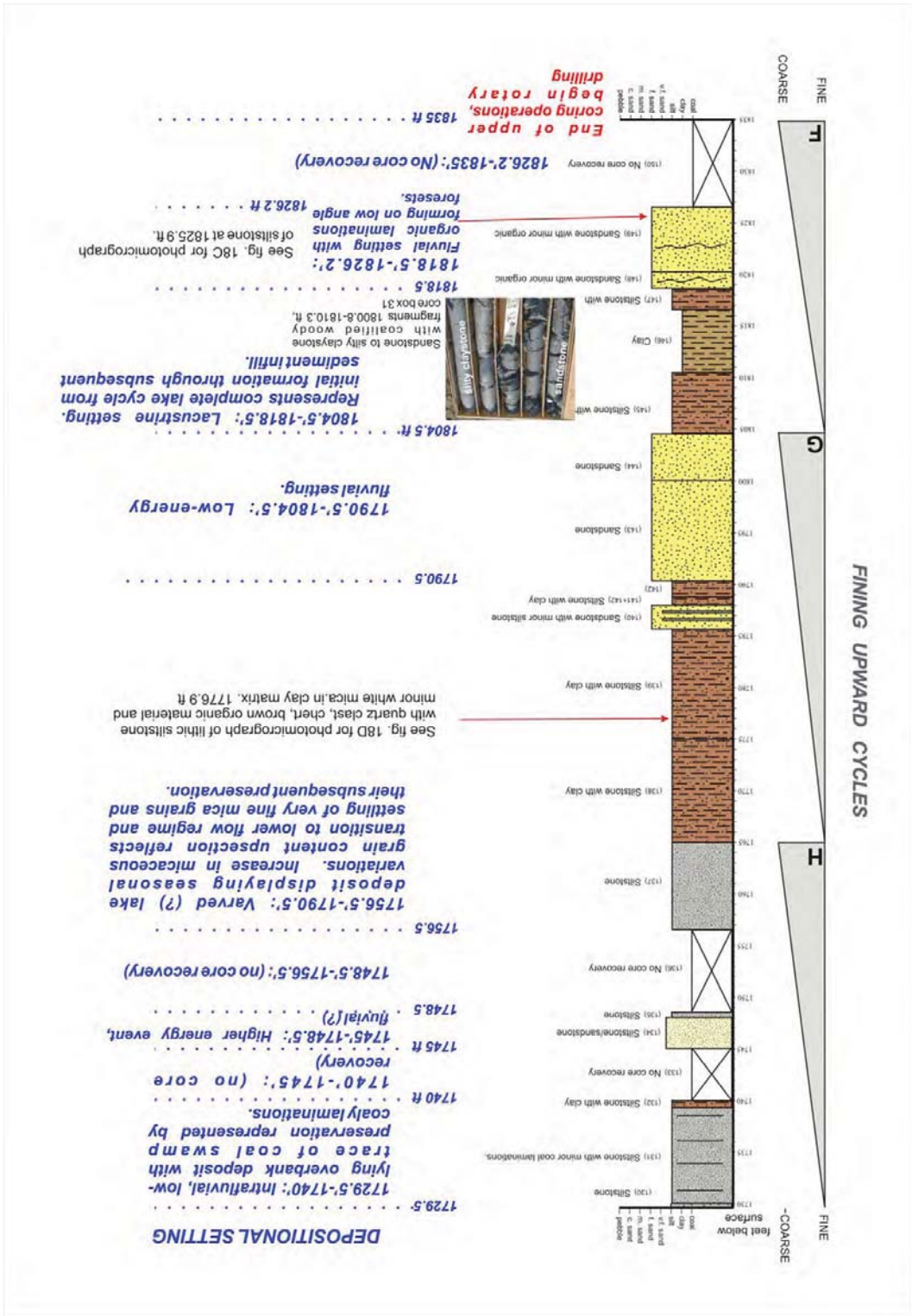


Figure 14. Graphic representation of lower Fort Yukon core and depositional settings for fining-upward cycles L and M, 1506 to 1601 feet below surface. See Fig. 6 for lithologic legend.

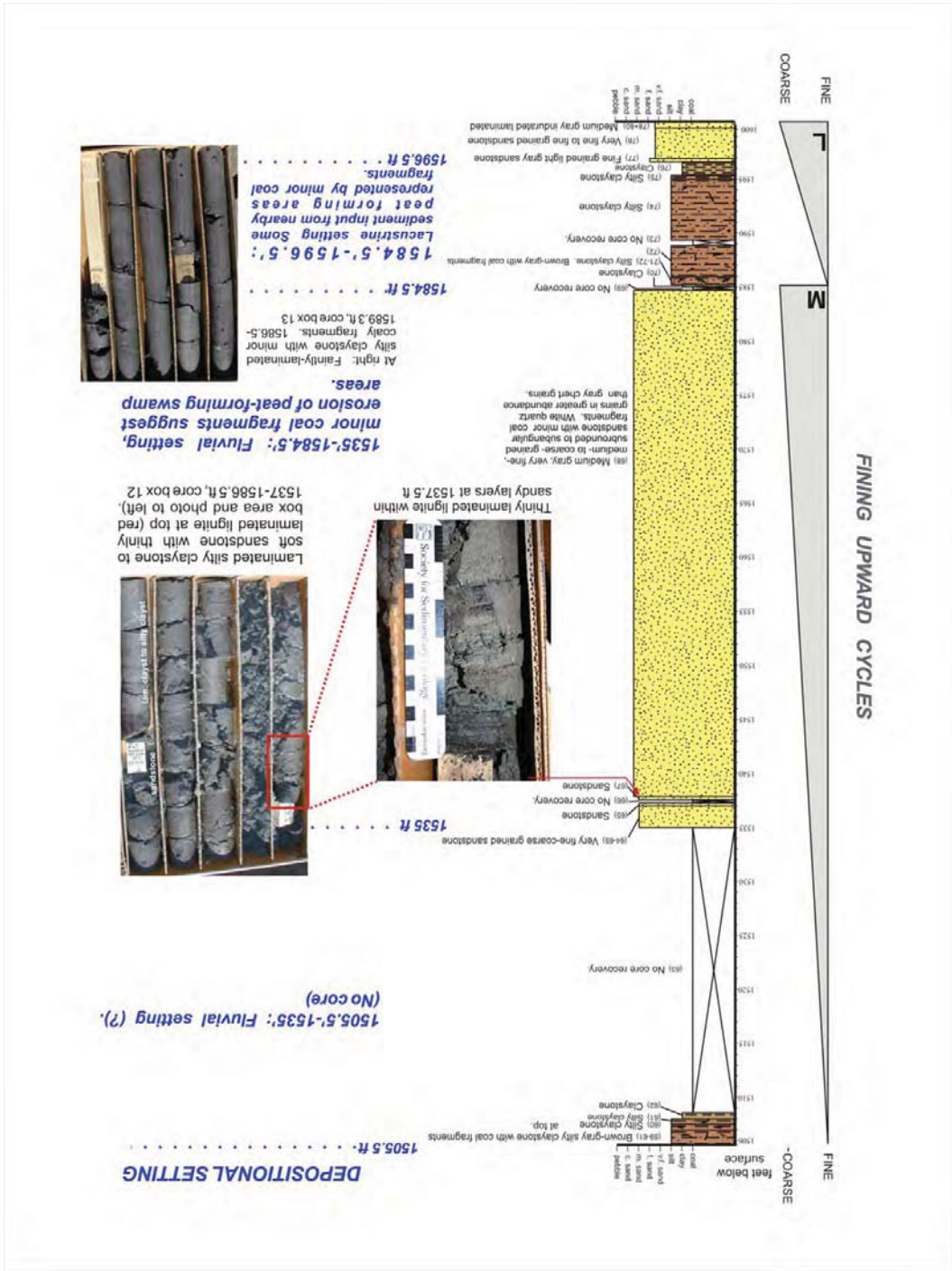
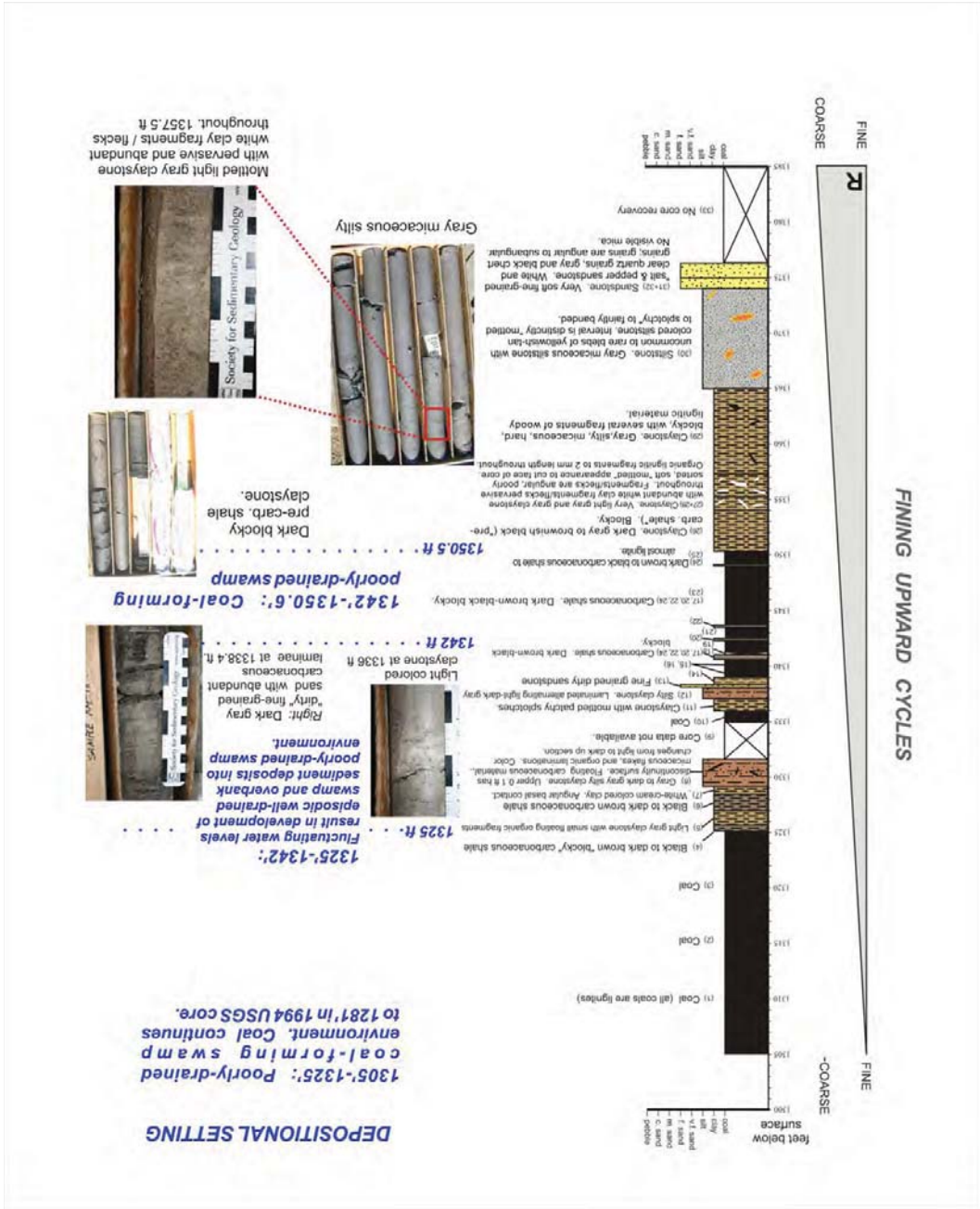


Figure 16. Graphic representation of lower Fort Yukon core and depositional settings for fining-upward cycle R, 1305 to 1385 feet below surface. See Fig. 6 for lithologic legend.



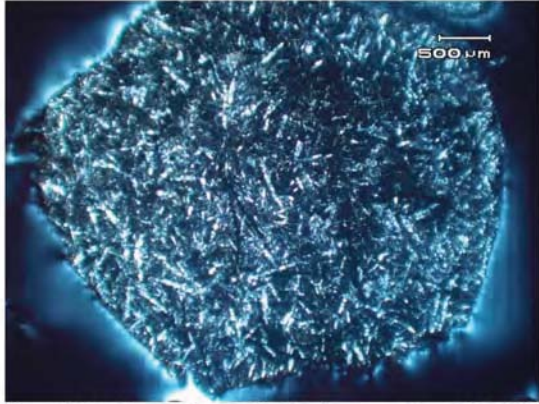


Figure 17A. Photomicrograph of grain mount from 2235-2245 ft:

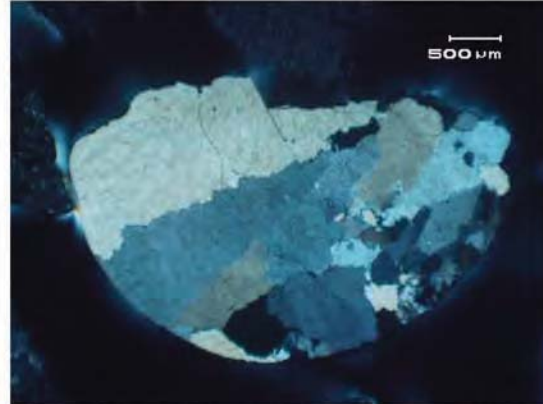


Figure 17B. Photomicrograph of grain mount from 2235-2245 ft: Quartz arenite-quartzite clasts.

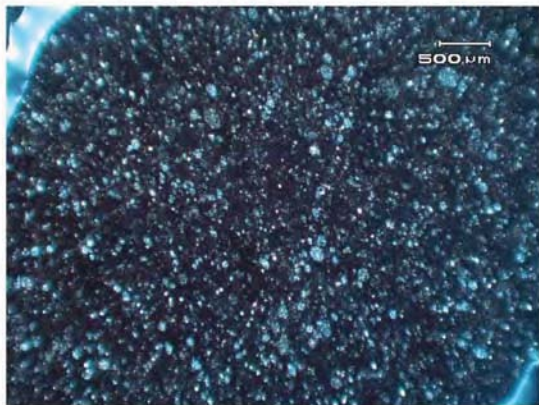


Figure 17C. Photomicrograph of cuttings from 2215-2225 ft: Conglomerate. Meta-siltstone clasts in grain mount. Grain mount clasts include sandstone, siltstone, chert with radiolarians, and cherty argillite.

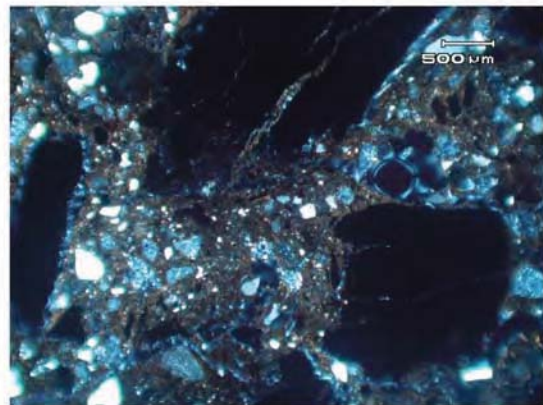


Figure 17D. Photomicrograph of grain mount from cuttings from 2135-2145: Silica fracture fill. Quartz and clay clasts. Clay matrix.

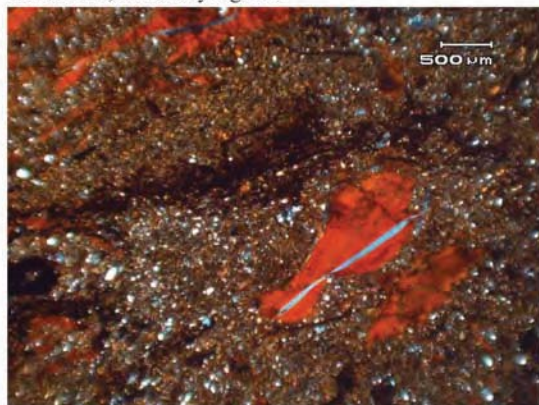


Figure 17E. Photomicrograph of grain mount from 1999.5 ft: Siltstone with oxidized organic debris. Quartz with lesser amounts of chert. White mica clasts. Matrix is silt, clay, and altered organic debris.

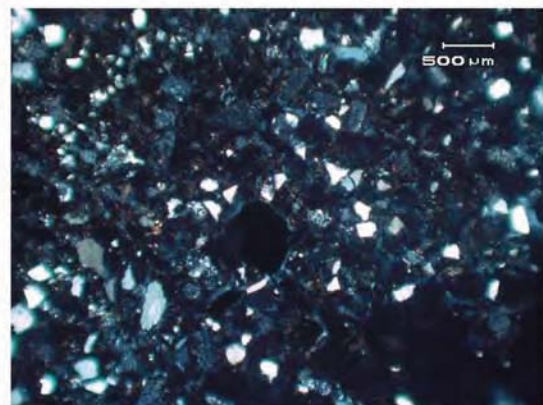


Figure 17F. Photomicrograph of grain mount. 1985-1995 ft: Chert and quartz. Traces of white mica and clay matrix.

Figure 17A-F. Photomicrographs of grain mounts from lower Fort Yukon core. See figures 7, 8, and 10 for stratigraphic position in core.

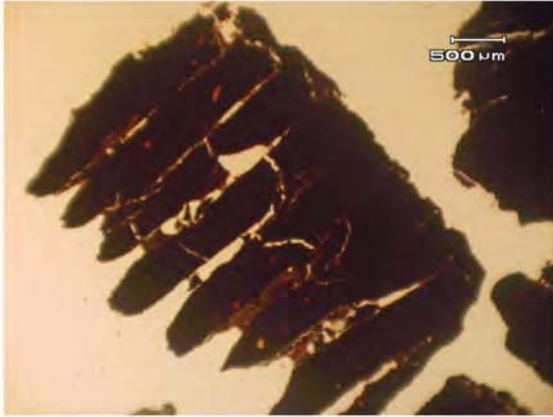


Figure 18A. Photomicrograph of grain mount from 1905'-1909': Organic material in carbonaceous coal to shale. Sample consists of 90-90% black to black-red organic debris with quartz clasts and clay.

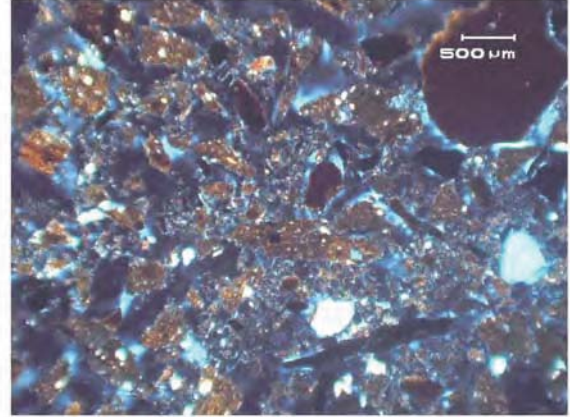


Figure 18B. Photomicrograph of clay-rich siltstone. Quartz clasts, organic material, abundant chert and minor white mica. 1845-1855 ft.

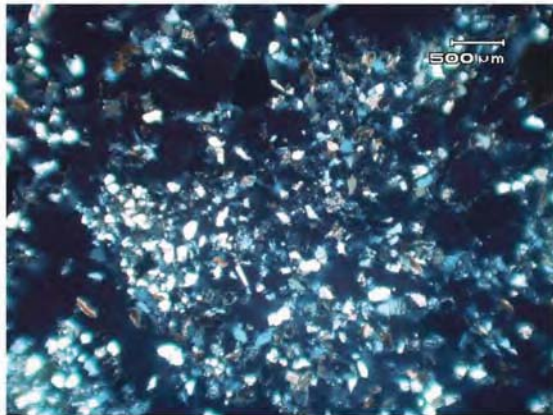


Figure 18C. Photomicrograph of siltstone with quartz chert and abundant organic debris. Minor white mica also present. 1825.9 ft.

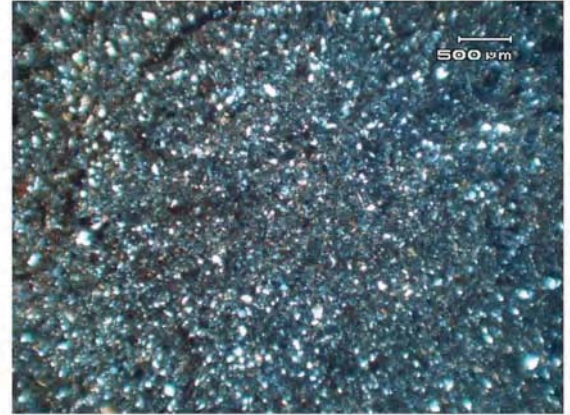


Figure 18D. Photomicrograph of lithic siltstone with quartz clast, chert, brown organic material and minor white mica in clay matrix. 1776.9 ft

Figure 18A-D. Photomicrographs of grain mounts from lower Fort Yukon core. See figures 11 and 12 for stratigraphic position in core.

DISCUSSION

We recognize 18 fining upward cycles (A-R) within the lower Fort Yukon core and cuttings that reflect episodic changes in base level within a fluvio-lacustrine-mire setting (see conceptual depositional model, fig. 19). Overall, the general pattern of sedimentation is fining upwards from sand- to silt-dominated fluvial deposits into eventual claystone to silty-claystone lacustrine or marsh deposits, and/or lignite or carbonaceous shale deposits representing a poorly-drained swamp environment. The fining upward cycles represent a decrease in energy up-section whereby stream flow and erosion cease and are overtaken by a rise in base level and subsequent peat formation.

The summary suite of depositional settings and their corresponding lithofacies [in brackets] recognized during this preliminary investigation of the lower Fort Yukon core Tertiary sediments are:

- Fluvial high-energy active channel [pebble sand conglomerate]
- Fluvial- seasonally active braided stream [sandstone and silty sandstone]
- Overbank crevasse splay [siltstone, clayey siltstone]
- Lacustrine or oxbow lake, ± varves [silty claystone, claystone]
- Well-drained shallow marsh [claystone, carbonaceous shale]
- Poorly-drained peat-forming mire [lignite, carbonaceous shale]

Our interpretations are based on a single core and it is difficult to establish the lateral extent of these facies. However, based on the seismic survey of Miller and others (2002), the major subsurface reflectors extend across the entire Fort Yukon area suggesting that the major facies are laterally extensive. Were a three-dimensional view of the Fort Yukon Tertiary possible with multiple drill holes, we would likely see lateral accretion of stream channel sands, overbank flood deposits, stream channel abandonment and the development of well-drained marsh, lacustrine and poorly-drained swamp (mire) environments. Rip-up clasts of coal at the base of channel sands suggest erosion of peat-forming swamp during higher energy lateral stream migration during base level fall.

Analysis of the sedimentary record preserved in this drill core and outcrops on the periphery of the basin will help to constrain depositional models that provide insight on the hydrocarbon potential of the Tertiary within the Yukon Flats.

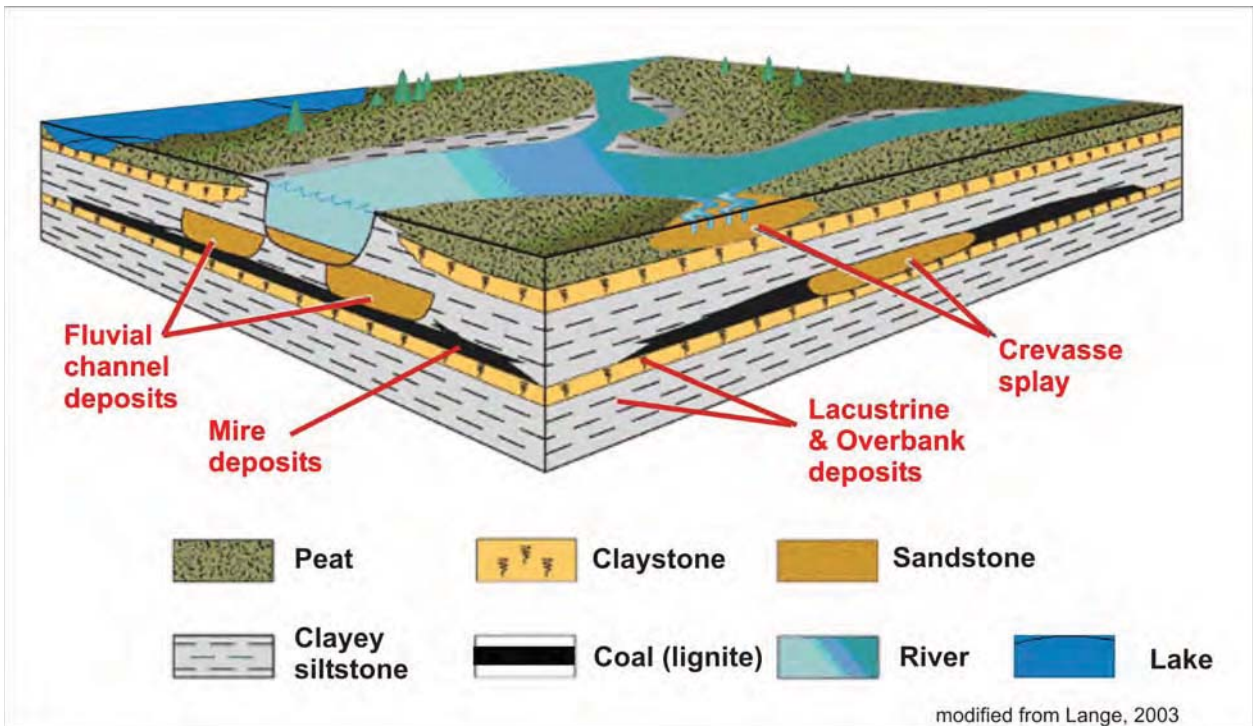


Figure 19. conceptual model for the Tertiary fluvial, lacustrine, and peat-forming mire settings represented in the lower fort Yukon core.

ACKNOWLEDGMENTS

We gratefully acknowledge the efforts of many people that have contributed to the drilling program at Fort Yukon Alaska. Charles Barker and Art Clark, U.S. Geological Survey, Denver CO. (USGS) were instrumental in planning, executing and completing the drilling project in Fort Yukon. Without their expertise and efforts, obtaining the 2004 drill core at Fort Yukon would not have been possible. Also participating in the on site coring operation geology were Beth Maclean, U.S. Bureau of Land Management-Alaska; Steve Roberts (USGS), Karen Clautice, Alaska Div. of Geological & Geophysical Surveys (retired); and Amy Rodman, Univ. of Alaska Fairbanks.

We thank Brent Sheets and James Hemsath from the U.S. Department of Energy, National Energy Technology Laboratory, Arctic Energy Office in Fairbanks, Alaska who provided both funding through a Federal grant (DE-FC26-01NT41248) and additional advice and support along the way. Dennis Witmer, Arctic Energy Technology Development Laboratory (AETDL) of the University of Alaska Fairbanks administered the grant and was also helpful throughout the process.

Robert Fisk, U.S. Bureau of Land Management-Alaska has been an integral part of the ongoing efforts in rural Alaska and his agency provided considerable financial support to make the project possible.

Without the considerable help and support of the U.S. Air Force 611th Air Support Group, based at Elemendorf Air Force Base (Anchorage) for the use of the drill site and facilities at the Fort Yukon Long Range Radar Site (LRRS) this project would not have been possible. We particularly thank Major James A. McCoy, Captain Trevis Bergert, Senior Master Sargent Miranda, Master Sargent Jeffrey Herrick, and Sue Striebich, along with all of the USAF people behind the scenes that helped to make this project feasible.

Curt McEwan, Operations Manager for ARCTEC Alaska, contractors for the Fort Yukon LRRS, along with Clay Shaw, Station Mechanic at the Fort Yukon LRRS, were extremely helpful to the process.

Rick Miller from the Kansas Geological Survey, who successfully completed a high-resolution shallow seismic survey at Fort Yukon in 2001, provided valuable interpretations on the subsurface geology.

A great deal of thanks goes to Dave Lee Thomas from the Village of Fort Yukon who provided invaluable assistance with advice and site logistics for the project. His help through the years has been immense and we are indebted to him for all he's done. James Kelly and Clarence Alexander of the Gwitchya Zhee Corporation were crucial in completing our work through all their help and assistance. Fannie Carroll, Fort Yukon City Manager, made possible the use of an old city dump for the drilling waste disposal and also made our work go smoothly with the help of city equipment and facilities. Assistance from the Gwitchyaa Gwichin Tribal Government's Davey James was greatly

appreciated. Jim Mery and Norm Phillips from Doyon Limited have continually provide information and support for our efforts in Fort Yukon. Finally, we would like to acknowledge all the help and the gracious reception from the people of Fort Yukon, especially Bonnie Thomas, Fannie Carroll, Rocky James, and Richard Carroll.

REFERENCES

- Barker, C., Clark, A.C., Maclean, B., Roberts, S., Clautice, K., and Rodman, A. in press, Canister Desorption Results From Well DOI-04-1A, Fort Yukon, Alaska, U.S. Geological Survey Open-File Report ____, 10 p
- Brabb, E.E., and Churkin, M., Jr., 1969, Geological map of the Charley River Quadrangle, east-central Alaska: U.S. Geological Survey Miscellaneous Geological Investigations Map I-573, scale 1:250,000.
- Brosgé, W.P., Reiser, H.N., and Yeend, W., 1973, Reconnaissance geologic map of the Beaver Quadrangle, Alaska: U.S. Geological Survey Miscellaneous Field Studies Map MF-525, scale 1:250,000.
- Clark, A.C., in press, Drilling Operations at the DOI-04-1a Well, Fort Yukon, U.S. Geological Survey Open-File Report ____, 6 p.
- Farmer, E.T., Ridgway, K.D. Bradley, D.C., and Till, A.B., 2003, Cretaceous-Early Eocene Two-Stage Basin Development, Yukon Flats Basin, North-Central Alaska [abs.]: Geological Society of America Abstracts with Programs, Vol. 35, No. 6, September 2003, p. 560.
- Hite, D.M., and E.M. Nakayama, 1980, Present and potential petroleum basins of Alaska: In Landwehr, M.L., (ed.), New Ideas, New Methods, New Developments: Exploration and Economics of the Petroleum Industry, v. 18, p. 511-560.
- Kirschner, C.E., 1994, Interior basins of Alaska, *in* Plafker, G., and Berg, H.C., eds., The Geology of Alaska: Boulder, Colorado, Geological Society of America, The geology of North America, v.G-1, p. 469-493.
- Lange, J.P., 2003, Stratigraphy, depositional environments, and coalbed gas resources of the Cherokee Group coals (Middle Pennsylvanian)-southeastern Kansas, Kansas Geological Survey, Open-file Report no. 2003-82, 158 p.
- Miller, R.D., Davis, J.C., Olea, R., Tapie, C., Laflen, D.R., Fiedler, M., 2002, Delineation of Coalbed Methane Prospects Using High-Resolution Seismic Reflections at Fort Yukon, Alaska, Kansas Geological Survey, Open-file Report No. 2002-16, 47 p., 83 figs.

- Reifenstuhl, R.R., 2006, Yukon Flats Basin, Alaska: Reservoir Characterization Study, Alaska Division of Geological & Geophysical Surveys Report of Investigation 2006-1, 25 p.
- Saltus, R.W., Phillips, J.D., Till, A., Stanley, R.G., and, Morin, R.L., 2004, Geophysical evidence that oceanic rocks underlie the Yukon Flats basin, Alaska [abs.]: Geological Society of America Abstracts with Programs, v. 36, no. 5, p. 495.
- Till, A.B., O'Sullivan, P.B., Bradley, D.C., and Roeske, S.M., 2004, Apatite Fission Track Evidence for Repeated Tertiary Movement on the Tintina Fault System, Alaska [abs.]: Geological Society of America Abstracts with Programs, Vol. 36, No. 5, p. 512.
- Troutman, S.M., and Stanley, R.G., 2003, Maps Showing Sedimentary Basins, Surface Thermal Maturity, and Indications of Petroleum in the Central Alaska Province, U.S. Geological Survey Miscellaneous Field Studies Map MF-2428, one sheet.
- Tyler, R., Scott, A.R., and Clough, J.G., 2000, Coalbed methane potential and exploration targets for rural Alaska communities: Alaska Division of Geological & Geophysical Surveys, Preliminary Interpretative Report 2000-2, 169 p., 1 sheet.

APPENDIX A. FORT YUKON CORE DESCRIPTION

Interval	Core Box	Depth	Interval Thickness	Predominant Lithology	Sample #	Photos	Color	Induration	Description	Thin Section Descriptions
1	1	1304.5 1314.5	10.0	COAL					Lignite (wrapped in plastic)	
2	1	1314.5 1315.0	0.5	X					Wooden block- Lost core (0.5 ft)	
3	2	1315.0 1325.0	10.0	COAL					Lignite (wrapped in plastic)	
4	3	1325.0 1325.6	0.6	CARB SHALE			Black to dark brown	med. hard	Black to dark brown "blecky" carbonaceous shale	
5	3	1325.6 1327.3	1.7	CLAYSTONE	04FY1327.0-1327.3	photos not recorded	light gray	med hard	Light gray claystone with small floating organic fragments at 1326.3. Grades upsection from lt gray to dk gray. White layer at 1327.0-1327.3. Gradational into carb "shale" above	04FYU 1327-1327.3 Organic claystone/organic shale. Epifaecal, massive, very well sorted. Brown and dark brown organic rich shale.
6	3	1327.3 1328.4	1.1	CARB SHALE			black to dark brown	med hard	Black to dark brown carbonaceous shale with abundant clay towards top and bottom	
7	3	1328.4 1328.8	0.4	"CLAYSTONE"	04FY1328.8-1329.0	photos not recorded	white to cream colored	med hard	White to cream colored clay - Angular basal contact	
8	3	1328.8 1331.6	2.8	SILTY CLAYSTONE	04FY1331.3		gray to dark gray	med hard	Micaceous flakes and organic lamination. Gray to dark gray silty claystone. Upper 0.1 ft has clayey siltstone. Floating fragments of carb up to 0.2" to 1" wide. Increases in darkness and mottling upsection.	
9	3	1331.6 1335.0	3.4	X					Wooden Block (lost 3.4 ft)	
10	4	1335.0 1336.0	1.0	COAL						
11	4	1336.0 1337.2	1.2	CLAYSTONE	04FY1336.3	833, 834	light tanish gray	med hard	light tanish gray claystone with organic (lignitic) fragments to beds ranging in size from 1/2 mm to 1/2". Interval has mottled patchy splotches. Claystone similar to claystone below. White possible lignina (ash) at 1336.3 (0.1 ft thick). Interval has little to no silt.	04FYU 1336.3 Organic rich siltstone. Quartz siltstone. 80% material.
12	4	1337.2 1338.3	1.1	SILTY CLAYSTONE		see core box photo for good picture	light gray to dark gray	med hard	Parallel-laminated light gray silty claystone and darker gray silty claystone varying amounts of small grain-sized organic material.	
13	4	1338.3 1338.5	0.2	SANDSTONE		835	dark gray	hard	Dark gray "dirty" fine-grained sand with very abundant carbonaceous material	
14	4	1338.5 1339.0	0.5	CLAYSTONE			dark gray and tan	med hard	Dark gray and tan mottled to "wispy" claystone (as below)	
15	4	1339.0 1339.7	0.7	COAL					Lignite (wrapped in plastic)	
16	4	1339.7 1340.7	1.0	COAL SAMPLE (wooden block)					presumed lignite	
17	4	1340.7 1341.0	0.3	CARB. SHALE		PHOTO 835 of whole core box	black to brownish black	med hard	Blocky black to brownish black carbonaceous "shale" or siltstone (similar to 1338.3 to 1338.5 interval)	
18	4	1341.0 1341.2	0.2	X					Wooden block (lost 0.2 ft)	
19	4	1341.2 1342.2	1.0	COAL				med hard	Lignite (wrapped in plastic)	
20	4	1342.2 1342.5	0.3	CARB. SHALE			dark brown to black	med hard	Dark brown to black carbonaceous "shale" with gray discontinuous "coaly" laminae	

APPENDIX A. FORT YUKON CORE DESCRIPTION

Interval	Core Box	Depth	Interval Thickness	Predominant Lithology	Sample #	Photos	Color	Induration	Description	Thin Section Descriptions
21	4	1342.5 1343.5	1.0	? COAL ?			?	?	Wooden block Sample 104-19	
22	4	1343.5 1343.7	0.2	CARB. SHALE			dark brown to black	med hard	Dark brown to black blocky carbonaceous shale same as 1342.2 to 1342.5 above.	
23	5	1345.0 1349.0	4.0	COAL	04FY1347.7-1348.0	PHOTO of whole core box	brownish black		Coal (light) wooden block in middle states Sample 104-20 for sample from 1346-1347	
24	5	1349.25 1349.25	0.25	CARB. SHALE			dark brown to black	med hard	Dark brown to black carbonaceous shale to almost lignite	
25	5	1350.25 1350.25	1.0	COAL					Coal sample 104-21 represented by Wooden block	
26	5	1354.1 1354.1	1.1	CARB. CLAYSTONE		828, 829, 830	dark gray to brownish black	med	Dark gray to brownish black carbonaceous claystone ("pre-carb. shale"). Blocky instead of fissile.	
27	5	1355.0 1355.0	1.1	CLAYSTONE			light grayish tan	med	Light grayish tan claystone (as below) with angular to rounded coal fragments from 1/2 mm to 3/4 inch in size throughout. Minor amount of gray clay matrix. No bedding discernable but some nodding near top of interval.	
28	6	1357.2 1357.2	2.2	CLAYSTONE	04FY1356.5	825,826,827	very light gray and gray	med hard	Very light gray and gray claystone with abundant white clay fragments/flecks pervasive throughout. Fragments/flecks are angular, poorly sorted, soft and lend a "mottled" overall appearance to cut face of core. Organic lignitic fragments to 2 mm length throughout.	04FYU 1356.5 Organic-rich siltstone. Epiclastic. Massive. Moderately sorted. Very fine, sub-rounded. Traces of white mica and organic rich siltstone.
29	6	1365.0 1365	7.8	CLAYSTONE			gray	hard	Gray silty micaceous claystone. Claystone is hard and block and has several fragments of woody lignitic material, particularly at 1361	
30	7	1374 1374.0	9.0	SILTSTONE			gray	hard	Gray micaceous siltstone with uncommon to rare blebs of yellowish-tan colored siltstone. Interval is indistinctly "mottled to spicdy" to faintly banded.	
31	7	1375.0 1375.0	1.0	SANDSTONE			S&P gray	very soft	Very soft fine-grained "salt & pepper" sandstone. White and clear quartz grains, gray and black chert grains; grains are angular to subangular. No visible mica.	
32	8	1376.2 1376.2	1.2	SANDSTONE	04FY1375-1385		S&P gray	very soft	Very soft fine-grained salt & pepper sandstone. Finer-grained than at 1375 in core box 7. Bottom 0.2 ft mostly gray siltstone with carbonaceous woody material. Last 0.2 ft carb. shale. NOTE: this interval is from somewhere between 1375 and 1385. Some consolidation.	04FYU 1375-1385 Grainy to fine grained sandstone. 10% very fine grained, 60% fine grained, 30% medium grained. Sub-angular. Siltstone fragments 20-30%. Plagioclase feldspar 1-3% with good looking twins. Quartz 70-80%.
33	8	1385.0 1385.0	8.8	X					Wooden block-Lost 9 feet of core in interval 1375-1385. Interval not determined run 13 below.	
34	8	1395.0 1395.0	10.0	SILTSTONE/SANDSTONE		823, 824	light gray	hard	Light gray siltstone, with wispy laminae and coaly fragments to 1/2"	
35	8	1395.0 1405.0	10.0	SANDSTONE w siltstone at base		821, 822	light gray	soft	wooden block-run 13 above, run 14 below 1 ft soft S&P fine to medium grained sandstone with black and gray chert. Bottom 0.7 feet is laminated siltstone & lignite in sub-mm laminae NOTE: lost core from this interval, presumable because of soft sand	

APPENDIX A. FORT YUKON CORE DESCRIPTION

Interval	Core Box	Depth	Interval Thickness	Predominant Lithology	Sample #	Photos	Color	Induration	Description	Thin Section Descriptions
36	8	1405.0 1415.0	10.0	SANDSTONE			medium gray	soft	0.45 of soft S&P sandstone same as above. NOTE: don't know where this sand is from, somewhere between 1405-1415 (see drilling notes)	
37	8	1415.0 1427.0	12.0	X					Wooden block. Lost 1415 to 1427, no recovery	
38	8	1427.0 1430.0	3.0	SANDSTONE			medium gray	soft	Silt & pepper sandstone same as below and above	
39	9	1430.0 1430.2	0.2	SANDSTONE			medium gray	soft	soft medium gray "salt and pepper look" sandstone; poorly sorted, white qtz, black chert, very angular grains, micaceous.	
40	9	1430.2 1431.4	1.2	SILTY CLAYSTONE			brownish gray	medium	Brownish gray silty, sandy claystone with sandy horizons near top of interval. Coal fragments from 1/2" to over 1". Coarsens upward.	
41	9	1431.4 1432.0	0.6	SILTSTONE/SANDSTONE			light gray	medium	Light gray siltstone to very fine sandstone with minor clay present. Faintly laminated (?). Salt & pepper: white qtz, black chert, micaceous, very angular grains	
42	9	1432.0 1433.5	1.5	SILTY CLAYSTONE		817, 818, 819	brownish gray	medium	Brownish gray silty, sandy claystone with sandy horizons near top of interval. Coal fragments to couple of inches. (same as in interval 1430.2-1431.4)	
43	9	1433.5 1435.0	1.5	X					Wooden block. Lost core 1433.5 to 1435.0	
44	9	1435.0 1443.0	10.0	X					Wooden block: Run 17 1435-1445 No recovery	
45	9	1443.0 1445.5	0.5	CLAYSTONE			gray to dark gray	medium	Gray to dark gray silty claystone, micaceous. Organic "preighter" at top	
46	9	1445.5 1448.7	3.2	SANDSTONE			medium to dark gray	soft	Medium to dark gray salt & pepper sandstone, soft, with white and clear qtz grains and dark gray to black chert grains NOTE: this part of core from 1445-1448.7 is from somewhere between 1445-149, we don't know where.	
47	9	1448.7 1489.0	40.3	X					Wooden block: Run 18 1445-1480 Recover 3.5 ft (above) Run 19 (below) recover 2 ft	
48	9	1489.0 1491.0	2.0	CLAYSTONE		813, 814, 815, 816 of mold growth in core	dark brownish gray	medium	Varved claystone as below	
49	10	1491.0 1491.6	0.6	CLAYSTONE/SILTY CLAYSTONE-MUD	04FY1491.0	809, 810, 811, 812	dark brownish gray	medium	Dark brownish gray claystone alternating with (lighter) brownish gray silty claystone on 1 to 2 mm scale. Has "varved" look. Distinctly laminated.	04FYU 1491 Siltstone, shale, claystone, organic rich. Epifaucic. Very fine grained material. Silt sized quartz and white mica.
50	10	1491.6 1493.0	1.4	CLAY-SILTSTONE	04FY1492.3	805, 806, 807, 808	brownish gray	medium	Brownish gray clayey siltstone. Distinctly laminated on 1 mm scale. Possible tephra at 1492.3, sampled for ash. Partially oxidized.	04FYU 1492 Siltstone/claystone. Epifaucic. Plane laminated. Poorly sorted. 90% very fine grained material, 10% fine grained material. Quartz 60% (90% monocrytalline, 10% polycrytalline chert), organic debris 20-30%. White mica 2-3%. Clay matrix?
51	10	1493.0 1495.85	2.85	SILTY CLAYSTONE			brownish gray	medium	GRADATIONAL CONTACT TO ABOVE Brownish gray claystone with varying amount of silt throughout, but minor. Has 1-2 mm laminations in places evident on "cut" surface. Appears to increase in silt content upward.	
52	10	1495.85 1496.1	0.25	X					Wooden block	
53	10	1496.1 1497.0	0.9	CLAYSTONE			dark brownish gray	medium	Dark brownish gray claystone (perhaps faintly laminated, very minor silt)	

APPENDIX A. FORT YUKON CORE DESCRIPTION

Interval	Core Box	Depth	Interval Thickness	Predominant Lithology	Sample #	Photos	Color	Induration	Description		Thin Section Descriptions
									GRADES UP INTO INTERVAL ABOVE	DESCRIPTION	
54	10	1497.0 1497.3 1497.3	0.3	SILTY CLAYSTONE			brownish gray	medium	GRADES UP INTO INTERVAL ABOVE brownish gray silty claystone		
55	10		3.7	SANDSTONE to SILTSTONE	04FY1489.0		brownish gray	medium	GRADES UP INTO INTERVAL ABOVE Very fine, sub-rounded to sub-angular consolidated siltstone-sandstone. Gray to brownish gray very fine sandstone to siltstone with minor clay content. Visible white quartz, clear quartz, black chert grains.	04FYU 1489 Very fine sandstone. Epiclastic, 80% quartz, traces of biotite, hornblende, white mica. Clay matrix. Igneous or metamorphic provenance?	
56	11	1501.0 1501.0	2.0	SILTY CLAYSTONE	04FY1502.0		medium gray	hard	Medium gray silty claystone (or clayey siltstone), nondescript but perhaps laminated with organics. Fairly hard core (indurated)	04FYU 1502 Rock thin section. 20% silt, 45% very fine grained material, 25% fine grained material and 5-18% medium grained material, 65% poly quartz, 35% mono quartz, trace plagioclase, white mica, siltstone clasts. Clay matrix with high birefringence. Lithic recycled with chert, siltstone, and minor plagioclase.	
57	11	1503.0 1503.0 1505.0	2.0	SANDSTONE			medium gray	soft	Medium gray sand with white quartz and chert (?). Soft sediment with laminations		
58	11	1505.0- 1505.6-	0.6	SANDSTONE			medium gray	soft	Same as above		
59	11	1505.6- 1507-	1.4	SILTY CLAYSTONE			brownish gray	medium	Brownish gray claystone becoming more silty in the upper 1m. Coaly fragments and darker brown color in the upper portion of the interval.		
60	11	1507-	0.5	SILTY CLAYSTONE			brownish gray	medium	Brownish gray claystone becoming more silty in the upper 1m. Coaly fragments and darker brown color in the upper portion of the interval.		
61	11	1507.5- 1507.5-	0.5	SILTY CLAYSTONE			brownish gray	medium	Medium gray to brownish silty clay with minor lignite fragments.		
62	11	1508- 1508.5- 1508.5-	27.0	CLAYSTONE			dark brownish gray	hard	Darker color than above.		
63	11	1535- 1535-	26.5						Wooden Block		04FYU 1509.3 Very fine grained sandstone and siltstone thin section. Epiclastic, massive, 80% silt, 20% very fine grained material. Sub rounded. 1% pore space. 80% quartz/chert, 20% micaceous clay matrix with traces of white mica. Lithic recycled.
64	11		2.0	SANDSTONE	04FY1537		medium gray		Very fine grained to coarse grained sub rounded to sub angular unconsolidated sands. Medium gray white quartz sand (chert?)	04FYU 1537 Grainmount. Epiclastic. 10% very fine material, 30-40% fine material, 35-40% medium grained material, 60-70% chert (locally with white mica attached), 30% quartz, 3-4% plagioclase, 1-2% meta-siltstone and traces of white mica. Clay cement? Lithic recycled.	
65	12	1537- 1537.2-	0.2	SANDSTONE				soft	Medium gray sandstone		
66	12	1537.2- 1537.5-	0.3	SANDSTONE					Wooden block (Art QW sample (coal?))		
67	12	1537.5- 1537.9- 1537.9-	0.4	SANDSTONE		801, 802, 803, 804	medium gray		GRADES UP INTO INTERVAL ABOVE grades into laminated lignite		
68	12	1584.8- 1584.8-	46.9	SANDSTONE	04FY1584.0		medium gray	soft	Medium grained to coarse grained sub rounded to sub angular unconsolidated sands. Medium gray soft sand, gray to medium gray with small grains sized coaly fragments. White chert in greater abundance than lean quartz and gray chert. Coal fragments or lignite?	04FYU 1584 Grainmount. Epiclastic. Moderately sorted, 10-20% very fine grained material, 25-30% fine grained material, 50% medium grained material, 70% chert, 25% quartz, 1-5% plagioclase. Traces of white mica and minor schist. Lithic recycled with minor metamorphic rock component.	
69	12	1584.8- 1585	0.2						Wooden Block		

APPENDIX A. FORT YUKON CORE DESCRIPTION

Interval	Core Box	Depth	Interval Thickness	Predominant Lithology	Sample #	Photos	Color	Induration	Description	Thin Section Descriptions
70	12	1585-1586.1	0.1	CLAYSTONE			brownish gray		Brownish gray claystone with mm laminations of lignite. Organic-lignitic layers and fragments	
71	12	1586.1-1586.0	0.9	SILTY CLAYSTONE			medium gray to brown	medium	Medium gray to brownish gray silty claystone, faintly laminated up to 1mm thick throughout. Rare swells. Coaly fragments up to 4mm in length. Minor yellowish-tan weathering "concretions".	
72	13	1586.0-1586	2.9	SILTY CLAYSTONE			medium gray to brown	medium	Medium gray to brownish gray silty claystone, faintly laminated up to 1mm thick throughout. Rare swells. Coaly fragments up to 4mm in length. Minor yellowish-tan weathering "concretions".	
73	13	1586.9-1589.3	0.4						Wooden Block (Art QW sample)	
74	13	1589.3-1595.0	5.7	SILTY CLAYSTONE	04FY1589.3		medium gray to brown	medium	Consolidated medium gray to brown-gray silty claystone, faintly laminated up to 1mm thick throughout. Rare small coaly fragments up to 4mm in length. Minor yellowish-tan weathering "concretions".	
75	14	1595-1595.2	0.2	SILTY CLAYSTONE			medium-dark gray		Missing core? See lith log box 13 at the bottom	
76	14	1595.2-1596.65	1.9	CLAY-SILTSTONE-SANDSTONE			medium gray		Medium to dark gray silty claystone	
77	14	1596.65-1596.9	0.3	SANDSTONE		795	light gray	soft	POORLY SORTED white quartz, gray quartz, and clay	
78	14	1596.9-1600.7	3.6	SANDSTONE			olive gray	soft	Light gray fine sandstone, faintly laminated, with sub-angular white quartz, clear quartz, and dark gray chert. Indurated.	
79	14	1600.7-1601.3	0.6	SILTY CLAYSTONE			medium to dark gray		Medium gray fine to very fine sandstone. More indurated than the coarser soft sandstone mentioned above. Minor olive gray color. Occasional very faint lamination.	
80	14	1601.3-1601.8	0.5	SANDSTONE			medium gray		Medium to dark gray silty claystone	
81	14	1601.8-1602.6	0.8	SILTY CLAYSTONE with SAND	04FY1602.6-1603.0		medium to dark gray		Very soft medium gray fine sand with white quartz, clear quartz, and micaceous flakes	
82	14	1602.6-1603	0.4	SANDSTONE and SILTSTONE	04FY1602.6-1603.0	793 to 800	medium gray		Clay, silt, and very fine grained sub rounded to sub angular micaceous sand. Medium to dark gray silty micaceous claystone.	04FYU 1602.6-1603 Very fine sandstone and siltstone grain mount. Epiclastic. 10% silt, 40% very fine grained sand, 50% fine grained material. 46% quartz, 50% clay, 10% organic material and traces of white mica. Lithic recycled.
83	14	1603-1603.7	0.7	SANDSTONE	04FY1603.0-1603.2		medium gray		Laminated medium gray sand and silt layers with clay. Finest upward with minor carbonaceous material within the laminations	
84	14	1603.7-1604.8	1.1	SANDSTONE and SILTSTONE					Fine grained sub rounded sand. Very soft medium gray fine sand with white quartz, clear quartz, and micaceous flakes	04FYU 1603-1603.2 Very fine grained sandstone, siltstone, and shale grain mount. Epiclastic. 40% silt, 60% very fine grained material. 80% chert/quartz. Traces of white mica, plagioclase, and clay. Lithic recycled.

APPENDIX A. FORT YUKON CORE DESCRIPTION

Interval	Core Box	Depth	Interval Thickness	Predominant Lithology	Sample #	Photos	Color	Induration	Description	Thin Section Descriptions
85	14	1604.8-1605.0	0.2	SANDSTONE	04FY 1604.8-1605.0	791, 792	Light gray	very soft	Silt and very fine grained sub rounded to sub angular unconsolidated sandstone. Light gray very fine grained sand with subangular white quartz, clear quartz, and dark gray chert.	04FYU 1604.8-1605. Very fine sandstone/siltstone grain mount. Epiclastic. 50% silt, 50% very fine grained material. 80% chert/quartz, plagioclase 1%, mica-clay, schistose fragments, 19%. Lithic recycled and metamorphic fragments.
86	15	1605.0-1609.6	4.6	SANDSTONE	04FY1605.0		gray to dark gray		Very fine grained to fine grained sub rounded to sub angular unconsolidated and partially oxidized sandstone. Soft, poor core preservation. Gray to dark gray.	04FYU 1605 Grain mount. Epiclastic. 50% very fine chert/quartz, 20% micas-clay. Lithic recycled.
87	15	1609.6-1609.8	0.2	CLAY-SILTSTONE					Coarsens upwards	
88	15	1609.8-1613	3.2	SANDSTONE			gray		Fine to medium grained gray sandstone with white quartz, clear quartz, and gray chert	
89	15	1613-1615							MISSING CORE	
90	15	1615-1615.5	0.5	SILTSTONE			gray to dark gray		Gray to dark gray micaceous siltstone with carbonaceous laminations up to 3mm thick	
91	15	1615.5-1616.8	1.3	SANDSTONE			gray		Fine to medium grained gray sandstone with white quartz, clear quartz, and gray chert	
92	16	1616.8-1617.7	0.9	SANDSTONE			gray		Fine to medium grained gray sandstone with white quartz, clear quartz, and gray chert	
93	16	1617.7-1620.6	2.9	SANDSTONE	04FY1617.7	786-789	gray		Fine to medium grained sub rounded to subangular unconsolidated gray sandstone with white quartz, clear quartz, and gray chert. Partially oxidized.	04FYU 1617.7 Grain mount. Epiclastic. 40% very fine grained material, 60% fine grained material. 80% chert/quartz, 20% white mica, plagioclase, and clay. Lithic recycled.
94	16	1620.6-1621.0	0.4	COAL			black		Laminated coals	
95	16	1621.0-1622.4	1.4	SANDSTONE			gray		Fine to medium grained gray sandstone with white quartz, clear quartz, and gray chert.	
96	16	1622.4-1624.1	1.7	SILTSTONE			gray to dark gray		Gray to dark gray micaceous siltstone with coaly laminations near the top of the interval	
97	16	1624.1-1625.9	1.8	SANDSTONE			gray		Fine to medium grained gray sandstone with white quartz, clear quartz, and gray chert.	
98	16	1625.9-1626.0							Wooden Block	
99	16	1626.0-1626.7	0.7	SANDSTONE			gray		Fine to medium grained gray sandstone with white quartz, clear quartz, and gray chert. Laminated coals and silts near the top of the interval	
100	17	1626.7-1633.8	7.1	SANDSTONE	04FY1631.0		gray	very soft	Fine to medium grained	
101	17	1633.8-1635	1.2						MISSING CORE	
102	17	1635-1637.5	2.5	SANDSTONE					Upper portion of interval has distinct sub mm laminations of coal. Fine to medium grained sand with white, clear, and gray quartz	
103	18	1637.5-1641.6	4.1	SANDSTONE	04FY1638.0		gray		Fine to medium grained sub rounded unconsolidated gray sandstone with organic laminations, white quartz, clear quartz, and gray chert.	04FYU 1638 Grain mount. 10% silt, 40% very fine grained material, 60% fine grained material. 80% chert/quartz, 20% minor white mica, plagioclase, and organic material. Lithic recycled.
104	18	1641.6-1643.5	1.9	SILTSTONE			gray		Gray silt with rare and very thin coaly laminations and fragments	
105	18	1643.5-1645.0	1.5	X					MISSING CORE	

APPENDIX A. FORT YUKON CORE DESCRIPTION

Interval	Core Box	Depth	Interval Thickness	Predominant Lithology	Sample #	Photos	Color	Induration	Description	Thin Section Descriptions
106	18	1645.0-1645.8	0.8	SANDSTONE					Fine to medium grained gray sandstone with white quartz, clear quartz, and gray chert.	
107	18	1645.8-1646.4	0.4	SANDSTONE					Fine to medium grained gray sandstone with white quartz, clear quartz, and gray chert.	
108	18	1646.4-1647.3	0.9	SANDSTONE with COAL					Laminated dull black coals with fine grained silty sandstone. While quartz with dark gray chert and coaly particles.	
109	18	1647.3-1647.9	0.6	SANDSTONE					Fine to medium grained gray sandstone with white quartz, clear quartz, and gray chert.	
110	18	1648.3-1648.3	0.4	SANDSTONE					Laminated dull black coals with fine grained silty sandstone. While quartz with dark gray chert and coaly particles.	04FYU 1648.1 Grain mount. 10% silt, 50 % very fine grained material, 40 % fine grained material. Chert 80%, 10% white mica and plagioclase, 10% organic material.
111	19	1650.3-1650.3	2.7	SILTSTONE and SANDSTONE	04FY1648.1-1648.3		gray	soft	Very fine grained sub rounded to sub angular unconsolidated sandstone with organics. Mostly fine to medium grained sandstone with white and clear quartz, dark chert, and coaly laminations in the top portion of the interval	
112	19	1650.3-1650.4							MISSING CORE	
113	19	1650.4-1650.9	2.5	SILTSTONE and SANDSTONE	04FY1655.7	778-779	gray		Micaceous gray siltstone grading upwards in the interval into dark gray to gray fine grained sandstone with subangular white, clear, and gray quartz and chert with fragments of partially coalified wood to carbonaceous shale. Uncommon concretions (see photo).	04FYU 1655.7 Grain mount. Epifaunal. 40% silt, 50% very fine grained material, 10% fine grained material, 80% chert. 10-20% organic debris. Lithic recycled?
114	19	1650.9-1651.3	4.2	CLAY			medium to dark gray	soft	Medium to dark gray clay with low silt content.	
115	19	1651.3-1655.0	3.7						LOST	
116	20	1675-1675.0	10.0	SANDSTONE with CLAY	04FY1685.7		gray to dark gray		Very fine grained to fine grained unconsolidated sands, silts, and clay with plant material. Gray to medium gray clay with minor silt and rare coalified wood fragments and uncommon yellowish-tan concretions	
117	21	1675-1675.2	3.2	CLAYSTONE			gray to dark gray		Gray to dark gray clay with variable silt content	
118	21	1675.2-1679.0	0.8	CLAYSTONE			gray		Gray clay with yellowish tan concretions	
119	21	1679-1679.4	0.4	CLAYSTONE			gray		Gray clay only	
120	21	1683-1683.6	3.6	SILTSTONE with CLAY	04FY1680-1680.2	777	light to dark gray		Alternating light and dark gray siltstone and clay laminations. Grades into grayish to yellowish siltstone with local coaly fragments. Unconsolidated with organics.	04FYU 1681.6 Grain mount. 80% very fine grained material, 80% chert, 20% quartz, 20% organics, clay matrix. Lithics recycled 04FYU 1680-1680.2 Grain mount. Epifaunal, plane laminated, 20% very fine grained material, 80% chert, 10-20% organic material and clay. Lithic recycled
121	21	1684.6-1684.6	1.6	CLAY-SILTSTONE	04FY1683.6-1683.7				DISCREPENCY WITH SAMPLE #, see lith log box 21	
122	21	1684.6-1685	0.4	CLAY-SILTSTONE	04FY1684.7-1684.8		light gray		Unconsolidated light gray clay rich siltstone. Distinctly lighter than above and below.	
123	22	1685-1685	10.0	SILTY CLAYSTONE	04FY1686.7-1686.8		gray to dark gray		Predominantly gray to dark gray silty clay with variable amounts of silt. Several random yellow concretionary zones.	

APPENDIX A. FORT YUKON CORE DESCRIPTION

Interval	Core Box	Depth	Interval Thickness	Predominant Lithology	Sample #	Photos	Color	Induration	Description	Thin Section Descriptions
124	23	1695-1705	10.0	SILTY CLAYSTONE	04FY 1697.4-1697.5	774-775	light to dark gray		Unconsolidated light gray to gray micaceous clay-siltstone with small iron rich concretions cm in size.	04FYU 1697.4 Shale with siltstone and organic material. Epiclastic, plane laminated, very poorly sorted. 95% very fine grained material. 60% quartz, 10% chert, 30% clay and white mica. Shale with visible white mica, some chert, and recycled lithic fragments.
125	24	1705-1706.5	5.5	SILTSTONE	04FY1705		gray		Micaceous in upper portion of the interval	04FYU 1705.9 Siltstone and very fine sandstone. Epiclastic, plane laminated, poorly sorted. 85% very fine grained material. 40% quartz, 40% chert, 10% clay and white mica, 10% organic debris.
126	24	1706.5-1712.3	5.7	SILTY CLAYSTONE			dark gray		Gray to dark gray silty clay with thin laminations of tan siltstone and fine grained gray to dark gray micaceous silts with abundant chert	
127	24	1712.3-1715	2.7	SANDSTONE					Gray to medium gray sand with minor organic laminations	
128	25	1715-1720	5.0						MISSING CORE	
129	25	1720-1729.7	9.7	SANDSTONE	04FY1726.6		medium gray to dark gray	very soft	Very fine grained sub rounded to sub angular sandstone. Medium gray to dark gray fine to medium grained sand with white and clear quartz and gray chert grains. Core is shattered and very soft. Localized carbonaceous plant material from 1728.7-1728.9.	
130	25	1729.7-1730	0.3	SILTSTONE			tan		Carbonaceous fragments and micaceous laminations	
131	26	1730-1739.3	9.3	SILTSTONE	04FY1734.9-1735.2	771-773	gray-tan		Grayish tan clay-siltstone. Carbonaceous material and clay laminations from 1734.9-1735.2. Micaceous clay with coal seams.	
132	26	1739.3-1740	0.7	SILTSTONE with CLAY			gray		Mostly gray silty clay	
133	26	1740-1745	0.5						MISSING CORE	
134	27	1745.0-1748.0	3.0	SANDSTONE	04FY1747.2-1747.3		gray to dark gray		Silt to very fine grained to medium grained unconsolidated sandstone. Fine to medium grained gray to dark gray sand.	
135	27	1748.0-1748.5	5.0	SILTSTONE	04FY1748.25	BANET	tan to medium gray		Silt to very fine grained sub rounded to angular sands. Tan to gray micaceous siltstone with carbonized plant fragments on bedding planes (laminated organics).	
136	27	1748.5-1756.5					gray to dark yellowish tan	soft	MISSING CORE	
137	27	1756.5-1765	9.5	SILTSTONE					Gray to dark yellowish tan micaceous siltstone lacking sedimentary structure	
									DESCREpancy between lith log box 27 and 28 concerning test core	
138	28	1765-1775	10.0	SILTSTONE with CLAY					Micaceous increase from below	
139	29	1775-1785.6	10.6	SILTSTONE with CLAY					Micaceous. Minor Brownish wood fragments	04FYU 1784.7-1784.8 Siltstone. Quartz 60-70%. White mica 10%. Feldspar (?). Brown organic material. Clay matrix.
140	29	1785.6-1788	2.4	SANDSTONE			medium gray		Medium gray fine grained sand with minor silt laminations	
141	30	1788-1788.8	0.8	SILTSTONE with CLAY			medium to dark gray		Very minor organic partings	
142	30	1788.8-1790.2	1.4	SILTSTONE with CLAY			medium to dark gray		Very minor organic partings	
143	30	1790.2-1800.8	10.6	SANDSTONE			medium to dark gray		Fine grained sand with rare woody plant fragments	
144	31	1800.8-1804.6	3.8	SANDSTONE	04FY1802.2		medium to dark gray		Fine grained sand with rare woody plant fragments	

APPENDIX A. FORT YUKON CORE DESCRIPTION

Interval	Core Box	Depth	Interval Thickness	Predominant Lithology	Sample #	Photos	Color	Induration	Description	Thin Section Descriptions
145	31	1804.6- 1810.3	6.2	SILTSTONE with CLAY			olive gray		Light olive gray to medium gray silty clay with rare woody and coalified plant fragments cm's in length. Woody fragments are visible on some bedding surfaces. Micaceous flakes in clay layers.	
146	32	1810.3- 1816.9	6.6	CLAYSTONE	04FY1816.9 and 04FY1815.2		medium gray		Clay	
147	32	1816.9- 1818.6	1.8	SILTSTONE with CLAY			light to medium gray		Fining upward medium to light gray silty clay	
148	32	1818.6- 1820.1	1.5	SANDSTONE		22-23	light to medium gray		Same as below	
149	33	1820.1- 1826.2	6.1	SANDSTONE	04FY1825.9				Silty sand with sparse organic laminations	Siltstone with quartz and abundant chert fragments. Abundant organic debris, minor white mica, and clay matrix.
150	33	1826.2- 1835	8.8	?					MISSING CORE	
151-158	34	1835- 1905	70.0	CLAYSTONE	04FY 1845-1855				End of upper coring...rotary down, box 34 is all cuttings	Clay rich siltstone. Quartz clasts, organic material, abundant chert, and minor white mica.
159	34	1905- 1909	4.0	COAL	04FYU 1905-1909				COAL	Organic material and carbonaceous coal/shale. 90-90% black to black-red organic debris with quartz clasts and clay.
160	35	1909- 1919	10.0	COAL					COAL	
161	36	1919- 1921	3.0	CLAYSTONE	04FY1919.5	20-21	medium to light gray		Black organic laminations and coalified wood fragments	
162	36	1921- 1924	3.0	CLAYSTONE			medium to dark gray		WOOD BLOCK AT 1924.2-1925	
163	36	1924- 1925.5	1.5	CLAYSTONE	04FY1924					
164	36	1925.5- 1929.4	3.9	SANDSTONE	04FY1925.5					
165	37	1929.4- 1935.8	6.4	SANDSTONE	04FY1935.8		olive to medium gray		Fine to very fine sand with clay	
166	37	1935.8- 1936.0	0.2						WOODEN BLOCK	
167	37	1936.0- 1938.0	2.0	SANDSTONE			olive to medium gray		Fine to very fine sand with clay	
168	37	1938- 1939	1.0	SANDSTONE	04FY 1938.3		olive to yellow		Olive gray to yellowish sand with gravel lag deposits. Pebbles are sub rounded and appear to be siltstone	Siltstone with very fine sandstone. Chert clasts are more abundant than chert, argillite, traces of plagioclase, traces of white mica, and clay fine on clasts.
169	37-38	1940.2- 1944.2	1.2	SANDSTONE	04FY1939.9		olive to yellow		Olive gray to yellowish tan fine grained sand with silt. Organics consist of coalified plant material.	
170	38	1944.2- 1944.2							MISSING CORE	
171	38	1950- 1950	5.8	CLAYSTONE			olive gray		Olive gray to yellowish tan fine grained sand with silt. Organics consist of coalified plant material.	
172	38	1950.8- 1950.8	0.8	CLAYSTONE			olive gray		Olive gray to yellowish tan fine grained sand with silt. Organics consist of coalified plant material.	
173	38	1950.8- 1951.3	0.5	SILTSTONE to SANDSTONE	04FY1951		olive gray		Wavy laminations and thin carbonaceous plant fragments	Siltstone with quartz, minor chert, organic material, traces of white mica, and clay matrix.
174	38	1951.3- 1952.0	0.8	SILTSTONE with CLAY	04FY1951.3		medium gray		Sub mm partings of fine sand	Siltstone with quartz and chert. Minor white mica and abundant clay matrix.
175	38	1952.0- 1952.5	0.5	SILTSTONE with CLAY			gray brown		Organic partings	
176	38	1952.5- 1952.9	0.4	SILTSTONE with CLAY	04FY1952.6		light brown		Salt and pepper texture	Siltstone with very fine sandstone. Clasts of chert and quartz with traces of white mica and plagioclase.

APPENDIX A. FORT YUKON CORE DESCRIPTION

Interval	Core Box	Depth	Interval Thickness	Predominant Lithology	Sample #	Photos	Color	Induration	Description	Thin Section Descriptions
177	38	1952.9-1953.3	0.4	SILTSTONE with CLAY			light brown		Amber?	
178	39	1953.3-1955	1.7	SILTSTONE with CLAY	04FYU 1954.8	13-14	light brown		Coal fragments	Chert, quartz, traces of white mica and plagioclase in a clay matrix.
179		1955-1970	15.0	SANDY-SILTSTONE TO CLAYSTONE					Based on gamma ray log interpretation. Fining upward sequence from siltstone to claystone.	
180	cuttings	1970-2010	40.0	SANDY-SILTSTONE	04FY 1965-1975				Siltstone to claystone with thin sandy interbeds 1'-2' thick.	
181	cuttings	1975-1985	10.0	SILTSTONE with CLAY	04FY 1975-1985				Minor coal fragments	
182	cuttings	1985-1995	10.0	SILTSTONE with CLAY	04FY 1985-1995		olive gray			Chert and quartz. Traces of white mica and clay matrix.
183	cuttings	1995-2005	10.0	SILTSTONE with CLAY	04FY 1995-2005		olive gray		Minor coal fragments	Siltstone with oxidized organic debris. Quartz with lesser amounts of chert. White mica clasts. Matrix is silt, clay, and altered organic debris.
184	cuttings	2005-2015	10.0	SILTSTONE with CLAY	04FY 2005-2015		olive gray		Silty claystone with coarse sand interbeds, minor coal fragments	
185	cuttings	2015-2025	10.0	CLAYSTONE	04FY 2015-2025					
186	cuttings	2025-2035	10.0	CLAYSTONE	04FY 2025-2035		olive gray		Minor coal fragments	
187	cuttings	2035-2045	10.0	CLAYSTONE	04FY 2035-2045		medium to dark gray			
188	cuttings	2045-2055	10.0	CLAYSTONE	04FY 2045-2055		white to medium gray		Minor coal fragments	
189	cuttings	2055-2065	10.0	SILTSTONE with CLAY	04FY 2055-2065		medium gray		Minor coal fragments	
190	cuttings	2065-2140		SANDSTONE and SILTSTONE					Interbedded sandstone and siltstone in zones 2-5 feet thick.	
191	cuttings	2075-2085	10.0	SILTSTONE with CLAY	04FY 2065-2075		medium gray		Minor coal fragments	
192	cuttings	2085-2095	10.0	SILTSTONE with CLAY	04FY 2075-2085		medium gray		Minor coal fragments	
193	cuttings	2095-2105	10.0	SILTSTONE with CLAY	04FY 2085-2095		medium gray		Minor coal fragments	
194	cuttings	2105-2115	10.0	SILTSTONE with CLAY	04FY 2095-2105		medium gray		Minor coal fragments	
195	cuttings	2115-2125	10.0	SILTSTONE with CLAY	04FY 2105-2115		medium gray		Minor coal fragments	
196	cuttings	2125-2135	10.0	SILTSTONE with CLAY	04FY 2115-2125		medium gray		Minor coal fragments	Silica fracture fill. Quartz and clay clasts. Clay matrix.

APPENDIX A. FORT YUKON CORE DESCRIPTION

Interval	Core Box	Depth	Interval Thickness	Predominant Lithology	Sample #	Photos	Color	Induration	Description	Thin Section Descriptions
*		2140-2170		SANDSTONE to SILTSTONE					Interbedded sandstone and siltstone in zones 2-5 feet thick. Overall, this interval is a fining upward sequence of sandstone at the base to a siltstone at the top and a thin claystone interval at the very top. Based on geophysical log interpretation.	
197	cuttings	2135-2145	10.0	CLAYSTONE	04FY2135-2145		medium gray		Minor coal fragments and random quartz grain	
198	cuttings	2145-2155	10.0	CLAYSTONE	04FY2145-2155		medium gray		Minor coal fragments	
199	cuttings	2155-2165	10.0	CLAYSTONE	04FY2155-2165		medium gray		Minor coal fragments and random quartz grain	
*		2175-2225		SANDSTONE with PEBBLES					Finely clean sand interval (could be a gravel zone) with pebbly sand interbeds of varying thicknesses ranging at 2170'-2220'. This horizon on shallow seismic data is a prominent reflector. Based on geophysical log interpretation.	
200	cuttings	2165-2170	10.0	CLAYSTONE	04FY2165-2175		medium gray		Minor coal fragments	
201	cuttings	2175-2185	10.0	GRAVEL	04FY2175-2185		multi-colored		Black, gray, white, yellow, brown angular to sub-angular pea gravel	
202	cuttings	2185-2195	10.0	GRAVEL	04FY2185-2195		multi-colored		Black, gray, white, yellow, brown angular to sub-angular pea gravel	
203	cuttings	2195-2205	10.0	GRAVEL	04FY2195-2205		multi-colored		Black, gray, white, yellow, brown angular to sub-angular pea gravel	
204	cuttings	2205-2215	10.0	GRAVEL	04FY2205-2215		multi-colored		Black, gray, white, yellow, brown angular to sub-angular pea gravel	
205	cuttings	2215-2225	10.0	GRAVEL	04FY2215-2225		multi-colored		Black, gray, white, yellow, brown angular to sub-angular pea gravel	Conglomerate. Meta-siltstone clasts in grain mount. Grain mount clasts include sandstone, siltstone, chert with radiolarians, and cherty argillite.
206	cuttings	2225-2260	35.0	SILTY CLAYSTONE					Silty claystone with same log appearance as 1950'-1955'	
207	cuttings	2225-2235	10.0	GRAVEL	04FY2225-2235		multi-colored		Black, gray, white, yellow, brown angular to sub-angular pea gravel	
208	cuttings	2235-2245	10.0	GRAVEL	04FY2235-2245		multi-colored		Black, gray, white, yellow, brown angular to sub-angular pea gravel	Conglomerate. Same as 04FYU2215-2225 including silicified limestone clasts exhibiting silicified sponge spicules. Quartz arenite-quartzite clasts also present.
209	cuttings	2245-2255	10.0	GRAVEL	04FY2245-2255		multi-colored		Black, gray, white, yellow, brown angular to sub-angular pea gravel. Coal fragments present.	Conglomerate. Same as 04FYU2235-2245, yet lacks limestone clasts and includes traces of white mica, chert, cherty argillite, and organic materials.
210	cuttings	2260-2287	27.0	SANDSTONE with PEBBLES					Sandy interval with pebbly sand interbeds	
211	cuttings	2255-2256	1.0	No Data						
212	cuttings	2265-2275	10.0	GRAVEL	04FY2265-2275		multi-colored		Black, gray, white, yellow, brown angular to sub-angular pea gravel. Coal fragments present.	
213	cuttings	2275-2285	10.0	GRAVEL	04FY2275-2285		multi-colored		Black, gray, white, yellow, brown angular to sub-angular pea gravel. Coal fragments present.	Epiclastic, very poorly sorted to poorly sorted medium grained sub-angular to sub-rounded radiolarian cherts. Clay and white mica
214	cuttings	2285-2287	10.0	GRAVEL	04FY2285-2287		multi-colored		Black, gray, white, yellow, brown angular to sub-angular pea gravel. Coal fragments present.	Epiclastic, poorly sorted, very coarse angular to sub-rounded sandstone to conglomerate chert and sandstone.

Oil & Natural Gas Technology

DOE Award No.: DE-FC26-06NT41248

Final Report

Five Kilowatt Solid Oxide Fuel Cell/Diesel Reformer

Submitted by:

Dennis Witmer
University of Alaska Fairbanks
ffdew@uaf.edu
907-474-7082

Thomas Johnson
University of Alaska Fairbanks

Prepared for:

United States Department of Energy
National Energy Technology Laboratory

December 31, 2008



Office of Fossil Energy



Five Kilowatt Solid Oxide Fuel Cell/Diesel Reformer Report

Final Report

Starting June 1, 2004
Ending Sept 30, 2008

Dennis Witmer
University of Alaska Fairbanks
ffdew@uaf.edu
907-474-7082

Thomas Johnson
University of Alaska Fairbanks

Report Issued December 2008
DOE Award Number
DE-FC26-01NT41248
Task Number
2.04.1

Submitted by:
University of Alaska Fairbanks
Institute of Northern Engineering
Arctic Energy Technology Development Laboratory
Building 814
Fairbanks, Alaska 99775

Disclaimer

This report was prepared as an account of work sponsored by an agency of the United States Government. Neither the United States Government nor any agency thereof, nor any of their employees, makes any warranty, express or implied, or assumes any legal liability or responsibility for the accuracy, completeness, or usefulness of any information, apparatus, product, or process disclosed, or represents that its use would not infringe privately owned rights. Reference herein to any specific commercial product, process, or service by trade name, trademark, manufacturer, or otherwise does not necessarily constitute or imply its endorsement, recommendation, or favoring by the United States Government or any agency thereof. The views and opinions of authors expressed herein do not necessarily state or reflect those of the United States Government or any agency thereof.

Abstract

Reducing fossil fuel consumption both for energy security and for reduction in global greenhouse emissions has been a major goal of energy research in the US for many years. Fuel cells have been proposed as a technology that can address both these issues—as devices that convert the energy of a fuel directly into electrical energy, they offer low emissions and high efficiencies. These advantages are of particular interest to remote power users, where grid connected power is unavailable, and most electrical power comes from diesel electric generators. Diesel fuel is the fuel of choice because it can be easily transported and stored in quantities large enough to supply energy for small communities for extended periods of time. This project aimed to demonstrate the operation of a solid oxide fuel cell on diesel fuel, and to measure the resulting efficiency.

Results from this project have been somewhat encouraging, with a laboratory breadboard integration of a small scale diesel reformer and a Solid Oxide Fuel Cell demonstrated in the first 18 months of the project. This initial demonstration was conducted at INEEL in the spring of 2005 using a small scale diesel reformer provided by SOFCo and a fuel cell provided by Acumentrics. However, attempts to integrate and automate the available technology have not proved successful as yet. This is due both to the lack of movement on the fuel processing side as well as the rather poor stack lifetimes exhibited by the fuel cells. Commercial product is still unavailable, and precommercial devices are both extremely expensive and require extensive field support.

Table of contents

Contents

Five Kilowatt Solid Oxide Fuel Cell/Diesel Reformer Report

Final Report

Disclaimer	1
Abstract	2
Table of contents	3
Executive Summary	5
Background	5
Goals and objectives	6
Selection of Fuel Cell Company	7
Selection of Reformer Company	8
Description of the INEEL Diesel Reformer.....	8
First demonstration attempt, October, 2004	10
Second Attempt.....	11
Development of the control system for the diesel reformer at SOFCo.....	18
Fuel cell demonstration program at UAF	19
Discussion and Conclusions	22
Acknowledgements.....	24
References.....	25
Appendix.....	26

List of Figures

Figure 1 Schematic of the 500 kW reformer at INEEL.....	9
Figure 2 Acumentrics Fuel Cell at INEEL, October, 2004. Energy Alternatives Jim Buckley is standing next to fuel cell unit.....	11
Figure 3 Setup in the parking lot at INEEL. Acumentrics fuel cell at left, SOFCo reformer at right. Natural gas supply in tank with wheels, the insulated line at the top is for the steam supply.....	12
Figure 4 Low Sulfur diesel label for fuel used at INEEL demonstration. Maximum sulfur content of 15PPM.....	13
Figure 5 SOFCo Diesel reformer, as installed at test at INEEL. Note the control system (named Mark) at the back end of the machine.....	14
Figure 6 Transition between natural gas and diesel reformat, showing transitions in temperature and mass flow signals.....	15
Figure 7 Graph showing some of the data collected during the run at INEEL. Here the fuel and air flows can be seen, showing the natural gas flow is shut off during the Syntroleum and ULSD runs, and the air flows are adjusted to maintain constant voltage and amperage.....	17
Figure 8 Stable operation of the Acumentrics fuel cell on Natural gas, Syntroleum Fuel, Low Sulfur Diesel fuel, and returning to natural gas, from the March 16, 2005 run at INEEL.....	18
Figure 9. Performance of new stack design, Acumentrics. Graph shoes improved voltage performance and higher achievable maximum current density for “triple chromite” configuration.....	20
Figure 10. Operation of test stack at Acumentrics, showing stable operation. X axis is time in hours, Y axis is single cell voltage in volts. Temperature is in degrees C.....	21

Executive Summary

Reducing fossil fuel consumption both for energy security and for reduction in global greenhouse emissions has been a major goal of energy research in the US for many years. Fuel cells have been proposed as a technology that can address both these issues—as devices that convert the energy of a fuel directly into electrical energy, they offer low emissions and high efficiencies. These advantages are of particular interest to remote power users, where grid connected power is unavailable, and most electrical power comes from diesel electric generators. Diesel fuel is the fuel of choice because it can be easily transported and stored in quantities large enough to supply energy for small communities for extended periods of time. This project aimed to demonstrate the operation of a solid oxide fuel cell on diesel fuel and to measure the resulting efficiency.

Results from this project have been somewhat encouraging, with a laboratory breadboard integration of a small scale diesel reformer and a Solid Oxide Fuel Cell demonstrated in the first 18 months of the project. This initial demonstration was conducted at INEEL in the spring of 2005 using a small scale diesel reformer provided by SOFCo and a fuel cell provided by Acumentrics. However, this demonstration was a temporary breadboard integration accomplished in the parking lot of a building, and lasted for only about 4 hours.

This initial demonstration was followed by other activities intended to improve the system integration and verify longer term operation. The fuel cell was shipped to Fairbanks to be operated on natural gas while waiting for the automation of the diesel reformer. The fuel cell operated for less than 40 hours before failure, was returned to the factory, then operated for just under 4000 hours before it failed again. The diesel reformer integration effort was even more problematic, as the proposing company changed management, and the funds requested in the initial proposal (\$250,000) were deemed inadequate for the necessary work by the new management.

Based on the experiences of this project, it appears that reliable, economic fuel cells operating on diesel fuel are still unavailable, and precommercial devices are both extremely expensive and require extensive field support. It is not clear if or when these devices will be developed to a point suitable for use in remote communities in Alaska.

Background

Even at the beginning of the 21st century, much of Alaska remains remote and undeveloped, unconnected to either the road system or to the electric power grid. Those who live in these remote areas of Alaska depend on diesel electric power generators, and their power costs are far higher than those of typical US consumers, with recent rates

exceeding \$1.00 per kW-hr in some communities. Environmental concerns are also an issue, both particulate emissions from the diesel exhaust, and the contamination of water supplies from spilled fuel [1].

In the late 1990's, Polymer Electrolyte Membrane (PEM) fuel cell suppliers (the type of fuel cells used in automobiles and busses) became interested in the rural Alaska energy problem as a possible ideal application for their products[2]. Small scale fuel cells are much quieter than internal combustion engines and could be placed in individual residences, and the waste heat from the fuel cell could be used to supply heat to the residence. However, after testing PEM fuel cell systems provided by several suppliers, it became apparent that these fuel cells were considerably less efficient than promised (22% rather than 40%) [3-5], and that they did not have the desired longevity, lasting a year at best [6]. Diesel reforming also proved problematic, and no long term demonstrations were successfully conducted on these fuels. However, diesel reformers provided by Idatech and by Dias Analytic were delivered and tested, though the performance period from each unit was only about 50 hours [2].

Solid Oxide Fuel Cells have been demonstrated for longer periods of time and have been shown to have better performance [7], with lifetimes of 68,000 hours (8 years) and efficiencies of 49% on natural gas. The DOE SECA program was designed to help the industry to develop commercial product and address basic research and development issues [8]. A demonstration was conducted in Fairbanks on a 5 kW SOFC provided by Fuel Cell Technologies of Kingston Ontario, with a successful run of 9200 hours on natural gas [9]. Conversations with industry representatives indicate that hydrocarbon reforming was proceeding, and that integrating a SOFC fuel cell and diesel reformer into a single unit could be done, but that the best fuel cell technology and reforming technology might not from the same suppliers.

Goals and objectives

The goal of this project was to advance the state of the art in fuel cells that could operated on logistical fuels. Solid Oxide fuel cells appeared to be more attractive than lower temperature fuel cells due to the high operating temperatures, so that the heat provided from the fuel cell would be of use for the reformation reaction. The project was proposed to proceed in three phases:

1. Demonstration of a 5 kW SOFC operating on diesel reformatte provided by the INEEL 500 kW diesel reformer (funded by the US Navy)
2. Development of a diesel reformer appropriately sized for use with the 5 kW SOFC .
3. Breadboard integration of the fuel cell and reformer.

While the ultimate goal of any program of this kind would seem to be the complete integration of the fuel cell and diesel reformer, it was quite apparent from discussions with suppliers that this integration required considerable attention to the details of integration to allow for proper heat and mass transfer to occur. Given the fact that the best reformer technology and the available fuel cells were not from the same company,

and that intellectual property issues were involved in the integration of the two, this project moved forward with more modest expectations, with the integration of the two parts only at a laboratory breadboard integration. This was intended to be a proof of concept, and allow information to be collected on the operation of the fuel cell and reformer, but not to be a finished product. One thing of interest was the heat management of the fuel cell, as SOFCs operating on natural gas use steam reforming, which is an endothermic reaction, cooling the system. In the proposed diesel reformer/fuel cell breadboard test, the reformation reaction occurs outside the fuel cell envelope, which means that additional air flow is required to maintain fuel cell temperature.

Selection of Fuel Cell Company

There are several potential suppliers of solid oxide fuel cells, but there are no solid oxide fuel cells that could currently be considered commercial devices (fixed price, fixed delivery date, fixed specifications and a warranty). The DOE SECA program[8] focusing on the development of solid oxide fuel cell systems was promoting the basic R&D of small scale SOFC systems, and their integration into 5 kW test packages, and so the participants in that program seemed to be the most likely sources for fuel cells.

UAF had previous experience with the products from Fuel Cell Technologies (FCT) of Kingston, Ontario, and was quite impressed with the system quality, efficiency and operating reliability of those systems. At the beginning of this program, however, FCT was experiencing difficulties in obtaining fuel cell stacks from their supplier to integrate into their system, and found itself unable to meet its commitments to its customers. When asked to provide a quote for a system for this program, the number given was about \$300,000—quite a handsome sum for a 5 kW power generator.

A second supplier, Acumentrics, of Westwood, Massachusetts (near Boston) actively pursued this proposed project, and was willing to provide a fuel cell at \$200,000 (quite a bit lower than FCT, but still a lot of money for a small generator). Acumentrics was a small electronics firm providing ruggedized uninterruptible power supplies to the military, but purchased SOFC technology from a group of New Zealand developers. The technology being developed at Acumentrics focused on low cost manufacturing techniques using small scale tubes, deposition of material layers with ceramic slurries, and slightly lower operating temperatures than some other SOFC systems.

Other fuel cell suppliers were also considered, including SECA participants such as Delphi, who is developing a planar SOFC. Rolls Royce Fuel Cell division was also approached. However, these companies were unwilling to provide a quote for a small scale unit for this program.

Based on cost and availability, Acumentrics appeared to be the best supplier for the SOFC, and was included in the original proposal.

Selection of Reformer Company

UAF has had some experience with diesel reforming in the past, and has developed a healthy respect for the difficulties in this task. While the transformation of natural gas to syngas is a routine operation in many petroleum refineries, and, in theory, any carbon source including coal or biomass can be converted to syngas, the development of small scale diesel reformers has proved problematic. The main issues is the complete vaporization and mixing of the diesel fuel with the reacting air or steam. In small scale reactors sized to match small fuel cells, the surface to volume ratio is large, and the probability of developing cold spots on walls is high, resulting in localized carbon deposition, which in turn nucleates the formation of more carbon. Once solid carbon forms, it is difficult to remove, as it is thermodynamically stable in the reducing environment of the reformer. Once it begins to form, it grows to cover the catalytic surfaces of the reactor bed, and eventually plugs the flow channels, stopping the reactor.

The US DOE Energy and Efficiency division spent considerable effort in 2001-2004 attempting to develop an on-board gasoline reformer for fuel cell powered vehicles. This strategy had the advantage of being able to use the conventional fueling infrastructure currently available in the US while also enabling the transition to hydrogen fuel cell power. However, entry into this market required that the resulting vehicles perform in ways similar to conventional automobiles, including rapid starts, reasonable fuel economy, and packaging of the systems within the expected envelope of a normal automobile. This effort was reviewed in 2004 and the program was canceled as the issues identified were deemed beyond the resources of the program at that time, and the focus shifted to on board hydrogen storage for automotive use.

One of the participants in the DOE EE program was SOFCo EFS, a division of McDermott, located in Alliance, Ohio. This company had been working on the problem of diesel reforming since the 1994, and had invested about \$60M in research in this area. During a site visit to the facility in March of 2002, a 50 kW gasoline reformer was installed in the laboratory for evaluation. Discussions indicated that this reformer worked well on gasoline, but the start-up times and the volume constraints required by the DOE were not met. However, it was indicated that operation on diesel fuel for stationary applications would be possible.

During the Fuel Cell Seminar in November, 2002, Lyman Frost from SOFCo and Robert Carrington from INEEL indicated interest in testing a SOFC on a slipstream from the diesel reformer currently being built at INEEL. This device was intended to operate a 500 kW PEM fuel cell, but that fuel cell had proved to be unobtainable.

Description of the INEEL Diesel Reformer

Phase 1 of this project was intended to show that a fuel cell system could operate on a reformat stream from diesel fuel. The original plan was to use a slipstream from a 500

kW diesel reformer being built at Idaho National Engineering and Environmental Laboratory, with funding from SOFCo and the Navy in October, 2004.

The development of this reformer was funded largely through a Navy program intended to demonstrate fuel cells for use on board ships. The Navy is particularly interested in providing auxiliary power to their ships for several reasons, both for use in port, and as a backup system to decrease vulnerability during battle. This project began in the late 1990s when PEM fuel cell manufacturers were promising compact, inexpensive fuel cells to be used in transportation applications[10]. A 500 kW fuel cell was proposed as being of the right size for urban bus applications, so the diesel reformer was sized to match.

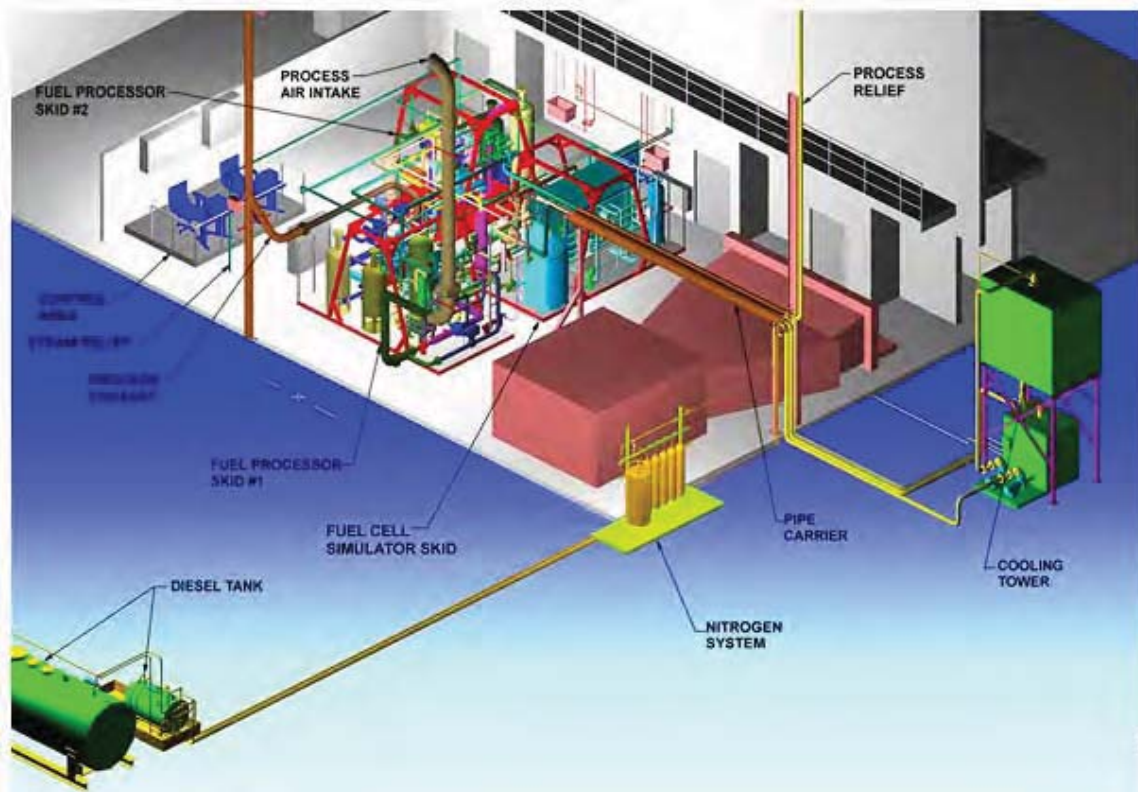


Figure 1 Schematic of the 500 kW reformer at INEEL.

By the time AETDL became involved with this project, the actual PEM fuel cell intended for the demonstration had been replaced with a simulated fuel cell—a reactor chamber that converted the reformat into heat and an exhaust stream similar to that from a fuel cell.

INEEL expressed interest in using a slipstream from the reformer to supply the 5 kW SOFC to demonstrate that the reformer could work with a fuel cell. The SOFC is actually an easier match with the diesel reformer, as SOFCs are more tolerant of carbon monoxide (SOFCs will convert CO and steam to Hydrogen and CO₂ in a spontaneous reaction inside the fuel cell stack, while PEM fuel cells are poisoned by CO levels above a few parts per million).

First demonstration attempt, October, 2004

The first attempt to demonstrate the operation of the Acumentrics Solid Oxide fuel cell operating on a slipstream of the INEEL 500 kW diesel reformer was conducted in October 2004. This date was chosen as it coincided with the time scheduled for a 100 hour test (approximately 1 working week) to demonstrate the stable operation of the diesel reformer as an important milestone in the Navy program.

The Acumentrics fuel cell was shipped to Idaho Falls in anticipation of the demonstration, and UAF personnel traveled to witness the demonstration and collect data.

Upon arrival at the INEEL facility, it became apparent that the expected level of progress had not been achieved. The reformer had been assembled, and filled a large bay of a building with hundreds of feet of piping and insulated reactor beds. A computerized control system had been built for both control and data acquisition. The fuel cell feed was installed as a port in the piping system at the appropriate point to divert about 1% of the total gas stream to the fuel cell.

However, this reformer failed to operate in a stable manner, and we were unable to demonstrate operation of the fuel cell from this reformer. The major reason for this appeared to be the instability created by dynamic issues related to the separation of the compressor and turbine used to move gasses through the system. In a typical turbine engine, there is a very small volume and no restrictions in the combustor zone, so increasing the fuel flow to the engine results in a very rapid increase in power delivered to the turbine, increasing the air flow into the system. This results in a stable acceleration of the engine. In the INEEL diesel reformer, a total of 200 feet of large diameter piping and 6 packed reactor beds had been installed between the compressor and the combustor. This created a large lag time between the addition of fuel to the system (into the first packed bed) and the subsequent arrival of this energy at the turbine. In fact, when diesel fuel was initially injected into the system, this fuel needed to be vaporized, increasing the backpressure on the compressor, but the fuel value of the fuel did not appear at the turbine until much later, perhaps minutes later. This made the reformer almost impossible to control (at a public meeting, one of the operators described running the system “like juggling snakes”, and when asked who designed the turbine he replied “Satan himself.”) Also contributing to the difficulty in controlling the system was the use of pneumatic valves for control (for safety reasons), which resulted in sluggish controls.

The fuel cell fared slightly better in this initial start-up attempt, with some shipping damage to the insulation package around the fuel cell stack noted. Also, during fuel cell start-up on natural gas, CO was detected inside the laboratory that was traced to the exhaust from the fuel cell (about 60 ppm was measured in the exhaust).



Figure 2 Acumentrics Fuel Cell at INEEL, October, 2004. Energy Alternatives Jim Buckley is standing next to fuel cell unit.

The attempt to run the fuel cell on a slipstream from the 500 kW reformer were abandoned after three days. The fuel cell was put back in the shipping crate and returned to the Acumentrics factory for repairs.

Attempts were made to operate the reformer for several weeks after the attempt to run the fuel cell, but the longest sustained run of the reformer was for 40 minutes.

Second Attempt

During a meeting at the Fuel Cell Seminar in November, 2004, a new demonstration strategy was developed, using a smaller 20 kW diesel reformer built by SOFCo at their Alliance OH facility, which would be shipped to INEEL for a demo. This was planned for early in January, 2005.

The Acumentrics fuel cell was returned to the factory, repaired, and a factory acceptance test was conducted during the last week in December, 2004 to verify that the fuel cell was operating properly.

SOFCo delayed shipping the diesel reformer, however, and so the demonstration was planned for mid March, with all participants being on site between March 14-16, 2005.

The diesel reformer and fuel cell were installed just outside the building at INEEL where the large diesel reformer was operating, in order to make use of some of the instrumentation installed for the larger unit.

Initial startup of the fuel cell and diesel reformer were attempted on Monday, March 14, with much of the day occupied with calibrating the mass flow lines needed for the diesel reformer. On Tuesday March 15, both the diesel reformer and the fuel cell were operational by mid afternoon, the fuel cell operating on natural gas, and the diesel reformer operating on low sulfur diesel, and a short test of about 45 minutes was conducted, with operation continuing long enough to approach thermal equilibrium.

On Wednesday, March 16, the fuel cell and diesel reformer were both started early, with the fuel cell operating on natural gas during the warm up (to baseline the fuel cell at the altitude) and the diesel reformer started on Syntroleum S2 fuel (no lubricity additive). After about 2 hours of independent operation, the reformat stream was directed into the fuel cell, and the system was operated on this fuel for about 2 hours. The feedstock for the diesel reformer was then switched to the low sulfur diesel fuel, and the system operated for another 2 hours to collect equilibrium data in this configuration.



Figure 3 Setup in the parking lot at INEEL. Acumentrics fuel cell at left, SOFCo reformer at right. Natural gas supply in tank with wheels, the insulated line at the top is for the steam supply.

It must be noted that there were some issues of concern in this demonstration. First, while the reformer was identified as a CPOX (Catalytic Partial Oxidation) device, these normally operate without the addition of steam, this reformer required steam for fuel vaporization. The addition of steam is also beneficial for the prevention of coking in reformers. However, requiring steam makes the technology less desirable from a remote field application viewpoint, as pure water is difficult to provide. This issue may disappear in a final version of the system where water vapor from the fuel cell exhaust could be used, as long as the mass flow balance could be shown to work.

A second issue is the efficiency demonstrated—the reformer was sized a bit bigger than the fuel cell, with about 9kW of diesel fuel flowing into the system, while the fuel cell was providing about 1.5 kW electrical energy out. This means that the fuel utilization during the demonstration was quite low, and further development is required if higher efficiencies are to be achieved.



Figure 4 Low Sulfur diesel label for fuel used at INEEL demonstration. Maximum sulfur content of 15PPM.

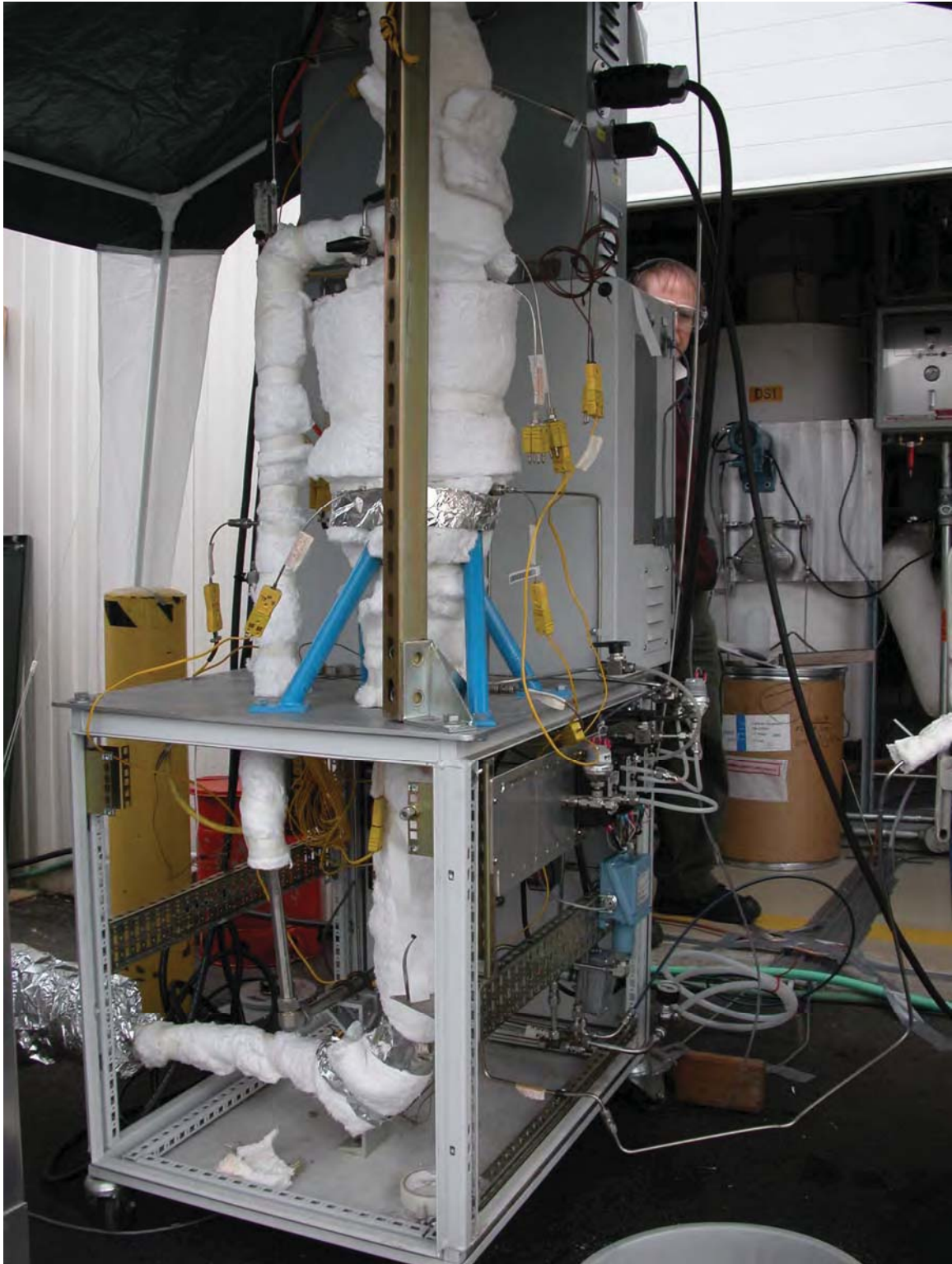


Figure 5 SOFCo Diesel reformer, as installed at test at INEEL. Note the control system (named Mark) at the back end of the machine.

Also, during the demonstration, the carbon monoxide detectors inside the building adjacent to the fuel cell and reformer indicated higher than normal readings. A portable detector was used to locate the source of this gas, (the reformer produces large amounts of CO during its normal operation, but this should be consumed in the fuel cell and converted to CO₂, but a leak could result in large amounts of CO being released into the atmosphere), and was found to be coming from the exhaust of the fuel cell. This was not expected, as the fuel cell should have been converting all the CO into CO₂ in the combustion zone after the fuel cell. (Later testing showed that the CO was actually leaking from the fuel cell stack area, due to incomplete sealing of the hot zone of the area).

However, the good news during this demonstration was that the fuel cell operated as expected, meaning that a steady output was obtained from the fuel cell during operation on both natural gas and the reformat stream from the small SOFCo reformer. The fuel cell was operated for a total of nearly six hours, with initial start up on natural gas, followed by stable operation on low sulfur diesel fuel and Syntroleum synthetic diesel fuels. The operation on the reformat gas required some adjustments in the air flow to the fuel cell, as internal reforming was not being done inside the fuel cell boundary, but these adjustments were made without difficulty. [11]

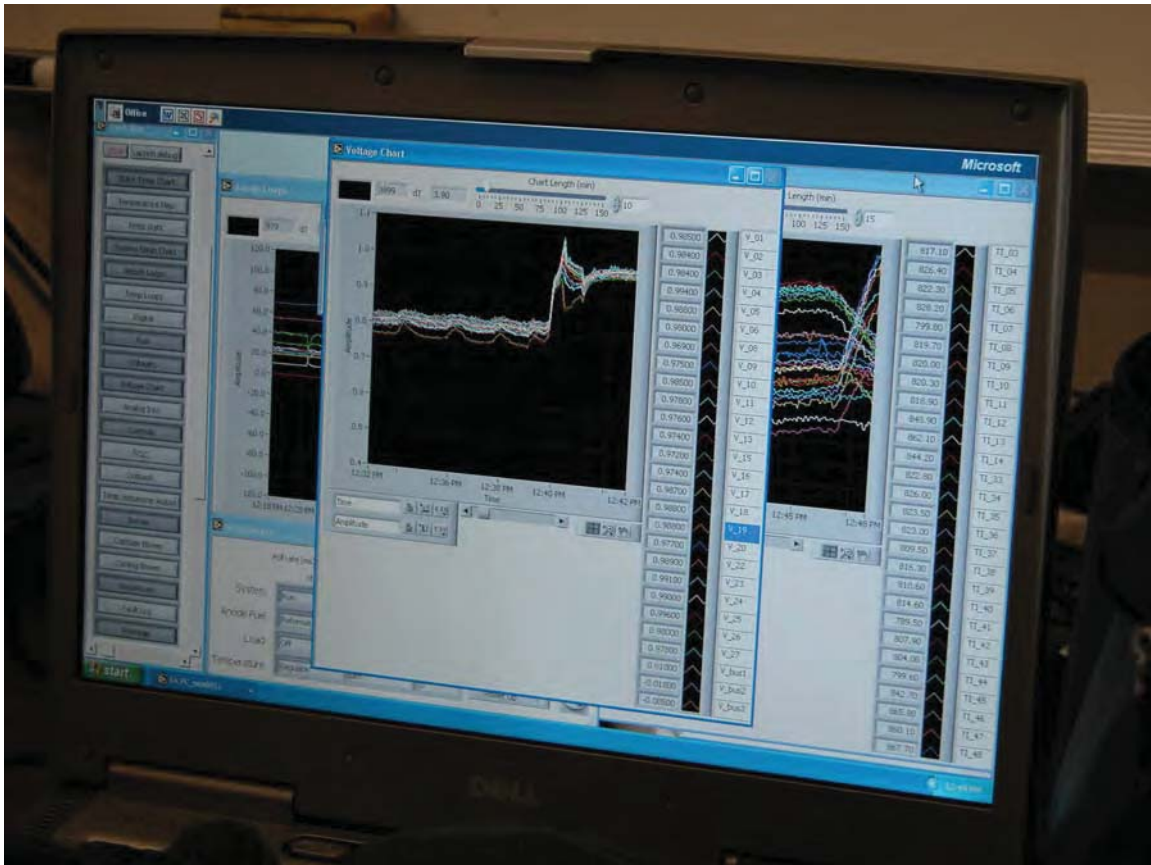


Figure 6 Transition between natural gas and diesel reformat, showing transitions in temperature and mass flow signals.

A press release was generated that very carefully stated that a successful demonstration had occurred:

Press Release Language

The US Department of Energy, The Arctic Energy Technology Development Laboratory (AETDL), the Department of the Navy, the Idaho National Engineering and Environmental Laboratory (INEEL), Acumentrics Corporation, and SOFCo Corporation successfully demonstrated the operation of a Solid Oxide Fuel Cell on reformat from diesel fuel on March 16, 2005 at INEEL in Idaho Falls, ID. This demonstration was part of a continuing effort to use readily available fuels to create electricity using highly efficient fuel cell technology.

During the demonstration, operation on two fuels was demonstrated, including conventional diesel fuel manufactured to the new EPA 2007 low sulfur spec, and a Fischer Tropsches synthetic fuel made by Syntroleum Corporation of Tulsa, Oklahoma. Both the fuel cell and reformer were stable on these fuels.

The efficiency measured during this demonstration was not at a desirable level—the reformer was sized a bit bigger than the fuel cell, with about 9kW of diesel fuel flowing into the system, while the fuel cell was providing about 1.5 kW electrical energy out. This means that the fuel utilization during the demonstration was quite low, and further development is required if higher efficiencies are to be achieved. In addition, some parasitics in the system (most notably the need for external steam for the reformer) were not accounted for in the demonstration evaluation (this function was intended to be incorporated into the final reformer design).

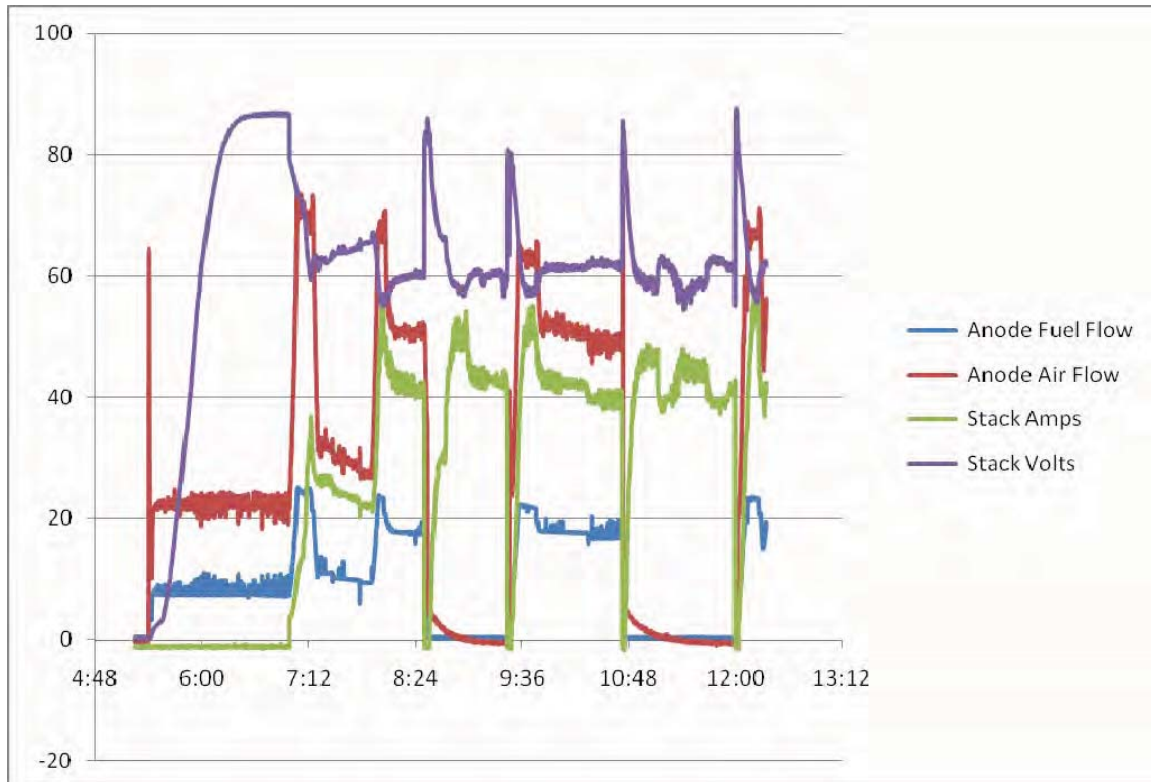


Figure 7 Graph showing some of the data collected during the run at INEEL. Here the fuel and air flows can be seen, showing the natural gas flow is shut off during the Syntroleum and ULSD runs, and the air flows are adjusted to maintain constant voltage and amperage.

In one sense, this demonstration met the “laboratory breadboard” demonstration goal listed as the end result in our initial proposal. However, there was also ample evidence of the need for additional work. The outstanding issues included automating the reformer to allow for continuous operation without the presence of an experienced operator, and conducting a long term test of at least 1000 hours to verify stable operation of the fuel cell stack on diesel reformat.

The project team then proposed continuation of the project towards a longer term demonstration of the reformer and fuel cell, to occur in Fairbanks. This proposal included two major pieces: development of the control system for the diesel reformer, and long term demonstration of the operation of the SOFC.

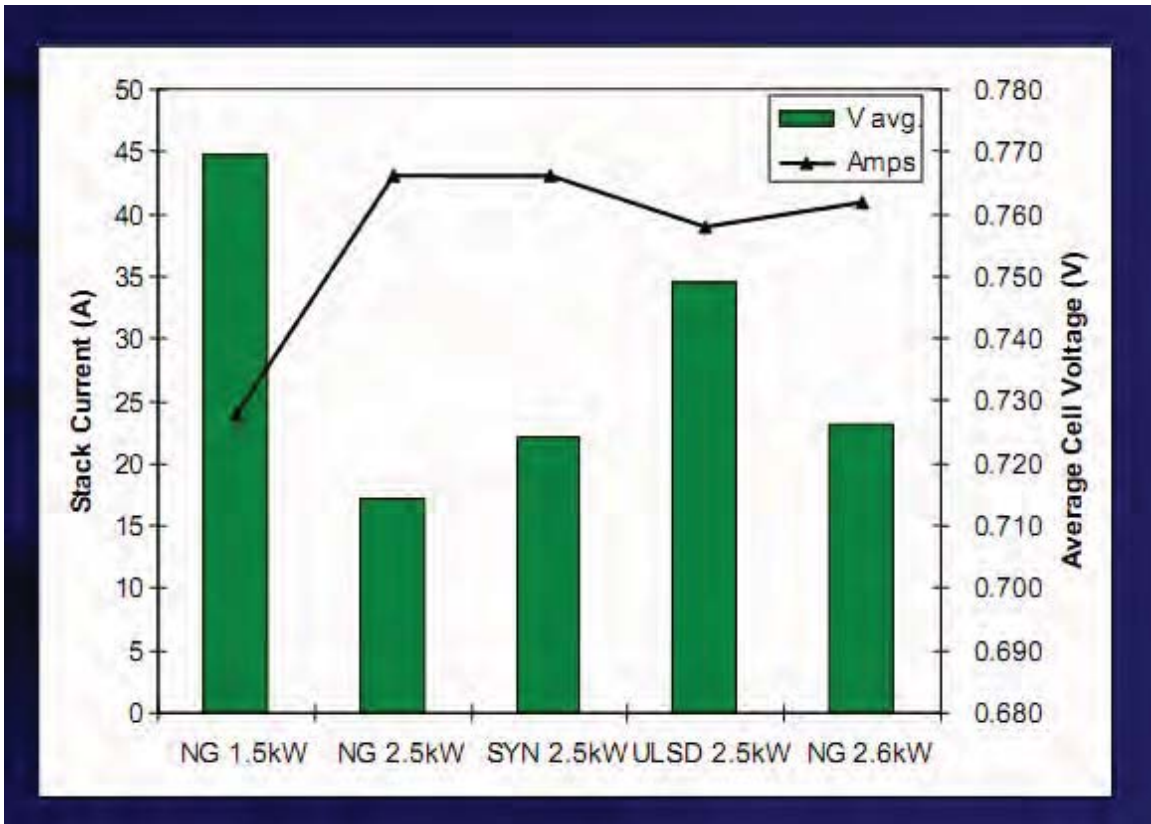


Figure 8 Stable operation of the Acumentrics fuel cell on Natural gas, Syntroleum Fuel, Low Sulfur Diesel fuel, and returning to natural gas, from the March 16, 2005 run at INEEL.

Development of the control system for the diesel reformer at SOFCo

In the initial proposal to the USDOE through the Arctic Energy Office at UAF, phase 1 of the demonstration was intended to be operation of the fuel cell on a slipstream from the 500 kW diesel reformer at INEEL, and phase 2 was for the development of a small scale diesel reformer by SOFCo, of Alliance Ohio.

After the successful operation of the small diesel reformer at INEEL, discussions were held with SOFCo about the scope of work for the development of the small diesel reformer. SOFCo has been involved in liquid hydrocarbon reforming for many years, and was a major participant in the US DOE EE program to develop on board reforming of gasoline for fuel cell powered vehicles in the early part of this decade. However, this program was abandoned when it became apparent that on board reforming was unlikely to meet some of the stringent requirements for operation on a vehicle, including weight, start up times, and gas purity.

SOFCo was also involved with the state of Ohio in developing an small SOFC system intended to provide auxiliary power to large trucks, especially for operation when the

trucks are not on the road (many truckers simply leave the engine at idle to provide power electrical power to the truck cab while the driver rests). Initial discussions with SOFCo centered on ways to combine the goals of these two projects so that a single development effort could result in deliverables for both programs, leveraging funding on both sides.

A sub-award document was prepared by UAF contracting with a \$250,000 budget and a performance period of 14 months, beginning in January, 2006, with delivery of the completed reformer to UAF for testing in the spring of 2007. Based on preliminary discussions between contracting groups, it was expected that this subaward SOW would be signed and returned quickly. However, this did not occur.

After several months, it became clear that SOFCo was not able to sign the subaward due to negotiations over the sale of the company. The existing management was unwilling to sign documents committing the company to the deliverables, but did indicate that the funds available in this award were part of the negotiations.

In April of 2007, it was announced that the new purchaser of SOFCo was Rolls Royce Fuel Cells. Given the interest that this company indicated in diesel reforming, it was expected that the sub-award would quickly be signed and returned to UAF. However, this did not occur. After several phone calls and discussions with the new management, it became clear that the issue was the new management considered the level of funding inadequate for completion of the proposed work. Rolls Royce proposed a budget requiring more than double the previously negotiated funding levels. Since this amount was considerably more than the funding available in the project, discussions were held with the USDOE Arctic Energy Office and NETL over a possible increase in the project budget to fund this effort. No funds were approved for this increase, so the sub-award documents were never signed.

Fuel cell demonstration program at UAF

After the successful completion of the operation of the Acumentrics fuel cell on diesel reformate in the INEEL parking lot, the fuel cell was put back into the shipping crate and shipped to Fairbanks. At this point in time, it was fully recognized that the delivery of the diesel reformer was some time away, but Acumentrics stacks had only been demonstrated for a maximum of 1500 hours. A decision was made to attempt to operate the fuel cell on natural gas while waiting for the delivery of the diesel reformer.

The fuel cell was installed at the Fairbanks Natural Gas facility in south Fairbanks, as the required utilities (natural gas, electrical supply, internet connections, exhaust lines, and waste heat recovery systems) were already installed, but the test site was vacant due to the recent failure of the FCT unit.

The unit was started on March 30, 2005, but ran for only 12 hours before it experienced a shutdown. A restart of the unit was attempted on April 6, but the unit did not start. Examination of the unit resulted in the discovery of a failed air supply fan, which was

replaced. A new fan was shipped, and a restart attempt occurred on May 5, 2005. During this attempt, a backfire occurred traceable to backpressure in the exhaust line, which caused instabilities within the fuel cell unit and a backflash of hot gases through fans designed only for ambient air. These fans melted, and needed to be replaced. In addition, a fan was placed in the hot exhaust line to lower the backpressure at the unit.

On May 16, the unit was restarted again. During start-up, it was noted that the fuel control valve was not functioning properly, but Acumentrics reps suggested that we open the valve full throttle and run anyway. The unit operated for about 12 hours before a voltage instability developed on one row of cells, indicative of a stack failure. Acumentrics did not seem particularly interested in repairing the stack.

In the fall of 2005, Acumentrics contacted UAF proposing to rebuild the fuel cell with a newly designed stack configuration. This new design was intended to shorten the electrical path between cells, reducing the ohmic losses in the stack, improving the efficiency of the system.

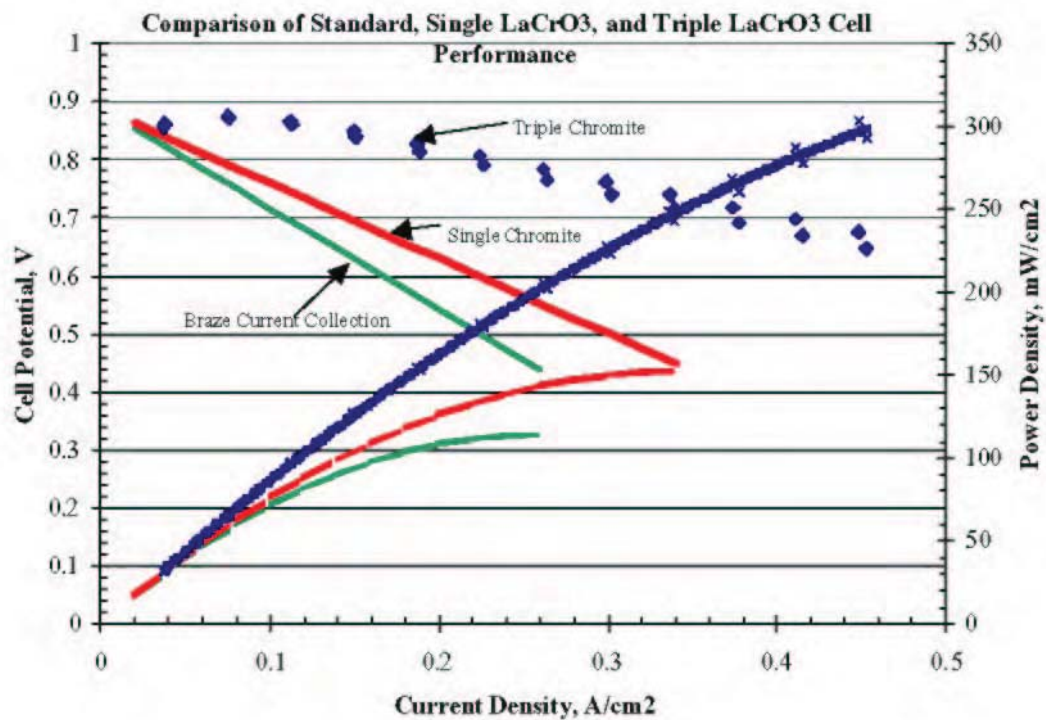


Figure 9. Performance of new stack design, Acumentrics. Graph shows improved voltage performance and higher achievable maximum current density for "triple chromite" configuration.

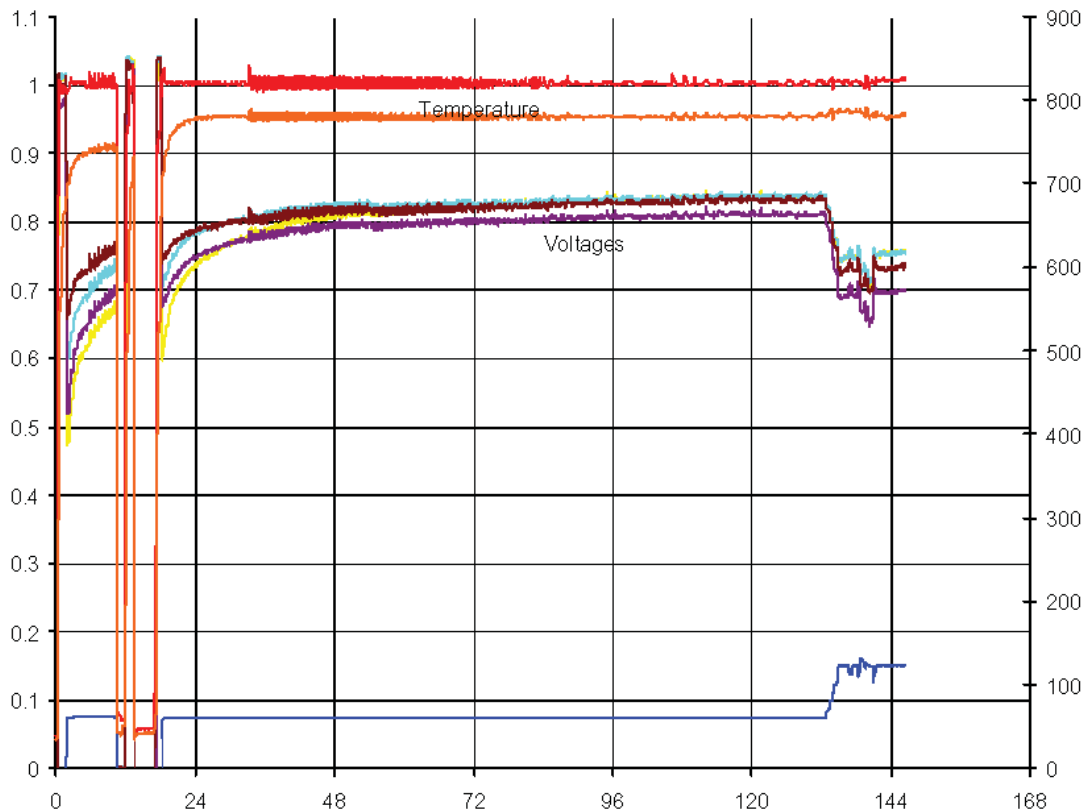


Figure 10. Operation of test stack at Acumentrics, showing stable operation. X axis is time in hours, Y axis is single cell voltage in volts. Temperature is in degrees C.

After some discussions and approval from DOE, the unit was shipped back to the factory for the rebuild in the Spring of 2006. The unit was rebuilt during the fall of 2006 and returned to Fairbanks in December of 2006 after a factory acceptance test.

The unit was started again on January 2, 2007. The details of this run are included in Appendix A. However, some general comments can be made.

First, the efficiency of the fuel cell operating on natural gas was much lower than expected—during the best run, near the beginning of the life of the fuel cell, the efficiency (based on total natural gas in to AC electricity out to the building) was 19.8%. During the longest run of 2700 hours, the efficiency was measured at 17.8%. Secondly, the fuel cell operated for a total of 3968 hours before the stack failed. While this is a considerable improvement from previous fuel cells developed by Acumentrics, it still falls far short of the 40,000 hour goal frequently stated as necessary for commercial markets.

After the stack failure in October 2007 discussions were held with the Acumentrics staff about what should be done with the unit. The AETDL process was nearing an end so additional funds were not available. It was apparent that operating a fuel cell on diesel fuel was not likely to happen. Also, the Acumentrics unit at Exit Glacier operating on propane experienced a stack failure, and could not be operated, and the Acumentrics factory was no longer supporting the cell design used in that stack. There were some funds left available for continued work, but not enough to support both projects. The decision was made to repair the stack in Fairbanks, but to operate it at Exit Glacier during the summer of 2008 on propane. The results from that demonstration can be found in the final report on that project. [12, 13]

Discussion and Conclusions

This results of this program can be best described as a mixed success. A solid oxide fuel cell was delivered to the program, and it operated on reformat from low sulfur diesel products for a few hours. A run of about 4000 hours was achieved on a small scale SOFC operating on natural gas.

However, the inability to achieve many of the aims of the program should also be noted: the initial attempt to operate fuel cell on the 500 kW diesel reformer failed because the reformer did not operate in a stable manner. The successful diesel demonstration lasted only a few hours. The fuel cell failed quickly after the initial demonstration when operated on natural gas. The reformer was not automated due to changing requirements for funding of this task. The rebuilt fuel cell achieved only about half the advertised efficiency (20% achieved compared to the 40% promised). These results demonstrate that the fuel cell industry has a long way to go before fuel cells will be inexpensive, reliable, and capable of replacing other technologies in commercial markets.

These results are consistent with others in the industry. Diesel reforming with Solid Oxide fuel cells was the focus of sponsored research during the early parts of this decade [14-17], but a web search at the time of this writing did not indicate much recent activity in this field. The waning enthusiasm for fuel cells in general and diesel reforming in particular is unfortunately traceable to the results obtained from programs such as this one.

The inability of the industry to develop commercial products is perhaps best indicated by the public announcement in June 2007 of the attempted sale of the Siemens Fuel Cell division. This group has been active in SOFC R&D since the mid 1970s, and has achieved many scientific and technical demonstration successes, and total corporate and government investment in this company is rumored to be well over one billion dollars. In 2000, they announced the building of a factory to produce hundreds of fuel cell systems per year for commercial deployment.

The reasons for this slow progress towards commercialization are many, but it is worth considering the differences between fuel cells operating on hydrocarbon fuels as compared to conventional combustion technologies.

For a combustion device such as a diesel generator or a gas turbine, the combustion reaction is a homogenous gas phase reaction that occurs when fuel and air are mixed and ignited. If one of these components is removed, the reaction stops, but usually the system simply stops with no permanent damage to the hardware. The engines are self aspirating, meaning that they pull in their own air supply by creating a vacuum by mechanical means. And the systems are robust with respect to the presence of impurities: the worst that usually happens if minor impurities are put into the system is that environmentally unfriendly products may result (think of acid rain caused by sulfur in fossil fuels), but the system continues to operate (an important safety feature in aircraft engines). The thermodynamic efficiency depends on the maximum temperature achieved, but this occurs in the gas phase, and the containing structures (the piston and cylinder walls in a diesel engine) remain much cooler, allowing the use of ordinary engineering materials (steel, cast iron, or even aluminum). And the combustion systems are compatible with a wide variety of naturally occurring hydrocarbon fuels, from natural gas to coal.

Fuel cells are electrochemical reactors, where air and fuel need to be supplied to reacting surfaces under carefully controlled conditions of temperature and pressure. The entire fuel cell stack must be maintained at temperature, so all materials used in the system must be capable of surviving on a long term continuous basis (at 800 degrees C, the temperature of solid oxide fuel cells, most metals experience rapid high temperature oxidation corrosion). The system is not self aspirating, so air must be supplied through an external blower or compressor (so much for the myth of no moving parts), and even short term interruptions in fuel or air can result in major damage to the system through chemical attack or thermal shock. Impurities are a major problem, as these impurities may block catalytic sites necessary for the gas-solid phase reactions. Small defects in the individual cells may create shorts, and the failure of a single cell is sufficient to stop the operation of the entire system. Care must be taken in starting and stopping the system to avoid thermal shock, although thermal cycling itself is somewhat damaging to the system. Hydrocarbon fuels do not react directly in fuel cell systems, so naturally occurring fuels must be reformed into hydrogen and carbon monoxide (syngas) in order to be used by the fuel cell.

The reforming reactions are complex, involving a mixture of a hydrocarbon, oxygen, and steam, but the exact reaction products are a complex function of temperature, pressure, flow rate, mixture ratios, hydrocarbon structures, and impurities. Natural gas is by far the easiest fuel to reform, but even this fuel in commercial purities contains sulfur in levels sufficient to contaminate many fuel cell systems. Heavier hydrocarbons, especially diesel fuels containing aromatic compounds, are especially difficult to reform, as the heavier molecules may condense out on cold wall surfaces and nucleate the formation of solid carbon particles, otherwise known as soot formation. This soot can quickly plug the channels in the reformer, stopping the reaction and the fuel cell. Soot formation can be suppressed by adding additional steam to the system, but creation of the steam is an energy parasitic on the system. In order for diesel reformers to be usable, they must be compact and cheap as well as efficient, but successful operation of diesel reformers to date have not included these attributes.

The successful commercial use of fuel cells requires that all these issues be addressed in a single system. There are no fundamental chemistry or physics laws preventing success, but the engineering challenges are daunting. In particular, the use of high purity exotic materials in fuel cells and reformers, the complex manufacturing processes needed to fabricate them, the intolerance of these systems to impurities, and the long lead time needed to prototype and test these systems all drive the development costs to very high levels. Given the billions of dollars that have been invested to date, it seems appropriate to evaluate the progress achieved and the cost, and compare to the future investments that need to be made if this technology is to succeed.

The goal of the Alaska Arctic Energy Technology Development Program was to determine if fuel cells are of use to the people living in remote communities as a more reliable and economic way of providing energy to residents of these communities. Based on the activities in this project, it appears that that the answer to this question is—not yet.

Acknowledgements

Special thanks to the industry partners and their employees who provided their skills and hardware to the program. These include:

SOFCo: Laurie Wessel, Thomas Flynn, and George Farthing

INEEL: Robert Carrington, Bob Cherry, and Lyman Frost

Acumentrics: Norm Bessette, Doug Schmidt, Tony Litka, and Rheese Foster

Energy Alternatives: Jim Buckley

Rolls Royce Fuel Cells: Mark Fleiner

-
- [m.](#)
8. SECA. *SECA Web Page*. 2006 [cited; Available from: <http://www.netl.doe.gov/technologies/coalpower/fuelcells/seca/>].
 9. FCT, *Press releases from www.fct.ca*. 2003.
 10. Frost, L. *Diesel Reformation at INEEL*. in *Alaska Rural Energy Conference, Fairbanks, Alaska, September 2002*. 2002.
 11. Schmidt, D., *Status of the Acumentrics SOFC program*, in *2006 Fuel Cell Seminar*. 2006: Honalulu, HI.
 12. Acumentrics. *Press Release 2008* [cited 2008 12/17/2008].
 13. Witmer, D., Thomas Johnson, Jack Schmid, *Analysis of Actual Operating Conditions of an Off-grid Solid Oxide Fuel Cell*. 2008, Arctic Energy Technology Development Laboratory: Fairbanks.
 14. Borup, R., Michael Inbody, Jose Tafoya, Dennis Guidry, and Jerry Parkinson, *Diesel Reforming with SOFC Anode Recycle*. The Electrochemical Society, 2004. **205 Meeting**.
 15. Borup, R., Michael Inbody, Jose Tafoya, Dennis Guidry, and Jerry Parkinson, *Diesel Reforming (for Solid Oxide Fuel Cell APU's)*. Los Alamos 2005.
 16. Di-Jia Liu, S.-H.S., & Michael Krumpelt, *Diesel Reforming for Solid Oxide Fuel Cell Application*. 2005: SECA Core Technology Peer Review Workshop, Tampa, FL.
 17. INL, D.N.R. *INL tests advanced fuel cell technology for industry*. 2005 [cited.

APPENDIX

Acumentrics Fuel Cell Demonstration Fairbanks

Run number: 1

start	1/4/2007 2:04:00 PM	Hours	48.816666	
				Efficiency: 10.78%
stop	1/6/2007 2:53:00 PM	Cumulative Hours	48.816666	
Electric start:	17335	Electric Meter end:	17410	Total kW hours 75
Gas meter start:	0	Gas meter end:	24	Gas x 100 tt3 24

Start up

Jim Buckley here for start up. Unit experienced rapid on-off cycling of start-up burner, issue solved by changing low temperature set point for burner start up. Significant odor detected from unit during start up.

Running notes:

Unit continued to give off a significant amount of irritating fumes during operation, CO sensors in room gave readings of up to 60 PPM CO during operation. Also, heat recovery coil was plugged, but the decision was made to deal with this issue during the next shutdown. Unit was not visible on the internet, Acumentrics personnel had no access to unit while running.

Shut down notes:

Unit shut down due to erratic cell voltage on two adjacent cell voltage taps. Data set revealed one cell at a negative voltage, the adjacent at nearly 2 volts, most likely due to loss of contact on lead.

Repair notes:

Cell voltage issue discovered to be incomplete crimping of lead to voltage tap. Wire was reattached with new crimp fitting, all other fittings checked for adequacy of crimping. Also installed internet access lines for communications, and attempted to rearrange insulation to prevent carbon monoxide from getting into building. Also replaced heat exchanger on top of fuel cell.

Planned Routine maintenance
Manufacturing defect

Control System
Balance of plant failure

Stack failure
Low Cell Voltage

Acumentrics Fuel Cell Demonstration Fairbanks

Run number: 2

start	1/31/2007 3:14:00 PM	Hours	502.41666	
				Efficiency: 19.82%
stop	2/21/2007 1:39:00 PM	Cumulative Hours	551.23333	
Electric start:	17410	Electric Meter end:	18479	Total kW hours 1069
Gas meter start:	24	Gas meter end:	210	Gas x 100 tt3 186

Start up

Make up air line installed in building near fuel cell, and significant airflow was entering the building through this. Unit failed to start on first several attempts--turned out that the igniter was not in proper position--unit started promptly when this was installed properly. CO measurements were much lower in the building. Coolant leak on heat recovery system discovered, patched with a clam type repair kit. Flammable gas detector inside the unit started beeping, adjusted cover to allow more air flow inside the unit.

Running notes:

2/1/07 Flammable gas detector beeping again, covers adjusted. Data computer shut down for several days after Windows automatic upgrade caused restart--lost data from 3 days. Fortunately the fuel cell was working fine through this event.

Shut down notes:

Cause of fuel cell shut down appeared to be low battery voltage--data set showed battery voltage sinking over last two or three days of run. System attempted to charge batteries, but could not meet building load at the same time, eventually shut off system at 42 volts on battery system.

Repair notes:

Batteries took charge, returned to normal state. Additional instrumentation placed on battery by UAF personnel. Measure battery currents, in and out, as well as voltage. Should allow for better observation of batteries in power management.

Planned Routine maintenance
Manufacturing defect

Control System
Balance of plant failure

Stack failure
Low Cell Voltage

Acumentrics Fuel Cell Demonstration Fairbanks

Run number: 3

start	3/8/2007 1:30:00 PM	Hours	251.15000	
				Efficiency: 11.28%
stop	3/19/2007 12:39:00 AM	Cumulative Hours	802.38333	
Electric start:	18596	Electric Meter end:	19090	Total kW hours 494
Gas meter start:	233	Gas meter end:	384	Gas x 100 tt3 151

Start up

Restart attempted after additional battery instrumentation added to system. Replaced main igniter after failed start attempt--unit started. At time of unit start-up, CO sensor reading 30 ppm.

Running notes:

Power logging system set up on 3/14/07. On 3/15/07, building smells acrid again, but CO sensors are reading 0 (discovered that they always read 0 when actual level is below 30 ppm)

Shut down notes:

Error log indicated fuse failure.

Repair notes:

Repair was complicated by lack of a bad fuse--required a lot of electrical system troubleshooting. Found a small diameter wire on fuse box burned off at fuse number 7. Repaired. Unit still did not start. Replaced control board with new board when heat damaged component discovered, but new board did not work due to changes in board design. Then a group of wires with burned insulation were found, turned out not to be the problem. Then discovered that one fuse had been moved by a single slot, most likely during troubleshooting. When fuse was placed in proper slot and old control board put back in unit, it started again.

Planned Routine maintenance
Manufacturing defect

Control System
Balance of plant failure

Stack failure
Low Cell Voltage

Acumentrics Fuel Cell Demonstration Fairbanks

Run number: 4

start	3/30/2007 11:30:00 AM	Hours	0	Efficiency:	0.00%
stop	3/30/2007 11:30:00 AM	Cumulative Hours	802.38333		
Electric start:	19090	Electric Meter end:	19090	Total kW hours	0
Gas meter start:	384	Gas meter end:	386	Gas x 100 tt3	2

Start up

Failed start due to installation of new control board, with different jumper configuration than previous board, causing a misread of the cell voltages. Stack got hot, but failed to take a load.

Running notes:

Shut down notes:

Repair notes:

Planned Routine maintenance
Manufacturing defect

Control System
Balance of plant failure

Stack failure
Low Cell Voltage

Acumentrics Fuel Cell Demonstration Fairbanks

Run number: 5

start	4/2/2007 1:37:00 PM	Hours	2767.0166	Efficiency:	17.81%
stop	7/26/2007 8:38:00 PM	Cumulative Hours	3569.3999		
Electric start:	19090	Electric Meter end:	24601	Total kW hours	5511
Gas meter start:	386	Gas meter end:	1453	Gas x 100 tt3	1067

Start up

4/2/07 Unit started after several failed attempts. These failed attempts resulted in either a complete failure of the ignition cycle, or erroneous voltage readings during start-up. Eventually the system was restored to proper electrical configuration, and it started.

Running notes:

Factory suggested that we increase the load to allow more heat to be generated by unit. However, when additional load was placed on the unit, battery voltage began dropping. Contact with factory, indicated that stack is limited to 80 amps, needed to reset current limit on unit to allow stack to supply additional current. Fuel utilization number very low.

5/4/07 As weather warms, fuel cell is starting to overheat the building. Temporary cooling done by opening garage door slightly.

5/17/07 Appears that a couple of the individual cell voltages are starting to drop out of the pack, going down to about .7 volts.

On Sunday, 6/17/2007. the load on the unit was increased by several hundred watts by turning on the building outside light. This caused a drain on the battery, and the fuel cell disconnected from the building load. After the battery was charged, the unit picked up the building again, and went through several cycles like this. On Tuesday, 6/19 the additional load was removed. This exercise seemed to damp out the low level cycles noted previously.

6/25/07 Noted that lowest 2 cell voltages have dropped to about .66 volts. Jim Buckley suggested running fuel cell at idle for two or three days.

7/11/07 Noted that voltages have dropped, with the lowest voltages going below 0.6 volts. E-mail from Stephan Worth at Acumentrics indicated that temperature of stack has changed due to a load change, and that they are working to get the temperatures and voltages back up.

Shut down notes:

On 7/25/07, the fuel cell appeared to be having problems with several cells. A discussion on 7/26/07 led to the decision to remove the load on the fuel cell for a few days to see if we could get the cells to recover. This strategy has apparently worked in the past for other fuel cell stacks. This was planned for implementation on July 27. However, when UAF personnel showed up to implement this plan, it was discovered that the fuel cell had faulted on a low cell voltage trip.

Low Cell voltage caused fault, probably cell 35.

Repair notes:

Plan to examine all voltage tap contacts to assure that voltage measurements received by the control system are accurate.

8/7/07 Attempt to restart fuel cell failed due to thermocouple located near heat exchanger fan. Disassembly of unit revealed that several thermocouple wires were heat damaged--hot gasses had melted fiberglass insulation, resulting in

Acumentrics Fuel Cell Demonstration

Fairbanks

Run number: 5

bare wires that crossed. Discussion with Acumentrics on 8/20/07 revealed that shutdown on July 27 was the result of voltage tap contact issues, as one row of cells dropped below .4 volts, while an adjacent row was climbing in voltage. Acumentrics recommended using silver paste to assure better contact between crimped connector and nickel voltage tap. Also repack insulation to assure less gas leakage.

8/28/07 On disassembly of the fuel cell insulation package, a gap between the recuperator and the downcommer was observed. This may be the source of leakage that caused the CO problems and the overheating inside the cabinet. Acumentrics recommends either removing shims to lower the recuperator, or to plug the gap with insulation.

8/22/07 Jim Buckley called--Exit Glacier stack row from failure in June ran fine back at the factory after the fuel lines were cleaned with a vacuum cleaner. Source of blockage unknown. Recommended that a forensics filter be used on the vacuum system to identify source of blockage.

Tom Johnson repaired unit, by removing insulation from left side of fuel cell unit, plugging leak noted, and replacing thermocouples affected by heat. Also recrimped voltage taps to hopefully prevent future issues with loose voltage taps.

Planned Routine maintenance
Manufacturing defect

Control System
Balance of plant failure

Stack failure
Low Cell Voltage

Acumentrics Fuel Cell Demonstration Fairbanks

Run number: 6

start	10/2/2007 11:00:00 AM	Hours	398.68333	
				Efficiency: 7.79%
stop	10/19/2007 1:41:00 AM	Cumulative Hours	3968.0833	
Electric start:	24601	Electric Meter end:	25012	Total kW hours 411
Gas meter start:	1453	Gas meter end:	1635	Gas x 100 tt3 182

Start up

Unit started up, but did not come up well. Appears that unit is starved for fuel, suspect that the problem may be fusing of the catalyst in the reformer section, as noted at the factory. Low voltage fault, cleared, unit continued to operate. Unit did not come up to full power level--unable to fully power the building lights--unit currently running a reduced power load, DC load of about 1500 watts, heater is cycling.

Running notes:

Unit seems starved for fuel. Not operating at full power.

10/12/07 unit doing funny oscillations, perhaps due to Acumentrics fooling with the unit... Low voltages on

Shut down notes:

10/20/07 Unit discovered non-operational by Jack Schmid.

Repair notes:

Plan to replace catalyst in pre reformer, but disassembly revealed no obvious damage to the reformer catalyst. No significant coking observed. It is not clear why the system is operating so poorly, but two cells are at very low voltage.

Unit not restarted. Eventually shipped to Exit Glacier to operate on propane in summer 2008 after an in-field stack repair.

Planned Routine maintenance
Manufacturing defect

Control System
Balance of plant failure

Stack failure
Low Cell Voltage

National Energy Technology Laboratory

626 Cochrans Mill Road
P.O. Box 10940
Pittsburgh, PA 15236-0940

3610 Collins Ferry Road
P.O. Box 880
Morgantown, WV 26507-0880

One West Third Street, Suite 1400
Tulsa, OK 74103-3519

1450 Queen Avenue SW
Albany, OR 97321-2198

539 Duckering Bldg./UAF Campus
P.O. Box 750172
Fairbanks, AK 99775-0172

Visit the NETL website at:
www.netl.doe.gov

Customer Service:
1-800-553-7681



Oil & Natural Gas Technology

DOE Award No.: DE-FC26-06NT41248

Final Report

Analysis of Actual Operating Conditions of an Off-grid Solid Oxide Fuel Cell

Submitted by:
Dennis Witmer
Thomas Johnson
Jack Schmid
University of Alaska Fairbanks

Prepared for:
United States Department of Energy
National Energy Technology Laboratory

December 31, 2008



Office of Fossil Energy



Analysis of Actual Operating Conditions of an Off-grid Solid Oxide Fuel Cell

Final Report

Starting June 1, 2004
Ending Sept 30, 2008

Dennis Witmer
University of Alaska Fairbanks
ffdew@uaf.edu
907-474-7082

Thomas Johnson
Jack Schmid

Report Issued December 2008
DOE Award Number
DE-FC26-01NT41248
Task Number 2.04.2

Submitted by:
University of Alaska Fairbanks
Institute of Northern Engineering
Arctic Energy Technology Development Laboratory
Building 814
Fairbanks, Alaska 99775

Disclaimer

This report was prepared as an account of work sponsored by an agency of the United States Government. Neither the United States Government nor any agency thereof, nor any of their employees, makes any warranty, express or implied, or assumes any legal liability or responsibility for the accuracy, completeness, or usefulness of any information, apparatus, product, or process disclosed, or represents that its use would not infringe privately owned rights. Reference herein to any specific commercial product, process, or service by trade name, trademark, manufacturer, or otherwise does not necessarily constitute or imply its endorsement, recommendation, or favoring by the United States Government or any agency thereof. The views and opinions of authors expressed herein do not necessarily state or reflect those of the United States Government or any agency thereof.

Abstract

Fuel cells have been proposed as ideal replacements for other technologies in remote locations such as Rural Alaska. A number of suppliers have developed systems that might be applicable in these locations, but there are several requirements that must be met before they can be deployed: they must be able to operate on portable fuels, and be able to operate with little operator assistance for long periods of time.

This project was intended to demonstrate the operation of a 5 kW fuel cell on propane at a remote site (defined as one without access to grid power, internet, or cell phone, but on the road system). A fuel cell was purchased by the National Park Service for installation in their newly constructed visitor center at Exit Glacier in the Kenai Fjords National Park. The DOE participation in this project as initially scoped was for independent verification of the operation of this demonstration.

This project met with mixed success. The fuel cell has operated over 6 seasons at the facility with varying degrees of success, with one very good run of about 1049 hours late in the summer of 2006, but in general the operation has been below expectations. There have been numerous stack failures, the efficiency of electrical generation has been lower than expected, and the field support effort required has been far higher than expected.

Based on the results to date, it appears that this technology has not developed to the point where demonstrations in off road sites are justified.

Table of Contents

Final Report	0
Disclaimer	1
Abstract	2
Executive Summary:	4
Background	4
Results:	5
Summer of 2003	5
Summer of 2004	5
Summer of 2005	7
Summer of 2006	8
Summer of 2007	12
Summer of 2008	13
Discussion and Conclusions	13
Acknowledgments	15
References	16

List of Figures

Figure 1 Department of Interior Alaskan Representative Cam Tooey at the Exit Glacier Visitor Center observing the operating Acumentrics fuel cell, May 26, 2004.	6
Figure 2 Graph showing the varying electrical demand at the Exit Glacier Visitor center. The spikes in demand are due to the arrival of busloads of tourist using the rest room facilities, causing the water pump to start.	7
Figure 3 Improvement in stack design resulting in improved polarization performance for the Acumentrics fuel cell stacks. Stack lifetime also improved as a result of this change in design.	8
Figure 4 Operation of the Acumentrics Fuel Cell at Exit Glacier during the summer of 2006. The run ended on September 22, 2006 in a deliberate shutdown at the closing of the visitor center at the end of the tourist season.	9
Figure 5 Performance of the fuel cell over a 1 week period, using hourly averaged data. Note that the fuel cell stack follows the load on a daily basis.	10
Figure 6 Polarization curve for the Acumentrics fuel cell during the 1300 hour run in late summer, 2006.	11
Figure 7 Linear Regression analysis of 3 periods of 1049 hour run showing the complete overlap of data from each period, or the absence of stack degradation during this period.	12

Executive Summary:

Fuel cells have been proposed as ideal replacements for other technologies in remote locations such as Rural Alaska[1-3]. A number of suppliers have developed systems that might be applicable in these locations, but there are several requirements that must be met before they can be deployed: they must be able to operate on portable fuels, and be able to operate with little operator assistance for long periods of time.

This project was intended to demonstrate the operation of a 5 kW fuel cell on propane at a remote site (defined as one without access to grid power, internet, or cell phone, but on the road system). A fuel cell was purchased by the National Park Service for installation in their newly constructed visitor center at Exit Glacier in the Kenai Fjords National Park. The DOE participation in this project as initially scoped was for independent verification of the operation of this demonstration.

This project met with mixed success. The fuel cell has operated over 6 seasons at the facility with varying degrees of success, with one very good run of about 1049 hours late in the summer of 2006, but in general the operation has been below expectations. There have been numerous stack and balance of plant failures, the efficiency of electrical generation has been lower than expected, and the field support effort required has been far higher than expected.

Based on the results to date, it appears that this technology has not developed to the point where demonstrations in off road sites are justified.

Background

Demonstrating the operation of a solid oxide fuel cell on a readily available, transportable fuel (not natural gas or hydrogen) has been a major milestone for use of this technology in Alaska. While the most desirable fuel in this application would be diesel fuel [4-6], propane is readily available in most remote communities in Alaska, typically used for residential cooking.

This project was funded largely by the Propane Research Council and the National Park service, and UAF and DOE were initially asked to participate only as an independent third party to verify data and assist with reporting requirements.

The fuel cell used in this project was built by Acumentrics Corporation[7, 8], of Westwood, Massachusetts (a suburb of Boston). This company has been in the fuel cell business since about the 1980s, but has been active in the solid oxide fuel cell industry only since about 2000.

There are some companies that have been investing in the solid oxide fuel cell industry for many decades, most notably Siemens Fuel Cells[9, 10], which has been working on developing tubular fuel cells since the mid 1970's. There have been some successes in this program[9], including a 69,000 laboratory demonstration of a stack, and field demonstrations of more than 30,000 hours, with electrical efficiencies of 46% on natural gas. However, the Siemens effort has never

resulted in a commercial product, due in large part to the cost of manufacturing the product. Much of the cost comes from the need to use high purity ceramic materials and the use of low throughput, high cost manufacturing techniques.

In 2000, the US DOE started the Solid Energy Conversion Alliance (SECA), intended to promote research and development efforts of planar solid oxide fuel cells, focusing on 5 kW systems[11]. This program used industry-university partnerships to address both basic materials research issues as well as the manufacturing cost/ system integration issues that need to be addressed for the creation of a commercial product.

Acumentrics Corporation began its efforts in the fuel cell area by concentrating right from the very beginning on cost reduction of the manufacturing processes, attempting to create fuel cells using conventional ceramic materials manufacturing techniques. It is clear to all involved in the fuel cell industry that product needs to both cheap and reliable. While Siemens elected to work on making fuel cells robust and degradation resistant, Acumentrics focused on cost reduction strategies right from the beginning.

Unlike companies that have deep corporate pockets, Acumentrics is a very small company, and found it necessary to place product in the field as quickly as possible in order to generate revenue for the company. In retrospect, it appears that the field deployments may have been a bit premature, but the experience gained through the course of this program has helped the company develop its product.

Results:

This demonstration project has occurred over several years, beginning in the summer of 2003, and continuing through the summer of 2008.

Summer of 2003

The National Park Service and the Propane Research Council funded the purchase of the 5 kW solid oxide fuel cell from Acumentrics Corporation, with the intent of installing it in the new visitor center at the beginning of the field season (mid-May), but delays at the factory prevented it from being shipped until late August. The fuel cell arrived at the Park, was uncrated and put into place in a special room for it. However, it was quickly discovered that the unit had suffered damage during shipping, and so after operating for a week, was put back in the crate and shipped back to the factory for repairs.

Summer of 2004

The fuel cell was shipped back to Alaska in mid-May for installation at the beginning of the visitor center season.

The National Park Service held a ceremony celebrating the opening of the new visitor center in late May, 2004, and the fuel cell was also unveiled at the same ceremony.



Figure 8 Department of Interior Alaskan Representative Cam Tooley at the Exit Glacier Visitor Center observing the operating Acumentrics fuel cell, May 26, 2004.

The fuel cell ran sporadically during the summer of 2004, for a total of about 350 hours. The major issues during this season were associated with the use of a steam reformer for propane. This reforming method is more efficient than partial oxidation reformers, but it requires careful management of the mass balance between the steam and the fuel.

By the fall of 2004, Acumentrics made the decision that the steam reformer needed to be replaced with a CPox reformer. This reforming method has the advantage of eliminating the need for mass flow control of steam, simplifying the design, and being of lower cost, but the disadvantage of reducing the reformer efficiency from about 80% to about 65%. Acumentrics and Energy Alternatives submitted a request to AETDL for an additional \$65,000 to cover this retrofit. The unit was once again shipped back to the factory for this retrofit.

Summer of 2005

The unit was again installed at Exit Glacier in the spring of 2005, and started in late May. Over the course of the summer, the unit operated for a total of 851 hours. In this period, a total of 395 gallons of propane were consumed by the fuel cell. This means that the electrical efficiency is about 11.2% based on propane at 90,000 btu/gallon. The other issue noted was the difficulty the fuel cell had due to the spikes in the electrical load caused by the nature of the facility. Since Exit Glacier is a very popular tourist destination, busloads of tourists arrive at the facility periodically during the course of a day. The first thing that happens when a busload of tourists stop is that all people on the bus head for the rest room facilities, and the water demand goes up rapidly. This in turn creates a huge surge in demand for electricity—as seen in the figure below.

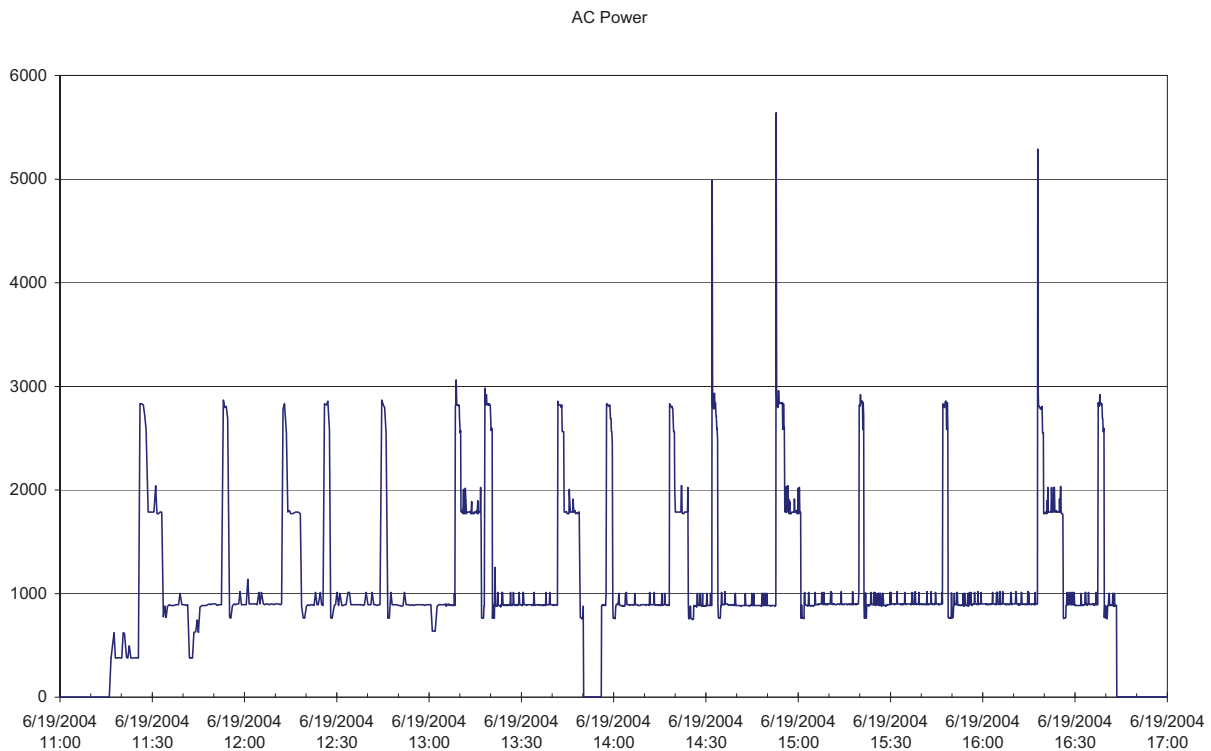


Figure 9 Graph showing the varying electrical demand at the Exit Glacier Visitor center. The spikes in demand are due to the arrival of busloads of tourist using the rest room facilities, causing the water pump to start.

The fuel cell was designed with some battery storage to absorb spikes in electrical loads, but these spikes were more intense than the batteries installed in the unit were able to manage. In mid-summer, additional batteries were added to the system, which helped the system.

A much larger issue, however, was the low efficiency during the course of the summer. Solid oxide fuel cells should be very efficient—the FCT fuel cell demonstrated in Fairbanks in 2003-04 had an efficiency of just below 40%, so the 11.2% number is very low. Acumentrics was aware of this low efficiency, and also was experiencing problems with short stack life—the maximum stack life at this point was only 1500 hours. To solve this problem, Acumentrics redesigned the entire fuel cell stack, with the major change being creating additional electrical

paths between fuel cell tubes to reduce ohmic losses. The results of this stack redesign can be seen in the figure below.

At meetings with Acumentrics in the fall of 2005, agreements were reached to ship the fuel cell back to the factory to retrofit the stack with one of the new design.

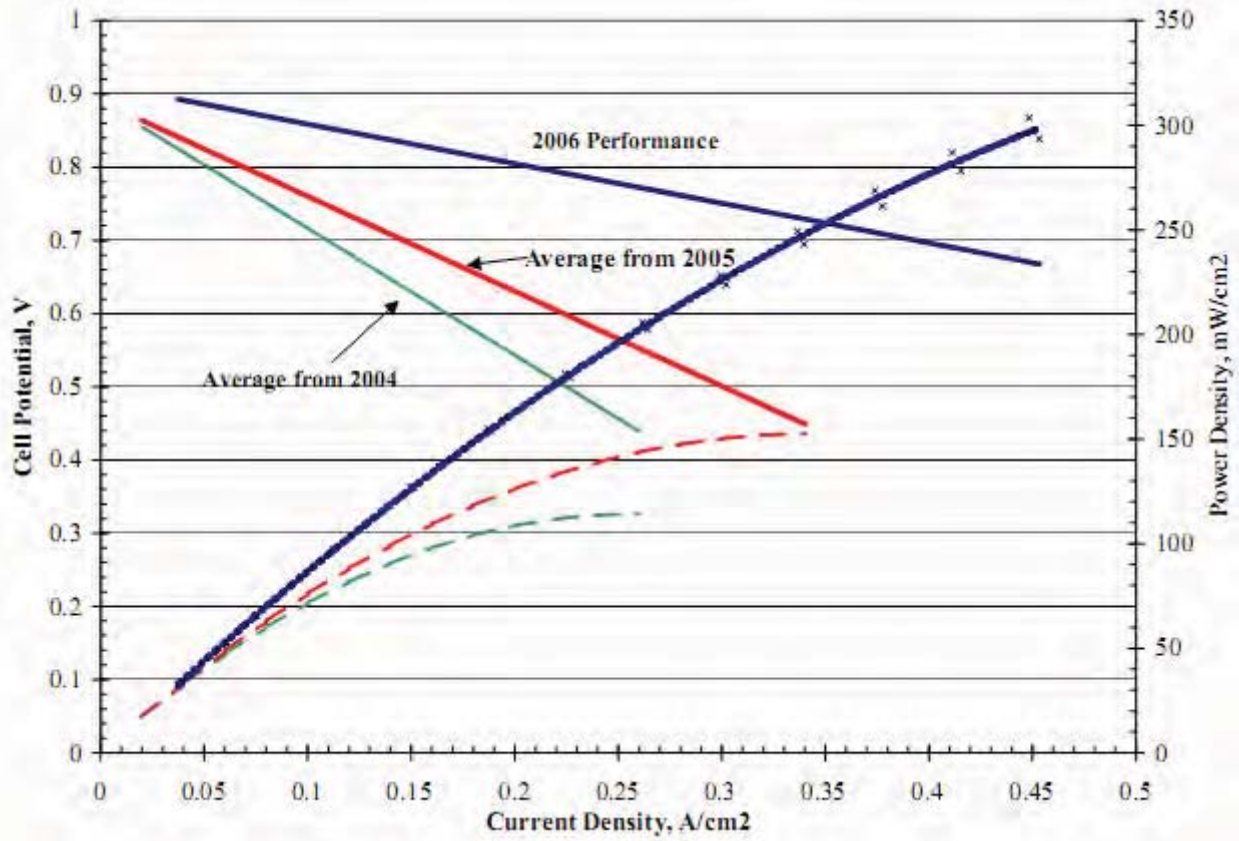


Figure 10 Improvement in stack design resulting in improved polarization performance for the Acumentrics fuel cell stacks. Stack lifetime also improved as a result of this change in design.

Summer of 2006

The retrofit of the fuel cell required for the fuel cell to be shipped back to Boston, but the road to the Exit Glacier visitor center is not plowed during the winter, so the fuel cell could not be shipped back until spring. The completed fuel cell was shipped back to Seward, and arrived for initial start-up on July 6. The fuel cell ran for about a week, but there were some issues with the electrical system.

On August 12, the fuel cell was started again, and ran for the remainder of the summer, until it was shut off for the closing of the visitor center at the end of the season. This run was 1049 hour long, and allowed for data collection with regards to the operation of the fuel cell. Figure 4 below shows the operational power output for the fuel cell for the whole summer.

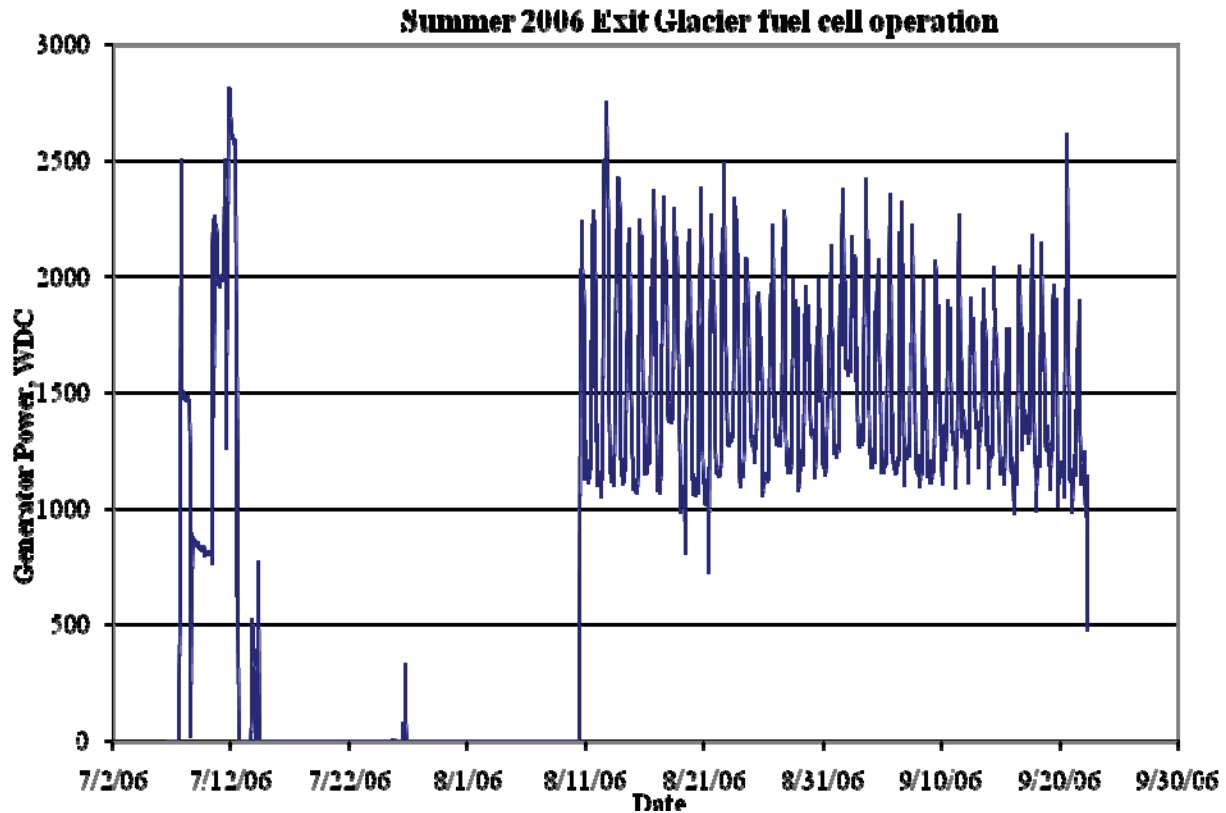


Figure 11 Operation of the Acumentrics Fuel Cell at Exit Glacier during the summer of 2006. The run ended on September 22, 2006 in a deliberate shutdown at the closing of the visitor center at the end of the tourist season.

Note that the fuel cell output varied between about 1200 watts and 2500 watts during the run, following the peak during the day, and operating at a lower level at night. The larger battery pack allowed for some smoothing of the peaks.

Alaska Generator Power

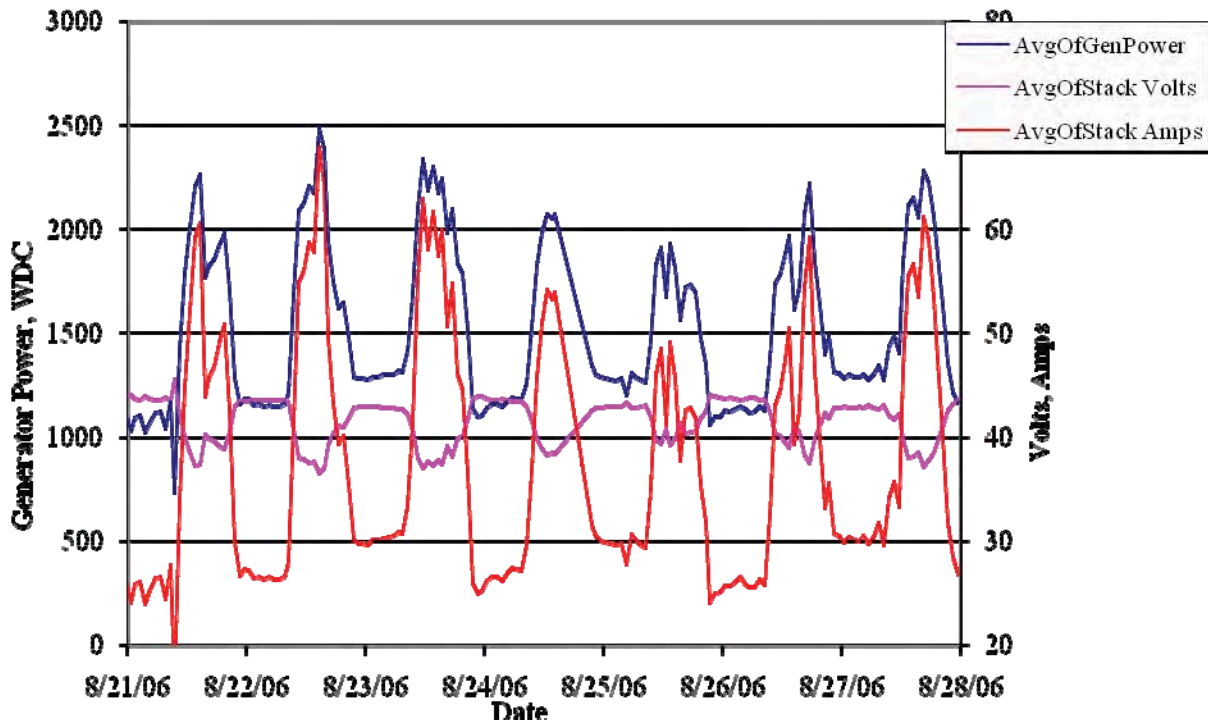


Figure 12 Performance of the fuel cell over a 1 week period, using hourly averaged data. Note that the fuel cell stack follows the load on a daily basis.

Figure 5 shows the performance of the fuel cell system, showing the smoothing of the power curve allowed by the addition of the larger battery system. While there are some abrupt changes in the current and voltage, the sharp spikes caused by the pump coming on when the busses show up.

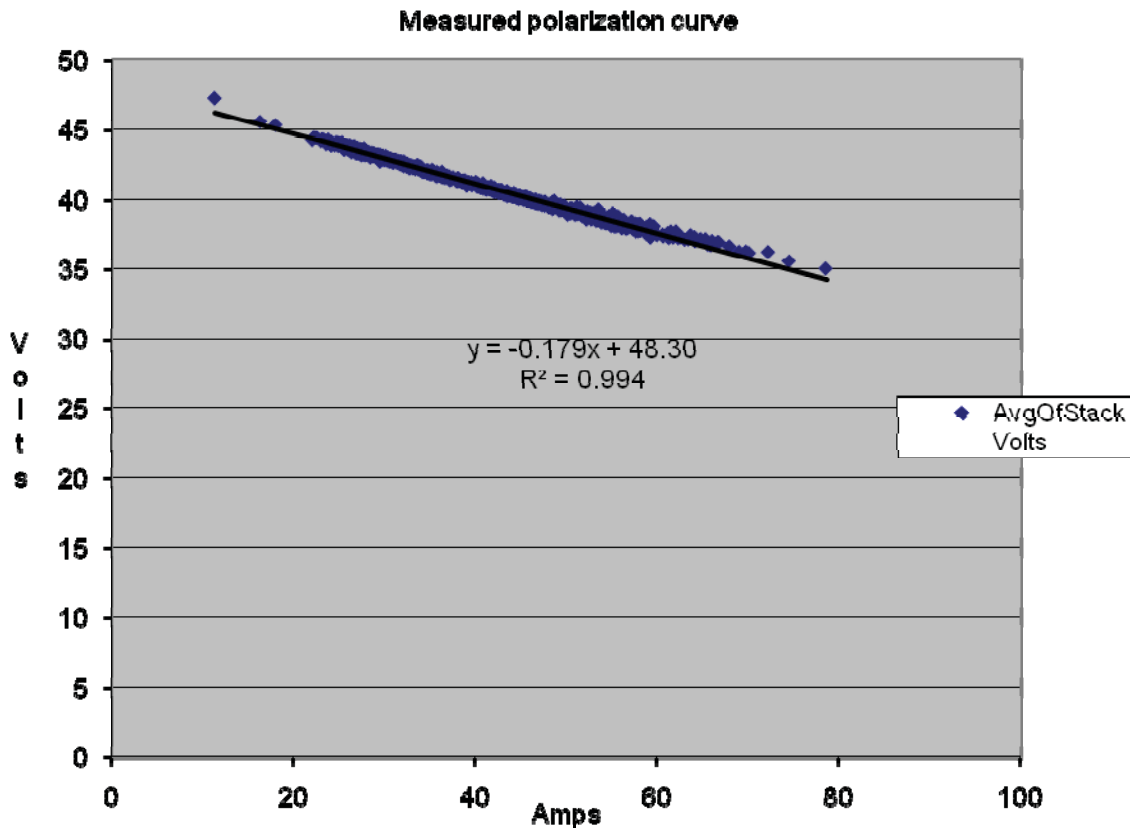


Figure 13 Polarization curve for the Acumentrics fuel cell during the 1300 hour run in late summer, 2006.

The polarization curve is very important in fuel cell evaluation as it provides information about the electrochemical reactions and the fuel cell efficiency. Figure 6 above shows the voltage vs. current for the stack during the 1049 hour run. The data appears very linear (as expected in the middle part of the polarization curve), and very stable (the points all lie along the same line, and do not appear to drift).

In order to see if the fuel cell is degrading over the time of the test, the polarization data can be used. For evaluating this, the data set was divided into three equal parts, and a linear regression analysis was done on each of these three data sets. The results of this analysis are shown in Figure 7 below. It appears that the three lines have nearly the same slope and intercept, indicating that the drift between the beginning and end of the run is minimal.

This data is consistent with reports from Siemens[11] where fuel cell stack performance actually improves slightly over the first 500 hours, then degrades at a rate of about .5% per thousand hours after that point.

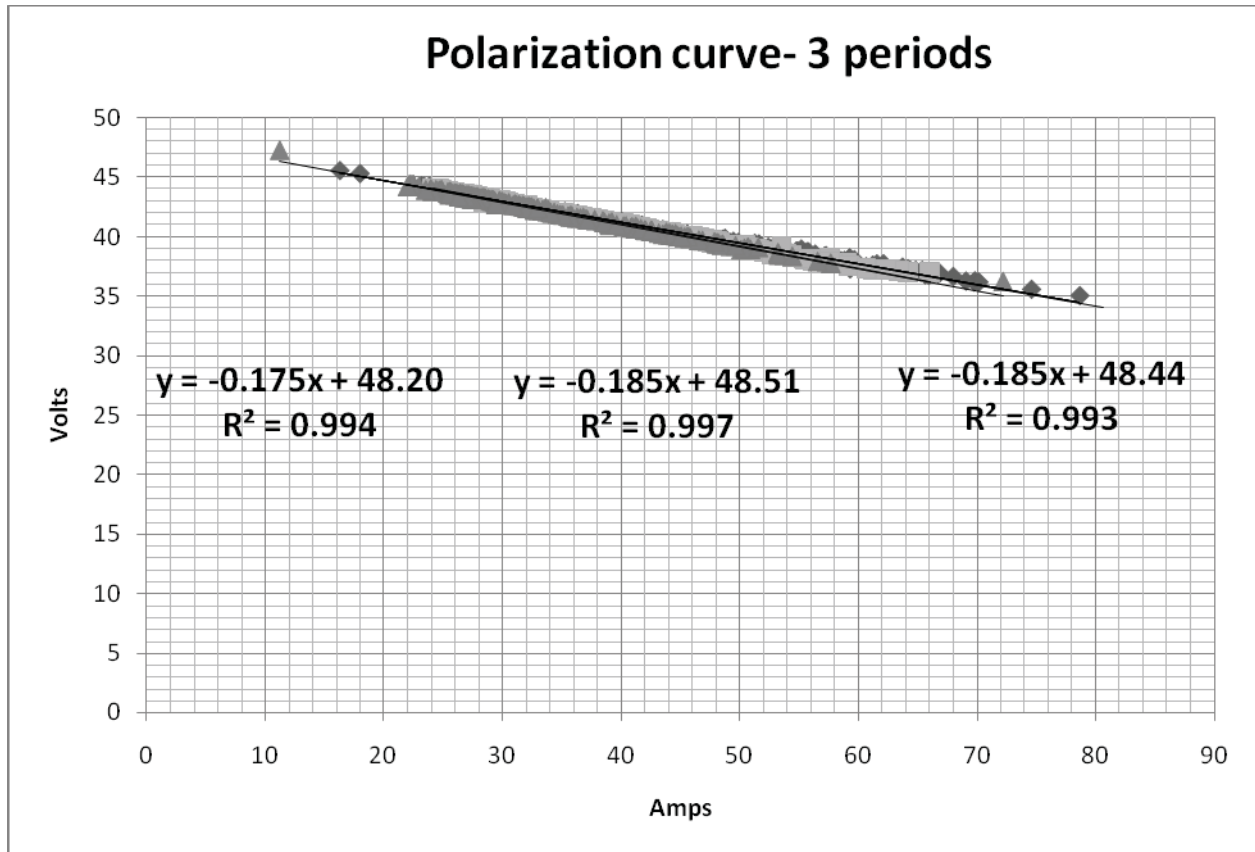


Figure 14 Linear Regression analysis of 3 periods of 1049 hour run showing the complete overlap of data from each period, or the absence of stack degradation during this period.

At the end of the season, the fuel cell was shut down with the expectation that it would start up in the spring, and the test would continue. A press release was issued to celebrate the successful test.

Summer of 2007

The fuel cell was left in place at the Exit Glacier Visitor center for the winter of 06-07, and start-up was attempted when the visitor center was opened in the spring. However, things did not go as planned. There was an initial failure of the heat exchanger on top of the unit on May 20, 2007, which required shipment of a new part from the factory. After restarting in early June, a second failure, this time in the stack occurred. Energy Alternatives representatives attempted to fix the unit in the field, but were unable to get the system operating properly. One bundle (of four) from the stack was removed and replaced with a new bundle. At the factory, the defective bundle operated as expected in testing, and the difficulties in the field were attributed to debris in the fuel lines.

Even after the bundle replacement, the system at Exit Glacier still did not function well. After mid July, efforts to keep the fuel cell operational were abandoned due to the lack of funds.

At the end of 2007, an assessment was made of the program at Exit Glacier. It appeared that further operation of the fuel cell at Exit Glacier would require returning the fuel cell to the factory yet again and rebuilding the stack, and none of the participating funding agencies had the patience or the funds for this. On the other hand, the fuel cell being operated on natural gas in Fairbanks [12] appeared to be in better shape, and could be repaired in the field. There was also some funding available due to the lack of a willing supplier of a diesel reformer. After discussions with the DOE, the decision was made to ship that fuel cell to Exit Glacier for operation on propane.

Summer of 2008

The final season of the demonstration at Exit Glacier began with the shipment of the fuel cell from Fairbanks to Seward in mid-May, 2008. The fuel cell was first installed in the NPS warehouse facility where repairs were made to the stack, including replacement of all of the thermocouples in the hot box area, replacing the fuel processor (thought to be the cause of failure in Fairbanks), rebuilding the insulation around the stack, and reattaching the voltage taps to the fuel cell stack.

The fuel cell was moved from warehouse to the Exit Glacier visitor center in late June, and started. However, the fuel cell never operated as well as expected this summer. The stack did not perform up to expectations, as it appeared that the fuel processor was not the problem, but rather that the stack had suffered degradation. Late in the summer, two rows of cells were operating at well below average voltage, so the software which normally shuts the system off to prevent damage to the stack was changed to allow the system to operate with the bad cells.

Discussion and Conclusions

After six summer seasons of operating a small SOFC at Exit Glacier, there have been some successes, but also clearly the need for additional development before these devices can be used in remote applications.

The successes include:

- The ability of the fuel cell to load follow a small building load
- Operation on propane, which is a transportable fuel
- Continuous operation of the fuel cell for more than a month unattended.

Additional development is needed in the following areas

- Significant cost reductions in capital cost of the fuel cell
- Increased reliability, preferably to the point where the fuel cell could operate for a year between maintenance
- Increased fuel cell stack life, preferably to the 40,000 hours advertised by the industry
- Increased system efficiency, preferably to the 40% advertised by the industry.

It is clear from this demonstration that the fuel cell industry is still far from achieving the promise of the technology. In the late 1990s, fuel cells were perceived by many as being on the verge of replacing the internal combustion engine with a cleaner, more efficient, environmentally friendly way of producing electrical power and propelling our vehicles. This excitement extended to Alaska, where people get their electrical power from expensive diesel generators. Many fuel cell advocates approached the Alaska congressional delegation looking for support for deploying this technology in the state.

The claims that fuel cell supporters make are: 1) Fuel cells are more efficient than combustion engines, 2) fuel cells are more reliable than mechanical engines because they have no moving parts, 3) fuel cells can be made cheaply in mass manufacturing, 4) fuel cells can be made sufficiently reliable for use in power generation and transportation applications, 5) fuel cells can be made to operate on conventional fossil fuels such as diesel fuel and coal through the use of gasification technologies.

Over the course of the past decade, the University of Alaska has been involved in testing a total of 11 fuel cells (plus attempting to test 2 additional fuel cells that have not been delivered). While this has been an interesting ride, it is safe to say that almost none of the promises of the fuel cell revolution have been achieved. Some of the claims of the fuel cell industry have nearly been verified—fuel cells are at least marginally more efficient than diesel generators (46% as compared to 40%) if they are operating on natural gas. They also are relatively clean as compared to combustion engines, not least in part because of their sensitivity to impurities such as sulfur, which require expensive chemical cleanup of fuel streams before they can be fed into the fuel cell.

However, the shortcomings of fuel cells are many. They still emit carbon dioxide if they are operated on hydrocarbon fuels (as most are). They need to have air and fuel supplied to them, and require the use of external blowers or compressors (so much for the no moving parts claim). So far, no manufacturer has succeeded in producing a sufficient number of fuel cells to achieve the favorable economics as compared to combustion engines (the closest is UTC with their Phosphoric Acid Fuel Cell, but these are still considerably more expensive than gas turbines, and they have not achieved significant market penetration.) And the reliability of fuel cells in field applications remains problematic—as the results of this study indicate. Also, the use of fuels heavier than natural gas remain problematic, though the results of this study are hopeful with regards to at least propane. The heavier diesel fuels and coal still have not been demonstrated in long term tests (the longest test on diesel fuel is approximately 1000 hours).

The fuel cell industry appears headed for retrenchment. The Siemens announcement that it was seeking a buyer for its fuel cell division in July of 2008 is the most dramatic evidence of this trend, but was preceded by announcement from GE that it was no longer pursuing fuel cells as a business line. Smaller companies have also failed, including Fuel Cell Technologies of Kingston Ontario, and many in the PEM fuel cell industry (H-Power, Dias Analytic and many others). Even the major players such as Ballard Power systems (current stock price of \$1.74, down from a high of \$140 per share in 1999) just fired their CEO, and Plug Power (current stock price of \$1.11, down from a high of \$146 per share in 2000) announced today that it was laying off one third of its work force (just before Christmas).

Given this attrition in the field, Acumentrics seems like a relative winner, recently announcing that it had been awarded approximately \$15,600,000 for research over the next three and a half years [13]. This level of funding represents about the quarterly operating expenses for some of the larger fuel cell companies, so the modest level of effort appears to be working in their favor.

It is clear that even the best fuel cells available today are not yet capable of replacing diesel generators in remote Alaskan villages, and that the challenges to develop reliable, robust products are many. It is also clear that the investment needed to overcome these challenges is significant, as fuel cell R&D has already absorbed several billion dollars.

However, some fuel cells, such as the UTC Phosphoric Acid system, are approaching commercial availability (though the rising price of natural gas in most markets would seem to limit their use). And the results of this study would seem to indicate that, given enough patience, a solid oxide fuel cell might one day be capable of operation in a remote location.

Acknowledgments

This work was a cooperative research project with the National Park Service and could not have succeeded without the continuing support of Tim Hudson, Chief of Maintenance of the Alaskan Region. Support also came from the Propane Research Council, with special support from Mr. Larry Osgood. Special thanks to the Acumentrics support from Norm Bessette, Tony Litka, Doug Schmidt, Rhys Foster. But the single individual most responsible for the successes of this project is Mr. Jim Buckley of Energy Alternatives, who developed the project and brought the partners together, and then supported the unit in the field with a grim determination to make the thing work.

This work could not have been done without the support of the US DOE, including the Arctic Energy Office with Mr. Brent Sheets, and the support of the SECA program manager Mr. Wayne Surdoval.

National Energy Technology Laboratory

626 Cochrans Mill Road
P.O. Box 10940
Pittsburgh, PA 15236-0940

3610 Collins Ferry Road
P.O. Box 880
Morgantown, WV 26507-0880

One West Third Street, Suite 1400
Tulsa, OK 74103-3519

1450 Queen Avenue SW
Albany, OR 97321-2198

539 Duckering Bldg./UAF Campus
P.O. Box 750172
Fairbanks, AK 99775-0172

Visit the NETL website at:
www.netl.doe.gov

Customer Service:
1-800-553-7681



References

1. Witmer, D., Jay Keller, and Ron Johnson, *Remote Area Power Program for Alaskan Villages*. National Hydrogen Association Annual Meeting, 1999.
2. Witmer, D., Ronald Johnson, Tristian Kenny, Chris Morgan, Baskar Neogi, Jose Reuter, Jack Schmid, Andy Lutz Dan Morse, Thomas Johnson, Steve Guthrie, Ron Johnson, and Jay Keller, *Rural Area Power Program (RAPP) Final Report*, in *University of Alaska Fairbanks*. 2002. p. 352.
3. Witmer, D., Thomas Johnson, Jack Schmid and Tristan Kenny, *Methanol Reformer/PEM Fuel Cell Project*, in *Arctic Energy Technology Development Laboratory*. 2006: Fairbanks, Alaska. p. 34.
4. Borup, R., Michael Inbody, Jose Tafoya, Dennis Guidry, and Jerry Parkinson, *Diesel Reforming with SOFC Anode Recycle*. The Electrochemical Society, 2004. **205 Meeting**.
5. Lutz, A., Robert Bradshaw, Jay Keller, and Dennis Witmer, *Thermodynamic analysis of hydrogen production by steam reforming*. *International Journal of Hydrogen Energy*, 2003: p. 159-167.
6. Witmer, D., *SMALL SCALE FUEL CELL AND REFORMER SYSTEMS FOR REMOTE POWER*, in *Other Information: PBD: 1 Dec 2003*. 2003: United States. p. Size: 14 pages; Format: Adobe PDF Document with Extractable Text.
7. Bessette, N., *Status of the Acumentrics SOFC Program*, in *SECA Annual Workshop*. 2006: Philadelphia, Pa.
8. Schmidt, D., *Status of the Acumentrics SOFC program*, in *2006 Fuel Cell Seminar*. 2006: Honolulu, HI.
9. Siemens. *Siemens Power Systems Web Site*. 2006 12/18/2006 [cited; Available from: <http://www.powergeneration.siemens.com/en/fuelcells/history/milestones/index.cfm>].
10. Singhal, S., *Discussion of Siemens Web site* 2002.
11. SECA. *SECA Web Page*. 2006 [cited; Available from: <http://www.netl.doe.gov/technologies/coalpower/fuelcells/seca/>].
12. Witmer, D., Thomas Johnson, Jack Schmid, *Five Kilowatt Solid Oxide Fuel Cell/Diesel Reformer Report, Final report to US DOE*, in *Arctic Energy Technology Development Laboratory*. 2008, University of Alaska Fairbanks: Fairbanks, Alaska. p. 26.
13. Acumentrics. *Press Release* 2008 [cited 2008 12/17/2008].

Alaska Coalbed Methane Water Disposal Methods: A Review of Available CBM Information, Disposal and Treatment Options for Alaska



Map of Alaskan coalfields and coal occurrences, from Flores et al, 2004.

Prepared for:

Arctic Energy Technology Development Laboratory

Technical Report: INE/AETDL 08.06

University of Alaska Fairbanks

September 2008



Alaska Coalbed Methane Water Disposal Methods: A Review of Available CBM Information, Disposal, and Treatment Options for Alaska

Topical Report

Reporting Period Start Date: December 15, 2004

Reporting Period Ending Date: December 15, 2007

*By: Michael R. Lilly¹, Debasmita Misra², Eric P. Robertson³, Robert Crosby⁴, Craig Wollard⁵,
Amanda Osborne⁵, and Kristie Holland¹*

1 Geo-Watersheds Scientific

2 University of Alaska Fairbanks, College of Engineering and Mines

3 Idaho National Laboratory

4 Remote Utilities Systems Group

5 University of Alaska Anchorage

Submitted: August 2008

DOE Award Number: DE-FC26-01NT41248

Submitted By:

Arctic Energy Technology Development Laboratory

University of Alaska Fairbanks

PO Box 755910, Fairbanks, AK 99775-5880

Prepared By:

Geo-Watersheds Scientific

PO Box 81538

Fairbanks, Alaska 99708

University of Alaska Fairbanks

College of Engineering and Mines

PO Box 755800, Fairbanks, AK 99775

Idaho National Laboratory

2351 N. Boulevard

PO Box 1625, Idaho Falls, ID 83415

Remote Utilities Systems Group

PO Box 80086

Fairbanks, AK 99708

University of Alaska Anchorage

Department of Environmental Quality Engineering

3211 Providence Dr., ENG 201, Anchorage, AK 99508

Prepared For:

US Department of Energy, National Energy Technology Laboratory

626 Cochran Mills Road, PO Box 10940

Pittsburgh, PA 15236-0940

Recommended Citation:

Lilly, M.R., Misra, D., Roberston, E.P., Crosby, R., Wollard, C., Osborne, A., and Holland, K.M. 2008, Alaska Coalbed Methane Water Disposal Methods: A Review of Available CBM Information, Disposal and Treatment Options for Alaska. University of Alaska Fairbanks, Institute of Northern Engineering. Technical Report INE/AETDL 08.06, Fairbanks, Alaska, 37 pp. + appendices.

Disclaimer:

This report was prepared as an account of work sponsored by an agency of the United States Government. Neither the United States Government nor any agency thereof, nor any of their employees, makes any warranty, express or implied, or assumes any legal liability or responsibility for the accuracy, completeness, or usefulness of any information, apparatus, product, or process disclosed, or represents that its use would not infringe privately owned rights. Reference herein to any specific commercial product, process, or service by trade name, trademark, manufacturer, or otherwise does not necessarily constitute or imply its endorsement, recommendation, or favoring by the United States Government or any agency thereof. The views and opinions of authors expressed herein do not necessarily state or reflect those of the United States Government or any agency thereof.

The contents of this report reflect the views of the authors, who are responsible for the accuracy of the data presented herein. This research was funded by the U.S. Department of Energy (DOE), National Energy Technology Laboratory (NETL). Funding and support was also provided by Geo-Watersheds Scientific (GWS) and Remote Utilities Systems Group (RUSG). The contents of the report do not necessarily reflect the views of policies of the DOE, NETL, GWS, RUSG or any local sponsor. This work does not constitute a standard, specification, or regulation.

The use of trade and firm names in this document is for the purpose of identification only and does not imply endorsement by the University of Alaska Fairbanks, DOE, NETL, GWS, RUSG or other project sponsors.

Abstract:

Energy costs in remote Alaskan communities and resource development operations are very high. With rising costs of transportation in Alaska and the resulting increase in diesel fuel costs, using local energy sources is becoming increasingly important. There are a number of villages and remote resource-development projects across Alaska that may benefit from the use of shallow coalbed methane (CBM) resources. CBM is normally developed from relatively shallow coal deposits. It is common for these deposits to have a mix of methane gas and water. The methane gas in these reservoirs will also have a greater affinity to absorb on the local coal (source rock) material and not be freely mixed with formation pore water. CBM reservoirs can have a wide variety of gas concentrations, relative to formation water. This may range from CBM reservoirs that have no produced water to manage, to reservoirs that require years of dewatering to produce economic amounts of gas. The management and methods of treating CBM produced water in arctic conditions is not well understood.

This report is intended to provide a review of existing information about treating CBM water in Alaska and other arctic regions. Alaska has had no commercial development of CBM resources to draw information from. Information from other arctic regions was reviewed to offset the lack of information associated with prior CBM development in Alaska. Another evaluation for this report was the potential use of CBM produced water as an additional resource for drinking water or non-potable water needs in rural communities or resource-development camps.

The review of CBM produced water quantity and quality indicate generalizations about what should be expected in rural Alaska communities is very difficult without site information about the CBM reservoir properties, formation water chemistry, infrastructure and needs in each setting. The production of CBM water can vary from near zero to requirements to pump for many years. The range of water quality can also vary from near drinking-water standards to water quality that could be very costly to treat. Currently, there are no good examples of developed CBM fields in the arctic that provide any innovative methods for managing produced water. The best future examples will likely come from arid regions where CBM produced water has a high value in water-poor areas. Treatment technologies for small-scale will be further developed. In Alaska, it will be important to obtain adequate reservoir-specific information on water-quantity estimates associated with development and production. Comparison with other CBM fields produced for full economic development will withdraw significantly greater amounts of water than CBM resources developed for isolated rural communities that are demand limited. It will also be important to characterize formation water quality and how it may vary over the development and production cycle. This information can then be used to evaluate how to integrate CBM produced water (both quantity and quality) in rural Alaska settings with existing water-treatment systems and technologies. The information sources summarized in this report were also used to develop an online resource for the University of Alaska Fairbanks at the Keith B. Mather Library. The CBM related resources are listed under the searchable bibliography indexes. Many of the references collected under this project were added to the library collection for access to future users. This online resource will help future CBM resource evaluation and development efforts in Alaska.

Contents

Executive Summary	1
Introduction.....	2
Objectives	6
Alaska Data Synthesis.....	7
Canadian Data Synthesis.....	10
Russian Data Synthesis.....	13
Other Cold Regions Data Synthesis.....	14
Potential Rural CBM Water Production, Treatment, and Disposal Methods	17
Rural Alaska Water Production Issues	17
Potential Rural CBM Water Production, Treatment, and Disposal Costs	19
Potential for Use of CBM Water as a Drinking Water Source in Rural Alaska.....	24
Outreach Activities	32
Summary and Recommendations	32
Acknowledgements.....	33
References.....	33

Figures

Figure 1. Structure and coal deposition are predicted to be similar for the San Juan and North Slope basins, as both of these basins are found along the Western Cretaceous Interior Seaway (from Tyler et al, 2000).	8
Figure 2. Total coal thickness of the Nanushuk Group, coal-bearing zones, western Colville basin. Coal thickness exceeds 300 ft south of the villages of Wainwright and Atqasuk (from Tyler et al., 2000)......	9
Figure 3. Location of the Chignik formation on the Alaskan Peninsula (from Tyler et al., 2000).	10
Figure 4. Major coal deposits of Canada.	11
Figure 5. Current coalbed methane plays in Western Canada.	12
Figure 6. Hard coal and coalbed methane deposits of Commonwealth of Independent States. ..	13
Figure 7. Coalbed methane resources distribution among basic coal areas of the former USSR.	14
Figure 8. Produced water management costs from Table 5, presented in graphical form.....	22
Figure 9. Existing village water treatment system construction cost (construction cost of water treatment systems divided by demand of villages, in gallons per day).	23
Figure 10. Example system flow chart for a water treatment and disposal system.	24

Tables

Table 1. CBM production summary of Zhaoyuang Block of Qinshui Basin, China (Reproduced from: Sanli et al., 2003).	15
Table 2. Volumes of collected, utilized and vented from the degasification station methane (losses of collected and non utilized methane) in 18 most gassy coal mines of USCB in 2001 (Reproduced from Krzystalik et al., 2003).	16

Table 3. Methane reserves of central Kazakhstan coal deposits (Reproduced from Mustafin et al., 2003).	17
Table 4. Disposal costs for produced water at offsite commercial facilities.	21
Table 5. Produced water management costs.	22
Table 6. Select water quality data for villages with surface water sources.	27
Table 7. Select water quality data for villages with non-surface water sources.	28
Table 8. Village water treatment system information.	29
Table 9. Estimated System Costs.	30

Appendices

Appendix I: Additional electronic searches- general CBM references	
Appendix II: Geologic information for US CBM reservoirs	
Appendix III: Water production/ disposal info for US CBM reservoirs	
Appendix IV: Summary of geologic information for potential Alaskan CBM resources	
Appendix V: Geologic information for Canadian CBM reservoirs	
Appendix VI: Geologic & water production/ disposal for Russian CBM reservoirs	
Appendix VII. CBM cold-region professional and research contacts	
Appendix VIII. Rural Alaskan community information	
Appendix IX. Endnote Reference Database (http://www.gi.alaska.edu/services/library/)	

Executive Summary

Energy costs in remote Alaskan communities and resource development operations are very high. With rising transportation costs and the resulting increase in diesel fuel costs, the potential for using local energy sources is increasingly important. There are a number of villages and remote resource-development operations (mines) across Alaska that may benefit from the use of shallow coalbed methane (CBM) resources. The Alaska Division of Geological & Geophysical Surveys investigated CBM potential in rural Alaska and reported over 35 rural villages which are situated on, or are immediately adjacent to, coal resources. This vast untapped resource of potentially 1,000 trillion cubic feet of methane statewide could provide low cost and relatively clean energy to rural Alaska for generations to come. In Arctic and Subarctic climate conditions, permafrost conditions, and remote rural areas, disposal costs would be an important factor. CBM is normally developed from relatively shallow coal deposits. It is common for these deposits to have a mix of methane gas and water. The methane gas in these reservoirs will also have a greater affinity to absorb on the local coal (source rock) material and not be freely mixed with formation pore water. CBM reservoirs can have a wide variety of gas concentrations, relative to formation water. This may range from CBM reservoirs that have no produced water to manage, to reservoirs that require years of dewatering to produce economic amounts of gas. The management of produced water and what methods exist in arctic conditions to deal with CBM related produced water is not well understood.

The effort presented in this report is intended in providing what is known about treating CBM water in Alaska and other arctic regions. Alaska has had no commercial development of CBM resources to draw information from or look at various case studies. Information from other arctic regions was reviewed to offset the lack of information associated with prior CBM development in Alaska. Another evaluation of this report was the potential use of the CBM produced water as an additional resource for drinking water or non-potable water needs in rural communities or resources development camps.

In rural Alaska, CBM produced water has a potential value to help supplement existing water sources. Cold winter temperatures cause water sources (lakes, rivers) to freeze in many cases. Communities then have to maintain large water-storage tanks to provide a winter water supplies. An additional task of this study was to evaluate the potential of using CBM produced water as a drinking water source in rural Alaska. We investigated potential CBM water quality to help evaluate this potential. Additionally, we summarized available drinking-water source-water quality from communities with known CBM potential. The treatment systems currently utilized in these communities and their approximate costs were summarized. Finally, we made an estimate of the number of communities and types of treatment systems that would be required to treat CBM water if it were to be adopted as a drinking water source.

In Alaska, the largest potential coal and coalbed methane resource base is located principally in the North Slope and Cook Inlet Provinces, where much is known about the thickness and continuity of coals in the subsurface. In Canada, the most advanced, and currently the only commercially viable, CBM projects are in the Palliser block of southern Alberta. Isolated attempts were undertaken in Russia and in the Ukraine to initiate methane recovery from coal

seams unrelated to coal mining activities. However, no plans have been found for the future development of the CBM resource located in the Pechorsky coal basin, which is the only major coal basin located within the colder northern region. Our research has resulted in obtaining information on the CBM fields and gas/water production of selected fields in China, Poland, and Kazakhstan, but there appears to be no information available on the management methods that are used for CBM water treatment and disposal in these areas, based on the review of the available literature.

The review of CBM produced water quantities and quality indicate that generalizations about what should be expected in rural Alaska communities is very difficult without site information about the CBM reservoir properties, formation water chemistry, and infrastructure and needs in each setting. The production of CBM water can vary from near zero to requirements to pump for many years. The range of water quality can also vary from near drinking water standards to water quality that could be very costly to develop. Currently, there are no good examples of developed CBM fields in the arctic that provide any innovative methods for managing produced water.

The best future examples will likely come from arid regions where CBM produced water has a high value in water poor areas, and treatment technologies for this scale will be further developed. In Alaska, it will be important to obtain adequate reservoir-specific information on water quantity development estimates associated with development and production. It will also be important to characterize the water quality in formation water and how that may vary over the development and production cycle. This information can then be used to evaluate how to integrate the CBM produced water (both quantity and quality) in rural Alaska settings and existing water treatment systems. The information sources summarized in this report were also used to develop an online resource for the University of Alaska Fairbanks at the Keith B. Mather Library. The CBM related resources are listed under the searchable bibliography indexes. Many of the references collected under this project were added to the library collection for access to future users. This online resource will help future CBM resource evaluation and development efforts in Alaska. This report is anticipated to serve as a resource for planning, understanding, and implementing environmentally sound water management practices of CBM produced water in Alaska.

Introduction

Coalbed Methane (CBM) is receiving increased attention as an energy source for Rural Alaska, and for commercial production in some areas of the state. An important issue to resolve for CBM production is water disposal or treatment methods. Little is known about what water chemistry characteristics should be anticipated, and what disposal or treatment methods are cost effective and meet the requirements of Alaska's arctic environment. High costs of water disposal or treatment could jeopardize the development of CBM resources in many rural areas of Alaska. The Alaska Division of Geological & Geophysical Surveys investigated CBM potential in rural Alaska and reported on over 35 rural villages which are situated on, or are immediately adjacent to, coal resources. This vast untapped resource of potentially 1,000 trillion cubic feet of methane statewide could provide low cost and relatively clean energy to rural Alaska for generations to

come. In Arctic and Subarctic climates, permafrost conditions, and remote rural areas, water-disposal costs would be an important factor. The potential resource will require solutions in water management for state and private producers to benefit from CBM utilization in Alaska.

Increases in the price of conventional fuel, such as diesel, has been of considerable concern especially in rural Alaska. Most of the rural Alaskan electricity needs are met through diesel. Extremely low temperatures in the winter season have made rural Alaska communities and households reliant on fuel to heat their homes and buildings as well as to generate electricity. They are confronted with the challenges of paying increasing retail fuel prices to meet basic survival needs. The United States Energy Information Administration reported that the nation's households, heated primarily with heating fuel, were paying approximately 32% more in 2005 than in 2004 (Division of Community Advocacy, 2005). With high unemployment and a limited local economic base, alternate energy resources, such as coalbed methane need to be explored to offset the increasing cost of diesel in rural Alaska.

In 1996 the State of Alaska directed the DGGs to evaluate the potential for coalbed methane (CBM) to meet the energy needs of roadless rural communities that currently depend on fuel oil for heating and electrical power generation. The DGGs evaluated the resource potential of frontier sedimentary basins using a CBM producibility model developed by the Texas Bureau of Economic Geology. A small coalbed gas field in a remote basin, that may be sub-commercial by industry standards, could represent a long-term energy resource for a village or for a major commercial enterprise. For development to occur, the costs of exploration, development, and production of coalbed gas must compare favorably to the existing cost of the current diesel fuel-based system. According to Tyler et al. (2000), Alaska's potential for CBM development may be as high as 1,000 trillion cubic feet, however, the actual number of methane-bearing coal basins and resources is not known and the producibility of the gas is not determined so far. According to Clough (2001), at least 25 roadless communities in Alaska have potential for coalbed methane resources. The Division of Geological and Geophysical Surveys (DGGs) of Alaska later identified at least 37 rural communities that are in the vicinity of methane bearing coal formations.

CBM is extracted from coal beds. In a conventional oil and gas reservoir, the resource is located and produced above a water contact. However, in CBM reservoirs, water often completely permeates the coalbeds and the gas is adsorbed into the grain surfaces of the coal due to the water pressure. Production of CBM usually requires dewatering of fractured coal seams. However, there are areas where dry gas has been produced from coal beds. Reduction of water pressure results in desorption of methane from the coal matrix resulting in flow of the gas towards the well bore.

The greatest concern and controversy associated with CBM development involves the large quantity of ground water that is produced along with CBM. The produced water is high in volume early in CBM development, but the volume of water is reduced during the life of the well operation. The disposal of this large amount of water is complicated by the fact that the water may vary in quality from meeting the federal drinking water standards up to extremely high concentrations of total dissolved solids (TDS). The majority of the water contains high levels of dissolved sediments and a high sodium absorption ratio. There are other problems involved with

the extraction of high quantity of groundwater, such as its impact on domestic water wells and natural springs, and water rights. The main problem, however, is what to do with this surplus water. According to All Consulting (2003), the management of CBM produced water is conducted using various water management practices depending on the quality of the produced water. In areas where the produced water is relatively fresh, a wide range of activities including direct discharge, storage in impoundments, livestock watering, irrigation, and dust control measures are used to handle the produced water. In areas where the water quality is not suitable for direct use, some operators are using treatment prior to discharge and injection wells to dispose of the fluids.

The major purpose of this report is to acquire, review and synthesize information on CBM water disposal and/or treatment issues that have been reported in CBM producing areas in cold climates. There is little information available for Alaskan CBM resources. Hence, this report is anticipated to serve as a resource for planning, understanding, and implementing environmentally sound water management practices of CBM produced water in Alaska.

Arthur et al. (2003) report that Alaska is new to coalbed natural gas production (first well in 1994) but has potential for development, and production would benefit remote rural communities as well as larger cities and towns. Reserve estimates for Alaska are as high as 1 quadrillion cubic feet of coalbed natural gas. Coals identified in 13 basins in Alaska are in the bituminous to lignite range with abundant water. Three of the basins – the western North Slope, the Alaskan Peninsula (southwest Alaska) and the Yukon Flats basin in central Alaska – contain the highest resources. CBM produced water disposal is a concern. Surface discharge is not a viable means because during the winter streams experience low flow rates. Water quality data from Alaska is limited, so studies would be required in most basins prior to CBM development.

Tyler et al. (2000) have discussed how CBM programs in rural Alaska will be beneficial in the profitable recovery of a local source of gas. The resource could be used as an alternative to more expensive and potentially environmentally damaging diesel fuel. The production of CBM might provide an opportunity to rural Alaskans to economically recover and possibly profit from this program. The development of CBM in rural Alaska may benefit in the creation of jobs, use of clean-burning energy, and reduction of methane emissions as a greenhouse gas.

What has not been considered extensively in the development of CBM as a resource for rural Alaskan communities is the management of the produced water. The question is, what is the quality and quantity of this water? If the quality is good, then could the inhabitants use this water as an additional resource for domestic and local industrial uses? If the quality is poor, then what would be the cost of treating the water? Would this create any financial constraints on the development of the resource, given the small community sizes it would cater to? If the water could be used as a resource, then would the production quantity pose a burden to the limited demand of the rural community? If so, then would it be possible to reduce the water production while producing sufficient gas to cater to the needs of the community? If the produced water was unsuitable as a resource, then what are the different approaches to dispose of this water without causing serious environmental impact?

While it is easy to consider a densely populated area for CBM resource development, rural Alaska poses quite a bit of challenge to utilization or treatment/disposal of the CBM produced water. With little experience with CBM resource development in Alaska, it is crucial to borrow lessons from other CBM producing regions, their environmental approaches, population that the resource caters to, and their management alternatives prior to scaling such information for application to a rural Alaskan development scenario.

This research was conducted under the direction and guidance of the US Department of Energy, National Energy Technology Laboratory, and Arctic Energy Office. Funding was provided for this research through the Arctic Energy Technology Development Laboratory of the University of Alaska Fairbanks.

The lead researchers of the project include UAF/UAA, GW Scientific, DGGS, RUSG, and INL. Literature and other information were obtained through the Geophysical Institute Library of UAF with the support of Julia Triplehorn. The basic information on the geology, potential CBM production sites, and CBM potential information on Alaska was provided by DGGS. Water quality information of rural communities and their current treatment options were obtained from research conducted by Craig Woolard. RUSG provided support in developing management models for the produced water for Alaskan rural communities. They also provided the group with internet support, development of questionnaires, and setting up the website for public information dissemination. INL provided information on Russian and Canadian experiences with CBM produced water.

The team consisted of personnel that led the direction of research and preparation of the document. The project team developed the direction and scope of the research that went into the report. The project team worked on the various portions of the report. Michael Lilly and Debasmita Misra prepared integration of the components. The team effort has been of immense help in structuring and finalizing the report. Listed below are the members of the project team.

- UAF/UAA
 - ✓ Dr. Debasmita Misra
 - ✓ Prof. Craig Woolard
 - ✓ Julia Triplehorn
- GW Scientific
 - ✓ Michael Lilly
 - ✓ Kristie Holland
 - ✓ Amanda Osborne
- Division of Geological and Geophysical Survey, Alaska
 - ✓ Dr. Jim Clough
- Remote Utilities Systems Group
 - ✓ Bob Crosby
 - ✓ Gary Whitton
- Idaho National Laboratory
 - ✓ Dr. Eric Robertson

A rigorous literature search was conducted using several databases with the help of Judy Triplehorn, Librarian, Geophysical Institute Library, UAF. The various databases searched (with keywords within parenthesis) are as follows:

- Cambridge Scientific Abstracts (coalbed methane)
- Cambridge Scientific Abstracts ((coalbed methane and (Alaska or Canada))
- Cambridge Scientific Abstracts (coalbed methane and water)
- Compendex (coal, bed, methane)
- Compendex (coalbed, methane, Alaska or Canada)
- Compendex (Exploitation of coal bed methane)
- Firstsearch Dissertations (coalbed and methane)
- Firstsearch Books-in-print (coal and bed and methane)
- Biblioline (coalbed or coal bed methane)
- Firstsearch ASTA (coalbed and methane)
- Firstsearch ASTA (Coiled tubing lowers completion costs for coalbed methane wells)
- Firstsearch ASTA (coalbed and methane)
- Firstsearch GeoRef ((coalbed and methane) and (alaska or canada))

Over 1449 references were identified from the search engines. Several of these references were procured and reviewed. All the references have been archived in an Endnote format for future search and query purposes.

Objectives

This report, on review and synthesis of CBM produced water management for rural Alaskan development addressed the following objectives:

- Define what water-management techniques are being used in other cold-climate regions
 - The scope of this objective was to review the current water-management practices adopted by CBM producers in other cold climates and the continental US. However, special attention would be given to the techniques adopted in cold climate environments.
- Alaska data synthesis
 - The scope of this objective was to gather information on coalbed methane resources of Alaska, its beneficiary rural communities, their energy demand, their water resources and demands, the quality of their resources, current treatment practices, and environmental constraints that would be limiting in adoption of their management practices.
- Canadian data synthesis
 - This objective was crucial in studying the CBM water management practices, water quality, and production quantity in Canadian cold climatic environments. Canadian geo-environmental conditions perhaps share the closest conditions to the coalbeds of Alaska. Information relevant to rural applications of water

management practices in Canada might be important to relate to Alaskan conditions.

- Russian data synthesis
 - Russian coalbeds are located in permafrost regions. Hence, synthesis of water management practice information from these CBM production sites could be beneficial in designing those for the Alaskan applications. It was presumed that Russian applications might have environmental similarities with Alaskan resources, especially in the small size of consumers and the vast amount of resource.
- Production, treatment, and disposal techniques and application for Alaska
 - This objective was designed to integrate all of the information from the other objectives in order to develop a suitable management option for CBM produced water for Alaskan rural applications.

Alaska Data Synthesis

Tyler, et al. (2000) stated in their report “Coalbed Methane Potential and Exploration Targets for Rural Alaskan Communities” that all rural Alaskan Basins have the potential for coalbed methane resource development. Their research utilizing the Bureau of Economic Geology (BEG) coalbed methane producibility model which was applied to rural Alaskan coal basins considered all the geohydrologic criteria available. They have accounted for six critical controls: tectonic/structural setting, depositional systems and coal distribution, coal rank, gas content, permeability, and hydrodynamics. Over the course of their research they have prioritized which of the five major coal provinces (including seven basins) were of primary importance in making a significant contribution to the rural Alaskan gas supply. The top ranking basins include: the Northern Alaska Province (Colville Basin), Upper Yukon Province (Yukon Basin), and the Alaska Peninsula Province (Chignik Basin). Those basins considered of secondary importance include: the Yukon-Koyukuk Province (Kobuk, Upper Koyukuk, and Lower Koyukuk Basins) and Nenana Province (Minchumina Basin). The coal types available in the primary coal basin areas range from Lignite and high volatile Bituminous to Subbituminous coal types from biogenic and thermogenic resources. While the secondary coal basins have Lignite and Subbituminous coal types from biogenic resources.

Most of Alaska’s coal was formed during the Cretaceous and Tertiary periods and is bituminous or subbituminous in rank. The largest potential coal and coalbed methane resource base is located principally in the North Slope and Cook Inlet Provinces, where much is known about the thickness and continuity of coals in the subsurface. Typical coal thickness was found to be between approximately 1-5 meters (3-16 ft) in these areas (Tyler et al., 2000). The Northern Alaska Coal Province, which includes the National Petroleum Reserve in Alaska (NPR), underlies up to an approximate 150,000 square kilometers (58,000 square miles) of the North Slope of Alaska. The major coal deposits mainly occur in two major areas: (1) the Arctic Foothills belt, which is located north of the Brooks Range; and (2) the Arctic Coastal Plain, which occupies the remaining area to the Arctic Ocean (Tyler et al., 2000). The Northern Alaska Coal Province is similar to the San Juan Basin located in the Rocky Mountain Foreland in both structural and depositional systems, as both of these basins are found along the flanks of the

Western Cretaceous Interior Seaway (Figure 1). About 150 coal beds of significant thickness, approximately 1.5-8.5 m (5 to 28 ft), have been documented along the North Slope, with a few beds measured at up to 12.192 m (40 ft) thick (Tyler et al., 2000). There is a wealth of subsurface data for the North Slope including more than 350 oil and gas exploratory wells, 2,500 development wells, and seismic data from near the Canadian border to the Chukchi Sea which has contributed substantially to the resource evaluation of the Colville Basin.

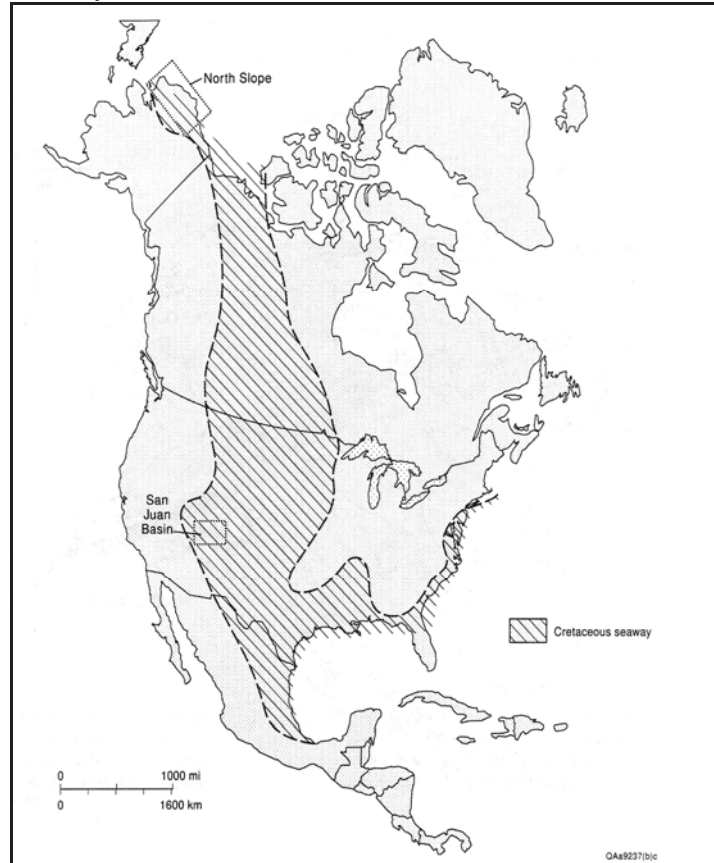


Figure 1. Structure and coal deposition are predicted to be similar for the San Juan and North Slope basins, as both of these basins are found along the Western Cretaceous Interior Seaway (from Tyler et al, 2000).

Generally, the lower and upper Cretaceous coals occur in two major sedimentary rock sequences: the Nanushuk Group (Early Cretaceous) and the Colville Group (Late Cretaceous). Given all of the available information, the primary potential coalbed methane resource occurs in the Cretaceous, Nanushuk Group coals within the western Colville Basin. The Nanushuk Group coals extend from the eastern boundary of NPRA to the Chukchi Sea coast and have the highest potential for coalbed methane resource development of rural Alaska (Tyler et al., 2000). Between Wainwright and Atkasuk and an area approximately 48 km (30 miles) south of these villages, the potential for coalbed methane resource development is high. Within this region, along the Alaskan Coastal Plain, the coals are found at depths suitable for exploration (Figure 2) (Tyler et al., 2000). In the Colville Basin, most of the Nanushuk Group coals will be in or near the permafrost zone. It is not yet known what effects permafrost and cold temperatures will have on gas flow from these coals, but low permeabilities in these shallow zones are predicted. The depths to the exploration targets should therefore be below the permafrost to depths not

exceeding 1,828.8 m (6,000 ft), an economic cut-off to depth of drilling based on the current activity in the lower 48 (Tyler et al., 2000).

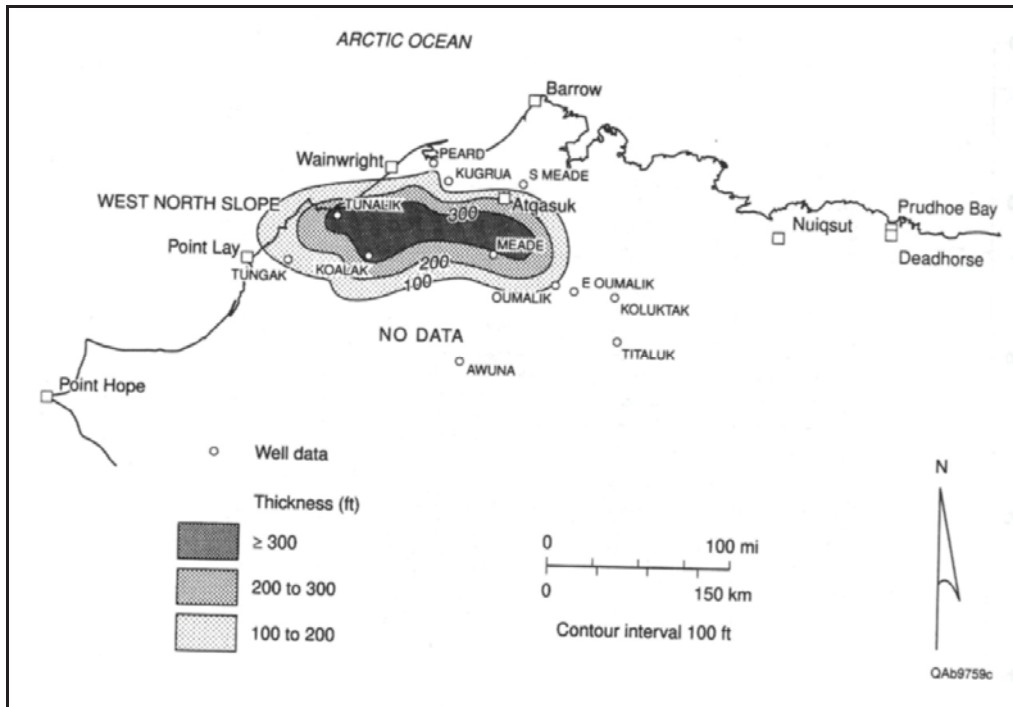


Figure 2. Total coal thickness of the Nanushuk Group, coal-bearing zones, western Colville basin. Coal thickness exceeds 300 ft south of the villages of Wainwright and Atqasuk (from Tyler et al., 2000).

The Yukon National Wildlife Refuge, south of the Brooks Range and north of the Alaska Range, consists of several distinct lithostratigraphic units and terranes, of which, the Yukon Flats Basin is considered important for oil and gas discovery (Tyler et al., 2000). The Yukon Flats basin is the largest interior basin in Alaska covering more than approximately 22,015 square kilometers (8,500 square miles). Oil and gas exploration of the Yukon Refuge show a complex assemblage of rock types, from all geologic time periods, however there is little to no subsurface data available. Using the limited subsurface and outcrop data, Tyler et al. (2000) inferred that coal-bearing rocks may underlie most of the Yukon Flats Basin, but they were unable to estimate coalbed thickness or coalbed methane potential. Although coals appear to be relatively thick (>6.4 m, (>21 ft)) and gassy in this area, it's possible that their thickness, lateral extent, and/or gas content are insufficient to support significant coal-gas production.

Along the Alaskan Peninsula, rocks of the Chignik Formation (Upper Cretaceous) are the prime coalbed methane targets (Tyler et al., 2000). The Chignik Formation is exposed in a long, narrow belt on the Alaska Peninsula between Pavlof Bay and Wide Bay, with two main coal fields, Chignik Bay and Herendeen Bay fields, approximately 160 km (99.42 miles) apart (Figure 3) (Tyler et al., 2000). The Chignik Bay coal field is the prime coalbed methane target and is generally in the bituminous rank except in localized areas of higher heat flow. Although Cretaceous coal may underlie a significant area of the Alaska Peninsula, the Chignik area is relatively unfavorable for coalbed methane exploration and development due to poor reservoir

rock continuity, the presence of intrusive/igneous rocks, and recent erosion in the area. In addition, due to the high annual precipitation rates and close proximity to the ocean, dewatering of permeable coal beds may prove to economically unfeasible (Tyler et al., 2000).

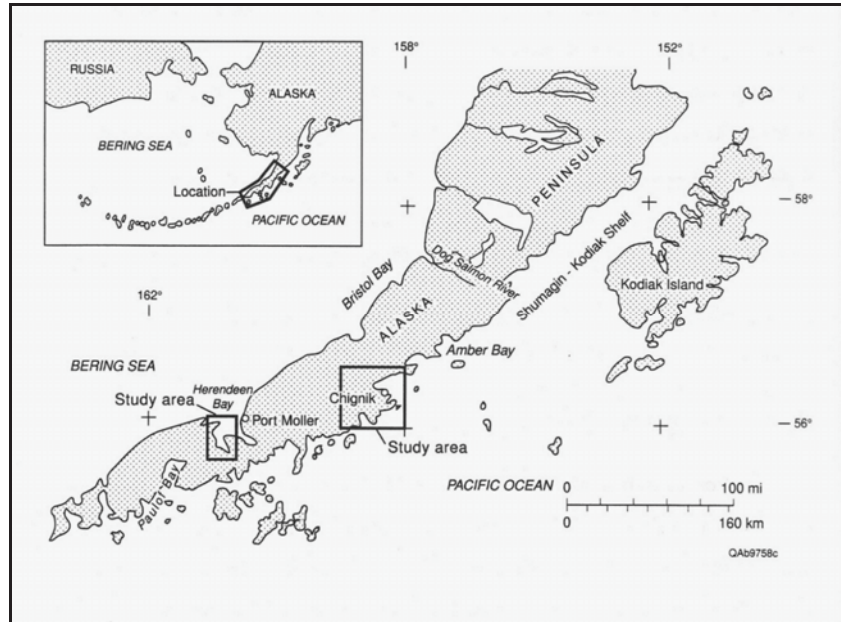


Figure 3. Location of the Chignik formation on the Alaskan Peninsula (from Tyler et al., 2000).

At the time of this report, there were no producing CBM fields in rural Alaska, or any exploration efforts that had collected or reported any specific water quality data. The few commercial CBM field developments in Southcentral Alaska were using downhole injection, so there were no water treatment methods being used applicable to rural Alaska.

Canadian Data Synthesis

Canada holds an estimated 7.3 billion short tons of recoverable coal reserves. The country produced 73.2 million short tons (Mmst) in 2002, down from a peak of 86.7 Mmst in 1997. A map showing the major coal deposit sites in Canada is shown in Figure 4. Coal production is concentrated in the western part of the country, specifically in Alberta (50% of production), British Columbia (30%), and Saskatchewan (15%).

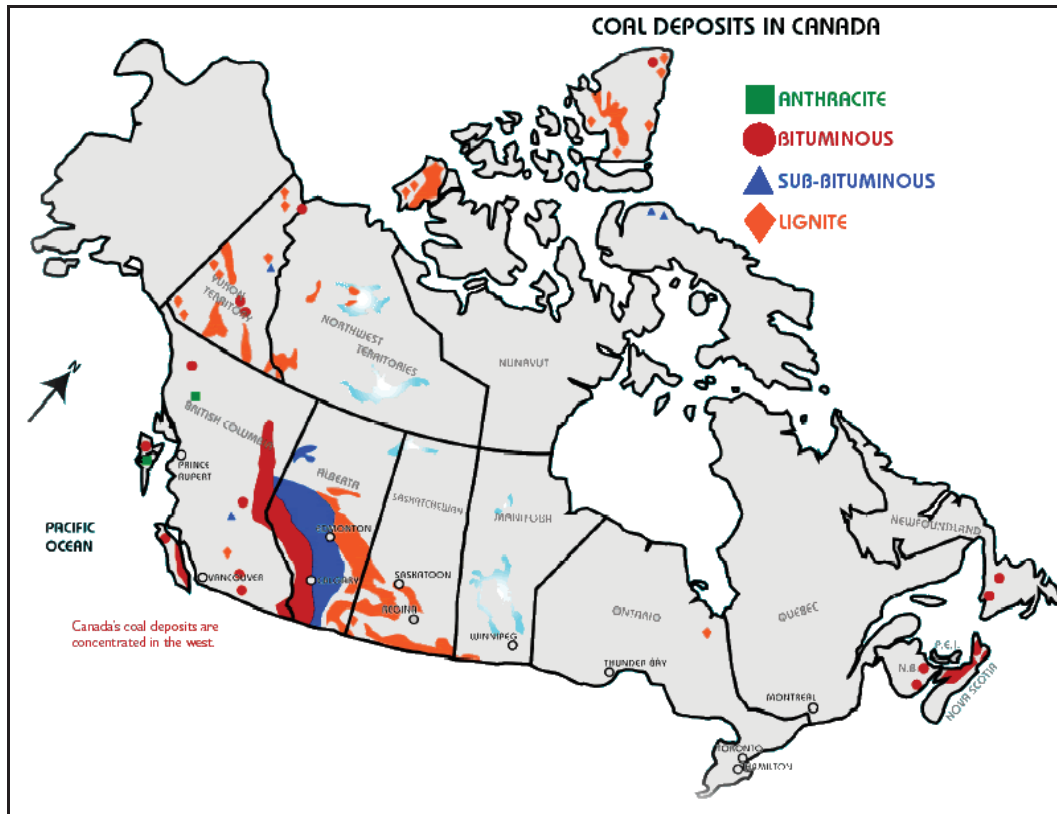


Figure 4. Major coal deposits of Canada.

Coalbed methane (CBM) production is still in its infancy in Canada, with the first wells drilled only in 1997. There is a strong belief that CBM production will eventually replace the decline in conventional natural gas production. In 2004, CBM production was at 100 Mmcf/d, with predictions that it could average over 1,400 Mmcf/d by 2010. Analysts estimated that Canada has 500 Tcf of recoverable CBM deposits, concentrated in British Columbia and Alberta (USDOE).

Figure 5 shows the current CBM plays in western Canada. The most advanced, and currently the only commercially viable, CBM projects are in the Palliser block of southern Alberta. However, there are more than 20 other publicly known projects investigating the commercial potential of CBM across Canada. CBM evaluation activity in British Columbia has lagged behind Alberta's somewhat, primarily due to a lack of oil and gas infrastructure and the wider distribution of the resource. Three areas that have seen activity in this province are: northeast British Columbia (Peace River), southeast British Columbia (Elk Valley) and Vancouver Island (Lang, 2002).

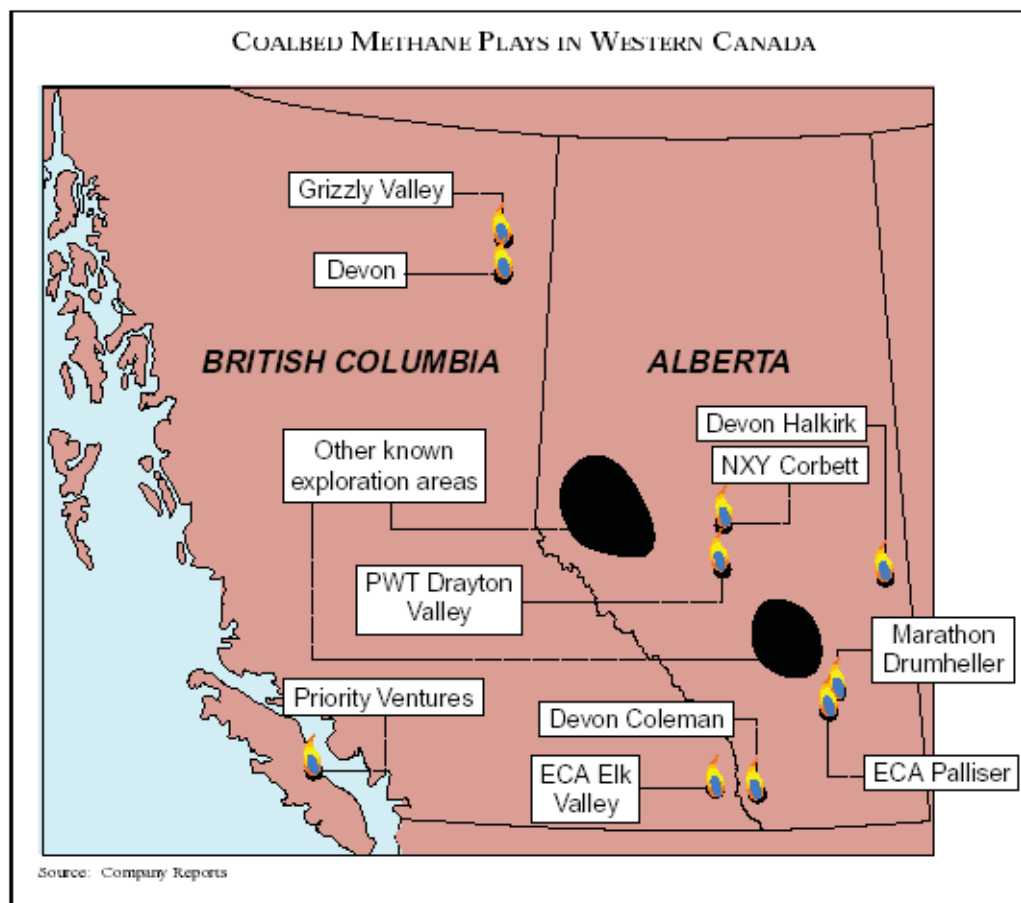


Figure 5. Current coalbed methane plays in Western Canada.

Currently there is no production of CBM or associated water in Alberta's permafrost regions. Most of the Alberta CBM production is in south central Alberta, primarily from coals that produce little to no water (Bastien, 2005). There is some production northwest of Edmonton (northwest-central Alberta), but this area is not in the permafrost zone, and this northwestern area has deeper production of saline water from coals, and is reinjected into nearby disposal wells (at a depth equal or greater than the CBM producing horizon). In northern Canada there have been some investigations of the CBM potential of some coal basins but there is no production at this time, and no plans to attempt production in the near future (Beaton, 2008).

All produced water in British Columbia, whether fresh or salt-laden brine, is deemed a waste and currently cannot be discharged into the environment except under specific authorization by the British Columbia Ministry of Water, Land and Air Protection. However, this ministry is proposing a Code of Practice (2004) to be administered and enforced by the Oil and Gas Commission that will authorize the surface discharge of some produced water from coalbed gas operations.

The Code will require the industry to consider the beneficial use of discharged water. The use of this water for irrigation, stream flow augmentation, or industrial purposes will be encouraged if

the quality is good enough or if the industry chooses to apply treatment to an acceptable level. In the proposed code, the maximum volume of discharge of produced water to a stream is limited by the amount of flow in the receiving stream. The code also includes standards that must be met for critical parameters (e.g., dissolved and suspended solids, toxicity, and dissolved oxygen). If the surface discharge standards are not met, then the produced water must be disposed of in underground formations deeper than the zone of extraction. Deep-well injection is regulated by the Oil and Gas Commission under the Petroleum and Natural Gas Act.

Russian Data Synthesis

Basic coal mining industries in the former Soviet Union were concentrated in four coal basins: Kuznetsk and Pechora, located on the territory of Russia, Donetsk sited in the Ukraine and Russia, and Karaganda coal basin situated in Kazakhstan (Figure 6). USSR coal output in 1989 made 730,899 thousand tons, 25.5 % of which belonged to Donetsk, 20.8% to Kuznetsk, 7% to Karaganda and 4% to Pechora coal basins.



Figure 6. Hard coal and coalbed methane deposits of Commonwealth of Independent States.

The total area of Donetsk coal basin is 12.8 million ac, with coal reserves amounting to 140.8 billion tons; Kuznetsk coal basin occupies the area of 5.69 million acre, incorporating 637 billion tons of coal reserves; Pechora coal basin total area is 19.2 million acre with coal reserves amounting to 265 billion tons; Karaganda coal basin area is 7.7 million acre with 32 billion tons of coal reserves. Assessed coal reserves (down to 1,800 meters depth) for these four coal basins

account for 473 Tcf. For Donetsk coal basin they amount to 34.0 Tcf, in Kuznetsk to 371.0 Tcf, in Karaganda to 14.2 Tcf and in Pechora to 53.8 Tcf (Figure 7).

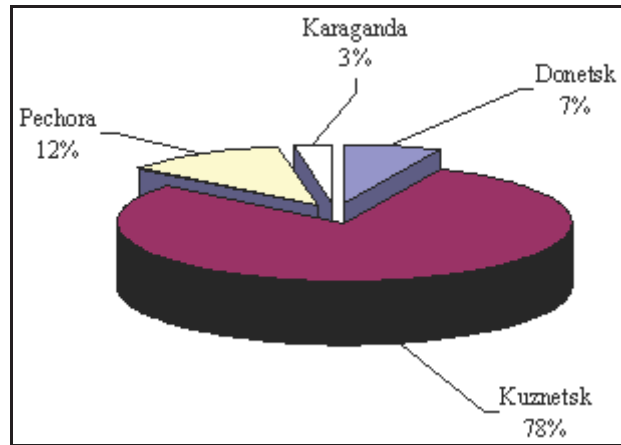


Figure 7. Coalbed methane resources distribution among basic coal areas of the former USSR.

Degasification systems' progress at coal mines of CIS countries are primarily aimed for securing mining work safety. Within recent years a decline of degasification work was observed due to the closure of gassy coal mines employing degasification systems; and coal output reduction resulting in a drop in coal mine methane.

Isolated attempts were undertaken in Russia and in the Ukraine to initiate methane recovery from coal seams unrelated to coal mining activities. In Kuzbass (in south-central Russia) in 1998 in the Erunakova region, the drilling of two pilot core holes was accomplished to 4,115 ft depth and drilling of the first commercial one is currently underway. Obtained test and research results demonstrated a high potential of stripped coal bearing strata for CBM recovery. Total coal seam thickness intersected by these wells is in excess of 244 ft; the in situ gas content was measured to be between 0.54 Mcf/t and 0.71 Mcf/t; and the permeabilities of the seam ranged from 20 mD to 150 mD. In case of positive results in pilot commercial wells exploitation, it is planned to drill 500 more wells on Russia's first coal-gas fields in Kuzbass.

No plans have been found for the future development of the CBM resource located in the Pechorsky coal basin, which is the only major coal basin located within the colder northern region.

Other Cold Regions Data Synthesis

Our literature survey has resulted in obtaining information on the CBM fields, gas and water production of selected fields in China, Poland, and Kazakhstan. According to Sanli et al. (2003), Qinshui Basin has become one of the most active areas for CBM exploration and development in China. In this area commercial CBM rates have been obtained with the maximum CBM rate of 16,000 cu. meters per day in a single well. No.3 and No.15 coal seams are two major pay-zones

in the area with both seams' burial depths being shallower than 1000 m with a stable distribution. No.3 coal seam's thickness ranges from 4.5 to 7 m, and No.15 ranges from 2.5 to 5 m. The coals in this area are anthracite. Gas contents are relatively high, ranging from 10 to 24 m³/t. The coal permeability extends generally from 0.1 to 5.7 mD, averaging 1 mD. Data on Qinshui Basin is provided in Table 1.

Table 1. CBM production summary of Zhaoyuang Block of Qinshui Basin, China (Reproduced from: Sanli et al., 2003).

Well	Days of Prod.	maxmium rate,m3/d	Averging Water Prod.,m3/d	Cum. Gas Prod.,m3
FZ-001	742	102.4	4.6	3698
FZ-002	727	13,648	7.1	1,580,000
FZ-003	712	2566	4.2	880,000
FZ-004	711	3524	4.5	720,000
FZ-005	711	388	14.7	73,000
FZ-006	709		50	38,000
FZ-007	732	1564	6	676,000
FZ-008	711	5719	13	1,430,000
TL-003	1687	6986	40	1,450,000
FZ-010	52		0.3	
FZ-011	47	767	7.5	1,679
FZ-012	45		8.6	
FZ-015	51		0.15	
FZ-016	35	312	8.9	1,367
FZ-017	46		20.5	
Total				6,853,744

In Poland, CBM was recovered through degasification of coalbeds in the Upper Silesian Coal Basin (USCB), located in the southern part of Poland. Total acreage of the basin is about 5,400 km². According to Krzystolik et al. (2003), Hard coal occurred in the formations of Upper Carboniferous. It was characterized in general by relatively good mining conditions. Average thickness of the seams was over 2.0 meters and their inclination was not higher than 10°. At present there are 42 operating coal mines, and their total output for the year 2001 was 103 million tons. Presently, regular degasification is being conducted in 18 - 20 hard coal mines, depending on the location of the coal faces, 17 of the above coal mines have central methane drainage stations on the surface. Methane intakes, its utilization and losses in the year 2001 are presented in Table 2.

Table 2. Volumes of collected, utilized and vented from the degasification station methane (losses of collected and non utilized methane) in 18 most gassy coal mines of USCB in 2001 (Reproduced from Krzystolik et al., 2003).

Lp	Coal mine	Volume of collected CH ₄		Volume of utilized CH ₄		Volume of vented CH ₄		Result %
		m ³ /min	m ³ /year	m ³ /min	m ³ /year	m ³ /min	m ³ /year	
1	Brzeszcze	67,90	35.666.928	67,90	35.666.928	0	0	100
2	Silesia	9,63	5.062.600	9,43	4.957.300	0,20	105.300	97,9
3	Weso ³ a	22,10	11.615.760	11,99	6.290.665	10,11	5.359.678	54,1
4	Halemba	9,10	4.654.619	4,47	2.286.799	4,63	2.367.820	49,1
5	Staszic	18,12	9.922.349	7,01	3.686.563	11,11	5.835.768	38,7
6	Bielszowice	10,46	5.496.051	1,21	636.585	9,25	4.859.466	11,6
7	Soenica	9,00	4.730.400	0	0	9,00	4.730.400	0
8	Budryk	26,00	13.666.100	0	0	26,00	13.666.100	0
9	ŒPsk	9,93	5.219.208	0	0	9,93	5.219.208	0
10	Szczyg ³ owice	13,02	6.843.904	0	0	13,02	6.843.904	0
Total		195,26	102.628.650	102,01	53.616.456	93,25	49.012.200	52,2
Coal mines of Rybnik Mining Area (pl: "ROW")								
1	Zofiówka	40,18	21.119.900	40,00	20.821.200	0,18	298.700	99,5
2	Jas – Mos	16,50	8.670.000	16,00	8.388.600	0,50	281.400	96,8
3	Pniówek	80,10	42.100.500	56,77	29.842.100	23,33	12.258.400	71,2
4	Marcel	17,80	9.356.560	11,82	6.212.940	5,98	3.140.620	67,2
5	Krupiński	38,30	20.124.000	22,04	11.586.100	16,26	8.537.900	57,6
6	Borynia	0,50	266.400	0,18	96.400	0,32	170.000	37,0
7	Jankowice	19,40	10.217.600	1,94	1.041.100	17,46	9.176.500	10,3
8	Chwa ³ owice	10,00	5.241.600	0	0	10,00	5.241.600	0
Total in ROW		222,80	117.103.680	148,75	78.183.000	74,05	38.920.680	66,8
TOTAL		418,06	219.732.330	250,76	131.799.450	167,30	87.932.880	60,0

According to Mustafin et al. (2003), the main Kazakhstan coal reserves are concentrated in the Central, Northern and Eastern regions of the country. The total reserves of these main coal mining regions are estimated at 30 billion ton and hypothetical reserves are at about 140 billion ton. Undiscovered coal methane resources for studied coal basins of Kazakhstan amount to 1.2-1.7 trillion m³. The main CBM reserves are concentrated in Karaganda and Ekibastuz basins, which contain 500-750 and 75-110 billion m³ respectively. CBM resources of Kazakhstan coal deposits, and prospects for gas extraction, are estimated at approximately 2 trillion m³, only to the depth of 1800 m. A half of these resources are contained in Karaganda coal-and-methane basins, and 47 billion m³ – in Ekibastuz Basin. The methane reserves of the central Kazakhstan are provided in Table 3.

Table 3. Methane reserves of central Kazakhstan coal deposits (Reproduced from Mustafin et al., 2003).

Basin, deposit, field	Coal reserves, million ton	Methane capacity m ³ /t	Methane reserves, billion m ³	Density of methane reserves, billion m ³ /km ²
1	2	3	4	5
Karaganda basin		10-30	~1000	0,28-0,7
FIST-PRIORITY OBJECTS				
Tentetskaya mold	1200,4	10-30	20,7	0,5
Deep horizons of Saranskiy field	3000	22-27	60	0,7
SECOND-PRIORITY OBJECTS				
Dubovkiy field	600	24-28	10.2	0.5
Deep horizons of Churubainurinskiy area	2327	24-27	55.4	0.4
Taldykudukskiy field	1800	10-30	36,4	0.6
FIST-PRIORITY OBJECT				
Ekibastuz coal basin (seams 1,2,3)	4800	14-20	47	1,3-3,1
OTHER OBJECTS				
Zavyalovskoye	529	17	14.6	0.03
Samarskoye	1300	25	26.0	0,12
Nurinskoye	491	12	5,9	0,17
Akzhar	421	15	3.4	0.1 1
Teniz-Korzunkolskiy basin	2600	25	45.0	0.26
Koitas	452	12	5.4	0,08

There is no information available on the management methods that are used for CBM water treatment and disposal in China, Poland, or Kazakhstan, based on the review of the available literature.

Most of the CBM production information is focused on gas production. Therefore, no technology on water disposal or treatment of the co-produced water has been discussed in the available literature.

According to the available literature, the CBM production in these regions is limited to coal mine degasification, except for the Chinese basin. No rural related applications have been recorded in their discussions.

Potential Rural CBM Water Production, Treatment, and Disposal Methods

Rural Alaska Water Production Issues

- Production reduction methods
 - The amount of water produced from existing CBM wells outside Alaska typically starts at a high volume and declines significantly once the coal seam becomes depressurized (Kuipers et al., 2004). Water flow rates depend on geologic features, coal seam permeability, completion and stimulation practices, and well pump size. Production usually peaks within the first month of pumping and then

decreases to 10 – 20% of the peak rate as the formation is depressurized. Water production rates also decrease with the development of adjacent wells that renders complementary dewatering in the formation (Gas Research Institute, 1993). Water production usually drops to a steady state after about 6 to 12 months of pumping. In CBM producing areas of the lower 48, the average water production ranges from less than 25 bbl/day/well to as much as 400 bbl/day/well.

- If we consider, hypothetically, that a CBM producing well in a rural Alaskan community produced 400 bbl/day/well (~16,800 gallons/day/well) and that the community's energy needs are met by this single well, then using the example of Clough (2001) for a medium-sized community of 700 people, the demand for water use for this community, assuming 40 gallons per person per day of use would total 28,000 gallons. Hence, if it is assumed that the community will depend partially on the CBM produced water as a resource, then the single well production would suffice as a resource for the community if the water is clean or treated to drinking water standards.
 - However, with more wells complementing the dewatering, the average production of water from the CBM wells would be much higher than the demand for use. In such a scenario, reduction of produced water would be a viable option. However, to the best of our knowledge, this option has not been researched for CBM recovery.
 - If however, the produced water needs to be disposed entirely, then environmental treatment costs would need to be considered in the economic evaluation. In such a scenario, lowering the amount of produced water would reduce environmental costs. Reduction in produced water is an area of active research in oil and natural gas production but has not been completely successful.
- Field logistics and drilling constraints
 - Alaska poses several constraints for development of CBM resources in rural communities. First and foremost is the high transportation cost to rural off-road locations. Most of the rural communities located near potential CBM resources are not on the state road system. Therefore, transportation of equipment for drilling and development of the basin is limited to water or air routes. Winter months are difficult for any fieldwork due to cold climate and snow conditions. Transportation in the winter is usually only possible via air routes, which might prove to be costly. The field season is also limited by the long winter months. Drilling in permafrost needs special familiarity. The success of a CBM development program in Alaska is best summarized by Tyler et al. (2000), "It is hypothesized that the first (one or two) wells drilled in the rural Alaskan exploration program will be the key to the future of coalbed methane development in the state. Fairways should therefore be targeted in the basin having the most available data (North Slope-Colville Basin) and the highest probability of penetrating thick, laterally continuous and gassy coal beds. Drilling a dry hole having little or no coal, or low gas contents, during early exploration attempts may severely retard future coalbed methane exploration and development in rural Alaska. The drilling program should proceed with the cooperation of local operators familiar with drilling in permafrost regions and with local organizations

that can provide additional data and information for complete evaluation of the coalbed methane potential.”

- Scaling issues associated with rural versus commercial production
 - Two issues are critical in scaling down a CBM project from a commercial production to a rural Alaskan operation. These are the amount of methane produced and the amount of water produced.
 - A commercial production caters to a population that is a few orders of magnitude larger than the typical rural community of Alaska. Hence, the demand for energy may also be equally low in Alaska. The constraint is how to produce the right amount of gas to meet the demand of the rural population without venting any excess amount to the atmosphere. This process would relate to assessment of the gas to water ratio of currently producing wells in order to plan for a suitable ratio based on the demand and supply of the rural communities. In the lower 48 CBM projects, the water to gas ratios vary from 0.03 to 2.75 (bbl/MCF) on average.
 - Once the energy demand is assessed, a certain water to gas ratio may be adopted for production of CBM in a rural community. The limitation of such a priori adoption may not be practicable depending upon the hydrogeology of the basin, the permeability of the coal seams and other geologic conditions. Production of water at a limited rate may not depressurize the coal formations appropriately; hence, production of methane might be hindered. As opposed, initial production of a high rate of water might be difficult to treat and/or dispose. Besides, control of the methane production might also be difficult. Without a complete assessment of the basins and their characteristics, it is not possible to conclude a specific scaling parameter for a particular basin and its associated rural community.

Potential Rural CBM Water Production, Treatment, and Disposal Costs

A review of the available literature indicates a high degree of variability in costs for CBM produced water treatment and disposal. Following are excerpts from one typical example. The first is from a white paper found at <http://www.netl.doe.gov/publications/>

Produced Water from Coalbed Methane (CBM) Production

“The quality of CBM produced water varies with the original depositional environment, depth of burial, and coal type (Jackson and Myers 2002), and it varies significantly across production areas. As CBM production increases and more water is produced, concern about the disposition of these waters on the receiving environment is increasing, since uncertainties abound regarding the impact of these waters, as regulators and operators try to ensure protection of the environment. CBM constituent data are growing, and many states maintain files with produced water data. Sources include the Colorado Oil and Gas Conservation Commission, the Groundwater Information Center at the Montana Bureau of Mines and Geology, the Utah Division of Oil, Gas, and Mining, and the Wyoming Oil

and Gas Conservation Commission. In addition, the U.S. Geological Survey (USGS) Produced Waters Database contains data on the composition of produced water and general characteristics of the volume of water produced from specific petroleum producing provinces in the United States (Breit et al. 1998). The data were originally compiled by DOE and the Bureau of Mines, and the USGS has reviewed, verified, and evaluated the reliability and quality of the data. However, information on the actual impacts of CBM discharges — which depend not only on produced water characteristics, but also on the characteristics of the receiving environment — are not well understood.”

Cost Rates (\$/bbl)

The cost of managing produced water after it is already lifted to the surface and separated from the oil or gas product can range from less than \$0.01 to at least several dollars per barrel. The following sections offer several examples of costs.

Offsite Commercial Disposal Costs

In 1997, Argonne National Laboratory compiled information on costs charged by offsite commercial disposal companies to accept produced water, rain water, and other “watertype wastes” (Veil, 1997b). The reported costs are assumed to be lower than or comparable to the costs available for onsite management by the operators themselves. Costs for disposing of these wastes are listed in Table 4. Overall, disposal costs are \$0.01-\$8/bbl, although most are \$0.25-\$1.50/bbl. The highest cost, \$8/bbl, is charged at one facility in Wyoming for particularly dirty wastes that need pretreatment before injection. The same facility charges as low as \$0.75/bbl for cleaner wastes. The lowest cost is charged by a nonprofit facility in California that operates as a cooperative for several member users. These costs are solely disposal costs; the cost of transporting the water to the facilities is additional.

By far, the most common commercial disposal method for produced water is injection. The range of costs for injection is the same as that described in the previous paragraph. Ten companies in Wyoming, five companies in Utah, and four companies in New Mexico use evaporation to dispose of produced water. The cost is \$0.25-\$2.50/bbl. Another New Mexico company uses a combination of evaporation and injection, at a cost of \$0.69/bbl. The nonprofit California company described above, which also uses a combination of evaporation and injection, charges \$0.01-\$0.09/bbl.

Six companies in Pennsylvania utilize surface water discharge options. Three of these companies treat and blend produced-water and discharge it directly through an NPDES permit. Another company treats the waste and discharges it to a sanitary sewer that leads to a municipal wastewater treatment plant. They charge \$1-\$2.10/bbl. Two municipal wastewater treatment plants accept water-type wastes but not produced water. They charge \$0.65-\$1.50/bbl. Another company in Pennsylvania spreads produced water on roads in the summer and discharges to a municipal wastewater treatment plant in the winter. This company charges \$1.30-4.20/bbl.

Costs for Rocky Mountain Region Operators

Jackson and Myers (2002, 2003) provide cost estimates for many produced water disposal methods that might be used in the states of Wyoming, Colorado, Utah, and New Mexico. Table 5 (see also Figure 8) is based on data from that paper. The majority of their reported costs range from \$0.01/bbl for surface discharge or evaporation to more than \$5.50/bbl for commercial waste haulers. The magnitude of the cost depends on the water chemistry, the regulatory requirements imposed, and the amount of treatment needed.

The cost of managing produced water after it is already lifted to the surface can range from less than \$0.01 to at least several dollars per barrel.

Table 4. Disposal costs for produced water at offsite commercial facilities.

State	Number of Facilities Using This Process	Type of Disposal Process	Cost ^a
CA	1	Evaporation/injection	\$0.01-\$0.09/bbl
KY	1	Injection	\$1/bbl
LA	23	Injection	\$0.20-\$4.50/bbl
NM	4	Evaporation	\$0.25-\$0.81/bbl
NM	1	Evaporation/injection	\$0.69/bbl
NM	1	Injection	\$0.69/bbl
OK	1	Injection	\$0.30/bbl
PA	3	Treat/discharge	\$1-\$2.10/bbl
PA	1	Treat/POTW	\$1.25-\$1.80/bbl
PA	1	POTW/road spread	\$1.30-\$4.20/bbl
PA	2	POTW	\$0.65-\$1.50/bbl
TX	9	Injection	\$0.23-\$4.50/bbl
UT	5	Evaporation	\$0.50-\$0.75/bbl
WY	10	Evaporation	\$0.50- \$2.50/bbl
WY	1	Treat/injection or discharge	\$0.96/bbl
WY	3	Injection	\$0.60-\$8.00/bbl

^a Costs are those reported by disposal company operators in 1997. Source: Veil (1997b).

Table 5. Produced water management costs.

Management Option	Estimated Cost (\$/bbl)
Surface discharge	0.01-0.80
Secondary recovery	0.05-1.25
Shallow reinjection	0.10-1.33
Evaporation pits	0.01-0.80
Commercial water hauling	1.00-5.50
Disposal wells	0.05-2.65
Freeze-thaw evaporation	2.65-5.00
Evaporation pits and flowlines	1.00-1.75
Constructed wetlands	0.001-2.00
Electrodialysis	0.02-0.64
Induced air flotation for deoiling	0.05
Anoxic/aerobic granular activated carbon	0.083

Source: Jackson and Myers (2002, 2003).

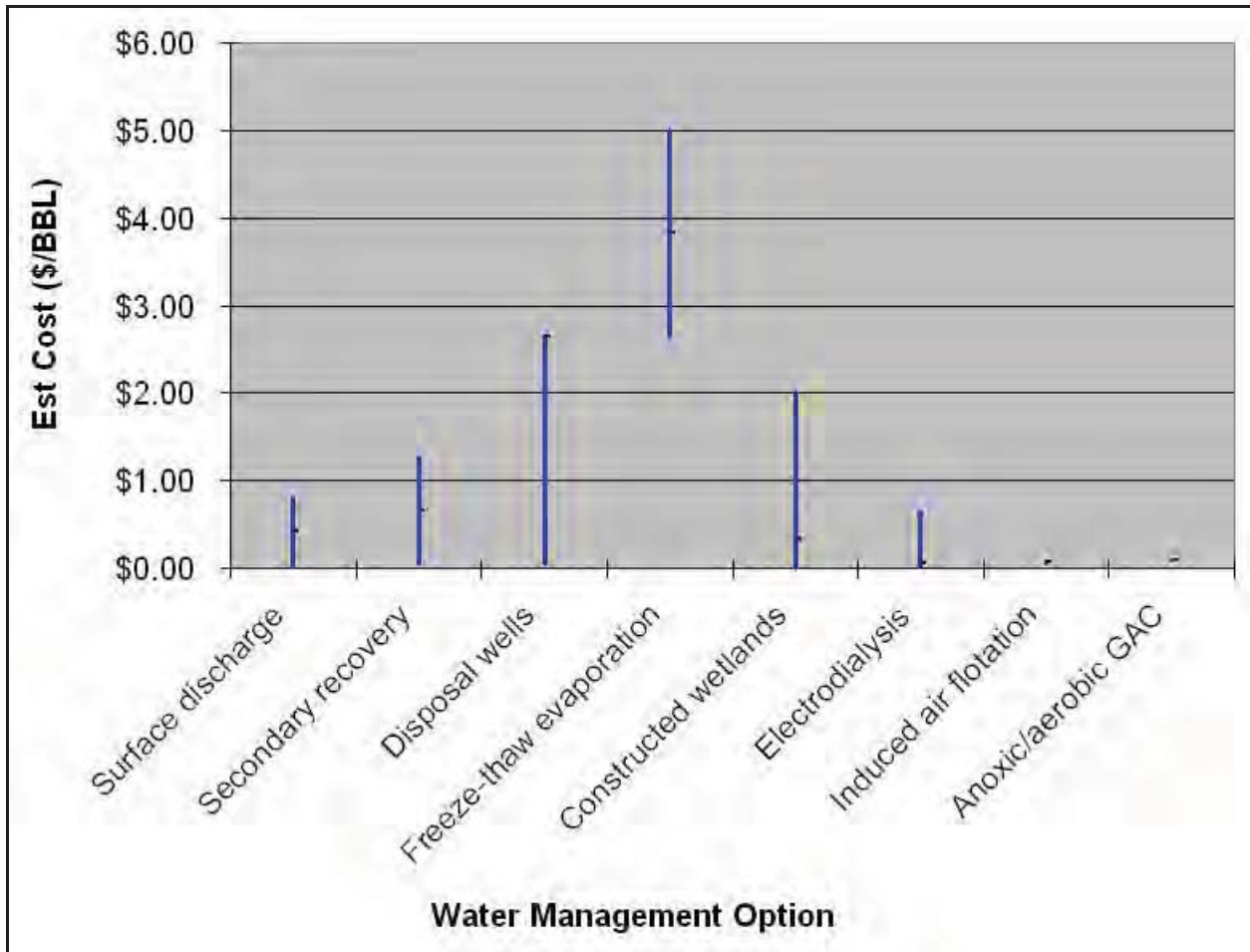


Figure 8. Produced water management costs from Table 5, presented in graphical form.

Rural Alaska costs issues and applicability for CBM water production

Available construction cost information for existing rural Alaskan village water treatment systems provided by the UAA Department of Environmental Quality Engineering indicates a similar degree of variability. The following chart (Figure 9) was generated by dividing the construction cost of water treatment systems in each of the listed villages by the demand, in gallons per day. Data was provided by UAA. An example flow chart of water treatment and disposal system is illustrated in Figure 10.

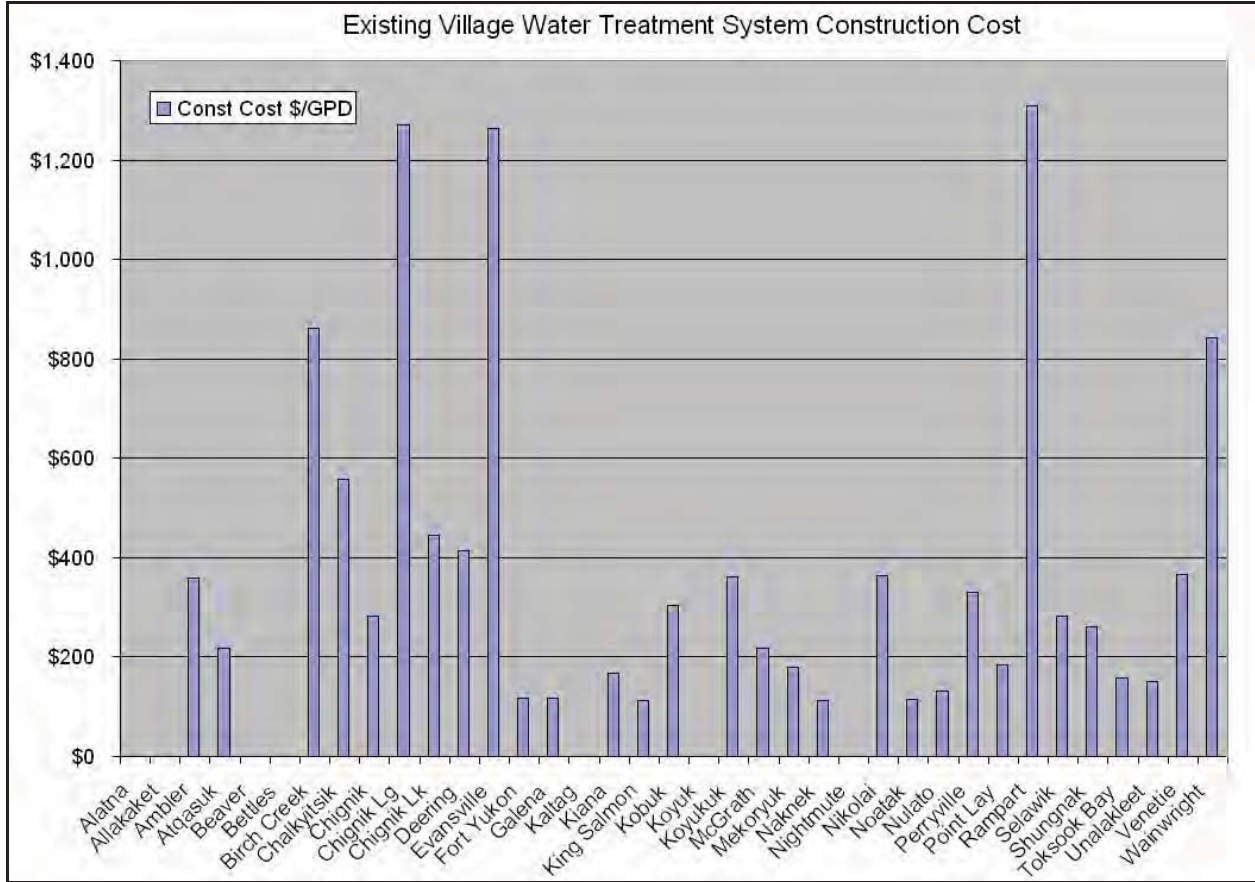


Figure 9. Existing village water treatment system construction cost (construction cost of water treatment systems divided by demand of villages, in gallons per day).

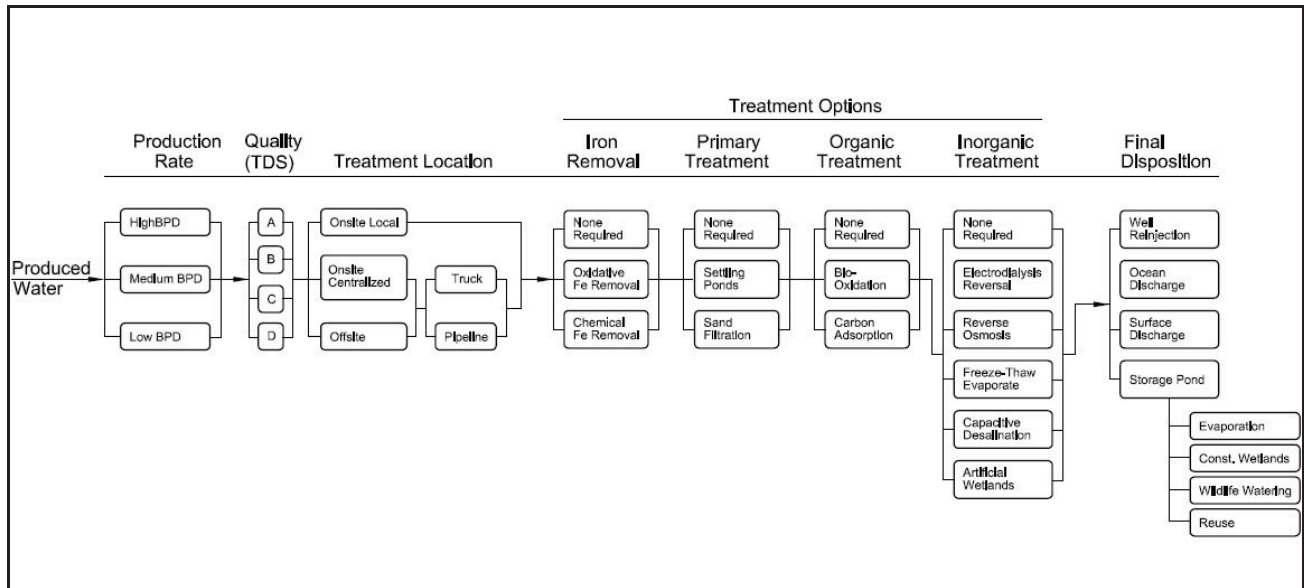


Figure 10. Example system flow chart for a water treatment and disposal system.

Potential for Use of CBM Water as a Drinking Water Source in Rural Alaska

In rural Alaska, coalbed methane (CBM) produced water might have value for use as a water source. Cold winter temperatures that cause water sources to freeze in many cases require villages to maintain large water storage tanks to provide a winter water supply. In addition, many surface water sources used by Alaska’s small communities contain high concentrations of natural organic material, referred to as “tundra tea” and often cause the formation of disinfectant byproducts during treatment (Jones, 2001). CBM produced waters would provide a constant thawed water source that could be treated and used year round, thereby decreasing storage requirements. Additionally, it is possible that the water quality generated from a CBM well could exceed the quality of the current water source, even in villages whose source is ground water under the influence of surface water, which is commonly plagued with high concentrations of iron, manganese, and arsenic.

The purpose of this study was to evaluate the potential of using CBM water as a drinking water source in rural Alaska. To evaluate this potential, we used the following approach. First, we investigated the potential CBM water quality. We then summarized the available current drinking water source water quality from villages with known CBM potential. The treatment systems currently utilized in these villages and their approximate costs were then summarized. Finally, we made an estimate of the number of communities and types of treatment systems that would be required to treat CBM water if it were to be adopted as a drinking water source.

Rural CBM Water Information

Information on specific characteristics of water co-produced with coalbed methane (CBM) in Alaska is lacking, so to estimate potential produced water quality, we reviewed the chemical content CBM produced waters from other locations. Among the most studied CBM waters are those produced by the following coal basins: Black Warrior, AL, Powder River, WY, Raton, NM, San Juan, CO, and Uinta, UT. Despite basin differences in coal formation type, geologic age and location, dissolved ions in these waters contain mainly sodium (Na), bicarbonate (HCO_3) and chloride (Cl). They are relatively low in sulfate (SO_4), and higher in sulfite (SO_3), (USGS 2000). Trace-element concentrations and volatile organic compounds are generally low (Van Voast 2003, Rice 2000).

High total dissolved solids (TDS) concentrations in CBM waters are commonly what exacerbate treatment issues and requirements. TDS concentrations can range from 200 mg/L to 170,000 mg/L (USGS, 2000). Unlike the other chemical characteristics of CBM produced waters, TDS concentration depends upon the depth of the coal beds, the composition of the rocks surrounding the coal beds, the amount of time the rock and water react, and the origin of the water entering the coal beds (USGS, 2000).

Without specific TDS data on CBM produced water in Alaska, it was necessary to assume (for the purposes of comparison and cost estimation) an average produced water quality. For this study, TDS concentrations modeled after CBM produced water in the Powder River Basin, WY, where TDS ranges from 370 to 1,940 mg/L, with a mean of 840 mg/L (Rice, 2000). Relative to other areas where CBM has been extracted, generated water in the Powder River Basin is of good quality, with a comparatively low TDS content.

Existing Village Water Supply Data

Tables 6 and 7 summarize the water-quality information available from rural villages proximate to CBM resources. Table 8 summarizes the basic village treatment system type and storage tank size. As shown in Table 6, thirteen of these villages obtain water from surface sources. Although occasional water quality issues are presented by high iron and manganese and total organic carbon (TOC), the general water quality is good. Treatment to drinking water standards is typically completed using basic granular media filtration and chlorine disinfection. Due to the high concentration of natural organic material in the surface water sources of the North Slope Borough villages of Wainwright, Point Lay and Atkasuk, these communities use a dual membrane microfiltration/nanofiltration system for treatment.

City and individual wells are used to provide water to the remaining villages (see Table 7). In these cases, the water is classified as groundwater or groundwater under the influence of surface water. Poor water quality or unreliable well flows are common, often due to poor well placement or aged equipment. Treatment to reduce high iron and manganese content is frequently required of these groundwater sources. Arsenic is another widespread groundwater contaminant in Alaska, but is not found to be an issue for the majority of villages identified near CBM reserves. In most cases, the green sand filters used by standard rural water treatment systems are sufficient to manage the high concentrations of these constituents and comply with

drinking water standards. Issues of taste and aesthetics still persist in some villages and individuals commonly use Brita or other household filters to improve palatability.

The data presented in Tables 6 and 7 suggest that even if CBM production in Alaska generates a high quality water, current water quality in all the villages will likely still exceed the CBM water quality. Produced water might offer relief from high iron, manganese, color and odor problems, but based on the review of other CBM operations; produced water will likely have a higher TDS content than most of the existing water sources. A financial advantage for water treatment will only be realized if CBM produced water quality in Alaska substantially exceeds the averages found elsewhere in the United States and Canada.

Costs for Various Water Treatment Systems

Capital costs estimates for village water-treatment systems were solicited from a cost estimator used by Alaska Native Tribal Health Consortium for feasibility studies. This function accounts for village specific constraints and corresponding pricing. Parameters included storage tank size, water treatment building square footage, and type and number of water source intakes. It generates a cost estimate that includes both equipment and construction. The estimates reported in Table 9 do not include equipment or construction costs associated with a washeteria, wastewater treatment, or any water distribution or sewer systems. The assumptions made in the preparation of these estimates included:

- Floor space requirements and corresponding square footage input was based solely on village population:
 - 400 ft² for populations less than 100
 - 900 ft² for populations of 100-249
 - 1225 ft² for populations of 250-349
 - 1600 ft² for populations of 350-500
 - 2500 ft² for populations of 500 or more

- All facilities built on conventional foundations of local gravel material.

Table 6. Select water quality data for villages with surface water sources.

Parameter	Source	TOC mg/L	Color PCU	TDS mg/L	Fe mg/L	Mn mg/L	Cl mg/L	As mg/L	Cond umhos /cm	Alk mg/L CaCO ₃	pH	Turb NTU	Reference
Drinking Water Std			15	500	0.3	0.05	250	0.05			6.5- 8.5		
Atkasuk	Imakruak Lake	4.59	10	100	<MRL	0.0112	<MRL			56.2	7.8	0.8	NTL Alaska, Inc. 2004
Chalkyitsik	Black River		10	170	1.1	0.19	6.6			135	7.7		HDR Alaska, Inc. 2001
Chignik	Indian Creek	0.53	5	33.8	0.25	0.01	5.5			15.5	8.22	0.76	CT&E Environmental Services 2000a
Deering	Inmachuk River	10.4	30		0.65	0.6			566	144	7.54	2.4	Menough 2001
McGrath	Kuskokwim River		5	235	2.79	0.581	0.512	0.01		144	7.4		CE2 Engineers, Inc. 2002
Nikolai	S.F. Kuskokwim R.		30	174	2.7	0.382	1.1			164	7.6	44	ANTHC 2005a
Noatak	Noatak River	4	<MRL	174		0.062					7.24	0.4	ANTHC 2003 & ANTHC 2004a
Perryville	stream		25						95		7.5		water sample 1980
Point Lay	Point Lay Lake	15	20	298	1.8	1.58	66.1		549	168		20	Analytica Group 2005a, North Slope Borough 1996
Selawik	Selawik River	19	350		1.62	0.102						16.6	CT&E Environmental Services 2003a
Shungnak	Kobuk River			80	0.11	0.114				60	6.6		NANA/DOWL 1998
Unalakleet	Powers Creek		25	32	0.684	0.0099	1.01			14.2	6.6	3.7	MWH Americas, Inc. 2002
Wainwright	Merekruak Lake	4.89											Analytica Group 2004a, ADEC 2001

Table 7. Select water quality data for villages with non-surface water sources.

Parameter	TOC mg/L	Color PCU	TDS mg/L	Iron mg/L	Mn mg/L	Cl mg/L	As mg/L	Cond umhos /cm	Alkalinity mg/L CaCO ₃	pH	Turbidity NTU	Reference
Drinking Water Std		15	500	0.3	0.05	250	0.05			6.5-8.5		
Alatna	6.52	70	264	2.01	0.519	<MRL	<MRL	402	241	7.6	9	CRW 1999, Columbia Analytical 1995
Allakaket				1.1	0.4							City of Allakaket 1998
Ambler			310	1.18	0.019	10	<MRL	270	246	7.5		Northern Testing Laboratories 1999a
Beaver	6.91		358	12.3	1.26	2.9	0.007		353	6.9		Northern Testing Laboratories 2000a
Bettles												
Birch Creek		200	183			<MRL	0.003	270	128		2.9	Northern Testing Laboratories 1999b
Chignik Lg	0.92		51.3	0.884	0.0715	7.58	0.001	120	20	7.5	5.6	CT&E Environmental Services 2000b
Chignik Lk	8	<MDL	99	0.03	<MRL	5.94	0.00887	350	50.56	8.4	1.34	ANTHC 2005b, GV Jones & Associates, Inc. 1986
Evansville		30	200	1.27	0.077	0.48	<MRL		182	7.61		Northern Testing Laboratories 2000b
Fort Yukon	10.7	80	191	2.6	0.67	<MRL	0.0094	379	210	7.7	14	Northern Testing Laboratories 2003
Gatena		47	177	4.67	0.184	2.1	0.00556		224	6.7		GV Jones & Associates, Inc. 2003
Kaltag			52.5	0.05	0.033				34.2	6.78	0.24	PDC, Inc. Consulting Engineers 2002
Kiana	1.2	<MRL	298	1.59	0.701				254	7.4	3.83	ANTHC 2004b
King												Analytica Group 2004b, CT&E
Salmon		55	186	17.2	0.0284	3.29	0.00364	220	124	7	4.4	Environmental Services. 2003b
Kobuk		140		5.4	0.51						40	ANTHC 2002
Koyuk			1750	0		860			200	7.5		Alaska Area Native Health 2002, Golder Associates 1998
Koyukuk	5.23		354	0.292	0.393	26.7	<0.005	705	360	7.78		PDC, Inc. Consulting Eng. 2004
Mekoryuk												
Naknek		20	100	2.33	0.0606	3.04	0.00874	160	75.5	7.5	19	CT&E Environmental Services 2003c
Nightmute		<MRL	144	0.07	14.3	5.48				7.35		Summit Consulting Services 2004
Nulato		5	115	0.05	0.02	0.357	0.005		85.8	6.77		CT&E Environmental Services 1997
Rampart		35	486	0.038	0.4135	<MDL	<MDL		350	7.75		ANTHC 2002b
Toksook By		10	118	0.69	0.067	8.3	<MRL		90.5	6.5		Analytica Group 2003
Venetie	<MRL	<MRL	218	<MRL	0.00473	1.52			178	7.5	<MRL	Analytica Group 2005b

Table 8. Village water treatment system information.

Village	Population	Storage Tank gallons	Treatment
Alatna	32	2,500	11 cartridge type filters (5 micron), no Fe/Mn removal or disinfection
Allakaket	90	100,000	green sand filter, chlorine, permanganate, treatment for Fe and Mn
Ambler	274	210,000	addition of liquid chlorine and fluoride prior to storage
Atqasuk	247		nanofiltration, microfiltration
Beaver	67	66,000	iron filter, manganese green sand filter, potassium permanganate, chlorination
Bettles	31	none	no public water treatment system
Birch			
Creek	43	80,000	filtration (pressure sand), chlorination
		95,000; school	
Chalkyitsik	84	80,000	Giardia filters, school WTP filters and chlorinates
Chignik	92	200,000	two 4' pressure sand filters (100gpm)
Chignik Lg	81	150,000	soda ash and chlorine
Chignik Lk	150	150,000	greensand filter, hypo chlorination
Deering	145	400,000	carbon filter, fill and draw; disinfection
Evansville	21	none	Culligan double water softener system
Fort Yukon	594	110,000	potassium permanganate, sand filter, chlorine, fluoride
Galena	717	97,000	greensand filter, chlorine, fluoride, activated carbon
Kaltag	211	200,000	two multi media filters, two giardia filters, fluoride
Kiana	394	200,000	chlorination
King			
Salmon	404		Amiad Pre-filter, air pump, aerator tank, kinetico macrolite filter
Kobuk	128	97,000	potassium permanganate, pressure sand filter, Cl, 80 gpm max
Koyuk	348	205,000	filters, chlorine
Koyukuk	109	5,000	chlorination
McGrath	367	500,000 and 75,000	polymer added, filter, chlorine, fluoride
Mekoryuk	198		
Naknek	601	none	none
Nightmute	232	44	chlorination system (designed to treat 6.1 gpm)
Nikolai	121	none	permanganate, hypo chlorination
Noatak	448	97,000	microfiltration, chlorination, fluoride to treat 25 gpm
Nulato	320		
Perryville	110	50,000	
Point Lay	251		nanofiltration, microfiltration
Rampart	21	35,000	Potassium permanganate, greensand filter, chlorination
Selawik	829	300,000	cationic polymer, 2 pressure sand filters, chlorine, fluoride
Shungnak	264	200,000	filters, chlorine (can treat 80 gpm)
Toksook			
Bay	561	212,000	greensand filter, potassium permanganate - 4' diameter
Unalakleet	728	1,000,000	polymer added, filter, chlorine (110,000gpd)
Venetie	188	428,000	sand filtration, cartridge filtration and chlorine
Wainwright	531	7,000,000 (3 tanks)	nanofiltration, chlorine, reverse osmosis, pH adjustment

Table 9. Estimated System Costs.

	Population	Current System Cost
Alatna	32	\$772,847
Allakaket	90	\$960,295
Ambler	274	\$1,656,445
Atqasuk	247	\$1,350,981
Beaver	67	\$904,302
Bettles	31	
Birch Creek	43	\$927,358
Chalkyitsik	84	\$1,172,993
Chignik	92	\$676,239
Chignik Lg	81	\$610,262
Chignik Lk	150	\$961,631
Deering	145	\$1,504,181
Evansville	21	\$663,450
Fort Yukon	594	\$2,365,938
Galena	717	\$2,108,520
Kaltag	211	\$1,260,922
Kiana	394	\$1,650,611
King Salmon	404	\$1,142,238
Kobuk	128	\$975,495
Koyuk	348	\$1,451,247
Koyukuk	109	\$985,512
McGrath	367	\$1,990,642
Mekoryuk	198	\$886,146
Naknek	601	\$1,688,300
Nightmute	232	\$1,001,562
Nikolai	121	\$1,100,906
Noatak	448	\$1,285,170
Nulato	320	\$1,056,107
Perryville	110	\$907,557
Point Lay	251	\$1,149,773
Rampart	21	\$687,659
Selawik	829	\$2,258,988
Shungnak	264	\$1,724,865
Toksook Bay	561	\$2,211,146
Unalakleet	728	\$2,729,826
Venetie	188	\$1,726,463
Wainwright	531	\$11,174,380

Potential for Combined Water Treatment Systems

Only in the North Slope Borough villages of Point Lay, Atqasuk and Wainwright are treatment systems already in place with the capacity to treat CBM waters with elevated TDS concentrations (assumed in this study to be 840 mg/L or greater). In all other villages, equipment additions and modifications would be required to current treatment systems in order to achieve drinking water standards. In those North Slope Borough villages, combined water treatment systems are feasible, but water production volumes and controlling them to meet only village demands might complicate the scenario. The cost benefits would need to evaluate both water and energy costs and demands.

All water generated from CBM would require some type of treatment prior to discharge, even that which is not used to meet a potable demand. The amount of water produced from CBM varies from basin to basin. In Colorado, a well in the San Juan Basin generates 1,050 gallons per day, but in Wyoming an average Powder River Basin well generates 16,800 gallons per day (USGS, 2000). The water production of a CBM well decreases with age, but the initial generation will likely exceed potable demand for many of the smaller Alaska villages. Since it would still require treatment, water generated in excess of village demand would drive an increased capacity for the water treatment system. To circumvent such expansion, a separate system could be used to treat unneeded CBM generated waters prior to surface discharge or use to serve non-potable needs. The overall water produced by CBM operations would need to account for the demand-limited condition at most village settings.

Rural Alaska Cost Issues and Applicability for CBM Water Production/Usage

Water quality analysis in rural villages identified on potential CBM resources indicates that current source quality will exceed even best case projected CBM water quality in all instances. High TDS content and saline characteristics of CBM produced water necessitate high-pressure treatment such as reverse osmosis or nanofiltration to achieve a TDS drinking water standard of 500 mg/L. Such sophisticated treatment equipment will make CBM water recycling financially and operationally impractical for rural Alaskan villages, except in those cases where the equipment already exists. Without accounting for the cost savings associated with reclamation and use of the produced methane gas as an energy source, reclaiming the generated waters would provide villages with little more than an expensive back-up water source.

Recycling CBM produced waters has possible financial merit in Wainwright, Point Lay and Atqasuk, where treatment systems with the capability to treat high TDS waters are already in use. Additionally, these North Slope Borough villages treat surface water which experiences seasonal unavailability and forces the villages to store and insulate large storage volumes to cover those supply periods. Replacing these seasonally unreliable surface water sources with a constant flowing CBM produced water, at least during the winter season, would alleviate large storage requirements and associated tank insulation and heating costs. The other ten villages that obtain drinking water from surface sources, as identified in Table 6, also have potential to gain benefits associated with reducing storage requirements. However, since current treatment systems are inadequate to treat anticipated high TDS concentrations, expensive upgrades and additions to water treatment systems would be required. The associated capital and construction

costs could be regained over time and their recovery would be greatly expedited if the generated methane were recovered to replace existing energy sources.

Outreach Activities

The project team gave various presentations at Alaska meetings to present interim project results. A CBM working group was also formed and held several meetings to help discuss project objectives and general CBM topics. The initial meeting was held in conjunction with the Rural Energy Conference in Valdez, Alaska. This meeting was followed by a workshop held at the Alaska Forum for the Environment Meeting in Anchorage, Alaska. An additional meeting was held at the International Arctic Research Center in Fairbanks, Alaska.

Professional society presentations were made at Alaska State Section meetings. These include the following presentations;

- Alaska Section, AWRA, 2005 Annual Meeting, April 7. Cordova
 - Alaska Coalbed Methane Water Disposal Methods: A Preliminary Review of available CBM information and disposal and treatment options for Alaska
- Alaska Section, AWRA, 2006 Annual Meeting, January 26. Anchorage
 - A Review of CBM Co-Produced Water Disposal Methods for Alaska

Summary and Recommendations

The primary purpose of this project was to determine CBM water disposal issues and potential solutions unique to Arctic environments. At the time of this report, there has not been any production scale CBM development in Alaska. Some early exploration efforts used down-hole methods for disposing of water produced during exploration. In search of experiences from other cold-region countries, we did not find any new treatment solutions to CBM produced water in the Arctic.

In doing this survey of information sources, we did discover some of the following points that should be noted in any development in Alaska, or other Arctic regions;

- CBM reservoirs can cover a very wide range of water quality and produced water characteristics. Evaluation of CBM produced water treatment and disposal options need to be based on reservoir-specific water quality and yield information.
- Exploration efforts need to include the collection of water samples to evaluate formation water chemistry.
- Disposal systems need to account for Arctic environmental conditions, such as prolonged winters with below freezing temperatures.
- In many Arctic regions, year-round water supplies are limited, particularly in continuous permafrost environments. The combination of exploration water chemistry and tests related to production yields with current water treatment approaches need to be evaluated

on a site specific conditions to evaluate economic reuse of CBM produced water for potable and non-potable water-use needs. These analysis need to take into account both water and energy utility economics.

- The application of water-treatment technologies for produced water from oil fields need to be applied to CBM produced water. Additionally, the application of water-treatment reuse systems in small arid systems also need to be considered for application in arctic communities, as some of the technologies from these systems may easily transfer small-scale treatment systems in the arctic.
- Permitting approaches need to treat the source-water discharge based on discharge water chemistry instead of the water source.

Acknowledgements

The authors would like to thank the Alaska Department of Natural Resources, Division of Geological and Geophysical Surveys, for providing valuable information about CBM resources in the state and other contact information throughout the project. We would also like to thank the International Arctic Research Center, Keith Mather Library, for the valuable help in US and International literature searches, organization and distribution of references during the project activities and serving as a long-term archive for project material and references to help benefit future efforts in CBM research.

References

ADEC Public Water Supply Program. 2001. Wainwright Water Sample Data. November.

Alaska Native Tribal Health Consortium. 2005b. Chignik Lake West Well Water Quality Sampling Results.

Alaska Native Tribal Health Consortium. 2004b. Kiana Well #1 Water Sample Analysis. May.

Alaska Native Tribal Health Consortium. 2005a. City of Nikolai Sanitation Facilities Master Plan. June.

Alaska Native Tribal Health Consortium. 2002b. Rampart Sanitation Facilities Master Plan – Final. September.

Alaska Native Tribal Health Consortium Division of Environmental Health and Engineering. 2003. Noatak, Alaska Water, Sewer & Solid Waste Facilities Master Plan – Update. May.

Alaska Native Tribal Health Consortium Division of Environmental Health and Engineering. 2004a. Construction Plans Sanitation Facilities. January.

- Alaska Native Tribal Health Consortium Division of Environmental Health and Engineering. 2002a. City of Kobuk Water Treatment Construction Plans. March.
- Alaska Area Native Health Service Office of Environmental Health and Engineering. 2002. A Sanitation Facilities Improvement Project Between the Alaska Area Native Health Service and the City of Koyuk, Alaska Project No. AN91-016/675. October.
- All Consulting, 2003. Handbook on Coal Bed Methane Produced Water: Management and Beneficial Use Alternatives, Prepared for Ground Water Protection Research Foundation, US Department of Energy, National Petroleum Technology Office and Bureau of Land Management.
- Analytica Group. 2003. Toksook Bay Water Quality Report. November.
- Analytica Group. 2005b. Venetie Water Quality Report Job # VEE.Q26VSW. April.
- Analytica Group. 2005a. Point Lay Fresh Water Lake Testing prepared for North Slope Borough – Public Works. May.
- Analytica Group. 2004b. King Salmon Domestic Well (Tibbets) Water Quality Report. September.
- Analytic Group. 2004a. Wainwright Water System North Lake Raw Water Results prepared for North Slope Borough-DMS. July.
- Arthur, D., Langhus, B., and Rawn-Schatzinger, V., 2003. Coalbed Natural Gas Resources and Produced Water Management, GasTIPS, p. 20-24.
- Bastien, P.A., O.F.R. Wirth, L. Wang, and G.W. Voneiff, 2005. “Assessment and Development of the Dry Horseshoe Canyon CBM Play in Canada,” *proc 2005 SPE Annual Technical Conference and Exhibition*, Dallas, Texas, U.S.A., 9-12 October 2005.
- Beaton, Andrew (*via personal communication with E.P. Robertson, INL, 2008*), Leader, Unconventional Gas and Oil Sands Section, Alberta Geological Survey, Alberta Energy and Utilities Board, 4999-98 Avenue, Edmonton, Alberta T6B 2X3, tel. 780-427-3272.
- British Columbia Ministry of Water, Land and Air Protection, 2004. *Code of Practice for the Discharge of Produced Water from Coalbed Gas Operations, CODE OF PRACTICE INTENTIONS PAPER – December 2004*, British Columbia Ministry of Water, Land and Air Protection.
- CE2 Engineers, Inc. 2002. Water and Sewer System Evaluation and Master Plan McGrath, Alaska. Test Well Log, Pump Test Results and Water Analysis.
- City of Allakaket. 1998. Project No. AN 98-L91. September.

- Clough, J.G., 2001. Coalbed Methane – Potential Energy Source for Rural Alaska, Alaska Geosurvey News, Vol. 5, No. 2, <http://www.dggs.dnr.state.ak.us>
- Columbia Analytical Services, Inc. 1995. Analytical Report Alatna Water Well. April.
- CRW Engineering Group. 1999. Technical Evaluation Alatna Water and Sewer (9975). October.
- CT&E Environmental Services Inc. 2000a. Laboratory Analysis Report, Chignik prepared for GV Jones & Associates, Inc. August.
- CT&E Environmental Services, Inc. 2003a. Selawik River Water Quality Report.
- CT&E Environmental Services Inc. 2000b. Chignik Lagoon Well #2 Analysis. June.
- CT&E Environmental Services, Inc. 1997. Nulato LTSL Water Tank Fill Water Quality Report. November.
- CT&E Environmental Services Inc. 2003c. Zimin Domestic Well in Naknek Water Quality Report. January.
- CT&E Environmental Services, Inc. 2003b. Tibbets Drinking Water Report. January.
- Division of Community Advocacy, 2005. Current Community Conditions: Fuel Prices Across Alaska, Report of the Commissioner, <http://www.commerce.state.ak.us/dca/pub/CommunityFuelReport2005.pdf>
- EPA. 2004. Federal Regulatory Programs for Coal Bed Methane Activities in Alaska. EPA 910-F-04-001, November.
- Flores, R.M., Stricker, G.D., and Kinney, S.A. 2004. Alaska Coal Geology, Resources, and Coalbed Methane Potential. U.S. Geological Survey, Reston, Virginia, DDS-77. <http://pubs.usgs.gov/dds/dds-077/>
- Gas Research Institute, 1993. Coalbed Methane Produced Water Management Guide – Treatment and Discharge to Surface Water: Black Warrior Basin, Alabama, Contract No. 5091-253-2215.
- Golder Associates. Water Resources Investigation Koyuk, Alaska. September.
- GV Jones & Associates, Inc. 2003. Galena Water Treatment System Modification and Expansion Options-Progress Memorandum No. 1-Final. March.
- GV Jones & Associates, Inc. & NANA/DOWL Engineers, LLC. 2000. Chignik Lake Water and Sewer System Feasibility Study. September.
- HDR Alaska, Inc. 2001. Village of Chalkyitsik Water and Sewer Feasibility Study. June.

- Jackson, L., and J. Myers, 2002, "Alternative Use of Produced Water in Aquaculture and Hydroponic Systems at Naval Petroleum Reserve No. 3," presented at the 2002 Ground Water Protection Council Produced Water Conference, Colorado Springs, CO, Oct. 16-17. Available at http://www.gwpc.org/meetings/meetings_special/PW02/Papers/Lorri_Jackson_PWC2002.pdf
- Jones, G.V., and Woolard, C.R. 2001. Cost Comparison of Nanofiltration Systems for Drinking Water Treatment in Small Communities, Sixth Annual Research and Development Conference on Rural Sanitation, Alaska Water Waste Water Management Association.
- Krzystolik, P., Mizra, A., and Skiba, J., 2003. Polish Methods of Methane Exploitation from the Coal-Mines and its Utilization in the Upper Silesian Coal Basin, Paper Number 0361, Proceedings of the 2003 International Coalbed Methane Symposium, Tuscaloosa, Alabama, USA.
- Kuipers, J.R., MacHardy, K., Mersch, W., and Myers, T., 2004. Coal Bed Methane- Produced Water: Management Options for Sustainable Development - A primer on coal bed methane-produced water disposal impacts and the feasibility of alternative strategies, Draft Report, Northern Plains Research Council, Billings Montana, pp.81.
- Lang, K., 2002. "Natural Gas Coalbed Methane: Non-US development heats up," Hart's E&P Net (September 2002).
- Menough, Jon. 2001. Long Term Study of Disinfection By-Product Formation Alaska Water and Wastewater Management Association International Research and Development Conference on Rural Sanitation. April.
- Mustafin, R.K., Alekseev, E.G., and Umarhajieva, N.S., 2003. Coal Methane – Potential Energy Prospects for Kazakhstan, Paper Number 0363, Proceedings of the 2003 International Coalbed Methane Symposium, Tuscaloosa, Alabama, USA.
- MWH Americas, Inc. 2002. Powers Creek Water Source Study. October.
- NANA/DOWL Joint Venture. 1998. Shungnak Sanitation Facilities Master Plan. November.
- Northern Testing Laboratories, Inc. 1999a. Ambler River Well Water Analysis. August.
- Northern Testing Laboratories, Inc. 2000a. Beaver Raw Water Analysis. July.
- Northern Testing Laboratories, Inc. 1999b. Birch Creek Water Analysis. September.
- Northern Testing Laboratories, Inc. 2000b. Evansville Community Sink Water Analysis. June.
- Northern Testing Laboratories, Inc. 2003. Ft Yukon Raw Water Analysis. May.

North Slope Borough. 1996. Capital Improvement Project Management. Village Water & Sewer Project Membrane Treatment Systems Procurement Manual. June.

NTL Alaska, Inc. 2004. Annual Raw Water Supply Test Results Atqasuk. July.

PDC, Inc. Consulting Engineers. 2004. Koyukuk Sanitation Facilities Master Plan. July.

PDC, Inc. Consulting Engineers. 2002. Kaltag Sanitation Facilities Master Plan. December.

Rice, C.A. Ellis, MS and Bullock, J.H., Jr. 2000. Water Co-Produced with Coalbed Methane in the Powder River Basin, Wyoming: Preliminary Compositional Data, US Geological Survey Open-File Report 00-372.

Sanli, F., Yongzhong, H., Shuian, Z., and Minzhai L., 2003. Technical Challenges of CBM Exploitation in the South Part of Qinshui Basin, Paper Number 0310, Proceedings of the 2003 International Coalbed Methane Symposium, Tuscaloosa, Alabama, USA.

Summit Consulting Services. 2004. Nightmute Water & Sewer Improvement Feasibility Study. August.

Tyler, R., Scott, A.R., and Clough J.G., 2000. Coalbed Methane Potential and Exploration Targets for Rural Alaska Communities, Preliminary Interpretive Report No. 2000-2, Division of Geophysical and Geological Surveys, pp. 169.

USGS. 2000. Water Produced with Coal-Bed Methane. FS-156-00, November.

US Department of Energy, 2005. Canada: Country Analysis Briefs (February 2005) Energy Information Association.

Van Voast, W.A. 2003. Geochemical Signature of Formation Waters Associated With Coalbed Methane, The American Association of Petroleum Geologists.

Veil., A. J., April 1997. Costs for Off-Site Disposal of Nonhazardous Oil Field Wastes; Salt Caverns Versus Other Disposal Methods. Argonne National Laboratory. Argonne, IL.

Water Sample, Perryville AK 1980.

Appendix I. References searched through Internet or other electronic search methods for general CBM references. These references were then searched for relevant content on CBM water disposal topics.

Reference Source	Database	Number of References Retrieved
OCLC First Search	Applied Science & Technology Abstracts	31
OCLC First Search	GeoRefS	352
CIRC	-	24
Cambridge Scientific Abstracts	NTIS	8
Biblioline	Arctic & Antarctic Regions	18
Biblioline	Arctic & Antarctic Regions	34
OCLC First Search	ASTA	31
Cambridge Scientific Abstracts	NTIS	39
Library Union Catalog	-	32
Miscellaneous	-	16
OCLC First Search	ASTA	231
OCLC First Search	ASTA	33
Engineering Village 2	Compendex	30
Engineering Village 2	Compendex	717
Engineering Village 2	Compendex	367
Cambridge Scientific Abstracts	Environmental Sciences and Pollution Mgmt	56

Reference Source	Database	Number of References Retrieved
Cambridge Scientific Abstracts	Conference Papers Index	51
Cambridge Scientific Abstracts	Environmental Sciences and Pollution Mgmt.	31
Cambridge Scientific Abstracts	Conference Papers Index	21
Cambridge Scientific Abstracts	NTIS	33
Cambridge Scientific Abstracts	NTIS	238
CIRC	-	8
DOE	-	20

Appendix II. Geologic information for selected US CBM reservoirs. Selected references are listed after this table.

US Basin Name	Regional Location	Type of CBM Resource	Formation Name(s)	Coal Rank or Type	CBM Depth Range	Water Production	Selected References
Powder River Basin (PRB)	Northwest	Secondary biogenic	Fort Union Fm.	Lignite to low-volatile bituminous	305 m (1,000 ft)	260 bpd per well	2, 7, 8, 9
San Juan Basin	Southwest	Thermogenic secondary biogenic	Fruitland Fm.	Subbit. B high-volatile	350-650 ft	130,000,000bbl cumulative	1, 3, 5, 6, 7, 11
Bull Mtn Basin	Northwest	-	Fort Union Fm.	Subbit.	-	-	2
Bighorn Basin	Northwest	-	Fort Union Fm.	High-volatile C bituminous	-	-	2
Wind River Basin	Northwest	-	Mesaverde and Meeteetse Fm.	Subbit. C to high-volatile C bituminous	1,150-5,615 m (3,770-18,410 ft)	-	4, 7
Raton Basin	S-Colorado, NE-New Mexico	-	Vermejo Fm. and Raton Fm.	High-volatile B & C bituminous	-	-	11
Vinta Basin	Utah	-	Mancos Shale & Mesaverde Group	High-volatile B to A bituminous	-	Excessive	5, 11

US Basin Name	Regional Location	Type of CBM Resource	Formation Name(s)	Coal Rank or Type	CBM Depth Range	Water Production	Selected References
Piceance Basin	Central	Thermogenic secondary biogenic	-	-	-	Low-High	9
Black Warrior Basin	Eastern	Thermogenic secondary biogenic	-	-	-	Less than 250 bpd	9, 11
Sandwash Basin	Southwest	-	-	-	-	High 200-1000 bbl/d	5

- 1-Ayers, W.B., Jr., and W.A. Ambrose, with assistance, 1990, Geologic Controls on the Occurrence of Coalbed Methane, Fruitland Formation, San Juan Basin *in* 1990, Geologic Evaluation of Critical Production Parameters for Coalbed Methane Resources: Part I, San Juan Basin, Final Report (August 1988-July 1989), Gas Research Institute, Chicago, Illinois.
- The Fruitland Formation in the San Juan Basin is a major producer of coalbed methane in the Western United States. Fruitland Formation waters are meteoric waters. Non-coastal waters reflect high alkalinities and low chlorinates. The distribution of low-chloride ground waters coincides with over pressured areas in the north-central basin. The area acts as a single hydrologic unit or homogeneous aquifer, but large local pressure gradients indicate that Fruitland strata may be hydraulically disconnected acting as a compartmentalized aquifer.
- 2-Bartow Chapman, Elizabeth and James R. Gruber, Jr., 1991, Coal and Coalbed Methane Resources of Montana: *in* Coalbed Methane of Western North America, Rocky Mountain Association of Geologists, Denver, Colorado.
- The report gives an overview of the coal and coalbed methane resources of Montana. Montana is the second largest coal resource in the United States with approximately 35% of the state having coal resources. A large portion of the coal is found in the Fort Union Formation and ranks from lignite to low volatile bituminous. Water production and disposal have minimal environmental concerns due to the related fresh water. The large majority of Coalbed Methane resources in Montana are in the Powder River Basin.
- 3-Dhir, Rahul, Matthew J. Mavor, Jay C. Close, 1991, Evaluation of Fruitland Coal Properties and Development Economics, San Juan Basin, Colorado and New Mexico *in* Coalbed Methane of Western North America: Rocky Mountain Association of Geologist, Denver, Colorado.
- The report documents the reservoir properties, deliverability, and development economics of four Fruitland Formation coal-gas wells in the San Juan Basin of Colorado and New Mexico. Detailed estimates of reservoir properties include pressure, thickness, ash content, gas content and storage, diffusion coefficients, permeability, cleat frequency and coal ranks. The application of more effective technologies would enable better access to the reservoirs and would significantly enhance gas recovery from the Fruitland Formation coal.
- 4-Johnson, Ronald C., Charles E. Barker, Mark J. Pawlewicz, Bonnie L. Crysedale, Arthur C. Clark and Dudley D. Rice, 1991, Preliminary Results of a Coalbed Methane Assessment of the Wind River Indian Reservation, Wyoming *in* Coalbed Methane of Western North America: Denver, Colorado
- The Wind River Indian Reservation, which occupies much of western Wyoming, contains significant amounts of coal deposits in the Upper Cretaceous Mesaverde and Meeteetse Formations. Preliminary results of coalbed methane occur at shallow depths in low-rank Mesaverde coals near Hudson, in the South Reservation. Desorbed gases are chemically dry (97.3%-99.7% methane) and contain minor amounts of carbon dioxide (0.61%-0.83%).

- 5-Kaiser, W.R., 1995, Hydrogeology of Coalbed Reservoirs, *in* 1995, Geologic and Hydrologic controls critical to coalbed methane producibility and resource assessment: Comparative studies of the San Juan, Greater Green River, and Piceance Basins, Gas Research Institute, Austin, Texas.
- Distribution of potential energy (hydraulic head) and mass (dissolved solids) identify regional ground-water circulation patterns and indicate permeability anisotropy. Reservoir conditions inferred from hydraulic gradient, pressure regime, and hydrochemistry. Hydrogeology is a major control on the occurrence and probability of coalbed methane, which is produced in a variety of hydrologic settings but is greatest from the artesian coal beds in association with discharge areas.
- 6-Oldaker, Paul R., 1991, Hydrogeology of the Fruitland Formation, San Juan Basin, Colorado and New Mexico: *in* Coalbed methane of Western North America, Rocky Mountain Association of Geologist, Denver, Colorado.
- The report is an overview of the hydrology of the Fruitland Formation in the San Juan Basin. The coal within the Fruitland Formation has a wide range of variation, which effects the variation of the formation's permeability (0.002-811 md). The depositional environments, structure, source organic material, etc all are factors of the coal's lithology and the Fruitland Formation's permeability. Water quality tests show a wide range in total dissolved solids. This is due to the basin having five major discharge areas and several flow paths with different resident times. The hydrology of the Fruitland Formation is determined by the topography, structure and climate.
- 7-Peterson, Kurt M., 1991, Coalbed Gas Development in the Western United States- An Update *in* Coalbed Methane of Western North America: Rocky Mountain Association of Geologists, Denver, Colorado.
- The western United States in general, with the San Juan, Piceance, Raton, Uinta, Green River, Wind River, and Powder River basins having particularly large coal reserves and have been and will continue to be the focus of coalbed gas development. With these increased interests in development of these basins, there have been many legal questions as to who has the rights to develop the basin. Careful and extensive analysis of land ownership records should identify the legal risks and the likelihood of disputes. Advanced negotiations are key to minimizing the legal risks associated with coalbed gas development.
- 8-Rice, C.A., M.S. Ellis, and J.H. Bullock, 2000, Water co-produced with coalbed methane in the Powder River Basin, Wyoming: preliminary compositional data [paper edition]: U.S. Geological Survey open file report 00-372.
- The report contains information of water and natural gas production from coal beds in the Powder River Basin (PRB). Water production in the PRB has had a ten-fold increase from 1997-2000. By the year 2000 PRB was producing 1.28 million barrels of water per day. Within the PRB the area of interest for gas and water production is in the Fort Union Formation's thick coal beds. Several wells were selected for water quality testing and results concluded that the water from coalbed methane wells pass EPA Drinking Water Standards.

- 9-Scott, Andrew R., Compositional Variability and Origins of Coal Gases, in *Geologic and Hydrologic controls critical to coalbed methane producibility and resource assessment: Comparative studies of San Juan, Greater Green River, and Piceance Basins*, Gas Research Institute, Austin, Texas.
- The composition of coal gases varies between wells, and vertically between coal beds within individual wells. The most effective conventional and hydrodynamic traps are perpendicular to migration pathways, indicating that an understanding of gas geochemistry and origins is critical in developing exploration strategies. The carbon isotopic composition of methane, ethane, propane, butane, and carbon dioxide in coal gases is often critical in determining gas origin and migration pathways.
- 10-Treman, C.M., N.H. Whitehead, III and S.E. Laubach, 1990, Regional Tectonic Setting of the San Juan Basin *in* 1990, *Geologic Evaluation of Critical Production Parameters for Coalbed Methane Resources, Part I, San Juan Basin, Final Report* (August 1988-July 1989), Gas Research Institute, Chicago, Illinois.
- Tectonic history influenced the Mesozoic and Cenozoic depositional patterns of coal occurrences. Tectonic events in the San Juan Basin of New Mexico and Colorado have controlled the distribution and orientation of folds and fractures in coals and adjacent rocks. An overall understanding of this basin will provide a basis for predicting coalbed methane occurrences and producibility.
- 11-Tyler, Roger, Andrew R. Scott, W.R. Kaiser, and Douglas S. Hamilton, 1995, *Geologic and Hydrologic controls critical to coalbed methane producibility and resource assessment: Comparative studies of the San Juan, Greater Green River, and Piceance Basins*, Gas Research Institute, Austin, Texas.
- The report is an overview of the composition of coal gases and coalbed methane development potentials of the San Juan, Greater Green River, and Piceance Basins in the western United States. It is a comparative study of the composition of the basins and their coalbed methane origins and migration patterns.

Appendix III. Water production and disposal information for selected US CBM reservoirs. Selected references are listed after this table.

US Basin Name	Regional Location	Number of producing wells	Water Production	Water Quality Information	Water Disposal Information	Selected References
San Juan Basin	Southwest	Many	Low-High	Sodium Bicarbonate	Re-injection into SWD wells.	2, 3
Black Warrior Basin	Eastern	Over 4000	Less than 250 bpd	Mineralized (Na, Cl, Bicarbonate)	Treated Surface Discharge, land treatment	2, 4, 5, 6
Sand Wash Basin	Southwest	-	High	-	-	3
Powder River Basin	Northwest	-	260 bpd per well	Ft. Union-ok Wasatch-poor	Surface Discharge	1, 6, 7
Greater Green River Basin	Central	-	High	Poor quality	Surface Discharge	6, 7
Piceance Basin	Central	-	High	Poor quality	Surface Discharge	6, 7
Central Appalachian Basin	Eastern	-	50 bpd per well	-	-	6, 7
Michigan Basin	Eastern	2700	-	-	Re-injection	6, 7

- 1- 2001, The Potential for Coalbed Methane (CBM) Development in Alberta, Alberta Department of Energy, September, 2001.
 - The Alberta Department of Energy commissioned a study in 2001 to examine the potential for Coalbed Methane (CBM) development. The province has vast resources of coal, an extensive natural gas distribution system and a growing demand for natural gas resources. The Alberta Energy and Utilities Board (EUB) estimates reserves of natural gas at 43 trillion cubic feet (tcf).
- 2- Dawson, F.M., 1995, Coalbed Methane: A comparison between Canada and the United States, Geological Survey of Canada-Bulletin 489.
 - The report is an overview of the geological characteristics of the San Juan and Black Warrior basins in the United States and highlights criteria that have allowed the development of coalbed methane productions from these regions. A similar overview is compared to the major Canadian basins in Alberta, Saskatchewan, the Maritimes, Yukon and the Northwest Territory. The United States basins and the Canadian basins are compared on elements of coal seam thickness, gas content, and highest coalbed methane potential.
- 3- Kaiser, W.R., D.S. Hamilton, A.R. Scott, Roger Tyler, & R.J. Finley, 1994, Geologic and Hydrologic Controls on the producibility of Coalbed Methane: Sand Wash Basin, Colorado and Wyoming, Journal of the Geological Society, London, Vol. 151, pp. 417-420.
 - Geologic and hydrologic comparisons of the San Juan and Sand Wash Basins of the United States indicates that; coal distribution, rank, gas content, ground-water flow, and structural settings are all critical controls on coalbed methane permeability. The report produces a basin-scale comparison of prolific and marginal production of the two basins.
- 4- Lawrence, Alonzo W., 1993, Coalbed Methane Produced-Water Treatment and Disposal Options, in Quarterly Review of Methane from Coalseams Technology, v. 11, no. 2 (April-June 1993).
 - The Gas Research Institution (GRI) and the Coalbed Methane Association of Alabama produced a study of produced water management in the Black Warrior basin. This study evaluated the six-treatment/discharge systems to develop a management guide for use in the basin's operations. In the San Juan basin, current disposal practices are reinjected into Class II saltwater disposal (SWD) wells under the Safe Drinking Water Act. The GRI has found that the volumes of water projected for coalbed gas activities may exceed the potential capacity of the existing disposal wells.

- 5- Pashin, J.C., W.E. Ward, II, R.B. Winston, R.V. Chandler, D.E. Bolin, R.P. Hamilton, and R.M. Mink, 1990 Geologic evaluation of critical production parameters for coalbed methane resources Part II, Black Warrior Basin, Chicago, IL, Gas Research Institute.
- Geologic evaluation parameters for coalbed-methane recourses in the Black Warrior basin of Alabama used an interdisciplinary approach that utilized coal quality, structure, sediment, and hydrologic data. Data suggests that productivity trends may be predictable. Several highly productive trends occur along northeast-oriented lineaments. These zones of enhanced permeability are related to fractures.
- 6- Reed, P.D., 1994, Compendium of Basins for the Potential Applicability of Jack W. McIntyres Patented Tool, Midland, TX, Geraghty & Miller, Inc.
- Completes wells produce methane wastewater brine. The water produced is usually treated and released into another body of water. The cost of these treatment facilities is very expensive to produce and maintain. However, a new process, patented by Jack W. McIntyre, has been produced to dispose of the water. The process utilizes a single well for both the production and water disposal. Fluids enter the wellbors, gas rises to the surface and the water is moved down into a disposal zone via gravity or mechanical pumping. This method allows for the simultaneous separation of gas and water disposal without the economic and environmental consequences of bringing the water to the surface.
- 7- Schwochow, Stephen D., Vito F. Nuccio, 2002, Coalbed Methane of North America II. Rocky Mountain Association of Geologists, The Rocky Mountain Association of Geologists.
- The report is an overview of coalbed methane potential as a gas resource. The report explores the geomorphology of drainage patterns and clues to coal gas natural fracture timing, orientation and locations. Chemical and isotopic compositions of water and implication for methane development in Fort Union and Wasatch Formations of the Powder River Basin are also discussed.

Appendix IV. Summary of Geologic information for potential Alaskan CBM resources. Selected references are listed after this table.

US Basin Name	Field Location	Type of CBM Resource	Formation Name(s)	Coal Rank or Type	Depth to CBM	Typical Coal Thickness	Selected References
Colville (North Slope)	Wainwright, Kukpowruk	Biogenic to Thermogenic	Lisbane-Nanushuk-Colville	Lignite to High-volatile Bituminous	Surface to >6000 ft.	5-10 ft.	1
Kobuk	West Kobuk, East Kobuk	Biogenic	Bergman/Kaltag	Lignite to Subbituminous	-	2-3 ft.	1
Upper Koyukuk	Tramway Bar	Biogenic	Bergman/Kaltag	Lignite to Subbituminous	-	3-12 ft.	1
Lower Koyukuk	Nulato	Biogenic	Bergman/Kaltag	Lignite to Subbituminous	-	<4 ft.	1
Yukon	-	Biogenic	Bergman/Kaltag	Lignites	-	<5 ft.	1
Minchumina	Little Tonzona	Biogenic	Usibelli	Subbituminous	-	20 ft.	1
Alaskan Peninsula	Chignik	Biogenic, Thermogenic	Chignik-Herendeen	Lignite, Anthracite to Bituminous	<9000 ft.	3-5-16 ft.	1

1-Tyler, R., Scott, A.R., Clough, J.G., 1997. Coalbed Methane Potential and Exploration Targets for Rural Alaskan Communities.

- A Department of Natural Resources Survey of coal bed methane potential in rural Alaskan communities. Including the number of villages and individuals in the area of interest and the distances to the nearest pipeline and roadways for access.

Appendix V. Geologic information for Canadian CBM reservoirs. Selected references are listed after this table.

Canadian Basin Name	Regional Location	Type of CBM Resource	Formation Name(s)	Coal Rank or Type	CBM Depth Range (m)	Water Production	Selected References
Vancouver Island	British Columbia	High volatile B bituminous to anthracite	Quinsam	-	500-1500	0.6%	6
Intermontane British Columbia	British Columbia	Semi-anthracite to Meta-anthracite	Bowser	-	-	2.5% - 5.3%	6
Intermontane British Columbia	British Columbia	High to medium volatile bituminous	Skeena	-	-	N/A	6
Intermontane British Columbia	British Columbia	High volatile C to B bituminous	Bowron River	-	700	N/A	6
Intermontane British Columbia	British Columbia	High volatile C to B bituminous	Merritt	-	-	N/A	6
Intermontane British Columbia	British Columbia	High volatile C to B bituminous	Tulameen	-	800	N/A	6
Rocky Mountain Front Ranges	SE British Columbia and SW Alberta	High to low volatile bituminous	East Kootenay	-	200-2000	0.9% - 1.4%	6

Canadian Basin Name	Regional Location	Type of CBM Resource	Formation Name(s)	Coal Rank or Type		CBM Depth Range (m)	Water Production	Selected References
				RO _{max}	Type			
Rocky Mountain Front Ranges	SE British Columbia and SW Alberta	High to low volatile bituminous	Crowsnest	-	67-380	N/A	6	
Rocky Mountain Front Ranges	SE British Columbia and SW Alberta	Low volatile bituminous to semianthracite	Cascade	-	400-1500	1.33% - 2.65%	6	
Rocky Mountain Front Ranges	SE British Columbia and SW Alberta	Low volatile bituminous to anthracite	Panther/Clearwater	-	500-1500	1.3% - 2.6%	6	
Inner Foothills	West-Central Alberta	Medium to low volatile	Nordegg	-	600-2600	1.2% - 1.6%	6	
Inner Foothills	West-Central Alberta	N/A	Cadomin-Luscar	-	500 - 2000	0.97% - 1.43%	6	
Inner Foothills	West-Central Alberta	Medium to low volatile bituminous	Smoky River	-	500-2000	1.3% - 1.7%	6	

Canadian Basin Name	Regional Location	Type of CBM Resource	Formation Name(s)	Coal Rank or		CBM Depth Range (m)	Water Production	Selected References
				Type	RO _{max}			
Inner Foothills	NE British Columbia	A bituminous to low volatile bituminous	Peace River	-	-	250 - 2000	1.0% -	6
							1.5%	
Outer Foothills	Alberta	High volatile bituminous	Belly River and Coalspur	-	-	250 - 2000	0.6% -	6
							0.75%	
Western Interior Plains	Alberta	Lignite to Bituminous	Mannville	-	-	<600 -	0.6% -	6
						>3000	1.2%	
Western Interior Plains	Alberta	Subbituminous C to high volatile C bituminous	Scollard	-	-	60 - 150	0.4% -	6
							0.75%	
Maritimes	Nova Scotia	High volatile bituminous A to medium volatile bituminous	Cumberland	-	-	150 - 800	0.75% -	6
							0.97%	
Maritimes	Nova Scotia	High volatile bituminous A to medium volatile bituminous	Pictou/Stellarton	-	-	600 - 1200	0.75% -	6
							0.97%	

Canadian Basin Name	Regional Location	Type of CBM Resource	Formation Name(s)	Coal Rank or Type		CBM Depth Range (m)	Water Production	Selected References
				RO _{max}	Type			
Maritimes	Nova Scotia	High volatile bituminous A to medium volatile bituminous	Sydney	-	-	500 - 2000	0.9% - 1.2%	6
Plains	Alberta	High-volatile C bituminous	Paskapoo (Obed)	-	-	0 - 500	0.48% - 0.63%	9, 5
Plains	Alberta	H-V bituminous C	Scollard (Ardley)	Variable water quality	-	0 - 700	0.5% - 0.65%	9, 1
Plains	Alberta	Subbituminous to H-V bituminous	Horseshoe Canyon (Carbon-Thompson & Drumheller)	Dry	-	0 - 800	0.39% - 0.65%	9, 10
Plains	Alberta	Subbituminous to H-V bituminous	Belly River (Lethbridge, Taber, & McKay)	TDS=139 mg/L	-	0 - 750	-	9
Plains	Alberta	Subbituminous to H-V bituminous	Upper Mannville	Water quality: Saline	-	800 - 2000	-	9

Canadian Basin Name	Regional Location	Type of CBM Resource	Formation Name(s)	Coal Rank or		CBM Depth Range (m)	Water Production	Selected References
				Type	RO _{max}			
Plains	Alberta	Subbituminous to H-V bituminous	Lower Mannville	-	-	750 – 3000	-	9
Foothills / Mountains	Alberta	H-V bituminous C	Coalspur	-	-	-	0.5% - 0.65%	3
Foothills / Mountains	Alberta	-	Brazeau	-	-	-	-	-
Foothills / Mountains	Alberta	H-V bituminous to Anthracite	Gates – Luscar	Water quality: variable	-	300 – 2500	1.05% - 1.89%	9, 7
Foothills / Mountains	Alberta	-	Moosebar – Luscar	-	-	500 – 2000	-	9
Foothills / Mountains	Alberta	-	Gladstone – Luscar	-	-	500 – 2000	-	9
Foothills / Mountains	Alberta	-	Cadomin – Luscar	-	-	500 – 2000	-	9
Foothills / Mountains	Alberta	-	Kootenay Group	-	-	1000 – 2000	-	9
Georgia	British Columbia	High-volatile B to A bituminous	Nanaimo Group	-	-	450-1500	0.64% - 0.72%	4
Big Horn	Alberta	Low-volatile bituminous	Luscar Group	-	-	>1.50%	-	7

1-Alberta Energy Utilities Board - Alberta Geological Survey, Earth Sciences Report: ESR 2003-04 - Chemical and Physical Hydrogeology of Coal, Mixed Coal-Sandstone and Sandstone Aquifers from Coal-Bearing Formations in the Alberta Plains Region, Alberta. Lemay, T.G. 2003.

- Unconventional gas resources are increasing in demand and importance. The natural gas developing companies in Alberta Canada face several challenges in the development of these unconventional gas resources. Land access, tenure, and economic developments are just a few of the obstacles that Alberta faces in its development and exploration of natural gas resources. Samples of coal, mixed coal-sandstone, and sandstone aquifers have been taken throughout Alberta. The resulting samples taken from Paskapoo-Scollard Formation aquifers have been shown to exceed Canada's water quality values in pH, sodium, manganese, and other precious metals. The preliminary analysis of the information available for pump testing has led to more informed and responsible decision-making regarding coal and sandstone aquifers.

2-Andrew Beaton: "Coal-Bearing Formations and Coalbed-Methane Potential in the Alberta Plains and Foothills," *CSEEG Recorder* (November 2003) p. 22 (http://www.cseg.ca/recorder/pdf/2003/11nov/nov03_05.pdf)

- Alberta contains substantial resources in the Plains and Foothills. Coal rank ranges from lignite in the eastern Plains up to low volatile bituminous and anthracite in the Foothills. Coalbed methane targets exist in the Scollard Formation, Horseshoe Canyon Formation and Coalspur coal zones of the Foothills. The maximum gas in place in Alberta is estimated at 1.42×10^{20} m³ (500 Tcf). Although this is a large number, the actual amount to be produced remains unknown due to limited data on gas concentrations and permeability.

3-Barry Ryan: "A Summary of Coalbed Methane Potential in British Columbia," *CSEEG Recorder* (November 2003) p. 32 (http://www.cseg.ca/recorder/pdf/2003/11nov/nov03_06.pdf)

- British Columbia has natural gas reserves of 9Tcf with additional undiscovered potential resources of 50 Tcf in the northeastern part of the province. Currently, the natural gas reserves of Canada and the United States are running out. The United States produces 8% coalbed methane out of all of the natural gases produced. This amounts to 1.56 Tcf/yr (2003). In Alberta and in British Columbia there are tremendous incentives to make CBM work. British Columbia alone has a CBM potential of over 3 billion tons. About 80% of British Columbia's coal resources lie within a number of upper Jurassic and lower Cretaceous coalfields in the foothills of the Rocky Mountains.

4-Cathy1-Bickford, C. Gwyneth, 1991, Coal Geology and Coalbed Methane Potential of Comox and Nanaimo Coal Fields, Vancouver Island, British Columbia in Coalbed Methane of Western North America: Rocky Mountain Association of Geologists, Denver, Colorado, pp.155-162.

- CBM of eastern Vancouver Island has contained high amounts of gas and coal. The two principal coalfields, Comox and Nanaimo, contain coal of Santonian and Campanian ages. The coals are soft, and the associated organic matter is rich in mudstones and gas bearing sandstone. Deeper drilling to a depth of 3,208 to 4,920 ft. is where this coal is found to persist.
- 5-"Canadian Minerals Yearbook 2003," Chapter 20.2, Catalogue no. M38-5/52E-PDF, ISBN 0-662-39197-7
- The total value of mineral commodities mined in Canada include, metals, nonmetals, and coal. In 2003 there was \$20.2 billion from these mines commodities as compared with the \$19.9 billion in 2002. However, the value of coal production has declined \$1.5 billion in 2003 from the \$1.6 billion in 2002 as the volume of coal production decreases.
- 6-Dawson, F.M., 1995. Coalbed Methane: A comparison between Canada and the United States, Geological Survey of Canada, Bulletin 489, pp. 60.
- Canada contains abundant coal resources spread throughout numerous basins in British Columbia, Alberta, Saskatchewan, the Maritimes, Yukon, and the Northwest Territories. Many of these basins contain coal suitable in quality and at a sufficient depth for coalbed methane reservoirs. However, only one well is in production currently. Canada's coal basins are ranked to have the highest coalbed methane potential for any region. A lack of information coal basins and CBM refinement has lead Canada to investigate the potential of its CBM resources.
- 7-Dawson, F.M., & W.D. Kalkrath, 1994, Coal rank, distribution, & coalbed methane potential of lower cretaceous luscara group, Bow River to Blackstone River, central Alberta foothills: Geologic Survey of Canada- Bulletin 473.
- The report gives a summary of the subsurface and surface mapping data collected from the Lower Cretaceous Luscar Groups coals from the Inner Foothills of Bow River to the Albert/British Columbia borders. The well samples indicate that coal rank is highly variable depending on the sample location and depth.
- 8-O.F.R. Wirth: "Exploration for Natural Gas from Coal in the Alberta Plains," presented at the AAPG Rocky Mountain Section Meeting -Rocky Mountain Natural Gas 2004, Denver Colorado August 9 to 11, 2004
- In February of 2003, MGV Energy Inc. was the first company in Canada to book natural gas from coal reserves. In November of 2003, production had exceeded 12 mmcf/d from the coals in the upper Cretaceous Horseshoe Canyon Formation and the Belly River Group. MGV also began CBM exploration in 1998. The meeting summarizes the coalbed methane potential of Alberta and it's near by plains.
- 9-O. Hoch: "The Dry Coal Anomaly - The Horseshoe Canyon Formation of Alberta, Canada," paper SPE 95872, proceedings of 2005 SPE Annual Technical Conference and Exhibition, Dallas Texas, 9-12 October 2005.
- The unique structure of the Horseshoe Canyon coal formation in Alberta, Canada has shown to be severely damaged by water influx and foams and normal permeability techniques have been unsuccessful. The approximate 12,000 sq. miles of the

Canyon are thought to contain 1-2 BCF per sq. mile. Nitrogen hydraulic fracturing is the only stimulation process that has had success in the formation thus far.

10- P.A. Bastian, O.F.R. Wirth, L. Wang, G.W. Voneiff: "Assessment and Development of the Dry Horseshoe Canyon CBM Play in Canada," paper SPE 96899, proceedings of 2005 SPE Annual Technical Conference and Exhibition, Dallas Texas, 9-12 October 2005.

- CBM plays an important role in Western Canada's conversion from an under-explored, and non-commercial resources to a major commercial resources has occurred over such a short time. In December of 2004, the Horseshoe Canyon CBM was estimated to be over 100 MMscfd of gas. The commercially developed wells were completed in 2003 and 2004. In 2005, wells are in excess of 3,000/year. Due to the unique and complex structure of the Horseshoe Canyon, assessment of the commercial viability and development has been difficult.

11-Richardson, R.J.H., 1991, Coal Resources and Coalbed Methane Potential of a Major Alberta Coal Zone in Coalbed Methane of Western North America: Rocky Mountain Association of Geologists, Denver, Colorado.

- The total Coal resources of Alberta have been estimated to be at 2.6 trillion short tons. The energy in this coal is 23 times that available in the province's remaining reserves of conventional oil and more than 3.7 times that of its massive oil sands deposits. The Ardley alone was calculated to have 468.5 billion short tons (425 billion tons) along a 250-mile-long subcrop on into the southwest side of the Alberta syncline. Deeper coal reserves have been found to contain large volume of gas below thick seams of dense peat moss growth.

Appendix VI. Geologic information of major Russian CBM reservoirs and water production and disposal information. Selected references are listed after this table.

Russian Basin Name	Regional Location	Type of CBM Resource	Formation Name(s)	Coal Rank or Type	CBM Depth Range (m)	Water Production	Selected References
Kuznetsk	South-central Russia	-	-	Hard coal	1,350	-	1
Pechora	North-central Russia	-	-	Hard coal	< 1800	-	1
Donetsk	Border of Russia and Ukraine	-	-	Hard coal	< 1800	-	1
Karaganda	Kazakhstan	-	-	-	< 1800	-	1
Artemovskoye	Habaravski Krai	Lignite	-	Brown coal	-	-	2
Partizanskoye	Primorsky Krai	Bituminous	-	Brown coal	450-620	-	2
Razdolnensky	Primorsky Krai	Bituminous	-	Brown coal	450-620	-	2
Tavritchanskoye	Primorsky Krai	Lignite	-	Brown coal	450-620	-	2
Podgorednen skoye	Primorsky Krai	Bituminous	-	Brown coal	450-620	-	2

1-“Status of Coalbed Methane Recovery and Utilization in the Former Soviet Union,” International Coal & Methane Research Center, <http://www.uglemetan.ru/HTML/WhitePapers.php>

2-“Coal Industry Status and Development Perspectives of Coalbed Methane Recovery and Utilization in Russia’s Far East,” International Coal & Methane Research Center, <http://www.uglemetan.ru/HTML/WhitePapers.php>

Appendix VII. CBM cold-region professional and research contacts.

Country	Name	Organization	Email Address	Phone	Address	Currently Working on CBM Issues	Currently Working on CBM Water Issues
Canada	Dr. Serge Guiot	Canadian National Research Council	serge.guiot@cnrc-nrc.gc.ca	514-496-6181	Not Known	No Reply Received	No Reply Received
Canada	Dr. Abdul Majid	Canadian National Research Council	Abdul.Majid@cnrc-nrc.gc.ca	613-993-2017	1200 Montreal Rd. Ottawa, ON K1A 0R6	Yes	Yes
Canada	Dr. Denis Groleau	Canadian National Research Council	denis.groleau@cnrc-nrc.gc.ca	514-496-6186	Not Known	Yes	Yes
Canada	Dr. Hongsheng Guo	Canadian National Research Council	Hongsheng.Guo@cnrc-nrc.gc.ca	613-991-0869	1200 Montreal Rd. Ottawa, ON K1A 0R6	No Reply Received	No Reply Received
Canada	Kevin Jonasson	Canadian National Research Council	Kevin.Jonasson@cnrc-nrc.gc.ca	613-993-6570	1200 Montreal Rd. Ottawa, ON K1A 0R6	No Reply Received	No Reply Received

Country	Name	Organization	Email		Phone	Address	Currently Working on	
			Address				CBM Issues	CBM Water Issues
Canada	Dr. William Keith	Canadian National Research Council	Bill.Keith@nrc-cnrc.gc.ca		705-762-2914	1200 Montreal Rd. Ottawa, ON K1A 0R6	No	No
Canada	Phillip M. Reece	Canadian National Research Council	Phill.Reece@nrc-cnrc.gc.ca		506-636-3367	1200 Montreal Rd. Ottawa, ON K1A 0R6	No Reply Received	No Reply Received
Canada	Dr. Michael Gattrell	Canadian National Research Council	Michael.Gattrell@nrc-cnrc.gc.ca		613-990-3819	1200 Montreal Rd. Ottawa, ON K1A 0R6	No	No
Canada	Curtis Evans	Alberta Department of Energy	N/A		403-297-8386	N/A	No Reply Received	No Reply Received
Canada	Tom Byrnes	Alberta Department of Energy	N/A		403-297-8479	N/A	No Reply Received	No Reply Received
Canada	Shirley	Alberta Department of Energy	N/A		403-297-2190	N/A	No Reply Received	No Reply Received

Country	Name	Organization	Email Address	Phone	Address	Currently Working on CBM Issues	Currently Working on CBM Water Issues
Russia	Oleg Tailakov	Uglemetan	tailakov@ugl emetan.ru	8 384 2 281366	ч Директор АНО "Углеметан", Д.Т.Н. ул. Рукавишник ова, 21 Кемерово, 650610	No Reply Received	No Reply Received

Appendix VIII. Geologic Information for Alaskan rural communities with or near potential CBM reservoirs. Selected references are listed after this table. CBM resource locations are general estimates, which would need to be evaluated by site-specific investigations.

Community or Village	Village		Approximate CBM Location	Geologic		Formation Name	Type of CBM Resource	CBM Depth Range	Selected References
	Regional Location	Basin and Field Name		Field Name	Basin and Field Name				
Alatna	North West	Rampart	Remote	Rampart	Bergman-Kaltag	Bituminous	No Data	6	
Allakaket	Central	Rampart	Remote	Rampart	Bergman-Kaltag	-	No Data		
Ambler	Northwest	Kobuk River	Immediate	Kobuk River	Bergman-Kaltag	Bituminous	No Data	1, 2, 4, 5, 6	
Atkasuk	North Slope	Northern Alaska Coal	Immediate	Northern Alaska Coal	Nanushuk-Colville	-	Surface to > 6000 ft	1, 2, 4, 5, 6	
Beaver	Central	Rampart	Immediate	Rampart	Bergman-Kaltag	Lignite	No Data	1, 5, 6	
Birch Creek	Central	Eagle - Circle	Immediate	Eagle - Circle	Bergman-Kaltag	-	No Data	1, 5, 6	
Bettles	Central	Rampart	Adjacent	Rampart	Bergman-Kaltag	Bituminous	No Data	1, 5, 6	
Chalkyitsik	Central	Eagle-Circle	Remote	Eagle-Circle	Bergman-Kaltag	Lignite	No Data	1, 5, 6	
Chignik	Aleutians	Chignik	Immediate	Chignik	Chignik	Subbituminous	< 9000 ft.	6	
Chignik Lg	Aleutians	Chignik	Immediate	Chignik	Chignik	Subbituminous	< 9000 ft.	6	
Chignik Lake	Aleutians	Chignik	Immediate	Chignik	Chignik	Subbituminous	< 9000 ft.	6	
Deering	Southwest	Chignik	Remote	Chignik	-	Bituminous		6	
Evansville	Central	Rampart	Adjacent	Rampart	Bergman-Kaltag	Bituminous	No Data	1, 5, 6	
Ft. Yukon	Central	Eagle - Circle	Adjacent	Eagle - Circle	Bergman-Kaltag	Lignite	1253	1, 5, 6	
Galena	Central	Nulato	Remote	Nulato	Bergman-Kaltag	Bituminous	No Data	1, 5, 6	

Community or Village	Village		Approximate Location	Geologic		Formation Name	Coal Rank or Type	CBM Depth Range	Selected References
	Regional Location	Field Name		Basin and Field Name	Basin and Field Name				
Kaltag	Western	Nulato	Adjacent	Nulato	Bergman-Kaltag	Bituminous	No Data	6	
Kiana	Northwest	Kobuk River	Adjacent	Kobuk River	Bergman-Kaltag	Bituminous	No Data	6	
Kobuk	Northwest	Kobuk River	Immediate	Kobuk River	Bergman-Kaltag	Bituminous	No Data	6	
Koyuk	Western	Nulato	Remote	Nulato	-	Bituminous & Lignite	-	6, 2	
Koyukuk	Western	Nulato	Local Occ. Adjacent	Nulato	Bergman-Kaltag	Bituminous	No Data	6	
McGrath	Central	Little Tonzona	Adjacent	Little Tonzona	-	Subbituminous	No Data	1, 5, 6	
Mekoryuk	Southwest	Rampart	Remote	Rampart	-	Subbituminous	-	6	
Nightmute	Southwest	Rampart	Remote	Rampart	-	Subbituminous	-	6	
Nikolai	Central	Little Tonzona	Immediate	Little Tonzona	Usibelli	Subbituminous	No Data	1, 5, 6	
Noatak	Northwest	Rampart	Remote	Rampart	-	Bituminous	-	6	
Nulato	Central	Nulato	Immediate	Nulato	Bergman-Kaltag	Bituminous	No Data	1, 5, 6	
Perryville	Southwest	Herendeen Bay – Unga Island	Remote	Herendeen Bay – Unga Island	-	Subbituminous	-	6	
Point Lay	North Slope	Northern Alaskan Coal	Adjacent	Northern Alaskan Coal	Nanushuk	Bituminous	Surface to >6000 ft	1, 2, 5, 8	
Rampart	Central	Rampart	Adjacent	Rampart	-	Bituminous	-	1, 5, 6	
Selawik	Northwest	Kobuk River	Adjacent	Kobuk River	-	Bituminous	-	6	
Shungnak	Northwest	Kobuk River	Immediate	Kobuk River	Bergman-Kaltag	Bituminous	No Data	6	
Toksook Bay	Southwest	Rampart	Remote	Rampart	-	-	-	6	
Tununak	Southwest	Rampart	Remote	Rampart	-	-	-	6	

Community or Village	Village		Approximate CBM Location	Geologic Basin and Field Name		Formation Name	Coal Rank or Type	CBM Depth Range	Selected References
	Regional Location	Location		Basin and Field Name	Field Name				
Unalakleet Venetie	Western	Remote	Remote	Nulato	-	Bituminous	-	6	1, 5, 6
	Central	Remote	Remote	Yukon	Bergman-Kaltag	Lignite	No Data		
Wainwright	North Slope	Immediate	Immediate	Northern	Nanushuk & Corwin	Subbituminous & Bituminous	-	1, 2, 5, 6	1, 2, 5, 6
				Alaska Coal					

- 1 – Huffman, A. C. Jr., Ahlbrandt, T. S., Pasternack, Ira, Stricker, G. D., and Fox, J. E., 1988, Sedimentology of the Nanushuk Group, North Slope, in Gryc, George (ed.), *Geology and Exploration of the National Petroleum Reserve in Alaska, 1974 to 1982*, U.S. Geological Survey professional paper 1399, p 281-298. <http://www.dggs.dnr.state.ak.us/pubs/pubs?reqtype=citation&ID=4007>
 - The Nanushuk Group is a regressive sequence of nonmarine, transitional and marine deposits, located on the North Slope of Alaska. The sedimentary rocks of the Nanushuk Group are exposed in an outcrop belt approximately 650 km long and 30-50 km wide. Coal beds are found within the Nanushuk Group and are commonly found in the transitional or nonmarine deposits ranging from about 1 m - 4 m thick.
- 2 – Merritt, R. D., 1986a, Evaluation of Alaska's coal potential, Alaska Division of Geological and Geophysical Surveys, Public-data file 86-92. <http://www.dggs.dnr.state.ak.us/pubs/pubs?reqtype=citation&ID=1293>
 - The report contains evaluations of Alaska's coal potential in different quadrangles throughout the state. The coal potential around Alaska is evaluated and ranked according to characteristics and locality of the deposit.
- 3 – Plafker, G., and Berg, H. C., 1994, Chapter 33, Overview of the Geology and Tectonic evolution of Alaska, *The Geology of North America Vol. G-1, The Geology of Alaska*, pp. 989-1021.
 - The report is an in-depth overview of Alaska's geology and tectonic evolution. One section of the report contains information about compositions and formation process of Alaska's different terrains. That is followed by descriptions of plutonic and volcanic belts, how interaction of oceanic and continental plates causes rotations and translations in Alaska, and finishes up with a tectonic evolution of Alaska from Precambrian time to the present.
- 4 – Sable, E. G., and Stricker, G. D., 1987, Coal in the National Petroleum Reserve in Alaska (NPR); Framework geology and resources, in Tailleux, I. L., and Weimer, Paul., eds., *Alaskan North Slope Geology*; Society of Economic Paleontologists and Mineralogists and Alaska Geological Society Book 50, p. 195-216.
 - The report focuses on the Corwin and Chandler formations within the National Petroleum Reserve in Alaska (NPR). The Corwin and Chandler formations are a part of the Nanushuk Group. They have bituminous to subbituminous coal ranks, with an estimated 2.7 trillion short-tons of coal. The river and delta dominated environment is very favorable to coal development. The report also contains a quick review on the physiography, drainage and climate of NPR. There are ground water issues due to the thick permafrost. Nearly all the fresh water comes from streams and lakes.
- 5 – Smith, T. N., 1995, Coalbed Methane Potential for Alaska Drilling Results for the Upper Cook Inlet, in INtergas '95: Proceedings of the International Unconventional Gas Symposium, p 1-21.
 - This document is an evaluation of Alaska's thirteen most promising coal basins based on coal rank, depth, seam thickness, and structure. Alaska's total coal estimate (5.5 trillion short-tons) is nearly half the U.S. total. The coal ranks from bituminous to

subbituminous and could produce 1,000 tcf of gas. The largest coal resource basins in Alaska are the North Slope Basin and Cook Inlet Basin. In a coalbed methane test well in the Cook Inlet Basin, gas content increased with depth. There is also a comparison of the coal's age and their coalbed methane potential within the different basins.

6 - Tyler, R., Scott, A.R., and Clough, J.G., 2000, Coalbed methane potential and exploration targets for rural Alaska communities: Alaska Division of Geological & Geophysical Surveys Preliminary Interpretive Report 2000-2, 177 p.

<http://www.dggs.dnr.state.ak.us/pubs/pubs?reqtype=citation&ID=2733>

- The document targets rural communities in Alaska for potential exploration of coalbed methane. The Bureau of Economic Geology created a model indicating the essential controls of coalbed methane producibility. The controls include: permeability, gas content, coal rank and gas generation, hydrodynamics, tectonic and structural setting, and depositional setting and coal distribution. With the application of the producibility model to all rural Alaskan coal basins, the North Slope has the highest potential for coalbed methane resource development.

IX. Utilization of Endnote Database for Reference Organization.

Project Endnote Use: The CBM project used the Endnote database to organize scientific and technical references from our reference searches. Julia Triplehorn of the UAF- Geophysical Institute Library was the primary contact for citation and copyright issues as well as guiding students on inputting Endnote information. Hardcopies of all information requested for the project has been archived at the library for project and public use. The information from the Endnote bibliography can be located at: <http://www.gi.alaska.edu/services/library/> under the “bibliographies (searchable)” link.

General Information about using Endnote: Endnote has been updated with references from many sources, to properly utilize the database it is recommended that you search for applicable resources, rather than generate a list of everything currently available. You must first open the desired “library” from the FILE menu. If you want to research a topic, you would select “Search References” from the REFERENCES menu, and proceed to enter your search information. For general topics, such as “water disposal”, the user should try searching ANY FIELD and using a combination of searches for the same topic (ex. water disposal, water and disposal). If you want to research information that has already been accessed by the CBM working group, you would search the codes listed below under their designated search fields. These codes have been set up specifically for tracking the references used by the project. From the “Search References” box, simply change ANY FIELD to one of the two fields below, and search by the listed codes.

To help code references with information related specifically to this project, we are using the “Research Notes” field in Endnote. The below codes are used to help with the “Research Notes” information and knowing if a reference is available for project team review.

RESEARCH NOTES:

Library- indicates the reference is available in the CBM Collection at the GI Library.

Electronic- indicates that an electronic copy is available.

CD- indicates a corresponding CD.

References- indicates that we have pulled further reference from the original resource.

ALTERNATE TITLE:

Specific Articles- indicates that specific articles have been pulled from a larger resource.

Oil & Natural Gas Technology

DOE Award No.: DE-FC26-01NT41248

Final Report

Field Exploration of Methane Seep Near Atqasuk

Submitted by:
Institute of Northern Engineering
University of Alaska Fairbanks
P.O. Box 755910
Fairbanks, AK 99775-5910

Prepared for:
United States Department of Energy
National Energy Technology Laboratory

January 2009



Office of Fossil Energy

